

This document is copyrighted material.

Permission for online posting was granted to Alaska Resources Library and Information Services (ARLIS) by the copyright holder.

Permission to post was received via e-mail by Celia Rozen, Collection Development Coordinator on December 16, 2013, from Kenneth D. Reid, Executive Vice President, American Water Resources Association, through Christopher Estes, Chalk Board Enterprises, LLC.

This symposium includes the following chapters directly relevant to the Susitna-Watana project:

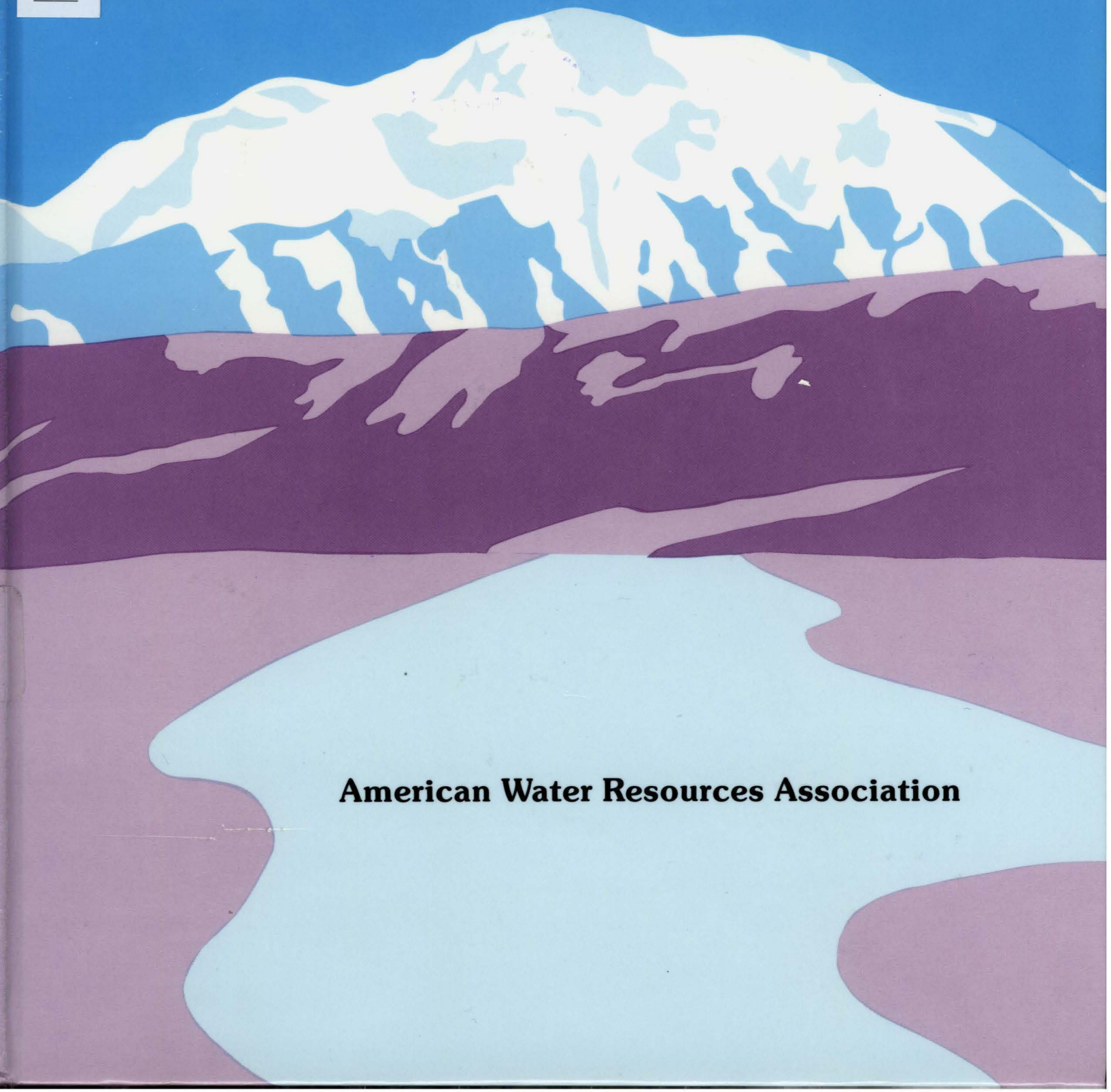
<i>The Susitna Hydroelectric Project simulation of reservoir operations,</i> by Yaohuang Wu, Joel I. Feinstein, and Eugene J. Gemperline	pages 3-11
<i>Hydrology and hydraulic studies for licensing of the Susitna Hydroelectric Project,</i> by Eugene J. Gemperline	pages 73-85
<i>Some aspects of glacier hydrology in the upper Susitna and Maclaren River basins, Alaska,</i> by Theodore S. Clarke, Douglas Johnson, and William D. Harrison.....	pages 329-337
<i>Forecasting the effects of river ice due to the proposed Susitna Hydroelectric Project,</i> by Ned W. Paschke and H.W. Coleman	pages 557-581
<i>Freezeup processes along the Susitna River,</i> by Stephen R. Bredthauer and G. Carl Schoch.....	pages 573-581

Proceedings: Cold Regions Hydrology

ARLIS



3 3755 000 53999 9



American Water Resources Association

GB
652
.P76
1986

PROCEEDINGS

of the

Symposium: Cold Regions Hydrology

UNIVERSITY OF ALASKA-FAIRBANKS, FAIRBANKS, ALASKA

Edited by

DOUGLAS L. KANE
Water Research Center
Institute of Northern Engineering
University of Alaska-Fairbanks
Fairbanks, Alaska



ARLIS
Alaska Resources
Library & Information Services
University of Alaska

3 3755 000 53999 9

Co-Sponsored by

- UNIVERSITY OF ALASKA-FAIRBANKS
FAIRBANKS, ALASKA
- AMERICAN SOCIETY OF CIVIL ENGINEERS
TECHNICAL COUNCIL ON COLD REGIONS ENGINEERING
- NATIONAL SCIENCE FOUNDATION
- STATE OF ALASKA, ALASKA POWER AUTHORITY
- STATE OF ALASKA, DEPARTMENT OF NATURAL RESOURCES
- U.S. ARMY, COLD REGIONS RESEARCH
AND ENGINEERING LABORATORY

Host Section

ALASKA SECTION OF THE AMERICAN WATER RESOURCES ASSOCIATION

The American Water Resources Association wishes to express appreciation to the U.S. Army, Cold Regions Research and Engineering Laboratory, the Alaska Department of Natural Resources, and the Alaska Power Authority for their co-sponsorship of the publication of the proceedings.

American Water Resources Association

5410 Grosvenor Lane, Suite 220
Bethesda, Maryland 20814

AMERICAN WATER RESOURCES ASSOCIATION TECHNICAL PUBLICATION SERIES
TPS-86-1

LIBRARY OF CONGRESS CATALOG CARD NUMBER: 86-70416

1986 COPYRIGHT BY THE AMERICAN WATER RESOURCES ASSOCIATION

All rights reserved. No part of this book may be reproduced in any form or by any mechanical means, without written permission by the publisher. These proceedings were published by the American Water Resources Association, 5410 Grosvenor Lane, Suite 220, Bethesda, Maryland 20814. The views and statements advanced in this publication are solely those of the authors and do not represent official views or policies of the American Water Resources Association; the University of Alaska-Fairbanks; the American Society of Civil Engineers, Technical Council on Cold Regions Engineering; National Science Foundation; State of Alaska, Alaska Power Authority; State of Alaska, Department of Natural Resources; and the U.S. Army, Cold Regions Research and Engineering Laboratory. Communications in regard to this publication should be sent to the Circulation Department of the American Water Resources Association, 5410 Grosvenor Lane, Suite 220, Bethesda, Maryland 20814, U.S.A.

PREFACE

Fascination with polar regions, along with potential commerce, first attracted arctic and antarctic explorers. However, most adventurers and their supporters soon concluded that resource development and trading in cold regions was not very profitable. In fact, the high latitudes of North America were viewed as a physical obstacle to trade routes between southeast Asia and Europe. Substantial time and effort was spent seeking the Northwest Passage.

Early commercial spirit faded with the decline of the fur trade and whaling, and with the depletion of the gold fields. The Second World War drew fresh faces to the North. Military activity and new resource development became the major motivating factors for population growth in cold regions. These activities stimulated the tremendous growth of scientific research on high-latitude phenomena over the last 40 years.

The first forms of economic activity in the North, such as whaling and gold mining, were performed by temporary inhabitants who frequently retreated southward to warmer climates. Slowly this mode of operation changed; people started to make the high latitudes their year-round home. New technology made living in these cold climates more tolerable during the winter. Modern transportation and communication reduced the perceived distance between the North and the rest of the world.

Since much of the increasing activity was affected to some extent by hydrologic phenomena, the need developed for both an understanding of hydrological processes dominated by snow and ice, and long-term data for hydrologically related design. Clearly, mid-latitude hydrology has attracted much more attention than high-latitude phenomena during the last few decades. This is rightfully so, since most people live at the mid-latitudes. Yet the search for natural resources now extends far beyond this zone of comfortable living. The greatest strides in our understanding of hydrologic processes are now being made in both cold and tropical climates. In cold regions, science has particularly advanced our understanding of the roles of snow and ice. Also, it is imperative that we precisely understand the contribution of the polar regions and the tropics to the global climate.

The objective of this symposium is to pull together researchers and practitioners in hydrology and closely related fields to discuss present hydrologic problems and interests. We are fortunate to have presentations from a large number of countries: Austria, Canada, Denmark (Greenland), England, Finland, Iceland, Japan, Norway, Sweden, USA and USSR.

A review of present hydrologic data reveals that most northern countries have very sparse networks for data collection. Most data are collected around population centers that are situated at relatively low elevations. The periods of record for most hydrologic data in cold regions are quite short relative to record lengths in temperate climates. Furthermore, instrumentation used to collect data often does not work satisfactorily in cold regions. A session on *Instrumentation and Data Collection*, and another on *Remote Sensing* will address many of these problems.

The sessions generally follow the logical divisions of the hydrologic cycle. Watershed input is covered in a session on *Precipitation — Snowpack — Soil Processes*. Along these same lines, glaciers that act as storage reservoirs during the winter and provide meltwater for runoff in the summer are included in the session on *Glacier Hydrology*. The importance of ablation and the conversion to runoff in the hydrologic cycle of cold regions are highlighted by a session on *Snowmelt Runoff*. Channel processes associated with sedimentation and ice are presented in one session on *Channel Hydraulics and Morphology*, and two sessions on *River Ice Hydraulics*. Surface storage in water bodies and associated processes are discussed in a session on *Reservoir and Lake Level Processes*. In the field of environmental hydrology, one session is devoted to *Water Quality*.

There are more than 20 additional papers in the poster session. These excellent papers could have fit into one of the other sessions if there had not been so many papers. The poster papers were selected by the technical chairman based solely on graphical criteria. For every session, snow, ice and frozen ground are the common threads that bind the symposium together.

Despite the fact that numerous books with ominous titles (*No Man's Land, Amid Snowy Waste, Ice Bound, Lost in the Arctic, Two Against the Ice, Nansen in the Frozen World, etc.*) have been written about the colder regions of the world, people venture forth in ever-increasing numbers. To treat this land properly, we need to develop a clearer understanding of its natural processes.

Douglas L. Kane
Editor, Technical Chairman

ACKNOWLEDGMENTS

As editor of this proceedings, I would like to thank several local AWRA members who have assisted me in making this publication possible: Brent Petrie (General Chairman) of the Alaska Power Authority; Stephen Mack (Co-Chairman Local Arrangements) of the Alaska Department of Natural Resources; James Aldrich (Co-Chairman Local Arrangements) of Arctic Hydrologic Consultants; Linda Perry Dwight; Stephen Bredthauer (Finance Chairman) and Jeffrey Coffin of R&M Consultants, Inc.; Ronald Huntsinger (Exhibits Chairman) of the U.S.D.I. Bureau of Land Management; and Charles Slaughter of the U.S.D.A. Institute of Northern Forestry. Two individuals that I would like to express special thanks to are Catherine Egan of the University of Alaska-Fairbanks and Charlene Young of AWRA for helping with all the details that are required to make the proceedings a reality.

Name	Affiliation	City/State/County
James Aldrich	Arctic Hydrological Consultants	Fairbanks, AK
Eric Anderson	U.S. National Weather Service	Silver Springs, MD
Gary Anderson	U.S. Geological Survey/WRD	Richmond, VA
George Ashton	U.S. Army CRREL	Hanover, NH
William Ashton	R&M Consultants, Inc.	Anchorage, AK
Lars Bengtsson	Uppsala University	Uppsala, Sweden
Carl S. Benson	University of Alaska-Fairbanks	Fairbanks, AK
Neil Berg	U.S.D.A., Forest Service	Berkeley, CA
David Bjerklie	University of Alaska-Fairbanks	Fairbanks, AK
Tim Brabets	U.S. Geological Survey/WRD	Anchorage, AK
Stephen R. Bredthauer	R&M Consultants, Inc.	Anchorage, AK
Edward J. Brown	University of Alaska-Fairbanks	Fairbanks, AK
Robert Burrows	U.S. Geological Survey/WRD	Fairbanks, AK
Darryl Calkins	U.S. Army CRREL	Hanover, NH
Robert F. Carlson	University of Alaska-Fairbanks	Fairbanks, AK
Edward F. Chacho	U.S. Army CRREL	Fort Wainwright, AK
George Clagett	U.S.D.A., Soil Conservation Service	Anchorage, AK
Jeffrey H. Coffin	R&M Consultants, Inc.	Anchorage, AK
Samuel Colbeck	U.S. Army CRREL	Hanover, NH
Keith R. Cooley	U.S.D.A., Agricultural Research	Boise, ID
Arthur G. Crook	U.S.D.A., Soil Conservation Service	Portland, OR
Larry Dearborn	Alaska Dept. of Natural Resources/DGGS	Eagle River, AK
Phil A. Emery	U.S. Geological Survey/WRD	Anchorage, AK
David C. Esch	Alaska Dept. of Transportation and Public Facilities	Fairbanks, AK
James L. Foster	National Atmospheric and Space Administration/GSFC	Greenbelt, MD
Andrew G. Fountain	U.S. Geological Survey	Tacoma, WA
John Fox	University of Alaska-Fairbanks	Fairbanks, AK
Thomas George	University of Alaska-Fairbanks	Fairbanks, AK
Joan P. Gosink	University of Alaska-Fairbanks	Fairbanks, AK
Raoul J. Granger	University of Saskatchewan	Saskatoon, Canada
Dorothy K. Hall	National Atmospheric and Space Administration/GSFC	Greenbelt, MD
Donald R. F. Harleman	MIT	Cambridge, MA

Name	Affiliation	City/State/County
William D. Harrison	University of Alaska-Fairbanks	Fairbanks, AK
Larry Hinzman	University of Alaska-Fairbanks	Fairbanks, AK
Mark Inghram	Alaska Dept. of Natural Resources/DGGS	Eagle River, AK
Peter Jordan	Consulting Services in Hydrology and Terrain Sciences	Vancouver, Canada
Douglas L. Kane	University of Alaska-Fairbanks	Fairbanks, AK
Bev D. Kay	University of Guelph	Guelph, Canada
Esko Kuusisto	National Board of Waters	Helsinki, Finland
Robert Lamke	U.S. Geological Survey/WRD	Anchorage, AK
Jacqueline D. LaPerriere	University of Alaska-Fairbanks	Fairbanks, AK
Stephen Mack	Alaska Dept. of Natural Resources/DGGS	Fairbanks, AK
David H. Male	University of Saskatchewan	Saskatoon, Canada
Eric A. Marchegiani	Alaska Power Authority	Anchorage, AK
Philip Marsh	National Hydrology Research Institute	Ottawa, Canada
Mary Maurer	Alaska Dept. of Natural Resources/DGGS	Eagle River, AK
Larry Mayo	U.S. Geological Survey/WRD	Fairbanks, AK
Mark Meier	University of Colorado	Boulder, CO
John M. Miller	University of Alaska-Fairbanks	Fairbanks, AK
Woodruff Miller	Brigham Young University	Provo, UT
James A. Munter	Alaska Dept. of Natural Resources/DGGS	Eagle River, AK
Gordon Nelson	U.S. Geological Survey	Anchorage, AK
Jerry Nibler	National Weather Service	Anchorage, AK
Mark Oswood	University of Alaska-Fairbanks	Fairbanks, AK
Bruce Parks	U.S. Geological Survey/WRD	Reston, VA
Eugene L. Peck	HYDEX	Fairfax, VA
Lawrence A. Peterson	L. A. Peterson and Associates	Fairbanks, AK
Brent Petrie	Alaska Power Authority	Anchorage, AK
William A. Petrik	Alaska Dept. of Natural Resources/DGGS	Eagle River, AK
Steven R. Predmore	U.S. Army Corps of Engineers	Buffalo, NY
Albert Rango	U.S.D.A./ARS/BARC-WEST	Beltsville, MD
David A. Robinson	Columbia University	Palisades, NY
Nigel Roulet	York University	Downsview, Canada
Larry Rundquist	Entrix, Inc.	Anchorage, AK
Henry S. Santeford	Michigan Technological University	Houghton, MI
Bernard A. Shafer	U.S.D.A., Soil Conservation Service	Portland, OR
Hung Tao Shen	Clarkson University	Potsdam, NY
David A. Sherstone	Inuvik Scientific Resource Centre	Inuvik, Canada
Charles W. Slaughter	U.S.D.A., Institute of Northern Forestry	Fairbanks, AK
Heinz G. Stefan	University of Minnesota	Minneapolis, MN
Jean Stein	Laval University	Quebec City, Canada
Robert Van Everdingen	Environment Canada, NHRI	Calgary, Canada
Patrick J. Webber	University of Colorado	Boulder, CO
Phyllis Weber	Alaska Dept. of Fish and Game	Fairbanks, AK
Peter J. Williams	Carleton University	Ottawa, Canada
Ming-Ko Woo	McMaster University	Hamilton, Canada
Sheri Woo	U.S.D.A. Forest Service	Berkeley, CA
Yaohuang Wu	Harza Engineering Co.	Chicago, IL
John Zarling	University of Alaska-Fairbanks	Fairbanks, AK
Chester Zenone	U.S. Geological Survey/WRD	Anchorage, AK

TABLE OF CONTENTS

RESERVOIR AND LAKE LEVEL PROCESSES

The Susitna Hydroelectric Project Simulation of Reservoir Operation	
— <i>Yaohuang Wu, Joel I. Feinstein, and Eugene J. Gemperline</i>	3
Reservoir Operations Planning in Snowmelt Runoff Regimes Based on Simple Rule Curves	
— <i>B. A. Shafer, P. E. Farnes, K. C. Jones, J. K. Marron, and F. D. Theurer</i>	13
Modelling Water Levels for a Lake in the Mackenzie Delta	
— <i>P. Marsh</i>	23
Short-Wave Heating of Lake Surface Water Under a Candelled Ice Cover	
— <i>J. P. Gosink and J. D. LaPerriere</i>	31
Hydrothermal Modeling of Reservoirs in Cold Regions: Status and Research Needs	
— <i>Donald R. F. Harleman</i>	39

WATER, SNOW AND ICE MANAGEMENT

Watershed Test of a Snow Fence to Increase Streamflow: Preliminary Results	
— <i>Ronald D. Tabler and David L. Sturges</i>	53
Survey of Experience in Operating Hydroelectric Projects in Cold Regions	
— <i>Eugene J. Gemperline, David S. Louie, and H. Wayne Coleman</i>	63
Hydrology and Hydraulic Studies for Licensing of the Susitna Hydroelectric Project	
— <i>Eugene J. Gemperline</i>	73
Ice Jam Flooding — Evolution of New York State's Involvement	
— <i>Russell E. Wege</i>	87
Hydrological and Ecological Processes in a Colorado, Rocky Mountain Wetland: Case Study	
— <i>Edward W. Rovey, Catherine Kraeger-Rovey, and David J. Cooper</i>	93
Seasonal Snow and Aufeis in Alaska's Taiga	
— <i>C. W. Slaughter and C. S. Benson</i>	101

INSTRUMENTATION AND DATA COLLECTION

Water Redistribution in Partially Frozen Soil by Thermal Neutron Radiography	
— <i>Michael A. Clark, Dr. Roger J. Kettle, and Giles D'Souza</i>	113
The Development and Use of "Hot-Wire" and Conductivity Type Ice Measurement Gauges for Determination of Ice Thickness in Arctic Rivers	
— <i>David A. Sherstone, Terry D. Prowse, and Harry Gross</i>	121

Recent Developments in Hydrologic Instrumentation	
— <i>Vito J. Latkovich and James C. Futrell II</i>	131
Problems Encountered and Methods Used in the U.S. Geological Survey for the Collection of Streamflow Data Under Ice Cover	
— <i>Ernest D. Cobb and Bruce Parks</i>	135
Simplified Method of Measuring Stream Slope	
— <i>Jacqueline D. LaPerriere and Donald C. Martin</i>	143

WATER QUALITY

Water Quality-Discharge Relationships in the Yukon River Basin, Canada	
— <i>Paul H. Whitfield and W. G. Whitley</i>	149
The Role of Snowcover on Diurnal Nitrate Concentration Patterns in Streamflow from a Forested Watershed in the Sierra Nevada, Nevada, USA	
— <i>Jonathan J. Rhodes, C. M. Skau, and D. L. Greenlee</i>	157
Reservoir Water Quality Simulation in Cold Regions	
— <i>C. Y. Wei and P. F. Hamblin</i>	167
Trophic Level Responses to Glacial Meltwater Intrusion in Alaskan Lakes	
— <i>J. P. Koenings, R. D. Burkett, Gary B. Kyle, Jim A. Edmundson, and John M. Edmundson</i>	179
Deep-Lying Chlorophyll Maxima at Big Lake: Implications for Trophic State Classification of Alaskan Lakes	
— <i>Paul F. Woods</i>	195
Factors Influencing the Quality of Snow Precipitation and Snow Throughfall at a Sierra Nevada Site	
— <i>Sheri Woo and Neil Berg</i>	201

POSTER SESSION

Primary Production, Chlorophyll, and Nutrients in Horseshoe Lake, Point MacKenzie, Alaska	
— <i>Paul F. Woods and Timothy G. Rowe</i>	213
Water Quality of Abandoned Mine Runoff: A Case Study of Alaskan Sites	
— <i>David B. Pott, Robert E. Lindsay, and Nicholas Pansic</i>	221
Thawing of Ground Frost on a Drained and Undrained Boreal Wetland Site	
— <i>L. E. Swanson and R. L. Rothwell</i>	231
Probability Distributions of Rain on Seasonally Frozen Soils	
— <i>John F. Zuzel</i>	237
Evidence of Groundwater Recharge Through Frozen Soils at Anchorage, Alaska	
— <i>James A. Munter</i>	245
Residential Well Development of a Low Permeability Bedrock Flow System	
— <i>William A. Petrik</i>	253
Hydrologic Monitoring of Subsurface Flow and Groundwater Recharge in a Mountain Watershed	
— <i>Michael E. Campana and Richard L. Boone</i>	263
Discharge Under an Ice Cover	
— <i>Henry S. Santeford and George R. Alger</i>	275

Hydrology of Two Subarctic Watersheds	
— <i>Robert E. Gieck, Jr. and Douglas L. Kane</i>	283
The Water Balance of the Upper Kolyma Basin	
— <i>V. K. Panfilova</i>	293
Water Balance and Runoff Analysis at a Small Watershed During the Snow-Melting Season	
— <i>H. Motoyama, D. Kobayashi, and K. Kojima</i>	297
Estimations of Snowmelting Rate in a Small Experimental Site	
— <i>N. Ishikawa, H. Motoyama, and K. Kojima</i>	305
A Methodology for Estimating Design Peak Flows for Yukon Territory	
— <i>J. Richard Janowicz</i>	313
Effects of Seasonally Frozen Ground in Snowmelt Modeling	
— <i>Knut Sand and Douglas L. Kane</i>	321
Some Aspects of Glacier Hydrology in the Upper Susitna and Maclaren River Basins, Alaska	
— <i>Theodore S. Clarke, Douglas Johnson, and William D. Harrison</i>	329
Regional Distribution of Stream Icings in Alaska	
— <i>K. G. Dean</i>	339
Estimation of Glacier Meltwater Hydrographs	
— <i>David Bjerklie and Robert Carlson</i>	345

PRECIPITATION — SNOW PACK — SOIL PROCESSES

Snow Surface Strength and the Efficiency of Relocation by Wind	
— <i>R. A. Schmidt</i>	355
Water Flow Rates, Porosity, and Permeability in Snowpacks in the Central Sierra Nevada	
— <i>Bruce J. McGurk and Richard C. Kattelmann</i>	359
In Situ Electrical Measurements of Snow Wetness in a Deep Snowpack in the Sierra Nevada Snow Zone of California	
— <i>James A. Bergman</i>	367
Measurements of Snow Layer Water Retention	
— <i>Richard Kattelmann</i>	377
Precipitation Measured by Dual Gages, Wyoming-Shielded Gages, and in a Forest Opening	
— <i>David L. Sturges</i>	387
The Mass Balance of Snow Cover in the Accumulation and Ablation Periods	
— <i>Esko Kuusisto</i>	397

CHANNEL HYDRAULICS AND MORPHOLOGY

Erosion Control for Placer Mining	
— <i>Larry A. Rundquist and N. Elizabeth Bradley</i>	407
Riverbank Erosion Processes of the Yukon River at Galena, Alaska	
— <i>William S. Ashton and Stephen R. Bredthauer</i>	415

SNOWMELT RUNOFF

Modelling Snowmelt Infiltration and Runoff in a Prairie Environment	
— <i>D. M. Gray, R. J. Granger, and P. G. Landine</i>	427
Using Real-Time (SNOTEL) Data in the NWSRFS Model	
— <i>Keith R. Cooley</i>	439
Theoretical Basis and Performance Evaluation of Current Snowmelt-Runoff Simulation Models	
— <i>T. W. Tesche</i>	449
Recent Developments in Snowmelt-Runoff Simulation	
— <i>Sten Bergström</i>	461

GLACIER HYDROLOGY

The Role of Glacierized Basins in Alaskan Hydrology	
— <i>C. Benson, W. Harrison, J. Gosink, S. Bowling, L. Mayo, and D. Trabant</i>	471
Glacier-Climate Research for Planning Hydropower in Greenland	
— <i>Roger J. Braithwaite and Ole B. Olesen</i>	485
A Forecast Procedure for Jokulhlaups on Snow River in Southcentral Alaska	
— <i>David L. Chapman</i>	491
Suspended Sediment Budget of a Glacier-Fed Lake — Eklutna Lake, Alaska	
— <i>Jeffrey H. Coffin and William S. Ashton</i>	501
Annual Runoff Rate from Glaciers in Alaska; A Model Using the Altitude of Glacier Mass Balance Equilibrium	
— <i>Lawrence R. Mayo</i>	509

REMOTE SENSING

Seasonal and Interannual Observations and Modeling of the Snowpack on the Arctic Coastal Plain of Alaska Using Satellite Data	
— <i>Dorothy K. Hall, Alfred T. C. Chang, and James L. Foster</i>	521
Operational Demonstration of Monitoring Snowpack Conditions Utilizing Digital Geostationary Satellite Data on an Interactive Computer System	
— <i>Milan W. Allen and Frederick R. Mosher</i>	531
Applying a Snowmelt-Runoff Model Which Utilizes Landsat Data in Utah's Wasatch Mountains	
— <i>Woodruff Miller</i>	541
Initiation of Spring Snowmelt Over Arctic Lands	
— <i>David A. Robinson</i>	547

RIVER ICE HYDRAULICS

Forecasting the Effects on River Ice Due to the Proposed Susitna Hydroelectric Project	
— <i>Ned W. Paschke and H. W. Coleman</i>	557

A Structure to Control Ice Formation and Ice Jam Flooding on Cazenovia Creek, New York	
— <i>Steven R. Predmore</i>	565
Freezeup Processes Along the Susitna River, Alaska	
— <i>Stephen R. Bredthauer and G. Carl Schoch</i>	573
Growth and Decay of River Ice Covers	
— <i>Hung Tao Shen and A. M. Wasantha Lal</i>	583
Ice Jams in Regulated Rivers in Norway, Experiences and Predictions	
— <i>Randi Pytte Asvall</i>	593
Hydrologic Aspects of Ice Jams	
— <i>Darryl Calkins</i>	603
Author Index	611

RESERVOIR AND LAKE LEVEL PROCESSES

THE SUSITNA HYDROELECTRIC PROJECT
SIMULATION OF RESERVOIR OPERATION

Yaohuang Wu, Joel I. Feinstein, and Eugene J. Gemperline¹

ABSTRACT: This paper presents the general concept and methodology used in the simulation of reservoir operation, which played an important role in the study of the Susitna Hydroelectric Project. The objective of the simulation was to find optimum operation rules which would meet projected energy requirements of the Alaska Railbelt, while at the same time satisfying flow regimes which would maintain habitat for resident and anadromous fish. Computer models were used for the simulation of reservoir operation on a monthly, weekly, and hourly basis, using streamflow records of 34 years. The results of the simulation allowed the selection of a preferred flow regime which could meet the projected energy requirements and also provide no net loss of habitat for the fish.

(KEY TERMS: reservoir operation modeling; rule curve; operating guide.)

flows in the summer for release during low flow periods in the winter when the energy demand is high. This alteration of the natural flow pattern would affect the quantity and availability of spawning, incubating, and rearing habitat for fish,

INTRODUCTION

The proposed Susitna Project consists of two tandem reservoirs on the Susitna River. The two proposed dam sites are the Watana site, a rockfill dam to be located at river mile 184 of the Susitna River, and the Devil Canyon site, a concrete arch dam 32 miles downstream from the Watana site as shown in Figure 1. The project would operate by storing the high natural

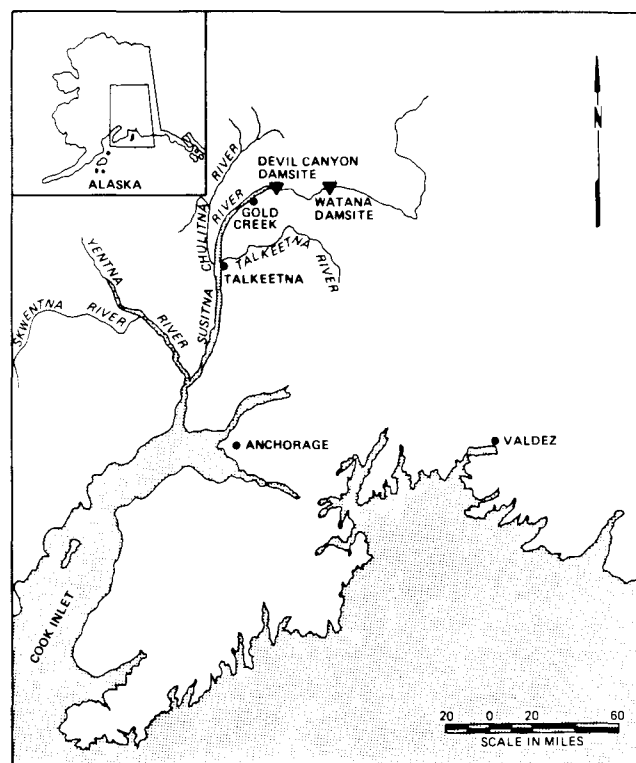


Figure 1. Susitna Project Location Map

¹ Respectively, Principal Engineer, DeLeuw, Cather and Company, 525 Monroe Street, IL 60606 (formerly Senior Power Planning Engineer of Harza Engineering Company); Power Planning Engineer, Harza Engineering Company, 150 South Wacker Drive, Chicago, IL 60606; and Manager of Hydrologic and Hydraulic Studies, Harza-Ebasco Susitna Joint Venture, 711 H. Street, Anchorage, AK 99501

primarily in the middle reach of the river. The impounding of water in the reservoirs and the alteration in flow patterns would also change water quality parameters associated with mainstem flow such as water temperature, turbidity, and suspended sediment. The simulation of water temperature, ice formation, and suspended sediment were conducted in a series of separate studies using the reservoir water levels and discharges from the reservoir operation study.

To mitigate the impacts on chum salmon spawning and incubation in side sloughs and chinook salmon rearing in side channels, eight different flow regimes were developed for evaluation (Alaska Power Authority, 1985). Each of the flow regimes was designed to provide a given amount of habitat for the fish species. Each flow regime consists of a series of weekly maximum and minimum flows through a year keyed to chum and chinook salmon life cycles. The maximum or minimum flows were specified at the Gold Creek station, which is located 15 miles downstream of the Devil Canyon site. Figure 2 shows the E-VI flow regime which was selected as the preferred alternative. Minimum summer flow requirements would provide flow stability and would maintain a minimum watered area for salmon habitat. Maximum winter requirements would provide flow stability and would minimize the potential for winter water levels to overtop side slough habitats affecting incubating and rearing chum salmon.

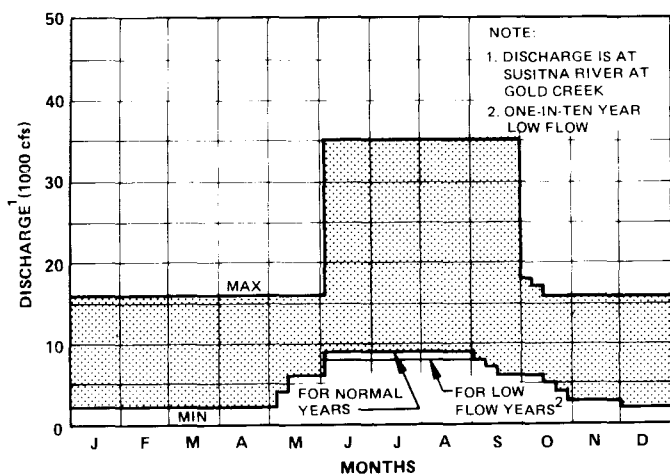


Figure 2. Environmental Flow Requirement, Flow Regime E-VI

The evaluation of the flow regimes was carried out by estimating the total cost to meet the projected Railbelt energy demand. These include capital and operating costs of the Susitna Hydroelectric Project, other generating facilities, and any mitigation measures required to meet the objective of no net loss of habitat value. Among the mitigation measures included in the evaluation of the alternative project flow regime were hatcheries and multi-level intakes for temperature and sediment control. Since the maximum and minimum flow constraints of the alternative flow regimes would restrict the seasonal distribution of Susitna energy production, the construction and operation of additional power plants to meet the system demand were also considered.

RESERVOIR OPERATION SIMULATION

Reservoir operation models simulate the reservoir storage, power generation, turbine discharge, valve release, and flood release as a function of time based on reservoir and power plant characteristics, power demand distribution, and environmental constraints. Cone valves may operate at each dam to satisfy an instream flow requirement or to keep the water surface elevation at the normal maximum level without having to use the spillway. These simulations are normally undertaken in two parts; long-term simulation and short-term simulation (Dondi and Schaffe, 1983). The long-term simulation for the Susitna Project uses a monthly program and a weekly program for simulating the operation for 34 years of streamflow record. The monthly program was used to determine the overall trend, while the weekly program was used for refinement of operation rules and to understand the behavior of the reservoirs and flows during critical periods. The short-term simulation used an hourly program to simulate the operation over a week, using the output from the weekly simulations as input data. The hourly program was designed for simulation of hourly generation to meet the daily peak and off-peak loads.

The monthly operation used a single rule curve as an operation guide to estimate the annual energy production and to

satisfy the monthly instream flow requirements. A rule curve indicates the desired reservoir water level in different months. The weekly operation program used an operation guide for seasonal adjustment of flows which produce a series of reservoir outflows with gradual changes. Operation guides consist of a series of rule curves to control the reservoir outflow. The hourly operation program used an hourly load curve as the upper limit of possible generation. The load curve was based on actual hourly load data and a load forecast. This program tested how well the energy obtained from the long term analyses could fit the hourly load curve, subject to environmental restrictions on the daily and hourly flow changes.

Power and energy production from the monthly simulation of the Susitna Project was used in the Railbelt expansion planning studies, which in turn was used in both the economic and financial analyses. Although monthly simulations were sufficient for these studies, they were not adequate to estimate environmental effects. Therefore, a simulation with a weekly time step was needed to generate input data for subsequent computer models used in the environmental impact studies. Other environmental studies required hourly discharge to estimate river stage fluctuations.

The monthly program was originally developed by Acres American for the Susitna feasibility study (Alaska Power Authority, 1982) and later improved by Harza-Ebasco Susitna Joint Venture. The weekly program was developed by Harza-Ebasco by using parts of the monthly program. The hourly operation program was developed by Harza-Ebasco. All of the programs were written in Fortran IV.

The Susitna project was scheduled to be built in three stages. First an initial Watana Project would be developed, followed by construction of Devil Canyon downstream. Finally, Watana would be raised to its ultimate height. The full reservoir areas for the low and high dams at Watana would be 19,900 and 38,000 acres respectively, and 7,800 acres at Devil Canyon. Because of the large reservoir surface area at Watana, release of a large quantity of water would cause a relatively small change in the project head. In contrast, Devil Canyon would have a small surface area, and would hence lose consid-

erably more head for the same volume of release. Consequently, the reservoir operation methodology attempted to keep the Devil Canyon reservoir close to its normal maximum operating level while using Watana's storage to provide the necessary seasonal regulation. Therefore, the modeling effort in both the single and double reservoir operation in monthly and weekly simulation was focused on the Watana operation. The operation levels of the reservoirs for the various stages are shown on Table 1.

Table 1

OPERATION LEVELS

	Normal	Environ-	Nominal		
Min-	Maxi-	Sur-	Plant	On-	
imum	mum	charge	Capac-	line	
<u>Level</u>	<u>Level</u>	<u>Level</u>	<u>ity</u>	<u>Date</u>	
(ft)	(ft)	(ft)	(MW)		
Watana					
Low Dam	1850	2000	2014	440	1999
Watana					
High Dam	2065	2185	2193	1110	2005
Devil					
Canyon	1405	1455	1455	680	2012

MONTHLY OPERATION MODEL

Monthly reservoir simulations were carried out to optimize project energy production subject to environmental flow requirements. The rule curve which would optimize energy production was determined by trial and error. The optimal energy production is a function both of the firm energy and total energy. Figure 3 shows a sample rule curve of the Watana reservoir.

During the simulation in each time step, the reservoir release has to satisfy the firm energy and environmental minimum flow requirement. If the end-of-month water surface elevation is lower than the corresponding rule curve elevation, only firm energy is produced and no additional

water is released. If the end-of-month water surface elevation is higher than the rule curve elevation, the water stored between these two elevations is released to generate secondary energy up to the system energy requirement.

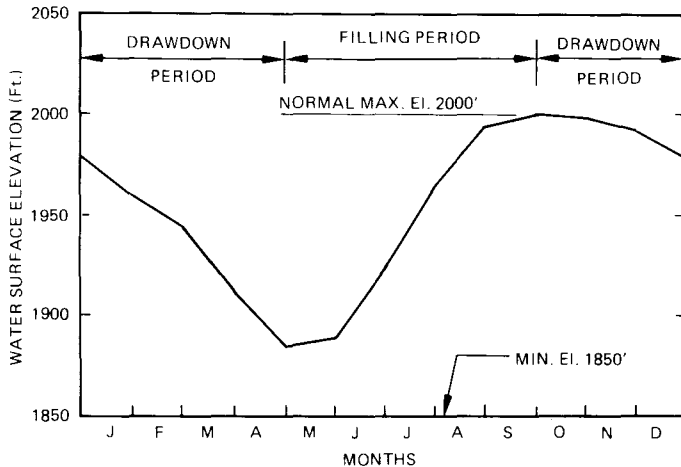


Figure 3. Example Rule Curve For Watana Operation, Year 2004

The dry season is from October to April and the wet season from May to September, as shown in Figure 4. The rule curve elevation at the end of September is at the normal maximum pool elevation because the reservoir is expected to be full at

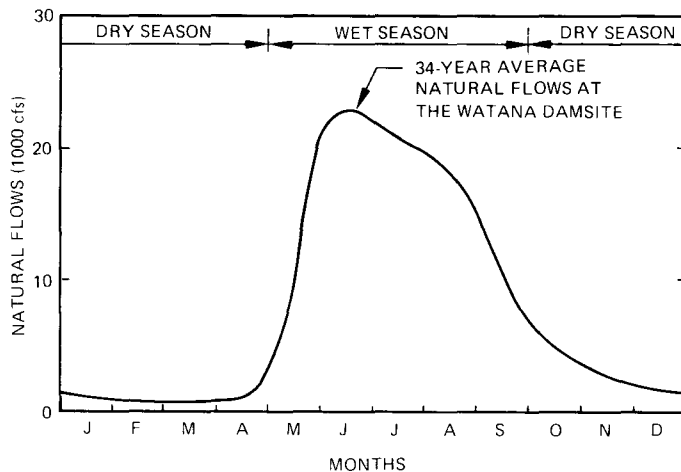


Figure 4. Natural Flows at Watana

the end of the wet season. In contrast, the rule curve elevation at the end of April is at its minimum because the draw-down is required for firm energy production in the dry season. The higher the minimum rule curve elevation (at the end of April), the greater the firm energy production. This is because the reservoir levels would be kept relatively higher and the storage available for firm energy would be more in the drought period. Alternatively, the lower the rule curve, the greater the total energy production. This is because there would be more active storage for flow regulation and less amount of spills on a long term basis. Various sets of rule curve elevations with various minimum elevations will give different values of firm energy and total energy. The acceptable minimum rule curve elevation for the Susitna Project was selected based on an operation in which the increase of total energy is about one percent when lowering the minimum elevation by five feet.

Once the maximum and minimum rule curve elevations were determined, the rest of the rule curve elevations were determined by a trial and error procedure to obtain an acceptable distribution of energy through the year. The operational strategy was to capture additional economic benefits through adjustments of the Susitna generation by leaving the residual thermal generation during each of two periods, the summer filling period and the winter drawdown period. As stated above, the reservoir would be almost full at the end of September and would be at the lowest levels at the end of April. Therefore, Susitna energy distribution during the filling period, May to September, and during the drawdown period, October to April, could be varied as a function of reservoir water surface variation without reducing total project energy production. It was assumed that it would be more economical to provide thermal energy by running the least-cost thermal units throughout a whole period rather than running them for part of the period along with other less efficient units. Also the system was assumed to be more reliable if the thermal requirement would be about the same from month to month. This would mean that investment in additional thermal capacity could be delayed as long as possible. Therefore, the energy distribution

was adjusted so that the Susitna energy production would maintain constant thermal generation in both the filling period and the drawdown period as much as possible.

The analysis of the project's benefits was based on its ability to meet energy requirements. These requirements were the total projected Railbelt system energy demand minus the energy production of existing hydroelectric facilities. Figure 5 shows the monthly distribution of energy requirements, and also indicates how the Susitna energy would be distributed throughout the year.

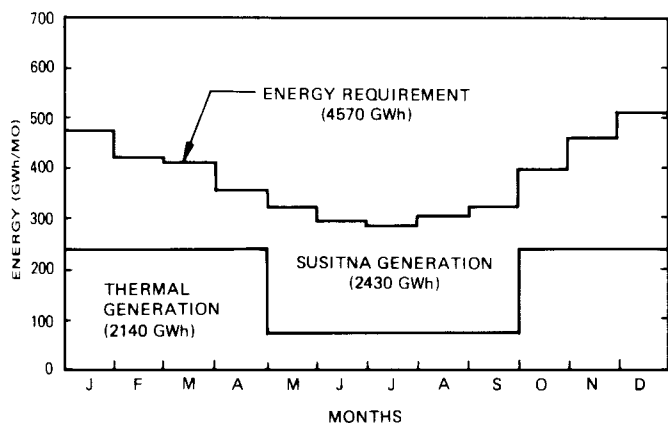


Figure 5. Monthly Energy Distribution, Watana, Year 2004

The rule curve approach is predictive because it attempts to achieve an end-of-month elevation which presumes some knowledge of the expected reservoir inflow during that period. The operation guide approach, which will be discussed below in conjunction with the weekly program, is non-predictive because it specifies a discharge rate through the powerhouse based on the reservoir elevation at the beginning of the period. The rule curve approach is easy to apply for simulation but can be operationally difficult to achieve, because reservoir inflows are difficult to accurately forecast. The operation guide approach is more difficult to model, but more closely approximates how the project would actually operate. The two approaches yielded similar power and energy results in many trial runs, so the monthly model (rule curve approach) was used for the economic and financial analyses in selection of the best scheme. The rule curve approach could not be used in the weekly simulations for the environmental studies because the release of the

storage above the rule curve elevation for the secondary energy would cause an unrealistic change of discharge between two consecutive weeks. The operation guide in the weekly simulation was designed to prevent these large changes.

WEEKLY OPERATION MODEL

The weekly operation model was primarily designed for simulation based on the operation guide. An operation guide is composed of a series of rule curves which are used as a guide for determining the turbine discharge in each week during the simulation. An example operation guide is shown on Figure 6. Each guide has two families of rule curves; increasing curves and decreasing curves. Each curve defines the reservoir level at which the powerhouse discharge should increase or decrease to a specified percentage rate of the expected powerhouse discharge. These specified percentage rates are in 20% intervals. The expected powerhouse discharges are a set of weekly discharges which would produce an expected distribution of energy production over a year. The single rule curve operation is based on the target firm energy; however, the operation guide uses 60% of the expected powerhouse discharge as the minimum discharge and 140% as the maximum normal discharge.

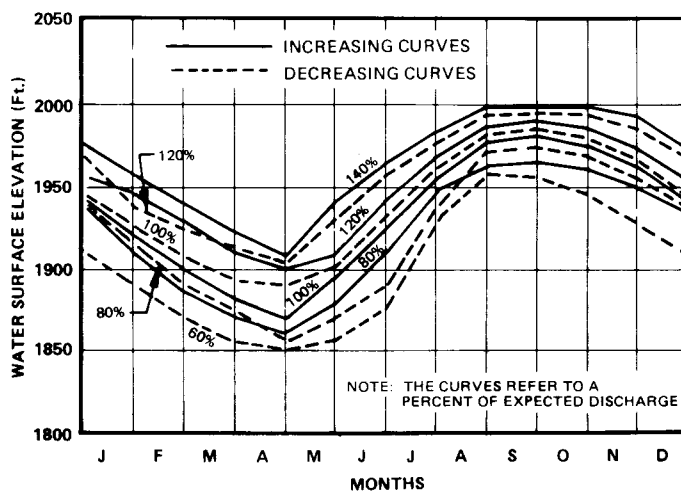


Figure 6. Operation Guide For Watana Operation, Year 2004

At the beginning of each simulation week, these curves are used to determine whether the current discharge rate is kept the same, increased to the next higher rate, or decreased to the next lower rate. The water surface elevation at the beginning of the week is put on the operation guide and compared with the elevations of increasing and decreasing curves. If the water surface elevation is higher than the elevation of the increasing curve of the next higher rate, the discharge is increased to that rate. If the water surface elevation is lower than the elevation of the decreasing curve of the next lower rate, the discharge is decreased to that rate. Otherwise, the discharge is kept the same. The change of rates in two consecutive weeks is limited to 20%. For example, if the discharge rate is at 100% of the expected powerhouse discharge in the preceding week, the rate may be changed to either 80% or 120% or stay at 100%. Because of the difference in elevation between the increasing curve of the next higher rate and the decreasing curve of the next lower rate, the rate will generally be kept the same for a few weeks. In contrast with the simulation using a single rule curve, an operation guide will give an outflow hydrograph with relatively gradual changes in the discharges.

A smooth curve giving the energy requirements throughout the year is shown on Figure 7. The average energy production of the Susitna Project in the drawdown and filling periods was determined from the monthly simulation. Similar to the monthly modeling, efforts were made to capture the additional economic benefits by leaving the thermal generation constant in both the drawdown period (October to middle May) and the filling period (middle May to September). In weekly runs the reservoir level is the lowest in the middle of May and full in most years at the end of September. The energy production in these two periods are inexchangeable, but redistributing energy production within either period does not cause additional valve and spillway releases or flow deficits. Adjustments of energy production within either period by leaving thermal requirements constant was assumed to increase the economic value of the project. Gradual changes of thermal energy requirements at the boundaries of

the filling and drawdown periods were considered for a smooth transition of the operation. The resulting weekly distribution of energy production over a year was used for computation of the weekly expected powerhouse discharge.

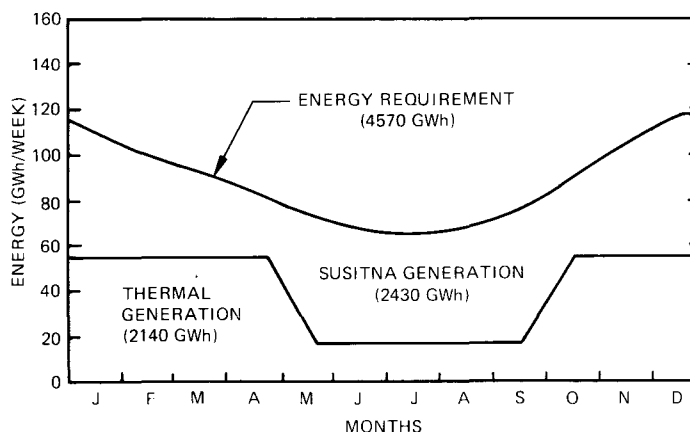


Figure 7. Weekly Energy Distribution, Watana, Year 2004

Development of an operation guide is an iterative process. An assumed set of rule curves for the operation guide were put into simulation initially to find flow deficits resulting from not satisfying the minimum flow constraints or from discharging less than the minimum powerhouse discharge (60% of expected discharge in the example). The curves were then gradually improved by satisfying these two requirements through the whole simulation period. The curves were again adjusted to maximize the average energy production and improve the energy distribution through the year. A good operation guide should provide: 1) turbine discharges close to the expected powerhouse discharge, 2) discharge rates generally constant for a period of at least several weeks, and 3) average energy production maximized.

Figure 8 shows the historical inflow hydrograph at Watana. Figure 9 shows the simulated outflow hydrograph of Watana operation for the load year 2004. The comparison of duration curves between the pre-project and post-project flows at Gold Creek Station is shown on Figure 10. Note that, through flow regulation by Watana, the high flows in summer would be substantially reduced and the low flows in the winter would be increased for power generation. The simulated outflows from Watana were, in general, consistent with

the expected discharges and there were no rapid changes of discharge except those during floods.

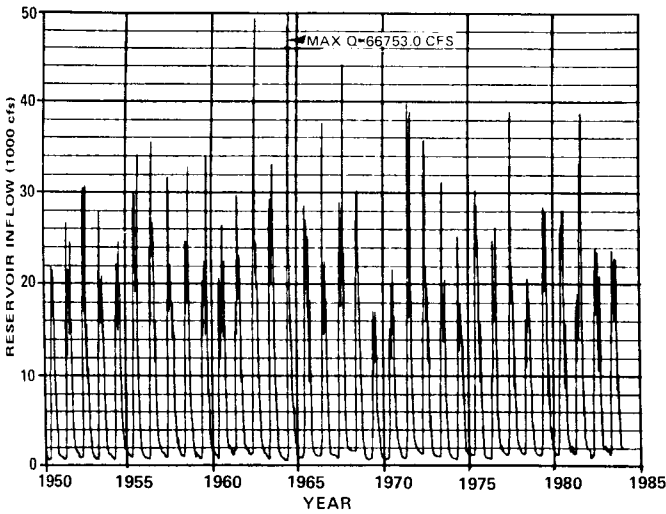


Figure 8. Watana Inflows

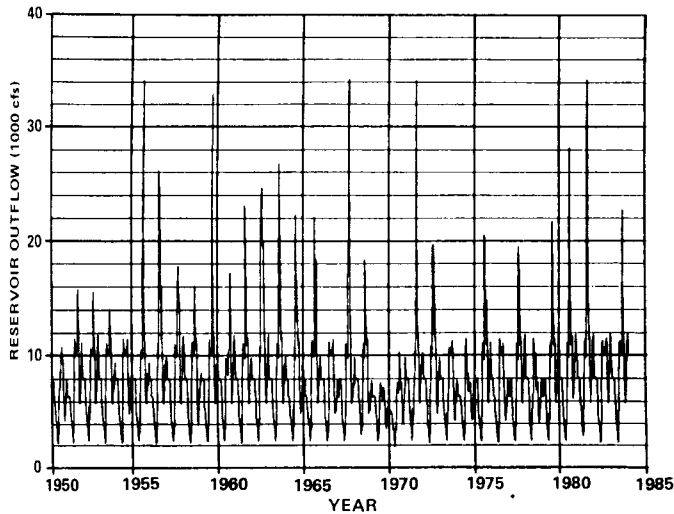


Figure 9. Watana Outflows, Stage I, Load Year 2004

HOURLY OPERATION MODEL

The hourly program modeled a reservoir operation over a week, using an hourly load curve (for the demand distribution within a week) as the upper limit of possible generation and discharges from

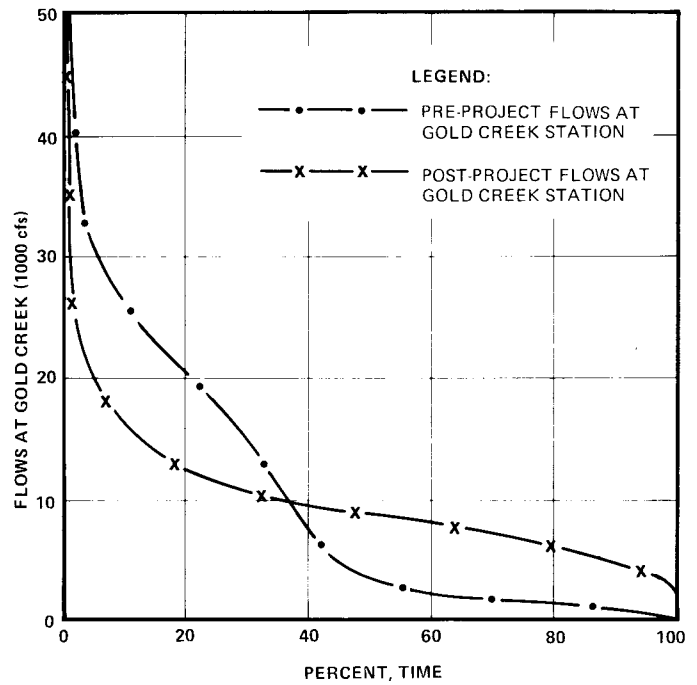


Figure 10. Duration Curves of Flows at Gold Creek

the results of weekly simulation as input data. Outflow fluctuations were restricted by maximum hourly and daily variation constraints. The model tests how energy obtained from the long term analyses can fit the hourly variation of demand with environmental constraints. The output was used in river stage fluctuation studies. An example of the output is plotted as shown in Figures 11 and 12 to aid in understanding the results. Figure 11 contains a plot of generation showing the system demand, the existing hydro generation, and Susitna Project generation. Figure 12 shows the reservoir discharge through the powerhouse and the valves, and the minimum flow required to meet the environmental requirements at Gold Creek.

The reservoir outflow constraints limit how the plant can operate in the system. For example, if the daily variation constraint is very small, then the plant is essentially base loaded, but if both hourly and daily variation constraints are large, the hydro plant can load follow. Load following operation means that the plant can increase or decrease its generation by following the hourly fluctuation of the system demand, and will leave the

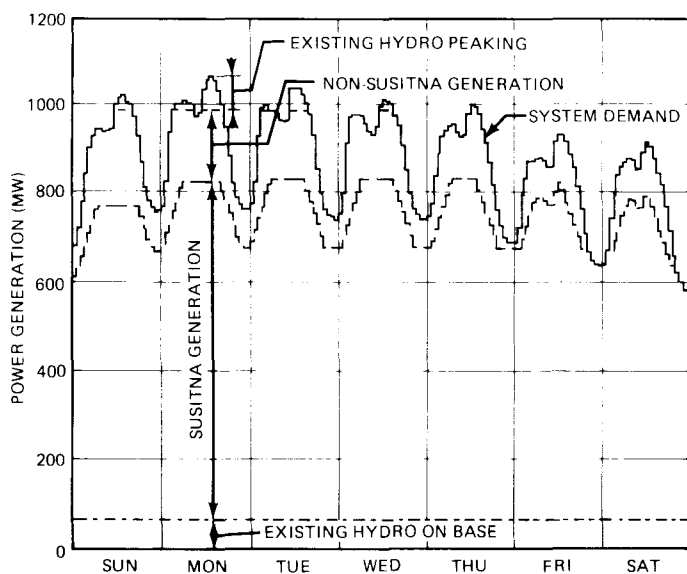


Figure 11. Hourly Power Generation

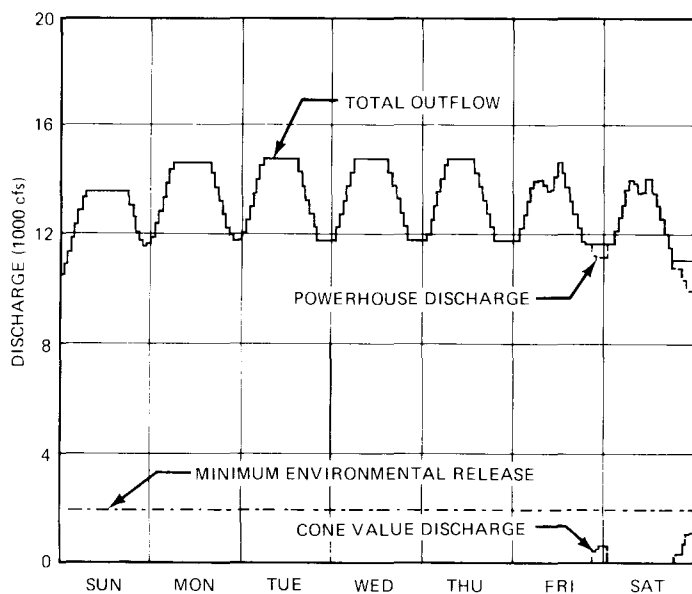


Figure 12. Hourly Reservoir Discharge

energy from other sources at constant capacity. Base loaded operation means that the plant generation is constant in principle, but a certain percentage fluctuation may be allowed. Load following operation would provide more

capacity value for the project than base loaded operation. Base loaded operation would provide stable flows in the downstream channel. Project operation is currently constrained to be base loaded with allowable variations of 20% in total project discharge within a week, therefore, providing stable flows and minimizing impacts to salmon.

Chum and sockeye salmon spawn in sloughs along the river. These sloughs collect sediment and organic matter throughout the normal course of the year, which make it difficult for the fish to spawn and may reduce egg survival. Naturally occurring floods clean out the sloughs and thus provide better habitat. The dams would tend to reduce these naturally occurring floods which may decrease the natural fish habitat. Some of the flow regimes incorporate spikes of flow to create artificial floods to clean the sloughs. The hourly program can also model these spikes as instream flow requirements at Gold Creek.

Input to the hourly model consists of the initial storage at the beginning of the week and the amount of water to be released during the week (obtained from the results of the weekly simulation). The program generates a curve called a template for use as a guide in simulation of hourly power generation. The first template is equivalent to the hourly system load minus the existing hydro production. Turbine release in each time step is determined from the energy requirement of the template. The turbine release is then checked with the flow constraints and the total release is adjusted to satisfy the constraints if there is any violation. After the first iteration with the template, the template is adjusted according to the ratio of the amount of water to be released and the total outflow in the previous iteration. The simulation is iterated with new templates until the outflow for the week is equal to the amount of water to be released for the week.

The hourly program modeled a single reservoir. When the Devil Canyon reservoir is in operation, the Watana plant will load-follow and the Devil Canyon plant will be base loaded. Therefore, the release from Devil Canyon would be stable and the variation of discharge on the downstream channel could be easily controlled. Because of low flow from Watana

in off-peak hours and high flow in peak hours, Devil Canyon will draw down in off-peak hours and fill in peak hours. The maximum drawdown for daily fluctuation at Devil Canyon was estimated at one-half foot.

The hourly program as well as the weekly program have provisions for flood operation. During a large flood when the reservoir is full, the reservoir inflow could be greater than the sum of turbine and valve capacities. If the spillway is used, nitrogen would be entrained in the water and there would be the potential for nitrogen concentration to exceed tolerable levels. In order to minimize use of the spillway, the reservoir is allowed to surcharge above the normal maximum level up to an environmental surcharge level. The environmental surcharge for Watana low dam would be 14 ft and that for Watana high dam would be 8 ft. These levels were determined on the basis of avoiding the use of the spillway in a flood of less than a 50-year return period. The spillway would not be open unless the water surface elevation reaches the environmental surcharge level.

In non-flood operation the valves would not release water unless it is necessary for the instream flow requirements. When the water surface elevation is at or above the normal maximum level, the excess water would be released from the valves. As the water starts to surcharge above the normal maximum level in a flood, the total outflow could be increased hourly at a special flood rate, designed to minimize impacts on the fishery from changes in flow and temperature, until the valves are fully open. However, the outflow would never be allowed to be greater than the peak discharge of inflow. As stated previously, if the water surface elevation reaches the environmental surcharge level, the spillway would be opened for release so that the outflow would be equal to inflow. The falling limb of the outflow hydrograph would also be constrained by an hourly decreasing rate for flood operation.

CONCLUSION

The monthly simulation with rule curve operation is simpler and less expensive than the others. It was effectively used in the economic analysis of the project.

The weekly simulation with the operation guide more closely simulates the discharge variations for the studies of environmental impacts. The operation guide restricts the discharge variation in a specified limit to secure the protection of fishery habitat. The simulation with the weekly model was successfully used for the evaluation of the flow regimes.

The hourly simulation was used to test how the energy obtained from the weekly analysis could fit the hourly load curve. It was also used for the study of peaking capacity with respect to the allowable fluctuation of discharge in the downstream channel.

Monthly, weekly, and hourly operation models are all indispensable in the study of the Susitna Hydroelectric Project.

REFERENCES

- Alaska Power Authority, 1985. Case E-VI Alternative Flow Regime, Susitna Hydroelectric Project, Volume 1 - Main Report, Document No. 2600.
- P.H. Dondi and G. Schaffe, 1983. Simulation and Optimization of a Series of Hydro Stations, Water Power and Dam Construction, Nov. 1983.
- Alaska Power Authority, 1982. Feasibility Report, Susitna Hydroelectric Project, Volume 1, Engineering and Economic Aspects.

RESERVOIR OPERATIONS PLANNING IN SNOWMELT RUNOFF REGIMES
BASED ON SIMPLE RULE CURVESE.A. Shafer, P.E. Farnes, K.C. Jones, J.K. Marron, and F.D. Theurer¹

ABSTRACT: Selecting appropriate storage and release rates for reservoirs in snowmelt runoff environments is a prerequisite to sound water management. A significant number of small impoundments, operated for single or multiple purpose use in the Western U.S., lack adequate management tools to guide this process each year. A methodology is presented to use seasonal streamflow volume forecasts issued by the U.S. Soil Conservation Service and National Weather Service to improve management capability at many of these reservoirs. The technique involves generating a family of simple rule curves for each forecast period. These curves permit operators to use predicted inflow volume to set target outflow rates that will enable them to reach a full reservoir after passage of the seasonal peak. Forecasts at three probability levels help establish the range of likely seasonal runoff events. The derivation of the curves is presented along with a mathematical algorithm to produce them objectively from historical inflow records. The rule curves provide an operational tool useful for developing effective water management plans for reservoirs where forecast information is available. Seven reservoir operating plans

have been developed and implemented using this procedure in Montana and Oregon. (KEY TERMS: reservoir management, rule curves, streamflow forecasts, snowmelt runoff.)

INTRODUCTION

Annual water supply in the Western U.S. is highly variable, often fluctuating between extremes. This inherent natural variability imposed by climate and topography makes it difficult for water managers to plan their operation to optimally use available runoff. The seasonal nature of runoff also complicates management because usually the bulk of flow occurs in only a four-month period (April-July typically) in response to melting mountain snowpacks. This snowmelt component produces from 50 to 85 percent of the region's annual runoff and is therefore the foundation of most water management decision-making.

Many water users have found it necessary to construct storage reservoirs that enable them to capture seasonal flow volumes and regulate releases consistent with annual demands. There are thousands of these reservoirs of all sizes in the West ranging from only

¹Respectively, E.A. Shafer, K.C. Jones, and J.K. Marron, Soil Conservation Service, 511 NW Broadway, Portland, Oregon 97209; P.E. Farnes, Soil Conservation Service, Federal Building, Bozeman, Montana 59715; and F.D. Theurer, Soil Conservation Service, 301 South Howes, Ft. Collins, Colorado 80522.

a few acre-feet up to millions of acre-feet in storage capacity. Most of the water held in storage in these impoundments is utilized for irrigation, hydropower production, municipal water supply, flood control, fisheries, recreation, or some combination of these uses. Often there is competition among uses for water held in storage, making it important for managers to apply the best analytical tools available to fill and empty reservoirs in a manner which maximizes beneficial water use and minimizes negative impacts. Inordinately high or low flows downstream from reservoirs caused by uninformed management are to be avoided if possible.

Reservoir capacities on snowmelt dominated streams are frequently smaller than average annual runoff. As a result, reservoir operators must balance their ability to store and eventually release runoff volumes with expected seasonal inflows on a recurring basis. A substantial number of irrigation reservoirs and multipurpose structures currently lack a formal management plan to guide this process each year. Instead a philosophy of "fill and spill" is adopted by default; this approach sometimes has disastrous consequences and does not take advantage of information on current hydrologic conditions that is readily available. Water supply forecasts based on snowpack, precipitation, temperature, and streamflow are made routinely by the Soil Conservation Service (SCS) and National Weather Service to aid reservoir managers in their decision-making. These predictions have not been effectively utilized in many cases. A major factor contributing to this situation was an inability to integrate the forecast information into a practical and easily applied scheme that could be understood by relatively unsophisticated operators.

A procedure has been developed to address this deficiency. It provides a means for reservoir operators who depend on snowmelt

runoff for all or a significant portion of their inflow to set outflow rates that enable them to meet storage goals based on streamflow forecasts. The technique is principally oriented toward improving management capability on small reservoirs whose primary function is to supply storage for agricultural interests. Reservoir management plans have been developed and implemented on six impoundments in Montana and one in Oregon using this procedure. One of these plans on Hebgen Lake in southwestern Montana has been in use for over ten years. It can also be applied to evaluate the feasibility of planned storage projects.

The methodology involves generating a family of simple rule curves which permit an operator to relate forecasted inflow volumes at three probability levels to target outflow rates. The target outflows are designed to help the operator reach a defined storage level (usually a full reservoir) after passage of the seasonal peak flow. Principles used to construct the curves are presented. A mathematical algorithm is described to produce the curves objectively from historical inflow records. A computer program that incorporates the rule curve algorithm, data input, data analysis, and curve plotting is explained.

RULE CURVE PRINCIPLES

Typically, snowmelt runoff begins on most streams from late March to early May, with the recession continuing into July or early August. Peak inflows usually occur between mid-May and early June. Although this flow pattern is annually repetitive, there is substantial variability in total volume and timing of runoff, making it necessary for reservoir operators to tailor their operations to prevailing conditions.

Examination of runoff hydrographs on snowmelt dominated

streams revealed that on an individual watershed there is a discernible consistency in hydrograph shape and time distribution for similar seasonal flow volumes. This observation implied that it should be possible to construct a stable relationship between seasonal volume and reservoir outflow settings to achieve a specific storage goal. In this context, seasonal volume serves as an index to hydrograph shape. To accommodate the need to reflect current conditions, relationships can be developed for several flow periods for which forecasts are routinely made; e.g., April-July, May-July, June-July.

Specifically, a relationship is desired for each forecast period to make it possible for an operator to select an outflow setting that would produce a specified storage level if the forecasted runoff actually occurred. Figure 1 illus-

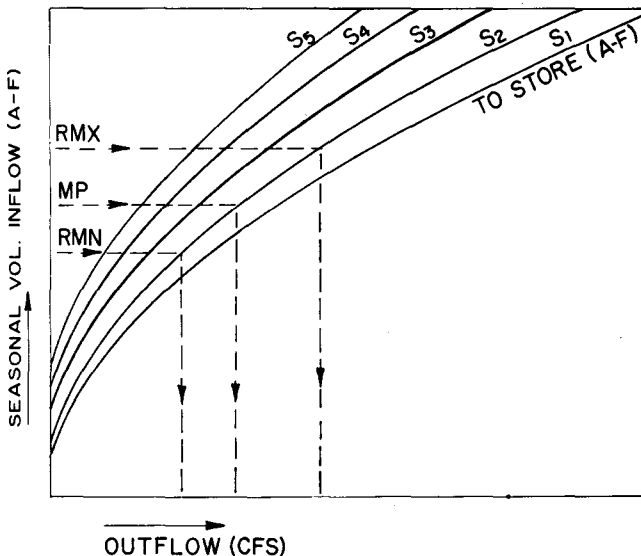


Figure 1. Conceptualized representation of how seasonal snowmelt runoff at three probability levels--RMX, MP, RMN--can be used with reservoir rule curves to arrive at reservoir outflow rates that meet storage goals. $S_1, S_2 \dots S_5$ are storage increments that an operator wishes to achieve during spring runoff. Note $S_5 > S_4 > S_3$, etc.

trates conceptually how an operator would use the forecast with a set of rule curves derived from an analysis of historical reservoir inflows. In actual practice, most probable (MP), reasonable minimum (RMN), and reasonable maximum (RMX) forecasts are made corresponding to 50, 90, and 10 percent exceedance probabilities. Entering the graph with these forecast values and moving horizontally to the volume of storage left to fill would produce a range of outflow rates. The rate chosen would be based on an assessment of local operating constraints and magnitude of runoff expected. This concept allows the reservoir manager to fill the reservoir while maintaining fairly constant release rates.

Besides determining outflow rates during the main runoff period, early season forecasts and reservoir operating curves can be used to determine desirable storage levels in the reservoir. When the present storage and forecasted runoff indicate an outflow less than that needed for downstream uses, it would be desirable to increase storage prior to spring runoff so these needs could be met. The largest storage level that would be desirable could be determined by reading the storage at the intersection of the forecast and upper range of desirable outflow.

RULE CURVE GENERATION

Development of operating rule curves depicted in figure 1 is unique for each reservoir. The first step to develop rule curves is to obtain a minimum of 10 years of daily reservoir inflow data that includes both high and low runoff seasons. Daily streamflow observations for only the snowmelt period satisfy the minimum data requirements. However, complete annual records are desirable to detect unusual runoff sequences that affect reservoir operation but are unrelated to snowmelt runoff.

For each year, individual storage versus outflow curves are constructed by selecting a series of outflow rates and tabulating the corresponding storage that would result given the seasonal inflow hydrograph. Storage volumes are obtained as the sum of all daily flows greater than or equal to the selected outflow rates. This stipulation prevents a drop in stored contents and implies outflow is set equal to inflow when the target release rate is higher than inflow. The storage-outflow data pairs are then plotted and a smooth line fitted to the points either by eye or a least square analytical method. Figure 2 illustrates this procedure for a single year's hydrograph. Setting outflow rates

of O_A, O_B, O_C, O_D results in storing volumes S_A, S_B, S_C, S_D (cross hatched area). In actual practice, many more points than four are generated to fit the storage-outflow curve. Figure 3 shows examples of six storage-outflow curves for a hypothetical stream based on April-July daily inflow data. High, low, and intermediate seasonal volumes are represented. From these relationships, operating curves can be created for specific storage levels; i.e., S_1, S_2, S_3, S_4 .

This task is accomplished by generating a series of seasonal volume-outflow rate data pairs for each incremental storage level, e.g., S_1 in figure 3, and fitting a smooth curve to the points. The process of generating the pairs is to select a desired storage level, and for each year, read the outflow setting required to produce it from the curves of figure 3. Doing so for a storage increment of S_1 results in outflow rates $O_1, O_2 \dots O_6$ corresponding to years 1971-76, respectively. Data pairs consisting of these seasonal volumes and associated outflow rates are plotted and a line fitted to the points either by eye or using a curvilinear least square regression method. Figure 4 shows an operating curve for the S_1 to store increment derived from the graphs of figure 3. Successive repetitions of this procedure for other storage increments produce a family of operating curves like those of figure 1. Families of curves for any desired seasonal flow period can be developed by the method outlined.

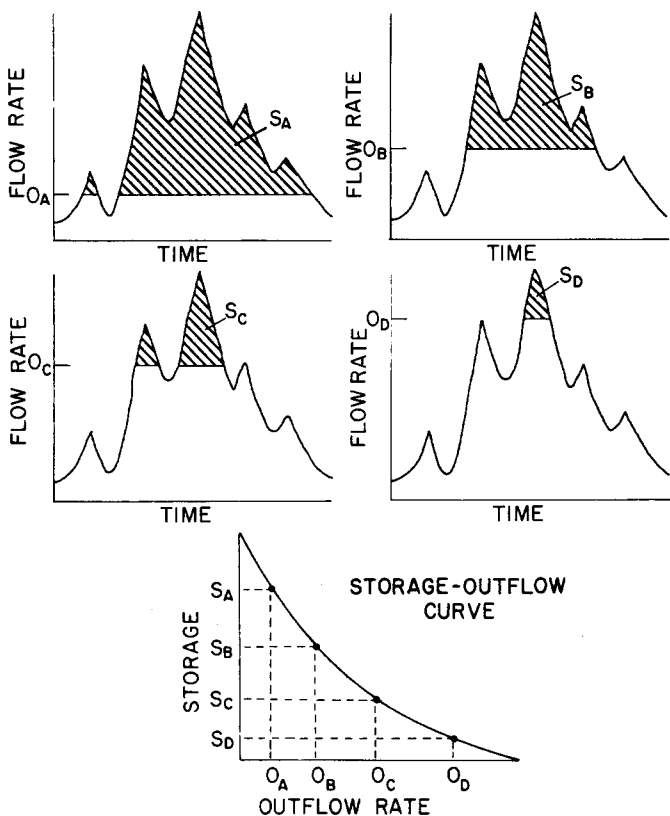


Figure 2. Storage vs. outflow curve constructed for each year of record by determining how much water could be stored at various release rates (O_A, O_B, O_C, O_D).

RULE CURVE ALGORITHM

Building on this conceptual understanding of the principles of operating curve development, an objective, automated technique to produce the family of curves is explained. The rule curve

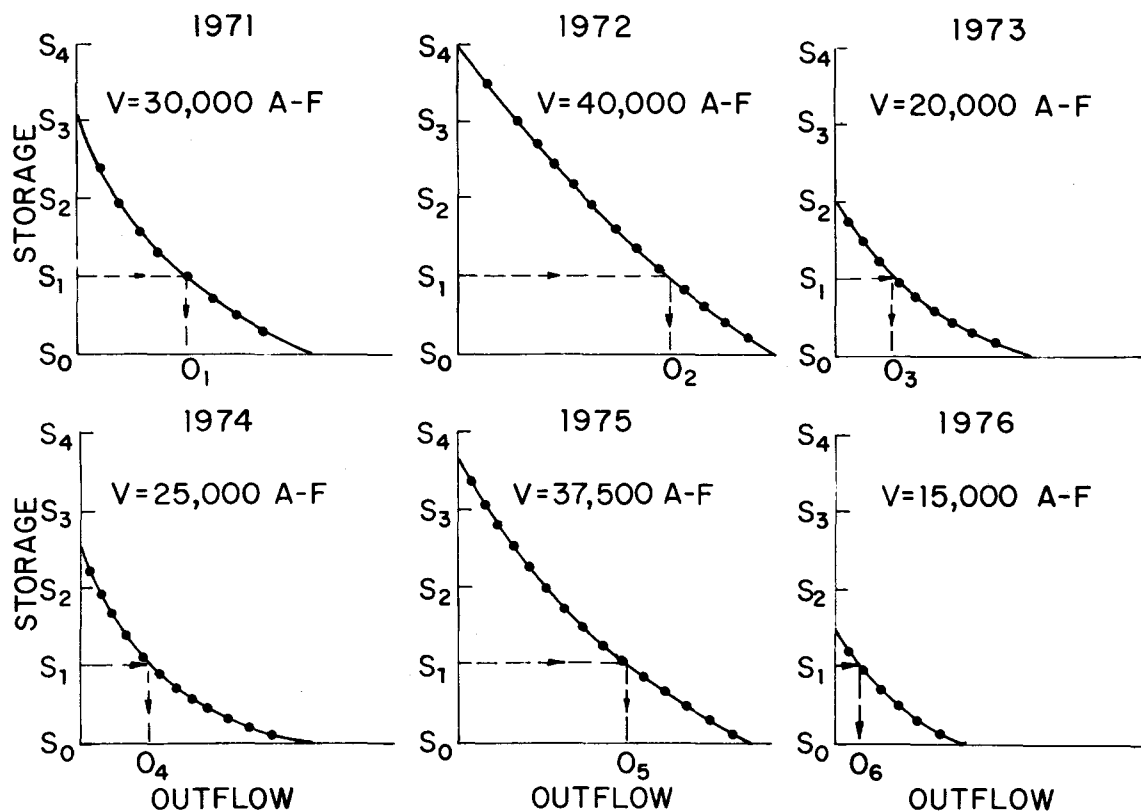


Figure 3. Six storage vs. outflow curves for a hypothetical stream illustrate how seasonal volume (V) influences shape. To produce the same storage level (S_1) each year, outflow rates are set at $O_1, O_2 \dots O_6$.

algorithm to generate the curves is constrained to be an analytical least square fit of a three-dimensional data set consisting of seasonal inflow volume, outflow rate, and storage level. The regression model relating these variables is:

$$T = a_1X + a_2Y + a_3Z \quad (1)$$

where $T = V - S$;
 $X = O$;
 $Y = (O)^{0.5}$;
 $Z = (O)(S)$;
 $V =$ total seasonal volume inflow to reservoir;
 $S =$ desired storage level;
 $O =$ outflow setting required to obtain desired storage level; and

a_1, a_2, a_3 are regression coefficients.

The transformed variables (X, Y, Z) were chosen to meet certain rational and/or observed behavior. The dependent variable, $T = V - S$, was chosen so that when the outflow setting was at or near zero, the predicted storage level would be at or near the inflow volume; i.e. $S = V$ when $O = 0$. The first independent variable, $X = O$, was set as a standard linear regression term. The second independent variable, $Y = (O)^{0.5}$, was set to reflect the observed curvature behavior between inflow volume (V) and outflow setting (O) for a given storage (S). The third independent variable, $Z = (S)(O)$, was chosen to reflect the skewness between the various storage level curves because they are not necessarily parallel.

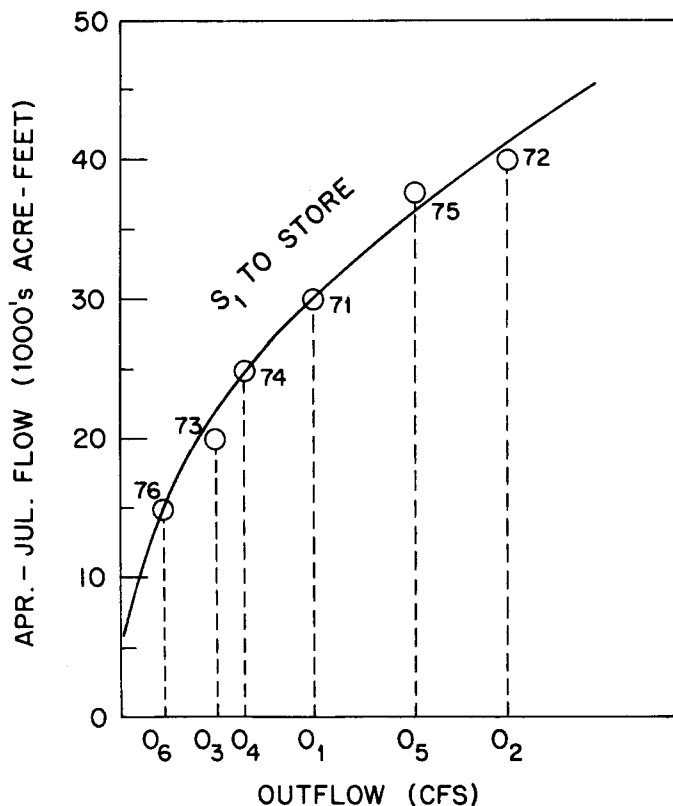


Figure 4. A reservoir rule curve for the S_1 storage level is generated from the graphs of figure 3 by plotting seasonal volume vs. release rate for each year of record.

A necessary step in obtaining the rule curve equation is to produce a three-dimensional matrix of seasonal volumes, storage, and outflow rates. These values are derived from the storage-outflow relationships for individual years (figure 3). A fifth degree least square polynomial regression procedure is used to objectively fit a curve to the storage-outflow data pairs for each year. It takes the form:

$$S = b_1O + b_2O^2 + b_3O^3 + b_4O^4 + b_5O^5 + b_6 \quad (2)$$

where $b_1, b_2, b_3, b_4, b_5, b_6$ are regression coefficients and S and O are as previously defined. It is now possible to employ a Newton iteration technique (Carnahan et

al., 1969) to find outflow rates at previously selected storage volumes for each year. This process yields the requisite three-dimensional matrix of data elements that is input to the rule curve algorithm.

The coefficients $a_1, a_2,$ and a_3 are found by solving the normal equations dictated by the form of the model in equation 1 (McCuen, 1985). The normal equations are:

$$a_1 \sum X^2 + a_2 \sum XY + a_3 \sum XZ = \sum XT \quad (3)$$

$$a_1 \sum XY + a_2 \sum Y^2 + a_3 \sum YZ = \sum YT \quad (4)$$

$$a_1 \sum XZ + a_2 \sum YZ + a_3 \sum Z^2 = \sum ZT \quad (5)$$

The summation (Σ) is carried out for p elements.

$$\text{where } p = l(m)n \quad (6)$$

l = number of years analyzed;

m = number of outflow rates chosen;

n = number of storage levels chosen.

The solution to the system of three simultaneous equations is given by finding the values of a_1, a_2, a_3 in the following matrix representation of the normal equations:

$$\begin{vmatrix} \sum X^2 & \sum XY & \sum XZ \\ \sum XY & \sum Y^2 & \sum YZ \\ \sum XZ & \sum YZ & \sum Z^2 \end{vmatrix} \cdot \begin{vmatrix} a_1 \\ a_2 \\ a_3 \end{vmatrix} = \begin{vmatrix} \sum XT \\ \sum YT \\ \sum ZT \end{vmatrix} \quad (7)$$

Gaussian elimination or matrix inversion can be used to solve for $a_1, a_2,$ and a_3 (Carnahan et al., 1969).

Having determined the regression coefficients, it is now possible to solve either directly or iteratively for any one of the original variables given the other two. In particular, we desire to produce the operating curves for specific storage levels. This requirement can be satisfied by fixing the storage level, incrementing through a range of seasonal volumes, and solving for outflow settings at each step using Newton's iteration method.

The rule curve algorithm has been subjected to verification tests to insure its mathematical integrity. In addition, validation

analyses have been conducted with actual data from various locations throughout the West.

ROMP PROGRAM

To facilitate SCS field personnel's ability to effectively utilize this procedure, a reservoir operation and management planning (ROMP) computer program was written. The program was designed to integrate data entry, streamflow screening, flow analysis, curve fitting, plotting, and error analysis. The initial version of ROMP was written in BASIC for Tektronix 4050 series graphics systems because they support high resolution screen and plotter graphical displays and were available in each of the SCS state offices in the Western U.S. A second version has been adapted to run on a Data General MV 8000 mini-computer with graphical output directed to a Tektronix 4105 color terminal. ROMP is fully menu driven making it easy for field personnel to use without extensive training.

ROMP's architecture is comprised of eight modules that are normally executed sequentially to produce a set of reservoir operating curves. Following is a list of the modules in the ROMP program:

1. Data Input
2. Hydrograph Plotting
3. Reservoir Inflow Correction
4. Flow Analysis
5. Storage vs. Discharge
6. Rule Curve Equation
7. Rule Curve Error Analysis
8. Rule Curve Plotting

RULE CURVE APPLICATION

It is instructive to go through an abbreviated example of developing and applying the results of the ROMP program. Middle Creek Reservoir in southwestern Montana is used to show how reservoir

operating curves are generated and how they guide the management decision making process. This reservoir is managed primarily for irrigation and municipal water storage but potential impacts on other interests affect how the project is operated.

Middle Creek Reservoir is on Hyalite Creek in the Gallatin River Basin. It has a drainage area of 27.4 square miles. The streamflow regime is dominated by snowmelt runoff. Reservoir capacity is 8,261 acre-feet. Daily inflow records are only available April-July for a 17-year period (1966-83, 1970 missing). The outlet tunnel will pass 800 cfs when the reservoir is full. However, considerable downstream erosion occurs at flows in excess of 400 cfs. A flow of 125 cfs is necessary to satisfy decreed water rights and irrigation demands. A minimum outflow of 25 cfs is required to support downstream fish populations. These operating constraints dictate that the desirable operating range for outflow be between 125 and 400 cfs during the irrigation season. Streamflow forecasts are issued for reservoir inflow monthly January through June.

Daily reservoir inflow data for the April-July period were entered from the keyboard using the ROMP Data Input module. The Flow Analysis, Storage vs. Discharge, and Rule Curve Equation modules were next executed sequentially to create the following rule curve regression equation for the April-July period:

$$S = [V - 7.4247 * O - 1537 * (8) \\ 00.5] / (1 + .0025 * O)$$

The rule curves shown in figure 5 were generated using equation 8 and the Rule Curve Plotting module. A similar procedure was followed to produce the May-July rule curves shown in figure 6. These two charts used in conjunction with streamflow forecasts provide the means to make outflow adjustments commensurate with anticipated runoff. Illustration

tions of how the operating curves might be used in a high snowpack year and low snowpack year are given for comparison.

Low Runoff Year

On March 1, assume the reservoir has 3,261 acre-feet of water in storage and the most probable (MP) April-July inflow forecast is 22,000 acre-feet or 76 percent of average. Average April-July inflow is 29,000 acre-feet. The reasonable minimum forecast (RMN) is 17,500 acre-feet; the reasonable maximum forecast (RMX) is 27,500 acre-feet. Subtracting current storage from the reservoir's capacity leaves 5,000 acre-feet required to fill the reservoir. Entering the April-July operating curves of figure 5 with RMN, MP, and RMX and moving horizontally to the 5,000 acre-feet to store curve yields release rates of 60, 110,

and 170 cfs, respectively. Based on these figures, a logical decision would be to store as much water as possible and to only release enough water to support a viable fishery.

By April 1, reservoir storage was increased by 200 acre-feet, thus requiring 4,800 acre-feet to fill the reservoir. The April-July forecast has been raised slightly to 18,000 acre-feet for RMN, 22,500 for MP, and 27,000 for RMX. Entering the April-July operating curves with these values indicates outflow settings of 67, 112, and 167 cfs, respectively. These figures show that only with above normal subsequent precipitation will the reservoir fill and meet withdrawal demands. Both outflow settings found with RMN and MP inflows are well below the minimum desirable outflow of 125 cfs necessary to satisfy downstream water rights. At this point, the decision would probably be made to continue storing as much as possible until May 1 forecasts are received.

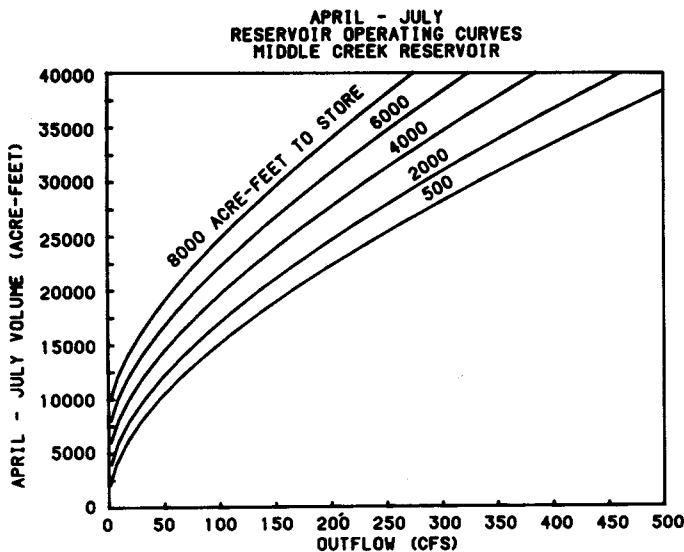


Figure 5. Reservoir rule curves for Middle Creek Reservoir, Montana, applicable for April-July runoff period. Curves were developed from 17 years data.

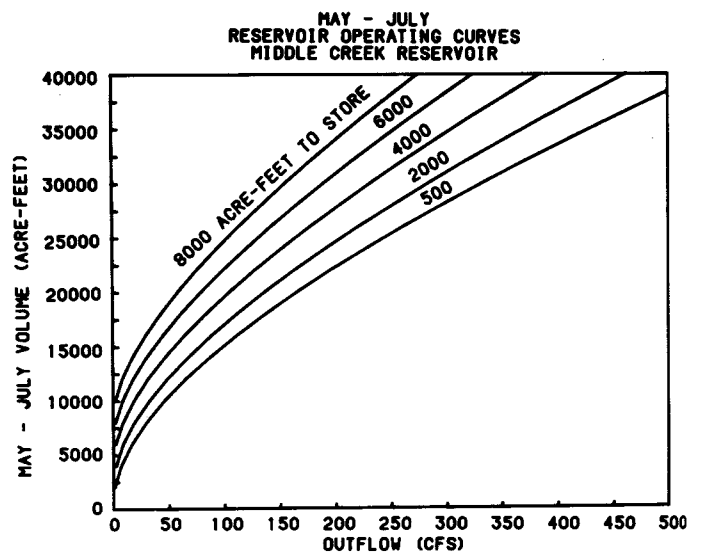


Figure 6. Reservoir rule curves for Middle Creek Reservoir, Montana, applicable for May-July runoff period.

During April, runoff was sufficient to provide an additional 500 acre-feet of storage leaving 4,300 acre-feet necessary to fill the reservoir. The May-July MP has been raised to 80 percent of normal or 21,500 acre-feet. The May-July average is 27,000 acre-feet. RMN is 18,000 acre-feet, and RMX is 25,000 acre-feet. Using May-July reservoir operating curves of figure 6, the outflows for RMN, MP, and RMX would be 75, 110, and 158 cfs, respectively. The decision would probably be made to maintain releases at the minimum levels dictated by fishery considerations and continue storing as much water as possible until irrigation and municipal withdrawal demands exceed inflow. With the expected low runoff, the probability of generating channel damaging flows in excess of 400 cfs is remote.

In such a low runoff year, when reservoir storage is low, demand for irrigation water may be greater than the outflow rates which would permit filling the reservoir. Water users must then decide whether they would rather use the water for early irrigation or to put it into storage for later delivery when crop consumptive demands are highest.

HIGH RUNOFF YEAR

On March 1, assume 3,000 acre-feet are needed to fill the reservoir and the April-July MP is 35,000 acre-feet or 121 percent of average. RMN and RMX are predicted to be 30,000 and 40,000 acre-feet, respectively. Entering figure 5 with these predictions yields outflows of 257, 300, and 410 cfs. These outflow rates are in the range that raises concern about the possibility of being forced into releases higher than are desirable later in the season. They also support the contention that there is likely to be plenty of water to fill the reservoir and satisfy all downstream requirements. The decision will probably be made to

hold the reservoir at the same level or decrease it a little by setting outflow equal to, or slightly greater than, inflow and wait until the April 1 forecasts are received.

When April 1 comes, the reservoir storage has dropped to a level requiring 3,300 acre-feet of water to fill. Streamflow projections of April-July runoff are for RMN, MP, and RMX values of 31,500, 35,000, and 39,500 acre-feet, respectively. Entering figure 5 with these numbers translates into potential release rates of 275, 335, and 395 cfs corresponding to RMN, MP, and RMX. The decision would likely be made to set outflow rates 10 to 15 cfs above inflow rates to begin reducing reservoir storage before runoff begins. Any significant increase in storage or leaving the reservoir at its present level could create a potentially hazardous situation if abnormally high precipitation and temperatures are experienced in the next several months.

On May 1, the MP is for a May-July flow of 130 percent of average or 35,000 acre-feet. RMN and RMX are for flows of 32,000 and 38,000 acre-feet, respectively. Reservoir storage has been reduced and there are 4,000 acre-feet of available storage. Using these figures in the May-July reservoir operating curves (figure 6) gives release rates ranging from 260 cfs for RMN to 351 cfs for RMX with an intermediate value of 305 cfs for MP. These numbers continue to indicate a heavy runoff but with a lessening probability that release rates will have to approach or exceed 400 cfs, the threshold at which damage occurs at downstream reaches in the channel. The decision would probably be made to set outflow rates about 300 cfs and continue to carefully monitor weather temperatures during the month for unusually warm conditions or heavy precipitation. If either of these events occurred, it would be appropriate to raise outflows to levels between 350 and 400 cfs.

Melting winter snowpack and spring and early summer rain are the primary sources of water in many locations in the West. Flows from these sources into a reservoir vary significantly from year to year and day to day within a given year depending on a number of factors. These include volume of water accumulated in the winter's snowpack, basin soil wetness, areal extent of snow cover, temperature conditions during the main snowmelt period, and the amount and rate of spring and early summer precipitation. Reservoir managers must assess these factors and the uncertainty they impose in terms of risks associated with storing too much or too little water. To the degree that operators can reduce uncertainty about future runoff, they incrementally reduce their exposure to risk. An analytical tool to help them define the magnitude and probability of runoff events several months in advance and the consequent implications for project regulation is highly desirable.

Ideally, reservoir operation would regulate outflow to minimize spilling excess water, satisfy senior downstream water rights, minimize erosion and downstream flooding, provide sufficient water for recreation, fisheries, and wildlife, and enable the reservoir to be full near the end of the high water period. Sometimes heavy snowfall or rain occur in late spring and may prevent achieving ideal outflow conditions each year to satisfy all these requirements. However, most of the time it is possible to successfully base each year's reservoir management on expected runoff conditions by using water supply predictions. During heavy snowpack years, downstream flooding can be reduced; in low snowpack years, effects of low runoff can be somewhat moderated.

A procedure has been developed and is being used operationally to assist reservoir operators to manage their facilities with seasonal forecasts of snowmelt runoff. Informed decisions can be made based on the probability of occurrence of seasonal flow volumes. The methodology employs reservoir operating rule curves that are generated from historical inflow data. The derivation of the operating curves has been explained and a mathematical algorithm to calculate them presented. An integrated, menu-driven computer program called ROMP has been developed to aid technical specialists in the development of these curves. Examples of how the curves might be used as guides in high and low runoff years are offered. Given reasonably accurate streamflow forecasts and knowing the amount of available storage space, a reservoir operator can use the family of operating curves to analyze available options objectively to help reduce uncertainty and manage exposure to risk.

Literature Cited

- Carnahan, B., H.A. Luther, and J.O. Wilkes, 1969. Applied Numerical Methods. John Wiley & Sons, New York, N.Y.
- McCuen, Richard H., 1985. Statistical Methods for Engineers. Prentice-Hall, Inc., Englewood, N.J. pp. 221.

MODELLING WATER LEVELS FOR A LAKE IN THE MACKENZIE DELTA

*P. Marsh*¹

ABSTRACT: A detailed hydrologic study of a perched lake in the Mackenzie Delta was carried out during the summer of 1985. The hydrologic regime of this lake may be divided into three distinct periods: flooding, discharge, and evaporation. Over the summer of 1985 the lake experienced a small negative water balance. However, if the lake was not flooded, it would have experienced a severe negative balance since evaporation exceeded precipitation. This type of lake is probably dependent on flooding to keep water levels at the present level. A simulation model, which accurately predicted water level over the summer period, could be used to predict the flooding frequency required to maintain lake levels.

(KEY TERMS: lake hydrology; water balance; Mackenzie Delta.)

become an issue as development proceeds in the Mackenzie Valley. A major concern is that pollutants introduced into the Mackenzie River upstream of or within the delta, will be distributed into Mackenzie Delta lakes by the vast distributary channel network. A second concern is that further flow regulation in the Mackenzie River system may have an effect on lake levels, as has already occurred in the Peace-Athabasca Delta (Peace-Athabasca Delta Group, 1972) with the resulting consequences to permafrost and wildlife habitat (Gill, 1973).

It is the purpose of this paper to describe the hydrological processes operating in a typical perched lake in the Mackenzie Delta. In addition a simulation model for predicting lake level will be presented.

INTRODUCTION

The Mackenzie Delta is dominated by the myriad of lakes which occur throughout its entire 65 by 180 km extent. These lakes play a significant role in the delta ecosystem. They affect the distribution of permafrost (Smith, 1976), support large populations of fish, mammals, and waterfowl (Gill, 1973; Peterson, Allison, and Kabzems, 1981), and provide storage for water, sediment, and pollutants. In spite of the importance of these lakes to the hydrology, geomorphology, and wildlife of the Mackenzie Delta, few hydrologic studies have been conducted to date. Mackay (1974) discussed the origin of Mackenzie Delta lakes and their general hydrologic characteristics, and Bigras (1985) has considered lake levels in the eastern sector of the Mackenzie Delta.

Changes in the natural environment of these delta lakes, though not a problem at present, may

MACKENZIE DELTA LAKES

Lakes dominate the physical landscape of the Mackenzie Delta both in sheer number and area covered. An analysis of aerial photographs for a typical 70 km² area southwest of Inuvik, N.W.T., showed that 282 lakes covered 50% of the surveyed area. Large river channels covered an additional 3% of the area, and land the remaining 47%.

Two common types of lakes, each with different hydrologic conditions, are found in this area. The primary factor controlling the lake type is the sill elevation between the lake and main channel. Even though only two lake types are described here, there is probably a continuum of lake types between the two.

The first lake type has a well defined, water filled channel connecting it to a main channel. As a result, the water level in the lake and main channel are similar. Due to small changes in the

¹ National Hydrology Research Institute, Environment Canada, Ottawa, Ontario, Canada, K1A 0E7.

relative level of the channel and lake they are constantly interchanging water. These connecting channels may become dry when the main channels reach low water levels in the fall. There are 61 connected lakes covering 39% of the surveyed area.

The second lake type is perched above the surrounding main channel and connected lake system. These perched lakes have small connecting channels which carry water into the lake for a one or two week period, but may discharge water to the main channel for an additional two to five weeks. Flooding is normally an annual event, but during years with low Mackenzie water levels and for lakes with the highest closure levels, overtopping and subsequent flooding may not occur every year. In the study area there are a total of 207 perched lakes, covering 8% of the area. Bigras (1985) called these perched lakes either low or high closure lakes depending on their sill elevation.

The land area contributing water to these lakes is generally small. In most cases the actual contributing area is hard to define since the land is very flat and the poorly defined drainage system is covered by dense vegetation.

In the study area there were also 14 lakes (4% of the area) which from the aerial photographs, could not be classified as either connected or perched.

STUDY AREA AND METHODOLOGY

Study area

Field work was carried out from early June to early September 1984 and 1985 at a typical perched lake (unofficial name NRC Lake) approximately 5 km southwest of Inuvik (Figure 1). This lake is about 2 m above the low water level of the surrounding connected lakes and channels. During the spring flood, the lake level may be over 2.5 m higher than in mid-summer. The small channel connecting NRC Lake to a nearby connected lake is active during and immediately after the flood period. For the rest of the year the channel is dry. During mid-summer NRC Lake is approximately 300 m in length, 220 m in width, has a mean depth of 0.88 m and maximum depth of 1.6 m, and is 0.069 km² in area. The basin surrounding the lake has an area of 0.43 km² and is covered by an open, mature spruce forest. The area surrounding the lake is underlain by permafrost in excess of 80 m in thickness (Johnston and Brown, 1964), and the active layer is up to 0.5 m deep by late summer. The zone beneath the lake is composed of unfrozen

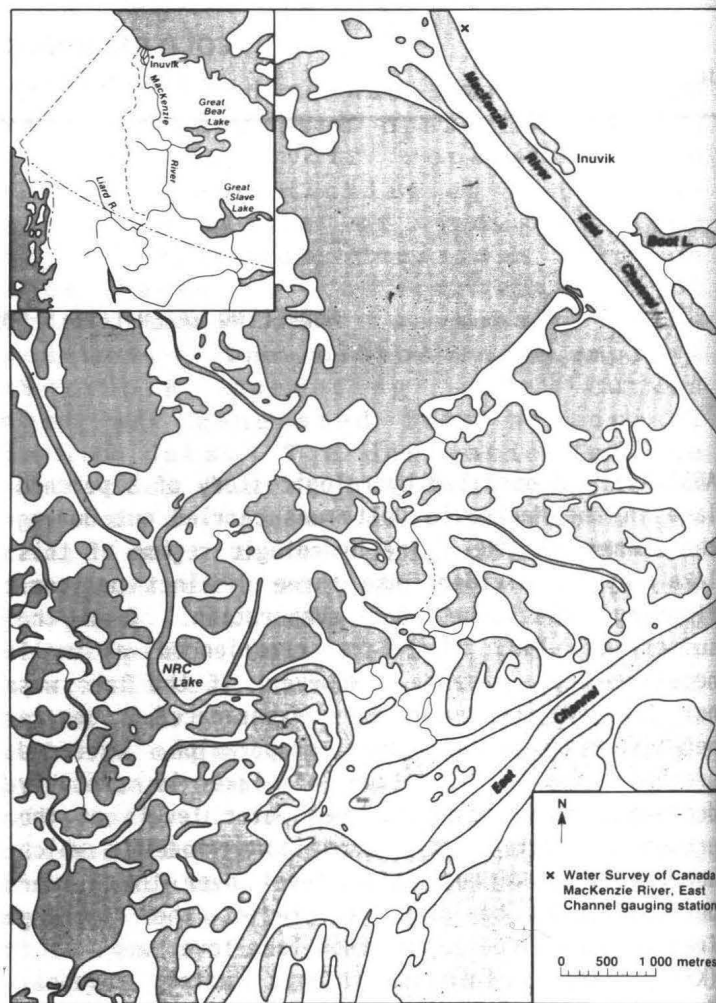


Figure 1. Location of the study site near Inuvik, N.W.T.

silts and clays (Johnston and Brown, 1964, 1965), with bedrock occurring at a depth of 80 m (Johnston and Brown, 1964).

In the Inuvik area, air temperature rises above 0°C in mid May (AES, 1982). Snowmelt and the first deterioration of ice on the Mackenzie River East Channel are initiated at this time and on average the river is clear of ice by June 5 (Allen, 1977). As warmer floodwater enters the lakes during spring breakup, the lake ice cover melts rapidly and lakes such as NRC Lake are usually ice free by early to mid-June. Air temperature falls below 0°C by late September (AES, 1982) and the lakes freeze shortly afterwards. The first permanent ice forms on the Mackenzie River East Channel by October 11 on average, and it is completely frozen by October 19 (Allen, 1977).

Field Methods and Instrumentation

Micrometeorological and hydrologic measurements were made from an instrument platform near the centre of NRC Lake and a 15.9 m tower at a forest site. A Campbell CR21 data logger recorded air temperature, relative humidity, wind speed, net radiation, solar radiation, precipitation, and water or soil temperature at both sites. Hourly averages of these parameters were obtained from measurements taken at 60 second intervals. A Stevens Type F water level recorder was used to record lake water level. Manual measurements were made of water and bed temperature from the lake surface to 4 m below the lake bed, soil moisture, supra-permafrost groundwater levels at sites around the perimeter of the lake, frost table, and surface flow in a small rill entering the lake. The lake discharge was measured a number of times in order to obtain a rating curve of discharge versus lake stage. In addition the lake outlet channel was surveyed to determine the sill elevation controlling inflow and outflow. Water level measurements for the Mackenzie River East Channel were obtained from Water Survey Canada.

Lake Water Balance

The lake water balance is given by

$$(1) P + E + Q_0 + Q_{in} + Q_{sp} + Q_{sb} + Q_s + e = ds/dt$$

where P is precipitation on the lake surface, E is evaporation from the lake surface, Q_0 is outflow discharge, Q_{in} is inflow discharge from the Mackenzie River, Q_{sp} is supra-permafrost groundwater flow to the lake from the surrounding active layer, Q_{sb} is sub-permafrost groundwater flow through the talik beneath the lake, Q_s is surface flow from the surrounding basin, e is an error term, and ds/dt is the change in lake storage. In all cases the terms have positive values when water is added to the lake and negative when removed from the lake. The \dot{P} , Q_{in} , Q_0 , and ds/dt terms were measured on an hourly basis. Methods to calculate E, Q_{sp} , and Q_s are given below. Since all terms were measured or calculated, the error term (e) could be calculated as a residual.

Water balance and groundwater studies at NRC Lake have suggested that sub-permafrost groundwater flow occurs. However, the volume is small because the lake bed is composed of fine grained material (Johnston and Brown, 1965) with a low permeability, and permafrost surrounding the lake is over 80 m thick (Johnston and Brown, 1964). Because of its

small magnitude, sub-permafrost groundwater will not be considered in this paper.

Evaporation

Evaporation was computed using the Priestley and Taylor (1972) approach as applied to northern forests by Rouse, et al. (1977), to shallow northern lakes by Stewart and Rouse (1976), and to arctic tundra by Marsh, et al. (1981). In this approach evaporation is calculated by

$$(2) E = a' [s/(s + g)] (Q^* - Q_g) / L_v \rho$$

where E is evaporation, s is the slope of the temperature - saturated vapor pressure curve, g is the psychrometric constant, Q^* is net radiation, Q_g is the ground heat flux, L_v is the latent heat of vaporization, ρ is water density, and a' is an empirical constant which relates actual to equilibrium evaporation (Marsh, et al., 1981). Various studies (Priestley and Taylor, 1972; Rouse, et al., 1977) have found that for saturated surfaces a' averages 1.26. The slope of the temperature - saturated vapor pressure curve (s) may be calculated as a function of air temperature (Dilley, 1968).

For the lake, Q_g was estimated from the change in water and bed temperature

$$(3) Q_g = \int_{z=0}^{z_0} c \, dT/dt \, dz$$

where z is the depth below the water surface and z_0 is the depth at which annual bed temperature amplitude equals zero, c is the bed or water heat capacity, and T is the bed or water temperature. Observations showed that over the summer period z_0 is approximately 4 m. Hourly averages were used for air temperature and net radiation in equation 2, and for water and bed temperature in equation 3.

The ground heat flux term varied greatly on a daily basis and must be included if hourly or daily evaporation is required. Over the summer period however, Q_g was small, accounting for only 3% of the available energy.

Surface and Supra-permafrost Groundwater Flow

Surface and supra-permafrost groundwater flow entered the lake in 9 small rills spaced around the

lake. Total surface flow into the lake was obtained by

$$(4) Q_s(T) = Q_s(m) (A / A(m))$$

where $Q_s(T)$ is the total surface flow entering the lake, $Q_s(m)$ is the measured surface flow, A is the total area contributing water to the lake (.43 km²), and $A(m)$ is the area contributing water to the measured rill (.021 km²).

Supra-permafrost groundwater flow (Q_{sp}) in a single rill was calculated from

$$(5) Q_{sp} = K dh/dl W D$$

where K is the hydraulic conductivity, dh/dl the hydraulic gradient, W is the width of the rill, and D is the thickness of the saturated portion of the active layer. Total flow into NRC Lake ($Q_{sp}(T)$) was then estimated by

$$(6) Q_{sp}(T) = Q_{sp} N$$

where N is the number of rills.

NRC LAKE HYDROLOGY

The hydrologic regime of NRC Lake during the period May to September may be divided into three distinct periods. During each period one process usually dominates the lake water balance. These periods are: (1) flooding regime, (2) discharge regime, and (3) evaporation regime.

Flooding Regime

During 1985 NRC Lake was flooded on May 21 (Figure 2), when the main channel water level rose above 3.813 m. After this date, water levels in NRC rose rapidly, reaching a peak of 6.363 m on June 2. Levels then declined quickly, reaching 4.25 m by June 9. After this date lake discharge was controlled by the outlet channel geometry, not by the Mackenzie River water level. Throughout this period, NRC Lake water level was similar to that measured by Water Survey of Canada on East Channel 5 km to the northeast (Figure 2). Prior to the removal of ice on East Channel (June 2), NRC Lake water level averaged .246 m higher than East Channel. From June 2 to June 9, the difference was only .136 m. For a 6.34 km channel length, the water slope was .00004 and .00002 respectively during this period. The river slope during the ice

covered period was considerably higher than the open water slope of .00002 measured in late summer.

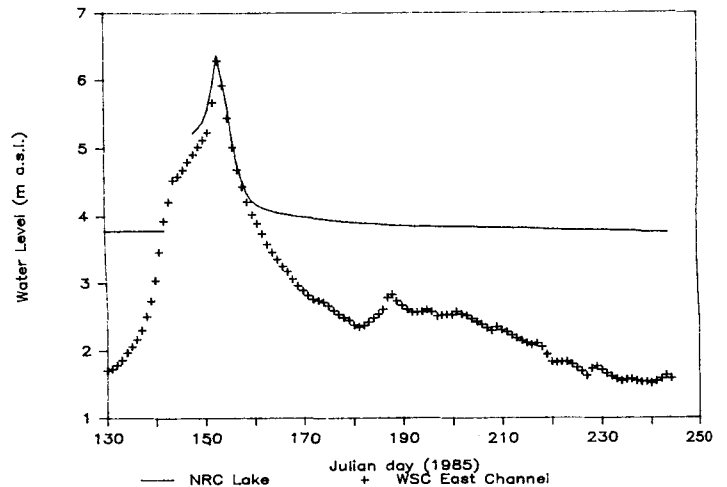


Figure 2. NRC Lake level and Mackenzie River East Channel level, May to September 1985. Julian Day 130 is May 10, 1985.

The lake water balance during this period (Table 1) is dominated by the influx of Mackenzie

TABLE 1. Water Balance, NRC Lake 1985.

Date	Inputs			Outputs			Error		
	P	Q_{sp}	Q_s	Q_{in}	Q_{sp}	Q_o			
May 21 - June 9	5	0	0	2578	0	-2113	0	465	-5
June 9 - Aug 4	22	9	239	0	0	-579	-185	-437	56
Aug 4 - Sept 1	4	0	0	0	0	0	-60	-62	-6
Total	31	9	239	2578	0	-2692	-245	-34	45

floodwater (2578 mm) and subsequent outflow (-2113 mm) as the Mackenzie level declined. Precipitation was only 5 mm and because of the lake ice cover, evaporation was close to zero. The overall result was to increase the lake storage by 465 mm. In addition the flood water saturated the land surrounding the lake. This flood water was the primary source of water entering the lake as surface and groundwater flow following the flood period. The water balance error term was only -5 mm.

Discharge Regime

After June 9, discharge from NRC Lake was controlled by the outlet channel geometry. The peak discharge on this date was $.20 \text{ m}^3/\text{s}$ and the flow declined gradually as the lake level dropped. Discharge ceased on August 4 when the lake level reached the sill elevation (Figure 2). Channel discharge of -579 mm was the dominant component of the lake water balance over this period (Table 1). After the lake ice cover was removed in early June evaporation became an important component of the lake water balance, with a total of -185 mm (Table 1).

When flood waters declined, water drained from the land into the lake. The surface flow totalled 239 mm from June 9 until June 20, while from June 9 to August 1 supra-permafrost groundwater flow contributed 9 mm to the lake. Drainage and evaporation from the surrounding forest was greater than precipitation and the active layer dried significantly over the summer.

During June and July, precipitation was only 22 mm . The result was that lake storage decreased by -437 mm over the period June 9 to August 4. The water balance error was 56 mm during this period. Small errors in determining surface inflow and channel discharge during the rapid decline in lake level could account for this error. Since the error is only 12% of the change in storage, it is acceptable.

Evaporation Regime

After August 4, groundwater inflow, surface inflow, and channel outflow had ceased. The only source of water was precipitation directly onto the lake surface and the only removal of water was by evaporation from the lake surface.

Predicted evaporation from August 4 to September 1 was -60 mm , precipitation was only 4 mm , and the change in lake storage was -62 mm . The residual error term was -6 mm (Table 2). Since the lake acted as a large evaporation pan, this period provided an excellent test of the Priestly-Taylor evaporation approach (equation 1). The predicted and measured evaporation were within 6 mm or 10% of each other. This is an acceptable result and justifies the use of this technique to calculate evaporation from lakes in the Mackenzie Delta.

Summer Period

Even though it received a large volume of floodwater in 1985, NRC Lake experienced a decline in storage of -34 mm from May 21 to September 1. The water balance components responsible for this are listed in Table 1 and are described below.

The Mackenzie River added a total of 2578 mm to the lake as flood water. Surface and groundwater flow, of which most was Mackenzie flood water draining from the surrounding land, added an additional 248 mm of water. Total water input from flooding was therefore 2826 mm . The only other source of water, precipitation on the lake surface, totalled 31 mm from May 21 to September 1. This was less than normal. At the AES Inuvik weather station for example, the June, July, and August precipitation was only 31 mm compared to the 30 year normal of 101 mm .

Most of the 2927 mm of water added to the lake, was discharged as channel flow which totalled -2692 mm . Evaporation was the second largest term, equalling -245 mm . Total calculated output was -2937 mm , and the water balance error term, calculated as a residual, was 45 mm . This is an acceptable error since it is such a small percentage of either the total input or output of the lake. However, it is a significant proportion of the measured change in lake storage. The lake is in fact in a very fine balance, with large inputs and outputs of water, but very small changes in storage from year to year.

PREDICTED NRC LAKE LEVEL

Simulation Model

Changes in lake level over the flooding, discharge and evaporation periods were predicted using: (1) adjusted East Channel water levels during the flooding period and (2) hourly water balance calculations for the remainder of the summer.

The model is initiated with a measured pre-melt lake level. In 1985 this was 3.785 m . Lake level remains constant until the channel water level rises above the NRC sill elevation (3.813 m) and the lake is flooded with Mackenzie River water. The lake level then equals the channel level, which is estimated from East Channel level adjusted for channel slope. A slope of $.00002$, determined from summer observations, was used. Once the lake level falls below the elevation where NRC Lake discharge is controlled by the outlet channel geometry

(4.25 m), the lake level is controlled by the lake water balance. The hourly lake levels were then calculated as

$$(10) \quad LS(t) = LS(t-1) + P + Q_{sp} + Q_s + E + Q_o$$

where LS is the lake stage at time t and (t-1). The other parameters, as defined earlier, are measured or calculated over the time period (t-1) to (t). Precipitation was measured at the lake, and groundwater, surface flow, and evaporation were calculated using equations 6, 4, and 2 respectively. Discharge was calculated from a relationship between stage and discharge. Observations showed that discharge ceased when lake level dropped below 3.813 m.

Results

Predicted NRC Lake level is similar to that observed over the entire summer period (Figure 3).

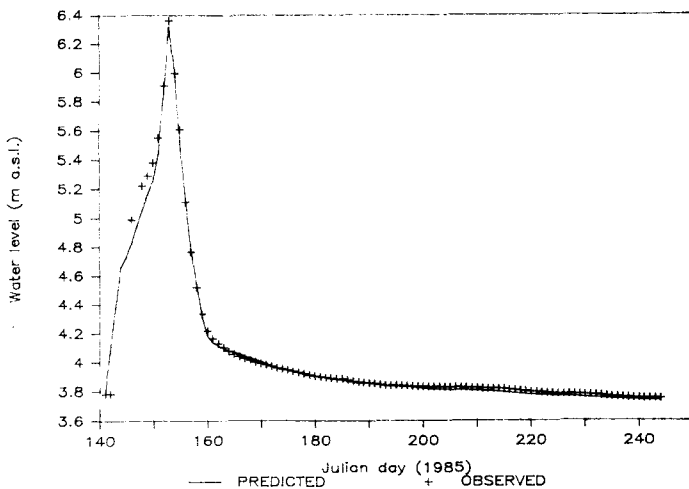


Figure 3. Observed and predicted NRC Lake level, May to September 1985. Julian day 140 is May 20, 1985.

The maximum differences between predicted and observed mean daily lake level during the flooding, discharge, and evaporation periods were only .176, .028, and .023 m. By the end of the simulation period the difference between observed and predicted was only .016 m. The largest error occurred in the flooding period when lake level was calculated using WSC East Channel level adjusted using an open water slope. During this period however, water slope varies as the channel changes from ice covered to open water. These changes in slope were not accounted for in the present model. However, considering the large changes in level

during this period, the error involved is relatively small.

DISCUSSION

The water balance listed in Table 1 shows that flooding contributes a large volume of water to NRC Lake. Low closure lakes like NRC Lake probably flood annually, however certain high closure lakes are flooded infrequently. The frequency of flooding, controlled by the lake sill elevation and the Mackenzie River flood level, could change if flow regulation occurred in the Mackenzie River Basin.

The water balance of a perched lake during a non-flooding year can be estimated from the NRC Lake data. In 1985, evaporation from NRC Lake was -245 mm and precipitation was 31 mm. Since in the absence of flooding the only significant input and output is precipitation and evaporation, the resulting change in storage at NRC Lake would have been -214 mm. Even in a year with normal precipitation, evaporation would probably exceed precipitation. In 1984 for example, a year with near normal precipitation, NRC Lake level decreased over the summer period. This implies that evaporation was greater than precipitation. Therefore, without flooding, water level in NRC Lake would be expected to decline significantly within a few years. This is probably true for most perched lakes.

This conclusion is substantiated by data from a perched lake 50 km southwest of Inuvik. This high closure lake was last flooded in June 1982. The lake does not have a surface outlet, but the lake level declined 1.43 m between June 3, 1982 and August 27, 1985 (Bigras, personal communication). The average summer decline of .36 m, is larger than the difference between precipitation and evaporation experienced at NRC Lake in 1985. This is probably explained by a higher evaporation rate at the southern site due to warmer air temperatures. Further work is required to substantiate this explanation. The important point from this example is not the rate of decline, but that without flooding it will probably be dry within a few years.

One aspect of the lake hydrological regime not included here is the snowmelt period. It is not known how much of the winter snowfall of approximately 130 mm water equivalent runs off into the lake during the spring melt. However the dry soil, low relief, and poorly defined drainage system must limit the runoff. Future work will

consider this aspect of the lake hydrological regime.

Perched lakes certainly do not require annual flooding, but they probably require flooding on a frequent basis to maintain water levels. The frequency of flooding required could be determined by running a version of the simulation model described earlier.

CONCLUSIONS

The primary conclusions of this paper are:

- (1) the lake sill elevation is a major factor controlling the hydrology of Mackenzie Delta lakes, determining the duration and magnitude of flooding
- (2) permafrost limits groundwater movement from NRC Lake, allowing it to remain perched above channel level for most of the year
- (3) because evaporation from the lake surface is greater than precipitation, the lake experiences a negative water balance. Without replenishment of water from the Mackenzie River during the spring flood, the lake level would probably decrease significantly within a few years
- (4) as a result of evaporation from the land surrounding the lake, surface and sub-surface drainage to the lake was small for much of the summer. Most of the drainage to the lake was a result of flooding of the land by the Mackenzie River
- (5) A simulation model was able to accurately predict lake level throughout the spring flood and summer period. This model, with a few additions, could be used to determine the frequency of flooding needed to sustain perched lakes in the Mackenzie Delta
- (6) perched lakes are susceptible to pollutants introduced from the Mackenzie River since these lakes are only flushed once per year

Acknowledgements: The generous logistical support of Polar Continental Shelf Project, Department of Energy, Mines, and Resources, and the Inuvik Scientific Resource Centre, Department of Indian and Northern Affairs is gratefully acknowledged. I would like to thank R. Smith, M. Suzor, and R. Storey for their assistance in the field.

REFERENCES

- Atmospheric Environment Service, 1982. Canadian climate normals. Volume 2, Temperature, 1951 to 1980. Environment Canada. 306 p.
- Allen, G.D., 1977. Freeze-up, break-up and ice thickness in Canada. Atmospheric Environment, Publication CLI-1-77, 185 p.
- Bigras, S.C., 1985. Lake regimes, Mackenzie Delta, NWT, 1981. National Hydrology Research Institute, Internal Report, Environment Canada, 39 p.
- Dilley, A.C., 1968. On the computer calculation of vapor pressure and specific humidity gradients from psychrometric data. Jour. of Applied Meteorology, 7, 717-719.
- Gill, D., 1973. Modification of northern alluvial habitats by river development. Canadian Geographer, 17, 138-153.
- Johnston, G.H., and R.J.E. Brown. 1964. Some observations on permafrost distribution at a lake in the Mackenzie Delta, N.W.T., Canada, Arctic, 17, 163-175.
- Johnston, G.H., and R.J.E. Brown. 1965. Stratigraphy of the Mackenzie River Delta, Northwest Territories, Canada. Geol. Society of America Bull., 76, 103-112.
- Mackay, J.R., 1974. The Mackenzie Delta area, N.W.T., Geol. Survey of Canada Misc. Report 23, 202 p.
- Marsh, P., W.R. Rouse, and M.K. Woo., 1981. Evaporation at a High Arctic site. Jour. of Applied Meteorology, 20, 713-716.
- Peterson, E.B., L.M. Allison and R.D. Kabzems., 1981. Alluvial ecosystems. In: Mackenzie River Basin Committee, Mackenzie River Basin Study Report Supplement 2, 129 p.
- Peace-Athabasca Delta Group. 1972. The Peace-Athabasca Delta, A Canadian Resource. 144 p.
- Priestley, C.H.B. and R.J. Taylor. 1972. On the assessment of surface heat flux and evaporation using large-scale parameters. Monthly Weather Review, 100, 81-92.
- Rouse, W.R., P.F. Mills, and R.B. Stewart. 1977. Evaporation in high latitudes. Water Resources Research, 13, 909-914.
- Smith, M.W., 1976. Permafrost in the Mackenzie Delta, Northwest Territories. Geol. Survey of Canada Paper 75-28, 34 p.
- Stewart, R.B. and W.R. Rouse, 1976. A simple method for determining the evaporation from shallow lakes and ponds. Water Resources Research, 12, 623-628.

SHORT-WAVE HEATING OF LAKE SURFACE WATER UNDER A CANDLED ICE COVER

J. P. Gosink and J. D. LaPerriere*

ABSTRACT: During spring, as the snow covering the lakes and rivers begins to melt from a positive surface heat balance, meltwater percolates through microcracks in the ice, initiating vertical channels through the ice. The ice develops into a porous fabric, known as candled ice, characterized by closely packed vertical "candles" of ice interspersed with channels of meltwater. Candled ice is quite transparent to short wave radiation, with optical extinction coefficients approaching those found in the lake water. This implies that the incident solar radiation can penetrate through the ice cover, warming the water immediately below the melting ice. La Perriere (1981) reported lake temperatures in excess of 6°C one to two meters below the base of the candled ice during field studies in Harding Lake, Alaska. This layer of water, although heated above the temperature of maximum density, appeared to be stable due to the slight density difference between the meltwater with low specific conductance, and the more saline lake water.

The stability of the under-ice water column is critical for lake overturn and subsequent reoxygenation of the lake. In a typical dimictic lake, overturn occurs during strong winds at or soon following complete disappearance of the ice. The overturn results in reoxygenation of the lake to near saturation levels. However, when near surface warming of the lake occurs through the candled ice column, the potential exists for initiation of summer stratification conditions below the ice cover, with a stable density structure in the water column. If the

wind stress over the lake is low as the final ice melts, it is possible that little or no overturn and reoxygenation of the lake water will take place. This situation occurred in Harding Lake in May 1975.

This paper presents the results of a one-dimensional heat balance study of the near surface water below candled ice. Short wave penetration of heat through the candled ice and into the underlying water column, latent heat effects, and thermal conduction and convection are considered. The model predicts the occurrence of a subsurface water temperature maximum close to 6°C at a depth one to two meters below the base of the candled ice. The analysis includes a discussion of convective stability in the meltwater layer below the melting ice cover. Velocities in the meltwater are shown to be between 0.1% and 10% of the corresponding Monin-Oubukhov velocity at a free surface.

(KEY TERMS: lake ice; candled ice cover; penetrative convection, surface mixing.)

INTRODUCTION

Thermal energy transfer at a snow or ice surface on a lake or river consists of heat flux due to sensible heat transfer, conduction through the snow and ice, latent heat exchange due to sublimation and melting or freezing, long-wave radiative exchange and short-wave radiative transfer. The short-wave transfer differs from the other modes of heat exchange in that attenuated short-wave radiation

*J. P. Gosink, Geophysical Institute, University of Alaska, Fairbanks, Alaska 99775-0800; J. D. La Perriere, Alaska Cooperative Fishery Research Unit, Arctic Health Research Building, University of Alaska, Fairbanks, Alaska 99775-0810.

penetrates through the surface, into the snow and ice, and ultimately into the underlying water column. If the snow layer is thick, then most of the available short-wave energy is expended warming or melting the snow layer. In spring, as the snow layer melts, an increasing amount of shortwave radiation is absorbed within the ice layer and in the underlying water column. The radiation absorbed in the ice raises the ice temperature to 0°C, and excess radiation results in melting at grain boundaries (Knight, 1962; Lyons and Stoiher, 1959). The effect of this melting process is to cause deterioration of the ice fabric (Ashton, 1985; Bulatov, 1970). The deteriorated ice becomes porous and assumes the appearance of closely packed "candles". Canded ice is substantially weaker than an intact ice layer.

La Perriere (1981) observed canded ice on Harding Lake during late spring, and measured water temperatures below the bottom of the ice layer. A somewhat surprising result was the discovery of a stable layer of water heated above the temperature of maximum density which had not mixed downward. It was hypothesized that the heat gain in the water was due to the transparency of the canded ice to short-wave radiation. It was further assumed that melting of the ice produced a shallow and relatively buoyant fresh water lens below the ice surface. Vertical water velocities were not measured; however, it was suggested that convective velocities due to buoyancy differences were minimal.

This article evaluates the mixing potential of the surface layer water. This is accomplished through an analytic model of heat transport in the water column with three modes of heat transport: conduction, convection and radiation. This model, in the form of an analytic solution to the governing equation, is previously unpublished. Scaling arguments are used to prescribe maximum and minimum limits for the convective velocity. Short-wave radiation and light extinction coefficients are approximated from typical measured values at the Harding Lake study site.

THEORY

Short-wave radiation penetrating into a water column is attenuated with depth according to Bouger's relation (Fischer et al., 1979). It is known that the light extinction is dependent upon the wave length (Hutchinson, 1957); however, for studies involving small changes in depth, a bulk extinction formula is appropriate. The usual form of the governing equation for short-wave radiation in water is:

$$S(y) = S_w \exp(-\alpha y) \quad (1)$$

where S_w is the radiation at the top of the water column, y is depth and α is the extinction coefficient. Measurements were made of the short-wave radiation in Harding Lake during summer 1976 (La Perriere et al., 1978). The extinction coefficients for various wavelengths ranged between 0.4 and 1.0 m^{-1} . For the present study, a value of 0.8 m^{-1} was assumed for all calculations.

The short-wave radiation at the top of the water column, S_w , is the radiative flux at the bottom of the ice layer. S_w is proportional to the radiative flux arriving at the top of the ice. Bulatov (1974) determined that the radiation attenuation in ice is dependent upon the radiative wave length. Several investigators (Warren, 1982; Grenfell and Maykut, 1977) measured radiative extinction in fresh and sea-water ice, and established empirical relationships defining the extinction as a function of depth in these media. The study by Grenfell and Maykut (1977) suggested that the bulk short-wave radiation attenuation in ice is defined by the formula:

$$S_i(y) = S_o \exp(-1.36 y^{.5}) \quad (2)$$

where S_o is the short wave radiation at the top of the ice. This implies that, for ice thicknesses less than 0.5 m, more than 40% of the short wave radiation at the ice surface penetrates into the water column and is absorbed there as heat. Furthermore, the short-wave radiation at the top of the water column, $S_w \approx S_o \exp$

$(-1.36 d \cdot 5)$ where d is the ice thickness. The short wave radiation flux given by equation (1) may be considered a distributed heat source in the water (Mellor, 1964; Tien, 1960).

The equation for heat transport in the water, including both conduction of heat and the short-wave radiation acting as a distributed source, may be written as follows:

$$K \frac{d^2 T}{dy^2} + \alpha S_w \exp(-\alpha y) = 0 \quad (3)$$

where K is the thermal conductivity of the water. This equation assumes that a steady state condition exists and that no convective heat transport is considered. The solution to the equation is straightforward (Carslaw and Jaeger, 1971):

$$T(y) = T_0 + y (T_1 - T_0)/b + S_w [1 - \exp(-\alpha y) - y(1 - \exp(-\alpha b))/b] / \alpha K$$

where the boundary conditions $T(0) = T_0$ and $T(b) = T_1$ have been applied, $y = 0$ is the position of the water-ice interface, and $y = b$ is a given water depth. The model defines a modified linear temperature distribution, such that the curvature in the profile is proportional to the short-wave radiative heating.

Two limitations of the model are the assumptions of steady-state conditions and that of no vertical convection. Clearly, the position of the water-ice interface changes with time as the ice melts, but the temperature at this position remains at the freezing point. This suggests that a solution to equation (3) in a coordinate system which moves upward at the rate that the ice is melting would be more appropriate. If the ice melting rate is assumed to be constant and equal to v , then a transformation of coordinates for the transient form of equation (3) results in the following quasi-steady equation:

$$\rho c v \frac{dT}{dy} = K \frac{d^2 T}{dy^2} + \alpha S_w \exp(-\alpha y) \quad (5)$$

where the coordinate y is measured from the moving ice-water interface, ρ is the water density, and c is the specific heat. Note that $v \approx Q/L$ where Q is the residual heat available for melting ($W m^{-2}$), and L is the volumetric latent heat of ice ($J m^{-3}$). Q can be determined as the melt rate of the ice by a heat balance approach. However the meteorological data required for a complete surface heat balance was not available for the Harding Lake study site. Since heat conduction through an isothermal ice cover is zero, a reasonable approximation of Q is S_w , the short wave energy flux transmitted through the ice. For example, if $S_w \approx 15 W m^{-2}$, then $v = 5 \cdot 10^{-3} m sec^{-1}$ or $0.5 cm day^{-1}$. This is a very small melting rate which possibly represents early springtime warming in central Alaska.

Another interpretation of equation (5) may be inferred when v is assumed to represent a vertical convective velocity in the water. With this interpretation, there are three modes of heat transfer: conduction, convection and short-wave radiation. If v is a gravitational velocity due to density differences, solutions of equation (5) would represent the complete convective-diffusive model with a distributed heat source. Therefore, the same equation, equation (5), is a model for the quasi-steady case with a moving phase front (when $v = S_w/L$) and for the convective case (when $v > S_w/L$). The solution to equation (5) when v is constant is:

$$T(y) = T_0 + (T_1 - T_0) \left[\frac{1 - \exp(vy/k)}{1 - \exp(vb/k)} \right] + T_{sw} [1 - \exp(-\alpha y)] - T_{sw} \left[\frac{(1 - \exp(-\alpha b)) (1 - \exp(vy/k))}{1 - \exp(vb/k)} \right] \quad (6)$$

where $k = K/\rho c$

$$T_{sw} = S_w/\rho c (k\alpha + v)$$

Equation (6) then represents a quasi-steady solution to the equation for heat transport in the water when all three

mechanisms of heat transfer are included: conduction, convection due to density differences and short-wave heating. The lower limit for v is the melting rate of the ice.

An upper limit for v may be found from Monin-Oboukhov scaling for velocity due to gravitational differences (Tennekes and Lumley, 1972; Fischer et al., 1979):

$$u_f = \left(\frac{S_w \beta g b}{\rho c} \right)^{1/3} \quad (7)$$

where β is the thermal expansion coefficient of water and g is the gravitational acceleration. u_f is often called the penetrative convective velocity and is a measure of the free-fall velocity due to density changes at the water surface. Monin-Oboukhov scaling has been used widely in geophysical applications (Turner, 1973; Fischer et al., 1979; Niiler, 1975) to estimate the mixing or penetration velocity in mixed layer dynamics. It may be considered an upper limit for the convective velocity under the ice layer. It is an upper limit since it does not include the effects of the surface drag which would be present at the water-ice interface.

Penetrative convection may be expected if the density differences associated with temperature change are sufficiently large to overcome viscous forces. The critical parameter for the initiation of convection when a temperature gradient equal to $\Delta T/b$ is imposed is the Raleigh number (Raleigh, 1916; Bear, 1972; Turner, 1973):

$$Ra_t = \frac{\beta \Delta T g b^3}{\nu} \quad (8)$$

where ν is the kinematic viscosity. Two other forms of the Raleigh number are pertinent in the present analysis. The first is a salinity Raleigh number associated with the melt water - lake water salinity difference (Turner, 1973):

$$Ra_s = \frac{\Delta \rho g b^3}{\rho \nu} \quad (9)$$

where $\Delta \rho$ is the density difference due to salinity variation between the melted ice and the lake water. The other pertinent Raleigh number is associated with an internal heat source as the cause of the gravitational convection (Turcotte and Schubert, 1982):

$$Ra_i = \frac{\alpha S_w \beta g b^5}{K \nu} \quad (10)$$

Each of these three Raleigh numbers have somewhat different critical values depending upon the assumptions made concerning boundary conditions. However, in all cases the critical Raleigh number is less than 5000. Estimates of these Raleigh numbers appropriate for Harding Lake are; $Ra_t = 5 \cdot 10^7$, $Ra_s = 0.0$, and $Ra_i = 10^7$. These estimates were obtained by assuming a temperature difference of 2°C across a 0.5 m water depth, a thermal expansion coefficient equal to $0.3 \cdot 10^{-5} \text{ }^\circ\text{C}^{-1}$, an electrical conductivity difference of $60 \mu \text{ mhos cm}^{-1}$, short-wave radiation equal to 10 W m^{-2} , and an extinction coefficient of 0.8 m^{-1} . According to the formulae given by Bennett (1976), this electrical conductivity difference implies a negligible salinity difference. These values correspond approximately to the measured quantities determined at Harding Lake by La Perriere et al. (1978). The estimated Raleigh numbers suggest that penetrative convection due to thermal gradients and radiative heating was indeed occurring, but that measured salinity differences were inadequate to account for gravitational convection.

RESULTS AND DISCUSSION

Upper and lower limits for the velocity v in equation (5) and (6) have been previously defined. The lower limit is the ice melting rate and the upper limit is the Monin-Oboukhov (M-0) convective velocity. Both these limits are dependent upon the heat exchange term S_w . In Table 1, a few values of melting rate and M-0 velocity are presented as a function of S_w .

Table 1. Minimum and maximum velocities

S_w (Wm^{-2})	Melting rate ($m\ sec^{-1}$)	M-0 velocity ($m\ sec^{-1}$)
5	$2 \cdot 10^{-8}$	$2 \cdot 10^{-4}$
15	$5 \cdot 10^{-8}$	$3 \cdot 10^{-4}$
50	$16 \cdot 10^{-8}$	$5 \cdot 10^{-4}$

Equation (6), which defines the temperature distribution with convection, conduction and heat source, is depicted in Figure 1 for the two limiting values

of v , i.e., $v_{min} = 3 \cdot 10^{-8} m\ sec^{-1}$ and

$v_{max} = 2 \cdot 10^{-4} m\ sec^{-1}$. The measured temperature distribution at the Harding Lake study site is also shown on the figure. The calculated temperature distribution for the lower limit velocity, v_{min} , is effectively identical to the zero convection solution, equation (4). This might have been anticipated through a consideration of the Peclet number, $Pe_{min} = v_{min} b/k \approx 0.3$, since Pe can be considered the ratio of convection to diffusion of heat. The calculated temperature distribution for the upper limit velocity, v_{max} , indicates an intensely mixed surface layer in which latent heat losses at the water-ice interface are rapidly transported downward.

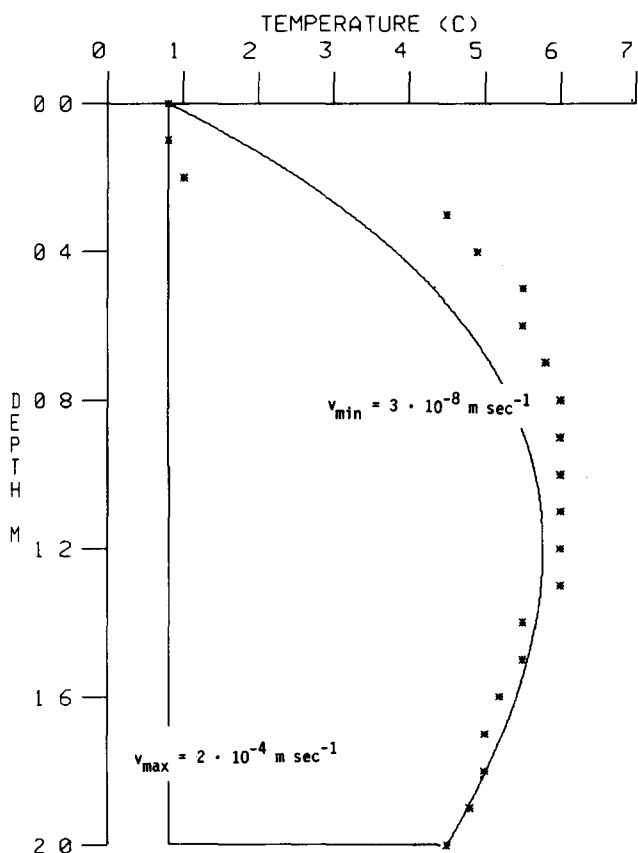


Figure 1. Measured (*) and calculated (-) temperature distributions under a candled ice cover in May, 1975. Depth is measured from the bottom of the ice, which was about 0.5 m thick. Both calculated temperature distributions are defined by equation (6). The assumed values for v ($v = v_{min}$ and $v = v_{max}$) are defined on the curves.

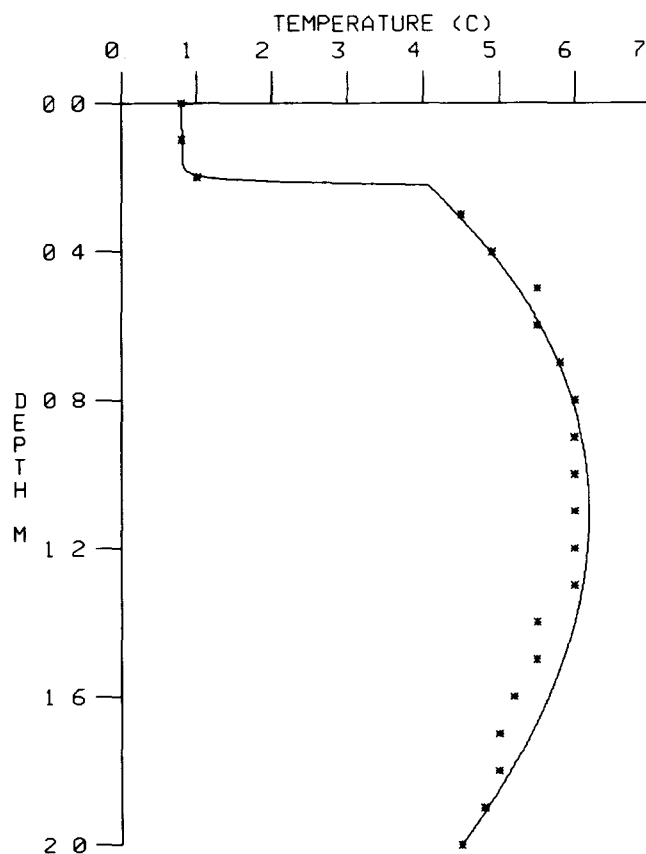


Figure 2. Measured (*) and calculated (-) temperature distributions under a candled ice cover in May, 1975. Depth is measured from the bottom of the ice, which was about 0.5 m thick. The calculated temperature distribution is defined by equation (6), with values of $v = 10^{-5} m\ sec^{-1}$ in the upper 0.2 m and $v = 10^{-7} m\ sec^{-1}$ in the lower 1.8 m.

The measured temperature distribution suggests that an intermediate value for convective velocity may more accurately define the heat transfer mechanisms. Furthermore, it appears that a larger velocity is indicated in the upper portion of the profile, and a somewhat smaller velocity below. In Figure 2, the calculated temperatures have been graphed with a convective velocity equal $10^{-5} \text{ m sec}^{-1}$ in the upper 0.2 m and equal to $10^{-7} \text{ m sec}^{-1}$ in the lower 1.8 m. These velocities for upper and lower layers are about 10% and 0.1% respectively of the associated Monin-Oboukhov velocity at a free surface. The agreement between the two layer convective model and the measured temperature distribution is excellent. The reasons for a greater convective velocity in the upper portion of the profile relative to the lower portion are not apparent. However, possible explanations may be related to deceleration due to viscosity or to the smaller heating in the lower portion associated with attenuated radiation penetration.

The upper 0.2 m may be interpreted to be a region in which the convection of cool water from the ice surface is sufficiently high to overcome the warming by short wave penetration. In effect, the time scale for removal of heat by convection is smaller than the time scale for heat generation by short wave penetration. This downward velocity is necessary to explain the positive curvature of the temperature profile in this region. Note that the application of equation (4), the zero velocity solution, to the upper layer would imply a negative curvature, contradicting the measured values of temperature.

In the lower layer, a smaller value of the convective velocity permits radiative heating and conduction to warm the water above the temperature of maximum density. The convection time scale in the lower region is smaller than the time scale for short wave heat generation.

Short-wave radiation penetration through a candled ice cover has the potential to raise the near ice water temperature above the temperature of maximum density. This occurred during a spring 1974 investigation of Harding Lake (La Perriere, 1981). The resultant density excess induced an instability with downward gravitational convective velocity. Density differences due to the measured salinity difference between lake water and melt water were negligible. However, the calculated Raleigh numbers for both conductive heat transfer and internal radiative heating were sufficiently high to ensure convective instability of the near-ice water. The appropriate convective velocity below the ice cover appears to be a small fraction of the Monin-Oboukhov velocity at a free surface. Apparently the ice-water interface acts to decrease the expected motion.

A new and previously unpublished solution of the heat transport equation with a heat source has been presented. Measured temperatures at Harding Lake under the ice cover show excellent agreement with the calculated temperatures, verifying the assumptions of weak convective instability under the ice cover and the penetration of radiative heating below the ice.

SYMBOL DEFINITIONS

b =	water depth [m]
c =	specific heat of water [$\text{J kg}^{-1} \text{ } ^\circ\text{C}^{-1}$]
d =	ice thickness [m]
g =	gravitational constant [m sec^{-2}]
k =	thermal diffusivity of water [$\text{m}^2 \text{ sec}^{-1}$]
K =	thermal conductivity of water [$\text{Wm}^{-1} \text{ } ^\circ\text{C}^{-1}$]
L =	volumetric latent heat of ice [J m^{-3}]
Q =	available heat for melting ice [W m^{-2}]

R_{ai} = Raleigh number for internal heat source, equ. 10 []
 R_{as} = Raleigh number for salinity, equ. 9 []
 R_{at} = Raleigh number for temperature gradient, equ. 8 []
 S = Short wave radiation in water, equ. 1 [$W m^{-2}$]
 S_i = Short wave radiation in ice, equ. 2 [$W m^{-2}$]
 S_o = Short wave radiation at ice upper surface [$W m^{-2}$]
 S_w = Short wave radiation at water surface or water-ice interface [$W m^{-2}$]
 T = water temperature [$^{\circ}C$]
 T_o = water temperature at $y = 0$ [$^{\circ}C$]
 T_l = water temperature at $y = b$ [$^{\circ}C$]
 u_f = Monin-Oboukhov velocity, equ. 7 [$m sec^{-1}$]
 v = velocity defined in text [$m sec^{-1}$]
 y = downward distance [m]
 α = short wave extinction coefficient in water [m^{-1}]
 β = thermal expansion coefficient of water [$^{\circ}C^{-1}$]
 ρ = average water density [$kg m^{-3}$]
 $\Delta\rho$ = density difference by salinity [$kg m^{-3}$]
 ν = kinematic viscosity of water [$m^2 sec^{-1}$]

Acknowledgements: Partial support for this work was provided by the Department of the Army under contract DAAG29-85-K-0260 and by State of Alaska funds through the Geophysical Institute, University of Alaska.

REFERENCES

- Ashton, G. D., 1985. Deterioration of Floating Ice Covers. *J. Energy Res. Tech.* 107:177-182.
- Bear, J., 1972. *Dynamics of Fluids in Porous Media*. American Elsevier Publ. Co., Inc., N.Y., 754 p.
- Bennett, A. S., 1976. Conversion of in-situ measurements of conductivity to salinity, *Deep Sea Res.* 23:157-165.
- Bulatov, S. N., 1970. Calculating the Strength of Thawing Ice Cover and the Beginning of Wind-Activated Ice Drifts (in Russian). *Trudy Vypysk* 74, *Gidrometeorologicheskoe Izdaniye*, Leningrad, p. 120.
- Carslaw, H. S. and J. C. Jaeger, 1971. *Conduction of heat in solids*, Oxford at the Clarendon Press, London.
- Fischer, H. B., E. J. List, R. Koh, J. Imberger and N. H. Brooks, 1979. *Mixing in Inland and Coastal Waters*. Academy Press, N.Y.
- Grenfell, T. C. and G. A. Maykut, 1977. The Optical Properties of Ice and Snow in the Arctic Basin. *J. Glac.* 18(80): 445-463.
- Hutchinson, G. E., 1957. *A Treatise on Limnology*. Vol. 1. Geography, Physics and Chemistry, Wiley, N.Y., 1015 p.
- Knight, C. A., 1962. Studies of Arctic Lake Ice. *J. Glac.* 4(3):319-355.
- La Perriere, J. D., 1981. Vernal Overturn and Stratification of a Deep Lake in the High Subarctic Under Ice. *In: Proceedings of the International Association for Theoretical and Applied Limnology, Congress in Japan, 1980*, pp. 288-292.
- La Perriere, J. D., T. Tilsworth and L. A. Casper, 1978. Nutrient Chemistry of a Large, Deep Lake in Subarctic Alaska. *Ecological Research Series Report EPA-600/3-78-088*. Environmental Protection Agency, Environmental Research Laboratory, Corvallis, OR 97330.
- Lyons, J. B. and R. E. Stoiber, 1959. The Absorptivity of Ice: A Critical Review: Scientific Report No. 3, Dartmouth College, Hanover, N.H., October 31, 1959; also, Air Force Cambridge Research Center Technical Note 59-656.

- Mellor, M., 1964. Properties of Snow. USA CRREL Report II-A1, Hanover, N.H.
- Niiler, P. P., 1975. Deepening of the Wind-Mixed Layer. J. Marine Res. 33(3):405-422.
- Raleigh, L., 1916. On Convection Currents in a Horizontal Layer of Fluid When the Higher Temperature is on the Under Side. Phil. Mag. 6(32):529-546.
- Tennekes, H. and J. L. Lumley, 1972. A First Course in Turbulence. The MIT Press, Cambridge, Mass.
- Tien, C., 1960. Temperature Distribution of Snow with Gamma Ray Radiation, USA CRREL Research Report 67, Hanover, NH.
- Turcotte, D. L. and G. Schubert, 1982. Geodynamics. John Wiley and Sons, N.Y.
- Turner, J. S., 1973. Buoyancy Effects in Fluids. Cambridge at the University Press, Cambridge, England.
- Warren, S. G., 1982. Optical Properties of Snow. Rev. of Geophys. and Space Phys. Vol. 20(1):67-89.

HYDROTHERMAL MODELING OF RESERVOIRS IN COLD REGIONS: STATUS AND RESEARCH NEEDS

Donald R. F. Harleman¹

ABSTRACT: A review of mathematical models for the prediction of the thermal structure and water quality of reservoirs in cold climates is presented. Recent research and research needs are discussed in the following subject areas: dynamics and thermodynamics of ice cover formation and decay, wind stress with weak stratification and wind stress attenuation due to ice formation, suspended sediment effects and local mixing and water quality effects.

(KEY TERMS: reservoir thermal stratification; reservoir water quality; cold region impoundments, ice cover formation; ice cover decay; heat transfer in ice.)

INTRODUCTION

The development of the cold regions of the earth for human habitation and for energy resources is proceeding at a rapid pace. Thus the potential for reservoir construction for hydroelectric development and water supply in high latitudes is greater than in the more developed temperate and tropical zones. There exists, therefore, a need for deterministic models to predict the physical, thermal and associated water quality aspects of impoundments in cold regions. The obvious starting point is the considerable body of knowledge that

has been accumulated over the past 30 years in the mathematical modeling of lakes and reservoirs located in mid-latitudes. The objective of this paper is to focus on the features of the modeling problem that are characteristic of, and in many cases, unique to cold climates. The first section will review a number of impoundment models that have been used in temperate zones with an emphasis on attempts that have been made to adapt them to cold region conditions. Subsequent sections will discuss some of the unique modeling problems such as the dynamics and thermodynamics of ice cover formation and decay; wind stress on weakly stratified lakes and attenuation due to ice growth; effects of suspended sediment inflows due to glacier melt; and localized mixing and overall water quality effects. In each case a brief literature review will be followed by a discussion of future research needs.

REVIEW OF ONE-DIMENSIONAL
RESERVOIR MODELS

Diffusion Models

Thorough documentation of the early history of hydrothermal modeling of impoundments has been given by Harleman (1982) and Orlob (1983). The first attempts at mathematically modeling

¹Ford Professor of Engineering, R. M. Parsons Laboratory, Department of Civil Engineering, Massachusetts Institute of Technology, Cambridge, Massachusetts 02139.

temperature distributions in deep, stratified impoundments were carried out in the late 1960's and early 1970's independently by Orlob and co-workers at Water Resources Engineers (WRE) and by Harleman and co-workers at MIT. The Orlob (1983) review documents one, two and three-dimensional modeling efforts and gives criteria for use of the one-dimensional approach in which the water body is assumed to be stratified in horizontal planes. In this paper attention will be restricted to one-dimensional models.

The classical advection-diffusion equation approach is illustrated by Figure 1 showing a one-dimensional schematization for a variable area reservoir with an inflow and one or more outflows.

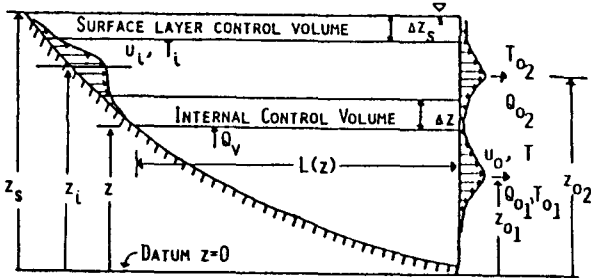
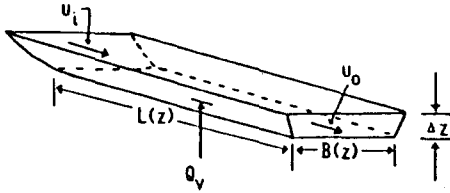


FIG. 1 - Schematization and control volume for mathematical model for reservoir temperature distribution.

The thermal energy equation for an internal element is given by Huber, Harleman and Ryan (1972) as

$$\begin{aligned} \frac{\partial T}{\partial t} + \frac{1}{A} \frac{\partial}{\partial z} (Q_v T) &= \frac{1}{A} \frac{\partial}{\partial z} \left(A E_z \frac{\partial T}{\partial z} \right) \\ &+ \frac{B(u_i T_i - u_o T)}{A} \\ &+ \frac{\phi_s (1-\beta)}{\rho c A} \frac{\partial}{\partial z} [A e^{-\eta(z_s - z)}] \end{aligned} \quad (1)$$

where T is temperature within the reservoir (T_i is inflow temperature), z is measured from a bottom datum (the surface elevation z_s is a variable), A is the horizontal area of the reservoir, E_z is the eddy diffusivity of heat and B is the width. Horizontal velocities due to inflow u_i and outflow u_o are computed by assuming Gaussian velocity profiles. The height of the Gaussian outflow profile is related to the vertical density gradient by selective withdrawal theory. The river inflow is mixed with water from the surface element in a specified ratio, changing both the volume and temperature of the inflow. The mixed inflow enters the water column centered at the elevation at which the reservoir density is equal to the mixed inflow density. Vertical velocities are computed from the continuity equation for each element, thus the vertical flow rate Q_v is given by

$$\begin{aligned} Q_v(z, t) &= B \int_0^z u_i(z, t) dz \\ &- B \int_0^z u_o(z, t) dz \end{aligned} \quad (2)$$

The last term in equation (1) represents the internal heat source due to the absorption of shortwave solar radiation. The terms ρ and c are the density and heat capacity of water, ϕ_s is the heat flux per unit area due to short wave radiation reaching the water surface, β is the fraction of that radiation absorbed in the surface (approximately 0.5) and $\eta(m^{-1})$ is the extinction coefficient which depends on water clarity.

The surface boundary condition, assuming that the water surface remains free of ice is given by

$$\begin{aligned} \rho c E_z \frac{\partial T}{\partial z} &= -\beta \phi_s - \phi_a + \phi_b \\ &+ \phi_e + \phi_c \text{ at } z = z_s \end{aligned} \quad (3)$$

where ϕ_a is the incoming atmospheric, or long wave, radiation which is completely absorbed at the surface; ϕ_b is the flux due to back radiation from the water surface; ϕ_e and ϕ_c are heat fluxes from the water surface due to evaporation

and convection. The latter three components are functions of the water surface temperature, wind speed and vapor pressure gradient. The bottom boundary condition, usually assumed to represent zero heat flux ($\partial T/\partial z=0$), and a specified vertical temperature distribution initial condition completes the mathematical specification.

Various empirical representations have been used for the vertical eddy diffusivity E_z . These range from assuming it to be a constant in both time and depth to assuming a functional relationship between E_z and the densimetric water column stability ($1/\rho \partial \rho/\partial z$). Harleman (1982) pointed out that in reservoirs having near surface inflows and relatively deep outlets the vertical heat convection term (the term to the left of the equal sign in equation 1) dominates the vertical diffusion term. The result is that the vertical temperature profiles are relatively insensitive to the vertical diffusivity. This is in contrast to lakes in which there is generally a high degree of sensitivity. Empirical evidence suggests that turbulent mixing induced by wind shear at the surface is highest in the near surface or epilimnion region. In addition, the epilimnion is frequently found to be well-mixed with little or no vertical temperature gradient at the surface. These observations, coupled with the lack of a generally satisfactory resolution of the problem of specifying $E_z=f(z,t)$, led to the development of mixed layer models in the latter half of the 1970's.

Mixed Layer Models

The surface mixed layer may be thought of as encompassing three zones: (1) the near surface region in which turbulent kinetic energy (TKE) is produced by wind shear as the stirring agent. The TKE is exported to the fluid below; (2) a central zone in which the TKE exported from above is used to homogenize the fluid; and (3) a thin frontal zone separating the turbulent interior from the quiescent fluid beneath the upper mixed layer. In this zone the remainder of the TKE exported from the surface, plus any that may be locally produced by the shear of the advecting mixed layer, less that

which is locally dissipated or radiated downward by internal waves, is used to entrain quiescent fluid into the mixed layer. Density instabilities, resulting from surface cooling, can also cause mixing through the production of turbulence associated with vertical buoyancy fluxes. This is known as penetrative convection mixing. The entrainment velocity u_e , defined as the time rate of increase of thickness, h , of the upper mixed layer, is $u_e = dh/dt$ and the problem is reduced to finding an expression for u_e .

Stefan and Ford (1975) at University of Minnesota developed a mixed layer model (MLTM) for application to small lakes. Independently, Harleman and Hurley-Octavio (1977), Bloss and Harleman (1979, 1980) and Imberger, et al., (1978) developed similar models at MIT (MITEMP) and University of California, Berkeley (DYRESM). All of these models consider the turbulent kinetic energy budget integrated over the thickness of the mixed layer. Parameterizations of the various processes leading to the production and decay of TKE result in expressions for the entrainment velocity u_e that are functions of the local and bulk Richardson numbers.

One of the differences between DYRESM and the previous mixed layer models was the change from a fixed or Eulerian layer system to a variable or Lagrangian grid in which each layer can expand or contract to balance the movement of water in and out of that layer. The advantages of the Lagrangian approach are twofold: (1) conservation of mass is improved because the need for addition or deletion of layers at the reservoir surface is removed, (2) numerical dispersion is reduced because no vertical flows between layers are required.

The mixed layer models have worked quite well for lakes and reservoirs in temperate climates. Admittedly there are a fair number of "constants" in the TKE budgets employed in the various models and these have yet to be assigned "universal" values. The following section will discuss attempts to modify existing models for cold region applications.

Modification of Existing Models for Cold Regions

In the mid 1970's the Orlob-WRE model was modified to include a freeze-thaw cycle for applications to two impoundments near the US-Canada border (Chen and Orlob, 1973) (Norton and King, 1975). An additional term for the heat exchange accompanying the change of state of water from liquid to solid was added to the heat budget equation (1). When freezing temperatures are reached, further loss of heat proportional to the latent heat of fusion, results in ice formation. Other surface heat transfer processes (e.g., evaporation) were modified to account for the ice sheet.

Findikakis, Locher and Ryan (1980) modified the MIT mixed layer model to include ice cover formation and melting. They noted that if wind mixing in the surface layer is underestimated, the simulated water surface temperature decreases at a faster rate than the observed, resulting in an early formation of ice in the reservoir. Their model and field data comparisons were made for Spada Lake, a reservoir on the Sultan river in Washington.

Additional modifications to existing models include a proposal by Ashton at CRREL (Ashton, 1982) to include an ice and snow cover in CE-QUAL-R1, the water temperature and quality model currently being used by the Waterways Experiment Station (Environmental Laboratory, 1981). The hydrothermal component of this model is a modified version of the Orlob-WRE model. The modifications to the original WQRRS model to form CE-QUAL-R1 include the change to a Lagrangian grid and the replacement of the eddy diffusivity approach by a mixed layer algorithm. (Ford, et al. 1980). Ashton's cold region modifications included the following "threshold conditions" to be met before an intact ice cover is established:

- volume averaged water temperature $< 2^{\circ}\text{C}$
- average wind speed $< 5 \text{ m/s}$
- average daily air temperature $< -5^{\circ}\text{C}$

Ashton states that the choice of water temperature less than 2°C requires that the water mass be cooled below the 4°C stability point due to surface cooling.

This criterion therefore implicitly considers the effect of wind mixing in retarding the initial formation of the ice cover. The requirement that the wind velocity be less than 5 m/s is based on his experience that strong winds prevent ice formation. The threshold air temperature of less than -5°C is a subjective one that allows the ice sheet to attain a thickness sufficient to resist break up. As soon as an intact ice cover is formed the wind stress is set equal to zero.

There has been an extension of DYRESM to include an ice cover by Patterson and Hamblin (1983). They allow the ice cover to gradually decouple the wind stress from the surface layer dynamics. A further modification to DYRESM to include suspended sediment as well as ice has been described by Wei and Hamblin (1986). Independently, Gosink (1986) formulated a snow and ice cover algorithm for DYRESM. These will be discussed in the following sections.

DYNAMICS AND THERMODYNAMICS OF ICE COVER FORMATION AND DECAY

Ragotzkie (1978) and Ashton (1980) have summarized the essential features of the heat budget of lakes including lakes with ice and snow covers. In the latter case the relevant heat flows are shown in Figure 2.

Once an ice cover has developed the thermal response of a lake or reservoir to climate undergoes a drastic change. Evaporation, a major component of the heat budget in an unfrozen lake, ceases and radiation becomes the primary mechanism of heat exchange. When snow is added to the ice cover the heat budget becomes much more complex. Sensible heat is stored in water, ice and snow and latent heat is stored in the ice and snow. Defining heat content per unit area on a base of 0°C , the "negative" sensible heat in ice is given by the product of its temperature below 0°C , its thickness, density (0.92 g/cm^3) and specific heat ($0.5 \text{ cal/}^{\circ}\text{C-g}$). Latent heat is equal to the mass of ice or snow per unit area times the latent heat of fusion for water (80 cal/g). Heat loss by outgoing longwave radiation from the

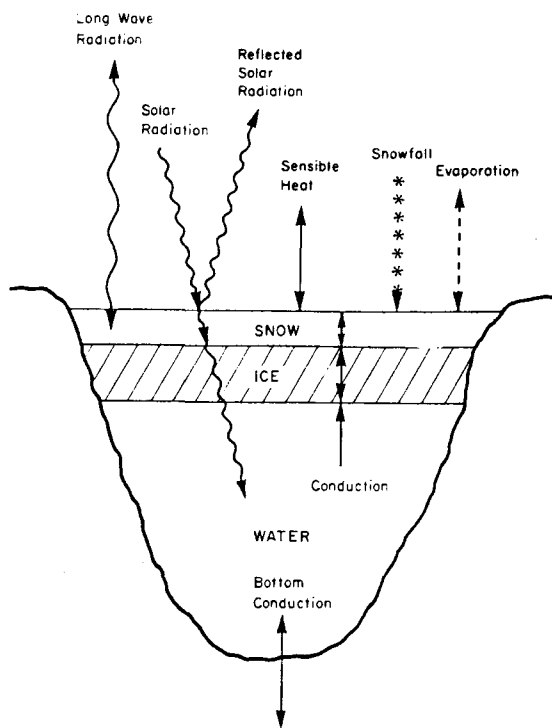


FIG. 2 - Heat Flows in a frozen lake

ice or snow surface results in the growth of the ice layer. Some heat enters the water by short wave solar radiation which is able to penetrate an ice cover. However, if the snow is present on top of the ice the change in the albedo effectively eliminates short wave penetration. One portion of this entering heat is stored in the water while another portion is lost by conduction back through the ice layer. Sensible and latent heat exchanges occur between the atmosphere and the snow or ice surface and snow accumulation represents a negative latent heat input that will have to be balanced by heat addition before the lake loses its ice cover in the spring. Adams and Lasenby (1978) also discuss the calculation of latent heat terms for ice and snow energy budgets.

Some of the earliest observations of the ability of short wave radiation to penetrate an ice cover were made in permanently ice covered Antarctic lakes by Shirtcliffe and Benseman (1964). Their measurements in Lake Bonney with a snow-free ice cover of approximately 3.5 m thickness, shown in Figure 3, indicate a maximum temperature of 7.5°C at a depth of 13 m. The density profile is stable

because the salt content of the lake increases with depth such that the density in contact with the ice is 1.0 g/ml, whereas at the lake bottom (30 m) the density is 1.2 g/ml. The absorption length for solar radiation (reciprocal of the extinction coefficient η in eq. 1) is 8.2 meters. The lake is therefore a natural "solar pond".

Stewart (1972) measured isotherms under ice covers in a number of small non-saline frozen lakes in New York and Wisconsin. These lakes show the typical temperature gradient from 0°C at the bottom of the ice cover to 4°C at the lake bottom. Stewart (1973) also measured isotherms under Lake Erie ice and found that in contrast to findings from smaller ice-covered lakes, Lake Erie has almost no winter vertical stratification. For example, in early March most of the lake water was less than 0.1°C. Stewart attributed this to the fact that even though the lake is covered extensively with ice there are irregular openings and cracks; and heat exchange and wind mixing are effective in preventing a stable winter stratification.

Wake and Rumer (1979 a) developed a mathematical model for the ice regime of Lake Erie that assumed a vertically mixed water column during the ice season (in accordance with Stewart's observations). They neglected super-cooling effects, snow accumulation on the ice cover and assumed temperature gradients in the ice cover and at the ice-water interface, when they exist, to be linear. They further assumed the ice cover to be static at all times and well drained during the ice dissipation period. The neglect of the effect of accumulated water on the dissipation rate was justified in an earlier study (Wake and Rumer, 1979 b). The model was two-dimensional in the plane of the lake surface and the outputs of the numerical model are water temperature and ice thickness during a 20 day ice growth period from January 1 and a 25 day period in the spring ice dissipation season. Wake and Rumer (1983) extended the model to account for ice transport and deformation due to wind and water stresses. They adopted a macroscopic continuum hypothesis for the fragmented ice field and coupled the thermodynamic model of the previous study with an ice

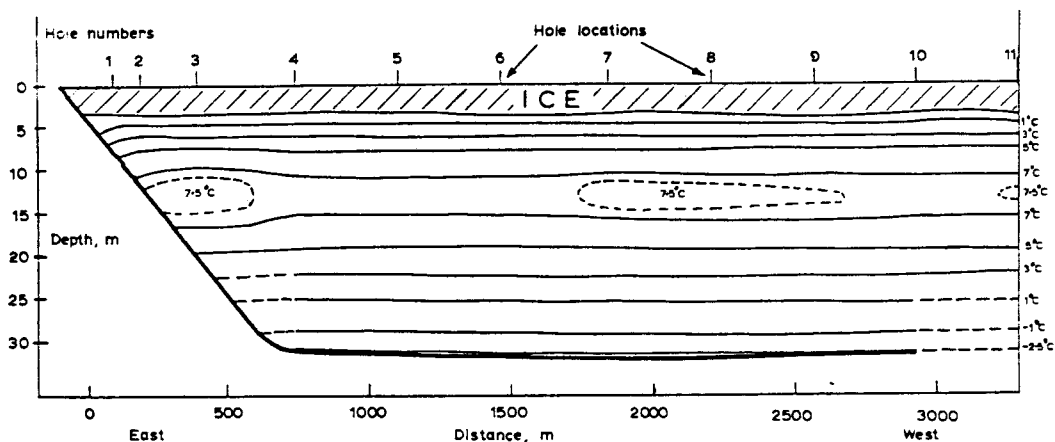


FIG. 3 - Vertical section of Lake Bonney showing isothermal profiles.

transport model. The hydrodynamic component produces two-dimensional ice drift velocity fields under time varying wind inputs. Additional outputs are areal ice concentration fields and areal internal ice pressure distributions. In a later paper Chieh, Wake and Rumer (1983) presented the calibration of the model using observed data from specific Lake Erie ice transport events during the winter of 1979. The simulation for the freezing period agrees quite well. During the melting period the simulation agrees well with the data when wind-driven surface currents and ice melt at the ice-water interface are included.

Very few model-prototype comparisons specifically directed at high latitude reservoirs with extensive periods of ice cover have been presented in the literature. Exceptions are the recent studies by Gosink (1986) and Wei and Hamblin (1986) using a data set for Eklutna Reservoir in south central Alaska. The measured temperature profiles were obtained by R & M consultants (1982) for the open water season and by Osterkamp and Gosink (1982) (unpublished field data) for the ice-covered season. Gosink (1986) developed a numerical model (DYRSMICE), a modification of DYRESM, in which the main modification is the incorporation of ice growth and dissipation. This requires a solution of the heat transport equations in the snow and ice layers as schematized in Figure 2. A quasi-steady assumption is used for the surface heat flux and the snow and ice temperatures. The heat

transfers are assumed to be in equilibrium recognizing that meteorological observations may be available on at most a daily basis at remote locations. For example, the governing heat transfer equation for temperature in the snow layer is

$$k_s \partial^2 T / \partial z^2 + \eta_s \phi_s \exp(-\eta_s z) = 0 \quad (4)$$

where k_s is the conductivity of snow, η_s is the short wave extinction coefficient in snow, z is the vertical coordinate, positive downward from the snow surface, and ϕ_s is the short wave radiation. The surface and bottom boundary conditions are $T(z=0) = T_s$ and $T(z=h_s) = T_i$ where h_s is the snow depth and T_i is the temperature at the snow-ice interface. Because of the steady state assumption an analytical solution to equation (4) can be obtained. Since T_s and T_i are not known a priori, they must be determined by simultaneous consideration of the surface heat fluxes and the temperature distribution in the ice layer. The latter requires solution of a heat transport equation similar to equation (4) for the lower ice layer.

Wei and Hamblin (1986) modified DYRESM to include a snow and ice cover in a similar manner. Their model includes turbulent transport of heat from water to ice due to the under-ice flow field generated by inflows and outflows and the formation of frazil ice. They compared, predicted and measured ice cover thickness as well as reservoir isotherms.

This section, on dynamics and thermodynamics of ice cover formation and decay, will conclude with a brief assessment of some future research needs in this area.

Prior to the formation of an ice cover, evaporation is one of the dominant terms in the heat budget. Fog may form in the surface layer above a lake or reservoir when the air becomes saturated due to the temperature having fallen to the dew point. Thus fog may occur with a higher frequency in cold climates with resulting condensation or negative evaporation. Research is needed on techniques for factoring in the occurrence of fog on surface heat exchange. Some research in this area has been done in connection with predicting the formation of fog induced by cooling ponds (Tsai, 1980).

Reservoirs used for pumped storage power production experience large daily fluctuations in water level. Very little is known about the effect of large water elevation changes on ice formation and decay. Karnovich et al. (1983) presented some operating experience on ice effects on pumped storage reservoirs in the USSR. There is a need for additional field data and analysis on this problem.

The prediction of the decay and deterioration of ice covers during spring melt appears to be a somewhat more difficult problem than the formation and growth of ice. Ashton (1983, 1985) has analyzed the deterioration process by applying an energy budget to determine when and where the ice temperature is below freezing and where it is at freezing but sufficient energy has been absorbed to melt a portion of the ice. The resulting ice porosity is related to failure stress and this may be used to predict the load-carrying ability of the ice sheet. Snow cover generally prevents solar radiation from penetrating to the ice cover; however, when the snow cover is gone conditions are set for deterioration to begin. It is unfortunate that data does not exist for the testing of these hypotheses.

In most aspects the application of mixed layer models, that have been developed and tested on temperate climate lakes and reservoirs, to cold region water bodies is straightforward. Two exceptions are (1) the effect of surface wind stress induced mixing under open water conditions with relatively weak stratification and (2) the attenuation of surface wind stress induced mixing due to the formation and growth of an ice cover.

Mixing with Weak Stratification

Lakes and reservoirs in temperate climates tend to stratify rapidly and strongly during the spring warming period. In summer, surface to bottom temperature differences of the order of 20°C are common. The resulting strong stratification effectively isolates the hypolimnion in regard to mixing. In fact, if a late spring temperature profile is used as an initial condition, it is usually found that heat transfer in the hypolimnion throughout the summer is adequately represented by molecular diffusivity. However, it has also been observed, during the short period of weak stratification following the spring overturn, that episodic mixing events are necessary to explain the slight warming of the hypolimnion. Because the period of weak stratification is a matter of a few weeks, data is scant and the question of hypolimnetic mixing has not received the attention it deserves. By an interesting coincidence, related to the non-linear temperature-density relationship for water, stability conditions in tropical water bodies are quite similar to those of cold regions. For example, a tropical lake having a maximum surface-bottom temperature range from 28° to 26°C has the same density stability as a northern lake

with a temperature range from 13° to 4°C. Harleman, Adams, Aldama and Bowen (1986) used Lewis' (1983) data from Lake Valencia, Venezuela (which has seasonal temperatures in the 28°-26°C range) for determining an improved hypolimnetic diffusion component for the MIT mixed layer model. The expression for E_z in equation (1) is

$$E_z = \frac{C_\alpha \rho_o u_*^3 A_s h^2}{P_s} \quad (5)$$

where C_α is a dimensionless (non-universal) parameter that probably depends on water body area and shape; u_* is the friction velocity, $u_* = (\tau_s/\rho)^{1/2}$, where τ_s is the water surface wind shear stress; A_s is the surface area; h , the total lake depth and P_s the potential energy of the stratification, defined by

$$P_s = \int_0^h [\bar{\rho} - \rho(z)] g A_s dz \quad (6)$$

where $\bar{\rho}$ is the volumetric mean density of the water body.

This parameterization of the hypolimnetic diffusivity which is capable of capturing episodic wind mixing events is similar to that proposed by Imberger and Patterson (1981) except that it was found to be unnecessary to include their local stratification effect. It is necessary to use an upper bound for E_z during isothermal conditions when P_s approaches zero. The value of $E_z = 1.10^{-4} \text{ m}^2/\text{s}$ (about 700 times the molecular diffusivity of heat) recommended by Imberger and Patterson (1981) was used. It is suggested that the diffusivity relation represented by equations (5) and (6) could be used for open water conditions in cold climates.

Farmer (1980) discusses some special features of mixed layer dynamics near the temperature of maximum density. In particular, he points out that as the temperature cools through 4°C, the surface buoyancy flux changes sign and the wind works to drive the heat deeper. Gosink (1986) in her discussion of modifications to DYRESM refers to the parameterization

of the surface stress term in the TKE budget and indicates that in high latitudes it may be necessary to introduce a Coriolis "cut-off" time scale to limit mixed layer deepening.

Wind Stress Attenuation Due to Ice Formation

Ashton's (1982) modification to CE-QUAL-R1 to induce ice formation based on "threshold conditions" has already been mentioned. Based on experience on Eklutna Reservoir, Gosink's (1986) modification to DYRESM differs in that she elects to modify the wind stress by applying a damping coefficient that decreases linearly from 1 to 0 as the calculated ice thickness increases from 0 to 10 cm. This allows for partial ice cover development in the early stages of formation. It would be interesting to see how well the modified model predicted the formation and growth of the Eklutna ice cover.

SUSPENDED SEDIMENT EFFECTS

Gosink (1986) noticed difficulties in calculating the heat balance in Eklutna Reservoir in the late summer which she attributed to an order of magnitude change in the short wave extinction coefficient caused by the inflow of high turbidity glacier melt water. Incorporation of this effect into a predictive impoundment model requires inclusion of a mass conservation equation for suspended sediment and modification of the equation of state to incorporate sediment as well as temperature effects on density.

Findikakis, Locher and Ryan (1980) added a suspended sediment mass balance equation in their modification of the MITEMP model for Spada Reservoir. They expressed particle concentration in turbidity units by assuming a linear relationship. The sediment inflows in this reservoir consisted of very fine clay material and they assumed that settling was negligible. In this aspect the situation may be similar so that encountered with "glacial flour" inflows. Dhamotharan and Stefan (1980) modified MLTM to include the simulation of

reservoir turbidity. The resulting model, designated RESQUAL, has been applied to Lake Chocot, Arkansas. The Corps of Engineers CE-QUAL-R1 model, previously discussed also contains suspended sediment as a state variable.

Wei and Hamblin (1986) extended DYRESM to include the concentration of suspended sediment. Density inversions resulting from suspended sediments are checked and mixed to establish stability. Settling velocities appropriate to the size range of the inflowing sediments are input to the model.

Additional research is needed into the settling characteristics of fine sediments characteristic of glacier fed reservoirs. Flocculation and coagulation effects must be recognized since much of the material of interest is outside of the discrete particle settling range.

LOCAL MIXING AND WATER QUALITY EFFECTS

The interaction between seasonal ice cover and hypolimnetic dissolved oxygen depletion in lakes and reservoirs is beginning to receive attention. Thomas and Orn (1982) report on DO conditions in the Greifensee, a Swiss Alpine lake. Disastrously low oxygen conditions result if low mixing during autumn cooling is followed by an early ice cover of long duration, succeeded by rapid stratification after the ice melt. Babin and Prepas (1985) report on efforts to model winter oxygen depletion rates in ice covered lakes in Canada.

Jain (1980) analyzed the plunging phenomena at the entrance to reservoirs using gradually varied two-layer flow theory. A limitation of this type of analysis is that it does not account for the three-dimensional lateral spreading characteristic of actual reservoirs. Fischer and Jensen (1983) made observations of reservoir inflow mixing in Lake Mead. A tributary inflow was dyed continuously for nine days and permitted computation of the entrainment into the inflow at the plunge point. They found that the entrainment flow was about equal to the inflow. However, a clear correlation between inflow slope, densimetric Froude number and other factors remains to be established.

Coleman and Armstrong (1983) measured horizontal diffusivities in a small, ice-covered lake by injecting a tracer as a point source under the ice cover. A number of studies have been carried out to investigate the effects of heated effluents or waste discharges into ice-covered water bodies. Ashton (1979) prepared a comprehensive report on the suppression of ice by thermal effluents. In the first part he considers the effluent to be fully mixed across the flow section while in the second part he assumed a side discharge. A similar study of mixing in the near bank zone is reported by Gerard, Putz and Smith (1985). Significant differences were found between open water and ice-covered conditions. Belore and McBean (1983) carried out laboratory experiments on entrainment of heated discharges at the ice-water interface. In contrast to open water conditions the dilution was found to have relatively little dependence on the discharge densimetric Froude number.

Wells and Gordon (1980) discussed the need for multi-dimensional reservoir models for water quality management using field data from two TVA reservoirs. They concluded that there was no justification for 3-D models, that under certain circumstances 2-D (longitudinal and vertical) models might be needed but that for the most part 1-D models were adequate.

CONCLUSIONS

A number of one-dimensional reservoir models have been modified to include cold region effects. In most instances the applications have been limited to temperate region lakes and reservoirs in which ice cover is a secondary effect of relatively short duration. It is clear that much additional research is needed for the prediction of temperature and water quality effects in high latitude regions in which ice cover is the dominant effect. In this respect the most pressing need is for field data. Theoretical advances necessary to improve mathematical modeling will continue to be limited by the sparcity of cold region lake and reservoir data.

A significant data collection resource that does not appear to have been adequately utilized is that of satellite observations. Stewart (1985) discusses a number of remote-sensing techniques that are directly applicable to ice observations. These have been widely used in oceanographic studies of the polar ice regions. The techniques include Landsat visible light scanners (VISSR) and radio-frequency radiation signals. The latter provide open water surface temperatures to an accuracy of 1°C, areal ice-open water concentrations and distinction between first year and multi-year ice. Synthetic-aperture radars accurately map reflectivity changes over areas 50 to 100 km on a side with resolution of 10-40 m

Simultaneous modeling and data collection efforts are vitally needed. It is unfortunate that research in lake and reservoir management has not had access to the data collection resources that have routinely been associated with oceanographic research in polar regions.

References

- Adams, W.P. and D.C. Lasenby, "The role of ice and snow in lake heat budgets," *Limnol. Oceanogr.* 23(5), 1978.
- Ashton, G.D., "Suppression of river ice by thermal effluents," CRREL Report 79-30, U.S. Army Corps of Engrs, Cold Regions Research and Eng. Lab., 1979.
- Ashton, G.D., "Freshwater, ice growth, motion and decay," Ch. 5, Dynamics of Snow and Ice Masses. Academic Press, 1980.
- Ashton, G.D., Details of an ice cover algorithm for the CE-QUAL-R1 reservoir water quality model, unpublished note, 1982.
- Ashton, G.D., "Lake ice decay," *Cold Regions Sci. and Tech.*, 8, 1983.
- Ashton, G.D., "Deterioration of floating ice covers," *Trans. ASME, Jour. of Energy Res.Tech.*, Vol. 107, June 1985.
- Babin, J. and E.E. Prepas, "Modeling winter oxygen depletion rates in ice-covered temperate zone lakes in Canada," *Canadian Jour. of Fish. and Aq. Sci.*, Vol. 42, No. 2, Feb. 1985.
- Belore, R.C. and E.A. McBean, "Physical modelling of dilution entrainment of heated discharges under ice," 20th IAHR Congress, Moscow, Vol. II, 1983.
- Bloss, S. and D.R.F. Harleman, "Effect of wind-mixing on the thermocline formation in lakes and reservoirs," Tech. Rep. No. 249, R.M. Parsons Lab., MIT, Nov. 1979.
- Bloss, S. and D.R.F. Harleman, "Effect of wind-induced mixing on the seasonal thermocline in lakes and reservoirs," 2nd Intern. Symp. on Stratified Flows, Trondheim, Norway, 1980.
- Chen, C.W. and G.T. Orlob, "Ecologic study of Lake Koochanusa," Rep. to US Army Corps of Engineers, Dist. of Seattle by Water Res. Eng., Inc., 1973.
- Chieh, S.H., A. Wake, and R. Rumer, "Ice forecasting model for Lake Erie," *Proc. ASCE, Vol. 109, Jour. of Waterway, Port, Coastal and Ocean Eng.*, No. 4, Nov. 1983.
- Coleman, J.A. and D.E. Armstrong, "Horizontal diffusivity in a small, ice-covered lake," *Limnol. Oceanogr.* 28(5), 1983.
- Dhamotharan, S. and H. Stefan, "Mathematical model for temperature and turbidity stratification dynamics in shallow reservoirs, ASCE Symp. on Surface Water Impound., Vol. I, Univ. of Minn., 1980.
- Environmental Laboratory, CE-QUAL-R1: "A numerical one-dimensional model of reservoir water quality; User's Manual," Tech. Rep. E-18-8, U.S. Army Engineer Waterways Exp. Station, Vicksburg, Miss., 1981.
- Farmer, D.M., "Mixed layer dynamics in a lake near the temperature of maximum density," 2nd Int. Symp. on Stratified Flows, Trondheim Norway, 1980.
- Findikakis, A.N., F.A. Locher and P.J. Ryan, ASCE, Symp. on Surface Water Impound., Vol. I, Univ. of Minn., 1980.
- Fischer, H.B. and A.R. Jensen, "Observations of reservoir inflow mixing," 20th IAHR Congress, Vol. IV Moscow, 1983.
- Ford, D.E. K.W. Thornton, A.S. Lessem, and J.L. Norton, ASCE, Symp. on Surface Water Impound., Vol. I, Univ. of Minn., 1980.

- Gerard, R., G. Putz and D.W. Smith, "Mixing in the near-bank zone of a large northern river," 21st IAHR Congress, Melbourne, Australia, 1985.
- Gosink, J.P., "Northern lake and reservoir modeling," submitted to Cold Regions Science and Technology, 1986.
- Harleman, D.R.F. and K.A. Hurley-Octavio, "Heat Transport Mechanisms in Lakes and Reservoirs," 17th IAHR Congress, Baden Baden, August 1977.
- Harleman, D.R.F., "Hydrothermal analysis of lakes and reservoirs," ASCE Proc. Vol. 108, No. HY3, 1982.
- Harleman, D.R.F., E.E. Adams, A. Aldama and J. Bowen, "Hypolimnetic mixing in a weakly stratified lake," R.M. Parsons Laboratory, MIT, (in preparation), 1986.
- Huber, W.C., D.R.F. Harleman and P.J. Ryan, "Temperature prediction in stratified reservoirs," Proc. ASCE, Vol. 98, No. HY4, 1972.
- Imberger, J., J. Patterson, B. Hebbert, and I. Loh, "Dynamics of Reservoir of Medium Size," Vol. 104, No. HY5, Proc. ASCE, 1978.
- Imberger, J. and J.C. Patterson, "A dynamic reservoir simulation model - DYRESM:5." Transport Models for Inland and Coastal Waters, H.B. Fisher (Ed.) Academic Press, New York, p. 542, 1981.
- Jain, S.C., "Plunging phenomena in reservoirs," ASCE, Symp. on Surface Water Impound. Vol. IV, Univ. of Minn. 1980.
- Karnovich, V.N., "Winter operation of pumped storage power plant basins and canals," 20th IAHR Congress, Moscow, Vol. II, 1983.
- Lewis, W.M., "Temperature, heat and mixing in Lake Valencia, Limnol. Oceanogr. (28), No. 2, 1983.
- Norton, W.R. and I.P. King, "Mathematical simulation of water temperature to determine the impact of raising an existing dam," Prog. in Astro. and Aero. (36), 1975.
- Orlob, G.T., (Ed.), Mathematical Modeling of Water Quality: Streams, Lakes and Reservoirs. (Ch. 7, "One-dimensional Models" by G.T. Orlob; Ch. 8, Two and Three-Dimensional Models by M. Watanabe, D.R.F. Harleman and O.F. Vasiliev) Wiley, 1983.
- Patterson, J.C. and P.J. Hamblin, "Simulation of a lake with winter ice cover," Env. Dyn. Rep. ED-83-043, Univ. of Western Australia, 1983.
- R & M Consultants, Inc., "Alaska Power Authority, Susitna Hydroelectric Project, Glacial Lake Studies," Report prepared for Acres American Inc., Buffalo, N.Y., 1982.
- Ragotzkie, R.A., Heat budgets of lakes, Ch. 1, in Lakes, Chemistry, Geology, Physics. A. Lerman (Ed.) Springer-Verlag, 1978.
- Shirtcliffe, T.G.L., and R.F. Benseman, "A sun-heated antarctic lake," Jour. of Geophy. Res., (69) No. 16, 1964.
- Stefan, H. and D.E. Ford, "Temperature Dynamics in Dimictic Lakes," Proc. ASCE, Vol. 101, HY1, 1975.
- Stewart, K.M., "Isotherms under ice," Verh. Internat. Verein. Limnol. 18, 1972.
- Stewart, K.M., "Winter conditions in Lake Erie with reference to ice and thermal structure and comparison to lakes Winnebago (Wisconsin) and Mille Lacs (Minnesota)," Proc. 16th Conf. Great Lakes Res., 1973.
- Stewart, R.H., Methods of Satellite Oceanography, Univ. of Calif. Press, 1985.
- Thomas, E.A. and C.G. Orn, "Ice cover and hypolimnetic reoxygenation in the Greifensee from 1950 to 1980," Schweizerische Zeitschrift fur Hydrologie, Vol. 44, No. 1, 1982.
- Tsai, Y.J., "Predictive Model of Fog Induced by Cooling Pond," ASCE Symp. on Surface Water Impound., Vol. II, Univ. of Minn.. 1980.
- Wake, A. and R.R. Rumer, "Effect of surface meltwater accumulation on the dissipation of lake ice", Water Resour. Res., (15) No. 2, 1979.
- Wake, A. and R.R. Rumer, "Modeling ice regime of Lake Erie," Proc. ASCE, Vol. 105, No. HY7, July 1979.
- Wake, A. and R.R. Rumer, "Great Lakes ice dynamics simulation," Proc. ASCE, Vol. 109, Jour. of Waterway, Port, Coastal and Ocean Eng., No. 1, Feb. 1983.
- Wei, C.Y. and P.F. Hamblin, "Reservoir water quality simulation in cold regions," Proc. Cold Regions Hydrology Symp., Am. Water Res. Assoc., Fairbanks, Alaska 1986.

Wells, S.A. and J.A. Gordon, "A
three-dimensional field evaluation
and analysis of water quality -
management and modeling implications
of the third-dimension," ASCE, Symp.
on Surface Water Impound., Vol. I,
Univ. of Minn. 1980.

WATER, SNOW AND ICE MANAGEMENT

WATERSHED TEST OF A SNOW FENCE TO INCREASE STREAMFLOW: PRELIMINARY RESULTS

Ronald D. Tabler and David L. Sturges¹

ABSTRACT: Although snow fences have long been proposed as a method to increase water yield, the feasibility of this practice has not been established. This paper reports hydrologic changes the first 2 years after construction of an 800-m-long snow fence, 3.78 m tall, on a 307-ha paired watershed having 10 years of pretreatment data. Although final assessment will require more years of study, initial treatment effects are so apparent that preliminary results are meaningful. Snow accumulation increased about 58%, and streamflow averaged 237% of that predicted by the pretreatment calibration with the control watershed. Flow duration on the ephemeral stream increased about 18 days. Overall water-yield efficiency of the snow fence drift averaged about 43%; however, the yield efficiency of the added snow was about 85%. To amortize the fence construction cost over a 25-year physical project life, the value of the new water would have to be about \$0.06721 per cubic meter. (KEY TERMS: snow fences; snow management; water yield improvement; blowing snow.)

INTRODUCTION

Although snow fences can augment water supplies by altering the distribution of snow, they also make "new" water available by reducing the evaporative losses from blowing snow particles (Tabler, 1973). In Wyoming, for example, more than half of the blowing snow evaporates over a transport distance of 3000 m (Tabler 1975). It should also be possible to pro-

long snowmelt runoff by using snow fences to increase snow depth. Indeed, snow fences may have been invented as a method to augment water supplies because, according to Brown (1983), the first known reference to snow fences was in an 1852 Norwegian publication describing snow fences to provide water for livestock. Another early reference was an article that appeared in an Alaskan newspaper (Seward Weekly Gateway, 1909) describing how miners used snow fences to augment water supplies for placer mining. Since then there has been considerable speculation on the possibility of using snow fences to increase water yield or local water supplies (Lull and Orr, 1950; Martinelli, 1959; Berndt, 1964; Costin, 1968; Tabler, 1968; Swank and Booth, 1970; Tabler, 1971; Tabler and Johnson, 1971; Martinelli, 1973; Rechar, 1973; Saulmon, 1973; Tabler, 1973; Cooley *et al.*, 1981; Sturges and Tabler, 1981). But despite these numerous references, no studies have shown an effect of snow fences on streamflow. The snow fence treatment on the only watershed-based study (Cooley *et al.*, 1981) was too small to have a significant hydrologic effect, leaving in question the feasibility of this form of snowpack management.

This paper reports hydrologic changes during the first 2 years after construction of a large snow fence on a "calibrated" paired watershed having 10 years of pretreatment streamflow data. Although final assessment will require more years of study, initial treatment effects are so apparent that preliminary results are meaningful.

¹Hydrologist and Research Forester, respectively, Rocky Mountain Forest & Range Experiment Station, Forest Service, USDA; 222 South 22nd Street, Laramie, Wyoming 82070.

STUDY AREA AND METHODS

The study watersheds are part of the Stratton Sagebrush Hydrology Study Area (41° 26'N, 107° 07'W), located about 32 km west of Saratoga in south-central Wyoming. Elevation of the gently rolling terrain ranges from 2320 m at the lowest stream gage, to 2440 m at the upper watershed divide. Annual precipitation averages 53 cm, about half of which falls as snow from November through March. Precipitation data are from a well-sited recording gage located in a forest grove about 4.5 km from the streamgage on the fenced watershed. Mean monthly values of precipitation, air temperature, and wind speed are shown in Figure 1. Because snow is blown off of windward slopes and ridges, and redeposited on leeward slopes and in topographic depressions, snow depths prior to melt range from a few centimeters on windward slopes to 6 m or more in topographically controlled deposition zones.

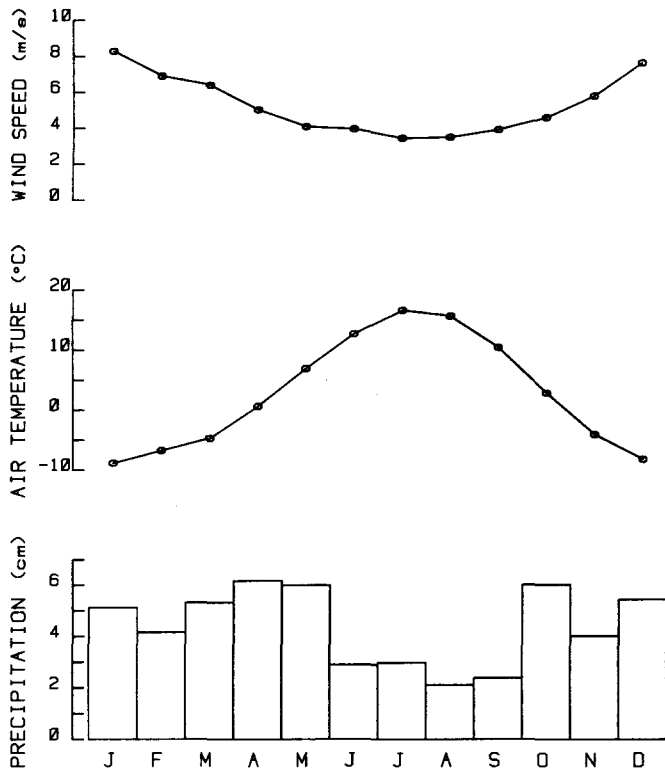


Figure 1. Mean monthly wind speed, air temperature, and precipitation at the Stratton Study Area, 1967-1981.

Soils developed in place from sandstone of the Brown's Park Formation, and have a loam or sandy loam texture in the A and B horizons. Both infiltration and soil stability are good. On moist sites, vegetation is dominated by mountain big sagebrush (*Artemisia tridentata* ssp. *vaseyana*) having a typical height of 60 cm. Wyoming big sagebrush (*A. t.* ssp. *wyomingensis*), typically about 20 cm tall, occupies upland areas where effective precipitation is less because of snow removal by wind.

Hydrologic data have been collected on the Stratton Study Area since 1967 when streamgages were installed on the two perennial streams, Loco Creek and Sane Creek, to determine the hydrologic effects of sagebrush eradication. Although a final publication on this aspect of the research is still in preparation, hydrologic characteristics of the area have been reported by Sturges (1975a, 1975b, 1979). Loco Creek (664 ha) has remained untreated, and serves as the control watershed for the study reported here. The 307-ha snow-fenced watershed (North Draw) is drained by an ephemeral stream charged primarily by snowmelt, with very little runoff from summer storms. This watershed has been continuously gaged since 1974, and remained untreated until the summer of 1983 when the snow fence was built.

The primary streamgages are 120-degree V-notch weirs having cutoff walls extending about 3 m below the surface and equipped with water-stage recorders. The entire weir pond, measurement section, and discharge apron of each streamgage are housed within a steel multiplate pipe arch (Figure 2) for protection against the deep snowdrifts in the stream channels (Johnson and Tabler, 1973). A Parshall flume was installed immediately above the snow-fenced channel reach in 1983.

Permanent snow courses have been measured since 1968 on Loco and Sane Creek watersheds. Measurements on two permanent snow courses crossing the lower North Draw channel were begun in 1969 and measurements began in 1979 on seven additional snow courses to better quantify channel snow storage in anticipation of the snow fence treatment. Although snow densities are measured each year along selected transects using a Federal snow sampler,

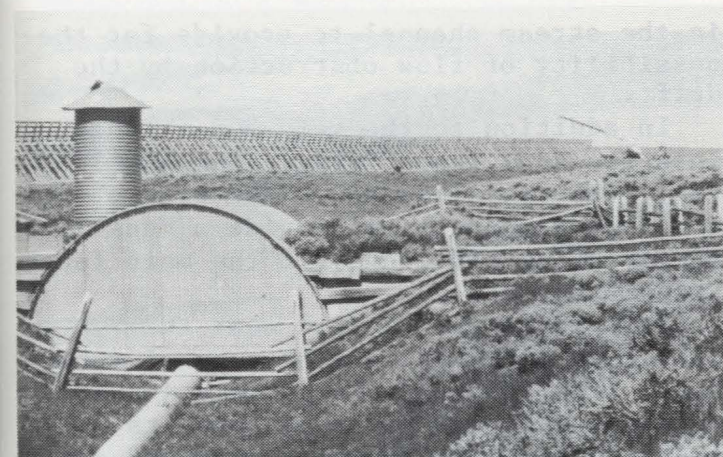


Figure 2. Construction of the 3.78-m-tall snow fence on North Draw watershed in 1983, with the streamgage shown in foreground.

these values are not representative of true snow densities in the deeper drifts because of measurement and sampling errors. Water-equivalents reported here are therefore calculated using the relationship between snow density and snow depth reported by Tabler (1985).

DESIGNING THE SNOW FENCE TREATMENT

The most logical location for a snow fence was such as to augment snow deposition along the lowest 815 m of the main stream channel. This section, having a mean azimuth of 292° , was closest to being perpendicular to the prevailing southwest winds, and natural snow storage capacity was inadequate to store all transported snow in winters with average precipitation. In addition, concentrating the snow in the primary channel would minimize snowmelt conveyance losses. This section of channel is the principal snow accumulation area on the North Draw watershed because it is incised about 6 m below the surrounding terrain. Snow depths elsewhere are controlled primarily by sagebrush height, and range from only a few centimeters to a meter or so at peak accumulation.

It is estimated that prior to fencing, the drift that formed in the incised channel contributed 60% of total discharge, even though 79% of the total watershed area lies above this section. Snow

storage capacity averaged about 78 m^3 of water-equivalent per meter of channel length, for a total of about $64,000 \text{ m}^3$ (52 acre-ft). Although the efficiency with which blowing snow was deposited in this topographic feature was unknown, a smooth snow surface extended across the channel in most years, implying a relatively low trapping efficiency by the end of the accumulation season and suggesting that a snow fence would increase deposition. Above this incised section, the channel branches into shallow tributaries that are nearly parallel to the wind and thus not as well suited to fencing. The length of the snow fence (800 m) was therefore dictated by the length of the incised channel. Although it would be possible to construct additional snow fence on the upper part of the watershed, we would expect the yield efficiency to be less than for fencing along the incised channel section.

The type of fence selected was the standard wood snow fence used by the Wyoming Highway Department since 1971 (Figure 2). This structure consists of horizontal boards 15 cm wide separated by 15-cm spaces, a bottom gap of approximately one-tenth of the fence height, and a 15-degree inclination downwind (Tabler, 1974). Net porosity (open area) of the structure, excluding the bottom gap, is about 48%. This type of fence was selected because it is known to be effective, economical to build and maintain, and has a known capacity and drift geometry (Tabler, 1980). At the time the snow fence treatment was designed, plans were available for heights of 1.83, 2.44, 3.17, and 3.78 m. The 3.78-m height was chosen as that required to store the maximum snow transport anticipated over the 25-year physical life of the snow fence, using the equation developed by Tabler (1975):

$$Q = 1515 P_r \left[1 - (0.14)^{R/3030} \right] \quad (1)$$

where Q is snow transport in cubic meters of water-equivalent per meter of width across the wind, P_r is relocated water-equivalent precipitation in meters, and R is the fetch or "contributing" distance in meters. This equation has been used to design successful snow fence systems for highway protection (Tabler and Furnish,

1982) and water supply augmentation (Sturges and Tabler, 1981), and to design snow fences on Alaska's North Slope, including the system constructed at the village of Wainwright in 1982. For the North Draw watershed, mean winter precipitation (November 1 through March 31) is estimated to be 0.24 m. Of this amount, about 16 cm would be retained by the vegetation, which averages about 45 cm tall. The maximum transport was estimated using a value for winter precipitation having an exceedance probability of 4% (return period of 1 year in 25), as computed from the frequency distribution reported by Tabler (1982). This value was 1.5 times the mean, or 0.36 m. P_r was then computed to be 0.20 m by subtracting the anticipated snow retention by vegetation (0.16 m). The fetch distance, R , was taken as the average distance (2000 m) between the North Draw channel and the nearest snow accumulation feature upwind. Although some blowing snow is expected to escape these upwind deposition areas, which are similar to the North Draw channel, using this fetch distance assured a conservative (low) estimate of snow transport.

Maximum snow transport was thus estimated from Equation (1) to be about 190 m^3 water-equivalent per meter of channel length. A 3.78-m-tall fence will store about 172 m^3 on level terrain if both windward and leeward drifts are considered (Tabler, 1980). Total storage capacity would therefore be about 250 m^3 per meter of fence length after adding the 78 m^3 storage in the channel. The extra storage capacity provided by using a 3.78-m-tall fence assured that most of the blowing snow would be deposited, because snow trapping efficiency does not decrease significantly until a fence is filled to about 80% of its capacity (Tabler, 1974).

The fence line was curved to parallel the stream channel at an average distance of 38 m (ten times the fence height) upwind (Figure 3). This placement was chosen to minimize the distance snowmelt runoff had to travel to the channel, while being far enough upwind that the drift would not be expected to block the stream channel in a winter with average (or below) precipitation. However, because it is necessary to gage the streamflow accurately for research purposes, perforated plastic drain pipe was installed

in the stream channel to provide for the possibility of flow obstruction by the drift.

In addition to the main 800-m fence, a separate snow fence, 112 m long and 3.8 m tall, was installed 200 m downwind of the North Draw channel to provide a measure of the trapping efficiency of the main fence (Figure 3).

This fence was located near the watershed boundary, and because of the small size of the drift in relation to total channel snow storage (and its distance from the channel) it would not be expected to have a discernible effect on streamflow. The fences were built during the 1983 summer after a calibration period sufficient to detect a 15% change in streamflow from snowmelt.

HYDROLOGIC EFFECTS OF THE SNOW FENCE

Nearly identical results were obtained the first 2 years after the fence was built, even though the 36 cm of precipitation the first winter (1983-84) was the highest in 14 years of record on the study area, and the 22 cm recorded the second winter was about average.

A comparison of snow accumulation on a single snow course in the incised channel section before and after fencing is shown in Figure 4. Based on the pretreatment relationship between maximum snow accumulation on two index transects on the control and treated watersheds (Figure 5), snow accumulation was 54% and 62% greater the first and second year after fencing, respectively, than would have occurred without the fence (Figure 6). Pretreatment data in Figure 5 are restricted to values at peak accumulation; after fencing, however, the snow courses have been measured on several dates each winter to provide an estimate of the future effect of treatment on snow retention. The ratio of the slopes of the snow accumulation relationships in Figure 5 suggests that before fencing, efficiency of the stream channel in trapping blowing snow averaged about 56% of that with the fence in place.

Peak snow water-equivalent volume stored by the downwind fence was less than the precipitation relocated between the fences in both posttreatment years,

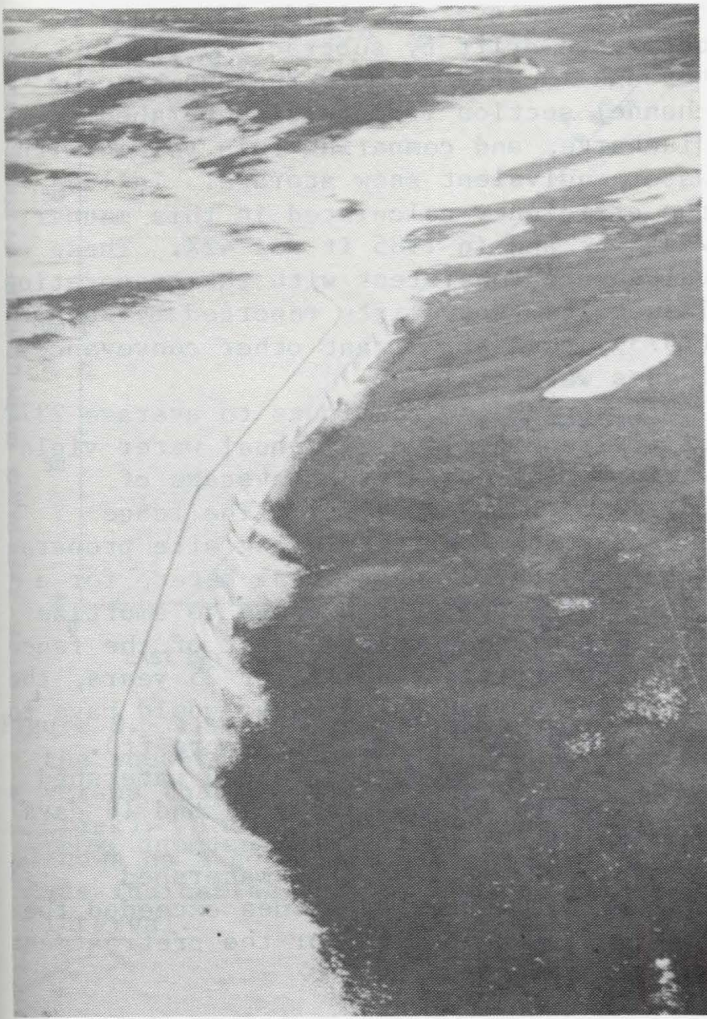


Figure 3. Aerial view of North Draw watershed on 25 March 1985, the date of peak accumulation. The wind is from the upper left, and the streamgage instrument shelter is visible near the bottom of the photo.

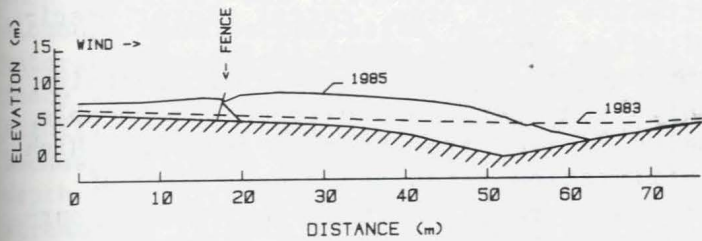


Figure 4. Snow profiles on a North Draw snow course before and after fencing, in years with similar winter precipitation.

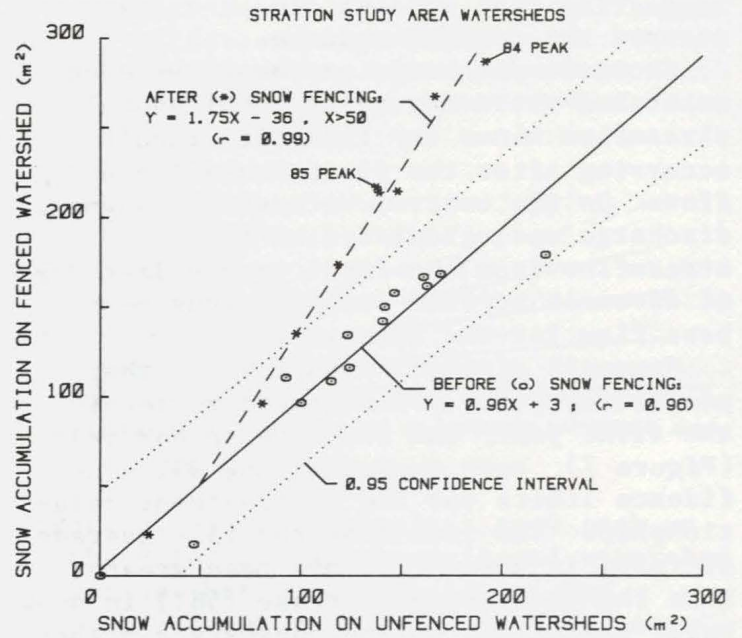


Figure 5. Snow accumulation on North Draw watershed (average cross-sectional area of two transects), versus the average of two transects on untreated watersheds. Data before fencing are at peak accumulation only. Posttreatment values include measurements taken through the accumulation periods as well as at peak accumulation. Dotted lines indicate the 95% confidence interval for the pretreatment regression.



Figure 6. Snowdrift on the lee side of the fence at time of peak accumulation in 1985. The top of the streamgage instrument shelter is visible in the background.

suggesting that no significant transport escaped the main snow fence.

Snowmelt discharge on the snow-fenced watershed was computed as total annual streamflow minus any rainstorm runoff occurring after the first cessation of flow. On the control watershed, snowmelt discharge was calculated as total streamflow from the first to the last day of snowmelt surface runoff, minus mean base flow for the interval.

Snowmelt discharge was 232% of that predicted by the pretreatment regression the first year, and 242% the second year (Figure 7), both exceeding the 99% confidence limits for the pretreatment relationship. The fact that the 137% average increase in streamflow has been greater than the percentage increase (58%) in snow water-equivalent volume suggests a higher efficiency of water yield from the additional snow caught by the fence. The ratio of the increase in streamflow to the

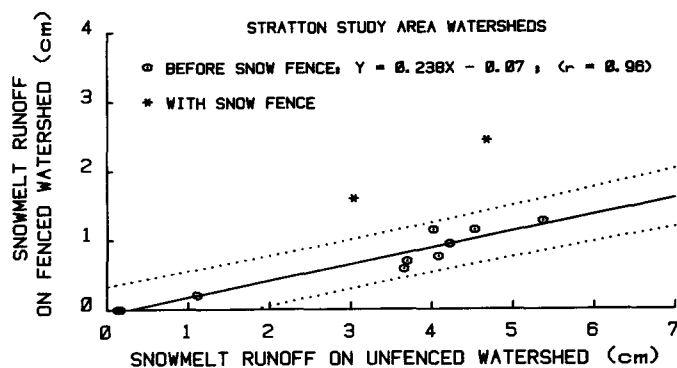


Figure 7. Annual snowmelt discharge on the snow-fenced watershed in relation to that on the control (Loco Creek). The pretreatment regression is shown as a solid line, with dotted curves indicating the 95% confidence interval.

increase in water-equivalent snow storage was 0.78 in 1984, and 0.92 in 1985, suggesting an average yield efficiency of 85%. This high efficiency is attributed to the fact that soil water recharge requirements are satisfied independently of the additional snow, and that evaporation losses are relatively small during the extended melt period. It is possible

to estimate overall yield efficiency of the fence drift by subtracting flow through the flume above the snow-fenced channel section from total watershed discharge, and comparing this volume with water-equivalent snow storage. In 1984 the efficiency calculated in this manner was 44%, and in 1985 it was 42%. These values are consistent with the evaporation losses from snowdrifts reported by Rechar (1975), suggesting that other conveyance losses were small.

If streamflow continues to average 237% of pre-fencing levels, annual water yield would be increased by an average of 28,200 m³ (22.9 acre-ft). The fence construction cost (including site preparation) was \$59.25 per lineal meter, for a total of \$47,390. In order to amortize the initial construction cost of the fence over the anticipated life of 25 years, the value of the increased water would have to be \$0.06721 per m³ (\$83 per acre-ft).

Flow duration on the fenced watershed was extended 19 days in 1984, and 18 days in 1985, based on the pretreatment relationship with the control watershed (Figure 8). Observed values exceeded the 95% confidence limits for the pretreatment relationship.

CONTRAST WITH AN EARLIER SNOW FENCE TEST

The dramatic streamflow effects of the North Draw snow fence contrast markedly with those from an earlier paired watershed test of snow fences conducted on Pole Mountain about 30 km east of Laramie, Wyoming. Located at 41° 15'N, 105° 21'W, at an elevation of about 2450 m, weather conditions were similar to those on the Stratton Study Area, except winter precipitation averaged about 15 cm. More importantly, however, the Pole Mountain soils are coarse and extremely permeable, being derived from Sherman granite. High infiltration rates and a deep zone of fractured rock result in very little surface runoff from snowmelt. After two small watersheds had been calibrated for 7 years (1963-1969), a 3.8-m-tall snow fence, 396 m long, was built on a 45-ha watershed in 1970. The second watershed, 36 ha in size, remained untreated. The design of the snow fence treatment (Tabler, 1971) was based on the same

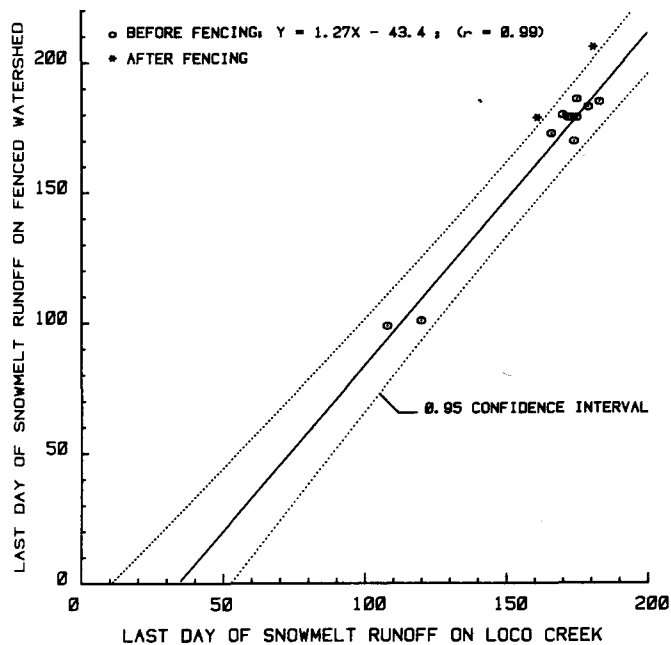


Figure 8. Last day of snowmelt runoff on the snow-fenced watershed (North Draw), versus that on the control (Loco Creek). The pretreatment regression is shown as a solid line, with dotted curves indicating the 95% confidence interval.

reasoning used for the North Draw fence, and eventually led to the development of Equation (1). This snow fence also was planned to augment snow deposition in the stream channel immediately above the streamgage, and was located about 20 m upwind from the channel centerline to minimize snowmelt conveyance losses.

Snow accumulation and streamflow were monitored for 4 years after treatment and then the study was discontinued in 1974. Although snow accumulation on the watershed approximately doubled after the fence was built (Figure 9), there was no significant increase in snowmelt discharge because all melt water percolated to such depth that it was not intercepted by the streamgage (Figure 10). Although the increased snow accumulation must have had some effect on groundwater, the treatment failed to increase local surface discharge. This comparison demonstrates that edaphic and geologic characteristics of the watershed must be considered when designing snow fence treatments to increase surface runoff.

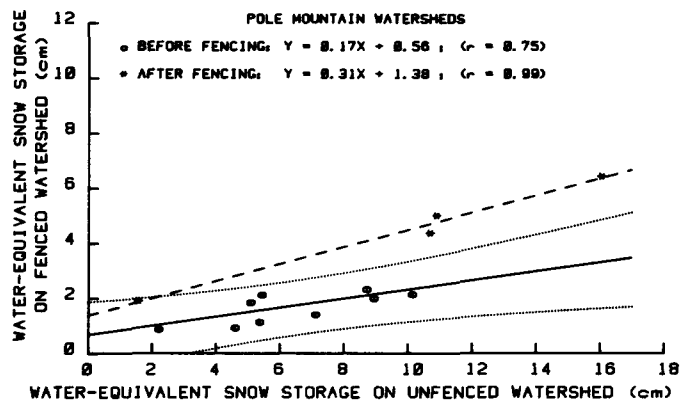


Figure 9. Water-equivalent snow pack on the Pole Mountain snow-fenced watershed versus that on the control. The pretreatment regression is shown as a solid line, with dotted curves indicating the 95% confidence interval.

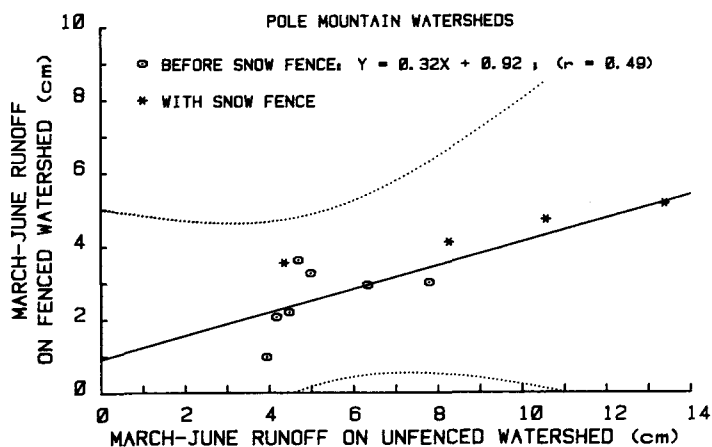


Figure 10. March-June (inclusive) streamflow on the Pole Mountain snow-fenced watershed, versus that on the control. The pretreatment regression is shown as a solid line, with dotted curves indicating the 95% confidence interval.

CONCLUSIONS

Although final conclusions must await additional years of study, it seems certain that the snow fence has significantly increased both quantity and duration of streamflow on North Draw watershed. Results the first 2 years after fencing indicate that the method and criteria used

to design the treatment were entirely satisfactory. Although the geology of North Draw watershed is probably ideal for realizing maximum benefits from this form of snowpack management, even larger increases in water yield are possible in areas having more snow transport, less natural snow storage capacity, or where longer fences can be built. Properly designed snow fence treatments appear to be a viable means of augmenting water supplies on windswept lands.

ACKNOWLEDGEMENTS

Research reported here was supported in part by the Bureau of Land Management, U.S. Department of the Interior. The Rocky Mountain Forest and Range Experiment Station laboratory at Laramie is maintained in cooperation with the University of Wyoming. Station headquarters is at Fort Collins, in cooperation with Colorado State University.

LITERATURE CITED

- Berndt, H. W., 1964. Inducing Snow Accumulation on Mountain Grassland Watersheds. *J. Soil and Water Conserv.* 19(5):196-198.
- Brown, R. H., 1983. Snow Fences: Then and Now. *J. Cultural Geog.* 4(1):87-98.
- Cooley, K. R., A. L. Huber, D. C. Robertson, and J. F. Zuzel, 1981. Effects of Snowdrift Management on Rangeland Runoff. In: *Proc. 49th Western Snow Conf.*, p. 55-64.
- Costin, A. B., 1968. Management for Improved Water Yield from Victorian High Mountain Catchments. *Victoria's Resources*, June-Aug. 1968:4-8.
- Johnson, K. L. and R. D. Tabler, 1973. An Enclosed Weir for Small Streams in Snow Country. *USDA For. Serv. Res. Note RM-238*. 8 p.
- Lull, H. W. and H. K. Orr, 1950. Induced Snow Drifting for Water Storage. *J. Forestry* 48:179-181.
- Martinelli, M., Jr., 1959. Some Hydrologic Aspects of Alpine Snowfields Under Summer Conditions. *J. Geophys. Res.* 64(4):451-455.
- Martinelli, M., Jr., 1973. Snow Fences for Influencing Snow Accumulation. In: *The Role of Snow and Ice in Hydrology. Proc. Symp. on Measurement and Forecasting*, WMO, Sept. 1972. Banff, Alberta. p. 1394-1398.
- Rechard, P. A., 1973. Opportunities for Watershed Management in Wyoming. *Proc. Irrig. and Drainage Div. Specialty Conf.*, April 22-24, 1973. Colorado State Univ., Fort Collins. *Amer. Soc. Civil Eng.* p. 423-448.
- Rechard, P. A., 1975. A Study of Evaporation from a Snowdrift. In: *Proc., Snow Management on the Great Plains Symposium*, July 29, 1975. Bismarck, N. Dak. *Great Plains Agric. Counc. Publ.* 73, p. 65-84.
- Saulmon, R. W., 1973. Snowdrift Management Can Increase Water-Harvesting Yields. *J. Soil and Water Conserv.* 28(3):118-121.
- Seward Weekly Gateway, 1909. Alaska Miners Store Snow. *Seward Weekly Gateway*, April 10, 1909. p. 2C2.
- Sturges, D. L., 1975a. Sediment Transport from Big Sagebrush Watersheds. In: *Proc. ASCE Irrig. and Drainage Div., Watershed Manage. Symp.*, August 11-13, 1975. Logan, Utah. p. 728-738.
- Sturges, D. L., 1975b. Oversnow Runoff Events Affect Streamflow and Water Quality. In: *Proc., Snow Management on the Great Plains Symp.* July 25, 1975. Bismarck, N. Dak. *Great Plains Agric. Counc. Publ.* 73, p. 105-117
- Sturges, D. L., 1979. Hydrologic Relations of Sagebrush Lands. *Proc. Symp. on the Sagebrush Ecosystem*, April 27-28, 1978. Logan, Utah. p. 86-100.
- Sturges, D. L. and R. D. Tabler, 1981. Management of Blowing Snow on Sagebrush Rangelands. *J. Soil and Water Conserv.* 36(5):287-292.
- Swank, G. W. and R. W. Booth, 1970. Snow Fencing to Redistribute Snow Accumulation. *J. Soil and Water Conserv.* 25(5):197-198.
- Tabler, R. D., 1968. Physical and Economic Design Criteria for Induced Snow Accumulation Projects. *Water Resources Res.* 4(3):513-519.
- Tabler, R. D., 1971. Design of a Watershed Snow Fence System and First-Year Snow Accumulation. In: *Proc. 39 Western Snow Conf.*, p. 50-55.

- Tabler, R. D., 1973. Evaporation Losses of Windblown Snow, and the Potential for Recovery. In: Proc. 41st Western Snow Conf., p. 75-79.
- Tabler, R. D., 1974. New Engineering Criteria for Snow Fence Systems. Transp. Res. Rec. 506:65-78.
- Tabler, R. D., 1975. Estimating the Transport and Evaporation of Blowing Snow. In: Proc., Snow Management on the Great Plains Symp., July 25, 1975. Bismarck, N. Dak. Great Plains Agric. Counc. Publ. 73, p. 85-104.
- Tabler, R. D., 1980. Geometry and Density of Drifts Formed by Snow Fences. J. Glaciology 26(94):405-419.
- Tabler, R. D., 1982. Frequency Distribution of Annual Peak Water-Equivalent on Wyoming Snow Courses. In: Proc. 50th Western Snow Conf., p. 139-148.
- Tabler, R. D., 1985. Ablation Rates of Snow Fence Drifts at 2300 Meters Elevation in Wyoming. In: Proc. 53rd Western Snow Conf., p. 1-12.
- Tabler, R. D. and R. P. Furnish, 1982. Benefits and Costs of Snow Fences on Wyoming Interstate-80. Transp. Res. Rec. 860:13-20.
- Tabler, R. D. and K. L. Johnson, 1971. Snow Fences for Watershed Management. In: Proc., Snow and Ice in Relation to Wildlife and Recreation Symp., February 11-12, 1971. Ames, Iowa. p. 116-121.

**SURVEY OF EXPERIENCE
IN OPERATING HYDROELECTRIC PROJECTS IN COLD REGIONS**

Eugene J. Gemperline, David S. Louie, H. Wayne Coleman¹

ABSTRACT: In response to operational and environmental concerns, a literature review, mailed survey and site visit have been made to evaluate the procedures adopted by operators of hydroelectric projects in cold regions similar to the Susitna Hydroelectric Project site. Four specific areas were addressed and are discussed in this paper.

- ° Reservoir and powerhouse operating procedures to mitigate ice jam related flooding,
- ° The effects of reservoir ice cover and bank ice on animal crossing,
- ° Management of reservoir ice cover to control cracking and the associated danger to animals, and
- ° Bank erosion resulting from reservoir and river ice movement. The effect of this movement on suspended sediment and turbidity levels.

Ice-related flooding is a major concern in cold regions and several comprehensive manuals have been published by concerned organizations. Summaries of the subjects covered in these documents are presented. In order to obtain more specific information on operating hydroelectric projects, a mail survey was conducted. Questionnaires were sent to hydropower utilities, water supply utilities, federal and state agencies for the environment, universities, research organizations, and

other organizations located in Canada, northern states in the United States, Europe, and Asia. The questions asked concerned ice management policies in use or being adopted, for operations or environmental purposes. The results of the survey are presented and discussed. Additionally, a site visit was made and discussions were held with operators of an existing hydro-power utility in Canada and an agency concerned with the operation. A summary of the results of those discussions is included.

(Key Terms: Cold Regions Hydrology, Hydroelectric Projects, Experience Survey, River Ice, Environmental Impacts, Reservoir Ice Cover.)

INTRODUCTION

The Susitna Hydroelectric Project is being proposed by the Alaska Power Authority to meet projected electrical energy demands in the Alaska Railbelt in the 21st century. The project would consist of two dams, powerhouses and appurtenant facilities, to be built in three stages on the Susitna River about midway between the principal load centers of Anchorage and Fairbanks. The upstream dam (Watana) would be an earth and rockfill structure about 270 m high having a six unit powerhouse capable of generating 1,110 MW at a flow of 650 m³/s. The downstream project would be located 52 km below Watana at the Devil Canyon site and would be a thin concrete arch having a height of 197 m and capability of 680 MW

¹Respectively, Manager Hydrologic and Hydraulic Studies, Harza-Ebasco Susitna Joint Venture, 711 H St. Anchorage, Alaska 99501; Chief Hydraulic Engineer, Harza Engineering Co.; Section Head, Hydraulic Design and Analysis, Harza Engineering Co., 150 S. Wacker Dr., Chicago, Illinois 60606.

at a flow of $430\text{m}^3/\text{s}$, through four turbine/generator units.

The Watana dam would be built in two stages. In the first stage the dam would be raised to 56m below its final height and four of the six units installed in the powerhouse. This would become operational in 1999. The second stage of the project would be the construction of the Devil Canyon dam and powerhouse. This would become operational in 2005. In the final stage, the Watana dam would be raised to its full height and the powerhouse completed. The average annual generation from the final project would be 6,900 gwh.

The project is located in the cold region of south-central Alaska. Air temperatures in the region are below freezing for seven months (October- April) and the river is subject to ice cover during this entire period. River flows during this period are normally low, but proposed project operation would result in much higher winter flows. The river ice regime would be altered due to both flow and temperature effects induced by the reservoir. Additionally, a large reach of the river to be impounded by the reservoirs (approximately 130 km) would be covered by a stable but large ice sheet as compared to the normal river ice cover composed of frazil pans and frozen slush.

As a result of these effects there was concern that wildlife inhabiting the basin area and anadromous fish (salmon) in the river downstream of Devil Canyon would be affected. Therefore, a series of hydrologic and hydraulic studies were undertaken to estimate the effects of project construction and operation on the river to aid biologists in their impact assessments. These included studies of project operation (Wu, et.al., 1986), studies of reservoir water quality including temperature, ice cover and suspended sediment (Wei and Hamblin, 1986), river temperatures for open water reaches of the river downstream of the dams (AEIDC 1983) and river ice processes (Paschke and Coleman 1986). A more complete description of the project, basin, river and the hydrologic studies is contained in a paper by Gemperline (1986).

In addition, there were several aspects of the proposed project's effects, beyond the scope of model studies, which were

addressed by a survey of experience in operating hydroelectric projects in cold regions. These concerns dealt with the effect of the reservoir ice cover on animals crossing the reservoir; the effect of potential powerhouse operation on the stability of the downstream ice cover, and the effect of ice cover on reservoir and river bank erosion.

The experience survey was carried out in three parts. In the first part a literature review was made of several ice management and ice engineering manuals compiled by U.S. and Canadian agencies. In the second part, a concise set of questions was developed and mailed to hydroelectric project operators in cold regions, environmental agencies, water supply utilities, universities, research organizations and others who might have information. The replies were compiled and evaluated. Follow-up phone calls and discussions were held which yielded additional information. In the third part of the study a visit was made to an operating hydroelectric project in a cold region. The results of the study were documented in a report (Harza-Ebasco 1985) and integrated with the modeling studies to determine the potential project effects during the winter and to evaluate proposed operating constraints.

LITERATURE REVIEW

Several organizations have published general information and guidelines for ice considerations in the design and operation of hydroelectric and other projects. These sources were reviewed:

1. Evaluation of Ice Problems Associated with Hydroelectric Power Generation in Alaska, Final Report to the State of Alaska Department of Commerce and Economic Development by J.P. Gosink and T.E. Osterkamp, of the University of Alaska Geophysical Institute.

The problems dealt with in this study pertain more to energy generation than to environmental concerns. There is discussion of problems related to hanging dams and ice jams which is of interest. Various methods for determining the open water reach downstream of a reservoir are discussed. A survey of hydropower plants

was conducted to determine potential ice-related problems and possible solutions.

2. Course Notes for Ice Engineering on Rivers and Lakes by the University of Wisconsin, Madison in cooperation with the U.S. Army Corps of Engineers, Cold Regions Research and Engineering Laboratory and the University of Wisconsin Sea Grant Institute.

The course notes include articles by leading authorities in the field of ice engineering, dealing with:

- a) formation and breakup of a river ice cover and methods for analyzing and solving associated problems,
- b) ice problems at hydroelectric structures, and
- c) mechanical properties of ice and ice forces on structures.

The notes provide a good compendium of potential ice problems and engineering solutions. However, they do not deal with environmental effects other than effects of flooding on human habitation.

3. Design and Operation of Shallow River Diversions in Cold Regions by the U.S. Department of the Interior, Bureau of Reclamation REC-ERC-74-19.

This report contains information on potential ice problems and design guidelines. Although the report is written for shallow river diversions, many of the design guidelines are applicable to hydroelectric projects as well. The report does not deal with environmental problems.

4. Winter Ice Jams on the Gunnison River, by the U.S. Department of the Interior, Bureau of Reclamation REC-ERC-79-4.

The report details ice jam flooding problems associated with operating projects and methods used in an attempt to alleviate the problem. The flooding affected residents along the reach of the Gunnison River between Blue Mesa and Taylor Park

reservoirs. Relationships were developed between ice jam location, weather conditions and level of Blue Mesa Reservoir water surface.

5. Ice Management Manual, by Ontario Ministry of Natural Resources.

This report includes guidelines for dealing with chronic ice problems including procedures for monitoring, predicting and acting on freeze-up and break-up ice jamming related flooding. It includes information on conditions causing ice jamming, explains causes and predictive methods for break-up, lists the data which should be collected in a monitoring program, and assesses the success rate of various remedial measures.

6. Ice Engineering by the U.S. Army Corps of Engineering, EM 1110-2-1612.

This is a very comprehensive report summarizing potential problems at all types of civil works structures including hydroelectric projects. The report provides guidance for the planning, design, construction, operation and maintenance of ice control and ice suppression measures and is used by the Corps of Engineers for their projects. The manual discusses ice formation processes, physical properties and potential solutions.

7. Behavior of Ice Covers Subject to Large Daily Flow and Level Fluctuations by Acres Consulting Services, Ltd. for the Canadian Electrical Association.

This report contains much valuable information on the types of problems encountered relative to river ice covers downstream of hydroelectric projects. An attempt was made to establish the state-of-the-art in predicting the stability of a river ice cover subject to flow and level fluctuations. Theoretical computations were made to establish stability criteria for the ice cover and to provide a means for developing guidelines for flow and level fluctuations to prevent ice cover break-up. The study concludes that:

"...generalized criteria do not exist at present, and designs cannot be prepared for many cases of ice structure, or shoreline, interaction."

The report concludes that extensive laboratory and field studies are necessary before a generally applicable model can be formulated and that the guidelines presented in the manual can be used to establish that field program. Site specific studies would also be required.

8. Reservoir Bank Erosion Caused and Affected by Ice Cover by Lawrence Gatto for the U.S. Army Corps of Engineers Cold Regions Research and Engineering Laboratory (Special Report 82-31).

This report describes a survey of reservoir bank erosion problems at various places throughout the world and provides a reference list. Many photographs of existing installations are presented. Criteria for various types of erosion are presented.

9. Proceedings of the Ice Management Seminar, January 30, 1980, London, Ontario by the Ministry of Natural Resources, Southwestern Region, London, Ontario.

This report provides the experience of many Canadian and U.S. experts in the field of ice management and control. Its scope is similar to Ice Engineering by the U.S. Army Corp of Engineers (6. above) and course notes for Ice Engineering on Rivers and Lakes (2. above).

Additionally, many articles available in the general literature were consulted. Some of these were provided by participants in the mail survey described later.

MAIL SURVEY

A mail survey was conducted to determine the experience of operators of hydroelectric projects in cold regions. The survey asked for information on the following four subjects:

1. Procedures or operating policies used in the control of ice levels in rivers

downstream and upstream of dams and hydropower plants caused by environmental water releases and power generating flow fluctuations in order to minimize the formation of ice jams and more importantly to minimize the associated flooding.

2. Environmental impact on terrestrial animals such as caribou, elk, bear, moose, etc., due to the formation of ice on wet reservoir banks exposed by reservoir drawdown or due to reservoir surface ice which has broken up at the banks. This ice may cause the animals to lose their footing and slip into the reservoir, resulting in injuries or drownings. What procedures, if any, have been taken to minimize this hazard?

3. The method of reservoir fluctuation management or precautions used in order to control the width of opening and pattern of crack development in the ice sheet such that after snowfall with cracks covered, the traversing animals would not fall into and be trapped in the cracks.

4. Problems of bank erosion caused by break-up and movement of ice resulting in increase of sediment in the reservoir and in the river downstream. What is the permissible degree of turbidity in parts per million or its equivalent that is acceptable for aquatic life such as salmon, trout, etc.?

The questionnaires were sent to hydro-power and water supply utilities; federal and state agencies for the environment, fish, wildlife, natural resources, energy, and inland waterways; universities; research organizations; and engineering companies located in each of the Canadian provinces and northern states in the United States, Europe and Asia, involved in ice engineering, and also selected concerned citizen groups. After a reasonable time lapse, follow-up letters were sent to some non-respondents. During the process of compiling the replies, telephone contacts were made in an attempt to clarify certain points.

Over 160 letters and telexes or cables

were sent to various organizations throughout the world, of which over 80 replies were received - 50%. This is considered a good response.

The replies were carefully reviewed and those that addressed the question(s) were tabulated; the rest of the respondents normally stated that nothing is known about the queried subject. Technical information in the replies was quite sparse although many respondents sent papers and manuals. Many respondents suggested names of persons and organizations to contact. In general, these suggestions were followed through. The following is a summary of the replies, organized by question.

Question No 1. - Reservoir Operating Procedures to Mitigate Ice Jam Related Flooding:

1. During freeze-up it is important that powerhouse discharges remain relatively high until a stable ice cover is formed, in the downstream river, at a high enough stage and of sufficient thickness and strength to allow full flexibility of discharge throughout the winter. Thereafter, the outflow may be reduced as required. This action permits the water to flow freely under the ice cover. When short term increased discharge is necessary, it should not exceed the discharge at ice cover formation until the ice cover has had a chance to strengthen as a result of heat loss and consolidation of ice blocks forming the initial cover. The consequences of increasing discharge over that at cover formation are the lifting of the ice cover, and a tendency to cause ice build-up. The ice build-up or hanging ice could result in increased back-water and ice jams during the break-up period.
2. During ice cover formation, the rate of freezing is monitored, and daily discharge is kept as constant as possible to reduce ice shoves at the leading edge of the ice cover and minimize flooding. If shoving should occur and water stage should increase, the discharge is moderated to reduce the hazards.

3. British Columbia Hydro attempts to coordinate ice break-up of the Peace River with the various tributaries on its river system. However, the timing and rate of break-up depend primarily on prevailing weather conditions and spring freshet flood peaks from the tributaries, and cannot be controlled at the dam. Therefore, extensive field observation posts at various stations have been established to monitor ice conditions. Where necessary and feasible, operations were modified in order to minimize hazards.
4. Each plant in the Manitoba Hydro system is associated with a unique set of operating policies. These policies are usually established out of concern for the environment, but also with recognition of a preferred mode of operation for power production purposes. Attempts to mitigate effects of flooding, etc. are made. If damage should occur, compensation procedures are adopted.
5. Ontario Hydro states that operational procedures at dams and hydroplants are still primarily based on operator's experience because the necessary understanding of ice jams is still not available.
6. Most respondents state that no attempts have been made to control ice levels to affect ice jamming or flooding.
7. Some respondents state that they have no written operating policy. Water levels are not regulated with effects on wildlife in mind, but only with the intent of providing required power generation or adequate water supplies for the users. Potential downstream effects at many of these sites are generally negligible because of sparse population or wildlife.
8. In other cases, operational constraints are employed to prevent the formation of hanging dams downstream of a hydro project or to reduce water levels upstream of the hanging dam after it forms. Hanging dams may result in high water levels which can

reduce the plant generating capacity, endanger the powerhouse, or result in flooding of areas adjacent to the river. These types of constraints include:

- o Inducing an early ice cover on the river upstream of known sites of hanging dams, by artificial means such as ice booms or other obstructions. When an ice cover forms, frazil ice production stops and the hanging dams, which result from frazil accumulation, are minimized.
 - o Inducing an early ice cover on the river by keeping powerhouse discharges low while the ice cover forms. This may result in more rapid ice cover advance, preventing further frazil production. After the ice cover is formed, powerhouse discharges can be increased.
 - o Preventing ice cover formation in sensitive areas by fluctuating discharges, continually breaking up the ice cover and keeping it downstream. This may result in higher water levels further downstream, but lower water levels in sensitive areas.
 - o Reducing discharges after a hanging dam forms in order to reduce water levels upstream of the hanging dam.
9. The Canadian Electrical Association and many plant operators indicated that powerhouse operations during the winter to maintain a stable cover would be site specific and require operating experience over a number of years. Reservoir discharge, climate conditions, channel morphology, and water temperature are all variables which must be considered.

Question No. 2. - Ice on Reservoir Banks:

In general, all organizations take no specific actions on their reservoirs to alter the state of ice on reservoir banks for wildlife safety reasons. Two organizations indicated sporadic cases of deer drowning within ice covered drawdown zones

but have no quantitative or documented information. Others reported no known problems with animal injuries or drowning as a result of reservoir drawdown.

Vattenfall (The Swedish State Power Board) reports some potential problems related to the need for reindeer to pass regulated rivers have been discussed when planning for new hydro power stations and in some cases the Power Board has constructed special reindeer bridges where "natural crossings" cannot be used anymore.

The Union Water Power Company reports, "The nature of reservoir freezing during drawdown does not allow wet reservoir banks to exist. The drawdown is gradual thus allowing solid freezing of the water. There are no exposed areas where an animal would become entrapped in a combination of wet mire and reservoir ice. At the time of freezing, the reservoir ice has formed sufficiently to support the weight of animals."

The United States Fish and Wildlife Service reports "There is the potential, if reservoirs freeze, for terrestrial animals to become stranded on ice and become easy prey to predators. Animal loss can be prevented by predator control, fencing of reservoirs and providing access to winter feeding areas away from iced surfaces."

Question No. 3. - Reservoir Management for Ice Crack Control:

All respondents except one state that no procedures are used to control cracks in reservoir ice that might be a hazard to animals. Also, most stated that no known problems with animals falling in cracks or openings along reservoirs have been documented. Many routes for migratory species do not cross existing reservoirs. Apparently, this is coincidental and not by choice of design because many of the reservoirs were in place prior to public awareness of environmental problems.

Kennebec Water Power Co., Maine states "In Maine, most large animals stay off the ice as they are unable to maintain mobility - especially the hooved animals."

At the Lucky Peak Dam, an irrigation and flood control structure in Idaho, many deer drownings occurred between its construction in 1956 and the institution

of measures to minimize the problem. The reservoir is reportedly in a major migration path and, up until about 10 ago, as many as 150-175 deer per year would drown in the reservoir. This was apparently caused by the animals crossing the reservoir when the ice cover was still thin. Pockets of unsupported ice or cracks apparently formed in the ice cover as the reservoir was being drawn down. Deer stepping on these areas would fall through the cover. Later, when the ice cover thickened, the problem ceased. The reservoir is now maintained at a stable level during cover formation to prevent the formation of these cracks or pockets. Deer drownings have reportedly been reduced to 5-10 animals per year.

At the Blue Mesa Reservoir in Colorado there has been one major incident of elk drowning during recent years. The exact cause is not known. However it appears, from the location where the elk were found, that they may have fallen through thin ice at the edge of the reservoir when the cover was first forming. It also appears that the elk do not normally travel on the reservoir and were there because of any of a number of reasons including a harsh winter and poaching hunters. The elk had apparently travelled at least a mile on the ice. The Blue Mesa Reservoir normally draws down continually through the winter by 40 to 100 feet. No measures have been instituted to control ice cover formation. Isolated instances of animals being trapped on the ice do occur and rescues have been made.

At the Revelstoke Hydroelectric Project in British Columbia, moose cross the impoundment ice with no apparent reluctance or difficulty when it is stable and generally avoid crossing when it is not. Many observations at this reservoir confirm that in almost all cases moose can climb out of the reservoir onto the ice after falling through weak spots. No ice related caribou mortalities have been noted at the Revelstoke Project. Woodland caribou readily cross the reservoir during the winter when ice conditions permit, individually or in groups of up to 20 animals.

Question No. 4 - Bank Erosion Due to Ice Movement:

The answers to this question dealt mostly

with the question of turbidity and not bank erosion. The report by Gatto (1982) was found to be the best source of information on bank erosion. Regarding turbidity, permissible levels are difficult to define and vary from province to province in Canada and from state to state in the U.S. Usually the levels are set for drinking water standards or human recreation standards and seldom for aquatic life.

The province of Ontario does not permit Secchi disc readings to change by more than 10%. Alberta's objectives suggest changes be less than 25 JTU's over seasonal natural background levels. These are drinking water standards.

The state of Michigan replied with information on maximum water surface fluctuations in impoundments for:

- o cold water rivers (salmon, char, trout, etc.) at 8"-10" per day
- o warm water rivers (bass, walleyes, etc.) at 12"-18" per day.

These criteria are based on experience in the state.

Many agencies stated that project operation results in turbidity increases over natural conditions during spring floods and ice movements but this is not within design control. The increase in sediment gives an apparent large increase in turbidity. However, turbidity changes due to project construction such as high velocity sediment sluicing operations, are more critical to fish. The agencies generally concluded that operational experiences gained each season, monitored by specialists, should be used to guide future operations.

Large amounts of bank erosion were experienced at Southern Indian Lake (Hecky, and McCullough 1984) as a result of wave action on an exposed permafrost shoreline. The Southern Indian Lake water level is nearly constant all year and the shoreline at one level is continually exposed to erosive forces from waves. The soils at Southern Indian Lake are predominately silty clay, with widespread permafrost at a depth of up to 10 m. The exposure of the permafrost to the warm water and waves melts the ice and creates "thermal niches" which contribute to

erosion. Soils eroded from the banks of Southern Indian Lake tend to stay in suspension and contribute to high turbidity levels because of their small grain size and low settling velocity. Additionally, the ratio of shoreline length to volume at Southern Indian Lake is very high compared to narrow deep reservoirs such as are proposed for Watana and Devil Canyon. Shoreline erosion which occurred at Southern Indian Lake would be expected to have a larger effect on suspended sediment concentrations than at narrow, deep reservoirs.

VISIT TO BRITISH COLUMBIA HYDRO AND PEACE RIVER TOWN

Officials of British Columbia Hydro in Vancouver and Alberta Environment in Peace River Town were visited. Information was obtained on operating policies of the W.A.C. Bennett and Peace Canyon Project and records of the flooding of Peace River Town which was related to wintertime operations of B.C. Hydro's upstream projects.

Conclusions regarding the effect of the Portage Mountain Development on Peace River ice conditions, are as follows:

1. Freeze-up staging on the order of several meters can result from consolidation of an ice front following severe flow fluctuations from a load following power plant.
2. This consolidation and associated staging can extend over a range of 100-150 km.
3. Such consolidations occur naturally to some extent, but can be more frequent and of greater magnitude with the higher winter power flows and if flow is fluctuated.
4. An important aspect of the freeze-up staging is flow surge from water released from storage under a backwater profile following consolidation of an ice front, resulting in unsteady flows which may be 1.5-2.0 times the steady flow.
5. The generally accepted procedure for operation in the vicinity of a sensitive area, is to maintain steady,

high power discharge while the ice front is passing through the area. Once the front is well upstream, and a competent cover has developed, which period may be 1-2 weeks depending on the air temperatures, load following operations can resume. The ice front is always subject to consolidation, but the sensitive area will be safe if the front is far enough upstream.

6. Break-up consolidation and jamming is much less controllable. Factors other than power releases can be more important, such as development of intervening flow from snowmelt, effects of tributaries, and rate of warming of air temperatures.
7. On the Peace River, the procedure on break-up seems to be to provide high, fluctuating flows as far as possible in non-sensitive areas. When approaching a sensitive area, it is desirable to reduce flow and hold steady until the front is downstream of the sensitive area.

SUMMARY AND CONCLUSIONS

The conclusions of this study are:

1. Reservoir operating procedures which are in use at other projects to mitigate downstream ice jam related flooding include:
 - a) Establishment of a stable ice cover on the downstream river early in the season during freeze-up. The ice cover should be high enough and strong enough to allow full flexibility of discharges throughout winter.
 - b) Operational procedures may also be employed to prevent hanging dams. These include inducing an early ice cover on the river upstream of known sites by artificial means, or by keeping powerhouse discharges low while the cover forms. Hanging dams may also be prevented in sensitive areas by fluctuating discharge to keep the ice cover broken up and downstream of the area.

- c) Measures to prevent release of ice from the reservoir to the river downstream. This ice, if released, could contribute to jamming downstream.

The Canadian Electrical Association and many plant operators indicated that powerhouse operations during the winter to maintain a stable cover would be site specific and require operating experience over a number of years. Reservoir discharge, climatic conditions, channel morphology, and water temperature are all variables which must be considered.

2. All respondents to the mail survey state that their organizations take no specific actions on their reservoirs to alter the state of ice on reservoir banks for wildlife safety reasons.

The Power Board in Sweden has provided reindeer bridges where "natural crossings" cannot be used. Two organizations indicated sporadic cases of deer drowning within ice-covered drawdown zones but have no quantitative or documented information. Usually, in Canadian provinces, animals have returned and crossed the reservoir prior to ice break-up. Others reported no problem of a similar nature. It was also noted that the freeze-up and break-up periods are dangerous times to cross the natural river.

3. All respondents except one state that their organizations take no actions to control cracks in reservoir ice cover that might be a hazard to animals.

A policy has been instituted at Lucky Peak Dam to minimize drownings of deer. This includes keeping the reservoir water level stable during the initial ice cover formation period, to prevent cracks or pockets of unsupported ice. Reservoir drawdown to required spring levels for flood control is accomplished either before initial ice cover formation, or after the cover has thickened sufficiently that the unsupported areas would be less of a hazard.

4. The report by L. Gatto (1982) indicates that local bank erosion can be expected in reservoirs which drawdown

continually in the winter. This is generally limited to the period during ice cover melt out when winds may blow the ice cover against the exposed banks. This would result in local increases in suspended sediments but would not affect the overall sediment load of the outflow significantly. Some erosion of bank material and vegetation removal also occurs in reservoirs with ice covers continually at one level because of thermal expansion and wind force induced "ice push" of the stable ice cover.

ACKNOWLEDGEMENT

This study was funded by the Alaska Power Authority and was carried out by the Harza-Ebasco Susitna Joint Venture. Particular thanks are given to all those respondents to the mail survey. The cooperation of British Columbia Hydro, and Alberta Environment is deeply appreciated, especially the help of C. V. Kartha and Les Parmly of the Hydrology Section of B. C. Hydro and Gordon Fonstad of Alberta Environment.

REFERENCES

- Alaska Power Authority, 1985, Before the Federal Energy Regulatory Commission, Application For Major License, Project No. 7114, The Susitna Hydroelectric Project, (Amended Draft) Exhibit E Chapter 2 Water Use and Quality, Section 3. Prepared by the Harza-Ebasco Susitna Joint Venture.
- Arctic Environmental Information and Data Center (AEIDC), 1983, Susitna Hydroelectric Project, Stream Flow and Temperature Modeling in the Susitna Basin, Alaska, for the Harza-Ebasco Susitna Joint Venture for the Alaska Power Authority.
- Gemperline, Eugene J., 1986, Hydrology and Hydraulic Studies For Licensing of the Susitna Hydroelectric Project, Proceedings of the Cold Regions Hydrology Symposium, American Water Resources Association, Fairbanks.
- Harza-Ebasco Susitna Joint Venture, 1985, Susitna Hydroelectric Project Survey of

Experience in Operating Hydroelectric Projects in Cold Regions, for the Alaska Power Authority.

Hecky, R.E., and G.K. McCullough, 1984, Effect of Impoundment and Diversion on the Sediment Budget and Nearshore Sedimentation of Southern Indian Lake, Canadian Journal of Fisheries and Aquatic Science, Vol.41.

Paschke, Ned W., and H. Wayne Coleman, 1986, Forecasting the Effects of River Ice Due to The Proposed Susitna Hydroelectric Project, Proceedings of the Cold Regions Hydrology Symposium, American Water Resources Association, Fairbanks.

Wei, C.Y., and P.F. Hamblin, 1986, Reservoir Water Quality Simulation in Cold Regions, Proceedings of the Cold Regions Hydrology Symposium, American Water Resources Association, Fairbanks.

Wu, Yaohuang, Joel I. Feinstein, and Eugene J. Gemperline, 1986, The Susitna Hydroelectric Project, Simulation of Reservoir Operation, Proceedings of the Cold Regions Hydrology Symposium, American Water Resources Association, Fairbanks.

**HYDROLOGY AND HYDRAULIC STUDIES
FOR LICENSING OF THE SUSITNA HYDROELECTRIC PROJECT**

Eugene J. Gemperline¹

ABSTRACT: The planning for and licensing of a major hydroelectric project require many hydrologic and hydraulic studies. These range from observations of existing conditions in the watershed, to estimates of project related effects on water use, water quality and impacts on the ecosystem. The number and breadth of these studies for a project located in a cold region is discussed. Examples of analyses used to predict changes to plants and animals resulting from the construction and operation of this major hydroelectric facility are presented. Hydrologic considerations in the design and operation of such a facility which are additional to considerations in a more temperate zone are included. For example, the effects of glaciers on streamflow and on sediment and the effects of ice on river stage and reservoir heat transfer are topics which are not addressed in temperate region hydro-projects. Evaluation of such a development in a cold region, therefore, requires the coordinated efforts of hydrologists, hydraulic engineers, fishery, wildlife and plant biologists.

(Key Terms: Cold Regions Hydrology, Hydroelectric Projects, Licensing, Environmental Impacts, Alaska Railbelt.)

INTRODUCTION

Project Description

The Susitna Hydroelectric Project has been proposed by the Alaska Power Authority to provide for the projected electrical

energy needs of the Railbelt region in the 21st century. The Railbelt region is the area of southcentral Alaska extending from Homer at the southern tip of the Kenai Peninsula to Fairbanks and including the large metropolitan area of Anchorage. The region is so-named because its principal cities are linked by the Alaska Railroad (Figure 1).

The project would consist of two dams, powerhouses and appurtenant facilities, to be located on the Susitna River about midway between Anchorage and Fairbanks. The upstream development at the Watana site is located 296 km (184 miles) upstream of the river's mouth at Cook Inlet. This dam would be an earth and rockfill structure and would be built in two stages. In the initial stage the dam height would be raised approximately 214 m (702 ft.) above its foundation to El. 617.2 m (2,025 ft. msl). A powerhouse with four turbine/generator units (units) having a total average capability of 440 MW at a discharge of approximately 340 m³/s (12,000 cfs) would become operational in 1999. This dam would be raised to El. 672.1 m (2,205 ft. msl) in the third stage of the project, following completion of the downstream dam. Two additional units would be added to the powerhouse increasing the total average generating capability of the Watana development to 1,110 MW at a discharge of approximately 650 m³/s (23,000 cfs). The two additional units would become operational in 2012. The downstream development at the Devil Canyon site is located 245 km (152 miles)

¹Manager, Hydrologic and Hydraulic Studies, Harza-Ebasco Susitna Joint Venture, 711 H St. Anchorage, Alaska, 99501 now at Stetson-Harza, 185 Genesee St., Utica, New York, 13501.

upstream of Cook Inlet. The dam at this site would be a thin concrete arch structure with a crest at El. 446 m (1463 ft. msl) 197 m (646 ft.) above its foundation. The downstream impoundment would extend to the upstream dam. The powerhouse at Devil Canyon would contain four units and have a total average generating capability of 680 MW at a flow of 430 m³/s (15,200 cfs). These units would become operational in 2005.

The Watana dam site is located in a broad U-shaped canyon and the Devil Canyon dam site is located in a narrow, steeply incised canyon. The Watana reservoir would provide the flow regulation for its own and the Devil Canyon powerhouses. The Devil Canyon dam would provide little flow regulation but would develop additional head. The Watana reservoir would impound 5.3x10⁹m³ (4.3x10⁶ ac-ft) of water in Stage I and 11.7x10⁹ m³ (9.5x10⁶ ac-ft) of water when it is raised in Stage III. The Devil Canyon dam would impound 1.4x10⁹ m³ (1.1x10⁶ ac-ft) of water (APA 1985).

History of Project

The proposed project is a result of a series of reconnaissance, prefeasibility and feasibility studies performed by various agencies of the Federal Government and the State of Alaska (Acres 1981). The initial reconnaissance level work by the U.S. Bureau of Reclamation (USBR) identified five damsites from a list of 25 as being most appropriate for further investigation. These sites were all located in the river reach upstream of the major confluences with the Chulitna and Talkeetna Rivers. These areas were considered appropriate because the site characteristics generally allow for high heads to be developed and substantial flow regulation to be achieved with dams located in relatively narrow canyons. Additionally, dams located in this reach would have less effect on the river's large anadromous fishery than dams at downstream sites. Later studies by the USBR, Alaska Power Administration and H. J. Kaiser Co. for the State of Alaska built upon the original USBR study with some slight refinements to the site locations. All proposed the Devil Canyon site as the initial damsite with upstream sites to be developed in the future. The

U. S. Army Corps of Engineers (COE) prepared comprehensive basin studies in 1975 and 1979 and proposed the damsites at Watana and Devil Canyon as the most appropriate. Following the COE's 1979 study the State of Alaska formed the Alaska Power Authority (APA) for the purpose of planning for the power needs of Alaska and developing the projects to meet the needs. The APA reassessed the previous studies and confirmed the conclusions of the COE. The initial License Application before the Federal Energy Regulatory Commission (FERC) was filed by the APA in 1983 (APA 1983). This application was amended to include refinements and staging the Watana dam (APA 1985). The latest application has recently been withdrawn in favor of a study of alternative energy sources for the region.

The Basin

The drainage basin upstream of the Devil Canyon site is located approximately between latitude 62°05' and 63°40' North and between longitude 146°10' and 149°30' West in south central Alaska, approximately 225 km (140 miles) north-northeast of Anchorage and 177 km (110 miles) south-southwest of Fairbanks (Figure 1). The drainage areas upstream from the Devil Canyon and Watana damsites are about 15,050 and 13,400 square kilometers, (5,810 sq. mi. and 5,180 sq. mi) respectively.

The basin is geographically bounded by the Alaska Range to the north and west, and the Talkeetna Mountains to the south and east. The topography is varied and includes rugged mountainous terrain, plateaus, broad river valleys and lakes. Mount McKinley (El. 6,194 m) is located on the northwest divide of the basin. Elevations within the basin upstream of the Devil Canyon site range from approximately 260 meters above mean sea level (850 ft, msl) at Devil Canyon site to over 2,100 meters, msl (7,000 ft. msl) near the head reach of the Susitna River.

Approximately 5% of this basin is covered by glaciers. Three major glaciers - West Fork Susitna, East Fork Susitna and Maclaren, exist in the basin. The landscape consists of barren bedrock mountains, glacial till-covered plains and

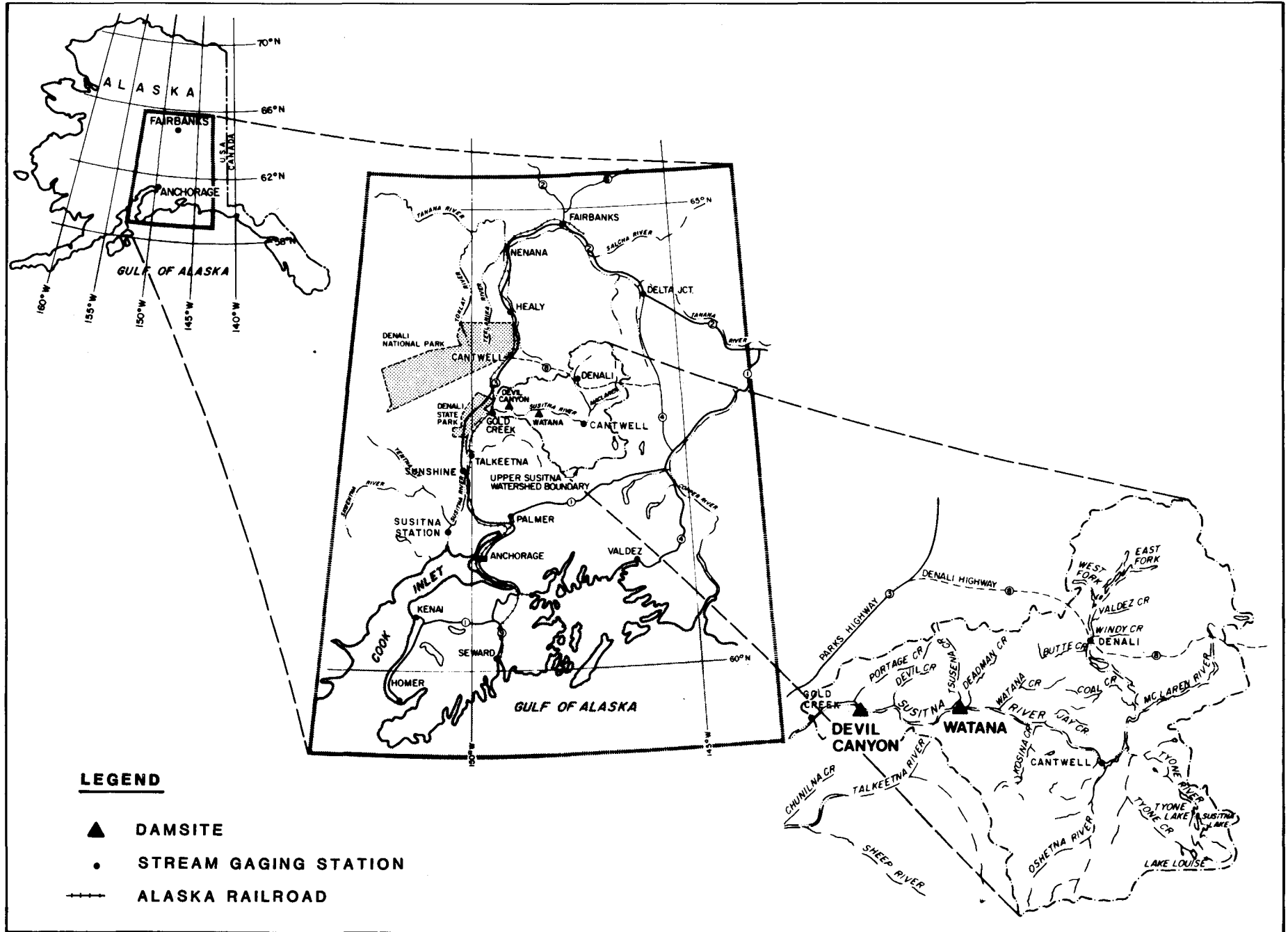


FIGURE 1

LOCATION MAP

exposed bedrock cliffs in canyons and along streams. Soils are typical of those formed in cold, wet climates and have developed from glacial till and out-wash. They include the acidic, saturated, peaty soils of poorly drained areas, the acidic relatively infertile soils of the forest and gravels and sands along the river. The basin is generally underlain by discontinuous permafrost.

The River

The Susitna River originates in the East Fork and West Fork Susitna Glaciers at an altitude of approximately 2,380 m (7,800 ft. msl) and travels a distance of about 512 km (318 miles) before discharging into Cook Inlet. The head waters of the Susitna River and the major upper basin tributaries are characterized by broad, braided, gravel flood plains below the glaciers. Several glacierized streams exit from beneath the glaciers before they combine further downstream. Below the confluence with the West Fork Susitna River, the river develops a split-channel configuration with numerous islands and is generally constrained by low bluffs for about 89 km (55 miles). The Maclaren River, draining the Maclaren Glacier and a few small lakes, and the non-glacial Tyone River draining Lake Louise and swampy lowlands of the south-eastern part of the basin, join the main river downstream of Denali. Below this confluence, the river flows west for about 155 km (96 miles) through steep-walled canyons before reaching the mouth of Devil Canyon. River gradients average about 0.3 percent in a 87 km (54-mile) reach upstream of Watana, about 0.2 percent from Watana to the entrance of Devil Canyon and about 0.6 percent in a 19 km (12-mile) reach between Devil Creek and the outlet of Devil Canyon.

The Susitna River is typical of glacial rivers with high turbid summer flow and low, clear winter flow. The discharge generally starts increasing during early May. The base flows during July through September are due to groundwater, glacial melt and melt of long term snowpack. Peak flows during this period are associated with general frontal type of thunderstorm activities. The river flow rapidly decreases in October and November as the

river freezes. The break-up generally occurs in early May. The May through June flows are caused by snowmelt combined with rainfall. Melting of snow, firn and ice from the glaciers has accounted for about 13% of the annual streamflow at Devil Canyon. The average summer and winter flows at a few selected stream gaging stations are given in Table 1. Figure 1 shows the locations of the stream gaging stations.

Project Operation

The project will operate by storing the high summer flows in Watana Reservoir to provide a dependable source of power in the winter for the Railbelt. The reservoirs will generally be full in late August or September and the Watana Reservoir will be drawn down throughout the winter. It will reach its lowest level in early May and begin to fill as river flows increase from snowmelt and rainfall. Filling will continue throughout summer until the water level reaches its normal maximum level. This can occur as early as late June in a wet year or as late as early September in a dry year.

When the reservoir is full, inflow in excess of power and environmental flow requirements must be released. High inflows in July and August may often exceed these requirements resulting in the need to release flows through outlet works to prevent the reservoir water level from encroaching on dam safety requirements. Table 1 compares natural and with-project flows for the Susitna River at Gold Creek for summer (May - September) and winter (October - April) periods based on 34 years of record and simulations of project operation (Wu et. al. 1986). Gold Creek is 26 km (16 miles) downstream of the Devil Canyon site and is the location at which environmental flow requirements will be gaged. There are no major tributaries between the damsites and Gold Creek.

Average monthly flows and floods during Stage I, II, and early Stage III would be similar. Energy demands are projected to increase in late Stage III and the summer flows would decrease accordingly.

Flood peak discharges would also be reduced due to the storage capacity of the Watana Reservoir as shown by Table 2.

Susitna River Gaging Station	Drainage Area	Summer (May - Sept)			Winter (Oct - Apr)		
		Natural	Stages I, II	Stage III	Natural	Stages I, II	Stage III
	(Sq. km)						
Near Denali	2,460	179	179	179	11.7	11.7	11.7
Near Cantwell	10,700	365	365	365	37.8	37.8	37.8
At Gold Creek	16,000	572	374	285	64.1	207	271
At Sunshine	28,700	1,380	1,180	1,090	153	296	360
At Susitna Station	50,200	2,680	2,480	2,390	354	497	561

Table 1. Average Summer and Winter Flows (m^3/s) at Selected Stream Gaging Stations for Natural and With-Project Conditions

Return Period (Years)	Natural ^{1/}		Gold Creek		Sunshine	
	Gold Creek	Sunshine	Stages I, II ^{2/}	Stage III ^{1/}	Stages I, II	Stage III
2	1,360	4,050	1,030	626	3,650	2,970
5	1,790	4,700	1,220	844	4,190	3,430
10	2,090	5,180	1,250	968	4,560	3,770
25	2,470	5,670	1,270	1,080	4,930	4,160
50	2,770	6,060	1,320	1,210	5,270	4,500

Table 2. Natural and With-Project Floods Susitna River (m^3/s)

^{1/} Annual series, occurs in May - June at Gold Creek and July - September at Sunshine.

^{2/} July - September series. Under natural conditions the highest peak floods occur in June as a result of snowmelt and precipitation runoff. Regulation of floods by the reservoir will delay the highest floods until the July - September period except in late Stage III. In late Stage III regulation by the project will be so large that July - September floods will be less than those in June.

Overview of Hydrologic Studies

The planning for and licensing of a major hydroelectric project require many hydrologic and hydraulic studies. The initial requirement, during the reconnaissance level studies, is for a reasonable estimation of streamflow quantity, time distribution and reliability. As the need for the project increases and the proposed sites must be screened to develop plans worthy of more detailed and costly investigation, the scope of the hydrologic studies must also increase. More accurate knowledge of flows is required in these prefeasibility level studies and potential project effects on the ecosystem must be more

accurately evaluated. For the feasibility and licensing level of work, the selected development will be compared to other projects on the bases of economic and engineering feasibility and environmental impacts. For a large, capital intensive project located in an ecologically sensitive area to survive comparison against smaller, less capital intensive projects with less visible environmental impacts requires accurate determination of the hydrologic resource available to produce energy and comprehensive studies of how project operation will affect the environment.

During feasibility and licensing of the project, hydrologic studies are carried out for three purposes: one, to develop

information on flows required to judge the project economics; two, to develop information necessary for the planning and preliminary design of project structures; and, three, to estimate potential project effects on the water resource and resulting impacts to humans, animals and plants which use the water.

From an engineering or project design standpoint there are many hydrologic considerations. The most important is the time distribution and reliability of river inflow and how this affects the need for active storage capacity in the reservoir. This was a factor in the selection of possible dam sites and in the scheduling of Watana dam construction ahead of Devil Canyon.

Other hydrologic considerations in design were the potential for glacial outbreak floods and the influence of mass glacial wasting on streamflows. The location of the project in a cold region with its great variation in summer and winter streamflows, the importance of snowmelt and glacier melt and the presence of glaciers which could surge or cause jokulhlaups has resulted in studies which would not be carried out in a more temperate climatic region.

The proposed project is located in a wilderness like area on a stream which supports a diverse anadromous fishery in a basin which contains much wildlife. The potential for affecting this ecosystem is an important issue and is addressed primarily by hydrologic and hydraulic studies coordinated with biologic studies. Such factors as the project influence on downstream flows, water temperature, sediment concentration, river ice regime, and dissolved gas concentration have been evaluated in great detail with hydrologic and hydraulic studies and have influenced the proposed project design and operation. Again, the breadth of these studies is larger in a cold region than in a more southerly area because of the occurrence of ice on the river and proposed reservoir, and its affect on water levels, river and reservoir temperatures.

Hydrologic studies will not end with project licensing. In fact, they will likely increase as project operators and fish and wildlife agencies seek to use the water resource to greater advantage. Efforts will be made to forecast reservoir

inflows (Hydex, 1985). Project effects on temperature, ice, sediment, etc. will be monitored and predictions made during licensing will be refined. Effects on fish and wildlife will be observed. Energy demand growth, now just a prediction, will occur. Project operation will need to be modified to meet the need for energy and to preserve and enhance the environment.

HYDROLOGIC STUDIES FOR PROJECT ECONOMICS

The hydrologic studies required to evaluate project economics center on three subjects: one, the quantity of flow in the river; two, the distribution of this flow throughout the year, and three, the reliability of this flow from year to year. These three factors along with the topographic features of a reservoir site (depth, volume, surface area) determine the average energy which can be generated, the reliable or firm energy, the amount of storage which must be provided in the reservoir and the manner of reservoir operation. The location of the Susitna Project in a cold region influences the three parameters.

The first parameter, average quantity of flow, is a function of precipitation, evaporation and transpiration since, over the long term, runoff must equal precipitation minus the other losses. This is largely controlled by the basins' geographic location, topography and large scale weather patterns. The main influences on the quantity of flow due to the cold climate, which are different than in a more temperate climate, would be the effects on evaporation and transpiration losses.

For the Susitna Project the estimation of streamflow quantities was relatively simple. The U.S. Geological Survey has collected streamflow information at a site near the proposed project since the potential project was first considered. Thus, thirty-four years of flow data are available (USGS, 1949-1984). These values were transposed to the project site using multi-site regression analyses (Harza-Ebasco 1985a).

While its location in a cold region may not affect the quantity of flow, the location does affect the distribution of flow within the year and the reliability

of flow from year to year. The location of the energy demand centers in a cold region also affects the demand for the power over a year and thus affects the project operation. In a warmer climate, such as in some areas of the 48 contiguous U.S. states, summer temperatures are typically hot enough to require air conditioning. These areas may experience their highest electrical energy demands in the summer. In contrast, the Alaska Railbelt has mild summers not requiring air conditioning. Winters are cold, long, and relatively dark resulting in highest electrical energy demands in December and January. This pattern of energy consumption is expected to continue in the future and contrasts with the pattern of streamflows.

The long period of subfreezing air temperature (October - April) results in extreme differences between summer (May - September) and winter streamflows. Average summer streamflows are 470 m³/s cfs compared to average winter flows of approximately 53 m³/s. Therefore, the Watana Reservoir must provide an active storage equal to 0.6 of the average annual inflow in order to provide a dependable capacity equivalent to 211 m³/s in the winter of a very dry year. While the extreme seasonal distribution of inflow results in the requirement of a large storage capacity, other factors offset this. These are the minimal net evaporative loss from the reservoir surface and the presence of glaciers and occurrence of long term snow pack. In effect, the river streamflow is regulated by the glaciers and snowpack. Studies were undertaken to estimate the net difference between evaporation from the reservoir surface and evapotranspiration from the same area under natural conditions (Harza-Ebasco 1985a). These established that net loss of water would be less than 0.1% of the annual inflow. Thus, this was not a factor in sizing the reservoir as in warmer climates.

Studies were also made to determine how the glaciers act to regulate streamflow (R&M 1981, 1982, Clarke et.al. 1985, Clarke, 1986). Although they cover only 5% of the basin they have a significant regulating effect. In wet years they tend to accumulate snowfall and in dry years they tend to waste. A study of the mass

balance of the glaciers was undertaken to determine whether there were any discernible trends in the glacier's behavior to indicate whether the streamflow estimates during the 34 years of record were influenced by any gain or loss of glacier mass. These studies were, by necessity, carried out on a reconnaissance level since the only aerial photos of the glaciers in 1949 were uncontrolled, and the only controlled photographs of the glaciers in 1980 comprised less than 5% of the glaciated area. Additionally, a reconnaissance level study of the glacier surface elevations was undertaken. These studies tended to confirm that the streamflow measurements were probably not unduly influenced by changes in the glacier mass (APA 1985). Studies were also made to determine the influence on project economics if the glacier melting were to diminish (Harza-Ebasco 1985b). These confirmed the project's viability even if the glaciers' mass balance were to change.

HYDROLOGIC STUDIES FOR PROJECT DESIGN

Basin hydrology affects the design of major project features in addition to reservoir size.

The most prominent hydraulic structure in a major hydroelectric project is the spillway or outlet works which must pass flood flows through the project without endangering the dam. In the Susitna Project there are two means for passing non-power releases. Outlet works controlled by fixed cone valves are planned at both dams to release all floods up to the 50-year event. Less frequent floods would be released through gated overflow spillways. The outlet works are provided so that the more frequent floods can be discharged to the river through the cone valves which disperse the flow over a large area and minimize the potential for elevated gas concentrations in the river downstream. High gas concentrations can be deleterious to the fish.

Hydrologic studies included development of the 50-year flood hydrograph for annual, spring and fall series and routing of these floods through the project reservoirs. These studies established the necessary outlet works and flood storage capacities (Harza-Ebasco 1985c).

Project spillways were designed to pass the Probable Maximum Flood (PMF) without endangering the dam as set out in guidelines of the COE and the U.S. Committee on Large Dams (COE 1965, USCOLD 1970). Hydrologic studies included estimation of the PMF hydrograph (Acres, undated) and routing of the PMF through the projects to establish required spillway capacities and surcharge levels (APA 1985).

An important factor in the PMF determination was the estimation of snowpack and the manner of snowmelt since the PMF would occur during the May-June period (Acres, undated). A probability approach was adopted to estimate the total snowpack during the event and snowmelt was assumed to occur in a manner to maximize runoff.

The PMF was estimated by assuming the maximum possible precipitation concurrent with a 1000-year snowpack and various antecedent conditions and the runoff routed through the basin. This is a standard, accepted method. However, in a glaciated basin, there is always the potential for a jokulhlaup or flood caused by the break-out of a glacially dammed lake. Discharges from such occurrences can be very high, potentially exceeding a PMF. Therefore, a survey was made to determine the potential for glacial dammed lakes which might affect the project (R&M 1981). The study indicated little likelihood of this.

Almost all large reservoirs are subject to some degree of sedimentation and the Susitna Reservoirs would be no exception. Hydrologic studies were made to estimate the suspended and bed load in the river (Knott and Lipscomb 1983, 1985) and to determine the effects on reservoir life (Harza-Ebasco 1984a, 1985d). The average annual sediment load of approximately 6.0×10^9 kg. (6.5 million tons) would require 1,400 years to fill Watana dead storage and 2,300 years to fill the Devil Canyon dead storage. The average suspended sediment concentration in the inflow is 800 mg/l and is comprised of a high percentage of very fine rock flour (27% less than 10 microns). This is the result of glacial weathering of underlain rock. This material has a very slow settling velocity (10^{-6} - 10^{-5} m/sec) and much is expected to remain in suspension in the reservoir. The trap efficiency of the

reservoir is expected to be about 80% - 90% (APA 1985) as contrasted to reservoirs of similar characteristics in areas with coarser sediment which have trap efficiencies near unity (USBR 1977). A mathematical model was developed, and is described below, to more accurately estimate the potential sediment concentrations downstream of the project, for estimating impacts to fish.

Another important project feature is the means of handling water during project construction. The diversion facilities will consist of tunnels to pass normal river flows around the construction areas and cofferdams at the upstream and downstream ends of the areas. These facilities will be sized using risk/cost analyses to minimize their cost and the potential losses resulting from failure. This means that cofferdam heights and tunnel sizes will be determined for various frequency floods to assign probabilities to the risk of failure. Another hydrologic consideration in diversion tunnel design is its elevation relative to the streambed and the potential for bed load material to become trapped in the tunnel, if it is set too low, thus reducing its capacity and affecting the hydraulics at the tunnel outlet. The Susitna tunnels have been located to prevent this (Wang, et. al 1986). The diversion facilities design must also consider the need to pass ice and the potential for ice jam floods. The diversion tunnel intakes at both Watana and Devil Canyon would be located on the outsides of bends for reasons of economy in tunnel construction. They are thus well located for passing incoming frazil ice in October and November and broken ice sheets in April and May (USBR, 1974). The tunnel sizes are believed wide enough (11 m.) to handle ice sheets during breakup. Nevertheless, careful consideration will be given to the intake design, to minimize potential jamming in this area.

Breakup jamming is also a potential problem downstream of the diversion tunnel. A bend in the river downstream of the tunnel outlet may provide a site for jamming of broken ice passed through the tunnel. Therefore, consideration was given to this and the downstream cofferdam crest elevation was set to prevent overtopping and flooding of the construction

site by water backed up behind the potential jam.

Other hydraulic considerations due to the project's location in a cold region are also primarily the result of ice. The design of the power intake towers includes heated floating ice booms to prevent ice forces on the trashracks and gates. The potential for entrainment of frazil and broken ice in the flow through the intake may dictate the submergence of the operating intake below the water surface at some times. However, as the intake has openings at several levels this will not preclude safe operation of the powerhouse.

HYDROLOGIC AND HYDRAULIC STUDIES FOR ENVIRONMENTAL IMPACT ANALYSIS

The primary environmental concern is the potential effect of the project on the downstream fishery. Other concerns include the project's potential effect on terrestrial wildlife and riparian vegetation. The mechanisms responsible for the potential impacts are the proposed project's effects on the quantity and quality of water in the Susitna River. The primary concerns relate to the potential impacts on river flows, floods, water temperature, river ice conditions, suspended sediments, turbidity, and river morphology.

Salmon utilize the peripheral areas of the river (such as sloughs which have favorable velocities, depths, temperatures, turbidities and substrates) for spawning, rearing and incubation. The amount of area available for fish use is related to the magnitude and stability of river flow. In conjunction with fisheries experts, who developed models of fishery habitat versus flow, the amount of habitat for all stages of project operation was estimated by simulating flows with project operation from initial construction to full use of project capacity, approximately 30 years (Trihey, et. al. 1985). Flow constraints were developed to provide fishery habitat of equal or greater value than natural conditions.

The quality of the water can also affect the fishery. For example, temperature can be lethal in the extremes or can affect fish growth. Suspended sediment can affect fish gills. Settling of

sediment in spawning beds can affect intergravel flow through these areas. Turbidity can provide protection from predators and can retard production of waterborne insects which provide food for the fish. The hydrologic and hydraulic evaluation of the effects of the Susitna Project on water quality were evaluated with a system of three models: a reservoir water quality model, a river temperature model and a river ice model.

Reservoir water quality was evaluated using the Dynamic Reservoir Simulation Model (DYRESM) (Imberger and Patterson, 1981). Modifications were made to the model to handle cold regions conditions and features of the Susitna Project (Harza-Ebasco 1984b Wei and Hamblin 1986). The model was modified to include:

- o Formation of an ice cover on the reservoir and winter stratification,
- o Outflow from the reservoir through multiple level offtakes, and
- o Simulation of suspended sediment including settling and the effect of sediment on density and thus, reservoir stratification.

This latter modification was necessary because of the small size of inflowing sediment and the need to estimate the downstream sediment concentration. A program of collection of hydrological and meteorological data was undertaken at Eklutna Lake (R&M 1985b) a small, glacially fed, lake-tap hydroelectric project near Anchorage to provide the data needed for development and testing of the modifications. Upon completion of testing, the model was applied to the proposed sites using hydrologic and meteorologic data collected for the purpose at the sites (R&M 1985a). Extensive studies were made, at the request of regulatory agencies, to provide information for evaluating impacts and to determine the most favorable method for operating the multi-level offtake.

Temperatures in the river downstream of the reservoirs were evaluated using the Stream Network Temperature Model (Theurer, et. al. 1984), driven by output from DYRESM. The modeled reach extended from the Watana and Devil Canyon dam faces to

Sunshine, 23 km (14 miles) downstream of the confluence with the Chulitna River a distance of about 160 km (100 miles). The potential for lethal temperatures to occur was found to not be a problem and the modeling effort focused on the potential for effects on growth. While the DYRESM model provided outlet temperatures on a daily basis, the SNTMP model was used on an average weekly basis. Several refinements were made to the SNTMP model as well (AEIDC 1983). These include:

- o Estimation of solar radiation from radiation incident at the edge of the atmosphere corrected for atmospheric and topographic effects,
- o Inclusion of frictional heating,
- o Inclusion of tributary temperature effects on mainstem temperature and regression modeling of tributary temperatures, and
- o Inclusion of air temperature lapse rates between the site of the temperature recorder and the upstream end of the study reach.

River temperatures were measured both in the mainstem and tributaries to allow calibration and verification of the model.

The SNTMP model was used to estimate river temperatures downstream of the reservoir throughout the year for all DYRESM simulations. In the summer the downstream end of the study reach was at Sunshine. Modeling of temperatures was not considered necessary downstream of that point because with-project temperatures were generally found to be within 1°C of natural. In the winter the downstream end of the SNTMP modeled reach was the location of 0°C.

Modeling of winter river conditions, with ice, was done using a model developed for the project (ICECAL) (Harza-Ebasco 1984c). This model computes the amount of ice produced, hydraulic conditions in the channel, development of border ice, formation of an ice cover from frazil ice and staging of water levels due to the ice cover. The model was used primarily to determine how peripheral habitat areas

would be affected by the increase in winter flows (from 60 m³/s - 250 m³/s) coupled with the change in the extent of ice cover. There was concern that increased water levels in the river area affected by ice would overtop peripheral habitat areas and introduce cold water into the sloughs thus stressing the salmonids. The results of the modeling allowed prediction of the impact, and development of mitigation measures.

During development and testing of the model an extensive program of field observations was carried out (R&M 1981-85) to develop information for verifying the model and to better understand the basic ice processes in the river.

Several other hydrologic studies were undertaken in conjunction with the evaluation of biologic impacts. A mailed survey was undertaken and a site visit was made to determine the experiences of other hydroelectric project operators in cold regions (Gemperline et. al. 1986). River-bed stability was evaluated to estimate potential aggradation and degradation (Harza-Ebasco 1984a, 1985e). This involved determination of bed load, bed material sizes and bed material transport equations. Impacts evaluated included the potential for aggradation near tributary mouths possibly affecting fish access and degradation in the mainstem possibly affecting peripheral habitat. Potential effects of project operation on riparian vegetation were evaluated using notes on vegetation types observed during river surveys. The observed elevations of various types of vegetation were correlated to river flows and floods. Based on a model of vegetation succession and predicted with project flood flows, the vegetation encroachment on the river was, to some degree, quantified.

CONCLUSION

This paper presents some of the more important hydrologic and hydraulic studies which have been made for the licensing of the Susitna Hydroelectric Project, including considerations because of the project's location in a cold region. For the purpose of the paper the studies were separated into those required for economic, analyses, engineering design and environmental impact analyses. However,

in reality, the studies were not separated. For example: the evaluation of fishery habitat and the establishment of minimum flows affected estimated project energy production; the design of power oftakes and release facilities affected estimated downstream water quality. Coordination was required between all participants to develop the information necessary for licensing of the project.

ACKNOWLEDGEMENT

The studies described in this paper were funded by the Alaska Power Authority. The studies were carried out by the Harza-Ebasco Susitna Joint Venture, R&M Consultants, Inc., the Arctic Environmental Information and Data Center, the U.S. Geological Survey and the University of Alaska Geophysical Institute. The support of all these organizations is deeply appreciated.

REFERENCES

- Acres American, Inc., 1981. Susitna Hydroelectric Project, Development Selection Report, for the Alaska Power Authority.
- Acres American Inc, undated. Susitna Hydroelectric Project, Feasibility Report, Hydrological Studies, Final Draft, Volume 4, Appendix A, for the Alaska Power Authority.
- Alaska Power Authority, 1983. Before the Federal Energy Regulatory Commission, Application for Major License, Project No. 7114, The Susitna Hydroelectric Project, prepared by Acres American Inc.
- Alaska Power Authority, 1985. Before the Federal Energy Regulatory Commission, Application for Major License, Project No. 7114, The Susitna Hydroelectric Project (Amended Draft), prepared by Harza-Ebasco Susitna Joint Venture.
- Arctic Environmental Information and Data Center (AEIDC), 1983. Susitna Hydroelectric Project, Stream Flow and Temperature Modeling in the Susitna Basin, Alaska for the Harza-Ebasco Susitna Joint Venture for the Alaska Power Authority.
- Clarke, T. S., D. Johnson, and W. D. Harrison, 1985. Glacier Mass Balances and Runoff In the Upper Susitna and Maclaren River Basins, 1981-1983, for Harza-Ebasco Susitna Joint Venture for the Alaska Power Authority.
- Clarke, Theodore S., 1986. Glacier Runoff, Balance and Dynamics in the Upper Susitna River Basin, Alaska, Thesis presented in partial fulfillment of the requirements for the degree of Master of Science, University of Alaska, Fairbanks.
- E. W. Trihey and Associates, 1985. Response of Juvenile Chinook Habitat to Discharge in the Talkeetna to Devil Canyon Segment of the Susitna River, for Harza-Ebasco Susitna Joint Venture for the Alaska Power Authority.
- Gemperline, E. J., D. S. Louie, and H. W. Coleman, 1986. Survey of Experience in Operating Hydroelectric Projects in Cold Regions, Proceedings of the Cold Regions Hydrology Symposium, American Water Resources Association, Fairbanks.
- Harza-Ebasco Susitna Joint Venture, 1984a. Susitna Hydroelectric Project Reservoir and River Sedimentation, for the Alaska Power Authority.
- Harza-Ebasco Susitna Joint Venture, 1984b. Susitna Hydroelectric Project, Eklutna Lake Temperature and Ice Study, with Six Months Simulation for Watana Reservoir, prepared for the Alaska Power Authority.
- Harza-Ebasco Susitna Joint Venture, 1984c. Susitna Hydroelectric Project Instream Ice, Calibration of Computer Model, for the Alaska Power Authority.
- Harza-Ebasco Susitna Joint Venture, 1985a. Susitna Hydroelectric Project, Case E-VI Alternative Flow Regime, Appendix D, Stream Flow Time Series, for the Alaska Power Authority.
- Harza-Ebasco Susitna Joint Venture, 1985b. Letter of June 4, 1985 to the Alaska Power Authority.

- Harza-Ebasco Susitna Joint Venture, 1985c. Susitna Hydroelectric Project, Flood Frequency Analyses for Natural and With Project Conditions, for the Alaska Power Authority.
- Harza-Ebasco Susitna Joint Venture, 1985d. Susitna Hydroelectric Project, Effects of the Proposed Project on Suspended Sediment Concentration, for the Alaska Power Authority.
- Harza-Ebasco Susitna Joint Venture, 1985e. Susitna Hydroelectric Project, Middle Susitna River Sedimentation Study, Stream Channel Stability Analysis of Selected Sloughs, Side Channels and Main Channel Locations, for the Alaska Power Authority.
- Hydex Corporation, 1985. Streamflow Forecasting Feasibility Study, for Harza-Ebasco Susitna Joint Venture for the Alaska Power Authority.
- Imberger, J. and J. C. Patterson, 1981. A Dynamic Reservoir Simulation Model - DYRESM: 5, in Transport Models for Inland and Coastal Waters, Chapter 9, Academic Press.
- Knott, James, M. and Stephen W. Lipscomb, 1983. Sediment Discharge Data for Selected Sites in the Susitna River Basin, Alaska 1981-1982, U. S. Geological Survey Open File Report 83-870 prepared in cooperation with the Alaska Power Authority.
- Knott, James, M. and Stephen W. Lipscomb, 1985. Sediment Discharge Data for Selected Sites in the Susitna River Basin, Alaska, October 1982 to February 1984 U. S. Geological Survey Open File Report 85-157, prepared in cooperation with the Alaska Power Authority.
- R & M Consultants, Inc, and W. D. Harrison, 1981. Susitna Hydroelectric Project Task 3 - Hydrology; Glacier Studies, for Acres American Inc., for the Alaska Power Authority.
- R & M Consultants, Inc. 1981-1985. Susitna Hydroelectric Project, Annual reports of Ice Conditions during Freezeup and Breakup, for Acres American, Inc. and Harza-Ebasco Susitna Joint Venture for the Alaska Power Authority.
- R & M Consultants, Inc, and W. D. Harrison, 1982. Susitna Hydroelectric Project; Task 3 - Hydrology; Glacier Studies, for Acres American Inc. for the Alaska Power Authority.
- R & M Consultants, Inc., 1985a. Susitna Hydroelectric Project, Processed Climatic Data, October 1983 - December 1984, for Harza-Ebasco Susitna Joint Venture, for the Alaska Power Authority.
- R & M Consultants, Inc. 1985b. Susitna Hydroelectric Project Glacial Lake Physical Limnology Studies, (Draft) for Harza-Ebasco Susitna Joint Venture, for the Alaska Power Authority.
- Theurer, F. D., K. Voos, and W. J. Miller, 1984. Instream Water Temperature Model, Instream Flow Information Paper 16, U. S. Fish and Wildlife Service (Draft).
- U. S. Committee on Large Dams, 1970. Criteria and Practices Utilized in Determining the Required Capacity of Spillways.
- U. S. Department of the Army, Corps of Engineers, 1965. Standard Project Flood Determinations, Engineering Manual No. 1110-2-1411.
- U. S. Department of the Interior, Bureau of Reclamation (USBR), 1974. Design and Operation of Shallow River Diversions in Cold Regions, REC-ERC-74-19.
- U. S. Department of the Interior, Bureau of Reclamation, (USBR) 1977. Design of Small Dams, (2nd ed.).
- U. S. Department of the Interior Geological Survey (USGS), 1949-1984. (Annual Reports) Water Resources Data for Alaska.
- Wang, B. H., S. R. Bredthauer, and E. Marchegiani, 1986. Design Problems in Gravel Bed Rivers, Alaska, Proceedings of the International Workshop on Problems of Sediment Transport in Gravel

Bed Rivers (In Press) 12-17 August
1985, Colorado State University.

Wei, C. Y., and P. F. Hamblin, 1986.
Reservoir Water Quality Simulation in
Cold Regions, Proceedings of the Cold
Regions Hydrology Symposium, American
Water Resources Association,
Fairbanks.

Wu, Y., J. I. Feinstein, and E. J.
Gemperline, 1986. The Susitna
Hydroelectric Project, Simulation of
Reservoir Operation, Proceedings of the
Cold Regions Hydrology Symposium,
American Water Resources Association,
Fairbanks.

ICE JAM FLOODING – EVOLUTION OF NEW YORK STATE'S INVOLVEMENT

Russell E. Wege¹

ABSTRACT: This paper outlines the development of New York State's involvement in assisting flood plain communities impacted by ice jam flooding. While this paper is neither a technical nor historical dissertation, the discussion illustrates the state's process by which state-of-the-art technology has been translated and communicated to village, town and city officials. This training effort has encouraged local government to help themselves and has substantially reduced the number of requests for federal and state assistance.

(KEY TERMS: involvement; ice jams; training.)

INTRODUCTION – BACKGROUND

The many large rivers in the northeastern United States encouraged colonial settlement in the floodplains. Nineteenth century industrialization and development brought a constant flow of immigration and the expansion of villages and cities in the floodplains. The transformation of forest land into agriculture and settlements modified both fluvial flow and ice related problems.

Records of fluvial flooding go back to in the colonial period. In New York State, ice jam flooding began to be recorded in the latter half of the 19th century. After the U.S. Department of Interior's stream gaging program was expanded, early in the 20th century, ice jam flooding was more frequently reported. Continued development in the floodplains increased the frequency of ice jam flooding and rapidly expanded the record of ice jam problems.

Economic development in New York State included several large public works projects that affected ice jam and fluvial flood events. Ashokan, the largest of several New York City water supply reservoirs, was completed in 1915. The 500-mile barge canal system, with its summit level storage reservoirs and control structures, was completed in 1918. The 42-square mile Great Sacandaga Reservoir, which regulates flow in the upper Hudson River, was completed in 1930. In addition, many private and utility-owned hydro projects were constructed throughout the state during the first quarter of the 20th century.

With the exception of the Great Sacandaga Reservoir, none of these projects was constructed specifically for flood control

purposes, although all had an important and mitigating impact on ice jam problems. These large pools of water stopped the moving ice from causing downstream jams and reduced frazil ice production by regulating stream flow. In addition, rivers channalized for navigation eliminated obstacles that previously had triggered ice jams.

New York winters may be described as ranging from moderate to severe. The up-state area, away from the coastal influence, annually receives 60-180 inches of snow. Winter months commonly record sub-zero temperatures. It is not uncommon for night temperatures to drop to -20°F and, on occasion, to -40°F in the mountain valleys.

Almost annually, New York will experience a mid-winter thaw during the 4th week of January. Temperatures will often rise into the 40's and even the 50's and sometimes last for several days. The mid-winter thaw can cause streams and rivers to rise, breaking up their ice cover. The ice begins to run, only to jam, flooding roads and, on occasion, forcing evacuations.

HISTORY OF STATE INVOLVEMENT

Until the mid 1930's, ice jam and fluvial flooding were considered a local problem and not a specific state issue. However, the great floods of 1935 and 1936 overwhelmed countless river communities and cities in several northeastern states. As a result, federal and New York State legislation in 1936 provided authority to develop local flood protection projects in severely damaged communities. Flooding problems were longer ignored by federal and state government.

The success of this legislation is reflected in the statistics. Over 80 flood control projects involving construction of 142 miles of improved channels and 105 miles of levees and walls have been constructed in New York over the last 45 years. However, New York's 1936 legislation limited state involvement to a cooperative partnership with the U.S. Army Corps of Engineers. The state does not have standing authority to construct flood control projects unless they are approved

¹New York State Department of Environmental Conservation, 50 Wolf Road, Albany, NY 12233-0001.

federal projects. There are 1480 communities that have been identified as being flood prone along the thousands of miles of rivers and tributaries in New York State. However, almost all of these communities will never qualify for a federal flood protection project and therefore, remain subject to ice jam and fluvial flooding events.

Without a legislative mandate for involvement, ice jam problems from the late 1930's to the late 1960's were viewed by the state as little more than winter statistics. This attitude was soon to change. A reorganization of state government in 1967 led to the development of a flood control bureau in the State Conservation Department. The new bureau had a small professional staff and was responsible for flood response training, operation and maintenance of flood control projects and advocating new federal projects on behalf of flood-damaged communities.

The first flood control project to address ice jam flooding was in the rural community of East Branch in the Delaware River Basin. During the winter of 1971 an ice jam so threatened the community that it made international news. The crisis was met jointly when the Army Corps of Engineers built an emergency levee on the right-of-way expeditiously obtained by the state.

The quick solution to the East Branch ice jam problem was unusual. More commonly, when communities made requests to the state for ice jam removal, the requests were simply forwarded to the Corps of Engineers. It was hoped that the federal agency would solve the problem. Rarely did that happen. However, the Corps usually did send a representative to look at the problem. The Corps soon realized that many of the requests were for minor ice jam problems that were not a serious threat to the health and well being of the community, so it began to develop criteria for federal involvement.

Eventually, the criteria authorized federal involvement in ice jam breaching only as a supplement to state, county and local efforts. This required local governments "to exhaust" local resources before federal involvement was authorized. However, the state did not have legislative authority, aside from state emergency powers, to spend money on ice jam problems and county governments were under similar restraints.

Since adoption of this federal policy several years ago, only two ice jam problems in New York State have qualified for federal intervention. Both cases took several weeks to satisfy federal requirements. The Corps policy has essentially eliminated federal involvement in ice jam mitigation work and has forced the state to be more responsive.

The Flood Control Bureau in the newly organized State Department of Environmental Conservation began to respond to community requests for assistance by sending a flood control engineer to look at the problem and offer technical assistance. By December of 1976, it had become official state policy to provide technical assistance to communities having ice jam problems.

It was during the early 1970's that an understanding of the causes of ice jams and the techniques to alleviate ice jam

flooding developed. This learning process was greatly enhanced by the cooperation of personnel from the Corps of Engineers Cold Regions Research and Engineering Laboratory in Hanover, New Hampshire.

By the mid 1970's, community requests for state assistance had become overwhelming. There were simply not enough experienced people to meet the need. This led to the development of a state training program, which has as its goal the development of field personnel trained in ice jam problems and mitigation measures. With more people trained, the state could respond more promptly with sound technical assistance.

Over the years, the training sessions have increased in frequency and improved in content. State field personnel invited local emergency management and community officials to attend the training sessions, which are held throughout the state. Class size is usually 20 to 30 people, but as many as 100, have attended these sessions. A brief description of the material covered in the training sessions is as follows.

TYPES OF ICE JAMS

Ice problems are dependent upon several factors: frost depth, amount of snow in the basin, amount and intensity of a rain storm, severity of winter temperatures, and rate of temperature rise. These factors play an interrelated role. Annual variances of any one of these conditions can spell the difference between major ice jam problems and no problem at all. Ice problems fit into two general categories:

A. *The warm weather breakup.* Runoff from a thaw or rain storm feeds water into the tributaries and rivers. The ice/ground contact weakens and begins to fail. Continued inflow begins to raise the ice sheet or inundate it, introducing upward forces. The ice sheet becomes unstable and begins to move and break up. The breakup develops into an ice run and will begin to move downstream until it meets an obstruction. There, the run will stop, back up water and usually breach. This is a true ice jam, where a jam forms and breaches, only to jam again downstream. This happens countless times each winter as small streams discharge into major river systems.

In general, high gradient streams will loose their ice cover sooner than low gradient streams.

B. *Cold weather blockage.* The most common and troublesome form of ice is called frazil. Research (Ice Engineering, 1982) has determined that ice nuclei crystals develop in waters moving 2 FPS or greater in an atmospheric environment of 20°F or less. These crystals are very cohesive and join together to form frazil. Frazil ice will stick to most objects. It forms collars around rocks and piers and sticks to the stream beds and banks. It adheres to broken pool ice and often forms masses greater than 10 feet thick in our larger rivers.

Hydro electric generation, with daily releases in cold weather, is a magnificent frazil ice generating machine. As an example, hydro generation on the West Canada Creek in Central New York annually produces frazil ice that fills a one-mile reach of a 300-foot wide channel to a depth of 8-15 feet. The resultant high water surface increases local ground-water depth and causes wet basements at Herkimer, a village some 25-miles downstream from the power dam.

Frazil ice can also develop into a hanging dam. This phenomenon usually occurs in a pool at the end of a rapids section in larger rivers. Frazil ice develops in the higher energy upstream reach and moves into the low velocity pool where it begins to float to the surface. The ice covered pool begins to collect frazil under the sheet ice. The hanging mass of ice severely restricts river flow, causes bottom scour, and often produces upstream backup and localized flooding.

Hanging dams are usually massive. One can assume that such ice blockages are the last to shear during the mid-winter or spring breakup. This stability often creates an obstruction that can quickly plug the restricted channel and produce a rapid backup of the river.

CAUSES OF ICE JAMS

- A. *Changes in stream slope.* New York is a headwater state. Many rivers originate in its mountain areas. Steep sloped streams produce both frazil and pool ice. The mid-winter or spring thaw can produce a runoff that rapidly breaks up the ice cover on these upland streams. Broken sheet ice and large masses of frazil ice move down the river system in a series of jams and breaches until the ice reaches the floodplain of a large river. Often the slope of the tributary flattens out at this point and the stream velocity decreases. The drop in velocity causes the larger pieces of ice to ground out which commonly triggers a jam in the tributary.
- B. *Bridge piers.* New York State has many old bridges with massive stone or concrete piers that are spaced closely together. These piers frequently catch large pieces of solid sheet ice and trigger jams behind the structure. Replacement structures now include more widely-spaced, piers which offer a higher probability of breaking or crushing of large pieces of ice, allowing them to continue down river.
- C. *Sheet ice.* New York State is blessed with over 7,000 lakes and ponds. In addition, hydropower development has created many run-of-river pools. Each pool, either natural or constructed stops ice. A jam will often occur at the point of entry. Usually, the backup is minor because the water will circumvent the jam and find entry into the pool at a nearby location. Lakes, reservoirs and ponds are especially beneficial in mitigating ice damage because they prevent moving ice from traveling further downstream.

- D. *Sharp bends.* The geometry of the stream channel is another factor causing ice jams. A river channel that suddenly loses one fourth of its width at a sharp bend has a high probability of stopping an ice run and plugging the channel. Flooding is the inevitable result.

- E. *Man-made obstructions.* Aside from bridge piers many New York rivers have other man-made obstructions. The 19th century timber industry drove countless wooden piles into river beds to anchor log booms. Thousands of these piles remain today and are capable of catching ice. In addition, stone filled wooden cribs and derelict dams dot the river beds in mountain rivers and streams. These also play a part in triggering ice jams.

- F. *Modified channel.* This type of problem could be classified as a man-made obstruction, but it is better discussed as a separate cause of ice jamming. It is usually associated with a new road bridge. Design engineers, intent on accommodating a high rate of flow, will widen the channel immediately above and below the structure. Such a change in stream bed geometry can have embarrassing and sometimes devastating results. The widened channel will often reduce stream velocity to the degree where the ice run may ground out and result in a jam at that point.

Several years ago the writer observed an ice jam in the Village of Mohawk that was almost 20 feet high and did enormous damage to many private homes. It was caused by doubling the width of a high gradient stream under a replacement bridge. The jam never touched the bridge but forced ice well above the elevation of the bridge railing.

This type of problem can be mitigated by including a low flow channel through the modified channel section. The low flow channel concentrates stream flow offering a good prospect for passing an ice run.

- G. *Combinations.* Rarely is there a single cause for an ice jam. It is not uncommon that three or even four causes are present. In addition, the triggering mechanisms can be spread over an extensive distance in large rivers. These possibilities need to be considered carefully prior to initiating any action.

WHAT GOES INTO A DECISION TO "DO SOMETHING"?

A very important part of ice jam training is to convey to local governments that federal and state agencies will not respond by breaching ice jams. Therefore, instead of focusing on big government resources, which are not there, local governments must turn to and focus on their own resources. Repeated communication of this message is changing the thinking of local interests and reduces the number of requests

for ice jam assistance. The federal and state government can be relied upon only for technical assistance.

Secondly, it is important to evaluate the damage potential of the ice jam. For example, does the jam threaten the property and well-being of a substantial number of people? A judgment concerning property damages must be made. It is one thing to worry about a few wet basements and it's another to evacuate a subdivision, cut off a hospital or shut down a major employer.

Finally, a judgment concerning public utilities and facilities such as roads must be made. The flooding of a low usage, rural town road is nowhere near as disruptive as flooding a primary road system.

State and federal technical assistance can assist a community in evaluating damages or potential damages. However, the decision to take action remains with local officials. The training sessions emphasize that point.

WHAT CAN BE DONE TO ALLEVIATE ICE JAM FLOODING?

The evaluation of what caused the jam and the significance of damages leads to the question, "what can be done to alleviate ice jam flooding?" A decision to "do something" costs money, requires time and planning, and incurs a certain degree of risk. Often the practicality of "doing something" is limited. The community which sends its public works personnel to the river's edge to throw dynamite onto the ice has no chance for success, although it may reap certain public relations benefits. Likewise, a community that faces a several mile long jam in a major river has little hope of success if it tries to breach the jam.

Let's look at the more realistic alternatives for alleviating damages.

A. *Raise or remove damage-prone materials and equipment.* If something can be moved out of harms way the recommendation is simple. As example, the writer advised the management of a paper company, which had stored \$1,000,000 worth of paper inventory on the riverbank, to relocate the inventory when an ice jam backed water to within two feet of the material.

B. *Emergency measure at the riverbank.* Often a jam will fill or even overflow the river channel. The top of the ice may be above the riverbank. Its massive extent precludes attempts to breach it. A temporary levee separating the river from the community will reduce damages and is a logical mitigation measure, provided the length of levee needed is not prohibitive. Planning time is required for this alternative, and it is particularly appropriate after a mid-winter breakup when there is a heavy snow pack which increases the danger of flooding in a spring runoff.

C. *Evacuation/Flood insurance.* All riverside communities should have emergency management plans. Such plans should include river stage elevations and indicate when evacuations are to begin. Evacuation is often the only feasible alternative to minimize the impact from ice jam flooding.

Public education and availability of flood insurance can minimize personal property losses. In New York State approximately 1460 of the 1480 flood-prone communities are participating in the National Flood Insurance Program. Eligibility for this program allows individuals to purchase insurance protection against flood damages.

D. *Ice jam breaching.* Our experience indicates that the best chance for successfully breaching a jam is to attack the jam immediately after it has formed. Methods of breaching a jam are outlined below. These methods are most applicable to small and moderate width rivers.

1. *Mechanical.* Many New York tributaries and rivers are shallow and have a stony bottom. We have found that the most effective way of breaching an ice jam in these shallow, hard bottom rivers is with bulldozers, beginning downstream and progressing upstream through the jam. It is not necessary to clear the entire river channel of ice. Construction of a pilot channel through the blockage is sufficient to breach the jam.

Clamshell buckets have also been used successfully in the area near bridges or along short stream reaches. The Town of West Seneca near Buffalo, New York, contracts for a small crane with a clamshell bucket during the winter months. As the ice begins to run, the contractor responds on short notice to the known ice jam location behind a shopping center. The equipment operator simply keeps the ice moving where it tends to ground out on a bar.

2. *Explosives.* Through the years, there has been much misuse of explosives by many communities attempting to breach ice jams. Research (Ice Engineering, 1982) by the Army Corps of Engineers has developed extensive information on the best way to breach ice jams with explosives. Briefly, the following principles should be followed when this alternative is considered.

a. Explosives must be placed under the ice. Explosives break ice by forming a gas bubble under the ice. The gas bubble lifts the ice, causing it to fail in shear.

- b. Blasting operations must be under the direct supervision of a licensed blaster.
- c. Blasting operations must begin at open water downstream of the problem area. This will allow broken ice to float away and results in a clean channel through the jam.
- d. Streamflow must be sufficient to carry away ice debris.
- e. Blasting should not be considered near structures. Several years ago the writer was informed of an incident that resulted in litigation after a village begin ice blasting operations near a greenhouse.
- f. Moderate temperatures are desirable. Cold weather will cause rapid refreezing of ice debris.
- g. Downstream effects need to be considered. Blasting may instantly release a large volume of water. Usually, such releases become insignificant a short distance downstream, but, if a downstream community experiences flooding from a high river stage coincidental to up-river blasting, litigation may result. The burden of proof will rest on the community doing the blasting.

3. *Dusting.* Dark material spread thinly over sheet ice will successfully weaken the ice, causing it to fail at the beginning of breakup, thus reducing the chances of its obstructing an ice run. However, dusting is not effective in breaking a mass of frazil or a true ice jam. The melting of a few inches of frazil or the top of a jam several feet thick has no effect on breaching the blockage.

4. *"Ducks."* The City of Buffalo has an amphibious vehicle. It has been used successfully to break up ice in the Niagara River. It has also been used to breakup competent sheet ice on low-gradient small streams. Success depends upon the availability of downstream open water and sufficient depth and flow to float the broken ice away. Without sufficient depth and flow, the machine will simply break the ice and push it into the mud, possibly increasing the ice jam potential.

5. *Imaginative solutions using reservoirs and hydro plants.*

- a. Reservoir releases for flushing out river ice have been suggested for years. Usually, these suggestions are made by laymen when considering a course of action to breach a troublesome ice jam. Only recently has the suggestion been developed into an apparent workable plan of

action for ice control. CRREL (Ferrick, 1985) is studying this technique in the Lake Luzerne/ Corinth reach of the upper Hudson River in eastern New York. Releases originate from the Great Sacandaga Reservoir through a cooperative effort with the owner of the reservoir, the Hudson River Black River Regulating District and the Niagara Mohawk Corporation, the regional electric power supplier. The purpose of the release is to break up and flush out early winter sheet ice in order to prevent development of thick sheet ice that may stop an ice run.

- b. Reservoir releases may also be employed to breach an ice jam. Water in deep reservoirs will be warmer than river water. A reservoir release introduces heat into the river system which widens the passage ways through the ice jam. Eventually, the roof of the ice jam will collapse thus, breaching the obstruction.

- c. New York's larger mountain rivers have numerous low-head hydro plants. On one occasion, near Corinth in eastern New York, a breach was accelerated when the pool containing an ice jam was lowered several feet. The drawdown introduced additional stress through the blockage and accelerated its breaching.

E. *Overflow channel.* Ice jams sometimes can be bypassed as a mitigation measure. Bypassing eliminates the expense of attempting to breach the blockage. Maintenance costs of a bypass channel may be minor compared to the cost of efforts to breach recurring jams.

A bypass channel involves the removal of trees and woody growth and the grading of a high flow channel downstream of a damage-prone area. A small bypass channel has been constructed by the City of Norwich, in central New York, as an outcome of the state ice jam training session. In addition, the Philadelphia District of the Army Corps of Engineers is planning a major bypass channel to protect the twin communities of Port Jervis, New York, and Matamoras, Pennsylvania, on the Delaware River. Three other bypass channels have been recommended by New York State engineers but have not been constructed as of this date.

Design criterions for ice jam bypass is in its infancy. The following design guidelines are suggested. The bypass channel should have a width between one-half to full channel width for rivers up to 200 feet wide. The width of the bypass channel can be substantially smaller than the natural channel for larger rivers. The entrance into the bypass channel should be wider than the bypass channel in order to insure bypass if jamming occurs at that location. The invert into

the bypass channel should be of sufficient elevation to exclude normal flow rates. Ideally, this elevation should be high enough to prevent masses of frazil ice from entering the bypass and low enough to accommodate a high water flow rate without damaging the upstream community.

- F. *Ice booms.* Aside from the large booms at the entrance of the Niagara River and in the St. Lawrence River, only one ice boom has been installed in New York State for ice control. Unfortunately, that boom was severely damaged by a late fall flood and is not operational at the present time. The boom is located in the upper Hudson River at Hadley and was constructed by state and local governments under the technical guidance of CRREL.

Ice booms are inexpensive structures that encourage development of upstream sheet ice. Sheet ice deters frazil development and is a barrier to an ice run. Favorable ice boom locations are at the downstream ends of pools, upstream from damage-prone areas.

SUMMARY

The success of ice jam training cannot be accurately determined. However, as a result of such training, many communities are recognizing state and federal limitations and, based on a better understanding of the causes of ice jams, are taking action to mitigate their ice jam problems. Local communities have removed channel obstructions and, in one case, have even constructed a bypass channel. In another community an ice boom was installed. In addition, approximately 1,460 flood-prone communities participate in the National Flood Insurance Program. State training has contributed significantly to an understanding and awareness of ice jam flooding. As a result, reports on ice jam problems and requests for state and federal assistance have steadily declined.

REFERENCES

- Ferrick, M., L. Lemieux, L. Gatto, and Mulherin, 1985. Hudson River Ice Management. 42nd Eastern Snow Conference, Montreal, Canada.
- Ice Engineering, Engineering and Design, 1982. Department of the Army Corps of Engineers Office of the Chief of Engineers, Ice Formation and Characteristics, pg. 2-2, October 15.
- Ice Engineering, Engineering and Design, 1982. Department of the Army Corps of Engineers Office of the Chief of Engineers, Ice Jams, pp. 3-3 to 3-5, October 15.

**HYDROLOGICAL AND ECOLOGICAL PROCESSES IN A COLORADO,
ROCKY MOUNTAIN WETLAND: CASE STUDY**

Edward W. Rovey, Catherine Kraeger-Rovey, David J. Cooper *

ABSTRACT: Wetlands of Cross Creek exist in the vicinity of and are controlled by flows in the main channel. Water levels in the creek have a seasonal cycle dominated by snowmelt runoff. Groundwater levels in the wetland rise and fall in response to water levels in the main channel and levels in the tributaries affected by backwater from Cross Creek. Vegetation communities have developed at locations in the wetlands related to depths of standing water or depths to ground water. Stream meandering also affects the wetlands. Large diversions of summer runoff proposed by the Homestake II will lower water levels in Cross Creek. Distribution of wetland plant species will change in response to the diminished creek water levels.

(KEY TERMS: wetlands, groundwater, snowmelt, vegetation communities, water levels.)

INTRODUCTION

Wetlands of the Cross Creek Valley exist high in the Colorado Rocky Mountains where the controversial Homestake II water diversion project is proposed (see Figure 1). The project is planned to annually divert 25 million cubic meters (20,000 acre-feet) of water from the Holy Cross Wilderness Area. Eleven miles of tunnels are planned beneath 4,270 meter (14,005 feet) high Mount of the Holy Cross to carry

snowmelt runoff to an adjacent watershed where existing storage and tunnel facilities will be used in the transbasin diversion of water to the cities of Colorado Springs and Aurora.

A general definition of wetlands is an area where soils are saturated for a duration and frequency that allows the establishment of vegetation adapted to saturated soil conditions. Federal law and Executive Orders are intended to regulate filling operations within wetlands.

This paper is written by the professional consultants retained by the Holy Cross Wilderness Defense Fund, a nonprofit organization, to evaluate the potential impacts of the project on wetlands. While the project proponents claim there will be no impact to wetlands below diversion points, it is our opinion, based upon research and evaluation completed to date, that removal of up to ninety percent of the natural streamflows at diversions will have significant, adverse impacts to wetlands downstream.

METHODS

Hydrologic and hydraulic calculations have been made of pre- and post-diversion flows (Sundeen and Fifer, 1981) from historical records at the creek mouth and projections into the upper basin. Stream

* Rovey and Kraeger-Rovey, hydrologists, Terra Therma Inc., 2927 W. 36th Ave Denver, CO 80211; Cooper, ecologist, 3047 Redstone Ln., Boulder, CO 80303

hydraulics were calculated using direct step backwater and uniform flow methods, channel slope, typical channel cross sections and reasonable flow resistance parameters. Groundwater hydraulic calculations were made with parameters obtained from a brief field investigation and seven laboratory tests of permeability from one wetland (Ward, 1983). Water table responses were analyzed using a standard drain algorithm.

AREA DESCRIPTION

Snow and snowmelt control the hydrologic regime of Cross Creek wetlands and surrounding areas. Eighty percent of the annual runoff occurs from late May through July (USGS, 1984). Though the region is cold due to the high elevation, there is no permafrost in the area. In fact, the wetland surface may not freeze due to the early, insulating covering of a snowpack. Wetland characteristics and those of surrounding areas are listed in Table 1.

Montane wetlands, as described by Kilburn (1983) and considered in this report, occur at locations where geologic outcrops have created erosion-resistant features that obstruct the gradient of the stream. Soils in the wetlands are

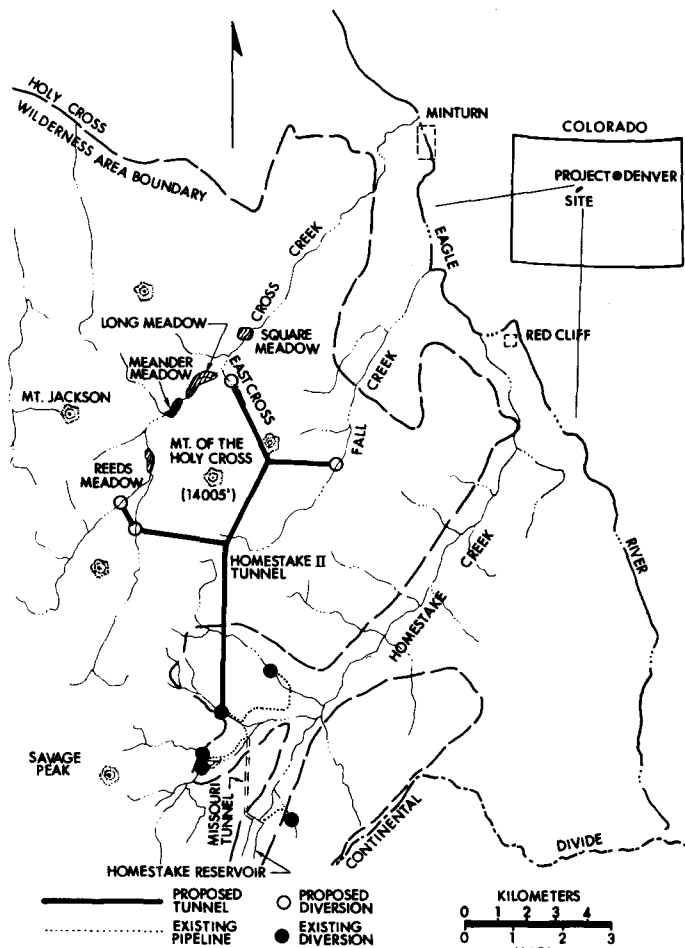


Figure 1. Wetlands and Vicinity Map

Twenty four homogenous stands of vegetation were selected, sampled and classified using standard Braun-Blanquet methods (Westhoff and van der Maarel, 1978). Depth to water table was measured in each stand. Gradient analysis, using the methods of Dix and Smiens (1967), was used to analyze the behavior of species along the water table/drainage gradient regime. Plant species nomenclature follows Weber (1976).

TABLE 1. Description of the Area

Wetland Elevation Range	2,900 to 3,070 m. (9,500 to 10,060 ft)
Mean Annual Precipitation	50 to 125 cm (20 to 50 inches)
Cross Creek Drainage Area	8,675 hectares (33.5 square miles)
Annual Runoff Volume	71 million cu. m. (58,000 acre feet)

primarily composed of silts with little clay-sized material (Ward, 1983).

Main stream channels have meandered across the wetlands leaving buried remnants of material varying from large boulders and gravels to some lenses of clay material. Slopes across lateral sections of the wetlands are nearly flat. Close inspection of the wetland surface reveals the existence of numerous tributary channels extending from the main channel of Cross Creek to the valley walls.

Six major communities comprise the bulk of the wetland vegetation. These are: (1) Ranunculus tricophyllus (water crowfoot) - Sparganium sp. community in shallow water averaging 10 cm in depth, but intermittently exposed during summer and fall; (2) Carex utriculata (bladder sedge) community is one of the most abundant communities in the wetlands. It

occurs in both marshes with mineral soils and fens with largely organic soil. Depth to water table averaged 16 cm; (3) Carex aquatilis (water sedge) community occupies a variety of habitats and was observed at an average depth to water table of 31 cm; (4) Calamagrostis canadensis (Canada reedgrass) community occupies sites with an average water table depth of 56 cm; (5) Calamagrostis canadensis - Mertensia ciliata (bluebell) community occupies the tops of levees and is characterized by coarse herbaceous dicots. Average water table depth was observed at 65 cm; (6) Salix planifolia (plane-leaf willow) community occupies the most well drained sites in the wetlands with an average water table depth of 70 cm.

RESULTS

WATER SOURCES AND TIMING

Snowmelt is the primary source of water to the wetlands. Snowmelt can be subdivided into components dependent on location and timing of the melt. Primary components are: onsite snowmelt, sideslope runoff and main channel flows. The other component contributing to wetland water sources is the growing season precipitation, i.e., rainfall, falling directly on wetlands.

Snowmelt on the wetland surfaces at 3,050 meters (10,000 ft.) elevation commences during early May (Kraeger-Rovey and Rovey, 1984). Melt calculations and observations indicate the 43 cm (17 in.) average water equivalent snowpack on the wetland surface can melt in two to three weeks. Using 7 deg. C (45 deg. F) as an indicator of the commencement of growth (SCS, 1970), the onsite snow melt is completed on the wetlands prior to wetland plant growth. This early snowmelt replenishes soil moisture deficiencies that are carried over from the previous growing season and is an adequate quantity to raise the shallow water table to the surface of the wetland. However, an adequate quantity of water is necessary but not the only condition sufficient to provide saturated soil conditions in the wetlands. Mechanisms of groundwater flow must be considered in determining how water drains or is retained within wetland

soils. Groundwater is discussed in a subsequent section.

Melt from sideslope areas above the wetlands contributes water to the wetlands during May through early fall. This sideslope water continues beyond the duration of active snowmelt due to the timing delay of melt water flowing through the porous medium of talus and rock slopes. Estimates of these sideslope contributions have been made using data generated from a water budget procedure (Enartech, 1983) and reported (Kraeger-Rovey and Rovey, 1984) as 13 cm (5 in.), 23 cm (9 in.), and 13 cm (5 in.) for typical wetland conditions during May, June and July, respectively. An evaluation of the mechanisms and factors controlling the sideslope flows was made. Numerous small tributaries were located leading from the valley walls to the main channel. The frequency of these wetland channels has been measured from air photos as one tributary channel per 60 m (200 ft) of wetland perimeter (Kraeger-Rovey, 1984) for those tributaries larger than 1.0 m (3 ft) wide and 0.3 to 1.0 m (1 to 3 ft) deep. Smaller rivulets are more abundant yet often not observed until walking across the wetland surface. A hydraulic analysis of these wetland channels determined their capacity to average four times the estimated sideslope contribution for the May to July period. Thus, the wetland channels could efficiently convey the sideslope contributions through the wetlands to the main channel absent high water in the main channel which back water up causing it to spread across the entire wetland surface.

Onsite, summer precipitation on wetland surfaces provides only a portion of the moisture requirement of wetland vegetation (Sundeen, 1983). Consumptive water requirements from the wetland surfaces were estimated to be 42 cm (16.5 in.) for the May through September period while the effective precipitation was 14 cm (5.5 in.) during that interval. The net water requirement of 28 cm (11 in.) must come from other sources. This water deficit applies to the plants and does not include the substantial amount of water to keep from draining the wetland soils.

The main channel of Cross Creek conveys streamflow through the wetlands and provides the two main mechanisms that maintain saturated soil conditions in the wetlands. Main channel flows overtop the natural streambank during the peak runoff season and during heavy rainfall periods as occurred in late July, 1985. These overbank flows saturate the wetlands during that time. The mechanism that provides the longest duration of wetland saturation is when the stage (stream level) is at or near bank full. High water level in the stream may not directly provide water to the wetlands but creates a backwater extending up the tributaries that flow across the wetlands, and also causes the groundwater table throughout the wetland to be maintained at a high elevation. These mechanisms are discussed in later sections of this paper.

WETLAND VEGETATION AND WATER LEVEL RELATIONSHIPS

Main Channel Flows and Backwater Characteristics. By early June the onsite wetland snowpack has melted and the remaining dependable sources of wetland water supply are sideslope runoff and high stream flows in the main channel of Cross Creek. Flow estimates at Reeds Meadow, the first major wetland below two of the Homestake II diversions in the upper portion of the watershed (see Figure 1) have been made. Table 2 shows the average June and July Cross Creek discharges, for natural conditions and with the depletions caused by Homestake II diversions.

TABLE 2. Cross Creek Flows at Reeds Meadow

Month	Natural Flow	Post-Diversion Flow
June	3.40 cu.m/s (120 cfs)	0.99 cu.m/s (35 cfs)
July	2.12 cu.m/s (75 cfs)	0.71 cu.m/s (25 cfs)

Water level variations due to diversions were evaluated. An analysis was made in Reeds Meadow where stream flow estimates are available and some surveyed information on the slope of the channel water surface profile was collected (Ward, 1983). Streamflow from Reeds Meadow discharges over a resistant rock outcrop at the lower end of the meadow. The outcrop appears to function as a weir with a steep increase in downstream gradient where the flow goes through critical depth. Using an approximate rock outcrop elevation of 3,060.20 meters (10,040 feet), a water surface slope of .05 percent (.0005), and constant channel cross sectional shape, backwater calculations were made to calculate the water surface elevations for the flow conditions shown in Table 2 for natural and post-diversion flows. The results are shown in Table 3 for a location 700 meters (2,300 feet) above the mouth of Reeds Meadow. This is a location where a transect of groundwater piezometers was installed (Ward, 1983).

TABLE 3. Water Surface Elevations in Reeds Meadow

Month	Natural Water surf.	Post-diversion Water surf.
June	3,061.50 m (10,044.3 ft)	3,061.01 m (10,042.7 ft)
July	3,061.29 m (10,043.6 ft)	3,060.86 m (10,042.2 ft)

The decrease in water surface elevation in Cross Creek channel is 0.49 meters (1.6 feet) for June and 0.43 meters (1.4 feet) for July. The average summer season decrease in channel water surface is 0.46 meters (1.5 feet).

Backwater effects, extending into the wetlands from the full-flowing main channel, provide the essential mechanism giving the wetlands access to sideslope runoff and controlling groundwater drainage from the wetlands. With the exception of a few isolated areas, the Cross Creek wetlands are traversed by a dense network of small to medium sized tributaries, ranging from 0.3 to 2.0 meters (1 to 6 feet) across and

from .15 (0.5 feet) to 1.5 meters (5 feet) deep. In every wetland, the aggregate capacity of these channels is many times greater than the total available sideslope runoff (Kraeger-Rovey, 1984). The high water level in Cross Creek "backs up" outflow from these side tributaries, prevents it from running downstream, and causes the sideslope runoff to spread over the surface of the wetlands during the growing season. If this backwater effect is eliminated, the network of tributary channels will very efficiently drain the sideslope runoff through wetlands into Cross Creek, leaving wetland surfaces literally high and dry.

The proposed diversions of Homestake II would substantially reduce peak runoff flows in Cross Creek to levels now typical in late summer and fall. The average reduction in water level in Cross Creek that is expected to result from the diversion has been estimated at about 65 cm (2.2 feet) (Ward, 1983). As a result, backwater restrictions into side tributary channels will be substantially reduced or, for the shallower tributaries, eliminated. The tributaries will be able to convey a greater portion of the sideslope runoff through wetland channels, substantially reducing or eliminating the portion that overflows onto wetland surfaces.

Groundwater Responses. Groundwater seepage provides the link between water levels in Cross Creek and its tributaries, and wetland soil saturation. The water-holding capacity of soils and alluvial material in the wetlands provides a time-delay between the drop in creek levels in mid-summer, and drainage of groundwater from the wetlands. If that time delay is sufficiently long, wetland soils may remain saturated for a considerable period of time after snowmelt has ceased. Prolonged moisture retention in the soils would reduce the wetland's dependancy on high water levels in the main creek channel.

A decrease in water level in a stream channel induces drainage from the adjacent streambank. With time, the subsurface gradient propagates away from the

streambank, eventually inducing drainage throughout the wetland area. As drainage occurs, the water table drops. Drainage occurs most quickly in areas close to a streambank, where the soil is permeable. Both these conditions predominate in the Cross Creek wetlands. Numerous observations have shown that in most areas, wetland groundwater levels respond very rapidly to changes in Cross Creek water levels, indicating that the hydrology is governed by permeable materials. Given the dense network of tributary channels in most wetland areas, no point is very far from a surface stream channel.

A range of permeability values for the Cross Creek wetlands was obtained from field testing and laboratory analysis of soil samples (Ward, 1983). Using a geometric mean of these permeability values 0.0065 cm/sec, the time delay of drainage was computed using a standard drain formula (Todd, 1967). The estimated time delay between a drop in channel water level of 70 cm (2 ft), and a decline in wetlands water table of 15 cm (0.5 ft) was computed for a range of distances from the nearest drainage channel. For a distance of 2.4 m (8 ft) from the channel, the water table would decline 15 cm (6 in) in about two hours. At a distance of 12 m (40 ft), the 15 cm water table decline would take about five days. Few wetland areas are farther than forty feet from at least one minor drainage channel.

The conclusion drawn from these calculations is that wetlands are strongly dependent on high creek levels for maintaining a high water table necessary for keeping wetland soils saturated. Except for a few isolated locations, the groundwater reservoir drains too quickly to provide any useful function in independently maintaining the wetlands.

Vegetation Response. The gradient analysis shown in Figure 2 plots the percent coverage of 6 key indicator species and community dominants along the water table/drainage regime gradient. This ordination gives a model of species behavior along the moisture gradient and outlines the niche of each species. It also gives a predictive model of change in species abundance if the water

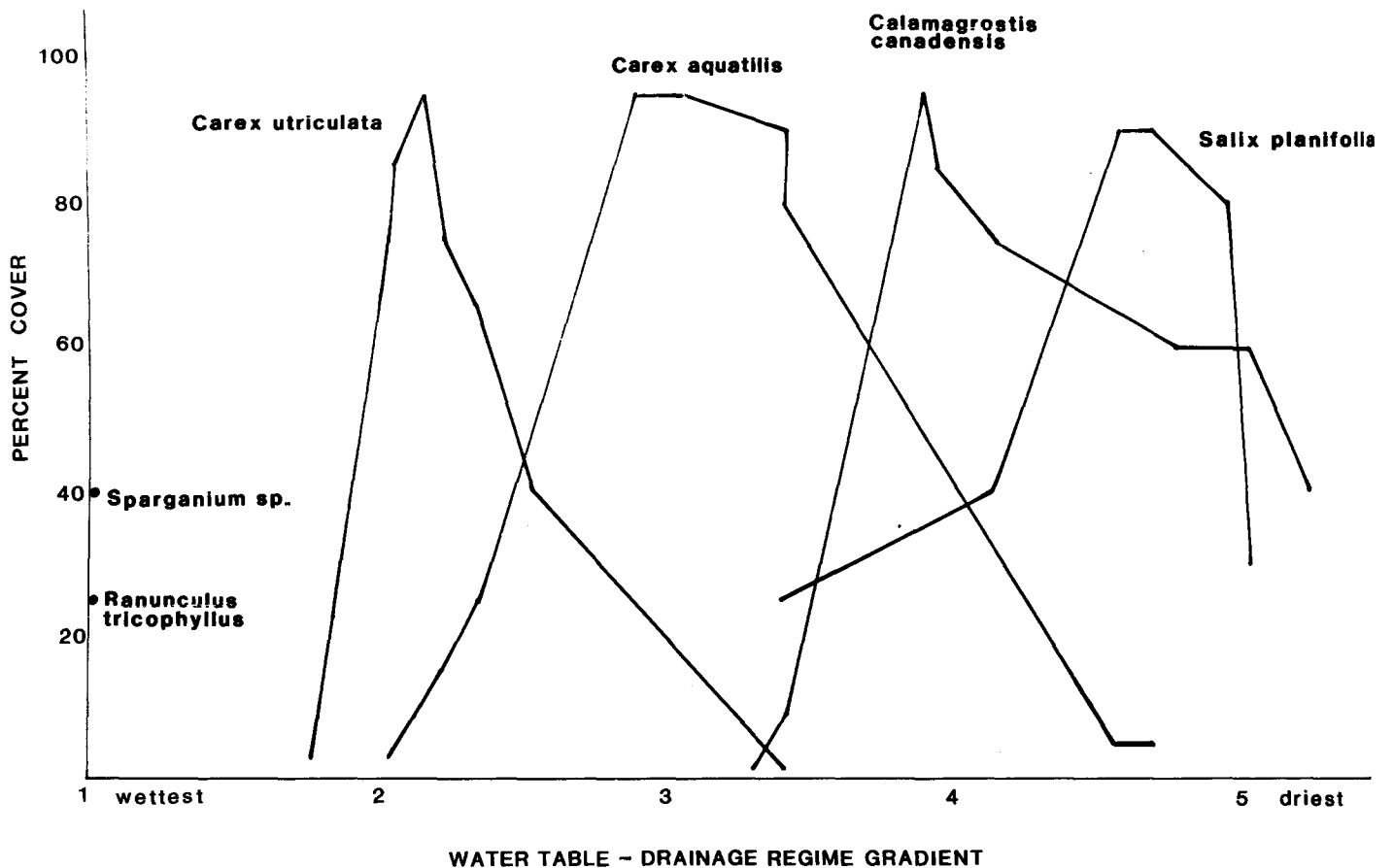


Figure 2. Gradient Analysis of Indicator Plant Species for Cross Creek Wetlands

table/drainage regime at any site were to change.

Figure 3 plots the average depth to water table or the depth of standing water for the 6 communities described here. The average difference between communities in depth to water table is 13.3 cm (5.2 in). Thus, small differences in water table relations make large differences in composition of the stands. It is hypothesized that any permanent change in summer water table depth greater than 13.3 cm will initiate secondary succession.

The pathway of secondary succession and the floristic change to be expected can be predicted using Figures 2 and 3. In general, succession would proceed from one species and community to the next up the water table/drainage gradient. For example, if the water table in Carex utriculata communities is dropped an average of 50 cm (20 in.), conditions similar to what presently support the

Calamagrostis canadensis-Mertensia ciliata community will develop on that site. If the water table dropped 15 cm, conditions similar to the Carex aquatilis would occur. Whether or not tree species would invade the wetlands is more difficult to predict since forests do not currently occur in the Cross Creek wetlands.

OTHER PROCESSES AFFECTING WETLANDS

High flows associated with spring runoff perform two functions essential to the maintenance of fen and marsh wetlands: (1) stream meandering and (2) overbank flooding in the meadows. Sustained high volume, high velocity flows, such as occur during spring runoff, provide the energy which allows streams to meander. Only under the influence of high flows are major sections of streambank dislodged, and sediment transported to form point bars.

The proposed Homestake II project will capture and divert the high flows associated with spring and early summer runoff. This will drastically reduce meandering and overbank flooding in the wetlands.

CONCLUSIONS

- (1) Main channel water levels are predicted to decrease an average 0.46 meters (1.5 feet) during the growing season as a result of the proposed Homestake II diversions,
- (2) Groundwater levels will decline in response to declining stream levels during the growing season,
- (3) The distribution of wetland plant species will change in response to declining groundwater levels during the growing season and some communities would probably die out,
- (4) Therefore, Homestake II will have an adverse effect on wetlands along Cross Creek.

REFERENCES

- Aqua Resources, Inc., 1984. Wetland Impact Evaluation for Homestake Phase II, prepared for Sacramento District, Corps of Engineers.
- Burke, R., H. Hemond, K. Stolzenbach, 1980. An Infiltrometer to Measure Seepage in Salt Marsh Soils. In: Estuarine and Wetland Processes, P. Hamilton and K. McDonald (Editors). Plenum Publishing Corp., New York, New York. pp. 413-423.
- Burton, T., 1985. The Effects of Water Level Fluctuations on Great Lake Coastal Marshes. In: Coastal Wetlands, H. Prince and F. D'Itri (Editors). Lewis Publishers, Inc., East Lansing, Michigan.
- Dix, R. L. and F.E. Smiens, 1967. The prairie meadow and marsh vegetation of Nelson County, North Dakota. Canadian Journal of Botany 45:21-58.
- Enartech, Inc., 1983. Stream and Wetland Hydrology - Homestake Phase II Project.

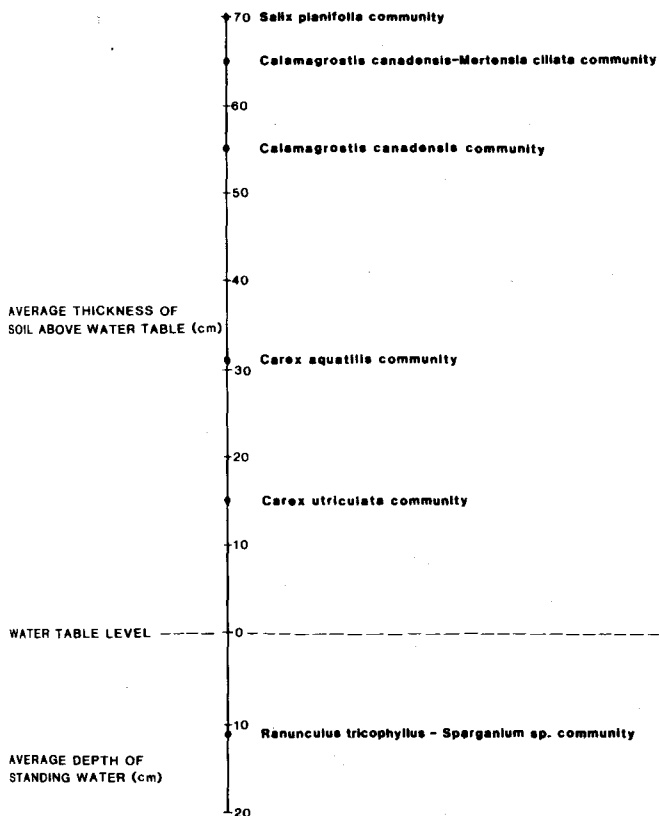


Figure 3. Average Water Table Depth or Standing Water Depth for Major Communities, late July-early August, 1985

Meandering reworks the floodplain sediments. This serves two critical ecological functions in the Cross Creek meadows. (1) By eroding high terrain, such as beaver dams and natural levees, the stream limits floodplain aggradation that, left unchecked, would eventually convert the floodplain into a river terrace. (2) Water provides the nutrients necessary to sustain the growth of the existing, fen-type and marsh-type vegetation. Absent this infusion of nutrients, the soils would become depleted, and the vegetation would be replaced with plant species that flourish in nutrient-poor soils.

Overbank flooding assures saturated soil conditions by maintaining high water levels during the growing season. Saturated soil conditions also prevent the invasion of upland plant species into wetland areas. Overbank flooding during the six-week, high streamflow period from late May to early July assures that wetland water levels are near the ground surface.

- Kilburn, P., 1983. Preliminary Ecological Investigation of Wetlands for the Homestake II Project, Eagle County, Colorado. International Environmental Consultants, Inc., Denver, Colorado.
- Kraeger-Rovey, C., E. W. Rovey, 1984. Microscale Engineering Analysis of the Holy Cross Wetlands.
- Rovey, E., C. Kraeger-Rovey, 1984. Comments of Draft Homestake II Wetland Report.
- Sundeen, K., R. S. Fifer, 1981. Homestake Phase II Fishery, Water, and Wetland Evaluation for Cross and Fall Creeks. USDA White River National Forest, Rocky Mountain Region.
- Sundeen, K., 1983. Analysis of Wetland Conditions - Fall and Cross Creeks. USDA White River National Forest, Rocky Mountain Region.
- Todd, D.K., 1967. Ground Water Hydrology. John Wiley & Sons, New York, New York.
- U.S. Department of Agriculture, Forest Service, White River National Forest, 1983. Final Environmental Impact Statement on Application for Land Use, Homestake Phase II Project.
- U.S. Department of Agriculture, Soil Conservation Service, Irrigation Water Requirements, Technical Release No. 21, April, 1967.
- U.S. Geological Survey, 1984. Flow Frequency Analysis of Discharge Records at Cross Creek near Miniturn, Colorado. WATSTORE Data Retrieval.
- Ward, J.R., 1983. Hydrological Investigation of Wetlands, Homestake I and II Projects, Eagle County, Colorado.
- Weber, W.A., 1976. Rocky Mountain Flora. University of Colorado Press, Boulder, Colorado.
- Westhoff, V., E. van der Maarel, 1978. The Braun-Blanquet Approach. In: Classification and Ordination of Communities. The Handbook of Vegetation Science, R. H. Whittaker (Editor). Junk, the Hague, pp. 617-726.

SEASONAL SNOW AND AUFEIS IN ALASKA'S TAIGA

C.W. Slaughter and C.S. Benson¹

ABSTRACT: The unglaciated taiga of central Alaska is subjected to seasonal snow and ice for 6 to 8 months of every year. Snow and ice thus play a major role in hydrologic regime. A typical taiga snowpack is less than 100 cm in depth, has a mean density at deposition of 0.05 to 0.10 g cm⁻³, and mean "ripe" density at time of spring snowmelt of less than 0.30 g cm⁻³. Low snowpack density (the result of intensive depth hoar formation in response to very steep vapor pressure gradients from base to surface of pack during the entire winter) contrasts with high-density (0.40 g cm⁻³) tundra snow at wind-affected taiga sites and in the high Arctic. Aufeis can occupy major sectors of stream channels and flood plains, and modifies hydrologic regime by temporary storage of groundwater (winter baseflow) and release of that water to streamflow after the snowmelt season. (KEY TERMS: snow; ice; aufeis; subarctic; taiga; hydrology.)

INTRODUCTION

Alaska has over 1.5 million km² of land, and extends through 20 degrees of latitude, from 51°N lat. at Amatsignak Island in the Aleutians to 71°N lat. at Barrow, and through 58 degrees of longitude from Hyder, on the Alaska-British Columbia border, to Attu at the tip of the Aleutian chain. The westernmost point on the Seward Peninsula is only 88 km from Asia; Little Diomed Island (U.S.) is only

3.7 km from Big Diomed Island (USSR). Mean annual runoff for the State is estimated at 9.8×10^{11} m³, or about one-third of the total estimated water yield of the entire United States. South-central and southeastern Alaska account for some 5.7×10^{11} m³ of water, while the Yukon and Kuskokwim River systems contribute about 2.5×10^{11} m³ (Hartman and Johnson, 1978).

Four major physiographic regions are recognized in Alaska (Wahrhaftig, 1965): the Arctic Coastal Plain, the Rocky Mountain System, the Intermontane Plateaus, and the Pacific Mountain System. Alaska may be divided into four climatic zones that roughly parallel the physiographic regions (Hartman and Johnson, 1978). The Arctic zone has a mean annual temperature of -12 to -15°C, generally low precipitation, and is subject to strong winds. The Interior zone is characterized by a continental climate; summers are short and warm, with air temperature occasionally exceeding 30°C, and winters are commonly long and cold with -40°C commonly and -50°C occasionally observed. Mean annual temperature is -10 to -5°C; precipitation varies from 25 to over 90 cm annually. The Transitional zone has less yearly temperature variation, higher precipitation and more cloudiness than the continental Interior, and is intermediate between the Interior and the Maritime zone of south-central and southeastern Alaska. The Maritime zone is characterized by relatively low variation in annual

¹Respectively, USDA Forest Service, Pacific Northwest Research Station, Institute of Northern Forestry, 308 Tanana Drive, Fairbanks, AK 99775-5500, and University of Alaska, Geophysical Institute, Fairbanks, AK 99775.

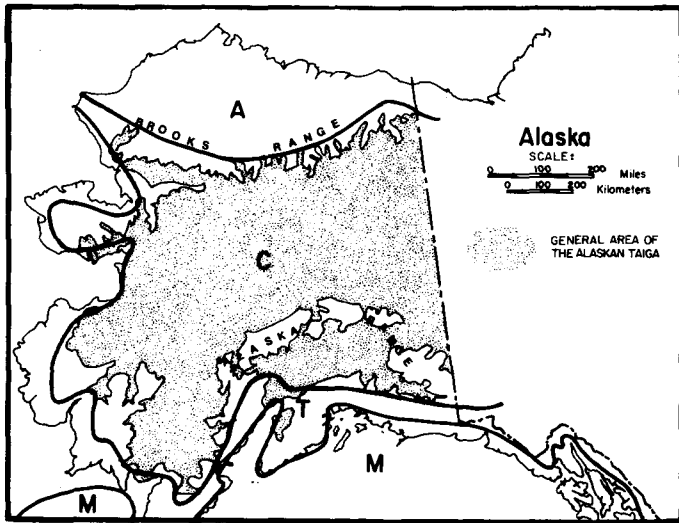


Figure 1. Distribution of taiga (after Viereck, 1973) and climatic zones (after Hartman and Johnson, 1978).
 A: Arctic; C: Continental;
 T: Transition; M: Maritime.

temperature, a great deal of cloudiness, high precipitation (to over 500 cm annually), and mean annual air temperature above 0°C.

The taiga (Figure 1) generally coincides with the Interior climatic zone and with Wahrhaftig's (1965) Intermontane Plateaus physiographic region. According to Viereck (1973), "In Alaska the taiga extends from the south slope of the Brooks Range southward to its border with the coastal forests, eastward to the border with Canada, and westward to a maritime tree line very close to the Bering and Chukchi Seas. Within this area of 138 x 10⁶ hectares, approximately 32%... is forested.... The unforested land consists of extensive bogs, brush thickets, grasslands, sedge meadows, and some alpine tundra." This region is composed of rolling, occasionally rugged uplands and extensive low-lying wetlands. The region was unglaciated in the Wisconsin Glaciation save for localized activity at high elevations. The taiga generally corresponds to the zone of discontinuous permafrost--perennially frozen ground--and periglacial geomorphic processes are active in the entire region. Permafrost is common on north-facing slopes and in poorly-drained lowlands but is generally lacking on southern exposures. The

proportion of frozen ground increases with latitude; only sporadic to discontinuous permafrost is found in the south, but permafrost is essentially continuous from the crest of the Brooks Range north to the Arctic Ocean.

TAIGA SNOW

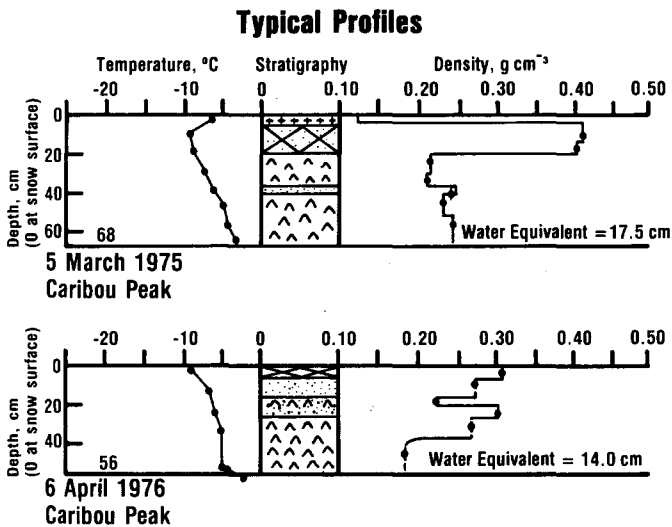
Snow is a dominant feature of the taiga and mantles the entire landscape for 6 to 8 months of every year, depending on specific location and year. Surface energy relationships which affect biological and physical processes, to say nothing of human activities, are markedly responsive to this seasonal snowpack.

Two primary northern snow types and regions are distinguished by Pruitt (1970): "taiga snow" and "tundra snow." Hare (1971) showed that density of taiga snowpacks in Canada reaches 0.25 to 0.30 g cm⁻³ in late winter, while density of tundra snow is consistently greater than 0.35 g cm⁻³. The seasonal snowpack of interior Alaska may be considered typical taiga snow: densities at initial deposition are low, 0.05 to 0.10 g cm⁻³, movement and reworking by wind is uncommon, and snowpack metamorphism is primarily through vapor transfer within the pack in response to strong vapor pressure gradients. Relatively warm soil (rarely below -5°C) at the base of the snowpack and cold ambient air produce steep vapor pressure gradients, with upward water vapor flux within the snowpack averages 0.025 g cm⁻³ day⁻¹ throughout the winter (Trabant and Benson, 1972; Trabant, et al., 1970). Final "ripe" snowpack density is commonly 0.20 to 0.28 g cm⁻³.

In contrast to taiga snow, "tundra" snow is commonly deposited during windy conditions, which lead to errors in measurement. Long-term climatic records have underestimated snowfall on Alaska's Arctic slope by a factor of three; the annual flux of windblown snow is on the order of 50 ± 20 t/m (Benson, 1982). A significant, but unknown, amount of snow is lost by sublimation during wind transport; in Wyoming, Tabler (1975) showed that about a third of windblown snow sublimated during transport. The typical structure of tundra snow includes

"Tundra" Snow

- above treeline, or otherwise exposed
- extensive re-working by wind
- higher density on windslab layer at top of pack
- relatively low density at base of pack



"Taiga" Snow

- generally below treeline
- low snow pack density
- little to no re-working by wind
- subject to strong air temperature inversions

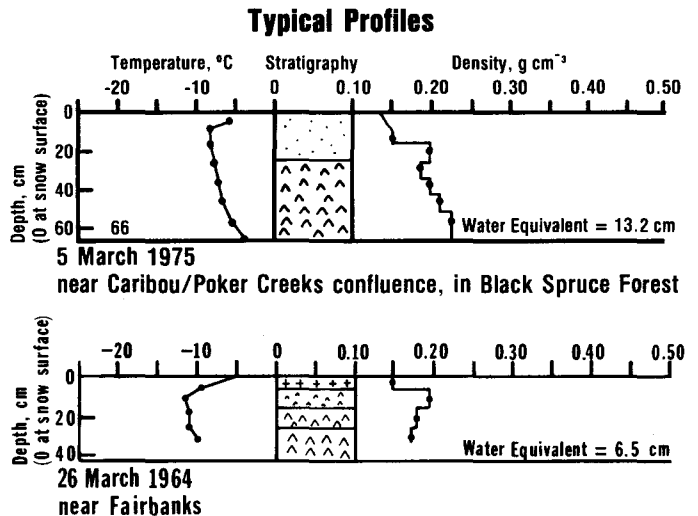


Figure 2. Typical taiga and tundra snowpack stratigraphy.

Stratigraphic Symbols

- ++++ New snow, some original crystal forms still recognizable.
- Fine or very fine grained (snow < 1 mm).
- Same as above, but very hard--a result of wind packing --often referred to as a windslab.
- Medium grained snow 1 to 2 mm.
- Depth hoar, coarse loosely-bonded crystals often with well developed crystal faces. Larger chevron patterns indicate larger crystal size.

a hard wind-packed layer with density 0.35 to 0.50 g cm⁻³ overlying a low-density depth hoar layer. Depth-hoar may be very thin while snow beneath the wind-packed layer is soft with grain size of about 1 mm. "Tundra" snow is very irregularly distributed. Stream valleys may be completely filled with dense (0.35-0.40 g cm⁻³), hard snow while adjacent slopes are snow-free (Benson, 1967; Liston, 1986; McKay and Findlay, 1971). Tundra snow prevails on the Arctic coastal plain of Alaska, and is also found in wind-affected settings in the taiga--areas above treeline (Benson, 1967) and in valleys subject to frequent cold-air drainage

winds, such as at Delta Junction, Alaska (Benson, 1972; Bilello, et al, 1970).

A "transitional" snow zone has been delineated by Benson (1982). This zone is climatically intermediate between the cold continental climate of the central Alaska taiga and the cold maritime climate of the western Alaska coast and Bering Sea. West of Koyukuk (158° W long.) in the Yukon-Kuskokwim delta, the temperature is higher and winds are stronger than they are farther east, and the climate becomes more maritime than continental. Many storms produce mixed rain and snow, and the snow cover is characterized by significant amounts of ice crusting, though depth hoar

is still developing at the ground surface (Benson, 1982).

Typical profiles of taiga and tundra snowpacks from interior Alaska sites are depicted in Figure 2. Tundra and taiga snowpack types may be closely intermingled. At many tree-line or otherwise wind-affected sites in the taiga, deep, high-density wind-drifted tundra snow grades rapidly to shallow, low-density taiga snow over very short distances (Benson, 1978).

SEASONAL ICE

Rivers and lakes in the taiga can have an ice cover for 5 to 7 months of the year. Floating ice, frazil ice, anchor ice, ice breakup events, and the hydraulic and thermal conditions attendant to these seasonal ice forms have received detailed attention elsewhere (Benson, et al, in preparation; Calkins, 1979; Michel, 1971; Osterkamp, 1975, 1978) and are not considered in the present discussion.

Another important seasonal ice phenomenon forms when water in or adjacent to a stream channel rises above the surface of an existing ice cover. Such an accumulation of ice, superimposed on the frozen surface of a stream, river, or sector of landscape is generally termed "aufeis" (Grey and MacKay, 1979) or "icing" (Carey, 1973); the Russian term "naled" is preferred by some authors (Akerman, 1982). Aufeis is commonly associated with permafrost-affected terrain. Comprehensive reviews of aufeis are provided by Carey (1973) and Grey and MacKay (1979). Kane et al. (1973) and Kane and Carlson (1977) summarize knowledge of mechanisms of aufeis formation. Aufeis is a circumpolar phenomenon, and has been studied or documented in locales ranging from Yukon (van Everdingen, 1982) to Spitsbergen (Akerman, 1982) to Mongolia (Froehlich and Slupik 1982).

Aufeis deposits are multilayered and may be several meters thick in streams that normally have water depths of 50 cm or less. In Alaska's taiga, aufeis is most commonly found in stream valleys and river floodplains. Extent and thickness of aufeis deposits in the taiga are generally less than for those on Alaska's

Arctic Coastal Plain (Dean, 1984) or in major north-flowing river systems of northeastern Siberia (Kane, personal communication).

HYDROLOGIC RELATIONSHIPS

Seasonal snow and seasonal ice constitute forms of detention storage for precipitation. The snowpack binds virtually all precipitation falling during the period from October through March in a veneer overlying most of the taiga landscape. This water may be redistributed vertically over short distances by snowpack metamorphism and depth hoar formation, and may be redistributed laterally by wind action. In either case, the redistribution is essentially local, and incoming precipitation, at least below treeline, is largely retained on the watershed of original deposition.

The hydrologic relationships of seasonal snow have been studied over many years in many settings. An extensive body of literature is available concerning snowmelt physical processes, snow/terrain/vegetation relationships, meltwater routing, conceptual and quantitative modeling, and engineering/resource management applications of this knowledge (e.g., Colbeck and Ray, 1979; Glen, 1982; Meiman, 1969; National Academy of Sciences, 1974; U.S. Army Corps of Engineers, 1956). The seasonal snowpack is subject to the same processes and physical laws in the taiga as in other regions. Major differences in snow hydrology, or in application of snow hydrology knowledge developed in more temperate settings, derive from several factors: the prolonged and continuous nature of the snow-cover season, extreme seasonal variability in energy available at the earth surface at high latitudes, the existence of cold soil (either seasonally or perennially frozen) at the base of the snowpack during most of the winter and during spring snowmelt, pronounced development of depth hoar in the snowpack, occurrence of aufeis in streams and valleys, and a relative paucity of quantitative data concerning precipitation and streamflow.

Depending upon the specific setting and year, snow covers the taiga for 6 to 8 months of each year. Often the ambient air temperature does not exceed 0°C from October through March. Average snow cover duration in the central Alaska lowlands (Fairbanks) is 214 days (Haugen, et al., 1982). Snowpack persistence is a direct response to availability of energy for warming and melting; the extreme seasonal variability of incoming short-wave radiation at high latitudes is well documented (Baker and Haines, 1969; Seifert, 1981). Daily short-wave radiation available at a horizontal surface at Fairbanks (Figure 3) varies from less than 200 W-hr m⁻² in December to over 5000 W-hr m⁻² in June (Wendler, 1981).

The winter climate of the lowlands of the taiga is typified by cold air and little wind. The snow-covered surface favors development of strong surface inversions which trap the calm, cold air in a surface layer between 50 and 100+ m thick. The snowpack lying within the altitude range of the inversion layer is subject to negligible winds, often through the entire winter. The snowpack is subjected to very low ambient air temperature at the air/snow interface--from -30 to -45°C is normal. The ground beneath the snowpack rarely becomes colder than -6 to -10°C, and strong temperature gradients prevail in the snow; this leads to vertical water vapor flux and extensive depth hoar development, with average density generally less than 0.20 g cm⁻². The steep temperature gradient within the snowpack is accompanied by a steep vapor pressure gradient, leading to vertical flux of water vapor of up to 0.025 g cm⁻² day⁻¹. This vertical flux of water leads to dessication of the underlying soil (Kane, et al., 1978; Trabant and Benson, 1972). Santeford (1979) reports that about 50% of water initially available in an organic soil-surface layer overlying permafrost migrates upward into the snowpack in the course of a winter. Such soil desiccation strongly influences the disposition of initial snowmelt water (Slaughter and Kane, 1979).

Spring, the period of rapid increase in solar insolation and day length, is accompanied by rising solar angle so that an increasing proportion of north-aspect

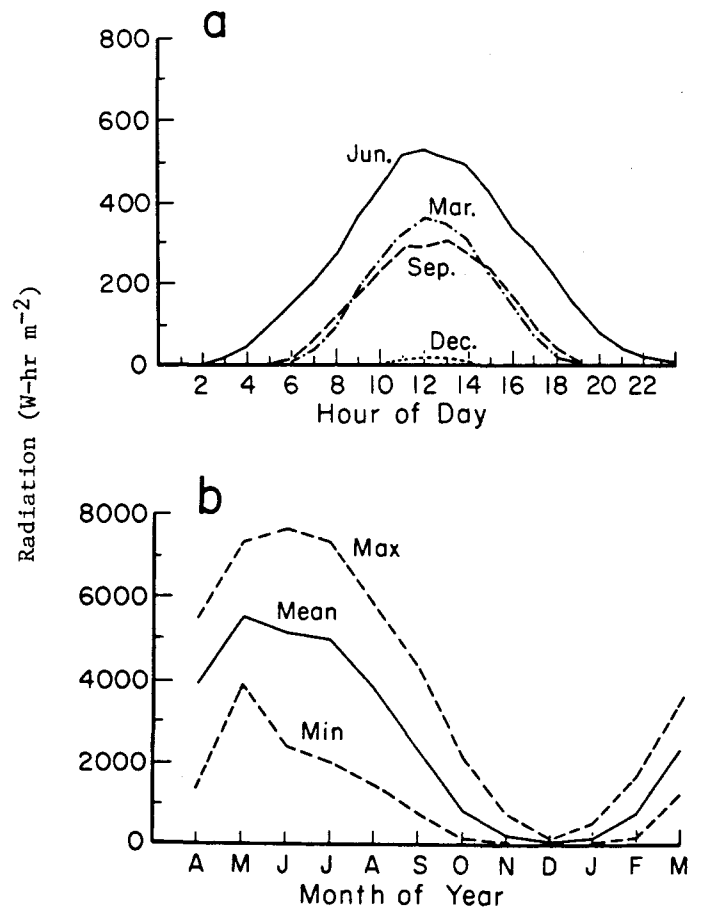


figure 3. (a) Hourly mean values of global radiation (horizontal surface) in December, March, June, and September, Fairbanks (65°49' N). (b) Daily sums (maximum, mean, minimum) of global radiation on a horizontal surface, Fairbanks (after Wendler 1981).

terrain is subject to the increasing energy load; this coincides with rapid decrease in surface albedo as the snow surface ages and settles, and twigs and branches become exposed and act as energy absorbing and reradiation media. The result is a relatively brief, intense snowmelt runoff season. The complete snowmelt runoff period can be as little as 7 to 10 days (Kane and Stein, 1984).

Disposition of meltwater is affected by presence of seasonally or perennially frozen ground. Kane and Stein (1983, 1984) demonstrated that antecedent (fall) soil moisture conditions affect volume of snowmelt runoff the following spring on small plots and on a large (5,132 km²) watershed in the discontinuous-permafrost

zone of Alaska. The proportion of snowmelt water that infiltrated into the soil mantle on a permafrost-free site was sharply reduced, with a concomitant increase in runoff, by increased soil moisture levels in the fall. The presence of permafrost similarly influences disposition of meltwater (and summer precipitation). Permafrost essentially precludes infiltration beneath the seasonally thawed "active layer," thereby restricting meltwater detention and transmission to the soil mantle (largely organic soils of low bulk density and high transmissivity) (Kane, et al., 1981; Slaughter and Kane, 1979). This effectively increases the proportional yield of meltwater in spring, relative to nonpermafrost catchments. In an upland watershed north of Fairbanks, a permafrost-free 5.2-km² basin yielded less than 50% as much total snowmelt runoff volume as did an equal-sized (5.7 km²) basin which is dominated by permafrost (Slaughter, 1981); the spring period of high flow lasted more than twice as long in the permafrost-dominated basin, 8 days versus 3 days.

Aufeis derives from groundwater sources (van Everdingen, 1982). Aufeis immobilizes water that is being yielded to the stream channel or to the ground surface during the winter and which would otherwise contribute to current streamflow. A consequence of aufeis formation in a catchment is solid-state storage of baseflow and diminution of streamflow during the winter and spring, with subsequent augmentation of streamflow when aufeis melts during spring and early summer.

The occurrence of aufeis has consequences for both hydrologic regime and geomorphic processes. Åkerman (1982) showed that aufeis has both direct and indirect geomorphologic effects. The physical presence of ice in stream channels and on floodplains during spring runoff may protect stream banks and adjacent ground surfaces from fluvial action, and may divert flow to landscape sectors not normally abraded by water---such as at the lateral margins of ice, perhaps far removed from the normal (ice-free) stream channel (Froehlich and Slupik, 1982; Kane and Slaughter, 1972). Such protection during major runoff events

may influence either local bed profile or local drainage patterns (Åkerman, 1982).

Presence of aufeis in combination with an ice cover on streams can produce marked effects on streamflow. Kane, et al. (1973) monitored pore water pressure in two stream valleys in discontinuous permafrost, and demonstrated a very dynamic system during the "frozen" period of aufeis formation and continuous ice cover on streams. Hydrostatic head variations as great as 2.1 m within a single week were recorded, reflecting changes in groundwater flow and subsurface conditions for flow in the aquifer/stream/aufeis system. Peaks in hydrostatic head were generally accompanied by an increase in formation or thickness of aufeis (Kane, et al., 1973). The water mass held as aufeis can be appreciable; in a central Alaska watershed of 104 km², aufeis covered 1% of the drainage area (Benson, 1978), comprised approximately 4% of total annual streamflow and 40% of expected winter streamflow (Kane and Slaughter, 1972). This ice melts more slowly than the adjacent snowpack, and thus contributes meltwater (release from storage) to the stream system over a period of weeks or even of several months into summer. Although aufeis cannot be reliably predicted in terms of intensity and magnitude, Sloan et al. (1975) monitored a transect across Alaska and demonstrated that aufeis has a tendency to recur at the same locations year after year; however, not all locations showed aufeis activity in every year of their study. A similar pattern of recurrence was documented by Slaughter (1982) in a central Alaska watershed.

SUMMARY

Seasonal snow and ice are dominant components in the annual hydrologic regime of Alaska's taiga. A veneer of snow covers the landscape for 6 to 8 months of the year and strongly affects energy balance at the earth surface. At high latitudes, rapidly increasing day length and solar angle combine with decreasing albedo to produce short-lived spring snowmelt runoff periods; the flood of record may result from snowmelt water encountering aufeis-blocked stream channels. Presence of permafrost and of

associated organic soil layers modifies translation of meltwater from snowpack to stream. Aufeis comprises another form of detention storage; the aufeis affects fluvial geomorphic processes, modifies winter base flow in streams, and provides meltwater well into summer months in some locations.

LITERATURE CITED

- Akerman, J., 1982. Studies on naledi (icings) in West Spitsbergen. pp. 189-202 In: Proceedings, 4th Canadian Permafrost Conference. The Roger J.E. Brown Memorial Volume. National Research Council of Canada, Ottawa.
- Baker, D.G. and D.A. Haines, 1969. Solar radiation and sunshine duration relationships in the north-central region and Alaska. Minnesota Agricultural Experiment Station Technical Bulletin 262.
- Benson, C.S., 1967. A reconnaissance snow survey of interior Alaska. UAGR-190. Geophysical Institute, University of Alaska, College, Alaska. 71 pp.
- Benson, C.S., 1972. Physical properties of the snow cover in the Ft. Greely Area, Alaska. SR-178, U.S. Army Cold Regions Research and Engineering Laboratory, Hanover, New Hampshire 24 pp.
- Benson, C.S., 1978. Studies on the seasonal snow cover of the Caribou-Poker Creeks Research Watershed during the winters of 1974-75 and 1975-76. Final Report. Geophysical Institute, University of Alaska, Fairbanks, Alaska. 38 pp.
- Benson, C.S., 1982. Reassessment of winter precipitation on Alaska's Arctic slope and measurements on the flux of wind blown snow. UAG R-288, Geophysical Institute, University of Alaska, Fairbanks, Alaska. 26 pp.
- Benson, C.S., W. Harrison, J. Gosink, S. Bowling, L. Mayo, and D. Trabant, in prep. Workshop on Alaskan hydrology: problems related to glacierized basins. Geophysical Institute, University of Alaska, Fairbanks.
- Bilello, M.A., R.E. Bates, and J. Riley, 1970. Physical characteristics of the snow cover, Fort Greely, Alaska, 1966-67. Technical Report 230, USA Cold Regions Research and Engineering Laboratory, Hanover, New Hampshire. 33 pp.
- Calkins, D.J., 1979. Accelerated ice growth on rivers. CR 79-14, U.S. Army Cold Regions Research and Engineering Laboratory, Hanover, N.H. 5 pp.
- Carey, K.L., 1973. Icings developed from surface water and ground water. Cold Regions Science and Engineering Monograph III-D3. USA Cold Regions Research and Engineering Laboratory, Hanover, New Hampshire. 65 pp.
- Colbeck, S.C. and M. Ray (editors), 1979. Proceedings, Modeling of Snow Cover Runoff. USA Cold Regions Research and Engineering Laboratory, Hanover, New Hampshire. 432 pp.
- Dean, K., 1984. Stream-icing zones in Alaska. Report of Investigations 84-16. Alaska Department of Natural Resources, Division of Geological and Geophysical Surveys, Fairbanks. 20 pp.
- Froehlich, W. and J. Slupik, 1982. River icings and fluvial activity in extreme continental climate: Khangai Mountains, Mongolia. pp. 203-211 In: Proceedings, 4th Canadian Permafrost Conference. The Roger J.E. Brown Memorial Volume. National Research Council of Canada, Ottawa.
- Glen, J.W. (editor), 1982. Hydrological aspects of alpine and high-mountain areas. IAHS Publication 138, International Association of Hydrological Sciences, Washington, D.C. 350 pp.
- Grey, B.J. and D.K. MacKay, 1979. Aufeis (overflow ice) in rivers. pp. 134-165 In: Canadian Hydrology Symposium 79--Cold Climate Hydrology. National Research Council of Canada, Ottawa.

- Hare, F.K., 1971. Snow-cover problems near the Arctic treeline of North America. Report Kevo Subarctic Research Station 6: 31-40.
- Hartman, C.W. and P.R. Johnson, 1978. Environmental atlas of Alaska. Institute of Water Resources/Engineering Experiment Station, University of Alaska, Fairbanks, Alaska. 95 pp.
- Haugen, R.K., C.W. Slaughter, K.E. Howe, and S.L. Dingman, 1982. Hydrology and climatology of the Caribou-Poker Creeks Research Watershed, Alaska. CRREL Report 82-26, U.S. Army Cold Regions Research and Engineering Laboratory, Hanover, New Hampshire. 34 pp.
- Kane, D.L., S.R. Bredthauer, and J. Stein, 1981. Subarctic snowmelt runoff generation. pp. 591-601 In: The Northern Community: A Search For a Quality Environment. Proceedings of the Specialty Conference. American Society of Civil Engineers.
- Kane, D.L. and R.F. Carlson, 1977. Analysis of stream aufeis growth and climatic conditions. pp. 656-670 In: Proceedings, 3d National Hydrotechnical Conference, Canadian Society for Civil Engineering. Quebec, Canada.
- Kane, D.L., R.F. Carlson, and C.E. Bowers, 1973. Groundwater pore pressures adjacent to subarctic streams. pp. 453-458 In: Proceedings, North American Contribution, 2nd International Conference on Permafrost. National Academy of Sciences, Washington, D.C.
- Kane, D.L., J.N. Luthin, and G.S. Taylor, 1978. Heat and mass transfer in cold regions soils. IWR-65, Institute of Water Resources, University of Alaska, Fairbanks, Alaska.
- Kane, D.L. and C.W. Slaughter, 1972. Seasonal regime and hydrological significance of stream icings in central Alaska. pp. 528-540 In: Proceedings, The Role of Snow and Ice in Hydrology. Banff, Alberta, Canada. UNESCO/WMO/IASH.
- Kane, D.L. and J. Stein, 1983. Water movement into seasonally frozen soils. Water Resources Research 19: 1547-1557.
- Kane, D.L. and J. Stein, 1984. Plot measurements of snowmelt runoff for varying soil conditions. Geophysica 20(2): 123-135.
- Liston, G., 1986. Study of the seasonal snow cover in the Upper Kuparuk drainage on Alaska's Arctic Slope. M.S. Thesis, University of Alaska, Fairbanks.
- McKay, G.A. and B. Findlay, 1971. Variation of snow resources with topography and vegetation in Canada. Proceedings, 39th Annual Western Snow Conference: 17-26.
- Meiman, J.R. (editor), 1969. Proceedings of the Workshop on Snow and Ice Hydrology. U.S./IHD Snow and Ice Work Group. Fort Collins, Colorado. 142 pp.
- Michel, B., 1971. Winter regime of rivers and lakes. Monograph 111-B1a, U.S. Army Cold Regions Research and Engineering Laboratory Hanover, New Hampshire. 130 pp.
- National Academy of Sciences, 1974. Advanced concepts and techniques in the study of snow and ice resources an interdisciplinary symposium. National Academy of Sciences, Washington, D.C. 789 pp.
- Osterkamp, T.E., 1975. Tanana River ice cover. pp. 201-209 In: Proceedings International Symposium on Ice Problems, IAHR, Hanover, New Hampshire.
- Osterkamp, T.E., 1978. Frazil ice formation: a review. J. Hydraulics Division, American Society of Civil Engineers 104 (HY-9): 1239-1255.
- Pruitt, W.O., 1970. Some ecological aspects of snow. pp. 83-89 In: Ecology of the subarctic regions: Proceedings of the Helsinki Symposium. UNESCO.
- Santeford, H.S., 1979. Snow-soil interactions in interior Alaska. pp. 311-318 In: Colbeck, S.C., and M. Ray (editors). Proceedings, Modeling of snow

- cover runoff. U.S. Army Cold Regions Research and Engineering Laboratory, Hanover, New Hampshire.
- Seifert, R.D., 1981. A solar design manual for Alaska. University of Alaska, Institute of Water Resources, Fairbanks, Alaska. 163 pp.
- Slaughter, C.W. and D.L. Kane, 1979. Hydrologic role of shallow organic soils in cold climates. pp. 380-389 In: Canadian Hydrology Symposium 79--Cold Climate Hydrology. National Research Council of Canada, Ottawa.
- Slaughter, C.W., 1982. Occurrence and recurrence of aufeis in an upland taiga catchment. pp. 182-188 In: Proceedings, 4th Canadian Permafrost Conference. The Roger J.E. Brown Memorial Volume. National Research Council of Canada, Ottawa.
- Slaughter, C.W., 1981. Snowmelt runoff estimation with time lapse photography. Pacific Northwest Section, American Geophysical Union. Central Washington University, Ellensburg, Washington.
- Sloan, C.E., C. Zenone, and L.R. Mayo, 1975. Icings along the trans-Alaska pipeline route. Open-File Report 75-87, U.S. Geological Survey, Anchorage, Alaska. 39 pp.
- Tabler, R.D., 1975. Estimating the transport and evaporation of blowing snow. pp. 85-104 In: Snow Management on Great Plains Symposium Proceedings. Publication 73, Great Plains Agricultural Council, Bismark, North Dakota.
- Trabant, D., C.S. Benson, and G. Weller, 1970. Physical-thermal processes in the seasonal snow cover of northern Alaska. pp. 328-332 In: Proceedings of the Twentieth Alaska Science Conference, College, Alaska. Alaska Division, American Association for the Advancement of Science.
- Trabant, D.C. and C.S. Benson, 1972. Field experiments on the development of depth hoar. pp. 309-322 In: Doe, B.R., and D.K. Smith (editors). Studies of Mineralogy and Precambrian Geology. GSA Memoir 135, Geological Society of America, Boulder, Colorado.
- U.S. Army Corps of Engineers. 1956. Snow Hydrology. Summary report of the snow investigations. North Pacific Division, U.S. Army Corps of Engineers. Portland, Oregon. 437 p.
- van Everdingen, R.O., 1982. Management of groundwater discharge for the solution of icing problems in the Yukon. pp. 212-226 In: Proceedings, 4th Canadian Permafrost Conference. The Roger J.E. Brown Memorial Volume. National Research Council of Canada, Ottawa.
- Viereck, L.A., 1973. Wildfire in the taiga of Alaska. Quaternary Research 3(3): 465-495.
- Wahrhaftig, C., 1965. Physiographic divisions of Alaska. Professional Paper 482, U.S. Geological Survey.
- Wendler, G., 1981. Solar radiation data for Fairbanks. Geophysical Institute Report, Solar Energy Meteorological Research and Training Site, University of Alaska. Fairbanks, Alaska.

INSTRUMENTATION AND DATA COLLECTION

WATER REDISTRIBUTION IN PARTIALLY FROZEN SOIL BY THERMAL NEUTRON RADIOGRAPHY

Michael A. Clark¹, Dr Roger J Kettle¹, Giles D'Souza².

ABSTRACT: Thermal neutron radiography has been utilised as a technique for determining relative water movements in partially frozen soil. The method is non-destructive and determinations of local water content can be made at any time throughout the test. The experimental test rig is designed so that the soil matrix can be uniformly irradiated by a thermal neutron beam, to obtain radiographs, which upon interpretation yield information on relative water / ice contents. Instrumentation is incorporated in the soil matrix in the form of psychrometer / thermocouples to record water potential, electrical resistance probes to enable ice and water to be differentiated on the radiographs and thermocouples to record the temperature gradient. Interpretation of the radiographs is accommodated using image analysis equipment capable of distinguishing between 256 shades of grey. Image enhancing techniques are then employed to develop false colour images which show the flow of water and development of ice lenses in the soil matrix. Water content determinations can then be made and plotted against potential measurements for each radiograph. From these graphs, using relevant theory, pore water distributions can be obtained and combined with water content data to give hydraulic conductivities.

(KEY TERMS: thermal neutron radiography; image analysis; hydraulic conductivities; partially frozen soil.)

INTRODUCTION

Hydraulic conductivity is a fundamental parameter of a soil. In an unfrozen soil it can be determined using a permeameter where water enters and leaves the

specimen via inlet and outlet reservoirs. However if the soil is subject to freezing conditions the reservoirs have to be maintained at sub-zero temperatures which results in the reservoir water freezing.

One way of preventing this is to add lactose to the water, this however limits the temperature range which may be examined and there is a danger of lactose molecules moving into the soil by molecular diffusion or by transportation by the flowing water.(Williams and Burt 1974).

In recent years techniques which dispense with the involvement of a permeameter have been developed. These have often incorporated the use of various forms of radiation to monitor the moisture flux within the soils. X-rays have been used to depict lead shot, imbedded in a soil subject to partial freezing, to give information on water redistribution during freezing (Yoneyama et al, 1983) and by using dual gamma-rays, water and density are monitored simultaneously and used to determine water flow in a freezing soil (Fukuda et al, 1980).

The techniques reported here have been introduced in earlier papers (Clark & Kettle, 1985a, 1985b). Neutron radiography is used to depict, on photographic plates, water / ice in a soil subject to partial freezing. Neutrons are absorbed by atoms according to their atomic weight. Hydrogen, the main constituent of water, has the lowest atomic weight of the elements and is the greatest absorber of neutrons. The cell and matrix are therefore made up of elements with low coefficients of neutron absorption so that the degree of exposure of the photographic plate is directly related to the water / ice content of the matrix.

Using the images and data, from instrumentation incorporated in the soil, information on water movements and hydraulic potentials can be obtained and developed to give hydraulic conductivities.

1: Department of Civil Engineering, Aston University, Aston Triangle, Birmingham, England.

2: Remote Sensing Unit, Bristol University, Bristol, England.

EXPERIMENTAL SET UP

The Snowcal (powdered chalk) matrix is housed in a rig made entirely of PTFE sheet and aluminium. Snowcal, PTFE and aluminium have low neutron absorption coefficients and are hence virtually 'transparent' to the thermal neutron beam.

The matrix is compacted, at approximately 10% water content, into six rectangular cross-section PTFE rings within a rectangular cross-section cell. The cell, made of PTFE for insulation and encased in aluminium for rigidity, forms the central portion of the experimental set up with similar lower and upper cells completing the main apparatus.

The lower cell contains a water bath and water temperature regulation unit and the upper cell contains a freezing head. Once the three cells are fitted together the apparatus is free from leaks and hence all water entering the central cell via the water bath (fed by a Mariotte vessel) remains in the matrix as water or ice.

End temperatures during the test are lowered to $+4^{\circ}\text{C}$ and -1°C by circulating ethylene glycol / water solution through the water temperature regulation unit and freezing head using cryostats. The central and upper cells are modified so that psychrometer / thermocouple probes, used to measure water potential, fit into the PTFE rings and protrude into the matrix. Any heave that occurs during the test is allowed to develop by the free vertical movement of the rings. The three cells comprising the main apparatus are illustrated in Figure 1.

The apparatus is located so that the flat sided central cell is irradiated by the neutron beam. To detect neutrons which pass through the cell and matrix an x-ray film plate and gadolinium intensifying screen are used, this is housed in a Light Tight Container (LTC) positioned behind the central cell.

A reference cell with three compartments containing snowcal at zero water content, 100% water content and the initial water content of the matrix is also in the line of the beam and appears on all the photographic plates. Attached to the reference cell is a watch on which the hands and hours are marked with small lengths of plastic tube, the plastic tubing has a high hydrogen content and hence shows up clearly on the radiographs, thereby providing a permanent record of the time of exposure. By comparing the grey shades of the matrix with the grey shades of the reference cell direct determination of water contents can be made. Incorporating the reference cell in this way eliminates any errors in developing or exposure time as each radiograph has its own built in reference standards.

As water and ice are depicted identically on the radiographs, it is necessary to distinguish between these two phases by determining the relative electrical resistance of the soil at various locations.

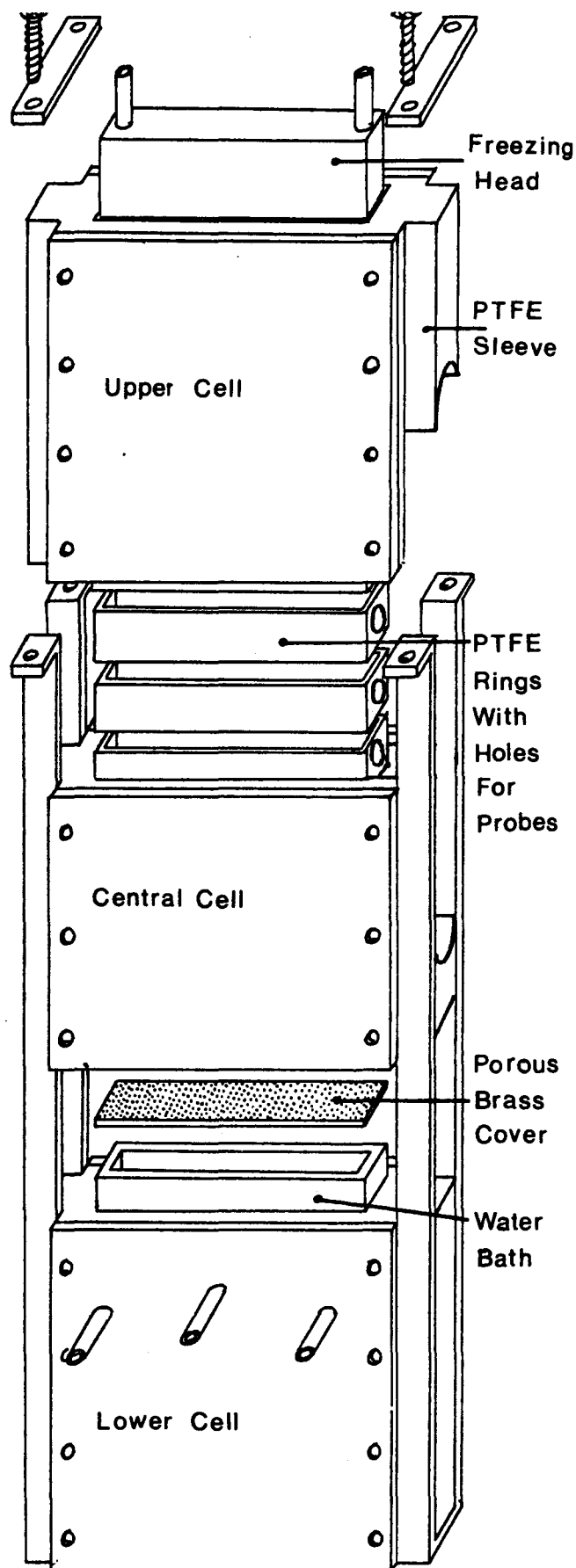


Figure 1 (Scale 1: 2)

The neutron beam has a large neutron intensity and requires a high degree of shielding. This is achieved using concrete blocks arranged to form a cavity for the apparatus.

The apparatus is surrounded by a series of copper pipes through which ethylene glycol/water mixture, at reduced temperature, is circulated to reduce the air temperature.

Access to the apparatus for positioning and removing the LTC is made possible by a narrow slot cut in the shielding. All connections to the instrumentation for the apparatus pass through a channel, formed in the shielding and re-filled with blocks of lead and paraffin wax.

The exposure time for each radiograph is accurately maintained using a paraffin wax beam stop to seal off the beam at the end of the exposure period. The radiographs obtained show the formation of the frozen fringe and as they are one to one images of the cell any heave associated with the partial freezing of the matrix can be measured directly from them.

INSTRUMENTATION

The water supply to the matrix is from a marriote vessel. Within the vessel a polystyrene float, connected to a linear motion potentiometer, rests on the water. In this way any water uptake by the matrix is represented by a movement of the float which is registered by the potentiometer and recorded on a chart recorder.

Wescor PST 55-30 psychrometers and a Wescor PR55 psychrometric microvoltmeter are used to measure water potential in the soil matrix. The psychrometers incorporate a small chromel constantan thermocouple concentrically mounted at the centre of a hollow cylindrical stainless steel bulb. This design is chosen as it minimises the effects of temperature gradients which adversely affect the suction readings. The single junction thermocouple permits measurement of these thermal gradients to enable correction of the suction readings. A calibration model for this type of thermocouple psychrometer has been developed by Brown and Bartos (1982) and has been used in this test.

Water potentials are measured with the psychrometers using the peltier effect. Water from the matrix is conducted through the bulb to the inner surface where it evaporates until the humidity approaches 100%. An electric current is passed through the thermocouple for fifteen seconds cooling the sensing junction slightly below ambient temperature so that water from the atmosphere surrounding the couple condenses on the thermocouple.

After cooling the condensed water evaporates which again cools the junction. This time however the cooling is a function of the rate of evaporation which is a function of the vapour pressure of the atmosphere which in turn is a function of the water potential of the matrix.

Copper-constantan thermocouples are located alongside the psychrometers to record the matrix temperature throughout the test.

The electrical resistance of the soil between the psychrometer probes is determined throughout the test to identify ice in the matrix. This is achieved through connections to the stainless steel shields of the psychrometers. The shields are insulated from the rest of the probe by a plastic casing and from each other by the PTFE rings which house them.

METHOD

The work has been carried out at the Universities of Manchester and Liverpool Research Reactor using a thermal neutron beam from a horizontal access hole, which gives a maximum neutron flux of $7.5 \times 10^7 \text{ n cm}^{-2} \text{ S}^{-1}$ at the radiographic position. An exposure time of 18 seconds is used for each radiograph at a reactor power of 100kw.

Loading the Matrix

With the three cells of the main apparatus in position and all instrumentation in place the matrix is loaded, via the upper cell, into the six 12.5 mm dep PTFE rings of the central cell. The matrix is compacted in ten equal layers. Each layer contains a specified quantity of matrix (dependent on the water content) and is compacted to a thickness of 7.5 mm. In this way the compaction is standardised and no compaction plane is incident with a ring intersection.

Test Procedure

With the apparatus positioned in the cavity formed in the concrete shielding, and all connections made to instrumentation and cooling equipment, cooled ethylene glycol/water solution is circulated through the copper tubing and left on overnight to lower and stabilise the matrix temperature. An initial radiograph is then taken before freezing is initiated. Freezing is achieved by circulating cooled ethylene/glycol solution through the freezing head. Subsequent radiographs are obtained at approximately half hour intervals throughout the test.

The same process is used to obtain each radiograph. With the LTC positioned behind the cell the beam stop is

withdrawn, allowing the thermal neutron beam to fall on the cell, and replaced after the exposure time of eighteen seconds has elapsed. When the LTC has radioactively 'cooled down' it is removed and the photographic plate developed.

Radiographic Materials

- FILM - 'KODAK' INDUSTREX CX, Medium Speed, fine-grain, high - contrast, direct exposure film.
- DEVELOPER - 'KODAK' LX 24 X-RAY DEVELOPER.
- STOP BATH - 'KODAK' LX INDICATOR STOP BATH
- FIXER - 'KODAK' FX - 40 X - RAY LIQUID FIXER
- HARDENER - 'KODAK' HX - 40 X - RAY LIQUID HARDENER

$$X_n = ((X - X_0) / (X_{100} - X_0)) \times 255$$

- where: X_n = New normalised digital count
 X = Old digital count
 X_{100} = Digital counts of 100% water content reference cell
 X_0 = Digital count of 0% water content reference cell

The soil matrix areas with water contents of 0% - 100% are thus enhanced to give a range of 256 grey levels. In order that the water content variations can be more easily seen the frames are density sliced in colour to give false colour images. Different colours are assigned to steps of 25 digital counts, ranging from red for levels of 0 - 25 inclusive and blue for levels of 225 - 255 inclusive.

RADIOGRAPH ENHANCEMENT AND ANALYSIS

Contact prints are made of the radiographs (negatives) and 35 mm slides (transparencies) made of these prints. The transparencies are used in a scanning microdensitometer. The size of the soil matrix on the original negative is 72.5 mm x 84 mm and on the 35 mm negatives this is reduced to 15 mm x 17.5 mm. The 35 mm negatives are scanned with a spot size of 100 μ m (0.1 mm) and hence the soil matrix area is covered by 150 x 175 pixels. Thus each pixel represents an area of 0.5 mm x 0.5 mm on the original negative.

The negatives are scanned at 3-D optical density, levels of 0 - 255 are assigned to the degree of brightness. The scanner sets white on the negative to zero and black to 255. Therefore the reference cell of 100% water content has higher digital count values than those of the 0% water content reference cell.

The scanned data are displayed on an I²S Image Analyser.

To account for any differences in exposure, printing and scanning, the frames are individually normalised using the 0% and 100% water reference cells.

For any one frame, the digital counts less than those within the 0% water reference cell are set to zero (black) and those equal to or greater than those within the 100% water reference cell are set to 255 (white) to produce an enhanced black and white image. Any values within these extremes are then linearly stretched so that the new digital count becomes:-

RESULTS

The preliminary results are in the form of three radiographs and their enhancements taken at various representative times throughout the freezing test.

The corresponding data are given in the following table.

TIME 10.24

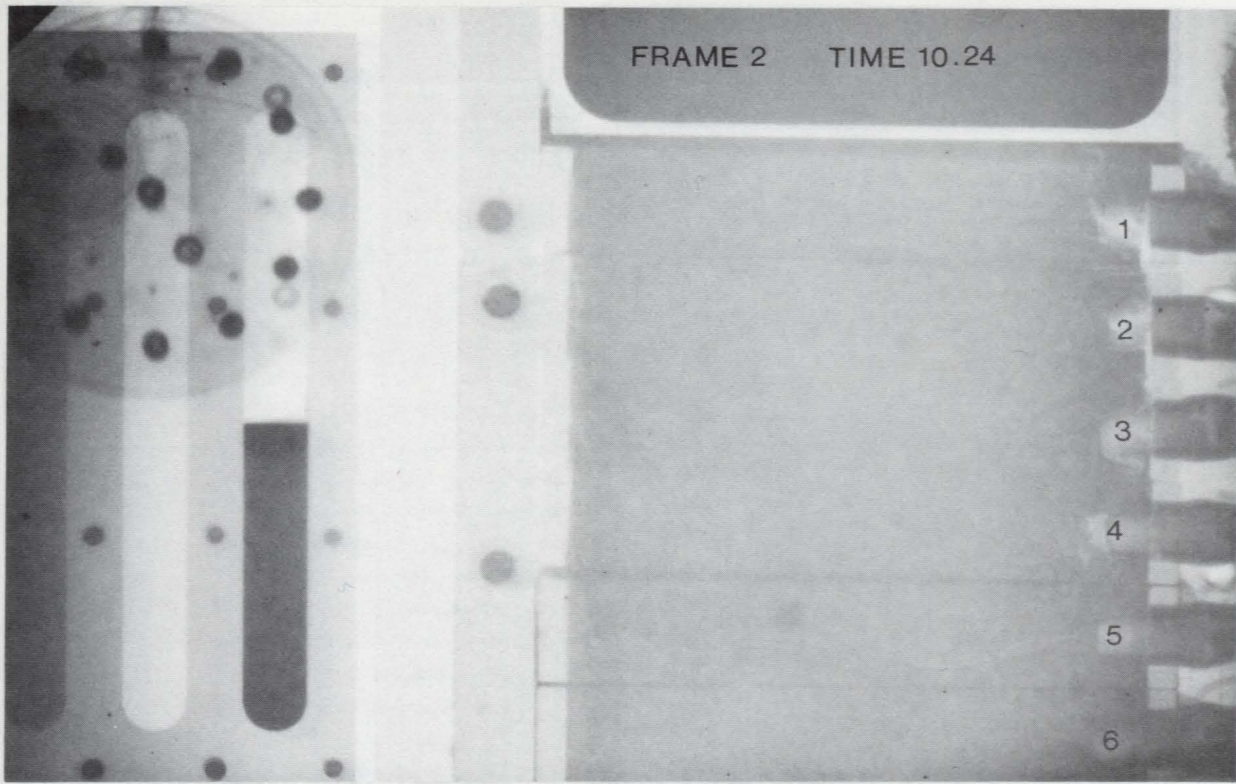
Psychrometer Position	Water Potential (Bar)	Elec. Res (K Ω)	Approx Water Content (%)
1	6.1	35	28
2	5.6	23	26
3	4.4	25	22
4	4.0	25	24
5	4.9	26	35
6	0.0		100

TIME 11.17

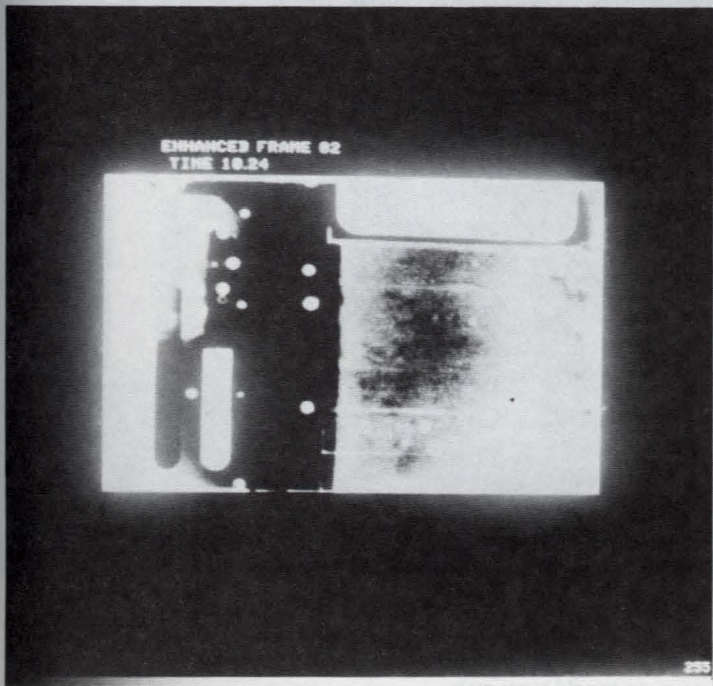
Psychrometer Position	Water Potential (Bar)	Elec. Res (K Ω)	Approx Water Content (%)
1	12.7	89	20
2	5.6	31	26
3	3.0	26	35
4	4.8	27	26
5	5.1	25	28
6	0.0		100

TIME 14.02

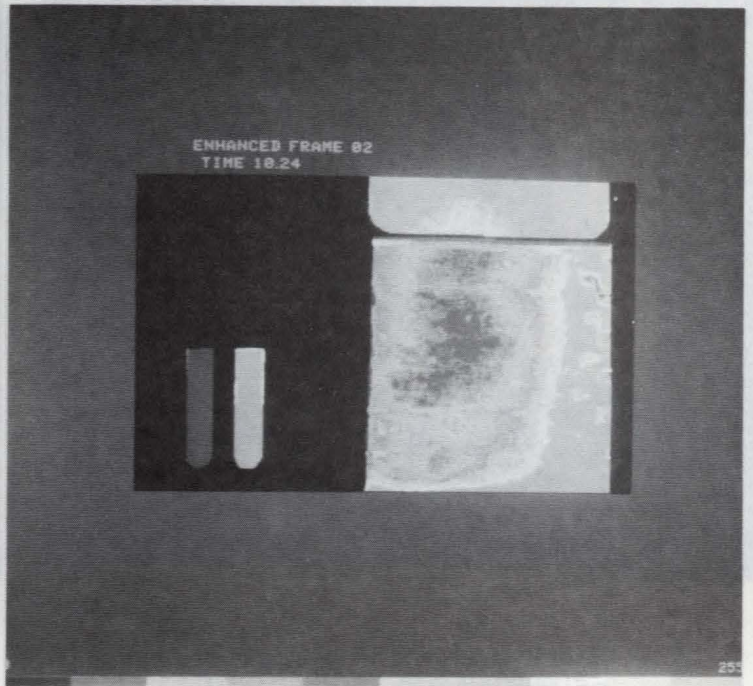
Psychrometer Position	Water Potential (Bar)	Elec. Res (K Ω)	Approx Water Content (%)
1	15.3	1100	95 (ICE)
2	7.8	480	20
3	5.0	25	12
4	4.8	29	16
5	5.2	25	18
6	0.0		100



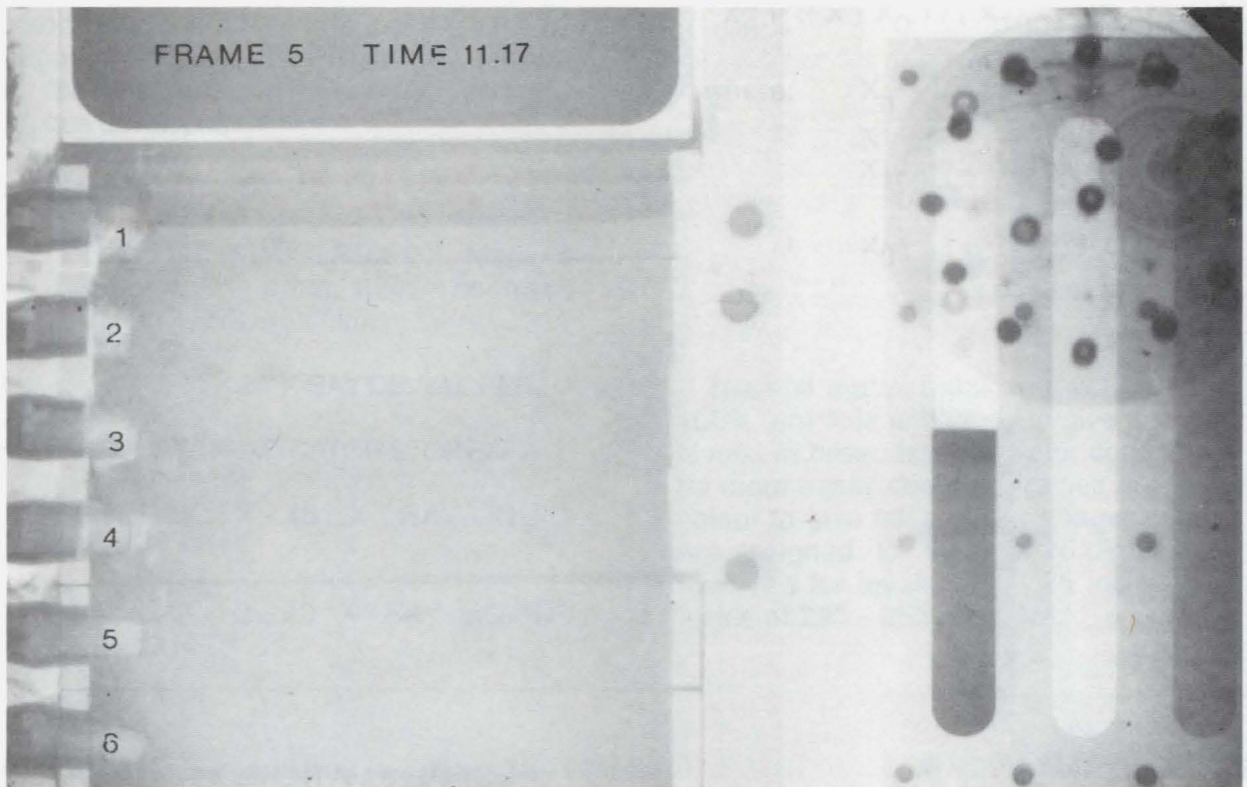
Radiograph taken at time 10.24



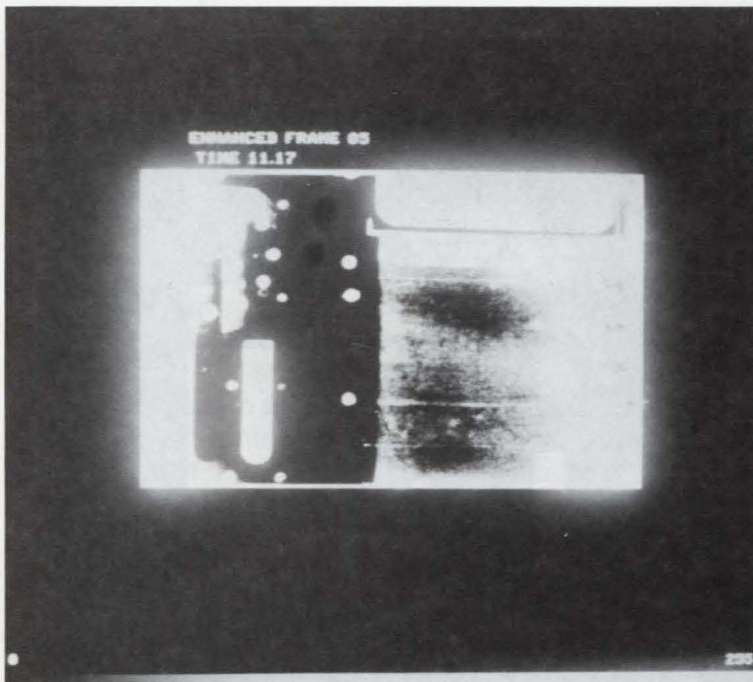
Black and White enhancement of radiograph



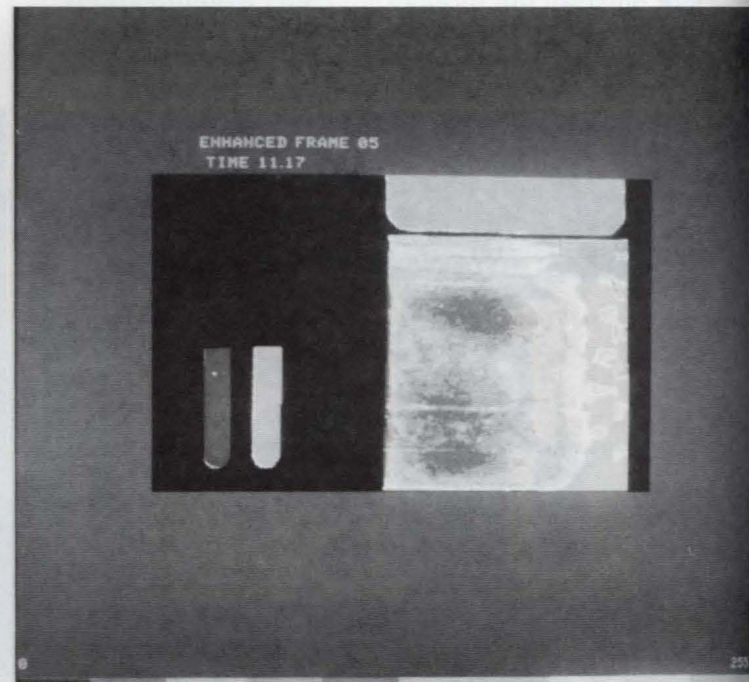
False colour enhancement of radiograph



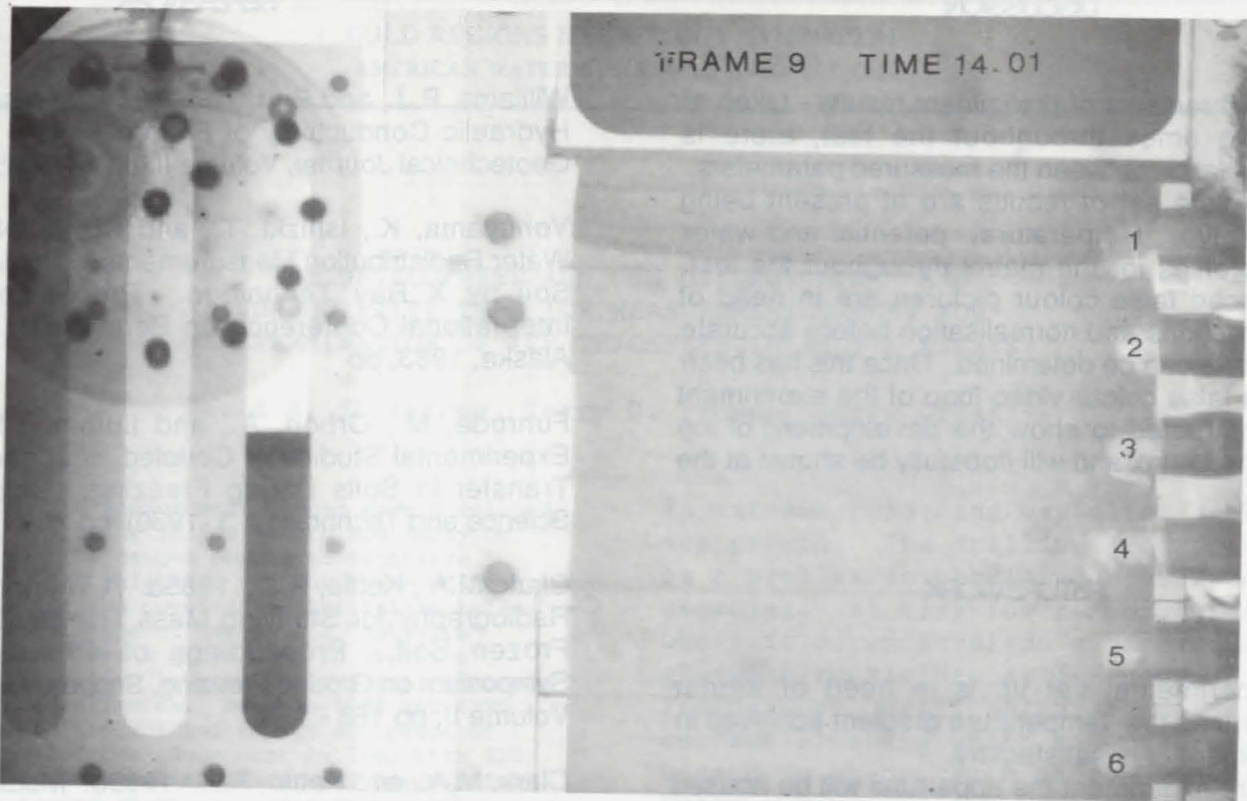
Radiograph taken at time 11.17



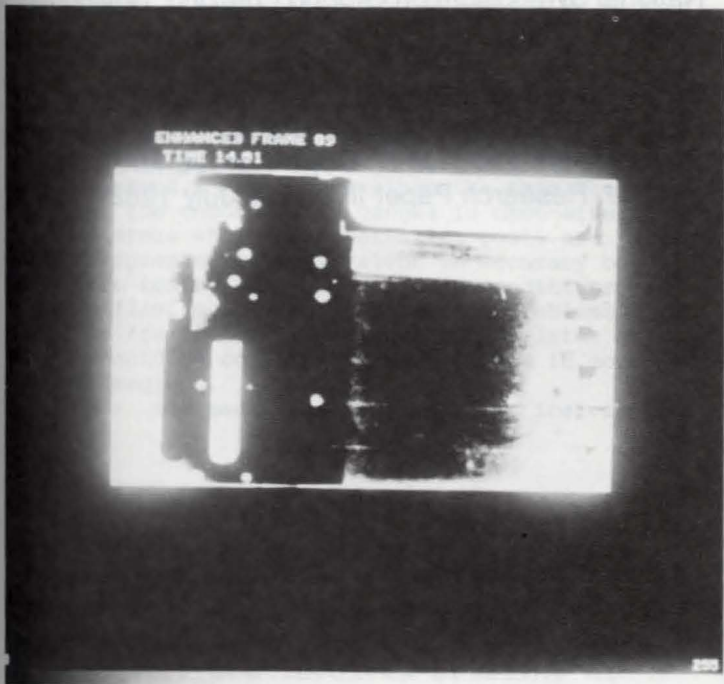
Black and White enhancement of radiograph



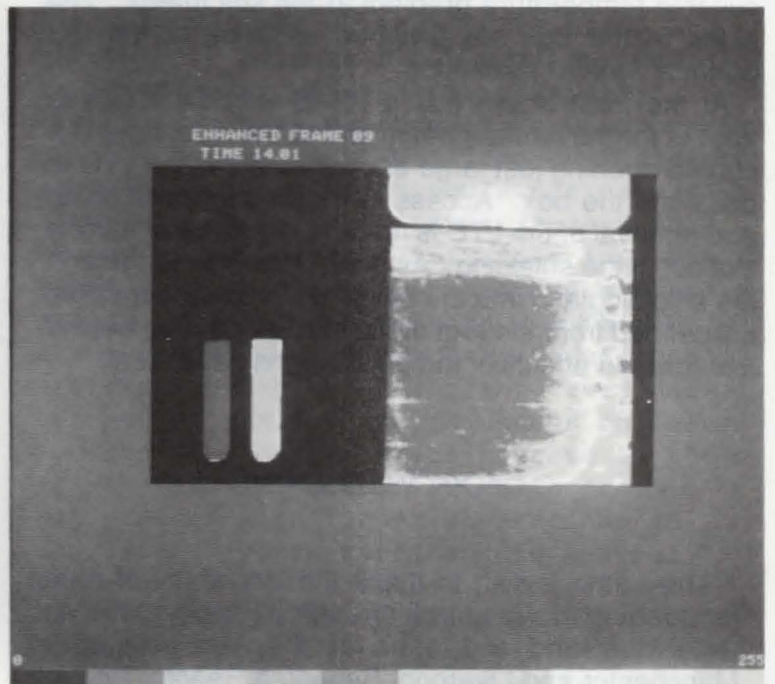
False colour enhancement of radiograph



Radiograph taken at time 14.01



Black and White enhancement of radiograph



False colour enhancement of radiograph

DISCUSSION

From the three sets of preliminary results - taken at representative times throughout the test, there is evident correlation between the measured parameters.

The complete set of results are at present being collated to give temperature, potential and water content profiles for the matrix throughout the test. The enhanced false colour pictures are in need of further corrections and normalisation before accurate water contents can be determined. Once this has been achieved a false colour video loop of the experiment will be constructed to show the development of ice lenses in the matrix and will hopefully be shown at the conference.

FUTUREWORK

The experimental set up is in need of further development as the temperature gradient achieved in this experiment is unsatisfactory.

In a future experiment the apparatus will be housed in an insulated wooden box fitted into the concrete shielding cavity, in order to further reduce the air temperature around the test rig and so facilitate a suitable temperature gradient in the soil matrix. The sides of the box are plywood sections containing paraffin wax for insulation.

At the front of the box a PTFE window provides access for the neutron beam and at the side there is a curved opening just large enough to allow the LTC to pass into the box. Access to the box for positioning and removal of the LTC is made possible by a narrow slot cut in the shielding. As the LTC is moved through the shielding and into the box it disturbs rubber strips, suspended from the roof of the slot, which drop behind it to form an effective temperature insulated seal.

ACKNOWLEDGEMENT

The authors wish to thank the University of Aston for funding this research through a Faculty grant and Dr Bates and the staff of the Universities of Manchester and Liverpool Research Reactor for their continued support.

REFERENCES

- Williams, P.J., and Burt, T.P., 1974. Measurement of Hydraulic Conductivity of Frozen Soils - Canadian Geotechnical Journal, Volume II, pp 647 - 650.
- Yoneyama, K., Ishizki, T., and Nishio, N., 1983 - Water Redistribution Measurements in Partially Frozen Soil by X Ray Technique. Proceedings of 4th International Conference on Permafrost, Fairbanks, Alaska, 1983, pp
- Fuhruda, M., Orhon, A., and Luthin, J.N., 1980. Experimental Studies of Coupled Heat and Moisture Transfer in Soils During Freezing. Cold Regions Science and Technology. 3 (1980) pp 223 - 232.
- Clark, M.A., Kettle, R.J., 1985a. A Thermal Neutron Radiography for Studying Mass Transfer in Partially Frozen Soil. Proceedings of 4th International Symposium on Ground Freezing, Sapporo, Japan, 1985. Volume II, pp 168 - 173.
- Clark, M.A., and Kettle, R.J., 1985b. Modifications to Equipment and Improvements in Facilities, used in the Study of Mass Transport in a Partially Frozen Soil by Thermal Neutron Radiography. Proceedings of 2nd National Symposium on Ground Freezing, Nottingham, England, 1985.
- Brown, R.W., and Bartos, D.L., 1982. A Calibration Model for Screen -Caged Peltier Thermocouple Psychrometers. U.S Dept Agriculture, Forest Service, Research Paper INT - 293 July 1982

THE DEVELOPMENT AND USE OF "HOT-WIRE" AND
CONDUCTIVITY TYPE ICE MEASUREMENT GAUGES FOR
DETERMINATION OF ICE THICKNESS IN ARCTIC RIVERS

David A. Sherstone, Terry D. Prowse, Harry Gross¹

ABSTRACT: Two ice measurement gauges were developed to assist in the study of ice growth and decay on arctic rivers. The gauges permitted successive measurement of ice thickness without the need to drill through the ice cover after initial installation. The first type of gauge is a "hot-wire" design, modified from a gauge used in southern Canada. It was proven to provide low-cost, accurate readings in cold climates. Between 1982 and 1986 modifications to the initial design and reuse of components reduced per gauge cost to less than \$20 per season. Measurement accuracy was approximately 0.5 cm. The second gauge, a conductivity probe was designed to speed data collection and permit remote reading of ice thickness. Parallel electrodes are installed vertically through the ice and allowed to freeze into the ice cover. The magnitude of electrical current carried between the electrodes is proportional to the length of electrode in the water while current carried by the ice is negligible. Ice growth is therefore proportional to the reduction in current flow. Four conductivity gauges were tested in the 1984-85 winter. Accuracy was comparable to that of the hot-wire gauges except in the re-freezing period. While more expensive than the hot-wire type, the conductivity gauges is cost-effective in remote areas where transportation costs are high. Although approximately equivalent in accuracy both gauges were tested only under arctic conditions in a calm flow regime, and performance problems related to frazil ice formation and mid-winter melt periods should be considered prior to use in more temperate regions.
(KEY TERMS: ice measurement; freshwater ice; arctic rivers.)

INTRODUCTION

Within the nordic countries, the most common and standardized method of measuring the thickness and basic stratigraphy of freshwater ice involves drilling of the ice sheet (Adams and Prowse 1986). Drilling has a number of drawbacks; it is time consuming, unpleasant and risky

in extreme cold, and may alter subsequent ice growth. The drilling procedure can be a problem in obtaining measurements, especially at very low temperatures (-25°) where it often involves a hazardous struggle with recalcitrant, gas-powered drills. Furthermore, drill holes often lead to surface slushing which can create a travel hazard in areas, such as the Mackenzie Delta, where the ice cover is extensively used for road transport.

The effects of slushing produced by drilling can also significantly affect the temporal and spatial patterns of ice thickness. Because the underlying water is often under hydrostatic pressure, either from surface snow loads or increases in upstream flow, drilling can initiate a slushing event which would not naturally occur. Under cold temperatures, the slushed layer of snow refreezes into an upper stratum of white ice thereby augmenting the total ice thickness. Although Adams and Prowse (1981) have found that artificial slushing of the snowcover does not affect maximum ice thickness on lakes because of a compensation process in the growth rates of black and white ice, it can produce significant aberrations in short-term growth rates and in spatial patterns of ice thickness. The effects of artificial slushing are probably much greater on rivers, because of the greater possibility of frequent and quite large overflows. Hence, measurement procedures which employ drilling preclude obtaining a record of "natural" ice growth on both

¹Respectively, D. Sherstone, Inuvik Scientific Resource Centre, P.O. Box 1430 Inuvik, Northwest Territories, Canada, XOE 0T0, T. Prowse and H. Gross, National Hydrology Research Institute, Environment Canada, Ottawa, Ontario, Canada, K1A 0E7

lakes and rivers.

To obtain an "undisturbed" sample, standard practice usually involves drilling a new hole at a slightly different location each time a measurement is made. However, the thickness of freshwater ice, especially river ice, is characterized by a considerable degree of local variability. In addition to variability introduced by white ice growth at the surface, the bottom topography of river ice can be quite variable due to, for example, frazil accumulations and melt-induced wave patterns. To minimize the effect of such spatial variability in the record of ice growth, measurements should be made at the same point each sampling period.

In view of the problems associated with drilling and the need to obtain repetitive samples from a single site, a number of measurement devices have been developed over the years. The approaches and instruments used by various countries are reviewed in Adams and Prowse (1986). This paper reviews the development and testing of two of these gauges under arctic conditions on channels of the Mackenzie Delta.

One of the primary design criteria for the gauges was that they provide an ice measurement without inducing artificial slushing. They were also to be inexpensive enough to be expendable. The first is a "hot-wire" resistance gauge similar to that used by Ramseier and Weaver (1975) in southern Canada, but redesigned for use under arctic conditions. The second gauge or "conductivity probe" was designed to speed data collection and offer the possibility of remote reading of ice thickness, either through inter-connecting a number of gauges to a central recorder or through a satellite data collection platform.

Hot-wire gauges have been used successfully in the Mackenzie Delta since 1982. The conductivity probe has been tested under temperate conditions on the Ottawa River in 1983-84, under arctic conditions in the Mackenzie Delta in 1984-85, and is now being evaluated under sub-arctic conditions in the Schefferville region of Quebec. Data from the Mackenzie Delta program are presented in Sherstone and Prowse (1986).

HOT-WIRE GAUGES

Design and Construction

The earlier device by Ramseier and Weaver (1975) was modified to make it less expensive, easier to assemble in the field and more compact (Figure 1). Major components of the probe include: a stand and base plate, electrical and heating (resistance) wires, contacts, and a weight. The wooden base plates are fabricated from common 2.5 X 10 cm lumber with each leg approximately 60 cm long. A wooden 2 cm thick plywood pad reinforces the junction of the support legs and is used to fix a threaded pipe flange to the assembly. The "L"-shaped pipe stand is made of two lengths of 2.5 cm mild steel pipe. The vertical section, 90 cm long, is joined to a 60cm horizontal pipe by a 90° elbow fitting. The wire is supported at the end of the horizontal bar through a slot in the pipe and retained by a threaded cap.

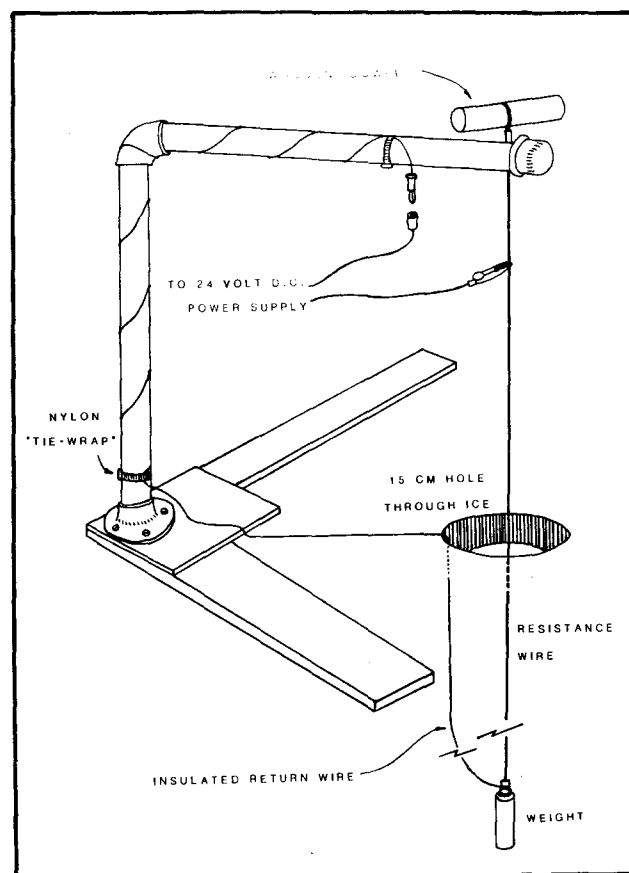


Figure 1. Schematic of Hot-Wire Ice Thickness Gauge (After Ramseier and Weaver, 1975) Details of Material and Construction are Provided in the Text.

The resistance wire (Chromel A; 18 gauge) is cut to a length slightly greater than the expected maximum ice thickness plus the height of the stand above the ice surface. A 275 - 300 cm wire is used in the Mackenzie Delta. The electrical circuit is created by fixing one end of an insulated wire to the horizontal pipe and joining (crimp-solder) the other end to the resistance wire at the weight assembly. The weight is currently constructed of steel rod, but any heavy material could be used.

Initial cost of the gauges is less than \$20 CDN., but many of the parts are retrievable which can further reduce costs. In the Mackenzie Delta, for example, parts recovered near the end of one winter season reduced the unit gauge price by 50% for the subsequent season.

Installation and Operation

Initial installation involves removing snow from an approximate 2 m² area. A 15 cm hole is drilled through the ice and the resulting slush used to freeze the base plate around the hole, with the end of the stand directly over the hole. The wire and weight assembly are lowered through the hole and the insulated wire is secured to the pipe frame with electrical "tie-wraps". Ideally, snow should not be replaced over the hole until the ice surface has refrozen. Otherwise, the mixture of water and snow will refreeze into a hummock of white ice not representative of surrounding ice stratigraphy and makes subsequent measurements difficult.

At installation, notes are made of the ice thickness, both white and black ice, and the amount of wire which can be pulled up before the weight strikes the base of the ice sheet. Subsequent measurements involve heating the resistance wire by attaching a battery, lifting the weight to the bottom, recording the amount of extended wire, and then lowering the weight again. Under cold conditions, the battery can be temporarily disconnected between raising and lowering the weight, thereby freezing the wire in a "measurement" position. The amount of ice growth at the base of the ice sheet between sampling dates is equal to the difference in the lengths of wire which can be exposed at the surface (Figure 2). The amount of white ice growth at the

surface is obtained by measuring the upward growth on the vertical portion of the pipe frame. Gradations on the pipe assist in measurement.

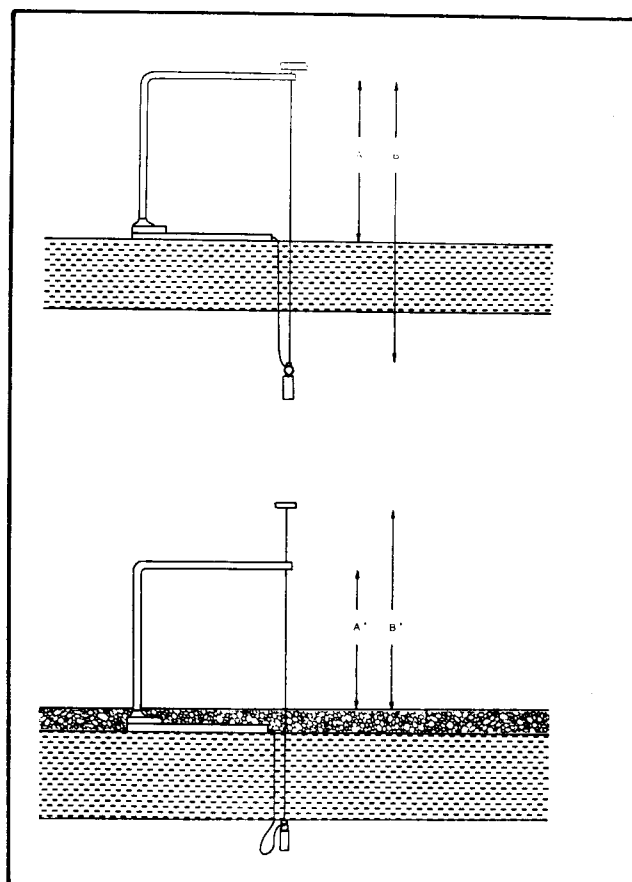


Figure 2. Measurement of Ice after Freeze-back of Installation Hole. Distance, A, and Length of Resistance Wire, B, are known at the time of installation. During use Measurements A', and B', are taken. Total Ice Thickness is thus B-B'; White Ice Thickness can be obtained from A-A'.

In southern Canada sufficient power can be supplied by a 12 volt battery to free the wire in a short period of time. However, under arctic conditions with ice thickness often exceeding 1.5 m and temperatures below -25°C, a 12 volt system requires 5 to 10 minutes to free the wire. A series electrical connection of two batteries (24 volts) can reduce the waiting period to less than 5 seconds.

Gauge Performance

In 1982-83 sixteen gauges were install

ed in the Mackenzie Delta (Sherstone 1984a). Four were located in a lake near Inuvik, ten in central Delta locations and two in a channel expected to experience thicker than normal ice. All gauges functioned flawlessly throughout the season.

In the following three years, twenty gauges were installed on major Delta channels with one gauge failure in each of the first two years (Sherstone 1984b, 1985). In 1983-84 a gauge wire could not be melted free for approximately six weeks during the coldest part of the winter. The cause of this partial failure is unknown, but a problem in one of the two crimp-solder junctions is suspected. In 1984-85, a gauge failed soon after installation probably due to a broken wire below the ice.

To assess the accuracy of the hot-wire gauges, test holes were drilled in close proximity at various times throughout the growth season. Gauge readings were within 3 to 4 cm of the values obtained by drilling. In view of the possible errors associated with the spatial variability of ice thickness, the gauge readings are considered satisfactory.

CONDUCTIVITY GAUGES

Design and Construction

The conductivity gauge was developed by the National Hydrology Research Institute, with final engineering and production undertaken by Richard Brancker Research Ltd. The theory of operation is that a pair of parallel electrodes immersed in water will pass an electrical current proportional to the length of the electrode in the water. As the water freezes downward, the ice forms an insulating layer thereby reducing the electrical current flow. Measurement of current flow yields the length of the electrodes still exposed to water and by simple subtraction from the known length of the electrodes, the ice thickness can be obtained.

Such a simplified approach ignores possible changes in the conductivity of water with temperature and solute load. To compensate for such variations, a second, shorter pair of reference electrodes is positioned below the measurement

electrodes and below expected freezing levels. The ratio of current flow between the measurement and reference electrode pairs will be the same as the ratio of their lengths in unfrozen water.

The gauge consists of two basic parts, an ice probe and a portable reader unit (Figures 3a, 3b, and 4). The bottom of the probe is a hollow plastic pipe which supports two (0.05 cm) diameter stainless steel tubes (AISI type 304) running down each side of the pipe. Plastic spacers separate the tubes from the pipe. All electrodes are wired to an electrical coupling head contained within a housing on the ice surface. The top of the housing is threaded and capped to protect the wiring from the elements.



Figure 3a. NHRI Conductivity Type Ice Thickness Probe. Note Clear Plastic Collar Base Plate, required because of large diameter hole in Ice cut in the ice.



Figure 3b. Electrical Coupling Head. When not in use a Protective Cap covers the Connectors.

Polyvinylchloride (PVC) plastic was used for the probe body because it can withstand low temperatures without becoming brittle, is easy to machine, inexpensive and readily available. Stainless steel tubing was used for the electrodes because it does not form an insulating oxide surface, as would aluminum, or corrode as copper or ferrous electrodes. As long as the water is not completely oxygen free, the stainless steel retains a stable passivated surface. It has sufficient electrical conductivity for this application and low thermal conductivity to minimize vertical heat transfer. Hollow tubing, rather than solid rod, contributes to the low thermal conductivity.

The reader unit contains electronic circuitry that automatically balances a Wheatstone bridge by means of precision resistors and reed relays. The results are displayed on LED's on the front panel. The use of resistors and a bridge reduces variations resulting from temperature

extremes. By making the bridge self-balancing, operator time is considerably reduced.

Current costs of the probes are approximately \$200 CDN and \$1,000 CDN for a reader unit. Design simplification and construction modifications are expected to reduce these costs, especially in the case of the probes.

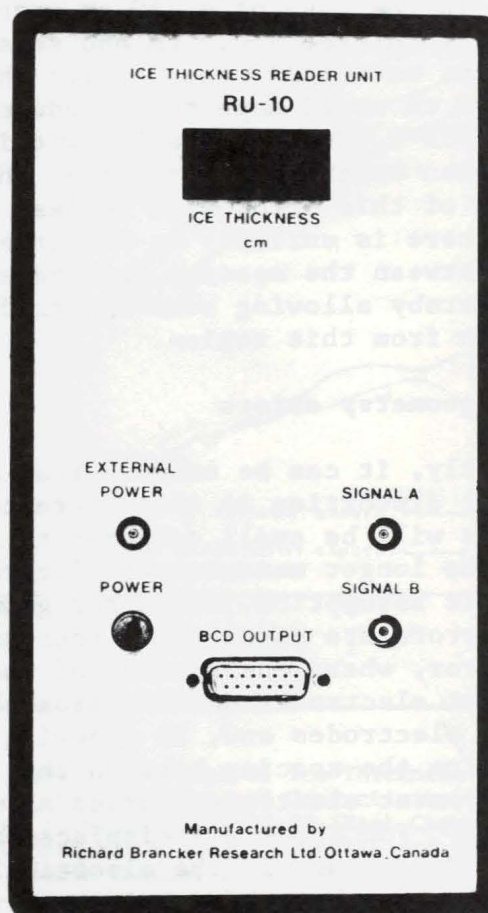


Figure 4. Reader Unit. Box measures 24.0 cm X 12.5 cm X 9.0 cm and weighs approximately 1.7 kg with batteries. The Reader Unit is connected to the Electrical Coupling Head by two 1.4 m Co-axial Cables.

Design Measurement Errors

There are four design and construction factors which might affect measurement accuracy: a) "staircase" errors, b) probe geometry error, c) water temperature gradient error, and d) ionic concentration gradient error. Space does not permit the derivation of each error but the results of some "worst case"

analyses are provided below.

a) Staircase error

The measurement electrodes are held in place by a series of spacers. Assuming perfect contact between the electrodes and spacers, there will be no electrical flow from the region of contact but the ice thickness will be underestimated by an amount equal to the total thickness of spacers in the unfrozen water. For example, in the case of a 150 cm probe with spacer thickness 0.5 cm and separation 10 cm, an initial measured ice thickness of 90 cm would have to be reduced by 3 cm (six 0.5 cm spacers lie within the unfrozen water). In practice, the magnitude of this error will be less because there is unlikely to be perfect contact between the spacers and the electrodes, thereby allowing some electrical conduction from this region.

b) Probe geometry errors

Firstly, it can be assumed that any bending or distortion in the reference electrodes will be small compared to that in the longer measurement electrodes. Noting this assumption, two other geometry related errors are possible: a constant offset error, where the spacing of the measurement electrodes differs from the reference electrodes and, b) a bowing error, where the spacing between the two measurement electrodes varies along the length. For the small displacements expected, any change in the electrical current flow can be taken as inversely proportional to the change in electrode spacing. Thus, any change in electrical current flow from irregular spacing will produce a corresponding change in the measured length of the water column.

With the 0.5 cm tubing, manufacturing tolerances for an electrode spacing of 3.8 cm is approximately 0.08 cm. The expected maximum offset and bowing errors in this case are 2.1% and 1.3% respectively.

c) Water temperature gradient error

The electrical conductivity of water increases with temperature. In a worst case scenario, the probe would encounter

a gradient of 4°C (freezing point to the temperature of maximum density for water) over the length of the electrodes. This results in a maximum error of approximately 4%. Much smaller temperature gradients and errors are normally to be expected.

d) Ionic concentration gradient

Changes in ionic concentration along the electrodes will affect measurement readings in the same way as a temperature gradient. Changes in conductivity resulting from the process of freeze-out are currently being examined at the Schefferville test site. For freshwater, it is expected that the effects of variations in ionic concentrations will not exceed that due to temperature variations (less than 4%).

Under most conditions, the combined error from the above four sources is expected to be less than 5%.

Installation and Operation

Installation of the conductivity probe is decidedly simpler than that for most other types of ice measurement devices. Site preparation involves clearing a small patch of snow and drilling a single hole through the ice which is sufficiently large (approximately 5 cm) to permit lowering of the probe and electrodes. In practice, a larger diameter hole will probably be drilled because of equipment availability and the need for a larger hole to permit inspection of the ice stratigraphy. Where large diameter holes are drilled, a collar can be placed between the probe and upper housing to support the device while refreezing occurs (see Figure 3a).

Notes are made of the initial thickness of white and black ice, and of the collar if one is used. Subsequent growth of white ice is noted on the upper housing. To obtain a measurement of ice thickness beneath the surface, the housing cap is removed and the reader unit attached to the electrode terminals. A complete reading requires less than one minute.

Gauge performance

In January 1985, four conductivity gauges with 1.5 m measurement electrodes were installed in the Mackenzie Delta. The gauges were located within 0.3 - 1.0 m of some previously installed hot-wire gauges. Initial reading of both gauge types was made 14 days after installation and then at 10 day intervals when weather permitted.

Removal of the gauges proved difficult. Even close to break-up, solar heating had not melted the gauges free. One complete gauge was recovered but this required extracting an approximate 90 kg ice block. Unfortunately, the other three gauges had to be severed at the housing-probe connection.

Records obtained from adjacent hot-wire and conductivity gauges are shown in Figure 5. In general, the data from the two types of gauges show similar trends in ice growth and ice thickness. The differences between readings can be ascribed to a number of factors related to gauge installation and spatial variations in sub-surface ice topography. However, because there was no way to visually inspect the ice sub-surface, it is only possible to speculate on the relative importance of these factors.

Firstly, differences in gauge readings at the start of the study period can be explained by the lengthy time required for refreezing in the holes used for installation of the conductivity probes. The conductivity probe will not provide an accurate reading of ice thickness until the entire ice stratum has refrozen. The presence of water within the hole will result in an under-prediction of ice thickness, such as that observed for gauge 84-02 during the refreezing period. By the time of the second reading at this site, both gauges were producing similar results. If the two types of gauges are installed at the start of the winter season, when the ice sheet is much thinner, the time required for a stabilization of readings will be significantly shortened.

Following the initial refreezing period, site 84-11 showed a consistent difference between the two gauge readings. Although this may have been related to the electrode circuitry in the

conductivity probe, it could also have been due to large local variations in ice thickness. The difference in thickness may be due to natural spatial variations in the sub-surface ice topography or from effects created by ice drilling during gauge installation.

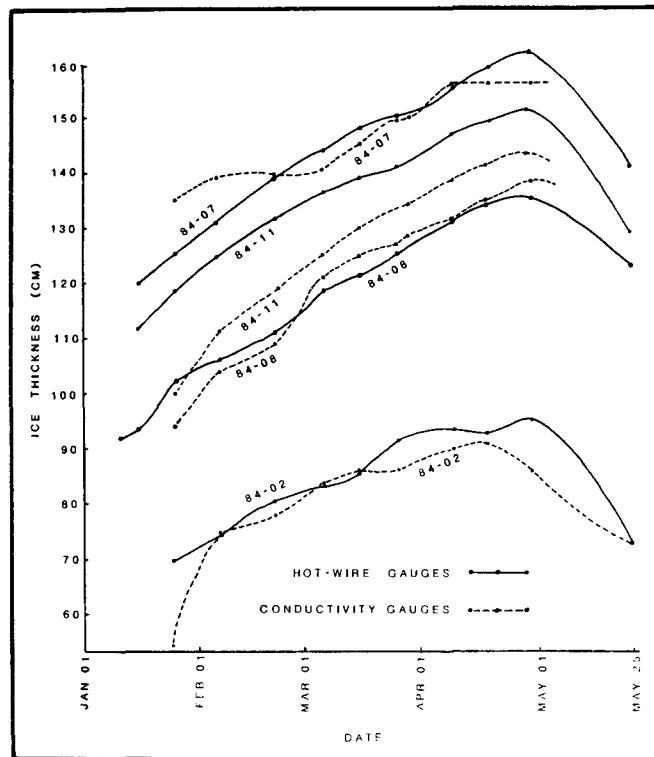


Figure 5. Graph of Ice Thickness Values obtained from Hot-Wire and Conductivity Gauges located at Gauge Sites 84-02 (East Channel), 84-07 and 84-08 (Oniak Channel) and 84-11 (Middle Channel). Winter 1984-85

During the spring period, hydrothermal melt at the base of the ice sheet can amplify local variations in ice thickness. Although water temperatures may only be a fraction of a degree above freezing, the river heat flux is often sufficient to produce large ripples on the base of the ice sheet. For example, Marsh and Prowse (1986) observed, on another part of the Mackenzie River system, ice ripples at the base of the ice sheet with amplitudes of up to 6 cm and wavelengths of approximately 20 cm. Under such conditions, differences of 12 cm could be expected between gauges, despite their close proximity. Furthermore, these ripples may be a transient feature which could further

complicate the gauge comparison. These type of effects may be responsible for the late season fluctuations in the data from site 84-02.

One final gauge problem is apparent for site 84-07 in Figure 5. By April 07 the readings from the conductivity probe stabilized near 155 cm. This was simply due to the ice thickness exceeding the length of the measurement electrodes.

Although the original objective of this project was to test the performance of the gauge under field conditions, the complications created by various hydroclimatic factors indicates that future calibration of the devices should be undertaken in a controlled laboratory environment. The field results, however, suggest that reliable readings can be obtained. Periodic confirmation of the readings by drilling is recommended, at least until variations in the record can be adequately explained.

DISCUSSION

The hot-wire gauges have been used in the Mackenzie Delta for four winters and can now be considered operational devices. The gauges are inexpensive, easily manufactured, largely recoverable and can be quickly read. They have resulted in increased productivity and reduced the danger to field personnel from exposure. The present network of 20 gauges, spread along 115 km of ice roads, can be monitored in one day, of which about two hours is spent in data acquisition. Previously, only five to eight holes could be completed by drilling in one day over the same route. Furthermore, drilling required almost twice as much time spent by field personnel exposed to the elements.

The conductivity gauge is still in a design stage but appears to hold considerable promise for reducing field time and speeding data collection, especially when integrated with data-loggers or satellite DCP's. It is hoped that design simplification will reduce the cost of the probes. However, even at the current price, the conductivity gauge can be cost-effective for application in remote areas where transportation costs are high.

Both gauges appeared to provide reliable ice thickness measurements. However, these tests were primarily restricted to arctic conditions within the calm flow regime of the Mackenzie Delta. A number of other performance problems may arise under different climatic and flow conditions.

For example, more turbulent flow on other rivers may lead to the production of active frazil which will adhere to portions of the gauges exposed beneath the main ice sheet. Frazil accumulations could quickly encase the gauge and render it useless. This problem does not develop on lakes or on rivers without open water zones necessary for frazil production. In case of the conductivity probe, turbulent water does, however, eliminate the errors produced by temperature and ionic gradients. These are most likely to be a problem in the case of lakes where there is little mixing beneath the ice sheet.

Mid-winter melt periods, which are common in more temperate climates, may also limit the usefulness of the conductivity probe. Absorption of solar radiation by the exposed gauge housing and heat conduction along the probe may result in the accumulation of water beside the electrodes. This water will increase current flow and result in an underprediction of the thickness of the surrounding ice sheet. Subsequent refreezing, however, should make this only a temporary problem.

REFERENCES

- Adams, W.P. and T.D. Prowse, 1981. Evolution and Magnitude of Spatial Patterns in the Winter Cover of a Temperate Lake. *Fennia*, 33, 117-128.
- Adams, W.P. and T.D. Prowse, with M.A. Bilello, E. Eliassen, S. Freysteinnsson, O. Laasanen, T. Pangburn, B. Raab, E. Tesaker and A. Tvede, 1986. Techniques for Measurement of Snow and Ice on Fresh water in Nordic Countries. Proceedings of the Sixth Northern Research Basins Symposium, Houghton, Michigan (in press).
- Marsh, P. and Prowse, T.D., 1986. Water temperature and heat flux to the base of river ice covers. National Hydrology Research Institute report,

- Environment Canada, Ottawa, 42 p.
- Ramseier, R.O. and Weaver, R.J., 1975.
"Floating Ice Thickness and Structure Determination - Heated Wire Technique" Technical Bulletin No. 88, Inland Waters Directorate, Environment Canada, Ottawa, 16 p.
- Sherstone, D.A., 1984 a. "Ice Thickness in the Mackenzie Delta, Winter 1982-83: Data Obtained From Hot-Wire Gauge Systems", Report 84-1, Inuvik Scientific Resource Centre, Dept. of Indian Affairs and Northern Development, Inuvik, Feb. 1984, 16 p.
- Sherstone, D.A., 1984 b. "Ice Thickness in the Mackenzie Delta, Winter 1983-84: Data Obtained From Hot-Wire Gauges", Report 84-4, Inuvik Scientific Resource Centre, Dept. of Indian Affairs and Northern Development, Inuvik, October 1984, 16 p.
- Sherstone, D.A., 1985. "Ice Thickness in the Mackenzie Delta: Winter 1984-85". Report 85-2, Inuvik Scientific Resource Centre, Indian and Northern Affairs Canada, Inuvik, Oct. 1985, 13 p.

RECENT DEVELOPMENTS IN HYDROLOGIC INSTRUMENTATION

Vito J. Latkovich and James C. Futrell II¹

ABSTRACT: The programs of the U.S. Geological Survey require instrumentation for collecting and monitoring hydrologic data in cold regions. The availability of space-age materials and implementation of modern electronics and mechanics is making possible the recent developments of hydrologic instrumentation, especially in the area of measuring streamflow under ice cover. Material developments include: synthetic-fiber sounding and tag lines; polymer (plastic) sheaves, pulleys, and sampler components; and polymer (plastic) current-meter bucket wheels. Electronic and mechanical developments include: a current-meter digitizer; a fiber-optic closure system for current meters; noncontact water-level sensors; an adaptable hydrologic data acquisition system; a minimum data recorder; an ice rod; an ice foot; a handheld sediment sampler; a lightweight ice auger with improved cutter head and blades; and an ice chisel.

(KEY TERMS: hydrologic instrumentation; electronics; water-level sensors; data acquisition system; microprocessor-based instruments.)

INTRODUCTION

The U.S. Geological Survey is the principal Federal organization responsible for providing water resources information. Through a system of data-collection programs, measurements of surface water, ground water, and water quality are made at more than 15,000 individual remote field locations throughout the nation. A large number of these locations are located in cold regions; necessitating measurements under extremely cold temperatures and even under ice cover. Continual modernization and automation of instrumentation is highly desirable and essential as a means of increasing overall organization effectiveness and efficiency. The purpose of this report is to briefly describe a few developments that are helping to keep the Survey up to date in hydrologic instrumentation.

DEVELOPMENTS BASED ON NEW MATERIALS

Synthetic-fiber sounding and tag lines are presently being field tested and evaluated. The material used is Kevlar (the use of brand names in this report is for identification purposes only and does not constitute endorsement by the U.S. Geological Survey), an aramid fiber that is extremely strong and lightweight. The sounding line will incorporate a 4-conductor wire internally for electrical signal transmission between the sounding sensor and recording/listening device. The tag lines vary in size and use from a 1/16-in.- diameter wading measurement line to 3/16-in.- diameter boat measurement lines that either float or are lead-weighted depending on the depth of submergence required. The wading line has a 300-lb breaking strength and a 600-ft length of line can be pulled taut with a 25-lb force.

Lennite, an ultra-high molecular weight polymer (plastic), has been tested and evaluated as a replacement for metal pulleys, sheaves, handles, and water-quality sampler components. This polymer can be machined in the same manner as metals. It is as durable and much less expensive than the metals.

Price AA and Pygmy current-meter bucket wheels have been developed using Lexan, another polymer that is very durable and easily molded. It has been observed during cold weather field tests that ice-covered polymer wheels warm up much faster in flowing water than the existing metal ones. The polymer wheels have solid cups (buckets) that have been laboratory-tested and shown to be almost nonresponsive to the vertical component of velocity. Also, ice buildup does not occur on the solid cups as it always does in the metal open-cups. Polymer wheels are extremely cost effective; an AA polymer wheel may cost about \$5 per copy versus \$125 for the metal version and a Pygmy polymer wheel may cost about \$3 per copy versus \$84 for the metal version.

¹Supervisory Hydrologist and Engineering Technician, Hydrologic Instrumentation Facility, U.S. Geological Survey. WRD, NSTL, MS 39529.

ELECTRONIC AND MECHANICAL DEVELOPMENT

A current-meter digitizer (CMD) was developed to automate streamflow velocity measurements. The CMD is a microprocessor-controlled unit that automatically records the current-meter revolutions, keeps track of time, and converts the results into real-time velocities. Meter-rating equations are preprogrammed into the CMD's memory for instant recall, dependent on the mode of recording (automatic or manual) and the type of meter being used. In the read-velocity mode, the hydrographer can rapidly assess variations in velocity by observing if the computed velocity numbers are changing or steady. The CMD straps to the hydrographer's waist or arm and may be operated while wearing mittens in temperatures down to -40° C.

The fiber-optic closure system, a near frictionless technique for monitoring current-meter bucket wheel revolutions, functions by rotating two U-shaped, fiber-optic bundles in conjunction with the movement of the bucket wheel. An infrared light-emitting diode and a photo transistor are used to sense light changes as the rotating fiber-optic bundles pass and block light transmission. Four pulses are generated for each bucket wheel rotation. An electronically clean, square wave is generated. The spacing between the rotating bundles and infrared sender/receiver is not critical. The upper housing of the system resembles an inverted cup that is sealed with O-rings to retard the entry of water and silt.

Traditionally, the U.S. Geological Survey has collected water-level (stage) data using floats, pressure devices, surface followers, and other devices. All of these sensors/devices require a physical connection from the stream to the data-recording system/shelter, which is not always practical due to restrictions on locating gaging stations and sensors.

The 1980 eruption of Mt. St. Helens and the ensuing problems of obtaining water levels in the surrounding streams due to the very unstable channels, prompted the Survey to explore the feasibility of using noncontact water-level sensors; i.e., no physical "connection" between the sensor/recorder and the stream.

To date three different noncontact technologies have been researched and developed: ultrasonic, laser, and radio frequency. Ultrasonic sensors are presently employed as early-warning flood and mudslide detectors as well as backup units for primary sensors. They do not operate within the Survey's required accuracy limits (± 0.01 ft) and cannot be used as primary water-level sensors. The units are interfaced to digital water-level recorders and/or data-collection platforms for near real-time data transmission. A laser sensor prototype was developed, but rejected as a primary sensor because it also could not meet the Survey's required accuracy limits. A radio-frequency sensor prototype has been developed and is awaiting field test and evaluation. This unit

holds the most promise of sensing water levels to an accuracy of ± 0.01 to ± 0.02 ft through a range of 5 to 50 ft, and it does not require compensation for temperature changes. Although the cost per unit may be high (up to \$9000 for the radio-frequency version), the long-term benefits should be worth the development effort and investment.

The Survey's current hydrologic field data-acquisition instrumentation lacks the capability, flexibility, and ability to utilize, and thereby interface with, state-of-the-art electronic sensors, and be software controlled. Present instruments are not adaptable to new operations and updated components. They are difficult to integrate into new system configurations and will not operate throughout the required ranges of environmental conditions. Reliability varies from instrument to instrument and site to site. The Adaptable Hydrologic Data Acquisition System (AHDAS) will be the Survey's solution to replacing the existing and obsolete punched-paper tape analog to digital recorder (ADR). AHDAS will be a microprocessor-controlled recorder/retriever system utilizing nonvolatile, solid-state data memory and intelligent control features. Memory capacity can be adjusted to fit specific measurement and parameter requirements. A Field Component (recorder) and Portable Field Interrogator (retriever) are the system's basic components. The system will interface to numerous sensors and be capable of multiple transmission modes. It will have a satellite communication interface capability, thereby requiring only a transmitter for operation. This development is a major effort by the Survey to take advantage of state-of-the-art electronics to modernize their data-collection instrumentation.

The Survey expressed a need for an inexpensive (\$400 per unit) ground-water-level recording system to monitor levels in small-diameter (2-in.) observation wells. The system should be easily installed, operated, and maintained for unattended periods up to 1 year. A minimum data recorder (MDR) is being developed that must meet the following performance specifications: (1) fit inside a 2-in. borehole or casing; (2) battery powered; (3) record the daily average water level and maximum and minimum (time-tagged) levels for the period of record; (4) operate unattended for at least a 12-month period; (5) employ one of a family of pressure transducers to cover a total range of water levels from 0 to 120 ft; (6) retrieve recorded data using an off-the-shelf portable computer; and (7) monitor water levels to an accuracy of ± 0.1 ft. The MDR will be a microprocessor-controlled recorder utilizing solid-state data memory. Future ground-water software development plans include an aquifer test program. Other potential applications for the MDR are recording flood hydrographs for small drainage-area discharge determination and short-term, reconnaissance-type streamflow appraisals.

The ice rod under development has several unique features. It is made from 7075-T6 aluminum, has a

7/8-in. outside diameter, is hollow, and each 4-foot section locks together with two screws that back out to fasten into mating holes in the second rod. This fastening method yields a smooth rod with no projections. The mating holes are drilled through the rod to allow ice that has formed during a velocity measurement to be pushed out of the opposing holes when the rod is disassembled. The total assembled length of the rod is 18.25 ft. Internal to the rod are mating, miniature, underwater connectors that carry the electrical signal from the meter to the CMD. The anodized rod is black with white markings and numbers, making visual observations very effective and efficient. An aluminum tail fin attaches to the rod immediately above the ice foot. This fin fits through a 6-in. ice hole when attached to the rod and can be used to check misalignment of the ice meter in flowing water when flow velocities beneath ice cover exceed approximately 1.0 ft³/sec. A stainless steel pointer-protector attaches to the top of the rod to assist in alignment of the meter into the flow streamline and prevents the entire assembly from falling through the ice hole due to accidental slippage. This device is keyed and may only be attached to the rod in one position that lines up with the buckets of the current meter as attached to the ice foot. A 20-ft cord attaches to the top of the rod with an underwater connector and is held by a restraining clamp on the pointer-protector. This cord resembles a large telephone handset cord and is rated to -40° C. The other end of the cord attaches to the CMD with a military-type threaded connector.

The ice foot was developed that attaches to the lower part of the ice rod to accept a current meter and to measure stream depth and ice thickness. An ice thickness gage is part of the ice foot and a circular plate mounted on this gage protects the cups of the ice meter when raised or lowered through slush ice. The zero of the rod is located at the hole used to mount the ice meter in the ice foot and aligns with the centerline of the ice-meter cups. The base of the ice foot is 0.25 ft below rod zero and the top of the ice thickness gage is 0.25 ft above rod zero.

Spacing of the ice thickness gage and the base of the ice foot from the buckets of the ice meter were determined by laboratory experiments. Movable plates were mounted above and below the meter while rating in a towing tank to determine the distance of noninterference of the plates with the performance of the meter. Six plate distances were tested from 0.100 to 0.183 ft. When the plates were spaced more than 0.150 ft from the centerline of the ice meter cups, no significant change in meter efficiency (meter revolutions divided by distance traveled) was measured. A spacing of 0.250 ft for the base and the ice thickness gage was selected for the convenience of the field person and is greater than the plate simulation testing for these items that might cause interference with performance of the ice meter.

A lightweight, handheld sediment sampler has been developed to operate through a 6-in.-diameter hole in the

ice. The sampler, a modification of the US DH-75 system, incorporates a tilting mechanism to allow insertion through the hole. The main section of the sampler is a modified ice rod; therefore, extensions can readily be added to accommodate streams of different depths.

Once the desired length of rod is in place, the handle to the pivot strap is pushed down and the sampler tilts to a vertical position. While in this position, the sampler will pass through a 5-in. augered hole. However, a 6-in. hole is more desirable for sampling ease. Once the sampler body is through the ice, the handle is released and the spring mechanism pulls the sampler to a horizontal position for sampling. The sampler is removed after tilting it back to the vertical position.

Field tests, including one on the Peace River in Alberta, Canada, have demonstrated that the tilt sampler functions at low temperatures and is a timesaving device.

A commercially available, lightweight, easily transportable Aqua-Bug ice auger has been tested and evaluated. The auger can be carried to remote sites where access is limited to backpacking, snowmobile, or aircraft and is used where ice thickness does not exceed 2.5 to 3.0 ft. The weight of the auger is approximately 30 lbs. It starts easily and runs smoothly at temperatures down to -40° C. Holes of 6 and 8 in. in diameter, 3.0-ft deep, have been augered with the unit, and it did not show any sign of "killing out" or working beyond its capacity/capability. Cutter heads and teeth were modified for field servicing and portability, as well as increasing cutting efficiency and effectiveness. Cutting rates varied from 0.3 to 0.9 in./sec depending on which prototype cutting head was used. The original auger had a gear reduction ratio of 35:1; since then the manufacturer has made several design changes including a new gear reduction ratio of 41:1. Also, the name has changed from Aqua-Bug to Tanaka. As a result of the redesign, four new Tanaka augers were purchased and are undergoing field test and evaluation. Results of the tests will be available in July 1986. The extension flights, cutter heads, and blades used for the Tanaka can also be used on the heavier Stihl Model 4309 auger which is the mainstay system in the United States and Canada. The Stihl auger is for heavy duty ice work (thicknesses greater than 3 ft).

A prototype ice chisel has been developed that has a hickory handle and is lightweight in comparison to existing steel-handle chisels. This chisel has a hardened steel blade that does not dull rapidly in silt-laden ice. The blade is made from type A-2 tool steel. The cutting edge is hardened to Rockwell C54 to C58, the approximate hardness of commercial cold chisel. After hardening, the cutting edge is surface-ground with water cooling to avoid altering the temper. This edge is ground at a 17.5-degree angle and honed to razor sharpness. The blade may be dressed with a file if severe nicks are not present. The weight of this chisel is concentrated at the blade for easier cutting.

The hickory shaft is a replacement shovel handle that is commercially available with the D-handle installed. It is 1.5 in. in diameter and is 6 ft long, not including the blade. The fasteners used to hold the shaft to the blade and the D-handle do not protrude and thus cannot snag the operator's mittens. The hickory shaft makes the chisel lighter and does not transmit severe cold to the hands like the steel handle of the existing chisel. For this reason the prototype chisel is easier to operate for extended periods in severely cold temperatures. The D-handle is useful in thick ice and helps to prevent the chisel from slipping through mitten-covered hands through the ice hole.

The basic design of this chisel is approximately 20 years old. It was originally conceived by Monty Alford, Water Survey of Canada, for use in the Yukon Territories and has

been perfected over many years of actual field use. The chisel was tested at Fairbanks, Alaska, by a Survey hydrographer with 25 years of ice-chiseling experience. He preferred the prototype chisel to the one he designed and has been using for many years.

SUMMARY

Space-age materials and proven state-of-the-art electronics (especially microprocessor technology) are making possible the many recent developments of hydrologic instrumentation, especially in the area of measuring stream-flow under ice cover. The Survey is taking advantage of those developments, while providing field personnel the proper methods to operate and maintain the new instrumentation.

PROBLEMS ENCOUNTERED AND METHODS USED IN THE U.S. GEOLOGICAL SURVEY
FOR THE COLLECTION OF STREAMFLOW DATA UNDER ICE COVER

Ernest D. Cobb and Bruce Parks

ABSTRACT: The U.S. Geological Survey is the principal Federal agency responsible for the collection and dissemination of streamflow data in the United States. An important part of this effort in cold climates is the collection of data under winter conditions when ice covers streams and rivers. Standard cup-type as well as vane-type current meters are used with various types of suspension equipment to make discharge measurements under ice. Safety hazards and a variety of ice conditions add to the difficulty in making winter streamflow measurements. Stilling wells and intake systems or manometers connected to gas-purge systems are commonly used to obtain winter stage records. Water in stilling wells tends to freeze and various methods are used to prevent this from happening. Current activities related to providing better tools and in documenting acceptable methods are presented.

(KEY TERMS: discharge measurement; ice cover; streamflow; anchor ice; ice break-up; frazil ice.)

INTRODUCTION

The Water Resources Division of the U.S. Geological Survey is the principal Federal agency responsible for the collection and dissemination of streamflow data. In cold climates, an important part of this effort is the collection of streamflow data under winter conditions

when ice covers streams and rivers. These data are used for water-supply studies, for waste-allocation studies, and for a number of other purposes. It is, therefore, important that the best efforts possible, within funding and manpower constraints, be used in the collection and analysis of winter streamflow data.

This paper discusses some of the problems in obtaining winter streamflow data and presents methods used in the collection and analysis of these data. Equipment developments and acceptable methods of documentation also are discussed.

The wide range of elevations and latitudes within the United States results in a large variety of winter conditions. Ice thicknesses of 2 to 3 meters are common in northern Alaska, while thicknesses of only a few centimeters may be found in streams in the more southern latitudes. Some streams are affected by ice for only a few days while those on the Arctic coast of Alaska are frozen from mid-September to early June. Because of this diversity in winter ice conditions, there are corresponding variations in problems in obtaining winter streamflow data in the United States. Many of these problems are discussed in the following sections.

DISCHARGE MEASUREMENTS

Sites for the measurement of discharge under ice cover usually are selected

Respectively, Office of Surface Water, 415 National Center, U.S. Geological Survey, Water Resources Division, Reston, Virginia 22092; and Office of Water Data Coordination, 417 National Center, U.S. Geological Survey, Water Resources Division, Reston, Virginia 22092.

during periods of open water. These sites are selected on the basis of channel and flow conditions; if the sites have been used in previous years, experience gained from ice conditions would also assist in site selection. It is usually difficult to determine horizontal angle corrections, so a site is selected where horizontal angles are minimized.

Prior to the discharge measurement, the exact location of the flow in the channel must be determined. In small streams, an entire cross section may be cleared of ice and open-channel techniques used to make the discharge measurement. In larger channels, or if the ice is quite thick, holes are drilled or chiseled across the section to determine the location and characteristics of the flow. If the flow characteristics are not suitable for a measurement at the site, a different site is chosen and the process is repeated.

After the site has been selected, 20 or more holes are drilled or chiseled across the section, prior to the start of the discharge measurement. Additional holes may be made during the measurement to better define the channel or flow characteristics. Most discharge measurements are made using a wading rod or an ice rod to suspend the current meter and to obtain depths in the section. The wading rod is used in shallow streams and rests on the bottom of the channel. The meter is raised and lowered on the rod. If an ice rod is used, the current meter is fixed at the bottom of the rod and the rod is raised and lowered from the ice surface and held at the proper location in the vertical. Cable-suspended measuring assemblies are used for larger streams. Some use is made of handlines for the suspension of the measuring assembly.

Data are obtained for the vertical distance from the top of the water in the hole to the bed of the channel, and for the distance from the water surface to the bottom of the ice or slush. The effective depth of flow is the difference in the two readings. The bottom of the ice or slush is determined by raising the current meter in the flow until the meter quits turning or by the use of an "L" shaped stick or other object that can be lowered through the hole in the

ice and raised until resistance is felt or sensed from the object coming into contact with the ice or slush.

Velocity measurements are made using a variety of current meters. Most current meters used by the Geological Survey are of the vertical-axis type. Electromagnetic velocity meters have been used a few times but have not proven to be reliable under some conditions (Wellen and Kane, 1983). Most measurements made under ice use a standard AA current meter, a pygmy current meter, or an ice meter. The AA and the pygmy meters are both cup-type meters while the ice meter is a vane-type meter. The ice meter is used primarily with rod suspension.

With rod suspension, velocities are obtained at 0.2 and 0.8 of the effective depths when depths are equal to or greater than 0.76 meters and at the 0.6 depth when depths are less than 0.76 meters. No coefficients are applied to the mean of the observed 0.2 and 0.8 depth velocities to obtain a mean velocity in the vertical. When the 0.6 depth method is used under ice cover, a coefficient of 0.92 is applied to the observed velocity to obtain the mean velocity in the vertical. The depth at which the 0.2 and 0.8 depth method is used with cable suspension is dependent on the distance above the bottom of the weight at which the current meter is set. Figure 1 shows a typical vertical-velocity curve under ice cover.

There are many problems associated with discharge measurements under ice cover that are not encountered at other times of the year. Difficulties with access to the station site may be one of the first problems encountered. Winter road conditions can be quite hazardous: roads can be icy or deep snow or drifts can cover the road. Helicopters or airplanes may be needed to get to some stations. Air travel has added hazards in the winter with high winds or poor visibility. When temperatures are below -40°C , equipment problems increase and efficiency decreases. Under these conditions, waiting for another day when weather conditions are better for working may be the best alternative. The field person is given the discretion to make decisions on what is safe or not safe to do relative to winter field work.

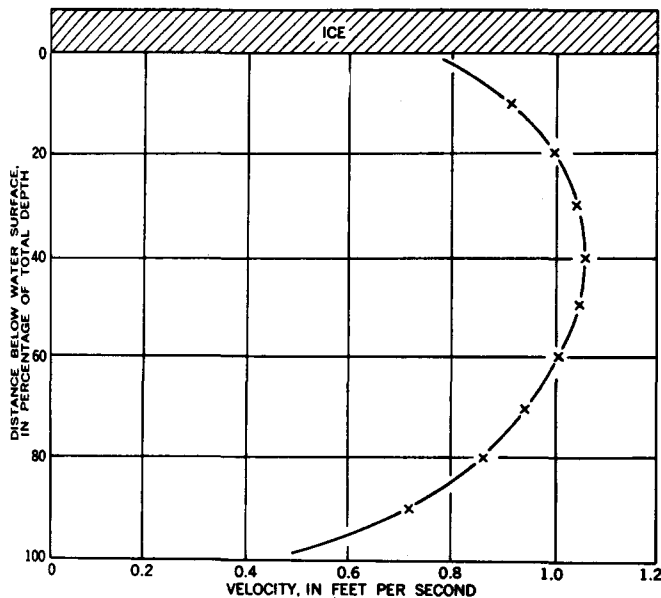


Figure 1. Typical Vertical-Velocity Curve Under Ice Cover (Rantz and others, vol. 1, 1982).

Although discharge measurements may be desirable during ice formation or break-up, the safety of the field personnel is the overriding concern during these potentially dangerous periods. During formation, the ice cover may not be complete or it may be too thin or weak to support field personnel and their equipment. If the stream is too deep or swift to wade, it is often better not to attempt to make a measurement. Discharge measurements can be difficult or impossible to make at times during ice breakup. Often, large pieces of ice will be carried by the current and can make measurement conditions dangerous to the field person or hazardous to equipment. As a result, it is sometimes impractical to make a discharge measurement during parts of the ice breakup. Time-saving measures, such as half counts and reducing the number of verticals, help reduce the time the current meter is in the water and exposed to potential damage from floating ice. Alternative methods of flow measurement, such as the timing of floating ice, and returning at a later time to measure the cross-sectional area and to determine the relation of surface velocities to the mean velocity, are considered.

Floating slush or frazil ice will collect in the cups of the AA and pygmy

current meters. This is usually not a problem with the vane-type ice meter. Floating slush ice is more of a nuisance than it is a hazard but is important because when it collects in cups of current meters, it causes the meter to indicate an erroneous velocity.

Slush ice can accumulate, sometimes to great depths, under a solid ice cover. When this occurs, a pole may be needed to move the slush aside so that the current-meter assembly can be lowered into the flow. Slush ice can enter and be trapped in current-meter cups as the meter is lowered through the slush. If it is realized that the slush is in the cups, it can sometimes be easily dislodged. If it is not detected, the measurement of velocity in that section probably will be in error.

Aufeis occurs when the stream freezes down to the streambed at a downstream point and water in the stream is backed up and flows over the top of the ice and freezes adding a new layer of ice on top. The process can be repeated many times until the ice can become several meters thick. When this condition exists, it may be very difficult to find the flowing water, especially if the flow is small. A great deal of chiseling or drilling in the ice may be required to find the flow.

Flow can sometimes occur between layers of ice. This creates a very difficult situation in which to make a discharge measurement, and the field person usually tries to find another location for the measurement. If a suitable site cannot be found, the field person may not be able to make a measurement. Sometimes, the flow between each layer can be measured and added to the flow measured in the other layers to obtain the total discharge. The accuracy of such measurements is usually poor.

Care must be used in finding the edges of flow under ice. If augers are used, the cutting blade can be easily damaged if it cuts into bed material near the edges of flow. Therefore, chisels often are used to cut through the ice near the banks. Sand often is imbedded in river ice. This sand will dull the cutting teeth on an auger. Therefore, the teeth must be readily sharpened by filing or

be readily replaced with a new set of sharp-cutting teeth.

When holes are drilled or chiseled in the ice, the water under the ice may flow up through the hole onto the surface of the ice. When this occurs, a variety of alternatives are considered. Usually, the flow will quit after a few minutes and the measurement can be made. Under some conditions, a snow dam can be formed around the hole keeping the water from flowing out of the hole. Sometimes, holes can be drilled about a stream width downstream that allow the pressure under the ice to be relieved. The system is allowed to stabilize before the discharge measurement is made.

When pressurized flow is found, there may be a modification in the shape of the vertical-velocity curve until the pressure is relieved. Making measurements at places where the water flows upward out of holes in the ice, during extreme cold, is very difficult because the water quickly turns to slush and freezes on the equipment and the field person.

When the current meter is moved from one hole to the next, there is a tendency for ice clinging to the meter to freeze, thus immobilizing the meter. The tendency for this to happen is reduced if the meter is quickly moved from one hole to the other. If ice has formed on the meter, the meter can be lowered into the water in the next hole and the ice will usually thaw after a while. Sleds on which a compartment is mounted in which the meter may be placed and that is heated using a propane heater may be used to keep the water on the meter from freezing while the meter is being moved between sections.

On large rivers when the ice is thick and the flow is swift and deep there are, at present, no practical ways of obtaining good discharge measurements. Some of these streams are 18 meters deep and have velocities of 3 meters per second. Wet-line corrections may be needed but cannot be readily determined, making depths difficult to accurately measure. The meter assembly may also move about excessively in the flow.

In high velocities and extreme depths, the current-meter assembly tends to be forced downstream by the current, away from the vertical position. The observed

depth is then incorrect and a wetline correction based on the observed angle of the suspension line relative to the vertical is used to adjust the depth readings and to adjust the meter position in the section. In a situation where thick ice exists, the angle of the suspension line from the vertical usually cannot be determined. The observable part of the line is stopped by the ice walls of the hole from taking the position it would assume if the meter assembly were suspended in open water.

The cost of obtaining discharge measurements in the winter can be considerably more than at other times. If hazardous conditions are anticipated or if large streams are to be measured, two or more field people are required to make a measurement that may normally be made by one person. It often takes more time to get to a gaging site in the winter than at other times and special transportation, such as aircraft or snowmobiles, may be needed. When extremely low temperatures are experienced, the field persons are less efficient than in milder weather. More time is needed to make a discharge measurement under ice cover because snow must be cleared, holes must be drilled in the ice, and additional information must be collected. Not only are winter discharge measurements more costly, but they also have greater uncertainty than those made under open-water conditions.

STAGE DATA

Stream stage data may be of limited value for streams that are affected by ice for extended periods of time. The data are of value during periods when anchor ice is forming and releasing and are also of value in determining when ice cover is forming and when it is breaking up. Most offices of the Geological Survey, except in parts of Alaska, attempt to collect stage data throughout the year. Stage records are obtained throughout the winter, in most areas, because thaws occur that result in open-water periods. Ice will also sometimes bridge over the water surface as the flow recession continues through the winter

season, providing open-water flow conditions. Both of these conditions may provide periods when a stage-discharge relationship is stable and defined. Data obtained during these periods can be extremely valuable in helping to analyze the data when ice cover exists.

Stage data usually are collected using stilling wells and intakes or manometers and gas-purge systems. Stilling wells often are set in the streambank with intakes from the well to the stream. Sometimes the well may be attached to the downstream side of a bridge or other structure and holes placed in the well to allow the water level in the stream to be reflected in the well. Where manometers are used, the gage shelter may be placed in a safe location some distance back from the stream.

Freezing of the intakes or of the water in the well is a major problem in collecting stage data under severe cold conditions. Attempts are made to locate the intakes low in the water column to prevent freezing. At times it is not possible to place the intakes in a position where they will not freeze. Heat tapes are sometimes wrapped around the intakes. If line current is not available, a generator can be connected to the heat tape to thaw the intakes if they have become frozen. Often the heat tape will become damaged after a period of time and will have to be replaced. The replacement of the heat tape can be a significant effort. In some places, the heat tape is used to thaw the intakes primarily so they will be open when the spring ice breakup occurs.

Oil cylinders were used inside stilling wells in the United States for many years to maintain a liquid column inside the well from which to obtain a stage record. This is no longer recommended because of the potential for spilling the oil and contaminating the stream.

A variety of other means are used to try to keep the water in the stilling well from freezing. Some use is made of styrofoam pellets poured into the well. This creates an insulating barrier between the colder air and the water. This is a messy and sometimes troublesome solution to the problem. Nitrogen gas is sometimes bubbled into the well to prevent ice formation. Where possible, an

insulated subfloor often is installed in the well below the frostline. This can be a very effective means of keeping the water in the well from freezing. Propane heaters are used in some wells. Where electricity is available, heat lamps or electric floating-tank heaters are sometimes used.

In areas where the stream has a steep gradient and where the stream water temperature is above freezing, such as downstream from a dam or a spring, stream water is brought into the stilling well through a pipe with its intake at an upstream point. This water is allowed to circulate through the well and is discharged through the stilling-well intakes. The pipe from the upstream should be smaller than the stilling-well intake so that the level of the water in the well can remain at the same level as the level in the stream at the gage. The warmer circulating water helps keep the water in the well from freezing. This method is best suited to gages having marginal well-freezing problems.

Stations using manometers and gas-purge systems sometimes have problems from ice forming over the orifice, especially if the flow of gas is cut off for a period of time. A more common problem occurs when moisture collects in a low spot of the gas-feed line and freezes, but this can be avoided by eliminating low points in the gas line.

Recorders

Recorders will often fail for a variety of reasons in severe cold weather. Clocks may quit because the lubricant gets stiff or battery efficiency is reduced because of the low temperatures. Various parts in the recording system may not be capable of operating in extreme cold. Some wires or other parts may become brittle and break during extreme low temperatures causing failure.

Recording systems operating in extreme conditions should have component parts that are specified and designed to function in those conditions. Many pieces of equipment currently available are not designed for the extreme conditions that are often experienced in the field.

Gage houses or recorder components often are insulated. This will not only

protect equipment, at times, from the most severe temperatures, but it also will reduce the shock due to large and fairly quick temperature changes. In addition, where electricity is available, heat lamps may be used in the shelter to keep temperatures from dropping too low. Otherwise, propane heaters may be used. Unless the propane heater contains features to stop the flow of gas if the flame goes out, the gage house can fill with gas and be a safety hazard to the next field person visiting the gage.

Stream Controls

When the control freezes, the stage record may lose much of its value because the stage-discharge relationship is no longer valid. In some of the more moderate winter areas, attempts are, therefore, made to keep the controlling section of the stream free from ice to maintain the stage-discharge rating throughout the winter. This is generally only practical on small streams. One approach to this is to create turbulence in the control section by installing a weir. Ice may form upstream and constrict the approach section, creating a shift to the rating.

A shelter is sometimes constructed over the control section of the stream. The lower part of this structure must be made of material that will move with the current if the stream rises while the shelter is in place. The shelter itself should be allowed to float off to one side of the control and be retained on the other side. This prevents loss of the shelter should a major rise of the stream take place while the shelter is still over the control. The shelter can be used to provide a small amount of insulation from the colder air outside of the shelter. This, together with the small amount of energy released as the water goes over or through the control section, may prevent the control from freezing. A propane heater also can be installed under the shelter to provide added heat.

When the control is a weir, ice will sometimes freeze over the weir and will freeze to a depth on the upstream side of the weir that is lower than the weir crest. When this occurs, siphoning of

water out of the pool upstream from the weir may take place until the upstream pool is lowered sufficiently to break the suction. The pool will then fill up and the cycle may repeat itself many times. This will produce a series of stage drops and rises on the stage record. The pattern is easily recognizable but the discharge during this time must be determined using other methods.

INTERPRETING STAGE AND FLOW RECORDS

The accuracy of flow records during winter months will generally be less than those collected during open-water periods. The accuracy will depend on the type of ice, the areal extent of the ice on the river, the duration of the ice cover, the number of discharge measurements obtained during periods of ice affect, the available information from surrounding streams and weather stations, and on a variety of other information that may be available to the analyst.

Usually, the records at stations least affected by ice are analyzed first. Those that are most affected, or most difficult, are analyzed last. This allows area flow trends to be better understood prior to analyzing the more difficult records.

Probably the most difficult periods of record to interpret are during ice-cover formation and during the spring breakup of ice. There is considerable variation in backwater during these periods. Large volumes of water may be discharged during the spring breakup in a short time. These added uncertainties during ice formation and breakup may significantly affect the error in the annual flow determinations.

The stage record collected during periods of anchor ice development and release is generally clearly recognizable. As anchor ice forms on the streambed during the night, it may produce an increase in water stage. In the morning when the streambed is warmed by shortwave radiation from the sun, the anchor ice will release and allow the water level to drop to its previous stage before the anchor ice formed. A line drawn between ice-free periods on the stage record, under these conditions, will allow a good estimate of the flow to be made (Rantz

and others, 1982, pp. 361-362). The rise due to anchor ice formation is slow compared to the fall when the ice is released. The flow records during these periods can be computed from the stage record with little loss of accuracy.

The most common method of computing discharge during periods of ice is the hydrographic and climatic comparison method. This involves the use of discharge measurements, comparisons with appropriate open-water records at other stations and climatic records, observer notes, power generation data, and other information that might help the analyst estimate flow.

If no stage record exists and where there are no nearby records with which to make hydrographic comparisons, an average recession curve may be used, so long as the fall recession continues through the winter without interruption. All discharge measurements and flow records for the period of record are plotted on a single hydrograph, and a curve is drawn that most approximately represents the suite of curves. The shape of this curve is then used to estimate a winter's record by drawing a line of the same shape through any measurements made during the period in question.

CURRENT ACTIVITIES

For the past several years, representatives from the Water Resources Division of the Geological Survey have been meeting with representatives from the Water Survey of Canada of the Water Resources Branch and with others to compare equipment and methodology and to look for better ways of collecting streamflow data under ice cover. Equipment from one agency has been, and is being, tested and tried by the other agency and vice versa. As a result, some equipment has been modified to improve data collection.

Another joint effort between the Geological Survey and the Water Survey of Canada is the preparation of a manual for the measurement of flow under ice cover. This manual will come out in the United States as a chapter in the "Techniques of Water-Resources Investigations" series.

There have been a number of recent developments in the area of equipment that have implications in the collection of flow data under winter conditions. Following is a brief discussion of a few of these developments in the United States.

The Geological Survey has been developing solid-cup bucket wheels for current meters. The solid cups will not allow slush ice to become trapped in the cups as it presently does in the hollow cups. It is expected that in the near future, the solid cups will be commonly used, especially for measurements under ice cover, in the United States.

Optic heads for counting current-meter revolutions have been developed. This current-meter option will allow recently developed digital counters to count and record meter revolutions, time, and velocity. Due to reduced drag resulting from use of the optic heads, the meters have a lower stall velocity, allowing lower stream velocities to be measured.

Fiberglass wading rods have been developed. These are lighter, easier to handle in cold weather, and have built-in electrical circuitry for the counting of current-meter revolutions. Ice rods for suspending a current meter through a hole in the ice have been redesigned to improve the readability of the distance markings on the rod and to improve the means of adding and disassembling sections to the rod.

Weight-suspension systems are being standardized. Considerable testing has been done on various systems in towing tanks to determine good suspension systems for use through ice. The Water Survey of Canada has developed a "tear drop" suspension assembly for use in small diameter holes in ice. This assembly is being examined by the Geological Survey for adoption in the United States.

Various power heads for ice augers, auger assemblies, and cutting bits are being tested. These tests are evaluating the weight of the units, reliability, ability to cut through ice, ease of assembly and disassembly, and of maintenance of effective cutting teeth.

Ice chisels, for use in the United States, have been redesigned based on work done in Canada. Wooden handles replace the steel handles previously used. The chisel balance has been improved by

placing the center of gravity nearer the lower end of the chisel. The angle of the cutting edge has been modified so that it cuts into the ice better while still retaining the strength of the blade.

Acoustic velocity meters are being tested in ice-covered rivers. This meter depends on the reception of an acoustic signal that has been transmitted across a stream at an angle, other than 90°, to the flow direction. The time of travel of the signal across the stream in the upstream and downstream directions are determined and the stream velocity computed from the time differential. This metering system should be of value for a number of stream-gaging sites.

The use of transducers is being investigated for the purpose of replacing the manometer with a transducer in connection with a gage-purge system. The transducer will be placed in the gage shelter and will measure the pressure transmitted by the gas-purge system. The use of transducers will allow for smaller gage shelters to be used and should make insulating or heating the shelter or equipment easier. The temperature of the transducer may have to be measured and recorded to make corrections to the transducer readings.

Dilution measurements of streamflow under ice have been successfully made on a few streams. Details of the method are described in the report by Kilpatrick and Cobb (1984). More testing is needed to determine the conditions where this method can be effectively used.

CONCLUSIONS

There are numerous problems with collecting streamflow records in the winter months in many parts of the United States. Nevertheless, these streamflow records are needed and every effort possible, within funding and manpower constraints, must be exerted to collect them. The collection of accurate winter records is highly dependent on the commitment of the people who collect them. Work is progressing on providing better equipment for the field person and on expanding documentation of accepted procedures for the collection of winter flow records.

REFERENCES

- Kilpatrick, Frederick A. and Ernest D. Cobb, 1984. Measurement of Discharge Using Tracers. U.S. Geological Survey Open-File Report 84-136. 73 pp.
- Rantz, S. E. and others, 1982. Measurement and computation of streamflow: Volume 1. Measurement of stage and discharge. U.S. Geological Survey Water-Supply Paper 2175. 284 pp.
- Rantz, S. E. and others, 1982. Measurement and computation of streamflow: Volume 2. Computation of discharge. U.S. Geological Survey Water-Supply Paper 2175. pp. 285-631.
- Wellen, Paula M. and Douglas L. Kane, 1983. A comparison of velocity measurements between cup-type and electromagnetic current meters. Report presented to the Annual Meeting of the Alaska Section, American Water Resources Association, Fairbanks, Alaska, November 10-11, 1983. 12 pp.

SIMPLIFIED METHOD OF MEASURING STREAM SLOPE

Jacqueline D. LaPerriere and Donald C. Martin¹

ABSTRACT: For use in measuring stream slopes in remote areas, surveyor's instruments such as a level or telescopic alidade are relatively cumbersome and delicate; furthermore, standard surveying methods require that an unobstructed line of sight be found or cleared. We describe a simple "carpenter's water level" that saves considerable effort. In comparisons with a surveyor's level to measure slopes over 10 m, measurements with our instrument were within 2% of those made with a surveyor's level for slopes of 2.46% and within 0.5% for slopes of 5.31%; and, within 2% for slopes of 4.24% over 20 m. (KEY TERMS: stream slope; field instrument.)

INTRODUCTION

To test a hypothesis that stream gradient is associated with the concentration of drifting benthic macroinvertebrates (David Zimmer, 1977, personal communication), one of us (J.D.L.) needed to measure stream slope (LaPerriere, 1983). During the first field season, stream reaches were specifically chosen because they had a clear line of sight that would enable surveying of the slope. In the following field season, sites were chosen for other characteristics, and an alternative method of measuring stream slope was sought. Rough surveying with a clinometer yielded unsatisfactory results. The use of a "carpenter's water level" (here called a slope-meter) suggested by William W. Mendenhall (Professor of Civil Engineering,

University of Alaska, 1979, personal communication), was then constructed, and used in the field. We describe the construction and use of this field instrument, and compare its accuracy with that of standard methods of measuring slope with a level and stadia rod.

METHODS AND MATERIALS

An ordinary level and stadia rod were used in tests of the accuracy of the field instrument. The slope-meter is made inexpensively from a length of transparent plastic tubing, two stoppers that fit the inner diameter of the tubing, two metersticks, some fiber-strengthened adhesive tape, and a length of unstretchable cord (polypropylene 1-cm in diameter is suitable).

The cord is taped to the base of the two metersticks so that they are set a pre-determined distance apart when the cord is pulled taut. When this distance does not exceed 10 m, the cord and tubing do not readily become entangled with each other, and the tube can be easily inspected visually for bubbles that might cause errors. The transparent tube (2 m longer than the pre-determined distance) is then placed parallel to the outstretched cord and taped to the top and base of each meterstick so that graduations on the metersticks can be seen through the tubing. Water is then added to the tube until it rises from 1/3 to 1/2 of the height of the metersticks when they are held side-by-side. (Water may have to be added or removed to facilitate readings). The stoppers are used

¹Respectively, Assistant Leader and Research Assistant, Alaska Cooperative Fishery Research Unit, 138 Arctic Health Research Building, University of Alaska, Fairbanks, Alaska 99775-0110. The Unit is jointly supported by the University of Alaska, Alaska Department of Fish and Game, and the U. S. Fish and Wildlife Service.

to hold the water between measurements.

In use, each of two persons places their meterstick at the wetted edge of the stream, laying the cord along the edge of the stream between them. Each person then reads the height of the water level on the meterstick and the difference between the two readings is the rise. Dividing the rise by the set distance between the two metersticks gives the slope. If slope needs to be surveyed for a longer specific distance, multiple readings are made in sequence. The downstream operator walks to the position of the upstream operator, who then walks upstream the set distance and lays the line on the wetted edge; the reading is then taken again. This procedure is repeated until the total distance has been covered.

The design of a more sophisticated carpenter's water level is presented by Walkotten and Bryant (1980). They also provide photos and sketches of their instrument in use.

RESULTS

We checked measurements made with this field instrument against those made with a surveyor's level and stadia rod. In measurements made by both methods in triplicate at three locations along halls with built-in wheelchair ramps in the Fine Arts Building of the University of Alaska, Fairbanks, (Table 1) the slopes determined were nearly identical (within 2% at slopes

of 2.46% and within 0.5% at slopes of 5.31% over a 10 m distance; and, within 2% at slopes of 4.24% over 20 m).

DISCUSSION

Slopes measured with the "water level" were not significantly different from those measured with a surveyor's level and stadia rod, even when two successive measurements (extending 20 m) were made at one location. We have used this instrument successfully in the field, where it can be laid out along a stream through riparian vegetation that would block a line of sight measurement with surveying instruments. The instrument is light and durable for use in remote field locations common in Alaska.

REFERENCES

- LaPerriere, J. D. 1983. Alkalinity, Discharge, Average Velocity, and Invertebrate Drift Concentration in Subarctic Alaskan Streams. *Journal of Freshwater Ecology* 2:141-151.
- Walkotten, W. J. and M. D. Bryant 1980. An Instrument to Measure Stream Channel Gradient and Profiles. U. S. Forest Service. Pacific Northwest Forest and Range Experiment Station. Research Note. 5 pp.

TABLE 1. Measurements of Slope at Three Locations by Two Methods

Location	METHOD					
	Level and Rod			Carpenter's Water Level		
	Rise (ft.)	Distance (ft.)	Slope (%)	Rise (cm)	Distance (m)	Slope (%)
1	0.79	32.8	2.41	24.5	10.0	2.45
	0.79	32.8	2.41	24.5	10.0	2.45
	0.79	32.8	2.41	24.7	10.0	2.47
2	1.74	33.0	5.27	52.8	10.0	5.28
	1.75	33.0	5.30	53.1	10.0	5.31
	1.74	33.0	5.27	53.4	10.0	5.34
3	2.78	66.5	4.18	84.7	20.0	4.24
	2.78	66.5	4.18	84.6	20.0	4.23
				85.0	20.0	4.25

WATER QUALITY

WATER QUALITY-DISCHARGE RELATIONSHIPS IN THE YUKON RIVER BASIN, CANADA

Paul H. Whitfield and W. G. Whitley¹

ABSTRACT: Weekly and biweekly water quality samples were collected at ten sites throughout the Canadian portion of the Yukon River basin during 1982-1983. The relationships between the water quality variables and discharge are examined. Most of the relationships between the variables and discharge are either oposite or negative and exhibit hysteresis, a few variables appear to be independent of discharge. A system of classification of the relationships, with potential causal mechanisms, is proposed.

KEY TERMS: Hysteresis, water quality-discharge relationships.)

INTRODUCTION

Water quality-discharge relationships are characteristic of the processes which result in the movement of materials into rivers and streams. Whitfield and Schreier (1981) found that such relationships formed open loops which persist from year to year and become progressively open with downstream distance. These relationships are described as exhibiting hysteresis, the lagging or leading (in time) of a physical effect in relation to its cause. This paper describes these processes and relationships throughout the Canadian portion of the Yukon River basin.

These relationships can lead to an understanding of how water quality is determined (eg. Davis and Zobrist, 1978; Hall, 1971; Johnson, 1979; Rieger and Olive, 1985; Toler, 1965; Whitfield and Schreier, 1981). Such an understanding is pertinent in the north where a general lack of data requires extrapolation to unsampled or poorly sampled basins. Understanding the dynamic processes which give rise to these relationships requires a knowledge of the entire seasonal nature of these systems.

Water quality data were gathered at ten sites at one week intervals (7 sites) and two week intervals (3 sites) during the Yukon River Basin Study. These data describe a basin largely unaffected by human activities. They were gathered to provide information about the seasonal and spatial variation in water quality, and are described by Jack *et al.* (1983).

This paper proposes a classification system to describe the relationship between water quality variables and discharge. These relationships exhibit varying degrees of hysteresis and dependence on discharge. The degree of hysteresis is approximated by measurement of the lag 1 autocorrelation coefficient. The classification system was developed from a sorting and grouping exercise. Hard to classify cases were also identified. A mechanism for classifying new cases on a statistical basis is demonstrated. Possible processes which result in water quality variables behaving in the described manner are proposed.

STUDY AREA

The Yukon River basin is the fifth largest river basin in North America, draining northwestern Canada into the Bering Sea through central Alaska. At the end of the Canadian portion of the basin the drainage area is 294,000 km² (113,500 sq miles) with an average annual flow of 2340 m³/sec (82,660 cfs) at Eagle, Alaska (U.S.G.S., 1984). Discharge data were obtained from published records (U.S.G.S., 1984; Water Survey of Canada, 1983; 1984).

The drainage basin consists of two distinct portions, the western portion drained by rivers dominated by the glaciers of the St. Elias Mountains (Wrangells) and the Coast Mountains; the remainder of the basin drains the Yukon Plateau and the Mackenzie mountains. The physiography of the basin

¹Respectively, Inland Waters Directorate, Environment Canada, 502-1001 West Pender Street, Vancouver, B.C., V6E 2M9; and Northern Affairs Program, Indian and Northern Affairs Canada, 200 Range Road, Whitehorse, Yukon Territory, Y1A 3V1.

is described in detail by Bostock (1948).

The water quality data described here were collected between August, 1982 and September, 1983. The procedures used to collect and analyse the samples are described by Jack *et al.* (1983) and are typical of those used by most water quality agencies. Whitfield (1983) evaluated a number of water quality sampling sites in the lower portion of the Yukon River and found that sampling at a one week interval provided the most representative data. The ten stations which had sampling frequencies of weekly or every two weeks were selected from the 21 sites sampled by Jack *et al.* (1983) and are shown in Figure 1. Samples were collected once every two weeks at three sites (Nordenskiold, Takhini at Highway #2, and Yukon River below Whitehorse) and once each week at the other seven sampling sites.

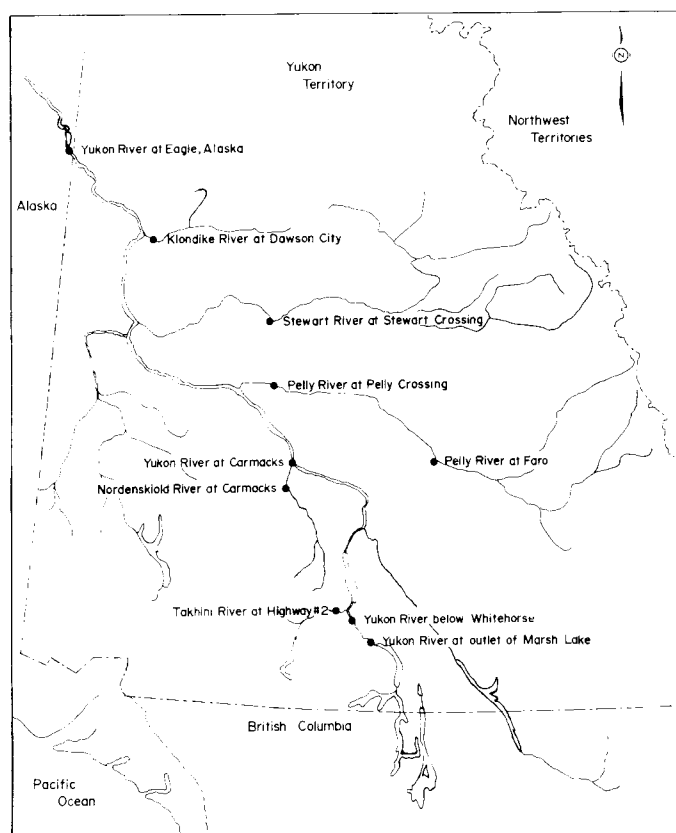


Figure 1. Study area showing sampling locations.

RESULTS AND DISCUSSION

Jack *et al.* (1983) collected data for some 37 water quality variables. We examined these records and eliminated those variables which had little or no variation, those variables where a substantial portion was either missing or less than detection limit, and those variables which provided redundant information. We then had 26 variables to evaluate for the ten

ivers. The variables that were examined were total alkalinity, total hardness, calcium (dissolved), sodium (dissolved), potassium (dissolved), chloride (dissolved), fluoride (dissolved), pH, specific conductivity, turbidity, colour, silicate (reactive), sulphate (dissolved), nitrate+nitrite, non-filterable residues, extractable arsenic and selenium, total dissolved nitrogen, total organic carbon, total inorganic carbon, total phosphorus, and total copper, lead, iron, manganese and zinc. Two additional data sets were subsequently eliminated for one river because of missing data. We then prepared log-log plots of each water quality variable against discharge, although for pH we used linear-log plots.

The 258 plots were roughly grouped on the basis of visual similarities. This generally resulted in similar stations and variables being grouped together. The grouping was complicated by a lack of agreement within variables across all stations. It became evident that the ten stations were best considered as two main groups; the first consisted of six "river" sites, while the second consisted of three "lake-fed" sites. One site, the Yukon River at Carmacks, was often difficult to classify into either of these groups. We believe that this site is substantially affected by Teslin and Labarge Lakes which are upstream of this site, and reflects a transition between the "lake-fed" type sites and the "river" type sites.

Variables from the "lake-fed" sites appeared to be independent of discharge and were either random or dependent on other processes. This view was subsequently modified when it was realized that what had appeared to be independence of discharge was simply low slope relationships, when compared to the "river" systems. Thus one of the important differences between the "river" sites and the "lake-fed" sites is that the "river" sites show more concentration variation in relation to discharge. This difference is due to the buffering and trapping processes in lakes.

The relationships between water-quality variables and discharge are much more evident for the six "river" sites. Here we found that every case could be placed into one of four groups: (1) having a positive relationship with discharge, and exhibiting clockwise hysteresis, (2) having a negative relationship to discharge, and exhibiting counterclockwise hysteresis, (3) having no relationship to discharge, but exhibiting episodic or sequential behavior, (ie. some order exists), or (4) appearing to be entirely random. We observed that the degree to which hysteresis was evident increased with distance downstream or with the magnitude of the discharge, confirming the result of Whitfield and Schreier (1981).

Yang *et al.* (1983) observed a reversal of the direction of the hysteresis for sediment-discharge relationships in the Yangtze River. The lagging of sediment was attributed to the timing of flooding and

irrigation of rice fields. Rieger and Olive (1985) examined sediment-discharge relationships during storm events in five small watersheds. They found several types of relationships; sediment led discharge in 41% of the cases, lagged in 13%, was in phase in 26%, and 41% of the cases had no identifiable pattern. Their results show multiple types of relationships within and between watersheds and storms. Rieger and Olive (1985) suggest that these complex responses are the result of several sediment transport mechanisms. Our results show indications of some of these complex responses. Since the basins that we considered are relatively large these complex responses at the storm event level are generally masked.

The grouping of the variables suggests that common mechanisms cause the observed behavior. The variables that exhibit the positive relationship with discharge, and the clockwise hysteresis are: non-filterable residues, turbidity, colour, total iron, copper, zinc, manganese, and lead, extractable arsenic, and total phosphorus. These variables are sediment related and suggest a relationship to erosional processes. The postulated mechanism can be described as follows: freshet snowmelt and surface runoff carry surface material over seasonally frozen soils into the streams, while during post-freshet the thawed soils allow precipitation to replenish groundwater thus contributing less sediment to the streams. Figure 2 is a log-log plot of total iron concentration against discharge. The broad open loop shown there is characteristic of this group of variables. Although the Yukon River at Carmacks was often difficult to classify in parallel to other stations, Figure 2 shows that this was not always the case. Figure 2 is typical of the hysteresis reported by Whitfield and Schreier (1981).

The variables that exhibit a negative relationship with discharge and a counterclockwise hysteresis are: total alkalinity, calcium, total hardness, sodium, specific conductivity, silicate, sulphate and total inorganic carbon. These variables are major ions, generally conservative, and have a relationship to groundwater (Whitfield and McNaughton, 1986). The postulated mechanism which results in the observed hysteresis is described as follows: snowmelt and surface runoff dilute groundwater during freshets; during post-freshet conditions concentrations increase with the increasing dominance of groundwater. These relationships are more evident in the Yukon Basin than Whitfield and Schreier (1981) observed in the Fraser River Basin of British Columbia because of the increased dominance of groundwater and the dominance of snowmelt as the source of water in this generally arid area. Figure 3 is a log-log plot of sulphate concentration against discharge for the Pelly River at Pelly Crossing. This figure is the classic case of the negative relationship of concentration with discharge and the counterclockwise

Yukon River at Carmacks, Y.T.

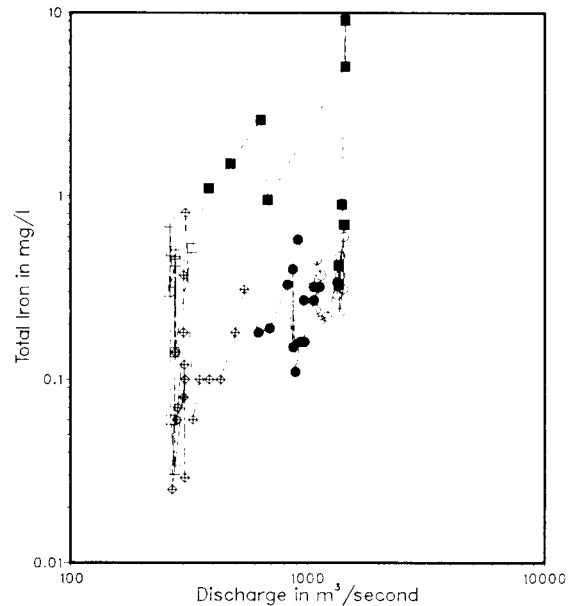


Figure 2. Clockwise hysteresis with a positive relationship to discharge. Points are joined in date order. [In Figures 2-9 the symbols indicate; □ -March-April, ■ -May-June, ○ -July-August, ● -September-October, ⊕ -November-February.]

Pelly River at Pelly Crossing, Y.T.

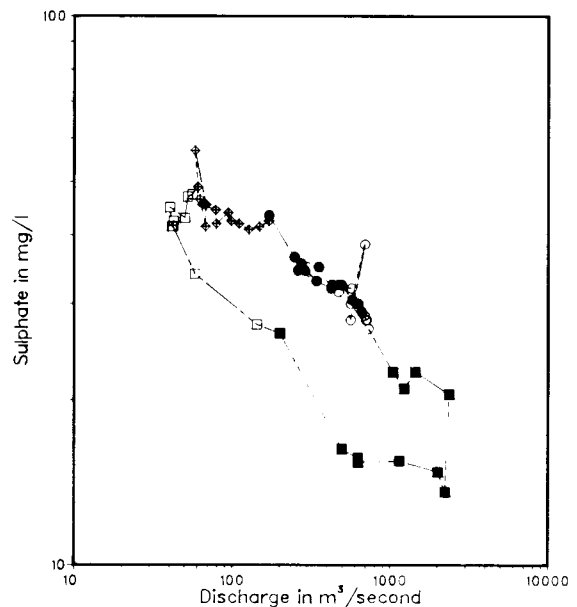


Figure 3. Counterclockwise hysteresis with a negative relationship to discharge. Points are joined in date order. Symbols are as given in Figure 2.

hysteresis. We observed that the "openness" of these loops increased with downstream distance, and/or increased magnitude of discharge.

The variables that exhibit no relationship to discharge, but show episodic or another form of ordered behavior are: chloride, fluoride, potassium, and total organic carbon. As a group, these variables are an odd assemblage. It is unlikely that the behavior of all four of these variables would be due to the same mechanism. Chloride patterns are typified as shown in Figure 4. These patterns are generally open loops with an apparent independence of discharge. Similar patterns were observed for potassium, suggesting a similar mechanism is active. Fluoride patterns were also highly characteristic, an example of which is given in Figure 5. The pattern shown in Figure 5 is typical of all fluoride series, each plot showed a crossover point in October–November forming a figure 8. Total organic carbon exhibited a pattern which tended to be bimodal in a fashion somewhat similar to fluoride. The first three variables are postulated to be controlled by a process which consists of constant input concentrations from atmospheric inputs which are subsequently modified by contact with soils. Thus the highest concentrations occur at the beginning of the spring thaw, and the lowest values at the time of freeze-up.

The variables that appeared to be independent of discharge and generally behaved in a

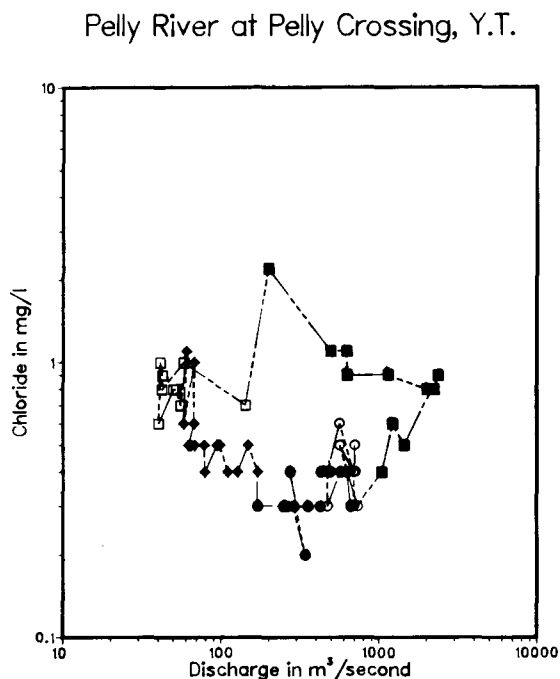


Figure 4. A typical pattern for chloride and potassium with discharge. Points are joined in date order. Symbols are as given in Figure 2.

Pelly River at Faro, Y.T.

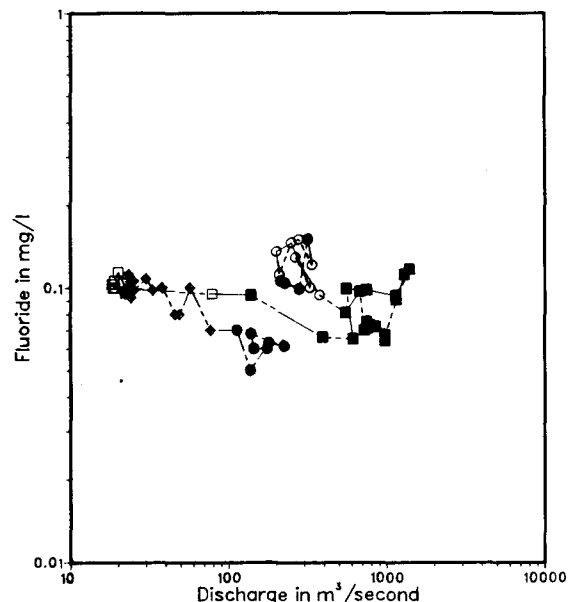


Figure 5. A typical pattern for fluoride with discharge. Points are joined in date order. Symbols are as given in Figure 2.

random manner are: total dissolved nitrogen, nitrate + nitrite, extractable selenium, and pH. Of these we observed two distinct patterns. The first, shown by pH and selenium was an apparent lack of variation, Figure 6 is typical of the results we obtained. The two nitrogen variables behave in very similar manners, partially due to their interrelated nature. Typical plots of both nitrate + nitrite and total dissolved nitrogen showed an independence of discharge but a great deal of variation with a definite episodic pattern. Figure 7 shows total dissolved nitrogen concentrations in the Yukon River at Eagle, Alaska. The high variation in concentration as well as several periods of episodic behavior are evident.

To illustrate the differences that exist between "river" and "lake-fed" systems we have included a plot of sulphate against discharge (Figure 8) which can be compared with Figure 3. Even though the range of sulphate concentrations is one to ten in Figure 8 as opposed to 10 to 100 in Figure 3, there is only the slightest hint of a decrease in sulphate concentration with increasing discharge. This property was common to all of the "lake-fed" systems, and for this reason we have considered them separately. With the exception of these differences in the slope of the relationship with discharge, variables such as sulphate behaved in generally the same manner as in "river" systems.

One of the common characteristics of the "lake-fed" sites is the behavior of the variables:

colour, turbidity, phosphorus and iron. These variables were observed to exhibit a pattern which we considered to be of a non-random nature. These variables have a large peak in spring (March–April) and sometimes a secondary peak in the late summer. The coincidence of these peaks with peaks in activity of biological processes in the lakes suggests that these variations are due to primary production within the lakes. Figure 9 is a plot of turbidity at the outlet of Marsh Lake which shows the peak in the early portion of the year and a secondary peak occurring at peak discharge in the late summer. This plot is typical of these four variables in the three "lake-fed" sites.

Although the classification scheme proposed has clear distinctions between the various groups, some cases remain difficult to place in single groups. These cases generally have a more closed than open structure and often contain crossovers and secondary loops. While this was particularly true for many variables for the Yukon River at Carmacks, several other cases also existed. Whitfield and Schreier (1981) designated many of the cases they considered as mixed (clockwise and counterclockwise hysteresis). The data which they considered consisted of many fewer observations (8) than we had available to us (26 – 55). We believe that although cases do exist which contain secondary loops, each and every case contains a dominant structure which allows it to be placed into one of the groups described.

Yukon River at Eagle, Alaska

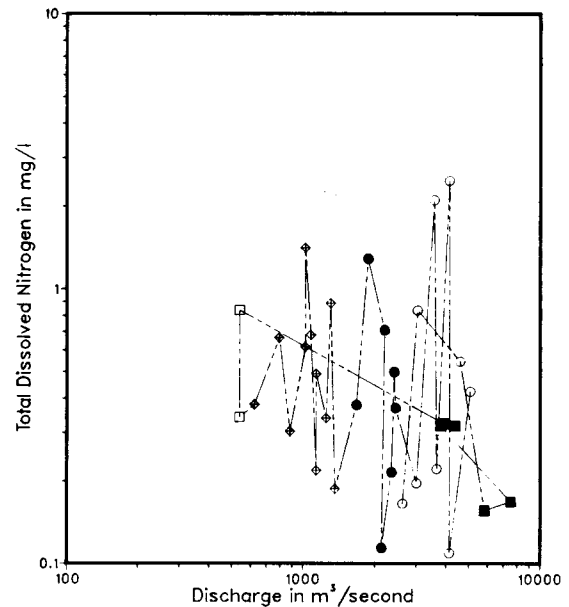


Figure 7. A typical pattern for nitrogen variables with discharge. Points are joined in date order. Symbols are as given in Figure 2.

Klondike River at Dawson, Y.T.

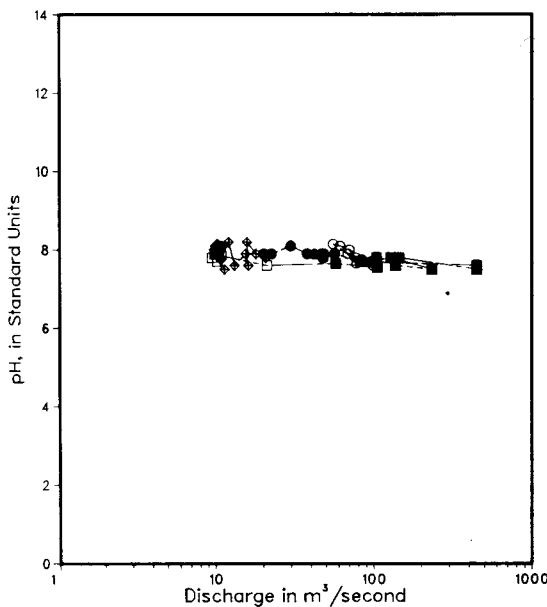


Figure 6. A typical pattern for pH and selenium with discharge. Points are joined in date order. Symbols are as given in Figure 2.

Yukon River at outlet of Marsh Lake

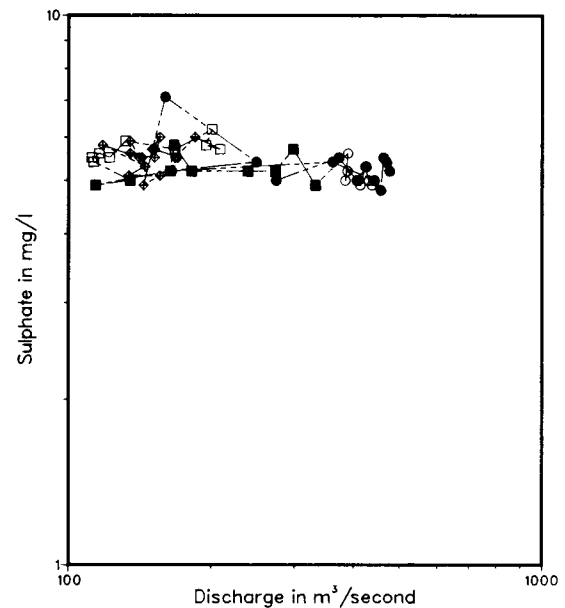


Figure 8. The relationship between sulphate and discharge at a "lake-fed" site. Points are joined in date order. Symbols are as given in Figure 2.

We were concerned that since the classification of individual cases required substantial judgement that a general application was not immediately practical. We then considered the basis for our proposed scheme on a more mechanistic basis. The first criterion in the classification is the behavior in relation to discharge and we had found three possibilities: (1) increasing concentration with increasing discharge, (2) decreasing concentration with increasing discharge, and (3) concentration independent of discharge. This property can be measured or estimated in a number of ways: simple correlation was thought to be the simplest, limiting the range to -1 to 1 and avoiding the problems of scale inherent in statistics such as slopes etc. The second classification criterion which was used has been alluded to as an ordering of sorts or a lack of randomness. This property is common in most sampled time series, such as those being described here. Whitfield (1984) examined the time series properties of these same series of data and found many of them to be highly autocorrelated. In its simplest form, autocorrelation at lag 1 is the correlation of each point in a series with the one immediately following, it also varies from -1 to 1 and also is dimensionless. These two classification criteria, or statistics, should be sufficient to place the classification of cases on a more rigorous basis. We then estimated both the correlation of each variable with discharge, and the autocorrelation of each

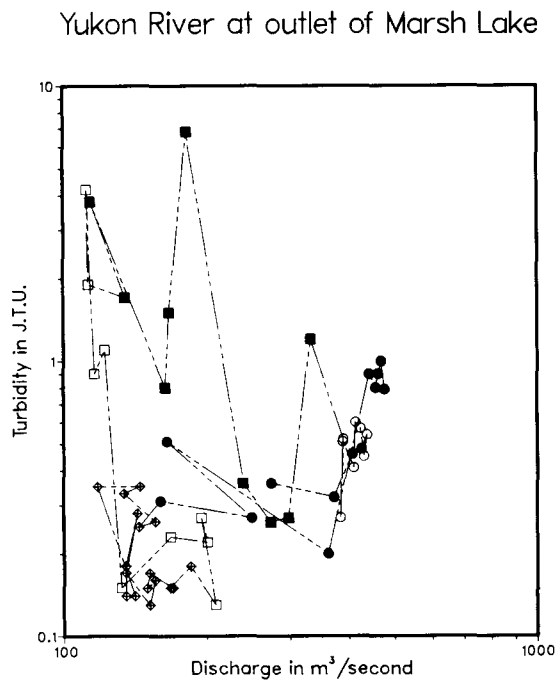


Figure 9. The relationship between turbidity and discharge at a "lake-fed" site. Points are joined in date order. Symbols are as given in Figure 2.

River Sites

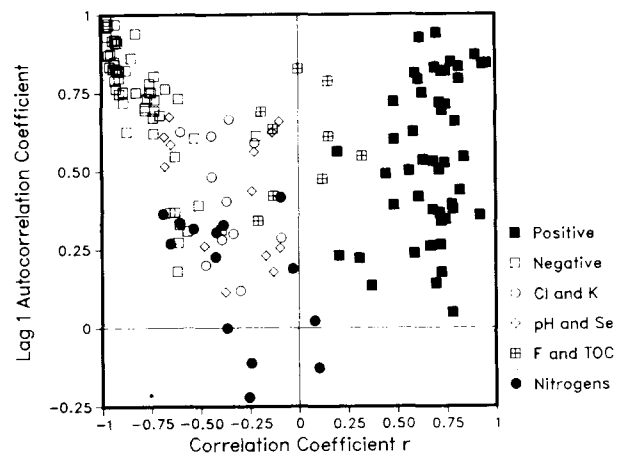


Figure 10. Relationship between correlation with discharge and autocorrelation within the grouped variables at "river" sites

Lake-fed Sites

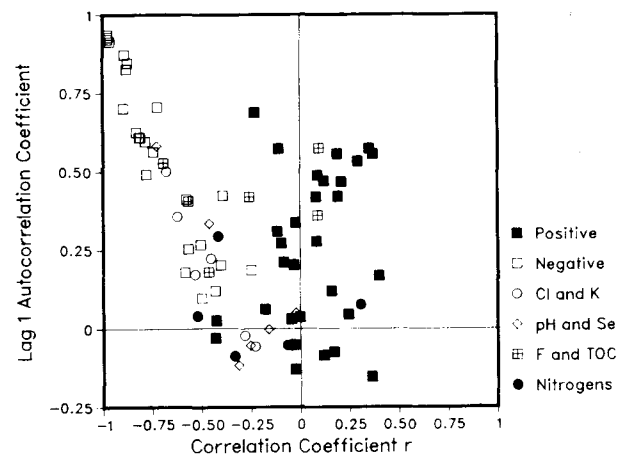


Figure 11. Relationship between correlation with discharge and autocorrelation within the grouped variables at "lake-fed" sites

variable. We then prepared two plots, one for the "river" sites (Figure 10), and one for the "lake-fed" sites (Figure 11). Variables were grouped according to the classification system described previously and common symbols used for each group. These figures both show that the proposed classification scheme fits fairly well with a description that would use the statistics describing the correlation to discharge, and the amount of autocorrelation within each series. It is not, however a perfect fit. There are several instances where a case would be classified differently, if only the statistical properties were used. These cases were also difficult to classify on a visual basis, and may be due to anomalous data.

CONCLUSIONS

There remain a number of limitations, concerns, and questions that need further consideration. One area that we are particularly concerned about is the lack of data from rivers that are directly glacially fed. Data from that type of system is needed to fully understand the range of variation present in the Yukon Basin. Some superimposed loops occur at high discharge rates, that might be attributable to the late summer glacial outflow.

There are limitations to the classification scheme using either the visual or the statistical approach. One of these is a problem of validation, *ie.* how can we confirm that a specific case is correctly classified? In the process of the original classification exercise we examined a number of cases which were odd. Classification of these is often not possible without an in-depth knowledge of the variable being considered. For example, during a portion of the year the data were at or near the detection limit and the loops therefore were flattened at one end, or the slope of the relationship to discharge appeared to change. Superimposed loops, related to storms and/or delayed discharges from higher elevations also confuse the relationships. Similarly, Rieger and Olive (1985) found numerous variations on hysteresis of sediment and discharge in storm runoff.

Perhaps of most concern is that the present classification system does not provide a feeling for the concentration disparity between rising and falling limbs of the annual hydrograph. In some cases the differences observed were of only minor importance, whereas in some, such as those shown in Figures 2 and 3, the differences are a factor of 2 to 10. The use of rigorous statistical techniques, such as time series methods will alleviate most of the inherent estimation problems (eg. Rieger and Olive, 1985).

This type of analysis has a number of important applications. First, it aids understanding of the seasonal variation of water quality variables with discharge. Variables can be grouped with others that behave similarly and distinguished from groups with different behavior. It identifies variables which are poorly understood such as fluoride, chloride, and other variables that appear to be independent of discharge. Secondly, with an understanding of the underlying processes and variation with the size of the stream, tentative extrapolation can be made to other areas and other variables. This is of particular value in northern Canada where data and understanding are limited. Thirdly, sampling can be directed towards variables and seasons in a knowledgeable way. In northern systems sampling is often most intensive in the spring and summer whereas many variables reach limiting values in the fall and winter.

The classification system described here is consistent with mechanisms postulated for each grouping, and these mechanisms are relevant processes in determining water quality in this subarctic region. Visual and statistical analysis both resulted in the same groupings. Variables associated with erosion demonstrate a positive relationship to discharge and a strong leading hysteresis. The dominance of groundwater in controlling the concentrations of many variables is reflected in broad open loops with negative slopes. Some variables were observed to be independent of discharge and some of these also demonstrated hysteresis. This taxonomy is consistent with that proposed by Whitfield and Schreier (1981), and the causal mechanisms are believed to be similar. The classification system proposed may allow the characterization of other areas with more limited sampling.

LITERATURE CITED

- Bostock, H.S. 1948. Physiography of the Canadian Cordillera, with special reference to the area north of the fifty-fifth parallel. Geological Survey of Canada Memoir 247.
- Davis, J.S., and J. Zobrist. 1978. The interrelationships among chemical parameters in rivers - analysing the effects of natural and anthropogenic sources. *Progress in Water Technology*. 10:65-78.
- Hall, F.R. 1971. Dissolved solids-discharge relationships. 2. Applications to field data. *Water Resources Research* 7:591-601.
- Jack, M., B.E. Burns, and T.R. Osler. 1983. Water Quality - Yukon River Basin. Yukon River Basin Study Water Quality Work Group Report No. 1. Indian and Northern Affairs Canada.
- Johnson, A. 1979. Estimating solute transport in streams from grab samples. *Water Resources Research* 15:1224-1228.
- Rieger, W.A., and L.J. Olive. 1985. Sediment responses during storm events in small forested watersheds. In: *Proceedings of the Statistical Analysis of Water Quality Monitoring Data*. October 1985.
- Toler, L.G. 1965. Relation between chemical quality and water discharge in Spring Creek, Southwest Georgia. U.S. Geological Survey Professional Paper 525-C:C209-C213.
- U.S. Geological Survey. 1984. Water Resources Data for Alaska. Water Year 1983. U.S. Geological Survey Water-Data Report AK-83-1.
- Water Survey of Canada. 1983. Surface Water Data, Yukon and Northwest Territories, 1982. Environment Canada.
- Water Survey of Canada. 1984. Surface Water Data,

- Yukon and Northwest Territories, 1983. Environment Canada.
- Whitfield, P.H., 1983. Evaluation of water quality sampling locations on the Yukon River. *Water Resources Bulletin* 19:115-121.
- Whitfield, P.H., 1984. Optimization of water quality monitoring the Yukon River Basin. Yukon River Basin Study Water Quality Work Group Report No. 2. Inland Waters Directorate, Environment Canada, Pacific and Yukon Region.
- Whitfield, P.H. and H. Schreier, 1981. Hysteresis in relationships between discharge and water chemistry in the Fraser River basin, British Columbia. *Limnology and Oceanography* 26:1179-1182.
- Whitfield, P.H., and B. McNaughton. 1986. Depression of dissolved oxygen under ice in two Yukon Rivers. *Water Resources Research* in press.
- Yang, Z.-S., J.D. Milliman, and M.G. Fitzgerald. 1983. Transfer of water and sediment from the Yangtze River to the East China Sea, June 1980. *Canadian Journal of Fisheries and Aquatic Sciences* 40(Supplement 1):72-82.

THE ROLE OF SNOWCOVER ON DIURNAL NITRATE CONCENTRATION PATTERNS IN
STREAMFLOW FROM A FORESTED WATERSHED IN THE SIERRA NEVADA, NEVADA, USA

Jonathan J. Rhodes, C. M. Skau, and D. L. Greenlee¹

ABSTRACT: In-basin hydrology was monitored intensively concurrent with chemical sampling for $\text{NO}_3\text{-N}$ concentrations in snow, vadose water, groundwater, overland flow and streamwater in a small headwater stream in the Sierra Nevada. Denitrification rates from a meadow within the watershed were measured in the field. Mean $\text{NO}_3\text{-N}$ concentrations were: 0.037 mg/l for snow; 0.001 mg/l for groundwater; and 0.097 mg/l for overland flow. $\text{NO}_3\text{-N}$ concentrations in the stream remained <0.001 mg/l except during the generation of hydrograph peaks by snowmelt. When the watershed was snow-covered, peak nitrate concentrations in the stream coincided with discharge maxima. As snowcover was melted off the lower watershed, nitrograph maxima became lagged behind peak discharge, a common pattern during snowmelt in the Sierra Nevada. The lagged pattern results from the operation of biological $\text{NO}_3\text{-N}$ removal mechanisms which are light- and/or temperature-sensitive. The removal mechanisms are denitrification, uptake by plants and in-stream uptake by periphyton; all have diurnal patterns of uptake after snowcover removal due to diurnal heating and irradiance. The removal mechanisms are dormant or steady beneath the insulating snowcover which excludes light, hence lagging does not occur during complete snowcover. By controlling both runoff mechanisms and light and heat delivery to the watershed, snowcover strongly affects concentration patterns of $\text{NO}_3\text{-N}$ during snowmelt.

(KEY TERMS: snowmelt chemistry; nitrate transport; aquatic biology; nutrient cycling; snowmelt runoff; small streams.)

INTRODUCTION

Runoff mechanisms generating streamflow from snowmelt are known to vary seasonally and areally in forested watersheds. The dominance of the particular mechanism in generating snowmelt runoff is dependent on antecedent hydrologic conditions, basin topography and the intensity and duration of snowmelt (Dunne and Black, 1971; Price and Hendrie, 1983). The mechanisms, such as subsurface and overland flow, involve different paths and widely divergent travel times prior to entering streamflow (Dunne, 1978). Water pathway and residence time are the strongest controls on water chemistry on both the geochemical and biological levels. Therefore, it is logical that water from different runoff regimes would have different chemical signatures. This is especially true when dealing with a non-conservative constituent, such as $\text{NO}_3\text{-N}$, which is strongly affected by biologic reactions. Stream chemistry should be a reflection of the type of mechanisms contributing to streamflow generation at a point in time and space. Snowcover greatly influences both runoff mechanisms and biology, hence it exerts a strong control on stream chemistry.

¹Respectively, Graduate Research Assistant, College of Forest Resources, University of Washington, Seattle, WA 98195; Professor of Watershed/Forestry, Department of Range, Wildlife and Forestry, University of Nevada Reno, Reno, Nevada 89512; and Hydrologist, Tahoe Regional Planning Agency, P.O. Box 1038, Zephyr Cove, NV 98448.

In 1982, a field study was initiated to investigate the hydrologic processes controlling nitrate export in streamflow from a high-elevation, forested watershed in the central Sierra Nevada, Nevada, USA. Nearby Lake Tahoe is currently undergoing cultural eutrophication due to accelerated nitrogen loading (Goldman, 1985). The ultimate objective of the research was to provide a scientific foundation for watershed management policies in the Lake Tahoe Basin. The more immediate goal of the study was to characterize the nitrate chemistry of precipitation, vadose water, groundwater, overland flow on hillslopes, and streamwater both temporally and areally. Concurrent with water quality sampling, intensive hydrologic monitoring was performed in order to determine how in-basin hydrologic processes affected the nitrate load in streamflow. The initial phase of the research identified denitrification within the subsurface system as a possible important component of $\text{NO}_3\text{-N}$ removal. Subsequently, summer and autumn denitrification rates in a wet meadow were measured. Results of the study help to elucidate the effect of snowcover and mechanisms of snowmelt runoff generation on chemical constituents strongly affected by biology and flowpath.

DESCRIPTION OF THE STUDY SITE

The experimental watershed is located in the Toiyabe National Forest on the east side of the Sierra Nevada, in Washoe County, Nevada, USA, and is approximately 3 km from Lake Tahoe (Figure 1). Elevations in the basin range from 2012 m at the stream outlet to approximately 2500 m at the upper divide. North-aspect slopes dominate the east-west trending watershed. Slope inclination varies from 20 to 50 percent.

A first-order stream drains the 0.80 km² watershed. The stream is fed by perennial springs and numerous ephemeral springs which flow during snowmelt and after heavy rain events. The flowing segments of stream channel expand and contract rapidly in response to snowmelt and drought. Snowmelt runoff is the dominant generator of streamflow. Peak

streamflow ranged from 3 l/s in late summer to 30 l/s during spring snowmelt.

Mean annual precipitation in the area is estimated to be 76 cm with approximately 85 percent falling as snow. The remainder of the precipitation usually falls in autumn rain events; summer storms are infrequent. Snowcover typically blankets the area from October to May.

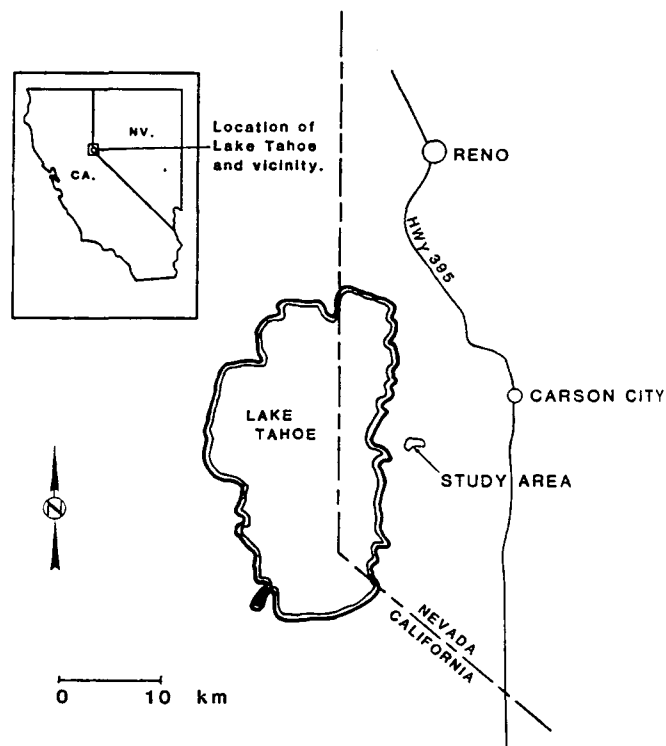


Figure 1. Location of the study area.

Soils are comprised of coarse, decomposing granodiorite. Infiltration rates and saturated hydraulic conductivity values in the soils are high (Rhodes, 1985). As in most forested, mountainous watersheds, overland flow rarely occurs except when the soil profile is completely saturated. Soil depths vary from 4 m on ridge axes to 0.5 m in the channels.

Vegetation is a mosaic of riparian zones, wet and dry meadows, and old growth conifers. The watershed outlet is dominated by a wet meadow flanking the riparian zone. The riparian zones contain alder (*Alnus tenuifolia*), willows (*Salix* spp.), horsetail (*Equisetum arvense*), and ferns (*Athyrium filix-femina*). The upper slopes support virgin stands of ponderosa pine (*Pinus ponderosa*), Jeffrey pine (*Pinus jeffreyii*), and

red and white fir (Abies magnifica and concolor). Alder is known to be a nitrogen fixer.

INSTRUMENTATION AND METHODS

Hydrology

Precipitation quantities were measured with a recording precipitation gage located in the lower wet meadow and augmented by a snow board network. Streamflow discharge at the watershed outlet was measured with a continuous stage recorder coupled with an 0.5 m H-flume. Groundwater levels were monitored via piezometers constructed of 5 cm ID PVC pipe screened at the terminus. Forty-six piezometers were located throughout the watershed with terminus depths ranging from 0.3 to 4 m. Depth to groundwater in the piezometers was measured in a non-recording manner; measurement frequency ranged from every 4 hours diurnally to monthly dependent on instrument location and season.

Water Chemistry

Soil water samples were collected by means of suction cells attached to porous ceramic cups. Details of sampler construction, preparation and installation can be found in Linden (1977). Forty samplers were used; they were located in 37 sites at depths ranging from 0.3 m to 3.3 m. The samplers were located in tandem with the piezometers. Measurement of groundwater levels during sampling allowed differentiation of samples into the vadose or groundwater regimes.

The site was visited approximately twice weekly during the winter and four times weekly during snowmelt. Samples of the stream chemistry at the outlet were taken during the visits and augmented by diurnal sampling during the melt events. Samples of precipitation were taken from snowboards within 24 hours of storm cessation. All soil water samplers were sampled monthly except during December, 1982, through February, 1983, due to instrument malfunction caused by the heavy snowpack. Prior to sampling, the soil water samplers were purged and a

vacuum was applied. Samples were taken from the soil water samplers within 48 hours of the application of a vacuum. Additional surface water samples were taken from the snowpack base, ephemeral channel segments, overland flow on saturated areas, and springs during the spring snowmelt. All water chemistry data presented is from sampling done October, 1982, through June, 1983. This period corresponds to the period of snowcover in the watershed during the year.

All samples were collected in polyethylene bottles which had been rinsed with diluted HCl and three sample aliquots prior to sample collection. Samples were immediately taken to the EPA-certified Water Lab of the Desert Research Institute for analysis. Samples were analyzed by ion chromatography. The method has been shown to give excellent agreement with liquid chemistry methods (Fishman and Pyen, 1979) and is accurate to ± 0.001 mg/l with a lower detection limit of 0.001 mg/l $\text{NO}_3\text{-N}$. Duplicate sample results were always ± 0.001 mg/l $\text{NO}_3\text{-N}$.

Denitrification

Denitrification was measured directly in-situ in the lower wet meadow using acetylene blockage techniques (Ryden, et al., 1978; Ryden, et al., 1979a; Ryden, et al., 1979b) using a soil chamber system constructed as recommended by Denmead (1979). Six pairs of sampling sites were arranged in a circle approximately 6 m in diameter and 8 m from the stream. Each sampling pair was sampled simultaneously during the sampling runs. Additionally, the following were also measured at the sampling area during each sampling run: 1) soil temperature at the 10, 25 and 50 cm depth with thermistor/thermometers; 2) depth to groundwater using piezometers; and 3) soil moisture content at 15 cm intervals to 2 m using a neutron soil moisture gage and aluminum access tubes. Displacement of N_2O gas from the samples and analysis with gas chromatography was done based on the procedures outlined by Ryden, et al. (1978). Measurements were taken during the summer of 1983 and summer through

autumn of 1984.

RESULTS

Hydrology

Precipitation amount over the watershed area was 103.7 cm of water equivalent. The snowpack was the greatest in over 100 years of record in the region for depth, water equivalent and persistence. Some snowcover remained in the watershed through June.

Groundwater was the dominant generator of streamflow both in time and space (Rhodes, et al., 1984). There was no indication of interflow; the dominant pathway of precipitation was through the vadose zone into groundwater and then to the stream (Rhodes, 1985). Soil temperatures at the 10 cm depth ranged from 2 to 3.5°C from December 1982 through January, 1983. Groundwater levels and soil moisture remained high through mid-winter; they were maintained by snowmelt at the pack base generated by heat flow from the soil (Rhodes, 1985). During spring snowmelt, piezometer data indicated areas of profile saturation expanded and overland flow was observed. Overland flow contributions to streamflow increased during spring snowmelt and were greatest during daily peak runoff (Rhodes, 1985).

Water Chemistry

Precipitation had a weighted mean concentration of 0.037 mg/l $\text{NO}_3\text{-N}$. Groundwater had consistently low $\text{NO}_3\text{-N}$ concentrations. Of 158 groundwater samples, 112 were below detection limits of 0.001 mg/l. Mean concentration in the groundwater was 0.001 mg/l $\text{NO}_3\text{-N}$. The $\text{NO}_3\text{-N}$ concentrations in the vadose zone were highly variable temporally and areally, ranging from < 0.001 mg/l to 1.06 mg/l $\text{NO}_3\text{-N}$ in 45 samples. Samples with high concentrations in the vadose zone were always restricted to areas with bare soils near the watershed boundaries (Rhodes, 1985). While alders are notorious nitrogen fixers, soil water samples from alder thickets did not have high $\text{NO}_3\text{-N}$ concentrations. Eight samples of

soil water were taken from the alder thickets in April and May, 1983. Only two samples had concentrations above detection limits, they were 0.001 and 0.004 mg/l $\text{NO}_3\text{-N}$.

Four samples of meltwater taken from the base of the snowpack gave a mean concentration of 0.093 $\text{NO}_3\text{-N}$, which is a reasonable enrichment given the meltwater fractionation of contaminants in the snowpack (Johannessen and Henriksen, 1978). Three grab samples of overland flow on saturated areas were taken in May 1983. These overland flow samples had a mean concentration of 0.097 mg/l $\text{NO}_3\text{-N}$. Sixteen samples from flowing stream segments in the upper watershed yielded a mean concentration of 0.011 mg/l $\text{NO}_3\text{-N}$ with a range of 0.002 to 0.026 mg/l $\text{NO}_3\text{-N}$. Concentrations in the stream at the outlet remained low except during snowmelt and rain events. Of 99 samples, 33 had concentrations > 0.001 $\text{NO}_3\text{-N}$ mg/l. Peak concentration in the stream at the outlet was 0.007 mg/l during the peak snowmelt period on May 18, 1983.

The nitrate budget for the period of investigation indicates uptake and/or removal of $\text{NO}_3\text{-N}$ is highly efficient. The $\text{NO}_3\text{-N}$ load to the watershed in precipitation was 450 g/ha from Sept. 1982 to June 1983. During this period, 48 g/ha was exported from the watershed in streamflow (Rhodes, 1985). Actual retention or removal of $\text{NO}_3\text{-N}$ within the system may actually be higher because inputs of $\text{NO}_3\text{-N}$ via dryfall and plant fixation were not quantified. Also, inputs of other nitrogen forms were not quantified and these forms, such as N_2 , $\text{NH}_4\text{-N}$, can be converted to $\text{NO}_3\text{-N}$ by nitrification.

Hydrograph and Nitrograph Relationships

From October, 1982, through March, 1983, streamflow generation was dominated by groundwater. Streamflow hydrographs exhibited no peaks and $\text{NO}_3\text{-N}$ concentrations were always < 0.001 mg/l.

A rain-on-snow event penetrated the snowpack on March 11, 1983. The event raised initially high groundwater levels and generated a streamflow peak subsequent to the development of profile saturation (Figures 2a and b). The

stream was sampled diurnally during this event. The $\text{NO}_3\text{-N}$ concentration in the stream peaked coincident with discharge and dropped rapidly afterwards (Figure 2a).

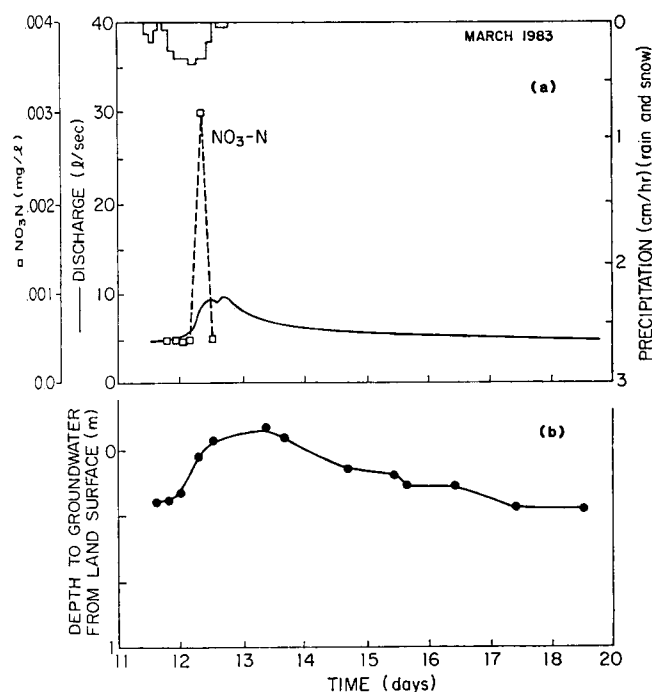


Figure 2. (a) Storm hydrograph, streamflow hydrograph and streamwater nitrograph, (b) Piezometric data from intensively monitored site for March, 1983 rain on snow event.

A pattern of elevated $\text{NO}_3\text{-N}$ concentrations coincident with peak daily snowmelt discharge emerged with the onset of snowmelt. When snowmelt generated daily discharge peaks, $\text{NO}_3\text{-N}$ concentrations in the stream rose above the detection limits; during periods of groundwater-generated flow, there were no hydrograph peaks and $\text{NO}_3\text{-N}$ concentrations remained below detection limits (Figure 3). This pattern of $\text{NO}_3\text{-N}$ concentration and stream discharge continued through May, 1983. With ongoing snowmelt, the extent of saturated area in the watershed expanded, concomitantly increasing both runoff and $\text{NO}_3\text{-N}$ concentrations at the stream outlet by increasing the overland flow component of runoff. However, peak $\text{NO}_3\text{-N}$ concentrations became lagged about 10 hours behind discharge peaks once snowcover was removed from the stream channel and the lower wet meadow in mid-May (Figure 4). Nitrograph and

hydrograph minima remained roughly coincident (Figure 4). The lagged nitrograph pattern is pervasive during peak snowmelt in streams in the Sierra Nevada (Coats, et al., 1976; Leonard, et al., 1979).

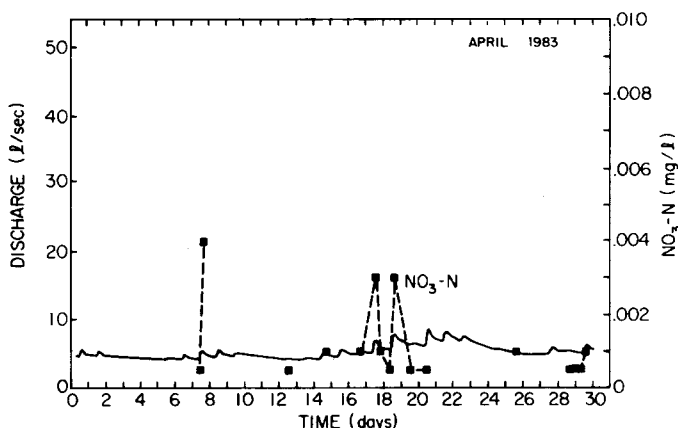


Figure 3. Streamflow hydrograph and streamwater nitrograph, April, 1983.

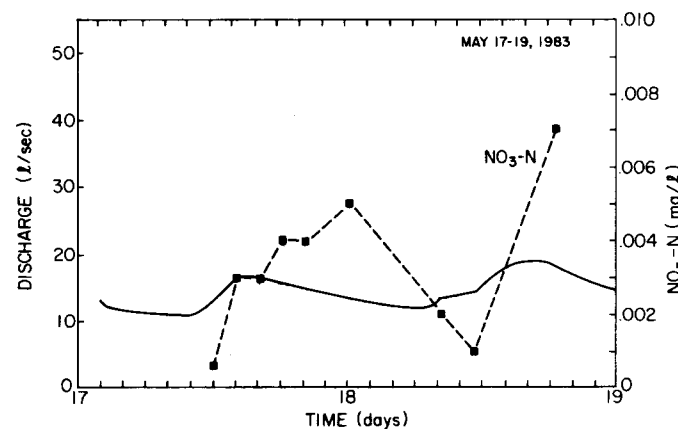


Figure 4. Streamflow hydrograph and streamwater nitrograph for diurnal sampling, May 17-19, 1983, at peak snowmelt.

Denitrification

During the 1984 sampling season, 109 samples of N_2O gas were taken from the meadow. Measured denitrification rates ranged from 0.14 to 2.94 g $\text{NO}_3\text{-N}/\text{ha}/\text{hr}$ with a mean of 1.26 g $\text{NO}_3\text{-N}/\text{ha}/\text{hr}$ (Greenlee, 1985). The rates had a strong diurnal variation (Greenlee, 1985). Rates peaked at about 13.30 PST and then dropped (Figure 5). The diurnal fluctuation of denitrification rates appears to be associated with soil temperature (Figure 5). Denitrification rates have

been found to be highly correlated with soil temperatures by other researchers (Freney, et al., 1978; Ryden, et al., 1978; Ryden, et al., 1979a; Ryden, et al., 1979b; Denmead et al., 1979). Of all the variables measured, soil temperature at the 10 cm depth gave the best correlation with denitrification rates. However, the correlation of temperature with denitrification was not particularly strong with $r = 0.66$ at the 0.01 confidence level (Greenlee, 1985). Denitrification rates had little diurnal variation on days with minimal variation in soil temperature (Greenlee, 1985).

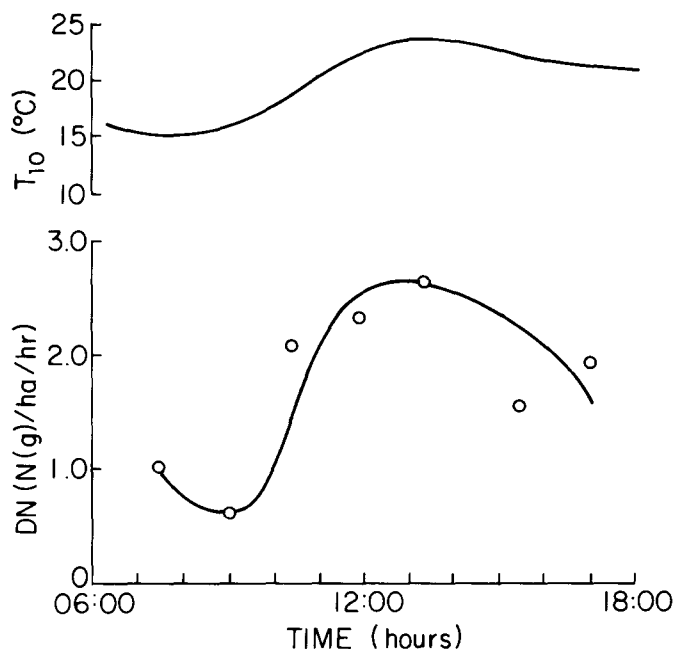


Figure 5. Denitrification rates (DN) for a 12 hour period on 9-18-84. The denitrification rates are averages for the two simultaneously sampled plots and are plotted in the middle of each sampling period. The temperature at 10 cm below the soil surface (T₁₀) is plotted for approximately each 1/2 hour period.

DISCUSSION

In light of the sampling results of water chemistry, the pattern of NO₃-N concentration with discharge during early spring snowmelt (Figure 3) is as expected. When only groundwater generated the streamflow flow, stream concentrations were similar to groundwater

concentrations. During the generation of hydrograph peaks a greater fraction of overland flow over saturated margins contributed to streamflow. Water reaching the stream by overland flow had higher NO₃-N concentrations because it bypassed the soil system, thus avoiding plant uptake and denitrification in the anaerobic subsurface environment. Due to the higher concentrations of NO₃-N in overland flow, in-stream NO₃-N concentrations increase with increasing overland flow contributions and peak coincident with maximum discharge (Figure 3). This also explains why NO₃-N concentrations increase with the increasing snowmelt runoff; i.e., because saturated area within the watershed expanded. This conclusion is strengthened by the snowmelt and water chemistry data from the water year '83-'84. During that year the shallow snowpack melted and retreated rapidly. Overland flow was not observed, snowmelt peaks were not generated and NO₃-N concentrations in the stream never rose above the detection limits of 0.001 mg/l NO₃-N (Melgin, 1985).

The lagging of nitrograph peaks after the discharge peaks in mid-May (Figure 4) is initially perplexing. Groundwater and vadose water during this period had concentrations less than the peak value in the stream; they could not have accounted for the lagged peak. The lagging only occurred after the lower wet meadow and stream channel were snow-free, allowing light penetration and diurnal warming. The lagged nitrograph pattern is hypothesized to result from the operation of NO₃-N removal during the day by biologic processes which are light- and temperature-sensitive and consequently have a diurnal pattern. Three biological processes are believed responsible for the removal of nitrate from water in the watershed: anaerobic denitrification in wet meadows; uptake by vascular macrophytes; and uptake by in-stream periphyton.

Denitrification is temperature-sensitive. While denitrification rates were not measured during the winter, the consistently low groundwater NO₃-N concentrations indicate denitrification was active. Results of the denitrification rate measurements also indicate rates would have been steady because soil

temperature varied little beneath the insulating snowcover (Rhodes, 1985). Upon partial snowcover removal, the upper 10 cm of soil in exposed areas heated from 1°C to 7°C from May 15 through 19, 1983 (Rhodes, 1985). Given the temperature and denitrification rate results, it is likely the nitrification rates increased dramatically due to the temperature increase during this period and that the rates had a diurnal fluctuation. The daily maximum denitrification rates in exposed areas probably occurred near solar noon as is the case with the rates measured during summer and autumn, 1984.

Uptake by terrestrial vascular macrophytes largely coincides with evapotranspiration rates, hence it is both light- and temperature-sensitive. Peak rates coincide with solar noon. In the Sierra Nevada, plants typically exert their maximum seasonal uptake after removal of snowcover. Hence, plant uptake was probably exerting a maximum effect during period when the stream nitrographs began to exhibit lagging.

NO₃-N uptake by periphyton has been shown to be proportional to solar irradiance (Triska, et al., 1983) and exhibits a periodicity of activity similar to that of phytoplankton in lentic water (Toetz, 1976). Most past research into nitrate uptake by periphyton and diel patterns of NO₃-N concentrations has been conducted during summer baseflow conditions (Manny and Wetzel, 1973; McColl, 1974; Duff, et al. 1983; Triska, et al., 1983; Sebetich, et al., 1984). However, it should be possible to extrapolate the research results on periphyton NO₃-N uptake to the study site because many periphyton species are well adapted to cold environments (Hynes, 1970). Research has shown NO₃-N uptake by periphyton is at a maximum near solar noon and rapidly drops to a minimum with the onset of darkness (Triska, et al., 1983). Active periphyton communities have been shown to exert a powerful control on nitrate transport in streams (McColl, 1974; Duff, et al., 1983; Triska, et al., 1983; Sebetich, et al., 1984). Streams affected by periphyton have NO₃-N concentrations with a distinct diel pattern; the maximum NO₃-N concentration occurs near midnight and the minimum during the day (Triska, et al., 1983; Sebetich, et

al., 1984). NO₃-N uptake appears to be greatest at low concentrations when the algae is nitrogen "starved" (McColl, 1974; Triska, et al., 1983; Sebetich, et al., 1984). Actively growing algal mats have higher uptake rates than mature mats (Duff, et al., 1983; Triska, et al., 1983). The algae have been shown to be opportunistic, rapidly increasing NO₃-N uptake with increasing NO₃-N supply (Triska, et al., 1983; Sebetich, et al., 1984).

Periphyton communities in the stream were observed by early May, appearing within a few days of snowcover removal from the stream channel. Sluggish, diffuse streamflow and open canopy conditions in the riparian zone prior to leaf emergence provided an ideal location for periphyton colonization. Given the above review of past literature, it is likely the algal mats exerted a pronounced effect on the nitrograph in mid-May. The communities were actively growing, shading was minimal, and the NO₃-N/P ratio in the stream was always less than 1 indicating intense nitrogen starvation.

In-stream uptake is likely. Chemistry-based hydrograph separation techniques (Pinder and Jones, 1968) and nitrate concentration data for overland flow and groundwater indicate the peak discharges would have been 99% groundwater generated. The estimate of the fraction of streamflow generated by groundwater is unrealistically high in light of the extent of saturated area and overland flow observed at the time (Rhodes, 1985). The hydrograph separation technique assumes an absence of uptake mechanisms. The higher NO₃-N concentrations in the upper watershed also suggest NO₃-N removal along the stream length. However, in the absence of accurate discharge measurements in these reaches, this evidence for NO₃-N removal is inconclusive.

All three biological removal mechanisms would have a diurnal peak near solar noon, which corresponds to the time of peak discharge and the anticipated nitrograph peak if NO₃-N removal were not occurring. The nitrograph without the operation of NO₃-N removal is hypothesized to appear as in Figure 6. Thus, the timing the the observed peak appears

to be due to diurnal $\text{NO}_3\text{-N}$ removal mechanisms superimposed on the nitrograph.

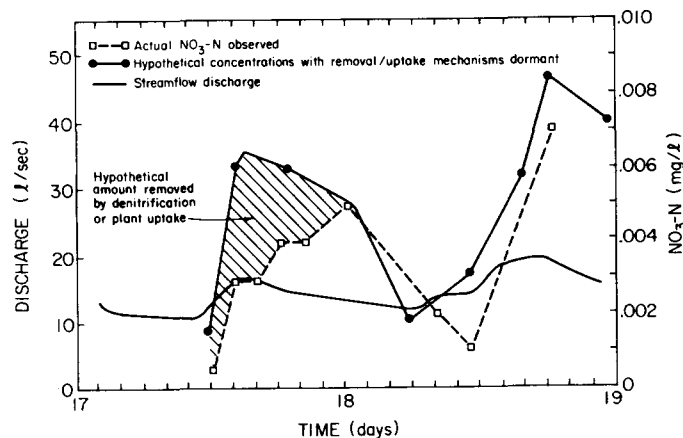


Figure 6. Stream hydrograph, actual streamwater nitrograph and hypothetical nitrograph without uptake/removal mechanisms.

Nitrogen undergoes a wide variety of biological transformations. In order to conclusively use $\text{NO}_3\text{-N}$ as flow path indicator, all forms of nitrogen in the nitrogen pool must be monitored. Plant fixation of N_2 and subsequent nitrification can contribute $\text{NO}_3\text{-N}$ to streamflow. However, our soil water data do not indicate such subsurface sources. All forms of nitrogen were not monitored. However, our combined hydrologic, chemistry and denitrification rate data strongly suggest that the lagging of peak $\text{NO}_3\text{-N}$ concentrations in streams behind daily discharge peaks is due to diurnally varying $\text{NO}_3\text{-N}$ removal and uptake mechanisms.

The nitrate removal mechanisms would have been nearly dormant under the snowpack. Periphyton were probably absent due to the exclusion of sunlight by the snowcover. Certainly diurnal fluctuations would have been essentially non-existent. Thus, an explanation is provided for the absence of lagging of peak nitrate concentrations earlier in the season when snowcover was complete.

CONCLUSIONS

Runoff mechanisms obviously exert a strong control on stream chemistry, especially in the case of reactive

constituents. Such control is evident in seasonal and diurnal patterns of stream flow and its $\text{NO}_3\text{-N}$ concentrations. Beneath a snowpack biological mediation of water chemistry is minimized by cooling the system and excluding light. Diel biological activity is steadied by the snowcover shielding the sun and insulating the soil system. Under snowcover, diurnal patterns of nitrate concentration are mainly a function of the type of mechanism generating runoff. However, with partial removal of snowcover within a watershed, light- and temperature-sensitive biological processes can alter the concentration patterns in streamflow generated solely by runoff mechanisms. Thus, on both the hydrologic and biological levels, the presence of snowcover exerts a pronounced influence on $\text{NO}_3\text{-N}$ concentrations which shift seasonally. Other chemical constituents which undergo biological reactions may be affected in a similar manner.

In most areas, $\text{NO}_3\text{-N}$ concentrations in streamflow increase with increasing discharge. In mountainous areas, peak annual discharge occurs during spring snowmelt. Streams in the Sierra Nevada export the major part of the annual $\text{NO}_3\text{-N}$ load during spring snowmelt (Leonard, et al., 1979; Rhodes, 1985). Denitrification and $\text{NO}_3\text{-N}$ uptake by periphyton can greatly affect $\text{NO}_3\text{-N}$ concentrations in streamflow and their distribution in time. Presently, data on these processes during complete snowcover and spring snowmelt is lacking. Considering the importance of the snowmelt period in annual hydrologic and chemical budgets of mountainous areas, research needs to be conducted to investigate the role of these $\text{NO}_3\text{-N}$ removal mechanisms in shaping snowmelt runoff chemistry.

ACKNOWLEDGMENTS

This study was supported in part by a grant from the Office of Water Research and Technology, U.S. Department of Technology, and in part by a grant from the McIntyre-Stennis program of the U.S. Department of Agriculture.

LITERATURE CITED

- Coats, R. N., R. L. Leonard, and C. R. Goldman, 1976. Nitrogen Uptake and Release in a Forested Watershed, Lake Tahoe Basin, California. *Ecology* 51:995-1004.
- Denmead, O.T. 1979. Chamber Systems for Measuring Nitrous Oxide Emission from Soils in the Field. *Soil Science of America Journal* 43:89-95.
- Denmead, O.T., J. R. Freney, and J. R. Simpson. 1979. Studies of Nitrous Oxide Emission from a Grass Sward. *Soil Science of America Journal* 43:726-728.
- Dunne, T. and R. D. Black. 1971. Runoff Processes During Snowmelt. *Water Resources Research* 7:1160-1172.
- Dunne, T. 1978. Field Studies of Hillslope Flow Processes. In: *Hillslope Hydrology*, M. J. Kirkby (Editor). John Wiley & Sons, New York, New York, pp. 227-293.
- Duff, J. H., K. C. Stanley, F. J. Triska, and J. A. Avanzino. 1983. The Use of Photosynthesis-Respiration Chambers to Measure Nitrogen Flux in Epilithic Algal Communities. *Verh. Int. Ver. Limnol.* 22:1436-1443.
- Fishman, M. J. and G. Pyen. 1979. Determination of Selected Anions in Water by Ion Chromatography. In: *Proceedings of the 21st Rocky Mountain Conference on Analytical Chemistry*, July 30, 1979, Denver, Colorado.
- Freney, J. R., O. T. Denmead, and J. R. Simpson. 1978. Soil as a Source or Sink for Atmospheric Nitrous Oxide. *Nature* 273:530-532.
- Goldman, C. R. 1985. Lake Tahoe: Increasing Fertility and Decreasing Transparency During a Quarter-Center of Lake Basin Development. *Eos* 66:114.
- Greenlee, D. L. 1985. Denitrification Rates of a Mountain Meadow Near Lake Tahoe. M.S. Thesis, University of Nevada Reno, Reno, Nevada.
- Hynes, H. B. N., 1970. *The Ecology of Running Waters*. University of Toronto Press, Toronto.
- Johannessen, J. and A. Henriksen. 1978. Chemistry of Snow Meltwater: Changes in Concentration During Melting. *Water Resources Research* 14:615-619.
- Leonard, R. L., L. A. Kaplan, J. F. Edler, R. N. Coats and C. R. Goldman. 1979. Nutrient Transport in Surface Runoff from a Subalpine Watershed, Lake Tahoe Basin, California. *Ecological Monographs* 49:281-310.
- Linden, D. R. 1977. Design, Installation and Use of Porous Ceramic Samplers for Monitoring Soil Water Quality. U.S.D.A. Technical Bulletin 562 10 pp.
- Manny, B. A. and R. G. Wetzel. 1973. Diurnal Changes in Dissolved Organic and Inorganic Carbon and Nitrogen in a Headwater Stream. *Freshwater Biology* 3:31-43.
- McColl, R. H. A. 1974. Self-Purification of Small Freshwater Streams: Phosphate, Nitrate and Ammonia Removal. *New Zealand Journal of Marine and Freshwater Research* 8:375-388.
- Melgin, W. 1985. The Influence of Hillslope Hydrology on Nitrate Transport in a Forested Watershed Near Lake Tahoe. M.S. Thesis, University of Nevada Reno, Reno, Nevada.
- Pinder, G. F. and J. F. Jones. 1968. Determination of the Ground-water Component of Peak Discharge from the Chemistry of Total Runoff. *Water Resources Research* 5:438-445.
- Price, A. G. and L. K. Hendrie. 1983. Water Motion in a Deciduous Forest During Snowmelt. *Journal of Hydrology* 64:339-356.
- Rhodes, J. J., C. M. Skau, and W. Melgin. 1984. Nitrate-Nitrogen Flux in a Forested Watershed--Lake Tahoe, USA. In: *Recent Investigations in the Zone of Aeration*. Proceedings of the International Symposium, Munich, West Germany, October 1984, P. Udluft, B. Merkel, and K. H. Prosl (Editors), pp. 671-680.

- Rhodes, J. J. 1985. A Reconnaissance of Hydrologic Nitrate Transport in an Undisturbed Watershed Near Lake Tahoe. M.S. Thesis, University of Nevada Reno, Reno, Nevada.
- Ryden, J. C., L. J. Lund, and D. D. Focht. 1978. Direct In-field Measurement of Nitrous Oxide Flux from Soils. *Soil Science of America Journal* 42:731-737.
- Ryden, J. C., L. J. Lund, and D. D. Focht. 1979a. Direct Measurement of Denitrification Loss from Soils: I. Laboratory Evaluation of Acetylene Inhibition of Nitrous Oxide Reduction. *Soil Science of America Journal* 43:104-110.
- Ryden, J. C., L. J. Lund, J. Letey, and D. D. Focht. 1979b. Direct Measurement of Denitrification Loss from Soils: II. Development and Application of Field Methods. *Soil Science of America Journal* 43:110-118
- Sebetich, M. J., V. C. Kennedy, S. M. Zand, R. J. Avanzino, and G. W. Zellweger. 1984. Dynamics of Added Nitrate and Phosphate Compared in a Northern California Woodland Stream. *Water Resources Bulletin* 20:93-101.
- Toetz, D. W. 1976. Diel Periodicity in Uptake of Nitrate and Nitrite by Reservoir Phytoplankton. *Hydrobiologia* 49:49-52.
- Triska, F. J., V. C. Kennedy, R. J. Avanzino, and B. N. Reilly. 1983. Effect of Simulated Canopy Cover on Regulation of Nitrate Uptake and Primary Production by Natural Periphyton Assemblages. In: *Dynamics of Lotic Ecosystems*, T. D. Fontaine and S. M. Bartell (Editors). Ann Arbor Science, Ann Arbor, Michigan, pp. 129-159.

RESERVOIR WATER QUALITY SIMULATION IN COLD REGIONS

C.Y. Wei and P.F. Hamblin¹

ABSTRACT: The requirements for environmental impact analysis associated with the license application of the proposed Susitna Hydroelectric Project have motivated a program of data collection, development and testing of a reservoir simulation model in two Alaskan basins. The model developed for simulating the temperature and suspended sediment distributions and ice and snow cover in lakes and reservoirs is based on the dynamic reservoir simulation model called DYRESM. The model was first applied to a known water body, Eklutna Lake, which had a number of properties in common with the proposed reservoirs. Comparison of simulations with field observations are presented. Excellent results were obtained and the general applicability of the model to the proposed reservoirs in a subarctic region is demonstrated. The model was then applied to the proposed Watana and Devil Canyon reservoirs. The influence of water quality requirements for downstream temperatures and suspended sediments on the reservoir behavior are discussed. Finally, the model's capability to simulate operation of the proposed multi-level intake structures under different meteorological and project operating conditions is demonstrated. The effect of the operating conditions on two water quality parameters, temperature and suspended sediment concentration, provides informa-

tion required to evaluate the influence of the project operations on fishery resources. The predicted ice-cover thickness served as input to terrestrial wildlife management planning.

(KEY TERMS: Eklutna Lake; glacially fed lake; hydroelectric project; multi-level intake; reservoir simulation, stratification; subarctic Susitna basin; suspended sediment concentration; temperature and ice.)

INTRODUCTION

The Susitna Hydroelectric Project has been proposed by the Alaska Power Authority in order to provide a dependable and economical source of energy for the Alaska Railbelt area. The project would consist of two dams, a 197 m (646 ft) high concrete arch dam at the Devil Canyon site and a 270 m (885 ft) high earth and rock-fill dam at the Watana site located on the Susitna River about midway between Anchorage and Fairbanks (see Figure 1) the principal load centers of the Railbelt region. It would be built in three stages and would ultimately provide 6,900 Gwh/year of energy with a firm capacity of 1,620 MW. The project and the basin are described in more detail by Gemperline (1986).

¹Respectively, Senior Hydraulic Engineer, Harza Engr. Co., 150 S. Wacker Dr., Chicago, IL 60606; and Research Scientist, National Water Research Institute, Canada Center for Inland Waters, 867 Lakeshore Road, Burlington, Ontario L7R 4A6.

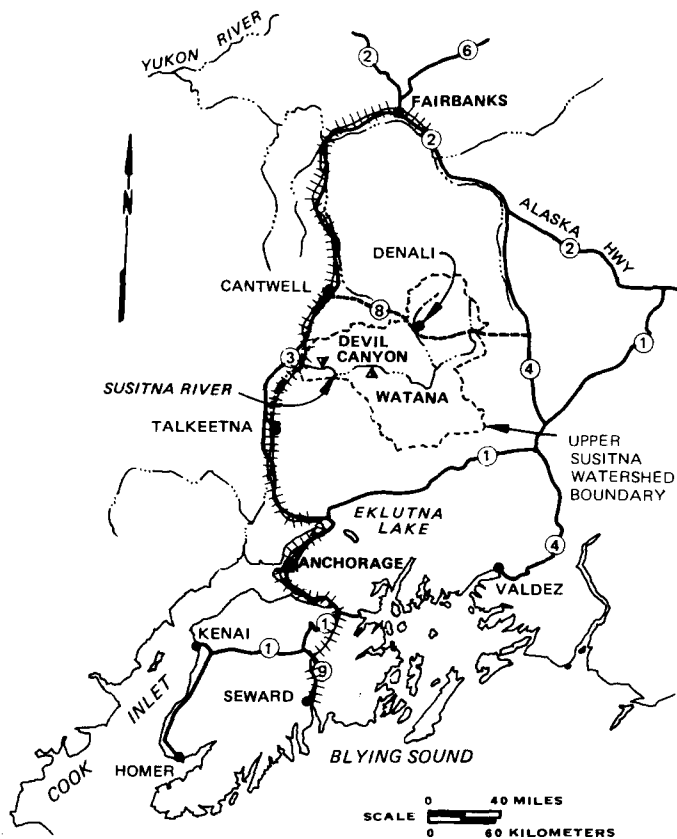


Figure 1. Location of the Proposed Susitna Hydroelectric Project and Eklutna Lake.

The potential effects of the Susitna Hydroelectric Project on the fishery resources of the Susitna River are an important concern in the development of the project. The potential effects include possible changes in both the quantity and quality of water in the Susitna River with respect to the fish and other wildlife habitats. The potential changes in river flows, water temperature, suspended sediment concentration, and ice conditions must be evaluated carefully in an environmental impact study associated with the license application of the project. Such concerns and needs have motivated a program to collect data at Eklutna Lake and in the Susitna Basin, to develop and test the DYRESM reservoir model and to apply the model to predict the temperature and suspended sediment regimes in the proposed Watana and Devil Canyon reservoirs. The DYRESM reservoir temperature simulation model has been extended and enhanced by adding capabilities to simulate suspended sediment con-

centrations in the reservoir, the winter ice-cover formation, and the operation of a multi-level intake for applications to the Susitna Project. Testing of the model with the Eklutna Lake data showed good agreement between predicted and observed outflow temperatures and winter ice-cover thicknesses.

Following successful tests of the DYRESM model, the model was applied to predict the temperature regimes of the proposed Watana and Devil Canyon reservoirs. The selective withdrawal capability of the proposed multi-level intake structures was simulated for different project operating conditions. To assist in the determination of the outflow turbidity the extended DYRESM model was applied to simulate the suspended sediment concentrations in the proposed reservoirs and the Eklutna Lake data collection program was expanded to provide sediment data for testing the model. Satisfactory results were obtained on the suspended sediment concentrations of the outflow. Further refinements of the analysis are also needed to improve the simulation of suspended sediment regime of the lake.

THE DYNAMIC RESERVOIR SIMULATION MODEL

The dynamic reservoir water quality simulation model, DYRESM, was originally developed by Imberger and Patterson (1981) and has been modified and enhanced by Harza-Ebasco Susitna Joint Venture to include simulations of multi-level intake operations, frazil ice inflow, and suspended sediment concentration. A snow and ice-cover algorithm as developed by Patterson and Hamblin was also incorporated in the DYRESM model. The basic features of the model are summarized as follows.

In the formulation of the modelling strategy of the model, the principal physical processes responsible for the mixing of heat and other water quality components are parameterized. This approach is in contrast to other simulation models which are largely empirically based. While the modelling philosophy employed in DYRESM requires a reasonable understanding of the

key processes controlling water quality, so that they may be parameterized correctly, this process related approach to modelling has the advantage that the resulting model may require less calibration and is more generally applicable than the empirically based methods. A second major consideration in model formulation has been to keep the computational overhead as low as possible in order to keep the running costs of the simulation of a number of variables over time periods of up to three years within reason. Thus, the basic time step of the model is one day although sub-daily time steps as short as one-quarter hour are allowed when required for model stability and accuracy.

The influence of ice and snow on the heat transfer across the water surface of a reservoir is taken into account by calculating the area of snow and ice cover and their thicknesses as a function of time. The effect of snow and ice cover on the heat transfer is to reduce the amount of short wave radiation reaching the upper layers of the reservoir through the reflective and absorptive properties of ice and snow and to reduce the cooling of the reservoir surface that would otherwise occur by providing a covering layer of reduced thermal conductivity. The reflective properties of the snow cover on short wave radiation are varied in time according to well established empirical relations involving snow age and snow temperature. A novel feature of the ice cover simulation model is the turbulent transport of heat from the water to the ice due to the under-ice flow field generated by inflows and outflows (Patterson and Hamblin, 1986). Additionally, since snow thickness is limited by the bearing capacity of the ice cover, snowfall beyond this limit is added to the water surface. The input of a volume of frazil ice is provided as a percentage of the daily inflow. The mass of ice contained in the inflow is computed and added to the existing ice thickness in both the cases of full or partial ice. In the latter case the frazil ice input is added to the ice cover until full ice cover is reached.

The horizontally averaged profiles of suspended sediment are changed in the model by three processes, namely by vertical mixing, by inflows and outflows and

by settling. The suspended sediment concentrations are solved based on a sediment transport equation and the water density calculations include the contributions from the suspended sediment as well as temperature. Density inversions resulting from suspended sediments are checked and mixed if required to establish a stable density distribution. Settling velocities are input appropriate to the size range of the inflowing sediments. The sediments are deposited on the bottom as they reach the bottom layer of the reservoir. The effective diffusivities of the sediment fractions are assumed to be identical with that of temperature.

APPLICATION TO EKLUTNA LAKE

To facilitate the testing of the DYRESM model on a existing glacially fed lake, Eklutna Lake was selected for an intensive field study (R&M Consultants, 1985(a)& (b)). Eklutna Lake, shown in Figure 2 is located approximately 48 kilometers (30 miles) northeast of Anchorage and 160 kilometers (100 miles) south of the project site. The purpose of testing the DYRESM model was to demonstrate the applicability of the model to the proposed reservoirs. Both the proposed reservoirs and Eklutna Lake are located in the south-central region of Alaska. Eklutna Lake is also operated for hydroelectric production and has a similar average residence time of 1.65 years to that of the Watana reservoir (1.77 years).

The testing of the DYRESM model was performed in two phases. In the initial phase, the basic DYRESM model for temperature and ice simulation was tested. In the second phase, the suspended sediment option was added to the model and the testing of the model was conducted in conjunction with the expanded sediment sampling and turbidity data collection program.

A meteorological and limnological data collection program was initiated in June 1982 which was designed specifically for model verification purposes. A major component of the field study was a weather station established at the south-east end of the lake. Besides the pertinent mete-

Testing of the DYRESM Model: Temperature and Ice

The DYRESM model was applied to simulate the average temperature distribution in Eklutna Lake for the period starting June 1, 1982 and ending May 30, 1983. An analysis of the initial results (Harza-Ebasco Susitna Joint Venture, 1984) led to several improvements of the model. These improvements included application of the Anderson incoming long-wave radiation equation instead of the Swinbank formula during the sub-freezing conditions (Tennessee Valley Authority, 1972) and incorporation of intake design and wind effects on temporal thermocline displacement in estimation of outflow temperatures.

The simulated and observed outflow temperatures are shown in Figure 3. In general, the differences between the predicted and observed winter outflow temperatures were within 0.5°C (1°F). However, summer deviations of up to about $+2.0^{\circ}\text{C}$ (3.5°F) also occurred, especially during and after high wind periods. The surface wind shear effects and the internal wave motions near the intake structure are extremely difficult to model with a one-dimensional approach and three-dimensional modeling is not considered practical.

The results also show an excellent correspondence between measured ice thickness and predicted ice thickness, being within the standard error of the observations except in March. The accuracy of the March prediction is difficult to evaluate. The only ice measurement available was made at Station 13 which is located near the north end of the lake (Figure 2). The

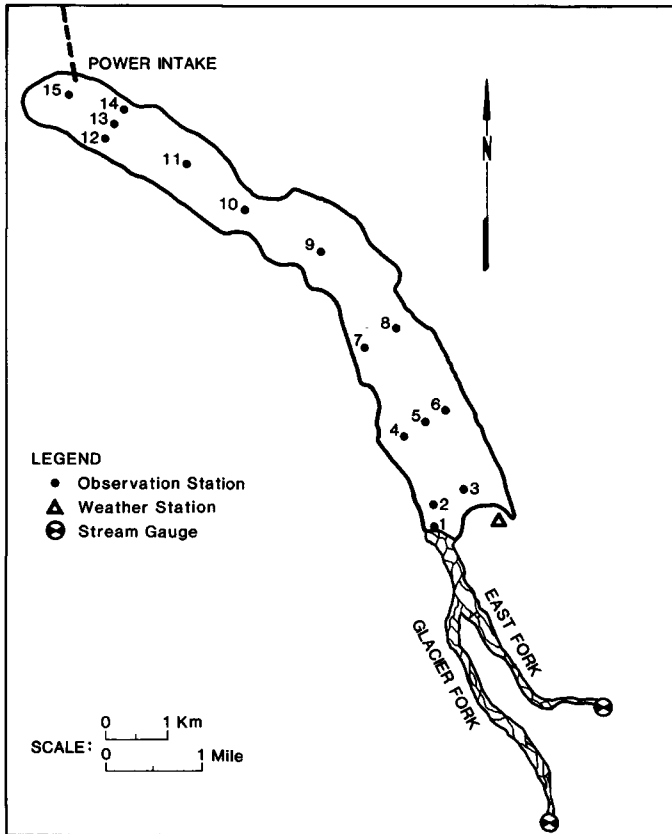


Figure 2. Location of the Observation Stations, Eklutna Lake

orological data such as solar radiation, air temperature, relative humidity, and wind speeds etc, these data also include daily inflow and outflow discharges and their temperatures, and suspended sediment concentrations as well as approximately monthly to semi-monthly surveys of lake temperature and turbidity profiles. In addition, occasional ice thicknesses were measured.

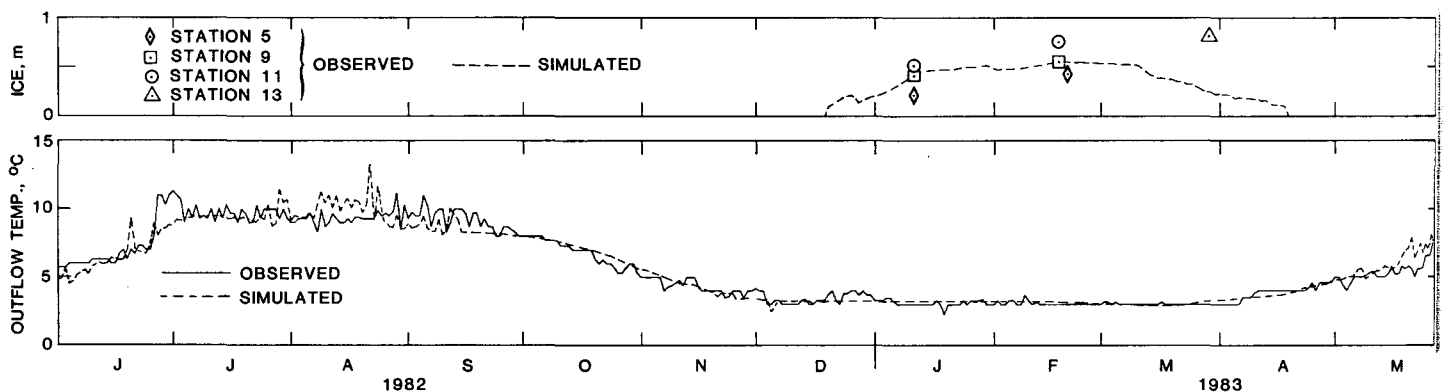


Figure 3. Observed and Simulated Eklutna Lake Ice Thicknesses and Outflow Temperatures.

relatively thick ice measured was probably due to local accumulation of rafted ice caused by persistent downlake winds. In addition to the outflow temperatures, the observed and simulated time history of temperature versus depth are shown in Figures 4(a)&(b). The general characteristics of the observed temperature regime are simulated reasonably well by the DYRESM model.

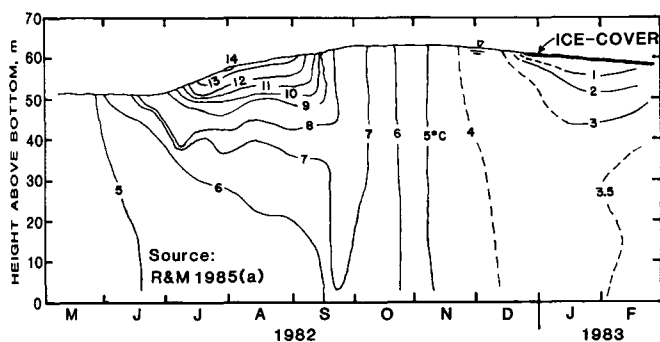
The results of the study demonstrate the applicability of the DYRESM model to simulate the hydrothermal behavior of a reservoir in the specific region of the Susitna Project. The study has also demonstrated the need for accurate climatic data to apply the model properly. The accuracy and reliability of field measurement instruments and data collection procedures must be maintained for the results to be useful.

Testing of the Extended DYRESM Model: Suspended Sediments

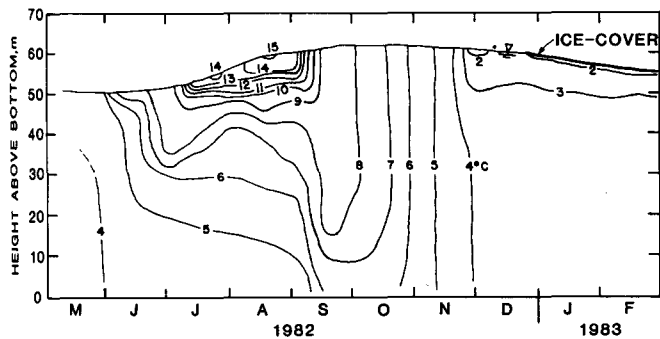
The extended DYRESM model was tested using the Eklutna Lake data to determine

its ability to simulate suspended sediment concentration of the outflows from the Susitna project. The hydrological and meteorological data collection program was continued (R&M Consultants, 1985(a)&(b), and Coffin and Ashton, 1986) with special emphasis on suspended sediment sampling for the period from May to November 1984. The total incoming suspended sediments were measured twice weekly. An empirical relation was established using these observed semi-weekly inflow suspended sediments and the corresponding discharges. This relationship was applied to estimate the daily total inflow suspended sediment concentration. These suspended sediment concentrations ranged from 0.15 to 570 mg/l in the inflow streams, and from 0.50 to 36 mg/l in the outflow. Peak values in the inflow occurred in late July or early August, and in the outflow in late July to mid-August. The winter inflow and outflow suspended sediment concentrations were on the order of 0.1 mg/l.

The total suspended sediment influent from both Glacier Fork and East Fork streams (Figure 2) were first divided into three groups representing three different particle size ranges. The particle size ranges selected were 0-3 microns, 3-10 microns and greater than 10 microns. Initial test runs indicated that particles greater than 10 microns would settle rapidly to the bottom of the lake and have little effect on the average suspended sediment concentration profiles. The greater than 10 micron sediments were therefore ignored in the study. The total incoming suspended sediments of each particle size range were then estimated based on the weighted particle size distributions determined from the samples taken from East Fork and Glacier Fork streams. These samples were obtained in three field trips made on July 21, August 28, and October 23, 1984. The daily particle size distributions were interpolated from these three basic distributions. To apply the extended DYRESM model, it was necessary to specify an initial vertical distribution of suspended sediment, the particle settling velocity, and the average density of the particle. Based on Stoke's law, a settling velocity of 1.5×10^{-6} m/s was used for the 0-3 micron sediments and 4.0×10^{-5} m/s for the 3-10 micron sediments. A particle specific gravity of 2.60 was



(a) OBSERVED (Station 9)



(b) SIMULATED

Figure 4. Observed (a) and Simulated (b) Isotherm Distribution in Eklutna Lake.

used in the study while the measured specific gravity varied from 2.50 to 3.00. The DYRESM simulations were made for 0-3 micron sediments and 3-10 micron sediments separately. The resulting outflow suspended sediments of these two separate analyses were then combined to yield the total outflow suspended sediment concentrations as shown in Figure 5. The predicted outflow suspended sediment concentrations were in reasonable agreement with data obtained from the powerhouse tailrace especially considering the coarse resolutions of the inflow concentrations. On two occasions, the field data show temporary increases in suspended sediment concentrations that were not predicted by the DYRESM model. Prior to these events, there were relatively heavy rains. A small stream which flows into the lake near the intake may have carried significant amount of sediments and caused the suspended sediment concentration to increase locally and temporarily at the intake area.

The suspended sediment influents were, later in a test study, neglected and the simulation was repeated. The resulting temperature distributions showed the influence of the suspended sediments to be insignificant. Hence, the suspended sediment inputs to a reservoir may be ignored in most cases in this region when only the temperature analysis is needed.

APPLICATION TO SUSITNA RESERVOIRS

Simulation of Temperature and Ice

Following the successful testing of the DYRESM model with the Eklutna Lake data, the model was applied to determine the temperature regimes in the proposed Watana and Devil Canyon reservoirs.

Fifteen years of hydrologic and meteorological data have been assembled and analyzed. The data collected at the Watana and Devil Canyon weather stations since 1982 (R&M Consultants, 1985(c)) were incorporated. In this paper, the hydrothermal and ice regimes of both reservoirs analyzed for the Case E-VI flow requirements are discussed. The Case E-VI flow requirements are considered as an optimal operating condition with respect to the

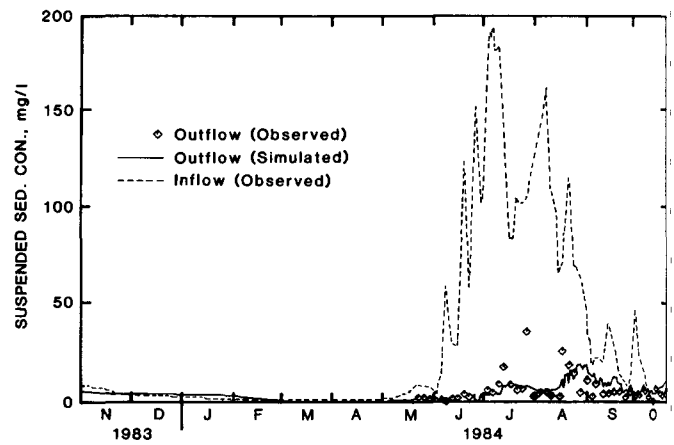


Figure 5. Observed and Simulated Outflow Suspended Sediment Concentrations from Eklutna Lake.

energy and instream flow requirements. The 1981-1982 inflow and meteorological conditions, which represent average to wet year conditions were used in the analysis. The energy demands considered included energy demands predicted for all three stages of project operation. Each study case was simulated for a period of two years starting in November.

The completed Watana reservoir would have a maximum depth of about 220 m (720 ft) with a total volume of about $1.16 \times 10^{10} \text{ m}^3$ (9.4×10^6 acre-ft). The Watana dam would be built to an intermediate height of 214 m (702 ft) above foundation in Stage I (scheduled for operation from 1999 to 2004) and raised to the final height in Stage III (scheduled for operation from 2012 onward). The Watana reservoir would have a maximum depth of about 165 m (540 ft) and total volume of $5.24 \times 10^9 \text{ m}^3$ (4.25×10^6 acre-ft) in the first and second stages. The Devil Canyon reservoir would be completed in Stage II (scheduled for operation from 2005 to 2011) and the maximum depth would be about the same as that of Stage I Watana reservoir. However, the total volume of the Devil Canyon reservoir would be about one-quarter of the Watana reservoir in Stage I or II and about one-tenth of the completed Watana reservoir.

The Watana control structure which would be located on the right abutment of the dam at about 46 m (150 ft) below the normal maximum reservoir level would include a multi-level powerhouse intake and a single-level outlet works (cone-valves) intake near the bottom of the structure.

The two-level powerhouse intake of the Devil Canyon reservoir would also be located near the normal maximum reservoir level, however, the outlet works intakes would be located at the center of the dam, about 168 m (550 ft) below the normal maximum reservoir level. The outlet works are provided to release flow, (a) to meet environmental minimum flow requirements when powerhouse flows are not adequate, and, (b) to release flood flows when the reservoir(s) are full and the powerhouse does not have the capability to pass the inflow. The outlet works are normally operated in July and August. Two intake operation policies were considered, namely, inflow temperature matching and warmest possible release. A reservoir operation study (Harza-Ebasco Susitna Joint Venture, 1985 (a)) was carried out to determine the inflow, outflow, and reservoir level of each reservoir for various project stage, energy demand, and the downstream flow requirements.

The temperature and ice simulations thus performed using the DYRESM model indicate that, regardless of the project operation schemes and project status (stages), both reservoirs would develop stratification in the summer months of June, July, August, and September. OvertURNS would occur in spring and fall followed by the formation of ice-cover in winter.

At Watana, the general aspects of the temperature behavior are similar to Eklutna Lake. The ice-cover would form in November and a total meltout would occur in May. A maximum ice thickness of 1.0 to 1.5 meters can be expected in March (Figures 6 & 8).

The multi-level intake structures proposed for the Watana reservoir for different project stages provide the project capability to release water selectively from various levels of the stratified water body in the reservoir. The Watana summer release temperatures can be approximately controlled to satisfy a predetermined objective. In the summer, the river inflows are more responsive to variations in the meteorological conditions than the reservoir due to the shallowness of the river. The river inflow warms up in the early summer and cools down in the late summer more rapidly than does the reservoir. Hence, the Watana discharge water would be colder in the early summer and

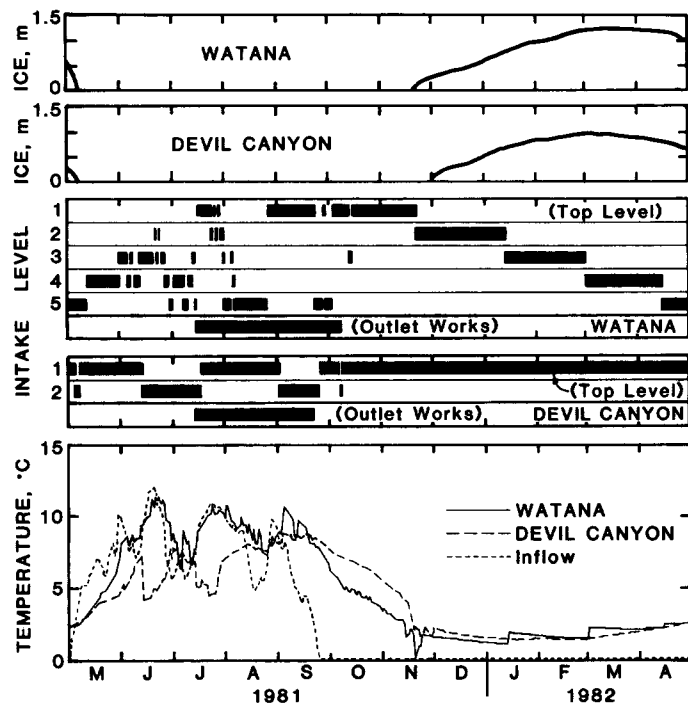


Figure 6. Simulated Susitna Project Intake Operations, Ice Thicknesses and Outflow Temperatures—Inflow Temperature Matching (Stage II).

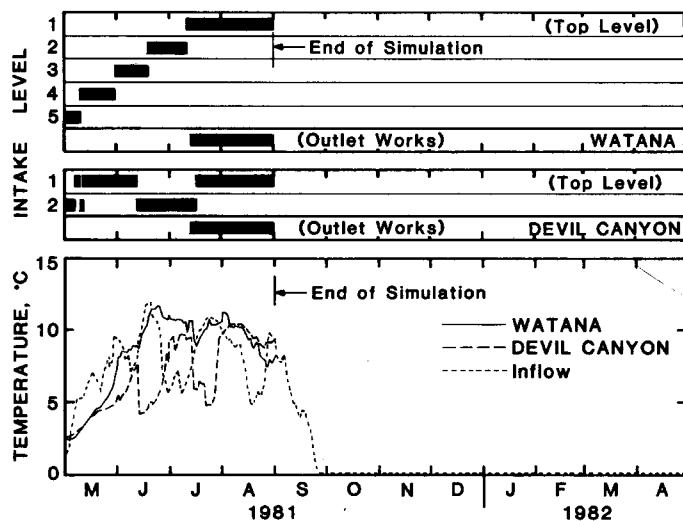


Figure 7. Simulated Susitna Project Intake Operations and Outflow Temperatures—Warmest Possible Release (Stage II).

warmer in the early fall than the natural river conditions. However, in most of the summer months (June, July and August) the Watana discharge temperatures can be regulated to approximate inflow temperatures through operation of the multi-level intake except in times when large releases are made through the outlet works (Figures

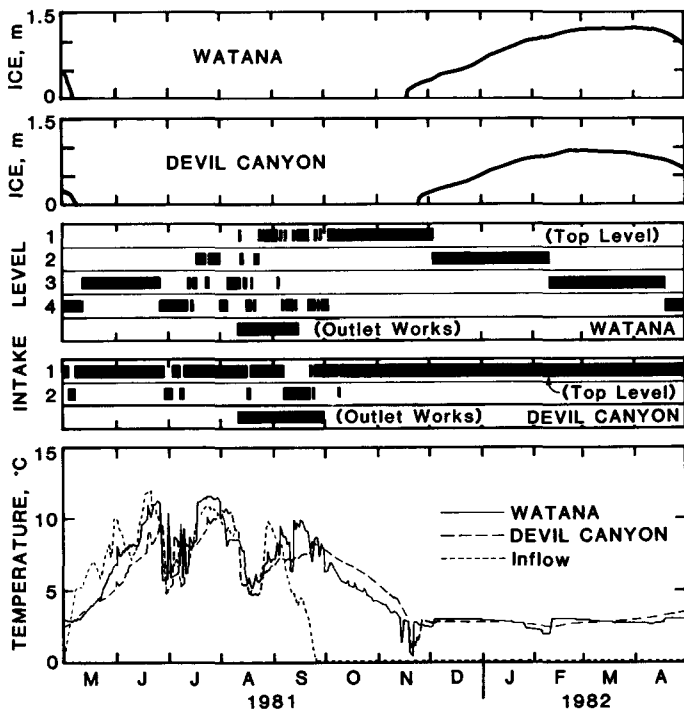


Figure 8. Simulated Susitna Project Intake Operations, Ice Thicknesses and Outflow Temperatures—Inflow Temperature Matching (Stage III).

6 & 8). In the winter, inflow temperatures would be near 0°C (32°F) and the reservoir temperatures in the reversed stratification zone would range from near 0°C (32°F) at the contact surface with the ice-cover to approximately 4°C (39°F) at the top of the hypolimnion. Therefore, the Watana discharge temperatures would be slightly warmer during the winter than natural river conditions. As a result, the discharge temperatures would range from approximately 5 to 12°C (41 to 54 °F) in the summer and approximately 0.5 to 3°C (33 to 37°F) in the winter depending on the project and meteorological conditions, and energy demand level.

When the Devil Canyon reservoir is completed, it will receive inflows from the Watana reservoir and the tributaries downstream of the Watana dam. Hence, the Devil Canyon main inflow would be cooler in early summer and warmer in early fall than the natural project inflows. In addition, relatively large summer discharges releasing water through deep low-level outlet works and the smaller size of the reservoir relative to Watana would reduce the summer average residence time and result in a larger variation in the

temperature of the hypolimnion than in Watana. The hydrothermal regime of the Devil Canyon reservoir especially in the hypolimnion would therefore, be more sensitive to the operation of the outlet works than Watana. The temperature in the hypolimnion would vary from 4 to 10°C (39 to 50°F) in the summer.

With relatively shallow warmer surface layer (epilimnion), the operation of the Devil Canyon intake would be less efficient in terms of selective withdrawal than Watana. Comparison of the Watana and Devil Canyon outflow temperatures are shown in Figures 6-8. In Figure 6, outflow temperatures predicted for Stage II conditions are shown. The operation of the powerhouse intake structures was simulated to match the release temperature with the natural inflow temperature. The summer outlet works operations and the relatively thin epilimnion reduced the effectiveness of the selective withdrawal using the multi-level intakes in both reservoirs. Similar effects were noted when releasing warmest possible water from the Devil Canyon reservoir in Stage II as demonstrated in Figure 7. In mid-June of 1981, the Devil Canyon intake releases were changed from the top-level ports to the bottom level ports due to decreased reservoir level and caused a 4°C (7°F) reduction in outflow temperature while the Watana release temperature rose steadily. Thus, the Devil Canyon releases can be up to 5°C (9°F) colder than the Watana releases in June and July. The effectiveness of the intakes is improved when the project is fully developed, the reservoir levels are more stable and the operations of the outlet works are less frequent in Stage III as shown in Figure 8.

Effect of Intake Operation on Winter Release Temperature

The ice-cover formation in a reservoir is strongly dependent upon the meteorological conditions prior to the surface freeze-up. At the fall overturn, the reservoir destratifies and becomes isothermal with a relatively uniform vertical temperature distribution. Mixing and further cooling would continue in a cold climate until the surface of the reservoir freezes. The presence of ice-cover pre-

vents further mixing and hence conserves the heat remaining in the reservoir. By changing the operating policy of the multi-level intake, the amount of heat stored in the reservoir prior to the freeze-up can be altered, to some extent, and hence the timing of the reservoir surface freeze-up and the subsequent winter release temperature can also be modified.

As an example, by releasing warmest possible water from the Watana reservoir in the summer less heat would be preserved in the water body in the period prior to freeze-up and the surface water temperature would be reduced to the freezing point sooner. Hence a freeze-up of the surface water may be induced, in some cases, about two weeks earlier than in the case of operating the intake by matching the inflow temperatures. With ice-cover formed two weeks sooner, more heat would be preserved for the remaining winter. Therefore, an increase of the outflow temperature of up to about 1°C (2°F) may be obtained.

Simulation of the Suspended Sediment Concentration

In addition to the outflow temperature of a reservoir, the turbidity level of the reservoir releases may also have an impact on downstream fisheries. Because of the nature of inflows to the glacially fed Eklutna Lake, the turbidity is mainly derived from the suspension of the glacial flour. To provide basic information for further assessment of the turbidity effects, the extended DYRESM model was applied to predict the suspended sediment concentrations of the Watana and Devil Canyon reservoir outflows. Based on the Eklutna Lake tailrace sediment data, the suspended sediments of the Watana reservoir outflow are expected to be comprised primarily of particles of size less than 3-4 microns. Larger size particles would generally settle out rapidly to the bottom without significantly affecting the average concentration levels in the reservoir and outflows. In the study, only sediments of up to 10 microns were analyzed and the solution procedure applied is

identical to that used in the Eklutna Lake study.

The total sediment influent to the Watana reservoir was estimated from the USGS data at Gold Creek gaging station based on the drainage areas. The average particle size distribution curve of the river suspended sediments available at the project area from the Cantwell station was used to determine the suspended sediment influent of each sediment group from the total suspended sediment influent. Fifteen percent of the total suspended sediment influent was assigned to 0-3 micron sediments and 12 percent to the 3-10 micron sediments (Harza-Ebasco Susitna Joint Venture, 1985(b)). The 1970, 1981, and 1982 flow conditions which represent the low sediment influent, high sediment influent, and average sediment influent years, respectively, were considered.

The operation of the multi-level intakes was simulated to withdraw the near surface water since it allows for withdrawal of water with the lowest level of suspended sediment concentration. Figure 9 shows the predicted project outflow suspended sediment concentration from the Devil Canyon reservoir for the Stage III condition. These analyses indicate that the suspended sediment concentration level of the summer release flows from the project would be decreased from the pre-project condition of about 60 to 3000 mg/l to about 50 to 200 mg/l. In the winter, the suspended sediment concentration level would be increased from a range of 1 to 80 mg/l to a range of 10 to 100 mg/l.

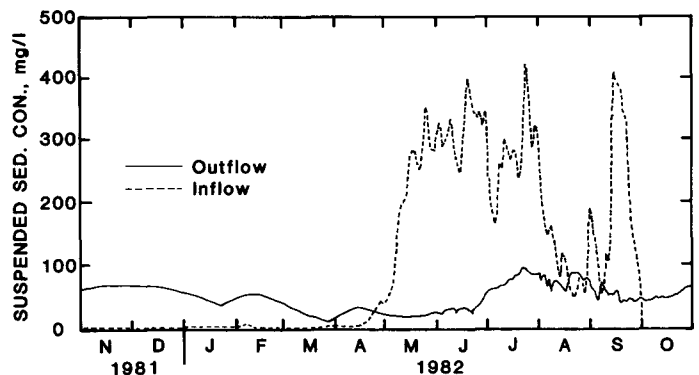


Figure 9. Simulated Susitna Project Outflow Suspended Sediment Concentrations (Stage III).

CONCLUSIONS

A dynamic reservoir simulation model suitable for water quality simulation in environmentally sensitive northern regions has been briefly outlined and applied to two Alaskan Basins. Comparisons of model simulations with field observations in Eklutna Lake are considered to be sufficiently satisfactory to permit utilization of the model for the design and environmental assessment of the proposed Susitna Hydroelectric Project in Alaska.

A number of novel aspects of the modeling of the behavior of northern lakes and reservoirs have been found in the study; namely, the insensitivity of the lake-wide heat budget to river-borne frazil ice, the possibility of controlling the date of freeze-up in reservoirs by altering the fall heat storage, the need for improved estimation procedures for incoming long-wave radiation, the requirement for the accurate specification of heat transfer between water and ice and the requirement for highly resolved measurements of suspended sediment loading in time.

The model has been applied to yield quantitative estimates of the thermal behavior of the proposed Watana and Devil Canyon reservoirs. The reservoir stratification and release temperatures simulated by the model have demonstrated the feasibility of utilizing the proposed multi-level intakes to control the downstream temperatures in consideration of the environmental needs most of the time. The outflow suspended sediment concentrations and ice-cover thickness have also been simulated with reasonable degrees of confidence to assist in the planning of the fishery and wildlife resources management.

ACKNOWLEDGEMENTS

The supports provided by the Alaska Power Authority, Harza-Ebasco Susitna Joint Venture, R&M Consultants, and the Manager of the Hydrologic and Hydraulics Studies of the Joint Venture, E.J. Gemperline in carrying out this study are deeply appreciated. The following engineers participated in the study at various stages: T.H. Hsu, D.L. Muirhead,

J.S. Kuo, M.F. Rogers, and J.H. Lin. Mr. W. Dyok also contributed in the initial stage of the study. Their contributions are acknowledged.

REFERENCES

- Coffin, J.H., and W.S. Ashton, 1986. Sediment Budget of a Glacier Lake, Eklutna Lake, Alaska. In: Proceedings of the Cold Regions Hydrology Symposium, American Water Resources Association.
- Gemperline, E.J., 1986. Hydrology and Hydraulic Studies for the Licensing of the Susitna Hydroelectric Project. In: Proceedings of the Cold Region Hydrology Symposium, American Water Resources Association.
- Harza-Ebasco Susitna Joint Venture, 1985(a). Case E-VI Alternative Flow Regime. Susitna Hydroelectric Project. Prepared for Alaska Power Authority.
- Harza-Ebasco Susitna Joint Venture, 1985(b). Effects of the Proposed Project on Suspended Sediment Concentration. Susitna Hydroelectric Project. Prepared for Alaska Power Authority.
- Harza-Ebasco Susitna Joint Venture, 1984. Eklutna Lake Temperature and Ice Study with six months simulation for Watana Reservoir. Susitna Hydroelectric Project. Prepared for Alaska Power Authority.
- Imberger J., and J.C. Patterson, 1981. "A Dynamic Reservoir Simulation Model - DYRESM:5," Transport Models for Inland and Coastal Waters, Chapter 9, Academic Press.
- Patterson, J.C., and P.F. Hamblin, 1986. Thermal Simulation of a Lake with Winter Ice Cover. To be published.
- R&M Consultants, Inc., 1985(a). Glacial Lake Physical Limnology Studies: Eklutna Lake, Alaska. Volumes 1 & 2. Susitna Hydroelectric Project. Prepared under contract to Harza-Ebasco Susitna Joint Venture for Alaska Power Authority.

R&M Consultants, Inc., 1985(b). Processed Climatic Data, October 1983 - December 1984, Eklutna Lake Station. Volume 7. Susitna Hydroelectric Project.

Prepared under contract to Harza-Ebasco Susitna Joint Venture for Alaska Power Authority.

R&M Consultants, Inc., 1985(c). Processed Climatic Data, October 1983 - December 1984, Watana Station and Devil Canyon Station. Volumes 4 & 5. Susitna Hydroelectric Project. Prepared under contract to Harza-Ebasco Susitna Joint Venture for Alaska Power Authority.

Tennessee Valley Authority, 1972. Heat and Mass Transfer between a Water Surface and the Atmosphere, TVA Report No. 0-6803, Tennessee Valley Authority.

TROPIC LEVEL RESPONSES TO GLACIAL MELTWATER INTRUSION IN ALASKAN LAKES

J. P. Koenings, R. D. Burkett, Gary B. Kyle, Jim A. Edmundson, and John M. Edmundson¹

ABSTRACT: Many large lake and riverine systems in Alaska are influenced by meltwater intrusion from glaciers and/or snow packs. Occluded within the ice or snow are sediments ranging in size from cobbles to colloids. Our interest centers on the colloidal sized particles since they are in large part responsible for the turbid nature of lakes. We found that turbidity, caused by inorganic particles, initiates significant impacts on aquatic production beginning with effects on temperature regimes, light profiles, and nutrient inputs. Specifically, glacial lakes with turbidity levels above 5 NTU are characterized by seasonally elevated phosphorus levels, but lowered areal primary production, reduced zooplankton densities, a restricted diversity within the macrozooplankton community, and lowered fish yields. In addition, because glacial lakes exhibit characteristics unique from clear water systems many of the cause/effect models derived for such lakes e.g. phosphorus input versus chlorophyll *a* response, must be corrected for light restriction and for forms of non-biologically available phosphorus prior to application on turbid systems. Finally, as both reduced zooplankton production and fish yield are tied to increased turbidity, a compressed euphotic zone needs consideration as a negative modifier of areal fish production estimates from glacial lakes.

(KEY TERMS: glacial silt, euphotic zone, turbidity, smolt yield, sockeye salmon.)

INTRODUCTION

Many of the freshwater lakes of the Pacific Rim support populations of anadromous

salmonids. In particular, the young or juveniles of the sockeye salmon (*Oncorhynchus nerka*) spend one to three years of in-lake rearing before emigrating as smolts to the ocean. Lakes classified as sockeye nursery areas have widely varying capacities to rear juveniles to smolts. The ability to understand and then predict, through empirical models, the juvenile rearing or carrying capacity of lake systems is important for either stock management or enhancement purposes.

A successful theory predicting potential fish yield must contain terms describing the effects of physical (e.g. solar radiation, temperature) and chemical (e.g. nitrogen and phosphorus), and of other groups of aquatic organisms in the water body (Mathisen 1972, Rigler 1982). Much effort has recently been spent on predictions of aquatic primary production from nutrient levels (Vollenweider 1976, Smith 1979), and then relating primary production to fish yield (Nelson 1958, McConnell et al. 1977, Hecky et al. 1981, Jones and Hoyer 1982, and Koenings and Burkett 1986). As turbidity imparted by inorganic particles has been described as a modifier of primary production (Goldman 1960, Oglesby 1977, Edmundson and Koenings 1985a, Grobbelaar 1985, and Koenings and Burkett 1986), we began to question the effect of increased turbidity on other levels of aquatic production in cold regions (Lloyd et al. 1986); and on the potential alteration of trophic linkages leading to fish yield in lakes turbid with silt.

Glacial lakes, located throughout Alaska, are a sub-set of oligotrophic sockeye nursery lakes that are distinguishable by characteristics derived from the large scale intrusion of glacial

¹Alaska Department of Fish and Game, FRED Division, P. O. Box 3-2000, Juneau, Alaska.

meltwater. These systems are turbid (>5 NTU) for much of the year by virtue of colloidal sized inorganic particles which remain suspended in the water column. The effect of such particles on the autochthonous production of natural lakes within cold regions is largely unknown, and is described here through comparisons with the well described limnological characteristics (Hutchinson 1957, Wetzel 1975, Likens 1985) and sockeye rearing capacities (Foerster 1968) of clear water systems. Herein, we develop cause/effect relationships at each trophic level (1°, 2°, and 3°) that act to separate turbid, cold-water lakes from geographically adjacent clear and organically stained systems. Such trophic level assessments are necessary because of the ever increasing pressure on the salmonid resources of Pacific Rim nations, and the concomitant need for alternative management approaches (Koenings and Burkett 1986).

METHODS AND MATERIALS

Limnological data were collected and analyzed by the State of Alaska, Department of Fish and Game, Limnology Program. The field and laboratory techniques are described in detail in the Fish and Game Limnology Manual (Koenings et al. 1986). In general, the sampling protocol was conducted at three week intervals during the ice-off to ice-on period, and at least once during mid-winter. Physical parameters included measurements of lake temperatures, light penetration, turbidity, and Secchi disk transparencies. Lake temperatures and dissolved oxygen levels were recorded at 1 m intervals to the lake bottom or to a depth of 50 m using a YSI model 51 temperature/dissolved oxygen analyzer. Both incident and reflected solar radiation (footcandles) were recorded at 0.5 m intervals from the surface to a depth equivalent to 1% of the sub-surface reading using a Protomatic submersible photometer. The algal light compensation point (depth) was defined as the depth at which 1% of the sub-surface active light [photosynthetically available radiation (400-700 nm)] penetrates (Schindler 1971).

Nutrient Chemistry

Water quality samples were collected from the 1 m depth and mid-hypolimnetic zone (minimum of two sampling stations) for the analysis of algal nutrients (phosphorus, nitrogen, silicon, and carbon) and other water quality parameters (e.g., pH, conductivity, alkalinity, and turbidity). In general, reactive phosphorus (P) analyses were determined using the molybdenum-blue method as modified by Eisenreich et al. (1975). Total-P analysis utilized the same procedure following acid persulfate digestion. The various components used to characterize total-P i.e., particulate, colloidal, and dissolved were analyzed after Koenings et al. (1986). Turbidity measurements were determined on samples collected from the 1 m strata using a model DRT-100 nephelometric turbidimeter.

Primary Production

Autochthonous primary production (algal standing crop) was estimated by chlorophyll a (chl a) analysis after the fluorometric procedure of Strickland and Parsons (1972). We used the low strength acid addition recommended by Reimann (1978) to estimate phaeophytin. Water samples (1-2 liters) were filtered through 4.25 cm GF/F filters to which 1-2 ml of a saturated MgCO₃ solution were added just prior to the completion of filtration. The filters were then stored frozen in separate plexi-slides for later analysis. Primary productivity (rate of carbon uptake) within the euphotic zone was determined through carbon-14 isotope experiments using three incubation depths i.e., surface (1 m), mid-euphotic, and the light compensation point. We utilized the light-dark bottle technique after Saunders et al. (1962) using 2-4 stations per lake with 6-8 sampling dates over the May-October period. Replicate clear and lightproof bottles containing 100 ml of lake water were labeled with 5.2 microcuries of NaH¹⁴O₃ and incubated in situ 4-6 hours. Samples were fixed with Lugol's acetate solution and filtered through a 2.5 cm GF/F filter. Filters were stored frozen in 20 ml polyethylene vials. Prior to analysis, filters were thawed, acidified, and then dispersed into

a toluene based scintillation cocktail. Algal carbon incorporation was quantified using a Packard model 3255 scintillation spectrometer. Volumetric uptake rates ($\text{mg C/m}^3/\text{day}$) were determined using the cumulative percent time productivity curve after Vollenweider (1965). Mean daily rates were determined from integrated areal productivity versus time plots.

Secondary Production

Zooplankton were enumerated from replicate 50 m or bottom to surface vertical tows using either a 0.2 m or 0.5 m diameter, 153 μ mesh conical zooplankton net. The net was pulled at a constant 1 m/s, and washed well before removing and preserving the organisms in 10% neutralized formalin (Haney and Hall 1973). At least two stations per lake were sampled 6-8 times during the open water period. Identification within the genus *Daphnia* followed Brooks (1957); of the genus *Bosmina* after Pennak (1978); and of the copepods after Wilson (1959), Yeatman (1959), and Harding and Smith (1974). Identification and enumeration consisted of counting triplicate 1 ml subsamples taken with a Hensen-Stempel pipet in a 1 ml Sedgewick-Rafter cell which was subdivided into transects. Finally, descriptions of laboratory experiments used in monitoring *Daphnia* reproductive success and survivorship under varying turbidity regimes are detailed in Edmundson and Koenings (1985b).

Tertiary Production

The Tustumena Lake sockeye fry stocking, smolt production, and fry distributional information were taken from reports by Flagg (1985), and Thomas et al. (1984). For other lakes, sockeye smolt production information was obtained from technical data reports available through the Alaska Department of Fish and Game. The rearing sockeye fry distributional data were obtained through the application of hydroacoustic assessment techniques (Kyle 1985). In short, this technique consists of recording fish signals on tape, in digital format, from a series of cross-lake transects using a scientific echosounder. The number of echoes represent individual fish which

can be converted to fish densities for each transect at various depth intervals. Finally, lake temperature profiles were measured to relate fry rearing temperatures to fry rearing depths.

RESULTS AND DISCUSSION

Primary Production

Primary production has been correlated with solar radiation (Brylinski and Mann 1973), temperature (Grobbelaar 1985), and nutrients (Schindler 1978) with Smith (1979) stressing the specific role of phosphorus in limiting primary productivity. In addition, phosphorus-chlorophyll (P-C) response models have in recent years provided lake investigators a useful tool in evaluating primary production responses to changes in nutrient loading (Sakamoto 1966, Dillon and Rigler 1974, Vollenweider 1976, and Prepas and Trew 1983). In general, lakes in the same geographic area with similar morphometric features and nutrient levels should have similar capacities for autochthonous primary production. Since factors limiting primary productivity could largely determine total system production (Hecky 1984) including the tertiary trophic level (Nelson 1958, McConnell et al. 1977), we were interested in the cause(s) for the decreased chlorophyll a (chl a) levels in glacial lakes compared to the clear water lakes. Thus, our investigations centered on processes by which glacial silt particles affect temperature regimes, light profiles, and the phosphorus cycle.

First, the most noticeable result of glacier meltwater intrusion is an increase in turbidity. Recent studies describing the nature of turbidity derived from glacier melt (Edmundson and Koenings 1985a) stress the strong correlations between turbidity and both particle size and concentration. In addition, we found that turbidity levels of from 5-60 NTU were largely due to particles (silt) within the 20-40 micron size class. Furthermore, electron micrographs of these sized glacial particles revealed irregular shapes with smooth planar surfaces. Particles with this structure are characterized by large surface area to volume ratios; and would

be less likely to settle out, thereby acting to enhance turbidities.

Large concentrations of these planar-structured particles reflect or backscatter a larger proportion of incident solar radiation compared to non-turbid lakes (Figure 1). We found the ratio of incident to reflected light in two clear water systems to equal 30:1 and 17:1 (Hidden and Leisure Lakes respectively) compared to a ratio of 3:1 in the glacial lakes.

Moreover, in Packers Lake (organically stained) this light ratio equalled 60:1. Thus, our data suggest that glacial lakes reflect or backscatter significantly more light than occurs in both types of non-turbid lakes. The effect of light reflection or backscatter may also have implications regarding temperature regimes. Hecky (1984) found that sediment induced turbidity, as a result of impoundment activities in Southern Indian Lake, not only decreased light levels, but also lowered seasonal mean lake temperatures 1-2°C. As penetrating solar radiation can directly warm lower layers to a depth of 10 m, the action of silt particles to reduce the depth of light penetration reduces deep heating (Ragotzkie 1978). Therefore, evidence suggests that lake temperatures (seasonal) can be both lower in glacial lakes and higher in stained lakes compared to clear water lakes solely as a result of increased/decreased light backscatter within surficial strata. Since photosynthesis is determined by a combination of temperature, light, and nutrients, the effect of turbidity induced backscatter in lowering glacial lake temperatures may in itself result in decreased primary productivity.

Second, a strong correlation was found between turbidity (NTU) and depth of light penetration expressed as euphotic zone depth (EZD) (Edmundson and Koenings 1985a, Lloyd et al. 1986). That is, turbidity levels were inversely correlated to EZD ($\text{Log EZD} = 1.23 - 0.66 \text{ Log NTU}$; $r^2 = 0.94$) and more importantly, even low turbidities (5-10 NTU) severely restrict light penetration (EZD). Edmundson and Koenings (1985a) established that turbidity levels >5-10 NTU and an EZD <6-4 m could be used to distinguish clear from glacial lakes. In turn, the adverse effect of turbidity restricted light regimes on areal aquatic productivity through various carbon-14

algal transfer and silt addition experiments has been shown by Goldman (1960, 1961), Tizler et al. (1976), and more recently by Edmundson and Koenings (1985a). In essence, areal carbon uptake rates within oligotrophic lakes decreased linearly with increasing turbidities i.e., reduced light levels (Koenings and Burkett 1986). Moreover, we found gross differences between clear and glacial lakes when comparing euphotic volume (EV) as a proportion of the total lake volume among various lake types e.g., clear, organically stained, and glacial (Table 1). For clear lakes (n=11) the EV ranged from 41-90% of the total with a mean value of 64%, whereas in the organically stained lakes (n=5) the EV ranged from 8-32% and averaged 21%. However, in the glacially influenced lakes (n=10) the EV ranged from a low of <1%, in a heavily glacial system (45 NTU), to 23% in semi-glacial lakes (5-10 NTU) yet averaged only 6.7%. Thus, the EV as a percentage of the total lake volume is significantly less in glacial lakes compared to non-turbid lakes. This severely restricts the volume of water capable of autochthonous production.

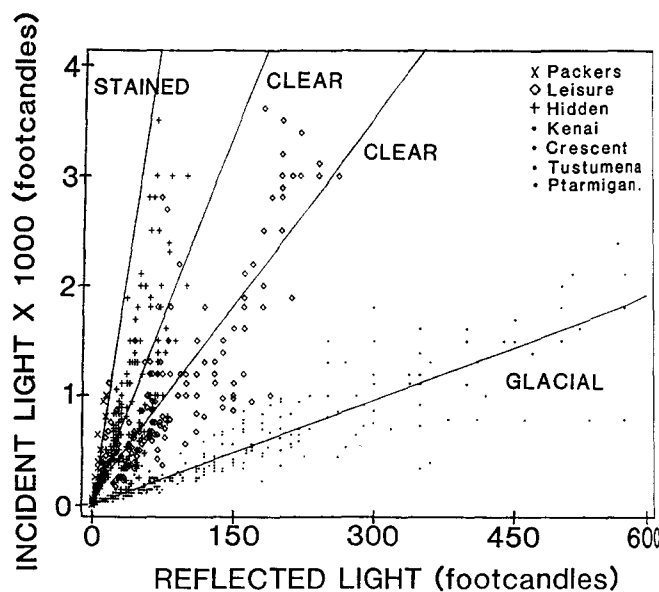


Figure 1. The relationship between incident solar radiation (400-700 nm) and reflected radiation (backscatter) from two clear water lakes (Hidden and Leisure), an organically stained system (Packers), and four glacially influenced lakes.

Table 1. A comparison of total surface area, water residence time, light compensation depth, and euphotic volume (EV) (expressed as a percent of total lake volume) between clear, organically stained, and glacially influenced Alaskan lakes.

Lake	Volume (m ³ x 10 ⁺⁶)	Lake type (water clarity)	Surface Area		Water residence time (yr)	Light compensation level (m)	Euphotic volume	
			(m ² x 10 ⁺⁶)	(acres)			(m ³ x 10 ⁺⁶)	(% of total)
Tustumena	37,000	Glacial	295.0	55,597	17.2	1.1	325.0	<1
Skilak		Glacial	99.0	24,463		1.5	148.5	<1(est.)
Kenai		Glacial	56.0	13,837		4.0	224.0	<1(est.)
Tonsina	726	Glacial	13.7	3,394	2.0	1.3	18.0	3
Tazlina	10,584	Glacial	155.9	38,528	3.8	1.6	249.4	2
Trail Lakes	124	Glacial	8.1	1,754	0.2	0.5	3.6	3
Klutina	3,020	Glacial	67.1	16,587	3.1	3.8	255.0	8

Eklutna	512	Semi-Glacial	14.0	3,458	1.8	3.0	42.0	8
Ptarmigan	125	Semi-Glacial	3.0	750	1.1	6.0	15.6	17
Crescent	389	Semi-Glacial	16.2	4,002	0.3	5.5	89.1	23

Bakewell	67	Organic Stain	2.8	692	0.4	4.5	12.6	19
Hugh Smith	198*	Organic Stain	3.2	800	1.1	5.0	16.0	8
Packers	26	Organic Stain	2.1	519	3.0	4.0	8.4	32
McDonald	197	Organic Stain	4.2	1,035	0.7	7.5	31.5	16
Falls	30	Organic Stain	1.0	254	0.5	9.5	9.0	29

Bear	19	Clear	1.8	445	0.8	9.5	17.1	90
Hidden	138	Clear	6.8	1,680	11.2	15.0	102.0	74
Upper Russian	122	Clear	4.6	1,137	1.1	13.0	51.0	42
Karluk	1,920	Clear	39.0	9,637	6.0	20.0	780.0	41
Tokun	38	Clear	1.8	448	1.0	16.0	25.0	65
Eshamy	122	Clear	3.6	890	2.7	20.0	72.0	59
Leisure	23	Clear	1.1	259	0.3	18.0	19.8	86
Larson	29	Clear	1.8	445	1.9	9.5	17.1	59
Sea Lion Cove	<1	Clear	0.1	19	0.3	6.9	0.3	80
Nunavauguluk	4,489	Clear	79.0	19,513	6.0	25.0	1,975	44

*Volume of the mixolimnion

Third, we were interested in the effects of glacial silt particles on nutrient (e.g., phosphorus) cycles. Our fractionation studies have determined that glacial particles are composed of significant amounts of inorganic particulate phosphorus (IPP) or rock phosphorus (Edmundson and Koenings 1985a). An example is the effect of glacial silt on the phosphorus cycle in Crescent Lake, a semi-glacial system which has a seasonally defined on/off glacier-melt cycle (Figure 2). Total phosphorus

(TP) levels increased from 4.5 µg/l in the spring (April-June) at a time of minimum glacier melt to 8.5 µg/l during the summer (July-September) at maximum glacier melt, and then decreased to 4.5 µg/l in winter (Figure 2a). In turn, total particulate phosphorus (TPP) which is comprised of inorganic (IPP) and organic (OPP) particulate fractions (Koenings et al. 1985) followed a similar trend i.e., increasing from 2.0 µg/l to 7.5 µg/l in mid-summer and decreasing to 1.5 µg/l

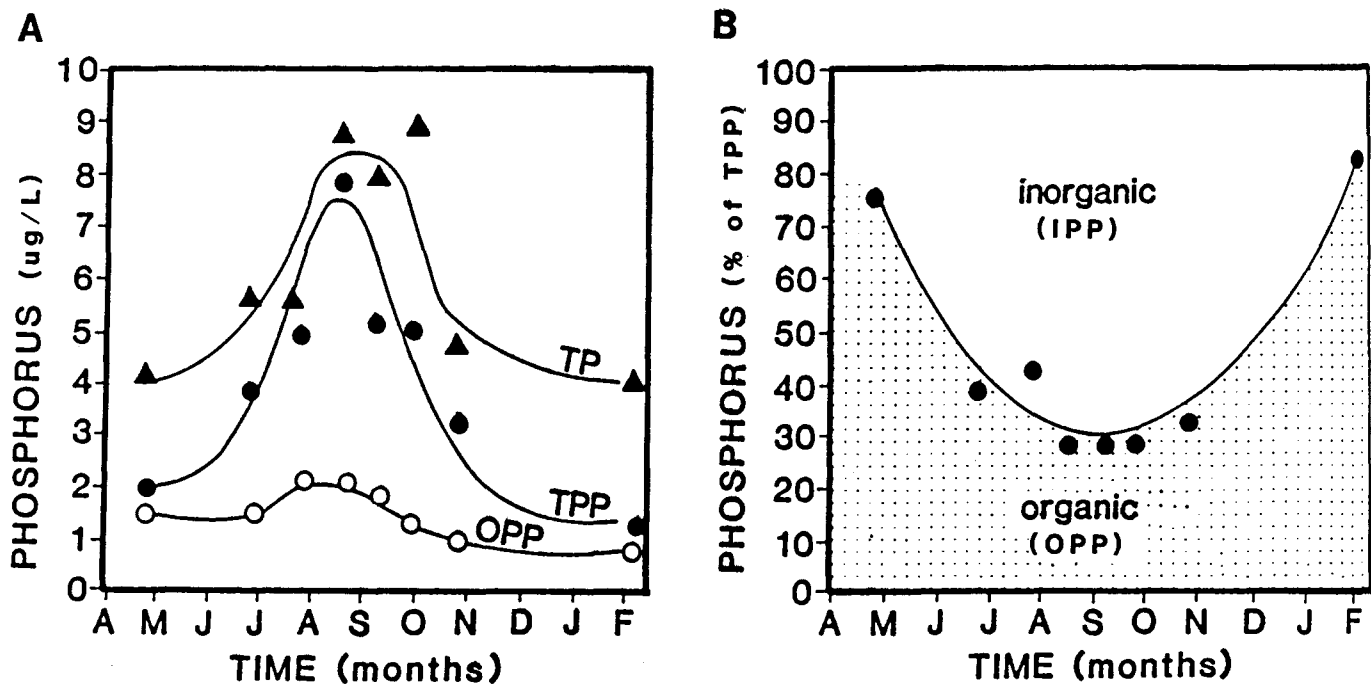


Figure 2. Seasonal phosphorus cycles in Crescent Lake (semi-glacial): (A) total phosphorus (TP) levels compared to total particulate phosphorus (TPP) and organic particulate phosphorus (OPP); and (B) seasonal fluctuations in inorganic and organic particulate phosphorus expressed as a percent of TPP.

in winter. However, seasonal fluctuations of OPP levels were minimal as concentrations remained between 1-2 $\mu\text{g/l}$. That is, while OPP comprised 80% of TPP during the spring and winter, IPP comprised 80% at the height of meltwater intrusion. Thus, the increase in TPP, and indeed TP, was due to increased IPP resulting from glacial melt during the summer (Figure 2b). Because of glacier melt, a significant amount of TP in the lake during the peak-growing season is comprised of non-biological IPP i.e., rock phosphorus.

Finally, phosphorus-chlorophyll *a* (P-C) regression analysis of glacial lakes initially showed little correlation between chl *a* levels and phosphorus concentrations. However, Edmundson and Koenings (1985a) observed that several semi-glacial lakes overlapped into the regression used to derive the clear-water lake P-C model. When these systems were excluded, a significant P-C relationship was derived for glacial lakes which showed the same basic trend established for clear water Alaskan lakes except for a significantly lower chl *a* response at equivalent

phosphorus levels (Figure 3a). To explain lower chl *a* levels, at particular P concentrations, in glacial lakes we felt corrections for IPP and light restrictions were appropriate. Using IPP corrected total phosphorus levels, the semi-glacial lakes fell entirely within the clear lake P-C response model, and justifiably, were excluded from the glacial P-C model. While a consideration of IPP resulted in a significant reduction between observed and predicted chl *a* levels in glacial lakes (Figure 3b), a substantial difference remained in lakes >5-10 NTU which could not be explained by IPP alone. Following the principle of Verduin et al. (1978) which considered the ratio of EZD to mean lake depth in P-C relationships, Edmundson and Koenings (1985a) found that this light correction factor further reduced the amount of chl *a* expressed per unit phosphorus concentration. That is, corrections for both IPP and restricted light combine to reduce 92% of the overall differences between observed chl *a*, and chl *a* predicted using clear water P-C models.

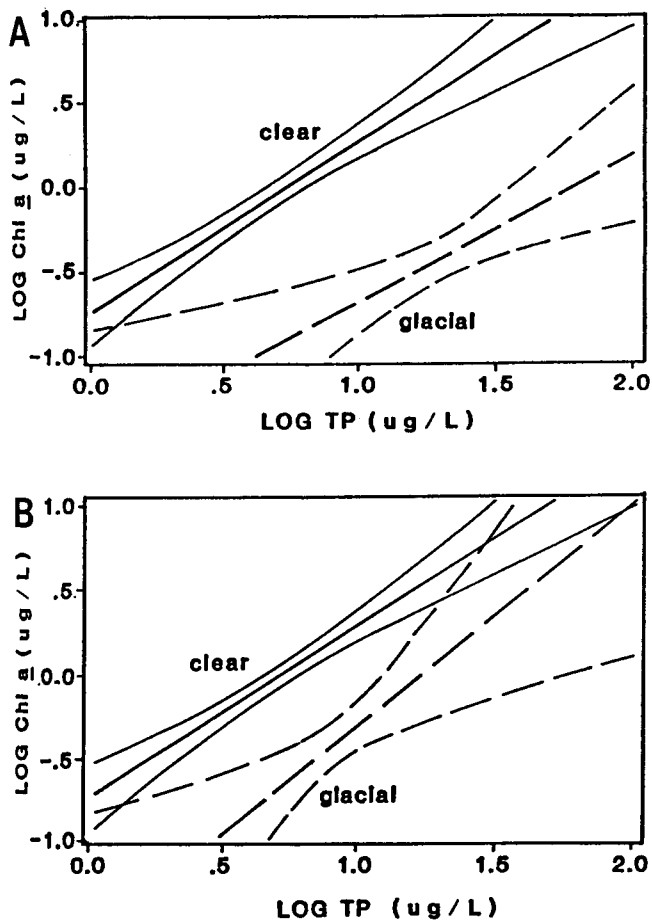


Figure 3. Phosphorus-chlorophyll *a* (P-C) response models, with 95% confidence limits, derived for clear water (—) and glacial lakes (---); (A) excluding the semi-glacial lakes, and (B) excluding the semi-glacial lakes and after correcting for IPP.

Secondary Production

A comparison of seasonal (May-October) mean macro-zooplankton densities from several oligotrophic lakes shows a decrease in euphotic zone depth and mean seasonal macro-zooplankton density with increased glacial influence (Figure 4). The clear water lakes (Karluk-Bear Lake) have an average EZD of 16 meters, and an average macrozooplankton density of 475,000 organisms/m². The organically stained lakes, along with those with some glacial influence (Ptarmigan-Kenai Lakes), have an average EZD of 5 meters and average macro-zooplankton density of 205,000 organisms/m² over the same time period. Finally, Tustumena and Upper

Trail Lakes, which are heavily influenced by glacial runoff, have an average EZD of 0.5 meters and average macro-zooplankton density of 23,500 organisms/m².

While light restrictions from glacial meltwater intrusion are associated with reduced macro-zooplankton densities, it is also evident that glacial silt affects macro-zooplankton diversity as well (Table 2). The macro-zooplankton species composition is conspicuous in the total absence of the non-discriminate filter feeding cladoceran species, specifically *Bosmina* and *Daphnia*, from the macro-zooplankton community in glacial lakes (6-45 NTU) while they are well represented in non-turbid (0-5 NTU) lakes. In contrast, the selective feeding species, represented by the copepods, are well represented in both lake types. Because both the turbid and non-turbid lakes possess similar oligotrophic lake features, i.e., low primary productivity, it appears that glacial meltwater produces additional conditions unfavorable for the survival of cladoceran species thereby enhancing the success of the copepods, particularly *Diaptomus* and *Cyclops*.

Laboratory tests designed to mimic the effect of in-lake glacial silt intrusion on *Daphnia* survival and reproduction, indicate that *Daphnia* are able to thrive under conditions of high turbidity (Figure 5). In these tests, *Daphnia* were exposed to varying levels of turbidity ranging from 0 to 60 NTU by the addition of increasing concentrations of glacial silt. The surprising result was that *Daphnia* survival and reproduction over time was most successful under the highest turbidity level of 60 NTU. This was attributed to silt particles providing sites for bacterial growth, thus, providing an unlimited food source which ultimately enhanced *Daphnia* survival and reproduction (Edmundson and Koenigs 1985b). These results indicate that silt by itself is not detrimental to *Daphnia* survival and reproduction when food levels are high.

That *Daphnia* cannot survive and therefore are not found in turbid Alaska lakes (Edmundson and Koenigs 1985b) whereas they thrive under turbid conditions in the laboratory, appears to be contradictory. However, the contradiction

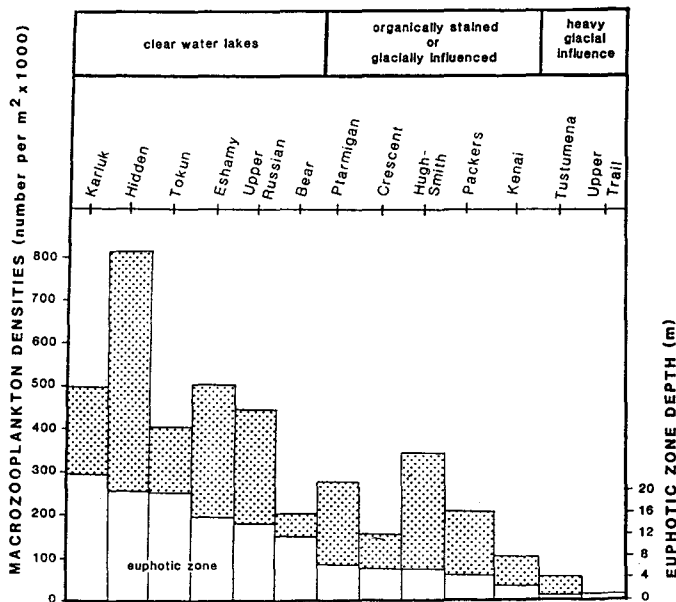


Figure 4. Comparison of seasonal mean macrozooplankton densities among clear lakes (mean EZD = 16 m), semi-glacial and organically stained lakes (mean EZD = 5 m), and lakes with heavy glacial influence (mean EZD = 0.5 m).

disappears when we consider the presence of glacial silt together with low level food conditions that exist in oligotrophic Alaskan lakes. Arruda et al. (1983) has shown that cladocerans survive well in turbid, southwestern United States reservoirs, where, under warm water conditions bacteria are able to colonize silt particles, thus providing an additional food source for foraging *Daphnia*. In colder Alaska lakes; however, conditions are not conducive to this type of association (Stockner 1983), thus cladocerans gain no benefit from ingested glacial silt particles. Moreover, studies conducted by Patalis and Salki (1984), before and after impoundment of Southern Indian Lake, a cold water, northern latitude lake, have shown a link between decreased water temperature and decreased macro-zooplankton density. In addition, McCabe and O'Brien (1983) have suggested that the ingestion of silt particles interferes with *Daphnia* survival and reproduction. Indeed, Edmundson and Koenings (1985b) have shown from both in situ and laboratory tests, where chl *a* levels were manipulated as well as

turbidity levels, that *Daphnia* survival and reproduction fared best under conditions of high chl *a* levels and low silt concentrations. Those exposed to low chl *a* levels and high silt concentrations suffered increased mortality rates and repressed reproduction severe enough to result in extinction.

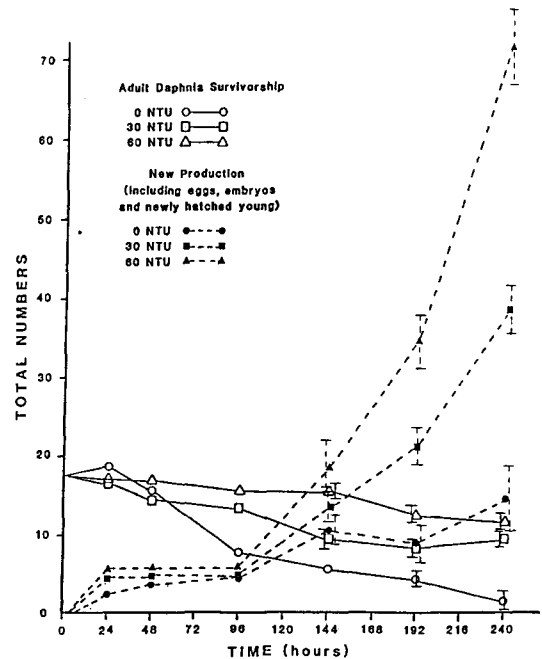


Figure 5. Laboratory experiments at 13°C showing adult *Daphnia* survivorship and reproduction when exposed to varying turbidities. Values are means of three replicates with the latter three dates represented by means \pm 1 S.E.

Investigations by Allen (1976) and Richman and Dodson (1983) have shown that under conditions of low food abundances copepod species have a competitive advantage over cladocerans. Cladocerans, which are non-discriminate filter feeders, must filter a large amount of water in order to obtain a small amount of food, wasting energy. In contrast, copepods, with a selective feeding strategy, inspect and ingest a lower number of individual particles per unit time, expending less energy. The non-discriminate and inefficient foraging strategy of cladocerans is adequate for survival and reproduction in Alaskan oligotrophic, clear water lakes (Table 2). However, high levels of suspended silt relative to food particles, results in the filtering and ingestion of

Table 2. Comparison of mean seasonal zooplankton community composition between glacial (>6 NTU) and non-turbid (≤5 NTU) lakes. Lakes exemplify an extensive data set [glacial (n = 18), non-turbid (n = 78)] that includes systems located throughout Alaska. Relative densities are: absent (-), ≤33% (+), ≥34% ≤66% (++) , and ≥67% (+++).

Taxa/Lake	Glacial Lakes (6-45 NTU)					Non-Turbid Lakes (0-5 NTU)				
	Tustumena	Kenai	Crescent	Grant	Ptarmigan	Hidden	Packers	Leisure	Karluk	Badger
<u>Cladocera:</u>										
<i>Bosmina</i> sp.	-	-	-	-	-	+	+	+++	+	+
<i>Daphnia</i> sp.	-	-	-	-	-	+	+	+	+	+
<i>Holopedium gibberum</i>	-	-	-	-	-	-	-	-	-	+
<i>Alona</i> sp.	-	-	-	-	-	-	+	-	-	-
<i>Polyphemus pediculus</i>	-	-	-	-	-	-	-	-	-	+
<u>Copepoda:</u>										
<i>Cyclops</i> sp.	+	++	+	++	++	+	+	+	+++	+++
<i>Diaptomus</i> sp.	+	+	-	-	++	+	++	+	+	+
<i>Epischura</i> sp.	-	-	-	-	-	+	+	-	-	-
<u>Rotifera:</u>										
<i>Kellicottia longispina</i>	+	+	+	+	+	++	-	-	-	+
<i>Asplanchna</i> sp.	-	-	+++	+	-	-	-	-	-	-
<i>Keratella</i> sp.	-	-	-	-	-	-	-	-	-	-
<i>Conochiloides</i> sp.	-	-	-	-	-	+	-	-	-	-

glacial silt particles of the size range of algal material normally consumed by cladoceran species. Under this regime, cladocerans are unable to obtain, from the total amount of material ingested, the required amount of energy necessary for long term survival.

Finally, we also suggest that the parthenogenic reproductive strategy of cladocerans is adversely influenced by glacial meltwater intrusion. The rapid reproduction of many broods of young is severely disrupted by the ingestion of silt particles which reduces the ability of cladocerans to meet the energy demands for this reproductive strategy. In contrast, the selective filter feeding and slow paced sexual reproductive strategy of the copepod species, requires less energy. This is especially germane under conditions of low food availability and high concentrations of suspended silt. Thus, it is the presence of suspended glacial silt particles in combination with low algal densities that results in the elimination of the non-discriminate filter feeding cladocerans from the macro-zooplankton community.

Tertiary Production

Density-dependent relationships between forage density, food type, and fish abundance infer differences in juvenile growth potential in lakes having different capacities for food production. In general, we would expect that sockeye salmon nursery lakes having higher capacities for forage (zooplankton) production would show higher sockeye growth rates (at comparable fry densities) than would lakes with lower capacities for zooplankton production. In addition to a high overall productive capacity for zooplankters, sockeye rearing lakes need to produce preferred zooplankters (i.e., cladocerans) for the most efficient energy transfer. While we acknowledge that density-dependent factors such as zooplankton abundance and type do effect sockeye production, recent comparisons between glacial and clear lakes reveal that density-independent factors may be as, or even more, important in limiting fish production.

A compilation of sockeye smolt sizes from clear, organically-stained, and glacial lakes, indicates that age 1 and age 2 smolts produced from glacial lakes are consistently small (Table 3). In

fact, the age 1 and age 2 smolts produced from clear or stained lakes were 16-104% and 22-135% greater in length respectively, than from glacial lakes. Considering the consistent production of near threshold-size smolts (Koenings and Burkett 1986) from differentially sized glacial lakes located in divergent geographic regions in Alaska, we believe that cooler juvenile rearing temperatures characteristic of glacial lakes, as well as limited forage, influences the size of smolts.

Table 3. Representative mean length and weights of sockeye smolts from clear, organically stained, and glacial lakes located throughout Alaska. Values were obtained over the entire outmigration period.

Lake	Geographic Region	Age 1		Age 2	
		Length (mm)	Weight (g)	Length (mm)	Weight (g)
<u>Clear</u>					
Hidden	Cook Inlet	143	27.3	200	83.9
Larson	Cook Inlet	86	5.1	123	16.5
Leisure	Cook Inlet	80	4.0	97	9.0
Tokun	P.W.S.	72	2.5	---	---
Eshamy	P.W.S.	76	3.4	101	7.8
Karluk	Kodiak	101	10.7	113	14.1
Frazer	Kodiak	76	3.1	103	7.9
Chilkat	Southeast	100	---	110	---
McDonald	Southeast	70	2.6	79	4.5
<u>Stained</u>					
Packers	Cook Inlet	97	8.5	132	21.2
Hugh Smith	Southeast	69	2.9	78	4.4
<u>Glacial</u>					
Tustumena	Cook Inlet	70	2.8	85	5.0
Crescent	Cook Inlet	68	2.8	76	3.8
Kenai	Cook Inlet	62	2.1	72	3.1
Tazlina	P.W.S.	72	---	73	---
Klutina	P.W.S.	64	---	72	---
Tonsina	P.W.S.	64	---	64	---
Chilkat	Southeast	65	---	70	---

P.W.S.- Prince William Sound

To illustrate the effect of a density-independent factor (rearing temperature) on sockeye production, we focused on smolts produced from Tustumena Lake (glacial); and fish growth relative to rearing temperatures in Hugh Smith Lake (stained). Rearing distribution studies were undertaken in Hugh Smith Lake because the sockeye smolts displayed only small differences in size or age structure in response to increased forage production resulting from nutrient enrichment. Diel patterns of vertical fry migration, obtained by hydroacoustic surveys, showed

that the majority of fry remained in cool rearing temperatures of 7°C or less (Peltz 1985). Furthermore, using the growth mode of Iwama and Tautz (1981) to predict age 1 smolt size based on lake rearing temperatures, the length of growing season, and the assumption of food satiated growth; Peltz (1985) found that over four years the predicted weight of age 1 smolts deviated from the observed by only 1-11%. These results indicate the potential for fry rearing temperatures to either control or at least strongly influence the growth of juvenile sockeye.

In glacially turbid Tustumena Lake, the 7.8 million sockeye fry initially stocked in 1979, along with the recruits from the 1978 escapement of 110,000 adults produced an estimated 400,000 + age 1 smolts in 1980. However, with the ever increasing fry rearing pressure on the zooplankton forage base; the smolt age compositions, and in particular, the smolt sizes have remained essentially unchanged. For example, from the production of only 2.3 million smolts in 1981 to 16.7 million in 1985, the age composition of age 1 smolts decreased by only 8%, while the size of age 1 smolts was identical, and the size of age 2 smolts decreased by about 5% (Figure 6). Considering that the initial 1981 smolts were near threshold-size, a density-dependent response to a seven-fold increase in the total number of smolts conceivably would have caused a shift in age structure to predominantly age 2 smolts. The lack of a density-dependent response suggests that a density-independent factor of cool rearing temperatures has a major influence on juvenile sockeye growth to smolt in this glacial lake.

These detailed seasonal and diel hydroacoustic surveys suggested that limits on juvenile fish growth rates within a season could be set by accumulated temperature units. Thus, both the rate of juvenile growth and the total growth within an annual period can be heavily influenced by in-lake rearing temperatures and the length of the open water period respectively. Considering the potential impact of an abiotic density-independent factor on the age and size of smolts (the end product of freshwater rearing); we hydroacoustically surveyed several sockeye nursery lakes for juvenile rearing distributions relative to temperature (Figure 7)

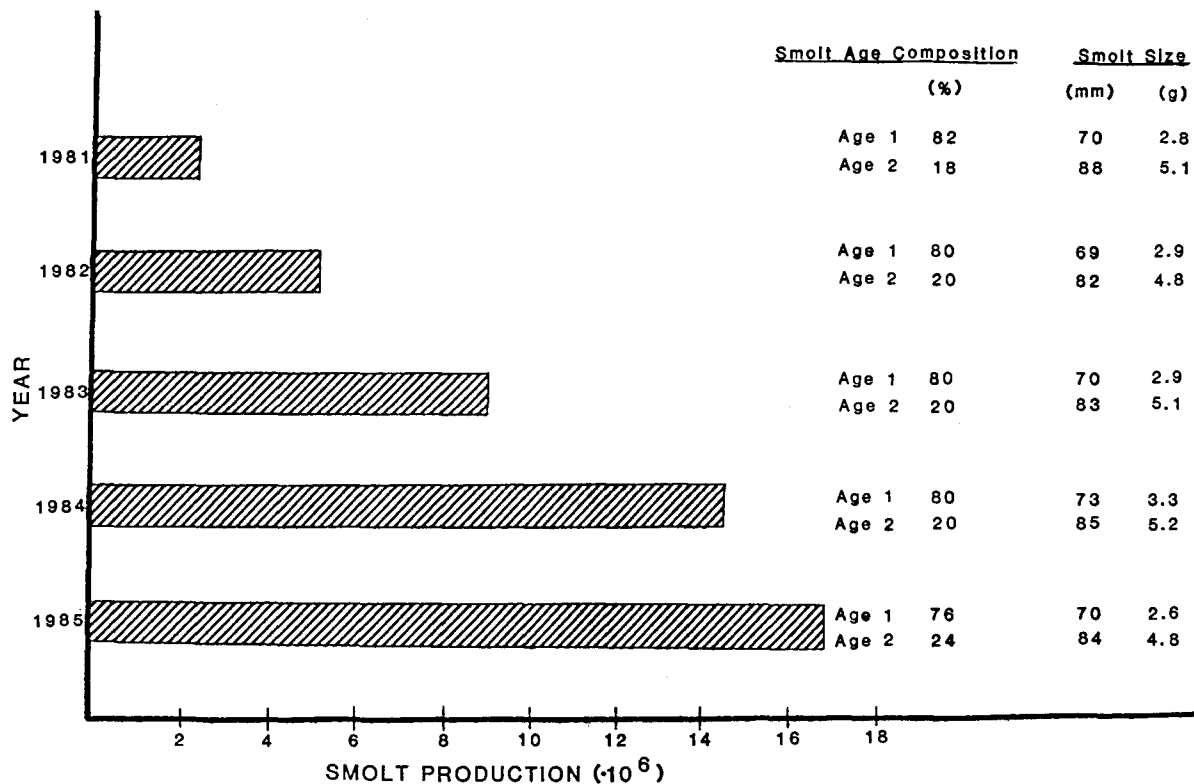


Figure 6. Summary of annual sockeye smolt production from Tustumena Lake (1981-1985) showing the constancy in smolt size and age composition despite significant increases in smolt numbers. Such unresponsiveness in smolt patterning (Koenings and Burkett 1986) to density increases is characteristic of a density-independent controlling factor(s).

Using the 7°C isopleth as a guide, lakes were ranked by actual fry rearing temperatures during July and/or August. We found that low rearing temperatures for juveniles were not confined solely to glacial systems, but that low rearing temperatures were consistent only within the glacial lakes surveyed. Despite the possibility that over a longer period of time, variations could occur which would correspondingly affect the growth rate, other investigators have found similar temperatures affecting sockeye growth (Clarke 1967, Brett et al. 1969). Although Brett et al. (1969) and Shelbourn et al. (1973) demonstrated that the optimum temperature for growth shifts to a lower temperature with a decrease forage base (which is applicable to glacial lakes), the findings of Biette and Green (1980) and Clarke (1978) showed at a reduced to moderate forage base, sockeye growth was enhanced under cyclic rearing temperatures. This is because to a large

extent energy expenditure is governed by activity (e.g. feeding) and temperature. Since metabolic rates are closely correlated to feeding rates in fish (Paloheimo and Dickie 1966) it is reasonable to assume that temperature will act as a major independent variable.

In addition to temperature being a factor in sockeye juvenile growth, it appears that juvenile feeding behavior is influenced by reduced light conditions in glacial lakes. Normally, in clear lakes sockeye fry are distributed near-surface at night while being dispersed through deeper strata during the day. This pattern of feeding behavior has been hypothesized to be a result of predator avoidance and/or the requirement of light for sockeye fry to locate zooplankton prey (Narver 1970, Eggers 1978). In glacially-turbid Tustumena Lake, rearing juveniles were distributed near surface during the day while being dispersed through deeper strata at night (Thomas

et al. 1984). In addition, the surface affinity of the fry was much greater in the fall than during the summer. Thus, the reduced hours of sunlight in the fall combined with the input of glacial silt over the summer, forced a greater percentage of foraging fry nearer the surface during the day. Although fish visibility is reduced by glacial silt, the presence of rearing fry nearer the surface during the day rather than at night allows for increased risk of capture by predators. Hence, in glacial lakes with substantial predator populations, the fry are at a great survival disadvantage having to balance the need to feed on sparse zooplankters with predator avoidance.

Finally, as discussed earlier, the intrusion of suspended glacial silt particles lowers areal primary productivity; a direct result of reduced light penetration. In turn, Koenings and Burkett (1986) showed that mean annual areal rates of photosynthesis for several oligotrophic lakes were highly correlated to euphotic zone depth (EZD). By combining lake surface area (m^2) with EZD (m) an index of potential system production, euphotic volume, was calculated. It was natural to assume that a comparison of fish production for different types of lakes (i.e., clear, organically-stained, and glacial) should be compared on the basis of euphotic volume rather than on an areal basis, to incorporate the affects of light (Figure 8). Smolt production based on lake surface area indicates a significant difference between lake types; however, the same smolt production based on euphotic volume shows that smolt production was more consistent across lake type. This emphasizes the concept that when sockeye lakes are defined as rearing area limited, they fall within the same general range of production when euphotic volumes are considered.

CONCLUSIONS

The immediate result of glacier melt-water intrusion is an increase in turbidity, a function of varying particle concentrations as well as size distributions. Suspended glacial silt has been found to dominate the phosphorus cycle, and to determine light regimes in glacially turbid (≥ 5 NTU) lakes. Specifically, our

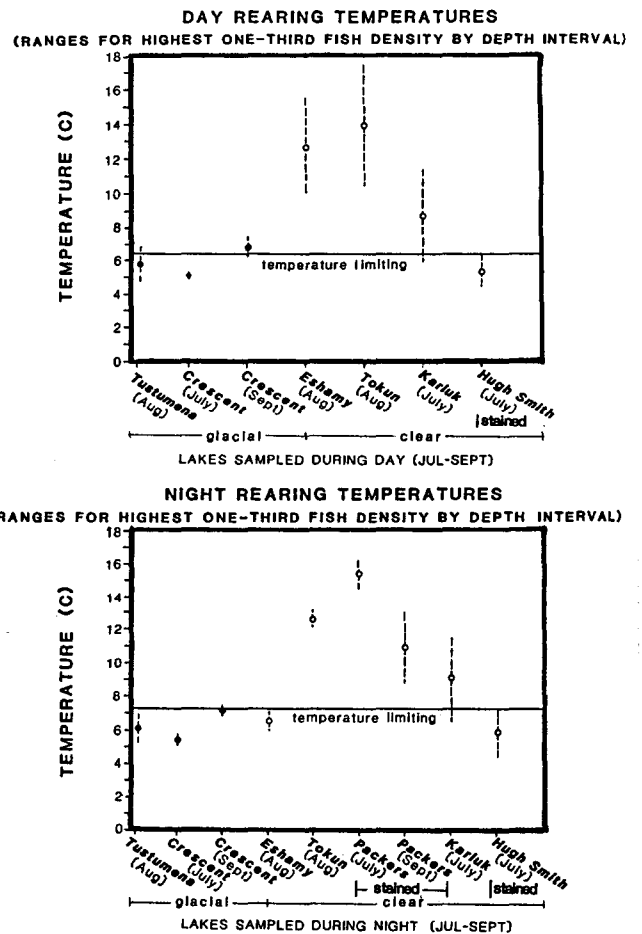


Figure 7. Diurnal in-lake juvenile rearing temperatures showing the greater potential for cooler temperatures to effect sockeye growth rates in glacial lakes compared to clear or stained systems.

fractionation studies have shown that rock phosphorus contained within the particulate inorganic fraction dominates the phosphorus cycle in glacial lakes; and the light compensation depth was found to be inversely related to turbidity levels thereby acting to define the extent of the euphotic zone. As a result, the euphotic volume, as a percent of the total lake volume, is significantly less in glacial systems compared to the non-turbid systems we examined. As a consequence, algal cell can spend considerable time in an aphotic zone that extends well beyond the critical mixing depth used to estimate the point where such mixing becomes a major primary production regulator in turbid waters (Grobbelaar 1985). Moreover, as light is attenuated rapidly in turbid waters, only a small amount of the energy flux is

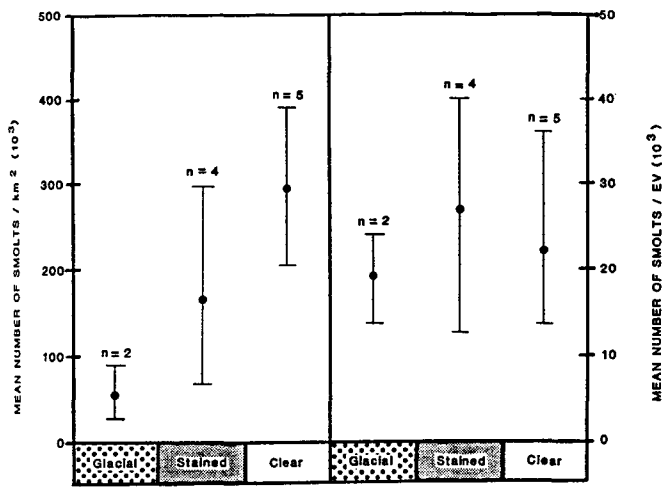


Figure 8. Sockeye smolt production from turbid, stained, and clear water lakes based on surface area (km²) and euphotic volume (EV) showing the reduced variation in smolt numbers between different lake types after correcting for the depth of light penetration.

available for photosynthesis (Grobelaar 1985). The high proportion of reflected light acts to compress the euphotic zone, but because of the abiotic nature of the particles involved a shallow euphotic zone does not indicate increased volumetric production. This is unlike clear water systems where increased turbidity is caused by dense concentrations of algal cells; and lost euphotic depth is compensated for by increased volumetric production (Koenings and Burkett 1986).

The effects of glacial silt were evident both on primary productivity (carbon uptake rates) and on primary production (chlorophyll *a*). That is, volumetric measurements of carbon uptake decreased with an increase in glacier melt influence. Moreover, when productivity rates were integrated over the euphotic zone, areal productivity was considerably reduced especially at the height of glacial meltwater influence. We also observed that summer period chlorophyll *a* levels were significantly less than those predicted using phosphorus-chlorophyll response (P-C) models derived from clear water lakes. The inconsistency between P-C models was found to be partially explained by the dominance of inorganic particulate phosphorus in the total

phosphorus cycle, and by a consideration of the ratio of euphotic volume:total volume. Thus, the magnitude of glacier meltwater intrusion results in decreased autochthonous production, and the increased oligotrophy of glacial lakes.

Lowered primary production also results in reduced densities of herbivorous macro-zooplankters which forage on the algal community. We have also found that filter feeding cladocerans e.g. *Bosmina* and *Daphnia* are uniquely absent from the zooplankton community of glacial lakes. While primary production and summer temperatures in glacial lakes are low, both are not beyond the lower limit we have observed for geographically similar clear water systems that contain robust populations of cladocerans. In addition, we have found cladoceran species to be absent from the zooplankton community of fishless but glacially turbid lakes. The overlapping size ranges of algal material and glacial silt allow ingestion of the glacial particles by non-discriminating filter feeders. Such an inefficient foraging strategy, especially when particle concentrations are high and algal numbers low, results in the eventual elimination of *Bosmina* and *Daphnia*. Thus, the macro-zooplankton community of glacial lakes consists entirely of the selective herbivore *Diaptomus* and the raptorial feeding *Cyclops*.

The adverse consequences of lowered autochthonous primary productivity is also felt at the tertiary level. A consequence of the restricted species composition with the sparse zooplankton community of glacial lakes, is a lowered rearing potential for sockeye salmon fry relative to clear water lakes. Goodlad et al. (1974), O'Brien (1979), Vinyard (1982), Koenings, and Burkett (1986) have found that planktivorous fish, given a choice, prefer cladocerans as prey species over copepod species. Since salmon fry, rearing in glacial lakes, must expend more time and energy capturing evasive copepod species; the areal rearing potential of these lakes is limited compared to clear water lakes. Thus, the restricted light regime of glacial lakes becomes an important factor in correcting areal rates of fish yield.

LITERATURE CITED

- Allan, J. D., 1976. Life History Patterns in Zooplankton. *Amer. Natur.* 110:165-180.
- Arruda, J. A., R. G., Margolf, and R. T. Faulk, 1983. The Role of Suspended Sediments in the Nutrition of Zooplankton in Turbid Reservoirs. *Ecology.* 64:1225-1235.
- Biette, R. M. and G. H. Green, 1980. Growth of Underyearling Sockeye Salmon, *Oncorhynchus nerka*, Under Constant and Cyclic Temperatures in Relation to Live Zooplankton Ration Size. *J. Fish. Res. Bd. Canada* 37:203-210.
- Brett, J. R., J. E. Shelbourn, and C. T. Shoop, 1969. Growth Rate and Body Composition of Fingerling Sockeye Salmon, *Oncorhynchus nerka*, In Relation to Temperature and Ration Size. *J. Fish. Res. Bd. Canada* 26:2363-2394.
- Brooks, J. L., 1957. The Systematics of North America *Daphnia*. *Mem. Conn. Acad. Arts. Sci.* 13:1-180.
- Brylinski, M. and K. H. Mann, 1973. An Analysis of Factors Governing Productivity in Lakes and Reservoirs. *Limnol. Oceanogr.* 18:1-14.
- Clarke, W. C., 1978. Growth of Underyearling Sockeye Salmon, *Oncorhynchus nerka*, On Diel Temperature Cycles. *Fish. Mar. Serv. Tech. Rep.* 780: 19 p.
- Dillon, P. J. and F. H. Rigler, 1974. The Phosphorus-Chlorophyll a Relationship in Lakes. *Limnol. Oceanogr.* 19:767-773.
- Edmondson, W. T. and G. G. Winberg (eds), 1971. A Manual for the Assessment of Secondary Productivity in Fresh Waters. International Biological Program Handbook. 12:358 p.
- Edmondson, J. A. and J. P. Koenings, 1985a. The Effects of Glacial Silt on Primary Production, Through Altered Light Regimes and Phosphorus Levels, in Alaska Lakes. p. 3-19. *In*: L. P. Dwight [chairman] Proceedings, Resolving Alaska's Water Resources Conflicts. Report IWR-108. University of Alaska-Fairbanks, U.S.A.
- Edmondson, J. M. and J. P. Koenings, 1985b. The Influences of Suspended Glacial Particles on the Macro-Zooplankton Community Structure Within Glacial Lakes. p. 21-35. *In*: L. P. Dwight [chairman] Proceedings, Resolving Alaska's Water Resources Conflicts. Report IWR-108. University of Alaska-Fairbanks, U.S.A.
- Eggers, D. M., 1978. Limnetic Feeding Behavior of Juvenile Sockeye Salmon in Lake Washington and Predator Response. *Limnol. Oceanogr.* 23:1114-1125.
- Eisenreich, S. J., R. T. Bannerman, and D. E. Armstrong, 1975. A Simplified Phosphorus Analysis Technique. *Environ Letters* 9:43-53.
- Flagg, L. B., 1985. Sockeye Salmon Smolt Studies, Kasilof River, 1985. Alaska Department Fish and Game, FRED Tech. Data Report (In Press).
- Foerster, R. E., 1968. The Sockeye Salmon, *Oncorhynchus nerka*. *Fish Res. Board of Canada Bull.* 162:422 p.
- Goldman, C. R., 1960. Primary Productivity and Limiting Factors in Three Lakes of the Alaskan Peninsula. *Ecol. Monogr.* 30:207-230.
- Goldman, C. R., 1961. Primary Productivity and Limiting Factors in Brooks Lake, Alaska. *Verh. Int. Ver. Limnol.* 14:120-124.
- Goodlad, J. C., T. W. Gjernes, and E. L. Brannon. 1974. Factors Affecting Sockeye Salmon (*Oncorhynchus nerka*) Growth in Four Lakes of the Fraser River System. *J. Fish. Res. Board of Can.* 31:871-892.
- Grobbelaar, J. A., 1985. Phytoplankton Productivity in Turbid Waters. *J. Plankton Res.* 7:653-663.
- Haney, J. F. and D. J. Hall, 1973. Sugar Coated *Daphnia*: A Preservation Technique for Cladocera. *Limnol. Oceanogr.* 18:331-333.
- Harding, J. P. and W. A. Smith, 1974. A Key to the British Freshwater Cyclopoid and Calanoid Copepods. *Sci. Publ. Freshwater Biol. Assoc.* 18:1-54.
- Hecky, R. E., E. J. Fee, H. J. Kling, and J. W. M. Rudd, 1981. Relationship Between Primary Production and Fish Production in Lake Tanganyika. *Trans. Amer. Fish. Soc.* 110:336-345.
- Hecky, R. E., 1984. Thermal and Optical Characteristics of Southern Indian Lake Before, During, and After Impoundment and Churchill River Diversion. *Can. J. Fish. Aquat. Sci.* 41:579-590.
- Hutchinson, G. E., 1957. A Treatise on Limnology. I. Geography, Physics, and Chemistry. John Wiley and Sons, Inc., New York. 1015 p.

- Iwama, G. K. and A. F. Tautz, 1981. A Simple Growth Model for Salmonids in Hatcheries. *Can. J. Fish. Aquat. Sci.* 38:649-656.
- Jones, J. R. and M. V. Hoyer, 1982. Sport Fish Harvest Predicted by Summer Chlorophyll *a* Concentration in Midwestern Lakes and Reservoirs. *Trans. Amer. Fish. Soc.* 111:176-179.
- Koenings, J. P. and R. D. Burkett, 1986. The Production Patterns of Sockeye Salmon, *Oncorhynchus nerka*, Smolts Relative to Temperature Regimes, Euphotic Volume, Fry Density, Forage Base Within Alaska Lakes. Proceedings, "Sockeye 85", International Sockeye Salmon Symposium, Nanaimo, British Columbia, Canada. November 18-22, 1985. (In Press.)
- Koenings, J. P., R. D. Burkett, G. B. Kyle, 1985. Limnology and Fisheries Evidence for Rearing Limitation of Sockeye Production in Crescent Lake, Southcentral Alaska, (1979-1982). Alaska Department of Fish and Game, Juneau, AK. FRED Technical Report No. 57. 113 p.
- Koenings, J. P., J. A. Edmundson, J. M. Edmundson, and G. B. Kyle, 1986. Limnology Field and Laboratory Manual: Methods for Assessing Aquatic Production. Alaska Department of Fish and Game, Juneau, AK. FRED Technical Report No. (In Press).
- Kyle, G. B., 1985. Abundance and Distribution of Juvenile Sockeye Salmon in Five Lakes Throughout Southcentral Alaska During 1982 and 1983 with Comments on the Use of Hydroacoustic Survey Information. Alaska Department Fish and Game, Juneau, AK FRED Technical Report No. (In Press).
- Lloyd, D. S., J. P. Koenings, and J. D. LaPerriere, 1986. Effects of Turbidity in Freshwaters of Alaska. *North American J. of Fish. Man.* (In Press).
- Likens, G. E. [ed.], 1985. An Ecosystem Approach to Aquatic Ecology. Springer-Verlag, New York, N.Y. 516 p.
- Mathisen, O. A., 1972. Biogenic Enrichment of Sockeye Salmon Lakes and Stock Productivity, *Verh. Internat. Verein. Limnol.* 18:1089-1095.
- McCabe, G. D. and J. W. O'Brien, 1983. The Effects of Suspended Silt on Feeding and Reproduction of *Daphnia pulex*. *American Midland Naturalist* 110:324-337.
- McConnell, W. J., S. Lewis, and J. E. Olson, 1977. Gross Photosynthesis as an Estimator of Potential Fish Production. *Trans. Amer. Fish. Soc.* 106:417-423.
- Narver, D. W., 1970. Diel Vertical Movements and Feeding of Underyearling Sockeye Salmon and the Limnetic Zooplankton in Babine Lake, British Columbia. *J. Fish. Res. Board Can.* 27:281-316.
- Nelson, P. R., 1958. Relationship Between Rate of Photosynthesis and Growth of Juvenile Red Salmon. *Science.* 128:205-206.
- Oglesby, R. T., 1977. Phytoplankton Summer Standing Crop and Annual Productivity as Functions of Phosphorus Loading and Various Physical Factors. *J. Fish. Res. Board Can.* 34:2255-2270.
- Paloheimo, J. E. and L. M. Dickie, 1966. Food and Growth of Fishes. II. Effects of Food Temperature on the Relation Between Metabolism and Body Weight. *J. Fish. Res. Board Can.* 32:869-908.
- Patalis, K. and A. Salki, 1984. Effects of Impoundment and Diversion on the Crustacean Plankton of Southern Indian Lake. *Can. J. Fish. Aquat. Sci.* 41: 613-637.
- Peltz, L., 1985. Evidence for Temperature Limitation of Sockeye Salmon, *Oncorhynchus nerka*, Growth in Hugh Smith Lake, Southeastern Alaska. Alaska Department of Fish and Game. Unpublished Report. 23 p.
- Pennak, R. W., 1978. Fresh-Water Invertebrates of the United States, 2nd Edition. John Wiley and Sons, New York 803 p.
- Prepas, E. E. and D. O. Trew, 1983. Evaluation of the Phosphorus-Chlorophyll Relationship for Lakes Off the Precambrian Shield in Western Canada. *Can. J. Fish. Aquat. Sci.* 40:27-35.
- Ragotzkie, R. A., 1978. Heat Budgets of Lakes, p. 1-18. In A. Lerman (ed.) *Lakes, Chemistry, Geology, Physics.* Springer-Verlag, New York, N.Y.
- Reimann, B., 1978. Carotenoid Interference in the Spectrophotometric Determination of Chlorophyll Degradation Products From Natural Populations of Phytoplankton. *Limnol. Oceanogr.* 23:1059-1066.
- Richman, S. and S. Dodson, 1983. The Effect of Food Quality on Feeding and Respiration by *Daphnia* and *Diaptomus*. *Limnol. Oceanogr.* 28:948-956.

- Rigler, F. H., 1982. The relation Between Fisheries Management and Limnology. *Trans. Amer. Fish. Soc.* 111:121-131.
- Sakamoto, M., 1966. Primary Production by Phytoplankton Community in Some Japanese Lakes and its Dependence on Lake Depth. *Arch. Hydrobiol.* 62:1-28.
- Saunders, G. W., F. B. Trama, and R. W. Bachmann, 1962. Evaluation of a Modified ¹⁴C Technique for Shipboard Estimation of Photosynthesis in Large Lakes. *Univ. Michigan, Great Lakes Res. Div., Spec. Rep. No. 8.* 61 p.
- Schindler, D. W., 1971. Light, temperature, and Oxygen Regimes of Selected Lakes in the Experimental Lakes Area, Northwestern Ontario. *J. Fish. Res. Bd. Canada* 28:157-169.
- Schindler, D. W., 1978. Factors Regulating Phytoplankton Production and Standing Crop in the Worlds Freshwaters. *Limnol. Oceanogr.* 23:478-486.
- Shelbourn, J. E., J. R. Brett, and S. Shirahata, 1973. Effect of Temperature and Feeding Regime on the Specific Growth Rate of Sockeye Salmon Fry, *Oncorhynchus nerka*, With a Consideration of Size Effect. *J. Fish. Res. Board Can.* 30:1191-1194.
- Smith, V. H. 1979. Nutrient Dependence of Primary Productivity in Lakes. *Limnol. Oceanogr.* 24:1051-1066.
- Stockner, J. G., 1983. Personal Communication. Department of Fisheries and Oceans, Fisheries Research Branch, West Vancouver Laboratory, 4160 Marine Drive, West Vancouver, British Columbia V7N 1N6.
- Strickland, J. D. H. and T. R. Parsons, 1972. A Practical Handbook of Seawater Analysis, 2nd Ed. *Fish. Res. Board of Canada Bull.* 167:310 p.
- Thomas, G. L., R. E. Thorne, J. McClain, and D. Marino, 1984. Hydroacoustic Measurements of the Density and Distribution of Juvenile Sockeye in Tustumena Lake, Alaska During 1984. University of Washington. *Fish Res. Inst. Contract No. 14-16-0007-83-5271.*
- Tizler, M. M., C. R. Goldman, and R. C. Richards, 1976. Influence of Sediment Inflow on Phytoplankton Primary Productivity in Lake Tahoe (California-Nevada). *Int. Revue Ges. Hydrobiol.* 61:169-181.
- Verduin, J., L. R. Williams, V. W. Lambou, and J. D. Bliss, 1978. A Simple Equation Relating Total Phosphorus to Chlorophyll Concentration in Lakes. *Verh. Internat. Verein. Limnol.* 20:352.
- Vinyard, G. L., 1982. Feeding Success of Hatchery-Reared Kokanee Salmon When Presented With Zooplankton Prey. *Prog. Fish Culturist.* 44:37-39.
- Vollenweider, R. A., 1965. Calculation Models of Photosynthesis-Depth Curves and Some Implications Regarding Day Rate Estimates in Primary Production Measurements. *Mem. Ist. Ital. Idrobiol. Suppl.* 18:425-457.
- Vollenweider, R. A., 1976. Advances in Defining Critical Loading Levels for Phosphorus in Lake Eutrophication. *Mem. Ist. Ital. Idrobiol.* 33:53-83.
- Wetzel, R. G., 1975. *Limnology.* W. B. Saunders Co., Philadelphia. 743 p.
- Wilson, M. S., 1959. Calanoida. p. 738-794. In: W. T. Edmondson [ed.], *Fresh-Water Biology*, 2nd ed. John Wiley and Sons, New York, N.Y.
- Yeatman, H. C., 1959, Cyclopoida. p. 795-815. In: W. T. Edmondson [ed.], *Fresh-Water Biology*, 2nd ed. John Wiley and Sons, New York, N.Y.

DEEP-LYING CHLOROPHYLL MAXIMA AT BIG LAKE:
IMPLICATIONS FOR TROPHIC STATE CLASSIFICATION OF ALASKAN LAKES

Paul F. Woods*

ABSTRACT: Concerns over potential eutrophication of Big Lake have arisen because the lake's shoreline is extensively developed with residences, most of which have individual, on-site septic systems. Such concerns led to a study of the lake's physical, chemical, and biological characteristics during 1983-84. The range in concentration from 418 chlorophyll *a* samples was 0.05 to 46.5 micrograms per liter. The east limnological station had significantly higher chlorophyll *a* concentrations in both years. The highest concentrations during each year at each station occurred in deep-lying chlorophyll maxima within the hypolimnion. Time-depth plots of chlorophyll *a* were used to illustrate the influence of sampling design on the calculation of the lake's mean chlorophyll *a* concentration. Three sampling designs that ranged from reconnaissance-level to *in vivo* fluorometric profiling yield mean chlorophyll *a* concentrations ranging from 1.16 to 4.96 micrograms per liter. The largest mean concentrations were calculated from samples collected throughout the euphotic zone; the other two sampling designs were restricted to the epilimnion and hence failed to sample the deep-lying chlorophyll maxima.

(KEY TERMS: chlorophyll; trophic level; eutrophication.)

INTRODUCTION

The proximity of Big Lake to the rapidly developing communities of Anchorage, Wasilla, Eagle River, and Palmer has encouraged residential development and intensive, year-round recreational use of this 1,213-hm² lake in the Matanuska-Susitna Borough of southcentral Alaska (Figure 1). Maintenance of the lake's water quality is essential because Big Lake receives about 16,000 person-days per year of fishing effort for salmonids such as rainbow trout (*Salmo gairdneri*) and Dolly Varden char (*Salvelinus malma*); in addition, the annual escapement of sockeye salmon (*Oncorhynchus nerka*) from Big Lake has reached nearly 200,000 fish in recent years (Engel, L.J., Alaska Department of Fish and Game, oral commun.,

1985). The rapid residential development of the lake's 27-km shoreline and its numerous islands has created concern over the potential for nutrient enrichment, or eutrophication, of Big Lake. Most of the approximately 1,000 permanent lake residents dispose of their wastewater via individual, on-site septic systems. Such concerns prompted the U.S. Geological Survey and the Alaska Department of Natural Resources, Division of Geological and Geophysical Surveys to conduct a cooperative study of Big Lake during 1983-84 with the following objectives: (1) to determine the lake's trophic state; (2) to interpret spatial and temporal trends in physical, chemical, and biological variables; and (3) to investigate the relation between phytoplankton primary production and selected limnological variables. An extensive data base of chlorophyll *a* concentrations was assembled during 1983-84 because this water-quality variable is germane to each of the three study objectives.

This paper describes trends in depth and time for chlorophyll *a* concentrations at the east and west limnological stations of Big Lake during 1983-84. These data are then used to show the influence of sampling design on the trophic state classification of Big Lake.

The 232-km² drainage basin of Big Lake is characterized by low-relief terrain with elevations ranging from approximately 40 to 168 m. Glacial deposits of sand and gravel underlie much of the area; muskegs are common in low-lying areas. Mean annual precipitation near Big Lake is 395 mm with July as the wettest month. July is also normally the warmest month (mean temperature = 14.4°C) and January is the coldest (mean temperature = -11.4°C). Ice as thick as 1 m covers the lake from late October through late May. Daylength varies from 5.5 hr on the winter solstice to 19.5 hr on the summer solstice.

The east basin of Big Lake has a maximum depth of 15 m and contains the lake's major inlet, Meadow Creek, and the lake outlet into Fish Creek (Figure 2). The lake's deepest point, 27 m, is in the west basin. The 1,213-hm² lake contains 112 hm³ and thus has a mean depth of 9.2 m.

*Hydrologist U.S. Geological Survey, 1209 Orca Street, Anchorage, Alaska 99501.

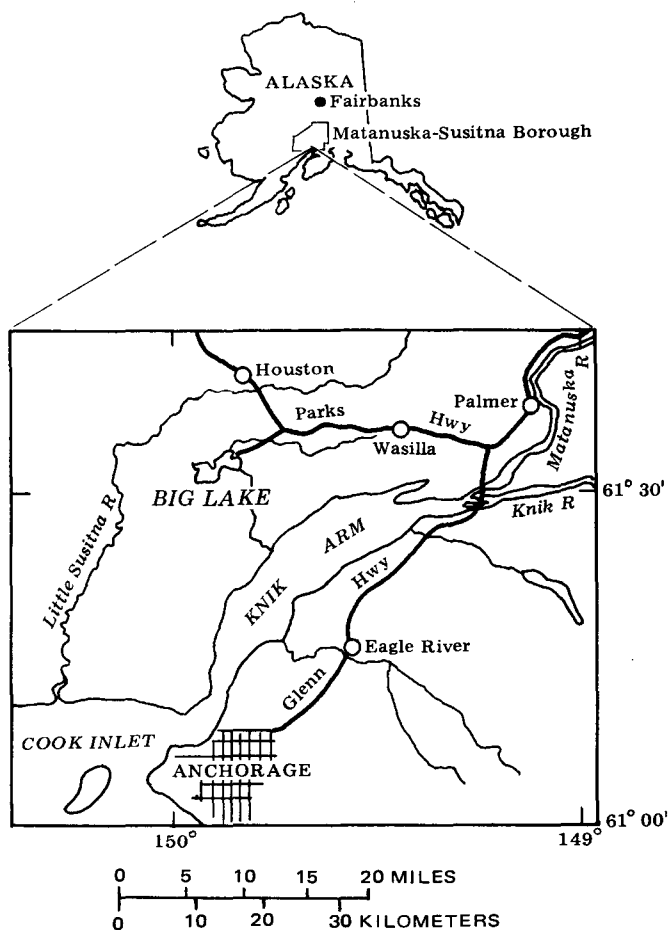


Figure 1. Location of Big Lake within the Matanuska-Susitna Borough of Southcentral Alaska.

METHODS

Sampling for chlorophyll *a* was done from January 1983 through December 1984 at the two primary limnological stations (Figure 2), one each in the lake's east and west basins. Samples were collected biweekly during the open-water season and approximately monthly when ice covered the lake. During 1983, numerous discrete-depth samples were obtained with an opaque Van Dorn sampler. In 1984, *in vivo* fluorometry was used to profile the water column for a qualitative description of chlorophyll *a*. Discrete-depth samples were then obtained at representative depths. The samples were analyzed fluorometrically for chlorophyll *a*, with correction for pheophytin, per methods in Wetzel and Likens (1979). Numerous other variables were also sampled during this study; these data are available in publications of the U.S. Geological Survey (1984, 1985).

RESULTS AND DISCUSSION

Chlorophyll *a* concentrations, in μgL^{-1} (micrograms per liter), at the east limnological station

ranged from 0.05 to 46.5 (mean = 3.9, $n = 101$) in 1983 and from 0.05 to 9.2 (mean = 2.6, $n = 102$) in 1984 (Figure 3). At the west limnological station, chlorophyll *a* concentrations ranged from 0.07 to 8.0 (mean = 1.8, $n = 108$) in 1983, and from 0.14 to 6.4 (mean = 1.7, $n = 107$) in 1984 (Figure 3). Parametric statistical tests indicated that chlorophyll *a* concentrations at the east limnological station were significantly higher than those at the west limnological station for both years. Chlorophyll *a* concentrations at the east limnological station alone did not differ significantly from 1983 to 1984; the same result was obtained for the west limnological station.

The lowest concentrations of chlorophyll *a* were measured between October and March, under ice cover. In mid-March, chlorophyll *a* concentrations began to increase in the upper 5 m of the lake even though an ice cover nearly 1 m thick still covered the lake. Chlorophyll *a* concentrations within the upper 5 m of Big Lake did not exceed 3.5 and 5.5 μgL^{-1} , respectively, at the west and east limnological stations throughout the study. The annual maximum chlorophyll *a* concentration was usually attained by the end of June, within a month of the melting of the lake's ice cover. During late July to early September 1983, however, the east limnological station experienced a second pulse of chlorophyll *a* that reached a peak concentration of 46.5 μgL^{-1} at a depth of 9 m.

The yearly maximum concentration of chlorophyll *a* at each limnological station occurred near the lower depth limit of the euphotic zone, defined here as the depth at which photosynthetically active radiation is 1 percent of that incident upon the lake's surface. Big Lake's deep-lying chlorophyll maxima were situated within the hypolimnion, in that the depth of the euphotic zone normally exceeded the depth of the epilimnion during late May through mid-September. Deep-lying chlorophyll maxima have been reported to occur under similar conditions in many lakes (Fee, 1976; Priscu and Goldman, 1983; Pick *et al.* 1984). These chlorophyll maxima have frequently been composed of flagellated, colonial algae of the subphylum Chrysophyceae (Fee, 1976; Pick *et al.* 1984). The 1983-84 limnological study at Big Lake included sampling for phytoplankton species composition and biomass at selected depths. The phytoplankton samples that were taken at the 10-m depth during the occurrence of the deep-lying chlorophyll maxima were dominated numerically by unidentified microalgae. The largest contribution to algal biomass was from the Chrysophyceae which were commonly represented by genera such as *Chromulina*, *Chrysochromulina*, *Dinobryon*, *Kephyrion*, and *Mallomonas*, all of which are flagellated organisms.

The occurrence of large concentrations of chlorophyll within a hypolimnion, that also contains part of the euphotic zone, may reveal the presence of photosynthetic bacteria; however, anoxic conditions also must exist because such bacteria are obligate anaerobes (Rheinheimer, 1974). The deep-lying

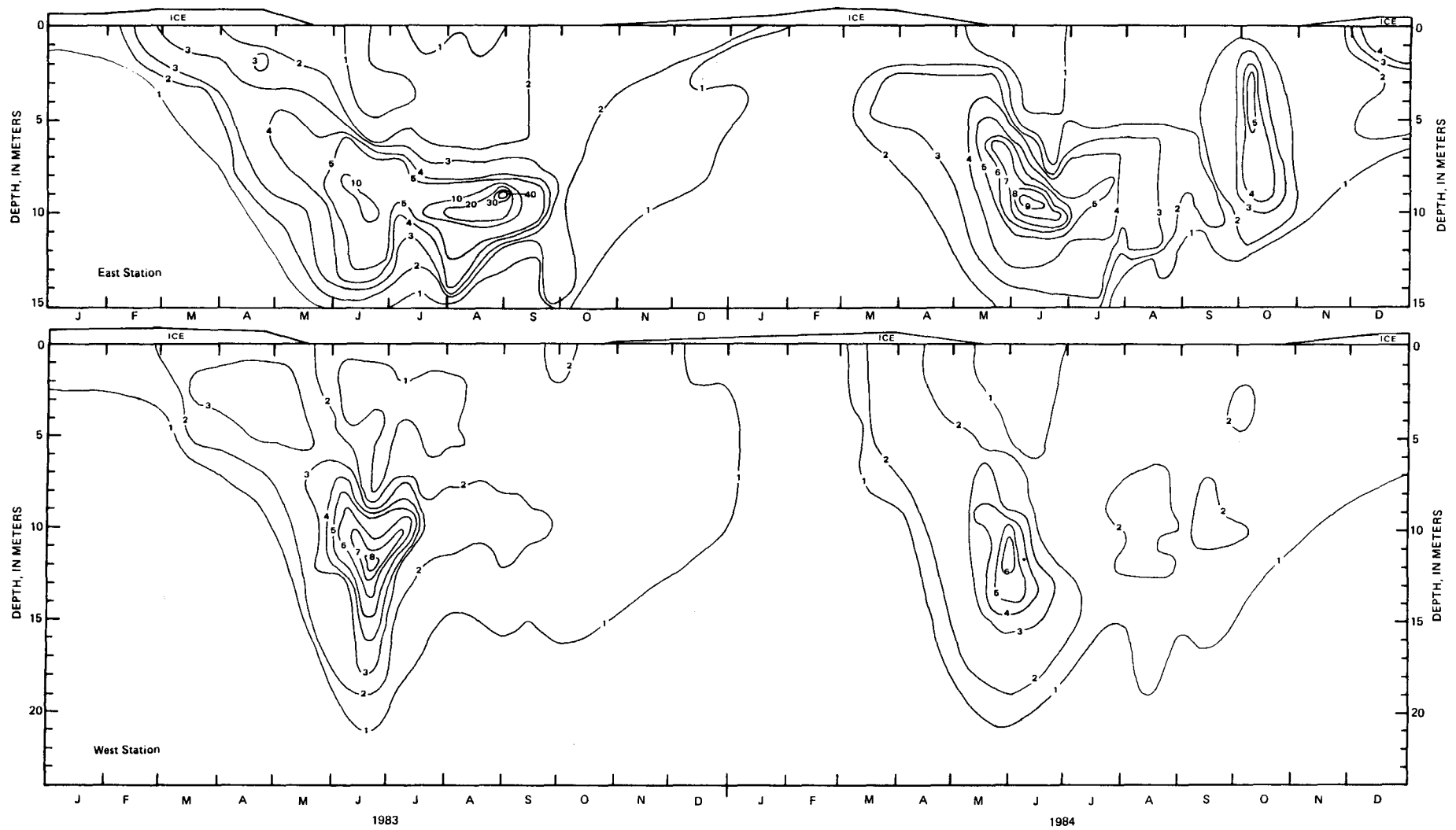


Figure 3. Time-depth plot of chlorophyll *a* concentrations, in micrograms per liter, during 1983-84 at the east and west limnological stations.

obtained with the second and third sampling designs are different for each station and year; however, the 95-percent confidence limits overlap and thus the mean concentrations are not significantly different. The mean concentrations of chlorophyll *a* obtained with the first sampling design are significantly larger than those obtained under the other two sampling designs except in two instances. There is a slight overlap in the 95-percent confidence limits for sampling designs I and II at the east limnological station during 1984. A similar overlap exists between sampling designs I and III at the west limnological station during 1983. A wide disparity also exists for the ranges of chlorophyll *a* concentrations obtained with the three sampling designs. The significantly larger mean values and the wide ranges in chlorophyll *a* concentrations obtained under the first sampling design are largely attributable to the deep-lying chlorophyll maxima in the hypolimnion that were not located by the other two sampling designs.

The mean concentration of chlorophyll *a* in a lake during the summer has often been used to categorize the lake's trophic state as either oligotrophic, mesotrophic, or eutrophic. An international workshop on the control of eutrophication recently concluded that chlorophyll *a* is a widely cited and accepted indicator of lake trophic state (Rast, 1981). Numerous trophic state categorizations based on chlorophyll *a* have been proposed; one of the more recent is that of Hern *et al.* (1981). These authors classify a lake as oligotrophic if its mean chlorophyll *a* concentration within the euphotic zone is less than 2.3 μgL^{-1} ; it is eutrophic if chlorophyll *a* exceeds 6.4 μgL^{-1} ; and the lake is mesotrophic if it contains between 2.3 and 6.4 μgL^{-1} . Application of this trophic state categorization to the chlorophyll *a* data in Table 1 yielded the following results. Sampling designs II and III categorized both limnological stations as oligotrophic during 1983-84 because the mean concentrations of chlorophyll *a* did not exceed 1.93 μgL^{-1} . Sampling design I also yielded an oligotrophic ranking for the west limnological station in both years; however, the east limnological station was mesotrophic in both years.

The differences in the results obtained by the three sampling designs have important implications for limnological studies in Alaska because deep-lying chlorophyll maxima do not appear to be unusual features. Woods (1985) reported the occurrence of metalimnetic dissolved-oxygen maxima, which may indicate deep-lying chlorophyll maxima, in six of nine small lakes in southcentral Alaska that he studied in 1982-83. Deep-lying chlorophyll maxima were verified by discrete-depth sampling in four of the nine lakes. A 1985 study of the primary productivity of Wasilla Lake in Wasilla, Alaska found a deep-lying chlorophyll maximum at the lower depth limit of the euphotic zone (Vaught, K.D., University of Alaska, written commun., 1985). The Alaska Department of Fish and Game has also discovered deep-lying chlorophyll maxima in southcentral Alaskan lakes (Koenings, J.P., Alaska Department of Fish and

Game, oral commun., 1985). Given the frequent incidence of deep-lying chlorophyll maxima, the trophic state of many Alaskan lakes may be underestimated if chlorophyll *a* sampling is restricted to the epilimnion or near surface region such as might occur in a reconnaissance-level study of numerous lakes.

Table 1. Comparison of chlorophyll *a* concentrations obtained by three different sampling designs during late May through September at Big Lake

Sampling design and statistics	Chlorophyll <i>a</i> concentrations, in micrograms per liter, at indicated limnological station and year			
	East 1983	West 1983	East 1984	West 1984
DESIGN I¹				
Mean	4.96	1.89	2.81	1.92
95% C.I.	3.13 - 6.79	1.56 - 2.22	2.38 - 3.24	1.69 - 2.15
Range	0.32 - 46.5	0.24 - 8.05	0.34 - 9.17	0.53 - 6.41
n	71	78	71	76
DESIGN II²				
Mean	1.92	1.26	1.93	1.41
95% C.I.	1.37 - 2.47	1.10 - 1.42	1.45 - 2.41	1.20 - 1.62
Range	0.93 - 8.52	0.33 - 2.04	0.79 - 7.17	0.53 - 2.88
n	30	30	27	27
DESIGN III³				
Mean	1.48	1.20	1.39	1.16
95% C.I.	1.07 - 1.89	0.84 - 1.56	1.10 - 1.68	0.90 - 1.42
Range	0.93 - 2.67	0.33 - 2.04	0.79 - 1.83	0.53 - 1.49
n	10	10	9	9

¹ Numerous samples (5 to 10) from euphotic zone taken biweekly. Profiles of water temperature, photosynthetically active radiation, and *in vivo* fluorescence used to select depths.

² Three samples from epilimnion (top, mid, bottom depths of epilimnion) taken biweekly.

³ Single, near surface sample taken biweekly.

REFERENCES CITED

- Fee, E.J. 1976. The Vertical and Seasonal Distribution of Chlorophyll in Lakes of the Experimental Lakes Area, Northwestern Ontario: Implications for Primary Production Estimates. *Limnology and Oceanography* 21(6): 767 - 783.
- Hern, S.C., V.W. Lambou, L.R. Williams, and W.D. Taylor. 1981. Modifications of Models Predicting Trophic State of Lakes: Adjustment of Models to Account for the Biological Manifestations of Nutrients. EPA-600/3-81-001.
- Pick, F.R., C. Nalewajko, and D.R.S. Lean. 1984. The Origin of a Metalimnetic Chrysophyte Peak. *Limnology and Oceanography* 29(1): 125 - 134.
- Priscu, J.C. and C.R. Goldman. 1983. Seasonal Dynamics of the Deep-Chlorophyll Maximum in Castle Lake, California. *Canadian Journal of Fisheries and Aquatic Sciences* 40(2): 208 - 214.
- Rast, W. (ed.). 1981. International Workshop on the Control of Eutrophication. International Institute for Applied Systems Analysis, Laxenburg, Austria. October, 1981.
- Rheinheimer, G. 1974. *Aquatic Microbiology*. J. Wiley and Sons, New York.

- U.S. Environmental Protection Agency. 1980. Clean Lakes Program Guidance Manual. U.S. Environmental Protection Agency, EPA-440/5-81-003.
- U.S. Geological Survey. 1984. Water Resources Data, Alaska Water Year 1983. U.S. Geological Survey Water-Data Report AK-83-1.
- U.S. Geological Survey. 1985. Water Resources Data, Alaska, Water Year 1984. U.S. Geological Survey Water-Data Report AK-84-1.
- Wetzel, R.G. and G.E. Likens. 1979. Limnological Analyses W.B. Saunders Co., Philadelphia.
- Woods, P.F. 1985. Limnology of Nine Small Lakes, Matanuska-Susitna Borough, Alaska, and the Survival and Growth Rates of Rainbow Trout. U.S. Geological Survey Water-Resources Investigations Report 85-4292.

FACTORS INFLUENCING THE QUALITY OF SNOW PRECIPITATION
AND SNOW THROUGHFALL AT A SIERRA NEVADA SITESheri Woo and Neil Berg¹

ABSTRACT: Regression analysis showed precipitation type (rain, snow, mixed rain and snow, hail/graupel) and latitudinal storm path to be important factors influencing both precipitation conductivity and nitrate solute concentration ($r^2 = 0.88$ and 0.80 , respectively) at a subalpine site near Lake Tahoe, California. Weaker relationships existed between both precipitation type and precipitation pH and sulfate solute concentration ($r^2 = 0.50$ and 0.32 , respectively). Storm duration, interstorm period, and precipitation amount and intensity were relatively unimportant explanatory variables. Vegetative influence on snow throughfall under forest canopy was minimal, compared to unaffected precipitation. Solute concentrations of H, SO_4 , Cl, and Ca in snow drip from two major conifers, lodgepole pine and red fir, were generally greater than precipitation in an open site. Contrary to studies in rain-dominated environments, snow drip chemistries between fir and pine were statistically different only for Ca.

(KEY TERMS: atmospheric deposition; lodgepole pine; throughfall chemistry; red fir.)

INTRODUCTION

Aquatic ecosystem responses to acidic deposition have been documented in Scandinavia, Canada, and the northeastern United States. Water quality degradation has resulted in fish kills and the inhibition of amphibian reproduction in snowmelt pools (Leivestad and Muniz, 1976; Pough, 1976). Terrestrial ecosystem responses have also been documented; declines in forest growth and increases in tree mortality have been associated with atmospheric deposition (Linzon and Skelly, 1985). Processes regulating atmospheric chemical loading differ in temperate versus frigid climates. Theoretical and empirical research shows evidence of

an acidic "pulse" or "spike" during snowmelt (Colbeck, 1981; Johannessen and Henriksen, 1978). Because concentration of solutes during snow metamorphism is likely, research on the effects of "acid rain" cannot be directly extrapolated to effects of acidic snow.

The extent of acidic deposition in upland areas in California is largely unknown but could be critical. Currently, in the Sierra Nevada of California, precipitation chemistry is routinely monitored at seven sites by two governmental agencies, the National Atmospheric Deposition Program and the California Air Resources Board. However, both agencies monitor two sites that lie in proximity, so on a large scale, only five locations represent a mountainous region of approximately 486,600 km². For comparison, this area is greater than the states of New Hampshire and Vermont combined. Although the authors realize that other monitoring sites may exist, known sites have not been located to determine chemical spatial variation.

Although the data base is inadequate to allow a comprehensive analysis of wetfall chemistry by precipitation type, the available data suggest that the pH of rainfall is lower than that of snowfall (Table 1).

All monitoring stations in the Sierra Nevada sample precipitation in forest clearings or "open sites." Standardization of sampling is an advantage inherent in monitoring networks. However, if determination of chemical loading into soil and water is a research or management objective, then precipitation sampling in forested areas is necessary. About 45% of the snow zone on the western slope of the Sierra Nevada is forested. Therefore, at ground level, little more than half of the area is currently monitored for acidic deposition. Without accounting for forest influences, chemical loading estimates, used to predict water quality effects, are inaccurate.

¹Respectively, Hydrologic Technician and Supervisory Hydrologist, Pacific Southwest Forest and Range Experiment Station, Forest Service, U.S. Department of Agriculture, P.O. Box 245, Berkeley, California 94701.

TABLE 1. Summary of Acidic Precipitation Research in California

Location	Mean pH ^a	Constituents	Sample type	Reference
Berkeley	4.66	SO ₄ NO ₃ NH ₄ Ca	Rain	McColl 1980
Hopland	5.10	"	"	"
Tahoe City	5.17	"	"	"
Davis	5.20	"	"	"
Menlo Park	5.20	SO ₄ NO ₃ Ca	Rain	Kennedy et al. 1979
Los Angeles	4.49	SO ₄ NO ₃ NH ₄ CA	Rain	Morgan and Liljestrand 1980
Riverside	4.97	"	"	"
Pasadena	4.41	"	"	"
Sierra Nevada (51 sites)	5.8	SO ₄ Ca	Snow	Feth et al. 1964
Sierra Nevada (26 sites)	5.6	SO ₄ NO ₃ Ca	Snow	Brown and Skau 1975
Los Angeles	3.6	NO ₃ SO ₄ Cl NH ₄ Na	Mist	Brewer et al. 1983
"	3.3	and K Ca Mg Pb Fe Ni	Fog	"
Warner Springs	3.74	NO ₃ -N NH ₄ -N Ca Mg	Rain	Ellis et al 1983
Central Sierra Nevada		Cl P NO ₃ SO ₄	Rime	Nachlinger 1984
Ward Valley	5.1		Snow?	Leonard et al. 1981
Eastern Sierra Nevada	3.7-4.9	NH ₄ Na Ca Mg K NO ₃	Rain	Melack et al 1982
"	5.7	and SO ₄ Cl	Snow	"
Central Sierra Nevada	5.3	NO ₃ SO ₄ Cl Alk Na	Snow	Berg and Woo 1985
"	4.9	and Ca Mg K	Rain	"
San Nicolas Island	5.0	NO ₃ SO ₄	Rain	Calif. Air Resources Board 1984
Lynwood	4.6	"	"	"
Pasadena	"	"	"	"
El Monte	"	"	"	"
Mt. Wilson	4.8	"	"	"

^a pH values are presented as they appear in the references. Some are averaged pH, and some are converted to H⁺ as $\mu\text{eq/L}$, averaged, then reconverted back to pH.

Studies of precipitation chemistry in forests are numerous, but most research relates to nutrient cycling problems, not acidic deposition. Hydrogen ion is an unimportant nutrient, and most early studies did not monitor pH. Hence, few studies have investigated the addition of hydrogen ion to snow surfaces under a forest canopy.

Though terminology in the literature varies, the authors prefer that of Zinke (1967) and Kittredge (1953). "Precipitation" is wetfall sampled in a forest clearing. "Forest throughfall" is that precipitation sampled under the forest canopy during a storm event. In a snowfall event, "drip" refers to intercepted snow precipitation that falls or drips from vegetation after the storm event.

Most throughfall studies document precipitation as rain. A few studies differentiate snow from rain, but their collection methods are unclear (Feller; 1977, Verry and Timmons, 1977; Jones, 1984) (Table 2). No studies involving the chemistry of snow precipitation, throughfall, and drip are known for the mountainous areas of California.

This paper examines the chemistry of two components of the hydrologic cycle: snow precipitation or snow throughfall and drip. Further, explanations for observed chemical differences are sought. Specific objectives of this study are

- To determine which, if any, meteorologic parameters are related to precipitation chemistry. Parameters considered are

TABLE 2. Summary of Throughfall pH Studies by Forest Type.

Forest type	Precip. pH ^a	Throughfall pH	Other constituents	Reference
Alder	6.1	6.0	NO ₃ NH ₄ org.N	Tarrant 1968
Conifer	6.1	6.1	"	"
Mixed	6.1	6.1	"	"
Sugar maple ^b	4.06	4.85	Ca Mg K Na NO ₃ NH ₄ org.N PO ₄ SO ₄ Cl	Eaton et al. 1973
Yellow birch	4.06	5.30	"	"
Beech	4.06	5.22	"	"
Eucalyptus	5.0	5.4	K Na NH ₄ Ca Mg Cu Fe Mn Zn NO ₃ H ₂ PO ₄ Cl HCO ₃ SO ₄	McColl and Bush 1978
Red oak ^c	5.6	4.45	Total reducing sugars,	Malcolm et al. 1968
Live oak	5.6	4.10	Total N, polyphenols	"
Longleaf pine	5.6	3.95	"	"
Beech	5.2	5.7	Na K Ca Mg Mn Cl SO ₄ PO ₄ Total N	Nihlgard 1970
Spruce	5.2	4.5	"	"
Douglas-fir ^d	5.20	5.28	NO ₃ Kjeldahl-N Na K Mg Ca Alk	Sollins 1980
Mixed western hemlock, redcedar (snow)	4.5	4.4	K Na Mg Ca Fe Mn NH ₄ Cl H ₂ PO ₄ NO ₃ SO ₄ HCO ₃ SiO ₂	Feller 1977

^a Precipitation is rain except for final entry.

^b Converted to pH units from mg/L.

^c Picked leaves were swirled in distilled water for 5 min. to simulate canopy drip.

Not standard procedure.

^d Converted to pH units from µg/L.

precipitation amount, intensity, density, and type; storm duration and type; and length of interstorm period.

To examine the vegetative influence on precipitation chemistry by comparing chemical differences between precipitation and forest throughfall, precipitation and drip under red fir, precipitation and drip under lodgepole pine, and red fir and lodgepole pine drip.

METHODS

The study was performed at the USDA Forest Service's Central Sierra Snow Laboratory (CSSL), elevation 2103 m, from January 1 to August 31, 1984. CSSL is located 25 km northwest of Lake Tahoe on the west side of the Sierra crest. Precipitation events are strongly influenced by maritime meteorologic conditions. Vegetation at this location consists of red fir (*Abies magnifica*) and lodgepole pine (*Pinus contorta*), with manzanita and ceanothus understory. Trees range up to 38 m in

height and are approximately 100 years old. Soils are slightly acidic, naturally well-drained coarse loams having moderately high subsoil permeability and very low substratum permeability. Available moisture holding capacity ranges from 3 to 7 cm.

Monitoring was conducted at two sites, a 0.3 ha clearing immediately west of CSSL and a forest site located about 250 m north of CSSL. During each storm event, precipitation and throughfall samples were collected from the open and forest sites. After each event, drip samples were collected under red fir and lodgepole pines. Multiple samples were collected throughout each storm, and subsamples (or "replicates") were also taken.

When precipitation occurred as snow, precipitation and throughfall samples were taken from the snowpack surface at each 10 to 12 cm snow accumulation interval. The samples were packed into linear polyethylene (LPE) bottles, capped, and later melted at room temperature. For snow events depositing less than 10 cm depth and for precipitation types other than snow, samples were collected from plastic lined collector boxes, not the snow surface. Sample collectors were not exposed to dryfall except as it may have occurred

concurrent with wetfall or drip.

After a snow storm, drip was collected using similarly lined plastic boxes. Two boxes were used for each tree species, and boxes were placed under the tree driplines, 1 to 1.5 m away from the trunks. Samples continued to be collected until snow was no longer visible in the trees. Tree selection depended on age and proximity to trees of other species. Chemical contributions from old, very mature trees are often greater than from younger trees (Mecklenburg and Tukey, 1964). Therefore, boxes were placed in small stands of pure fir or pine having trees of medium height and age.

Precipitation, throughfall, and drip samples were analyzed for pH, conductivity, and alkalinity at CSSL within 24 hours after collection. Acidity was measured with a Fisher Analog pH meter equipped with a combination flowing junction reference electrode. (Trade names and commercial products are mentioned solely for information. No endorsement by the U.S. Department of Agriculture is implied.) Conductivity was measured with a Weather-Measure Wheatstone bridge conductivity meter. Alkalinity was determined by color titration. In addition, precipitation, throughfall, and drip samples were analyzed for major cations and anions (Ca, Mg, Na, K, NO_3 , SO_4 , and Cl). Samples were stored frozen in LPE bottles and cation solute concentrations were later determined by atomic absorption spectrophotometry. Nitrate and sulfate solute concentrations were analyzed by molecular absorption spectroscopy. Chloride solute concentrations were determined by color titration.

Precipitation amount, duration, and time from previous storm were read from the recording charts of a weighing bucket precipitation gauge. Precipitation intensity was calculated from the same charts, using the time span of each sample as the base interval. Snow density was measured by two snow boards. Precipitation type was visually observed and recorded. Storm types, classification of storms based on latitudinal source area and path, were assigned by observing the track of low pressure areas from satellite photos (Monteverdi, 1976).

Snowmelt volume was calculated from stream discharge records for a tributary of Onion Creek, 7 km from CSSL. Snowmelt timing was determined through analysis of runoff into snowmelt lysimeters located in the open site at CSSL (Kattelmann, 1984).

RESULTS AND DISCUSSION

Variance in Chemistry Data

Low solute concentrations of all monitored constituents led to uncertainty about the quality of

the chemistry data set. Analytical accuracy was determined by comparing the sum of cations with the sum of anions, i.e., by an ionic balance (Figure 1). A regression using all 100 observations implies fair accuracy ($r^2 = 0.86$), but the points are not evenly distributed throughout the range of the ionic sums. When a separate regression is run on those points with a cation sum of less than 200 $\mu\text{eq/L}$ (93 observations), $r^2 = 0.63$.

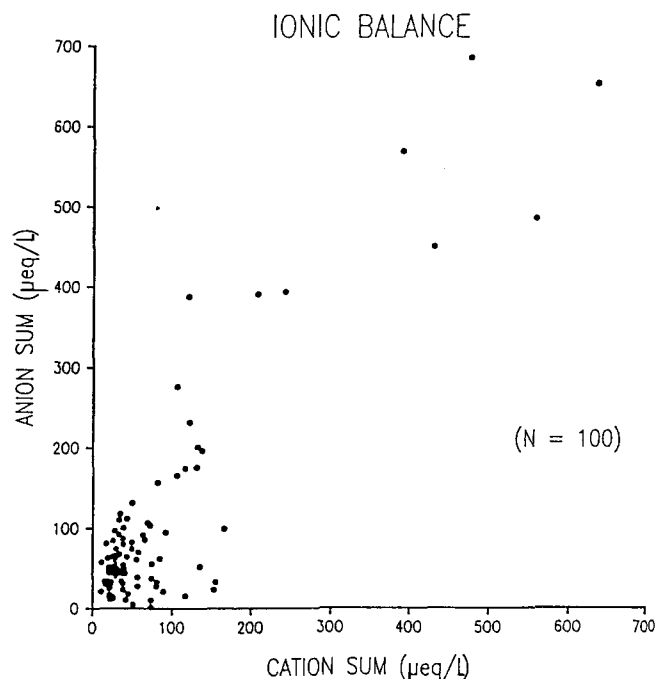


Figure 1. Ionic balance, the sum of anions versus the sum of cations. r^2 for all points is 0.86; r^2 for points less than 200 $\mu\text{eq/L}$ is 0.63. High accuracy is implied by a straight line of slope = 1 and intercept = 0.

To check analytical precision, 66 subsamples, or replicates, were analyzed. Unfortunately, standard deviations varied with the magnitude and range of each element (Table 3). For example, calcium in drip samples exceeded calcium in precipitation (mean drip calcium = 49 $\mu\text{eq/L}$; mean precipitation calcium = 6 $\mu\text{eq/L}$). The standard deviation for drip calcium was correspondingly lower than for precipitation (SD drip calcium = 6 $\mu\text{eq/L}$; SD precipitation calcium = 9 $\mu\text{eq/L}$). In general, higher analytical uncertainty exists in precipitation than drip data. This is not surprising, if one considers that precipitation values were very close to analytical detection limits.

Chemical data in low concentrations require careful analysis, given the lack of precision and accuracy inherent in the methods of current technology. Extreme care must be taken in sampling and handling to prevent contamination. Also, the

inherent variation in the data, which increases with decreasing concentration, sometimes requires sophisticated statistical analyses. One should recognize that in many water chemistry data sets, uncertainty is high when concentrations are very low. The variability found within this data set is taken into account in all further analyses.

TABLE 3. Subsample Analytical Variation, by Sample Type.

	Sample type									
	H ^a	Alk ^b	Cond ^c	NO ₃	SO ₄	Cl	Ca	Mg	Na	K
<u>Open precipitation</u>										
Mean	4.6	22.0	4.5	0.7	4.1	13.1	11.0	9.8	10.7	2.5
SD ^d	0.5	3.0	1.3	0.3	6.3	15.3	9.4	24.7	11.8	2.1
DF ^e	21	16	21	18	13	16	15	14	7	16
<u>Forest throughfall</u>										
Mean	4.6	15.6	5.4	0.8	7.8	19.1	13.3	22.4	13.1	3.5
SD	0.5	2.1	1.5	0.5	6.5	10.7	12.1	28.9	5.7	1.9
DF	15	12	14	12	9	11	11	10	6	10
<u>Drip from fir</u>										
Mean	20.0	1.0	36.0	0.0	66.0	43.3	49.4	37.4	41.1	23.8
SD	2.6	1.9	4.7	0.1	4.8	5.9	6.3	17.6	48.8	8.2
DF	8	5	8	5	5	5	4	4	4	4
<u>Drip from pine</u>										
Mean	12.5	1.8	22.1	0.9	25.5	28.0	25.3	12.9	31.6	10.1
SD	1.6	—	2.0	0.1	2.4	9.4	2.8	3.0	10.0	3.8
DF	9	3	10	6	6	6	6	6	6	6

^a Units are µeq/L unless otherwise noted.

^b Alkalinity in µeq/L as bicarbonate.

^c Conductivity in µS/cm at 25°C.

^d Standard deviation.

^e Degrees of freedom.

Meteorological Parameters Related to Precipitation Chemistry

Multiple regression was used to evaluate the relative importance of various meteorological parameters governing precipitation chemistry. Given the large standard deviations in chemical analyses, regressions were run using only pH, conductivity, NO₃, and SO₄ as the dependent variables. Conductivity and pH are broad, general indicators of water quality. NO₃ and SO₄ are suspected primary precursors to acidic deposition. Of the meteorological parameters, precipitation intensity, duration, amount, density and type were chosen because they may characterize a storm's ability to scavenge pollutants. Storm type, a variable

classifying storms by latitudinal path, was chosen because source area determines the potential amount of pollutants entrained. Storm type represents source area and temperature, and chemical differences are expected when these parameters vary. The time between storms, the interstorm period, is a measure of atmospheric loading before rainout or washout processes occurred. Lastly, a random number variable was included to evaluate the statistical relevance of each variable.

Of the eight independent variables, all combinations of five variables were run against each dependent variable (pH, conductivity, NO₃, and SO₄). Two hundred eighteen combinations were possible, and subsets of "best fits" were selected. The frequency of occurrence of each independent variable in each regression was noted, and importance evaluated. A variable occurring less frequently than the random number variable was considered "unimportant" (Table 4).

TABLE 4. Frequency of Meteorological Variables Related to Precipitation Chemistry.

Meteorological variables	Dependent variable			
	pH	Cond. ^a	NO ₃	SO ₄
Intensity	8	16	9	5
Amount	14	16	16	5
Duration	11	16	9	5
Interstorm period	10	16	16	5
Snow density	8	10	9	5
Precipitation type	23	42	27	16
Storm type ^b	18	16	9	5
Random number ^b	7	16	9	5
r ²	0.45-0.50	0.83-0.88	0.75-0.80	0.27-0.32
SE	0.17	3.09	0.81	6.28
n ^c	25	42	27	16

^a Conductivity in µS/cm at 25°C.

^b Random number included in the independent variable set.

^c Number of values in the "best fit" subset.

r² values were high for conductivity and NO₃, but low for pH and SO₄. For pH, only 50% of the variability could be accounted for by the regression. Twenty-five combinations of the independent variables were within 0.05 of the highest r² (0.50). Precipitation type and storm type were the two variables most used, and therefore evaluated as "important." Conductivity had the highest r² value (0.88); the only important variable was precipitation type. NO₃ regressions were similar to the conductivity results, with precipitation type the only important factor. Only 32% of the SO₄ variation could be accounted for by the regression. Precipitation type and storm type

were again the variables occurring most frequently.

Precipitation type and, to a lesser extent, storm type were important variables related to precipitation chemistry. Regression analysis serves to identify relationships between variables, it cannot ensure cause and effect between variables. However, it is not unreasonable to speculate that different precipitation types have different scavenging capabilities, and that precipitation type thereby influences precipitation chemistry. In this data set, four types of precipitation were classified: snow, rain, mixed rain and snow, and hail/graupel. Upon inspection, we observe that rain and hail/graupel are associated with lower pH and higher conductivity, NO₃, and SO₄.

Precipitation type may, alternatively, be the product of atmospheric conditions that affect precipitation chemistry. Atmospheric temperature and humidity are factors governing precipitation type, perhaps one of these factors directly governs precipitation chemistry. That storm type is a parameter of secondary importance supports this interpretation. Low latitude storms are generally warmer, with low pressure paths over Hawaii and southern California. High latitude storms generally come from the Gulf of Alaska, and are usually quite cold. Mid-latitude storms, as the term implies, are in the middle range of storm paths and temperatures.

Vegetative Influences on Precipitation Chemistry

Field Observations. Precipitation, throughfall, and drip were collected for 11 storms. A significant delay occurred (sometimes 2 days) between the collection of open precipitation and forest throughfall during a storm, and fir and pine drip collected after a storm. The separation of forest throughfall and drip was justified; snow generally stayed on vegetation once in contact with it. Therefore, snow falling to the forest floor during an event had little or no contact with vegetation. This generalization is true because snow in this area is often heavy and wet, wind rarely was strong enough to blow snow off vegetation.

Drip samples contained water in both solid and liquid form. Differences in drip phase were apparent between tree species. Fir needle and branch configuration held more snow longer relative to pine. Fir drip was often liquid in form, while pine drip tended to be in snow "clumps." Often, fir drip was yellow, seeming to correspond to the amount of liquid in the drip sample. Drip which fell as liquid was yellower. Yellow drip was never observed under pines.

Four hypotheses were formed on the basis of the reviewed literature. The statistical significance of chemical differences between precipitation and

forest throughfall, precipitation and red fir drip, precipitation and lodgepole pine drip, and fir and pine drip were examined by paired t-testing. No chemical trends within storms were observed, so constituent concentrations within storms were averaged to obtain a representative chemical signature for each storm. By averaging values for each storm, data files of 10 constituents for 4 sample types for 11 storms were created.

Results from Hypothesis Testing. Results from paired t-tests for the four hypotheses are summarized (Table 5). Each column corresponds to one of the tested hypotheses; note that one- and two-sided t-tests were employed. Delta refers to the mean differences calculated from n number of storms. Although n is always small (< 9 in all cases), there were from 2 to 7 samples averaged for each storm. An arbitrary significance level was chosen ($\alpha = 0.05$), but the reader is encouraged to assign "significance" based on the mean differences and standard errors, and on management objectives.

The uncertainty in some of the analytical methods casts doubt on the precision and accuracy of mean differences and significance levels. In the discussion of the four hypotheses that follows, the conclusions are tempered by the magnitude of analytical variation.

TABLE 5. Mean Differences in Chemistry between Snow Precipitation, Forest Throughfall, and Drip from Red fir and Lodgepole pine.^a

Element	Precip-tr ^b		Precip-drip _{fir} ^c		Precip-drip _{pine} ^d		Drip _{fir-pine} ^e	
	delta	n	delta	n	delta	n	delta	n
H	-0.18	6	-12.20	8 *	-9.05	8 *	3.16	8
Alk.	-1.39	6 *	10.27	6 *	8.41	5 *	-0.79	5
Cond.	-0.83	6	-19.50	8 *	-15.16	8 *	4.31	8
NO ₃	-0.18	5	0.35	6	-0.66	6	-1.01	6
SO ₄	-4.10	6	-23.70	6 *	-7.63	6 *	16.00	6
Cl	-11.40	6	-21.70	6 *	-8.60	6	13.10	6 *
Ca	-7.20	6	-26.10	5 *	-7.30	6	16.20	5 *
Mg	-26.40	6	-17.10	5	-1.45	6	14.20	5
Na	-1.22	4	-23.20	5	-10.50	6	13.80	5
K	-1.30	6	-16.10	5 *	-4.40	6 *	10.80	5

^a Delta = arithmetic difference, n = number of storms, * = significance at $\alpha = 0.05$, units: alkalinity in $\mu\text{eq/L}$ as HCO₃, conductivity in $\mu\text{S/cm}$, all others in $\mu\text{g/L}$.

^b Ho: no chemical difference between open precipitation and forest throughfall. H1: difference exists.

^c Ho: no chemical difference between open precipitation and drip from red fir. H1: precipitation alkalinity > red fir drip alkalinity. H1: precipitation H, conductivity, NO₃, SO₄, Cl, Ca, Mg, Na, K < those of red fir drip.

^d Ho: no chemical difference between open precipitation and drip from lodgepole pine. H1: precipitation alkalinity > lodgepole pine alkalinity. H1: precipitation H, conductivity, NO₃, SO₄, Cl, Ca, Mg, Na, K < those of pine drip.

^e Ho: no chemical difference between drip from fir and pine. H1: fir drip alkalinity < pine drip alkalinity. H1: fir drip H, conductivity, NO₃, SO₄, Cl, Ca, Mg, Na, K > those of pine drip.

Precipitation and Forest Throughfall. At $\alpha = 0.05$, no statistical differences existed between precipitation from the "open" site and forest throughfall for any constituents except alkalinity (Table 5). Standard deviations for precipitation and throughfall were small for H, alkalinity, and conductivity with respect to their mean values, but were large for NO_3 , SO_4 , Cl, Ca, Mg, Na, and K (Table 3). Therefore, we cannot definitively conclude that no differences exist for the anions and major cations. However, all mean differences are fairly small (Table 5, column 1), and in very few cases would a difference of the magnitude cited have any practical meaning (note that units for cations and anions are $\mu\text{eq/L}$). We conclude that no practical difference exists between precipitation and forest drip H, conductivity, and alkalinity, and that indications point to no difference in NO_3 , SO_4 , Cl, Ca, Mg, Na, and K as well.

A difference between open precipitation and forest throughfall was not anticipated, because forest throughfall had little or no contact with vegetation. This result agrees with that of Jones (1984).

Precipitation and Red Fir Drip. Statistically significant differences between precipitation and drip from red fir are implied for H, alkalinity, conductivity, SO_4 , Cl, Ca, and K (Table 5). Analytical precision, indexed by standard deviations, for fir drip was good for H, conductivity, SO_4 , Cl, and Ca (Table 3). Precipitation standard deviations are small only for H, alkalinity, and conductivity. Also taking into account the magnitude of the mean differences, we conclude that practical and statistical differences exist between precipitation and fir drip for H, alkalinity, and conductivity, and that H and conductivity are greater in fir drip than in precipitation. Alkalinity is less in fir drip than in precipitation. Sulfate, Cl, Ca, and K differences were statistically significant, but uncertainty in measurement of these constituents for precipitation makes a definitive conclusion impossible. Poor precision for Mg and Na prevented any definite conclusions.

The results of these tests agree with those found in the literature. Rain throughfall and drip under conifer species have been found to be more acidic than the ambient precipitation (Nihlgard, 1970; Malcolm and McCracken, 1968). This is probably due to leaching and/or washing of organic acids from conifer vegetation surfaces. Washing and leaching would also cause an increase in drip conductivity. Differences in SO_4 between precipitation and fir drip are not surprising because SO_4 is a major nutrient and fairly mobile.

Precipitation and Lodgepole Pine Drip. Results from chemical comparison between precipitation and drip from lodgepole pine are similar to results from precipitation and fir drip (Table 5, column 3). Balancing the importance and magnitudes of analytical standard deviations, mean differences, and significance levels, we definitely conclude that H and conductivity are greater in pine drip than in precipitation. Alkalinity is less in pine drip than in precipitation. Statistical difference is implied for SO_4 and K, but mean differences are not large, and standard deviations for these constituents in precipitation are also large. No conclusions are drawn for the other constituents.

Discussion of expected results for the above hypothesis parallels the discussion of results for chemical differences in precipitation and fir drip. Briefly, pine drip was likely to be more acidic than precipitation due to leaching and washing processes.

Fir and Pine Drip. Few statistically significant differences were implied between red fir and lodgepole pine drip chemistry (Table 5), but mean differences for the major anions and cations ranged from 10 to 16 $\mu\text{eq/L}$, except for NO_3 . Except for Na and Cl, analytical precision was good for fir and pine drip. A practical and statistical difference between drip from fir and pine is indicated for Ca. No difference is indicated for H, alkalinity, and conductivity. No conclusions are attempted for the other constituents.

Field observations led to expectations of practical differences between fir and pine drip. Snow stayed longer on the fir canopy than on the pine canopy. And as intercepted snow became drip, pine drip had a greater fraction of solid ice than fir drip. Because liquid drip comes into contact with vegetation more thoroughly than ice, fir drip samples were expected to have lower pH, and higher conductivity. Although trends were toward lowered pH and elevated conductivity in fir drip, the magnitudes of the analytical standard deviations may have masked the differences. The literature review also led to expectations that throughfall and drip chemistry would be species dependent. However, in most studies cited, events of rain and throughfall, not snow and drip, were observed (Parker, 1983). Rain throughfall comes into more intimate contact with trees than snow drip, perhaps a difference exists between fir and pine throughfall, but only a small difference exists between fir and pine drip.

CONCLUSIONS AND SUMMARY

From this study, the following conclusions are drawn:

- Precipitation type (rain, snow, hail/granpel) is related to precipitation conductivity and nitrate concentration ($r^2 = 0.88$ and 0.80 , respectively). A weaker relationship exists between precipitation type and pH and sulfate concentration ($r^2 = 0.50$ and 0.32 , respectively). Storm type is a related variable of secondary importance.

- Variability in chemical analysis often masks trends or relationships in water samples with very low concentrations. This variability must be taken into account during subsequent statistical analysis.

- No practical difference exists between precipitation from an open site and forest throughfall for conductivity, alkalinity, and H. For the major cations and anions, no difference is implied, but analytical error is high, and a conclusive statement is not possible.

- Acidity, conductivity, and SO_4 concentrations are greater in fir drip than in precipitation. Alkalinity is lower in fir drip than in precipitation. Statistical analyses and the magnitude of mean differences imply that Cl, Ca, and K are also greater in fir drip than in precipitation.

- Acidity and conductivity are greater in pine drip than in precipitation, and alkalinity is less in pine drip than in precipitation. The SO_4 difference was statistically significant, but the mean difference was small. Potassium difference was also statistically significant, but analytical variation for K in precipitation was high.

- No statistical or practically significant differences were found between fir and pine drip for H, conductivity, and alkalinity. A difference in Ca is indicated, but nothing can be said for the other constituents.

The results of this study suggest further investigation of precipitation chemistry by precipitation type. Vegetative influences on precipitation chemistry may also be modified by precipitation type. If estimation of chemical loading into surface water and soil is an objective, then the influence of different vegetative species on throughfall and drip chemistry should be studied.

ACKNOWLEDGMENTS

This research was supported in part by the Division of Atmospheric Resources Research, Bureau of Reclamation, U.S. Department of Interior.

Without the attention to detail and careful sample handling procedures followed by R. Osterhuber, T. Mihevc, and R. Kattelmann, this study would not have been completed. We are also thankful for the field assistance provided by D. Azuma and M. Pack.

LITERATURE CITED

- Berg, N.H., and S. Woo, 1985. Acidic Deposition and Snowpack Chemistry at a Sierra Nevada Site. In: Proc. West. Snow Conf., Boulder, Colorado, Colorado State University, Ft. Collins, Colorado. pp. 76-87.
- Brewer, R.L., R.J. Gordon, L.S. Shepard, and E.C. Ellis, 1983. Chemistry of Mist and Fog from the Los Angeles Urban Area. *Atmospheric Environ.* 17(11):2267-2270.
- Brown, J.C., and C.M. Skau, 1975. Chemical Composition of Snow in the East-Central Sierra Nevada. Cooperative Report Series Publication No. AG-1, Center for Water Resources Research, Desert Research Institute, Reno, Nevada. 13 p.
- California Air Resources Board, 1984. Second Annual Report to the Governor and the Legislature on the Air Resources Board's Acid Deposition Research and Monitoring Program. State of California, Air Resources Board, Sacramento, California. 85 p. plus appendices.
- Colbeck, S.C., 1981. A Simulation of the Enrichment of Atmospheric Pollutants in Snow Cover Runoff. *Water Resources Research* 17(5):1383-1388.
- Eaton, J.S., G.E. Likens, and F.H. Bormann, 1973. Throughfall and Stemflow Chemistry in a Northern Hardwood Forest. *Journal of Ecology* 61:495-508.
- Ellis, B.A., J.R. Verfaillie, and J. Kummerow, 1983. Nutrient Gain from Wet and Dry Atmospheric Deposition and Rainfall Acidity in Southern California Chaparral. *Oecologia* 60:118-121.
- Feller, M.C., 1977. Nutrient Movement through Western Hemlock-Western Redcedar Ecosystems in Southwestern British Columbia. *Ecology* 58:1859-1866.
- Feth, J.H., S.M. Rogers, and C.E. Roberson, 1964. Chemical Composition of Snow in the Northern Sierra Nevada and Other Areas. USGS Water Supply Paper 1535-J. 39 p.
- Hansen, E.A., and A.R. Harris, 1975. Validity of Soil-Water Samples Collected with Porous Ceramic Cups. In: Proc. Soil Science Soc. Amer. 39:528-536.
- Johannessen, M., and A. Henriksen, 1978. Chemistry of Snow Meltwater: Changes in Concentration during Melting. *Water Resources Research* 14(4):615-619.
- Jones, H.G., 1984. The Influence of Boreal Forest Cover on the Chemical Composition of Snowcover. In: Proc. East. Snow Conf., Washington, D.C.

- Eastern Snow Conference, pp. 126-138.
- Kattelmann, R.C., 1984. Snowmelt Lysimeters: Design and Use. In: Proc. West. Snow Conf., Sun Valley, Idaho. Colorado State University, Ft. Collins, Colorado. pp. 68-79.
- Kennedy, V.C., G.W. Zellweger, and R.J. Avanzino, 1979. Variation of Rain Chemistry During Storms at Two Sites in Northern California. *Water Resources Research* 15(3):687-702.
- Kittredge, J., 1953. Influences of Forests on Snow in the Ponderosa-Sugar Pine-Fir Zone of the Central Sierra Nevada. *Hilgardia* 22(1):1-99.
- Leivstad, H., and I.P. Muniz, 1976. Fish Kill at Low pH in a Norwegian River. *Nature* 259:391-392.
- Leonard, R.L., C.R. Goldman, and G.E. Likens, 1981. Some Measurements of the pH and Chemistry of Precipitation at Davis and Lake Tahoe, California. *Water, Air, and Soil Pollution* 15:153-167.
- Linzon, S.N., and J.M. Skelly, 1985. Effects of Gaseous Pollutants on Forests in Eastern North America. In: Abstracts, Muskoka Conference '85, International Symposium on Acidic Precipitation, Muskoka, Ontario. pp. 277-278.
- Malcolm, R.L., and R.J. McCracken, 1968. Canopy Drip: A Source of Mobile Soil Organic Matter for Mobilization of Iron and Aluminum. In: Proc. Soil Science Soc. Amer. 32:834-838.
- McCull, J.G., 1980. A Survey of Acid Precipitation in Northern California. Final Report for Contract A7-149-30, California Air Resources Board.
- Mecklenburg, R.A., and H.B. Tukey, 1964. Influence of Foliar Leaching on Root Uptake and Translocation of Calcium-45 to the Stems and Foliage of *Phaseolus Vulgaris*. *Plant Physiology* 39:533-536.
- Melack, J.M., J.L. Stoddard, and D.R. Dawson, 1982. Acid Precipitation and Buffer Capacity of Lakes in the Sierra Nevada, California. In: Proc. Amer. Water Res. Assoc. Symp. Hydromet., Bethesda, Maryland. pp. 465-472.
- Morgan, J.J., and H.M. Liljestrang, 1980. Measurement and Interpretation of Acid Rainfall in the Los Angeles Basin. W.M. Keck Lab., Division of Engineering and Applied Science, California Institute of Technology, Pasadena. Rept. No. AC-2-80, February, 1980. 54 p.
- Monteverdi, J.P., 1976. The Single Air Mass Disturbance and Precipitation Characteristics at San Francisco. *Monthly Weather Review* 104:1289-1296.
- Nachlinger, J., 1984. Rime Accumulation and Chemical Composition in a Subalpine Forest. Unpublished report, University of Nevada, Reno. 18 p.
- Nihlgard, B., 1970. Precipitation, its Chemical Composition and Effects on Soil Water in a Beech and Spruce Forest in South Sweden. *Oikos* 21:208-217.
- Parker, G.G., 1983. Throughfall and Stemflow in the Forest Nutrient Cycle. In: Advances in Ecological Research, Volume 13. A. MacFadyen and E.D. Ford (eds.), pp. 58-120.
- Pough, F.H., 1976. Acid Precipitation and Embryonic Mortality of Spotted Salamanders, *Ambystoma maculatum*. *Science* 221(4235):68-70.
- Sollins, P., C.C. Grier, F.M. McCorison, K. Cromack, Jr., and R. Fogel, 1980. The Internal Element Cycles of an Old-Growth Douglas Fir Ecosystem in Western Oregon. *Ecological Monographs* 50(3):261-285.
- Tarrant, R.F., K.C. Lee, and W.B. Bollen, 1968. Nutrient Cycling by Throughfall and Stemflow Precipitation in Three Coastal Oregon Forest Types. USDA Forest Service Res. Pap. PNW-54. Portland, Oregon. 7 p.
- Verry, F.S., and D.R. Timmons, 1977. Precipitation Nutrients in the Open and Under Two Forests in Minnesota. *Canadian Journal of Forestry Research* 7:112-119.
- Zinke, P.J., 1967. Forest Interception Studies in the United States. In: Forest Hydrology, Proceedings of a National Science Foundation Advance Science Seminar, University Park, Pennsylvania, pp. 137-161.

POSTER SESSION

PRIMARY PRODUCTION, CHLOROPHYLL, AND NUTRIENTS
IN HORSESHOE LAKE, POINT MACKENZIE, ALASKA*Paul F. Woods and Timothy G. Rowe**

ABSTRACT: A limnological study of Horseshoe Lake was started in 1985 to determine the relation between nutrients and primary production in the 64.8 square-hectometer lake prior to and after any influx of dairy wastes produced by the nearby Point MacKenzie Agricultural Project. This paper documents results from data collected from June through September 1985 at Horseshoe Lake's east arm, the part of the lake nearest the agricultural project. Concentrations of total phosphorus, dissolved inorganic nitrogen, and chlorophyll *a* were characteristic of oligotrophic lakes as was integral primary production, which ranged from 44.2 to 104.5 milligrams of carbon per square meter per day. The ratio of dissolved inorganic nitrogen and dissolved orthophosphorus indicated that phytoplankton growth was limited by nitrogen, not phosphorus. Concentrations of dissolved chloride, instead of nitrate are used as the primary tracer of dairy wastes because the nitrogen budget of Horseshoe Lake may be augmented by nitrogen fixed by the dense stands of alder trees (*Alnus spp.*) that occupy the lake's 7.5 kilometer shoreline.

(KEY TERMS: eutrophication; ground-water pollution; primary productivity; chlorophyll.)

INTRODUCTION

The Point MacKenzie area within the Matanuska-Susitna Borough of southcentral Alaska (Figure 1) is characterized by undulating, low-relief terrain containing numerous muskegs, ponds, and lakes; most of the area is underlain by thick glacial deposits. Several large dairy farms have recently begun operation at Point MacKenzie as part of the 5,666 hm^2 Point MacKenzie Agricultural Project. The dairy wastes generated by the farms are placed in excavated manure lagoons where the potential exists for these wastes to leach into the shallow ground-water system and eventually to reach nearby ponds and lakes. Dairy wastes characteristically are rich in nitrogen and phosphorus, two nutrients that are closely associated with eutrophication, or nutrient enrichment, of lakes.

Horseshoe Lake is immediately adjacent to the west boundary of the Point MacKenzie Agricultural Project and the lake's northeast shoreline is about 1,500 m southwest of a dairy farm's manure lagoon. The first dairy cows arrived at this farm in the autumn of 1984; prior to construction of the farm the area adjacent to Horseshoe Lake was essentially undeveloped. Water-quality data collected at Horseshoe Lake during 1981-82 indicated that the western arm of the lake had low concentrations of dissolved oxygen in its hypolimnion (Glass, 1983). These results suggest that the lake may have a limited capacity to assimilate additional nutrients because the lake's oxygen deficit will be intensified by significant increases in biological productivity.

The U.S. Geological Survey and Division of Geological and Geophysical Surveys of the Alaska Department of Natural Resources recognized the potential for nutrient enrichment of Horseshoe Lake by an influx of manure lagoon leachate and thus began a cooperative limnological study of Horseshoe Lake in October 1984. A major goal of the project is to assess limnological conditions in the lake prior to the anticipated arrival of manure lagoon leachate. If leachate is detected the project will then study the response of the lake's biological productivity to the increased loading of nutrients. The purpose of this paper is to document the results of the first year of limnological sampling in Horseshoe Lake's east arm, the part of the lake nearest the dairy farm manure lagoon (Figure 2).

Horseshoe Lake is U-shaped and has a surface area of 65.2 hm^2 , a volume of 1.9 hm^3 , and a mean depth of 2.9 m. The west and east arms of the lake are, respectively, 7.5 and 5.5 m deep and are connected by a shallow channel. The lake has no defined inlet streams; its single outlet stream drains to the Little Susitna River. Dams have been constructed by beavers at the lake's outlet and between the east arm and an adjacent pond. The Alaska Department of Fish and Game reports that the lake is accessible to anadromous salmonids, particularly silver salmon (*Oncorhynchus kisutch*).

The climate of Point MacKenzie can be characterized by climatological data gathered at Anchorage,

*Hydrologists, U.S. Geological Survey, 1209 Orca St., Anchorage, Alaska, 99501

which is 20 km southeast of Horseshoe Lake (Table 1). Mean annual precipitation is 366 mm, and September is the wettest month. The mean annual air temperature is 1.8°C with July having the highest mean monthly air temperature of 14.5°C. Horseshoe Lake is ice covered generally from mid-October to mid-May.

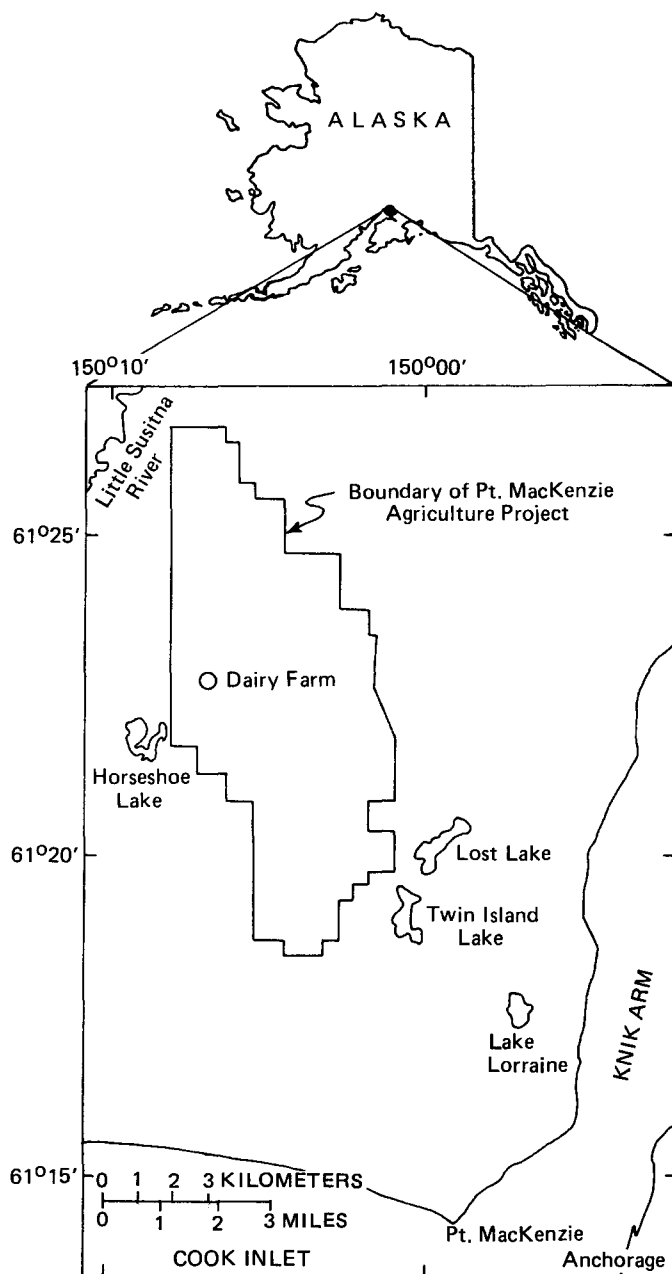


Figure 1. Location of the Point MacKenzie Agricultural Project and Horseshoe Lake, Matanuska-Susitna Borough of Southcentral Alaska.

METHODS

A limnological sampling station was located over the deepest part of the lake's east arm (Figure 2). Sampling was conducted six times between early June and mid-September 1985 on a tri-weekly

schedule. The 5.5 m deep water column was profiled at 0.5 m intervals for water temperature, dissolved-oxygen concentration, and photosynthetically active radiation (PAR). The PAR data were measured using a spherical quantum sensor and were used to determine the extinction coefficient and the depth of the euphotic zone, defined here as the depth at which *in situ* PAR is 1 percent of the PAR incident upon the lake's surface. Water column transparency was measured with a 20 cm Secchi disc.

Water samples were collected from 1 m beneath the surface and 0.5 m above the lake bottom. Methods described in Koenings *et al.* (1985) were used to analyze the water samples for the following constituents: total phosphorus, dissolved orthophosphorus, dissolved ammonia, dissolved nitrite plus nitrate, and total ammonia plus organic nitrogen. Dissolved chloride was determined for the 1-m depth samples per methods in Skougstad *et al.* (1979). Chlorophyll *a* samples were collected at depths of 1, 2, 3, and 4 m and were analyzed fluorometrically, with correction for pheophytin, per Wetzel and Likens (1979). Phytoplankton species composition was determined per Greeson (1979) from samples collected at depths of 1, 2, 3, and 4 m.

Primary productivity of phytoplankton was measured *in situ* using the carbon-14 light and dark bottle methodology described in Koenings *et al.* (1985). Incubations occurred between 1000 and 1600 hours and were 4 to 5 hours in duration. Incubation depths were 1, 2, 3, and 4 m. Following incubation the 125 mL samples were filtered onto glass-fiber filters and then assayed using a liquid scintillation spectrophotometer. Concentrations of inorganic carbon were analyzed on an infrared carbon analyzer. The amount of PAR incident at the lake surface was recorded for the incubation period as well as the entire 24 hours of the sampling date. The hourly rates of primary productivity were expanded to daily rates based on the ratio of incubation PAR to daily PAR.

Additional limnological data have been collected as part of this study at other stations on or near Horseshoe Lake (Figure 2). These additional data are available within the U.S. Geological Survey's WATSTORE water-quality data computer system.

RESULTS AND DISCUSSION

The ice cover on Horseshoe Lake was completely melted by May 25, 1985. By the June 4 sampling trip the temperatures in the water column of the east arm sampling station ranged from 10.3 to 13.5°C. The maximum surface and near-bottom temperatures of 19.6 and 17.5°C, respectively were measured on July 19. During the September 18 sampling trip the east arm was isothermal at 10.3°C. Ice re-formed on the lake in mid-October. The six temperature profiles showed that the east arm did not stratify thermally from June through September 1985. Glass (1983) also found that Horseshoe Lake's east arm did

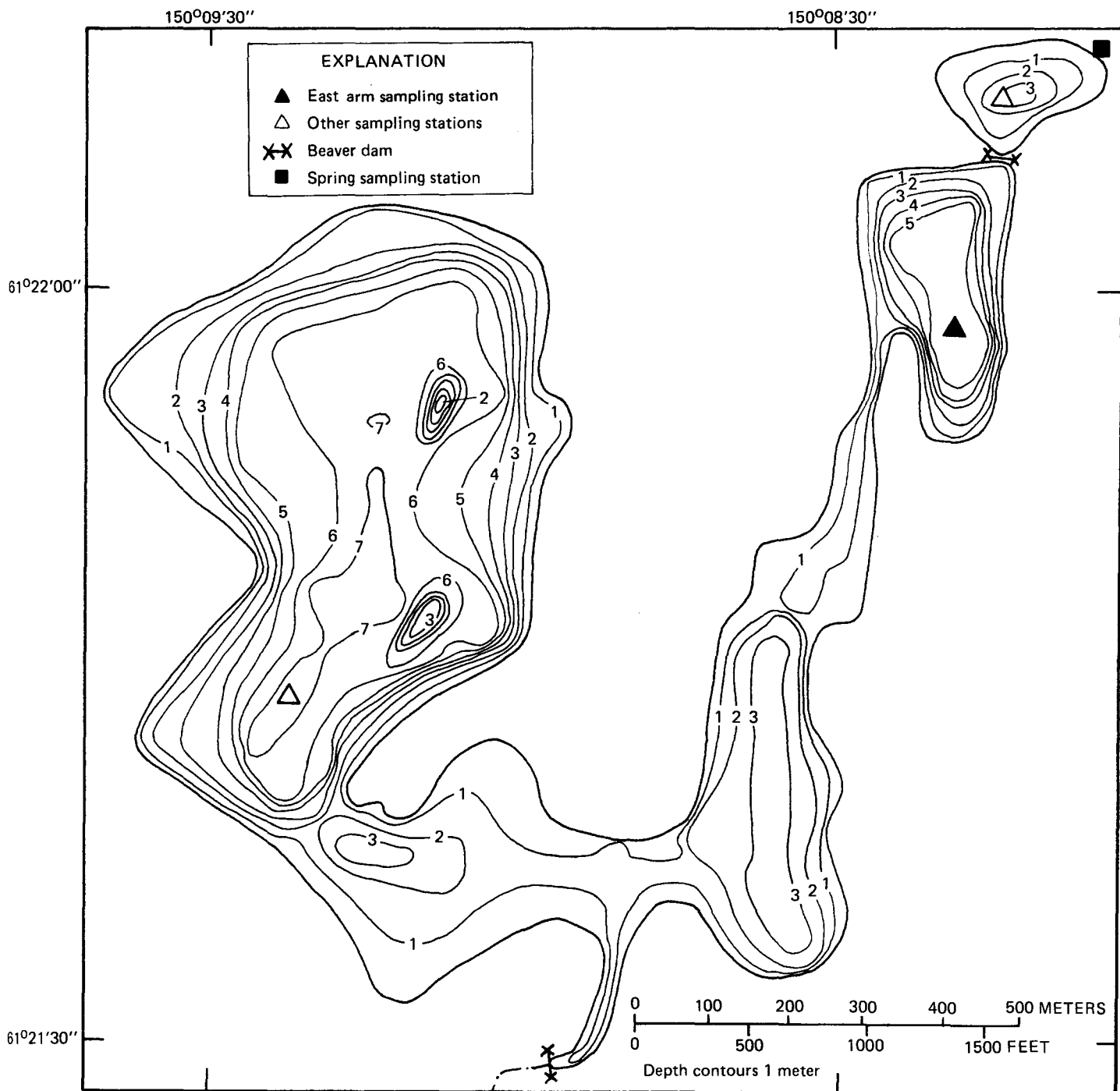


Figure 2. Bathymetric map of Horseshoe Lake and location of the east arm sampling station.

not stratify from June through September 1981. This lack of thermal stratification is attributable to the shallowness of the east arm and to Horseshoe Lake's exposure to strong winds, which are characteristic of the area.

Water column transparency ranged from 4.2 to 5.2 m. The euphotic zone extended to the lake bottom on all six sampling trips. The penetration of PAR to the lake bottom, even on cloudy days, was a consequence of the low values of extinction coefficients which ranged from 0.33 to 0.45 m^{-1} .

Dissolved-oxygen concentrations ranged from 5.4 to 14.6 mgL^{-1} (Figure 3). Concentrations less than 9 mgL^{-1} occurred during August in water deeper than 4 m. Percentage saturation of dissolved oxygen was as high as 141 percent and as low as 58 percent (Figure 4).

Concentrations of nitrogen and phosphorus and nitrogen to phosphorus ratios for depths of 1 and 5 m are shown in Table 2. There were only minor differences between nutrient concentrations at depths of 1 and 5 m on any given sampling date.

Table 1. Air temperature and precipitation characteristics during June through September 1985 near Horseshoe Lake

Month	Monthly precipitation ¹ (millimeter)		Monthly mean air temperature ¹ (°C)	
	Long-term mean ²	1985	Long-term mean ²	1985
June	27.4	25.6	12.4	11.1
July	50.0	25.2	14.5	14.7
August	53.6	89.9	13.4	12.9
September	62.2	80.5	9.0	8.7

¹ Data recorded at Anchorage WSCMO AP (U.S. Department of Commerce, issued annually)

² Period of record is 65 years.

Total phosphorus concentrations ranged from 6.4 to 14.0 $\mu\text{g L}^{-1}$ (mean = 9.1) whereas dissolved orthophosphorus concentrations ranged from 1.4 to 4.1 $\mu\text{g L}^{-1}$ (mean = 2.4). The range and mean of dissolved nitrite plus nitrate concentrations were, respectively, 0.7 to 2.8 and 1.6 $\mu\text{g L}^{-1}$. Dissolved ammonia concentrations ranged from 1.0 to 18.8 mg L^{-1} (mean = 5.6). Nitrogen to phosphorus ratios ranged from 1.2 to 6.5 (mean = 2.7) with the lowest values computed for August 28, the date with the lowest combined concentrations of dissolved nitrite plus nitrate and dissolved ammonia. When nitrogen to phosphorus ratios are less than 5, nitrogen limitation of phytoplankton photosynthesis and growth is indicated (Rast and Lee, 1978). Concentrations of dissolved chloride at the 1 m depth averaged 3.2 mg L^{-1} within a range of 2.7 to 3.6 mg L^{-1} .

The distribution of chlorophyll *a* in the east arm is shown in Figure 5; concentrations ranged from 0.9 to 4.1 $\mu\text{g L}^{-1}$ with a mean of 2.7 $\mu\text{g L}^{-1}$. The highest concentrations on a given sampling date occurred in the lowermost depths. The mean concentration of chlorophyll *a* for each sampling date was inversely correlated ($r = -0.91$, P less than 0.05) with Secchi disc transparency.

The taxonomic composition and percentage occurrence of phytoplankton are listed in Tables 3 and 4, respectively. Based on number of cells per liter, Chrysophyta was the dominant phylum on all sampling trips. The Bacillariophyceae, or diatoms, were most abundant on the first five sampling trips and they were mainly represented by the pennate diatom *Nitzschia*. *Dinobryon*, of the Chrysophyceae, dominated the phytoplankton on September 18. Within the Chlorophyta, *Ankistrodesmus* commonly was the most abundant whereas *Anabaena* tended to dominate the Cyanophyta. The mean number of cells per liter for the water column ranged from 178,875 on July 19 to 262,825 on September 18. The number of cells per liter at each of the four depths was uncorrelated with chlorophyll *a* concentrations.

Integral primary production of phytoplankton in the 5.5 m deep euphotic zone ranged from 44.2 to 104.5 $\text{mg C m}^{-2} \text{d}^{-1}$ (Figure 6) and was uncorrelated with daily PAR, which ranged from 19.6 to 42.7 Em^{-2} . The lack of correlation was likely due to

photoinhibition of primary production in the near-surface samples on sunny days. Primary production on a given day was highest at depths of 3 or 4 m on the four sampling dates that were sunny or partly sunny. The remaining sampling date, August 7, was cloudy with rain; its highest rate of primary production was at 1 m. Primary production in $\text{mg C m}^{-3} \text{d}^{-1}$, ranged from 28.8 at 1 m on August 7 to 1.5 at 2 m on July 19. Hourly specific primary production (primary production normalized for chlorophyll *a* concentration) at the depth of maximal primary production varied from 0.33 to 0.64 $\text{mg C (mg chlorophyll } a)^{-1}$.

Several of the limnological variables measured at Horseshoe Lake have been extensively used to classify the trophic state of lakes. Based on criteria listed by Taylor *et al.* (1980) and Wetzel (1975) the east arm of Horseshoe Lake is oligotrophic, or nutrient-poor (Table 5). The range in daily integral primary production falls within ranges cited for other oligotrophic lakes by LeCren and Lowe-Connell (1980) and Wetzel (1975).

The occurrence of nitrogen limitation and the oligotrophy of Horseshoe Lake's east arm support the concerns expressed over the possibility of eutrophication via leachate from the dairy farm manure lagoons. The principal constituents emanating from animal feedlot wastes are the nutrients nitrate and phosphorus plus chloride and occasionally, heavy metals; however, because of its mobility, nitrate is the only nutrient that enters the ground-water system in substantial quantities (Miller, 1980). Chloride is a conservative constituent that is also highly mobile in ground water and thus serves as a reliable tracer of contamination (Canter and Knox 1985). Any significant increases in the dissolved chloride concentration in the east arm would constitute evidence that manure lagoon leachate had entered Horseshoe Lake. Similar increases in nitrate concentrations in the lake would not necessarily provide reliable evidence of contamination because nitrate is a non-conservative constituent in that it is an important nutrient for aquatic plant growth. In addition, nitrate may be added to Horseshoe Lake from the numerous alder trees (*Alnus spp.*) which inhabit much of the lake's 7.5 km shoreline. Goldman (1961) reported that the

Table 2. Nutrient concentrations and nitrogen to phosphorus ratios at depths of 1 and 5 meters in the east arm of Horseshoe Lake during June through September 1985

Date	Depth (meters)	Nutrient concentrations (micrograms per liter)				Nitrogen to phosphorus ratio ¹
		Total phosphorus	Dissolved orthophosphorus	Dissolved nitrite + nitrate	Dissolved ammonia	
June 5	1	7.4	2.4	2.3	4.6	2.9
	5	10.1	4.1	2.3	8.3	2.6
June 26	1	10.8	3.2	1.2	18.8	6.5
	5	14.0	2.9	2.3	15.4	6.1
July 19	1	7.5	2.2	0.7	3.0	1.7
	5	11.1	1.6	0.7	4.3	3.1
August 7	1	9.0	1.4	0.7	2.2	2.1
	5	10.4	2.3	0.7	3.3	1.7
August 28	1	7.0	2.0	1.3	1.0	1.2
	5	8.6	2.3	2.3	1.0	1.4
September 18	1	6.9	3.0	2.8	4.3	2.4
	5	6.4	2.0	1.3	1.2	1.2

¹(Dissolved ammonia and dissolved nitrite plus nitrate): (Dissolved orthophosphorus)

Table 3. Taxonomic composition of phytoplankton¹ in the east arm of Horseshoe Lake during June through September 1985

Phylum Chlorophyta	Phylum Chrysophyta
<i>Ankistrodesmus</i>	Sub-phylum Chrysophyceae
<i>Crucigenia</i>	<i>Dinobryon</i>
<i>Starastrum</i>	<i>Diceras</i>
<i>Scenedesmus</i>	Sub-phylum
<i>Cosmarium</i>	Bacillariophyceae
<i>Franceia</i>	<i>Coscinodiscus</i>
other Chlorophyta	<i>Nitzschia</i>
Phylum Cyanophyta	<i>Cymbella</i>
<i>Anabaena</i>	<i>Tabellaria</i>
<i>Chroococcus</i>	<i>Pinnularia</i>
<i>Gloeocapsa</i>	<i>Amphipleura</i>
<i>Oscillatoria</i>	<i>Gomphonema</i>
other Cyanophyta	<i>Synedra</i>
Phylum Pyrrophyta	other Bacillariophyceae
<i>Glenodinium</i>	
<i>Ceratium</i>	
other Pyrrophyta	

¹Taxonomic classification per Prescott (1970)

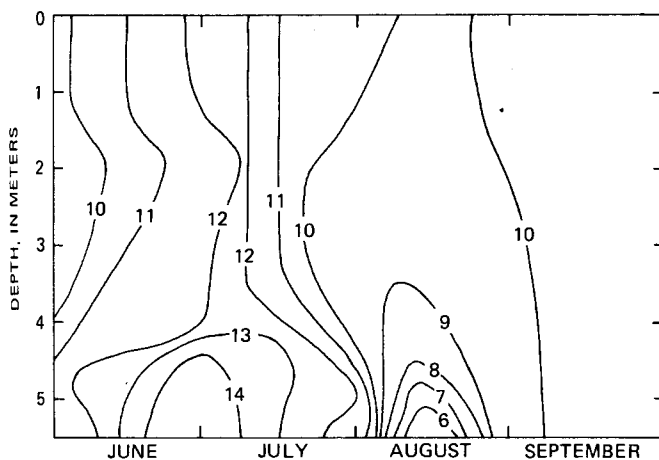


Figure 3. Time-depth plot of dissolved-oxygen concentration (mgL^{-1}) in the east arm of Horseshoe Lake during 1985.

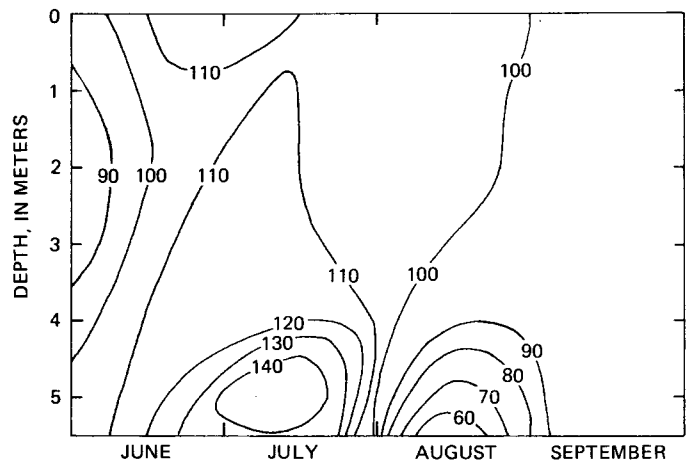


Figure 4. Time-depth plot of percentage saturation of dissolved oxygen in the east arm of Horseshoe Lake during 1985.

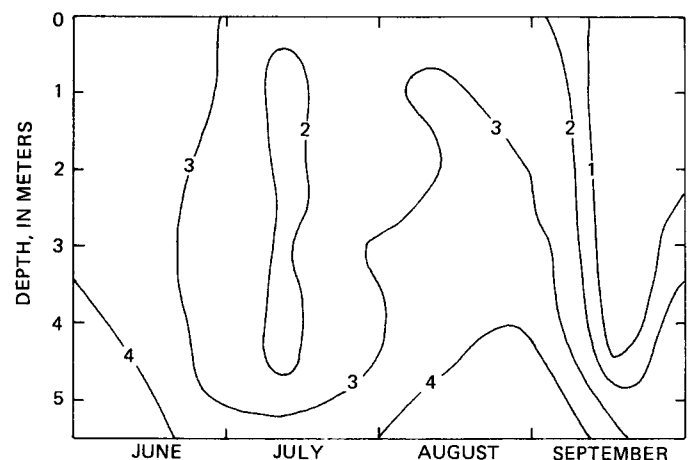


Figure 5. Time-depth plot of chlorophyll a concentration (μgL^{-1}) in the east arm of Horseshoe Lake during 1985.

Table 4. Percent occurrence of phytoplankton, based on cells per liter, in the east arm of Horseshoe Lake during June through September 1985

Date	Mean number of cells per liter	Mean percent occurrence by taxonomic design ¹				
		Chlorophyta	Cyanophyta	Pyrrhophyta	Chrysophyta	
					Chrysophyceae	Bacillariophyceae
June 5	223,850	21.9	0	0.5	18.1	59.5
June 26	216,150	13.9	8.8	0.9	1.8	74.6
July 19	178,875	37.9	14.9	1.1	3.0	43.1
August 7	256,625	28.0	28.1	0.6	3.4	39.9
August 28	257,550	36.7	11.8	0.3	12.7	38.5
September 18	262,825	10.4	1.7	0	68.3	19.6

¹Based on four samples from depth of 1, 2, 3, and 4 m.

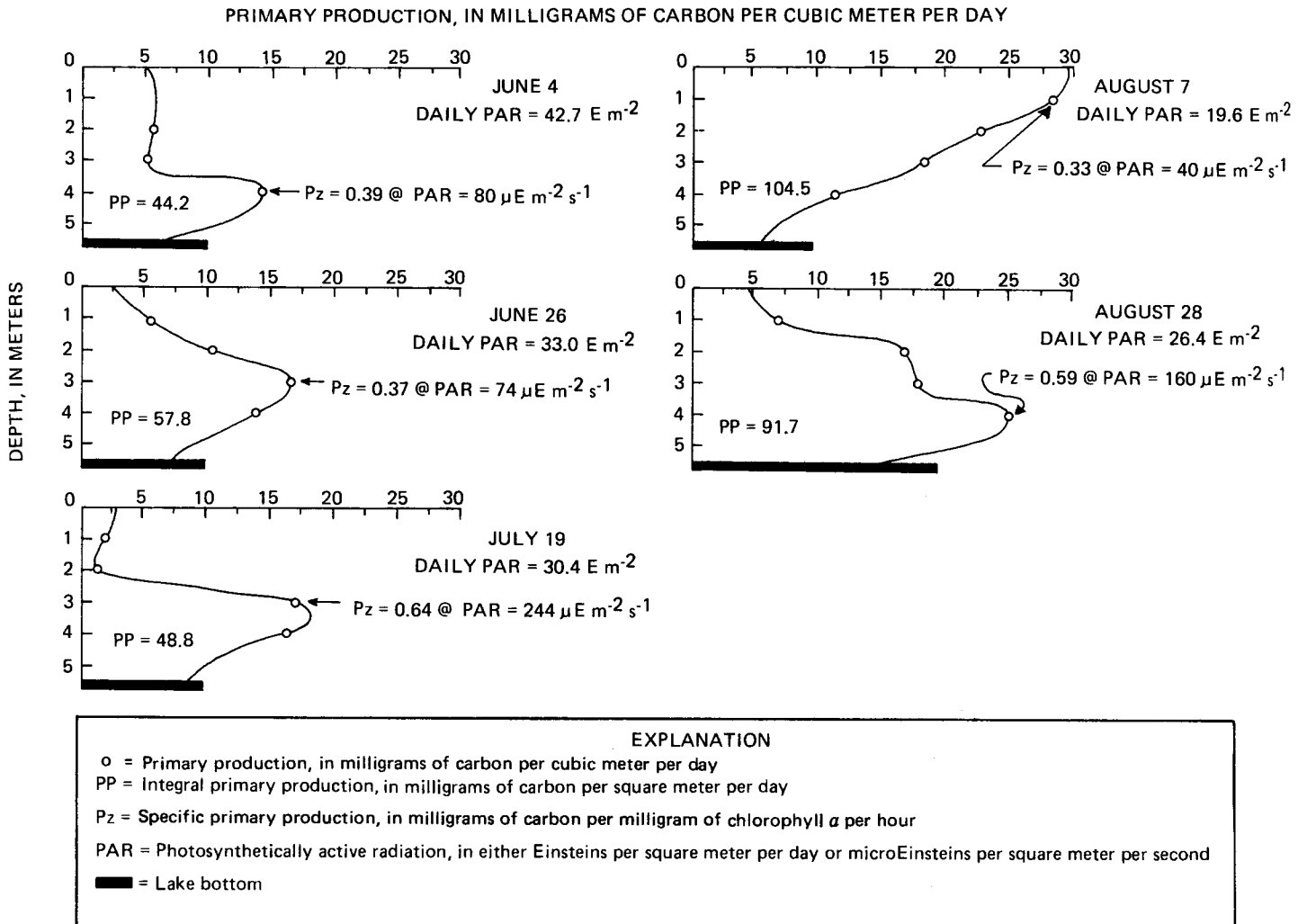


Figure 6. Depth distribution of daily primary production in the east arm of Horseshoe Lake during 1985.

Table 5. Trophic state designation for east arm of Horseshoe Lake based on selected variables
[source: Taylor *et al* (1980), Wetzel (1975)]

Trophic state	Total phosphorus concentration (microgram per liter)	Inorganic nitrogen concentration (microgram per liter)	Chlorophyll <i>a</i> concentration (microgram per liter)	Secchi disc transparency (meter)	Integral primary production (milligram carbon per square meter per day)
Oligotrophic	<10	<200	<7	> 3.7	50-300
Mesotrophic	10-20	200-650	7-12	2.0-3.7	250-1,000
Eutrophic	> 20	500-1,500	>12	<2.0	>1,000
Mean value in east basin of Horseshoe Lake, June through September 1985	9.1	7.2	2.7	4.7	66.4

primary production of Castle Lake, California was enhanced by nitrogen leached from leaf litter and soils associated with alder trees. Burns and Hardy (1975) reported that alders are capable of fixing nitrogen at annual rates between 56 and 156 kg ha⁻¹. At Horseshoe Lake the leaching of nitrogen from leaf litter and the shoreline area may be enhanced because beaver activity has raised the lake's water level enough to inundate lowlying shoreline areas.

Water-quality data have recently been collected from a spring adjacent to the pond at the northeast shoreline of Horseshoe Lake (Figure 2), however, it is not known if this spring delivers ground water that may eventually be contaminated by the manure lagoons. The spring's mean nitrate concentration is 73.2 µgL⁻¹ and its mean dissolved chloride concentration is 1,400 µgL⁻¹ (Table 6). A recent report by Madison and Brunett (1985) serves to put a perspective on the mean nitrate concentration of this spring. They statistically analyzed the nitrate concentrations from 87,000 wells in the United States and assumed for classification purposes that concentrations less than 200 µgL⁻¹ represent natural background values whereas concentrations larger than 3,100 µgL⁻¹ may indicate contamination by human activities. In Alaska only 5.2 percent of the 1,205 wells analyzed had nitrate concentrations exceeding 3,100 µgL⁻¹; 60.9 percent had nitrate concentrations less than 200

µgL⁻¹. Thus, the spring's nitrate concentrations can be assumed to represent uncontaminated ground water.

Water-quality sampling will continue at the spring as well as at the limnological stations to develop an understanding of the spatial and temporal variability of Horseshoe Lake's water-quality characteristics prior to the anticipated arrival of manure lagoon leachate. There are also plans to install a series of wells between the manure lagoon and Horseshoe Lake to allow water-quality sampling of the shallow ground-water system.

REFERENCES CITED

- Burns, R.C. and R.W.F. Hardy. 1975. Nitrogen Fixation in Bacteria and Higher Plants. Springer-Verlag, New York.
- Canter, L.W. and R.C. Knox, 1985. Septic Tank System Effects on Ground Water Quality. Lewis Publishers. Chelsea, Michigan.
- Glass, R.L. 1983. Hydrologic Data for Point MacKenzie Area, Southcentral Alaska, October 1983. U.S. Geological Survey Open-File Report 83-142 update.

Table 6. Concentrations of dissolved nutrients and chloride in a spring adjacent to Horseshoe Lake during 1985

Sample Date	Concentration of dissolved constituent (microgram per liter)			
	Nitrite plus Nitrate	Ammonia	Orthophosphorus	Chloride
August 7	62.0	<1	2.7	1,300
August 28	66.8	<1	3.9	1,400
September 18	77.0	<1	5.4	1,500
October 7	86.9	<1	6.7	1,400
Mean	73.2	--	4.7	1,400

- Goldman, C.R. 1961. The Contribution of Alder Trees (*Alnus tenuifolia*) to the Primary Production of Castle Lake, California. *Ecology* 42:282-288.
- Greeson, P.E., (ed.). 1979. A Supplement To -- Methods for Collection and Analysis of Aquatic Biological and Microbiological Samples (U.S. Geological Survey Techniques of Water-Resources Investigations, Book 5, Chapter A4). U.S. Geological Survey Open-File Report 79-1279.
- Koenings, J.P., J.A. Emundson, J.M. Edmundson, and G.B. Kyle. 1985. Limnological Methods for Assessing Aquatic Production. Alaska Department of Fish and Game. Division of Fisheries Rehabilitation, Enhancement and Development. Technical Report.
- LeCren, E.D. and R.H. Lowe-McConnell. 1980. The Functioning of Freshwater Ecosystems. Cambridge University Press, Cambridge.
- Madison, R.J. and J.O. Brunett. 1985. Overview on the Occurrence of Nitrate in Ground Water of the United States in U.S. Geological Survey, National Water Summary 1984. U.S. Geological Survey Water-Supply Paper 2275, pp. 93-105.
- Miller, D.W. (ed). 1980. Waste Disposal Effects on Ground Water. Premier Press, Berkeley, California.
- Prescott, G.W. 1970. How to Know the Freshwater Algae. Wm. C. Brown Co. Publishers, Dubuque, Iowa.
- Rast, Walter and G.F. Lee. 1978. Summary Analysis of the North American (U.S. Portion) OECD Eutrophication Project: Nutrient Loading-Lake Response Relationships and Trophic State Indices. U.S. Environmental Protection Agency, EPA-600/3-78-008.
- Skougstad, M.W., M.J. Fishman, L.C. Friedman, D.E. Erdmann, and S.S. Duncan. 1979. Methods for Determination of Inorganic Substances in Water and Fluvial Sediments. U.S. Geological Survey Techniques of Water Resources Investigations. Book 5, Chapter A1.
- Taylor, W.D., V.W. Lambou, L.R. Williams, and S.C. Hern. 1980. Trophic State of Lakes and Reservoirs. U.S. Environmental Protection Agency. Environmental Monitoring and Support Laboratory. Technical Report E-80-3.
- U.S. Department of Commerce. Issued annually. Climatological Data, Alaska.
- Wetzel, R.G. 1975. Limnology. W.B. Saunders Co., Philadelphia.
- Wetzel, R.G. and G.E. Likens. 1979. Limnological Analyses. W.B. Saunders Co., Philadelphia.

WATER QUALITY OF ABANDONED MINE RUNOFF:
A CASE STUDY OF ALASKAN SITESDavid B. Pott, Robert E. Lindsay, and Nicholas Pansic¹

ABSTRACT: The purpose of this study was to evaluate surface water quality and soil chemistry of two abandoned mined areas in interior Alaska and to use these data to help develop reclamation alternatives for the sites. Soil and water chemistry data from the sites indicated that no major pollutants were threatening nearby water courses. Leaching of mineral salts is occurring at both sites, with Na being the predominant cation found. Spoil materials at both sites are oxidized and neutral to slightly acid. Emphasis in the lower-48 states is upon rapid establishment of vegetation on disturbed lands with barren spoils viewed as reclamation problems. In colder climates advancement of vegetation cover onto barren areas often requires years even with the most optimum soil conditions. The reclamation alternatives selected for the two sites discussed in this study emphasized removal of safety hazards rather than extensive regrading and topsoiling which would have destroyed existing vegetation and disturbed soil profiles which had been developed in the years since mining.

(KEY TERMS: mining; land reclamation; runoff; water quality; sodium; Alaska.)

INTRODUCTION

Surface mining of coal and hard minerals disturbs large quantities of earth and the pedogenic processes that have been occurring there for millenia. Mining exposes parent and secondary minerals and greatly accelerates their weathering processes. Runoff from surface mines is a recognized source of pollution for streams and rivers.

Water quality impacts from mining are associated with soil erosion and oxidation of pyritic materials, which causes production of acids and leaching of salts and toxic metals (Anderson and Hawkes, 1985; Down and Stocks; 1977; Hadley and Snow, 1974; Letterman and Mitsch, 1978; Nordstrom, et al., 1979). The types and severities of water quality impacts vary with mine geochemistry and hydrology, receiving water quality and quantity, and mine reclamation measures. There are numerous reports of mine runoff water quality in temperate and subtropical regions but, we have found a paucity of information on water quality impacts from mines in cold regions.

We recently were given an opportunity to perform an environmental assessment and engineering design for reclamation of two abandoned surface coal mines in the interior region of Alaska. This study was funded through the Alaska Abandoned Mined

¹Respectively, Pott and Pansic, Harza Engineering Company, 150 S. Wacker Drive, Chicago, Illinois 60606; and Lindsay, Harza Engineering Company, 900 W. 5th Avenue, #700, Anchorage, Alaska 99501.

Lands Program. This paper presents a case study of two of these sites. The investigation program is described, water quality and soil chemistry data are presented, and site-specific problems are identified. Quantitative analyses of the sites' soils and runoff were made to characterize the severity of the problem at each site. We assessed the feasibility of reclamation of the mines. The nature of the sites, given their soil and hydrologic conditions, determine to a large extent the potential to revegetate and reclaim the sites to "acceptable" conditions.

STUDY AREAS

The mine sites studied are known as Diamond Mine and Dunkle Mine. Their locations are shown in Figure 1. Diamond Mine comprises three surface coal mine areas; the east, central, and west pits (Figure 2). Dunkle Mine

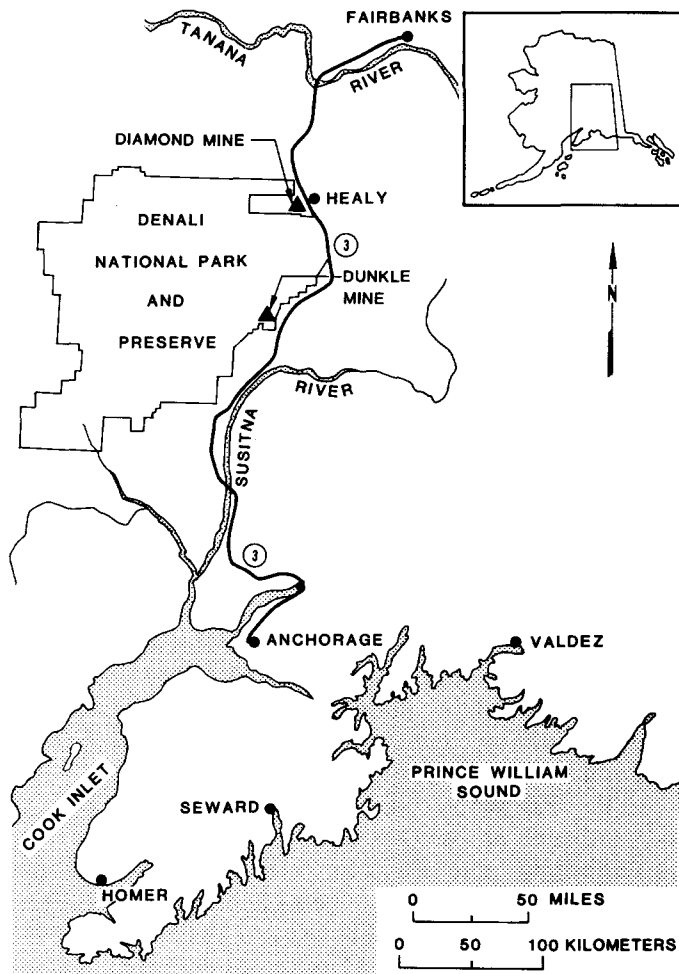


Figure 1. Map Showing Location of Study Areas.

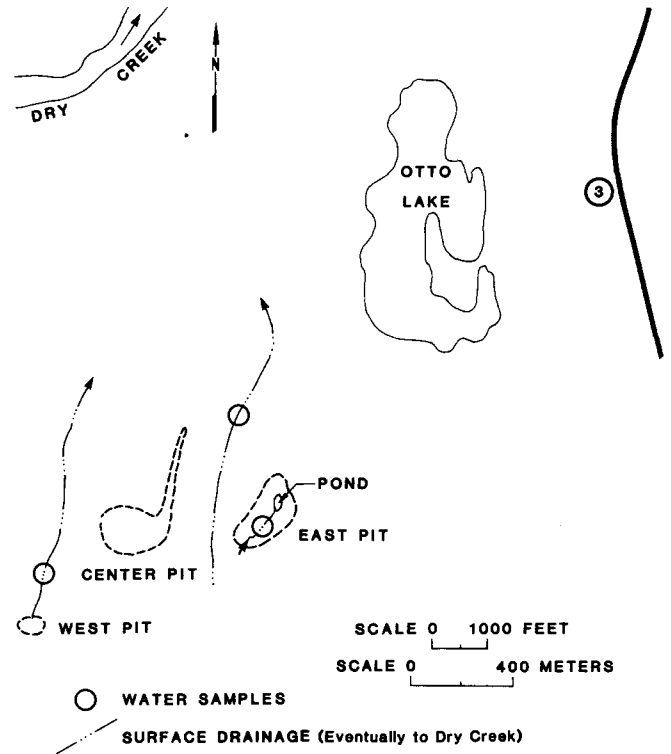


Figure 2. Diamond Mine Map Showing Water Sampling Locations and Surface Drainages. Soil Samples Were Taken at Each Pit.

consists of both a surface mine and underground workings. Dunkle is located within the eastern boundary of Denali National Park and Preserve (Figure 3).

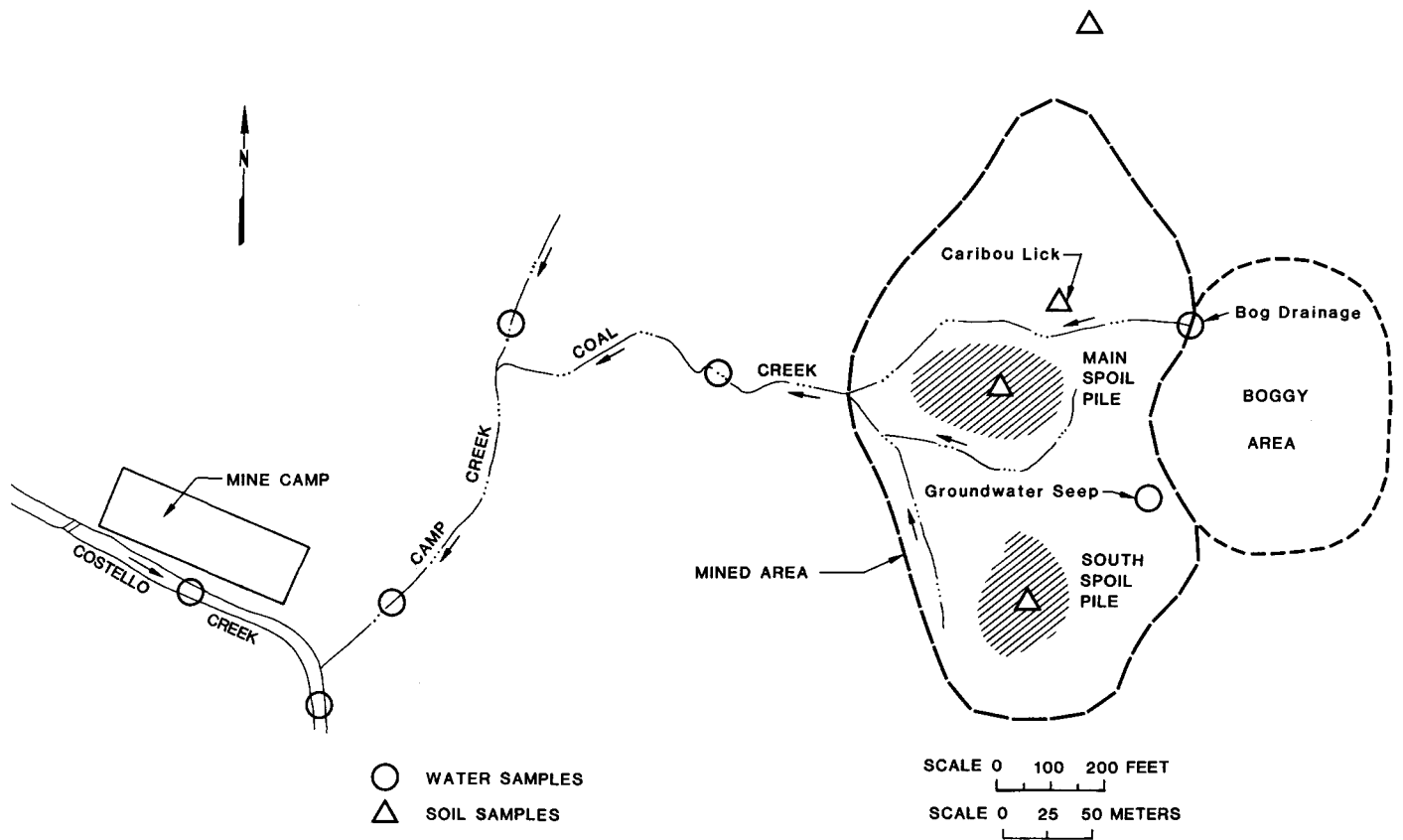


Figure 3. Dunkle Mine Map Showing Soil and Water Sampling Locations and Surface Drainages.

INVESTIGATION PROGRAM

The investigation program for the study included the following major tasks:

- o Comprehensive literature review;
- o Field survey and sample collection;
- o Water and soil chemical analyses;
- o Environmental assessment; and
- o Reclamation evaluation.

Published literature was reviewed to provide background for the study effort. Few materials, however, pertained specifically to Alaska or cold regions applications.

The field survey team included a reclamation specialist, an environmental chemist, a landscape architect, and a geotechnical engineer.

METHODS

Soil

Surface soils were grab sampled and composites were made, each representing barren and vegetated areas in each pit or spoil pile of the mines. In some cases, we took samples of subsurface (0.75 m) materials. Soils were analyzed for the following:

- | | |
|------------------|----------------------------|
| o Organic matter | o Cation exchange capacity |
| o Phosphorus (P) | o Sulfur (S) |
| o Potassium (K) | o Manganese (Mn) |
| o Magnesium (Mg) | o Iron (Fe) |
| o Calcium (Ca) | o Aluminum (Al) |
| o Sodium (Na) | o Zinc (Zn) |
| o Hydrogen (H) | |

The soils were dried at room temperature prior to being passed through a 2 mm sieve. Na, K, Mg, and Ca were extracted

using 1 N ammonium acetate, buffered to pH 7. Zn, Mn, and Fe were extracted using 0.1 N HCl while exchangeable Al was extracted with 1 N KCl. The soil extracts were analyzed for metals by flame atomic absorption spectrophotometry, according to Black (1965). Organic matter, cation exchange capacity (CEC), total S, total P and soluble salts were also measured by methods detailed in Black (1965). A 1:1 water to soil mixture was made for pH measurement with a glass membrane electrode and pH meter.

Water

Water samples for metal analysis were collected in acid-washed polyethylene bottles, and acidified with 2 ml concentrated HNO₃ per liter. These samples were filtered through 0.45 micron pore filters and analysed via inductively coupled plasma emission spectrophotometry. The metals we attempted to quantify included sodium, potassium, calcium, magnesium, aluminum, iron, manganese, and strontium. The technique also allowed quantification of the nonmetals phosphorus and silicon.

Dissolved oxygen, temperature, and conductivity were measured using field meters (Yellow Springs Instrument Co., Yellow Springs, Ohio). A glass-membrane pH potentiometer was also used in the field (Fisher Scientific Co., Pittsburgh, PA). Total acidity was titrated to the phenolphthalein end point (Hach Chemical Co., Loveland, CO).

RESULTS AND DISCUSSION

Complete results of the field sampling and data collection are detailed in the project reports (Harza Engineering Co., 1984a and 1984b). Tables 1 through 4 present some data relevant to this discussion.

The water chemistry data of the two mines show various levels of impact from the mining and disturbance of the soils.

Toxic Hazard Evaluation

The streams draining the Diamond Mine are moderately hard and neutral, not unlike area streams draining non-mined lands. Of the three samples taken, none exceeded Alaska's primary maximum contaminant concentration standards for metals and in only one case was a secondary maximum contaminant concentration standard exceeded. The secondary standard of 0.05 mg/l Mn was found to be exceeded by a factor of 11.6 in the stream draining between the east and center pits at Diamond Mine (0.58 mg/l Mn). This level of Mn is not toxic to most aquatic life (USEPA, 1976).

At Dunkle Mine, we found there to be no violations of primary contaminant standards. There were, however, five instances in which the secondary standards were exceeded: three violations of the Fe standard and two violations of the Mn standard. Both of these metals are notoriously associated with mine drainage. The concentrations we found were not hazardous. Coal Creek below the mined area had 0.37 mg/l Fe, slightly above the 0.3 mg/l standard. The other four violations were not likely related to the mining activities. They came from two samples: the bog water above the mine and groundwater seep at the high-wall. These two samples both contained Fe and Mn in excess of the secondary standard.

Leaching of Soluble Salts

It is apparent that the spoils at both mined sites are leaching salts into the nearby creeks. Much of the data suggests this. Sodium seems to be the main cation being leached at both sites. At Dunkle Mine, notice (in Table 3) the dilution of Na from the first order recipient stream, Coal Creek, to the third order Costello Creek. The high levels of extractable Na in the barren spoil piles are the probable source of this leached Na.

Spoils of both mined sites are oxidized and neutralized according to the mine classification in USEPA (1973). Soluble

TABLE 1. Soil Analyses of Dunkle Mine.

Sample Location	Organic Matter (%)	Soil pH (S.U.)	Cation Exchange Capacity (meg/100g)	Na	K	Ca	Mg	Al	Fe	Mn	P	S	Soluble Salts (mmhos/cm)
Undisturbed vegetated area north of mine	5.6	4.5	3.6	46	98	140	47	267	113	80	5	24	0.2
Main spoil pile barren areas	7.5	6.0	16.0	780	139	690	774	7	193	49	69	387	4.1
225 Main spoil pile vegetated areas	4.9	6.5	6.6	69	126	610	290	7	171	59	74	79	0.5
Main spoil pile subsurface	2.7	7.8	6.5	200	113	540	326	8	182	58	77	83	0.8
South spoil pile barren areas	1.9	7.4	7.3	116	113	550	462	7	178	144	73	300	1.6
South spoil pile vegetated areas	8.1	5.6	9.7	76	142	760	348	7	162	40	66	47	0.5
Caribou lick	3.6	7.5	5.9	42	80	830	169	7	206	120	60	12	0.3

TABLE 2. Soil Analyses of Diamond Mine

Sample Location	Organic Matter (%)	Soil pH (S.U.)	Cation Exchange Capacity (meg/100g)	Na	K	Ca	Mg	Al	Fe	Mn	P	S	Soluble Salts (mmhos/cm)
					(Elemental concentrations are in mg/kg)								
West pit barren areas	5.9	5.6	9.5	130	130	550	440	8	157	34	27	169	0.7
West pit vegetated areas	7.9	5.2	7.3	51	98	500	217	21	207	37	8	10	0.2
Center pit barren areas	8.4	5.5	13.5	280	145	680	604	9	222	35	26	196	0.8
Center pit vegetated areas	8.6	5.7	9.8	141	166	560	466	8	179	31	8	33	0.4
East pit main gob pile barren areas	9.0	4.7	12.6	42	89	660	302	19	180	49	4	20	0.3
East pit vegetated areas	8.6	5.0	11.7	40	110	850	260	27	175	72	7	15	0.2
East pit main gob pile subsurface (.75m)	8.5	5.6	10.9	46	98	700	433	20	188	53	4	14	0.3

TABLE 3. Water Analyses of Dunkle Mine. A dash indicates that the datum was not collected.

Sample Location	Conductivity (umhos/cm)	pH (S.U.)	Total Acidity (as mg/l CaCO ₃)	Na	K	Ca	Mg	Al	Fe	Mn	P	Si	Sr
(Elemental concentrations are in mg/l)													
Costello Ck. upstream of Camp Ck.	99	7.5	<17	3.1	<1.0	19	7.6	<0.05	0.09	<0.05	0.15	1.6	0.17
Camp Ck. up- stream of Coal Ck.	44	7.2	<17	2.0	<1.0	8.7	2.3	<0.05	0.16	<0.05	<0.05	2.6	0.07
Coal Ck.	110	7.4	34	6.5	<1.0	18	2.4	<0.05	0.37	<0.05	<0.05	2.8	0.23
227 Camp Ck. down- stream of Coal Ck.	48	6.8	<17	2.2	<1.0	9.0	5.0	<0.05	0.17	<0.05	<0.05	2.6	0.08
Costello Ck. downstream of Coal Ck.	97	7.5	<17	2.8	<1.0	18	6.7	<0.05	0.16	<0.05	<0.05	1.8	0.16
Groundwater seepage into mine	125	-	-	1.4	1.1	40	8.4	0.42	0.68	0.11	0.19	4.4	0.17
Boggy surface water entering mine	28	6.0	54	0.68	<1.0	4.9	0.93	0.06	4.8	0.22	<0.05	3.8	<0.05

TABLE 4. Water Analyses of Diamond Mine.

Sample Location	Conductivity (umhos/cm)	pH (S.U.)	Total Acidity (as mg/l CaCo ₃)	Na	K	Ca	Mg	Al	Fe	Mn	P	Si	Sr
West pit runoff	57	7.1	<17	1.0	<1.0	14	4.1	<0.05	0.17	<0.05	0.08	2.9	<0.05
East pit runoff	235	7.4	<17	1.5	3.9	34	17	<0.05	0.21	<0.05	<0.05	5.2	0.06
Stream passing through east and center pits	312	6.6	69	2.2	1.1	51	3.9	<0.05	<0.05	0.58	0.09	2.8	0.16

salts are apparently one limiting factor to complete natural revegetation. Comparison of the soluble salt levels in barren and vegetated spoils confirms this.

Although we have found no soil and water chemistry data from past studies, we would expect weathering and pedogenic processes to occur much more slowly in colder regions like these sites than in more temperate areas. The Dunkle Mine hasn't been worked since the early 1950's; the Diamond Mine since 1972. Runoff from neither mine site appears to have yet receded to background salt levels. For comparison, Brown et al. (1984) found runoff from revegetated Texas Gulf Coast lignite mined spoils to return to natural levels within 4 to 15 months.

One interesting point concerns the chemistry of the runoff entering Dunkle Mine from a bog above the site. This water showed the lowest pH and highest acidity of any other sample at the site. This sample also contained a low level of Ca, a high concentration of iron, and low conductivity. Although we did not measure dissolved organic matter, these parameters and the dark tea-colored nature of the water suggested the presence of substantial quantities of humic substances. Humic substances are known for their acidity and ability to preferentially complex Fe over Ca (Schnitzer and Khan, 1972; Alberts and Giesy, 1983).

Reclamation Evaluation

Traditional reclamation of abandoned mined lands has emphasized regrading spoil piles to original contour, covering barren or toxic sites with soil, and establishing vegetation to stabilize and reduce erosion and drainage through toxic materials. However, in many cases, results of such practices may be undesirable. Emphasis in the lower-48 states is upon rapid establishment of vegetation cover on disturbed lands with barren or slowly revegetating spoils viewed as reclamation problems. While this may be true in other parts of the country, the same

criteria do not necessarily apply in cold regions.

Soil formation along with vegetation establishment and growth are often slow, requiring years to accomplish the same degree of cover which can be obtained in one growing season in warmer climates. Regrading of problem spoils identified in this study may actually create worse problems. Soil profiles which have developed through the vegetational influences of aggregate formation and accumulation of organics would be destroyed, and the resulting compaction of the spoil would inhibit infiltration and percolation of water. Exposure of phytotoxic materials which may be present deep within spoil areas would negate any amelioration which has resulted from years of surface weathering and leaching.

Soil and water parameters of both the Diamond and Dunkle mines were examined carefully to aid in developing reclamation alternatives which met a basic goal of abating problem conditions in a cost-effective manner. Recommended reclamation alternatives for both sites were limited to the removal of public safety (unsound structures) and aesthetic problems.

In the case of the Diamond Mine, water quality and soil parameters did not indicate the need for extensive reclamation. The site had several extensive barren areas and many of them were being reclaimed by invasion of surrounding vegetation. The preferred reclamation alternative involved removal of existing or potential public safety hazards while leaving barren spoil areas unreclaimed. A sub-alternative to the preferred alternative included removal of a highwall which was visible from a major highway. Water quality would be adversely affected by transport of sediments if this work were carried out.

The Dunkle Mine also exhibited extensive barren spoils which, in most traditional reclamation plans, would be candidates for extensive regrading and topsoiling. However, soil and water quality sampling of the site did not indicate the need for this type of reclamation. The preferred reclamation alternative included work to remove several collapsing structures considered to be safety problems.

CONCLUSION

In this study, we examined field conditions of two abandoned surface mine sites in interior Alaska. These data were evaluated to assist in preparation of reclamation plans.

Spoils at both Dunkle and Diamond Mines were apparently oxidized and neutralized. There was some leaching of soluble salts, but no evidence of toxic metal problems at either site was found.

Natural revegetation has begun at both sites. Regrading and seedings of slopes was not recommended. Our reasons for this included the slow development of vegetative cover in cold regions, the possible exposure of unoxidized or acidic materials, and the likelihood of increased soil erosion at the sites. A number of unsafe collapsing structure existed at both mines; the preferred reclamation alternative involved removal of these public safety hazards.

ACKNOWLEDGEMENT

The authors gratefully acknowledge the support of our client, the Division of Mining of the Alaska Department of Natural Resources, in funding the reclamation study and allowing us to publish our findings. The comments of J.T. Passage and two anonymous reviewers were most helpful.

LITERATURE CITED

- Alberts, J.J. and J.P. Giesy, 1983. Conditional Stability Constants of Trace Metals and Naturally Occurring Humic Materials: Application in Equilibrium Models and Verification with Field Data. In R.F. Christman and E.T. Gjessing (Editors), Aquatic and Terrestrial Humic Materials. Ann Arbor

- Science, Ann Arbor, MI. pp. 333-348.
- Anderson, M.T. and C.L. Hawkes, 1985. Water Chemistry of Northern Great Plains Strip Mine and Livestock Water Impoundments. Water Resources Bulletin 21:499-505.
- Black, C.A. (Editor), 1965. Methods of Soil Analysis Part 2 - Chemical and Microbiological Properties. Amer. Soc. Agron. Inc., Madison, WI. 1572 pp.
- Brown, K.W., J.C. Thomas, and L.E. Deuel, Jr., 1984. Chemical Characteristics of Surface Runoff from Soils and Revegetated Lignite Mine Spoils. Journal of Soil and Water Conservation 39 (2):146-149.
- Down, C.G. and J. Stocks, 1977. Environmental Impact of Mining. John Wiley, New York, New York.
- Hadley, R.F. and D.T. Snow (Editors), 1974. Water Resources Problems Related to Mining. American Water Resources Association, Symposium Proceedings No. 18, Minneapolis, Minnesota, 236 pp.
- Harza Engineering Company, 1984a. Diamond Mine Engineering Design Alternatives and Environmental Assessments. Alaska Dept. Natural Resources, Division of Mining, Anchorage, AK.
- Harza Engineering Company, 1984b. Dunkle Mine Engineering Design Alternatives and Environmental Assessments. Alaska Dept. Natural Resources, Division of Mining, Anchorage, A.K.
- Letterman, R.D. and W.J. Mitsch, 1978. Impact of Mine Drainage on a Mountain Stream in Pennsylvania. Environmental Pollution 17:53-78.
- Nordstrom, D.K., E.A. Jenne, and J.W. Ball, 1979. Redox Equilibria of Iron in Acid Mine Waters. In: E.A. Jenne (Editor), Chemical Modeling in Aqueous Systems. Speciation, Solubility, and Kinetics. American Chemical Society, ACS Symposium Series 93, Washington, D.C. pp. 51-79.
- Schnitzer, M. and S.V. Khan, 1972. Humic Substances in the Environment. Marcel Dekker, New York, N.Y. 327 pp.
- U.S. Environmental Protection Agency (USEPA), 1973. Methods for Identifying and Evaluating the Nature and Extent of Non-Point Sources of Pollutants. USEPA, Washington, D.C. 261 pp. (As referenced in Down and Stocks, 1977).
- U.S. Environmental Protection Agency (USEPA), 1976. Quality Criteria for Water. USEPA, Washington, D.C. 501 pp.

THAWING OF GROUND FROST ON A DRAINED AND UNDRAINED
BOREAL WETLAND SITEL. E. SWANSON AND R. L. ROTHWELL¹

ABSTRACT: A study of ground frost levels in a drained and undrained boreal wetland site near Slave Lake, Alberta showed significant delay of thaw as well as lower temperatures at 40 and 60 cm depths in the drained area. The undrained area froze to greater depths than the drained area but thawed more rapidly. In the lower hydraulic conductivity portion of the drained area, 16.7 % of the sample points retained ice throughout the summer and were still frozen at the time of ground re-freezing in the fall. Thickness of the frozen layer appeared to be related to hydraulic conductivity as well as drainage. Thawing from underneath the frozen layer accounted for 38 % of total thaw in the undrained area.

(KEY TERMS: peatland drainage, ground frost, soil temperatures.)

INTRODUCTION

Alberta contains extensive areas of forested and nonforested organic soils, the majority of which are located in the northern half of the province. These sites are characterized by surficial organic deposits 0.3-4.0 m deep and water table levels within 0.1-.3 m of the ground surface throughout most of the year. The thermal properties of surficial peats in these areas are highly variable, with water content being the principal determining factor. Thermal conductivity is very low in dry peat (0.105 J/m s °C), but is much higher in moist peat (0.432 J/m s

°C) and frozen peat (Lee, 1978). Moist conditions in autumn and winter promote heat transfer out of the soil, but drying of surficial peat in summer inhibits heat transfer into soil. This lowers mean annual soil temperature and promotes formation of zones of permafrost (Brown, 1977).

Discontinuous permafrost occurs in Alberta north of about 57° latitude (Fisheries and Environment Canada, 1978), however localized patches of permafrost may be found south of this boundary in areas where surface peats dry in summer (Zoltai, 1971; Brown, 1965). Because of the thermal imbalance caused by the insulating effect of dry peat, practices which cause the extreme drying of surficial peats, such as drainage for agriculture and forestry, could be expected to lower mean annual substrate temperatures, possibly promoting the formation of discontinuous permafrost south of established limits.

A study was conducted to evaluate the effect of drainage on freeze/thaw cycles and frost depth on a boreal wetland site. Because of the significant differences in thermal properties between wet and dry peat, it was hypothesized that freeze/thaw cycles should be significantly different between drained and undrained areas, with the thaw in the drained area being delayed due to lower soil temperatures caused by the insulating layer of dry surficial peat. It was also desired to know if frost depths and freeze/thaw cycles were related to the spacing of ditches or hydraulic conductivity within the drained area.

The site selected for study was a peatland fen complex located 36 km south-east of the town of Slave Lake, Alberta,

¹Respectively, Graduate Student and Professor, Department of Forest Science, University of Alberta, Edmonton, Alberta, Canada, T6G 2E2

55° 10' latitude. This area is characterized by forest cover of black spruce (*Picea mariana*), tamarack (*Larix laricina*) and bog birch (*Betula glandulosa*). Peat deposits range from 0 to 4 m in depth. In the spring of 1984 a peatland drainage project was implemented in the area by the Alberta Forest Service in which an area approximately 0.5 km² was drained. Ditch spacings of 25 m and 40 m were used, based on saturated hydraulic conductivity classes of the peat.

METHODS

Frost recession was determined as described by FitzGibbon (1981). This method involved augering through the frozen peat in spring to determine total frost thickness, then monitoring the recession of the upper frost boundary throughout the summer by probing. Probing was done with a 5 mm diameter rod which passed easily through the peat but did not penetrate a frozen zone. Sampling began May 9-12, 1985, prior to the start of frost recession. Measurements were obtained at 64 sites using an ice auger and probe. Depth to the upper frost boundary was measured by probing on a weekly basis throughout the summer season. Frost recession was judged completed when repeated probings and temperature measurements could not detect the presence of frost.

Sampling began May 9-12, 1985. Sample points were located in three distinct areas: the 25 m spacing zone; the 40 m spacing zone; and an adjacent undrained zone. Transects of 20 sample points (10 hollows, 10 hummocks) were established in each zone. Hummocks and hollows were 16 to 52 cm different in elevation and had unique microclimates and site characteristics. Beginning June 15, 1985 a second transect of 36 sample points (18 hollows, 18 hummocks) was established in each of the areas to determine if site disturbance from foot traffic affected earlier observations.

Substrate temperature profiles were measured at four hummocks and four hollows in each of the three areas. At each point, thermocouples were installed

at depths of 10, 15, 45, and 60 cm below the ground surface. Temperatures were recorded biweekly throughout the summer using a handheld digital multimeter and a small electronic reference junction. During July and August a datalogger was used to monitor diurnal temperature fluctuations. Temperatures were recorded at hourly intervals continuously for approximately one week at one hummock in each of the three zones.

Precipitation was monitored using a Belfort Universal rain gauge placed at the southern edge of the drained area. Water table levels were obtained from a network of recording water wells maintained by the Department of Geology, University of Alberta.

RESULTS

Water table height was 20 to 50 cm lower in the drained area than the undrained. Average water table levels for the summer were 55 and 20 cm below the ground surface for the drained and undrained areas respectively. Water table responses to precipitation in all areas were pronounced, with the return of the water table to prestorm levels occurring within 4-5 days. Summer rainfall (May to October) for 1985 was 207 mm, 40% lower than the 63 year average of 350 mm.

Probe surveys for total frost thickness in the three zones on May 9-10 showed average frost thicknesses in the 40 m spacing zone to be significantly less than in both the 25 m spacing or undrained zones (Scheffe's test, 0.05 level). Mean frost thicknesses were 41.6 cm in the undrained, 36.7 cm in the 25 m spacing and 22.4 in the 40 m spacing. Associated standard errors were 2.63, 2.68 and 2.63 respectively. Ice structure in the 40 m spacing was often granular, while in the 25 m spacing and the undrained zones layers of solid, concrete ice were evident.

Frost recession was most rapid in the undrained area. This was most evident in the hollows (Fig. 1). During the period May 10-June 13, 1985, average depth to the frost table decreased 16.9 cm in the undrained area hollows, versus 7.4 cm and 7.8 cm for the 25 and 40 m spacings

respectively. The corresponding averages for the hummocks were 17.5 cm, 11.8 cm, and 9.8 cm. Frozen soil was detected more frequently in the 25 m spacing zone throughout the summer (Fig.2) than in the other areas. At the onset of frost formation in early October, 16.7% of the sample points in the 25 m spacing still retained ice. In the undrained area frozen soil was found at 2.3% of the sample points at this date. Frozen soil was not detected in the 40 m spacing zone after September 10, 1985. Transects which were started in May showed a slightly higher thaw rate than those started in June, suggesting some trampling might have occurred while sampling.

Thermocouple readings indicated soil temperatures in the surface 10 cm were warmer in the drained area than in the undrained area. Midday peat temperatures at 10 cm depth in the drained areas were 0 to 4.4 °C warmer than in the undrained area for most of the summer (Fig. 3). It was only in late August that midday temperatures at 10 cm were warmer in the undrained area.

Soil temperatures below 10 cm were warmer in the undrained area than in the drained area throughout most of the summer (Fig. 3). The same trend was observed by Pessi (1958) in a drained peatland in Finland. Maximum temperature differences of 4.9 and 4.3 °C at 40 and 60 cm respectively occurred in late July.

The maximum diurnal temperature fluctuation was greater in the drained areas than in the undrained. Fluctuations of up to 20 °C in a single day were recorded in the drained areas at the 10 cm depth (Fig.4). In the undrained area amplitudes of only 4 °C were observed at 10 cm. At 25 cm depth diurnal fluctuations of 8 °C were recorded in the drained areas versus less than 1 °C in the undrained area. Temperature fluctuations at the 40 and 60 cm depths in all areas were small, rarely exceeding 1 °C/day.

Frost recession occurred from both above and below in all zones, with thaw from below accounting for as much as 38 % of total thaw in the undrained area. Table 1 shows the maximum depth of frost penetration as determined on May 9-10, as well as the total depth of thaw from above, and the resulting percentages of

thaw which must have occurred from above and underneath. The depth of thaw from above is the position of the frozen layer one week prior to total thaw. Percent thaw from above is (thaw from surface/initial depthx100), and percent from below is (100-percent thaw from above) and represents the proportion of the total thaw which occurred from beneath the frozen layer. The final frost depth a week prior to complete thaw is indicative of the total depth of thaw from above since, in most cases, the frozen layer was so thin at this point that it could be penetrated with the probe using only light finger pressure.

	Initial lower frost depth (cm)	Depth of thaw from above (cm)	Percent of thaw from:	
	Mean std. error	Mean std. error	above	below
Undr.	56.3 (2.98)	35.0 (2.43)	62%	38%
40 m	36.9 (2.69)	26.8 (2.34)	73%	27%
25 m	52.0 (2.93)	35.9 (2.51)	69%	31%

Table 1. Thaw from beneath the frozen layer; maximum depth of frost penetration in winter and total depth of summer thaw.

DISCUSSION

Frost recession was slower in the drained areas than in the undrained area because the dry surficial peat acted as a barrier to conductive heat transport into the soil. The effectiveness of dry peat as an insulator is well documented (Rigg, 1947; Benninghoff, 1952; Brown, 1963; MacFarland, 1969; Moore and Bellamy, 1974). Thermal conductivity of peat decreases greatly with reduced water content (Lee, 1978). Therefore heat transport into the dry surficial peat would be limited to convective processes (vapor diffusion and rainfall), which can be slow and are extremely difficult to measure (Brown, 1963).

Frost recession was most rapid in the undrained area, even though its ice thickness was greater than the drained areas. The faster recession was attributed to the higher water content and

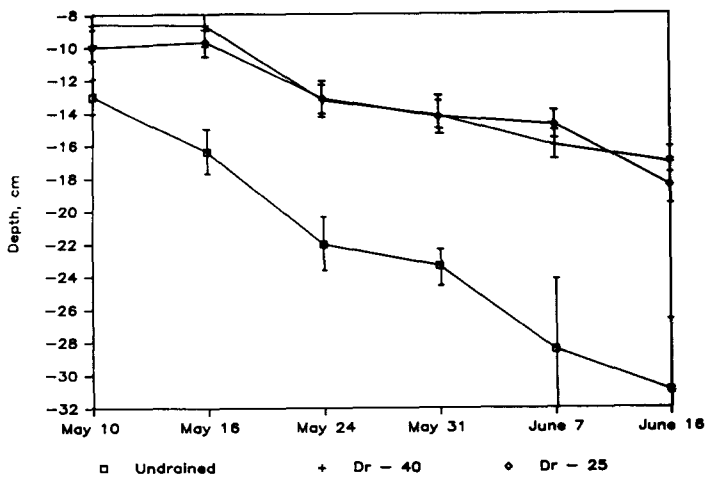


Figure 1. Frost recession rates in hollows for the undrained, drained - 40 m and drained - 25 m spacing areas.

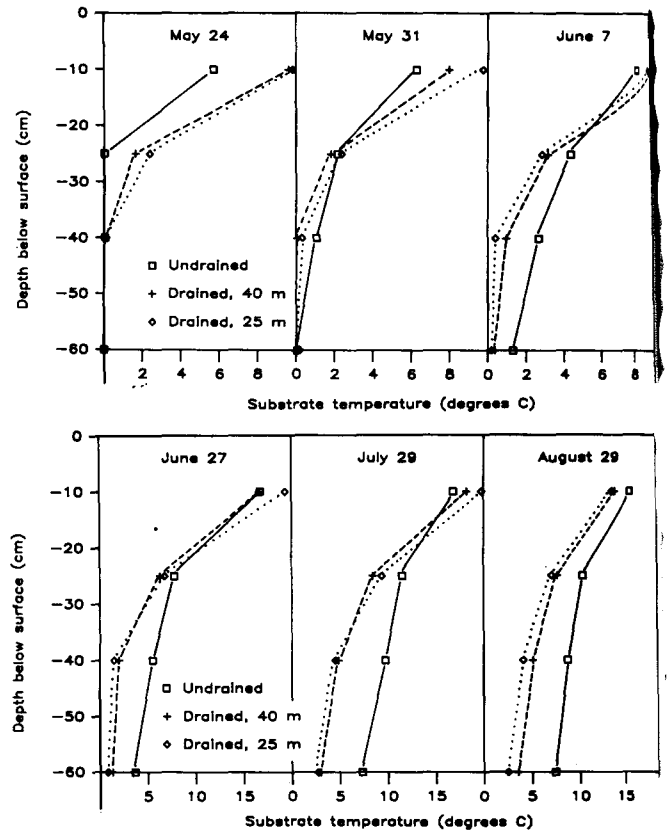


Figure 3. Midday substrate temperature profiles for various days throughout the summer, 1985.

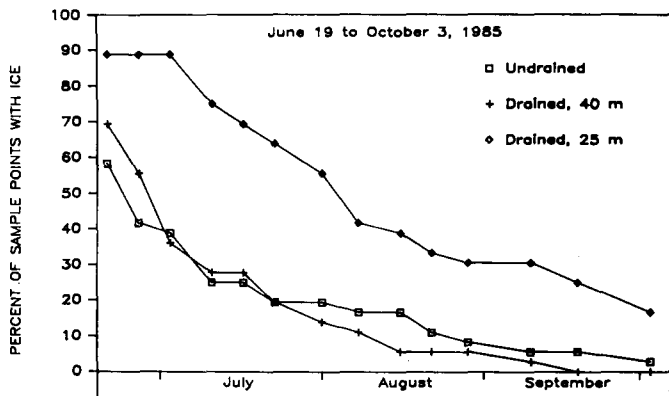


Figure 2. Frost recession shown as percentage of sample points in each area where ice was detected. Percentage is (number of sample points where ice was detected / total number of sample points) x100.

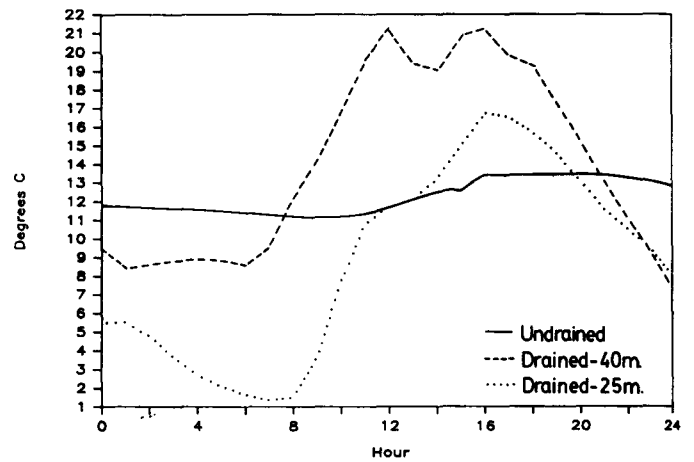


Figure 4. Diurnal temperature variation at 10 cm depth in the undrained, drained - 40 m and drained - 25 m spacing areas.

resultant higher thermal conductivity of the surface peat in the undrained area. Differences in water content of the surface peats between the drained and undrained areas were amplified by the unusually low rainfall levels observed during the study season. In the drained area the surface peat dried out as a consequence of lower water table levels, and rainfall events were too infrequent and too rapidly drained away to have any significant wetting effect. Higher water table levels in the undrained area were sufficient to maintain a moist layer of surface peat in spite of low rainfall levels.

Frost recession in the 40 m spacing area was more rapid than in the 25 m spacing. This occurred ostensibly because of less ice and lower frozen water contents in the 40 m spacing area. The ice in the 40 m spacing was thinner and appeared to be porous in structure, possibly because of the peat's higher saturated conductivity, which with drainage resulted in a rapid removal of water from the peat substrate. The more extensive ice in the 25 m spacing was in part attributed to its lower saturated conductivity which would lessen drainage and make more water available for freezing. Average saturated hydraulic conductivities for the 40 m and 25 m spacings were respectively .35 and .18 m/day (Toth, 1986).

The presence of remnant frost in the undrained area in early October (at 2.3 percent of the sample points) was attributed to low summer precipitation in 1985. Summer rainfall for 1985 (May-October) was 40% below the 63 year average for the Slave Lake region. As a result, some surface peat material in the undrained area dried out, albeit to a much lesser extent than occurred in the drained area. In a wetter year frost recession would probably occur earlier and at a faster rate on all sites because of latent and convective heat transfer (e.g. evaporation and precipitation) into the peat substrate.

Thawing of ground frost from above and below was evident in all of the study areas. As the study area is located in a fen complex, subsurface groundwater flow should be expected. FitzGibbon (1981) found 40% of thaw to occur from beneath

the frozen layer in a fen in Saskatchewan, whereas in a nearby bog (with no subsurface flow) no thaw from below was observed. FitzGibbon concluded that thaw from below was produced by heat exchange from groundwater. The lesser amounts of thaw from below in the drained areas compared to undrained in the present study (27.4 % and 31.0 % versus 37.8 % ; see Table 1) possibly was the result of less heat exchange with ground water in the drained area due to a lower water table.

Analysis of temperatures in this study reflected the same trends as observed for frost. Surficial peat temperatures in the undrained area at 10 cm were generally cooler than in the drained area. This is likely due to greater evaporation rates near the surface in the undrained area. Also, more heat energy is required to warm the peat in the undrained area due to higher water contents and hence higher specific heat and heat capacity. Temperatures and the rate of warming at lower depths (25-60 cm) were greater in the undrained area because of its higher thermal conductivity. The wide diurnal temperature fluctuations at 10 cm depth may be attributed to the reduced thermal capacity of the peat in the drained area.

The effects of evaporative cooling appeared to be restricted to the upper 10 cm. The undrained area was cooler at the surface due in part to greater evaporation rates, however at greater depths the higher thermal conductivity of the moist, albeit cool, surface peat in the undrained area resulted in higher temperatures at depth and more rapid thaw relative to the drained area. Evaporation played a more important role in drying of the surface peat, which lowered its thermal conductivity and restricted the flow of heat into the subsoil.

The results of this study contain implications for peatland management and utilization in Northern Alberta. The timing of frost recession and snowmelt runoff are of hydrological interest. Snow melt and associated runoff occur on average from mid to late April, when most peatlands are still frozen (Figure 5). The impermeable frost layers act as barriers to infiltration of snowmelt and recharge of peatlands. This explains the rapid snowmelt runoff from peatlands compared to more prolonged runoff from adjacent mineral

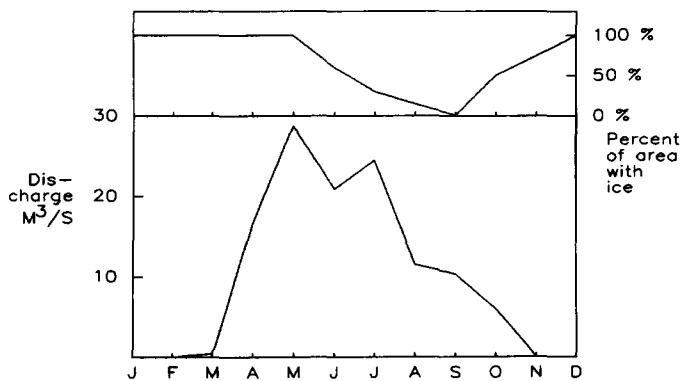


Figure 5. Seasonal runoff and frost occurrence at Saulteaux study area.

soil sites where infiltration is possible. Furthermore, it emphasizes the importance of summer precipitation as a source of recharge for peatlands and maintenance of peatland ecosystems.

Drainage of peatlands in Northern Alberta must be approached cautiously. A consequence of drainage will likely be the alteration of summer thermal regimen in the area, with surface layers warmer than the undrained condition but subject to much wider diurnal fluctuation, and temperatures at lower depths depressed below those of the undrained condition.

Drainage under conditions of shallow humic peats of low hydraulic conductivity could lower substrate temperatures enough to induce localized permafrost. The area chosen for this study is well south of both the established limits of discontinuous permafrost and the 0 °C mean annual air temperature isotherm, yet 16.7 % of the sample points in the 25 m spacing zone retained ice year-round. Permafrost occurring naturally in Northern Alberta is confined mainly to peatlands, specifically where drying of surface peat occurs in summer (Brown, 1977). One would suspect that peatland drainage, which causes the drying of surface peat, could easily induce permafrost formation in this region. Further study is needed to verify specific effects of drainage on thermal regimen, for example with respect to peat type and local hydrology.

The production of localized permafrost would be detrimental to the objectives of drainage for agriculture and forestry. A frozen layer near the surface would inhibit root penetration and reduced

temperatures would slow metabolic activity. The significance of alterations to thermal regime caused by drainage needs to be investigated relative to silvicultural and horticultural requirements of species planned for management on peatlands.

REFERENCES

- Benninghoff, W. S., 1952. Interaction of Vegetation and Soil Frost Phenomena. *Artic* 5:34-44.
- Brown, R. J. E., 1963. Influence of Vegetation on Permafrost. *Proc. Int. Conf. Permafrost, Lafayette, Ind.*
- Brown, R. J. E., 1965. Permafrost Investigations in Saskatchewan and Manitoba. *Nat. Res. Council, Dev. Bldg. Res., Tech Paper 193.*
- Brown, R. J. E., 1977. Muskeg and Permafrost. In: *Muskeg the Northern environment in Canada*, N. W. Radforth and C. O. Brawner ed. University of Toronto press. pp. 148-163.
- FitzGibbon, J. E., 1981. Thawing of Seasonally Frozen Terrain in Central Saskatchewan. *Can J. Earth Sci.* 18:1492-1496.
- Fisheries and Environment Canada, 1978. *Hydrologic Atlas of Canada*. Printing and Publishing, Supply and Services Canada.
- Lee, R. 1978. *Forest Microclimatology*. Columbia University Press, New York.
- MacFarlane, I. C. (ed.), 1969. *Muskeg Engineering Handbook*. Univ. of Toronto press.
- Moore, P. D., and D. J. Bellamy, 1974. *Peatlands*. Springer - Verlag, New York.
- Pessi, Y., 1958. On the Influence of Bog Draining Upon Thermal Conditions in the Soil and in the Air Near the Ground. *Acta Agric. Scand.* 8:359-374.
- Rigg, G. B., 1947. Soil and Air Temperatures in a Sphagnum Bog of the Pacific Coast of North America. *Am. J. Bot.* 34:462-469.
- Toth, J. 1986. Personal communication. Department of Geology, University of Alberta, Edmonton, Alberta.
- Zoltai, S. C., 1971. Southern Limit of Permafrost Features in Peat Landforms, Manitoba and Saskatchewan. *The Geological Assoc. of Canada, Special paper no. 9*, pp. 305-310.

PROBABILITY DISTRIBUTIONS OF RAIN ON SEASONALLY FROZEN SOILS

John F. Zuzel¹

ABSTRACT: A method to quantify daily rainfall amounts associated with different antecedent conditions and the relationships between daily rainfall, frozen soil, snow on the ground and runoff are presented. The procedure incorporates a daily soil frost simulation model which predicts the presence or absence of soil frost from daily weather records with algorithms for extracting rain and rain-on-snow events in the presence or absence of frozen soil from these same records. The presence or absence of soil frost was simulated for a 30 yr period using National Weather Service records for Moro, Oregon. Model output was used to characterize the occurrence of soil frost at the test site and as input to the algorithm for classifying daily precipitation events. Probability distributions for rain and rain on snow in the presence or absence of soil frost are presented. Rain-on-snow events were associated with 57% of the yearly peak discharges at a nearby crest gage. Daily precipitation amount and snow depth jointly accounted for 72.6% of the variance in runoff peaks at the crest gage site.

(KEY TERMS: soil frost, simulation models, frequency analysis, rain on snow, winter runoff.)

INTRODUCTION

Occurrence of frozen soils is an extremely important consideration in understanding runoff and soil erosion in mid-latitude climates characterized by low winter temperatures and shallow transient snowpacks. Rain on snow in the presence or absence of frozen soil or rain on frozen ground have been factors in many significant floods in the Pacific Northwest region (Johnson and McArthur, 1973).

Soil frost or frozen soil occurs when the surface freezes and moisture migrates from the deeper soil layers to the freezing front and then freezes.

Infiltration rates in frozen soil are determined partly by the structure of the soil frost and the soil water content at the time of freezing (Storey, 1955). Trimble et al., (1958) proposed four terms to describe soil frost structure: granular, honeycomb, stalactite, and concrete. Concrete frost has a dense structure resulting in a very low permeability and is the most common type of soil frost formed in bare agricultural soils (Storey, 1955; Trimble et al., 1958). In contrast, the loose porous structure of granular frost allows water to infiltrate readily.

In an infiltration experiment in northeast Oregon, Pikul et al., (1985) reported no infiltration in a fall seeded Walla Walla silt loam (Typic Haploxeroll, coarse-silty, mixed, mesic) winter wheat (*Triticum aestivum* L.) plot with 13 cm of concrete frost present. In contrast, an infiltration rate of 3 cm per day was observed when the soil was not frozen. In a forest soil, Kane and Stein (1983) reported an infiltration rate of about 17 cm per day in a low total moisture content, frozen, Fairbanks silt loam.

In parts of the Pacific Northwest east of the Cascade Mountains and in parts of the Intermountain West, concrete frost is characteristically formed on bare agricultural soils; thus frozen soils play a major role in runoff production, soil erosion, and sedimentation.

The study reported here was conducted using historical and recent field data near Moro, Oregon (Figure 1), in the southern portion of the Columbia Plateau (USDA, 1981). The area is characterized by humid winters and dry summers with relatively low rainfall intensity, usually less than 4 mm per hour (Horner et al., 1957). Average annual precipitation for Moro is 288 mm of which 70% occurs during the November through April period. The winter climate is also characterized by a shallow transient snow pack subject to several accumulation and melt cycles each

¹Hydrologist, U.S. Department of Agriculture, Agricultural Research Service, Columbia Plateau Conservation Research Center, P.O. Box 370, Pendleton, Oregon, 97801.

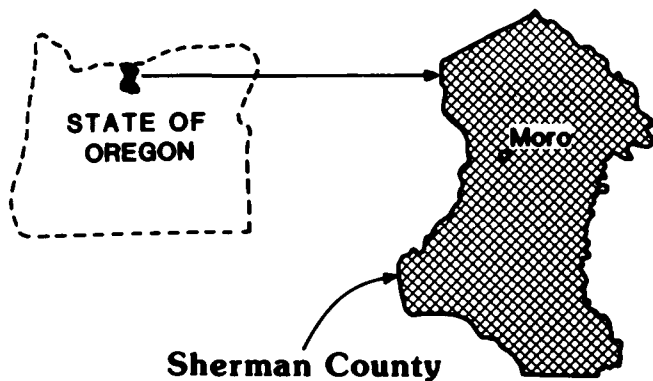


Figure 1. Location of the study site in northcentral Oregon.

winter. Frozen soils are common and occur nearly every year. The winter runoff from steeply-sloping croplands and rangelands in the Pacific Northwest can result in serious soil erosion and sedimentation and can be the major flood producing mechanism in some watersheds. Quantitative descriptions of the rainfall amount and frequency associated with winter runoff events are lacking and are essential for more accurate predictions of runoff, soil erosion and sedimentation. The objectives of the research reported here were to quantify daily rainfall amounts associated with different antecedent conditions and to investigate the relationships between daily rainfall, frozen soil, snow on the ground and runoff.

METHODS

Daily weather data, including maximum and minimum air temperatures, precipitation, snowfall and snow on the ground were obtained from National Weather Service records for Moro, Oregon for 1948 through 1978. Missing data were estimated from the nearest weather station record which contained the necessary variable. Also, crest gage data for 1959 through 1978 for Gordon Hollow at DeMoss Springs, Oregon, were obtained from the U.S. Geological Survey, Water Resources Division records. The crest gage records contained only the water year peak discharge so lesser peaks that occurred during the period of record were not available. The crest gage site was located 2 km north of Moro, Oregon, and has a drainage area of approximately 23 km². Elevation of the basin varies from 475 to 664 m while the elevation of the Moro weather station is 560 m.

During each of the five winters of 1980 to 1984, plot runoff, soil erosion, weather variables, soil

temperatures, and soil frost were monitored in farm fields located near Moro, Oregon (Figure 1). Each year a different site was instrumented because the cropping practice in this area is to seed winter wheat every other year in a particular field. In alternate years, these fields are not tilled after harvest but remain covered with crop residue over winter. In the fall of the seeding year, the fields are tilled and planted to winter wheat; the surface residue and plant cover is minimal during these winter seasons. This procedure produced soil frost data from plots with similar surface conditions for between year comparisons. All sites were within 2 km of the Moro weather station. Each site was instrumented to continuously record air temperature and relative humidity at 1 meter above the surface. Precipitation and soil temperature at about 5 cm below the soil surface were also monitored (Zuzel et al., 1982). Daily solar radiation was monitored at the calibration site in 3 of the 5 test years. Frost depth was measured weekly or more often using frost tubes (Ricard et al., 1976). Visual determination of soil frost by hand sampling was also performed as needed to provide a check on frost tube measurements. Snow depth and snow water equivalent were measured weekly using procedures for sampling very shallow snow (USDA, 1973). This field data set was used to verify a daily soil frost simulation model which predicts the presence or absence of soil frost from daily weather records. The soil frost model was described by Cary (1982) and the required inputs are maximum and minimum air temperature, snow depth and solar radiation. The model predicts net daily heat flux across the soil surface. The cumulative daily heat flux is then used to predict the presence or absence of soil frost. Negative values of cumulative soil heat indicate the presence of soil frost while positive values indicate an unfrozen soil. Since solar radiation is not included in daily weather records, a method was developed to predict daily values of solar radiation from potential radiation and daily air temperature range.

The model requires an initial value of soil heat at the beginning of each yearly run and an empirical, site specific constant which accounts for the effects of cover and other soil physical properties. The site constant was obtained by maximizing the number of days the model correctly predicted the presence or absence of soil frost over a 5-year field calibration period using the 1980-1984 field data set for input and validation. Initial soil heat was estimated using the average soil temperature and heat capacity of the top 30 cm of soil.

Soil frost for a 30-year period (1948-1978) was then simulated using National Weather Service records for Moro, Oregon. Daily maximum air temperature,

minimum air temperature and snow on the ground for November through March, 1948 to 1978 were used in the simulation. The field verified site constant and initial soil heat were not varied from year to year. Model output was used to characterize and quantify soil frost at the Moro site and as input to the algorithm for classifying precipitation events.

Precipitation events were classified as: 1) rain on snow, soil frozen; 2) rain on snow, soil thawed; 3) rain on frozen soil, no snow; and 4) rain on unfrozen soil, no snow. The algorithm used to classify the precipitation events is presented in Figure 2.

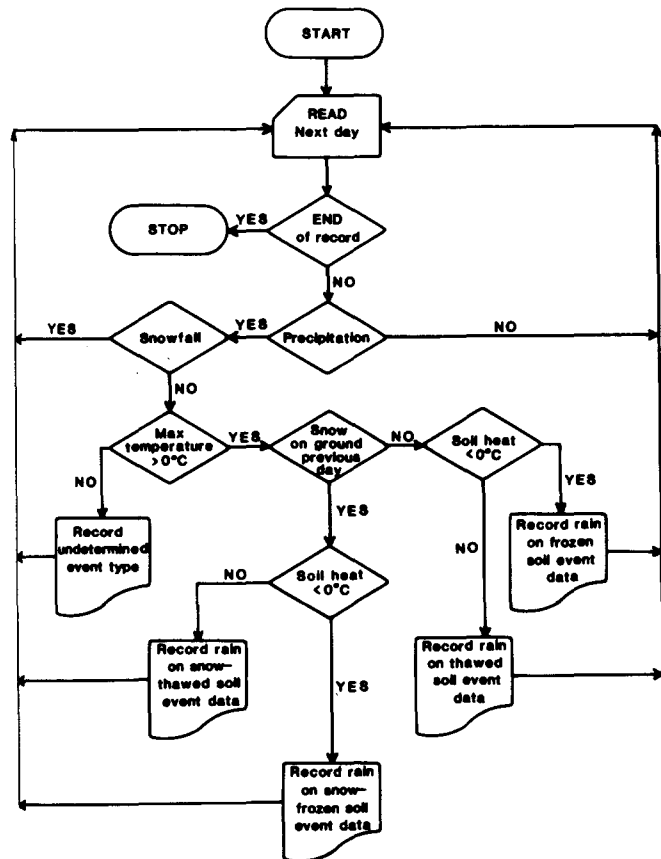


Figure 2. Flowchart of the algorithm used to classify types of precipitation events from weather records and cumulative soil heat.

The conditions which must be met for a rain-on-snow event to have occurred are that precipitation has occurred but snowfall has not; the maximum air temperature was greater than 0°C; and snow was present on the ground the previous day. The conditions which must be met for a rainfall event to have occurred are that precipitation has occurred but

snowfall has not, the maximum air temperature was greater than 0°C and snow was not present on the ground the previous or current day. In both cases, the cumulative soil heat is used to determine whether the soil is frozen or not. The undetermined event type occurs when precipitation was not recorded as snowfall and the maximum air temperature was less than 0°C (Figure 2). This situation can be interpreted as freezing rain or sleet which is a fairly common occurrence in the Pacific Northwest. It is also possible that this event type simply reflects an error in the historical record.

Probability distributions for the maximum annual series of rain on snow and rain on bare ground were fit to theoretical distributions for both the frozen soil and thawed soil cases. The events produced by the algorithm were correlated with the crest gage record from Gordon Hollow at DeMoss Springs, Oregon. The dates of peak discharge listed in crest gage records are not always exact, so detailed examination of weather records was necessary to determine or confirm the date of the peak in all cases.

RESULTS AND DISCUSSION

For the 1980-1984 calibration period, a site constant of 1.0 and an initial soil heat of 4190 kJ/m² produced the maximum number of correct predictions of the presence or absence of soil frost when compared to the field observations. Overall, the model correctly predicted the presence or absence of soil frost 80 percent of the time for the 5 year calibration period (Table 1).

Model output for the 30 year weather record at Moro, Oregon suggests that frozen soil occurs every winter at this site. The soil was frozen from 6 to 116 days per year with an average of 57 days per year. Freeze-thaw cycles (other than diurnal cycles) varied from 1 to 7 cycles per year.

The distribution of predicted soil frost by months shows that historically, January has the highest incidence of soil frost; the soil was frozen 67% of the time. Also, model output indicates that the soil was frozen more than 50% of the time in both December and February.

Between 6 and 116 days per year of frozen soil can be expected at Moro, Oregon. The results of the simulations for number of frozen soil days per year were fitted to a normal distribution (Figure 3). The estimated parameters of the distribution are also shown in Figure 3.

In order to test the goodness of fit of the normal distribution, a correlation analysis was performed using the exceedance probabilities derived

TABLE 1. Topographic characteristics of sites near Moro, Oregon used to verify the frost prediction model.

Site and winter number	Elevation (meters)	Year	Slope (percent)	Aspect (degrees)	Frost prediction ^{1/} (percent)	Distance from Moro weather station (km)
1	561	1979-1980	14	S40W	83	0
2	567	1980-1981	11	S61W	82	.5
3	539	1981-1982*	24	N65E	91	2
4	539	1982-1983*	24	N65E	63	2
5	539	1983-1984*	24	N65E	80	2

^{1/}Percent of days between 1 November and 31 March in which frost occurrence was correctly predicted.

* Same site.

from model output and the theoretical exceedance probabilities. This test yielded a correlation coefficient of 0.976. The chi square test indicated that the hypothesis of a normal distribution could not be rejected at the 5% significance level. An obvious difference between the distributions exists in the lower tail because the theoretical distribution is unbounded while the model derived data has a lower

bound of 6. From these analyses we concluded that the normal distribution can, with the indicated parameters (Figure 3), be used to represent the simulation model distribution for the number of frozen soil days per year.

Analysis of the Moro weather record using the algorithm shown in Figure 2 produced the results presented in Table 2. A rain-on-snow event with either frozen or thawed soils occurred in 28 of the 30 years of record at this location; a probability of occurrence in any year of 0.93. Rain on frozen soil in the absence of snow cover occurred in 25 of the 30 years ($P=0.83$). Rain on snow with frozen soil had an occurrence probability of 0.73, while rain on snow with thawed soils had a probability of 0.57 (Table 2).

The annual series of maximum precipitation for each year of occurrence were extracted for all event types except the undetermined. Summary statistics are presented in Table 3. Because all of the annual series are noticeably skewed, the data were fit to the lognormal, gamma, and 3-parameter lognormal distributions. The 3-parameter lognormal distribution produced the best fit in all cases. Goodness of fit was subjectively judged by comparing observed data parameters with parameters obtained using data generation techniques. Goodness of fit was statistically assessed using the chi-square statistic with 10 class intervals defined so that the expected number of observations in each class interval was the same. The hypothesis that the 3-parameter lognormal distribution describes the data could not be rejected for any of the event types at the 5% significance

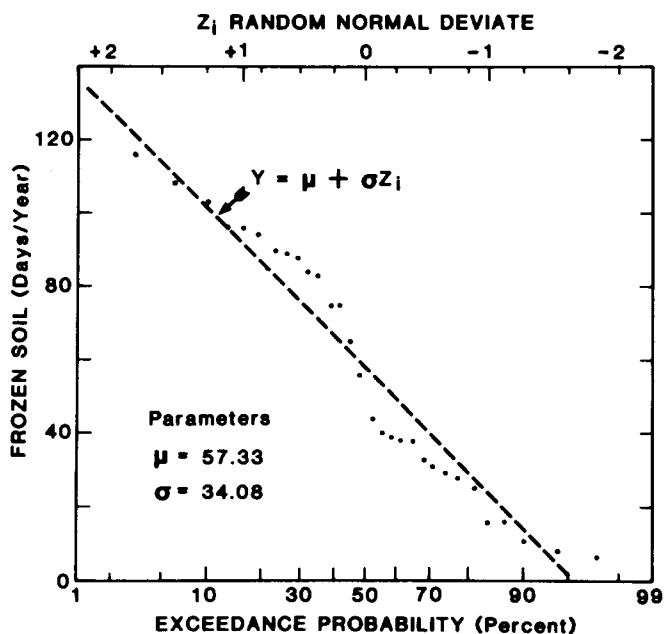


Figure 3. Cumulative frequency and fitted theoretical distribution of the number of frozen soil days per year at Moro, Oregon.

TABLE 2. Results of daily rainfall event classification for Mono, Oregon for the November-March time period, 1948-1978.

Event type	Number of Events		
	Frozen soil	Thawed soil	Total
Rain	259 (.83)	829 (1.00)	1088 (1.00)
Rain-on-snow	95 (.73)	38 (.57)	133 (.93)
Undetermined	---	---	39

Numbers in parentheses indicate the probability of occurrence in any year.

while the distribution for rain on thawed soils in the absence of snow can be described by:

$$Y = (e^{3.23221 + .30419Z} - 10.525) \quad (4)$$

Equations such as 1 through 4 can be used directly to generate daily precipitation amounts using Monte Carlo simulation. This is done by allowing Z to deviate randomly. The simulated data can then be used as inputs for physically based runoff, erosion and sediment models.

The crest gage data analysis for Gordon Hollow provided an estimate of the precipitation amount necessary to produce runoff as well as suggesting the relationships between runoff peak, snow on the ground, and daily rainfall amount. The gage had been in operation since 1959 and of the 20 yearly peak discharges recorded through 1978, five years had no

TABLE 3. Summary statistics for 8 rain-on-snow runoff events at Gordon Hollow at DeMoss Springs, Oregon.

Variable	Mean	Median	Std. Dev.	Max.	Min.	r
Precipitation (mm)	14.98	13.97	8.74	32.00	5.3	0.890
Average Air Temperature (°C)	4.87	4.50	1.96	8.00	3.0	-0.318
Maximum Air Temperature (°C)	8.62	8.00	2.88	12.00	4.0	-0.147
Antecedent snow on ground (cm)	6.87	3.00	7.72	25.4	2.5	0.637
Peak Discharge (m ³ /sec)	9.1	4.3	10.4	27.9	1.2	1.00

level. The theoretical and observed distributions for rain on snow with thawed soil, rain on snow with frozen soil, rain on frozen soil, and rain on thawed soil are presented in Figures 4 through 7. The cumulative frequency distribution for rain on snow with thawed soils is:

$$Y = 0.57 (e^{2.14767 + 0.61338Z} - 4.825) \quad (1)$$

where Y is maximum precipitation (mm) and Z is a standard normal deviate. The distribution for rain on snow with frozen soils is:

$$Y = 0.73 (e^{2.89757 + 0.39667Z} - 10.39) \quad (2)$$

and for rain on frozen soil in the absence of snow:

$$Y = 0.83 (e^{2.67804 + 0.51327Z} - 6.964) \quad (3)$$

flow, one peak discharge occurred in June and 14 occurred during the November through March period. The analysis showed that 8 of these 14 events (57%) were the result of rain on snow while the remaining 6 events were the result of rain with no snow cover. Moreover, the soil was frozen during 7 of the 8 rain-on-snow events and frozen during 1 of the rainfall events. Peak discharges ranged from 1.2 to 27.9 m³/sec with a mean of 9.1 m³/sec, while precipitation ranged from 5 to 32 mm with a mean of 15.0 mm. Statistics of the rain-on-snow runoff events are shown in Table 3 as well as the correlation coefficients for each variable with peak discharge.

A regression analysis using antecedent snow on the ground and precipitation amount as independent variables and peak discharge as the dependent variable produced the results shown in Table 4. Average air temperature and maximum air temperature were also included to show the relative importance of these variables in rain-on-snow events. It should be noted that while both antecedent snow on the ground

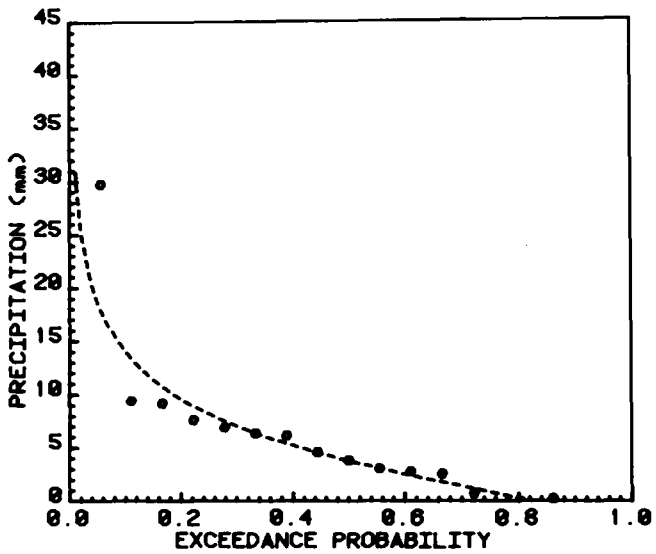


Figure 4. Cumulative frequency and fitted theoretical distributions of the annual series for rain on snow with thawed soils.

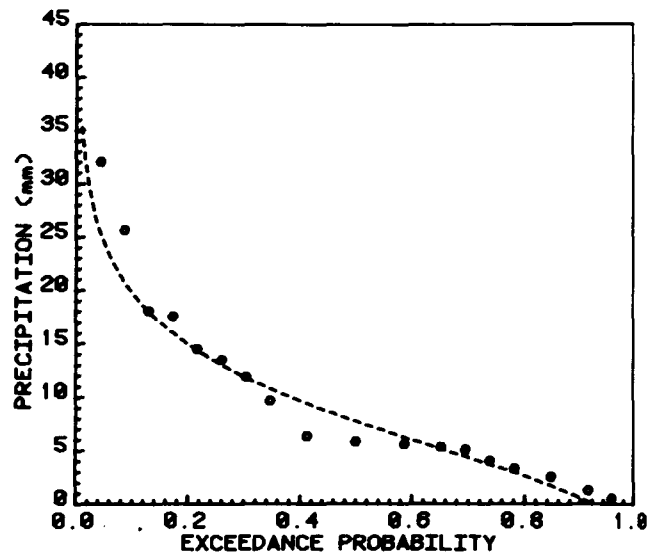


Figure 5. Cumulative frequency and fitted theoretical distribution of the annual series for rain on snow with frozen soils.

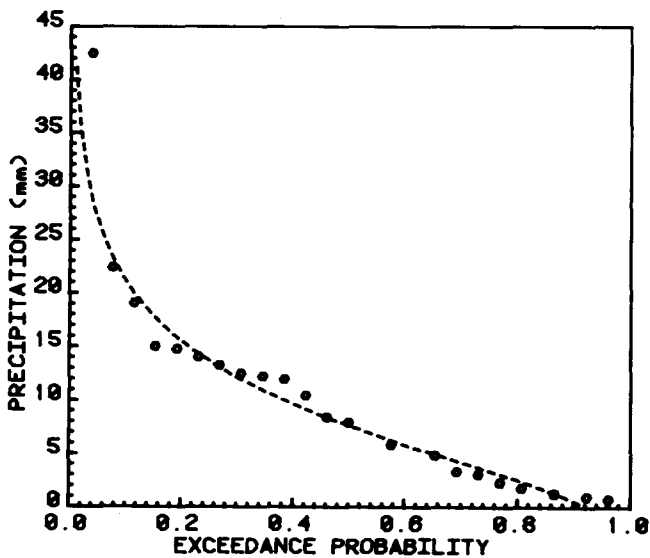


Figure 6. Cumulative frequency and fitted theoretical distributions of the annual series for rain on frozen soils in the absence of snow cover.

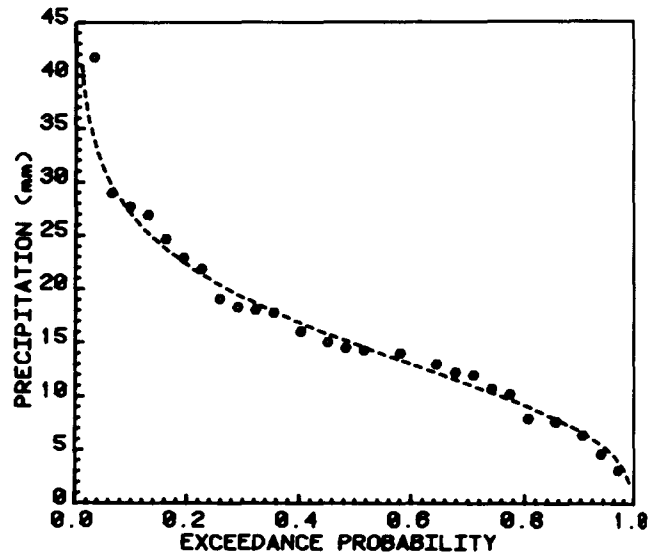


Figure 7. Cumulative frequency and fitted theoretical distribution of the annual series for rain on thawed soils in the absence of snow cover.

and precipitation each explain a significant percentage of the observed variation in peak flow, the combination of both does not increase explained variance to a significant degree. This is probably because the values of snow on the ground are concentrated at 3 to 5 cm. If more snow data in the mid and higher ranges were available, snow on the ground would probably assume more significance.

TABLE 4. Coefficients of determination for 2 independent variables on peak discharge at Gordon Hollow near DeMoss Springs, Oregon.

Variable	r ²
Antecedent snow on ground (cm)	40
Precipitation (mm)	79
Both	80
Average Air Temperature (°C)	10
Maximum Air Temperature (°C)	2

SUMMARY AND CONCLUSIONS

A daily soil frost simulation model which predicts the presence or absence of soil frost from daily weather records was combined with algorithms for extracting rain and rain-on-snow events in the presence and absence of frozen soils from these same records. Overall the soil frost portion of the model correctly predicted the presence or absence of soil frost 80 percent of the time for a 5-year (1 November to 31 March) calibration period.

Soil frost for a 30-year period was simulated using National Weather Service historical daily weather records for Moro, Oregon; within 2 km of the field calibration site. Daily maximum air temperature, minimum air temperature, and snow on the ground for November through March, 1948 to 1978 were used in the simulation. The field verified site constant and initial soil heat were not varied from year to year. Model output was used to predict soil frost at the Moro site and as input to the algorithm for classifying daily precipitation events.

Results showed that historically, frozen soils occurred every year and the soil was frozen an average of 57 days per year. The highest incidence of frozen soil occurs during January when the soil was frozen 67 percent of the time followed closely by February (53%) and December (51%). The number of freeze-thaw cycles other than diurnal cycles varied from 1 to 7 per year with an average of 3 per year for the simulation period. Frequency distributions

of the number of days per year with frozen soils were fit to a normal distribution.

Event analysis produced 133 rain-on-snow events of which 95 occurred while the soil was frozen. Rain on snow occurred in 28 of the 30 years of record at this location (P=0.933). The average number of events per year was four. However, the amount of precipitation was less than 2.5 mm for 50% of these events. Rain-on-snow events were associated with 57% of the yearly peak discharges at a nearby crest gage in operation from 1959 through 1978. Daily precipitation amount and snow depth jointly accounted for 72.6% of the variance in runoff peaks at this site. Probability distributions for rain on snow and rain on frozen ground were fit to three parameter lognormal distributions for both the frozen soil and thawed cases.

The model described in this paper is simple, easy to use and requires only the readily available input data of daily maximum and minimum air temperature, precipitation, snowfall and snow on the ground. It can be used in any area where a complete historical weather record is available to estimate the parameters of the probability distributions. Model output should prove useful in runoff and erosion prediction and in the design of erosion control, water conservation and drainage facilities. Equations 1-4 can be used directly to generate daily precipitation inputs for physically based runoff, erosion, and sediment production models. Freeze-thaw cycle information can be used in planning structures or roadbeds in areas where frost heaving is a potential problem.

REFERENCES

- Cary, J. W. 1982. Amount of soil ice predicted from weather observations. *Agric. Meteorology* 27:35-43.
- Horner, G. M., W. A. Starr, and J. K. Patterson. 1957. The Pacific Northwest wheat region. In *Soil, The Yearbook Of Agriculture*. U.S. Dept. Agr., Washington, D.C., pp. 475-481.
- Johnson, C. W. and R. P. McArthur. 1973. Winter storm and flood analyses, Northwest Interior. In *Proc. Hyd. Div. Spec. Conf. Hydraulic Engineering and the Environment*. Am. Soc. Civil Eng., pp. 359-369.
- Kane, D. L. and J. Stein. 1983. Water movement in seasonally frozen soils. *Water Resources Res.* 19:1547-1557.
- Pikul, J. L., Jr., J. F. Zuzel, and R. N. Greenwalt. 1985. Water infiltration in frozen soil. In *Columbia Basin Agricultural Research, Oregon*

- Research Experiment Station Special Report 738, pp. 6-11.
- Ricard, J. A., W. Tobiasson, and A. Greutorex. 1976. The field assembled frost gage. Tech. Note. Cold Regions Res. Eng. Lab. Corps of Eng., U.S. Army, Hanover, New Hamp., 7 pp.
- Storey, H. C. 1955. Frozen soil and spring and winter floods. In Water, The Yearbook of Agriculture, U.S. Dept. Agr., Washington, D.C., pp. 179-184.
- Trimble, G. R., Jr., R. S. Sartz, and R. S. Pierce. 1958. How type of soil frost affects infiltration. J. Soil and Water Conserv. 13:81-82.
- U.S. Dept. of Agriculture. 1973. Snow survey sampling guide. Agr. Handbook 169. Washington, D.C., pp. 26-27.
- U.S. Dept. of Agric. 1981. Land Resource Regions and Major Land Use Resource Areas of the United States. Agr. Handbook 296, Washington, D.C., pp. 6-7.
- Zuzel, J. F., R. R. Allmaras, and R. Greenwalt. 1982. Runoff and soil erosion on frozen soils in northeastern Oregon. J. Soil and Water Cons. 37(6):351-354.

EVIDENCE OF GROUNDWATER RECHARGE THROUGH FROZEN SOILS AT ANCHORAGE, ALASKA

James A. Munter¹

ABSTRACT: Three water-level observation wells located within the Municipality of Anchorage, Alaska have exhibited distinctive and anomalous water-level rises during January 1985, in conjunction with mid-winter thaws accompanied by precipitation events. One of the wells exhibited similar behavior during January, 1984. The magnitude of the rises is about 20-60 percent of the total annual water level fluctuation of each well. The surficial geologic materials near each well are at least moderately permeable under thawed conditions but are frozen near the land surface during the January events. The data suggest that the absence of available water may be the primary reason for the absence of groundwater recharge in areas where soils are frozen during part of the year, rather than the reduced permeability of frozen soils.

(KEY TERMS: recharge; frozen soils; groundwater; Anchorage; Alaska.)

INTRODUCTION

Groundwater recharge is poorly understood in many geological and climatological environments, yet is of importance for many applications, including water-supply assessment, runoff or flood forecasting, and waste-disposal evaluation. The rate of groundwater recharge is influenced by seasonally frozen soils in areas where several months of subfreezing temperatures occur. Zenone and Anderson (1978) suggest that frozen soils can act

"as a relatively impermeable barrier that temporarily restricts ground-water recharge". Kane and Stein (1983) demonstrated that the rate of infiltration is based on soil texture and total soil moisture (water and ice) conditions, with high ice-content soils having a relatively low permeability. Because low ice-content or fractured frozen soils may occur in many settings, the process of groundwater recharge through frozen soils is of considerable interest. In this paper, the geologic and climatologic conditions surrounding anomalous mid-winter episodes of rising water levels in three observation wells within the Municipality of Anchorage, Alaska, are presented. Examination of these conditions may prove useful for evaluating groundwater recharge processes in other areas.

OBSERVATION WELLS

Three water-level observation wells within the Municipality of Anchorage are described in this paper (fig. 1). The Potter Marsh wells were drilled in 1984 as observation wells for the Alaska Division of Geological and Geophysical Survey (DGGs) under a contract with a local water-well driller, and the Ravenwood well was drilled in 1983 as a water-supply exploration hole by a driller contracted by the Anchorage School District.

¹Hydrogeologist, Alaska Department of Natural Resources, Division of Geological and Geophysical Surveys, P.O. Box 772116, Eagle River, Alaska 99577.

TABLE 1. Log of Ravenwood Observation Well.

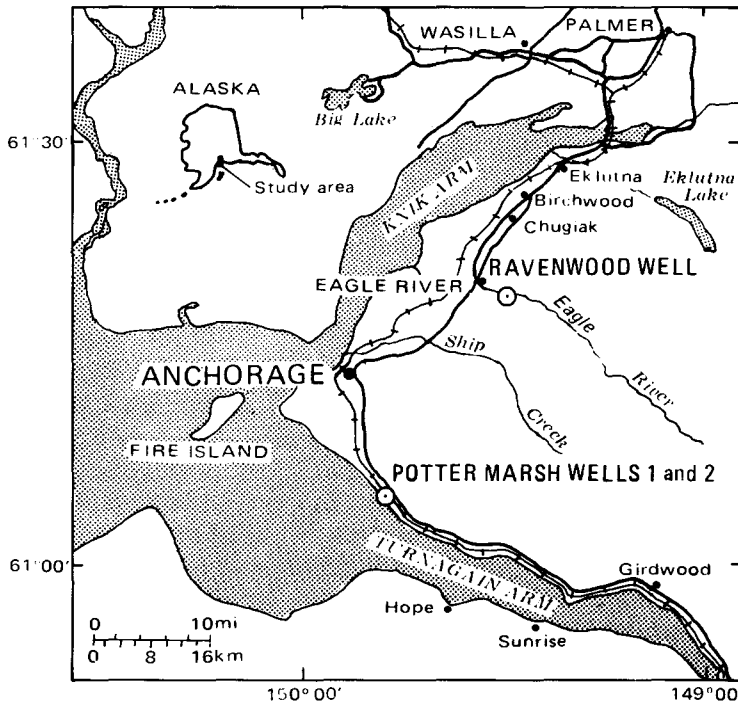


Figure 1. Locations of observation wells.

Ravenwood Well

The Ravenwood well was drilled on a bench-like ground moraine deposit composed principally of diamicton (Schmoll and others, 1980) that is 118 m in elevation above the Eagle River at its closest point. Surface runoff in the vicinity of the well occurs at a low rate because of the mostly forested conditions, but follows the land surface towards the Eagle River, located 900 m south of the well. A driller's log of the well, with casing data, is presented in Table 1. Two relatively shallow intervals in the well were screened and tested.

The depth of the well was sounded during 1984 and 1985, and was found to be 13.4 m, suggesting that sediments had infiltrated into the well during test pumping, and had not been removed. The well was successfully slug-tested to assure its adequacy as a reliable observation well.

The aquifer tapped by the Ravenwood well, called the Ravenwood aquifer by Munter (1984), has also been tapped by

Depth interval (m)	Material description
0.0-0.3	Organic topsoil
0.3-3.7	Silty gravel-loose
3.7-6.1	Gravelly silt
6.1-11.0	Silty gravel with water, 2.2×10^{-2} l/s \pm
11.0-13.7	Gravelly silt, hard
13.7-14.6	Sandy gravel with water, 2.2×10^{-1} l/s \pm (screened)
14.6-16.5	Gravelly silt, hard
16.5-17.4	Silty gravel with water 8.8×10^{-3} l/s \pm (screened)
17.4-18.6	Gravelly silt, hard
18.6-26.5	Gravelly silt, hard 8.8×10^{-3} w/seepage 3.5×10^{-2} l/s
25.6-87.8	Gravelly silt, hard to silty sand, some with water seepage
87.8	Boulder, casing stopped driving
87.8-107.6	Gravelly silt, hard
107.6-109.1	Sandy gravel with water - won't stand open

Depth interval (m)	Casing information
0.0-13.1	15 cm ID steel casing
13.1-14.6	No.100 slotted screen (2.54mm slot openings)
14.6-16.2	13cm ID steel casing
16.2-17.7	No.100 slotted screen (2.54mm slot openings)
17.7-18.3	13cm ID steel casing
18.3-26.8	Steel casing, backfilled with clean gravel
26.8-29.9	Steel casing, backfilled with cement grout
29.9-87.8	Steel casing, backfilled with silty gravel

Well completed March 29, 1983.

other residential wells in the vicinity. The aquifer is relatively flat-lying, with the thickness of the overlying confining unit increasing to about 30 m to the

north, toward the Eagle River valley margin. The Ravenwood aquifer is a few meters, or less, thick. A zone of ground-water discharge from the Ravenwood aquifer occurs about 300 m southeast of the Ravenwood well, where the land surface drops steeply to the river level and the Ravenwood aquifer is inferred to subcrop beneath the surficial soil mantle.

The sediments overlying the Ravenwood aquifer are described as moderately well drained to moderately poorly drained, with low surface runoff by Zenone and others (1974). Numerous single-family domestic septic systems operate in the vicinity of the Ravenwood well without apparent difficulty, suggesting that the surficial diamicton deposits in the area have at least moderate permeability under thawed conditions.

Potter Marsh Wells 1 and 2

The Potter Marsh wells 1 and 2 are located on artificial fill between the Old Seward Highway and Potter Marsh in south Anchorage (fig. 1). The geologic materials near the wells are of highly variable composition, from dominantly silty to dominantly gravelly fill, and are fairly level and well drained at an elevation about 10 m above the level of the marsh. The wells are about 2 m apart, about 5 m from the road ditch of the Old Seward Highway, and about 80 m from Potter Marsh.

A small tributary to Potter Marsh passes within about 100 m of the well site, and is about 3-4 m lower in altitude than the land surface at the well site. The wells are located outside of a small alluvial fan associated with the stream, suggesting that streamflow does not directly affect water levels in the wells. The wells were drilled with an air rotary drilling rig, and logs are shown in Table 2 and Table 3.

The abundance of dark grey silt in the sediments penetrated by well 1, and the location of the site near Turnagain Arm, suggest that most of the sediments at the site are of glaciomarine or glaciolacustrine origin.

TABLE 2. Log of Potter Marsh Observation Well 1.

Depth interval (m)	Material description
0.0-1.5	Dark grey silty gravel fill
1.5-2.7	Dark grey silt, damp
2.7-3.0	Grey gravel
3.0-8.7	Dark grey silt, moist, with clay, sand, and gravel
8.7-10.7	Dark grey, silty, fine-grained sand, with coarse sand to gravel
10.7-11.6	Light grey, silty, very fine-grained sand, with sand and occasional gravel
11.6-12.8	Dark grey, silty, sandy gravel
12.8-13.7	Dark grey, medium-to coarse-grained sand, with subangular to angular gravel. Yield tested by airlift method at 1.3×10^{-3} - 2.2×10^{-2} 1/s for 25 min. Cased with 15 cm ID steel casing to 13.7 m below land surface.

Well drilled and logged May 22, 1984.

TABLE 3. Log of Potter Marsh Observation Well 2.

Depth interval (m)	Material description
0.0-1.5	Dark brown gravelly sand fill
1.5-2.4	Dark grey silty gravel fill
2.4	Wood fragment
2.4-3.5	Gravel and water, yield tested by 2 airlift method at 8.8×10^{-2} to 1.8×10^{-2} 1/s for 30 min. Cased with 15cm ID steel casing to 3.0 m below land surface.

Well drilled and logged May 22, 1984.

Water-level Monitoring Equipment

Water-level data described in this paper were recorded with a microprocessor attached to a float and pulley system that senses water-level changes. The float and pulley system causes the shaft of a potentiometer to rotate, which is sensed by the microprocessor. The microprocessor converts the signals into digital data that are stored on an erasable solid state memory module. The module is periodically retrieved from the field, and the data are processed with DGGS computer facilities. Water-levels recorded by the microprocessor are converted to a common datum and verified for accuracy with wetted-steel tape measurements.

WATER LEVEL AND CLIMATOLOGIC DATA

Water-level data collected at the Potter Marsh and Ravenwood wells during water years 1984 and 1985 are shown in Figure 2.

The data show that the largest water-level rises in the Ravenwood well occur during the March-April and August-September periods for water years 1984 and 1985. These periods correlate with significant episodes of snowmelt and rainfall, respectively, in the Anchorage area. Less distinctive periods of rising water levels are evident from the Ravenwood well data for January 1984, and from the data from all three wells for January 1985. The magnitude of these water-level rises varies from about 20 to 60 percent of the range of the annual water-level fluctuation for each well. The water-level rises are anomalous episodes in the otherwise gradual decline of groundwater levels during the winter months.

For more than two months prior to the January episodes of rising water level, temperatures in Anchorage were mostly subfreezing (NOAA, 1983; NOAA, 1984b), indicating that surficial soils near the well sites were probably frozen. Selkregg (1974) shows that soils in Anchorage are

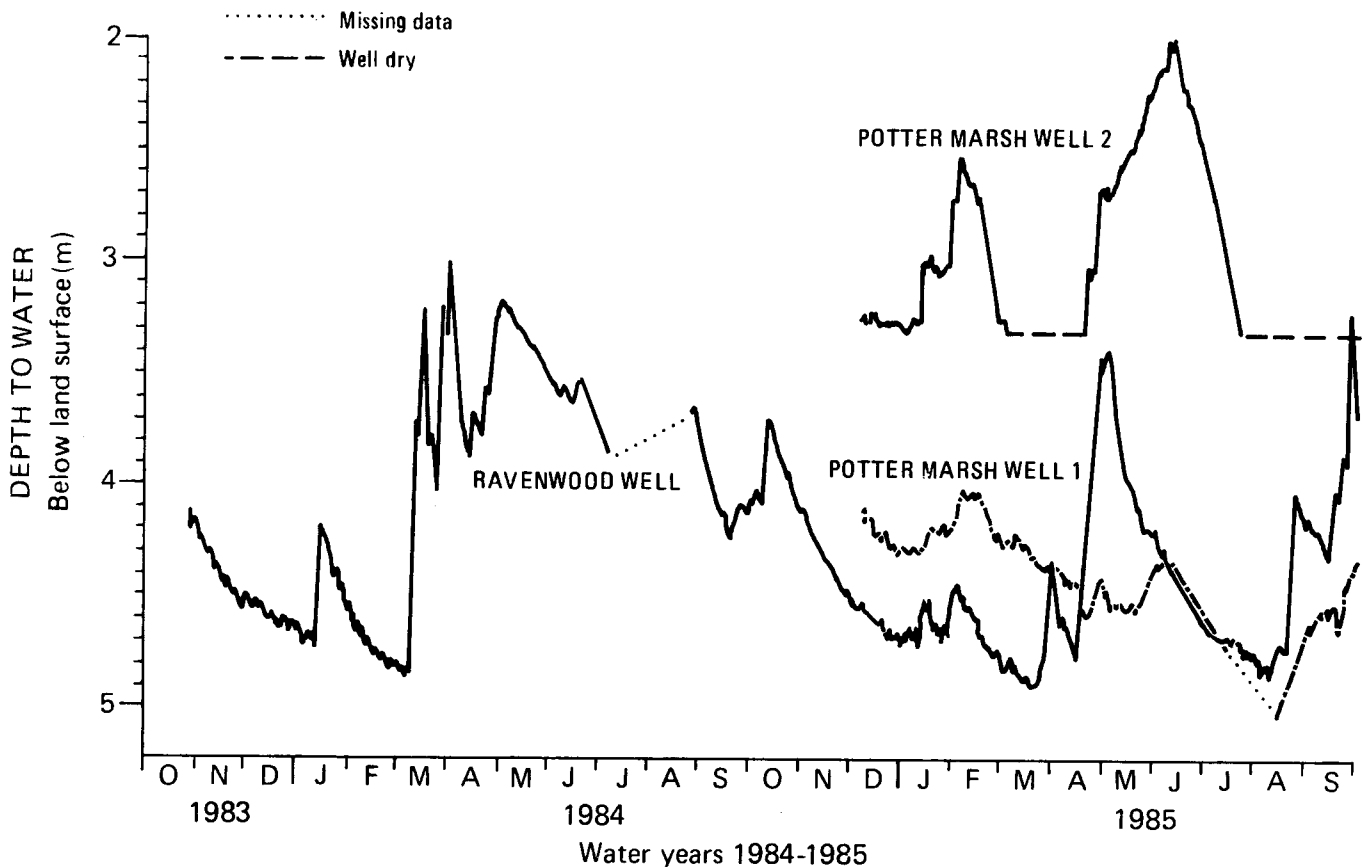


Figure 2. Water-level data from observation wells, water years 1984-1985.

frozen to an average depth of more than 0.6 m during January.

Water-level data collected at the Ravenwood well during January, 1984, are shown in Figure 3, with climatological data obtained at the Anchorage International Airport in west Anchorage (NOAA, 1984a). Subsequent to above-freezing temperatures on January 11 and 12, 1984, and 0.53 cm of precipitation (including 9.1 cm of snow) on January 11, the water-levels in the Ravenwood well began to rise during the first few hours of January 13. The water level continued to rise through January 14, with above-freezing temperatures that prevailed during this period, some or most of the precipitation recorded on January 11 and 14 must have fallen as rain, or melted soon after falling as snow, thus becoming available for percolation through the snowpack and infiltration into the ground.

January 1985 had two distinct periods of above-freezing days accompanied by precipitation events and rising water levels

in the Ravenwood and Potter Marsh wells 1 and 2 (Figure 4). The initial rise of water levels in the Ravenwood well and Potter Marsh well 2 occurred on January 10, the warmest day of a 6-day thaw on which 0.20 cm of precipitation (with no measureable snow) fell (NOAA, 1985). Water-level rises that also occurred during late January were during or shortly following above-freezing temperatures and measureable amounts of precipitation. Observed water levels in Potter Marsh well 1 show a subdued, yet distinguishable pattern of fluctuation similar to those observed in the Ravenwood well and Potter Marsh well 2 (Figure 2, Figure 1).

DISCUSSION

Water-levels in observation wells can respond to a variety of stimuli, both natural and man-induced. Pressure phenomena such as air entrapment, tides, external loading, earthquakes, or barometric effects last, at most, a few days (Freeze and Cherry, 1979, pp. 230-233), in

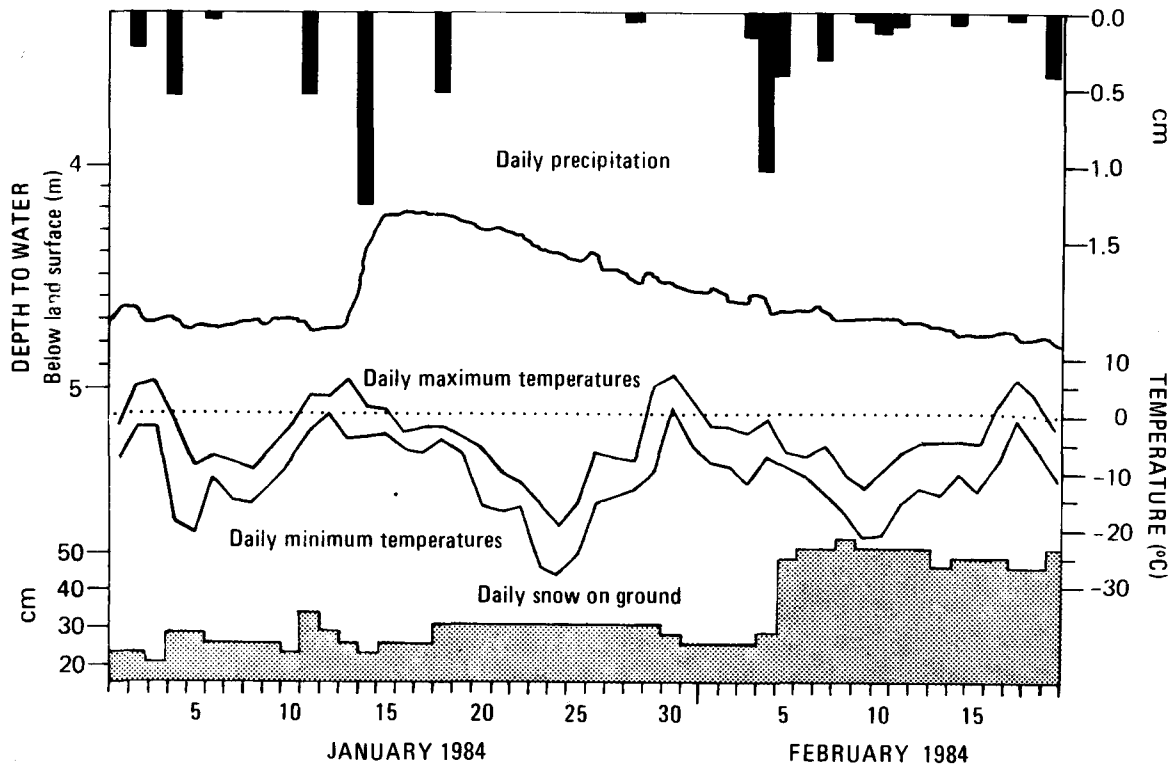


Figure 3. Water-Level Data from the Ravenwood Well and Climatological Data from the Anchorage Weather Service Meteorological Office, Anchorage International Airport.

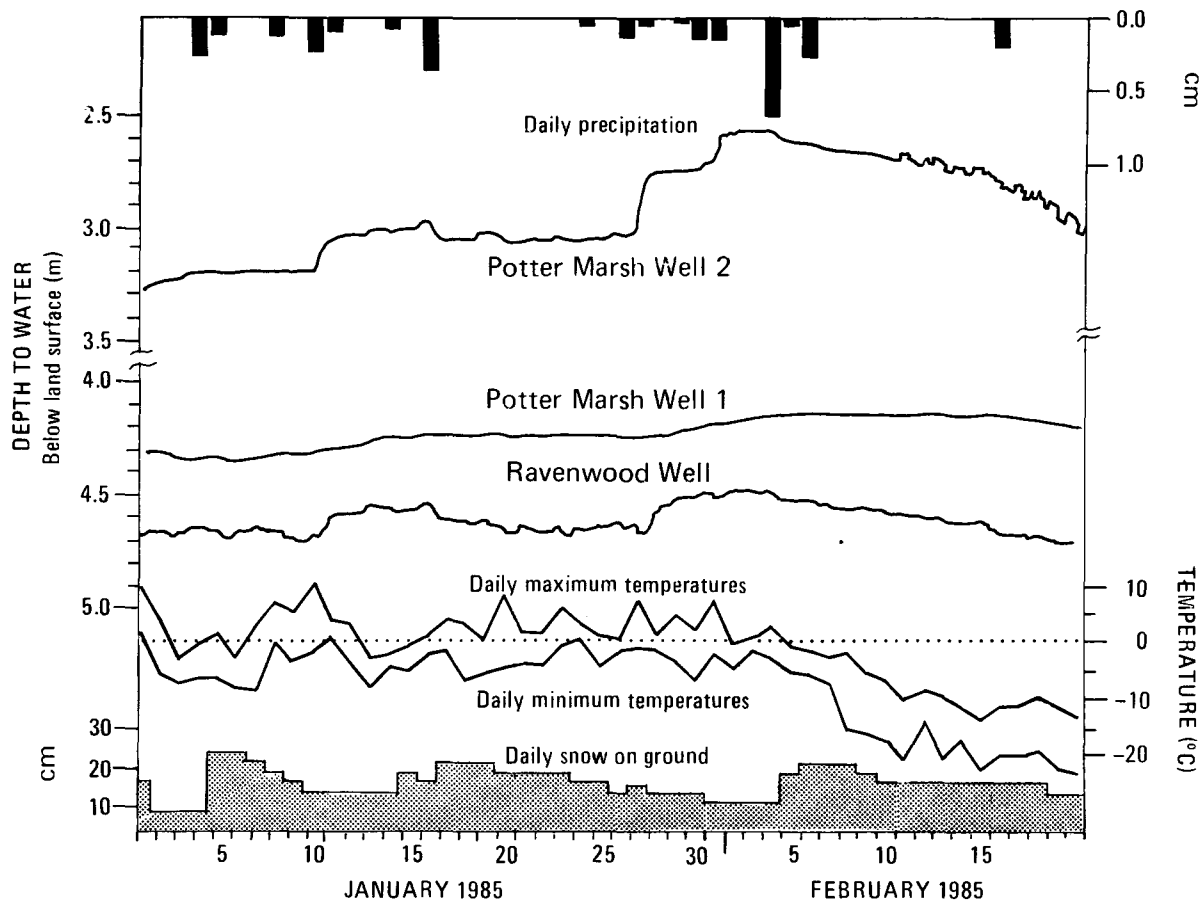


Figure 4. Water-Level Data from Observation Wells and Climatological Data from Anchorage Weather Service Meteorological Office, Anchorage International Airport.

contrast with the elevated water levels that persisted for weeks at the observation wells. No pumping, dewatering, or artificial recharge is known to have occurred near the observation wells that could have resulted in the observed water levels. Schneider (1961) has suggested that melting at the base of the seasonal frost layer within a few days of the onset of above-freezing air temperatures can result in a significant amount of groundwater recharge. In Anchorage, several periods of above-freezing temperatures that were devoid of precipitation clearly result in level or steadily declining water levels (Figure 3, Figure 4). This suggests that either the above-freezing weather did not persist long enough to cause melting at the base of the frost layer or that the moisture content of the soils at the base of the frozen soil layer were too low to contribute significantly to groundwater recharge. In either case, the

Anchorage data do not support the hypothesis that the initial surge of groundwater recharge is attributable to melting at the base of the seasonal frost layer. The data shown in Figures 2 through 4 exhibit strong correlations between above-freezing temperatures, precipitation, and rising water-levels during midwinter, a period usually characterized by groundwater recession conditions. Although the present study did not include detailed tracking of moisture and temperature conditions in soils, the elimination of other mechanisms leaves direct groundwater recharge resulting from surface water infiltration and percolation as the most reasonable explanation of the observed water-level rises.

The responsiveness of the water levels in the three monitoring wells to the climatic conditions is related to the thickness and type of strata that overlie

the aquifers that are tapped. With about 3 m of unsaturated gravelly fill overlying the aquifer, Potter Marsh well 2 shows a response to precipitation events within a few hours to a day. Recharge probably occurs in close proximity to the Potter Marsh wells because of the local distribution of the artificial fill.

The Ravenwood well responds to climatic conditions in a matter of a few hours to a day or two. This would seem to be relatively rapid, considering the thickness (about 6 m) of till in the area and the relatively low hydraulic conductivity of till. Freeze and Banner (1970) noted the occurrence of relatively rapid recharge through till, and postulated that fracture flow may be a significant component of flow through till deposits. At the Ravenwood site, fractures may have been present in the unfrozen till above the Ravenwood aquifer, or in the frozen soils near the land surface or both.

Potter Marsh well 1 responds sluggishly to climatic conditions because of the thickness and low permeability of sediments penetrated by the well (Table 2). The fact that the water-level in the well responds at all, however, illustrates the importance of recharge to aquifers typically considered to be confined and relatively unaffected by short-term surficial hydrologic processes.

Annual low water levels in the Ravenwood well occur during March of both years of record, immediately prior to major spring snowmelt episodes. The recharge events that occurred during January of 1984 and 1985 caused the elevation of the annual low water level in the Ravenwood well to be higher than it otherwise would have been because of the long and gradual recession of the hydrograph from the recharge events (Figure 2). The elevation of the annual low water level is important because numerous residential wells tapping the Ravenwood aquifer have a low tolerance to water-level declines because of relatively low static water levels (Munter, 1984). The occurrence of mid-winter groundwater recharge could prevent difficulty for some Anchorage domestic well

owners with shallow wells and low static water levels.

CONCLUSIONS

Groundwater recharge is concluded to have occurred through frozen soils at Anchorage, Alaska during mid-winter periods of above-freezing temperatures and precipitation, some of which occurred as rain. Significant recharge is not evident during mid-winter periods of above-freezing temperatures devoid of precipitation.

The primary factor governing groundwater recharge in areas where soils are at least moderately permeable and frozen may be the availability of significant quantities of water at the land surface. Because soils of at least moderate permeability are widespread, the major reason for the lack of recharge in most areas where soils are frozen during part of the year is probably the unavailability of water, rather than the reduced permeability of frozen soils.

Mid-winter groundwater recharge at Anchorage may constitute a significant percentage of total annual groundwater recharge during some years. Inaccuracies may result if the effects of mid-winter recharge are ignored during consideration of seasonal water-level fluctuations for water-supply or waste-disposal purposes, or runoff forecasting.

ACKNOWLEDGEMENTS

The author thanks Larry L. Dearborn, Gary S. Anderson, and an anonymous reviewer for helpful reviews of the manuscript.

LITERATURE CITED

Freeze, R.A., and Banner, J., 1970. The Mechanism of Natural Ground-Water Recharge and Discharge 2. Laboratory Column Experiments and Field Measurements. *Water Resour. Res.* 6(1): 138-155.

- Freeze, R.A., and Cherry, J.A., 1979. Groundwater. Prentice-Hall, Inc., Englewood Cliffs, N.J., 604 pp.
- Kane, D.L. and Stein, J., 1983. Water Movement into Seasonally Frozen Soils. Water Resour. Res. 19(6): 1547-1557.
- Munter, J.A., 1984. Ground-water Occurrence in Eagle River, Alaska. Alaska Dept. of Natural Resources, Div. of Geological and Geophysical Surveys, Report of Investigations 84-21. 15 pp.
- NOAA, 1983. Climatological Data, Annual Summary, Alaska, 1983. U.S. Dept. of Commerce, National Oceanic and Atmospheric Admin. 69(13).
- NOAA, 1984a. Climatological Data, Annual Summary, Alaska, January, 1984. U.S. Dept. of Commerce, National Oceanic and Atmospheric Admin. 70(1).
- NOAA, 1984b. Climatological Data, Annual Summary, Alaska, 1984. U.S. Dept. of Commerce, National Oceanic and Atmospheric Admin. 70(13).
- NOAA, 1985. Climatological Data, Annual Summary, Alaska, January, 1985. U.S. Dept. of Commerce, National Oceanic and Atmospheric Admin. 71(1).
- Schmoll, H.R., Dobrovolny, E., and Gardner, C.A., 1980. Preliminary Map of the Middle Part of the Eagle River Valley, Municipality of Anchorage Alaska. U.S. Geological Survey Open-File Report 80-890.
- Schneider, R., 1961. Correlation of Ground-Water Levels and Air Temperatures in the Winter and Spring in Minnesota. U.S. Geological Survey Water Supply Paper 1539-D, 14 pp.
- Selkregg, L., 1974. Alaska Regional Profiles, Southcentral Region. University of Alaska, Arctic Environmental Information and Data Center. 255 pp.
- Zenone, C., Schmoll, H.R., and Dobrovolny, E., 1974. Geology and Ground Water for Land-Use Planning in the Eagle River-Chugiak Area, Alaska. U.S. Geological Survey Open-File Report 74-57. 25 pp.
- Zenone, C., and Anderson, G.S., 1978. Summary Appraisals of the Nation's Ground-water Resources-Alaska. U.S. Geological Survey Professional Paper 813-P. 28 pp.

RESIDENTIAL WELL DEVELOPMENT OF A LOW PERMEABILITY BEDROCK FLOW SYSTEM

William A. Petrik¹

ABSTRACT: Complaints of inadequate domestic well yields in the hillside area of Eagle River, Alaska, prompted a survey of existing water well data, measurement of water levels in private domestic wells, and interviews with homeowners regarding water use and water shortage problems. Water levels were measured in 59 domestic wells during August and September, 1985. Fifty-six of these wells were drilled into bedrock. The depths of the wells vary from 11 to 215 m (36 to 706 ft). Well logs show unconsolidated sediments above the McHugh Complex metamorphic rocks to vary in thickness from 0.3 to 37 m (1 to 121 ft). Aquifers within the McHugh Complex rocks have virtually no primary permeability and low to very low secondary permeability. Reported well yields vary from 0.01 to 1.32 l/s (0.1 to 21.0 gpm). The median well yield is 0.13 l/s (2.0 gpm).

Comparison of 50 original reported static water levels to 1985 measurements indicate current water levels are an average of 0.3 m (1 ft) above originally reported values. This is not considered to be a significant change. No definitive areal trend of either rising or falling levels exists. Apparent water level changes exhibit an irregular areal distribution, are commonly many meters (tens of ft) in magnitude, and cannot be consistently correlated with any known factor.

Domestic water use is highly variable and shortages have occurred, indicating that some wells are inadequate for domestic needs.

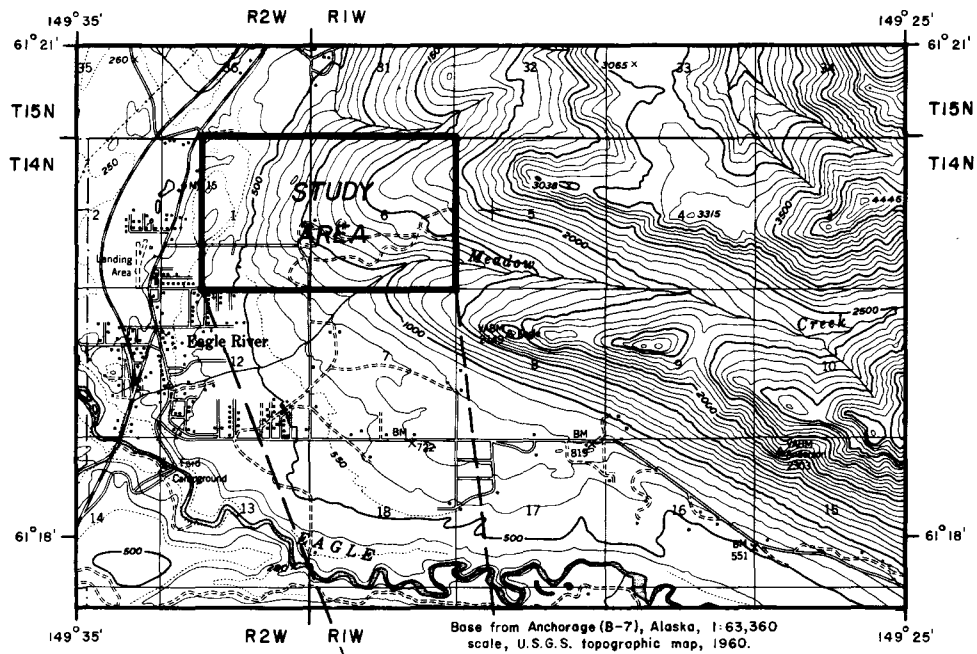
(KEY TERMS: aquifer; primary permeability; secondary permeability; water levels.)

INTRODUCTION

The community of Eagle River is located 24 km (15 mi) from downtown Anchorage, Alaska. Eagle River has experienced much growth in the last decade. Increased concentrations of residences now occupy the moderately sloped hillsides surrounding the core of the town. On the hillside, most water is provided by private domestic water wells. Along the north hillside area closest to Eagle River, many reports of domestic water well levels declining and wells going dry have been received by the Alaska Department of Natural Resources (DNR). Beginning August 28, 1985, DNR's Division of Geological and Geophysical Surveys (DGGS) conducted a five week field survey of domestic water wells to determine the nature of these problems and their implications.

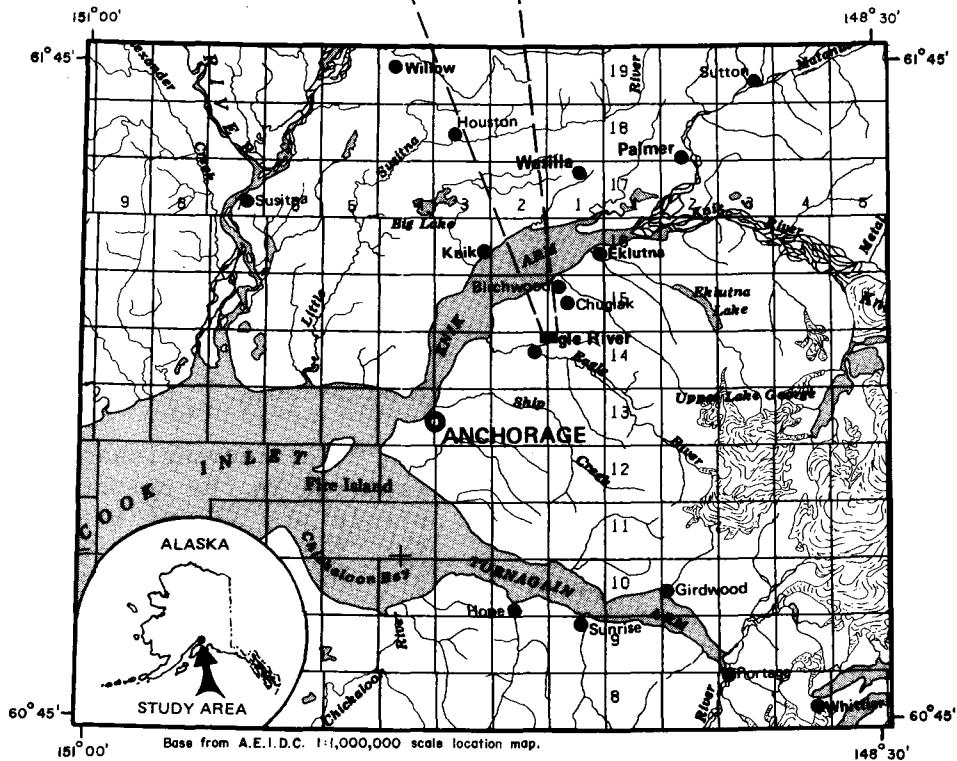
This reconnaissance level study was centered in the Meadow Creek drainage area within the SE $\frac{1}{4}$ of Sec. 1, T14N, R2W, and Sec. 6, T14N, R1W, Seward Meridian (Figure 1). On a smaller scale, the study area is bounded by Eagle River Loop Road and Meadow Creek on the south, the concealed Border Ranges fault on the west (Updike, 1986), and Chugach State Park and limits of residential construction on the north and east (Figure 2).

¹Hydrologist, Alaska Department of Natural Resources, Division of Geological and Geophysical Surveys, Water Resources Section, P.O. Box 772116, Eagle River, Alaska 99577.



CONTOUR INTERVAL
100 FEET (30.5 METERS)

SCALE



SCALE

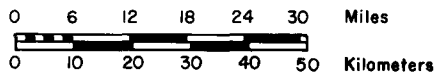
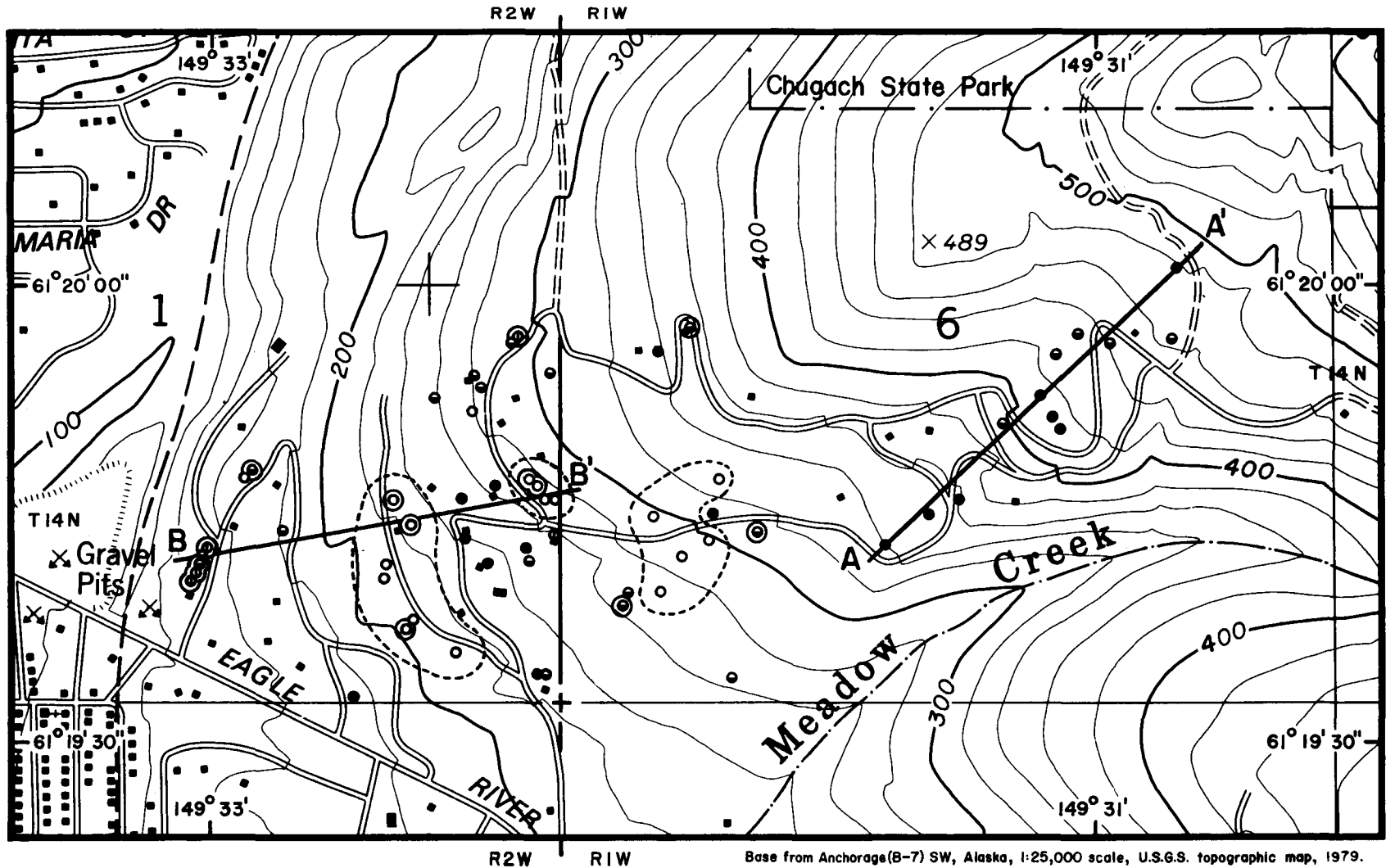


Figure 1. Location map of the study area.

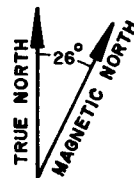
Figure 2. Study area location map with locations and yield data of measured wells, lines of section, and areas of very low yield wells.



Base from Anchorage(B-7) SW, Alaska, 1:25,000 scale, U.S.G.S. topographic map, 1979.

LOCATION OF WELLS AND REPORTED YIELDS

- | | | | |
|---|---------------------------|---|---------------------------------------|
| ○ | <1 Gallon per Minute | ⊙ | No yield data available |
| ○ | <.06 Liters per Second | ⊙ | Deepened, blasted or replacement well |
| ● | 1-3 Gallons per Minute | ⊖ | Area of very low yield wells |
| ● | .06-.19 Liters per Second | | |
| ● | >3 Gallons per Minute | | |
| ● | >.19 Liters per Second | | |



Approximate Mean Declination, 1979

SCALE 1:12,500



CONTOUR INTERVAL 20 METERS (66 FEET)

A ——— A' Line of Section

----- Approximate location of the Border Ranges Fault (Updike, 1986)

The mountains immediately surrounding this area are composed of McHugh Complex (Jurassic /Cretaceous) rocks (Zenone and others, 1974). The lithologies of this complex include weakly metamorphosed siltstone, conglomeratic sandstone, graywacke, arkose, greenstone, metachert, and argillite (Magoon and others, 1976). Strikes in this area generally trend between N60E and N90E and dips range from 45N to 90N (Updike, 1986). Three joint alignments have been noted nearby in this rock complex a few miles up Eagle River valley. Joint strikes and dips are: N34W, vertical; N80E, 80NW; and N38E, 46S, respectively (Updike, 1986).

Flow systems encountered within the McHugh Complex lithologies have virtually no primary permeability and low to very low secondary permeability. As reported on drillers' logs, water enters wells through fractured zones in bedrock. Most wells are reported to have two or more zones of water inflow (Figure 3).

Within the study area, the McHugh Complex is overlain by glacial alluvium, younger glacial moraine deposits, and colluvium (Zenone and others, 1974). According to drillers' well logs, these surficial deposits vary in thickness from 0.3 to 37 m (1 to 121 ft) in the study area. The thickest surficial deposits occur over the eastern portion of the study area (Section AA' and BB', Figures 2 and 3). Calculated from drillers' well logs, the median depth through these unconsolidated deposits to the McHugh Complex is 7.3 m (24 ft).

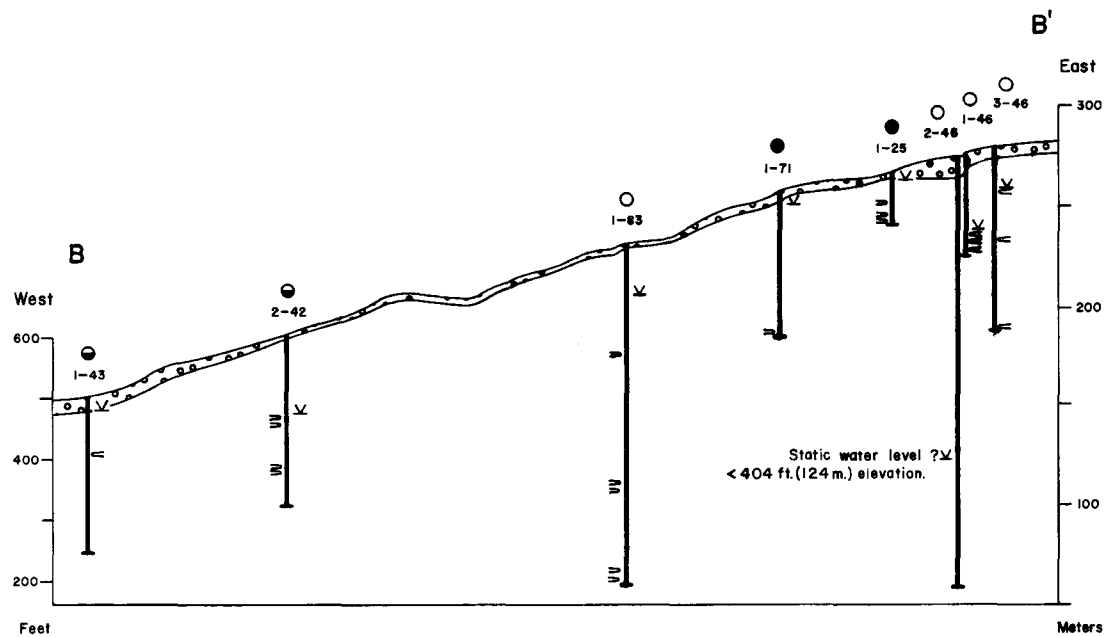
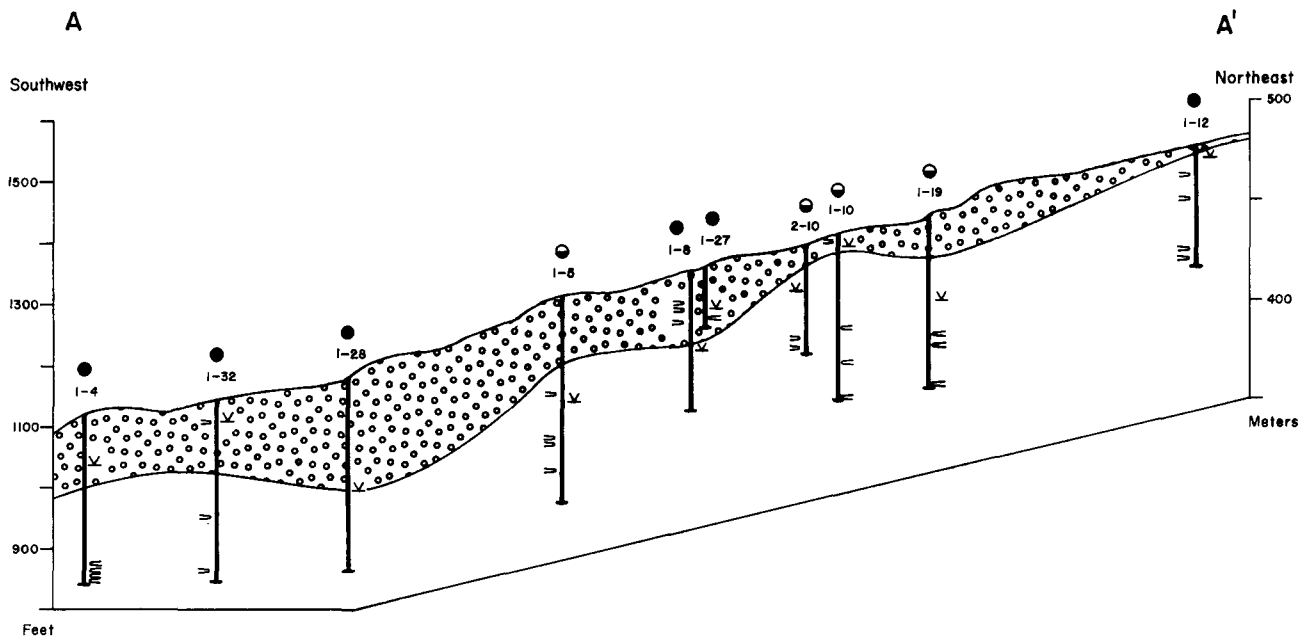
The slope of the study area is dominantly moderate (15-25 percent) with minor steeper areas (25-45 percent). The study area is dominantly hummocky terrain with some smooth to rolling uplands, mountain ridges and valleys, and river bluffs along Meadow Creek. Generally, stable slope conditions exist, except steeper areas and bluffs are possibly unstable, and potential for landslides or rockfalls exists (Zenone and others, 1974).

After initial reports of domestic water well problems were received by DNR, the Water Resources Section of DGGGS selected specific wells for obtaining water level measurements. Prior to measurement, homeowners were questioned for information regarding water quantity or quality problems, length of residence in the home, number of residents in the home, household water consumption patterns, and knowledge of neighbors having well problems. Water levels were measured in 59 domestic water wells to the nearest three thousandths of a meter (hundredth of a foot). A 152 m (500 ft) electric water level indicator (sounder) was utilized for measuring water levels in most wells, and a chalked steel tape was used for the rest.

Homeowners were asked not to use their water while measurements were being made and readings were taken only if the well pump had not run within 30 minutes. Water level measurements were checked by taking a second reading five minutes after the initial reading.

In some instances, the electrode of the sounder encountered rust and condensed water on the inside of the well casing, making it difficult to discern when contact with the water surface was made. To obtain a more reliable reading, a steel tape that was chalked for the first 6 m (20 ft) was used, and contact with the water was generally obvious. In an attempt to maintain consistent measurements, sometimes the steel tape was used to find the general water level first, then the sounder would be used for the final measurement.

Driller-reported static water levels were sometimes lacking and often ambiguous because the methods of measurement were variable and undocumented. Some drillers estimated the height of water column in the well, and others measured the depth from the top of the well casing. Familiarity with individual drillers' methods allowed adjustment of the data to a common



Legend

- Domestic Water Wells
- I-71 Well Identifier
- ∇ 1985 Measured Static Water Level
- \Rightarrow Driller-Reported Zones of Water Inflow
- Glacial Deposits and/or Colluvium
- Mc Hugh Complex

Reported Well Yields	
\circ	< 1 Gallons per Minute < 0.06 Liters per Second
\bullet	1-3 Gallons per Minute .06-.19 Liters per Second
\bullet	> 3 Gallons per Minute >.19 Liters per Second

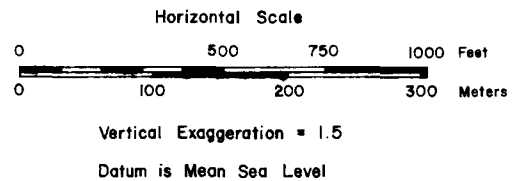


Figure 3. Generalized geologic sections showing well depths, yields, 1985 water levels, zones of water inflow, and overburden thickness.

datum. Accuracy of reported yield data is questionable for many of these wells because of varying methods by drillers to estimate yield. In addition, driller measured static water levels may have been taken prior to total recovery of a newly drilled well. Any resulting inaccuracy is most likely to occur in low yield wells.

Drillers' well logs were the primary source of domestic water well information. Domestic water well logs were obtained from the U.S. Geological Survey and DGGs Water Resources Section offices, Municipality of Anchorage Department of Health and Human Services, Alaska Division of Land and Water Management, drilling companies, and directly from the homeowners. Most well logs document the common domestic water well information including drilling company, driller, landowner, legal description of property, date of drilling, depth of well, lithologies encountered and their respective depths, estimated yields, casing size, casing depth, static water levels, and well pumping test results.

RESULTS

Water Level Changes

Of 59 water levels measured, 50 had original static water levels that were reported on their well logs by the driller. Comparison of original static water levels to 1985 measurements indicate no definitive trend of either rising or falling levels. Water levels lower than those reported by the driller were found in 22 wells. The declines ranged from 0.1 to 58 m (0.3 to 189 ft) with a median decline of 4.6 m (15.2 ft). Water levels in 29 wells were found to be higher than the static water level reported by the respective driller. Increases range from 0 to 39 m (127 ft), with a median increase of 4.3 m (14.1 ft). Using 49 wells, the median change was an increase of water level of 0.2 m (0.7 ft). Water level measurements made during this survey varied from 1.4 to 89 m (4.5 to 292 ft) below land surface (bls). One well showed a water level decline of at least 87 m (286 ft) when compared to the original

reported water level. The absolute decline was undeterminable because the 152 m (500 ft) limit of the well sounder was reached before the water level could be measured (Well 2-46, Figure 3).

Using data from 49 wells where original data were available, measured water levels in the hillside area of Eagle River indicate an average reading 0.3 m (1 ft) higher than levels reported by drillers. However, no distinctive area of either increasing or decreasing static water levels was found. Fluctuations exhibit a highly irregular areal distribution and appear to be independent of total well depth or distance drilled into bedrock.

Well Depths, Yields, and Flow Systems

Water levels were measured in 59 domestic water wells of which 56 were drilled into bedrock. Total well depths vary from 11 to 215 m (36 to 706 ft) bls with a median of 84 m (277 ft). Water yield of different inflow zones in a well is reported cumulatively. Reported total well yields vary from 0.01 to 0.76 l/s (0.1 to 12.0 gpm). The median reported yield of 53 wells is 0.13 l/s (2.0 gpm). Although the data exhibit a wide distribution, they suggest that the lowest yielding wells typically exhibit the greatest changes in water levels (Figure 4). The data also suggest that reported well yield decreases with the increasing distance that a well is drilled into bedrock (Figure 5). Existing hydrologic data for the Chugiak-Eagle River area indicate median yield for bedrock wells is 0.13 l/s (2.0 gpm) and 0.63 l/s (10.0 gpm) for aquifers in unconsolidated sediments (Johnson, 1979).

A continuous groundwater flow system was undefinable in this study area after examination of available data including cross sections and drillers' well logs. Moreover, existing flow systems in this area are isolated, variable, and randomly occurring. Adjacent wells with only several meters (tens of ft) separating them show drastically different potentiometric surfaces (e.g., wells 1-46 and

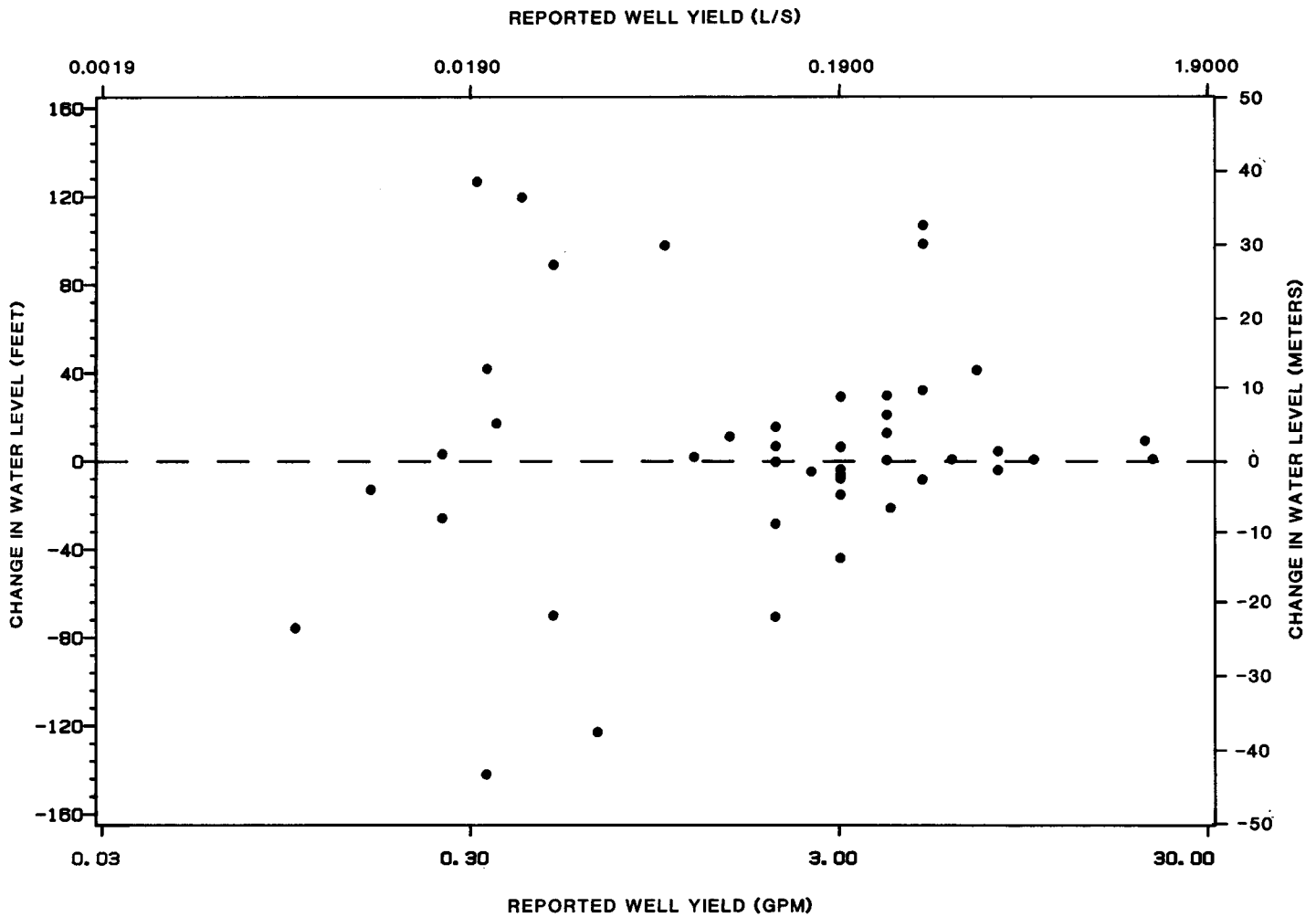


Figure 4. Relationship of water level change with increasing well yield (well yield axes are psuedo-logarithmic scale).

2-46, Figure 3). This strongly suggests a lack of fracture connectivity in rocks in this immediate area. Further evidence for poor hydraulic connectivity is the distinctly separate elevations of groundwater inflow in adjacent wells (Figure 3) and the fact that a few dry wells have been drilled.

Water level Changes in Shallow Wells

Figure 6 shows a plot of the change of water levels with respect to the distance the well was drilled into bedrock. Very similar results were found when plotting change of water level versus total well depth. Based on 1985 water level measurements, all wells less than 43 m (141 ft) deep exhibited no decreases in static

water levels when compared with driller reported levels. Of nine wells less than 43 m (141 ft) deep, three wells are cased to bedrock, two wells are cased into bedrock, three bedrock wells are not cased into bedrock, and the remaining well has insufficient casing data. The increases varied from 0 to 3.9 m (12.7 ft) with the median and average increase of 1.4 m (4.5 ft). Yields of these wells varied from 0.1 to 1.3 l/s (2.0 to 21.0 gpm) with a median of 0.4 l/s (6.0 gpm). These wells did not show decreases because their reported yield is relatively high. In addition, above average precipitation during July and August, 1985, could cause an increase of water levels in shallow wells as a response to groundwater recharge.

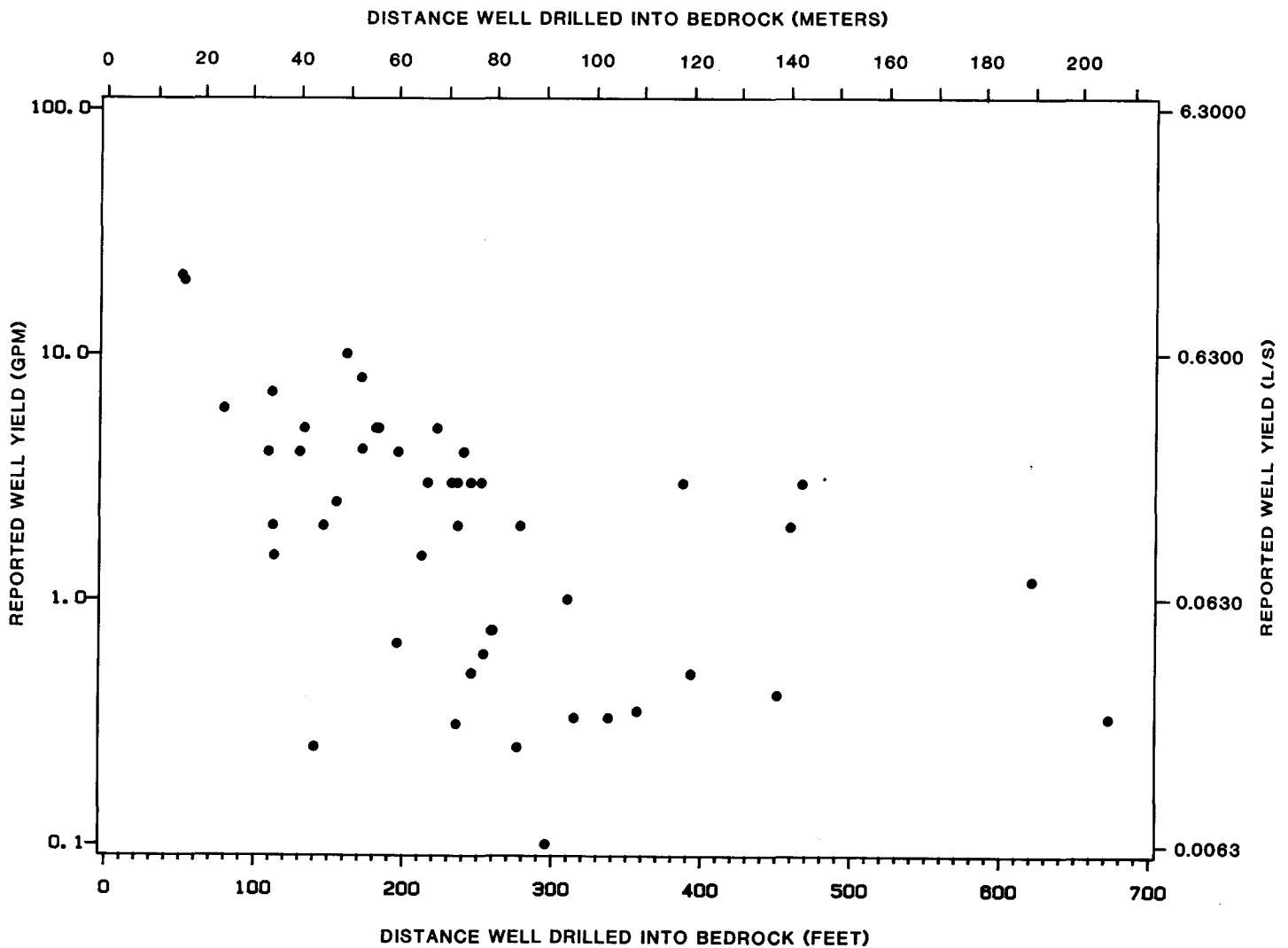


Figure 5. Inverse relationship between well yield and the depth the well was drilled into bedrock (well yield axes are psuedo-logarithmic scale).

Well Age Characteristics

The oldest well measured was drilled in June 1971 and the newest in June 1985. The average well age at the time of the survey was 6.75 years. No relationship is apparent between well age and change in water levels. Older wells do not have greater changes in water levels than younger wells. The hypothesis that newer wells are depleting available water supplies and dewatering existing wells is not supported by the data. In addition, no direct correlation was evident when comparing the long term precipitation data with changes in water levels.

Water Usage

Households reporting low water quantities available from their wells had varying water use habits and estimated well yields. Of 53 homeowners interviewed, 18 have wells with reported yields of 0.06 l/s (1.0 gpm) or less (Figures 2-6). Some of these households reported above average water consumption that included daily showers and laundry, car washing, and lawn watering, and did not have sufficient amounts of water for their needs. Average water consumption in the lower elevation of Eagle River is approximately 455 liters (120 gallons) per person per day (Munter, 1984).

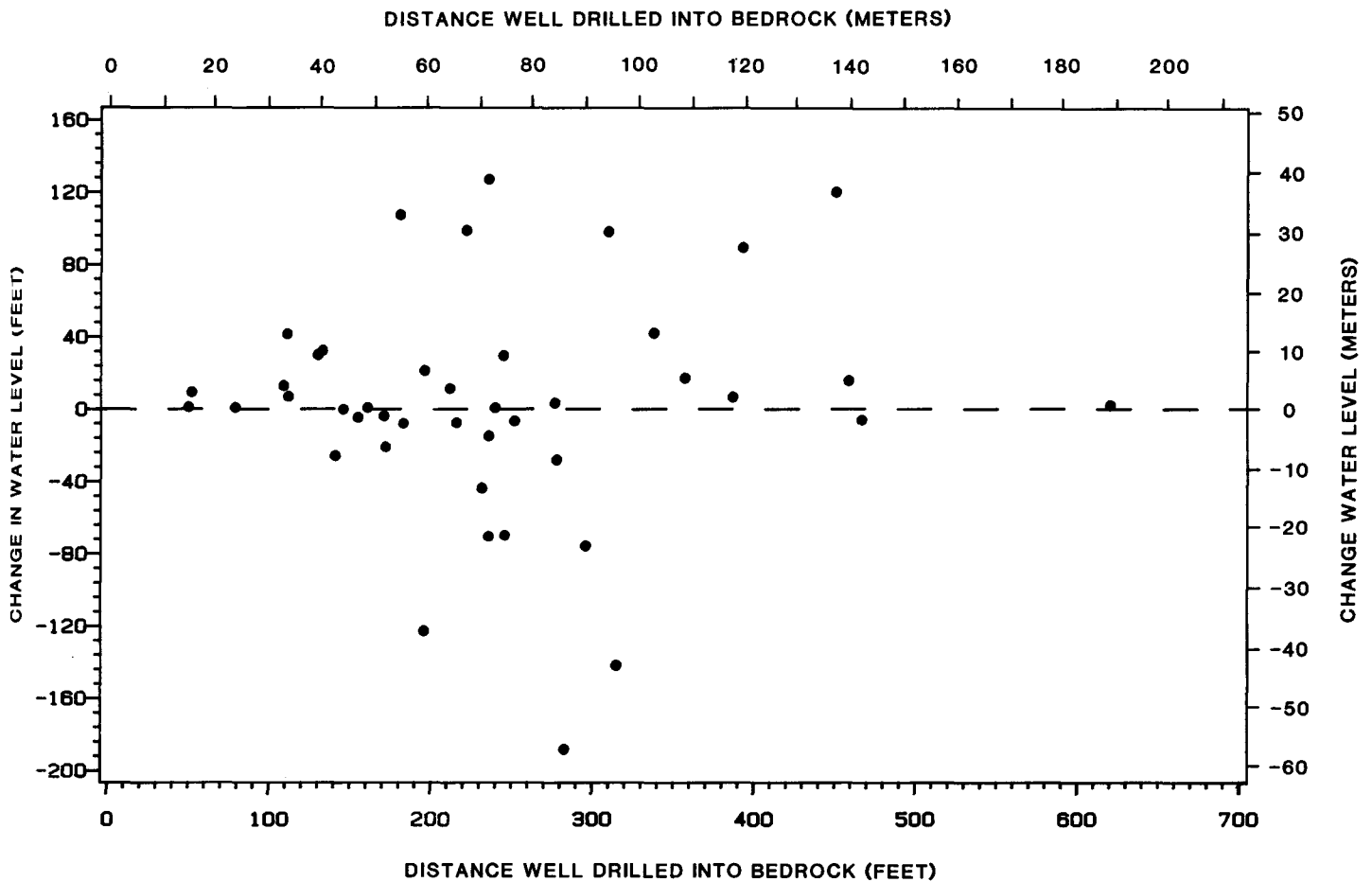


Figure 6. Change in water level plotted against distance well drilled into bedrock (shallow wells had no decrease in water levels).

Three areas of very low yield water wells [less than or equal to an estimated 0.06 l/s (1.0 gpm)] are outlined in Figure 2. Two of these areas are also characterized by reported below average water usage. Below average water usage is characterized by daily drinking and cooking needs, and washing dishes and showering on a limited non-daily basis. Two areas of low water use include residences in Broadwater Heights Subdivision and Seidler Subdivision No. 1. The third area, characterized by average water usage, is in the center of the southwest quarter of Sec. 6.

wells in the area exhibited significant yield increases. Yield in the first well increased from 0.04 to 0.19 l/s (0.6 to 3.0 gpm) as reported by the driller after it was deepened from 84 to 137 m (275 to 448 ft). The second well was deepened from 92 to 171 m (300 to 560 ft) and the reported yield increased from 0.01 to 0.02 l/s (0.1 to 0.3 gpm). The third well was deepened from 53 to 122 m (175 to 400 ft) and the reported yield increase was negligible. One other low yield well in the Meadow Creek area drainage was acidized and another blasted. In each case, reported yield was insignificant.

Attempts at Increasing Well Yield

Some wells that have failed have subsequently been deepened, blasted, acidized, redrilled, or abandoned. After deepening, two of three very low yield

CONCLUSIONS

The average change in static water levels in the study area in the past 15 years is insignificant. Changes in water levels are large at many wells and tend to

decrease with increasing yield. These large fluctuations of water levels in this area apparently are linked to the low yield of the wells. It appears that their water levels are affected most of the time by on-site domestic use. In addition, after 43 m (141 ft) depths, water level changes are independent of total well depth or distance well was drilled into bedrock and exhibit irregular areal distribution throughout the area.

Isolated complaints of declining water levels in the study area are legitimate. All of the problems of water acquisition in this area are a result of drawing from a low permeability bedrock aquifer. Three areas of declining water levels are characterized by unusually low-yield wells and varying water-use habits. Also, it has been determined that declining water levels are not a function of well age. Evidence indicates that water level changes are most affected by water usage in low-yield wells.

The problem of insufficient water supply has mostly been alleviated by deepening existing wells, drilling new or supplemental wells, or implementing more conservative water-use habits.

No unified continuous flow system in the study area has been definable based on existing data. All wells less than 43 m (141 ft) deep showed relatively stable water levels over a period of years. These shallow wells also are relatively high yielding and derive water from unconsolidated sediments as well as bedrock. An inverse relationship exists between well yield and distance well drilled into bedrock, suggesting that the option of drilling deeper to obtain water may not be as successful as drilling a new well at a different location.

Too often, the reliability and accuracy of historic water yield and water level data are questionable. Some of the original driller-reported water level readings and estimated yields at time of drilling are considered unreliable because very low permeability results in long periods (days) of water level readjustment after the stresses of drilling or yield

testing. Periodic remeasurement of levels and yields would further assist definition of the response of the aquifer, to residential pumping stress versus performance problems of specific wells. Baseline data collected by this study should, in time, help resolve long term water level trends, affects on the groundwater system, its relationship to domestic water usage, and lead to more confidence in the foregoing correlations.

Acknowledgements

The author would like to thank the residents of the study area for their courtesy and cooperation during acquisition of field data. Special thanks go to Jim Munter and Larry Dearborn of DGGs for their technical editing, review, and comments while compiling this manuscript.

LITERATURE CITED

- Johnson, P., 1979, Hydrogeologic data for the Eagle River-Chugiak area, Alaska: U.S. Geological Survey, Water Resources Investigations 79-59, 17 p.
- Magoon, L.B., Adkison, W.L., and Egbert, R.M., 1976, Map showing geology, wildcat wells, Tertiary plant fossil localities, K-AR dates, and petroleum operations, Cook Inlet Area, Alaska: U.S. Geological Survey, Miscellaneous Investigations Series, Map I-1019 (Sheet 1 of 3).
- Munter, J.A., 1984, Ground-water occurrence in Eagle River, Alaska: Alaska Division of Geological and Geophysical Surveys, Report of Investigation 84-21, 15 p.
- Updike, R.U., 1986, Division of Geological and Geophysical Survey Engineering Geology Section, oral communication.
- Zenone, C., Schmoll, H.R., and Dobrovolsky E., 1974, Geology and ground water for land-use planning in the Eagle River-Chugiak area, Alaska: U.S. Geological Survey Open-File Report 74-57, 25 p.

HYDROLOGIC MONITORING OF SUBSURFACE FLOW AND GROUNDWATER RECHARGE
IN A MOUNTAIN WATERSHEDMichael E. Campana and Richard L. Boone¹

ABSTRACT: The mountainous regions of the Great Basin are major water sources for the drier, lower-elevation regions. These mountain watersheds, which receive much of their precipitation as snow, serve not only as surface water catchments but also as source areas for much of the groundwater recharge received by the valley-fill aquifers in the intermontane basins. An understanding of the hydrologic processes in the mountain watersheds, particularly those occurring during winter, is requisite before hydrogeologists can understand and quantify recharge to the valley-fill groundwater reservoirs. A small-scale study conducted in a Sierra Nevada watershed just east of Lake Tahoe utilized four major groups of instruments to delineate infiltration, recharge and subsurface flow contributions to streamflow. Foremost among the groups was an automated tensiometer-transducer system. Tensiometers were linked to a central scanning valve via hydraulic tubing, which was buried to protect against freezing. The investigation indicated that deep percolation/groundwater recharge occurred beneath the snowpack during the winter months but could not determine how much of it discharged locally and how much flowed off-site, perhaps as part of a deeper system. The experience gained during the study has greatly aided continuing studies in the same area.

(KEY TERMS: groundwater recharge; mountain watershed hydrogeology; snowpack; infiltration.)

INTRODUCTION

The mountainous regions of the Great Basin are important sources of water for the dry, lower-elevation regions. The mountain watersheds, which receive substantially more precipitation than their low elevation counterparts, serve as catchments for the intermontane basins and source areas for the few large perennial streams in the Great Basin. However, their importance with respect to the groundwater resources of the region is often overlooked. Just as they serve as source areas for surface water, so do they function as catchments for much of the groundwater recharge received by the basin-fill alluvial aquifers. And, since much of the precipitation received by the mountainous regions is in the form of snow, an understanding of the interrelationships among the snowpack, snowmelt and subsurface flow in mountain watersheds is requisite before hydrogeologists can hope to quantify mountain-block recharge on a large scale. In addition, a knowledge of the different recharge and subsurface flow pathways is necessary to understand subsurface and surface water quality in mountain watersheds. In the Eastern Sierra Nevada, where the study was conducted, an important aspect with regard to subsurface flow paths concerns the disposition of acid rain derived from the large metropolitan areas to the west. The Eastern Sierra Nevada also serve as a major catchment for the western Great Basin

¹Respectively, Water Resources Center, Desert Research Institute, P.O. Box 60220, Reno, NV 89506 and Department of Geological Sciences, Mackay School of Mines, University of Nevada, Reno, NV 89557; and U.S. Environmental Protection Agency, 345 Courtland St. N.E., Atlanta, GA 30365.

in Nevada. We believe that this study represents the first attempt to identify the year-round subsurface flow regime in an Eastern Sierra Nevada mountain watershed and as such, is important in guiding future efforts along similar lines.

A hillslope in a small watershed was instrumented with a variety of instrument groups. The hydrologic regime of the hillslope was monitored from summer through winter with emphasis on delineating the hydrologic processes occurring during winter. Particular attention was paid to the following: 1) identifying cold-season groundwater recharge; 2) determining contributions of subsurface flow to streamflow during the winter; and 3) gaining a qualitative understanding of the subsurface flow processes operating at the site. Acquisition of experience in the installation, use and maintenance of the instrumentation, especially during the winter, was also a major objective of the study.

DESCRIPTION OF STUDY AREA

The study area is located on a hillslope having a northeast aspect along Clear Creek in Carson City, Nevada (Figures 1 and 2). The site is just east of Lake Tahoe approximately 9.5 km west of downtown Carson City, Nevada, in the Toiyabe National Forest. The experimental site (Figure 2) lies at an elevation of about 2000 m in the north-trending Carson Range of the Sierra Nevada and is underlain by Cretaceous granodiorite. Andesitic and dacitic dikes and plugs are abundant throughout the Carson Range and evidence of this is seen in a contact zone in the northwest portion of the site.

The average annual precipitation is about 75 cm/y; approximately 80% of this total occurs as snow. More than 50% of the total precipitation falls during January, February and March. Summer maximum temperatures can be as high as 37°C; minimums can be as low as -9°C. During the winter, high temperatures can reach 21°C; lows can approach -35°C.

Soils in the area are part of the Toiyabe-Rock outcrop complex and the Corbett-Toiyabe association. The Toiyabe soil is shallow and well-drained, formed in residuum from the granodiorite. The

soil has a surface layer of gray, stony loamy coarse sand approximately 10 cm thick. Below this is a layer of gray loamy coarse sand, gravelly coarse sand, and sand approximately 18 cm thick. Weathered granodioritic bedrock occurs at a depth of 28 cm. The Corbett soil is moderately deep and well-drained, formed in colluvium derived from weathered granodioritic bedrock. The surface layer of dark grayish-brown stony loamy coarse sand is about 20 cm thick. The next layer consists of about 80 cm of light gray gravelly and cobbly loamy coarse sand. Weathered granodioritic bedrock is found at a depth of 100 cm.

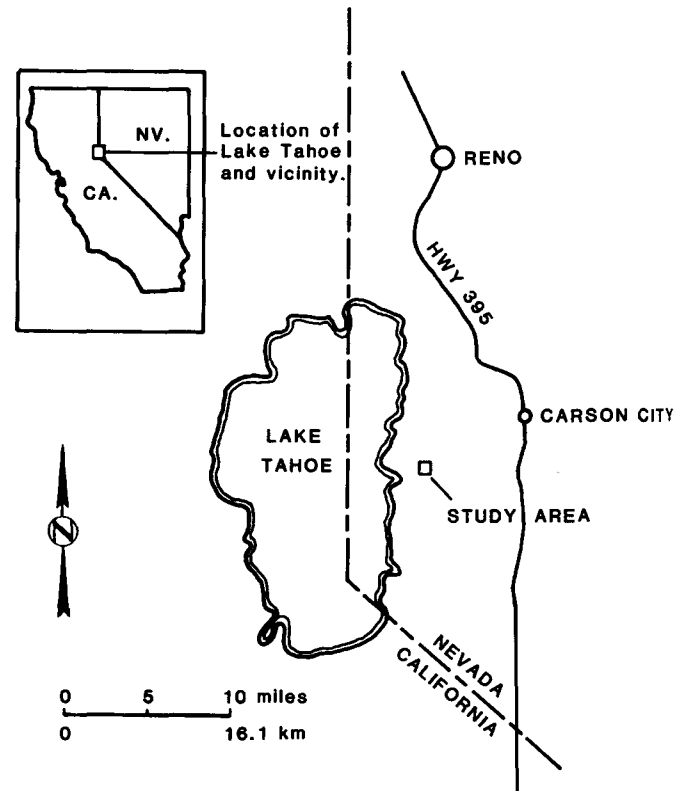


Figure 1. Location of Study Area.

Native vegetation of the area is characterized by Jeffrey pine (*Pinus jeffreyi*), lodgepole pine (*Pinus murrayana*), white fir (*Abies concolor*) and willow (*Salix* sp.) with an understory of antelope bitterbrush (*Purshia tridentata*), sagebrush (*Artemesia tridentata*), green manzanita (*Arctostaphylos patula*), tobacco brush (*Ceanothus velutinus*), horsetail (*Equisetum arvense*) and a variety of grasses.

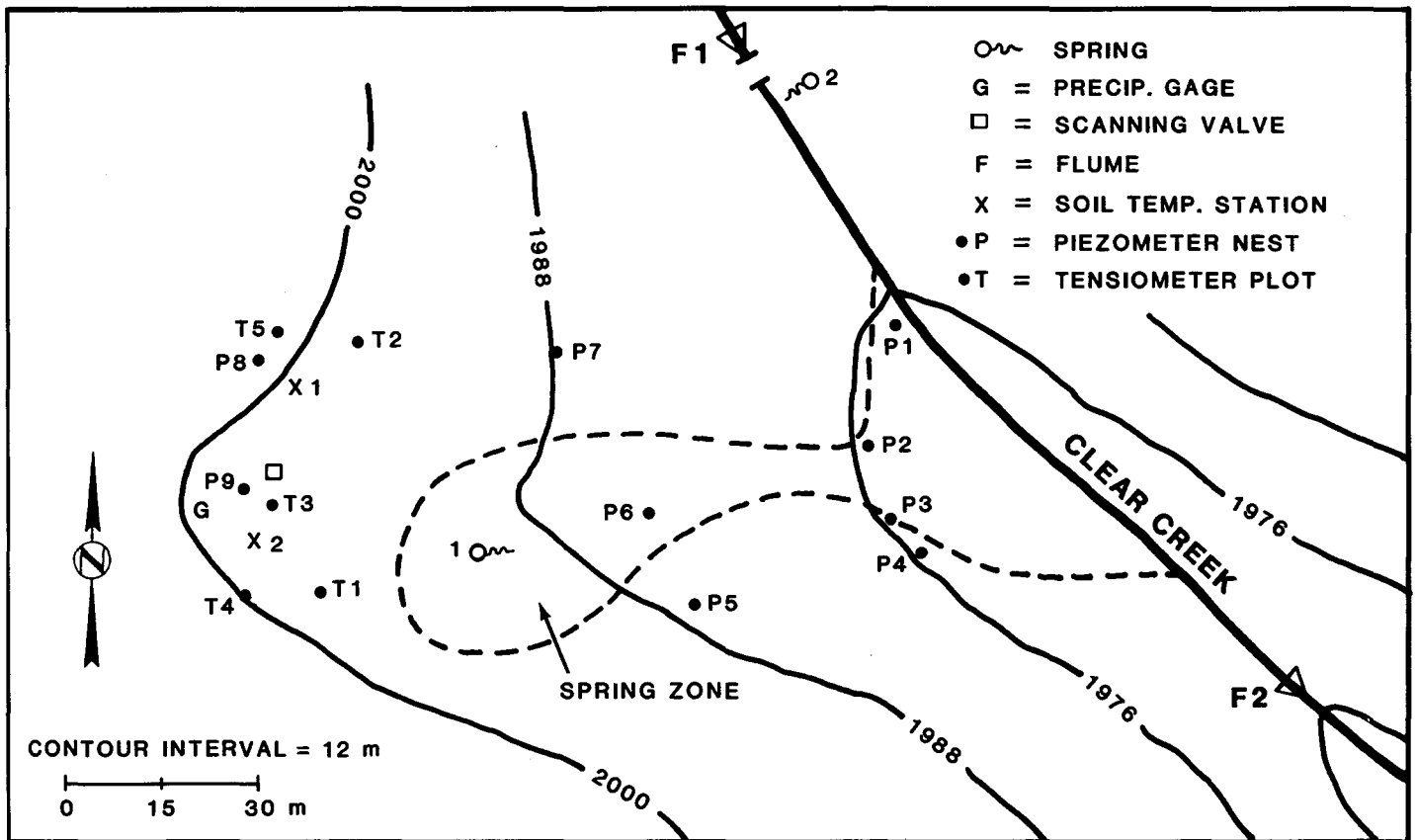


Figure 2. Map of Experimental Site.

Within the study area, a spring zone discharges into Clear Creek, a steeply incised perennial stream which has its headwaters at Snow Valley Peak (2,827 m). Clear Creek flows eastward into Eagle Valley where it enters the Carson River. The Clear Creek watershed has an area of 39 km² and delivers an average annual water yield of $4.8 \cdot 10^{-3}$ km³ into Eagle Valley.

INSTRUMENTATION

Four major groups of instruments were used at the site. The installation, operation and performance of the equipment, particularly during the winter, were a major objective of the study in addition to the purely hydrologic considerations. Since this study represented an early attempt at year-round surface/subsurface hydrologic monitoring in the Sierra Nevada, future studies (ongoing at the present time) would benefit from the mistakes and experience of the authors.

Piezometer nests provided data on vertical hydraulic gradients in the saturated zone and changes in groundwater levels. Flumes (H-type) were placed on the perennial stream to determine streamflow gains/losses through the experimental site. Vertically-distributed psychrometers in the soil provided temperature gradients.

The last major instrument group consisted of 5 tensiometer nests linked to a central 24-port hydraulic scanning valve by 1.6 mm OD flexible vinyl tubing (Figures 3 and 4). Trenches at least 45 cm deep were dug for tubing installation to reduce the possibility of freezing during the winter months. A total of 22 tensiometers and two reference reservoirs were used in the soil moisture monitoring system. The outlet of the scanning valve was connected to a differential pressure transducer, whose output was connected to a strip chart recorder. Lead-acid batteries were used for power. The scanning valve-transducer assembly was installed in a wooden box, insulated and buried about 50 cm deep. The batteries

and recorder were housed in an enclosure placed above the average snow level. In this manner, the entire tensiometric system was completely automated. The system used is similar to ones described by Anderson and Burt (1977) and Williams (1978); more detailed information can be found in Boone (1983). Monitoring was initiated in July 1982 and extended through March 1983.

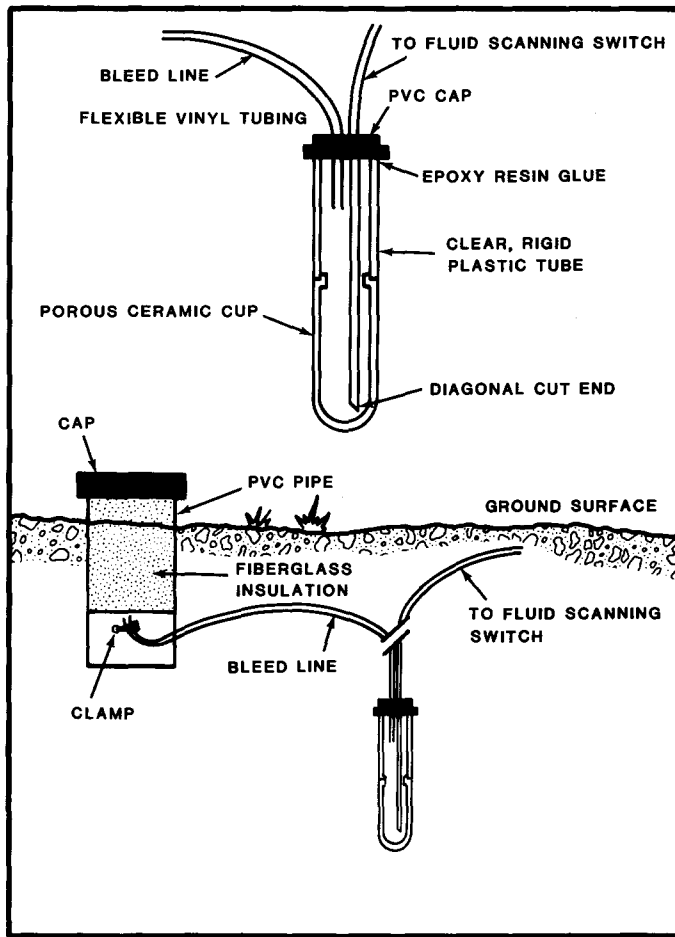


Figure 3. Tensiometer Construction and Arrangement (after Williams, 1978).

RESULTS AND DISCUSSION

Temperature Data

Temperature data, collected at two different sites, indicated gradual decreases in soil temperature throughout the study period. At no time, however, except for a few days in November, did

soil temperatures fall below freezing. Frozen soil was not observed at the snow/soil interface after the first snowfall in early November. The insulating effect of the snow (which averaged over one meter deep at the end of the study) was the major reason for the unfrozen soil. A slush layer was observed at the snow/soil interface, but it had metamorphosed to a granular, icy layer by mid-December. At station 1, the temperature gradient decreased from $3.9^{\circ}\text{C}/\text{m}$ in October to $1.6^{\circ}\text{C}/\text{m}$ in March; at the other station, the decrease was from $2.6^{\circ}\text{C}/\text{m}$ to $2.3^{\circ}\text{C}/\text{m}$.

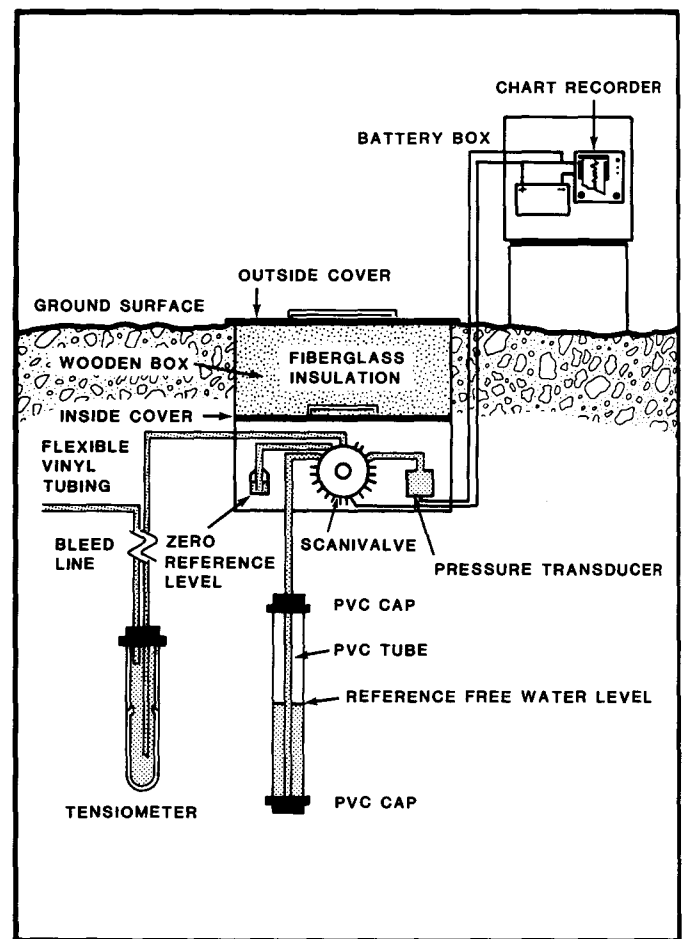


Figure 4. Automatic Tensiometer-Transducer System (after Williams, 1978).

The limited temperature data, coupled with the tensiometric data, suggest that the soil heat flux may have been suffi-

ent to melt the base of the snowpack in some areas and permit infiltration into the soil. The icy layer referred to earlier may have been discontinuous or not entirely impermeable.

Tensiometric Data

Tensiometric data from plots 3 and 4, which are representative of the entire site, and precipitation data (expressed as liquid water equivalent) are shown in Figures 5 and 6. Tensiometry established that from July to about early November, hydraulic gradients in the soil alternated between upward (response to evapotranspiration) and downward (response to precipitation/infiltration events). During this time, the tensiometer-transducer system performed well, although the system occasionally had to be shut down to purge it of air. This period essentially served as a "shakedown" period to ensure that the system worked well.

In November, matric potential at all soil depths decreased slightly from the near-zero or near-saturated conditions which resulted from the October storms. From November 1982 through February 1983 matric potential values remained fairly constant between -2.0 to -8.0 centibars with a downward hydraulic gradient. However, a slight increase in matric potential for most depths beginning around November 19th to 20th did occur due to the precipitation events of November 18th and 19th (6.9 cm total) and November 21st and 22nd (at least 1.3 cm total). Additional pulses of deep percolation may have occurred as a result of the storm (rain-on-snow) events of December 20th to the 21st (2.9 cm total) and January 24th to the 26th (1.6 cm total), but the data from plots 3 and 4 do not indicate this; these pulses are more evident from the piezometric data. Conditions at plot 4 were generally similar to those at plot 3 throughout most of the study period.

The maintenance of a downward hydraulic gradient in the soil in the vicinity of tensiometer plots 3 and 4 from November through February indicates that deep percolation (potential groundwater recharge) occurred through this period. This downward movement of water occurred under near steady-state conditions which were occa-

sionally disrupted by additional pulses of moisture movement due to precipitation events. In addition, soil moisture movement occurred at relatively high values of matric potential, indicating flow under "slightly" unsaturated conditions. It should be noted that the term "slightly" is subjective, since the lack of data did not permit the determination of the degree of saturation of the soil during this period of downward flux. Although moisture characteristic curves for the site soils were unavailable, comparison with those for soils of similar texture indicated that degrees of saturation were around 0.90 and that the soil hydraulic conductivity represented nearly-saturated conditions.

Piezometric Data

Unlike the tensiometric data, hydraulic head data from the piezometer nests were temporally discrete and obtained manually. This proved difficult at times during the winter because of deep snow conditions. Unfortunately, piezometric data in close proximity to the main tensiometer plots (3 and 4) were unavailable. Piezometer nest 1, located on the banks of Clear Creek, indicated horizontal flow throughout the study period; piezometer nest 6 indicated a slight upward gradient throughout the study. For illustrative purposes, data from nests 2, 3 and 4 are most useful and are shown in Figure 7. Piezometer nest 2 showed an upward gradient, while nests 3 and 4 indicated downward gradients. In each nest, the datum for hydraulic head is the bottom of the deepest piezometer.

Each of the nests in Figure 7 shows a fairly quick response to storm events during the late summer and fall. Piezometer nest 4 indicates the most change, probably because of its close proximity and direct hydraulic connection to Clear Creek. Increases in water levels in nest 4 probably reflect a rise in the water table within sediments of the stream channel, similar to a buildup of the zone of saturation along a stream bank as described by Chorley (1978). Piezometer nest 4 is located in that part of the channel occupied by Clear Creek during high discharge. Nest 4 also shows a rapid

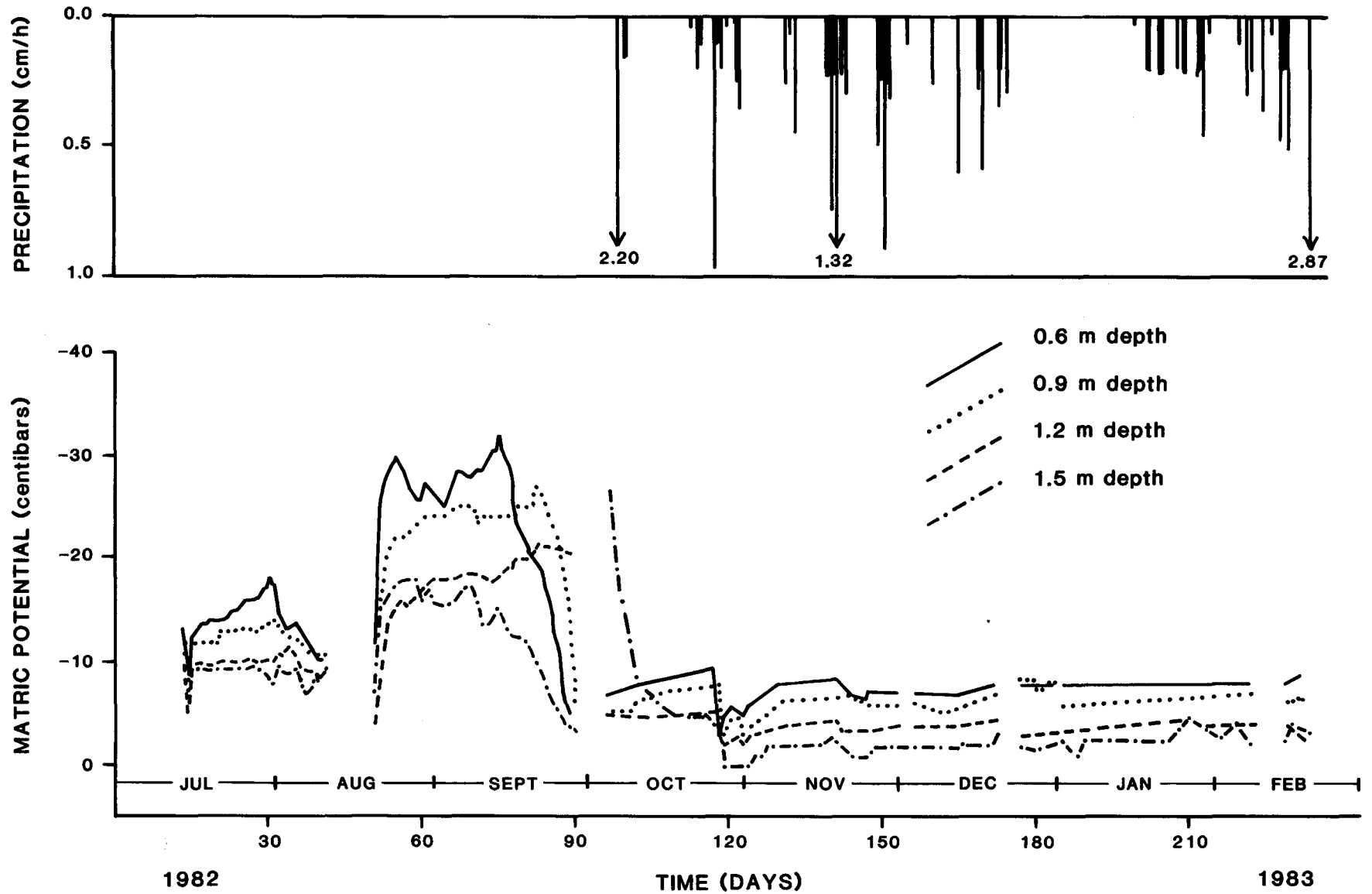


Figure 5. Site Precipitation and Tensiometric Data for Plot 3.

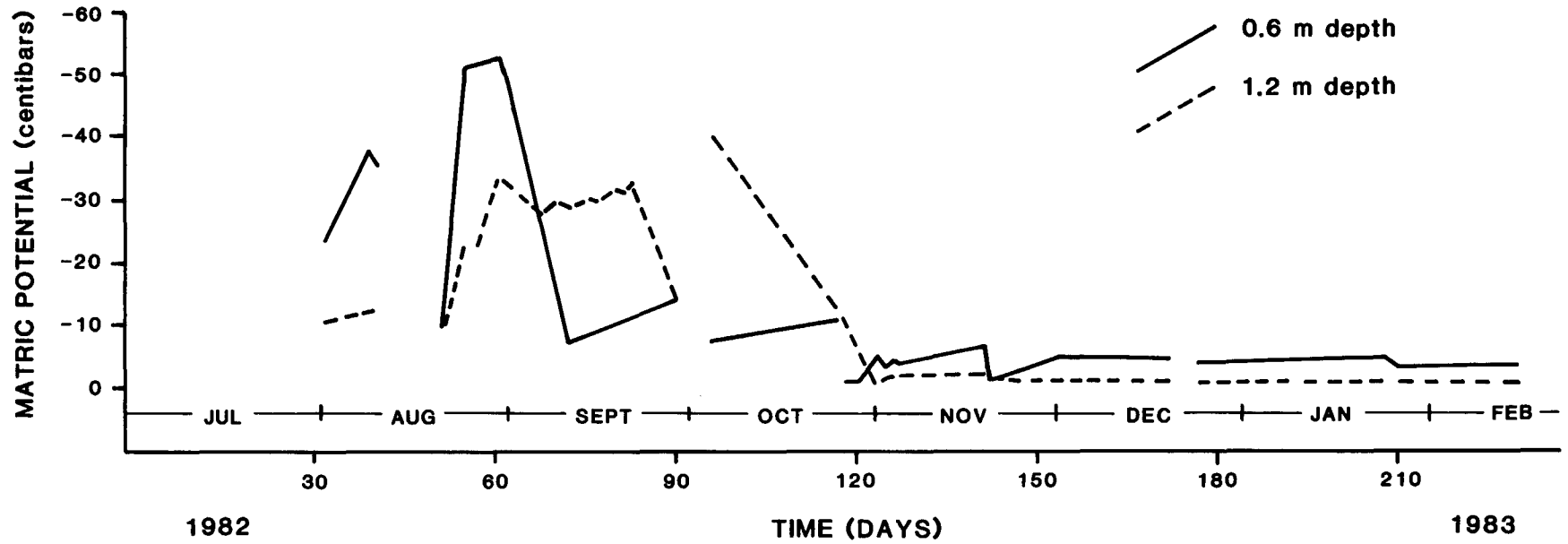
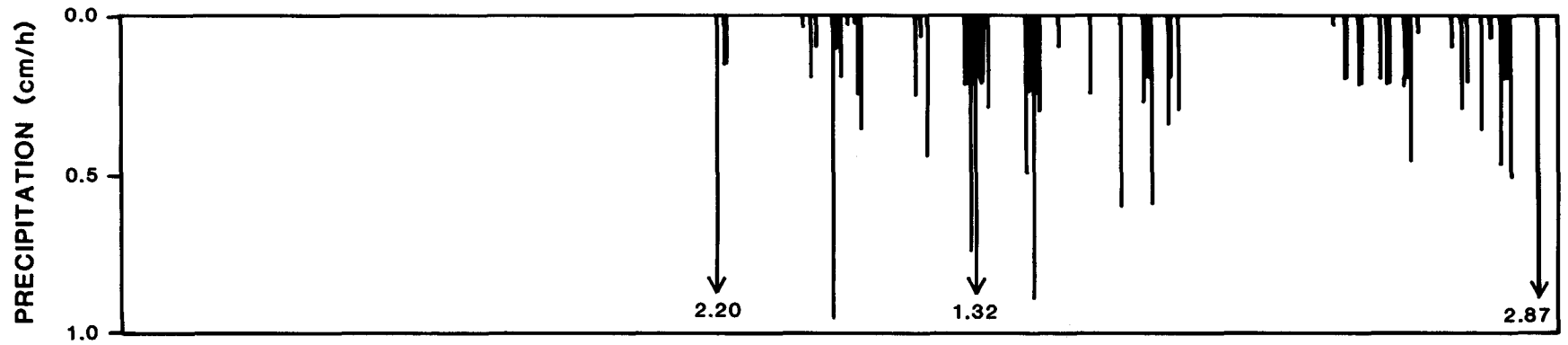


Figure 6. Site Precipitation and Tensiometric Data for Plot 4.

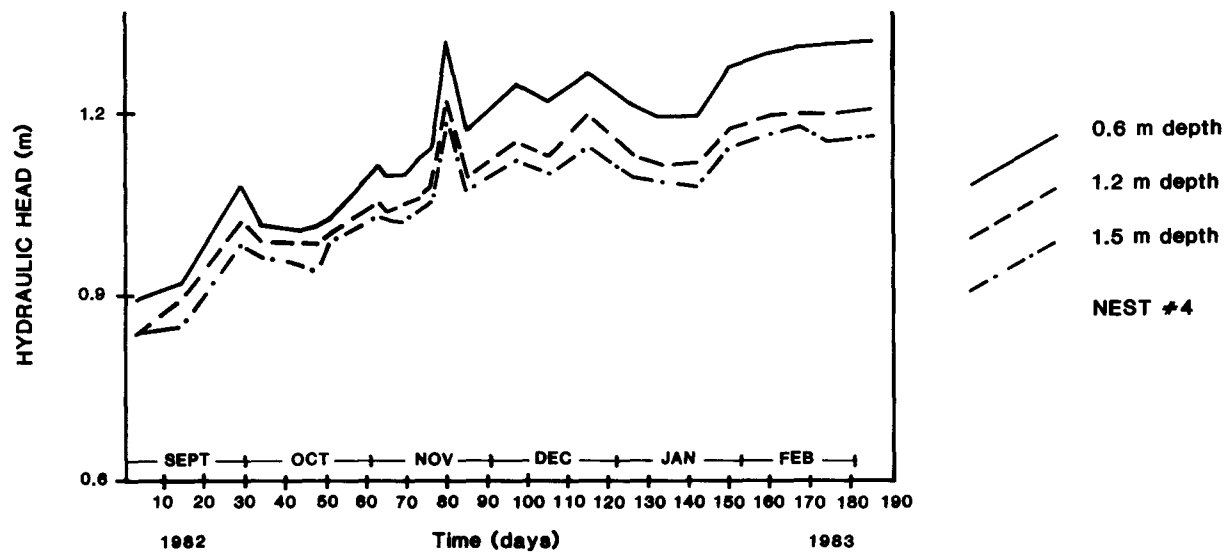
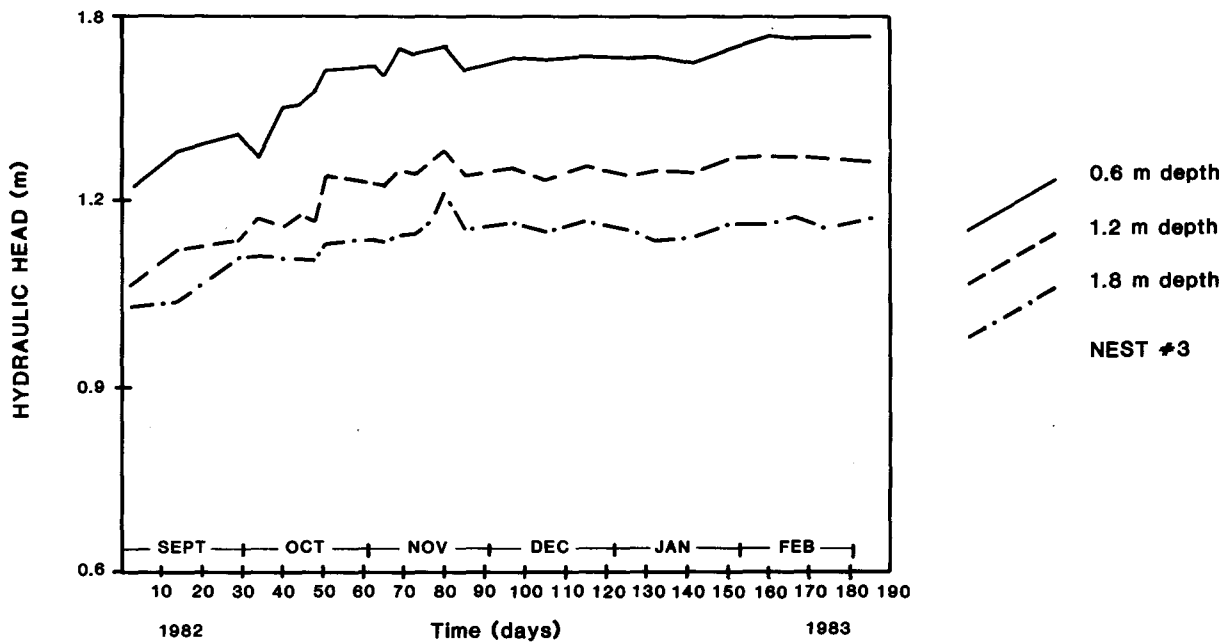
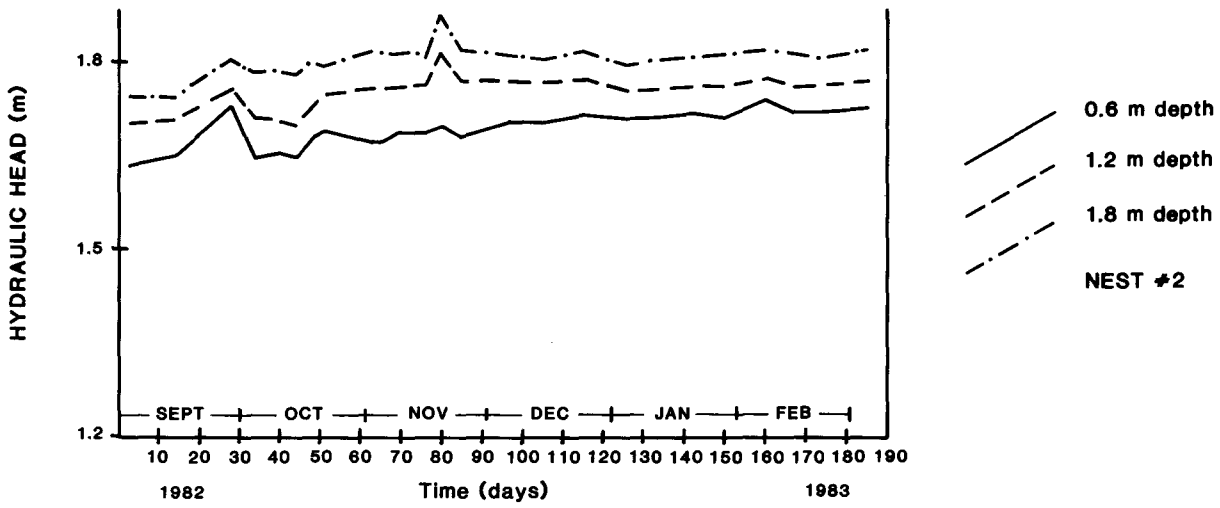


Figure 7. Hydraulic Head Data for Piezometer Nests 2, 3 and 4.

response to the aforementioned rain-on-snow events of late December, 1982 and late January, 1983. Nests 3 and 6 also showed overall water level rises from the beginning to the end of the study period. This indicates a rise in the saturated zone of the spring zone, possibly due to increased recharge associated with an areal shift in recharge/discharge areas. It is also possible that the increasing heads could have been the result of lateral unsaturated flow from upslope.

During piezometer installation, a confining clay layer approximately 5 to 10 cm thick was found about 2.4 m below the surface near piezometer nest 2. Groundwater existed above and below this layer. A similar clay layer was found at approximately 0.75 m below the surface near the top of the spring zone (approximately 15 m southeast of tensiometer plot 3). Assuming horizontal continuity, this clay layer could extend below the tensiometer plots at a depth of approximately 5.5 to 7.6 m and may play a major role in groundwater transmission in this area. This clay layer results in a groundwater system similar to an unconfined aquifer overlying a confined aquifer and was probably very significant in the development of this spring zone. The spring zone is a slump-type structure, the top of the zone being the edge or main scarp of the slump. These types of structures have been observed in other spring areas in the Clear Creek watershed. A perched water table atop the clay layer, coupled with the steep incision of Clear Creek, may have resulted in slope oversteepening and slumping.

It is possible that groundwater flows through the unconfined system below the tensiometer plots and contributes to streamflow. Water detected in the ten-foot piezometer of nest 8 around early February seems to confirm such a conclusion. The water table had risen approximately 0.08 m above the bottom of this piezometer by early March. The rapid response in piezometer water levels to storms could be a combination of recharge directly onto the spring zone and contribution of groundwater from this flow system. A medium for direct hydraulic connection between recharge and this groundwater system could be the thinner soils found on topographic spurs farther upslope.

Surface Water Data

Streamflow data were collected from two H-type flumes installed on Clear Creek about 160 m apart. Errors in discharge determination resulted from sedimentation in the flume, which changed the approach velocity and altered the stage-discharge relationship. Other sources of error were present, although sedimentation was undoubtedly the dominant one. The flume errors could account for the discharge differences between the two flumes, so the streamflow data were inconclusive and of little use.

RECHARGE IMPLICATIONS

The tensiometric data from plots 3 and 4 indicated that deep percolation (potential groundwater recharge) occurred beneath the snowpack during the winter. The hydraulic gradients in the soil at these plots were directed downward during the period from approximately November to March. Furthermore, with the exception of a few pulses of percolation from precipitation events, the downward gradient at each site was approximately constant, as was the matric potential at a given depth. These data indicate that deep percolation was occurring at this time, as was groundwater recharge. No piezometric data or deep (greater than a depth of 1.5 m) matric potential data are available from the immediate vicinity of plots 3 and 4, so recharge to the groundwater reservoir was not actually observed. However, the soil hydraulic data suggest recharge occurred, because soil-moisture movement was occurring under approximate steady-state conditions, which indicates that the soil was serving primarily as a "transmission zone".

Frozen soil was not observed during the study period, so water movement through the soil was possible. Although the slush layer at the snow/ground interface gradually metamorphosed to a granular, icy layer by mid-December, a transformation that would seem to preclude infiltration from the snowpack, dye studies suggest that such ice layers are not entirely impermeable but possess various permeabilities which force water to take a more circuitous route to the soil

(Langham, cited in Male and Gray, 1981, p. 398). Fracturing in the ice layers would also permit the movement of water into the soil.

CONCLUSIONS

The major conclusion of the study is that deep percolation, and thus, groundwater recharge, occurred beneath the snowpack during the winter months; furthermore, the rain-on-snow events provided additional pulses of infiltration superimposed on the steady downward deep percolation. Because this observation is mostly qualitative, more investigation is needed into winter-season recharge. This phenomenon is often overlooked in hydrologic studies/budgets in the Sierra Nevada, the Great Basin and perhaps other regions as well. The study could not determine how much recharge eventually discharged into Clear Creek and how much flowed off-site, perhaps as part of a deeper subsurface flow system.

The automatic tensiometer-transducer system exhibited rapid response, and although some problems, such as tensiometer failures, did occur, future studies can build on our experiences. A major constraint on the use of the system is the trenching required in order to bury the hydraulic tubing below the frost line. Trenching was labor-intensive and time-consuming since much of it had to be done manually. As suggested by others (McKim, et al., 1976; 1980), this could possibly be circumvented by the use of an ethylene glycol (antifreeze) - water mixture, although more research is needed to assess the effects, if any, of such a mixture on the soil matric potentials. The use of 1.6 mm OD vinyl tubing placed limits on the areal extent of the system because of the frictional head losses. The authors' experience leads them to recommend the use of 3.2 mm OD nylon tubing in similar studies; cost constraints prevented its use in the present study. Studies along the lines reported here are continuing, because this research spanned less than one year and sampled a winter that produced one of the heaviest snowfalls on record. The instrumentation at the site has been expanded and monitoring continues.

ACKNOWLEDGEMENTS

Many people assisted in this study and deserve thanks; however, without the help of C.M. Skau none of this would have been possible. Karla Cosens and Christine Stetter provided invaluable, excellent-quality assistance throughout the preparation of this manuscript. The Toiyabe National Forest of the U.S. Department of Agriculture allowed access to its land for the study; the Carson Ranger District of the U.S. Forest Service was most helpful. Financial support was provided by the Office of Water Research and Technology, U.S. Department of the Interior (Grant #14-34-0001-1244); the U.S. Geological Survey's Great Basin Regional Aquifer Systems Analysis (RASA) Program; and the Desert Research Institute, University of Nevada System.

REFERENCES

- Anderson, M.G. and T.P. Burt, 1977. Automatic Monitoring of Soil Moisture Conditions in a Hillslope Spur and Hollow. *Jour. of Hydrology*, 33:27-36.
- Boone, R.L., 1983. Groundwater Recharge and Subsurface Flow Processes on a Hillslope in the Clear Creek Watershed, Eastern Sierra Nevada. Unpublished M.S. Thesis, University of Nevada-Reno, 164 pp.
- Chorley, R.J., 1978. The Hillslope Hydrological Cycle. In: *Hillslope Hydrology*, M.J. Kirkby (ed.). John Wiley & Sons, pp. 1-42.
- Male, D.H. and D.M. Gray, 1981. Snowcover Ablation and Runoff, In: *Handbook of Snow*, D.M. Gray and D.H. Male, (eds.). Pergamon Press, pp. 360-436.
- McKim, H.L., R.L. Berg, R.W. McGraw, R.T. Atkins and J. Ingersoll, 1976. Development of a Remote-Reading Tensiometer/Transducer System for Use in Sub-freezing Temperatures. In: *Proceedings of the Second Conference on Soil Water Problems in Cold Regions*. American Geophysical Union, Washington, D.C., pp. 31-45.
- McKim, H.L., J.E. Walsh and D.N. Arion, 1980. Review of Techniques for Measuring Soil Moisture in situ. U.S. Army Corps of Engineers Special Report 80-31, Cold Regions Research and Engin-

Engineering Laboratory, Hanover, NH, 17 pp.
Williams, T.H.L., 1978. An Automatic
Scanning and Recording Tensiometer
System. Jour. of Hydrology,
39:175-183.

DISCHARGE UNDER AN ICE COVER

Henry S. Santeford and George R. Alger¹

ABSTRACT: In 1983, the authors proposed a theoretically based model, augmented with a conventional resistance equation (Manning's equation), to relate the stage to discharge on ice covered rivers. A cooperative field study was established with the U.S. Geological Survey and U.S. Army, Cold Regions Research and Engineering Laboratory to test the proposed model. The results of this first winter season indicate that the average difference between the predicted and measured discharge values was within the limit of error of the discharge measurement (± 3 percent). The model was also applied to unpublished historic records of the USGS for the same sites. Although there are traditionally only 2 to 4 data points per winter season, the results were the same as those reported for the more extensive study.

(KEY TERMS: ice cover; stage-discharge relationships.)

INTRODUCTION

Many hydrologists view the collection of discharge data as a routine type of operation. For the open water condition, a stage vs. discharge relationships is developed for the chosen gage location. Then a simple monitoring of stage can be used to develop a continuous record of discharge. Through periodic checks of actual discharge measurements and appropriate quality control, reliable records can be obtained.

However, when an ice cover forms on an open channel, the stage vs. discharge relationship which had existed for the open water condition is no longer valid. The presence of the ice cover alters the size and shape of the rigid boundary in contact with the moving water. This, in turn, causes the energy slope to steepen. In addition the ice cover which is generally assumed to be floating, has a buoyant displacement causing a further increase in stage. These two factors -- increased resistance and buoyant displacement -- often work together to produce a stage associated with ice covered conditions which is larger than the stage which would have existed at the same discharge for the open water condition. This increase in stage is often termed "ice induced backwater" or merely "backwater".

Through the years a number of techniques have been developed in an attempt to relate the open water and ice covered stage vs. discharge relationships. All of these early techniques suffer from the same general problems. First, none of the older techniques considers the buoyant displacement of the ice. Consequently, the buoyant displacement of the ice (distance from equivalent free water surface to underside of the ice cover) is not generally measured at the gage location. Secondly, none of the early techniques can be shown to be theoretically sound, i.e. they are merely based on regression analysis or curve fitting. And thirdly, all of the

¹Both, Department of Civil Engineering, Michigan Technological University, Houghton, Michigan 49931.

early techniques assume that the same functional relationship exist from the time of the first appearance of ice at freeze-up through the breakup period. A simple analysis of the flow regime clearly indicates that at freeze-up and again at breakup, the flow must be both unsteady and non-uniform as the transition is made between the open water and ice covered conditions (Santeford and Alger, 1983). However, once the transition is complete, a stable period exists during which there is a fixed relationship between the open water and ice covered conditions. The authors have term this "the period of stable ice control" (Santeford and Alger, 1984a, 1984e, 1984d).

Many of the water survey agencies in the northern hemisphere rely on the interpretative discharge technique to estimate winter discharge records. Actual discharge measurements are made at routine time intervals, often once per month. The actual discharge measurement is made at a convenient location, not necessarily at the gage cross-section. Consequently, the information necessary to correct for the buoyant displacement of the ice at the gage is not always available from the field data. The winter discharge record is then constructed by sketching a hydrograph between the plotted discharge values obtained at the time of the routine (monthly) measurements. The hydrologist is aided in his sketching by the stage record, local air temperature records, precipitation data, and discharge measurements from nearby streams. The procedure is very time consuming and highly dependent upon the skills of the hydrologist.

In 1983, the authors proposed an analytical technique which would provide a direct conversion from winter stage records to discharge. The model was based on a theoretical analysis of open channel flow augmented by a conventional resistance equation (Manning's equation). Using unpublished records of the U.S. Geological Survey encouraging results were obtained for data from several selected streams in Michigan's Upper Peninsula (Santeford and Alger, 1984b; Alger and Santeford, 1984). Based on these preliminary findings a

detailed study was initiated with the aid of the U.S. Geological Survey and the U.S. Army Cold Regions Research and Engineering Laboratory.

Three gaging sites were chosen for use in the initial study (Figure 1). At each site the frequency of discharge measurement was increased from once per month to as many as 3 per week. Warm weather conditions hampered the data collection efforts at the Red Cedar site. Thus, only the two northern stations will be discussed in the summary (see Santeford, Alger and Stark, 1986).

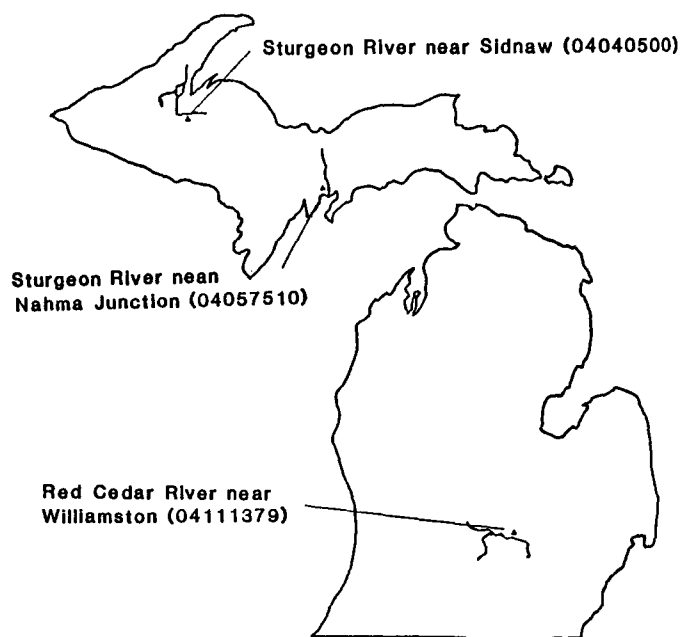


Figure 1. Map of Michigan showing location of study areas.

THE PROPOSED MODEL

Earlier works of the authors have shown that for the same discharge, the ratio between the open water mean hydraulic depth (D_o) and the ice covered mean hydraulic depth (D_i) is a constant termed the ice adjustment factor (IAF).

$$D_o/D_i = \text{constant} = \text{IAF} \quad (1)$$

The magnitude of the IAF will be site specific depending upon the location of the gaging site related to the control sections and the geometry of the gaging section.

Using a cross-section obtained at the gage location and the open water rating curve it is a simple matter to construct functional relationships between stage, discharge, area, top width, and mean hydraulic depth. These relationships can be presented either as mathematic functions or in tabular form as shown in Table 1 for the Sturgeon River near Nahma Junction.

During the ice covered period the stage record is influenced by the buoyant displacement of the ice as well as the increase in energy slope resulting from the added resistance offered by the ice cover. Thus, before the stage record can be used to predict discharge, it must first be corrected for buoyant displacement. Since most natural rivers do not have regular prismatic cross-sections and further since the density of the ice cover is not a constant, the term "float depth"

will be introduced to account for the buoyant displacement.

In the development of equation 1, a key element was the under ice area available to the flow. For the given under ice area there is a stage which would exist if the buoyant displacement of the ice was not present. That value of stage is termed GH_i . If the actual recorded stage is termed GH_w , it follows that

$$GH_w - GH_i = \text{float depth.}$$

Since GH_i is the desired term, it is more convenient to express the relationship as

$$GH_i = GH_w - \text{float depth} \quad (2)$$

Float depth can be defined as the correction which when applied to the actual stage reading yields a corrected stage with the appropriate area available to the flow.

When an actual discharge measurement is made on an ice covered stream, the under ice flow area and the actual stage

Table 1. Ice correction data table for Sturgeon River near Nahma Junction.

Stage (ft)	Discharge (ft ³ /s)	Area (ft ²)	Top Width (ft)	Mean Hydraulic Depth (ft)
4.10	86.0	99.1	60.3	1.64
4.09	84.4	98.4	60.2	1.63
4.08	82.8	97.8	60.2	1.63
4.07	81.2	97.2	60.2	1.62
4.06	79.6	96.6	60.1	1.61
4.05	78.0	96.0	60.1	1.60
4.04	76.4	95.4	60.1	1.59
4.03	74.8	94.8	60.0	1.58
4.02	73.2	94.2	60.0	1.57
4.01	71.6	93.6	59.9	1.56
4.00	70.0	93.0	59.9	1.55

(GH_w) are both known quantities. Entering a relationship such as shown in Table 1 with the under ice area, one can readily obtain GH_i and thus the float depth. The float depth can also be obtained through field measurements of the ice cover. The procedure consists of measuring the distance from the free water surface to the under side of the ice cover at numerous location along the gage cross-section. From these data one can compute the cross-sectional area occupied by the ice. For the given stage the total wetted area is known and the area available to the flow can be found as the residual. If the float depth is a known quantity or can be estimated for periods between measurements, then the adjusted stage record can be used to give a direct indication of discharge similar to what is done for the open water condition.

However, it is often more convenient to use only one rating curve for summer and winter condition and apply a correction for the ice covered condition. The ice adjustment factor (IAF) is that correction factor.

The IAF is also readily obtained from field data. Here a simple illustrative example is used to demonstrate the procedure. On February 11, 1985, the USGS measured discharge at the Sturgeon River near Nahma Junction and reported the following data:

Discharge = 83 cfs
 Stage (GH_w) = 4.92 ft
 Float Depth = 0.89 ft

Therefore:

$$GH_i = GH_w - FD$$

$$= 4.92 - 0.89 = 4.03 \text{ ft}$$

From Table 1 at a stage of 4.03 ft, the mean hydraulic depth is 1.58 ft. Since this value is for an ice covered condition, it represents D_i . Returning to Table 1 with discharge equal to the measured value of 83 cfs, the mean hydraulic depth that would have existed for open water condition, D_o , is found to be 1.63 ft.

Then: $IAF = D_o/D_i = 1.63/1.58 = 1.03$

If conditions are stable, the IAF should be a constant for any given gage location. Furthermore, the adjusted stage vs. discharge relationship for the ice covered condition should correspond to the open water relationship.

Because of the general requirements used in selecting favorable gaging sites, most gages which exhibit an ice effect on the stage vs. discharge relationship also experience a period of stable ice control. However, there are exceptions. As mentioned previously, freeze-up and breakup will produce unstable conditions at all gage location. In addition, the nature of the control section and the resulting water surface profile can also result in unstable conditions. For example: (a) a gage located along an M-2 profile upstream of a rapids or riffle which remained free of ice; and (b) a gage located in an ice covered channel a short distance downstream from the outlet of a lake. In both cases there will be a family of rating curves depending upon the buoyant displacement of the ice. Space limitation do not allow for a full discussion of the various water surface profile which can exist for ice covered condition. A full discussion of ice effects on water surface profile and thus stable vs. unstable condition is presented in: Stark, 1986; Santeford, Alger and Stark, 1986; and Santeford, 1986.

RESULTS

As mentioned previously, during the 1984/85 winter season the frequency of winter discharge measurement was increased. The actual number of measurements varied with each of the test sites. The measured stage vs. discharge data are shown in Figure 2 for the Nahma Junction site. The relationship could be described as a "shot gun pattern". The stage values were then adjusted for both float depth and increased resistance (i.e. IAF) and replotted in Figure 3. It will be noted that very close agreement is obtained with the open water rating curve. The IAF for each measurement was computed. The mean value was 1.03 with a standard deviation of 0.01. Using the mean value

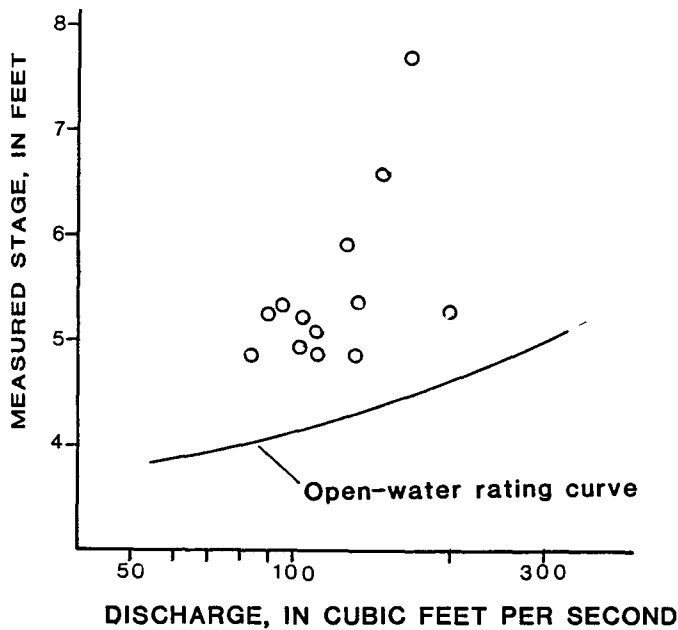


Figure 2. Semi-log plot of stage and discharge data collected during the 1984-85 winter season for the Sturgeon River near Nahma Junction.

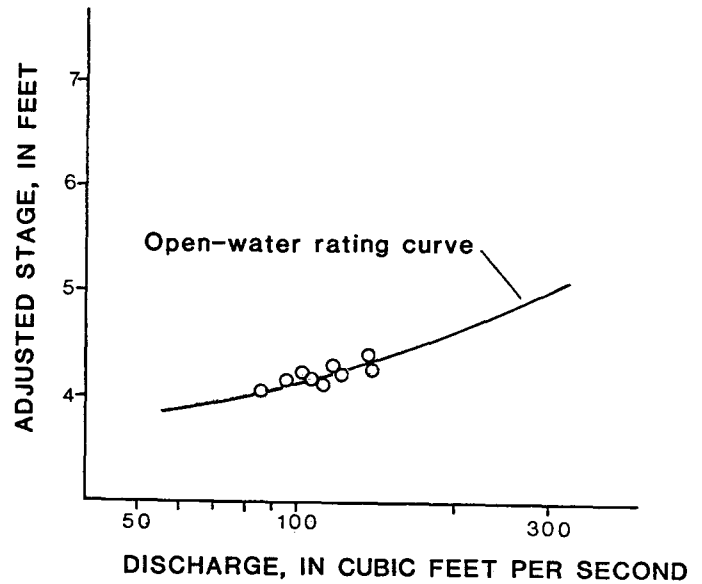


Figure 3. Adjusted stage vs. discharge relations for the 1984-85 winter for the Sturgeon River near Nahma Junction.

for the IAF and a linear interpolation of float depth between successive readings, the hydrograph of Figure 4 was computer generated from the stage hydrograph. The actual measured discharges are also shown.

Previous studies by the authors had used the unpublished records of USGS for the same station. Using the raw field data from the monthly measurement for the ice covered condition for the period 1970-75, the mean value of the IAF was computed to be 1.02 with a standard deviation of 0.02. This is basically the same as that found for the more extensive study during the 1984/35 winter season.

At the time of this writing only a portion of the data for the 1985/36 winter season was available. Here again, the IAF has a value between 1.02 and 1.03.

Of the 3 sites used in this study, the Sidnaw site received the most intensive study. Results similar to those shown for Nahma Junction were also obtained for the data from the Sidnaw

site. The ice adjustment factor was found to be 1.00 (mean value).

As part of the analysis of the Sidnaw data it was assumed that field measurement (i.e. float depth and discharge) were made on January 4 and again on January 29. A linear interpolation of float depth was used for all intervening days. Using the actual stage record and the interpolated float depth the model was used to predict the discharge for the intervening days. These results are shown in Table 2. Also, shown in Table 2 are the actual measured discharges on 9 different occasions during the 26 day time period. The average error between predicted and measured discharge was 2.9 percent. Under the best of field condition, it is generally assumed that a discharge measurement will have an error of ± 3 percent. Thus, the average error between the predicted and measured values of discharge was within the limits of error of the discharge measurements.

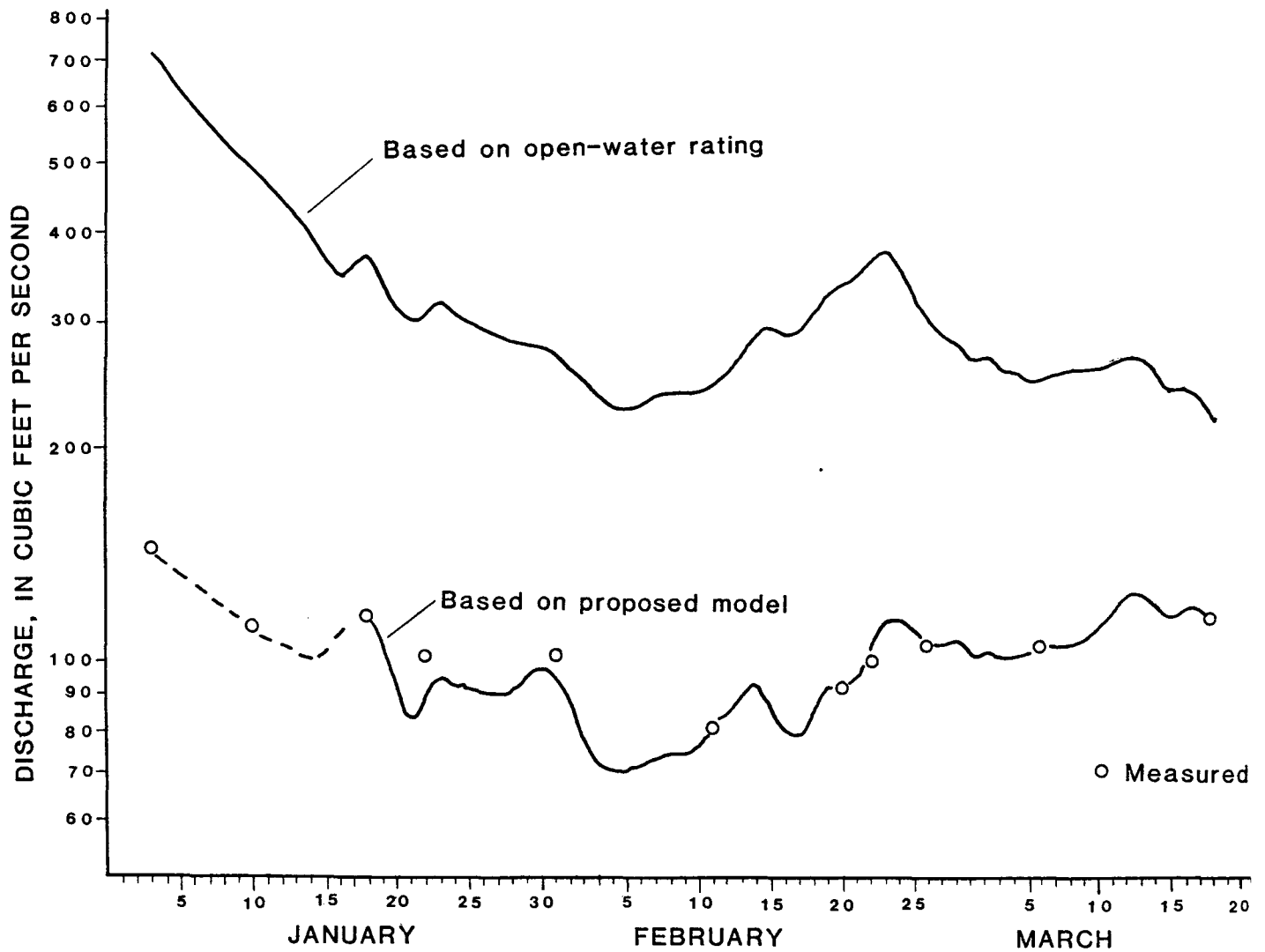


Figure 4. Hydrographs for the 1934-85 winter for the Studreon River near Nahma Junction

SUMMARY AND CONCLUSIONS

In 1983, the authors proposed a theoretically based model to relate stage on an ice covered river to discharge. When the condition at the gage can be classified as "a period of stable ice control" a simple relationship exists between the open water and ice covered rating curves based on mean hydraulic depth. However, the stage records for the ice covered period are influenced by a buoyant displacement resulting from the floating ice cover. In order to develop a rating curve for the ice covered

period, the stage records must first be corrected for the buoyant displacement.

In order to test the model, frequent discharge measurements were made on two different rivers in Michigan's Upper Peninsula. In both cases the results show that the average difference between predicted and measured values was within the expected limits of error associated with a discharge measurement ($\pm 3\%$). A review of unpublished historic records of the U.S. Geological Survey for the period 1970-75 showed that the same relationships existed for the historical record as were

Table 2. Comparison between predicted and measured discharge during January, 1985 for the primary gage at Sidnaw, Michigan.

Date	Stage (ft)	Discharge (ft ³ /s)		Error	
		Predicted ^a	Measured	(ft ³ /s)	Percent
January, 1985					
4	4.23	66.1	65.9	0.2	0.3
5	4.19	61.4			
6	4.18	60.3			
7	4.26	69.4			
8	4.27	70.6	66.7	3.9	5.7
9	4.23	65.7			
10	4.19	61.0			
11	4.16	57.0			
12	4.13	54.7	57.2	2.5	4.5
13	4.11	52.8			
14	4.10	51.7			
15	4.12	53.6	52.9	0.7	0.1
16	4.12	53.6			
17	4.11	52.5			
18	4.13	54.3			
19	4.15	56.2	53.6	2.6	4.7
20	4.11	52.2			
21	4.08	49.3			
22	4.08	49.3	50.7	1.5	3.0
23	4.09	50.1			
24	4.13	53.8			
25	4.13	53.8			
26	4.14	54.6	55.4	0.8	1.4
27	4.12	52.6			
28	4.12	52.6			
29	4.11	51.5	49.7	1.8	3.6
Average Error:				1.75	2.9

^a Predicted discharge is based on an assumption that discharge and float depth were measured only on January 4 and 29. A linear interpolation of float depth was used for all intervening days.

found in this study. Thus, although the data base for any given winter season may only contain a few actual discharge measurements the results confirm that a consistent relationship exists between the appropriate open water and ice covered rating curves.

ACKNOWLEDGMENT

The authors gratefully acknowledge the cooperation and support of the U.S. Geological Survey and the U.S. Army Cold Regions Research and Engineering Laboratory.

REFERENCES

- Alger, G. R. and H. S. Santeford, 1984, "A Procedure for Calculating River Flow Rate Under an Ice Cover," Proceedings: IAHR Ice Symposium, Hamburg, Germany, August 27-31, Vol. 1, p. 389-398, Discussion: Vol. III, p. 443-450.
- Santeford, H. S., 1986, "Stage, Discharge and Ice," Proceedings: Sixth Northern Research Basins Symposium/Workshop, Houghton, MI, January 26-30, 1986 (In publication).
- Santeford, H. S. and G. R. Alger, 1983, "Effects of An Ice Cover - A Conceptual Model," Proceedings: Frontiers in Hydraulic Engineering, ASCE Hydraulics Division Specialty Conference, Cambridge, MA, August, p. 242-247.
- Santeford, H. S. and G. R. Alger, 1984a, "The Hydraulics of River Ice - A Summary," Proceedings: Fifth Northern Research Basins Symposium, Vierumaki, Finland, March 19-23, p. 3.25-3.56.
- Santeford, H. S. and G. R. Alger, 1984b, "Predicting Flowrates in an Ice Covered Stream," Proceedings: Third International Specialty Conference on Cold Regions Engineering, ASCE/CSCE, Edmonton, Alberta, April 4-6, Vol. III, P. 1031-1043.
- Santeford, H. S. and G. R. Alger, 1984c, "Hydraulics of Breakup," Proceedings: Workshop on Hydraulics of River Ice, Fredericton, New Brunswick, June 20-21, p. 95-112.
- Santeford, H. S. and G. R. Alger, 1984d, "Hydraulics of Freeze-up," Proceedings: Water for Resource Development, ASCE Hydraulics Division Specialty Conference, Coeur d'Alene, Idaho, August 14-17, p. 574-578.
- Santeford, H. S., G. R. Alger and J. A. Stark, 1986, "Ice in Streams -- Its Formation and Effects on Flow," U.S. Geological Survey, Water Resources Investigation Report (in publication).
- Stark, J. A., 1986, Streamflow During a Period Stable Ice Control, A Master's Thesis, Michigan Technological University, Houghton, Michigan.

HYDROLOGY OF TWO SUBARCTIC WATERSHEDS

Robert E. Gieck Jr. and Douglas L. Kane¹

ABSTRACT: A water balance can provide information needed for sound water resource management. Two interior Alaskan watersheds located on Ester Dome west of Fairbanks, Alaska were studied from May 1982 to June 1984 to assess possible groundwater recharge. Numerous hydrologic measurements were made, but basically runoff and precipitation were measured and evapotranspiration was calculated using climatic variables. Generally, light showery precipitation and high evapotranspiration rates preclude or severely limit groundwater recharge during the summer months. Only during periods of substantial rainfall is groundwater recharge possible. During snowmelt every year, the groundwater recharge potential is quite high because of water stored in a snowpack that has accumulated over a 6 month period and evapotranspiration demands are minimal. (key terms: water balance; recharge; runoff; evapotranspiration; snowmelt)

INTRODUCTION

For much of interior Alaska's history, the most serious water resource problem has been to supply sufficient water for economic exploitation of its mineral resources. Recently, as rural lands have been developed for more diverse uses, the adequate and equitable supply of water for many types of use has become a serious concern. The Ester Dome area west of Fairbanks is an excellent example of such

an area. Here traditional mining operations, growing residential population, potential industrial development, agriculture, and wildlife must compete for the limited water resources available.

Water balances were calculated for two basins on Ester Dome to provide information about the area's water resources. A water balance is a valuable tool for managers and engineers who must make decisions about the area's water resources. Current problems can be solved, and future problems avoided by understanding the interrelationships of climate, runoff, groundwater storage, and land use. Of particular importance is groundwater recharge. Groundwater is the primary source of domestic water in the area; placer miners and wildlife rely on streamflow and surface storage.

STUDY AREA

Ester Dome is located within the Yukon-Tanana Upland of interior Alaska, at latitude 64° 53' north and longitude 148° 02' west. The area lies north of the George Parks Highway and approximately 11 Km west of Fairbanks within the Fairbanks Mining District. While much of the area remains undeveloped, several portions have been extensively modified by human activities.

Vegetation is typical of the Yukon-Tanana Uplands. The well-drained, south-facing slopes support forests of Paper Birch (*Betula papyrifera*), White Spruce

¹Graduate Research Assistant and Associate Professor Respectively, Institute of Northern Engineering, University of Alaska, Fairbanks, Alaska 99775-1760.

(*Picea glauca*), and Quaking Aspen (*Populus tremuloides*). The relatively sparse undergrowth consists of shrubs and forbs. The valley bottoms have shallow slopes of poorly drained soils, and the north-facing slopes support forests of Black Spruce (*Picea mariana*), with occasional Paper Birch, Green Alder (*Alnus crispus*), willow (*Salix* spp.), and Larch (*Larix larecena*). The undergrowth consists of a thick mat of mosses, lichens, tussock grasses, and shrubs.

The geology of the Ester Dome area was described by Forbes (1982). The bedrock is primarily crystalline schists of the Yukon-Tanana metamorphic complex. The mineral soils of the area are composed of layers of micaceous loess originating from the glacial outwash plains of the Tanana Valley to the south. Unconsolidated soil thickness varies from 5 cm to over 55 m. Permafrost is usually absent on the south-facing slopes. Discontinuous permafrost is encountered over much of the valley floor and on north-facing slopes. Well logs of the area show permafrost begins as shallow as 60 cm and can extend to depths beyond 45 m. Massive ground ice occurs in the area (Pewe, 1982).

Ester Dome lies within an area of continental climate characterized by warm summers and winters of severe cold. The average annual temperature at Fairbanks International Airport (133 m msl) is -3.3 °C, with an average precipitation of 24.7 cm and an average annual snowfall depth of 169 cm.

Two watersheds were studied on Ester Dome. Ester Creek is a 26.2 square-Km basin (21 percent permafrost) with a mean elevation based on area of 378 m. Happy Creek is a 25.0 square-Km basin (57 percent permafrost) with a mean elevation based on area of 216 m.

Two 73.4 square-m runoff plots were observed during snowmelt. These permafrost-free plots were located in the Goldstream Valley about 8 Km northeast of Ester Dome at an elevation of 290 m.

METHODS AND MATERIALS

The water balance equation for a basin and specific time period can be written as

$$P - I \pm F \pm E - RO \pm SS \pm GW = 0 \quad (1)$$

where

- P = precipitation
- I = interception losses
- F = lateral flux of water across soil boundaries
- E = evaporation, condensation, or actual evapotranspiration
- RO = runoff
- SS = change in soil moisture storage
- GW = change in groundwater storage.

Equation 1 can be simplified by selecting the boundaries of the soil volume to define a watershed, thus eliminating the lateral soil water flux (F) term. Precipitation (P), soil moisture (SS), interception (I) and evaporation (E) were combined into a single surplus precipitation term (SP). This term represents precipitation input after accounting for evaporation losses and changes in soil moisture. The total evaporation demand or potential evapotranspiration (PET) is controlled by the amount of energy available for evaporation. The interception term is included in PET since basically all interception evaporates in our case. When PET demand exceeds precipitation, stored soil moisture is used to fulfill the demand. Soil storage was established at 10.2 cm (Thorntwaite and Mather, 1955). When soil moisture storage is exhausted, actual evapotranspiration (AET) is less than PET. Precipitation in excess of PET is returned to soil moisture storage until the full 10.2 cm capacity is reached. The remaining precipitation is surplus precipitation (SP). Considering these simplifications equation 1 reduces to

$$SP - RO \pm GW = 0. \quad (2)$$

Potential evapotranspiration (PET) values were estimated from evaporation pan measurements. Pan data were adjusted using a 0.7 pan coefficient that was determined from a detailed mass balance for the upper one meter of soil calculation using equation 1. Soil moisture data from the runoff plots for June and July 1984 were used to obtain this pan coefficient. When pan evaporation data were not available, potential evapotranspiration was estimated using the Thorntwaite method (Dunne and Leopold, 1978). Local water balances (equation 2) were calculated monthly excluding the winter months.

Evaporation from the snowpack or condensation during snowmelt was estimated using an equation suggested by the U.S. Army Corps of Engineers (1956). This method was used for the 1983 data from start of snowmelt (15 April) until the disappearance of snow at the lowest elevations (28 April). Due to missing pan evaporation data in 1984, this method was used from 26 April until 17 May. The pan coefficient was used to adjust measured pan evaporation after these dates.

Runoff volumes were calculated by multiplying the mean discharge of a time period by the length of the time period. Discharge measurement sites were established on Happy Creek and on Ester Creek. Discharge measurements were taken using standard cup-type current meters. Measurements of discharge were made one to three times daily during snowmelt or heavy rainfall runoff events. Discharge was measured each week during mid-summer and fall. Additional snowmelt runoff data were collected at the runoff plots in Goldstream Valley.

Snowpack water equivalents were determined at snow courses designated by elevation along the existing road network. Snowpack water equivalents were obtained using an Adirondak snow sampler. The reported amounts of snow water equivalent are averages obtained for eight to ten measurements at each course.

In the late-spring of 1982, eight meteorological sites were established in the Ester Dome area to collect precipitation data. Summer precipitation data were collected using both standard 20.3 cm dipstick and tipping bucket raingages. These sites were: Coutts (2), Ester Dome Road (3), Gedney (4), Rice (6), Stone (7), Swainbank (8), Ester Dome Summit (10), and Nugget Creek (13) (bracketed numbers show site location in Figure 2). The following year 4 additional sites were added: Quartz (11), Lasonsky (12), Willow Creek (14), and St. Patrick Creek Road (15). Additional precipitation data were obtained from the U.S. Department of Commerce, National Weather Service, Alaska Climatological Summaries.

Annual precipitation was obtained by adding the summer precipitation at each site to the maximum snowpack water equivalent prior to ablation. Air temperature and relative humidity were measured

at the Ester Dome Summit site (10) using a recording hygrothermograph. Evaporation data were obtained at the Ester Dome Summit (10) using a standard 122 cm diameter by 25.4 cm deep evaporation pan, stilling well and hook gage. Additional evaporation data were obtained from the University of Alaska-Fairbanks, Agricultural Experiment Station (1).

Linear regressions were developed by comparing short term meteorological data collected on site to data obtained at nearby stations with longer periods of record. Regression lines were calculated using the least squares method. Significance of fit was determined by t-test at the 95 percent confidence level.

Soil tensions were obtained at the Stone (7) and Gedney (4) sites weekly using tensiometers installed at regular depths (20, 40, and 60 cm) during the summer of 1982. Summer 1984 soil moisture data were obtained in the upper one meter of soil from a long-term study taking place at the Goldstream Valley runoff plots. These data were collected using time domain reflectometry (Stein and Kane, 1983).

Three unpumped wells were monitored on Ester Dome: the Swainbank site (8), and the upper and lower wells at the St. Joe American Mine on Henderson Road. The depth to the piezometric surface in the wells was measured using both an acoustic well probe and a well tape. The wells were monitored during the 1981-1982 water year by Northern Testing Laboratories Inc. using a well tape.

RESULTS

The water balances in Ester Creek watershed, Happy Creek watershed and the runoff plots for the 1983 and 1984 snowmelt periods (calculated using equation 2) are given in Table 1. The distribution of snowmelt is shown on a percentage basis in Figure 1. Precipitation, evaporation and soil storage amounts end at the disappearance of the snowpack, while runoff quantities include the recession portion of the snowmelt hydrograph.

Monthly water balances were calculated for each basin. Precipitation and actual evapotranspiration were estimated for the mean watershed elevations to give average basin conditions. Runoff was calculated

Component (cm)	Ester Creek		Happy Creek		Plot 1		Plot 2	
	83	84	83	84	83	84	83	84
Snow Water Equiv. (+)	15.5	12.7	13.7	10.7	12.4	9.9	14.7	9.9
Soil Deficit (-)	1.0	1.5	5.6	3.6	3.6	2.5	3.6	2.5
Runoff (-)	3.8	2.8	3.6	3.0	3.0	2.5	4.8	1.5
Actual Evaporation (-)	1.5	1.8	1.5	1.8	1.5	1.8	1.5	1.8
Snowmelt Period								
Groundwater Recharge	9.2	6.6	3.0	2.3	4.3	3.1	4.8	4.1

Table 1. Snowmelt period water balances (15 April to 25 May 1984).

from streamflow measurements. Table 2 presents the 1983 water balance for the two watersheds.

Total annual precipitation is plotted in Figure 2. Isohyets have been superimposed over elevation contours to show the distribution of precipitation in the area.

An average pan coefficient of 0.7 was obtained from mass balance calculations using soil moisture data. Detailed soil moisture measurements at the runoff plots allowed us to make this determination.

Regression analyses show that precipitation increased as elevation increased. Snowfall increased 14 percent per 100 m increase in elevation. Rainfall increased 11 percent per 100 m increase in elevation. The air temperature lapse rate was $-0.83\text{ }^{\circ}\text{C}$ per 100 m increase in elevation.

a) Ester Creek watershed.

Component (cm)	APR	MAY	JUN	JUL	AUG	SEP	OCT-MAR	NET ANNUAL (cm)
P	15.5	0.5	1.9	5.6	10.9	3.0	0.0	(37.4)
PET	1.6	9.2	9.9	8.4	3.3	1.9	0.0	(34.3)
P-PET	13.9	-8.7	-8.0	-2.8	7.6	1.1	0.0	(3.1)
SSi	9.2	10.2	1.4	0.0	0.0	7.6	8.7	
SSF	10.2	1.4	0.0	0.0	7.6	8.7	8.7	
Δ SS	1.0	-8.7	-1.4	0.0	7.6	1.1	0.0	(-0.5)
AET	1.6	9.2	3.3	5.6	3.3	1.9	0.0	(24.9)
SP	12.9	0.0	0.0	0.0	0.0	0.0	0.0	12.9
RO	0.8	2.8	0.6	0.4	1.1	2.0	3.3	11.0
GW	12.1	-2.8	-0.6	-0.4	-1.1	-2.0	-3.3	1.9

b) Happy Creek watershed.

Component (cm)	APR	MAY	JUN	JUL	AUG	SEP	OCT-MAR	NET ANNUAL (cm)
P	13.7	0.4	1.7	4.9	9.6	2.6	0.0	(32.9)
PET	1.5	9.7	10.4	6.9	3.3	2.2	0.0	(34.0)
P-PET	12.2	-9.3	-8.7	-2.0	6.3	0.4	0.0	(-1.1)
SSi	4.9	10.2	0.9	0.0	0.0	6.3	6.7	
SSF	10.2	0.9	0.0	0.0	6.3	6.7	6.7	
Δ SS	5.3	-9.3	-0.9	0.0	6.3	0.4	0.0	(1.8)
AET	1.5	9.7	2.6	4.9	3.3	2.2	0.0	(24.2)
SP	6.9	0.0	0.0	0.0	0.0	0.0	0.0	6.9
RO	2.0	1.6	0.3	0.03	0.03	0.5	0.03	4.5
GW	4.9	-1.6	-0.3	-0.03	-0.03	-0.5	-0.03	2.4

SSi = initial soil moisture and SSf = final soil moisture.

Table 2. Monthly waterbalances April 1983 to March 1984.

DISTRIBUTION OF SNOWMELT

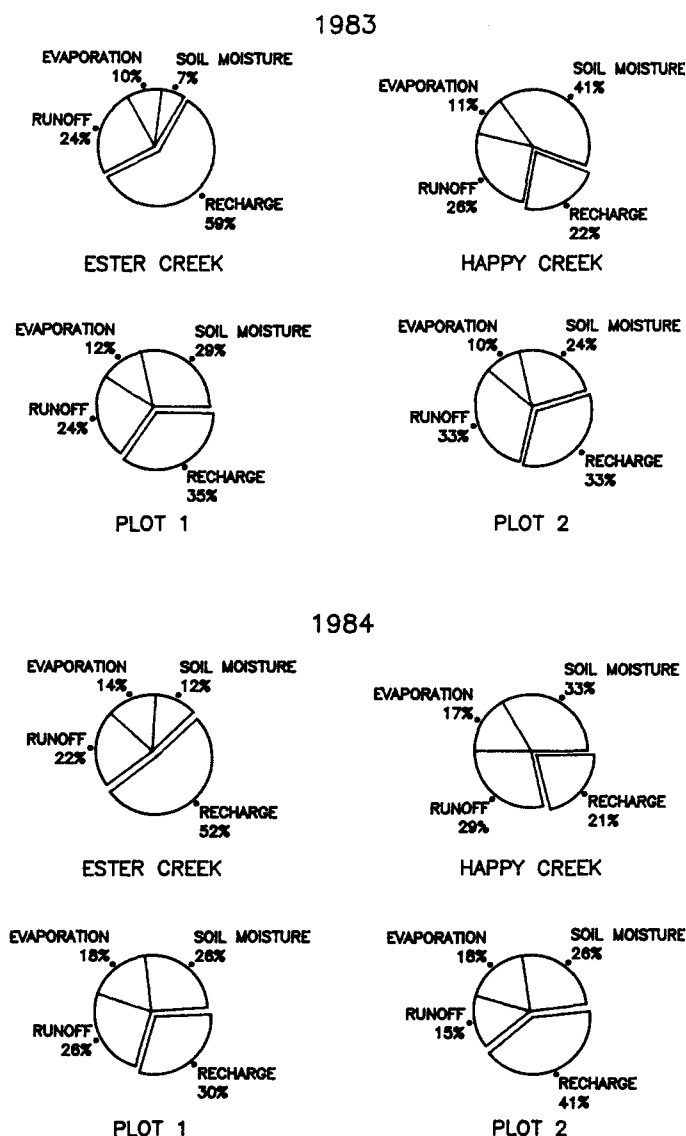


Figure 1. Distribution of 1983 and 1984 snowmelt.

Monthly evapotranspiration decreased by 3.5 percent per 100 m increase in elevation.

DISCUSSION

Winter Period

Potential groundwater recharge is unlikely during the winter in interior and northern Alaska. Unless significant melting of the snowpack occurs, which is

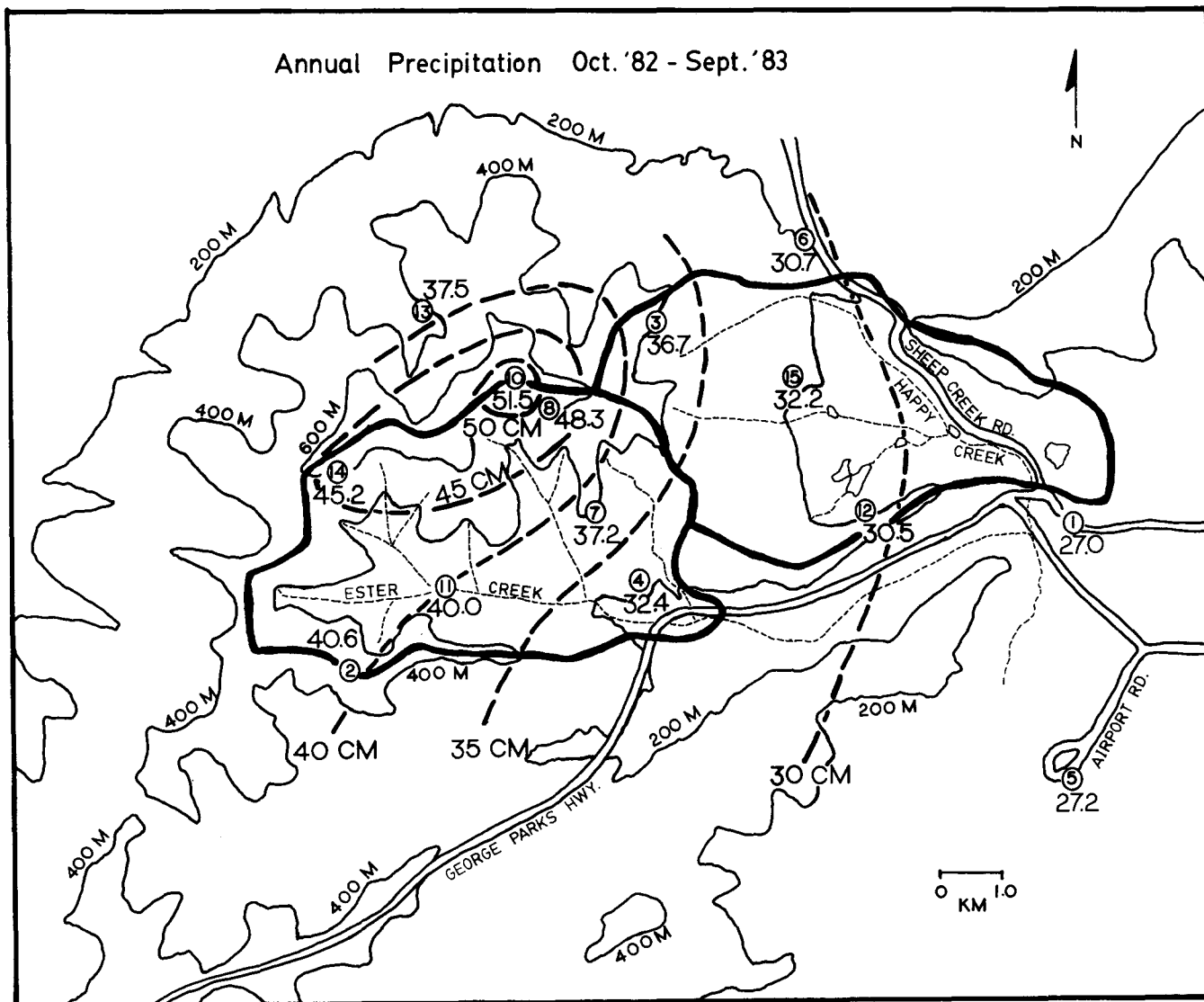


Figure 2. Site locations and precipitation distribution. Heavy dashed lines are isohyets and heavy solid lines are watershed boundaries.

quite rare, all precipitation remains frozen and stored at the surface as snow or ice. Snow accumulation generally begins in late September or early October, depending upon elevation. Due to cold air temperatures and very low insolation, snowmelt does not usually begin until mid-April. By late April or early May, sufficient energy is provided by rising air temperatures and increased insolation for melt to begin.

Without snowmelt inputs, winter is a period of net loss of stored groundwater. Groundwater storage changes through the runoff component as baseflow. The gradual drop of water tables in observed wells is evidence for the lack of winter ground-

water recharge and loss of groundwater storage as baseflow. The magnitude of winter baseflow is generally unknown, since ice-covered streams and aufeis accumulations prevent accurate stream gaging. However, a reasonable recession constant was estimated and applied to baseflow at freeze-up, so a crude estimate of winter baseflow was made for each basin.

The water balance equation for the winter months is very simple. All terms in the equation estimating groundwater recharge are zero except runoff (RO), which is equivalent to the baseflow.

Snowmelt Period

Significant infiltration can occur during snowmelt despite the extensive seasonal frost (Kane and Stein, 1983). Steady and gradual melt of accumulated winter precipitation, while evaporative demands are low, provides soil moisture recharge. Soils saturate rapidly and infiltration rates, although relatively low, allow water to enter the soil. Some of the snowmelt infiltration may be used later to satisfy evapotranspiration demand.

The Ester Creek watershed more efficiently retained snowmelt infiltration in 1983 and 1984. At least 50 percent of the snowpack became recharge in the Ester Creek watershed, while less than 22 percent of the snow water equivalent became recharge in the Happy Creek watershed. Several factors contributed to the disparity in recharge effectiveness. The higher mean elevation of Ester Creek watershed gives it a relatively higher snowpack water equivalent and a lower soil moisture deficit. Also, permafrost in the Happy Creek watershed reduced the area contributing to groundwater recharge, and increased the proportion of runoff.

Runoff dominates water balance losses during this period. Peak annual stream discharge usually occurs during the snowmelt period in interior and northern Alaska. Happy Creek snowmelt peak discharges occurred earlier, were higher, and receded earlier. More snowmelt runoff occurred in Happy Creek watershed, despite its lower terrain and gentler slopes.

Geologic mapping of the area and well logs show that permafrost underlays much of Happy Creek lowland. Aerial photography of Ester Dome was used to estimate the areal distribution of permafrost within each basin (NASA, 1978). Vegetation type was used as an indicator of permafrost-prone areas. The percentage of the basins with permafrost were: Ester Creek watershed 21 percent and Happy Creek watershed 57 percent.

Much of the infiltration in the Happy Creek basin may result in recharge to suprapermafrost water, with recharge not reaching the deeper subpermafrost groundwater. In comparison, Ester Creek watershed is dominated by well-drained, south-facing, permafrost-free soils.

Well data indicate that at least some of the snowmelt infiltration reaches the water table. The wells, one near the summit of Ester Dome and two along a ridge dividing the two basins, showed a rise in the late spring snowmelt season.

Summer-fall Period

Summer-fall hydrologic season was a time of net water loss. The water balance during this period was dominated by high potential evapotranspiration. Summer precipitation tended to be light and showery, providing scattered rainfall followed by dry periods. Fall precipitation, on the other hand, can be heavy and sustained. August has the highest average monthly precipitation in interior Alaska. However, the average August precipitation is lower than the average maximum snow water equivalent. Evapotranspiration demand exceeded precipitation throughout the summer months at lower elevations in 1982 and 1983. Early summer evapotranspiration was nearly equal to the 1982 and less than the 1983 precipitation in the upper elevations.

Long hours of daylight, warm air temperatures and low relative humidity maintained high demand for soil moisture. By mid-August, the evapotranspiration demand drops rapidly. Deciduous vegetation generally loses its leaves and stops transpiring in late August, and actual evapotranspiration may be less than the potential. If large precipitation events occur late in the period, as happened in August 1983, groundwater recharge is possible. Without significantly above-normal precipitation events, evapotranspirative losses probably still exceed inputs in the lower portions of the basins. Kane and Stein (1984) found that large September precipitation events, if they occur close to freeze-up, retard recharge the following spring, thereby offsetting any potential gains in groundwater storage. Basically, ice in the soil pores by reduces the infiltration the following spring.

Long term average data and the regression equations were used to estimate long term average conditions at all elevations on Ester Dome. Early summer (May and June) had greater PET losses than precipitation inputs at all elevations. July was

a transition month, precipitation just exceeded PET at the highest elevations. August and September, however, had PET less than precipitation over most of the area. PET exceeded precipitation only at the lowest elevations. The soil moisture gains in August and September do not totally replace the soil moisture lost in May, June and July. Both the average (4.7 cm) and highest recorded summer precipitation (15.7 cm) (both for August) are lower, respectively, than the average (10.7 cm) and highest recorded (24.9 cm) 1 April snow water equivalent. Compared to the April relationship, which includes the average March 31 snow water equivalent (USDA Soil Conservation Service, 1984) and average April precipitation, it becomes obvious that (at least on a long-term basis) the snowmelt period (usually April) is the most significant recharge period -- even when 20 to 30 percent runoff losses are taken into account.

The calculated 0.7 pan coefficient is lower than the 0.81 coefficient for well-watered rapeseed at Delta Junction, Alaska calculated by Braley (1980). He concluded that all summer precipitation was used to satisfy evapotranspiration demand at his low elevation sites. Our plots, where the 0.7 pan coefficient was determined are located in a mixed stand of Aspen, Birch and White Spruce on a well-drained, south-facing slope.

The Thornthwaite method was used to estimate monthly potential evapotranspiration when pan data were unavailable in the early summer. Thornthwaite's method tends to underestimate the amount of potential evapotranspiration in early summer and overestimate fall potential evapotranspiration. Patric and Black (1968) found a similar disparity at the Agricultural Experiment Station using long-term average data.

Soils became steadily dryer throughout 1982, a year of steady precipitation input. It is unfortunate that soil moisture data were not obtained for the summer of 1983, since extremely light precipitation occurred early in the summer followed by heavy fall precipitation. However, suction lysimeters used to obtain soil water for a study of the groundwater geochemistry of Ester Dome (McCrum, 1985), indicated relatively dry soils with tensions greater than 50 cm of water

throughout the summer. After the late August precipitation event, the suction lysimeters easily withdrew soil water, and tensions were less than 50 cm. Therefore, relatively wet soils were present in late August and September after heavy precipitation. Some recharge could have occurred.

A major flaw in treating the soil as a storage reservoir is that recharge can occur when soils are not saturated. The rate of recharge in unsaturated soils is dependent on soil moisture content and pressure gradients. Dry Fairbanks silt loams (less than 20 percent moisture by volume) have hydraulic conductivities less than 1×10^{-4} cm per second (Kane et al., 1978). So without high pressure gradients, recharge is small. The greatest potential for summer recharge occurs when a large input of water causes large pore pressure gradients.

This occurred in late-August 1983. Over 13 cm of precipitation fell at the highest elevations (above 600 m) from 20 August to 1 September 1983. Potential evapotranspiration was only 1.3 cm, leaving a precipitation excess of about 11.7 cm. The Swainbank well (640 m elevation) response was dramatic during this rainy period, rising over 46 m. The lower elevations received substantially less precipitation and higher potential evaporation demand. Less than 10 cm of precipitation fell on the lowest areas (below 250 m) from 20 August to 30 September. The estimated potential evapotranspiration was about 3.1 cm during this period. Table 2 shows that at the mean elevation of both watersheds (Happy Creek 216 m and Ester Creek 377 m) the soil had been completely depleted of stored moisture prior to this precipitation.

Neither basins' average input of precipitation fully replenished the soil moisture deficit. Due to the high pressure gradients between the upper and lower soils, some recharge must have occurred. Some of this summer recharge remained in soil storage until after freeze-up and some became runoff. Considering these losses, the summer recharge must have been less than the snowmelt recharge.

The 1983 water balance suggests that significant recharge in the summer-fall period is unlikely, especially at lower elevations. High potential evaporation demand early in the summer depletes stored

soil moisture. Heavy precipitation is required to overcome evapotranspiration demand and replenish depleted soil moisture if recharge is to occur.

Runoff losses are relatively small during the summer months. Baseflow is often considered to be an estimate of groundwater recharge in a steady-state system. The 1983 annual baseflow estimates were: Ester Creek 8.9 cm and Happy Creek 1.8 cm. Baseflow nearly equaled the 9.1 cm of estimated snowmelt groundwater recharge (Table 1) in Ester Creek watershed. The Happy Creek baseflow is much lower than the 3.0 cm of estimated snowmelt recharge, perhaps because of the large area of permafrost within the basin.

CONCLUSIONS

On and around Ester Dome (an area west of Fairbanks, Alaska) mining, and both residential and potential industrial development must compete for a limited water resource. Recent concern about the just and adequate distribution of water in the area has illuminated the need for more complete water resource information. Areas in the Yukon-Tanana upland adjacent to Fairbanks, such as Ester Dome, are of particular interest as development occurs because of limited groundwater storage in fractured schist aquifers.

There are several basic questions which should be answered before sound water management decisions can be made in developing areas. How much water is there? How and when does it get there? How and when does it leave? A water balance can partially answer these questions. Two watersheds on Ester Dome (Ester Creek and Happy Creek) were instrumented to collect data necessary for water balance calculations. Data collection began in June 1982 and ended in June 1984. Water balances were calculated, solving for groundwater recharge. An annual water balance was made from a synthesis of 1983 water balances.

Conclusions for the seasonal periods and annual synthesis were:

1) The snowmelt period was the primary time for significant groundwater recharge. This was a time of net gain in the area's water resources. The water

balance during this period was dominated by high runoff. Steady input of melt from the winter's accumulation of snow and low evaporation rates provided significant groundwater recharge, despite the reduced infiltration rates of the frozen soils caused by seasonal frost.

2) The summer-fall period was dominated by high rates of potential evapotranspiration. This period was one of net loss to the area's water resources. Light precipitation and high rates of evapotranspiration kept early and midsummer groundwater recharge very low. Groundwater recharge may occur in the late summer and fall as potential evapotranspiration rates decline, given sufficient precipitation input. Areas of higher elevation, where evapotranspiration is lower and precipitation greater, are more likely to have significant potential groundwater recharge.

3) The winter period is dominated by baseflow. All precipitation inputs are temporarily stored at the surface as ice or snow. Without snowmelt inputs the winter period was one of continual and significant water loss in the watersheds studied.

4) The upper elevations (above 600 m) of the Yukon-Tanana Uplands may receive twice the precipitation observed by the National Weather Service at the International Airport. The precipitation increases per 100 m increase in elevation were: snow pack water equivalent 14 percent and rainfall +11 percent. Monthly potential evapotranspiration decreased by 1.7 to 3.5 percent per 100 m increase in elevation. The average environmental lapse rate was 0.83 °C per 100 m. The Swainbank well rose in response to snowmelt and following concentrated rainfall in the fall. Receding water tables were observed in the winter and early to mid-summer.

REFERENCES

Braley, W. A. 1980. Estimates of evapotranspiration from barley and rapeseed in interior Alaska. M.S. Thesis. University of Alaska, Fairbanks, Ak.

- Dunne, T., and L. B. Leopold. 1978. Water in environmental planning. W.H. Freeman and Co.
- Forbes, R. B. 1982. Bedrock geology and petrology of the Fairbanks Mining District, Alaska. Alaska Department of Natural Resources, Division of Geological and Geophysical Surveys. Open-file Report 169.
- Kane, D. L., R. D. Seifert, and G. S. Taylor. 1978. Hydrologic properties of subarctic organic soils. University of Alaska, Institute of Water Resources Report 88.
- Kane, D. L., and J. Stein. 1983. Water movement into seasonally frozen soils. Water Resources Research. 19(6):1547-1557.
- Kane, D. L., and J. Stein. 1984. Plot measurements of snowmelt for varying soil moisture conditions. Geophysica. 20(2):123-136.
- McCrum, M. A. 1985. A chemical mass balance of the Ester Creek and Happy Creek watersheds on Ester Dome, Alaska. M.S. Thesis. University of Alaska, Fairbanks, Ak.
- NASA. 1978. Aerial Photo of Ester Dome. 23-317, JSC 386 Jul., 78 Alaska Cir. 60.
- Patric, J. H., and P. E. Black. 1968. Potential evapotranspiration and climate in Alaska by Thornthwaite's classification. USDA, Forest Service, Pacific Northwest Forest and Range Experiment Station, Juneau, Alaska. Forest Research Paper PNW-71.
- Pewe, T. L. 1982. Geologic Hazards of the Fairbanks Area, Alaska. State of Alaska Department of Natural Resources, Division of Geological and Geophysical Surveys. Special Report 15.
- Stein, J., and D. L. Kane. 1983. Monitoring the unfrozen water content of soil and snow using time domain reflectometry. Water Resources Research. 19(6):1573-1584.
- Thornthwaite, C. W., and J. R. Mather. 1955. The water budget and it's use in irrigation. The Yearbook of Agriculture, Water. U.S. Department of Agriculture. U.S. Government Printing Office, Washington, D.C. pp. 346-358.
- US Army, Corps of Engineers. 1956. Snow hydrology, summary report of the snow investigations. U.S. Government Printing Office, Washington, D.C.
- USDA Soil Conservation Service. 1984. Snow surveys and water supply outlook for Alaska as of April 1, 1984. Portland, Ore.

THE WATER BALANCE OF THE UPPER KOLYMA BASIN

V. K. Panfilova¹

ABSTRACT: The water balance must be estimated for the economic development of cold regions. The sparse hydrometeorological network in these regions requires indirect methods to estimate the water balance. The author used runoff and its coefficients for the Upper Kolyma Basin (99,400 square km). Instead of evaporation data for this area, the author used the balance method with due account of the orientation and wetting of the main tributaries in the Upper Kolyma Basin. The water balance components differ with region and with different landscape zones. (KEY TERMS: water balance; precipitation; runoff; evaporation; landscape zone.)

INTRODUCTION

The Upper Kolyma valley is one of the most developed regions of the North-Eastern part of the USSR. The further development in the mountainous areas of this region demands a more profound research of natural resources, especially of water resources. The hydrometeorological service concentrated in the Kolyma valley and the middle mountain areas (above 600 m). This network does not provide for adequate data concerning the different water economy accounts. This paper describes the elements and structures of water balance distributions in the different high-altitude zones of the region. The work is of great practical importance because there is no mutual estimation of the water balance elements for this region.

REGIONAL PHYSIOGRAPHICAL FEATURES

The water balance depends on some natural features of the region. The Upper Kolyma Basin is the middle mountain land with average height of 927 m and the maximum height up to 2,200 m. The annual precipitation varied from 200 to 400 mm. About 60-70 percent of annual precipitation falls during the warm season (May-September). The rigorous climatic conditions promote the total spread of permafrost. By September, the upper permafrost limit is: 60-70 cm below the surface with moss vegetation; 120-130 cm below the surface with trees and shrubs on loam; and 150 cm below the surface of the rudaceous rocks and alpine tundra.

Permafrost provides a natural impermeable layer that hinders water exchange between surface water and that of subpermafrost zone. This water exchange is possible only in limits of valley taliks of the rivers with catchment areas more than 7,000 square km. During the cold season (October-April), other rivers are frozen up to the bottom.

The rivers of the Upper Kolyma Basin are fed by rain and snowmelt; up to 95 percent of its runoff occurs during the May-September period. During the cold season, aufeis is formed from suprapermafrost water; 5-10 percent of annual runoff is stored as aufeis. The volume of growth of the aufeis depends on talus area in some river basins (Kuznetsov and Nasybulin, 1970).

¹Problems Research Laboratory for Northern Development, Geography Faculty, Moscow State University, Moscow, 119899, USSR.

Areas of talus are widespread in the region. These areas exhibit a larger infiltration capacity, lesser evaporation and good conditions for water condensation. Up to 30 percent of Upper Kolyma Basin is covered by talus.

River runoff is formed in the specific landscape zones of the region: alpine- tundra zone (above 1,500 m); elfin wood- tundra zone (1,500-1,000 m); larch open woodlands zone (1,000-600 m); larch taiga zone (600-400 m); willow-chosenia forests, larch open woodlands ("mari") and grass moor along the flood plains.

DATA AND METHODS

Observations in the study area were conducted by the Kolyma Water Balance Station on catchments from 0.30 to 21.2 square km and four catchments from 100 to 1,750 square km. The observation results depict the hydrological cycle (Kuznetsov, et al. 1969). A number of scientists attempted to account for the normal annual precipitation and runoff for the different observation periods throughout the Upper Kolyma Basin (Garzman and Ryabchikova, 1972).

The author used the following equation for the water balance:

$$P = R + E$$

where P, R and E are the normal annual precipitation, runoff and evaporation, respectively. This approach allows linking the water balance elements of the Upper Kolyma Basin.

Precipitation. The corrected data of 53 meteorological stations provided normal annual precipitation accounts. Most stations are located near the Kolyma mainstream. On the uplands--at the western, south-western and southern parts of the Kolyma Basin--the precipitation observations were not carried out. The meteorological stations are located at 600-800 m on the western part of the basin, and 200-400 m on the eastern one. Only one station, with representative observations is located at 1,220 m. The author used the method of "collective regional analogy" to determine the depth of rainfall at the different altitudes. This method is based on the regional

dependence of the precipitation from the sea-level elevation. The met-stations grouping made on the area data for right- and left-bank, and western and eastern tributaries of the Kolyma River revealed that in three main areas, $P = f(A)$ (where A is the met-station's sea-level elevation):

I. The western part, left bank of the Kolyma-Ayan-Yuryakh (14,140.2 square km) and Berelekh basins (9,829.9 square km);

II. The western part, right bank of the Kolyma-Kulu (15,654 square km), Tenke (4,450 square km) and Detrin (6,626.6 square km) basins. This area is divided into two subareas: IIa) Kulu Basin and IIb) Tenke and Detrin basins.

III. The eastern part, left-bank tributaries basins--Debin (5,444 square km), Tascan (11,911.8 square km) and right bank basins--Bokhapcha (13,600.0 square km), Orotukan (2,340.9 square km), Srednekan (1,728.5 square km). Normal annual precipitation in all of these basins is somewhat greater than in western ones.

For these areas, the relationship of $P = f(A)$ for the regions are as follows: 3.27 (I), 0.60 (IIa), 0.47 (IIb), 0.29 (III).

The existing met-stations network does not allow for reliable extrapolation in the "precipitation-elevation" relationship. We used the indirect method for precipitation accounting--on the basis of runoff and its resultant coefficients.

Runoff. The mean weighted elevation of the studied basins are 600-800 m (the eastern part) and 900-1,200 m (the west). Consequently, the precipitation data are sufficient for the 400-800 m elevation zones, but the runoff data are representative for the 900-1,200 m zones.

For $R = f(A)$, we used the runoff data of 125 rivers. All observations were reduced to annual series. These rivers were grouped on the basis of catchment area: 35 percent of rivers have the catchment area less than 10 square km, 50 percent have less than 50 square km, 60 percent have less than 100 square km, and 78 percent have less than 500 square km (in increasing summation). In accordance with the position of the catchment of the mean weighted elevation, there are three main groups of rivers: 38 percent of the

river's catchments are located in the 600-900 m elevation range; 52 percent in 900-1,200 m range and 10 percent in 1,200-1,400 m range.

The runoff data from 125 rivers reveal its distribution for each main tributary of the Kolyma. We have obtained representative curves for $R = f(A)$ for the Berelekh, Ayan-Yuryakh, Debin Tascan, Kulu, Detrin and Srednekhan basins. There are no direct data for the Tenke, Bokhapcha and Orotukan basins, so we used the analogy between the runoff distribution and the elevation of the neighbouring basins.

The combined analysis of $P = f(A)$ and $R = f(A)$ confirmed the existence of the regional boundaries for regions I, IIa, IIb, differing in the precipitation data. In the eastern region, differences in the character of the vertical runoff distribution were found. We divided this region into four subregions: IIIa) Tascan Basin; IIIb) Debin Basin; IIIc) Bokhapcha Basin; IIId) Orotukan and Srednekan basins.

The long combined "precipitation-runoff" observations were carried out on the Kolyma water balance station in the Kulu Basin. We used these data to determine the runoff coefficients for different elevational landscape zones. Nasybulin (1976) demonstrated that the hydrological conditions of the water balance station are representative throughout the Upper Kolyma Basin. This result has enabled us to use the regional runoff coefficient (IIa) for the other regional accountings. These calculations show the precipitation and runoff distributions depend on an area's elevation.

We have tabulated the accounting depths of precipitation and runoff using regional curves of $P = f(A)$. Since no evaporation data are available for the Upper Kolyma Basin, we determined the amount of evaporation in mm as the precipitation-runoff difference for the vertical zones. On the basis of values of P , R , E , we then determined α (the runoff coefficient) and β (the evaporation coefficient) for the same vertical zones of each subregion. See the accounting examples in Table 1.

The calculations were used to map the water balance of the Upper Kolyma. With these water balance maps and the landscape map planimetry made it possible to

TABLE 1. The elements of water balance distribution and structure in subregion IIId.

Elev A(m)	Precip P(mm)	Run R(mm)	Evap E(mm)	α	β
400	500	150	350	0.30	0.70
600	595	260	335	0.44	0.56
800	640	370	270	0.58	0.42
1000	675	450	225	0.67	0.33
1200	705	520	185	0.74	0.26
1400	730	570	165	0.78	0.22
1500	750	590	160	0.80	0.20

determine the mean weighted values of the water balance structure for different landscape zones (Table 2).

RESULTS

Both precipitation and runoff in Regions II and III increased with the elevation. In Region I, runoff increased with the elevation, but the precipitation decreased down to 1,100 m above sea level. This event is typical for the enclosed valleys like the Berelekh Basin. Besides, Region I is located in the western and northwestern parts of the Upper Kolyma Basin and is the farthest area away from the eastern and the northeastern humid flows. Higher than 1,100 m, the pluviometric coefficient has positive values, which is confirmed by $R = f(A)$. This phenomenon may be explained by the transport of humid air masses to high elevations.

The precipitation and runoff values in the Upper Kolyma Basin increase eastward and to the right-bank areas. The Orotukan and Srednekan basins receive the most precipitation. In the western part of the Upper Kolyma Basin, the evaporation is less than in the eastern parts because talus and scree cover most of the small river basins in the west.

DISCUSSION

This study provides the water balance

TABLE 2. Water balance for different landscape zones.

Region, subregion	Landscape (percent)					Water Balance elements (mm)				
	1	2	3	4	5	Precip P	Run R	Evap E	α	β
I	20.2	2.4	42.5	12.0	22.9	330	180	150	0.55	0.45
	21.8	6.9	33.5	7.1	30.8	375	200	175	0.53	0.47
IIa	36.0	1.0	33.7	8.9	20.5	375	220	155	0.59	0.41
IIb	31.6	0.5	29.6	10.9	27.3	410	240	170	0.59	0.41
	37.7	0.2	31.8	12.7	24.8	425	255	165	0.60	0.40
IIIa	16.2	4.1	28.4	17.3	34.0	500	210	290	0.42	0.58
IIIb	24.2	4.6	36.3	8.0	27.0	490	210	280	0.43	0.57
IIIc	33.3	2.2	34.3	10.3	20.0	545	265	280	0.48	0.52
IIId	26.2	3.7	40.4	15.1	14.5	570	290	280	0.51	0.49
	31.9	5.3	28.0	10.2	24.2	560	280	280	0.50	0.50
Upper Kolyma Basin	27.2	2.7	32.5	11.6	26.1	433	233	200	0.54	0.46

1 - alpine-tundra; 2 - elfin wood tundra; 3 - larch open woodlands; 4 - larch taiga; 5 - willow chosenia forests, larch open woodlands ("mari") and grass moor of flood plains.

for the Upper Kolyma Basin and the distribution of water in the landscape zones of the basin. These results are interesting for practical purposes, but the results include all errors and inaccuracies stemming from the water balance method used for estimating evaporation. Determined as the remainder term of the equation, the evaporation value includes all precipitation and runoff errors and other parameter effects of the water balance. In the Upper Kolyma Basin, the many talus slopes condense some amount of moisture. If this amount is ignored, this leads to understating the water supply term in the water balance. Besides that, the orographic differentiation of water balance elements has been determined for the main tributaries of the Kolyma only. It proved impossible to take into consideration the slope orientation. These shortcomings may be eliminated by more detailed water balance investigations.

REFERENCES

- Garzman, I.N., T.N. Ryabchikova, 1972. On Mean Annual Runoff and Precipitation Distribution on the Upper Kolyma Territory and the Northern Coastal Zone of the Okhotsk Sea. Transactions of the Far Eastern Hydro-Meteorological Institute. 39:5-17 [in Russian].
- Kuznetsov, A.S., Sh.S. Nasybulin and A.I. Ipat'eva, 1969. The First Results of the Upper Kolyma Basin Water Balance Investigations. Transactions of Magadan Hydro-Meteorological Observatory. 2:21-37 [in Russian].
- Kuznetsov, A.S., and Sh.S. Nasybulin, 1970. The Runoff Formation Peculiarities on the on the Rivers of the Upper Kolyma Basin. Transactions of Magadan Hydro-Meteorological Observatory. 3:52-65 [in Russian].
- Nasybulin, Sh.S., 1976. The Kolyma Water Balance Station's Runoff Data Representativity for the Upper Kolyma Territory. "The Natural Resources of the Soviet North-East". Vladivostok. [in Russian].

WATER BALANCE AND RUNOFF ANALYSIS AT A SMALL WATERSHED
DURING THE SNOW-MELTING SEASONH. Motoyama, D. Kobayashi and K. Kojima¹

ABSTRACT: The amount of snow water equivalent, the snowmelting rate and the stream discharge were measured at a small watershed (11.2km²) during four snowmelting seasons. Water balance and runoff analysis were made on the basis of hydrological observations. Some important characteristics of the water balance were found as follows; (1) 90% of the snowmelt in the watershed ran off in both heavy and light snow seasons; (2) the amount of evaporation was estimated to be less than 1% of the total amount of snowmelt; (3) in the middle of the snowmelting season, the several days accumulated snowmelt amount equaled the snowmelt runoff without a change of groundwater storage in the watershed. (4) The simulation of daily snowmelt runoff was successful by using the same runoff model for three years. (KEY TERMS: snowmelt; water balance; snowmelt runoff; runoff tank model.)

INTRODUCTION

It is well recognized that snowcover constitutes a vital part of water resources; therefore, accurate forecasting of the amount of runoff water is indispensable for making efficient use of meltwater and forestalling damage due to snowmelt flooding in snowy regions.

The total amount of snowcover just before the snowmelting season in experimental watersheds has been measured and forecasting of snowmelt runoff has been attempted by many investigators (Leaf, 1971, Rango, 1983, Sugawara et al., 1984). A prerequisite for forecasting of snowmelt runoff is to clarify the water balance of a watershed, but there are still many unknown factors at present. In a few papers, water balance is discussed on the basis of the observed snowmelt amount in the watershed and the stream discharge (Ono and Kawaguchi, 1974).

The present study was conducted for the following purposes: (1) to clarify the water balance of a watershed during the snowmelting season on the basis of observed hydrological data, (2) to simulate the daily snowmelt runoff.

INSTRUMENTS

The observations were carried out at an experimental watershed located in the northern part of Hokkaido, Japan (44°23'N, 142°17'E, drainage area 11.2km², elevation range 280-630m a.s.l., average slope angle 11.0°, shown in Fig. 1) during the period from April to May in the years 1981, 82, 83, 84.

¹Institute of Low Temperature Science, Hokkaido University, Sapporo, 060, Japan.

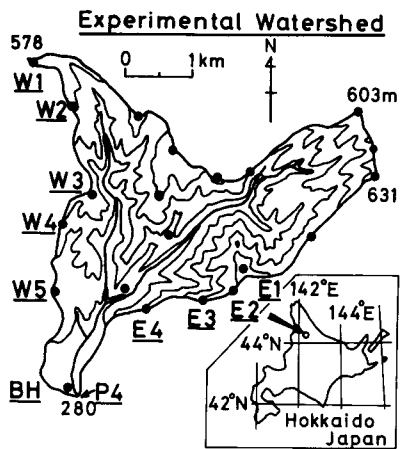


Figure 1. Location map of the experimental watershed. Solid circles indicate the measuring points of snow water equivalent and the snowmelting rate. BH station for meteorological observations. P4 water gauge station.

1) Snow Water Equivalent Observations in the Watershed

Total volume of snow cover in the watershed was obtained in mid-April, before the melting season, every year. The snow water equivalents (HW) at about twenty sampling points in the watershed (Fig. 1) were measured. Some ten measurements of the depth made with a snow sonde gave an average snow depth (HS) while three or four measurements of the average snow density made with a snow sampler gave the average density () at a point. The snow water equivalent is calculated as follows,

$$HW = HS \quad (1)$$

2) Observations of Snowmelt Amount in the Watershed

The snowmelt amounts were also measured at about twenty points in the watershed (Fig. 1). The height of snow depth (HS) and snow density () between 0-5 and 5-10cm below the snow surface were measured temporarily, so that the snowmelt amount between the measuring period was calculated as follows,

$$m = \Delta(HS) \quad (2)$$

where $\Delta(HS)$ means the height of lowering snow depth during the measuring period.

3) Observations of Melting Rate at the Lower Station (BH)

Melting rates were continuously observed by four different methods at BH station: (a) snow stake method, (b) lysimeter method, (c) snow pit observations, (d) heat balance calculations. Details were described as follows.

(a) Snow stake method: Height of snow depth (HS) and snow density between 0-5 and 5-10cm below the snow surface () were observed at 0900 and 1700 every day, so that the snowmelt amount (m) could be calculated by the equation $m = \Delta(HS)$, where (HS) means the height of the lowering snow depth during the period of 0900-1700 or 1700-0900.

(b) Lysimeter method: Amounts of runoff water from the snowpack were measured using two types of shallow lysimeters, one buried in the ground, 90 x 90cm area, and the other buried in the snow, 80 x 80cm area. Collected meltwater was measured by tipping bucket rain gauge.

(c) Snow pit observations: Snow pit observations were done once or twice a month. The snow density and water content profiles were obtained.

(d) Heat balance calculations: Neglecting the conductive heat flux through the snow cover during the snow-melting season, the heat energy balance equation at the snow surface is written as follows,

$$QT = QR + QA + QE, \quad (3)$$

where QR is the net radiation, QA is the sensible heat flux and QE is the latent heat flux. The values of QT usually become negative values at night when the meltwater of the surface layer refreezes and the snow temperature decreases below 0 C, but this negative values of QT are compensated by the positive values of QT the next morning. Each component is obtained as follows, QR : direct measurement by net pyrradiometer, QA and QE : calculation by bulk formulae obtained for this region (Ishikawa et al. 1982) $QA=0.0096(T_1-T_0)V_1$ MJ/m²h and $QE=0.02(E_1-E_0)V$ MJ/m²h, where T_1 (°C), E (mb), and V_1 (m/s) are air temperature,

vapour pressure and wind speed at 1m height above snow surface, and T (C) and E (mb) are surface snow temperature and surface vapour pressure, respectively.

4) Stream Discharge

Stream discharge at the outlet of the watershed (P4, Fig. 1) was measured with a self-recording stage recorder.

5) Other Observations

Precipitation was measured by tipping bucket rain gauge at BH station.

WATER BALANCE DURING THE SNOWMELTING SEASON

The water balance was calculated from the beginning day of the snow survey to the day of complete disappearance of snow from the watershed.

1) Water Balance Equation

The water balance for the snowmelting season at the watershed is written as:

$$\Sigma M + \Sigma R = \Sigma Q + \Delta E + \Sigma ET + \Delta Sd, \quad (4)$$

where M is the total amount of snow-melt, which equals the total amount of snow water equivalent at the beginning day of the water balance, ΣR is the total precipitation, ΣQ is the total amount of runoff depth, ΔE is the mass transfer at the snow surface (evaporation +, condensation -), ET is the total evapotranspiration in the watershed, ΔSd is the change of groundwater storage (gain +, loss -).

2) Each Component

The snow water equivalents (HW) obtained at about twenty points on the watershed are plotted against the altitude (z) in Fig. 2. The linear relation-

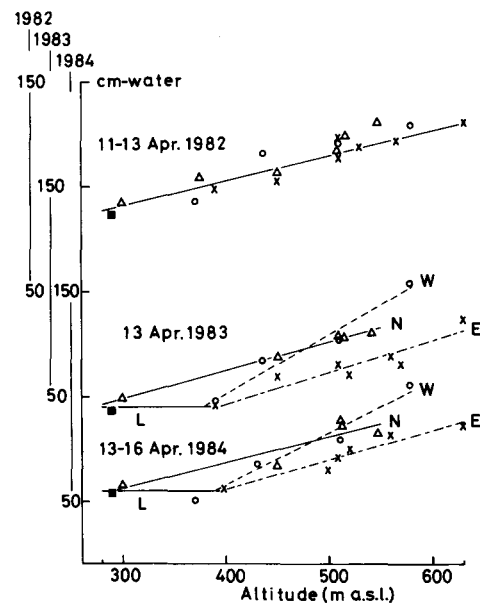


Figure 2. Altitude distribution of snow water equivalents in 1982, 83, 84. The linear relationship between the altitude and snow water equivalent was classified by four sub-watersheds, except in 1982. (open circle: west, open triangle: north, cross: east, solid square: lower region).

ship between them can be classified by four sub-watersheds (West, North, East and Lower regions) except in 1982, a heavy snow season. The altitude distribution of the sub-watershed area A(z)

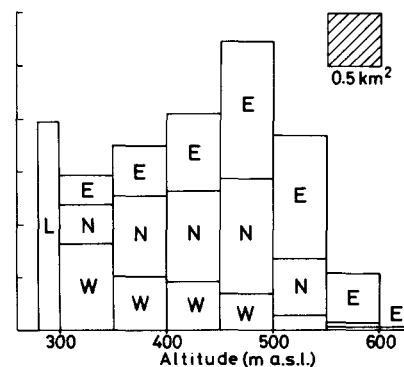


Figure 3. Altitude distribution of sub-watershed area. Square of oblique line indicates the area of 0.5km (W: west, N: north, E: east, L: lower region).

Table 1. Water balance ($\Sigma M + \Sigma R = \Sigma Q + \Delta E + \Sigma ET + \Delta Sd$, where M: snowmelt, R: precipitation, Q: runoff, E: evaporation or condensation at the snow surface, ET: estimated evapotranspiration, Sd: estimated groundwater storage)

	ΣM	ΣR	ΣQ	ΔE	ΣET	ΔSd	$\Sigma Q / (\Sigma M + \Sigma R)$
13 Apr.-15 Jun. 1982	106	14	110	1	2	7	0.92
13 Apr.-30 May 1983	60	13	68	0	2	3	0.93
14 Apr.- 5 Jun. 1984	67	3	53	-1	2	16	0.76

(cm-water)

is shown in Fig. 3. The total snow water equivalent can be calculated as follows,

$$HW = \int HW(z)A(z)dz \quad (5)$$

The total snow water equivalent in the watershed (including rain water) was 1.34×10^6 m³-water (120cm-water for areal mean) in 1982, a heavy snow season, but it was 7.6×10^5 m³-water (68cm-water) in 1983 and 7.8×10^5 m³-water (70cm-water) in

1984, which were seasons of little snow (Table 1).

The values of R, E and ET were assumed to be the same in all places. The amount of R was observed at BH station continuously. The value of E can be calculated by the empirical formula using the meteorological data at BH station, $E = Q_E / L_s$, where Q_E is the latent heat flux and L_s is the heat of sublimation. The amount of ET was assumed to be 1mm/day (Arai, 1980) after the day of disappearance of snow at BH station.

Total amount of snowmelt runoff was calculated by two methods. In one method that the runoff amount was accumulated during the snowmelting season, and in the other the snowmelt runoff was separated from the hydrograph, which was indicated the area of oblique line part in Fig. 4.

3) Results

The values of water balance components obtained are represented in Tables 1 and 2. Results shows that 80 - 100% of the snowcover in the watershed ran off in the three years with heavy and little snow (Fig. 5). one characteristic

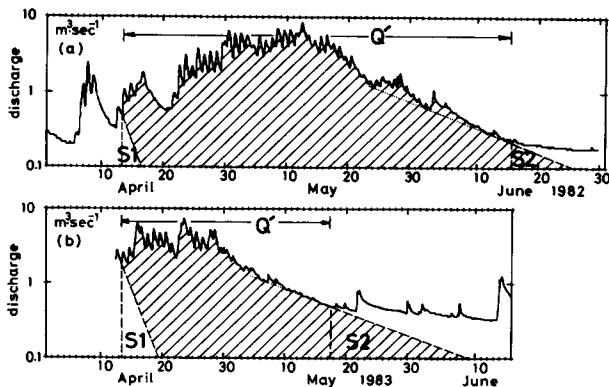


Figure 4. Separations of snowmelt runoff from the runoff hydrograph, indicated by the areas of oblique line part.

Table 2. Runoff coefficient of the snowcover in the watershed. S1, S2, Q' are shown in Fig. 4. Q: snowmelt runoff. I: snowmelt(M) + rain(R).

	S1	S2	Q'	$Q = Q' + S2 - S1$	$I = M + R$	Q/I
1982	1	2	110	111(1)	120	0.93
1983	3	5	62	64(2)	68	0.94
1984	1	4	53	56(3)	70	0.80

(cm-water)

(1) 13 Apr.-15 Jun. (2) 13 Apr.-17 May

(3) 14 Apr.- 4 Jun.

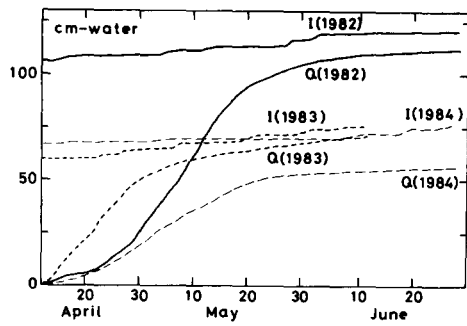


Figure 5. Accumulated runoff depth (Q) and accumulated precipitation in addition to areal mean snow water equivalent on 13 April (I). (Solid line: 1982, thick broken line: 1983, thin broken line: 1984).

of the water balance during the snowmelting season was that the amount of water loss from the watershed (evapotranspiration etc.) was less than that in other seasons.

The total amount of mass transfer at the snow surface was found to be less than 1% of the input (amount of snowmelt + rain) to the watershed during the snowmelting season. The loss values of snowmelt energy by evaporation during the daytime were usually compensated for by the gain values achieved by condensation during the night.

CHARACTERISTICS OF WATER BALANCE DURING THE MIDDLE OF THE SNOWMELTING SEASON

The water balance at the watershed is written as,

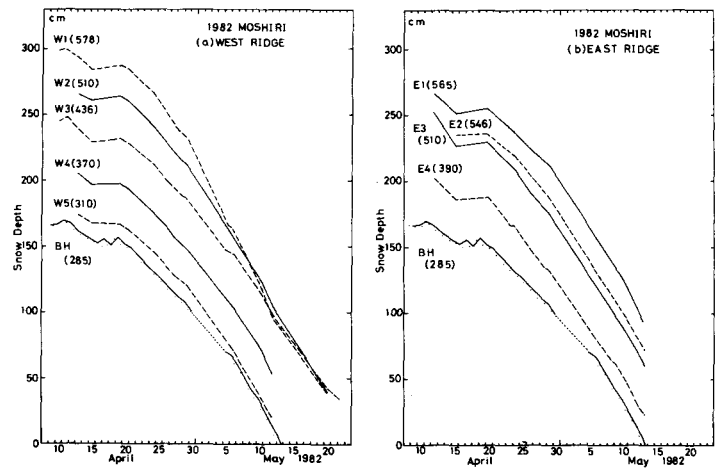


Figure 6. Variations of snow depth in 1982. The figures in parentheses indicate the altitude. Observational sites are shown in Fig. 1.

$$\Sigma M + \Sigma R = \Sigma Q + \Delta E + \Delta Sd + \Delta Sd', \quad (6)$$

where ΣM , ΣR , ΣQ , ΔE and ΔSd are explained in section 3.1. $\Delta Sd'$ is the change of liquid water storage in a snowpack.

The amount of snowmelt in a watershed was obtained by the snow stake method ($m = \Delta(HS) \cdot \rho$, Eq. 2) along with the altitudinal distribution of watershed area (Fig. 3). Examples of time variation of snow depth are shown in Fig. 6. The altitudinal difference between the top and the bottom of the watershed was only 300m, but the difference of snow depth became more than 1m.

The values of water balance components obtained are represented in Table

Table 3. Water balance during the middle of snowmelting season. ($\Sigma M + \Sigma R = \Sigma Q + \Delta E + \Delta Sd + \Delta Sd'$, where M: snowmelt, R: rain, Q: runoff, E: evaporation or condensation at the snow surface, ΔSd : change of groundwater storage, $\Delta Sd'$: change of liquid water storage in a snowpack)

	ΣM	ΣR	ΣQ	ΔE	$\Delta Sd + \Delta Sd'$	$\Sigma Q / (\Sigma M + \Sigma R)$
24 Apr.-29 Apr. 1982	12.1	0.3	9.6	0.0	2.8	0.77
29 Apr.-10 May 1982	39.4	2.6	40.8	0.3	0.9	0.97
16 Apr.-19 Apr. 1983	11.2	0.3	11.4	-0.2	0.3	0.99

(cm-water)

3. In the middle of the snow-melting season, melting rates were 20-40mm-water/day, the accumulated snowmelt water equaled the accumulated snowmelt runoff for several days, without a change of groundwater storage in the watershed.

RUNOFF ANALYSIS OF DAILY AMOUNT

We devised a runoff model for the snowmelting season in 1982 and tested the propriety of this model during the same season in 1981 and 1983.

1) Determination of the Daily Amount of Snowmelt

The daily snowmelt amounts obtained by four different methods at BH station showed different values from each other (over 10-20% differences, Fig. 7). The

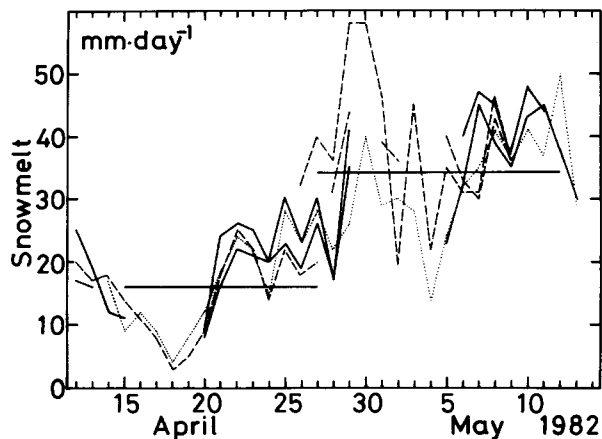


Figure 7. Daily snowmelt obtained by four different methods. (solid line: snow stake method, broken line: lysimeter method, horizontal thick solid line: snow pit observations, dotted line: heat balance calculations).

horizontal profiles of snow structure or ice layer were varied from one observational place to another, in spite of the smallness of the experimental site. But the snowmelt amounts that accumulated for several days did not vary from each other. We obtained accurate daily snowmelt values by comparing the results

obtained from different methods.

Input water for the runoff analysis is decided on the basis of the snowmelt amounts at BH station. Usually the snowmelt amount at BH station was nearly equal to the areal mean value of the watershed. But in 1982, the snowmelting rate of the upper region was larger than that of the lower region for a long period, so that the input water was 1.1 times as large as the snowmelting at BH station from 12 April to 12 May in 1982 (Fig. 8).

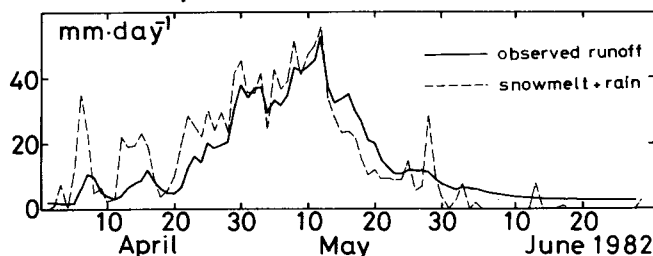


Figure 8. Areal mean daily snowmelt (added daily precipitation, broken line) and daily runoff depth (solid line) in 1982.

2) Determination of the Runoff Model

Sugawara's "tank model" was used here to calculate the runoff during the snowmelting season (Sugawara et al., 1984). A series of two storage type tanks was adopted, in which the upper tank had three outlets, two on the side for runoff and one on the bottom for infiltration, and the lower tank consisted of two outlets, one on the side and the other on the bottom (Fig. 9). The daily input water (snowmelt + rain) supplied to the

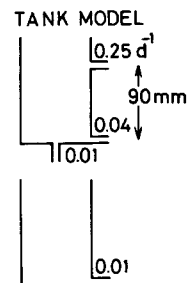


Figure 9. Derived tank model. Coefficients of tank's outlets are in units of day.

upper tank every day and runoff water discharged from the outlets on the side. The distinguished attenuation constants of the recession curves in the runoff hydrograph were applicable to the runoff coefficients of tank's outlets. The runoff $Q(t)$ at time t is expressed as,

$$Q(t) = Q_0 e^{-\alpha t} \quad (7)$$

where Q_0 is the runoff at time 0, $1/\alpha$ is a time constant (relaxation time). Other parameters of the tank structure were decided by the trial and error method until the calculated discharge fit well the observed one for the case of 1982.

3) Remnant Area of Snowcover and the Evapotranspiration in the Late Snow-melting Season

After the snowcover disappeared in the lower region, the remnant area of snowcover decreased. The decreasing rate of snowcover area can be modeled as shown in Fig. 10, which is based on the characteristics of recession curves of the runoff hydrograph and temporary snow line observations. The evapotranspiration was assumed to be 1mm/d after the day of disappearance of snow at BH station.

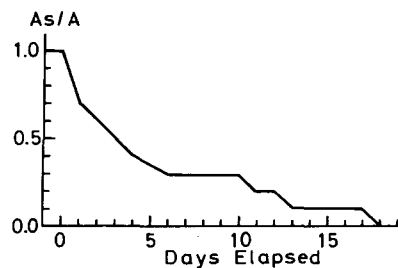


Figure 10. Remnant area of snowcover in the watershed (abscissa: elapsed time after the day of snowcover disappeared in the lower region, ordinate: ratio of remnant area of snowcover, as , to watershed area, A).

4) Results

The observed and calculated hydrographs in 1982 are plotted in Fig. 11, where the solid line indicates the

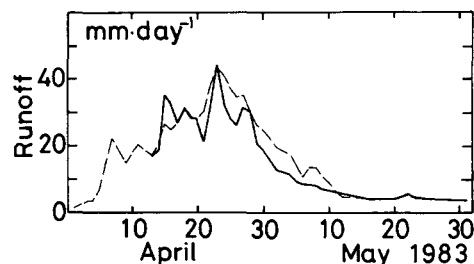
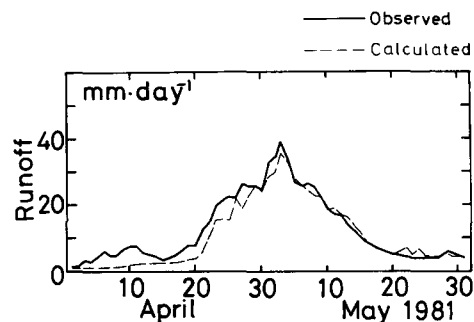
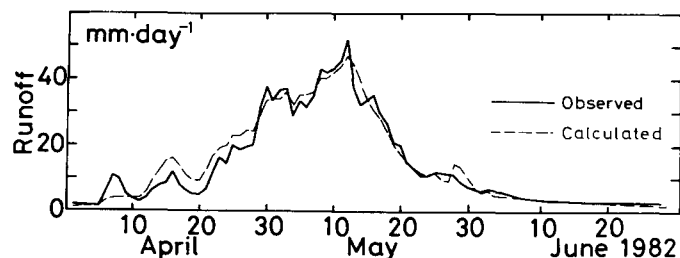


Figure 11. Daily runoff depth in 1982 and 81,83. (solid line: observed runoff depth, broken line: calculated runoff depth by using tank model in Fig. 9).

observed hydrograph and the broken line is the calculated one. Without changing the tank structure, the simulations of daily snowmelt runoff were successful in both 1981 and 1983. We considered an analogy between the tank structure and the runoff process as follows: The upper tank has two runoff outlets and the lower tank has one. Runoff coefficients of these outlets were decided by the recession curves of the hydrograph at various ranges of runoff amounts. It seemed that the runoff from the lower tank corresponded to the groundwater flow from the deep level, and the runoff from the upper tank was the groundwater flow from the shallow level.

CONCLUDING REMARKS

We measured the amount of snow water equivalent, the snowmelting rate and the stream discharge at a watershed during four snowmelting seasons. Water balance and runoff analysis were made on the basis of observed hydrological data. The following results were obtained.

1. 90 % of the snowcover in the watershed ran off in the three years with heavy and light snow.

2. The total amount of mass transfer at the snow-surface was estimated to be less than 1% of the input (amount of snowmelt + rain) to the watershed during the snowmelting season.

3. In the middle of the snowmelting season, melting rates were 20 - 40 mm-water/day, the accumulated snowmelt water equaled the accumulated snowmelt runoff for several days, without a change of groundwater storage in the watershed.

4. A tank model was used to calculate the runoff process. The simulation of daily snowmelt runoff was successful for the three year period without changing the tank structure.

ACKNOWLEDGMENTS

The authors are grateful to the staff members of the Uryu Experimental Forest of Hokkaido University for their help in these observations, and they also wish to thank Dr. N. Ishikawa of the Institute of Low Temperature Science for his helpful advice and useful suggestions.

REFERENCES

- Arai, T., 1976, Nippon no mizu. Sanseido, Tokyo (in Japanese).
- Ishikawa, N., S. Kobayashi and K. Kojima, 1982, Measurement of sensible heat flux in the snow-melting season I. Low Temperature Science, Ser.A, 41: 109-116 (in Japanese with English summary).

Leaf, C. F., 1971, Areal snow cover and disposition of snowmelt runoff in central Colorado. USDA For. Serv. Res. Pap. RM-66, Rocky Mt. For. and Range Exp. Sta., Fort Collins, Colo. 19pp.

Ono, S and R. Kawaguchi, 1974, Syoryuiki ni okeru choseturyo suitei to 'sinrin no eikyo' no kaiseiki. Ringyo Sikenjo Touhoku Siba. Nenpou: 114-119 (in Japanese).

Rango, A., 1983, Application of a simple snowmelt-runoff model to large river basins. 51st Annual Meeting Western Snow Conference, Vancouver, Washington: 89-99.

Sugawara, M., I. Watanabe, E. Ozaki and Y. Katsuyama, 1984, Tank model with snow component. Research Notes of the National Research Center for Disaster Prevention, 65: 1-293.

ESTIMATIONS OF SNOWMELTING RATE IN A SMALL EXPERIMENTAL SITE

N. Ishikawa, H. Motoyama and K. Kojima¹

ABSTRACT: Estimations of hourly and daily snowmelt were achieved by using the heat balance method and bulk meteorological parameters at a small experimental site. The results were compared with actual snowmelt and runoff amounts. Calculated snowmelt by use of the heat balance method explained variations of actual snowmelt for short- and long-term periods. Hourly variations of snowmelt could not be predicted by using simple formulae. However, daily variations could be explained by the daily mean and maximum air temperatures, in which lower limit of snowmelt occurrence was obtained. During the intensive snowmelt season the predominant percolation velocities of snowmelt water were measured to be 0.25-0.45 cm/min, which implies that a large lag time of 3-4 hours was required for melting water to reach the bottom of a 60-80 cm snow cover. The lag time depended on the melt intensity of the surface and the depth of snow. (KEY TERMS: heat balance; degree-day factor; discharge; percolation velocity.)

difficult to obtain snowmelt in a watershed of wide area, therefore many estimating techniques have been developed (Motoyama, et al., 1983, Granger and Male, 1978, Price, et al., 1976). Net radiation at a melting snow surface plays the most important role on the snowmelt process (Kojima, et al., 1971), while the sensible heat and the latent heat are smaller in magnitude than the radiation except in very warm and wet conditions (Takahashi, et al., 1981). However, for the sake of simplicity many empirical formulae using only air temperature have been proposed for estimation of snowmelt (Yamaguchi, 1971, Oura, et al., 1969, Ishii, 1959). Appropriate empirical equations have still not been established (Kojima, et al., 1983). In this paper the relationships between snowmelt and bulk meteorological parameters have been examined. The estimated snowmelt was compared with actual snowmelt and discharge at the small experimental site. These methods were tested in advance of application to the whole watershed.

INTRODUCTION

The estimation of snowmelt amount in a whole watershed is of increasing importance in forecasting snowmelt floods, as well as providing for the efficient use of snow as a water resource in a mountainous region. It is logistically

INSTRUMENTATION

Measurements of surface snowmelt, runoff and meteorological parameters were carried out at the small experimental site (about 400 m² area) during the intensive period of snowmelt from 1980 to 1985. The site is located at the

¹Institute of Low Temperature Science, Hokkaido University, N-19, W-8, Sapporo, 060, Japan.

lowest part of Bifukazawa River watershed (about 11.2 km² in area) in Uryu-River in northern part of Hokkaido, Japan (45°N, 140°E). The topography of the area is surrounded by mountain ridges with an altitude difference of about 250 m. The general winter climate is characterized by very cold air temperature (the minimum air temperature is below -35 °C) and well developed snow pack (the maximum snow depth is over 200 cm). The snowmelt season lasts from the middle of April to the middle of May.

1) Measurements of surface snowmelt

In order to obtain the short term (hourly) variations of snowmelt the following parameters were measured every one or two hours a day during the snow-melting season in 1985: Surface depression (Δh), liquid water contents (W) and snow density (ρ). The liquid water content of snow was measured by using the calorimeters designed by Akitaya (Akitaya, 1978). Snow stake readings were done twice a day (09h, 17h) to determine the long term (daily) variations of snowmelt during six different snowmelt seasons from 1980 to 1985.

2) Measurement of heat balance components

Micro-meteorological observations were carried out at the site to derive the heat balance components at the snow surface. Observations were taken as follow: dry and wet bulb air temperature (ventilated platinum resistance thermometers), wind speed (an ultra sonic anemometer, three-cup anemometers and a wind vane), dew point temperature (Lithium chloride dew points meters), sensible heat flux (ultra sonic anemo-thermometers), global and reflected solar radiation (pyranometers), net radiation (a net radiometer), surface temperature (an infrared thermometer) and conductive heat flux in snow (heat flow transducers). All meteorological data were measured at 20 sec intervals and averaged for 5 minutes by a data logger.

3) Measurement of discharge from snow cover.

Discharge of the snowmelt water can be obtained by a snow lysimeter

(Herrmann 1978). In this investigation two shallow lysimeters (size was 90 cm x 90 cm) were used, one of which was buried just below the ground surface, and the other in the snow. Meltwater was collected in rain gauges and recorded automatically.

4) Measurement of the percolation velocity of meltwater through the snowcover.

Observation of the rate of downward movement of meltwater through snow cover was made by using a dye-stuff (eosine powder). A small amount of the dye was spread on the melting snow surface, which dissolved instantaneously and percolated into the snow cover. Even if the dyed portion of the snow surface was limited, it was covered with a certain amount of snow for eliminating albedo changes. Measurement of the length of dyed depth every 0.5-1 hour gave the percolation velocity of meltwater.

OBSERVATIONAL RESULTS

1) The relationship of snowmelt with heat balance

The amount of water content in snow (W), snow density (ρ), and surface depression (Δh) were measured at one or two hour intervals. The density of snow just below the snow surface (0-5 cm) gave the nearly constant value of 450 kg/m³ during the observation period.

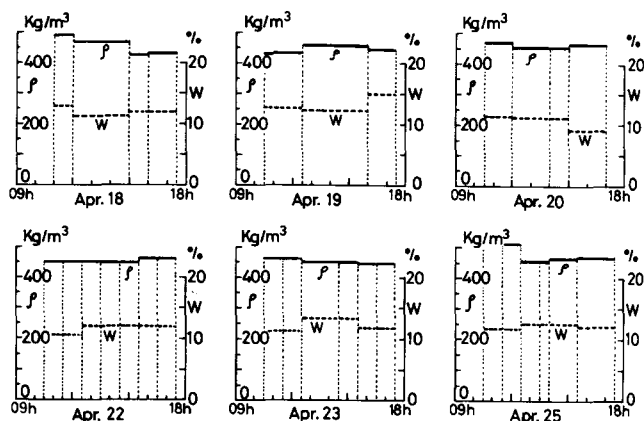


Figure 1. Variations of liquid water content and densities of snow cover. (18-25, April, 1985, Moshiri)

The liquid water content near the surface changed 9-15 % according to the time and weather condition (Fig.1). Using these values, surface snowmelt (M) was obtained directly ($M = (1-W)\Delta h \cdot \rho$), and hourly snowmelt (ΔM_h) at different weather conditions are shown in Fig. 2.

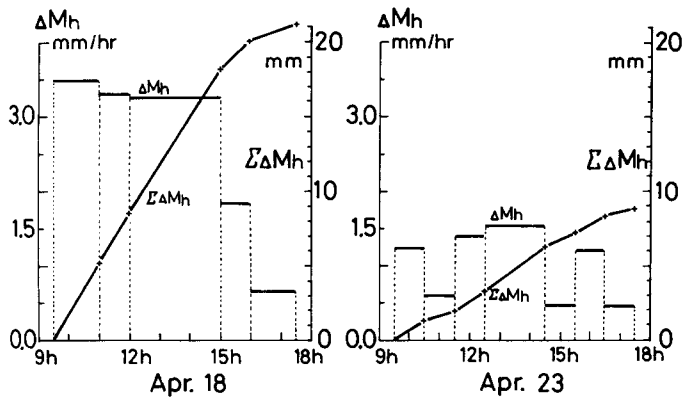


Figure 2. Hourly snowmelt measured by stake. (18-25, April, 1985, Moshiri)

Hereafter the method by stake measurement is called the direct method. The maximum value of snowmelt occurred near noon and ranged from 3.3 mm/hr on a clear day (18 Apr.) to 1.5 mm/hr on a cloudy day (23 Apr.). The total daily snowmelt ($\Sigma\Delta M_h$) was about 22 mm on the clear day and 9 mm on the cloudy day.

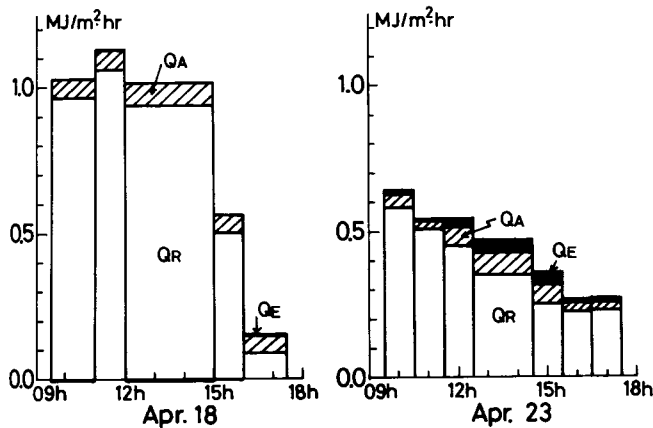


Figure 3. Hourly variation of each heat balance component.

Q_R : net radiation amount
 Q_A : sensible heat flux
 Q_E : latent heat flux of condensation or evaporation of water vapor
 (18-25, April, 1985, Moshiri)

Heat balance components were obtained during the same intervals when the stake measurement were carried out. Their time variation appears in Fig. 3. For the procedure radiation was measured by a net radiometer and sensible heat flux was measured by an ultra sonic anemometer. Latent heat flux for condensation or evaporation of water vapor was estimated by the empirical equation which was established for the experimental site before (Motoyama, et al., 1983). The sign of each component means that the positive and the negative show the flux towards and away from the snow surface, respectively. The main component of heat balance is due to net radiation (Q_R) (80-95 % during the intensive snowmelting season). Next in importance is the sensible heat flux (Q_A), while the latent heat flux of condensation or evaporation (Q_E) is small in magnitude and does not contribute much to the snowmelt as shown in figure 3. A previous investigation (Kojima, 1979) showed that the conductive heat flux in snow cover and the heat from rainfall were usually very small in the season, therefore snowmelt (M) can be estimated by the following heat balance equation:

$$M = Q_R + Q_A + Q_E,$$

where the positive sign of M shows snowmelt, and the negative sign indicates refreezing of meltwater in the snowcover. Figure 4 shows the comparison of hourly snowmelt obtained by stake measurement and the heat balance method. Their agreement is fairly good, but during the morning of clear days, values from stakes are lower than from the heat balance determination. With clear weather conditions, radiative cooling occurs at night, and the liquid water content near the surface tends to refreeze. Thus the so called ice crust layer forms. Even if heat balance becomes positive in the early morning, surface snowmelt does not occur before the crust layer warms up to 0°C . Neglecting the conductive heat flux in eq.(1) might be one of causes of this discrepancy.

While the heat balance method is pointed out as a suitable technique for estimating snowmelt, it is too complicated to use. Therefore, we consider a practical technique by using empirical

formulae requiring only bulk meteorological parameters.

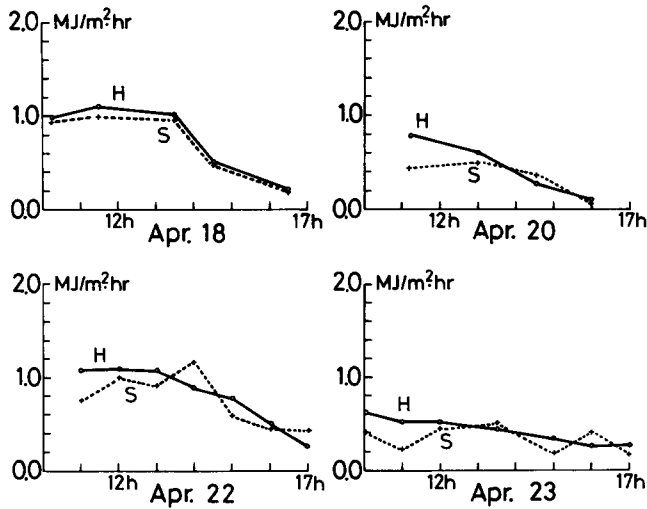


Figure 4. Comparison of snowmelt estimated by heat balance and obtained by stake method. (18-25, April, 1985, Moshiri).

H: heat balance method
S: stake method

2) The relationship of snowmelt with bulk meteorological parameters

i) Hourly snowmelt

Many investigators reported empirical formulae requiring only air temperature, but the most suitable formula, or melting coefficient termed "degree day factor" has not been established yet. In this investigation hourly values of snowmelt and meteorological parameters were accumulated during daily snow-melting period of a day. Figure 5 shows relationships between accumulated values of hourly snowmelt and bulk meteorological parameters (hourly mean air temperature (T_a) and hourly net radiation), which appeared during each day. The relationships between snowmelt and net radiation were expressed by empirical equations with high correlation coefficients. As mentioned before net radiation plays the most important role of the heat balance during the snowmelt season at the experimental site. The empirical constants (degree-hour factor) obtained on each day are similar for the entire observation period. From this figure it can be seen that the estimation of such short term snowmelt (hour-

ly) might be calculated by using only net radiation amounts. Correlation between accumulated values of hourly snowmelt and hourly air temperature are high, however linear regression lines change with individual days. Therefore, it is not possible to estimate hourly snowmelt by using only air temperature.

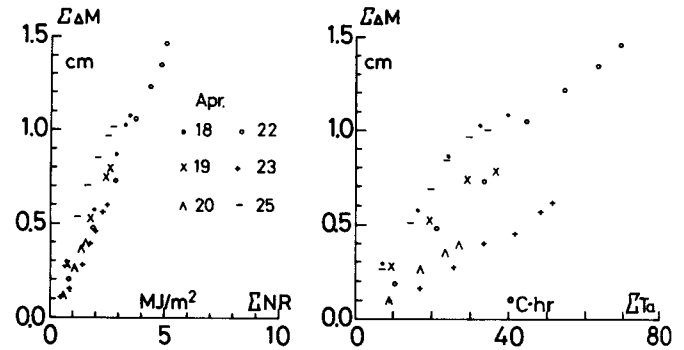


Figure 5. Relations of accumulated hourly snowmelt with bulk meteorological parameters.

a) net radiation
b) hourly mean air temperature
(18-25, April, 1985, Moshiri)

ii) Daily snowmelt

Figure 6 shows the relationship of daily snowmelt (ΔM) with the daily mean (T_d) and the daily maximum (T_{max}) air temperatures, respectively. The regression lines are expressed by the following equations:

$$\Delta M = -4.1 + 3.0 T_{max} \quad (\text{mm} \cdot \text{d}^{-1})$$

$$\Delta M = 4.1 \cdot (3.0 + T_d) \quad (\text{mm} \cdot \text{d}^{-1})$$

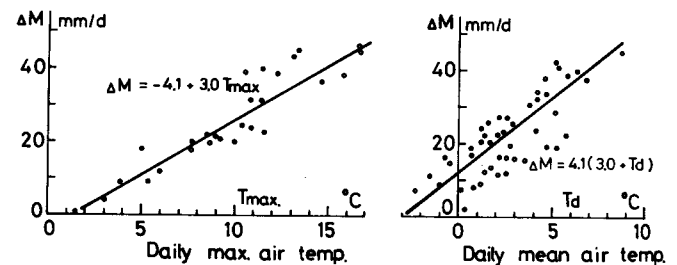


Figure 6. Relations of daily snowmelt with the air temperature.

a) daily maximum air temperature
(1980, Moshiri)
b) daily mean air temperature
(1980-1982, Moshiri)

These equations illustrate that the daily maximum air temperature $T_{max}=1.4^{\circ}C$ might be an approximate criterion of apparent snowmelt. Furthermore,, daily snowmelt occurs when the daily mean air temperature T_d is higher than $-3^{\circ}C$.

iii) Estimation of long-term snowmelt

Estimation of long-term snowmelt was done using bulk meteorological parameters. Unfortunately, no observational data of snowmelt exist, only depression of snow surface for long periods. Snow density near the surface was almost constant during the intensive snowmelt seasons. Therefore, depression of the surface were adopted instead of the snowmelt data. Figure 7 shows regression curves between accumulated surface depression and bulk meteorological parameters, where daily mean (T_d) and the daily maximum (T_{max}) of air temperature and daily amounts of net radiation (NR) were selected as bulk meteorological parameters. These values were accumulated for 10-14 days just before the day

when snowcover melted away from the experimental site, summarizing three different years (1983-1985). In comparison with short-term snowmelt, better relations appeared between bulk meteorological parameters and snowmelt. The relationships between accumulated surface depression ($\Sigma\Delta h$) and the net radiation for three years are shown by broken lines. The mean regression curve which is shown by the solid line can be expressed by

$$\Sigma\Delta h = 0.93 \Sigma NR + 0.98, \quad r=0.990$$

It is clearly shown that regression curves obtained at different years fitted well with the mean. Linear relations were obtained among accumulated amounts of surface depression ($\Sigma\Delta h$), daily mean air temperature (ΣT_d), and daily maximum temperature (ΣT_{max}). It is noted that the empirical coefficients can change slightly each year. Mean regression curves for three years (solid lines) can be expressed by

$$\Sigma\Delta h = 1.38 \cdot \Sigma T_d + 1.24 \quad (r=0.980)$$

$$\Sigma\Delta h = 0.62 \cdot \Sigma T_{max} - 2.51 \quad (r=0.975)$$

From these equations the amount of long-term snowmelt can be estimated by using bulk meteorological parameters.

3) Comparison of discharge with the surface snowmelt

An accurate method is still not available for measuring snowmelt continuously, therefore, discharges from a snow cover are used as an indicator of snowmelt in this paper. Figure 8 shows the variation of net radiation (NR) and discharge measured by a lysimeter (GL). Rainfall for every 30 minutes (P) are plotted on the same figure. Weather conditions during the observational period were mostly cloudy except April 22nd which was clear: Rain-fall on April 23rd was 0.5 mm, and on April 24 18 mm. Large discharge appeared during 24th of April in contrast to net radiation. Heat amounts of snowmelt due to rainfall (Q_p) can be estimated by the equation

$$Q_p = 70 \cdot T_a \cdot P / \Delta t \quad (W/m^2),$$

where T_a is the air temperature and P is the precipitation amount (mm) for Δt period (min). The mean air temperature was $2.7^{\circ}C$, and the maximum precipitation for 30 min was 2.3 mm at April 24th. It means that the heat of $14.5 W/m^2$ re-

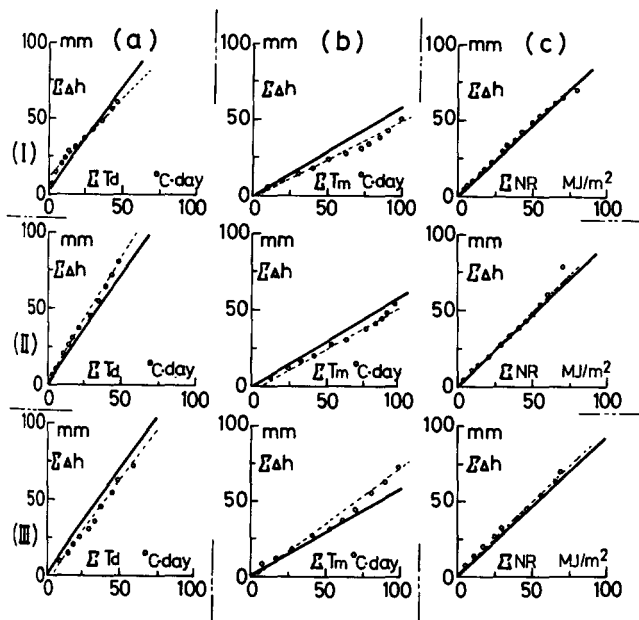


Figure 7. Relationships of accumulated daily surface depression with accumulated bulk meteorological parameters (from 1983(III) to 1985(I)).

- a) accumulated daily mean air temperature
 - b) accumulated daily maximum air temperature
 - c) accumulated daily net radiation
- solid lines: means for three years

leased from rainfall, which did not contribute much to snowmelt as mentioned before. Therefore, it can be said that most of discharge was due to the precipitation and not snowmelt. Large time differences are seen between the variations of net radiation and discharge. The lag time between the initial raise is about 4-5 hours, but the peak time difference is about 1-1.5 hours. The lag time is considered as the traverse time of meltwater from the surface to the bottom of snowcover. The former depends on the depth of snow cover and the intensity of surface snowmelt (Kojima, 1984).

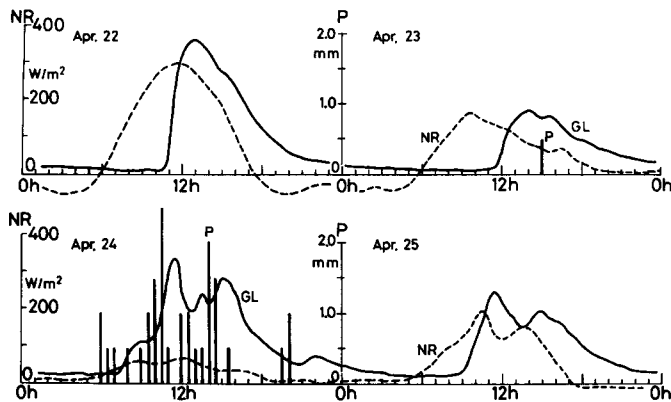


Figure 8. Hourly variations of net radiation (NR), discharge amounts (GL), rainfall (P). (22-25, April, 1985, Moshiri)

Some investigators have described the movement of snowmelt water through snow cover previously. In order to determine the percolation velocity of melt water, Wakahama, et al. (1968) measured time variations of liquid water content in a snowcover, and Fujino (1968) measured the time change of snow electro-conductivities after spreading some markers over the snow surface. Theoretical analyses of meltwater movement was done by Yoshida (1965) and Colbeck (1972). Wankiewicz (1979) reviewed the process of meltwater percolation in detail. From their works it can be said that the percolation velocity of snowmelt water depends on many factors: snow density, liquid water content, surface snowmelt rate and snow stratigraphy. In this investigation two kinds of dyes (eosine

and waterblue) were used to determine percolation velocity. After spreading small amounts of dye over the surface or inside the snowcover, the length of the colored depth was measured by snow pit observations after a specific time interval. Figure 9 shows the variation of percolation velocity of meltwater at specific depths (0.1m, 0.3m, 0.5m) and isopleths. Under clear conditions the percolation velocity at the upper part of the snowcover was much larger than in the lower part, and the maximum velocity appeared around noon. During cloudy conditions the velocity was almost constant at each depth. In this investigation the predominant percolation velocity of 0.25-0.45 cm/min was obtained. This means that it takes 3-4 hours for the surface meltwater to reach the bottom of a snow cover of a 60-80 cm depth (Fig. 8). Therefore, such a lag time effect should be corrected when comparing the surface snowmelt and discharge, especially for a shorter time durations.

Snowmelt obtained by three methods are compared with each other in Fig. 10.

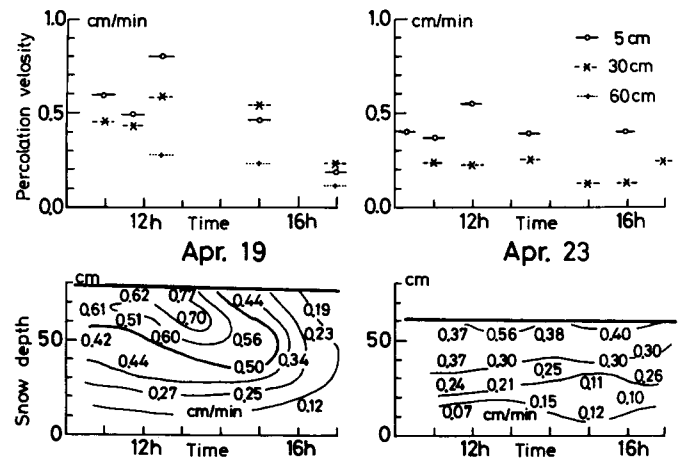


Figure 9. Percolation velocity of surface snowmelt.
upper: time variation of the velocity at 5 cm, 30 cm and 60 cm below the snow surface
lower: isopleths of the velocity
left: fine weather, right: overcast (April, 1985, Moshiri)

The abscissa shows the estimated snowmelt by using the heat balance, and the ordinate shows the snowmelt from the stake reading (direct method), and dis-

charge. These values are accumulated during 8 days just before the day of complete snowmelt.

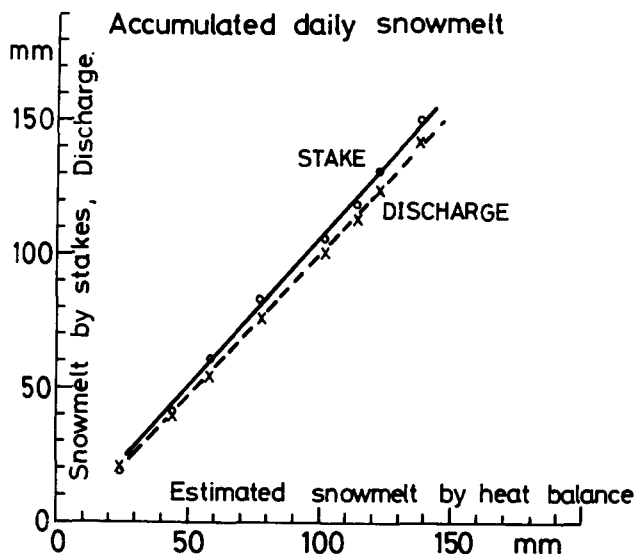


Figure 10. Comparison of estimated snowmelt with actual snowmelt and discharge. (18-25, April, 1985, Moshiri)

The estimated snowmelt by heat balance method coincided well with actual snowmelt from the stake reading and discharge measurements. It shows that the discharge from the bottom of snowcover can be taken as the surface snowmelt at the intensive snowmelt periods if it takes for a longer period of time, such as 24 hours.

CONCLUSION

Surface snowmelt during intensive snowmelting periods was estimated by using the heat balance method and bulk meteorological parameters. These were compared with the actual snowmelt and discharge at the small experimental site. The results are as follows:

- 1) Estimated snowmelt by heat balance or a simple formula using net radiation fitted well with the actual snowmelt. The relationship between calculated and observed snowmelt, accumulated for 8 days, could be represented by linear regression curve with a high correlation coefficient ($r=0.990$).
- 2) Short term variations of snowmelt

could not be explained by simple formulae using air temperature only. However, the daily snowmelt during intensive melt periods were explained by the daily mean and daily maximum air temperatures, respectively. Furthermore, long term snowmelt, accumulated for 10-14 days up to the day of snow disappearance, correlated well with the accumulated daily air temperature. From the work above the approximate criterion of apparent daily snowmelt occurrence is 1.4°C for daily maximum air temperature, and -3°C for daily mean air temperature. 3) Hourly snowmelt estimated by the heat balance method and simple equations were compared with snowmelt discharge from the bottom of snow cover. The lag times ranged from 3 to 4 hours, but they depended on intensities of snowmelt, and the depth of snow cover. For long periods such as 10-14 days good relations were found between estimated snowmelt and daily discharge, especially for accumulated ones.

ACKNOWLEDGMENTS

Authors would like to express their sincere thanks to Moshiri Branch of Uryu Experimental Forest, Hokkaido University for their logistic support to the investigations, and to Dr. K. Fujino, Institute of Low Temperature Science for his useful comments on the measurement of the percolation velocity of melt water. They also thank Misses A. Ohmori and N. Ochiai for the preparation of the manuscript.

REFERENCES

- Akitaya, E., 1978. Measurements of Free Water Content of Wet Snow by Calorimetric Method. *Low Temp. Sci.* 36:103-111.
- Colbeck, S.C., 1972. A theory of Water Percolation in Snow. *J. Glaciol.* 11:369-385.
- Fujino, K., 1968. Measurement of Flow Down Speed of Melt Water in Snow Cover. *Low Temp. Sci.* 26: 87-100.
- Granger, R. J., and D. H. Male, 1978.

- Melting of a Prairie Snowpack. J. Appl. Meteor. 17: 1833-1842.
- Herrmann, A., 1978. A Recording Snow Lysimeter. J. Glaciol. 20: 209-213.
- Ishii, Y., 1959. Studies on Snow Melting. Fundamental Research of Snow Cover. Hokkaido Electric Power Co. and Sapporo District Meteor. Observatory: 1-84.
- Kojima, K., D. Kobayashi, H. Aburakawa, R. Naruse, K. Ishimoto, N. Ishikawa, S. Takahashi, 1971. Studies of Snow Melt, Runoff, and Heat Balance in a Small Drainage Area in Moshiri, Hokkaido.II. Low Temp. Sci. 29: 159-176.
- Kojima, K. 1979. Mechanism of Snow Melting and Heat Budget. Note Meteor. Res. 139: 1-33.
- Kojima, K., H. Motoyama, and Y. Yamada, 1983. Estimation of Melting Rate of Snow by Simple Formulae Using only Air Temperature. Low Temp. Sci. 42: 101-110.
- Kojima, K., and H. Motoyama, 1983. Time Lag of Meltwater Percolation through a Snow Cover. Low Temp. Sci. 43: 181-194.
- Motoyama, H., D. Kobayashi, and K. Kojima, 1983. Water Balance at a Small Watershed during the Snowmelt Season I. Low Temp. Sci. 42: 123-133.
- Oura, H., K. Kojima, D. Kobayashi, R. Naruse, and N. Ishikawa, 1969. A Study of Snow Melt in Ikutora. Low Temp. Sci. 27: 143-162.
- Price, A. J., T. Dunne, and S. C. Colbeck, 1976. Energy Balance and Runoff from a Subarctic Snowpack. CRREL Rept. 27: 1-29.
- Takahashi, S., A. Sato, and R. Naruse, 1981. A Study of Heat Balance on the Yukikabe Snow Patch in the Daisetsu Mountains. Seppyō, 43: 147-154.
- Wakahama, G., T. Nakamura, and Y. Endo, 1968. Infiltration of Melt Water into Snow Cover II. Low Temp. Sci. 26: 53-75.
- Wankiewicz, A., 1979. A Review of Water Movement in Snow. Proc. Modeling of Snow Cover Runoff. S.C.Colbeck and M.Ray (Editors). U.S.Army CRREL, Hanover, NH, 26-28. Sept. 1978: 222-252.
- Yamaguchi, H., and S. Hasegawa, 1970. A Study on Snowmelt Runoff. Rep. Civil Eng. Res. Inst. 64: 1-174.
- Yoshida, Z., 1965. Infiltration of Melt Water in Snow Cover. Low Temp. Sci., 23: 1-16.

A METHODOLOGY FOR ESTIMATING
DESIGN PEAK FLOWS FOR YUKON TERRITORYJ. Richard Janowicz¹

ABSTRACT: A simple methodology based on a regional approach was sought for estimating peak flows for the design of hydraulic structures in Yukon Territory. This procedure is needed for the design of projects with relatively short design lives such as those associated with placer mining operations as well as more conventional hydraulic design situations. Because of its varied use a simple, readily transferable method was desired. Single station flood frequency analyses were carried out on 90 hydrometric stations with at least six years of record using a two parameter lognormal theoretical probability distribution which is believed to be the most appropriate for sparse data regions. Simple linear regression relationships were developed between maximum annual instantaneous discharge at selected return periods and drainage area for two hydrologic regions. An attempt was made to improve on these relationships through the inclusion of a storage index factor which accounts for the relative location of lake or swamp storage within a basin as well as the size of the storage. The inclusion of this parameter in the developed relationships was statistically significant. Multiple linear regression equations were developed for the Interior and Western Mountains hydrologic regions and the Territory as a whole. (KEY TERMS: regional approach; hydraulic design; placer mining operation; two parameter lognormal theoretical probability distribution; sparse data region; storage index factor.)

INTRODUCTION

Functional relationships were developed for estimating peak flows in the Yukon Territory. This information is needed for the safe and economical design of hydraulic structures such as bridges, culverts, dams, diversion

channels and road embankments. Methods which are traditionally used in more populated southern areas are not applicable in many areas of Yukon Territory due to the relatively small hydrometeorological data base and unique hydrologic regime types associated with subarctic and arctic environments. There are 94 hydrometric stations within the Territory or one station for every 5100 square kilometers. Most of these are relatively recent; however, with 47 of the total established within the last ten years. The mean record length is 12.4 years. Of the total number of hydrometric stations, 20 are partial record stations operated primarily on small streams. Hydrometric station locations are noted in Figure 1.

Relatively few stations exist in the northern part of the Territory; however, the available data indicates a differing hydrologic response between northern and southern regions. This is presumably due to the presence of underlying permafrost which becomes more dominant with increasing latitude. The boundary between the zone of continuous and discontinuous permafrost coincides approximately with 67° latitude as noted in Figure 1. Hydrometric station density decreases significantly north of the Ogilvie Mountains which coincides approximately with 65° latitude.

The majority of the peak flow design estimates required annually in Yukon Territory are needed for placer mining operations. Of the 300 Yukon placer operations most are on small streams with drainage areas less than 150 square kilometers. Since hydraulic structures associated with the placer

¹Water Resources Division, Northern Affairs Program, Indian and Northern Affairs Canada, Whitehorse, Yukon Territory, Y1A 3V1.

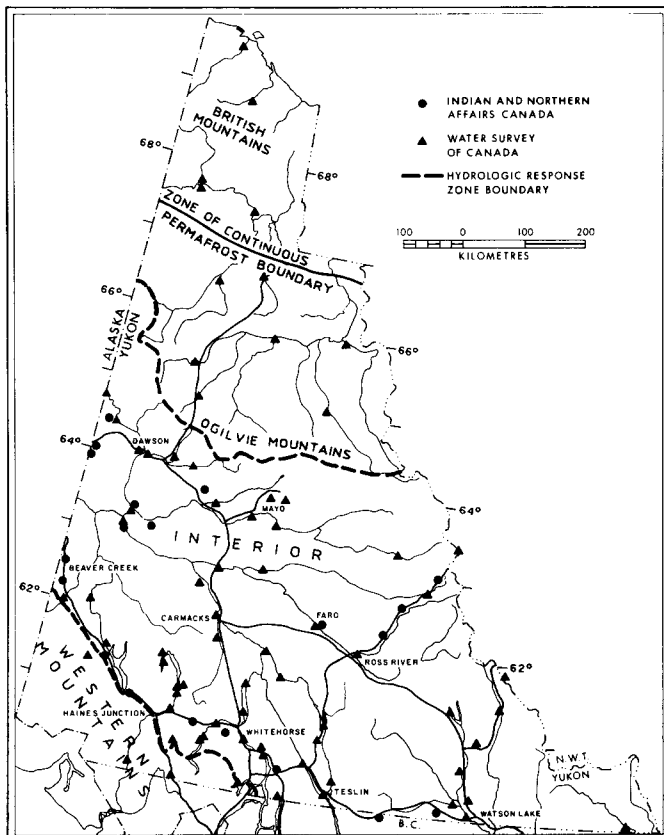


Figure 1. Yukon Territory existing hydrometric stations and hydrologic zones.

mining industry have relatively short design lives (two years), safety considerations and the economic impact of failure are less than other design problems.

The objectives of this study were to develop a simple methodology for estimating peak design flows for all Yukon watersheds. A simple criteria was desired since the placer mining industry would be a major user with design applications primarily associated with short design life projects. Use of this methodology would not be limited to placer operations; however, and a reasonable degree of confidence in the technique and subsequent design estimates is required.

Because of its anticipated varied application a lower or upper limit to drainage basin size was not used as a criteria in selecting hydrometric

stations for analyses. The application of the developed relationship is intended to be used for all hydraulic design situations for at least preliminary design purposes. If safety or economic considerations merit, and given a sufficient amount of data, other techniques should be investigated. The developed methodology is expected to provide estimates of flows for ungaged basins with a reasonable degree of accuracy and confidence throughout most of Yukon Territory.

SETTING

Streamflow in Yukon Territory is generally characterized by peak flows in spring or summer as a result of snowmelt and glacial inputs. Smaller systems are susceptible to peak flows in response to rainfall inputs while intermediate size basins may experience secondary rainfall peaks in addition to the freshet. Streamflow decreases to a minimum in March or April though groundwater inputs generally maintain winter flows in all but the smallest streams. Most streams are generally ice covered from late October to April.

Two primary hydrologic regimes have been identified in the Territory south of the Ogilvie Mountains. For discussion purposes these are referred to as the Interior and Western Mountains hydrologic regions. In the southwestern area of the Territory, streams which drain the St. Elias and Coast Mountains experience a rapid increase in streamflow discharge during the early summer in response to snowmelt at lower elevations. Flows increase in magnitude to a peak in later summer due to glacial melt at higher elevations.

The St. Elias and Coast Mountain drainages may be considered separate subregions of the Western Mountains hydrologic region. Streams draining the St. Elias Mountains have shorter response time than the Coast Mountains; therefore, exhibit a flashy response due to temperature and precipitation inputs during the summer. The Coast Mountains have smaller glacierized areas and longer stream lengths which in combination with the natural regulation

provided by the extensive lake systems tend to remove this variability.

Streams which drain the remainder of the southern region are characterized primarily by a rapid rise in discharge in the spring due to snowmelt inputs. Peaks generally occur in June, after which time summer rainfall maintains high flows for a few weeks. Small basins throughout the southern Territory may experience rainfall peaks, while intermediate basins may experience secondary peaks due to summer rainfall.

The available data indicates an increase in peak flows with increasing latitude north of the Ogilvie Mountains. This is presumably due to the increasing presence of underlying permafrost as it becomes more dominant. The dominance becomes complete within the direct Arctic drainage north of the British Mountains as indicated by the recorded unit discharge which is the highest in the Territory.

DEVELOPMENT OF REGIONAL RELATIONSHIPS

Single Station Analysis

Single station flood frequency analyses were carried out using all hydrometric data in Yukon Territory with at least six years of record. Sample data was obtained from Water Survey of Canada (WSC) and Indian and Northern Affairs Canada (INAC) computer files current to 1983. In addition selected peripheral stations in British Columbia and Alaska were used to supplement the Yukon data. Peak flow events produced by glacier outburst floods and ice jams were not included in the analysis. Records were not screened for mixed populations and outliers. A computer program initially developed by Environment Canada (Condie, Nix and Boone, 1976) and revised in 1981 was used for the analyses. The program utilizes the plotting formula:

$$T = \frac{N + 0.5}{m - 0.24}$$

where T is the return period, N is the sample size and m is the rank. The developed routine fits four theoretical probability distributions to the sample data using the method of maximum likelihood. The two parameter lognormal probability distribution was selected for the present study on the basis of previous work which included the development of a goodness of fit criteria based on classical tests (Janowicz, 1983). For application in sparse data regions it is believed that two parameter probability distributions are superior to those with three parameters due to the generally smaller data sets which make it difficult to fit the more complex distributions.

Regionalization Procedure

Hydrologic regions as defined by Janowicz (1984) were used as the basis for the development of the regional relationships. In the former study sufficient data were available to statistically define two hydrologic regions only within the Territory. As discussed above it is known that the hydrologic response of northern areas varies considerably from southern regions. This is indicated by the few available hydrometric stations in the northern part of the Territory, though these are insufficient in number to provide a statistical definition.

Janowicz (1984) used multivariate statistical analyses to define the hydrologic regions. A cluster analysis was initially used to define rudimentary statistical groups. Input parameters included a timing parameter and selected sample statistics of the annual mean daily flow series divided by drainage area. Only stations with a minimum of ten years of record were used.

The analysis yielded two well defined groups with evidence of a third transitional group. These essentially correspond in area to include the stations draining the Coast Mountains as the most significant group, with the St. Elias stations forming the weaker transitional group. The third group consisted of the remaining stations.

Multiple discriminant analysis was then used to amend boundary locations. It was determined that too few stations existed in the St. Elias region to yield a statistical distinction from the Coast Mountains. These were combined to form the Western Mountains region.

Region boundaries were adjusted during subsequent analyses. Two statistically defined hydrologic zones were obtained with relatively high degrees of accuracy. The defined hydrologic regions are shown in Figure 1.

Simple Linear Regression

Simple functional relationships between mean annual maximum instantaneous discharge at selected return periods, and drainage area were developed for the hydrologic regions discussed above. Of the physical watershed parameters, drainage area is generally the most significant and can be readily extracted from topographic maps. The least squares simple linear regression analyses were carried out on a Hewlett Packard 9826A micro-computer using the HP statistical library and graphics package. Because of the inverse relationship between drainage area and unit flood events, a curilinear relationship was initially sought using a polynomial curve fitting routine. Best results were obtained; however, with a linear fit using logarithmically transformed data. Values of the standard error of estimate were calculated using logarithmic units and represent the relative goodness of fit provided by the developed relationships.

It became apparent during the analyses that several of the outliers represented hydrometric stations with considerable upstream lake storage. Both data groups were screened for stations with significant upstream storage. These were used to form a third group of 13 stations. The analysis was repeated with 53 and 24 stations for the Interior and Western Mountains regions respectively.

The analyses were successful yielding values for the coefficient of determination (r^2) of 97, 94 and 86 percent for the Interior, Western Mountains and storage controlled responses respectively, with standard errors of estimates of 6.1, 8.1 and 11.4 percent respectively. Plots of mean annual maximum instantaneous discharge against drainage area, with 95 percent confidence limits, are presented in Figures 2 to 4 for the three response types.

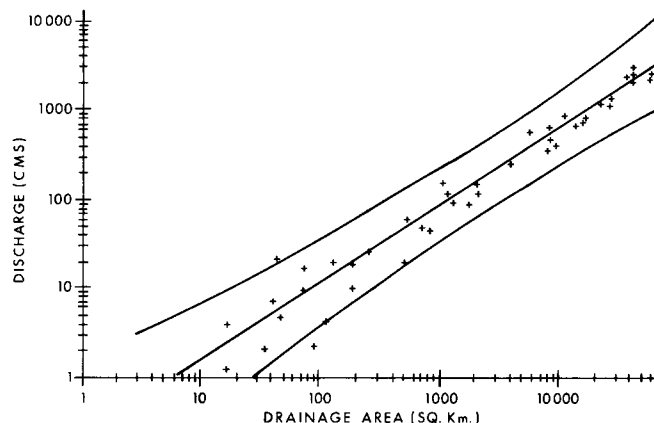


Figure 2. Mean annual maximum instantaneous discharge and 95 percent confidence limits for the Interior hydrologic region.

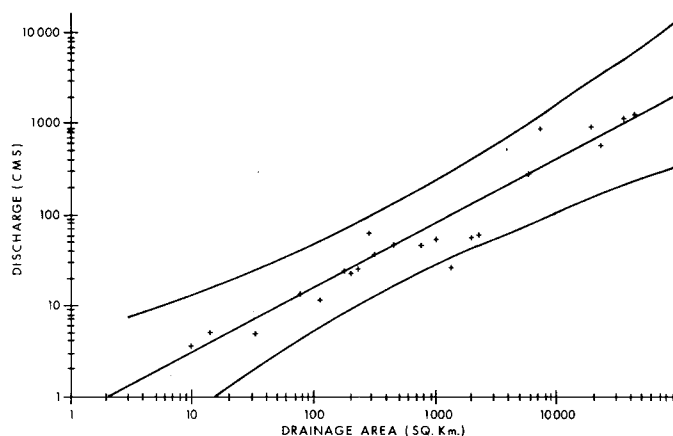


Figure 3. Mean annual maximum instantaneous discharge and 95 percent confidence limits for the Western Mountains hydrologic regions.

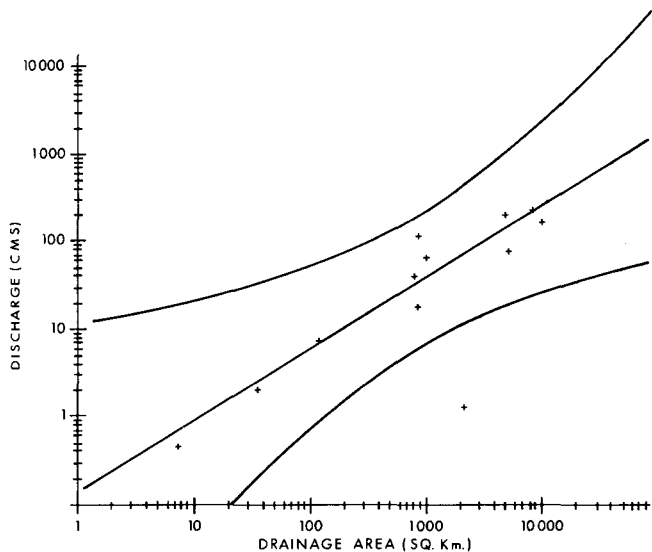


Figure 4. Mean annual maximum instantaneous discharge and 95 percent confidence limits for Hydrometric stations with significant upstream lake storage.

These relationships provide a means of obtaining design peak flow estimates with a reasonable degree of confidence for ungaged basins throughout most of the Territory. The developed relationships are presented in Table 1.

Table 1. Summary of Simple Linear Regression Equations.

$$Y = a(\text{AREA})^b$$

DEPENDENT VARIABLE		REGRESSION CONSTANT	REGRESSION COEFFICIENT		STANDARD ERROR OF ESTIMATE
Y		a	b	r ²	(PERCENT)
MEAN	1	0.226	0.865	0.97	6.1
ANNUAL	2	0.617	0.707	0.94	8.1
FLOOD	3	0.139	0.817	0.86	11.4
2-YEAR	1	0.188	0.876	0.96	6.5
	2	0.467	0.736	0.94	8.3
3	0.091	0.862	0.87	11.8	
	5-YEAR	1	0.301	0.856	0.97
2	0.971	0.676	0.92	7.9	
	3	0.200	0.798	0.86	11.3
10-YEAR	1	0.385	0.850	0.97	6.4
	2	1.430	0.640	0.91	8.4
3	0.305	0.760	0.84	11.5	
	50-YEAR	1	0.629	0.811	0.96
2	2.670	0.594	0.89	9.5	
	3	0.633	0.704	0.81	11.9

- 1 - INTERIOR
- 2 - WESTERN MOUNTAINS
- 3 - LAKE CONTROL

Storage Index Factor

Since lake storage appeared to have a considerable effect on peak flows within the study area, this

parameter was investigated further with the intention of improving the developed relationships.

Surface storage within a watershed is provided by lakes, swamps and reservoirs in addition to the stream channel itself and depression storage. In northern permafrost areas the thick organic mat which makes up the active layer also provides considerable storage. These storage systems attenuate peak flows by increasing the duration of the streamflow event. The relative degree of attenuation depends on the amount of storage and its location within the basin. Poulin (1971) found that a storage parameter which represented the location of the storage system with respect to the point of interest, as well as the size, provided a better index of attenuation than the amount of storage alone. The use of this index was investigated in an attempt to better define the relationships presented above. For the purpose of this study the index is defined as the relative amount of watershed drainage area, in percent, which is controlled by the upstream lake or swamp. The lake or swamp is required to have an area equal to or greater than one percent of the upstream area controlled by it. This parameter is defined in Figure 5.

The storage index factor has a range in values from 0 to 100 percent for both hydrologic regions. The mean is 31.2 and 68.1 percent for the Interior and Western Mountains hydrologic regions respectively. The greater values within the Western Mountains region are a result of a program carried out in the 1960's to establish hydrometric stations at lake outlets for the purpose of assessing hydroelectric potential in the area.

In a study carried out jointly by Environment Newfoundland and Environment Canada (1984), the investigators found this parameter to be quite significant. With 17 independent parameters it was most often entered by the stepping routine after drainage area as the second most significant variable. The study indicated; however, that in a particular region, estimates diverged considerably when this parameter fell below 55 percent.

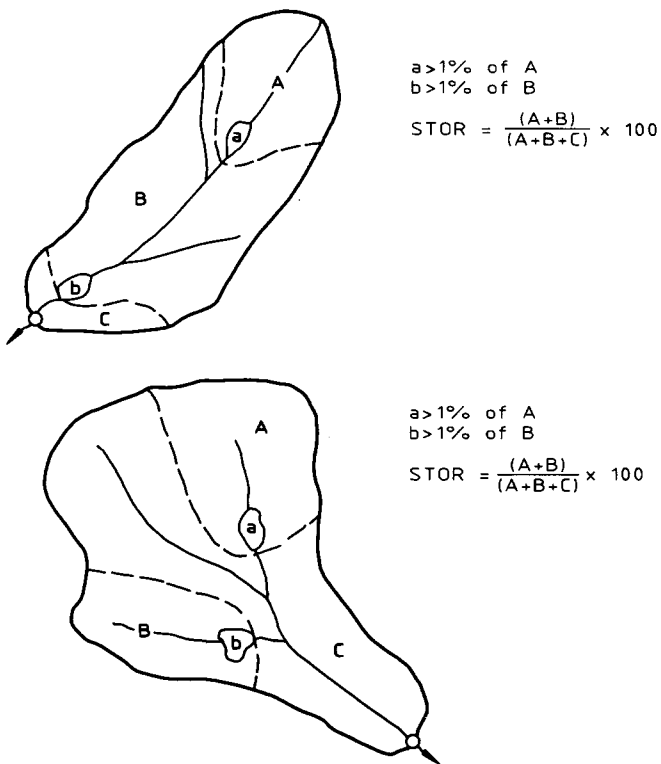


Figure 5. Determination of storage Index factor (after Poulin, 1971).

Multiple Linear Regression

Further analyses were carried out using the storage index factor in an attempt to improve the developed relationships. The stepwise multiple linear regression analyses were carried out using a program from the Biomedical Program series (Dixon and Brown, 1979). The general form of the equation is:

$$Y = a + b_1x_1 \dots b_nx_n$$

where Y is the dependent variable, a is a regression constant, x_1, x_n represent the values of the independent variable, and b_1, b_n are regression coefficients. The value of the F-statistic was set to allow the entry of independent parameters which were within the 99 percent level of significance. It was found that by logarithmically transforming the streamflow and drainage area data,

which had values with a range of up to five orders of magnitude, a better fit was generally obtained. The storage index data was not transformed. The general form of the transformed equation then becomes:

$$\ln Y = 1na + b_1 \ln x_1 \dots b_n \ln x_n$$

which in the present case becomes:

$$\ln Y = a + b_1 \ln x_1 + b_2 x_2.$$

Relationships were developed between mean annual maximum instantaneous discharge at selected return periods and the independent parameters of drainage area (AREA) and the storage index factor (STOR) at selected return periods. Relationships were developed for the two defined hydrologic regions as well as the Territory as a whole, for use in the region between the Ogilvie and British Mountains. The developed equations are presented in Table 2.

The best results were achieved for the Interior region as indicated by values of the standard error of estimate and the coefficient of determination. Though the entry of the storage index factor accounts for a small portion of the variance, the difference is significant at the 99 percent level. The use of this parameter reduced the standard error of estimate from 11.3 to 9.3 percent for the mean annual flood. Similarly there was an increase in the coefficient of determination from 0.916 to 0.945.

The development of an improved relationship for the Western Mountains hydrologic region using the storage index factor was more difficult than for the Interior region. It was discovered that the data representing intermediate sized basins draining the St. Elias Mountains detracted considerable from the general trend. By removing these four stations (White River, Kluane River, Alsek River and Kathleen River) the storage index factor was then readily entered into the relationship by the stepping function. These basins contain relatively large glacialized

Table 2. Summary of Multiple Linear Regression Equations.

$$\text{LnY} = a + b_1 \ln(\text{AREA}) + b_2 (\text{STOR})$$

DEPENDENT VARIABLE		REGRESSION CONSTANT	REGRESSION COEFFICIENT		STANDARD ERROR OF ESTIMATE	
Y		a	b ₁	b ₂	r ²	(PERCENT)
MEAN	1	-2.013	0.947	-0.0120	0.945	9.3
ANNUAL FLOOD	2	-0.172	0.574	0.0082	0.944	10.9
	3	-1.182	0.831	-0.0050	0.921	12.2
2-YEAR	1	-2.097	0.954	-0.0124	0.941	9.7
	2	-0.364	0.584	0.0090	0.947	11.0
	3	-1.356	0.845	-0.0048	0.920	12.5
5-YEAR	1	-1.757	0.943	-0.0121	0.947	9.1
	2	0.193	0.562	0.0072	0.939	11.0
	3	-0.844	0.819	-0.0056	0.920	12.1
10-YEAR	1	-1.591	0.939	-0.0120	0.947	9.0
	2	0.486	0.551	0.0063	0.930	11.4**
	3	-0.583	0.807	-0.0060	0.917	12.2
20-YEAR	1	-1.442	0.935	-0.0120	0.948	8.9
	2	0.796	0.524	0.0067	0.909	12.7**
	3	-0.340	0.792	-0.0061	0.909	12.6
50-YEAR	1	-1.299	0.933	-0.0118	0.946	9.1
	2	0.938	0.538	0.0047	0.901	13.0*
	3	-0.163	0.790	-0.0068	0.909	12.5
100-YEAR	1	1.190	0.930	-0.0116	0.943	9.3
	2	1.179	0.523	0.0041	0.888	13.4*
	3	0.047	0.776	-0.0069	0.901	12.8

1 - INTERIOR
 2 - WESTERN MOUNTAINS
 3 - COMBINED

* - NOT SIGNIFICANT
 ** - SIGNIFICANT TO 95%

areas and subsequently generate high peak flows. Additional support for the removal of these stations is provided by the observed distinction between the two subregions making up the Western Mountains region as noted during the regionalization procedure.

With the four station removed the developed relationship is statistically

significant at the 99 percent level. The entry of the storage index factor reduced the standard error of estimate from 12.6 to 10.9 percent for the mean annual flood. Similarly there was an increase in the coefficient of determination from 0.922 to 0.944.

A relationship was developed for the Territory as a whole using the

combined data sets of 61 stations. The relationship is intended for application to areas north of the Ogilvie Mountains. Because of the limited data base north of the Ogilvie Mountains and the increasing dominance of permafrost with increasing latitude, care should be exercised in applying the developed equation within this region. It should not be used for estimating design flows north of the British Mountains within the direct Arctic drainage. The developed relationship is statistically significant at the 99 percent level. The entry of the storage index factor reduced the standard error from 12.8 to 12.3 percent for the mean annual flood. Similarly the coefficient of determination increased from 0.913 to 0.921.

DISCUSSION

Simple and multiple linear regression relationships were developed for estimating peak flows in most areas of Yukon Territory. The developed relationships are based on a single station flood frequency analysis which was carried out on 90 hydrometric stations with at least six years of record. The two parameter lognormal theoretical probability distribution was selected for use in this study since it is believed to be the most appropriate for sparse data regions.

Relationships between annual maximum instantaneous discharge at selected return periods and drainage area were developed for two statistically defined hydrologic regions and a third group of hydrometric stations with relatively large areas of lake storage. Because of the considerable effect of lake storage in attenuating peak flows, it was believed that the addition of this parameter to the developed relationships would result in a significant improvement. The analyses were repeated using a storage index factor as a second independent variable. The storage index factor represents the location as well as the

size of the storage feature within a watershed.

The inclusion of the storage index factor parameter in the developed relationships was statistically significant. Multiple linear regression equations were developed for the Interior and Western Mountains hydrologic regions. A relationship using the combined data was developed for use outside these regions. The analyses were generally good as indicated by the relatively low standard error of estimates and the high coefficients of determination. The developed equations provide a simple method of estimating peak flows with a reasonable degree of accuracy for most areas of Yukon Territory.

REFERENCES

- Condie, R., G.A. Nix, and L.G. Boone, 1976 (with revisions 1981). Flood Damage Reduction Program - Flood Frequency Analysis. Water Planning and Management Branch, Inland Waters Directorate, Environment Canada, Ottawa, Ontario.
- Dixon, W.J. and M.B. Brown. 1979. Bio-medical Computer Programs - P - Sries, University of California Press, Berkeley, California.
- Janowicz, J.R. 1983. Peak Flow Regionalization for Alaska. Unpublished M.S. Thesis. Fairbanks, Alaska.
- Janowicz, J.R. 1984. Yukon River Basin Hydrometeorologic Data Network Assessment. Yukon River Basin Study - Hydrology Report #2. Indian and Northern Affairs Canada. Whitehorse, Yukon.
- Newfoundland Environment and Environment Canada. 1984. Regional Flood Frequency Analysis for the Island of Newfoundland. St. John's, Newfoundland.
- Poulin, R.Y. 1971. Flood Frequency Analysis for Newfoundland Streams. Water Planning and Operations Branch, Department of the Environment. Ottawa, Ontario.

EFFECTS OF SEASONALLY FROZEN GROUND IN SNOWMELT MODELING

Knut Sand and Douglas L. Kane¹

ABSTRACT: The Swedish HBV-3 runoff model was used for simulations of runoff during snowmelt periods in the Chena River Basin in interior Alaska. The model was calibrated using data from 1969-1974. The initial simulations showed a poor ability to simulate both snowmelt runoff and rainfall runoff events. Because frozen soils have much lower infiltration and storage capacities than unfrozen soils, the soil moisture routine in the model was modified to accept seasonally varying soil parameters. This modification substantially improved the runoff simulations. The model was tested with meteorological data from 1982-1985 using the modified soil moisture routine. The simulations in the test period were of approximately same prediction quality as the simulations in the calibration period, and provided good estimates of runoff generated by both snowmelt and rainfall. (KEY TERMS: runoff model; snowmelt; soil moisture; seasonal frost; frozen soil)

INTRODUCTION

High-latitude basins are characterized by winter precipitation storage in the form of snow on the ground and by seasonally frozen ground. The runoff regime is strongly influenced by these two factors. Application of a mathematical runoff model in these basins requires a model with separate accounting

routines for snowmelt and soil moisture. The snowmelt and the soil moisture routines are closely linked together, and successful modeling of snowmelt runoff strongly depends upon correct response from both routines and upon a correct interaction between the routines.

Physical characteristics--such as infiltration capacity and soil moisture storage capacity of most soils--change drastically when the soil undergoes freezing or thawing. Kane and Stein (1983) found for Fairbanks silt loam that the infiltration rate increased by a factor of 10-100 (depending on the soil ice-content) when going from frozen to unfrozen state. So far, this fact has not been seriously considered in the development of snowmelt runoff models.

The objectives of this study were:

1. determine how well a mathematical runoff model with its original snowmelt and soil moisture routines simulates runoff during snowmelt in a basin characterized by a seasonal snowpack and extensive seasonal frost; and
2. modify the soil moisture routine of this model to hopefully improve the runoff simulations.

¹Respectively, Research Engineer, Norwegian Hydrotechnical Laboratory, N-7034 Trondheim-NTH, Norway, and Associate Professor, Institute of Water Resources/ Engineering Experiment Station, University of Alaska-Fairbanks, Fairbanks, AK 99775-1760.

We selected Chena River Basin (Figure 1) as test basin for this study because of the availability of hydrologic and meteorological data. The basin is located near Fairbanks in interior Alaska and has a total area of 5,125 square km. It typically has a seasonal snowcover lasting for about six months of the year and extensive seasonal frost every winter. Wind-deposited silt loam is the dominant near-surface soil in the area. Many of the valley bottoms and north-facing slopes are underlain by permafrost. Much of the watershed is forested with tree line at about 600 m (msl). Poorly drained soils exist on most permafrost sites, and well-drained soils occur in permafrost-free areas. Moss and organic material cover all mineral soils at varying depths; depths are generally greater for permafrost sites.

We chose a distributed version of the HBV runoff model for our study (HBV-3). The model is used in many Scandinavian watersheds (Bergstrom, 1976), and it has also been applied to watersheds in Switzerland (Braun, 1985). We selected this model because it has a simple structure and requires relatively little data input. For most northern basins, availability of hydrological and meteorological data is a critical factor in model selection. The model's structure is graphically illustrated in Figure 2.

The soil moisture routine in the model has the following parameters:

- FC - maximum soil moisture storage (mm)
- LP - limit for potential evaporation (mm)
- BETA - empirical coefficient (no units)

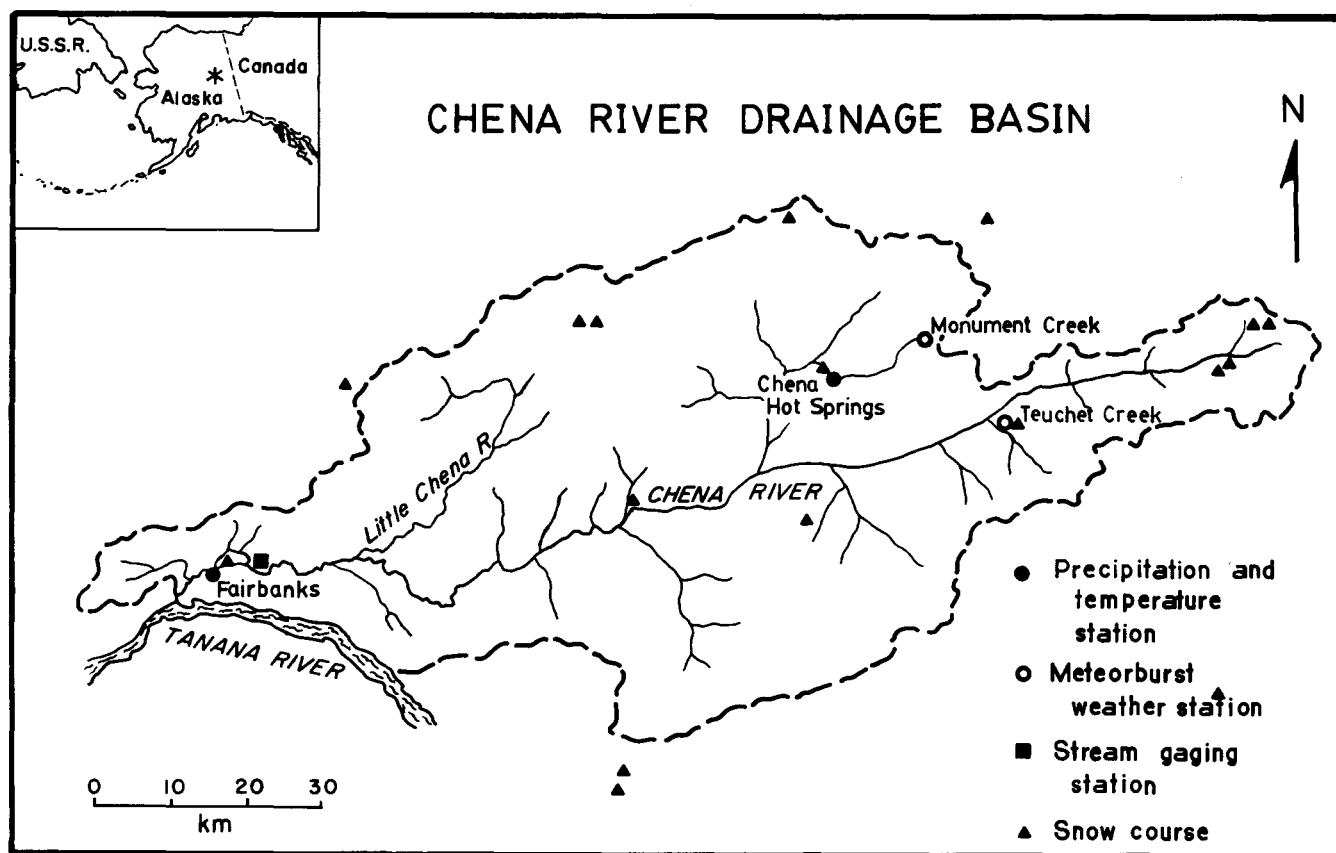


Figure 1. Chena River drainage basin showing data collection sites.

The outflow from the soil moisture zone is achieved by the following free parameters:

- K0, K1, K2 - storage discharge parameters (no units)
- UZL - limit for fast drainage, upper zone (mm)
- PERC - percolation capacity into lower zone (mm/day)

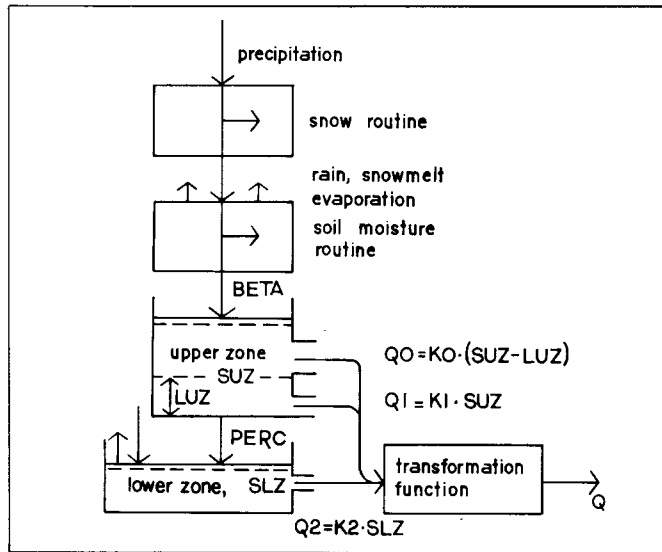


Figure 2. Schematic presentation of the HBV-3 model.

INPUT DATA

The HBV model requires daily values for precipitation and air temperature (daily mean), and monthly estimates of potential evaporation. An estimate of the initial conditions in the basin at the beginning of the simulation period is also necessary. These variables are:

- Snowpack depth (mm)
- Water content of snowpack (mm)
- Soil moisture storage (mm)
- Upper zone storage (mm)
- Lower zone storage (mm)
- Transformed discharge₃ (m³/s)
- Recorded discharge (m³/s)

We used precipitation and air temperature data from meteorological stations at Fairbanks Airport and Chena Hot Springs for 1969-1974 (NOAA, 1969-1974) and from

Fairbanks Airport, Monument Creek and Teuchet Creek for 1982-1985 (NOAA, 1982-1985; U.S. Army Corps of Engineers, 1985; and U.S. National Weather Service, 1985). Estimates of potential evaporation were made based on observations from University of Alaska, Agriculture Experiment Station (NOAA, 1969-1974). River discharge observations were obtained from gage No. 15493000 Chena River at Fairbanks (U.S. Geological Survey, Water Resources Division, 1969-1974 and 1982-1985). Snow cover depth and water content observations from snow courses within the basin were also used (Soil Conservation Service, 1969-1974 and 1982-1985).

CRITERIA FOR PERFORMANCE OF MODEL

The model uses a numerical criterion (Sutcliffe and Nash, 1970) to indicate model efficiency, or the agreement between the recorded and the simulated hydrograph.

$$R^2 = \frac{F_0^2 - F^2}{F_0^2} \quad (1)$$

where

- R^2 = efficiency of model
- F_0^2 = sum of squares of residuals between observed and computed discharges
- F^2 = sum of squares of residuals between observed discharge and mean of observed discharge during the simulation period.

The value of R^2 will range from minus infinity to +1, where +1 represents complete agreement between the observed and the simulated hydrograph. In addition to the numerical criterion, we gained valuable knowledge from inspection of the plotted hydrographs.

TABLE 1. Results from simulations (R^2 -values).

Year	Calibration	Test	R^2 -original model	R^2 -modified model
1969	X		0.14	0.80
1970	X		0.62	0.68
1971	X		0.48	0.89
1972	X		0.52	0.90
1973	X		0.04	0.83
1974	X		0.53	0.88
Average (6 years):			$R^2 = \frac{0.53}{0.39}$	$R^2 = \frac{0.88}{0.83}$
1982		X		0.80
1983		X		0.77
1984		X		0.74
1985		X		0.77
(Average (4 years):				$R^2 = \frac{0.77}{0.77}$

DISCUSSION

We calibrated the HBV model with available data from 1969-1974. Only the months April, May and June each year were simulated. To improve the simulations, we modified the model by introducing a seasonal variation in the parameters of the soil moisture routine (FC, LP, BETA and PERC). Finally, the modified version of the model was tested with data from 1982-1985.

The modified model improved the simulations in the calibration period substantially. The simulations in the test period were also satisfactory. The

results of the modelling effort are shown in Table 1. Soil moisture parameter values that produced these results are shown in Table 2.

When calibrating the original model, we got an underestimation every year of snowmelt runoff in the early part of the simulation period, and an overestimation of rainfall runoff in the late part of the period (see Figure 3). We assumed that this was because the soil moisture parameters are set as constants in the model, while they actually exhibit seasonal variation. In this case, it means that the model used too high an infiltration capacity when the ground was frozen, and too low an infiltration

TABLE 2. Values of the soil moisture parameters in the original and the modified model.

Parameter	Original model	Modified model	
		Frozen soil	Unfrozen soil
FC (mm)	265	190	320
LP (mm)	265	190	320
BETA (-)	3	8	2
PERC (m/day)		0.4	2.5

CHENA RIVER AT FAIRBANKS

April 1 - June 30 1972

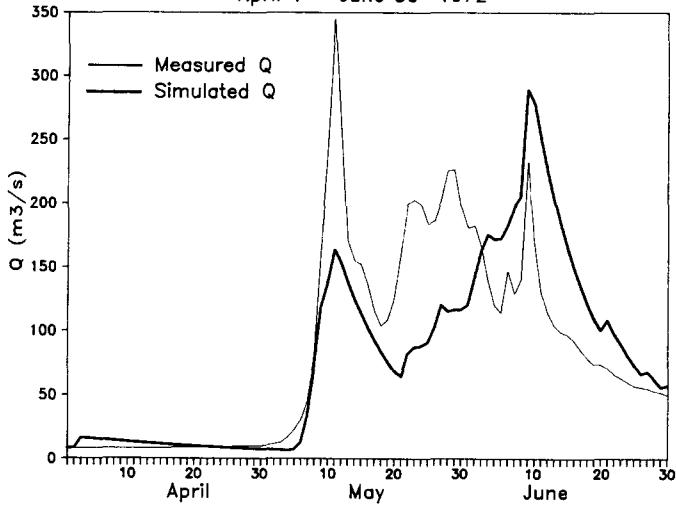


Figure 3. Runoff simulation 1972, original model.

capacity when the ground was thawed.

We recalibrated the soil moisture routine and then only examined simulation of snowmelt runoff occurring early in the period. We recalibrated the soil moisture routine again, and then simulated the rainfall runoff events in the latter part of the period (see Figure 4). This gave two sets of soil moisture parameters, one set for frozen soil conditions and one set for unfrozen soil conditions. Figure 5 shows the hydrograph simulation when the soil moisture parameter sets for frozen and unfrozen soil are combined; parameters for frozen soil are used in the first part of the modeling period, and parameters for unfrozen soil are used in the last part of the period. The point in time when the soil moisture parameters should be changed from the frozen to unfrozen case were, for all the years in the calibration period, determined from inspection of hydrographs only.

Our assumption is that we should change the soil moisture parameters when the seasonally frozen soil layer is partially thawed. We estimated this from:

1. the amount of snow on the ground and ice in the frozen soil at the beginning of the snowmelt season; and

CHENA RIVER AT FAIRBANKS

April 1 - June 30 1972

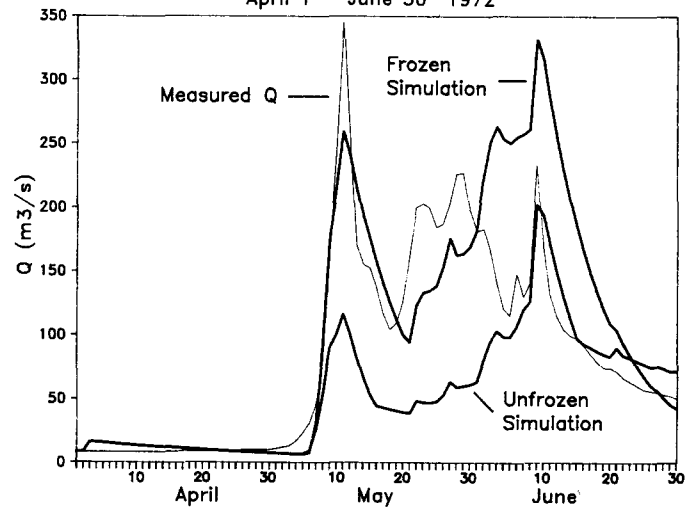


Figure 4. Runoff simulation 1972, with soil moisture parameters for both the frozen and unfrozen state.

2. the amount of incoming energy available for melting.

Lacking observations of ice content in the frozen soil, we estimated the total amount of snow and ice from the following parameters:

- P_s = precipitation previous September (mm)
- DD_f = accumulated degree-days of freezing during the previous winter ($^{\circ}\text{C}\cdot\text{days}$)
- S_d = water equivalent of the snowpack at the start of snowmelt (mm)

The amount of incoming energy available for melting can be expressed as degree-days of melting:

$$DD_m = \text{accumulated degree-days of melting from start of snowmelt } (^{\circ}\text{C}\cdot\text{days})$$

Using data from the calibration period (six years), we found the following regression equation for the required input of energy for melting.

$$DD_m = -88.2 + 0.125*S_d + 0.139*P_s + 0.053*DD_f + 1.319*DD_f/S_d \quad (2)$$

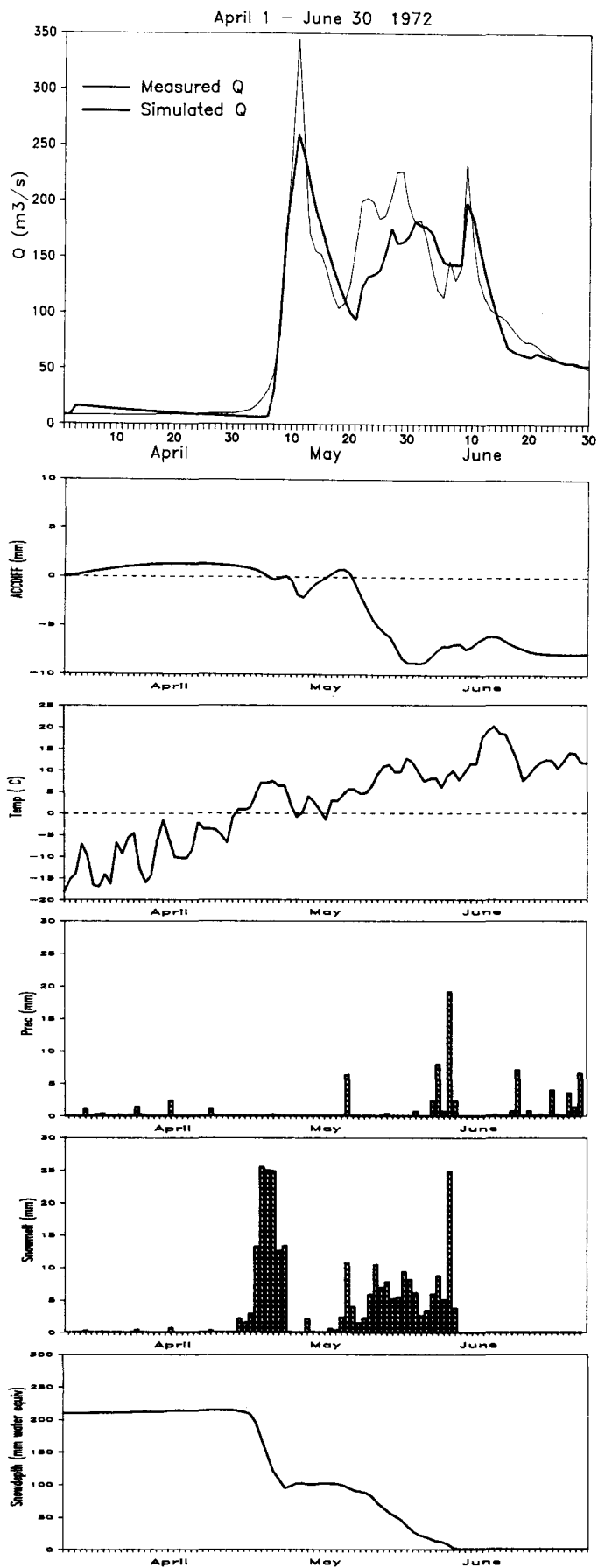


Figure 5. Modified runoff calibration, 1972.

which gave a correlation of $r^2 = 0.95$.

Using just six years of data from the calibration period is a minimal amount of data to confirm the validity of Equation (2). However, we used Equation (2) for predicting the time to change the soil moisture parameters in the test runs (1982-1985). Figure 6 shows the simulation of the hydrograph for one of the years (1984) the modified model was tested for the Chena River basin.

CONCLUSIONS

We demonstrate that improvements in model simulations of snowmelt and rainfall runoff can be made by introducing seasonal variation into selected soil moisture parameters in the HBV model. The main reason for this is that substantially different hydraulic properties exist between frozen and unfrozen soils and in our case extensive seasonal frost is also present. For our watershed, fine grained soils are predominant and, therefore, higher moisture levels occur than for coarser soils. Further improvements in the modifications to the model could be made by having a gradual transition between the frozen and unfrozen conditions instead of the abrupt change we used.

ACKNOWLEDGMENTS

Funds for this study were provided by U.S. Geological Survey. The Norwegian Hydrotechnical Laboratory and the Royal Norwegian Council for Industrial and Technical Research supported the time Mr. Knut Sand spent at University of Alaska-Fairbanks as a visiting research engineer. Dr. Sten Bergstrom, Swedish Meteorological and Hydrological provided us with a copy of the HBV-3 model and advice. U.S. Army Corps of Engineers and U.S. National Weather Service in Anchorage provided precipitation and air temperature data.

April 1 - June 30 1984

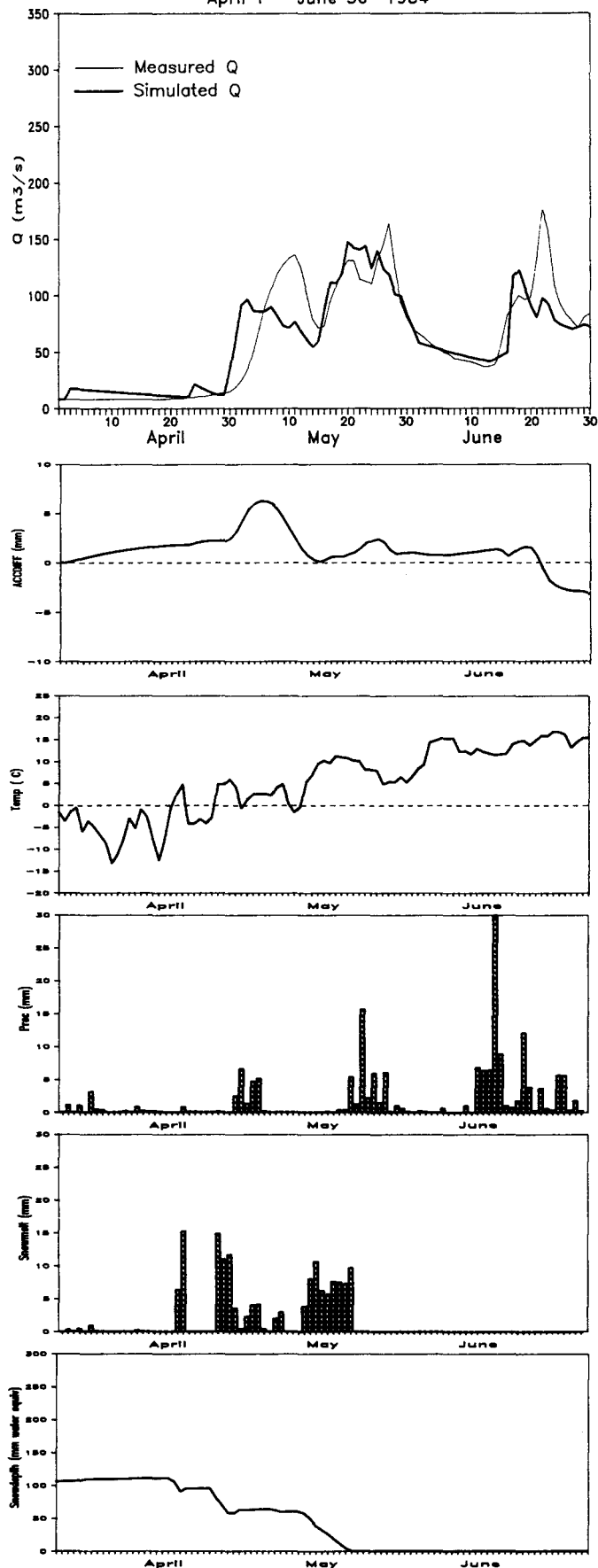


Figure 6. Test runoff simulation, 1984.

LITERATURE CITED

- Bergstrom, S., 1976. Development and Application of a Conceptual Runoff Model for Scandinavian Catchments. Swedish Meteorological and Hydrological Institute, Norrkoping, Sweden, Report No RH07.
- Braun, L.N., 1985. Simulation of Snowmelt-runoff in Lowland and Lower Alpine Regions of Switzerland. Geographisches Institut, Eidgenossische Technische Hochschule, Zurich, Switzerland, Heft 21.
- Kane, D.L., and J. Stein, 1983. Field Evidence of Groundwater Recharge in Interior Alaska. Proceedings, Permafrost: 4th International Conference. National Academy Press, Washington, DC.
- National Oceanic and Atmospheric Administration, U.S. Department of Commerce. Climatological Data, Alaska 1969-74. Vol. 55-60.
- National Oceanic and Atmospheric Administration, U.S. Department of Commerce. Local Climatological Data, Fairbanks, Alaska. International Airport, 1969-1974 and 1982-1985.
- Soil Conservation Service, U.S. Department of Agriculture. Snow surveys and water supply outlook for Alaska. 1969-1974 and 1982-1985.
- Sutcliffe, J.V., and J.E. Nash, 1970. River Flow Forecasting Through Conceptual Models. Part I - A Discussion of Principles. Journal of Hydrology, 10(1970), 282-290.
- U.S. Army Corps of Engineers. Precipitation and Air Temperature Data From Meteor-burst Stations in Chena River Basin. Unpublished data.
- U.S. Geological Survey, Water Resources Division. Water Resources Data, Alaska. Water years 1969-1974 and 1982-1985.
- U.S. National Weather Service. Precipitation and Air Temperature Data From Meteor-burst Stations in Chena River Basin. Unpublished data.

SOME ASPECTS OF GLACIER HYDROLOGY
IN THE UPPER SUSITNA AND MACLAREN RIVER BASINS, ALASKA

Theodore S. Clarke, Douglas Johnson and William D. Harrison¹

ABSTRACT: Proposed hydroelectric development on the Susitna River, Alaska, has raised interest in the glaciers that form its headwaters. Three separate aspects of the hydrology of these glaciers are addressed here. First, long-term glacier shrinkage, which releases water that is not renewable in the normal sense, appears to have produced on the order of 3-4% of the total Susitna River flow above the Gold Creek gauge site since stream gauging began. Second, the major glaciers of the basin are surge-type and have the potential to produce, in a few months, up to 30 times the estimated annual sediment input into the proposed Watana Reservoir. The next surge of one of the glaciers, Susitna, is predicted in the first decade of the next century. Third, winter precipitation varies by a factor of two among the glaciers, Maclaren Glacier receiving the most. (KEY TERMS: Glacier shrinkage, glacier surges, sediment supply, precipitation variations.)

INTRODUCTION

This paper describes, in part, the results of a study of the glaciers that head the Susitna and Maclaren rivers (Figures 1 and 2). It addresses three separate topics: (1) whether the glaciers have changed in volume since stream gauging began on the Susitna River, (2) if and when any of the glaciers in the area may be expected to surge, and how surges might affect the Susitna River, and (3) how precipitation varies throughout the area. A previous paper provides glacier runoff and mass balances estimates (Clarke and others, 1985). Early phases of the work are described by R & M and Harrison (1981) and R & M and Harrison (1982) and summarized by Harrison and others (1983). The material presented here should be considered an update to these three early papers.

Glaciers cover about 790 square kilometers or 5.9% of the basin area above the proposed Watana dam site, 5.2% of the area above the proposed Devil Canyon site, and 4.9% of the area above the Susitna River gauge located at Gold Creek (Figure 1). Field

measurements of precipitation, snow accumulation, ice melt, glacier speed, and surface elevation were made on most of the major glaciers in the basin during 1981, 1982 and 1983.

1. LONG-TERM GLACIER VOLUME CHANGE

Long-term glacier volume change is an important part of any hydrologic feasibility or planning study because it may have a significant impact on projected water supply. In general, glaciers have decreased in size during the last half century. Consequently, water to their basins has been supplied out of ice storage. As the glaciers approach equilibrium with the present climate, the amount of water from storage approaches zero. This has led, in some instances, to an overestimation of water supply (Bezinge, 1979). It seems that before long-term water availability is predicted from stream gauge records, smoothed trends of glacier release or storage of water over the period of record should always be subtracted. This reduces the problem to a conventional one of long-term prediction for an unglacierized basin, although, of course, even the conventional approach is susceptible to errors caused by climate change. Mayo and Trabant (1986) present evidence that a definable climate change took place in the Alaska Range in the Gulkana Glacier region, starting about 1976.

Volume change estimates for the Susitna basin are based on measurements on an unnamed glacier, commonly referred to as East Fork Glacier (Figure 2), which makes up only 5% of the total glacierized surface. Previous estimates of its volume change over the period 1949 to 1980 were made from photogrammetric data (R & M and Harrison, 1981; Harrison and others, 1983). These estimates suggested an average change in thickness of -50 ± 18 m. If this were typical of the other glaciers, then 13% of the Susitna River flow at the Gold Creek gauge site would have been from glacier storage. Since this seems unreasonably large, two other methods for estimation of volume change were

¹Theodore S. Clarke, Douglas Johnson and William D. Harrison, Geophysical Institute, University of Alaska-Fairbanks, Fairbanks, Alaska 99775-0800.

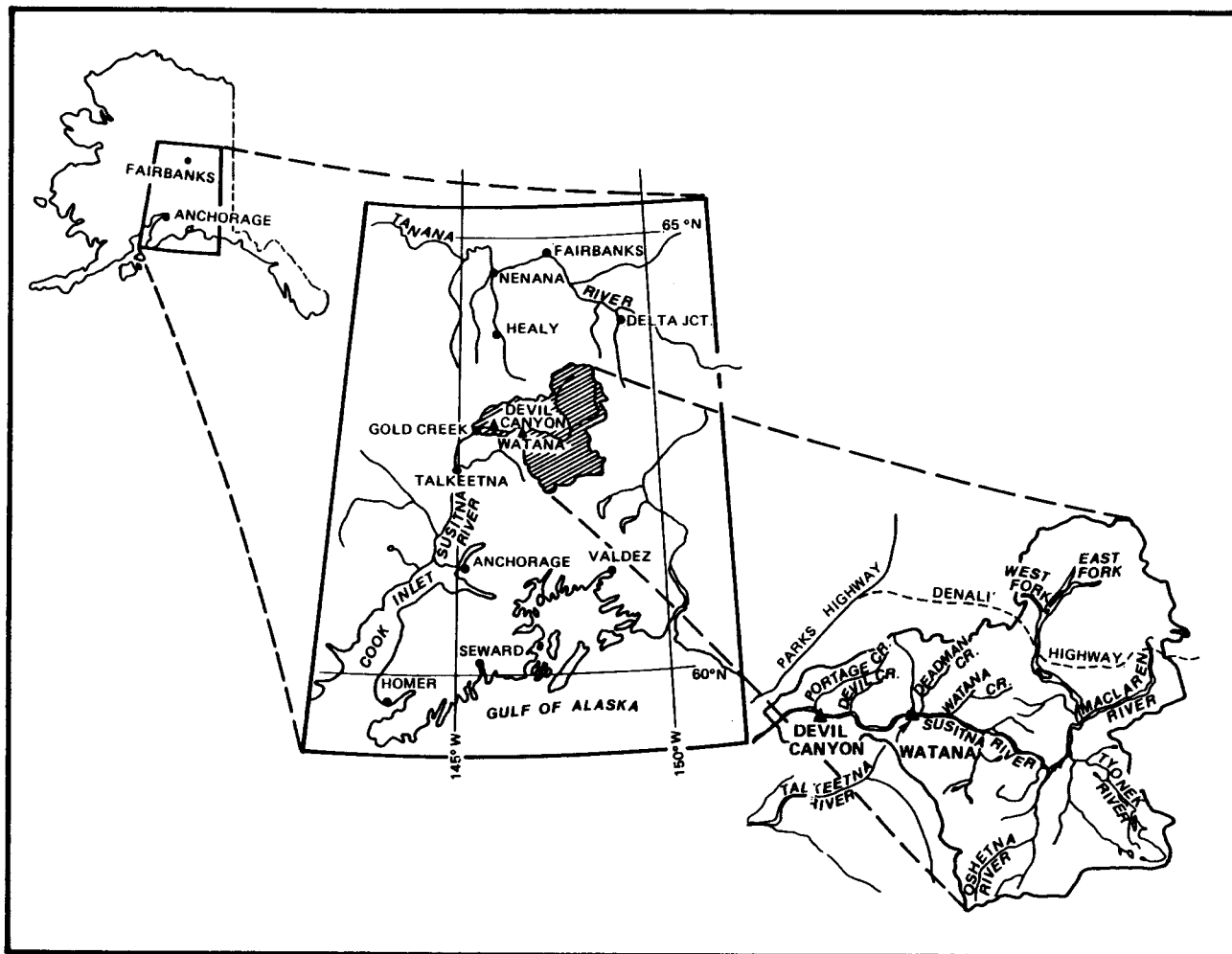


Figure 1. Location map. (From Acres American, 1982.)

applied. The first used direct measurement of glacier surface altitude; the second used the runoff precipitation model of Tangborn (1980).

Direct Measurement of Glacier Surface Elevation

In 1982 surface elevations were measured at several points on East Fork Glacier as a check of those estimated photogrammetrically from 1980 photos in the earlier work. Elevations were measured with a helicopter and its altimeter. Measurement points were located either by Brunton compass bearings to map identifiable features or by theodolite and established control points. The altimeter was calibrated periodically on rock points of known elevation. The results are shown in Table 1.

The results agree with those from the 1980 photos except at the highest point. According to the altimeter data, this point has remained at roughly the same elevation since 1949 when the U.S. Geological Survey maps were made, but the data provided by the photogrammetric method show this point to have lost 40 m of elevation. This discrepancy might be explained by the fact that the 1980

aerial photographs of East Fork Glacier show almost no contrast in its accumulation area. This makes it difficult to identify the surface accurately in these smooth snowy areas. Also, one might expect the accumulation area of a "normal" (non surge-type) glacier in retreat to remain at roughly the same elevation because a decrease in annual balance over the surface of a glacier affects the volume of ice transported by the glacier in a way that accumulates down-glacier.

The change in volume of the glacier was obtained by comparing the altimetry data with elevations obtained from 1949 photos. Unlike the 1980 photos, the 1949 photos are of very good quality. The elevations obtained from these early photos agree with published map elevations and are therefore probably accurate. In practice, the volume change was computed by determining a thickness change versus elevation relationship, multiplying it by the area per elevation interval determined from the map, and finally, by integrating over the elevation interval spanned by the glacier.

Taking the altimetry data as the more reliable, the average thickness change of East Fork Glacier comes out to -13 m water equivalent for the 1949 to

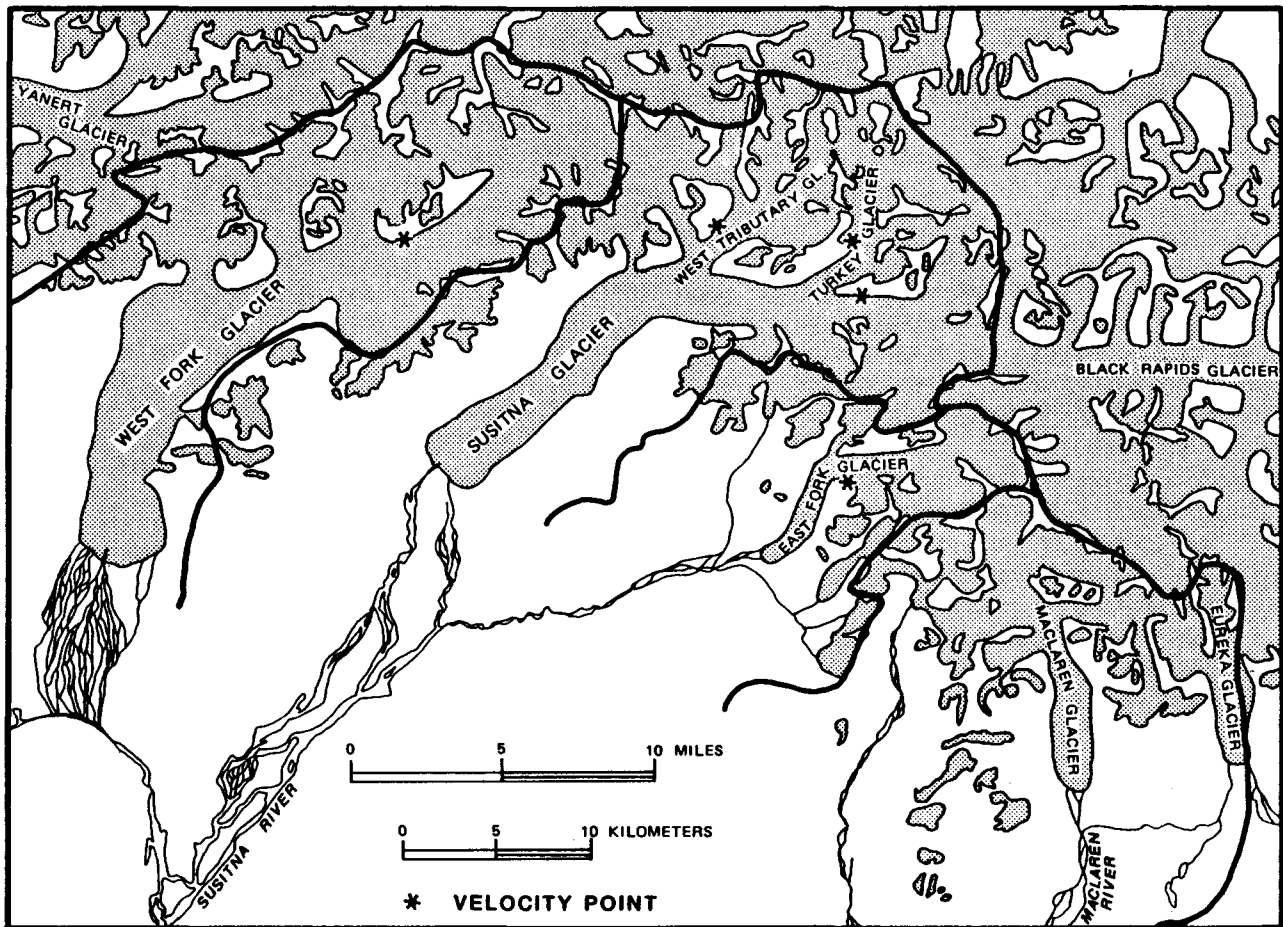


Figure 2. Glacier names, locations and drainage divides. Glacier center line velocity was measured where indicated. The points on the figure were placed next to the glaciers for clarity. (Modified from Harrison and others, 1983.)

1982 period, rather than the -50 m for the 1949 to 1980 period estimated by the previous work. If this 13 m of water equivalent loss is again extrapolated over the remaining 95% of the ice in the basin (with suitable caution) then, on the average, about 3 or 4% of the Susitna River flow at Gold Creek has been due to glacier recession as opposed to the 13% of the earlier estimates. This estimate has very large errors associated with it since it is based on four points on a glacier that makes up only 5% of the ice in the basin. However, it does seem more reasonable considering that the glacier runoff over the 1981 to 1983 period, when the glaciers were in approximate equilibrium, totaled only about 13% of the flow at the Gold Creek gauge site (Clarke and others, 1985).

Tangborn Runoff-Precipitation Model

Tangborn (1980) has suggested a model for determining long-term historical glacier balances by comparison of adjacent glacierized and unglacierized basins. The model works by determining differences in runoff that do not correspond to precipitation changes, and these differences are assumed to be

caused by changes in storage of water as glacier ice. The annual precipitation in each basin is determined by using a representative precipitation station and determining a coefficient that corrects for precipitation differences between the basins and the precipitation station. The sum of evaporation, transpiration and condensation, per unit area, is assumed to be the same for both basins. The coefficient can be determined if runoff from both basins and glacier volume change are known for a period of at least 1 year and if a suitable precipitation station exists.

The model was tested against published mass balances of nearby Gulkana Glacier for the period from 1967 to 1977 (Meier and others, 1980). Six different precipitation stations and three different unglacierized basins were checked for the best possible fit of the model. Phelan Creek was used as the glacierized runoff station since this drains Gulkana Glacier. The best correlation between calculated and measured balance occurred when Taiketna precipitation station was used with the unglacierized basin Ship Creek near Anchorage ($r^2 = 0.77$). Further details are given by Clarke (1986).

Table 1. Comparison of photogrammetric data (R & M and Harrison, 1981; Harrison and others, 1983) to helicopter altimetry data on East Fork Glacier. The surface elevation changes for the altimetry data are for the period from 1949 to 1982; the surface elevation changes for the photogrammetric data are for the period from 1949 to 1980. A loss of elevation is indicated by a negative sign.

<u>East Fork Glacier</u>		
Location on Glacier Center Line (1949 Map Elevation) (m)	Elevation Change Altimeter (m) (1949 to 1982)	Elevation Change Photogrammetry (m) (1949 to 1980)
1080	-74 ± 18	-67 ± 18
1390	-43 ± 18	-32 ± 18
1590	-51 ± 18	-78 ± 18
2050	+16 ± 18	-40 ± 18

In applying the model to the Susitna basin, there was a considerable uncertainty in what the actual balance was for the period from 1981 to 1983. The measurements, for all ice in the basin, came out to +0.06 m water equivalent when summed over the 3-year period, but the cumulative uncertainty for the 3-year period was 0.6 m (Clarke, 1986). In Tangborn's model this uncertainty plays a large role in the resulting change in glacier mass for the period from 1950 to 1983. These dates were chosen because 1950 is the first year from which complete runoff data are available for the Susitna River at Gold Creek. If it is assumed that balance for the period from 1981 to 1983 was +0.06 m, then the average loss from the glaciers above the Susitna River at Gold Creek gauge site for the period from 1950 to 1983 was -16 m water equivalent. If the balance was +0.66 m, then the average loss comes out to -9 m, and if the balance was -0.54 m, then a calculated balance of -22 m water equivalent results.

The results of the two methods of volume loss estimation are summarized in Table 2. They are uncertain, but not inconsistent. They imply that 3 to 4% of the water flow at Gold Creek between 1949 and 1980 came from ice storage. This amount is

within the stream gauging error and would therefore probably not be significant in terms of projected water supply.

II. GLACIER SURGES

The major glaciers of the Susitna basin are West Fork, Susitna, "East Fork", Maclaren, and Eureka (Figure 2). All except East Fork are listed by Post (1969) as being surge-type. Surges are sudden episodes of rapid glacier speed triggered by some internal instability, during which ice movement may be hundreds or thousands of meters within a few months. The effects on sediment and water supply, particularly the former, may be substantial.

There are some descriptive reports of high sediment production during glacier surges (Uskov and Kvachev, 1979; Shcheglova and Chizhov, 1981) and two direct measurements. Humphrey (1986) reported that the 1982-1983 surge of Varlegated Glacier, Alaska, released as suspended sediment the equivalent of about 0.3 m of eroded rock from the bed of that glacier. Björnsson (1979) reported an erosion rate of 0.014 m/yr from the surge of Bruarjökull Glacier

Table 2. Summary of glacier shrinkage estimates by two different methods.

<u>Method</u>	<u>Time Span</u>	<u>Area Covered</u>	<u>% Total Glacierized Area</u>	<u>Thickness Loss</u>	<u>Error</u>
Altimetry	1949- 1982	East Fork Glacier	5	13 (m)	large, see text
Runoff Precipitation Model	1950- 1983	all glaciers in basin	100	16	+6, -7 if model applicable

in Iceland. The two measurements differ by more than an order of magnitude, but both are extremely high when compared to sediment production in non-surge years. Although Variegated Glacier is considerably smaller than Susitna Glacier, both are narrow valley glaciers underlain by faults. If Variegated Glacier is representative of the Susitna basin, then a surge of the 250 km² Susitna Glacier could release as much as 200 x 10⁹ kg of suspended sediment into the Susitna River, assuming a rock density of 2.7 x 10³ kg/m³. This is 30 times the estimated annual sediment influx, including bed load, of 6.8 x 10⁹ kg (5.8 x 10⁶ m³) into the proposed Watana Reservoir (R & M, 1982).

There is little direct evidence about the effect of surges on water supply. However, there are three potential effects. First, there should be a temporary increase in melt water because of the increase in ablation area that accompanies some surges. Second, the extreme crevassing that occurs during a surge temporarily increases effective surface area, and therefore ablation. Third, surges release stored water (Kamb and others, 1985), although it is not clear whether this water comes from long-term storage or merely from the most recent summer season.

Given these effects of surges on sediment and water supply, it seems worthwhile to review the past history of surges in the Susitna basin, and what it may imply for the future, particularly since surges tend to be periodic (Meier and Post, 1969). West Fork Glacier is known to have surged sometime shortly before 1940 when Bradford Washburn photographed it. Susitna Glacier underwent a strong

surge between 1949 and 1954 (Post, 1960); photos that we recently examined indicate that the surge was complete by July, 1952. Maclaren Glacier underwent a weak surge or strong "pulse" in 1971 (Mayo, 1978).

Surface speed measurements on West Fork, Susitna, and East Fork glaciers indicate flow regimes that reflect the surge behavior of the first two. For both of these glaciers the rate of ice flow from the accumulation area is considerably less than the rate of snow accumulation there (Table 3). This indicates a thickening of the accumulation area that will probably be terminated by another surge. The velocity data and details of how accumulation and outflow were calculated are given by Clarke (1986).

West Fork Glacier

The disequilibrium of West Fork Glacier evident in Table 3 is consistent with its past behavior. Oblique aerial photographs of the terminus, taken by Bradford Washburn in 1940, show it to be extremely broken up and chaotic (see Clarke, 1986). This information, along with the looped moraine pattern, is conclusive evidence that a surge took place. Post (written comm. to Steven Wilbur, 1984) places the surge in 1937. Close inspection of 1981 NASA color infrared aerial photographs shows at least three successive terminal moraines, each of which was very likely caused by a successively weaker surge. Unfortunately, the periodicity of the surges cannot be estimated quantitatively because little

Table 3. Comparison of annual ice flow through several cross sections to the annual accumulation above the sections. The location of each cross section is shown as a velocity point on Figure 2. Surface center line velocity is assumed to be caused by 50% internal deformation and 50% basal sliding. All quantities are given in water equivalents. The cross sections are slightly below the accumulation areas and are shown as velocity points on Figure 2.

Glacier Name	Average Annual Ice Flow May 1981- June 1983 (m ³ /yr x 10 ⁶)	Annual Accumulation Above the Cross Section (m ³ /yr x 10 ⁶)			Volume Change Above Cross Section (1981-1983 average) (m ³ /yr x 10 ⁶)
		1981	1982	1983	
West Fork	54 ± 21	98 ± 33	82 ± 33	113 ± 33	+44 ± 39
Susitna, Main Branch	14 ± 6	50 ± 19	34 ± 19	71 ± 19	+38 ± 20
Susitna NW Trib.	36 ± 14	21 ± 15	- -	- -	- -
Susitna Turkey Trib.	72 ± 28	89 ± 15	70 ± 15	- -	- -
East Fork	31 ± 12	- -	20 ± 13	25 ± 13	- -

Information exists for West Fork Glacier prior to the Washburn photographs. Moffit (1915) gives a brief description of the glacier as it was in 1913 but nothing to indicate a surge had occurred recently. If its recurrence period is similar to the 50 or so years for Susitna Glacier, discussed below, a surge may be expected fairly soon.

Susitna Glacier

Susitna Glacier, unlike West Fork, has a complex set of tributaries that were studied individually, as summarized in Table 3. It can be seen that the main branch of Susitna Glacier is transporting only a fraction of the accumulated snow down-glacier. This would indicate that either this branch of the glacier is the one causing the surges, or it is at least a reservoir that depletes during a surge. Altimetry data collected in the accumulation area of Susitna Glacier also show this branch to be accumulating mass. A gain of 56 ± 18 m of elevation from 1956 to 1982 was measured by comparing 1982 altimetry data to 1956 map elevation data (Clarke, 1986). This translates to a gain of $93 \pm 30 \times 10^6$ m³/yr, which is reasonably consistent with the average rate of gain of $38 \pm 20 \times 10^6$ m³/yr for the 1981 to 1983 period (Table 3). Examination of moraine patterns confirms that this basin did indeed contribute a large quantity of ice to the last surge. Figure 3 depicts the moraine patterns on Susitna Glacier before and after the early 1950's surge. Before the surge, ice motion in the main trunk above Turkey tributary appeared to be very small, with relatively vigorous flow from Turkey pinching it off. After the surge, a large volume of ice had clearly advanced from the basin of the main branch. A large volume of ice appears to have come from Turkey tributary also, and Northwest tributary appears to have contributed very little ice, if any, to the surge. These observations indicate that flow and accumulation in Northwest tributary were probably in equilibrium before the surge, the main branch was far out of equilibrium, and Turkey tributary was somewhere in between.

There are two reasonably quantitative approaches to determining Susitna Glacier's surge period. First, the lobe created in the moraines of the main glacier by Northwest tributary had an area of about 4.0 km² in 1949. A surge of the main glacier took place about 1951, as already noted. By 1980 the new lobe had grown to an area of about 2.0 km² (Figure 3). Assuming the surge occurred in 1951, and assuming the present glacier speeds to be similar to those in the past, a period of roughly 60 years is indicated. Second, close inspection of the same lobe in 1949 aerial photographs shows about 47 ogives to have passed from Northwest tributary into the main glacier trunk (see Clarke, 1986). Ogives, or Forbes bands, are known to form on an annual basis (Nye, 1958). Again assuming the surge occurred in 1951, a surge return period of 49 years is indicated. It could be argued that Northwest tributary surges independently, but the slow growth

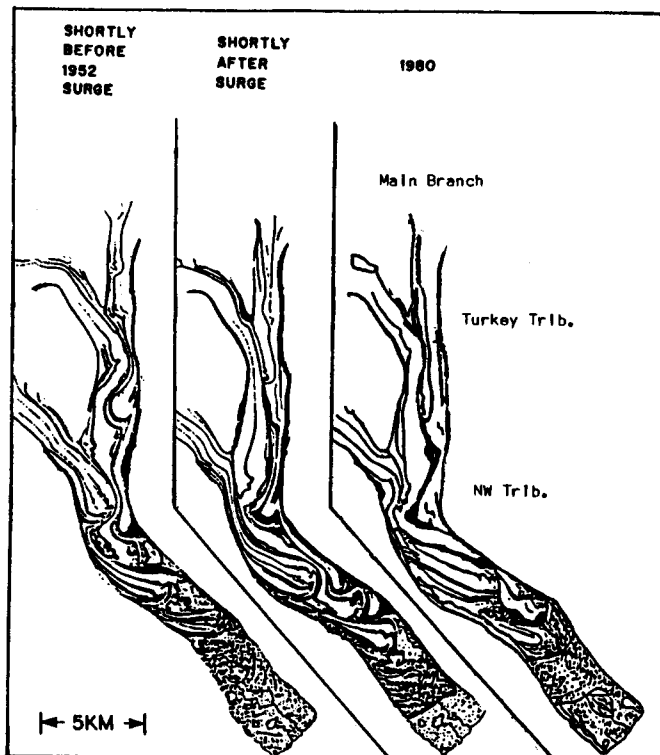


Figure 3. Evolution of moraine patterns on Susitna Glacier. Left and center diagrams are from Meier and Post (1969). Right diagram is sketched from National Aeronautics and Space Administration photographs. (Modified from Harrison and others, 1983.)

of its new lobe and the balance between accumulation and flow makes this seem unlikely (Table 3). The next surge would therefore be expected within the first decade of the next century.

East Fork, Maclaren and Eureka Glaciers

East Fork Glacier is probably not a surge-type glacier, as suggested by the approximate balance in Table 3, and by evidence from the displacement of surface features that the speed has not changed much since 1949 (R & M and Harrison, 1982).

Both Maclaren and Eureka glaciers are thought to be weak surge-type glaciers; they do not surge on the order of kilometers like Susitna and West Fork. As noted previously, Maclaren Glacier underwent a "pulse" in 1971 (Mayo, 1978). No speed measurements were made on these glaciers.

III. PRECIPITATION VARIATIONS

Another interesting aspect of glacier hydrology in this basin is the large difference in winter precipitation among the different glaciers. In the late winter of 1981, 1982 and 1983, snowpack thick-

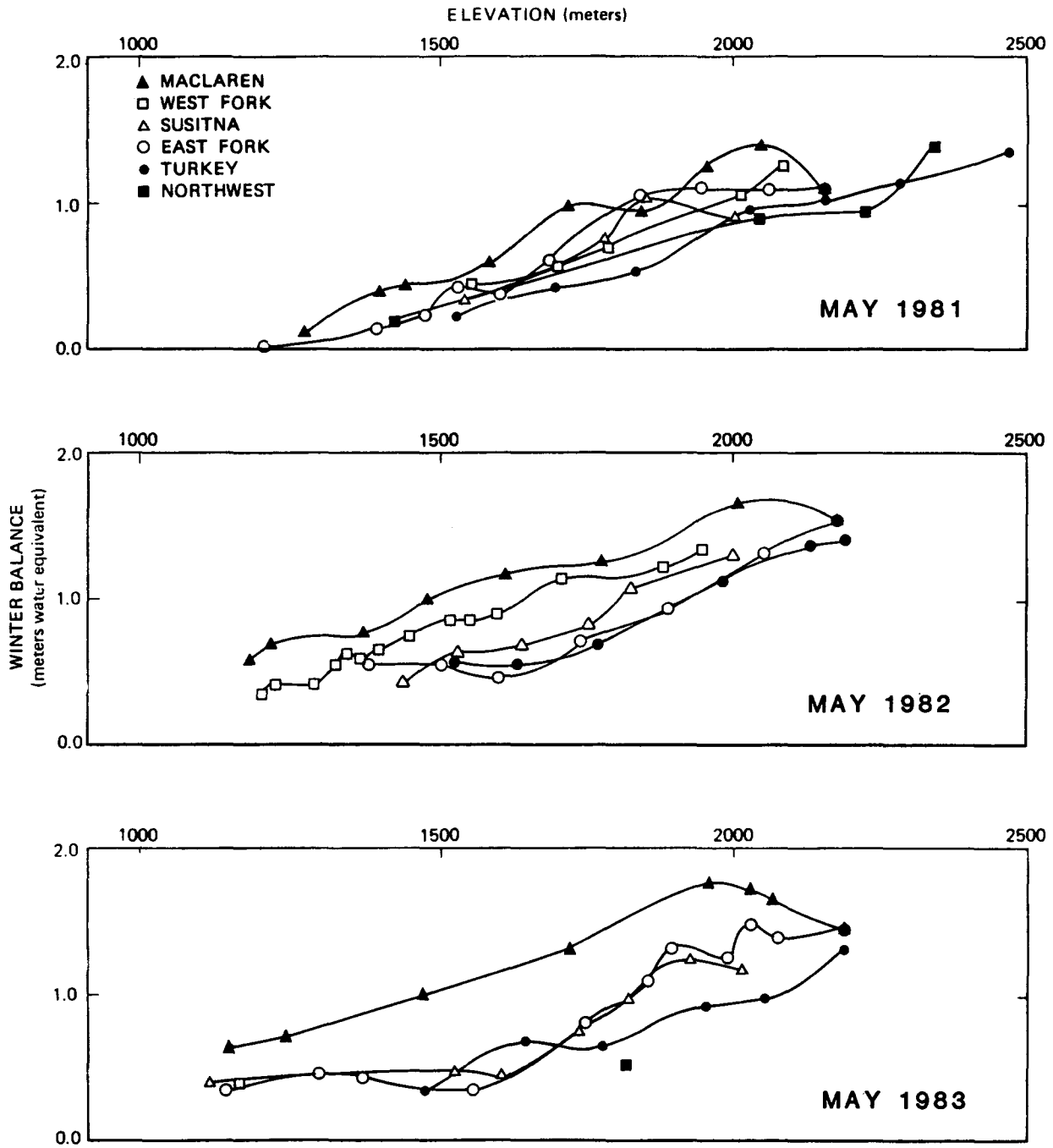


Figure 4. Winter accumulation versus elevation as determined from snow probe data. (Top figure is modified from R & M and Harrison, 1981; middle figure is from R & M and Harrison, 1982.)

ness was measured by probing at several points along the center line of each glacier, and snowpack density was measured at representative points on each glacier. The water equivalent thickness at each point is plotted in Figure 4. These data are reasonably consistent with more accurate snow depths measured at a few sites where stakes were maintained.

Generally the winter precipitation gradients are the same from glacier to glacier, about 1.2 mm water equivalent per meter of elevation, but the absolute amount of water varies considerably from glacier to glacier. Maclaren Glacier consistently received the most precipitation, and the two steep south-facing tributaries of Susitna Glacier consistently received the least. An orographic effect created by the Clearwater Mountains, which divide the tributary Maclaren River basin from the Susitna River basin, may direct moisture toward Maclaren Glacier and reduce precipitation in the Susitna basin to the west. It is worthwhile to note that because Maclaren Glacier had a positive mass balance of nearly 0.3 m/yr and the others had generally negative balances, it produced less runoff over the study period even though it received considerably more precipitation (Clarke and others, 1985).

IV. DISCUSSION AND CONCLUSIONS

An attempt has been made here to (1) determine whether the glaciers that head the Susitna and Maclaren rivers have changed in volume since stream gauging began on the Susitna River, (2) determine when these surge-type glaciers may surge again, and what the effects of surges are likely to be, and (3) describe variation in winter precipitation throughout the area. The conclusions are as follows:

1. The elevation change due to glacier wasting seems to be on the order of -10 to -15 m water equivalent for the 1949 to 1983 period for East Fork Glacier rather than the -50 m estimated by R & M and Harrison (1981) and Harrison and others (1983) for the 1949 to 1980 period. This amounts to 3 or 4% of the total flow of the Susitna River at Gold Creek rather than 13%. This quantity seems more consistent with the fact that during 1981, 1982, and 1983, when the glaciers were in approximate equilibrium, the average runoff from the Susitna basin glaciers was about 13% of the total Susitna River flow at Gold Creek (Clarke and others, 1985).
2. West Fork and Susitna are surge-type glaciers. If sediment output during a surge of Susitna Glacier, for example, is similar to that of Varlegated Glacier, a single surge may produce about 30 times the estimated average annual sediment influx into the proposed Wetana reservoir. The rates of transport and dispersion of such a large sediment influx are unknown. A surge of Susitna seems likely

because about two-thirds of the snow accumulating in the basin of its main branch is not being transported out (Table 3), and the accumulation area of this same branch has gained approximately 56 m of elevation since the last surge. If past history is any indication, it appears that Susitna Glacier has a surge period of 50 to 60 years, which places the next surge sometime between the years 2000 and 2010. It is also likely that West Fork Glacier will surge in the future, but no quantitatively determined period can be placed on it since no data are available for the period prior to its 1937(?) surge.

3. Accumulation varies considerably from glacier to glacier, with Maclaren Glacier receiving more winter precipitation than any of the other glaciers. Generally, the winter precipitation gradients are the same throughout the basins, about 1.2 ± 0.1 mm water equivalent/m elevation, but each glacier's accumulation versus elevation curve is shifted vertically with respect to the accumulation axis. The shift ranges over about 0.5 m water equivalent (Figure 4).

REFERENCES

- Acres American Inc., 1982. Susitna hydroelectric project; feasibility report. Final draft report for the Alaska Power Authority, Anchorage, Alaska. 8 vols.
- Bezing, A., 1979. Grande Dixence et son hydrologie, la collection de données hydrologiques de base en Suisse, Association Suisse l'aménagement des eaux. Service Hydrologique National, 19 pp.
- Bjornsson, H., 1979. Nine glaciers in Iceland. *Jökull* 29:74-80.
- Clarke, T. S., 1986. Glacier runoff, balance and dynamics in the upper Susitna River basin, Alaska. M.S. Thesis. University of Alaska, Fairbanks, 98 pp.
- Clarke, T. S., D. Johnson and W. D. Harrison, 1985. Glacier runoff in the upper Susitna and Maclaren River basins, Alaska. In: L. P. Dwight, 1985. Resolving Alaska's Water Resources Conflicts. Proceedings. Alaska Section, American Water Resources Association. Institute of Water Resources/ Engineering Experiment Station, University of Alaska, Fairbanks. Report IWR 108. 212 pp.
- Harrison, W. D., B. T. Drage, S. Bredthauer, D. Johnson, C. Schoch and A. B. Follett, 1983. Reconnaissance of the glaciers of the Susitna basin in connection with proposed hydroelectric development. *Annals of Glaciology* 4:99-104.
- Humphrey, N. F., 1985. Suspended sediment discharge from Varlegated Glacier during its surge and pre-surge phases of motion. A contribution to the workshop on Alaska hydrology, 10-13 April, 1985. In preparation.

- Kamb, B., C. F. Raymond, W. D. Harrison, H. Engelhardt, K. A. Echelmeyer, N. Humphrey, M. M. Brugman and T. Pfeffer, 1985. Glacier surge mechanism: 1982-1983 surge of Variegated Glacier, Alaska. *Science* 227(4686):469-479.
- Mayo, L. R., 1978. Identification of unstable glaciers intermediate between normal and surging glaciers. Academy of Science, USSR, Section of Glaciology, Proceedings of the International Workshop on Mechanism of Glacier Variations, Pub. 33, p. 47-55 and 133-135.
- Mayo, L. R. and D. C. Trabant, 1986. Recent growth of Gulkana Glacier, Alaska Range, and its relation to glacier-fed river runoff. Short paper for U.S. Geological Survey Water Supply Series. In press.
- Meyer, M. F. and A. S. Post, 1969. What are glacier surges? *Canadian Journal of Earth Science* 6:807-817.
- Meyer, M. F., L. R. Mayo, D. C. Trabant and R. M. Krimmel, 1980. Comparison of mass balance and runoff at four glaciers in the United States, 1966 to 1977. Academy of Science, USSR, Section of Glaciology, Report of the International Symposium on the Computation and Prediction of Runoff from Glaciers and Glacial Areas, Pub. 38, p. 138-143 and 214-216.
- Moffit, F. H., 1915. The Broad Pass Region, Alaska. U.S. Geological Survey Bull. 608. 80 pp.
- Nye, J. F., 1958. A theory of wave formation on glaciers. *IASH* 47:139-154.
- Post, A. S., 1960. The exceptional advances of the Muldrow, Black Rapids and Susitna glaciers. *Journal of Geophysical Research* 65:3703-3712.
- Post, A. S., 1969. Distribution of surging glaciers in western North America. *Journal of Glaciology* 8(53):229-240.
- R & M Consultants, 1982. Alaska Power Authority, Susitna Hydroelectric Project; Appendix B.8, Reservoir Sedimentation. Report for Acres American, Inc., Buffalo, NY, 49 pp.
- R & M Consultants and W. D. Harrison, 1981. Alaska Power Authority Susitna Hydroelectric Project; task 3 - hydrology; glacier studies. Report for Acres American, Inc., Buffalo, NY, 30 pp.
- R & M Consultants and W. D. Harrison, 1982. Alaska Power Authority Susitna Hydroelectric Project; task 3 - hydrology; glacier studies. Report for Acres American, Inc., Buffalo, NY, 22 pp.
- Shcheglova, O. P. and O. P. Chizhov, 1981. Sediment transport from the glacier zone, central Asia. *Annals of Glaciology* 2:103-108.
- Tangborn, W. V., 1980. Two models for estimating climate-glacier relationships in the North Cascades, Washington, USA, *Journal of Glaciology* 25(91):3-21.
- Uskov, Ju. S. and V. I. Kvachev, 1979. The didal surging glacier. Data of Glaciological Studies, Chronicle, Discussion. Academy of Sciences of the USSR, Section of Glaciology of the Soviet Geophysical Committee and Institute of Geography, Pub. 36, p. 170-175.

REGIONAL DISTRIBUTION OF STREAM ICINGS IN ALASKA

K. G. Dean

ABSTRACT. Stream-icing zones in mainland Alaska were mapped based on analysis of multi-date Landsat imagery. Mapped features include late winter overflow, residual ice-sheets and braided streams possibly susceptible to icings. Results of the 1:250,000 scale mapping were generalized and the regional distribution of icings displayed.

Almost all icings occur in or near upland or mountainous terrains. The Brooks Range and northeastern Alaska have the largest and greatest number of occurrences. The number and size of icings generally decrease to the south except in the vicinity of the Alaska Range. In northern Alaska many icings develop east of the Colville River but few to the west. This difference appears to be related to the availability of freshwater. In interior Alaska occurrences are numerous but small and are restricted to tributary stream channels. (Key Terms: Stream-icings, aufeis, naleds, Landsat, Alaska)

INTRODUCTION

Stream icings, also referred to as aufeis or naleds, are seasonal flood phenomena that develop in high latitude and alpine regions. Icings form when the hydrostatic pressure of water in aquifers or streams is sufficiently large to force water through its ice cover. These hydrostatic pressures largely result from restriction of water flow and the hydraulic gradient in stream channels and aquifers (generalized from Carey, 1973, and Harden et al., 1977). Factors of climate, hydrology, geology, permafrost, and topography influence icing occurrence and behavior (Carey, 1973).

Icings occur during subfreezing temperatures and result in the flooding of stream channels and adjacent low-lying areas. The flooding can extend many kilometers beyond the source of the extruded groundwater. The flood waters do not generally drain but freeze in place. This process repeats itself many times during a winter, often causing the accumulation of extremely thick sheets of ice; for example, 5 m along the Echooka River (Sloan et al., 1976).

Icings are a detrimental phenomena. They constitute hazards that can disrupt transportation and communication, hinder field exploration programs, and present difficult engineering problems for drilling operations, pipelines, roadways, buildings and other structures in arctic and subarctic regions. Icings may also indicate the presence of groundwater seeps or springs and perennially flowing water, which are potentially valuable resources. The intent of the

study reported here was to map the location and extent of icings in Alaska and to discuss their distribution.

PREVIOUS INVESTIGATIONS

Many investigators have mapped or studied icing conditions in Alaska. Existing knowledge concerning occurrence, control and prevention of icings was summarized by Carey (1973). Large icings in Alaska and Canada have been mapped and studied by Dean (1984 a&b); Harden et al. (1977); Childers et al. (1975); Van Everdingen (1975); Leffingwell (1919); and Hall (1976; 1980). Icings along the trans-Alaska pipeline route were mapped by Sloan et al. (1976). Local icings have been studied by Slaughter (1982); Carlson (1979); Kane et al. (1973); Kane and Carlson (1977); and Corbin (1977); Stringer et al. (1985).

METHODS AND PROCEDURES

Large stream-icing zones in Alaska were mapped at a scale of 1:250,000 based on analysis of multi-date Landsat imagery. These features include late-winter overflows and residual ice sheets that range from 6 to 40,500 hectares (20 to 100,000 acres) in areal extent; braided streams that are susceptible to icings were also mapped (Figure 1).

The icings were interpreted from Landsat MSS (multispectral scanner) data recorded during the 1972 to 1982 late-winter, spring, and summer seasons. The location and maximum extent of icings were mapped regardless of frequency and timing of occurrences. Most icings tended to recur at the same location each year, although the extent did vary. Selected images with minimum cloud cover and extensive icings were enlarged to 1:250,000 scale and used as primary data sources for each plate. Landsat images at 1:1,000,000-scale that were recorded on dates not selected for enlargement provided additional information.

Visible-wavelength (band 5) data were used to map residual ice after spring thaw (Figure 2). These ice sheets appear white on band 5 images due to their high reflectance compared with surrounding vegetation, soil, or rock. Occasionally, the ice even had a higher reflectance than nearby snow cover.

Landsat images recorded in near-infrared wavelengths (band 7) were used to map late-winter overflows (Figure 3). Active overflows appear dark gray to black due to absorption of these wavelengths

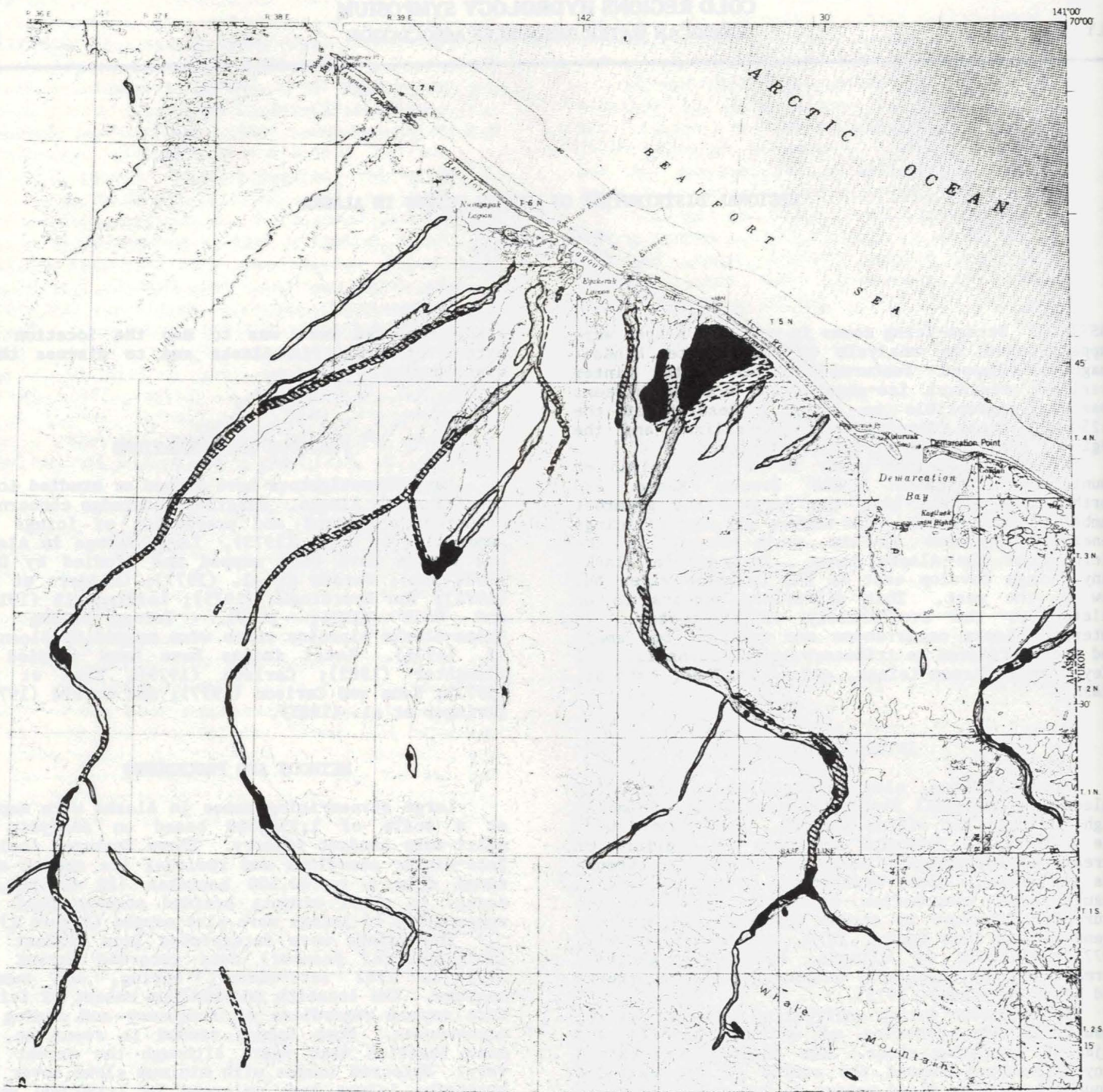


Figure 1. Stream icings in the vicinity of Demarcation Bay. Solid areas indicate residual ice sheets; hatched areas indicate overflows, and open areas indicate braided streams possibly subject to stream icings.

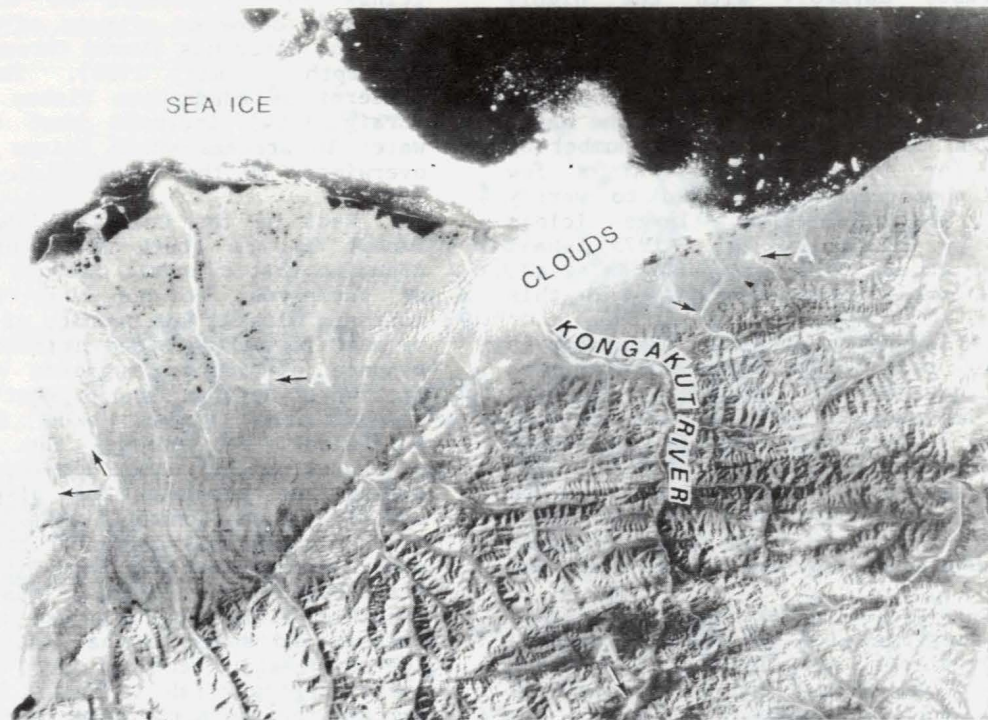


Figure 2. Summer Landsat image (band 5) of the Demarcation Bay area. Residual ice sheets (A) are bright and coincide with overflows displayed in Figure 3. Numerous unlabeled ice sheets are present.



Figure 3. Winter Landsat image (band 7) of the Demarcation Bay area. Stream overflows (B) are dark and coincide with ice sheets displayed in Figure 2. Several unlabeled overflows are present.

by water. The dark signature in the infrared wavelengths contrasts markedly with the highly reflective snow and ice.

Very limited field observations were made during this investigation. Crosschecking of features observed on images, and discussions with individuals familiar with specific areas helped refine the maps. In some areas, cloud cover restricted the number of images available for interpretation. At a few locations, aerial photographs were used to verify occurrences. At specific sites, large icings previously mapped by Childers et al. (1975), Hall (1976; 1980), Sloan et al. (1976), and Harden et al. (1977), compare favorably with those mapped in this investigation.

The presence of confusing spectral signatures in some areas may have resulted in misinterpretations; these areas are queried on the maps. Surface features that may be confused with or mask residual ice sheets include snow cover (usually at higher elevations), snow drifts along flood plains, river ice, gravel, and vegetation. Features that may be confused with late winter overflows include dense spruce forests; dense, leafless brush along streams; unfrozen stream channels; exposed clear ice; and exposed ground.

Overflows were observed on late-winter images in areas where large residual ice sheets were mapped. Typically, the overflows are located in stream valleys (river or spring icings) and their extent is larger than the residual ice sheets.

Icings are often associated with braided streams (Carey, 1973) and may cause braided-stream patterns to develop (Harden et al., 1977). Boundaries of flood plains thought to be susceptible to icings were delineated by braided patterns on topographic maps and Landsat images and by proximity to icing zones. Typically, streams that are susceptible to icings are finely rather than coarsely braided, and usually, meandering streams in mountainous regions with relatively short, braided segments are affected by icings in the braided reach. If springs are also present, icings are probably responsible for the braided patterns. In mountainous regions, bifurcated channels were also observed in icing areas.

REGIONAL DISTRIBUTION

Approximately 700 stream-icings were mapped. The locations of icings were plotted on a small-scale map of Alaska to display the regional distribution (Figure 4). The highest concentration and largest occurrences are associated with Alaska's two major mountain systems, the Brooks Range and the Alaska Range. The number and size of icings decrease away from these two mountainous regions. The largest icing is in northeast Alaska and affects an area greater than 40,500 hectares (100,000 acres). Few icings were mapped in low-lying areas that are not in the immediate proximity of hills and mountains. In interior Alaska most of the icings are confined to small tributary stream valleys which contrasts with occurrences to the north where icings develop along primary and tributary streams. Generally, the number and size of icings steadily decrease to the south with those in the vicinity of the Alaska Range being the exception.

Northern Alaska, which includes the Brooks Range and the Arctic Coastal Plains, has the greatest density of occurrences but the distribution differs east and west of the Colville River. East of the river, icings develop in most streams throughout the Brooks Range and on the coastal plain. Numerous

springs in the area are located at sites where icings form (Childers et al., 1975). Calcium carbonate deposits on some of these icings suggest that the water has flowed through calcareous bedrock at depth (Hall, 1980). The coastal dispersal patterns of anadromous fishes in the Beaufort Sea (Craig, 1984) indicate that there is sufficient water in streams where icings develop for fish to overwinter in this area (P.C. Craig, pers. comm., 1985).

West of the Colville River few icings occur except on the south flank of the Brooks Range. Assuming that climatic factors and the distribution of permafrost do not vary significantly across northern Alaska, the paucity of icings is apparently related to geologic and hydrologic conditions. The absence of icings suggests that there are few freshwater springs, and/or that flow of water within streams and stream beds is not constricted sufficiently to produce the required hydrostatic pressures or that water does not flow in the streams during the winter. The dispersal patterns and species of anadromous fishes west of the Colville River are markedly different from those found to the east, which coincides with the difference in the distribution of icings. This may be related to possible differences in the number of freshwater sources and suggests that water beneath the winter ice-cover is lacking or not sufficient for overwintering fish. Thus, icings may indicate streams that do not freeze to the bottom at least in arctic regions.

CONCLUSIONS

Stream icings are common throughout Alaska and usually recur near the same locality annually. Their areal extent may vary each year. The highest frequency and greatest density of icings occur in the Brooks Range, the northeast coastal plain and foothills. The largest icings also develop in this area. Few icings occur in the western coastal plain and foothills. Generally, the number and size of icings steadily decrease southward, except in the Alaska Range, where there are numerous stream icings. In interior Alaska, icings are numerous but relatively small and are restricted to tributary stream valleys. Almost all large icings occur within or near upland or mountainous regions and often along finely braided streams.

In northern Alaska many icings coincide with the location of known freshwater springs and hence icings may indicate the location of springs in other areas. The distribution of these northern icings also coincides with the dispersal patterns of anadromous fishes. This suggests that streams with icings are winter habitats of anadromous fishes.

ACKNOWLEDGEMENTS

The author wishes to thank Dr. W.J. Stringer, T.H. George and C. Helfferich for their helpful comments. The initial mapping of stream-icing zones was funded by the Alaska Division of Geologic and Geophysical Surveys.

LITERATURE CITED

Carey, K.L., 1973. Icings Developed from Surface Water and Ground Water. Cold Regions Research and Engineering Laboratory Monograph 111-D3,

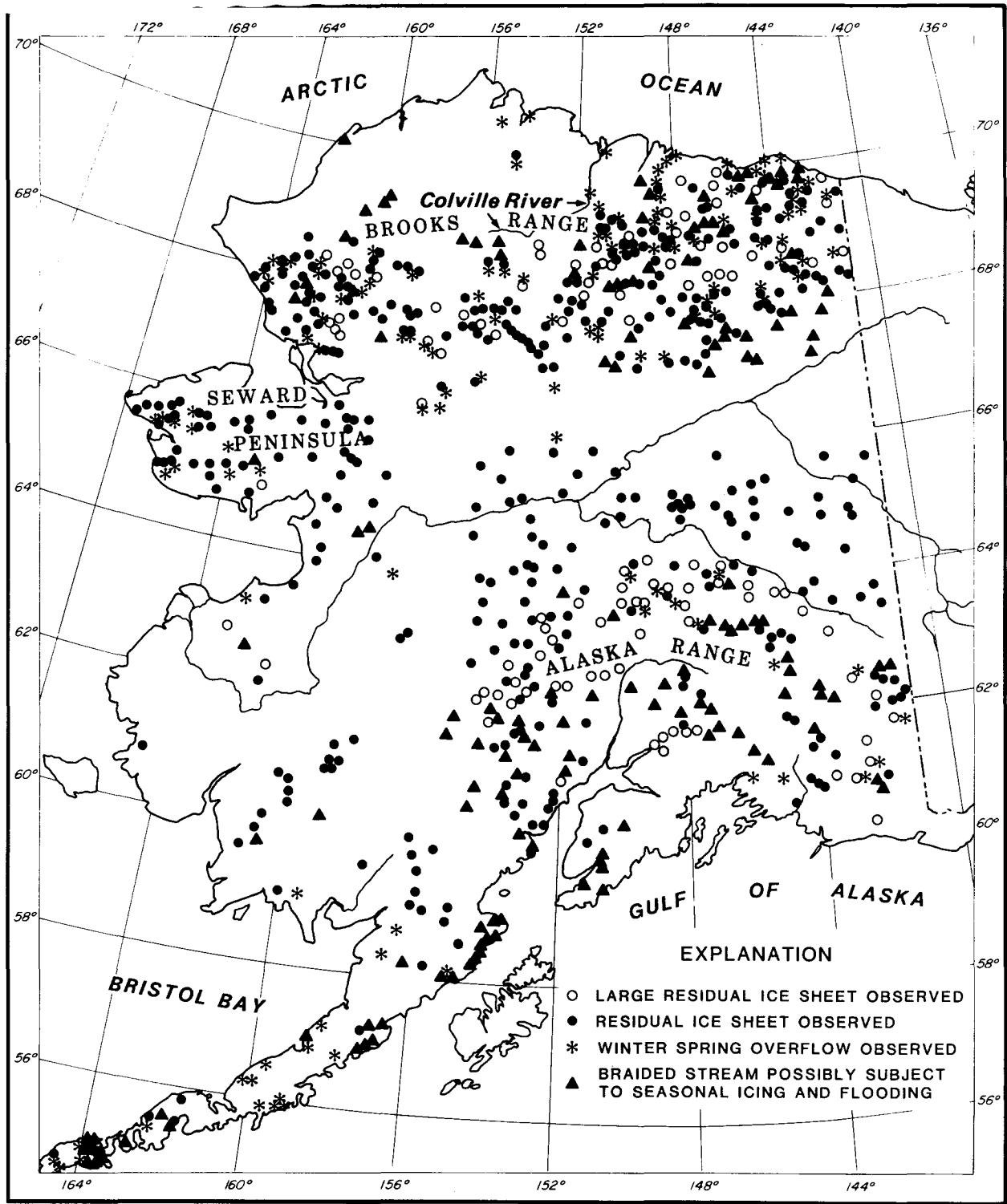


Figure 4. Regional distribution of icings in Alaska.

- Hanover, NH, 67 pp.
- Carlson, R.F., 1979. A Theory of Aufeis and Bed Erosion. In Canadian Hydrology Symposium 79, Cold Climate Hydrology. National Research Council of Canada, Ottawa, 197-205.
- Childers, J.M., Sloan, C.E., Meckel, J.P., and Nauman, J.W., 1975. Hydrologic Reconnaissance of the Eastern North Slope, Alaska. U.S. Geological Survey, Open-File Report 77-492, 65.
- Corbin, S.W., 1977. The Thermal Regime of a Stream in Central Alaska. M.S. thesis, University of Alaska, Fairbanks, 144 pp.
- Craig, P.C., 1984. Fish Use of Coastal Waters of the Alaskan Beaufort Sea: A Review, Transactions of the American Fisheries Society, 113:265-282.
- Dean, K.G., 1984a. Stream-icing Zones in Alaska. Alaska Division of Geological and Geophysical Surveys Report of Investigations 84-16, Fairbanks, AK, 20 pp. + 1 map.
- Dean, K.G., 1984b. Alaskan Stream Icings. The Northern Engineer, 16(1):3-7.
- Hall, D.K., 1976. Analysis of Some Hydrologic Variable on the North Slope of Alaska Using Passive Microwave, Visible and Near-infrared Imagery. In Proceedings of the American Society of Photogrammetry. Falls Church, VA, 344-361.
- Hall, D.K., 1980. Mineral Precipitation in North Slope River Icings. Arctic, 33:343-348.
- Harden, D., Barnes, P., and Reimnitz, E., 1977. Distribution and Character of Naleds in Northeast Alaska. Arctic, 30:28-40.
- Kane, D.L., Carlson, R.F., and Bowers, C.E., 1973. Groundwater Pore Pressures Adjacent to Subarctic Streams. In Proceedings for the North American Contrib., 2nd International Conference on Permafrost. National Academy of Science, Washington, D.C., 453-458.
- Kane, D.L., and Carlson, R.F., 1977. Analysis of Stream Aufeis Growth and Climatic Conditions. In Proceedings of the Third National Hydrotechnology Conference. Canadian Society for Civil Engineers, Quebec, 656-670.
- Leffingwell, E.K., 1919. The Canning River Region, Northern Alaska, US Geological Survey Prof. Paper 109, 251pp + maps.
- Slaughter, C.W., 1982. Occurrence of and Recurrence of Aufeis in an Upland Taiga Catchment. In Proceedings of the Fourth Canadian Permafrost Conference. March 1-6, 1981, Calgary, Alberta, Canada. National Research Council of Canada, Ottawa, 182-188.
- Sloan, C.E., Zenone, C., and Mayo, L., 1976. Icings Along the Trans-Alaska Pipeline Route. U.S. Geological Survey Prof. Paper 979, 31 pp.
- Stringer, W.J., T.H. George and R.M. Bell, 1985. An Aufeis Case Study. The Northern Engineer, 17:25-29.
- Van Everdingen, 1975. Use of ERTS-1 Imagery for Monitoring of Icings, N. Yukon and N.E. Alaska. In Research Program, Hydrology Research Division, Canadian Inland Waters Directorate, Water Resource Branch, Ottawa, Canada, Report Series No. 42, 75-87.

ESTIMATION OF GLACIER MELTWATER HYDROGRAPHS

David Bjerklie and Robert Carlson¹

ABSTRACT: The melt component of daily hydrographs from glaciers was estimated using a multiple regression model. The model was developed for one basin using a period of record over which precipitation was not a significant contributor to the streamflow. The input variables were the average daily temperature and the log of the previous day's flow. The model was then applied to subsequent years of temperature data to test its applicability. The melt estimates from the model simulations were compared with other independent estimates. The results indicate that estimation of melt using the simple multiple regression model presented here is a useful method which gives annual melt volumes that are similar to the other estimates and allows the daily determination of melt flow. The capability of the model to predict daily melt flows should be evaluated more thoroughly because of the model's high degree of sensitivity to error in input data and to changes in model parameters, and because of the model's overly simple design.

(Key Terms: melt; hydrograph; glacier)

OBJECTIVE

We investigated the use of a simplified technique to estimate melt flow hydrographs from glacierized basins. Daily temperature is often the only and the most detailed data available for many areas of Alaska. Multiple linear regression was used to evaluate mean daily temperature as an index to predict daily melt from the Phelan Creek basin, Alaska. This stream has been gaged by the USGS since 1966 and has included a systematic study of Gulkana glacier, which comprises 61% of the basin.

INTRODUCTION

There have been numerous efforts to model streamflow and melt from glacierized basins (Fountain and Tangborn, 1985). Modeling techniques have ranged from purely stochastic to purely deterministic, and have been concerned with time frames ranging from one day to many years.

The major source of ablation energy

¹Institute of Northern Engineering, Water Research Center, University of Alaska-Fairbanks, Fairbanks, Alaska 99775-1760.

is net radiation (Mayo and Pewe, 1963), however, in some cases temperature is more highly correlated with ablation than net radiation (Braithwaite, 1981). Modeling ablation with a simple linear temperature relationship of the form

$$\text{ablation} = B_0 + B_1(\text{temperature}) \quad (1)$$

where B_0 and B_1 are regression coefficients can explain up to half of the variance and has been applied in areas where there is sparse glaciologic and hydrologic data (Braithwaite, 1981).

Multiple regression analysis using the log of the previous days discharge, daily precipitation, daily temperature, daily incoming solar radiation and daily average vapor pressure as independent variables to predict daily streamflow, from a basin in Switzerland with 54% glacier area, explained up to 94% of the variance (Lang and Dayer, 1985). Lang and Dayer found that the previous days streamflow was a better predictor of streamflow than was the average daily temperature even though the basin area was only 34.5 square kilometers.

This paper will examine the use of a statistical multiple regression model to predict melt flows from Gulkana Glacier. Daily streamflows and daily temperatures were available for the basin as well as ablation estimates from glacier stake observations, from the USGS.

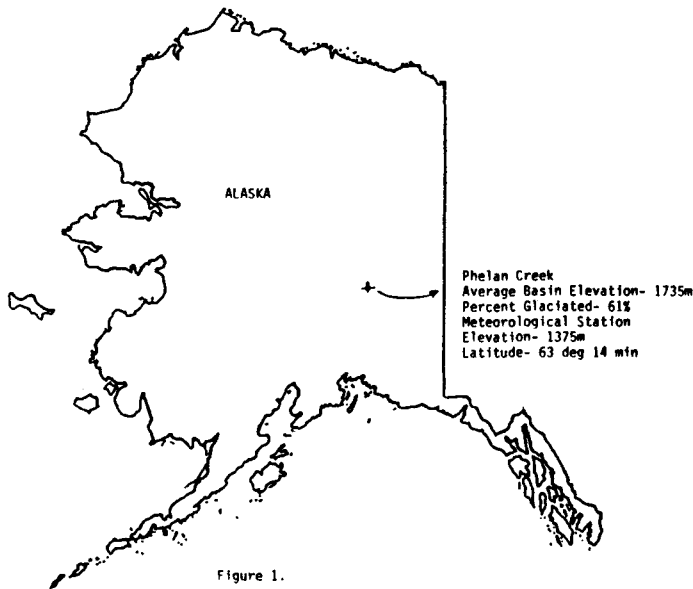


Figure 1.

The primary objective of this paper is to develop a means to estimate the melt component of the hydrograph. Periods of record were chosen for analysis during times of maximum melt contribution and minimum rainfall runoff contribution so that the hydrograph was dominated by the melt component. We assumed that the groundwater component was negligible in mountainous glacierized basins. The periods of record met the criterion that no more than 5% of the total flow over the period fell as precipitation. Under this criteria no spikes obviously associated with a rainfall runoff event were evident, and the volume of flow from rainfall runoff was minimal. In addition, no peaks were seen that did not also correspond to an increase in temperature.

These data provided a means to independently analyze the melt component of the hydrograph. Regression analyses were run on streamflow and temperature data in order to determine the best prediction model. The regression model used was of the form

$$y = B_0 + B_1(X_1) + B_2(X_2) \dots B_n(X_n) + e \quad (2)$$

where B_0 , B_1 and $B_2 \dots B_n$ are regression coefficients and y is the dependent variable, X_1 and $X_2 \dots X_n$ are independent variables, and e is the residual (Davis, 1986). We found that, similar to Lang and Dayer (1985), the log of the previous days streamflow ($\ln Q_1$) and the daily temperature (T) provided the best results (Table 1).

The longest period of record was that for Phelan Creek in 1977. This period also showed the best r squared value and smallest standard error of the estimate.

TABLE 1

Multiple Regression Results of Average Daily Temperature and the Natural Log of the Previous Days Flow vs the Natural Log of the Days Flow.

Stream	Period of Record	Regression Equation	R squared
Phelan Cr.	May 13-Sept 5 1977*	$\ln Q = .146 + .878 \ln Q_1 + .049 T$.987
Phelan Cr.	May 15-Jun 30 1969*	$\ln Q = .192 + .855 \ln Q_1 + .041 T$.976
Phelan Cr.	Jun 1-Jul 31 1976*	$\ln Q = .355 + .825 \ln Q_1 + .041 T$.906

$\ln Q$ = natural log of streamflow
 $\ln Q_1$ = natural log of previous days streamflow
 T = average daily temperature

* For periods of record with total precipitation volume of 5% or less of the volume of flow.

The 1977 Phelan Creek data were divided into three independent data subsets consisting of the June, July and August data. These data subsets were analyzed using multiple linear regression to determine if there was any time dependent difference in the regression results (Table 2). The regression coefficients indicate that temperature played the greatest role as a predictor variable in August and the least in June, indicating that the temperature-melt relationship changes through the summer. This agrees with known phenomena, i.e., as the summer progresses, more ice with a lower albedo is exposed and melt is enhanced. This also explains some of the variation among data sets seen in the initial regression results for Phelan Creek.

TABLE 2

Multiple Regression Results for Phelan Creek 1977 data Separated into Monthly Subsets.

Time Period	Regression Equation	R squared	Correlation of $\ln Q$ vs $\ln Q_1$, vs T
May 13-Jun 30	$\ln Q = .185 + .818 \ln Q_1 + .035 T$.991	.995 .675
Jul 1-Jul 31	$\ln Q = .240 + .893 \ln Q_1 + .039 T$.940	.935 .444
Aug 1-Sept 5	$\ln Q = .466 + .796 \ln Q_1 + .076 T$.934	.927 .793

The phenomenon of snow and ice melt is more complex than is suggested by the simple model produced from the regression analyses here. However, the goodness of fit of these regression models seems to indicate that they would prove useful for determining the melt component from river basins with significant glacierized areas. To test this hypothesis, a standard regression model was adopted. The regression results from the Phelan Creek 1977 summer data was used as the model because the results were the best statistically and the data encompassed the entire melt season.

QUANTITATIVE EVALUATION

The regression model was used to predict sequences of melt flows for the ablation seasons (May 15 to September 15) for five years of Phelan Creek data, including the 1977 calibration data. The results are shown in Figure 2 along with temperature sequences, precipitation and actual streamflows. In general, it appears that the model predicted melt peaks that were also seen in the actual flow sequences (related to temperature peaks). The model did not predict peaks associated with precipitation events. However, precipitation in this basin can fall as snow or rain, and can exist as both for a given storm at different elevations in the basin. Thus it is not necessarily true that a peak in streamflow would be associated with a precipitation event.

Numerous discrepancies are apparent by inspection between the predicted hydrographs and the actual hydrographs in terms of peak height and timing during periods of no precipitation and therefore melt only. Because of the interference of precipitation events, there is no sound statistical means to evaluate the predictive accuracy of the model. Thus, the only means to determine how well the model did was to compare the melt estimates with melt estimates determined using different means.

Three independent ablation estimates were used to evaluate the model's

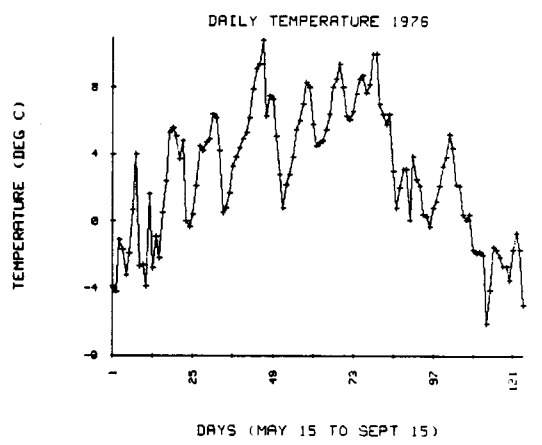
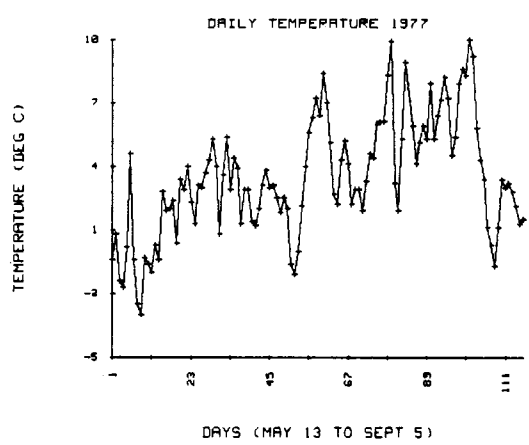
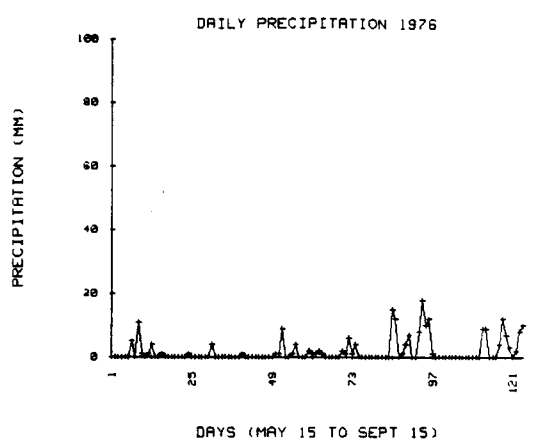
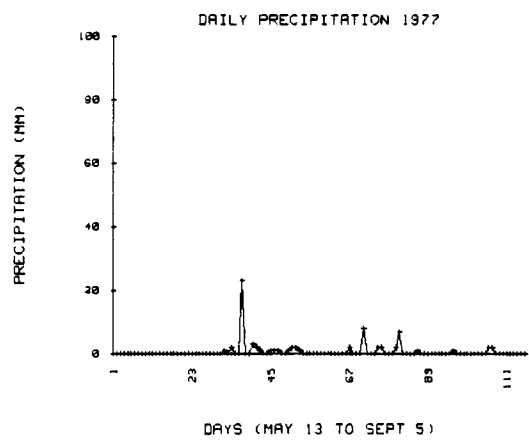
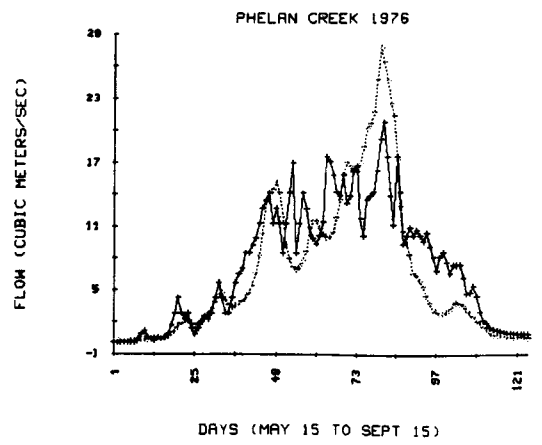
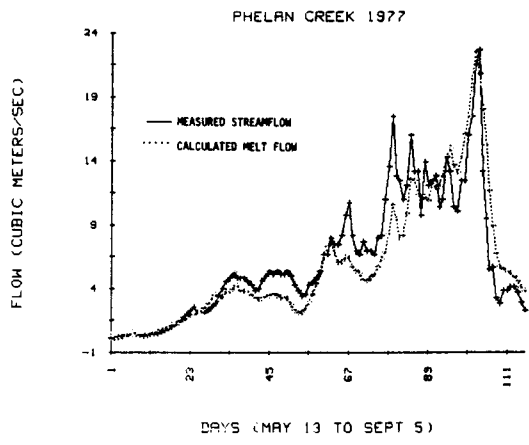


Figure 2.

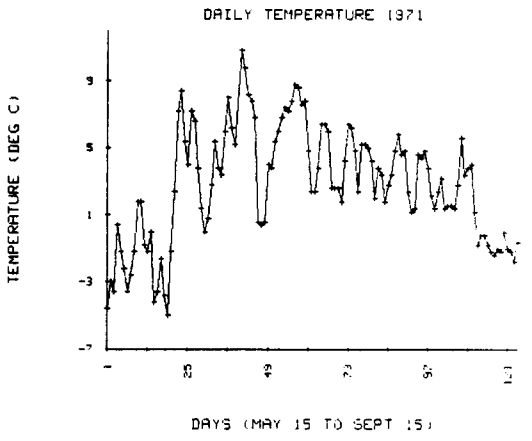
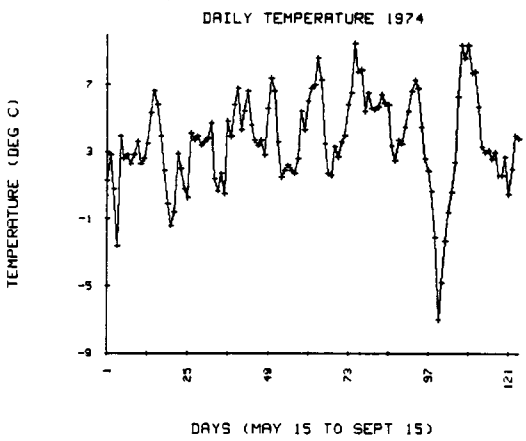
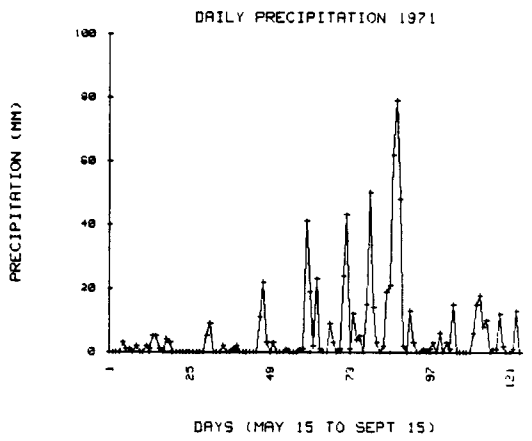
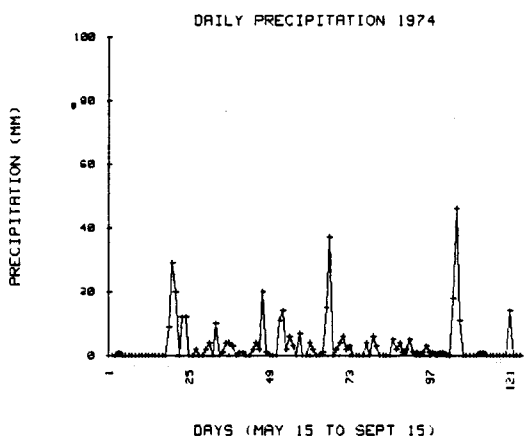
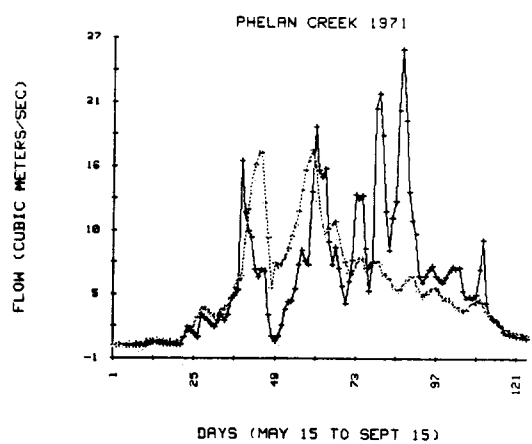
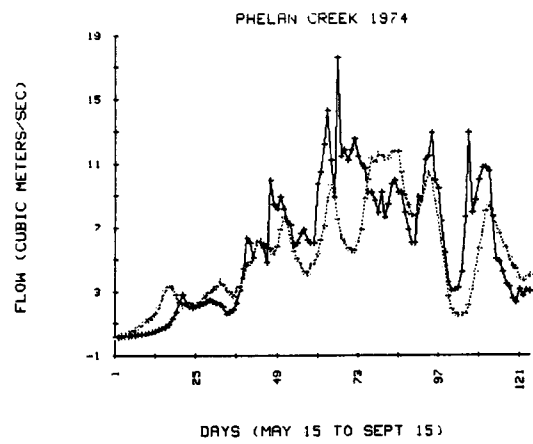


Figure 2 (cont.).

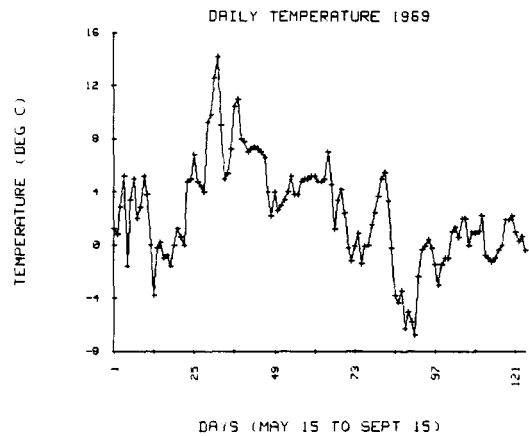
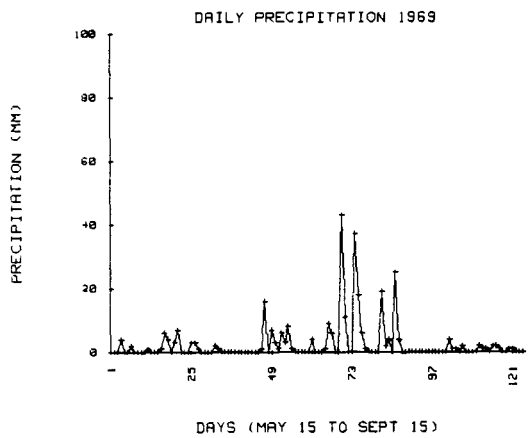
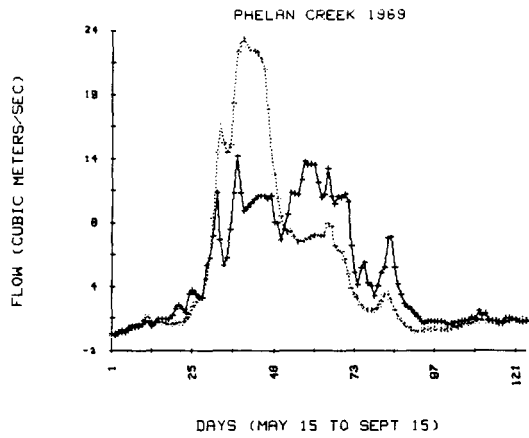


Figure 2 (cont.).

predictions. The best available estimate was from the glacier stake estimate of total melt volume over the ablation season provided by the USGS (Mayo, personal communication). In addition to this for comparative purposes, a predictive ablation model based on average ablation season temperature (Mayo and Trabant, 1984) was used to estimate the melt volume over the ablation season. Baseflow volumes were also computed over the ablation season. The baseflow was assumed to represent water released from storage, which would include the melt component. Groundwater contribution was assumed to be negligible in this basin due to the mountainous terrain.

The results of the estimates of melt season ablation by the four methods are shown in Table 3. The best approximation of the glacier stake estimate for all five years was provided by the multiple regression model (model simulation). However, the model estimates were fairly close to each other and to the glacier stake estimate, with the exception of the model presented by Mayo and Trabant (1984) for 1976 (alternative model). The baseflow estimates were consistently conservative.

TABLE 3

Melt Estimate Comparisons (meters).

Stream	Model Simulation	Glacier Stake	Alternative Model	Baseflow
Phelan Cr. 1969				
May 15-Sept 15	1.77	1.64	1.35*	0.96
Phelan Cr. 1971				
May 15-Sept 15	1.80	1.47	1.57*	1.24
Phelan Cr. 1974				
May 15-Sept 15	1.76	2.00	1.91*	1.43
Phelan Cr. 1976				
May 15-Sept 15	2.27	2.47	1.57*	1.73
Phelan Cr. 1977				
May 13-Sept 5	1.86	1.96	1.82*	1.58

* Estimated from USGS ablation model developed for Wolverine glacier (Mayo, 1984). Seasonal Ablation = $0.19 + 0.43T_a$ where T_a = avg. summer temp. R-squared = 0.65

SENSITIVITY ANALYSIS

A series of simulations were conducted after changing values of the data input and the regression

coefficients of the model in order to evaluate the sensitivity of the model to the model parameters and input data. The results of this analysis are shown in Table 4. It can be seen that minor changes in the data input as well as changes in the coefficients result in significant changes in the quantitative value of the flow simulations. The qualitative character of the simulation does not change, however, except when the B1 coefficient (associated with the lnQ1 variable) is altered. From this it can be concluded that, due to the sensitivity of the model to changes in model parameters and variables, it is probably not wise to apply the model developed in one basin to another, unless generalized information is all that is needed.

It is possible that a more extensive study can define the variation in coefficients with climatic and physiographic variables in order to render the model more generally applicable.

Using temperature and the previous day's flow as predictors of a melt hydrograph seems to be a workable method for estimating the contribution of the glacierized portion of basins to streamflow. However, the model needs to be calibrated more accurately to better predict the total volume of melt from glacierized areas. Discrepancies in the timing and peaks of predicted melt flow indicate that the modeling approach used here is limited by the simplistic indexing of melt with temperature. In addition, due to the model's high sensitivity to model parameters and the temperature input data, the model must be evaluated for individual cases, since each case can include data biases and differences in terrain and microclimatic conditions that could presumably effect the melt temperature relationship. An advantage of the use of the predictive model described in this paper is its capability to predict daily flow. This would enable the calculation of missing data and enable the continuous monitoring of the hydrologic conditions in glaciers. In addition, it might enable more detailed management of water from glacierized basins.

TABLE 4

Results of Sensitivity Analysis of Simulations.
Model form $y=B0+B1(X1)+B2(X2)$.

Model Used	Peak Flow	Minimum Flow
$\ln Q = .146 + .878 \ln Q1 + .049 T^*$	1.5	.01
$\ln Q = .146 + .800 \ln Q1 + .06 T$	0.6	.01
$\ln Q = .300 + .878 \ln Q1 + .049 T$	5.0	.01
$\ln Q = 0.00 + .878 \ln Q1 + .049 T$	0.4	.01
$\ln Q = .146 + .600 \ln Q1 + .049 T$	0.1	.01
$\ln Q = .146 + 1.00 \ln Q1 + .049 T$	2.7EE13	.01
$\ln Q = .146 + .878 \ln Q1 + .035 T$	0.7	.01
$\ln Q = .146 + .878 \ln Q1 + .060 T$	2.6	.01
$\ln Q = .146 + .878 \ln Q1 + .049 T$ +1 degree bias in T data	2.1	.01
$\ln Q = .146 + .878 \ln Q1 + .049 T$ +2 degree bias in T data	3.2	.01
$\ln Q = .146 + .878 \ln Q1 + .049 T$ -1 degree bias in T data	1.0	.01
$\ln Q = .146 + .878 \ln Q1 + .049 T$ -2 degree bias in T data	0.7	.01

* Model used for simulations.

REFERENCES

Braithwaite, R.J., 1981. On Glacier Energy Balance, Ablation, and Air Temperature. *Journal of Glaciology*, Vol. 27, no. 97. 9 pp.

Davis, J.C., 1986. *Statistics and Data Analysis in Geology*. 2nd Edition, John Wiley and Sons, New York. 646 pp.

Fountain, A.G. and W.V. Tangborn, 1985. Overview of Contemporary Techniques. Pages 27-41 in G.J. Young. *Techniques for Prediction of Runoff from Glacierized Areas*. IAHS publication no. 149.

Lang,H. and G. Dayer, 1985. Switzerland Case Study. Pages 45-59 in G.J. Young. Techniques for Prediction of Runoff from Glacierized Areas. IAHS publication no.149.

Mayo,L. and T.L. Pewe, 1963. Ablation and Net Total Radiation, Gulkana Glacier, Alaska. Chapter 43 in Ice and Snow Properties, Processes and Applications. MIT Press, Cambridge, Mass.

Mayo,L. and D.C. Trabant, 1984. Observed and Predicted Effects of Climate Change On Wolverine Glacier, Southern Alaska. Pages 114-123 in G.P. Juday and G. Weller. The Potential Effects of Carbon Dioxide-Induced Climatic Changes in Alaska, Proceedings of a Conference. Univ. of Alaska, Fairbanks, Alaska. University of Alaska misc. publication 83-1.

U.S. Geological Survey, Water Resources Div. 1969-1977. Water Resources Data for Alaska. Report AK-69-1 through AK-77-1.

Young,G.J., 1985. Overview. Pages 3-23 in G.J. Young. Techniques for Prediction of Runoff from Glacierized Areas. IAHS Publication no.149.

PRECIPITATION – SNOW PACK – SOIL PROCESSES

SNOW SURFACE STRENGTH AND THE EFFICIENCY OF RELOCATION BY WIND

R. A. Schmidt¹

ABSTRACT: An automated system developed by Martinelli and Ozment samples forces required to fracture grains from a snow surface. The device has sufficient sensitivity to measure differences in surface erodibility under saltating drift. Such measurements help explain differences in the efficiency with which wind transports snow.

(KEY TERMS: snow; blowing snow; drifting; snow strength; transport efficiency.)

INTRODUCTION

Wind-drifting snow is part of the hydrologic cycle in cold regions of planet Earth and two aspects of the process particularly significant to hydrologists are: (1) the reduction in effective precipitation caused by evaporation during transport and (2) the nonuniform distribution of the snow that remains after redeposition. Methods to predict these effects often require estimates of snow transport rate as a function of wind speed, from which the duration of drifting is computed for a given depth of snowfall.

The efficiency with which wind moves snow may be defined by the ratio of drift rate to wind energy. Experiments that measured drift rate and wind speed showed that after snowfall, transport efficiency increased as surfaces became hardened by the drift process (Schmidt, 1986). Drift efficiency seemed closely related to momentum lost by saltating particles on impact with the surface.

The wind energy required to maintain saltation over a hard, old snow surface as opposed to a soft, new snow surface is

analogous to the effort one exerts to keep a ball bouncing on a hard floor, in contrast to a foam pad. When a drift particle's impact fractures a new particle from the surface, kinetic energy is lost and the total momentum of new and old particles is less than when the particle rebounds without producing a fracture.

Surface hardening increases the probability that a surface grain is bonded too strongly to be ejected by the impact of a saltating drift particle. The hardening of the surface under drifting snow occurs (1) by mechanical reduction of the size and complexity of the precipitation crystals, and (2) through cohesion and subsequent bond growth by sintering. Laboratory experiments on these processes allow us to make general statements about how the hardening will proceed in relation to time, temperature, humidity, and particle size. However, the nonhomogeneity of both snow particles and surface configurations produces a distribution of strengths in bonds attaching the most exposed grains that is more easily measured than predicted.

A device useful for surface hardness observations should measure the same range of force particle impacts produce in saltation on a snow surface. Such forces may be estimated by assuming central, elastic collision of ice spheres (Schmidt, 1980). Impact velocities ranging from threshold (near 2) to 10 m s^{-1} or more may be expected, considering the wind speed near the top of a saltation trajectory. Sizes of saltating snow particles average near 0.2 mm diameter (Schmidt 1981). Forces up to 1 N seem possible (Figure 1), with the greatest number of impacts around

¹Rocky Mountain Forest and Range Experiment Station, 240 West Prospect, Fort Collins, Colorado, 80526, U.S.A.

0.1 N. The corresponding range of a load cell (in grams force) is also indicated on the figure.

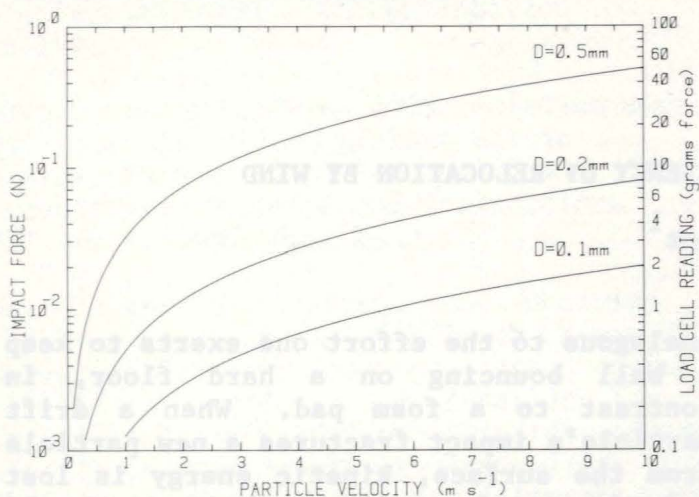


Figure 1. Estimated impact forces of two ice spheres with diameter D in a central, elastic collision where one sphere is stationary and the other has the speed indicated on the abscissa (Schmidt, 1980).

METHOD

Several hardness gages measure the resistance to penetration of snow by a hard conical probe. These devices sample a much deeper layer than that interacting with saltating drift. Martinelli and Ozment (1984, 1985a, 1985b) developed a method of rapidly sampling forces required to fracture individual grains from a snow surface *in situ* (Figure 2). A sensitive load cell measures the force on a solid plastic sphere 20 mm in diameter, driven toward the surface at 0.5 mm s^{-1} by a stepper motor. Comparing output voltage from the load cell with its no-load value, the system detects contact of the probe and the surface with a sensitivity of $9.8 \cdot 10^{-4} \text{ N}$ (a touch of 0.1 gram force). Surface detection starts a probe-travel counter and arms a break-detector that changes state when a surface failure reduces resistance against the probe by a specified amount ($2.94 \cdot 10^{-3} \text{ N}$ for these experiments). Probe travel and maximum force at failure are held for measurement and the probe is retracted while data are recorded on magnetic tape and printed for inspection by the system operator.

Each measurement takes approximately one minute. The probe may be repositioned within the support cylinder (Figure 2) to take many samples around the circumference of a circle 8 cm in diameter. An array of four thermistors measures surface temperature in the center of the sampling area. Approximately 100 measurements are possible before recharging batteries. The operator controls the instrument with a bar code reader that permits sampling under blizzard conditions without removing gloves or mittens. Data are transferred electronically to a desk-top computer for analysis.

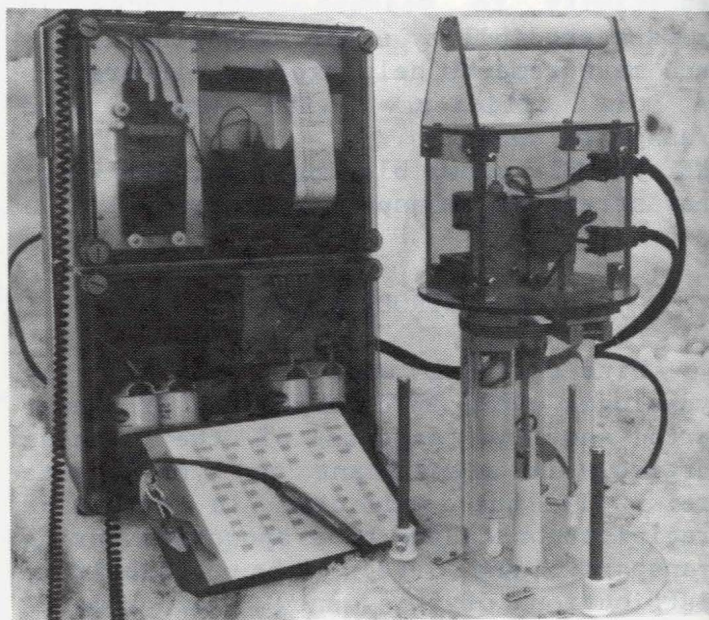


Figure 2. Photograph of the Martinelli-Ozment surface strength tester. During operation, the electronics are carried on a small sled.

Cold room experiments in which a television camera viewed interactions of the probe with surface grains confirmed sufficient sensitivity of the instrument to detect fractures of individual grains from the surface (Martinelli and Ozment, 1985a). As those authors note, the probe contacts surface grains at points that give a range of moment arms around the fracture fulcrums, adding to the large variance of these measurements. The same is true of saltation impacts.

RESULTS

Martinelli and Ozment (1985b) provide extensive measurements on snow surfaces to confirm the useful range of the instrument. Their experiments suggest a linear relationship between force at failure and distance the probe traveled between surface detection and fracture. The constant of proportionality varies widely.

During drifting in January and February, 1985 at Diamond Lake in southeastern Wyoming I sampled strengths on several pairs of surfaces, using the Martinelli-Ozment system. As an example, Figure 3 compares the distribution of surface strengths on (a) the upwind (eroding) face of a moving snow dune and (b) measurements near the top of the same dune, where deposition was occurring. Data consist of three replications of nine samples at each location. Figure 4 shows the relationship of probe travel and fracture force for the data of Figure 3. Both surface strengths and probe travels were smaller on the eroding face.

CONCLUSIONS

The device developed by Martinelli and Ozment provides both the sensitivity and speed to sample snow surface strength sufficiently that different surface conditions may be compared. For example, forces required to fracture grains from the windward face of an eroding snow dune were less than those on a surface depositing immediately downwind of the dune crest. Such data will help explain the large variations in snow transport efficiency.

ACKNOWLEDGEMENT

The usefulness of the instrument results from many clever solutions of both mechanical and electronic design problems by Mr. Arnold Ozment, who expertly machined the system and also helped with field measurements.

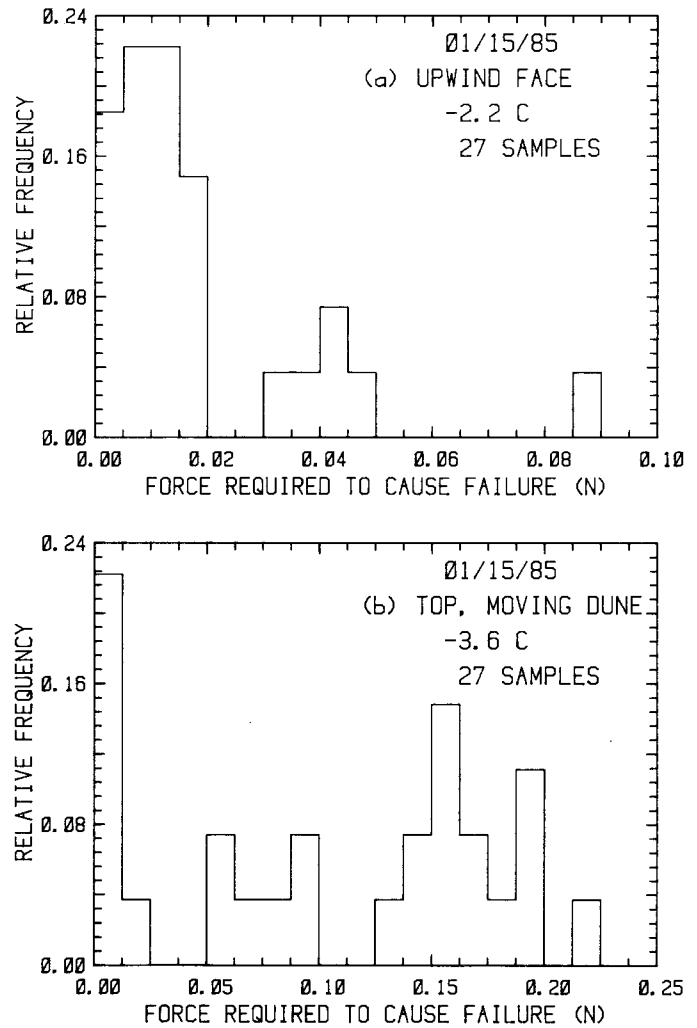


Figure 3. Distributions of forces that caused fracture of surface grains or bonds for (a) upwind (eroding) face and (b) top of a moving snow dune where deposition was occurring.

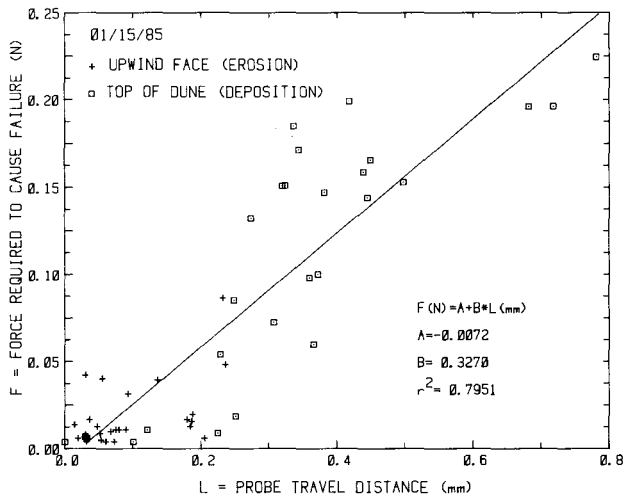


Figure 4. Forces that caused surface fracture were greater and the probe traveled farther on the deposition surface, for measurements in Figure 3.

REFERENCES

- Martinelli, M. and A. D. Ozment, 1984. Controlling Snow Surface Measurements with a Handheld Calculator. Cold Regions Sci. and Technol. 9(3):277-281.
- Martinelli, M. and A. D. Ozment, 1985a. Laboratory Test of a Motorized Snow Surface Hardness Gage, Cold Regions Sci. and Technol. 10(2):133-140.
- Martinelli, M. and A. D. Ozment, 1985b. Some Strength Features of Natural Snow Surfaces that Affect Snow Drifting, Cold Regions Sci. and Technol. 11:267-283
- Schmidt, R.A., 1980. Threshold Wind-speeds and Elastic Impact in Snow Transport. J. Glaciol. 26:453-467.
- Schmidt, R.A., 1981. Estimates of Threshold Windspeed from Particle Sizes in Blowing Snow. Cold Regions Sci. and Technol. 4:187-193.
- Schmidt, R.A., 1986. Transport Rate of Drifting Snow and the Mean Wind Speed Profile. Boundary-Layer Meteorol. 34(1986) 213-241.

WATER FLOW RATES, POROSITY, AND PERMEABILITY IN SNOWPACKS
IN THE CENTRAL SIERRA NEVADABruce J. McGurk and Richard C. Kattelmann¹

ABSTRACT: The equivalent permeability of spring snowpacks near Soda Springs, California was estimated from snowpack outflow data and calculated surface melt. The equivalent permeability results agree with reported values of intrinsic permeability and were found to decline an order of magnitude (from 5×10^{-9} to 5×10^{-10} m²) during spring snowmelt. Values of a permeability parameter also changed significantly over the melt seasons, and these values can be used in operational application of meltwater routing procedures. Water drainage from snowpacks was about three times as rapid in the early season than in the late season. The decreasing importance of flow channels with time may be responsible for this change in drainage speed.

(**KEY TERMS:** snowpack permeability, snowmelt, water movement through snow, snowpack porosity.)

INTRODUCTION

Snow cover runoff is forecasted daily by several agencies using a variety of methods. Many of the forecasting techniques currently used depend on empirical relations and perform adequately under typical or moderate weather and snow conditions. These procedures can produce serious errors, however, during unusual or extreme conditions such as rain-on-snow events. Yet these are also the times when the need for accurate prediction is greatest. Development and application of forecasting techniques based on physical measurements may offer the best hope of improving prediction accuracy during these extreme events.

Transmission of water through snow is among the processes that need to be considered in a comprehensive model of snow cover runoff. This

process is most important during extreme events and in areas of deep snow and rapidly responsive streams (Anderson, 1979). The study of water movement through snow based on porous media flow theory was pioneered by Colbeck in the 1970's (Colbeck, 1972). Some knowledge of the snow's permeability is required before the porous media flow models can be adapted to a snow cover. Laboratory measurements of permeability, however, are virtually impossible to perform accurately due to the triple-phase nature of snow as well as the physical changes that occur during the seasonal metamorphism of the snowpack. Nevertheless, snow permeability has been estimated in a variety of ways, and the reported values cover three orders of magnitude (Table 1). The nonhomogeneity of snowpacks in the Sierra Nevada and most other mountain ranges mandates that porosity and permeability be estimated *in situ* and throughout the melt season.

Snowpack permeability can be estimated by a procedure (described later) that requires hourly data on both snow surface water input and basal outflow, water travel duration and distance, and snowpack density. When the procedure is used with isolated columns of homogeneous snow (Colbeck and Davidson, 1973; Denoth and Seidenbusch, 1978), an intrinsic or saturated permeability may be estimated. When the procedure is used with data from a heterogenous, layered snowpack, the results could be termed a snowpack equivalent permeability rather than an intrinsic permeability, but this distinction is seldom made. At the end of the melt season, the permeability of snowpacks in California and Vermont were found to be in the range of 1 to 4×10^{-9} m² (Colbeck and Anderson, 1982). The permeability of snow to air has been found to be strongly dependent on the metamorphism of the snow and to change over time (Conway and Abrahamson, 1984). Intrinsic permeability is believed to be

¹ Pacific Southwest Forest and Range Experiment Station, Forest Service, U.S. Department of Agriculture, P.O. Box 245, Berkeley, California 94701.

determined mainly by grain size (Shimizu, 1970) and to change quickly during the early part of the melt season (Dunne *et al.*, 1976). On the basis of observations of extensive channeling in Sierra Nevada snowpacks (Gerdel, 1954, Kattelmann, this proceedings), we wondered if the gross permeability of the snowpack might change over time as the flow network is altered.

The procedures developed by Colbeck (1972, 1978, 1979) to model the routing of water vertically through a snowpack require separate estimates of permeability and porosity or of a parameter $k^{1/3}/\phi_e$, which is the quotient of the cube root of intrinsic permeability and the effective porosity

(proportion of the pore volume available for water movement). This parameter can be derived from the procedure Colbeck and Anderson (1982) used and, as a single value, characterizes an important property of the snow. Colbeck (1978) suggested that typical values be assigned to this parameter for use in operational forecasting and that they would change as the snowpack matures. This paper describes a study that, in part, attempted to find some representative values of this parameter to allow the application of both simple lag equations (Colbeck, 1978) and comprehensive routing programs (Tucker and Colbeck, 1977).

The study area, the U.S.D.A. Forest Service's

TABLE 1. Snow porosity and permeability values by snow description.

Snow Description	Porosity	Permeability ($\times 10^{-9}, m^2$)	Method	Source
Loose new dry snow	0.86	4	Permeameter	Bader et al (1954)
Fine grain old dry	.59	2		
Medium grain old dry snow	.68	6		
Coarse grain old dry snow	.67	10		
Newly fallen snow	.85	4	Permeameter	Kuroiwa (1968)
Fine grain snow	.7	0.06-8		
Large grain snow	.6	3-16		
Glass beads 1.0 mm	.37	.9	Not reported	de Vries [cited by Wankiewicz (1979)]
Not reported		.6	Shimizu (1970)	Price (1977)
Disaggregated wet <1 mm	.49-.58	.06-.7	Calculated from	Denoth and Seiden-
Disaggregated wet 1 mm	.44-.50	.9-3	column drainage	busch (1978)
Disaggregated wet >1 mm	.48-.49	1-10	Calculated from	Denoth <i>et al.</i> (1979)
Disaggregated wet 3 mm	.52	25	column drainage	
Disaggregated wet .65g/cm ³	.32	.1	Calculated from	Colbeck and
Disaggregated wet .62g/cm ³	.36	.3	column drainage	Davidson (1973)
Not reported	-	10-30	Not reported	Bengtsson (1981)
Midwinter 0.5-1 mm	.64-.84	2-3	Permeameter	Kattelmann (1981) ¹
Early spring 1 mm	.60-.65	3		
Late spring >1 mm	.39-.51	1		
Spring snowpack .48g/cm ³	.47	2.6	Calculated from	Colbeck and
Spring snowpack .50g/cm ³	.45	2	snowpack input	Anderson (1982)
Shallow snowpack .41g/cm ³	.55	3	and outflow rates	

¹ Kattelmann, R.C., 1981. Hydrology of Compacted Snow. Unpublished MS Thesis, University of California, Berkeley, California. 91 pp.

Central Sierra Snow Laboratory (CSSL), Soda Springs, California, accumulates deep seasonal snowpacks. It is in the forested snowpack zone on the west slope of the Sierra Nevada at 2100 m and is subject to a maritime climatic influence. Between storms, warm, sunny weather often leads to the formation of surface melt-freeze crusts, which become buried by subsequent snowfall to produce a highly stratified snowpack. Occasional midwinter rain or radiation-induced melt is often sufficient to produce snowpack outflow in any month (Smith, 1974). Rain or meltwater percolating downward from the surface becomes concentrated into distinct flow channels at the layer interfaces (Colbeck, 1979). The resulting snowpack and its internal flow network are highly variable spatially and continue to change as spring snowmelt progresses.

METHODS

Solar radiometers and other meteorological equipment at the study site provided hourly average data required by a radiation budget model to estimate hourly surface melt flux. Study intervals were selected from 1984 and 1985 on the basis of data availability and weather. Because melt is easiest to model during clear weather, the 14 intervals selected were mostly sunny with temperatures above 0°C. To match the melt outflow pattern, the modeled 24-hour intervals started at 0800 hours. Meltwater outflow was collected by several 2 m melt pans resting on the soil surface and plumbed into tipping buckets. Each pan was filled with gravel to allow rapid lateral flow, and the travel time from pan to tipping bucket was approximately 2 minutes. Because outflow from the pans varied somewhat in timing and quantity, an overall average time/outflow depth hydrograph was calculated. An isotopic profiling snow density gauge was used to measure average snowpack density and daily depth (Kattelmann et al., 1983).

The theory of porous media flow has been applied to liquid water flow through snowpack, to derive permeability and porosity (Colbeck and Anderson, 1982; Colbeck and Davidson, 1973; Price, 1977). Because the snow's unsaturated permeability must be known for the application of usual methods for describing flow, typical methods of estimating permeability cannot be used. However, because snow is a large-grained material, gravity forces override tension gradients, so capillary flow can be ignored (Colbeck, 1972).

As surface melt and percolation occur, the vertical rate of movement for a melt flux value u is given by (Dumne et al., 1976)

$$\left. \frac{dz}{dt} \right|_u = \frac{n}{\phi_e} \left(\frac{\rho_w g k}{\mu} \right)^{(1/n)} u^{(n-1/n)} \quad (1)$$

where n is a power law exponent (often assumed to be 3) that relates snow water saturation and intrinsic saturated permeability to relative or unsaturated permeability

$$k_w = k_s \phi_e^n \quad (2)$$

and effective porosity is a function of total porosity and irreducible water saturation

$$\phi_e = \phi(1 - S_{wi}) \quad (3)$$

If a meltwater flux u is estimated for the snow surface, and the elapsed time is known until an equivalent flux is released from the base of the snowpack, a ratio parameter $k_w^{1/3}/\phi_e$ can be estimated with equation 1. To this end, 14 melt/outflow events were selected from CSSL records for 1984 and 1985. Before the events were plotted, night freeze crust water equivalents were subtracted from the 0800 and 0900 hours of the calculated melt. The hourly melt values were then adjusted so that the total daily melt equalled the daily observed outflow. The effect of this adjustment was tested with one study interval and found to change travel times uniformly and by only a minor amount. Travel times for selected flux values were calculated by plotting the melt and outflow fluxes on a single graph and estimating the delay between melt and outflow for equivalent flux values (Figure 1).

Recession-limb wave speeds were calculated by dividing snowpack depth by travel times for decreasing late afternoon fluxes between 1 and 4 mm/h (Colbeck and Anderson, 1982; Dumne et al., 1976), and log-log plots of flux versus wave speeds were prepared (Figure 2). Least-squares fitting of a line to the points produced slopes of the lines for comparison with the theoretical value of 0.67, the flux exponent in equation 1 when n is equal to the integer value 3. Porosity was calculated from snow density, liquid water, and irreducible water saturation using equation 2 and

$$\phi = \frac{\rho_s - \rho_i}{\rho_w S_w - \rho_i} \quad (4)$$

Irreducible water saturation equals water content divided by porosity and is assumed to be 0.07 (Colbeck and Anderson, 1982). By inserting a wave speed and a matching flux value into equation 1, the $k_w^{1/3}/\phi_e$ ratio was obtained. The saturated permeability was then estimated by multiplying the flow parameter by the estimated effective porosity

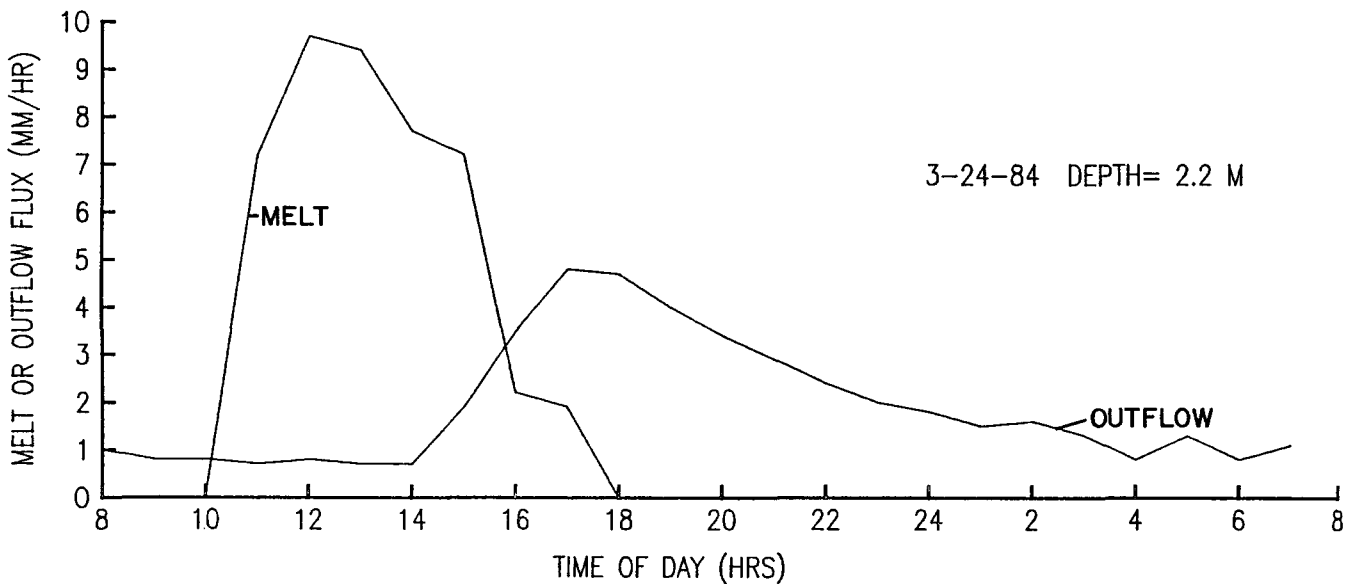
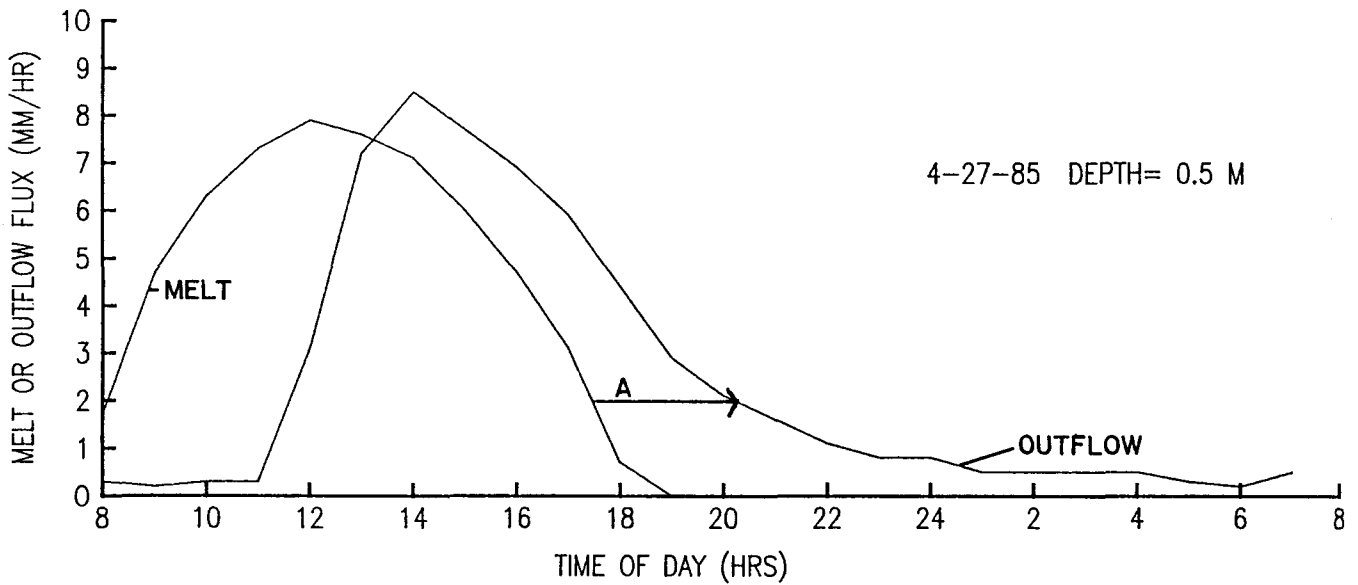


Figure 1. Melt and outflow flux for two days at the Central Sierra Snow Laboratory, Soda Springs, California. At A, a flux of 2 mm/hr has a travel time of over 3 hours through a snowpack 0.5 m in depth, and the wave speed is 5.2×10^{-5} m/s.

$$k_{est} = \left(\frac{k^{1/3}}{\phi_e} * \phi_{e_{est}} \right)^3 \quad (5)$$

Average porosities and permeabilities were calculated for each of the 14 events.

RESULTS AND DISCUSSION

Slope

The slopes of the lines in the log-log plots of flux and wave speed are indicative of the suitability of

an n value of 3 in equation 1 (Figure 2), but higher n values might be more suitable. The slopes are based on flux values of 1.11×10^{-6} m/s (4 mm/h) or less. Slopes ranged from 0.63 to 1.02 and had a mean value of 0.79 and a standard deviation ($n = 14$) of 0.11. No seasonal trend was apparent (Table 2), and even on successive days values were variable and occasionally quite different. When flux rates in excess of 4 mm/h were included in the least squares fitting, the calculated slope value increased.

While the portions of the curves that were analyzed were all monotonically decreasing (see Figure 1 for samples), one event (4-15-84) produced a slope value in excess of 1.0 (Table 2). Values greater than 1.0 indicate increasing flux rates and

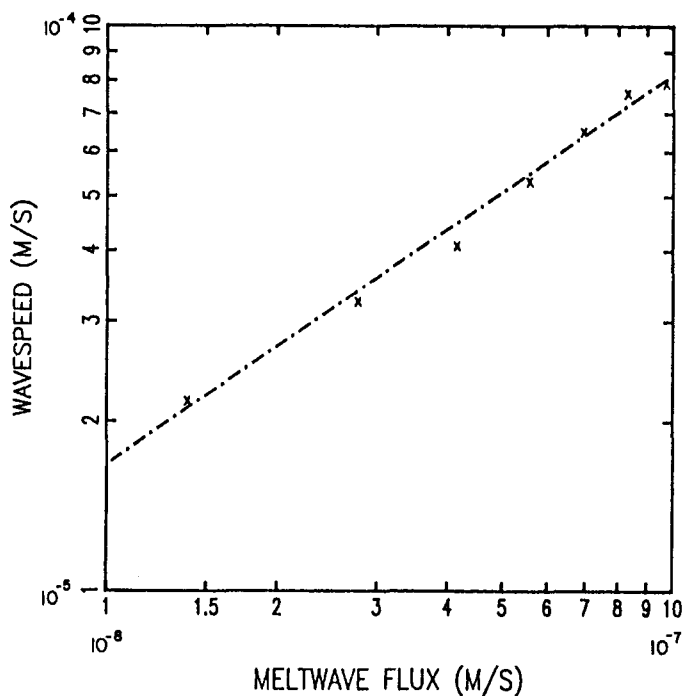


Figure 2. Calculated meltwave flux values and observed wavespeeds for 4-27-85. Line has theoretical slope of 0.67, while fitted value is 0.70.

imply the formation of a shock wave, which was clearly not the case. For this reason as well as for comparability with other literature values, a slope of 0.67 was used in equation 1 for the derivation of ϕ_e and k . The actual slope values were tested, but they were not used because they caused the effective porosity and the permeability/porosity ratio to deviate markedly from expected and literature values.

Once flux rates dropped below approximately 4 mm/h, a divergence between melt and outflow curves was observed, and only those points from the diverging curves were used in the calculation of slopes, porosity, and permeability. Steep slopes, often in excess of 1.0, resulted from including fluxes greater than 4 mm/h. Plots of melt and outflow flux often showed a constant delay (parallel lines) from the peak values down to about 5 mm/h (Figure 2, 4-27-85). This behavior fails to conform with theory that higher flow speeds result from higher flux values and higher water saturation values. The 4-27-85 event's outflow flux decreased from 7 mm/h (1.9×10^{-6} m/s) to 3.5 mm/h, yet the calculated wave speed changed insignificantly from 8.2×10^{-5} to 8.0×10^{-5} m/s. This situation was seen in over a quarter of the events analyzed.

TABLE 2. Depth, density, effective porosity, flow parameter, permeability, and derived slopes for study intervals at the Central Sierra Snow Laboratory, Soda Springs, California.

Date	Depth (m)	Density (kg/m ³)	ϕ_e ($S_{wi}=.07$)	$k^{1/3}/\phi_e$ ($\times 10^{-3}, m^{2/3}$)	k ($\times 10^{-9}, m^2$)	Derived Slope
3-23-84	2.2	420	0.55	2.6	3	.81
3-24-84	2.2	420	.55	2.7	3	.64
4-14-84	1.9	420	.55	2.5	3	.83
4-15-84	1.9	430	.54	2.5	3	1.02
4-22-84	1.8	420	.55	2.3	2	.82
5-11-84	.9	440	.52	1.7	0.8	.84
5-12-84	.8	440	.52	1.5	.5	.79
3-31-85	2.1	340	.63	4.1	18	.67
4-5-85	1.6	380	.59	2.6	4	.75
4-6-85	1.5	380	.59	2.9	9	.76
4-13-85	1.0	390	.58	2.7	4	.95
4-14-85	.9	390	.58	2.2	2	.86
4-27-85	.5	410	.56	1.5	.6	.70
4-28-85	.4	410	.56	1.2	.3	.63

The value of the exponent n has been extensively debated because it is crucial in converting saturated permeability to unsaturated permeability. Because the slopes of the lines should be 0.67 if the value of n in equation 2 is 3, these slopes fail to support the choice of n as being equal to 3 (Table 2 and Figure 3). Colbeck and Anderson (1982) found an n of 3.3 but concluded that, due to the ease of calculations with the integer value and the marginal improvement in fit, the value of 3 was preferable. Literature values of n range from 1.4 to 4.6 (Table 3). Values of n for sand samples

Table 3. Literature values of n for water flow through snow.

n	Sample	Source
>3.5	Spring snow	Jordan, 1983
2.8	Glacial firn	Ambach <i>et al.</i> , 1981
4-5	Derived	Morris and Godfrey, 1979
1.4-4.6	Metamorphosing snow	Denoth <i>et al.</i> , 1979

varied from 2.5 to 7 and were even greater for fine textured soils (Mualem, 1978). Our mean slope of 0.79 can be used to estimate an n value of 4.8.

Effective Porosity

Because effective porosity is inversely related to snow density when the irreducible water saturation is held constant, effective porosity declined from 0.65 to 0.52 as density increased from 330 to 440 kg/m³ during the spring melt and densification of the snowpack. Accurate estimation of effective porosity is dependent on accurate estimations of density and irreducible water saturation. Average density of the snowpack was measured as accurately as possible with an isotopic density gauge 1 to 6 m from the snowmelt lysimeters. In the range of densities encountered in the study, measured densities should have been within ± 20 kg/m³ of the actual density. This level of uncertainty affects calculated effective porosity to the extent of ± 0.02 . While irreducible water saturation was assumed to be 0.07 (Colbeck and Anderson, 1982), it is almost certainly between 0.04 and 0.10. Values of 0.02 and 0.08 have been considered the limits of irreducible water saturation (Ambach *et al.*, 1981). Thus, uncertainty in the calculated effective porosity due to uncertainty in the irreducible water saturation is less than ± 0.03 . Because of the uncertainties due to density measurement and the value of irreducible

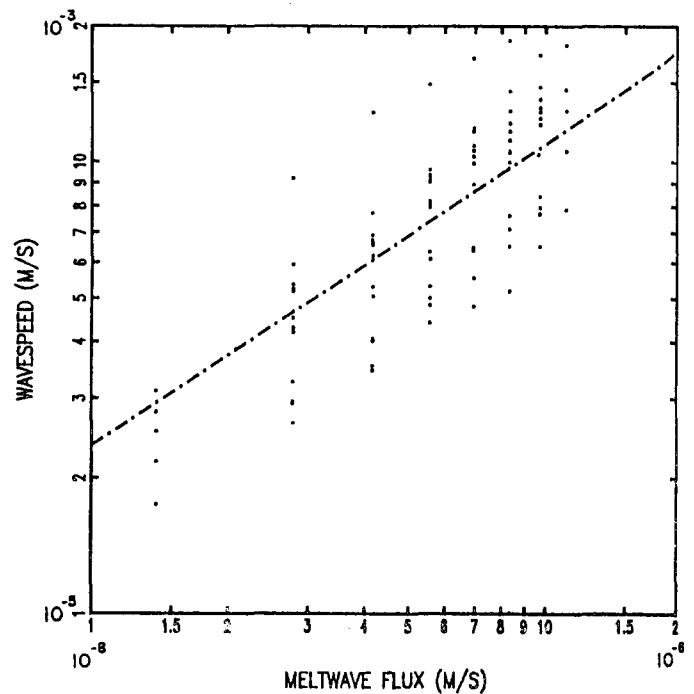


Figure 3. Wavespeeds from fluxes between 0.5 and 4 mm/hr. Line has slope of 0.67, while fitted slope is 0.79.

water saturation, the seasonal changes in the estimated porosity values should be viewed only as trends.

In turn, uncertainty in the calculated effective porosity leads to uncertainty in the permeability. Calculated permeability was found to be fairly sensitive to effective porosity, decreasing from 5.8×10^{-9} to 4.5×10^{-9} m² as effective porosity changed from 0.60 to 0.55 (a density change of 50 kg/m³). Therefore, uncertainties about density and irreducible water saturation contribute an uncertainty₂ to calculated permeability of about $\pm 1.5 \times 10^{-9}$ m² in the range of values encountered.

Permeability

The equivalent snowpack₉ permeability values ranged from 0.3 to 18×10^{-9} m², and agree well with most of the reported values (Table 1). The permeability values showed a strong seasonal trend in both years: permeability decreased as the snowpack transmitted water over time and became more dense (Table 2). The trend was uniform in 1984, with the values changing almost an order of magnitude from March to April. Colbeck and Anderson (1982) also found permeability decreased with increases in density. In 1985, little surface melt occurred until the end of March, and the high value on 3-31-85 may indicate that little water flowed through the snowpack before this time. Further, low peak flux values (less than 3.5 mm/h) may have

compromised the calculational technique somewhat. The snowpack melted out earlier in 1985 than in 1984, but the end-of-melt permeability values were similar.

The ratio parameter, $k^{1/3}/\phi_e$, decreased during both melt seasons, supporting Colbeck's (1978) hypothesis that this parameter characterizes snowpack properties and changes with time. Further, the values in both seasons were close to $2.8 \text{ m}^{2/3}$ when regular daily melt outflows were first observed, and fell to approximately $1.5 \text{ m}^{2/3}$ when the snow depth neared 0.5 m. The differences in this parameter within the pairs of data is of a magnitude comparable to that found by using 1954 CSSL lysimeter data (Colbeck and Anderson, 1982). The technique employed herein is simply not precise enough to eliminate variations of this magnitude, and additional seasons will be required to confirm the observed seasonal trend.

Wave Speed

Wave speeds (time between a given flux at the surface and an equal value of outflow, divided into the snowpack depth) were calculated for fluxes between 1 and 4 mm/hr. On a few of the days, peak flux was less than 4 mm/hr, and only two wave speeds were calculated. In 1984, wave speeds were approximately 6, 10, and $18 \times 10^{-3} \text{ m/s}$ at respective fluxes of 1, 2, and 4 mm/hr in March and declined to about one-half of these values for the same fluxes by May. Wave speeds in March were somewhat higher in 1985 than in 1984 but dropped to essentially the same May values as in 1984 (3, 5, and $9 \times 10^{-3} \text{ m/s}$ at fluxes of 1, 2, and 4 mm/hr, respectively). These May 1985 wave speeds were about one-third of their March counterparts. Jordan (1983) found average wave speeds of 3 to $10 \times 10^{-3} \text{ m/s}$ at fluxes of 1 to 3 mm/hr during the late snowmelt season.

The decline in wave speed over the course of the melt seasons was opposite what might be expected from decreases in porosity alone. Wave speed is inversely related to effective porosity (Colbeck, 1978) so that as porosity declines in the melt season, wave speed should increase. Based on Colbeck's equation for wave speed at a given flux, for a flux of 3.3 mm/hr and a permeability of $0.6 \times 10^{-9} \text{ m}^2$, wave speed increased insignificantly from 23 cm/hr to 26.5 cm/hr for a decline in the effective porosity of 0.65 to 0.55 (Price, 1977). In 1985, as effective porosity dropped from 0.64 to 0.56, we observed a decrease in wave speed from 68 cm/hr to 22 cm/hr at a flux of 3 mm/hr. We hypothesize that the observed decrease in wave speeds is due to the transition from a channel-dominated flow system in the early season to more widespread matrix flow in the later part of the

melt period. If the same surface flux is concentrated in channels of small areal proportion instead of distributed over most of the snow, then flow would be more efficient and faster in the channels than throughout the snow volume. The channels would tend to consist of larger diameter grains (and thus larger pore spaces) and would have higher water saturations than the entire mass of snow. Both of these conditions favor increased flow efficiency.

CONCLUSIONS

Equivalent permeabilities of spring snowpacks at a Sierra Nevada site declined from $5 \text{ to } 10 \times 10^{-9} \text{ m}^2$ at the onset of continued melt to about $0.5 \times 10^{-9} \text{ m}^2$ before snow cover disappeared. Similarly, the parameter $k^{1/3}/\phi_e$ decreased from about $2.8 \times 10^{-3} \text{ m}^{2/3}$ to about $1.5 \times 10^{-3} \text{ m}^{2/3}$ over the two melt seasons. A value of this parameter, interpolated from the results presented here, could be used in meltwater routing procedures, as suggested by Colbeck (1978). The exponent n, relating intrinsic permeability and effective saturation to unsaturated permeability, was found to be higher than the commonly used value of 3 and to be strongly dependent on the flux range chosen for analysis. As expected, the effective porosity decreased during both seasons, but by only a small amount.

The results presented here support Colbeck and Anderson's (1982) conclusion that deep Sierra Nevada snowpacks drain more slowly than reported by Bengtsson (1981). However, they seem to drain two to three times more rapidly in the early part of the melt season than they do near the end of the season. We hypothesize that as flow becomes more uniform throughout the snowpack with aging, flow is less efficient and a greater volume of snow drains at a slower rate than when channels dominate the flow. Thus, channeling, in addition to layering and densification, must be considered in defining an equivalent permeability for the snow cover.

NOTATION

$dz/dt _u$	wave speed or rate of propagation of a given value of u.
k	saturated permeability, m^2 .
k_w	unsaturated or relative permeability to water, m^2 .
n	exponent, often assumed to equal 3.
S_e	effective saturation.
S_w^e	water saturation as fraction of pore volume.

S_{wi}	irreducible water saturation.
g	gravity, 9.8 m/s.
t	time, s.
u	volume flux of water, m^3/m^2-s .
z	depth, m.
ρ_i	ice density, $0.917 Mg/m^3$.
ρ	water density, $1 Mg/m^3$.
ρ_s	snow density, Mg/m^3 .
ϕ	porosity.
ϕ_e	effective porosity.
μ	viscosity, $10.1 \times 10^{-4} N-s/m^2$
$\rho g/\mu$	flow factor, $5.47 \times 10^6/m-s$.

REFERENCES

- Ambach, W., M. Blumthaler, and P. Kirchlechner, 1981. Application of the Gravity Flow Theory to the Percolation of Melt Water through Firn. *Journal of Glaciology* 27(95):67-75.
- Anderson, E.A., 1979. Streamflow Simulation Models for Use on Snow Covered Watersheds. *In: Proceedings Modeling of Snow Cover Runoff*, S.C. Colbeck and M. Ray (Editors). U.S. Army Cold Regions Research and Engineering Laboratory (CRREL), Hanover, New Hampshire. pp. 336-350.
- Bader, H., R. Haefeli, E. Bucher, J. Neher, O. Eckel, and C. Thams, 1954. Snow and Its Metamorphism. U.S. Army Corps of Engineers, SIPRE Translation 14. 303 pp.
- Bengtsson, L., 1981. Snowmelt Generated Runoff from Small Areas as a Daily Transient Process. *Geophysica* 17(1-2):109-122.
- Colbeck, S.C., 1972. A Theory of Water Percolation in Snow. *Journal of Glaciology* 11(63):369-385.
- Colbeck, S.C., 1978. The Physical Aspects of Water Flow through Snow. *Advances in Hydroscience* 11:165-207.
- Colbeck, S.C., 1979. Water Flow through Heterogeneous Snow. *Cold Regions Science and Technology* 1:37-45.
- Colbeck, S.C. and E.A. Anderson, 1982. The Permeability of a Melting Snow Cover. *Water Resources Research* 18(4):904-908.
- Colbeck, S.C. and G. Davidson, 1973. Water Percolation through Homogeneous Snow. *In: The Role of Snow and Ice in Hydrology: Proceedings of the Banff Symposium, UNESCO-IAHS*. pp. 242-256.
- Conway, H. and J. Abrahamson, 1984. Air Permeability as a Textural Indicator of Snow. *Journal of Glaciology* 30(6):328-333.
- Denoth, A. and W. Seidenbusch, 1978. A Method for the Determination of the Hydraulic Conductivity of Snow. *Zeitschrift fur Gletscherkunde und Glazialgeologie* 14(2):209-213.
- Denoth, A., W. Seidenbusch, M. Blumthaler, and P. Kirchlechner, 1979. Some Experimental Data on Water Percolation through Homogeneous Snow. *In: Proceedings Modeling Snow Cover Runoff*, S.C. Colbeck and M. Ray (Editors). U.S. Army CRREL, Hanover, New Hampshire. pp. 253-356.
- Dunne, T., A.G. Price, and S.C. Colbeck, 1976. The Generation of Runoff from Subarctic Snowpacks. *Water Resources Research* 12(4):677-685.
- Gerdell, R.W., 1954. The Transmission of Water through Snow. *Transactions American Geophysical Union* 35:475-485.
- Jordan, P., 1983. Meltwater Movement in a Deep Snowpack 1. Field Observations. *Water Resources Research* 19(4):971-978.
- Kattelmann, R.C., 1986. Measurements of Snow Layer Water Retention. *Proceedings AWRA Cold Regions Hydrology Symposium*. (accepted)
- Kattelmann, R.C., B.J. McGurk, N.H. Berg, J.A. Bergman, J.A. Baldwin, and M.A. Hannaford, 1983. The Isotope Profiling Snow Gage: Twenty Years of Experience. *In: Proceedings of the 51st Western Snow Conference*. pp. 1-8.
- Kuroiwa, D., 1968. Liquid Permeability of Snow. *IAHS Publication* 79. pp. 380-391.
- Morris, E.M. and J. Godfrey, 1979. The European Hydrological System Snow Routine. *In: Proceedings Modeling of Snow Cover Runoff*, S.C. Colbeck and M. Ray (Editors). U.S. Army CRREL, Hanover, New Hampshire. pp. 269-278.
- Mualem, Y., 1978. Hydraulic Conductivity of Unsaturated Porous Media: Generalized Macroscopic Approach. *Water Resources Research* 14(2):325-334.
- Price, A.G., 1977. Snowmelt Runoff Processes in a Subarctic Area. *McGill University Sub-Arctic Research Paper* 29. 106 pp.
- Shimizu, H., 1970. Air Permeability of Deposited Snow. *Low Temperature Science, Series A* 22:1-32.
- Smith, J.L., 1974. Hydrology of Warm Snowpacks and their Effects upon Water Delivery...Some New Concepts. *In: Advanced Concepts in the Study of Snow and Ice Resources*. H.S. Santeford and J.L. Smith (Editors). National Academy of Sciences, Washington, D.C. pp. 76-89.
- Tucker, W.B., III and S.C. Colbeck, 1977. A Computer Routing of Unsaturated Flow through Snow. *U.S. Army CRREL Special Report* 77-10, Hanover, New Hampshire. 39 pp.
- Wankiewicz, A., 1979. A Review of Water Movement in Snow. *In: Proceedings Modeling Snow Cover Runoff*. S.C. Colbeck and M. Ray (Editors). U.S. Army CRREL, Hanover, New Hampshire. pp. 222-252.

IN SITU ELECTRICAL MEASUREMENTS OF SNOW WETNESS IN A DEEP SNOWPACK
IN THE SIERRA NEVADA SNOW ZONE OF CALIFORNIAJames A. Bergman¹

ABSTRACT: A twin-disc sensor that measures changes in snow capacitance has been developed for the determination of in situ snow wetness. In its current form the sensor is capable of measuring water in transit from rain-on-snow and spring melt, surface diurnal melt water flux, and the gradual wetting of snow as the winter season progresses. Wetness increases of up to 2 percent by volume and subsequent snowpack drainage has been measured during and after rain-on-snow. Surface diurnal melt water flux ranging from 0.5 to 2 percent volume wetness has been measured consistently by sensors near the snow surface. All buried sensors indicated an average seasonal progressive snow wetting of about 2.5 percent volume wetness. A sensor was calibrated in snow by spraying incremental additions of water on a sensor-snow block. A good linear response was indicated by an r^2 of 0.998. Based on snow calibration values, sensor volume wetness compared favorably with freezing calorimetry volume wetness. After 35 comparative measurements, wetness from the sensors averaged 2.6 percent while calorimetry volume wetness averaged 2 percent.

(KEY TERMS: capacitance; snow wetness; snow; free water; Sierra Nevada.)

INTRODUCTION

The threat of damaging floods from excessive snowpack outflow caused by rain-on-snow and excessive spring melt combined with ever increasing demands on the variable Sierra Nevada snow zone water supply, have created a need for in-place monitoring of the more elusive snow-water relationships. Snow wetness (free water, liquid water) and water flow routing through snow are two of the most difficult snowpack properties to measure. During rain-on-snow and spring melt, the speed at which these two components increase may indicate the severity of snowpack outflow and when it may occur.

The metamorphic state of a snowpack can significantly affect the quantity and timing of snowpack outflow. Internal snowpack structure and layer development are a potential hinderance to water flow through snow (Berg, 1982). The structure of layers in the early winter snowpack may not be as complicated as the structure that develops by early spring. By mid-to-late season there may be as many as 10 to 15 major storm layers and associated ice lenses, creating a highly structured snowpack that is more likely to retard rain and meltwater flow. Flow channel development may reduce the time it takes for rain and meltwater to reach the soil (Kattelmann, 1985). Rain-on-snow in the Sierra Nevada snow zone occurs mostly in December and January, before snowpack structure becomes very complicated. Flow channels produced by rainwater flowing in this portion of the snowpack may remove some of its retarding effect on subsequent water flow. This inconsistent snowpack water flow and the seasonal variation in snow accumulation create a need for methods that measure water in transit and suspended liquid water within the snowpack.

Most measurements of snow wetness, including water in transit (surficial meltwater, rainwater) employ sampling methods that destroy the snowpack. They include heating and freezing calorimetry, dilution of an acid or dye, centrifugal extraction, and portable plate and comb shaped capacitors (resonators) of various sizes. During the sampling procedure, the extraction of the snow sample interrupts the natural water flow paths within the snowpack. This compromises the integrity of the snowpack and excludes that portion from further free-water analysis. The majority of these methods are excellent for point wetness measurements and sensor calibration but they cannot be used to continually track in situ snow wetness and water in transit throughout the winter.

During the past decade, methods have been developed to measure in situ snow wetness in essentially undisturbed snow. Linlor (1980)

¹Hydrologist, Pacific Southwest Forest and Range Experiment Station, Central Sierra Snow Laboratory, P.O. Box 66, Soda Springs, California 95728.

developed an electromagnetic system for measuring snow wetness based on the attenuation of microwaves in the 4 to 12 GHz frequency range. Over these frequencies, the attenuation of microwaves by snow varies proportionally with the amount of liquid water associated with the ice. A system of horizontally opposed transmitter-receiver pairs was installed at different heights above the soil surface before snowfall to track the movement of free water with the sensor array. Although this method showed promise, it was complex, inconsistent and data reduction was difficult. Linlor also tried to determine gross snow wetness by placing a transmitter on the soil surface and measuring the vertical microwave attenuation by the snowpack. The main problem encountered with this method was the deflection/reflection of the microwave beam by intervening ice lenses. The results were inconsistent and the measurements were difficult to obtain.

Snow wetness has been studied by measuring changes in the electrical potential or capacitance of snow (Ambach and Denoth 1972; Denoth, et al. 1984; and Linlor and Smith 1974). Snow capacitance was measured by inserting closely spaced parallel plates of various sizes into the snow. Radio frequencies used varied between 1 and 20 MHz. At frequencies below 10 MHz, grain size and shape combined with the quantity of liquid water present to influence the capacitance reading. At frequencies above 10 MHz, the effect of grain size and shape was effectively eliminated. The parallel plate sensors work well when inserted into the snow, but because they are destructive, they do not appear to be suitable for in situ wetness measurements.

This paper describes the development of a permanently mounted electrical instrument with widely spaced discs that measures in situ snow wetness by monitoring changes in snow capacitance. In theory, the instrument was modeled after hand held plate resonators.

THEORY

Dry snow, as a conductor, has a specific capacitance for a given induced charge. The ability of snow to carry an induced charge is determined by its wetness. Therefore, given a specific charge, the potential of snow to carry this induced charge should be directly related to the amount of liquid water in it. Capacitance may be stated as the ratio of a charge on a positive plate of a condenser to the difference of potential from a corresponding negative plate. Thus, snow wetness can be determined by measuring capacitance between two closely spaced parallel plates or by measuring the

field capacitance surrounding thin discs.

The electrical field flux surrounding a thin disc is the basis for this sensor design. The field extends outward from the flat outer portion of each disc and then loops back toward the negative side of the sensor, in this case the mast (Figure 1). Field flux from the inner portion of the discs has a more direct path to the negative side of the sensor. Significant field flux occurs within approximately 3 radii of each disc and thus covers a larger volume of snow than the measurement field of parallel plate capacitors.

SENSOR DESIGN AND MEASUREMENT METHODS

A twin-disc sensor was designed to measure a large (0.04 m^3) volume of snow while withstanding snow loads of up to 0.15 Kg/cm^2 . The discs are

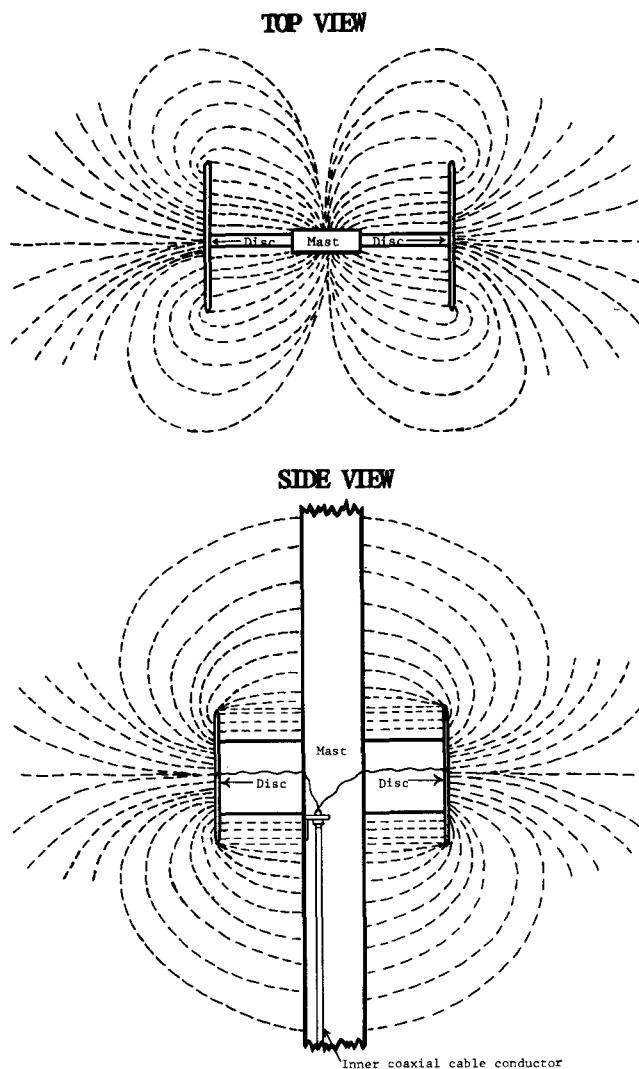


Figure 1. Three Dimensional Electrical Field Surrounding a Twin-Disc Sensor.

fabricated from T6 aluminum, 3 mm thick and 10 cm in diameter. An acrylic spacer, 2 cm thick and 10 cm long, attaches and electrically isolates each disc on opposite sides of a T4 aluminum channel mast (Figure 1). The discs may be considered as the positive side of the sensor and the mast the negative side.

During the 1983-84 winter, eight sensors were mounted 61 cm apart on a 5 meter high mast, beginning at 30 cm above the soil surface. During the 1984-85 winter, each sensor was mounted on its own mast and three measurement depths were duplicated. For the 1985-86 winter, three of the sensors had their 10 cm discs replaced with discs 15 cm in diameter to increase the resolution of the sensor.

The capacitance field surrounding each twin-disc sensor is measured by a Hewlett-Packard, Model 4342A, Q meter. (Trade names and commercial products are mentioned only for information. No endorsement by the U.S. Department of Agriculture is implied.) It is a stable solid state voltmeter which is connected across an internal variable capacitor (portion of the tuned circuit), to measure the reactive voltage in terms of the circuit Q. The coil portion of the tuned circuit is connected externally and represents the unknown to be measured. By inserting low impedance in series with the coil and high impedance in parallel with the capacitor, the parameters of the unknown components (twin-disc sensor) can be measured in terms of their effect on circuit Q and resonant frequency in units of picofarads (pf). Accuracy of the Q meter capacitance circuit is ± 0.1 pf.

To minimize distortion of the capacitance readings, the effect of the coaxial transmission line on signal stability was determined. Ideally, the signal will not be distorted if the standing wave ratio (SWR) of the transmission line remains below 0.25. Standing wave ratios of 0.25 to 0.50 may cause a slight distortion of the capacitance readings. During winter 1983-84 a wavelength of 555 meters, which corresponds to a frequency of 5.4 KHz, was used to measure snow capacitance. The SWR of the transmission lines, whose length varied from 8.3 to 12.6 meters, was 0.015 to 0.023. The frequency of 10.7 MHz, which corresponds to a wavelength of 30 meters, was used in winter 1984-85 and is being used for 1985-86. At this frequency, SWR's for the signal transmission lines vary from 0.27 to 0.42 indicating a possibility for distortion of the capacitance readings.

Distortion caused by signal line SWR's above 0.25 should remain relatively constant and be directional. If this is the case, then capacitance readings from all sensors will be slightly distorted in one direction only, causing the measurement peak

to shift in the direction of the distortion. This should not significantly affect sensor response to changes in wetness.

Capacitance readings may also be influenced by the size and shape of snow particles. Because snow metamorphosis is continual, its effect may vary and be omnidirectional. And because the direction in which the measurement peak shifts is not known, recorded sensor response to changes in wetness is somewhat unreliable. For this reason, frequencies above 10 MHz are used for measuring snow capacitance.

SENSOR CALIBRATION

Since all sensors are made from the same materials, the calibration results from one twin disc sensor is used to represent all sensors. In February 1984, one sensor attached to the center of a 76 cm portion of the mast material, was inserted into a cubic meter box of kiln dry fine sand. Measured amounts of water in increments equal to 1.7 percent by volume, were added to the sand until a maximum detectable wetness of about 7 percent was reached. Due to scale limitations, the Q meter could not accurately detect changes beyond 7 percent volume wetness in sand. After each incremental addition, the admixture was stirred to distribute the moisture evenly. At each wetness level capacitance measurements were continually made until sensor variation and instrument drift were accounted for (Table 1). A plot of the sand wetness calibration values indicated a good linear fit (Figure 2). An R^2 of 0.822 denotes the relationship of sand wetness to capacitance change. Due to Q meter detection limits, this correlation could not be continued past 7 percent volume wetness. The average capacitance change for each 1 percent volume wetness increase in sand is 12.1 pf.

During February 1985 the sensor that was calibrated in sand was tested for response to liquid water in snow. After completely saturating a 0.027 m³ snow block, a minimum capacitance reading was obtained. Capacitance readings were then obtained after a 45 minute drainage period and again after overnight drainage. Response was quite abrupt when a large quantity of water was applied (Table 2). After 45 minutes, capacitance values were close to those at the beginning of the test.

In early March 1985, the same sensor was calibrated in a 46 cm by 46 cm by 31 cm volume (0.064 m³) of moderately dry snow. Water was applied with a small adjustable hand sprayer in increments equivalent to 0.5 percent volume wetness or 320 ml. After each application of water, capacitance values were observed until a minimum

TABLE 1. Sensor Calibration, in Sand, at a Frequency of 5.4 KHz.

Wetness Percent Volume	No. of Replicate Meas.	Meas. Mean (pf)	Total Capacitance Change (pf)	Difference Between Meas.	Standard Deviation S_x	Standard Error of Mean $S_{\bar{x}}$
0	5	444.6	0	0	0.075	0.033
1.73	6	422.5	22.1	22.1	0.373	0.152
3.46	6	395.8	48.8	26.7	1.377	0.562
5.19	27	373.6	71.0	22.2	6.226	1.198
6.92	61	361.5	83.1	12.1	6.583	0.843

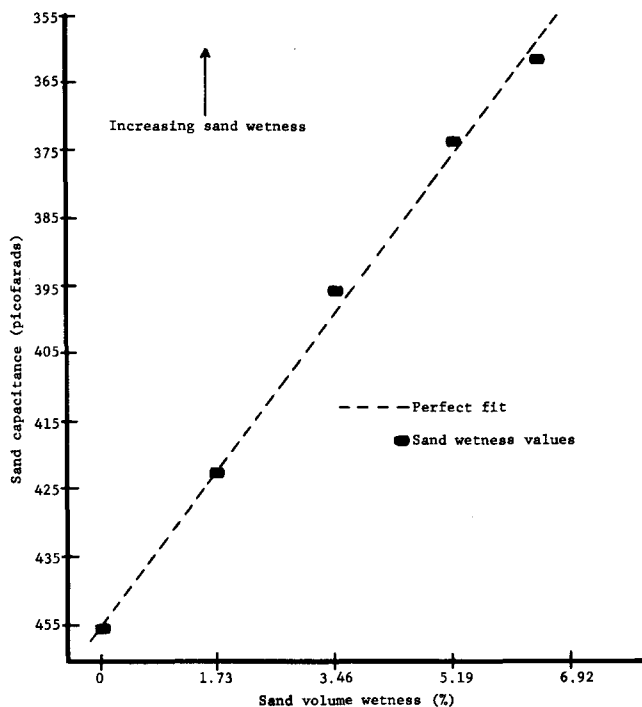


Figure 2. During Sensor Calibration in Sand, Capacitance Change and Sand Volume Wetness were Closely Correlated.

TABLE 2. Sensor Response Test, in Snow, at a Frequency of 10.7 MHz.

Snow Wetness	Measured Capacitance (pf)	Total Capacitance Change (pf)	Difference Between Measurements
Air	181.6	0	0
Mod. Dry Snow	160.2	21.4	21.4
Saturated Snow	91.5	90.1	68.7
Drain 45 Min.	145.1	36.5	-53.6
Drain Overnight, Sub-freezing	167.0	14.6	-21.9

reading was obtained. Application ceased after snow wetness reached 3.75 percent by volume. The sensor-snow block was measured after draining for 45 minutes and after draining overnight at

subfreezing air temperatures. The relationship between wetness and capacitance change showed excellent linearity ($R^2=0.994$) (Figure 3, Table 3). The capacitance reading after the sensor-snow block had drained for 45 minutes indicated that the snow retained about 1 percent by volume of the applied water. But, overnight drainage at subfreezing temperatures reduced snow wetness to below the initial level at which snow calibration began. Snow drainage can be rapid (Tables 2 and 3). The capacitance values were very close after draining for 45 minutes and overnight. Air and overnight drainage capacitance values, in both tests, were almost identical, indicating good repeatability of the sensor-snow measurement system. The average capacitance change for each 1 percent volume wetness increase in snow was 3.75 pf.

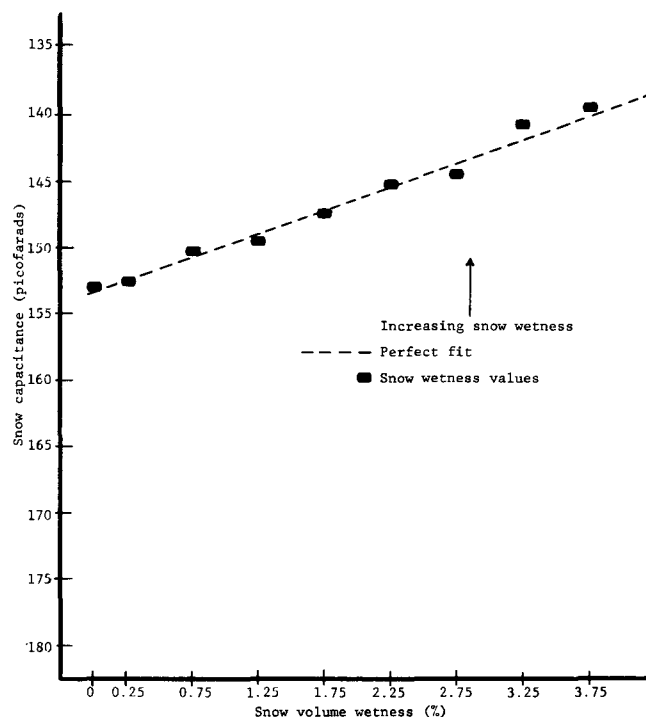


Figure 3. During Sensor Calibration in Snow, Capacitance Change and Snow Volume Wetness were Directly related.

TABLE 3. Sensor Calibration, in Snow, at a Frequency of 10.7 MHz.

Wetness Percent Volume	Measured Capacitance Change (pf)	Total Capacitance Change (pf)	Difference Between Measurements
Air	181.7	0	0
Mod. Dry Snow	153.1	28.6	28.6
0.25	152.7	29.0	0.4
0.75	150.7	31.0	2.0
1.25	149.0	32.7	1.7
1.75	147.1	34.6	1.9
2.25	145.6	36.1	1.5
2.75	144.0	37.7	1.6
3.25	141.4	40.3	2.6
3.75	139.0	42.7	2.4
Drain 45 Min.	148.2	33.5	-9.2
Drain Overnight, Subfreezing	165.6	16.1	-17.4

Results of the sand and snow calibrations show that sensor response to wetness change is much greater in sand than in snow. Sensor response is

influenced by the dielectric constant of the measured material. The dielectric constant of sand (quartz) is about 4.2 while that for snow (ice) is about 88. This may cause a difference in the electrical absorptivity of the two materials when mixed with water. Sand and snow have dissimilar water retention properties, and surface tension characteristics. This may cause more water to be retained by sand for a given volume, resulting in greater sensor response.

Because snow is the measured medium, wetness values from the calibration in snow will be used.

MEASUREMENT SITE

Capacitance is being measured at the USDA Forest Service's Central Sierra Snow Laboratory (CSSL), located at 2100 m elevation in the north central Sierra Nevada of California (Figure 4). The influence of maritime air masses at this location cause winters of long duration and deep snowpacks. Snow comprises about 85 percent of the total yearly precipitation. Snowstorms are usually large, intense and of low wetness. Midwinter rain-on-snow normally occurs at least once per season. The

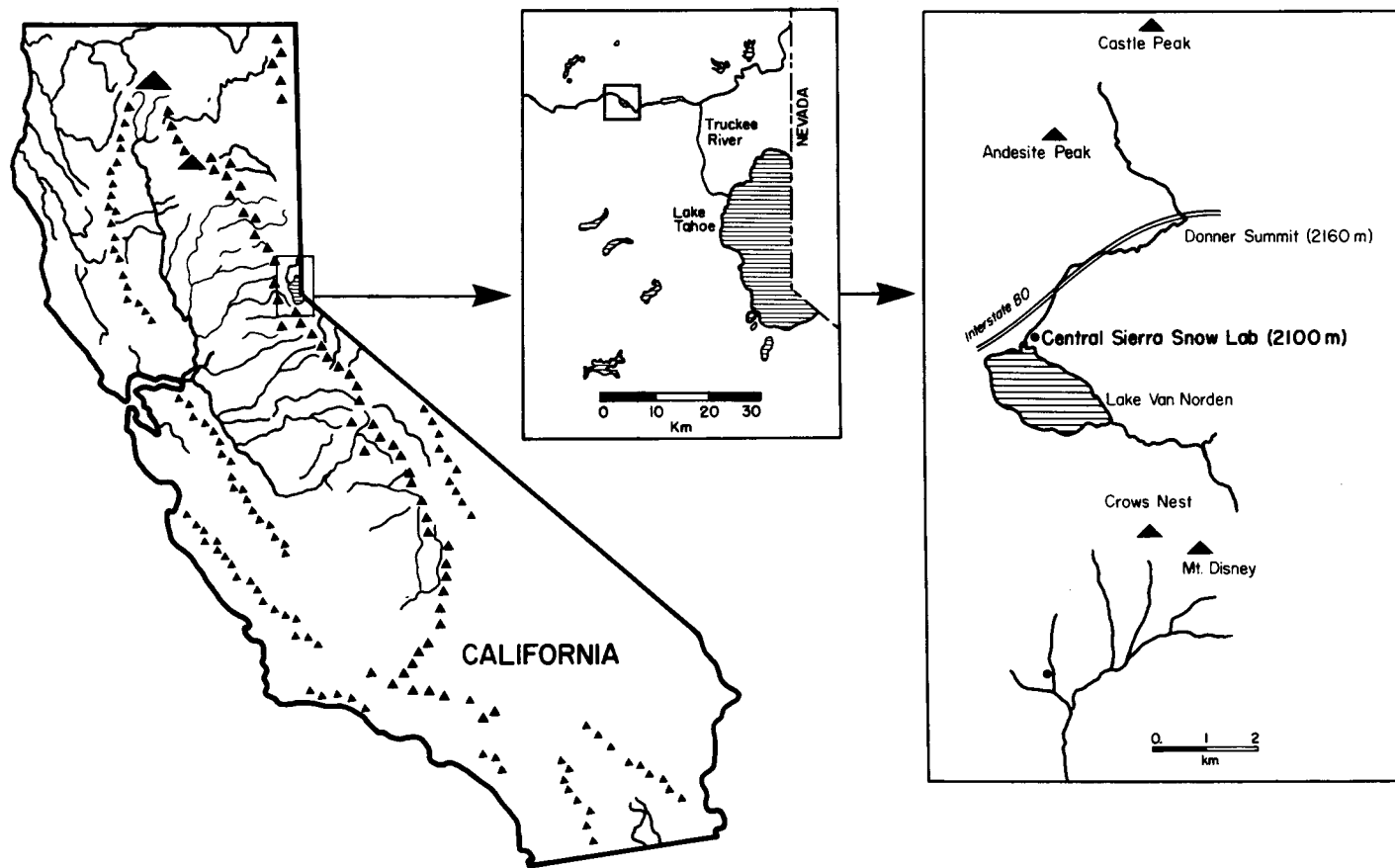


Figure 4. The Central Sierra Snow Laboratory is Located at 2100 m Elevation, in the North Central Sierra Nevada, Near Soda Springs, California

seasonal snowpack begins to accumulate in November, with major accumulation from January through March. An average peak snow depth of 305 cm and snow water equivalent of 90 cm is reached by early April.

RESULTS AND DISCUSSION

1983-84 Snow Season

Eight sensors were installed on a 5 m high mast. Initial data indicated that the buried sensors responded to a wetness increase, from water in transit, during a 3.2 cm rain-on-snow event in late December 1983. Three sensors located at 30 cm, 90 cm, and 150 cm above the soil surface showed an increase in wetness (capacitance decrease) during rainfall (Figure 5). The sensor nearest the snow surface decreased by 8.9 pf, which is equivalent to a 2.4 percent volume wetness increase when based on snow calibration values. The sensor nearest the soil surface decreased by 2.4 pf, indicating a liquid water increase of 0.65 percent volume wetness. And, the sensor buried midway in the snowpack showed a 6.1 pf decrease, for a 1.6 percent increase in volume wetness. After rain ceased, the sensors regained about two-thirds of the lost capacitance indicating that some snowpack drainage had occurred.

Decreasing wetness from the snow surface downward may be due to the establishment of water flow paths (Kattelmann, 1985). The greater number of surficial flow channels caused by the mechanical

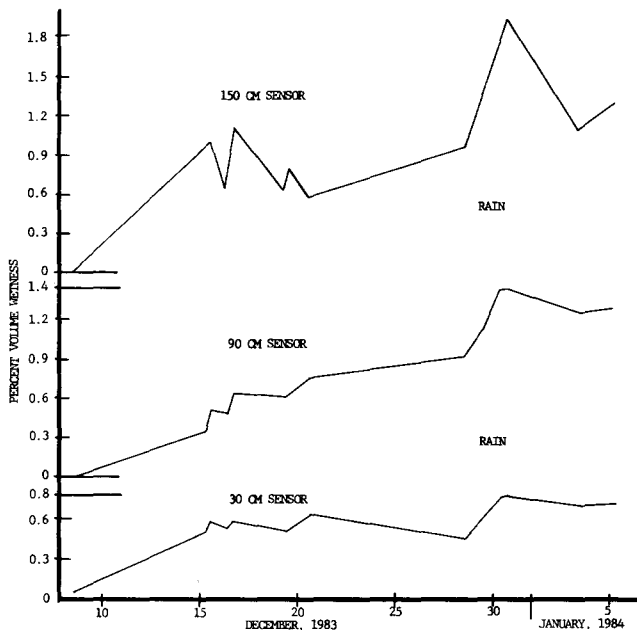


Figure 5. Three Buried Sensors responded to a 3.2 cm Rain-On-Snow event in December 1983.

action of rainfall may be considerably reduced by the time the rainwater reaches the lower portions of the snowpack. As the smaller flow pathways combine and form larger channels, the distance between them increases causing liquid water to become more difficult to detect because of a greater amount of dry snow between the wet pathways. Therefore, more than one sensor at each level may be necessary to monitor suspended and flowing water accurately.

Freezing calorimetry measurements were made during May to check sensor operation (Table 4). Sensor wetness was determined by subtracting snow capacitance from capacitance in air, assuming that the capacitance of totally frozen dry snow is close to that of air. Based on snow calibration values, data indicate good correlation between average wetness from all sensors and average wetness from freezing calorimetry. These results need to be put in the proper context: snow samples used in freezing calorimetry were obtained from an area of snow 10 m away from the sensors, and freezing calorimetry wetness may vary as much as ± 0.5 percent by volume because of user error and equipment limitations (Bergman, 1978). The above factors are likely to cause most of the variation between individual comparative measurements.

One of the basic problems of mounting a large number of sensors on a single mast is weight and sun cupping of snow around it. Due to reflected solar radiation, large melt cups formed around the mast midway through the winter. The melt cup may have affected the flow of water around the sensor mast by acting as a large flow path, causing overmeasurement. The melt cup probably reduced the magnitude of measured diurnal meltwater flux because the sensor became exposed while it was below the snow surface. The height of the mast combined with the weight of the sensors caused considerable swaying in high winds. This tended to cause air gaps around the sensor nearest the snow surface, resulting in lower wetness readings at that level.

The temperature of the Q-meter was found to affect sensor capacitance values. Colder Q meter temperatures resulted in lower capacitance readings and vice versa. To compensate for this effect, capacitance values from a twin-disc sensor always in air were averaged. Capacitance values from all other sensors were adjusted according to the deviation of the sensor in air from its average over the measurement season.

1984-85 Snow Season

To eliminate the influence of sun cupping and swaying of the mast, each sensor was mounted on top

TABLE 4. Comparison of Sensor Wetness and Wetness from Freezing Calorimetry.

Date	Height Above (cm)	Sensor wetness Sand Percent Volume	Snow Percent Volume	Calorimetry Wetness Percent Volume
-Measured at a frequency of 5.4 KHz.-				
4/20/84	30	0.6	1.9	1.4
π	90	0.7	2.2	0.4
π	210	0.5	1.5	2.4
4/23/84	30	0.8	2.1	0.4
π	90	0.8	2.7	2.1
4/27/84	30	0.6	2.1	0.9
π	90	0.7	2.3	2.5
4/30/84	30	0.7	2.1	3.1
π	90	0.8	2.4	1.3
5/02/84	30	0.7	2.1	1.0
π	90	0.7	2.3	0.7
5/04/84	30	0.7	2.3	0.9
π	90	0.7	2.3	0.7
5/10/84	30	0.8	2.4	2.7
5/11/84	30	0.8	2.5	3.7
5/16/84	30	0.8	2.5	1.3
Partial Ave.		0.7	2.3	1.7
-Measured at a frequency of 10.7 MHz.-				
4/18/85	30	0.9	3.0	2.5
π	30	1.0	3.1	2.5
π	90	0.8	2.7	2.0
π	90	1.2	3.7	2.0
π	30	0.9	3.0	3.6
π	30	1.0	3.1	3.6
π	90	0.9	2.7	3.3
4/19/85	30	0.9	2.9	3.1
π	30	1.0	3.1	3.1
π	90	0.8	2.5	2.9
4/22/85	30	0.9	3.0	1.8
π	30	1.0	3.1	1.8
π	90	0.7	2.3	2.2
4/26/85	30	0.9	2.9	0.5
π	30	1.0	3.2	0.5
Partial Ave.		0.9	2.9	2.3
Overall Average		0.8	2.6	2.0

of its own mast. Once buried, the mast stopped swaying and the sensor was not exposed until snowmelt. To better represent the snowpack and to check sensor response and repeatability, duplicate measurements were made at 30, 60, and 90 cm above the soil surface (Table 4). Excavation of a sensor near the snow surface indicated that sensor-snow contact was excellent. All disc, spacer, and mast surfaces showed complete contact with the snow. Even the snow directly below the 2 cm thick spacer maintained good contact. Apparently, the lateral pressure from the surrounding snowpack exerted

enough force to close the gap that formed during settling.

Throughout the winter, all of the buried sensors indicated a slow increase in wetness up to 1.5 percent by volume (Figure 6). As the snow

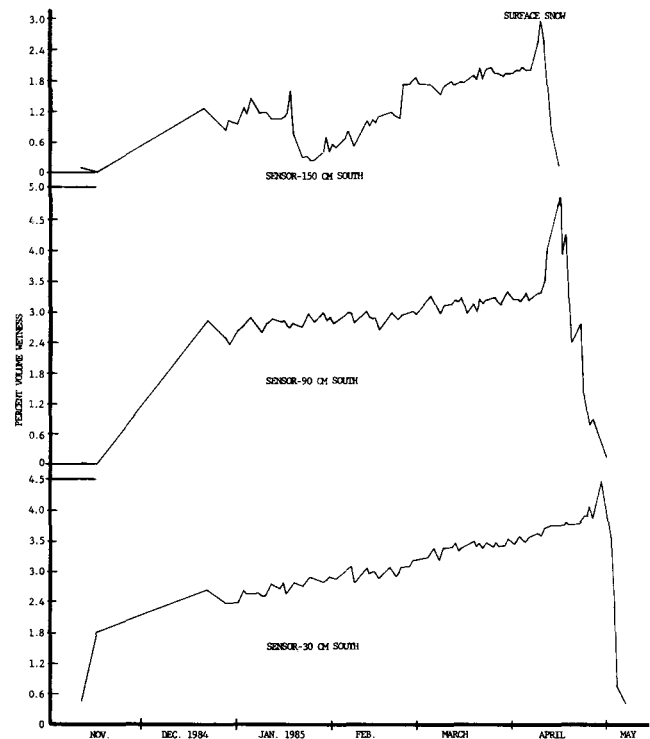


Figure 6. Snow Volume Wetness Gradually Increased During the 1984-85 winter.

surface neared each sensor, it showed a diurnal liquid water flux of up to 2 percent by volume (Figure 7). This wetness flux is attributed to meltwater infiltration and drainage during springtime freeze/thaw and is corroborated by basal outflow data collected from six melt pans situated

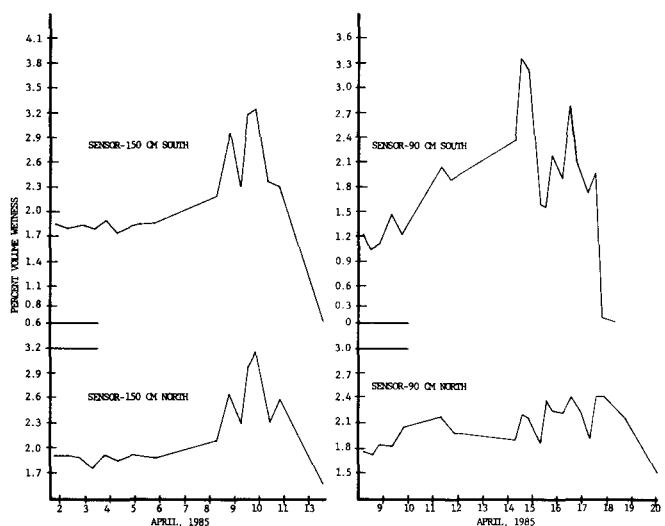


Figure 7. Four Twin-Disc Sensors Responded to Surface Diurnal Meltwater Flux.

beneath the snow, on the soil surface.

During April, wetness from sensors and wetness from freezing calorimetry were compared. Data indicate good sensor response when snow calibration values are used (Table 4), but sensors appear to undermeasure when sand calibration values are used.

Wetness values were higher in 1985. This may be due to several factors other than an actual increase in liquid water. Because the measurement frequency was changed from 5.4 KHz to 10.7 MHz, the influence of the size and shape of the ice particles was eliminated, possibly increasing measured wetness. Individual sensor/mast mounting eliminated mast sway and sun cupping from solar re-radiation, allowing for better sensor-snow contact and thus higher wetness readings.

1985-86 Snow Season

The sensor and monitoring system were refined for this winter season. Three of the sensors retain the original 10-cm diameter discs while three others, at matching levels, have 15 cm discs. The larger discs should increase the resolution of the sensor and respond more quickly to changes in wetness. A chart recorder is being used to continuously monitor the sensor nearest the snow surface, to track diurnal variations in wetness and to measure wetness during unattended periods.

Data collected so far this season indicate a gradual increase in snow wetness (Figure 8). Wetness increase appears to be about 1 percent greater from the two sensors with the 15 cm diameter discs. This implies that larger diameter discs have a higher degree of response to the presence of

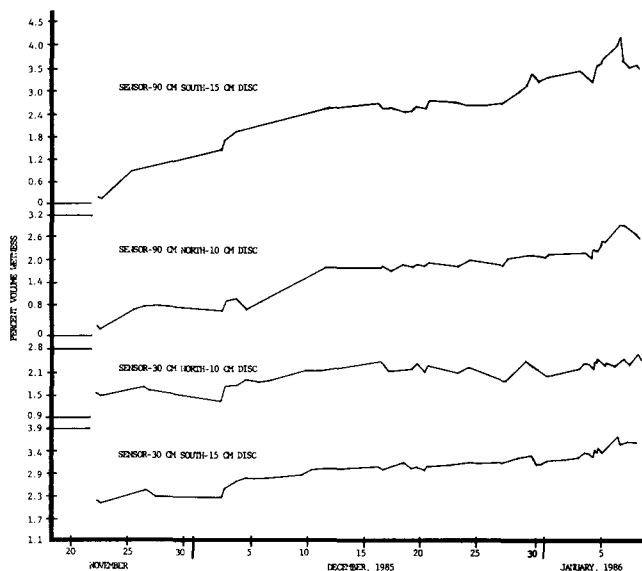


Figure 8. Snow Volume Wetness Gradually Increases During the 1985-86 Winter.

liquid water. The actual wetness values may not be as meaningful until a calibration of the sensor with the 15 cm discs is made.

The magnitude of wetness fluctuation caused by diurnal freeze/thaw did not seem to be affected by the difference in the size of the sensor discs (Figure 9). Wetness at the sensor with the 15 cm discs, located 150 cm above the soil surface, did not seem to fluctuate to any greater extent than it did at the sensor with the 10 cm discs. In fact, wetness at the 10 cm disc sensor varied more. High snow surface variability may be the cause for the equal response from the different size sensors, because the sensors are separated horizontally by about 2 m.

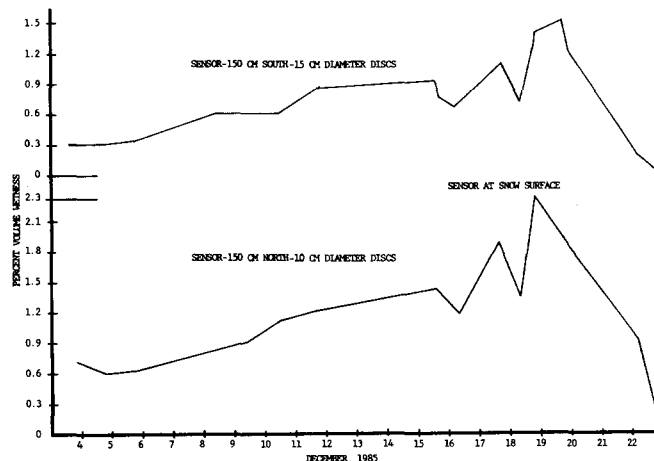


Figure 9. Surface Liquid Water Flux Measured by Different Size Sensors.

Two rain-on-snow events have occurred this season. A 1.9-cm rainfall on December 28, 1985 caused a slight response from the sensor with the 15 cm discs located at 90 cm above the soil surface and a more marked response from the sensors located at the 30 cm level (Figure 10). The detection of increasing wetness and the indication of drainage after the rainstorm were greatest in the deeply buried sensors and indicates that water flow was greater in these areas. Water flow in the upper snowpack was more variable. One sensor responded, while the other did not respond at all. This strengthens the conviction that early season water flow in snow is extremely variable, spotty and may be restricted to flow channels.

A 4.5-cm rainfall on January 5, 1986 caused just the opposite response. Both of the upper level sensors showed a large increase in wetness. More liquid water was indicated by the sensor with the 15 cm discs. The response of the more deeply buried sensors was variable but to a much lesser degree than the shallow sensors. The more intense rainfall probably created more flow paths in the upper half of the snowpack. As the rainwater infiltrated

downward in fewer but larger flow channels, liquid water detection became more difficult. At both levels, the sensors with the 15 cm discs indicated the most liquid water.

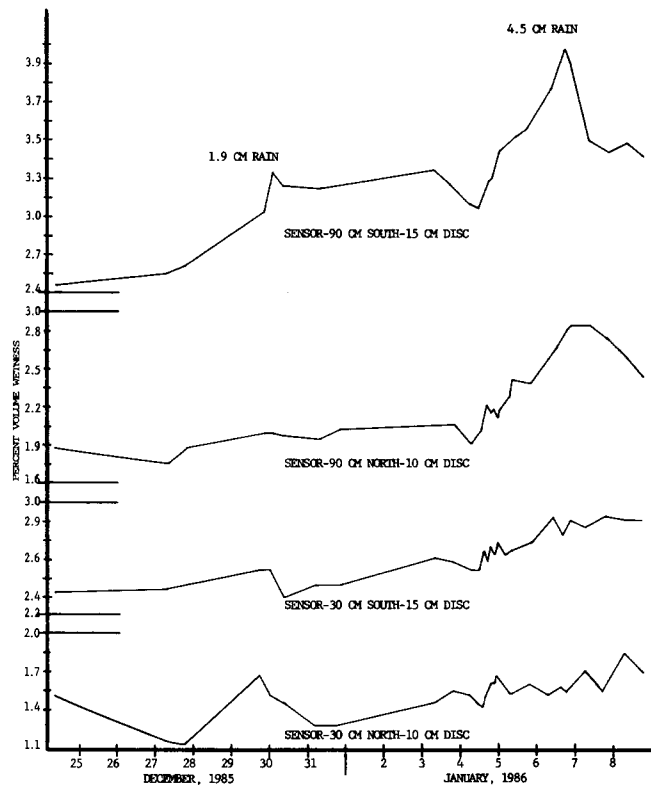


Figure 10. Sensor Response to Two Rain-On-Snow Events During the 1985-86 winter.

CONCLUSIONS

Data from 3 years indicate that buried twin-disc sensors respond to gradual changes in snow wetness and sharp rises in liquid water from rain-on-snow and springtime diurnal freeze/thaw. Snowpack drainage was indicated by the sensors after each rain-on-snow event. Wetness determined by individual sensors compared favorably with that determined by freezing calorimetry, especially when average values were compared. During calibration, one twin disc unit with 10 cm diameter discs showed a good linear response to incremental changes in snow wetness. The sensors are capable of consistent measurements and can indicate lateral variability in snowpack liquid water.

The calibration of the sensor with the 15 cm discs is scheduled for April 1986. Wetness measured by buried sensors will be compared with wetness values obtained by one of the more recent methods, probably acid dilution. If received in time, wetness measurements will be made by A. Denoth's new

hand held resonator and compared with twin-disc sensor wetness. More field work is needed to find the maximum practical disc diameter and the best available recording equipment. A complete remote system is planned for installation in the near future.

REFERENCES

- Ambach, W., and A. Denoth. 1972. Studies on the Dielectric Properties of Snow. *Zeitschrift fur Gletscherkunde und Glazialgeologic* 8(1):113-123.
- Berg, N. H., 1982. Layer and Crust Development in a Central Sierra Nevada Snowpack: Some Preliminary Observations. *In: Proceedings of the Western Snow Conference, Reno, Nevada, pp. 180-183.*
- Bergman, J. A., 1978. A Method for the Determination of Liquid Phase Water in a Snowpack Using Toluene Freezing Calorimetry. Masters Thesis. University of Nevada (Reno).
- Denoth, A., A. Foglar, P. Weiland, C. Matzler, H. Aebischer, M. Tiuri, and A. Sihvola, 1984. A Comparative Study of Instruments for Measuring the Liquid Water Content of Snow. *Journal of Applied Physics* 56(7):2154-2160.
- Kattelmann, R. C., 1985. Observations of Macropores in Snow. *Annals of Glaciology* 6:272-273.
- Linlor, W. I., 1980. Permittivity and Attenuation of Wet Snow Between 4 and 12 GHz. *Journal of Applied Physics* 51(2):2811-2816.
- Linlor, W. I., and J. L. Smith, 1974. Electronic Measurements of Snow Sample Wetness. *In: Advanced Concepts and Techniques in the Study of Snow and Ice Resources. National Academy of Sciences. Washington, DC. pp. 729-739.*

MEASUREMENTS OF SNOW LAYER WATER RETENTION

Richard Kattelmann¹

ABSTRACT: The water holding capacity of a snowpack determines the initial runoff response to snowmelt or rain-on-snow. Early streamflow generated from these events has been difficult to forecast due to limited understanding of snowpack water retention. To identify the likely range of water holding capacity of newly deposited snow layers, water was artificially applied to small plots, and water retention was determined by a change-in-density technique. All of the average water retention values from fresh snow on level ground ranged from 0 to 5 percent by volume. About two-thirds of these values were 2 percent or less. Concurrent applications of dyed water suggested that relatively little (<20 percent) of the snow volume conducted water. Other observations indicated that cold content was not fully satisfied before water left a given snow layer and that losses from water input continued long after snowpack outflow started as the wetted volume increased.

(KEY TERMS: Snowpack water storage, snowpack water movement, snowmelt runoff, rain-on-snow, snow hydrology.)

INTRODUCTION

The capability of snow to retain rain and meltwater is a major uncertainty in streamflow forecasting. This liquid water holding capacity of snow appears to be a highly variable phenomenon depending on the development of the snowpack and its properties at a given time. Estimates of water holding capacity range from 0 to more than 10 percent by volume. The retention capacity of a snowpack within this range can influence streamflow response to rain or melt enormously. This initial response is difficult to forecast.

The fundamental objective of this investigation was to obtain some idea of the range of water retention of fresh snow under a particular application regime. This case study measured the

approximate water holding capacity of 15 storm layers over 3 years. Most of these layers were measured successively over several days as metamorphism progressed.

EARLY STUDIES

A quotation from Snow Hydrology (U.S. Army Corps of Engineers, 1956: 314-315) summarizes the basic principles regarding water holding capacity:

Liquid water entering a cold snowpack freezes within the pack, becomes part of it, and increases the temperature within the snowpack. Snow at 0°C will impound additional water on crystal surfaces and in air spaces as hygroscopic and capillary water. Such water (held against gravity) also becomes part of the snowpack and is retained until the snow has melted. Pockets or cells of snow which are cold and dry may exist in an otherwise wet snowpack as the result of ice planes which have not yet disintegrated to allow the snow to become fully conditioned... Neither the retentivity or permeability of the snow is constant. Therefore, the transmission rates and water storage capacity of the snow vary with the character or the stage of the metamorphism of the individual snow layers."

The first significant work on the water holding capacity of snow was done by Gerdel [1945, 1949, and 1954] at the Central Sierra Snow Laboratory (CSSL). Among Gerdel's contributions was the distinction of surface tension (adsorbed or hygroscopic water) capacity from capillary capacity. He reasoned that new low density snow could retain water as surface films but the voids in such snow were too large to hold much water by capillarity. He argued that high retention of rain in fresh snow (e.g., Church, 1941; Horton, 1941; Wisler and Brater, 1949) should be

¹ Pacific Southwest Forest and Range Experiment Station, USDA Forest Service, P.O. Box 245, Berkeley, California 94701.

considered as a very short-term phenomenon resulting from surface tension or, more likely, ponding of water at the soil surface.

Several other studies included measured or estimated values of water holding capacity, generally as a minor topic [deQuervain, 1973; Wankiewicz, 1979]. Reported measurements and estimates of snowpack water retention vary widely [Table 1]. Wankiewicz [1979] listed the following as factors possibly influencing water holding capacity: drainage interval, snow texture, impurities, impeding layers, isolated dry cells, and attraction of moisture up to a refreezing surface.

deQuervain [1973] listed snow density, grain size, grain shape, specific surface of snow grains, specific number of grain contacts, and pore width as important influences. Snow with fine grains holds more water than does coarse grained snow and "an optimum dry density for maximum storage obviously exists" [deQuervain, 1973: 209].

Only two major studies known to date dealt exclusively with snowpack water holding capacity. Sulahria [1972] measured water retention as the difference between dry density and wet density after artificially applying water to a snowpack and

TABLE 1. Reported Determinations of Water Holding Capacity (WHC)

NEW SNOW			
<u>Description</u>	<u>WHC (by volume)</u>	<u>Determination Method</u>	<u>Source</u>
New	0.5	Residual water content	Gerdel and Codd (1945)
New	0-5(x=1)	Residual water content	Ebaugh and DeWalle (1977)
New	0-12	Change in density	Sulahria (1972)
Dry	1-10	Change in density	Smith and Halverson (1969)
35% density	2	Estimate	U.S. Army C.O.E. (1956)
Cold, arctic	4	Change in density	Marsh (1982)
New fine grain	4.7	Calculated from theory	Colbeck (1975)
20-25% density	5-6	Residual water content	Bengtsson (1981)
32% density, new	6.5	Residual water content	deQuervain (1973)
Above interfaces	10	Residual water content	Wakahama (1975)
13% density	10	Estimate	Kuzmin (1948)
OLD SNOW			
<u>Description</u>	<u>WHC (by volume)</u>	<u>Determination Method</u>	<u>Source</u>
35% density	0	Inflow-outflow	Himmel (1951)
Wet	0-4	Change in density	Smith and Halverson (1969)
Isothermal arctic	0-8	Change in density	Marsh (1982)
Old	0-40	Change in density	Sulahria (1972)
Wet	1-2	Residual water content	Gerdel (1954)
Wet	1-2	Estimate	U.S. Army C.O.E. (1956)
Wet	1-2	Residual water content	Leaf (1966)
Beginning to thaw	1.2	Inflow-outflow	Price, <u>et al.</u> (1979)
Wet	1.2-3.5	Residual water content	Gerdel (1945)
Wet	2-3	Estimate	Boyer and Merrill (1954)
Wet	2-3	Residual water content	Ambach and Howorka (1965)
Wet	2-3	Residual water content	Lemmelé (1973)
50% density 2-3 mm	2.5	Residual water content	deQuervain (1973)
Wet	3-4	Residual water content	Ambach (1965)
Wet	4-5	Residual water content	Bengtsson (1981)
Large gr. refrozen	4.7	Calculated from theory	Colbeck (1975)
45% density	6	Estimate	Kuzmin (1948)
Wet	6	Residual water content	Ambach (1963)
41% density, 1mm	8	Residual water content	deQuervain (1973)
53% density, wet	10	Residual water content	Wankiewicz (1976)

allowing it to drain. Areas of 1 m² in different locations in the Carson Range of the Sierra Nevada were irrigated on 13 occasions. Density, temperature, and grain size before irrigation and wet density after irrigation were measured at 5 cm intervals throughout excavated profiles. Other indices were calculated from meteorological observations at the sites.

Using multiple regression analysis, Sulahria developed a predictive equation for fresh snow and another for metamorphosed subfreezing snow. These equations had R² values, for his data set, of .886 for fresh snow and .755 for old snow. The equations relate water retention to dry density and to several terms involving different temperature measurements. These temperature terms included the mean snow surface temperature, the calculated cold content, average storm temperature, average temperature gradient of the snow layer, and the time weighted temperature [degree-days] of the snow layer.

Sulahria observed ponding of water on discontinuities and layer interfaces, flow along such layers on sloping terrain, and vertical channels conducting water within the snowpack. Fresh snow close to freezing and older snow that fell at low temperatures, but subsequently warmed to near freezing, had maximum water retention capacity. Other important observations were the occurrence of channels in homogeneous dry snow after water was applied; the small wetted volume of very cold snow after irrigation; the presence of subfreezing dry zones after water was observed to flow out of the pack; the warming of these zones within 24 hours; and the predictability of stratigraphic discontinuities within the pack that may retain large quantities of water.

The other known study of water holding capacity was a laboratory investigation of liquid water transmission and retention in new snow [Ebaugh and DeWalle, 1977a and 1977b]. Snow samples were irrigated with a rainfall simulator in a controlled temperature laboratory. Water application rate, snow temperature, rain temperature, sample depth, and time distribution of outflow volume were recorded. Regression equations were developed for water holding capacity, lag time, and routing coefficients. Initial snow density was the best predictor [of those monitored] for water holding capacity. They estimated liquid water holding capacity as

$$24 * [\text{initial snow density (g/cm}^3\text{)}] - 2.91$$

and found that it varied from 0 to 4.95 percent by volume with an average of 1.026 percent.

In the past decade, significant progress was achieved in understanding how liquid water interacts with snow [Colbeck, 1978; Wankiewicz, 1979; and Jordan, 1983a]. Water flows through snow primarily

in response to gravity. The gravity theory of water percolation through snow [Colbeck 1972] uses Darcy's law for one dimensional unsaturated flow:

$$u = -K [d/dz + 1]$$

where the flux u [m/s] is proportional to the sum of the capillary pressure gradient $[d/dz]$ and the gravitational pressure gradient $[1 \text{ m/m}]$. The constant of proportionality $[K]$ is the unsaturated hydraulic conductivity. Gravity drainage is predominant during steady or decreasing flow, and the capillary pressure gradient may be ignored except at very low flux $[10^{-8} \text{ m/s}]$ or at some interfaces [Colbeck, 1974]. Experiments demonstrated that a negligible capillary pressure gradient exists throughout the snowpack as a whole, but significant pressure gradients may occur at major pressure or textural discontinuities [Wankiewicz, 1978b].

In calculations of flux and the speed of the flux wave, the water retention or "irreducible water content" [Colbeck, 1972] becomes important in determining the proportion of the pore volume occupied by mobile [as opposed to retained] water. With greater volumes of water available for flow, the permeability increases rapidly [Colbeck, 1978a]. Values of the irreducible water content are usually assumed [Dunne, et al., 1976; Jordan, 1983a]. Modeling of water flow through snow based on the gravity flow theory has been extended to include the effects of ice layers and flow channels [Colbeck, 1979; Marsh, 1982], increasing flow [Jordan, 1983b], and refreezing and water retention [Bengtsson, 1982].

Inherent variability in snow water holding capacity may be high. The irreducible water content of uniform sand varied widely [Wankiewicz, 1979] based on data from Mualem [1978]. Additionally, water holding capacity should not be assumed to be a constant quantity. The presence of liquid water induces metamorphism of the snow grains [Wakahama, 1968], which in turn alters the ability of the snowpack to retain water against gravity. This grain growth and resultant increase in pore sizes reduce the amount of water that can be held by capillary forces and also increase the permeability of the snow to water [Marsh, 1982]. Therefore, water that is initially held may slowly be released as the physical structure of the snow changes.

STUDY AREA AND CONDITIONS

The study was conducted at the Central Sierra Snow Laboratory [CSSL], a facility of the Pacific Southwest Forest and Range Experiment Station near Soda Springs, California. The CSSL is located near the crest of the Sierra Nevada at 2100 m where Interstate Highway 20 crosses the range near Donner

Pass. The area is subject to a maritime climatic influence and accumulates deep seasonal snowpacks. Annual precipitation consists mostly of snow and averages about 150 cm. Average maximum seasonal snowpack water equivalent is about 110 cm (Smith and Berg 1982). Warm periods of several days to one or two weeks usually occur between storms and allow melt-freeze crusts to develop. These crusts become buried by subsequent snowfalls and result in strongly layered, heterogeneous snowpacks. Warm storms with high elevation freezing levels occasionally deliver rain to the snowpack, further altering its structure and raising the snowpack temperature to about 0°C.

The study was conducted during the winters of 1983 through 1985. 1983 was one of the wettest years on record in the study area. 1984 and 1985 were drier than average with prolonged interstorm dry periods. In 1983, storm temperatures ranged from -1 to -3°C, and snow densities at the time of irrigation were mostly 20 to 30 percent. In 1984, the three storms studied occurred at temperatures of -4, -7, and -10°C, and the densities of the layers ranged from 14 to 26 percent. Snowfall contributing to the 1985 layers occurred at -6 to -9°C. All snow densities in 1985 were less than 20 percent at the time of measurement.

DEFINITIONS

In this paper, the terms "water holding capacity" and "water retention" are considered equivalent and are used to include both water frozen when it enters a cold snowpack (that satisfying the "cold content" or "heat deficiency") and liquid water held against gravity (the "irreducible water content"). In this context, the question of interest is how much water will be retained by the snowpack for a given period of time, given some input of liquid water. Water holding capacity by volume [cm³ water/cm³ snow] = water holding capacity by weight [g water/g dry snow] x dry snow density [g snow/cm³ snow] / density of water [1 g water/1 cm³ water].

METHODS

The study approach was to apply water artificially over an area of snow, allow it to drain, and then compare the densities of samples collected in the wetted volume to densities of corresponding snow that was not irrigated. The difference in density, after correcting for settling in the presence of water, was attributed to water retained by the snow. This case study was limited

to a level area of less than 200 m² in a forest clearing at the CSSL.

Measurements were made only in layers of snow deposited by a single storm. The study was concerned with how much water could be held by snow with relatively consistent properties throughout its volume. Thus, interstorm boundary layers had to be avoided as did storm layers with obvious discontinuities [such as grain size changes caused by dramatic shifts in storm temperature]. Storm layers had to be of sufficient depth [minimum 50 cm] at the time of the first water application to allow sequential measurement of the same storm layer over several days.

The volumes of the snow that were irrigated were completely undisturbed portions of the snowpacks except for removal of the surface snow in some instances. Thus, the margins and base of the irrigated area were not physically isolated in any way from the remainder of the snowpack. The application of water alone defined the area that was altered. The extent of this area was determined by visual inspection. Only the central portion of the wetted areas was sampled for density, and no samples were taken within 15 cm of the surface perimeter of the irrigated area. Although irrigation usually took place on the natural surface, occasionally surface snow had to be removed before irrigation to avoid the water routing problems of surface crusts or to expose a layer which had been buried by subsequent snowfall. Snowfall in excess of one-half meter usually stopped measurements in buried layers. The measurement site was kept level by filling all pits before storms.

Both the water application and the density sampling procedures were revised a few times during the study as problems were noticed or improvements incorporated [Table 2]. Thus, the results are not comparable between seasons to the degree that they are dependent on the measurement technique and sampling procedures.

A series of pilot tests were made in 1982. Those tests included comparison of different density sampler volumes, selection of area and intensity for water application, and limited study of the effects of layer interfaces, drainage intervals, and compaction. The results of these tests provided the basis for the initial design of the study.

In 1983, two plots of 1 m² area were irrigated following snow storms of adequate depth with a hand-operated pump sprayer. Water to a depth of 2 cm was distributed as evenly as possible over the area in about 45 minutes, for an overall application rate of 2.7 cm/hr. Instantaneous intensities were somewhat higher because the spray nozzle was in motion and less than the entire area

was being sprayed at any given instant. The snow was irrigated in the late afternoon, covered with 3 sheets of 2 cm-thick expanded styrene and thin plastic film and allowed to drain overnight. A comparison area within a couple of meters was physically isolated from the wetted area by a metal sheet driven vertically into the snow to prevent any lateral flow of water. The comparison areas were covered in the same manner as the irrigated areas.

After 14-18 hours of drainage, an access pit was excavated on the edge of each 1 m² area. Cylindrical samplers were inserted horizontally to obtain up to 12 snow samples from the central 50 cm x 70 cm portion of the area. The samplers had an inside diameter of 10 cm, were 24.7 cm long, and enclosed a volume of 1940 cm³. The snow at the ends of the cylinders was cleanly cut with a thin metal blade, and the sample was removed for weighing. The average settlement of the wetted area (in excess of undisturbed settlement) was estimated to the nearest centimeter by measuring the vertical distance to the wetted surface from a straight edge held at a level as close as possible to the surface of the surrounding unwetted snow. In cases where a definite boundary (such as a buried crust) existed within 50 cm of the surface, several measurements

were made of the depth to the buried layer and averaged. Settlement was assumed to have occurred in the top 20 cm.

The water retention by volume was considered to be the difference between the mass of a unit volume of wetted snow and the mass of a unit volume of dry snow. In practice, the mean of the weights of the unwetted samples was subtracted from the mean of the weights of the samples of wetted snow. This difference was then divided by the sample volume to obtain the water retention on a volumetric basis (grams [or cm³] of water per cm³ of dry snow). Alternatively, the same result is obtained as the difference between the mean wet and dry densities. This value can be divided by the dry snow density to obtain the water retention on a weight basis (grams of water retained per gram of dry snow), if desired.

In order to correct for water induced settling, the mean of the weights of wet snow or the mean wet snow density must be multiplied by a factor that accounts for the more concentrated mass in the given volume. That is, if no settling occurred, less mass would be found in the same volume than is actually measured. This factor is computed as the quotient of the difference between depth of the layer in which the settling occurs (usually assumed to be 20

TABLE 2. Summary of Measurement Techniques and Results

Storm Date	Treated Plots/Day	Control Plots	Plot Area [m ²] & Irrigation Method*	Sampling Method & Volume*	Days Measured	Mean WHC [percent]
2-7-83	1	1	1 A	C	1	1
2-9-83	2	1	1 A	C	1	3
2-13-83	2	1	1 A	C	1	5
2-18-83	2	2	1 A	C	3	2,3,4
3-2-83	2	2	1 A	C	3	2,3,3
3-7-83	2	2	1 A	C	3	1,2,3
5-5-83	1	1	1 A	C	1	1
2-12-84	2	2	1 A	D	2	0,0
2-16-84	2	2	1 A	D	3	1,2,2
2-21-84	2	2	1 A	D	4	1,1,2,2
1-28-85	1	2	20 B	E	2	2,3
2-1-85	1	2	20 B	E	1	2
2-9-85	1	2	20 B	E	3	1,5,5
3-8-85	1	2	20 B	E	4	1,2,2,5
3-26-85	1	2	20 B	E	4	2,3,4,5

*A = pump sprayer B = hose w/ spray nozzle C = up to 12 samples of 1940 cm³
D = one 25,000 cm³ sample E = up to 30 samples of 13,000 cm³

cm] and the depth of settlement [to the nearest centimeter] divided by the depth of the layer [(20 minus settling depth)/20]. Often, no settling was observed and a default factor of 0.95 (1 cm in 20 cm) was used. The water retention value is very sensitive to the settlement factor.

For 1984, an automatic water applicator was designed and constructed based on drop forming needle-type rainfall simulators. In trials, the applicator failed to distribute water evenly and was abandoned. The pump sprayer was used again in the same manner as in 1983. A single large sample was excavated and weighed in each of two application areas and in the unwetted snow. The sampler was a rigid metal square (50 x 50 x 10 cm) that proved to be easier to use than the small samplers of 1983. A metal sheet was first inserted into an exposed pit wall at the edge of the irrigated area at a depth greater than 10 cm. Then, the sampler was inserted from above until contact with the sheet was made on all sides. Next, a second metal sheet was inserted along the upper edges of the square cutter, and the surrounding snow was excavated, allowing removal of the sample volume. The 25,000 cm³ volumes of snow were weighed, and water retention values were calculated in the same manner as in the previous year.

In 1985, a single 20 m² area was irrigated before each measurement day. A spray nozzle was used that produced a relatively even distribution of water over the application area (25 percent more water at the center than near the edges). The nozzle was operated at household line pressure through a hose attached to a tripod. Applications of 1-hour duration resulted in about 2-cm water depth over most of the area and up to 2.5 cm in the central few square meters. Water was applied in the late afternoon and allowed to drain overnight. When possible, the same layer of snow was irrigated in new plots on successive days to determine change in water retention over time.

A metal sheet was inserted horizontally at approximately 20 cm depth at the edge of the area to be wetted, before irrigation. A second plate was similarly inserted in snow that was not to be irrigated. The depths from the snow surface to the four corners of each plate were recorded before irrigation and again before sampling the next day. The difference between the overnight settling depths of the irrigated snow and the natural snow was used to correct the water retention in a manner similar to that described for 1983. Generally, settlement in the dry snow was from 0.5 to 1 cm per 10 cm of original depth, and settlement in the wetted snow was about twice that in the dry snow.

After 12 to 14 hours of drainage, large volume density samples were removed from both the natural

and irrigated snow and then weighed. Sections of flue pipe, 15 cm in diameter by 90 cm long, were inserted horizontally to obtain snow volumes of approximately 13,000 cm³. Great care was required to keep the samplers horizontal during insertion. The depths from the surface to the top of the sampler at each end were measured. If these depths differed by more than 1 cm, the sample was discarded. Sometimes, up to half of the potential samples were discarded to ensure that the same layer of snow was sampled throughout the area. Generally, 12 samples were obtained in the natural snow and up to 30 in the wetted snow, depending on the number of samples discarded. Water holding capacity by volume was then computed in the same manner as in 1983.

RESULTS

In 1983, 13 sets (two areas of the same snow layer irrigated at the same time) of measurements were obtained from seven storm layers before they became naturally wetted. In 11 of the 13 sets, the mean of the measured water retention values was 3 percent or less by volume. Water retention was 4 or 5 percent in the other two sets.

In the relatively dry winter of 1984, few storms were suitable for measurement. Only three storm layers were sampled, and 13 sets of measurements were obtained. In 9 of the 13 cases, the mean of the measured water retention values was 1 percent or less. The mean of the other 4 sets was 2 percent. On two occasions, measurements were obtained from topographic depressions where water was believed to have concentrated. The snow at these sites retained about 10 percent water by volume. At only 1 meter directly upslope from these sites, the snow had retained less than 1 percent water by volume.

In 1985, 14 sets of measurements were obtained from five storm layers. Measured water holding capacity by volume was 1 or 2 percent on 7 days, 3 percent on 2 days, and 4 or 5 percent on 5 days. Successive measurements of three of the layers over several days indicated increasing then decreasing water retention for the data observed. Water holding capacity was at a minimum (1 - 2 percent) 1 to 2 days after deposition, increased to a maximum (4 - 5 percent) after 2 to 3 days, and then decreased to nearly zero within 5 to 7 days, as the grains enlarged and midwinter melt percolated into the layers. In a fourth layer, water retention was already up to 5 percent when first measured 2 1/2 days after the end of the storm.

In 1983 and 1984, the absolute difference between plots was generally 1 percent or less. In a few cases, the difference was 2 percent. Because at most three applications were made at any one time,

assessing the natural variability of the water retention property or separating physical variability from possible problems with the experimental technique was not possible. Further work on this subject would require much greater attention to sampling design and a more uniform water application system.

Within the irrigated areas, the densities of small-volume samples (up to 30 in number) varied greatly. Densities in a single irrigated volume often ranged from the dry snow density (usually 0.25 g/cm³ or less) up to 0.60 g/cm³, over distances of only a few centimeters. Coefficients of variation ranged from 20 to 140 percent. This wide variation in snow density was most apparent with smaller volume (500 - 2000 cm³) samples. Visual inspection of the samples revealed that the high density samples included a large proportion of wet, nearly slushy, snow of large grain size (1 - 2 mm). The low density samples either lacked entirely or included only a small proportion of obviously wetted snow. Concurrent applications of dyed water to other areas of snow during the water retention experiments permitted documentation of the proportion of the snow volume that becomes wetted. A preliminary evaluation of these data suggested that less than 20 percent of the snow volume became wetted within 12 hours of the water application.

During the 3 years of this study, only two rain storms occurred when the snow was not already saturated. In one storm, 9 cm of rain fell over a 15-hour period, on snow 1 to 10 days old in the surface meter. About 5 cm of water was retained by the snowpack. Only 1 cm of rain fell on fresh snow during the other storm and all of it was retained by the snowpack. The near-surface snow layers had water holding capacities of 3 to 5 percent by volume during these events, as determined by changes in snow density (corrected for settling) over the storm periods. Snow pits excavated after the events revealed that much of the snow did not become wetted during the storms.

DISCUSSION

All of the average water retention values obtained from fresh snow on level ground ranged from 0 to 5 percent by volume. About two-thirds of these values were 2 percent or less. It appears that layers of fresh, low-density snow sampled in this study were not capable of retaining more than 5% liquid water by volume, 12-18 hours after high intensity application. In most cases, the layer water retention may have been less than 2 percent. These values tend to be at the lower end of the range of values reported for fresh snow and closer to common values for old snow (Table 1). In a

practical sense, water retention of 2 to 5 percent by volume means that a 50-cm thick snow layer could retain only 1 to 2.5 cm of rainfall. Results from the two rain events suggest that the high intensity artificial application of water did not seriously bias the apparent water retention as compared with low intensity rainfall.

The high variability of density in the wetted volumes and observations of widely distributed flow conducting channels indicated that relatively little (less than 20 percent) of the snow volume became wetted within 24 hours of water application. Thus, the distribution of water and the wetted proportion of the total volume may have been more important to total water holding capacity than the water retention of that part of the snow that actually conducted water. If snow that became fully wetted retained 30 percent water by volume, then a layer 50 cm thick that became 10 percent wetted could have held 1.5 cm of water, and one that became 20 percent wetted could have held 3 cm of water. The proportion of snow occupied by flow channels is being studied at CSSL. In the High Arctic, flow fingers covered about 22 percent of horizontal snow sections (Marsh, 1982).

Data collection was not structured in a way that allowed statistical evaluation. The only obvious influence on water holding capacity was natural wetting opportunity. As natural melt occurred, the measured water retention declined to zero. Surface melt occurs at the study site on most clear days throughout the winter (Smith, 1974). This input of water satisfies the water holding capacity and also increases density, grain size, and temperature. Thus, water retention declined coincidentally with increased age, density, grain size, and temperature, if meltwater input was the fundamental cause of the decline. Snow layer age is the most readily determined factor and, in general, water retention approached zero within a week if the layer had not been buried by subsequent snowfall. At elevations below that of the study site (2100 m), the water holding capacity would probably be satisfied even faster. Because only thick snow layers that were not buried by additional snowfall could be measured, the range of snow conditions sampled was relatively small. A greater number of replicated plots under a wider span of conditions would help to better understand the water retention process.

OBSERVATIONS AND CONJECTURES

During the study, a variety of qualitative observations were made opportunistically. While many of these observations lacked sufficient detail to support definitive statements, they provide some

direction for future studies. They also provided the basis for some ideas concerning various processes involved in snowpack water storage.

Slope angle appeared to be a critical factor in water movement and storage in snow. With even slight slopes (about 5%), a large proportion of the applied water was routed laterally downslope along one or more nearly imperceptible layers in the snow. Such flow reduced the wetted volume directly beneath the application area to less than the wetted volume in sample sites that were on level ground. Water flow apparently became more concentrated on slopes due to the opportunity for lateral downslope movement.

This study did not include interlayer boundaries. Water is known to be retained at layer interfaces where texture changes abruptly between fine-grain snow and underlying coarse-grain snow [Wakahama, 1968, 1975; Colbeck, 1973]. Concentration and storage of substantial quantities of water at such interfaces has been observed near the study area [Kattelmann, 1985]. Water storage at these layer boundaries and at the snow-soil interface may be more important than water storage in the snow layers. There is historical evidence that snowpacks can occasionally store large quantities of liquid water. If the snow matrix has insufficient capacity to account for these episodes of moderated water release to streams, then the interfaces are the next place to look.

A few periods of record from snowmelt lysimeters at CSSL indicate that water continues to drain from a saturated snowpack for several days after surface water input has ceased. This slow drainage could be expected from theories of declining flux due to declining liquid water content [Colbeck, 1972] and snow metamorphism in the presence of liquid water [Wakahama, 1968]. Therefore, it may be better to think of water "detention" by snow rather than water "retention", at least above the long-term "irreducible water content" [Colbeck, 1972].

Conversely, slow drainage from the wetted portion of the snow could be partially offset by increasing the wetted volume. Eventually, the entire snow mass comes into contact with liquid water, and some of this water will be stored around the newly wetted grains. The length of time for the entire snow matrix to become wetted following the development of the initial flow channels has not been directly measured. Results of a model study indicated that a deep isothermal snowpack becomes thoroughly wetted about 4 days after channels have penetrated the snow [Marsh, 1982]. Thus, losses from surface water input apparently can continue to occur after water has started to drain from a snowpack.

In a similar manner, liquid water continues to be stored in the snow matrix by freezing long after water begins to drain from the snowpack. Following the irrigation of subfreezing snow, dry sections of snow at the pre-application temperature were found on several occasions during the study. Snow temperatures as low as -4°C have been recorded up to 48 hours after substantial snowpack outflow had been recorded from snowmelt lysimeters at CSSL in 1985. Isolated cells of subfreezing snow in freely draining snowpacks have also been noted by other investigators (e.g., U.S. Army Corps of Engineers, 1956). Cold content or heat deficit must be satisfied eventually, but these observations indicate that water can be released before the entire snowpack warms to 0°C .

CONCLUSIONS

Measurements from 15 storm layers indicated that the total water retention capacity of fresh snow was almost always 5 percent or less by volume and usually less than 2 percent for the study conditions. Relatively little (perhaps less than 20 percent) of the snow conducted water within 18 to 24 hours following application of water. A limited number of observations indicated that topographic slope may reduce the wetted volume and water holding capacity below these values found for snow on level ground. No consistent relationships between water retention and other snow characteristics were suggested by the data. In developing forecasting techniques for snowpack water release, future research should be directed towards determining the effects of slope, snowpack structure, channel development, and snow/soil interactions.

Time is a critical consideration in assessing snowpack water storage. The intensity of the water input to the snow surface probably affects the distribution of water and the development of channels through the snowpack. For example, less water is probably stored if 5 cm of rain falls in an hour rather than if it falls uniformly over a day. This storage should be considered as temporary. Detention in the snow can distribute the rainfall or snowmelt over a longer period of time than in the absence of snow cover and thereby reduce the flood peak downstream. However, the ultimate volume of runoff may not be changed very much. Similarly, the heat deficit and irreducible water content of the whole snowpack must be satisfied, but not necessarily as a condition for snowpack water release. Some of the water input at the surface that enters dry snow can be frozen or held by capillary forces at the same time as other portions of the water are flowing through previously wetted channels to soil and streams.

ACKNOWLEDGEMENT. This research was supported by the USDI Bureau of Reclamation Office of Atmospheric Resources Research and Calif. Air Resources Board.

REFERENCES

- Ambach, W., 1963. Messungen des freien wassergehaltes in schneedecke. Expedition Glaciologique Internationale au Groenland 1957-60. 4[4]:174-180.
- Ambach, W., 1965. Research on the energy balance and free water content of a winter snowpack during ablation (a translation). Unpublished manuscript on file at the Central Sierra Snow Laboratory.
- Ambach, W. and F. Howorka, 1965. Avalanche activity and free water content of snow at Obergurgl. International Association of Hydrological Sciences [IAHS] Publication 69:65-72.
- Bengtsson, L., 1981. Snowmelt generated runoff from small areas as a daily transient process. *Geophysica* 17(1-2):109-122.
- Bengtsson, L., 1982. Percolation of meltwater through a snowpack. *Cold Regions Science and Technology* 6:73-78.
- Boyer, P. and P. Merrill, 1954. Storage effect of snow on the flood potential from rain falling on snow. U.S. Army/Weather Bureau Cooperative Snow Investigations Technical Bull. 17. 22 pp.
- Church, J.E., 1941. The melting of snow. *Proceedings of the Central Snow Conference. Michigan State College. Vol. 1: 21-32.*
- Colbeck, S.C., 1972. A theory of water percolation in snow. *Journal of Glaciology* 11(63):369-385.
- Colbeck, S.C., 1973. Effects of stratigraphic layers on water flow through snow. *CRREL Research Report 311. Hanover, New Hampshire. 13 pp.*
- Colbeck, S.C., 1974. The capillary effects on water percolation in homogenous snow. *Journal of Glaciology* 11(67):85-97.
- Colbeck, S.C., 1975. Analysis of hydrologic response to rain-on-snow. *CRREL Research Paper 340. Hanover, New Hampshire. 13 pp.*
- Colbeck, S.C., 1978. The physical aspects of water flow through snow. *Advances in Hydroscience* 11: 165-205.
- Colbeck, S.C., 1979. Water flow through heterogeneous snow. *Cold Regions Science and Technology* 1:37-45.
- Colbeck, S.C., E.A. Anderson, V.C. Bissell, A.G. Crook, D.H. Male, C.W. Slaughter, and D.R. Wiesnet, 1979. Snow accumulation, distribution, melt and runoff. *EOS, Transactions, American Geophysical Union* 60(21):465-468.
- deQuervain, M.R., 1973. Snow structure, heat, and mass flux through snow. *In: The Role of Snow and Ice in Hydrology—Proceedings of the Banff Symposium, UNESCO-WMO-IAHS, pp. 203-226.*
- Dunne, T., A.G. Price, and S.C. Colbeck, 1976. The generation of runoff from subarctic snowpacks. *Water Resources Research* 12:677-685.
- Ebaugh, W.P. and D.R. DeWalle, 1977a. Laboratory investigation of rainfall retention and transmission in fresh snow. *Institute for Research on Land and Water Resources. NTIS PB-268 703. Pennsylvania State University, University Park, Pennsylvania. 62 pp.*
- Ebaugh, W.P. and D.R. DeWalle, 1977b. Retention and transmission of liquid water in fresh snow. *In: Proceedings, Second Conference on Hydrometeorology in Toronto (American Meteorological Society, Boston), pp. 255-260.*
- Gerdel, R.W., 1945. The dynamics of liquid water in deep snowpacks. *Transactions, American Geophysical Union* 26(Part 1):83-90.
- Gerdel, R.W., 1948. Physical changes in snow cover leading to runoff, especially to floods. *IAHS Publication 31 (General Assembly of Oslo), pp. 42-53.*
- Gerdel, R.W., 1954. The transmission of water through snow. *Transactions, American Geophysical Union* 35(3):475-485.
- Gerdel, R.W., and A.R. Codd, 1945. Snow studies at Soda Springs, California. *Annual Report of Cooperative Snow Investigations of the U.S. Weather Bureau and University of Nevada-Reno.*
- Himmel, J.M., 1951. Lysimeter studies of rain-on-snow phenomena. *Cooperative Snow Investigations Research Note 4.*
- Horton, R.E., 1941. The role of snow, ice, and frost in the hydrologic cycle. *Proceedings of the Central Snow Conference. Michigan State College. Vol. 1:5-21.*
- Jordan, P., 1983a. Meltwater movement in a deep snowpack. 1. Field observations. *Water Resources Research* 19(4): 971-978.
- Jordan, P., 1983b. Meltwater movement in a deep snowpack. 2. Simulation model. *Water Resources Research* 19(4): 979-985.
- Kattelman, R.C., 1985. Wet slab instability. *In: Proceedings of the International Snow Science Workshop. Aspen, Colorado pp. 102-108.*
- Kuzmin, P.P., 1948. Snowmelt research and calculation. *Proceedings of the State Hydrological Institute. Issue 7(61). Cited in Kovzel, A.G., 1969. A method for the computation of water yield from snow during the snowmelt period. Floods and their computation. IASH Publication 85(2): 568-606.*
- LaChapelle, E.R., 1969. *Field Guide to Snow*

- Crystals. University of Washington Press, Seattle, Washington.
- Leaf, C.F., 1966. Free water content of snow pack in alpine areas. Proceedings of the 34th Western Snow Conference. pp. 17-24.
- Lemmela, R., 1973. Measurements of evaporation-condensation and melting from a snow cover. In: The Role of Snow and Ice in Hydrology: Proceedings of the Banff Symposium, UNESCO-WMO-IAHS pp. 870-879.
- Male, D.H. and D.M. Gray, 1981. Snowcover ablation and runoff. In: Handbook of Snow. Pergamon Press Canada, Ltd. pp. 360-436.
- Marsh, D., 1982. Ripening processes and meltwater movement in arctic snowpacks. Ph.D. Thesis. McMaster University. 179 pp.
- Muallem, Y., 1978. Hydraulic conductivity of unsaturated porous media: generalized macroscopic approach. Water Resources Research 14(2):325-334.
- Perla, R.I. and E.R. LaChapelle, 1984. Dilution method for measuring liquid water in snow. Proceedings of the 52nd Western Snow Conference. pp. 80-85.
- Perla, R.I. and M. Martinelli, Jr., 1976. Avalanche Handbook, USDA Forest Service Agriculture Handbook 489. 254 pp.
- Price, A.G., L.K. Hendrie, and I. Dunne, 1979. Controls on the production of snowmelt runoff. In: Proceedings Modeling of Snow Cover Runoff. S.C. Colbeck and M. Ray, [Editors]. U.S. Army CREL, Hanover, New Hampshire. pp. 257-268.
- Smith, J. L., 1974. Hydrology of warm snowpacks and their effects upon water delivery...some new concepts. In: Advanced Concepts and Techniques in the Study of Snow and Ice Resources, H. S. Santaford and J. L. Smith [Editors]. pp. 76-89. National Academy of Sciences, Washington, D.C
- Smith, J.L. and N.H. Berg, 1982. Historical snowpack characteristics at the Central Sierra Snow Laboratory, a representative Sierra Nevada location. The Sierra Ecology Project, Vol. 3, Part 2. USDI-Bureau of Reclamation, Sierra Cooperative Pilot Project. 44 pp.
- Smith, J.L. and H.G. Halverson, 1963. Hydrology of snow profiles obtained with the profiling snow gage. Proceedings of the 37th Western Snow Conference, pp. 41-48.
- Sulahria, M.B., 1972. Prediction of water retention capacity of high elevation snowpacks on the east side of the Sierra Nevada. Unpublished Ph.D. dissertation. University of Nevada at Reno. 115 pp.
- U.S. Army Corps of Engineers, 1956. Snow Hydrology. 436 pp.
- Wakahama, G., 1968. The metamorphism of wet snow. IAHS Publication 79 [General Assembly at Bonn], pp. 370-378.
- Wakahama, G., 1975. The role of melt-water in densification processes of snow and firn. International Symposium on Snow Mechanics. IAHS Publication 114, pp. 66-72.
- Wankiewicz, A., 1976. Water percolation within a deep snowpack--Field investigations at a site on Mt. Seymour, British Columbia. Unpublished Ph.D. dissertation. University of British Columbia. 177 pp.
- Wankiewicz, A., 1978a. Water pressure in ripe snowpacks. Water Resources Research 14(4): 593-599.
- Wankiewicz, A., 1978b. Hydraulic characteristics of snow lysimeters. Proceedings of the 35th Annual Eastern Snow Conference, pp. 105-115.
- Wankiewicz, A., 1979. A review of water movement in snow. In: Proceedings, Modeling of Snow Cover Runoff. S.C. Colbeck and M. Ray [Editors]. U.S. Army Corps of Engineers, CREL, Hanover, New Hampshire, pp. 222-252.
- Wisler, C.O. and E.F. Brater, 1949. Hydrology. John Wiley and Sons. pp. 186.
- Work, R.A., 1948. Snow-layer density changes. Transactions American Geophysical Union 29(4):525-546.

PRECIPITATION MEASURED BY DUAL GAGES, WYOMING-SHIELDED
GAGES, AND IN A FOREST OPENING

David L. Sturges¹

ABSTRACT: Precipitation measured by dual gages and a Wyoming-shielded gage in exposed locations was compared to that measured in a nearby forest stand. The Wyoming shield provided adequate protection from wind for rain, but not for snow. The Wyoming-shielded gage measured 37% to 53% of actual precipitation between November and March, when air temperatures were well below freezing and monthly wind speeds were at a maximum. Analysis of individual snowfall events indicated that undermeasurement was directly related to wind speed. The precipitation deficit increased about 7% for each 1 meter per second increase in wind speed for storms with air temperatures below -2°C.

Estimates of precipitation determined from dual gages were not statistically different ($p < 0.05$) from measurements in the forest stand in 8 of 12 months.

(KEY TERMS: precipitation gages; precipitation measurement; Wyoming shield; dual gages; precipitation undermeasurement; snow.)

INTRODUCTION

Accurately measuring precipitation falling as snow is a difficult task. Turbulence in the windstream created by the gage causes snow particles to be deflected over or around the gage, so that precipitation is undermeasured. Various types of shields have been developed to reduce the deleterious effects of wind. The shield devised by Alter (1937) and modified by Warnick (1953) is widely used in the United States. Precipitation is

still undermeasured, however, if snowfall is accompanied by wind (Larson and Peck 1974).

A shield specifically designed for gages operated in an exposed, windy environment was developed at the University of Wyoming (Rechard and Wei 1980). Use of the Wyoming shield at Barrow, Alaska tripled estimates of winter precipitation compared to measurements from unshielded gages (Benson 1982). Black (1954) earlier had noted that snow on the ground at Barrow contained two to four times as much water as indicated by measured precipitation.

Hamon (1973) believed actual precipitation could be computed from data collected at shielded and unshielded gages through use of a calibration coefficient to account for the influence of wind, and he developed the following relationship:

$$\ln\left(\frac{U}{A}\right) = B \ln\left(\frac{U}{S}\right) \quad (1)$$

where A is computed precipitation, U is precipitation at the unshielded gage, S is precipitation at the shielded gage, and B is the calibration coefficient with a value of 1.73. The use of data from shielded and unshielded gages to estimate precipitation is known as the dual gage procedure.

Relatively few studies rigorously evaluated the performance of precipitation gages in exposed locations. Gages protected by a Wyoming shield and a modified Alter shield measured 80% and 55%, respectively, of precipitation measured by a gage protected with a Nipher shield, a

¹Research Forester, Rocky Mountain Forest and Range Experiment Station, Forest Service, USDA, 222 South 22nd Street, Laramie, Wyoming 82070.

significant undermeasurement ($p < 0.05$) compared to the Nipher-shielded gage. The study was conducted at the Regina, Saskatchewan, airport, over five winters (Jones 1984).

Sturges (1984) compared precipitation measured by a Wyoming-shielded gage located on windswept rangeland with that measured in a nearby forest stand. Both gages measured similar precipitation for rainfall events. However, undercatch at the Wyoming-shielded gage was significant ($p < 0.05$) in months with snowfall. Between November and March, the Wyoming-shielded gage caught only 40% to 60% of precipitation measured in the forest opening. A linear relationship existed between wind speed and the under-measurement of precipitation when individual snowfall events were analyzed.

Hanson et al. (1979) compared precipitation computed by the dual gage method with that measured by a gage equipped with a Wyoming shield. Similar quantities of precipitation were measured by the two procedures.

OBJECTIVE

This study compared precipitation measured in a forest stand with that measured on adjacent windswept rangeland by dual gages and by a gage protected with a Wyoming shield.

STUDY SITES

Twin Groves

The Twin Groves site lies on a gently sloping bench just off the northern flank of the Sierra Madre mountain range ($41^{\circ}21'N$, $107^{\circ}10'W$) 30 km west of Saratoga, Wyoming. Forest-protected gages were located in an 18-ha stand of lodge-pole pine within an opening 0.75 tree height in diameter (Figure 1). Trees were about 15 m tall.

The gage protected by the Wyoming shield was placed 970 m upwind from the forest-protected gage and 360 m from the tree margin for the prevailing wind direction. Rangeland dominated by sagebrush about 30 cm tall surrounded the stand of trees. Elevations at forest-protected and

Wyoming-shielded gages were 2,465 and 2,445 m, respectively.

Foote Creek

The Foote Creek site lies off the eastern flank of the Medicine Bow mountain range, 67 km northwest of Laramie ($41^{\circ}36'N$, $106^{\circ}15'W$). The forest-protected gage was placed in a stand of aspen, willow, and alder bordering Foote Creek. Trees surrounding the gage were about 7 m tall and the gage was placed in an opening 0.5 tree height in diameter.

The gage protected by the Wyoming shield and the dual gages were placed on shortgrass prairie rangeland. The Wyoming shield was 195 m from the forest-protected gage. Dual gages were 6.1 m apart and about 48 m from the Wyoming shield (Figure 1). Elevation at the study site was about 2,360 m.

STUDY METHODS

Precipitation was recorded continuously by gages with an orifice 20.3 cm in diameter. The chart drum, driven by a stepper motor controlled by a quartz crystal, rotated every 8 days. The orifices of forest-protected gages and dual gages were 3 m above the ground while orifices of gages protected by the Wyoming shield were 2.3 m above the ground. The forest-protected gage at Foote Creek was shielded by a modified Alter shield as were gages at Twin Groves after November 1982. The shielded dual gage was equipped with a modified Alter shield which was further modified to constrain baffles so that their lower end pointed towards the precipitation gage at a 30° angle (Hamon 1973).

Gages at Twin Groves were usually serviced monthly and gages at Foote Creek were serviced bimonthly. Interval precipitation indicated by the chart trace was corrected to match interval precipitation determined from weighing the reservoir bucket at the start and end of each service interval. Chart precipitation recorded in the forest opening at Twin Groves was corrected to match precipitation measured by the nonrecording gage for the service interval. Comparison of interval precipitation determined from the

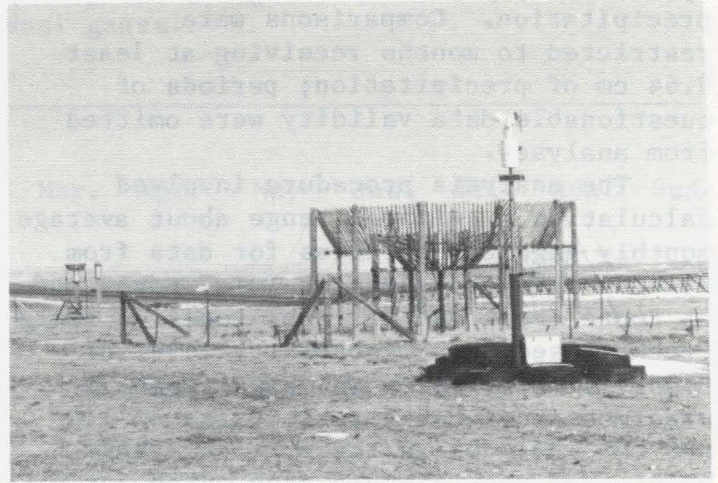
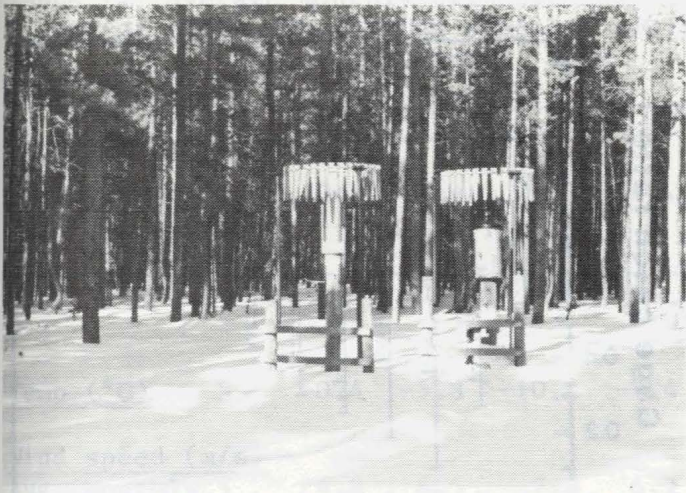


Figure 1. Forest-protected precipitation gages (standard and recording) at Twin Groves (left); precipitation gage protected by a Wyoming shield and the dual gages at Foote Creek (right).

change in bucket weight and recorded on the chart, provided an internal check on data consistency. The reservoir of each gage was charged with antifreeze to prevent freezing of precipitation and with transformer oil to prevent evaporation.

Wyoming shields were built to specifications of Rechar and Wei (1980). Two concentric rings of Canadian snow fence 1.2 m in height with a solid density between 40% and 50%, surrounded the precipitation gage. The outer ring was 6.1 m in diameter and the top of the fence was 2.6 m above the ground surface, while the inner ring was 3.05 m in diameter and 2.3 m above the ground surface. The outer and inner rings of snow fence inclined towards the precipitation gage at angles of 30° and 45° from vertical, respectively.

Wind speed, wind direction, and air temperature were recorded by a mechanical weather station located near the Wyoming shield. Sensors were 2 m above the ground surface at Twin Groves and during the first year of study at Foote Creek. The sensor was then moved to a 3-m height when dual gages were installed. Independent time control marks were placed on the chart at 6- or 12-hour intervals by a

marking system that was accurate to about 2 minutes per month.

DATA COMPARISONS AND ANALYSES

Comparisons of precipitation measurements in the forest opening with those from the Wyoming-shielded gages were based on a 9-year record period extending from November 1976 to October 1985 at Twin Groves, and a 4-year record period extending from November 1981 to October 1985 at Foote Creek. Data from dual gages were available from November 1982 to October 1985.

Freese (1960) and Reynolds (1984) describe use of the chi-square statistic to evaluate the accuracy of a new estimating or analysis procedure compared to a standard procedure. This analysis was used to determine if precipitation measured by an exposed gage was significantly different from precipitation measured in the forest opening. Analyses were based on monthly gage catch ratios calculated by dividing monthly precipitation measured at the exposed gage by precipitation measured in the forest opening. A ratio of 1.0 indicated the two gaging

systems measured identical quantities of precipitation. Comparisons were restricted to months receiving at least 0.64 cm of precipitation; periods of questionable data validity were omitted from analyses.

The analysis procedure involved calculating a critical range about average monthly gage catch ratios for data from Wyoming-shielded gages at Twin Groves and at Foote Creek and for dual gages at Foote Creek, based on a probability level of 0.05. Precipitation was significantly undermeasured when a ratio value of 1.0 was not included in the critical range about each mean monthly gage catch ratio. The correction for bias (average precipitation undermeasurement) described by Freese (1960) was applied if the average monthly gage catch ratio was less than 0.9.

RESULTS

Twin Groves and Foote Creek had similar climatic characteristics (Table 1). Average annual precipitation was 56 cm at Twin Groves and 59 cm at Foote Creek, with 75% of the total falling as snow. Average annual temperatures were about 2°C. Wind speeds were at a maximum in winter months and averaged more than 6 meters per second (m/s) between November and March. Prevailing wind direction was from the southwest at Twin Groves and from the west at Foote Creek.

Wyoming Shield

Monthly gage catch ratios for the Wyoming-shielded gage exhibited a cyclic pattern through the year (Tables 2 and 3). The ratio was about 1.0 in summer months, decreased to about 0.4 in midwinter, and then progressively increased until summer. Precipitation was significantly undermeasured ($p < 0.05$) between October and May at Twin Groves and at Foote Creek (Figure 2). Monthly ratios ranged from 0.35 to 0.54 between November and March when air temperatures were well below freezing, and monthly wind speeds were at a maximum. The shield did provide adequate protection for rainfall events in June, July, and August because the ratio was about 1.0.

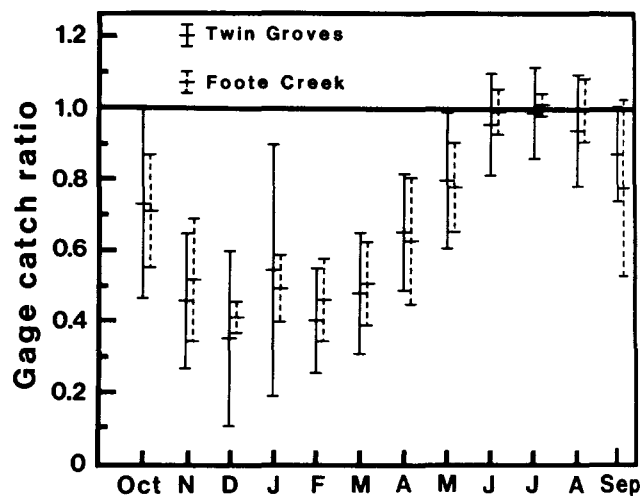


Figure 2. Average monthly gage catch ratios and associated critical ranges (0.05 probability level) for precipitation gages protected by a Wyoming shield at Twin Groves and Foote Creek.

Dual Gage

The average monthly gage catch ratio for precipitation determined from dual gage data was less than 1.0 throughout the year, but the critical range about mean monthly values included a ratio value of 1.0, except in October, November, May, and June (Table 3). Monthly analyses were based on 3 years of information and so results are not as representative of variability in yearly climatic characteristics as data from the Wyoming shield. The hypothesis that dual gages provide the same estimate of monthly precipitation as measured in the forest opening was accepted in 8 out of 12 months.

Relationship of Windspeed to Gage Catch at the Wyoming-Shielded Gage

Precipitation measurements at the Wyoming-shielded gage were both greater and smaller than precipitation measurements in the forest opening for individual rainfall events (Figures 3 and 4). Storm wind speed was not related to gage catch at either study site.

In contrast to rainfall events, undermeasurement of precipitation falling

TABLE 1. Average monthly climatic characteristics at the study sites and calculated precipitation for Wyoming-shielded gages and dual gages.

Parameter	Years of record	Twin Groves											
		Oct.	Nov.	Dec.	Jan.	Feb.	Mar.	Apr.	May	Jun.	Jul.	Aug.	Sep.
<u>Temp (°C)</u>	5	-0.4	-5.8	-10.2	-9.4	-9.2	-5.4	-1.2	3.3	8.9	13.8	14.0	8.2
<u>Wind speed (m/s)</u>													
Avg. monthly	5	4.8	6.5	7.8	6.2	7.2	5.9	5.1	4.4	3.9	3.2	3.2	4.3
Avg. storm	*	5.9	5.8	7.6	4.5	7.8	6.8	5.9	5.2	5.6	3.2	4.4	5.4
<u>Precipitation (cm)</u>													
Actual	10	5.6	4.9	5.2	4.9	3.9	6.5	5.6	6.6	2.4	4.0	3.0	3.6
Wyo shield	***	4.1	2.2	1.8	2.7	1.6	3.1	3.6	5.3	2.3	3.9	2.8	3.1
		Foote Creek											
<u>Temp (°C)</u>	4	2.9	-3.4	-7.5	-7.5	-6.6	-3.4	-0.3	8.3	11.8	17.6	18.0	9.8
<u>Wind speed (m/s)</u>													
Avg. monthly	4	5.8	7.4	8.6	8.4	8.0	7.3	6.1	5.5	4.6	4.0	4.1	5.2
Avg. storm	**	4.3	4.7	7.4	5.9	4.4	5.3	5.9	6.0	2.8	5.5	3.9	4.5
<u>Precipitation (cm)</u>													
Actual	8	5.0	5.6	5.1	4.6	3.1	7.1	6.4	9.7	2.4	4.2	3.0	3.3
Wyo shield	***	3.6	2.9	2.1	2.3	1.4	3.6	4.0	7.5	2.4	4.2	3.0	2.6
Dual gages	***	3.8	4.7	5.0	4.4	2.7	6.5	5.3	7.3	2.1	4.1	2.9	2.5

*From 7 to 24 individual storms were analyzed in a month.

**From 5 to 17 individual storms were analyzed in a month.

***Actual precipitation measured in forest opening multiplied by average monthly gage catch ratio.

TABLE 2. Mean monthly gage catch ratios (Precip. at Wyoming shield/precip. in forest opening) at Twin Groves, and critical range (0.05 probability level) associated with mean monthly gage catch ratio.

Year	Oct.	Nov.	Dec.	Jan.	Feb.	Mar.	Apr.	May	Jun.	Jul.	Aug.	Sept.
1976		**	0.693									
1977	0.799	0.630	.173	1.105	0.557	0.694	0.914	*	*	*	*	*
1978	1.067	.439	.409	*	.318	.449	.663	0.740	0.943	1.104	0.961	0.708
1979	.751	.409	.362	0.616	.509	.564	.589	.724	.791	1.000	.802	.788
1980	.688	.623	.558	.523	.449	.427	.581	.780	**	0.978	.947	.993
1981	.817	.548	.296	.338	.402	.557	.632	.814	.908	.882	1.087	1.000
1982	.557	.411	.209	.586	.373	.347	.533	.761	1.120	1.010	**	.856
1983	.863	.381	.253	.313	.270	.537	.676	.601	1.000	1.029	.821	.915
1984	.428	.224	.228	.354	.481	.439	.731	.882	.951	.814	1.016	.887
1985	.602			.513	.270	.302	.552	1.075	.964	1.068	.927	.759
n (year)	9	8	9	8	9	9	9	8	7	8	7	8
Avg.	.730	.458	.353	.543	.403	.480	.652	.797	.954	.986	.937	.871
Critical range	+0.265***	+0.189	+0.245	+0.353	+0.147	+0.170	+0.164	+0.191	+0.142	+0.127	+0.156	+0.132

*Data missing.

**Less than 0.64 cm precipitation in service interval.

***Precipitation measured by Wyoming-shielded gage significantly less than in forest opening if monthly ratio \pm critical range does not include a ratio value of 1.0.

as snow by the Wyoming-shielded gage was significantly related ($p < 0.05$) to storm wind speed when air temperatures were below -2°C (Figures 3 and 4). The data set included 79 events at Twin Groves; maximum wind speed was 11 m/s and minimum air temperature was -19°C . There were 54 events at Foote Creek; maximum wind speed was 11.3 m/s and minimum air temperature was -25°C . The gage protected by the Wyoming shield caught about half as much precipitation as measured by the forest-protected gage for winds 5 m/s, and less than a quarter as much precipitation for winds 10 m/s.

The relationship between wind speed and the deficit in gage catch for storms with temperatures between $+2^{\circ}\text{C}$ and -2°C was weaker than for storms with temperatures below -2°C though correlation coefficients were statistically significant (Figures 3 and 4). Data sets included predominantly snowfall events. The deficit in measured precipitation at the Wyoming-shielded gage increased about 5% for each 1 m/s increase in wind speed.

DISCUSSION AND CONCLUSIONS

The study was based on comparisons of precipitation measured in a small forest opening to reduce the deleterious effects

of wind on gage performance, with precipitation measured in exposed locations. This approach was the one Hamon (1973) used when determining the calibration coefficient to relate precipitation measured by shielded and unshielded gages to actual precipitation. The relationship between the actual vertical flux of precipitation and that measured in the forest stand is, of course, unknown, as it is for all studies utilizing this approach.

Average monthly gage catch ratios were utilized to develop a function to predict undermeasurement of precipitation at gages protected by a Wyoming shield through the year (Figure 5).

$$\text{Undermeasurement}(\%) = 3.177 + 0.218X + \frac{6.616X^2}{10^3} - \frac{5.258X^3}{10^5} + \frac{1.140X^4}{10^7} - \frac{6.578X^5}{10^{11}} \quad (2)$$

where X is the number of days past August 16.

Though the independent variable is number of days past August 16, the expression implicitly defines the effect of air temperature in determining whether precipitation falls as rain or snow and the effect of wind on gage performance in months with snowfall. It is applicable to sites with climatic conditions reasonably

TABLE 3. Monthly gage catch ratios for the Wyoming-shielded gage and for dual gages (Precip. at Wyoming shield or dual gage/precip. in forest opening) at Foote Creek, and the critical range (0.05 probability level) associated with mean monthly gage catch ratios for Wyoming shield and dual gage data.

Year	Oct. Ratio		Nov. Ratio		Dec. Ratio		Jan. Ratio		Feb. Ratio		Mar. Ratio	
	Wyo shield	Dual gage	Wyo shield	Dual gage	Wyo shield	Dual gage	Wyo shield	Dual gage	Wyo shield	Dual gage	Wyo shield	Dual gage
1981			0.485		0.452							
1982	0.662		.567	0.812	.381	1.073	0.566		0.548		0.477	
1983	.896	0.838	.675	.983	.434	1.106	.529	1.015	.422	0.639	.574	1.206
1984	.590	.695	.340	.705	.382	0.749	.387	0.891	.530	1.405	.594	0.880
1985	.693	.761					.490	.969	.344	.614	.385	.677
n (years)	4	3	4	3	4	3	4	3	4	3	4	3
Avg.	0.710	0.765	0.517	0.833	0.412	0.976	0.493	0.958	0.461	0.886	0.507	0.921
Critical range	<u>+0.159*</u>	<u>0.081*</u>	<u>+0.172</u>	<u>+0.159</u>	<u>+0.044</u>	<u>+0.198</u>	<u>+0.094</u>	<u>+0.080</u>	<u>+0.116</u>	<u>+0.509</u>	<u>+0.117</u>	<u>+0.282</u>

Year	Apr. Ratio		May Ratio		Jun. Ratio		Jul. Ratio		Aug. Ratio		Sep. Ratio	
	Wyo shield	Dual gage										
1981												
1982	0.577		0.897		1.043		1.000		0.903		1.000	
1983	.844	1.005	.700	0.804	0.959	0.890	1.048	1.033	1.060	0.966	0.895	.957
1984	.564	0.853	.685	.709	1.026	.777	0.998	0.920	.950	.900	.600	.472
1985	.523	.647	.830	.760	.926	.927	.990	0.995	1.059	1.084	.607	.875
n (years)	4	3	4	3	4	3	4	3	4	3	4	3
Avg.	0.627	0.835	0.778	0.758	0.988	0.865	1.009	0.983	0.993	0.983	0.776	.768
Critical range	<u>+0.178</u>	<u>+0.204</u>	<u>+0.125</u>	<u>+0.054</u>	<u>+0.063</u>	<u>+0.089</u>	<u>+0.031</u>	<u>+0.061</u>	<u>+0.088</u>	<u>+0.095</u>	<u>+0.247</u>	<u>+0.294</u>

*Precipitation measured by Wyoming-shielded gage or dual gages is significantly less than in forest opening if monthly ratio ± critical range does not include a ratio value of 1.0

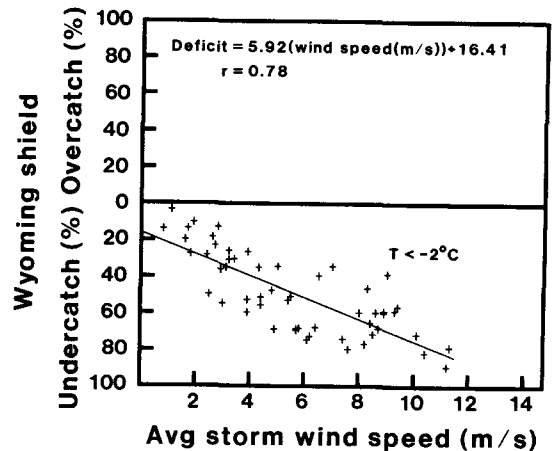
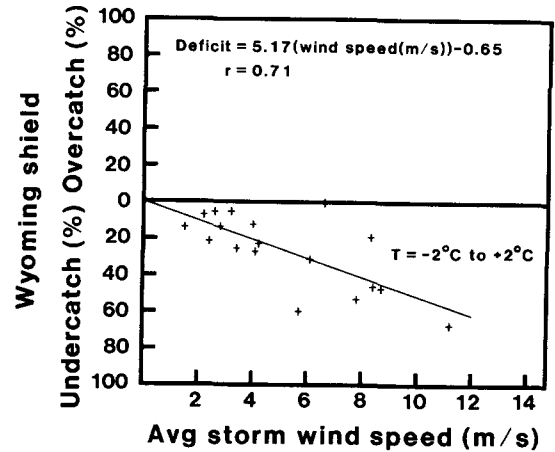
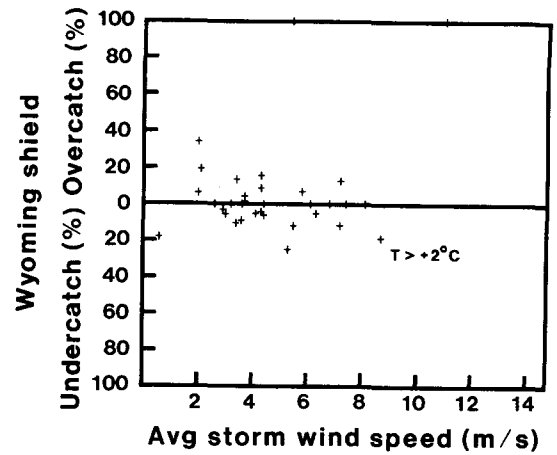
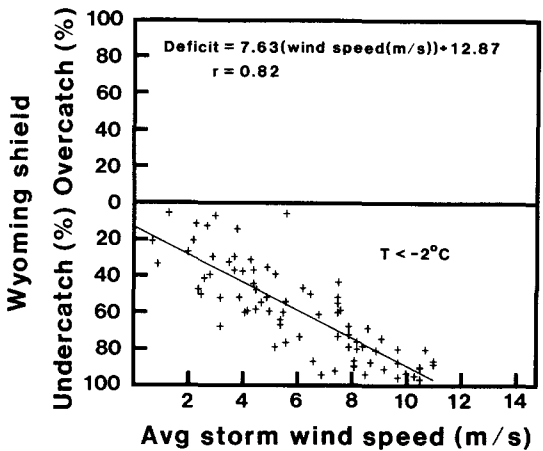
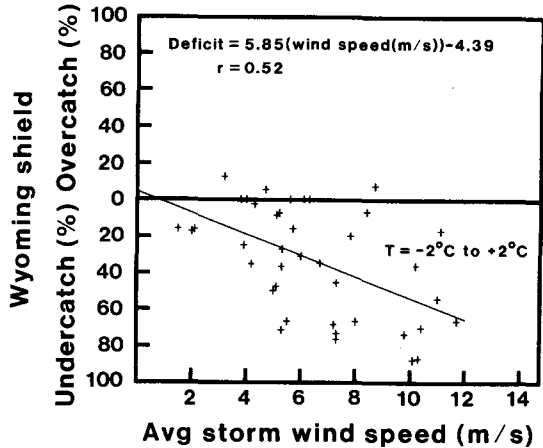
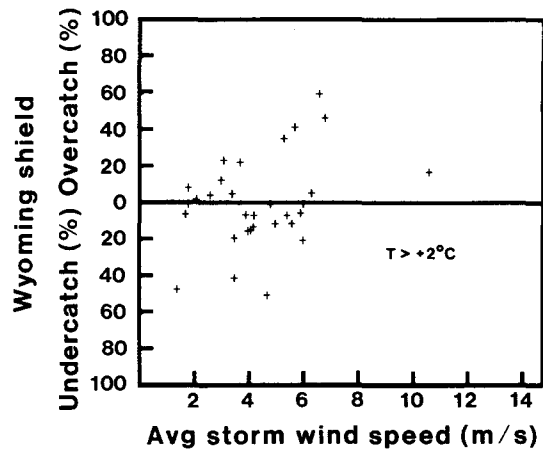


Figure 3. The relationship between wind speed and performance of the Twin Groves precipitation gage protected by a Wyoming shield. Precipitation events were stratified into three temperature regimes. Top--temperatures greater than $+2^{\circ}\text{C}$. Middle--temperatures -2°C to $+2^{\circ}\text{C}$. Bottom--temperatures less than -2°C .

Figure 4. The relationship between wind and performance of the Foote Creek precipitation gage protected by a Wyoming shield. Precipitation events were stratified into three temperature regimes. Top--temperatures greater than $+2^{\circ}\text{C}$. Middle--temperatures -2°C to $+2^{\circ}\text{C}$. Bottom--temperatures less than -2°C .

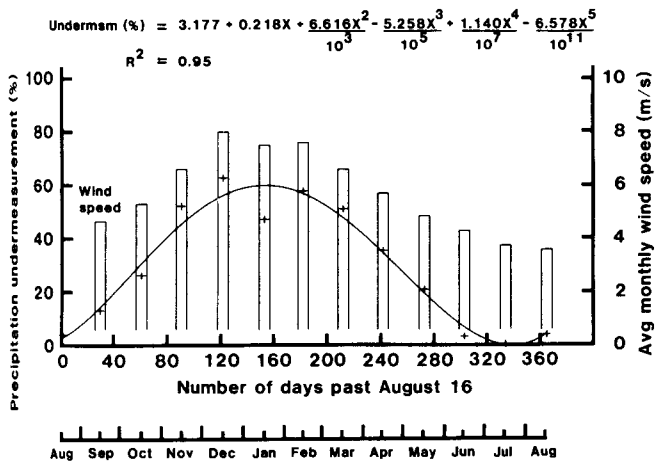


Figure 5. Undermeasurement of precipitation through the year as a function of the number of days past August 16. Average monthly wind speed is also shown.

similar to those in Table 1. Information about precipitation undermeasurement in relation to monthly wind speeds can be used to estimate undermeasurement in locations where climatic conditions are appreciably different from monthly averages in this study (Table 1). The relationship is based on average monthly gage catch ratios, so precipitation estimates for individual storms may be in considerable error if meteorological conditions during storms are not representative of average monthly conditions.

From a theoretical standpoint, precipitation should be measured without error in the absence of wind regardless of gage location or type of shielding. Wind speed had no effect on the quantity of precipitation measured at the Wyoming-shielded gage when precipitation fell as rain (Figures 3 and 4), a finding that agrees with results based on monthly gage catch ratios.

Intercept values for precipitation data collected at the Wyoming-shielded gage at storm temperatures between $+2^{\circ}\text{C}$ and -2°C were not significantly different from zero, in accordance with the theoretical relationship (Figures 3 and 4). However, there was a significant ($p < 0.05$) precipitation deficit in the absence of wind at both study sites for storms with temperatures below -2°C . Just 3 of

79 events at Twin Groves and 6 of 54 events at Foote Creek were accompanied by winds less than 2 m/s, and study data poorly defined the relationship between wind speed and precipitation undermeasurement for low wind speeds. Correlation coefficients between wind speed and gage undercatch were not as strong for precipitation falling between $+2^{\circ}\text{C}$ and -2°C as for precipitation falling at lower temperatures. The presence of some rainfall events in this data set probably contributed to the poorer relationship, but at the same time tended to pull the regression line towards the origin.

Hanson et al. (1979) found that similar quantities of precipitation were measured by a Wyoming-shielded gage and by dual gages for both rainfall and snowfall events. Precipitation calculated from dual gages at Foote Creek was usually not significantly different from actual precipitation, but gages protected by a Wyoming shield significantly undermeasured precipitation falling as snow. Thus, under study conditions, the dual gage approach was superior to use of a Wyoming shield to measure winter precipitation.

As Hanson et al. (1979) reported, the legibility of the pen trace of a Wyoming-shielded gage was greatly superior to the pen trace of the shielded member of the dual gage setup. Wind-induced vibrations caused the pen of the shielded gage to "paint" a line up to 1 cm wide, which obscured all detail of the pen trace. After 1 year of operation, support for the fixed windshield was separated from the post supporting the gage and the gage-support post was firmly guyed. These modifications vastly improved the quality of the chart trace and made it comparable to the trace of the Wyoming-shielded gage.

The Wyoming shield provides adequate protection from wind if precipitation falls as rain. Summer precipitation at Foote Creek was nearly identical in exposed and forest-protected locations and monthly critical ranges were narrower than those for Twin Groves (Tables 2 and 3), a reflection of the close physical proximity of Foote Creek gages. Twin Groves gages were about 1 km apart, and much of the between-storm variation reflected random, small-scale differences in storm patterns.

Precipitation received as snow measured in gages protected by a Wyoming shield should be considered a conservative estimate of actual precipitation. Undermeasurement can be a significant source of error if precipitation information is used as input data for hydrologic models, or used as a design parameter for snow control engineering purposes. For example, precipitation measured at the Wyoming shield in months when snow relocation is an important hydrologic process, averaged 47% of that measured in the forest opening. The severity of undercatch increases with increasing wind speed. Thus, undercatch would be more severe on the plains than in areas where wind is not such a dominant feature of the environment.

ACKNOWLEDGEMENTS

The Foote Creek study site is located on land belonging to the Bear Creek Cattle Company of McFadden, Wyoming; their interest and gracious cooperation with study efforts is appreciated. The Rocky Mountain Forest and Range Experiment Station laboratory at Laramie is maintained in cooperation with the University of Wyoming. Station headquarters is at Fort Collins, in cooperation with Colorado State University.

LITERATURE CITED

- Alter, J. C., 1937. Shielded Storage Precipitation Gages. *Monthly Weather Review* 65:262-265.
- Benson, C. S., 1982. Reassessment of Winter Precipitation on Alaska's Arctic Slope and Measurements on the Flux of Wind Blown Snow. Report UAG R-288. Geophysical Institute, Univ. of Alaska, Fairbanks.
- Black, R. F., 1954. Precipitation at Barrow, Alaska, Greater Than Recorded. *Trans., Amer. Geophysical Union* 35:203-206.
- Freese, F. 1960. Testing Accuracy. *Forest Science* 6:139-145.
- Hamon, W. R., 1973. Computing Actual Precipitation. *In: Distribution of Precipitation in Mountainous Areas. Vol. I, p. 159-174. World Meteorological Organization No. 326.*
- Hanson, C. L., R. P. Morris, and D. L. Coon., 1979. A Note on the Dual-Gage and Wyoming Shield Precipitation Measurement System. *Water Resources Research* 15:956-960.
- Jones, K. H., 1984. A Comparison of Various Snow Gauges on the Canadian Prairies Over Five Winters. Environment Canada Atmospheric Environment Service, Scientific Services Regina, Saskatchewan. Report No. CSS-R84-04.
- Larson, L. W. and E. L. Peck., 1974. Accuracy of Precipitation measurements for Hydrologic Modeling. *Water Resources Research* 10:857-863.
- Rechard P. A. and T. C. Wei., 1980. Performance Assessments of Precipitation Gages for Snow Measurement. *Water Resources Series No. 76, Water Resources Research Institute, Univ. of Wyoming, Laramie.*
- Reynolds, M. R. Jr., 1984. Estimating the Error in Model Predictions. *Forest Science* 30:454-469.
- Sturges, D. L. 1984. Comparison of Precipitation as Measured in Gages Protected by a Modified Alter Shield, Wyoming Shield, and Stand of Trees. *In: Western Snow Conference Proceedings 1984. p. 57-67.*
- Warnick, C. C., 1953. Experiments with Windshields for Precipitation Gages. *Trans. Amer. Geophysical Union* 34:379-388.

THE MASS BALANCE OF SNOW COVER IN THE ACCUMULATION AND ABLATION PERIODS

Esko Kuusisto

ABSTRACT: The mass balance of snow cover is affected by solid and liquid precipitation, mass flux from the soil, the net amount of snow transport by wind, evaporation (and sublimation) and water yield from the snow cover. The present status of knowledge of these components is reviewed. Even the measurement of their point values is still far from accurate, and areal estimates are very inadequate. — Gauge measurements normally underestimate solid precipitation at least by 20 %, but corrections based on in situ meteorological observations and gauge characteristics can lead to monthly values with an error of less than ± 5 %. Mass flux from the soil rather rarely occurs to such an extent that it would significantly affect the mass balance of the snow cover. Transport of snow by wind can essentially affect the areal distribution of snow cover even in partially forested basins. The combined evaporation from snow cover, interception storage and windborne snow can amount to several tens of millimeters per season. Water yield from snow cover is due to liquid precipitation and to three snowmelt components. Of these components, the basal snowmelt is a very inadequately known phenomenon which can cause considerable losses from the snow cover during the accumulation period.

(KEY TERMS: snow cover, snow accumulation, evaporation, interception, snow transport.)

INTRODUCTION

Snow — Nature's white, porous reservoir. In the Northern Hemisphere, the average maximum extent of snow cover is on land about 49×10^6 km² and at sea about 15×10^6 km² (Untersteiner, 1984). Thus one quarter of the hemisphere and one half of its land area is covered with snow in midwinter. The average maximum mass of the Northern Hemisphere's snow cover is about 9.5×10^{15} kg, giving an average maximum water equivalent of 150 mm.

Snow cover has a variety of influences. To the hydrologist, the most important is its role as a major source of streamflow. In Finland the spring runoff amounts to 40–60 % of the total annual runoff. Practically all annual flood peaks in northern Finland and 70–80 % in the south of the country are due to snowmelt.

Snow-soil interactions are very important both hydrologically and hydrochemically. The water immobilized in the snow

cover and the materials reaching the snow by wet and dry deposition are rapidly released during the ablation period. When meltwater penetrates the soil profile, its ion composition may change drastically. Therefore the study of the quality of groundwater and of the whole subsurface runoff is closely connected with snow accumulation and snowmelt (Soveri, 1985).

Usually, the snow scientist is mainly interested in the water equivalent of the snow cover. He or she is glad if a reasonably accurate estimate of an areal mean of water equivalent can be obtained.

However, estimates of the different components of the mass balance of the snow cover are also important. Simulation of the accumulation of snow cover for snowmelt-runoff models is crude without a knowledge of all the component processes. The areal distribution of the snow cover is determined by the micro-, meso- and macroscale heterogeneity of different mass balance components. This distribution is becoming increasingly important in snowmelt-runoff models, particularly if it is necessary to know the true origin of the water discharged during the spring flood. Even if successful forecasting of the magnitude of the flood is possible without this knowledge, the increasing use of hydrological models together with water quality models requires a thorough understanding of runoff formation.

In operative snowmelt-runoff models, two different approaches are used to estimate the areal water equivalent at the beginning of the melting season. Either a snow accumulation model is used or the areal water equivalent is estimated on the basis of snow surveys. A discrepancy of several tens of millimeters between these two results frequently occurs (Vehviläinen, 1986), and the model user finds it difficult to decide which value he should start with.

Part of the discrepancy is due to poor knowledge of the different processes affecting the mass balance of the snow cover in the accumulation model. It is of considerable significance to flood formation, which process has had the greatest influence. Losses from the snow cover to the underlying soil due to basal snowmelt are not losses from the point of view of flood formation, whereas losses due to evaporation are. The economic value of the correct information on the type of losses involved may be considerable.

THE MASS BALANCE EQUATION

The mass balance of the snow cover can be expressed by the equation:

$$W = P_s + P_l + M_g + D - E - Y \quad (1)$$

where:

- W = water equivalent of the snow cover, both in solid and liquid form
- P_s = solid precipitation
- P_l = liquid precipitation
- M_g = mass flux from the soil
- D = net amount of snow transport
- E = evaporation
- Y = water yield from the snow cover

All the components can be interpreted as accumulated values since the formation of the snow cover. The components P_s and P_l are normally considered to include rime deposition and condensation, respectively, because these are inevitably included in measurements by precipitation gauges (WMO, 1965). The component D also includes that part of the intercepted snow which later falls down onto the snow surface. Evaporation includes sublimation; in fact all of this component is sublimation in the case of dry snow and most of it even in the case of wet snow.

The component Y is the sum of the following processes:

- melting at the base of the snow cover
- melting within the snow cover
- melting at the snow surface
- liquid precipitation into the snow cover

Only the water produced by the first process is immediately released from the snow cover. The other components are released with a delay and attenuation which depend on the retention of liquid water within the snow cover.

SOLID PRECIPITATION

It is well known that the aerodynamic error of precipitation gauges is much greater for solid than for liquid precipitation. Even gauges equipped with a wind shield often underestimate the amount of snowfall by 20–30 per cent. In very open sites with high wind speeds, unshielded gauges have been reported to catch only one third of the snowfall (Benson, 1982).

The aerodynamic error also increases with decreasing temperature as a result of the change in structure of snow particles (Sevruk, 1982). If data on both these meteorological variables – wind speed and air temperature – are available, a rather reliable estimate of the true amount of winter precipitation can be obtained for shielded gauges, except in very open terrain. For example in Finland the detailed studies carried out by the Finnish Meteorological Institute and the Hydrological Office have made us believe that the accuracy of monthly precipitation in winter is often better than $\pm 5\%$. When exceptionally heavy snowstorms occur, the accuracy may be considerably lower.

Overestimation of solid precipitation may sometimes occur due to the catch of windborne snow by the gauge. Sevruk (1982) has presented corrections due to this phenomenon for the Tretjakov gauge as a function of wind speed and the duration of the storm. For example, with a wind speed of 10 m s^{-1} and duration of 12 h, the correction is 1.1 mm.

LIQUID PRECIPITATION

Liquid precipitation into the snow cover during the accumulation period is a rather frequent phenomenon in many regions. It can usually be estimated rather accurately with ordinary gauges. The percentage correction of gauged liquid precipitation in Finland is slightly higher in winter than in summer. This is due to a larger proportion of drizzle in winter.

The liquid water retention capacity of snow cover in Finland is normally 5–6 % by volume at the beginning of the ablation period (Lemmelä, 1970). Although it is smaller in the accumulation period due to a lower snow density, liquid precipitation is often retained and no water yield from the snow cover occurs. In Helsinki the liquid precipitation during a three month winter period (December 16 – March 16) averaged 31 mm in 1958–79. Only 8 mm of this amount was released (Kuusisto, 1984).

During the ablation period, liquid precipitation may be an essential factor in flood formation. These rain-on-snow events can cause serious flooding e.g. in the Columbia River Basin (Harr, 1981). In Finland heavy falls of rain are not common during snowmelt; rainfall normally represents only 8–12 per cent of the total water yield.

MASS FLUX FROM THE SOIL

An upward water movement within the soil towards the freezing front is a phenomenon which has been known for several decades. In recent years, it has been studied e.g. by Mageau and Morgenstern (1980), and Kane and Stein (1983). This movement may extend through the soil-snow interface and add to the water equivalent of the snow cover.

Santeford (1978) reported that in interior Alaska the average magnitude of the vapor transport from below to the snow cover was about 30 mm of water during the winter season. This moisture originated mainly from the organic soil and moss layer. The thickness of this layer was reduced from 25 cm by about one half as a result of the desiccation and compaction processes.

The temperature gradient near the soil-snow interface must probably be rather large for the upward vapor transport to occur. In addition, a significant moisture source must also be available.

MELTING AT THE BASE OF THE SNOW COVER

Heat flux from the soil or shortwave radiation penetrating through the snow can cause melting at the base of the snow cover. In Finland the latter can be significant only in the ablation season, but the former process may occur throughout the winter.

In heavy clay soil below the depth of maximum soil frost penetration, the heat flux at Jokioinen in southern Finland averaged 2.8 W m^{-2} in November–April in 1964–70 (Fig. 1). It decreased steadily throughout the winter so that the average flux in April was only 50 per cent of that in November.

Similar values have been reported elsewhere in southern Finland. The flux decreases towards the north due to the smaller storage of heat in the soil during the summer, in Lapland the flux is typically around 1.0 W m^{-2} . Thus the upward heat flux could theoretically cause considerable basal melting, in southern Finland over 20 mm/month and in Lapland 5–10 mm/month.

The amount of basal snowmelt is determined by the energy balance at the base of the snow cover. Upward heat losses through the snow cover often exceed the heat flux from the soil, resulting in the formation of soil frost.

The release of latent heat in the formation of soil frost essentially affects heat fluxes in the upper soil layers. Part of this energy is conducted downwards, leading to an increase in soil temperature below the freezing front, this phenomenon was already observed by Keränen (1920). The remainder is conducted upwards, retarding the freezing process and also leading to melting of soil frost or snow, if the heat losses through the snow cover decrease.

Studies by Solantie (1976) and Kuusisto (1984) can be used to derive areal estimates of basal snowmelt in Finland during the period December 16 – March 16. In the western coastal areas with a thin snow cover, basal snowmelt within this three month period is 10–15 mm. In southern Finland it is about 20 mm, in eastern Finland where the snow cover is thicker it amounts to 25–35 mm. Despite thick snow covers, the smaller heat flux from the soil and the lower air temperatures restrict the basal snowmelt to 10–25 mm in Lapland.

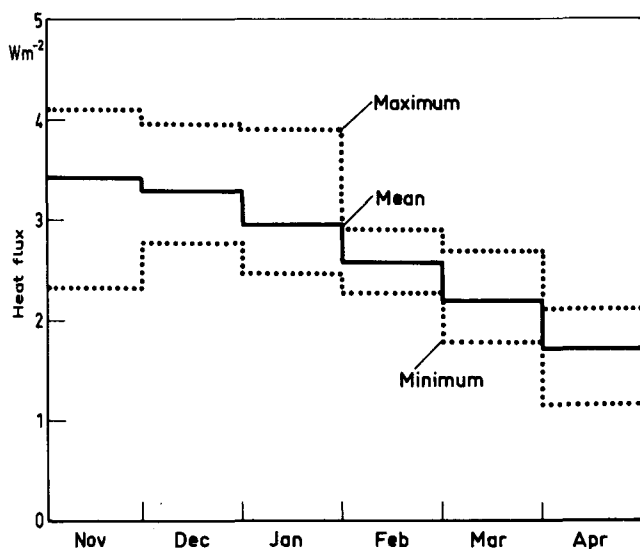


Figure 1. The average and extreme monthly heat fluxes below the depth of maximum soil frost penetration at Jokioinen (61° N , 23° E) in 1964–70.

At the base of a shallow snow cover, the heat flux is normally directed downwards during the ablation season (Weller and Holmgren, 1974; Granger and Male, 1978; Ohmura, 1982). Part of the shortwave radiation penetrating through the snow cover then causes melting of the soil frost.

SNOW TRANSPORT BY WIND

«...several kilometers long, up to 20 m wide and 10 m deep, they may contain from 20 to over 100 metric tons of water equivalent per meter of length along the bank.»

This is how Benson (1982) described the snow drifts on the banks of the Meade River near Barrow, Alaska. On the Canadian Prairies, Steppuhn and Gray (1978) estimated the potential transport fluxes during the winter season to vary between 2.6 and 22 tonnes/m.

There are three modes of snow transport by wind: ground creep, saltation and turbulent diffusion. Generally, it is accepted that most of the snow is transported by the two latter modes and mainly within a few centimeters above the snow surface (Gray and al, 1978).

If there is no crust on the snow surface, even a fairly light wind ($3\text{--}5 \text{ m s}^{-1}$) may initiate snow transport. The formation of a crust by refreezing of meltwater inhibits transport, but for new snow above such crust it may again be very effective.

The high water equivalents in snow drifts can cause serious errors in gamma snow surveys. Uryvaev and al (1969) gave an example of a 10 % underestimate with drifted snow. Fritzsche and al (1975) showed for an average water equivalent between 50 and 250 mm that underestimates up to 50 % could occur if the ratio between the water equivalent of drifted and non-drifted areas became larger than 4. A correction to the results of gamma surveys can be applied, if ground information is available on the water equivalents of snow drifts (Cork and Loijens, 1980).

EVAPORATION

Total evaporation (E_{tot}) during the accumulation and ablation periods consists of the following components:

$$E_{\text{tot}} = E_s + E_g + E_t + E_i + E_b \quad (2)$$

where:

- E_s = evaporation from snow cover
- E_g = evaporation from bare ground
- E_t = transpiration
- E_i = evaporation of intercepted water or snow
- E_b = evaporation of windborne snow

Of these components, E_s affects directly, E_i and E_b indirectly the mass balance of snow cover.

A rather accurate method for the measurement of evaporation from snow cover is the use of evaporation pans. Different kinds of pans have been used (e.g., Croft 1944, Nyberg 1966, Lemmelä 1970, Kaitera and Teräsvirta 1972). The pans used by the Finnish Hydrological Office are lathe-turned from

white plastic, they consist of double cylinders which are adjustable according to variations in snow depth. Their surface area has been 500 cm².

The other components of Eq. (2) are much more inadequately known than direct evaporation from snow cover. In the case of continuous snow cover and sub-zero temperatures, E_g and E_t can obviously be neglected. On the other hand, evaporation of intercepted or windborne snow can under certain conditions be much greater than evaporation from the snow cover itself. In Finland it has been estimated that the storage of intercepted snow in a coniferous forest may reach areally averaged values as high as 45 mm (Seppänen, 1959). At this level of maximum storage, the albedo of the forest is very high, thus reducing the net energy available for evaporation. Therefore the most favourable conditions for E_i may occur at intermediate values of interception storage. For example at an albedo of 0.40 the rate of evaporation from the interception storage could theoretically reach 1.9 mm d⁻¹ in southern Finland. With a canopy cover of 50 %, this would mean an areal value of almost 1.0 mm d⁻¹.

Snow particles transported by wind are subject to evaporation losses, which may be considerable. Tabler (1975) estimated that 37, 57 and 75 per cent of relocated snow in Wyoming evaporated over transport distances of 1500, 3000 and 4600 m, respectively.

The availability of energy and the presence of a vapor pressure gradient largely determine the evaporation from snow. In midwinter, both these conditions are unfavourable in Finland (Fig. 2). In the whole country, the radiation balance is negative from November to March. However, days with a positive radiation balance occur even in midwinter, and small amounts of evaporation can occur.

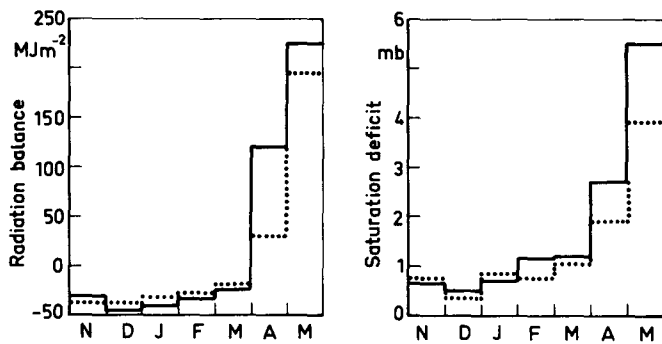


Figure 2. The monthly averages of the radiation balance and saturation deficit in southern Finland (solid line) and in northern Finland (dashed line) in November–April in the period 1971–80.

In the ablation period, energy supply and saturation deficit are sufficient for evaporation. In that period, a good correlation exists between daytime evaporation from snow cover and the dewpoint temperature (Fig. 3). In an experimental field in southern Finland, this dependence took the form:

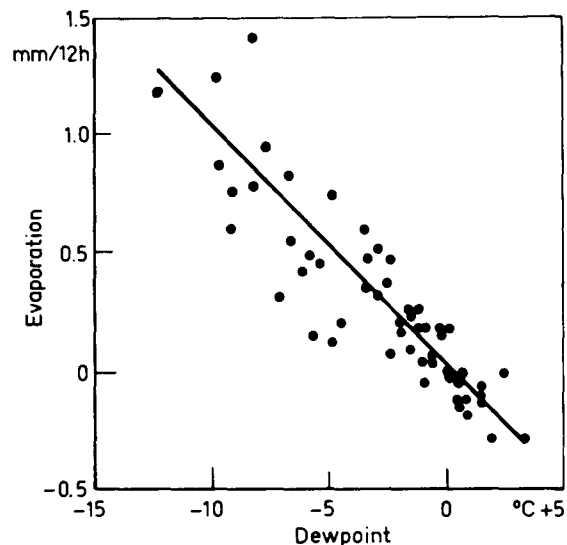


Figure 3. The dependence of daytime snow evaporation on the dewpoint temperature during ablation period in southern Finland.

$$E_s = -0.10 T_d + 0.02 \quad (3)$$

where E_s is expressed as mm/12 h and the dewpoint temperature T_d in °C.

Table (1) summarizes the monthly estimates of different components of evaporation in southern Finland in January–April. The total evaporation during these months amounts to 39 mm in open field areas and 49 mm in forests. Direct and indirect losses from snow cover are 18 mm in open areas and 36 mm in forests. Most of these losses occur during the ablation period.

Depending on climatic and physiographic conditions, either evaporation or condensation may prevail during snowmelt (Table 2). For the whole melting season, the average mass exchange due to evaporation-condensation rarely exceeds 1.0 mm d⁻¹. In a single day, both evaporation and condensation may exceed 2.0 mm (e.g. de La Casiniere, 1974; Moore and Owens, 1984).

INTERCEPTION

Interception of solid and liquid precipitation by tree canopies often has a considerable indirect influence on the mass balance of the snow cover. In a coniferous forest, the interception storage formed by snow and rime can have an areal water equivalent of several tens of millimeters. The portion of snowfall intercepted can reach 20–30 % from the seasonal total (Braun, 1985).

There are five processes by which the intercepted snow may leave the canopy (Miller, 1965):

TABLE 1. Estimated values of different evaporation components in southern Finland in winter and spring months.

Component	Estimated value of the component (mm/month)									
	Open field					Forest				
	J	F	M	A	Total	J	F	M	A	Total
E_s	0	1	6	4	11	0	0	3	4	7
E_g	0	0	2	18	20	0	0	0	6	6
E_t	0	0	0	1	1	0	0	0	7	7
E_i	0	0	0	0	0	3	5	8	12	28
E_b	1	2	3	1	7	0	0	1	0	1
E_{tot}	1	3	11	24	39	3	5	12	29	49

- falling of blowing of dry snow
- sliding or falling of partly melted bodies of snow
- dripping of flowing of meltwater
- vapor flux from meltwater film
- vapor flux from snow

The last two processes result in the component E_i in Eq. (2). This component may be considerably greater than evaporation from snow cover. Many facets of tree crowns are perpendicular to the solar radiation, and therefore they obtain more shortwave energy than horizontal surfaces. The large surface-to-volume ratio of the intercepted snow and high wind speeds at the canopy level also enhance evaporation.

Several methods have been applied in studying the removal mechanisms of intercepted snow. Goodell (1959) used weighing method, he found a 60 % loss in less than 3 hours, the whole loss being due to evaporation. Hoover and Leaf (1967) used time sequence photography. They concluded that mechanical removal predominated evaporation. Miller (1965) estimated that the removal of intercepted snow by sliding proceeded at the rate of about 2 mm h^{-1} , while removal by evaporation seldom exceeded 1 mm d^{-1} .

AREAL VARIABILITY OF MASS BALANCE COMPONENTS

Three different scales can be distinguished in the areal distribution of snow cover:

1. Microscale variability. This can be defined as the variation of snow properties over a homogeneous area. This area can be a section of an open field, located far enough from the edges of the surrounding forest. It can also be a forested area, consisting of trees of approximately equal age and spacing, or a slope with a constant angle in any terrain type. Characteristic linear distances of microscale variability range from a few centimeters up to 100 m.
2. Mesoscale variability. This is mainly caused by variation of physiographic factors: terrain types, slopes, aspects, variations in forest density etc. The characteristic linear distance of mesoscale variability depends on the scale of variation of physiographic factors. In Finland it usually ranges from a few tens of meters to several kilometers.

3. Macroscale variability. This depends mainly on the variation of climatological factors over a region. Typical scales in Finland are from a few kilometers (coastal effects) to hundreds of kilometers.

These three types of variability have been discussed by several authors (e.g. Gray and al. 1978, Gottschalk and Jutman 1979), but the definition of characteristic linear distances varies. — All components of the mass balance of snow cover vary in all these scales.

Consequently the water equivalent of the snow cover has a considerable micro-, meso- and macrovariability, all of which have been rather extensively investigated. On the other hand, only a few studies have been made on the variability of the different components, particularly in micro- and mesoscale.

Let us consider a small, partially forested river basin in Finland. If it is not located on the coast, the macroscale variability can be neglected. The following estimates of the effect of the variability of each component on the overall variability of the water equivalent in micro- and mesoscale can be made:

	microscale	mesoscale
P_s	moderate	small
P_l	small	small
M_g	small	small
D	large	large
E	small	moderate
Y	moderate	moderate

Even in a sheltered environment, the transport of snow by wind can often cause considerable areal variability of the water equivalent. In microscale this is manifested by ripples and ridges with a variety of forms, plus depressions around trees and other obstacles. In mesoscale the accumulation of drifted snow may occur e.g. in river beds and near the edges of an open field.

Uneven radiative melting can cause considerable variations in water yield both in micro- and mesoscale. Solid precipitation is unevenly distributed in microscale in a coniferous forest, whereas its mesoscale distribution is rather even (if differences in altitude are small). Evaporation from intercepted snow in the forest or from snow transported by wind in the open can also have a moderate mesoscale effect on the distri-

TABLE 2. The average daily values of snowmelt and snow evaporation in different climatic and physiographic conditions.

Reference	Site	Elevation (m)	Observation period	Average melt mm d ⁻¹	Average evaporation mm d ⁻¹
Gold and Williams (1960)	Open field (Canada), 45° N	100	March 1959	7	0.60
Treidl (1970)	Open field (Michigan), 46° N		January 23, 1969	15	- 0.64
Dewalle and Meiman (1971)	Forest opening (Colorado), 39° N	3 260	June 1968	50	0.18
de La Casiniere (1974)	Open field in mountains (France), 46° N	3 550	July 1968	16	0.28
	Open field in mountains (Spain), 41° N	1 860	April 1970	10	0.49
Granger and Male (1978)	Open field in prairies (Canada), 51° N		Melting season 1974	8	0.09
			Melting season 1975	5	0.17
			Melting season 1976	3	0.05
Hendrie and Price (1978)	Deciduous forest (Ontario), 46° N		April 1978	10	0
Kuusisto (1978)	Open field (Finland), 60° N	60	Melting seasons 1968-1973	7	0.03
Harstveit (1981)	Open field in mountains (Norway), 60° N	435	April-May 1979-1980	12	0
			- cloudy days	23	- 0.70
			- clear days	7	0.19
Braun and Zuidema (1982)	Small basin, 23 % forest (Switzerland), 47° N	800	Days with intense snowmelt, 1977-1980	23	- 0.54
Eaton and Wendler (1982)	Open field (Alaska), 65° N		April 1980	3	0.24
Kuusisto (1982)	Open field (Finland), 61° N	104	Days with intense snowmelt, 1959-1978	14	- 0.03
	Open field (Finland), 67° N	178		15	0.41
Moore and Owens (1984)	Open field in mountains (New Zealand), 43° N	1 450	Melting season 1982	31	- 0.91
Vehviläinen (1986)	Small basin, 82 % forest (Finland), 64° N	120	Melting seasons 1971-1981	5	0.08

bution of the snow cover.

In Finland the coefficient of variation of the areal water equivalent ranges in small basins typically from 0.2 to 0.5 during the period of maximum snow accumulation (Kuusisto, 1984). No quantitative estimates of the contribution of each mass balance component to these values have been made.

RESEARCH AND DATA NEEDS

It is obvious that fundamental measuring problems still exist in connection with all the components of the mass balance of the snow cover. This is true even for point measurements, but overwhelming difficulties arise when it is attempted to estimate areal values.

Some new methods of measurement will probably be developed in the future. The attenuation of transmitted gamma radiation in the canopy at different elevations can be measured to study evaporation from the interception storage. A gamma transmitter placed at the soil-snow interface can perhaps give the water equivalent accurately enough to indicate the magnitude of basal snowmelt or mass flux from the soil. The development of aerodynamic models together with observations on the structure of snow particles may improve the accuracy of

gauged solid precipitation (Carlsson and Svensson, 1984).

Accurate areal modelling of all the processes affecting the mass balance of the snow cover will, however, remain too complex for many years. Therefore the measurement of the water equivalent of snow will maintain its key role in snow accumulation studies, and new, more accurate methods for these measurements should be developed.

However, the practical value of the knowledge of the component processes will also increase. Such knowledge will help to diminish and interpret correctly the discrepancies between modelled and measured water equivalents of snow cover. This information is also needed in the study of the chemical composition of the snow cover and in the forecasting of the effects of snowmelt on water quality.

The need for the management of snow cover for different purposes (water supply, water quality, transportation, avalanche prevention) will also increase in some areas. This management requires improved knowledge of some processes affecting the mass balance of the snow cover, particularly snow transport by wind.

REFERENCES

- Benson, C., 1982. Reassessment of winter precipitation on Alaska's Arctic Slope and measurements on the flux of wind blown snow. Univ. of Alaska, Inst. of Geophysics, Report R-288, 26 p.
- Braun, L., 1985. Simulation of snowmelt-runoff in lowland and lower alpine regions of Switzerland. ETH, Geographical Institute, Zürich, 168 p.
- Braun, L. and P. Zuidema, 1982. Modelling snowmelt during advection-melt situations in a small basin. Proc. Symp. Hydr. Research Basins, Bern, vol. 3, pp. 771-780.
- Carlsson, B. and U. Svensson, 1984. Wind correction factors for snow precipitation gauges. Fifth NRB Symposium, Vierumäki, Finland, March 19-23, 1984, pp. 1.15-1.30.
- Cork, H. and H. Loijens, 1980. The effect of snow drifting on gamma snow survey results. *Journal of Hydrology* 48, pp. 41-51.
- Croft, A., 1944. Evaporation from snow. *Am. Met. Soc. Bulletin* 25, pp. 38-42.
- de La Casiniere, A., 1974. Heat exchange over a melting snow surface. *Journal of Glaciology* 13(67), pp. 55-72.
- Dewalle, D. and J. Meiman, 1971. Energy exchange and late season snowmelt in a small opening in Colorado subalpine forest. *Water Resources Research* 7(1), pp. 184-188.
- Eaton, F. and G. Wendler, 1981. The heat balance during the snowmelt season for a permafrost watershed in interior Alaska. *Archives for Meteorology, Geophysics and Bioclimatology* 31, pp. 19-33.
- Fritzsche, A. and E. Feimster, 1975. Snow water equivalent surveys of the Souris River Basin. EG & G Report EGG-1183-1668 (Prepared for U. S. National Weather Service).
- Gold, L. and G. Williams, 1960. Energy balance during the snowmelt period at an Ottawa site. *IAHS Publ.* 51, pp. 288-294.
- Goodell, B., 1959. Management of forest stands in western United States to influence the flow of snow-fed rivers. *IAHS Publication* 48, pp. 49-58.
- Gortschalk, L. and T. Jutman, 1979. Statistical analysis of snow survey data. *SMHI Rapport* RHO 20, 41 p.
- Granger, R. and D. Male, 1978. Melting of a prairie snowpack. *Journal of Applied Meteorology* 17(12), pp. 1833-1842.
- Gray, D. and al., 1978. Snow accumulation and distribution. *Modelling of Snow Cover Runoff*, Hanover, New Hampshire, 26-29 September, 1978, pp. 3-33.
- Harr, R., 1981. Some characteristics and consequences of snowmelt during rainfall in western Oregon. *Journal of Hydrology* 53, pp. 277-304.
- Harstveit, K., 1981. Studier av snøsmelting i Dyrdaalen 1979 og 1980. Norsk Hydrologisk komité, Rapport 9, 25 p.
- Hendrie, L. and A. Price, 1978. Energy balance and snowmelt in a deciduous forest. *Modelling of Snow Cover Runoff*, Hanover, New Hampshire, 26-29 September, 1978, pp. 211-221.
- Hoover, M. and C. Leaf, 1967. Process and significance of interception in Colorado subalpine forest. *Proc. Int. Symp. on Forest Hydrology*, Pergamon Press, pp. 213-222.
- Kaitera, P. and H. Teräsvirta, 1972. Snow evaporation in southern and northern Finland, 1969-71. *Aqua Fennica* 2, pp. 11-19.
- Kane, D. and J. Stein, 1983. Water movement into seasonally frozen soils. *Water Resources Research* 19(6), pp. 1547-1557.
- Keränen, J., 1920. Über die Temperatur des Bodens und der Schneedecke in Sodankylä. Helsinki, 200 p.
- Kuusisto, E., 1978. Optimal complexity of a point snowmelt model. *Symposium on the Modelling of Snow Cover*, Hanover, New Hampshire, 26-28 September, 1978, pp. 205-210.
- Kuusisto, E., 1982. Temperature index, energy balance – or something else? *Symposium on the Use of Hydrological Research Basins in Planning*, Sept. 21-23, 1982, Bern.
- Kuusisto, E., 1984. Snow accumulation and snowmelt in Finland. *Publ. of the Water Research Institute* 55, Helsinki, 149 p.
- Lemmelä, R., 1970. On the snowmelt runoff and groundwater formation on a glacial-fluvial esker in southern Finland. *Univ. of Helsinki, Dept. of Geophysics*, 119 p (in Finnish).
- Mageau, D. and N. Morgenstern, 1980. Observations on moisture migration in frozen soils. *Can. Geotechn. Journal* 17, pp. 54-60.
- Miller, D., 1965. The heat and water budget of the Earth's surface. *Advances in Geophysics* 11, pp. 175-302.
- Moore, R. and I. Owens, 1984. Controls of advective snowmelt in a maritime alpine basin. *J. of Climate and Applied Meteorology* 23, pp. 135-142.
- Nyberg, A., 1966. A study of the evaporation and condensation at a snow surface. *Arkiv för Geofysik* 4, Stockholm.
- Ohmura, A., 1982. Climate and energy balance on the arctic tundra. *J. of Climatology* 2, pp. 65-84.
- Seppänen, M., 1959. On the quantity of snow lodging on branches in pine dominated forest during the time of snow destruction in Finland. *IAHS Publication* 48, pp. 64-68.
- Sevruk, B., 1982. Methods of correction for systematic error in point precipitation measurement for operational use. *WMO, Operational Hydrology Report* 21, Geneva, 91 p.
- Solantie, R., 1976. The computation of the water balance of Finland in the period 1931-60. *Univ. of Helsinki, Dept. of Geophysics*, 350 p (in Finnish).
- Soveri, J., 1985. Influence of meltwater on the amount and composition of groundwater in quaternary deposits in Finland. *Publ. of the Water Research Institute* 63, Helsinki, 92 p.
- Steppuhn, H. and D. Gray, 1978. Modification of a conceptual model to estimate the sublimation potential for wind-transported snow. *Univ. of Saskatchewan, Div. of Hydrology*, Saskatoon.
- Tabler, R., 1975. Estimating the transport of blowing snow. *Univ. of Nebraska, Research Committee of Great Plains Agricultural Council*, Publication 73, pp. 85-117.
- Treidl, R., 1970. A case study of warm air advection over a melting snow surface. *Boundary-Layer Meteorology* 1, pp. 155-168.
- Untersteiner, N., 1984. The cryosphere. In 'The Global Climate', ed. by J. Houghton, Cambridge Univ. Press, pp. 121-140.
- Uryvaev, V. and al., 1969. Principal errors of airborne gamma surveying of snow cover. In 'Determination of the water equivalent of snow cover', ed. by L. Verzhinina and A. Dimakhsyan, Jerusalem.
- Vehviläinen, B., 1986. Modelling and forecasting snowmelt floods for operational purposes in Finland. *Second Scientific Assembly of IAHS, Budapest*, July 2-10., 1986.
- Weller, G. and B. Holmgren, 1974. The microclimates of the arctic tundra. *Journal of Applied Meteorology* 13, pp. 854-862.
- WMO, 1965. Guide to hydrometeorological practices. No. 168 TP 82, Geneva, 281 p.

CHANNEL HYDRAULICS AND MORPHOLOGY

EROSION CONTROL FOR PLACER MINING

Larry A. Rundquist and N. Elizabeth Bradley¹

ABSTRACT: Techniques for the control of nonpoint-source sediment pollution are reviewed for application to placer mines in northern environments. Erosion-control techniques are divided into three categories: drainage control, site grading, and stockpile protection and location. Drainage control serves two primary functions: 1) to exclude unpolluted water from the mine site and 2) to direct water that has become polluted within the site through a treatment system prior to discharge to the receiving waterbody. Drainage-control techniques include stream channel diversions, bedrock drains, overland-flow diversion structures and settling-pond systems. Site grading serves to reduce the height, steepness, or length of erodible slopes, thereby reducing the potential for erosion of the slope. Site grading should be conducted concurrent with the mining operation to reduce erosion potential. Locating and protecting stockpiles to minimize contact with waterbodies also reduces nonpoint-source sediment pollution. Stockpiles of vegetation, organic overburden, fine-grained inorganic overburden, oversized rocks, and fines removed from settling ponds may be retained for use in site rehabilitation; stockpiles of these materials should be located away from erosive waterbodies or protected with erosion-resistant materials.

(KEY TERMS: erosion control; nonpoint-source pollution; placer mining; drainage control; stockpiling.)

INTRODUCTION

Placer mining has historically increased turbidity in downstream receiving waters. Much attention has been directed at studying and regulating the water quality of the point-source discharges from placer-mining operations, with minimal study or control of nonpoint-source pollution. However, nonpoint-source pollution may cause substantial water quality degradation. Recent advances have been made in the control of nonpoint-source pollution from agriculture, silviculture, and urban construction. Measures proven to be effective in controlling sediment discharge resulting from these applications may be useful in reducing the erosion potential from mined areas.

The term "nonpoint-source pollution" is used in this paper to include all stream turbidity, suspended sediment, and siltation (deposition

of solids on the stream bed) resulting from soil erosion caused by human activity that cannot be traced to a single discharge point. Point-source pollution, in contrast, is highly localized with an origin that can be traced to an identifiable point where the polluted discharge reaches a body of water. For example, turbid effluent from the outlet of a settling pond is a point-source pollution, while sediment washed off an exposed hillside is nonpoint-source pollution.

A placer-mining operation typically removes upland and riparian vegetation and the soils overlying alluvial gravel deposits. Overburden is stripped to expose the gold-bearing gravels, which are processed to separate the placer deposits from the lighter alluvium. The mining process results in unvegetated slopes and steep piles of overburden and alluvium that contain fine particles, which are easily eroded during rainstorms and flood events. Tailing and overburden piles typically are located within the active floodplain and are susceptible to erosion by the stream during break-up and high flow events. Without proper erosion control, the fine particles will enter the local drainage system. Unlike point-source pollution, the nonpoint-source pollution from exposed and unstabilized slopes may continue long after the operation of the site has ceased.

This paper presents a summary of information obtained during a study to develop best management practices to minimize nonpoint-source pollution from placer mining. The best management practices are documented in a reference manual (Rundquist et al. 1986a) and a supporting technical report (Rundquist et al. 1986b). The development of the best management practices was based on a review of literature in the fields of mining engineering, drainage and erosion control, hydrology and hydraulics, aquatic and terrestrial biology, and aquatic and terrestrial-habitat rehabilitation. The

¹Senior Consultant and Staff Engineer, respectively, at Entrix, Inc., Business Park Blvd., Suite 6, Anchorage 99503

literature review focused on references with application to the control of nonpoint-source pollution in stream valleys in Alaska or other northern environments.

The study was designed to provide guidance to resource-management agencies reviewing placer mining permit applications, with particular emphasis placed on the control of nonpoint-source pollution and site rehabilitation. The study results also will assist placer miners in the development of mining plans that include design elements for nonpoint-source pollution control and site rehabilitation.

If appropriate erosion-control procedures for surface-water drainage, grading, and stockpiling are outlined during the planning phase and implemented during site operation, nonpoint-source pollution can be substantially minimized. Appropriate measures most often include: development of drainage systems; proper diversion of stream channels; construction, maintenance, and rehabilitation of an adequate settling-pond system; grading of tailings piles; and siting and protection of stockpiles. Site-specific conditions at a placer-mining site dictate which techniques are most effective at each site. The following sections of this paper present general techniques for drainage control, site grading, and stockpile placement for placer-mining operations.

DRAINAGE CONTROL

A comprehensive erosion-control plan to limit nonpoint-source pollution should focus on drainage control. Drainage control has two objectives: to divert water around a mine site in order to minimize the amount of water that contacts erodible material within the site and to collect all turbid water within the site to allow for treatment prior to discharge to the stream.

Prior to the initiation of mining activity, a drainage plan should be developed which delineates the surface-flow pattern around and through the site. This plan is useful in evaluating the need for, and location of, drainage-control structures. It can also be used when designing a plan to reestablish the drainage pattern during site rehabilitation.

Channel Diversion

Instream disturbances at a mining site should be avoided. If mining in a stream channel is necessary, the surface flow should be diverted and isolated from the mining activity prior to the initiation of mining within the existing stream channel. The

diversion channel should be sited, designed, constructed, and operated to avoid excessive erosion or deposition, to contain floods within the range of acceptable site risks, and to meet fish-passage requirements if fish are present. An overflow channel near the diversion channel may be constructed to divert potential flood flows around the settling ponds and any other structures, such as the camp, to be protected. The overflow channel can function as an access road within the site except during flood flows in excess of the diversion channel design flood.

The location for the diversion channel will depend on the physical characteristics of the site, the equipment available to construct the channel, and the proposed sequence of site operation. Preferably, the stream should be placed permanently into a newly constructed or rehabilitated stream channel. At sites where mining cuts are narrower than the entire floodplain, a permanent stream channel could be constructed on the mined portion of the floodplain prior to mining the other portion. Whenever possible, the stream should be diverted only once to minimize impacts to fish and wildlife. Design criteria for a diversion channel are presented in Rundquist et al. (1986a and 1986b) and Simons, Li, and Associates (1982).

Overland Flow Diversion

Surface runoff from the valley walls should be intercepted and diverted around the site. Gullies or other topographical features which may concentrate runoff can provide significant amounts of flow during or after rainfall events. Overland flow can also result from melting permafrost, groundwater seepage, and snowmelt. A drainage system can divert most of the surface runoff around the site and retain the remaining sediment-laden water within the site. Upslope berms may be used to divert water around the site (Herrick et al. 1974, Becker and Mills 1972). In areas of permafrost ditches draining the intercepted flow should follow the contours closely to avoid degradation. Overland flow may also be diverted by stockpiles of strippings and overburden pushed uphill onto the valley walls and out of the active mining areas (Figure 1). Overland flow interception structures formed in this manner should be protected from erosion.

Drainage structures in areas of permafrost will likely transport significantly larger amounts of water than those in non-permafrost areas, and should be sized accordingly. Areas of permafrost exhibit rapid responses to precipitation. In a study of similar sized streams with and without permafrost, Slaughter

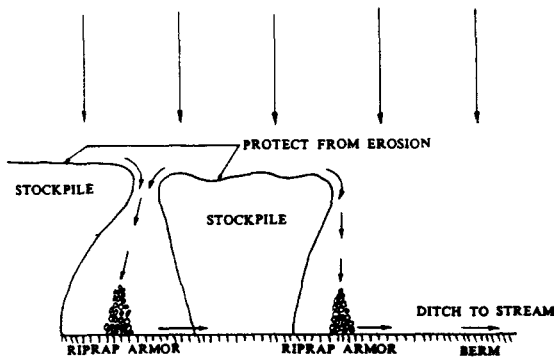


Figure 1. Using stockpiles to divert overland flow.

et al. (1983) found that the presence of permafrost resulted in increased amounts of overland flow. Due to the large amounts of flow and the potential for drainage structure failure caused by the degradation of permafrost, additional maintenance of drainage structures may be required in areas of permafrost; drainage structures should be inspected regularly.

Groundwater Diversion

Groundwater flow should also be diverted around the mining site. Combinations of both surface and subsurface drainage control will likely provide better and more economical results for erosion control (USSCS 1979). Bedrock drains located upstream of the excavation area may be used to divert groundwater before it seeps into the excavation area. While the bedrock drain should generally be only deep enough to prevent down valley seepage from flowing into the active mining area, the drain should be designed to have sufficient capacity for augeis growth. The bedrock drain may be backfilled with cobbles and large gravels to act as a french drain (Sowers 1979). The water collected in an upstream bedrock drain can be routed around the mine site in a ditch which flows into the stream downvalley (Figure 2). A series of bedrock drains may be dug throughout the mining site to collect additional groundwater infiltration from the valley walls (Peele 1941). However, groundwater or surface water which contacts unstabilized slopes or enters the excavation area must be collected and treated with other turbid water within the site.

Site Drainage

Water in contact with surfaces disturbed by mining will likely become sediment laden and

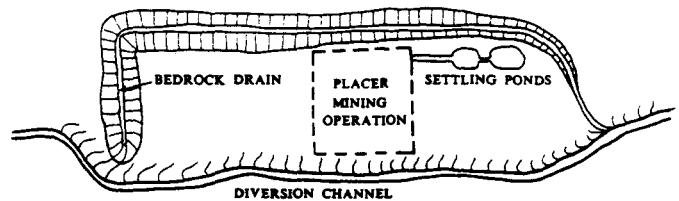


Figure 2. Bedrock drain routing groundwater flow around mine site.

turbid. Therefore, water that is not diverted around the site will require treatment prior to discharge. Overland flow resulting from precipitation or groundwater upwelling within the site should be routed into settling ponds. Settling-pond systems should be designed to retain all sediments originating on the site. Efforts to prevent water from becoming sediment laden appear to be more efficient than efforts to treat sediment-laden water (Vesilind and Peirce 1982).

Concurrent with mining activity, or at least at the end of each mining season, the overland flow drainage pattern should be reestablished and stabilized. Surface-water control is the primary concern in the design of the drainage pattern. Any water that is detained or impounded within the site will reduce the rate and amount of surface runoff (Beasley 1972) and thus reduce erosion. Storage of water will occur when small depressions or terraces along the contours are constructed (Frank Moolin and Associates 1985). Site grading should reestablish a drainage pattern to limit sediment contributions to the system (Figure 3).

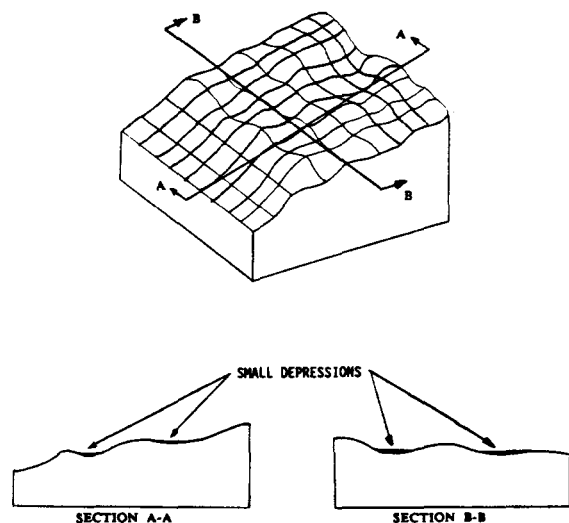


Figure 3. Grading should create a drainage pattern with small depressions.

Settling Ponds

Although settling ponds are essential to the control of point-source pollution, they are also an important aspect of nonpoint-source pollution control. Settling ponds are used to clarify water which has been used in mining activities such as sluicing or hydraulicking which produce point-source pollution. Settling ponds should also be used to clarify sediment-laden surface water and seepage from excavated or stripped areas which would otherwise contribute to nonpoint-source pollution. Surface water and seepage from the mining area must be controlled to limit nonpoint-source pollution; all sediment-laden water produced on the site should be routed through the settling pond system. However, the flow of unpolluted water into a settling pond should be minimized to increase the settling pond efficiency.

SITE GRADING

Grading tailing piles and steep, excavated slopes within the mining site will reduce erosion and encourage revegetation (Becker and Mills 1972). A grading plan should describe the sloping and contouring necessary to reestablish desired elevations within the site and to provide for an appropriate drainage pattern. The mining site should be graded to cause surface water from erodible areas to flow through the settling-pond system. Site grading should be done concurrent with mining activity, at the conclusion of each cut, or at least at the end of each mining season. Grading during mine operation will benefit seasonal erosion control; if tailings are properly placed and graded during mining, additional grading will not be necessary upon site closure.

Slope Modifications

Step slopes and tailing piles should be graded as soon as possible. Surface erosion from slopes is greatest during the first year following disturbance (Cook and King 1983). Reducing the steepness of tailing piles will significantly reduce surface-water pollution (Vesilind and Peirce 1982). A slope of 3 horizontal to 1 vertical or less is recommended (Becker and Mills 1972, Dryden and Stein 1976). Large piles of stripped loess with thawing ice lenses should be graded to slopes of 3 to 1 when placed. Slopes that are steeper toward the top and shallower toward the bottom are preferred as they have been shown to have less sediment loss than flat slopes or slopes that are steepest at the base (Haan and Barfield 1978, Meyer and Romkens 1976).

Grading steep slopes will also reduce potential slope failures which can release large amounts of sediments into nearby streams. Slope failures are generally avoided with 3 to 1 slopes (Schwab 1982). In addition, earth-moving equipment such as front end loaders and bulldozers are able to operate on slopes as steep as 3 to 1 (Johnson 1966).

Permafrost material that will be removed after thawing should be graded to a shallow grade to minimize erosion during thawing. Adjacent permafrost materials that will not be removed should not be graded; they should be left as a cut face for the duration of adjacent mining operations (Figure 4). This will minimize the area of permafrost degradation adjacent to the mine site by reducing the surface area of permafrost exposed to warm air, water, or solar radiation and minimizing disturbance to the insulating vegetation on the top of the cut bank. The length of time that the cut face is exposed should be minimized, especially in ice-rich permafrost terrain. Tailings should be pushed up against the cut face following the conclusion of mining at that location to insulate the cut face (Figure 4).

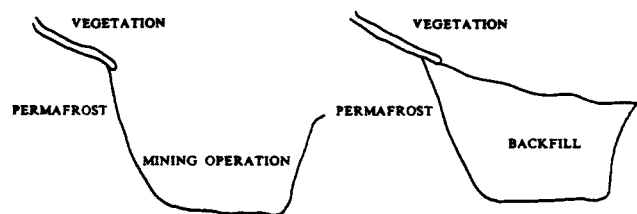


Figure 4. Site grading during and after mining adjacent to permafrost terrain.

Terracing and furrowing parallel to the contours should be incorporated in site grading, particularly outside the active floodplain, to reduce the effective length of the slope and thus decrease further erosion (Figure 5). Backsloping terraces encourage deposition of eroded soils (Beasley 1972). Small furrows (trenches) approximately 0.5 ft in depth and spaced closely together along the contours of the slope can effectively reduce erosion (Doyle 1976, Becker and Mills 1972, Cuskelly 1969).



Figure 5. Terraces and furrows on side slopes.

Contoured tailing piles and steep slopes should be roughened or scarified to reduce erosion by increasing water infiltration, minimizing slope failures, and encouraging natural revegetation (Rutherford and Meyer 1981, Troeh et al. 1980). Tailing piles should be reduced in height to minimize abrupt variations in surface elevations.

Timing of Grading

Site grading during site operation most likely will be more cost effective and efficient than site grading at the end of each mining season since the equipment will already be in the immediate vicinity; grading at the completion of each cut rather than at the end of the mining season will discourage repeated handling of material. Frequent moving and handling material will increase the time and costs involved in grading. In addition, a lesser amount of material will be handled at one time. Tailing piles and overburden may be mixed and graded together unless required for use in site rehabilitation. Progressive site grading can realize the benefits of improved erosion control and vegetation reestablishment (Johnson 1966).

STOCKPILE PLACEMENT

Proper placement and protection of stockpiles will minimize erosion of the stockpiles, ensure maximum retention of materials for site rehabilitation, and minimize distances that stockpiled materials must be moved during site rehabilitation. Stockpile placement and protection, if properly planned and executed, will help control erosion.

General Recommendations

Stockpile locations should be identified after consideration of drainage patterns and the eventual use of the material. Stockpiles should be located in areas where they can be easily protected and where rehandling will be minimized. Stockpiles should preferably be located where the results of the site assessment work indicate unproductive material. The amount and type of material required during site rehabilitation should be estimated to determine the quantities of each material to be stockpiled.

Nonpoint-source pollution from stockpiles can be minimized through proper siting and containment procedures. The principal objective is to select sites where the stockpiled material is protected from surface flow, including active stream channels and runoff

from rain or snow melt. Stockpiles should also be located and protected according to the acceptable risks at the site. Stockpiles should generally be located in elevated areas away from flood waters such as on the valley walls or in flat areas where flood waters often have shallow depths and low velocities. Stockpiles should not be located near an active channel or within the active floodplain where high flows could erode the sediments. Areas of concentrated surface runoff should also be avoided. Armoring the lower slopes of the stockpiles with cobbles, large rocks, or logs available on site is suggested if protection is needed (Joyce et al. 1980). An armoring layer of cobbles, large rocks, or logs may inhibit the erosion of fine sediments. Organic material and settling pond fines may have a high moisture content and may require containment berms around the perimeter of these stockpiles.

Location of stockpiles should also minimize handling. Properly choosing washplant, screening plant, grizzly, or stacker locations and the directions in which tailings are pushed can result in stockpiling in the proper location without expending additional equipment time for material redistribution.

Recommendations for Specific Materials

Materials stockpiled for use in site rehabilitation include six types of material that can be removed from a work area. These are: 1) trees (greater than 6 inches in diameter at breast height); 2) small trees, shrubs, and grasses with the top layer of organic soil; 3) shallow soils, often containing a mixture of fine organic and inorganic material; 4) large quantities of fine inorganic material, such as deep loess deposits; 5) oversize inorganic material such as large boulders; and 6) fines removed from settling ponds. If the top layer of organic soil is very thin, the upper six inches of the surface material should be removed and stockpiled with the shrubs and grasses. Depending on the area where the mine is located, one or more of these categories may not be present.

Large trees require little protection since surface flow past a stockpile of trees will not substantially contribute to nonpoint-source pollution. Stockpiles of trees should be placed in an area where they will not interfere with the mining operation and be available to enhance stream and floodplain habitats during site rehabilitation after the site is closed. Large trees should be stockpiled separately from other types of material and not mixed with other organic material during temporary storage. In some cases, the trees can be used to

construct log crib containment berms for smaller organic material.

The most common forms of vegetation that are removed during a placer mining operation are the small trees and shrubs that occupy previously undisturbed floodplain riparian zones. Proper stockpiling and protection of this material is important since it will serve as the stock for natural revegetation, and since the material is easily eroded. When feasible, the amount of time of exposure of stripped slopes should be minimized to reduce erosion. The small trees, shrubs, and grasses should be piled with the top layer of organic soil in a protected location. Placing these two types of materials together accomplishes several objectives. First, the woody material will provide some protection for the organic soil from wind and surface water erosion. Second, many species of shrubs and grasses will continue to grow within the stockpile. This will improve the survival rate of vegetation placed during site closure. Third, when the shrub layer and surface soil are removed together, disturbance of the root zones will be reduced, thus enhancing survival of the vegetation. This material should be kept moist to maintain the viability of the woody slash.

The shallow soils located beneath the top layer of organic soil and often consisting of fine organic material, sands, and perhaps some gravel and cobble should be piled separately from the trees and the shrub-organic soil piles. This material should be protected since it can be eroded easily. If necessary, large rocks can be used for protection along the side slopes of the piles. Containment berms may also be constructed around the stockpiles.

At some locations deep deposits of loess, or fine inorganic soil, must be removed to expose placer-bearing gravels. In these situations the large volume of material that must be handled dictates that it be moved a short distance and only handled once. Typically, the most efficient handling of this material is to push it up the valley side slopes into fan-shaped, flat-topped mounds (Figure 1). At sites where large volumes of this material must be handled, final stockpile locations should provide maximum protection from wind and surface-water runoff which can easily erode this material. If organic rehabilitation material is limited at the site, portions of this loess material may be used both as a leveling layer and as a seedbed to enhance vegetative recovery.

In situations where highly erodible stockpiled material cannot be protected using berms

and riprap as described, temporary seeding and fertilizing using annual grasses may be useful to help stabilize this material.

SUMMARY

If appropriate erosion-control procedures for surface-water drainage, grading, and stockpiling are outlined during the planning phase and implemented during site operation, nonpoint-source sediment pollution can be substantially minimized at a placer-mining site. Appropriate measures include the following:

1. Divert active channels around the site in a diversion channel if the active channel bed is to be mined; a one-time diversion into a final rehabilitated stream channel is recommended to minimize impacts to fish and wildlife.
2. Intercept and divert surface runoff around the site to prevent contact with erodible soils.
3. Intercept and divert groundwater around the mining activity using bedrock drains.
4. Route sediment-laden water within the mining site into settling ponds using proper grading.
5. Design settling ponds to accommodate all point- and nonpoint-sources of sediment-laden waters within the site in order to assist in the control of nonpoint-source pollution.
6. Grade the site concurrently with site operation. Steep slopes and tailing piles should be graded to reduce their height, slope steepness, or slope length to leave an undulating terrain. Roughening the surface reduces erosion potential and encourages natural revegetation.
7. Locate or protect stockpiles of materials to be used for rehabilitation to minimize erosion potential while minimizing distances that materials must be moved during site rehabilitation.

ACKNOWLEDGMENTS

This paper was based on the Technical Report and Reference Manual produced during the Best Management Practices for Placer Mining Study funded by the Alaska Department of Fish and Game, Habitat Division in Fairbanks, Alaska.

The authors wish to thank their colleagues in this study for their contribution. We also want to thank the reviewers of this paper, the Technical Report, and the Reference Manual.

REFERENCES

- Beasley, R.P. 1972. Erosion and Sediment Pollution Control. The Iowa State University Press. Iowa.
- Becker, B.C. and T.R. Mills. 1972. Guidelines for Erosion and Sediment Control Planning and Implementation. Prepared for Office of Research and Monitoring U.S. Environmental Protection Agency. Washington, D.C. EPA-R2-72-015.
- Cook, M.J. and J.G. King. 1983. Construction Cost and Erosion Control Effectiveness of Filter Windrows on Fill Slopes. Intermountain Forest and Range Experiment Station Research. Ogden, Utah. Note: INT-335.
- Cuskelly, S.L. 1969. Erosion-control Problems and Practices on National Forest Lands. Trans. Am. Soc. Agric. Eng. 12(1): 69-70, 85.
- Doyle, W.S. 1976. Strip Mining of Coal: Environmental Solutions. Noyes Data Corporation. Park Ridge, New Jersey.
- Dryden, R.L. and J.N. Stein. 1975. Guidelines for the Protection of the Fish Resources of the Northwest Territories During Highway Construction and Operation.
- Frank Moolin and Associates, Inc. 1985. Best Management Practices Manual on Erosion and Sedimentation Control. Prepared for the Alaska Power Authority.
- Haan, C.T. and B.J. Barfield. 1978. Hydrology and Sedimentology of Surface Mined Lands. University of Kentucky. Lexington, Kentucky.
- Herricks, E.E., J. Cairns, and V.O. Shanholtz. 1974. Preplanning Mining Operations to Reduce the Environmental Impact of in Use Drainage on Streams. In: Water Resources Problems Related to Mining. R.F. Hadley and D.T. Snow (eds). American Water Resources Association. Minnesota.
- Johnson, C. 1966. Practical Operating Procedures for Progressive Rehabilitation of Sand and Gravel Sites. National Sand and Gravel Association.
- Joyce, M.R., L.A. Rundquist, and L.L. Moulton. 1980. Gravel Removal Guidelines Manual for Arctic and Subarctic Floodplains. Prepared for U.S. Fish and Wildlife Service by Woodward-Clyde Consultants.
- Meyer, L.D. and M.J. Romkens. 1976. Erosion and Sediment Control on Reshaped Land. Proc. Third Federal Inter-Agency Sedimentation Conference, Water Resources Council. Washington, D.C.
- Peele, Robert. 1941. Mining Engineers' Handbook. John Wiley and Sons, Inc. New York.
- Rundquist, L.A., N.E. Bradley, J.E. Baldrige, P.D. Hampton, T.R. Jennings, and M.R. Joyce. 1985a. Best Management Practices for Placer Mining. Reference Manual. Prepared for the Alaska Department of Fish and Game.
- Rundquist, L.A., N.E. Bradley, J.E. Baldrige, P.D. Hampton, T.R. Jennings, and M.R. Joyce. 1985b. Best Management Practices for Placer Mining. Technical Report. Prepared for the Alaska Department of Fish and Game.
- Rutherford, C. and K. Meyer. 1981. Revegetation on Gold Dredge Tailings, Nyc, Alaska. Prepared for BLM, Anchorage, Alaska.
- Simons, Li and Associates, Inc. 1982. Surface Mining Water Diversion Design Manual. Prepared for U.S. Department of the Interior Office of Surface Mining.
- Slaughter, C.W., J.W. Hilgert, and E.H. Culp. 1983. Summer Streamflow and Sediment Yield from Discontinuous-Permafrost Headwaters Catchments. Proc. Fourth Annual Conference on Permafrost 1983. Fairbanks, Alaska.
- Sowers, G.F. 1979. Soil Mechanics and Foundations: Geotechnical Engineering. MacMillan Publishing Co., Inc. New York.
- Troeh, F.R., J.A. Hobbs, and R.L. Donahue. 1980. Soil and Water Conservation for Productivity and Environmental Protection. Prentice-Hall, Inc. New Jersey.
- U.S. Soil Conservation Service. 1979. Drainage of Agricultural Land. Water Information Center, Inc. Port Washington, NY.
- Vesilind, P.A. and J.J. Peirce. 1982. Environmental Engineering. Ann Arbor Science. Michigan.

RIVERBANK EROSION PROCESSES ON THE YUKON RIVER AT GALENA, ALASKA

William S. Ashton and Stephen R. Bredthauer *

ABSTRACT: Periodic measurements of riverbank recession on the Yukon River at Galena, Alaska have been made since 1946. Intensive studies of channel shape and riverbank erosion were conducted in 1959, 1984 and 1985. Erosion rates varied from 0.3 m/yr (1.0 ft/yr) at banks with developed vegetative protection (peat or bank debris) to 10.8 m/yr (35.5 ft/yr) at steep banks with active thermoerosional niching. Comparison of channel profile measurements from June 1984 and June 1985 indicate that the thalweg did not significantly change location or elevation during a 10-year recurrence interval flood.

(**KEY TERMS:** thermoerosional niching; subarctic; Alaska; Yukon River; erosion.)

INTRODUCTION

Galena, Alaska is located on the downstream end of an 11 km (7 mi) long meander of the Yukon River (Figure 1). Erosion control structures were first installed in the early 1960's by the U.S. Army, Corps of Engineers, when bank erosion threatened to undermine a flood control dike protecting the airfield from ice jam floods. The upstream key at the end of the airstrip is a series of sheet pile cells. Bank protection extends 793 m (2,600 ft) downstream of the sheet pile cells, and consists of a variety of designs, including the use of rock riprap and of gravel-filled 55 gallon oil drums. Both designs have a sheet pile wall at the toe.

Since 1946, there have been sixteen sets of riverbank erosion measurements of the Yukon River at Galena. During 1984

and 1985, detailed measurements were made of the channel geometry, bed material and riverbank erosion rates at sites studied since 1946. The following is a summary of riverbank erosion processes observed during 1984 and 1985, and of data collected since 1946.

STUDY AREA

The area climate is continental subarctic, with mean annual temperatures of -4.7 degrees C (23.6 degrees F) and mean annual precipitation of 329 mm (13.0 in). Snowfall averages 1500 mm (59.1 in) per year. Galena lies in a wide flood plain composed of fine to coarse grained deposits on a 11 km (7 mi) long bend of the Yukon River.

The study area has four physiographic phases, each with distinct permafrost, drainage, vegetation, and engineering characteristics. Each of these phases is temporary (relative to geologic time) and somewhat evolutionary in nature due to permafrost, flooding, river meandering, and associated vegetative changes. As the phases become older, ice-rich permafrost becomes more prevalent (Weber and Pewe, 1970).

The river is constrained by mountains for approximately 330 km (200 mi) upstream of Galena, flowing in a confined channel until reaching the Yukon-Koyukuk Lowlands, where the river meanders for about 67 km (40 mi) until again becoming confined by the mountains. The drainage area of the Yukon River at Galena is approximately 676,000 sq km (261,000 sq mi).

Twenty-three years of streamflow data

* Respectively, Hydrologist and Senior Civil Engineer, R&M Consultants, Inc., 5024 Cordova Street, Anchorage, Alaska 99503.

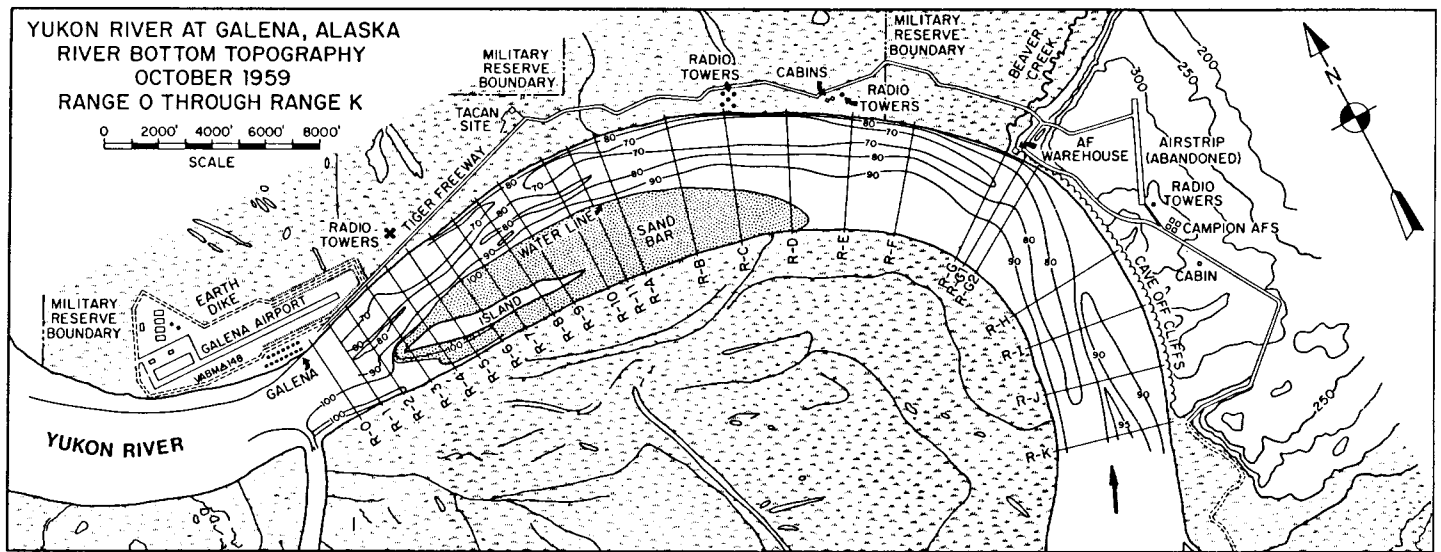


FIGURE 1. BOTTOM TOPOGRAPHY (IN FEET) AND RANGE LINES, GALENA, ALASKA, OCTOBER 1959. RANGES O THROUGH G WERE RESURVEYED JUNE 1984, AND RANGES 4 THROUGH 10 WERE RESURVEYED JUNE 1985. KALA SLOUGH ENTERS THE YUKON FROM THE LOWER LEFT.

are available at Ruby, approximately 80 km (50 mi) upstream of Galena and with a drainage area of approximately 671,000 sq km (259,000 sq mi). Mean annual flow is 4,730 cms (166,900 cfs), with average daily values ranging from a winter minimum of 480 cms (17,000 cfs) to a peak of 27,500 cms (970,000 cfs). As is typical of most subarctic rivers, the Yukon River has low flows in the winter, with flows sharply increasing at breakup in May. Peak flows normally occur in early June, steadily decreasing throughout the summer except for occasional late summer peaks.

The bankfull stage is approximately 38 m (125 ft) at Galena. However, at water levels of 34 m (112 ft), water begins to flow into old channels and lake beds on the north bank. Ice jams occur frequently in the area, with the maximum recorded stage of 40.5 m (133 ft) occurring during an ice jam in 1971.

Galena is in the zone of discontinuous permafrost. The mean annual freezing index is approximately 3000 degree-days C. Mean monthly air temperatures range from -24.2 degrees C (-1.5 degrees F) in January to 15.3 degrees C (59.6 degrees F) in July. Water temperatures rise rapidly shortly after breakup, reaching 10 degrees C (50 degrees F) by early June and up to 17-20 degrees C (63-68 degrees F) in late July or early August. The temperatures

then steadily decline, dropping to freezing in mid to late October. Freezeup occurs in November. Annual maximum observed ice thicknesses range from 830-1,400 mm (32-55 in). Breakup dates range from May 1 to May 28.

BANK AND BED MATERIAL

Data on bank and bed materials are available from the literature and from a drilling and bed material sampling program conducted in 1984 and 1985 (Weber and Pewe, 1970; R&M Consultants, 1985; Ashton, 1985). Generalized soils profiles near the new townsite (range 7) and upstream of the townsite (Range B) are shown in Figures 2 and 3, respectively.

The upper bank material is primarily composed of silt with some sand. The material becomes coarser in the lower layers, grading into sand, gravelly sand, and sandy gravel. Surface bed materials collected from the river with a 152 mm (6-inch) pipe dredge reflect two distinct types of surface bed material from the north bank to the south bank. Material gathered near the north bank consists of a well-graded mixture of gravel from 25.4 to 50.8 mm (1-2 inch) gravel down to fine sand, with median diameters ranging from 0.7 to 10.5 mm. Material found farther

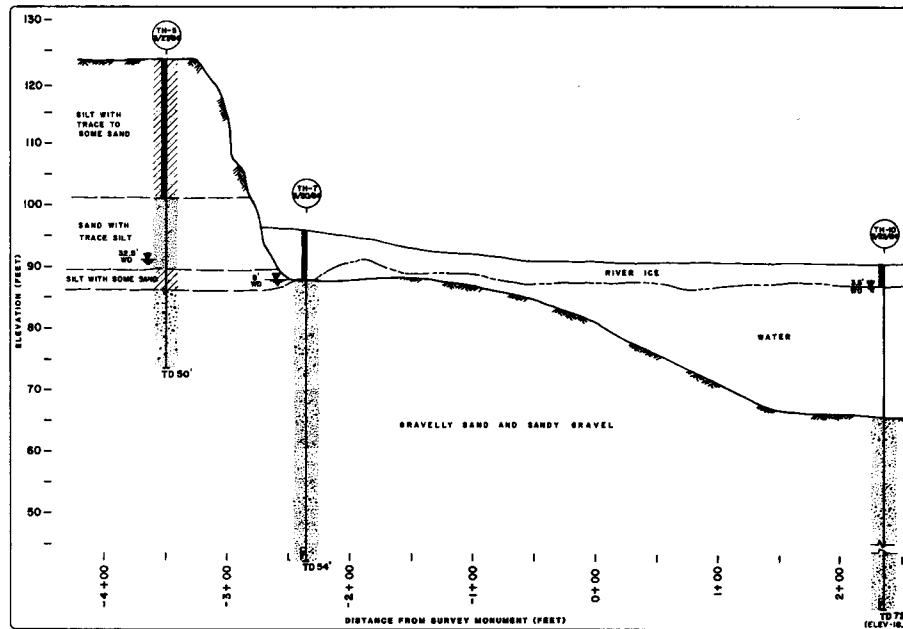


FIGURE 2. GENERALIZED SOIL PROFILE AT RANGE 7, LOOKING UPSTREAM, NEAR THE NEW GALENA TOWNSITE (R&M CONSULTANTS, 1985).

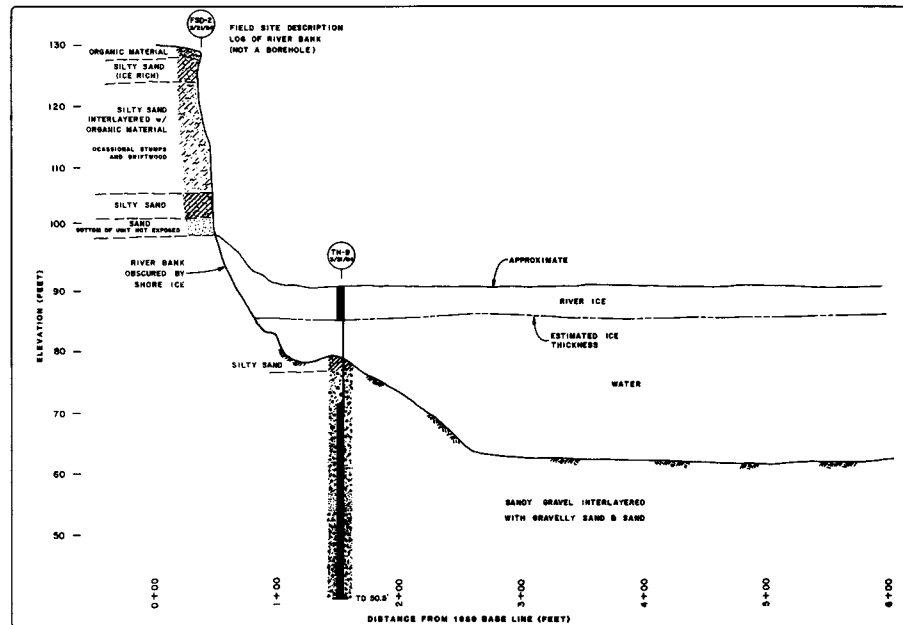


FIGURE 3. GENERALIZED SOIL PROFILE AT RANGE B, LOOKING UPSTREAM (R&M CONSULTANTS, 1985).

out in the channel consists of fairly uniform medium to fine sand. Sub-bed material collected in the main channel is primarily a mixture of fine gravel grading to fine sand.

Permafrost was encountered to elevation 30.9 m (101.2 ft.) along the bank at Range 7, but was not encountered below the main channel down to an elevation of 5.7 m (18.8 ft.). This is typical of permafrost patterns on large, migrating northern rivers, and has been reported for the Mackenzie River by Smith and Hwang (1973). The large heat mass of the water in the summer maintains a large thaw bulb beneath the river channel. Significant degradation of the permafrost on the north bank is not evident because the material is eroded away before the bank has a chance to thaw. However, permafrost was found at Range B at elevation 21.9 m (72 ft.), only 2.4 m (8 ft.) below the streambed. With the rapid bank erosion in this area, the bed would have been exposed for 4-6 years, and therefore it would be anticipated that the depth of thaw would have been greater.

EROSIONAL PROCESSES

General

The erosion processes observed on the Yukon River near Galena are similar to those described for other large northern rivers, as summarized in Lawson (1983). Lawson describes the erosion of perennially frozen streambanks as being comprised of three zones: bluff, transitional, and bank. The bluff zone is above high water, the bank zone is below low water and the transitional zone is the area between the two. There is no frequency of occurrence associated with these water levels. Therefore, for a specific location each zone is identified by field observations.

Observations During 1984 and 1985

For the Yukon River at Galena the bank zone is below elevation 97 ft (29.6 m) and the bluff zone is above elevation 120 ft (36.6 m). The transition between the bank zone and the transitional zone corresponds with the change in bank mate-

rial from sand and gravelly sand to silt and sandy silt. The following discussion concentrates on the erosion processes in the transitional zone.

During the breakup flood there is little or no bank erosion. Between Range 0 and Range 5 (Figure 1), an ice shelf along the north bank prevents moving ice from hitting the bank (except along the sheet pile cells at Range 4). Upstream of Range 5, ice is hitting the bank, but since the bank is frozen and water temperatures are still near 0 degrees C (32 degrees F), little erosion or thermoerosional niching occurs.

Water temperatures increase rapidly once ice is out of the river, reaching 10 degrees C (50 degrees F) less than 2 weeks after the 1984 breakup. Water levels are generally highest in June (except for ice jams), and the flow is against the frozen upper silt layer of the bank. The warm water rapidly thaws the frozen silt, which is carried away by the current and waves, forming thermoerosional niches of up to 5-7 m (15-20 ft) in depth.

The niching continues until the soil can no longer support the weight of the frozen cantilevered block, which then fails. Once the block fails, it thaws and the material is washed downstream. Depending on river stage and the bank material, the soil blocks provide the freshly exposed bank face limited protection from niching due to waves and currents, and no protection against thermal niching. During June 1984 niching progressed 0.4 m (1.3 ft) into a freshly exposed frozen silt bank in 24 hours due to thermal action and small waves (less than 5 cm high).

The rate of erosion varies throughout the meander bend, from little or no erosion at Ranges 4 and G to maximum rates at Range B through D (Table 1). The major portion of the thermoerosional niching occurs during the high water after breakup and into June and early July. The rate of niching decreases as water levels and nearshore velocities decrease, and as the larger bank material is exposed. During 1985 the water level stayed higher for a longer period than in 1984, with consequently more erosion (Patrick, 1985).

During June 1985, cross-section measurements and a thalweg profile were made at a discharge of 21,300 cms (754,000

TABLE 1. EROSION RATES NEAR GALENA, ALASKA

Range	1984 Erosion m(ft)(1)			1984-1985 Erosion m(ft)(1)		Average Erosion Rate
	June to July	July to October	Total	October 1984 to June 1985	1963-1983(2)	m/yr(ft/yr)
4	0.0	0.0	0.0	0.0		0.0
5	0.15(0.5)	0.5(1.5)	0.6(2.0)	1.2(4.0)		2.0(6.5)
6	1.4(4.5)	0.9(3.0)	2.3(7.5)	4.6(15.0)		3.7(12.0)
7	0.3(1.0)	2.7(9.0)	3.0(10.0)	2.6(8.5)		4.1(13.5)
8	3.4(11.0)	0.9(3.0)	4.3(14.0)	7.6(25.0)		4.0(13.0)
9	0.6(2.0)	1.2(4.0)	1.8(6.0)	(3)		4.4(14.5)
10	1.7(5.5)	1.5(5.0)	3.2(10.5)	7.9(26.0)		4.7(15.5)
11A	0.15(0.5)	0.15(0.5)	0.3(1.0)	(4)		4.1(13.5)
A	0.6(2.0)	1.8(6.0)	2.4(8.0)	(4)		4.4(14.5)
B	1.8(6.0)	5.9(19.5)	7.8(25.5)	(3)		4.4(14.5)
C	4.9(16.0)	0.8(2.5)	5.6(18.5)	10.8(35.5)		6.1(20.0)
D	0.9(3.0)	5.9(19.5)	6.9(22.5)	3.5(11.5)		4.6(15.0)
E	0.3(1.0)	0.0	0.3(1.0)	--		3.5(11.5)
F	0.0	0.0	0.0	0.0		2.3(7.5)
G	0.0	0.0	0.0	0.0		0.8(2.5)

(1) Measured from survey monument on north bank.

(2) Determined by comparison of aerial photographs from 1963 and 1983, R & M Consultants, 1985.

(3) Monument destroyed

(4) Monument underwater

From: Ashton, 1985.

cfs) at Range 7, with a total flow of approximately 22,600 cms (800,000 cfs) including flow through Kala Slough. This flow is approximately the 8-10 year recurrence interval flood and reached an elevation of 120 ft (36.6 m). The high water levels provided an opportunity to compare the bed elevations and bluff erosion between Ranges 4 and 10 with that which occurred during 1984, when the maximum flow was 11,400 cms (403,000 cfs) and the maximum water surface elevation was 113 ft (34.4 m). At Ranges 5 through 10 the bluff and transitional zone (elevation 27.4 m (90 ft.) to top of bank) eroded 1.2 to 7.9 m (4 to 26 ft), while the channel shape below elevation 27.4 m (90 ft.) was approximately the same as in June 1984. While there was no general lowering of the bed evident at these sites during the June 1985 flood, it was apparent that the bluff zone was eroding at a more rapid rate than measured during 1984 (Figures 4 and 5 and Table 1).

Historic Erosion Rates

At Range 7, the U.S. Army, Corps of Engineers has collected bank erosion rates since 1946 (Table 2). These measurements indicate an average annual erosion rate at Range 7 of 4.8 m/yr (15.6 ft/yr), ranging from 0.3 m/yr (1.0 ft/yr) in 1965 to 9.1 m/yr (30 ft/yr) in 1968. During our study we measured 3.0 m/yr (10.0 ft/yr) during 1984.

Comparison of aerial photography obtained in 1963 and 1983 indicates the long term upper bank erosion ranging from 0.8-6.1 m/yr (2.5-20 ft/yr) (Table 1). During 1984 the upper bank erosion was observed to vary from 0.3-7.8 m (1-26 ft) for the same area. The areas with low erosion rates (Ranges 11A and E) were located on an old slough channel filled with peat and at a bank protected by debris, respectively.

Erosion in any individual year varies, depending on the water stage, wind

420

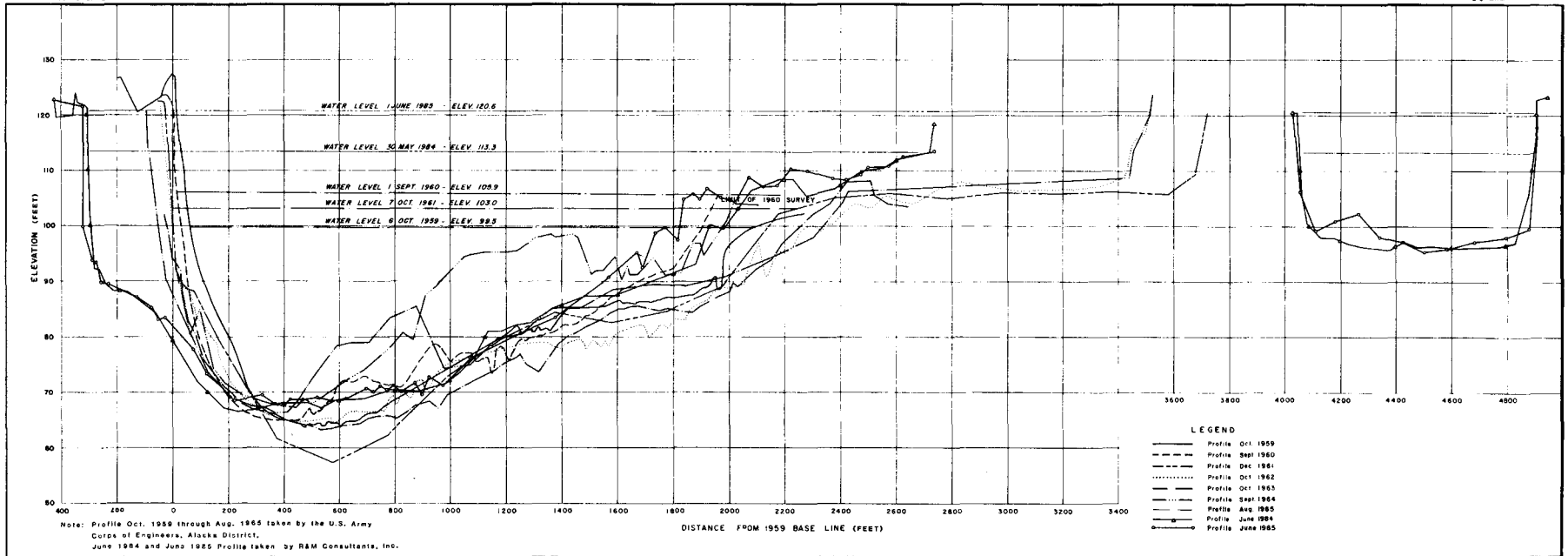
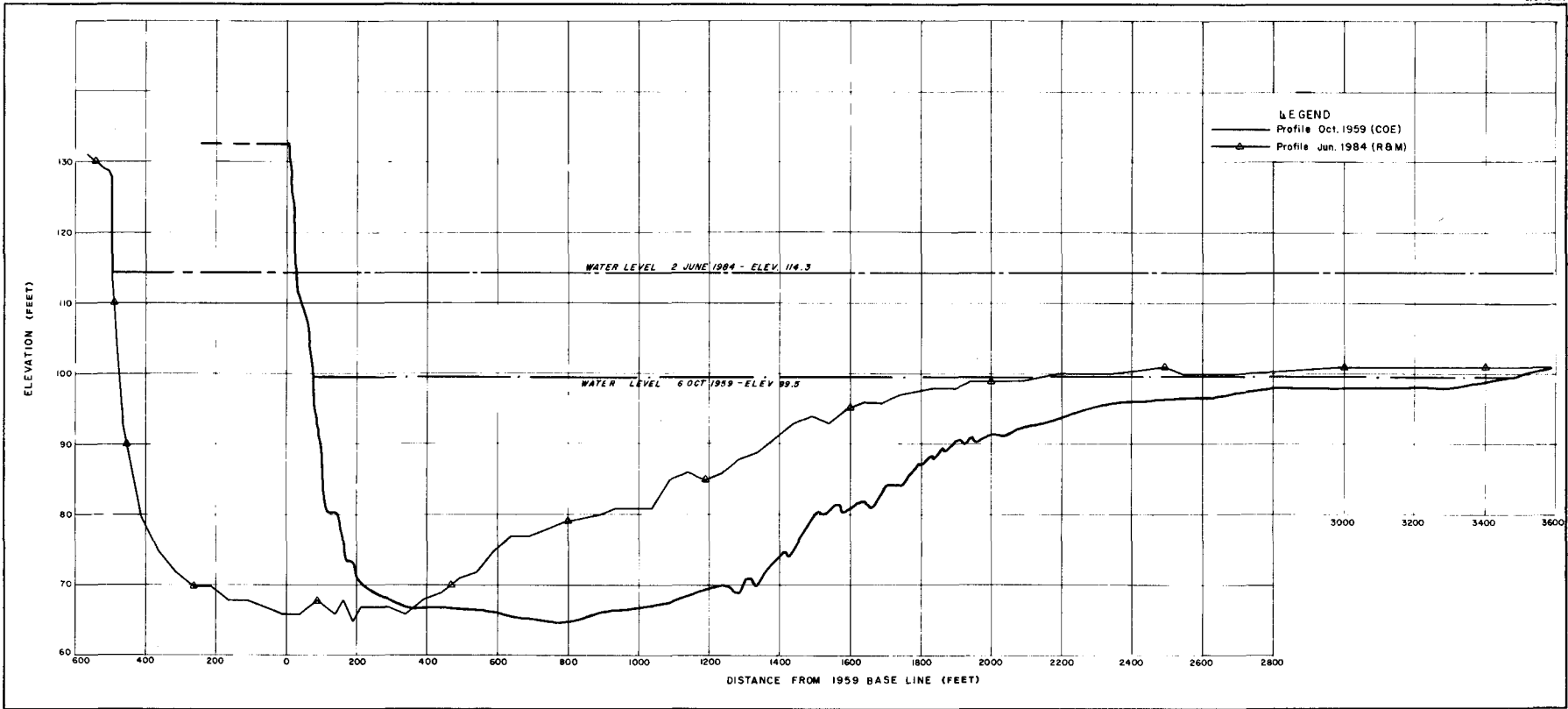


FIGURE 4. BOTTOM PROFILES, RANGE 7, LOOKING UPSTREAM (R&M CONSULTANTS, 1985).



421

FIGURE 5. BOTTOM PROFILES, RANGE C, LOOKING UPSTREAM (R&M CONSULTANTS, 1985).

TABLE 2. HISTORICAL EROSION RATES, RANGE 7

<u>Date</u>	<u>Period of Erosion Years</u>	<u>Amount of Bank Eroded m(ft)</u>	<u>Annual Rate m/yr(ft/yr)</u>
Winter 1946			
October 1959	12.8	70.1(230)	5.5(18)
September 1960	0.9	4.3(14)	4.9(16)
October 1961	1.1	6.4(21)	5.8(19)
October 1962	1.0	2.1(7)	2.1(7)
October 1963	1.0	4.9(16)	4.9(16)
October 1964	1.0	5.8(19)	5.8(19)
August 1965	0.8	0.3(1)	0.3(1)
July 1966	0.9	5.8(19)	6.4(21)
July 1967	1.0	1.5(5)	1.5(5)
February 1969	1.6	14.6(48)	9.1(30)
February 1974	5.0	15.2(50)	3.0(10)
June 1977	3.3	12.2(40)	3.7(12)
August 1978	1.2	9.1(30)	7.6(25)
September 1982	4.1	18.3(60)	4.6(15)
TOTALS	35.7	171(560)	4.8(15.6)

From: U.S. Army Corps of Engineers, 1983.

and amount of exposed bank silt. Rapid upper bank erosion is typically caused by a combination of high water and wind driven waves. Ott (1981) reports up to 13.7 m (45 ft) of erosion during a 3 day storm, and local residents report erosion of up to 36.6 m (120 ft) in one year (H. Strassburg, 1984). Comparison of long-term erosion rates with the depth of thermoerosional niches observed in 1984 indicates that on the average the upper bank goes through one cycle of thermoerosional niching and block slumping per year. The amount of slumping at any specific location is dependent on the localized bank stratigraphy.

SUMMARY

Observations of bank erosion processes along the Yukon River near Galena, Alaska found erosion rates similar to those summarized in Lawson (1983). The rates varied depending on water stage, frequency of wind waves, bank stratigraphy, and location along the meander bend. During 1984, bluff recession varied from 0.3 m (1 ft) in areas with developed bank vegetative cover (peat

soil or vegetative bank debris) up to 7.8 m (25.5 ft) in areas with steep banks and thermoerosional niching.

Channel cross-sections taken in 1984 and 1985 indicated that the bed elevation remained at approximately the same elevation in the study area during a 10-year recurrence interval flood, likely due to the relatively large bed material found near the north bank. However, rapid bluff erosion occurred due to the high water stages.

ACKNOWLEDGMENTS

Data used in this paper were collected during an erosion control study and design for the Alaska Department of Transportation and Public Facilities. Special thanks to boat operators Dan Patrick and Harvey Strassburg for their local insights of the Yukon River.

REFERENCES

- Ashton, W.S. 1985. Galena field trip
June 1-3, 1985. Memo to V.
Gretzinger and S. Bredthauer. R & M
Consultants, Inc. June 6, 1985.
14 pp.
- Lawson, D.E. 1983. Erosion of perennially
frozen streambanks. CRREL Report
83-29. Hanover, New Hampshire, 22
pp.
- Ott Water Engineers, 1981. Plan of study,
Yukon River erosion control at
Galena, Alaska. Prepared for U.S.
Army, Corps of Engineers, Alaska
District. Anchorage, Alaska, 25 pp.
with appendices.
- Patrick, D. 1985. Personal communication.
July 1985.
- R&M Consultants, Inc. 1985. Galena bank
stabilization, Project No. K-83513.
Final Report. Prepared for Alaska
Department of Transportation and
Public Facilities. 2 volumes.
Anchorage, Alaska.
- Smith, M.W. and C.T. Hwang. 1973.
Thermal disturbance due to channel
shifting. In Proc. 2nd International
Permafrost Conference. National
Academy of Sciences. pp. 51-59.
- Strassburg, H. 1984. Personal communica-
tion. October 1984.
- U.S. Army, Corps of Engineers, 1983.
Galena streambank protection, Galena,
Alaska. Section 14 Reconnaissance
Report. Anchorage, Alaska.
- Weber, F.R. and T.L. Pewe. 1970.
Surficial and engineering geology of
the central part of the Yukon-
Koyukuk lowland, Alaska. Department
of the Interior. U.S. Geological
Survey, Miscellaneous Geological
Investigations Map I-590.

SNOWMELT RUNOFF

MODELLING SNOWMELT INFILTRATION AND RUNOFF IN A PRAIRIE ENVIRONMENT

*D.M. Gray, R.J. Granger and P.G. Landine**

ABSTRACT: The development of an infiltration model for frozen soils and its application for predicting streamflow from snowmelt in a Prairie environment is discussed. The model assumes frozen soils can be grouped to three broad classes according to their infiltration potential: Unlimited - cracked or highly porous soils capable of infiltrating all the snow water; Limited - the infiltration potential of a soil depends primarily on the snowcover water equivalent and the ice content of the soil layer, 0-300 mm at the time of melt; and Restricted - a soil containing an impermeable layer that inhibits infiltration. Field measurements of soil water changes during snowcover ablation are used to support the concept and a prediction equation for soils of Limited potential is described. Estimates of infiltration quantities and runoff volumes determined by the model are compared with corresponding estimates which were either "observed" or "calculated" by a mass balance analyses of data collected on areas ranging in size from 35 m² to 11.4 km². The agreement in values suggest the model is capable of giving estimates of areal infiltration of acceptable accuracy for operational purposes. It is demonstrated that the performance of the NWSRFS and SSARR operational models in simulating streamflow from snowmelt on a Prairie watershed is markedly improved with the use of the infiltration algorithm.

(KEY TERMS: infiltration model, frozen soils, snowmelt streamflow simulation)

INTRODUCTION

Water generated by the melt of a shallow snowcover is an important component of the hydrological cycle of the Prairie region. It can be viewed as having either detrimental or beneficial effects. On the one hand, because of such factors as the poor relief and drainage development of the region, the presence of frozen soils at the time of melt, and the rapid ablation of the snowcover, direct runoff from snowmelt can lead to serious flooding, erosion and drainage problems. Conversely, snowmelt runoff provides a valuable source of water for domestic, livestock, and irrigation purposes as well as a wildlife habitat. It is estimated that 80-85% of the average annual volume of "local" surface runoff over much of the southern semi-arid region of western Canada is derived from snow.

A number of models have been developed for synthesizing streamflow from snowmelt. For example: the U.S. National Weather Service River Forecast System, NWSRFS (U.S. Department of Commerce, 1972; Anderson, 1973; Peck, 1976); the Streamflow Simulation and Reservoir Regulation Model, SSARR (U.S. Army Corps of Engineers, 1972); the Hydrological Engineering Center HEC-1 Flood Hydrograph Package (U.S. Army Corps of Engineers, 1973); the U.S. Department of Agriculture Hydrograph Laboratory Model USDAHL-74 (Holtan et al., 1975); the HBV of the Swedish Meteorological and Hydrological Institute (Bergström, 1979) and the UBC Watershed and Flow Model (Quick and Pipes, 1973). Of the existing systems no single model has

*Division of Hydrology, University of Saskatchewan, Saskatoon, Saskatchewan, Canada, S7N 0W0.

been adopted for universal use. Ongoing tests are being conducted by the World Meteorological Organization and other bodies on the performance of a number of the "better-known" models in different physiographic and climatic regions of the world.

Each model differs from another, either as it calculates hydrological components or simulates the various processes involved. A main factor contributing to the differences is that many models were developed for a specific set of physiographical conditions, e.g. climate, topography, vegetation and soil type. Consequently, a model developed in a mountainous area will not usually give reliable streamflow simulations for a Prairie watershed; nor should it be expected.

Direct runoff from snowmelt can be regarded as the last step in a series of events beginning with snowcover accumulation and including the processes of interception, ablation, evaporation, infiltration, and the storage of meltwater by the snowcover, soil, surface depressions and channels. It is not surprising then that the simulation of snowmelt runoff has been most successful where there is abundant, uniformly-distributed snow and pronounced topographical relief, i.e., where there is the least opportunity for other processes to be major components. The opposite situation exists on the Prairies. The snowcover is shallow and relatively large estimation errors of snowcover depth and water equivalent frequently occur, there is poor relief and the losses to evaporation, infiltration and depression storage may be comparable in magnitude with the total water content of the snowcover.

Thus, at least for the Prairie region, the performance of a model in simulating streamflow rates and volumes from natural catchments is often directly related to the accuracy with which infiltration is evaluated. In most operational systems infiltration is estimated by empirical equations such as those reported by Horton (1940) and Holtan (1961), soil moisture accounting routines, or from relationships that index antecedent groundwater storage conditions and the soil moisture storage potential to the base flow recession characteristics of the streamflow hydrograph. Two main problems arise in applying these procedures to watersheds in northern and

west-central Canada, namely; (1) no attempt is made to distinguish differences in the infiltration process to frozen soils and (2) many streams are ephemeral, i.e. flow occurs only following a rainfall or snowmelt event and therefore the recession properties of the hydrograph do not properly index the soil moisture storage potential of a basin at the time of runoff.

Anderson and Neuman (1984) used a frost index to calculate the reduction in percolation rates of frozen soils, and showed that this routine improved the performance of the NWSRFS Sacramento SMA model in simulating runoff on a basin with frozen soil. They suggest, however, that further improvements in modelling runoff from areas with frozen ground will probably require a more physically-based approach.

The following material presents a model for describing infiltration to frozen soils based on such an approach and focuses on the effects of the model in improving the simulation of streamflow rates and volumes from snowmelt in a Prairie environment. Many of the results presented have been reported by Granger and Gray (1984) and Gray et al. (1984, 1985 b, c) and the reader is referred to these publications for more complete details.

DEVELOPMENT OF A SIMPLE PHYSICALLY-BASED MODEL

Granger et al. (1984) and Gray et al. (1985b) outlined the development and testing of a simple physically-based model describing snowmelt infiltration to frozen soils. They based their model on approximately fifteen years of study by the Division of Hydrology, University of Saskatchewan, of the snow hydrology of the Prairie region, including a comprehensive field investigation of infiltration to frozen soils in the Dark Brown and Brown soil zones of the region, and on the results of infiltration studies under similar climatic regions of the USSR reported in the literature (Motovilov, 1978, 1979; Popov, 1973). The authors postulated that frozen soils may be grouped into three broad categories with regard to their infiltration potential, namely: Restricted, Limited and Unlimited (Fig. 1). Restricted - infiltration is impeded by

an impermeable layer, such as an ice lense at the soil surface or within the soil near the surface. For practical purposes the amount of meltwater that infiltrates can be assumed negligible and most of the snowcover water equivalent goes to direct runoff and evaporation.

Limited - infiltration is governed primarily by the snowcover water equivalent and the frozen water content of the shallow layer of soil, 0-300 mm.

Unlimited - a soil containing a high percentage of large, air-filled, non-capillary pores or macropores at the time of melt and most or all of the snow water infiltrates. Examples of those soils are dry, heavily-cracked clays and coarse, dry sands.

Granger et al. (1984) found for medium to fine-textured, uncracked frozen soils in which entry of meltwater is not impeded by ice layers (i.e. the Limited case) that: (a) the average depth water penetrated the soil during the melt period was 260 mm (standard deviation = 100 mm), (b) infiltration was relatively independent of soil texture and land use and (c) the amount of snowmelt infiltration was inversely related to the average moisture content of the soil layer, 0-300 mm, at the time of melt (θ_p). With respect to the last point, it was observed that infiltration does not result in saturation of soil depth penetrated by the infiltrating meltwater. The maximum degree of saturation of the layer can be approximated by the expression $(.6 + .4\theta_p)$, which reflects the trend for drier soils to reach moisture levels much less than saturation. The existence of an inverse relationship between infiltration and the ice content of a soil has been demonstrated or postulated by several researchers (Willis et al., 1961; Kuznik and Bezmenov, 1963; Gillies, 1968; Shipak, 1969; Romanov et al., 1974, Motovilov, 1979; Granger and Dyck, 1980; Kane, 1980 and Kane and Stein, 1983). Based on their findings, Granger et al. (1984) derived a set of equations defining the relationship between snowmelt infiltration (INF) snowcover water equivalent (SWE) and the premelt moisture content of the 0-300 mm soil layer (θ_p). For practical purposes and cases where $SWE > INF$, these results can be approximated by the equation:

$$INF = (1 - \theta_p) SWE^{0.584} \quad (1)$$

in which INF and SWE are in mm and θ_p is the degree of pore saturation cm^3/cm^3 . The equation is based on measurements of soil water changes from 130 sites made over a 7-y period. It has a correlation coefficient of .85 and gives a standard error of the estimate between calculated and measured values of 5.5 mm.

Equation 1 can be solved for INF when SWE and θ_p are known. Snowcover data are generally available or obtainable. The premelt moisture content, however, is not routinely observed and thus must be estimated from other measured variables. Gray et al. (1985a) showed that changes may occur in the moisture regime of a Prairie soil over winter because of moisture losses from the soil surface layer, infiltration of water from mid-winter snow-melt or rain events, and the migration of water in response to soil freezing. They showed, however, that in the absence of mid-winter infiltration events the soil moisture of the 0-300 mm layer in the fall (θ_f) could be used to index the moisture content (ice) at the time of melt (θ_p). The "best-fit" regression equations describing the relationships between the two variables were, for fallow lands:

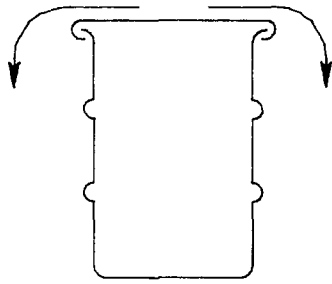
$$\theta_p = -5.05 + 1.05\theta_f, \quad (2a)$$

and for stubble lands:

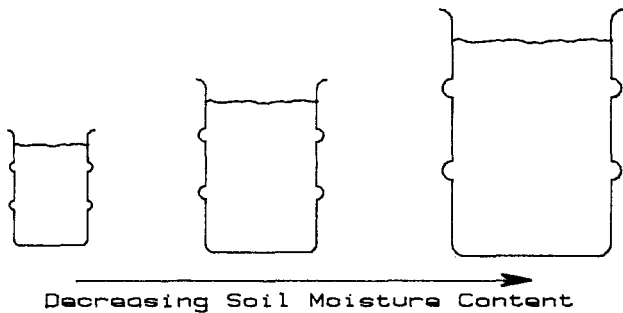
$$\theta_p = 0.294 + 0.957\theta_f, \quad (2b)$$

in which θ_p and θ_f are expressed as a percent moisture by volume. The values of the correlation coefficient and the standard deviation from regression of Eqs. 2a and 2b are 0.85 and 0.91, and 3.29 and 3.38% by volume respectively.

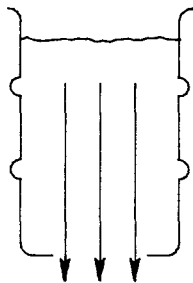
Figure 2 shows field measurements of infiltration plotted against snowcover water equivalent for the different categories of infiltration potential used by the model. In Figs. 2a, 2b and 2c the "x"-axis describes the relationship for the restricted case ($INF = 0$) and the 45° line, the unlimited case ($INF = SWE$). The infiltration data given in Fig. 2a were obtained from measurements of soil moisture changes made at sites where there was visual evidence that an ice lense or impeding layer



(a) RESTRICTED: infiltration is low, runoff potential is high.

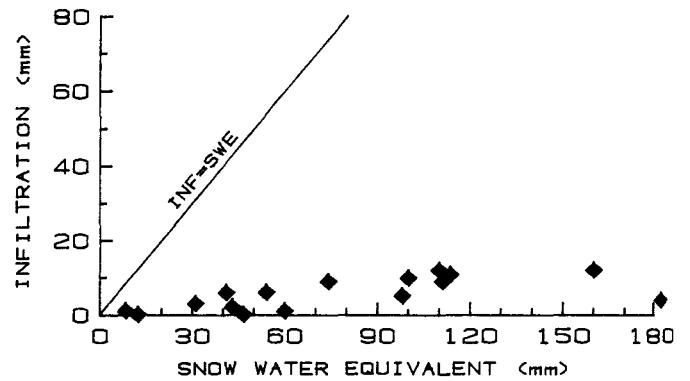


(b) LIMITED: infiltration governed by ice content of soil and snow water.

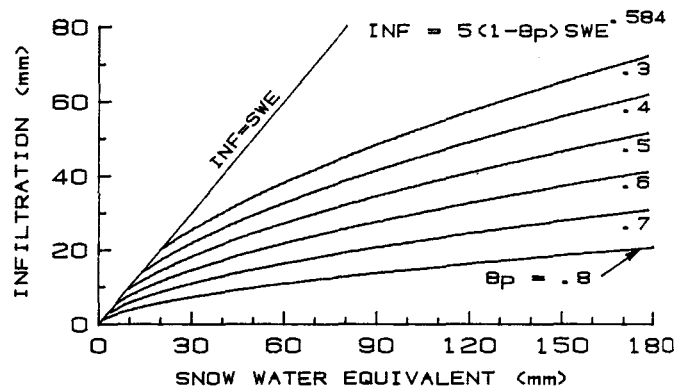


(c) UNLIMITED: soil can infiltrate all or most of the meltwater.

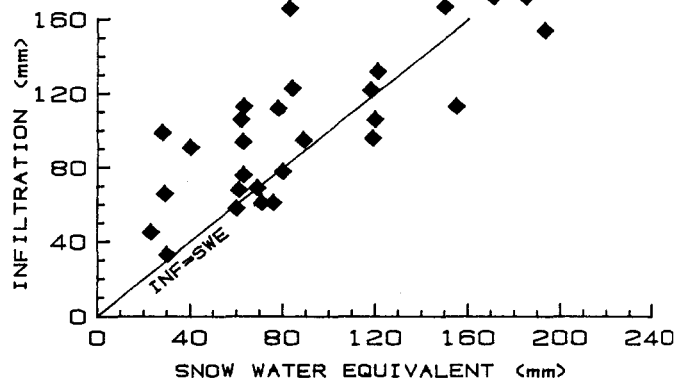
Figure 1. Conceptual model of the infiltration potential of frozen Prairie soils: (a) Restricted, (b) Limited and (c) Unlimited (after Gray et al., 1984).



(a) RESTRICTED



(b) LIMITED



(c) UNLIMITED

Figure 2. Infiltration measurements for the three classes of frozen Prairie soils: (a) Restricted, (b) Limited and (c) Unlimited. (Note: θ_p is the relative degree of saturation expressed in m^3/m^3 .)

was present and the closeness of the points to the "x"-axis support the assumption of very little infiltration for this soil condition. Conversely, the data presented in Fig. 2c, the Unlimited case, were obtained from measurements made in severely-cracked, heavy, lacustrine clays and represent moisture increases in the crack and adjacent soil. The fact that infiltration is greater than the snowcover water equivalent at many sites is possible because of runoff from outside the area of moisture measurement entering the crack directly and lateral flow along a crack. It is believed the data confirm the assumption that $INF = SWE$ for the soil condition. Figure 2b shows the family of curves described by Eq. 1, the Limited case. It is interesting to note in the figure that in a frozen soil at a given moisture content the incremental increase in snowmelt infiltration per unit increase in snowcover water equivalent decreases with an increase in SWE; as well there is a decrease in the ratio of INF to SWE.

TESTING OF MODEL

The ability of the model to simulate areal snowmelt infiltration to landscape units of uniform landuse was tested by comparing the infiltration quantities from Eq. 1 with those calculated by a mass balance approach applied to data collected from eleven small runoff plots ranging in size from 35 to 4000 m². It was found that the infiltration quantities obtained by the two methods were associated with a correlation coefficient of .73 and a standard error of the estimate of 7.2 mm. Also, it was noted that plot size appeared to have little effect on the difference between the estimates. The level of correlation obtained is encouraging considering the small sample and the fact that the initial soil moisture was estimated from a single measurement within each plot.

The initial tests of the infiltration model on a heterogeneous area involved water balance calculations using data collected during 1974 and 1975 on the Creighton Tributary, a small watershed (11.4 km²) located in the semi-arid region of western Saskatchewan. Certain features concerning the data available for the watershed and its physical characteristics

facilitated the approach: (a) in 1974 and 1975 comprehensive snow surveys had been undertaken to establish the snowcover water equivalent by procedures outlined by Steppuhn and Dyck (1974); (b) measurements of "fall" soil moisture content, made with a neutron gauge at 23 sites in fields located immediately adjacent to the watersheds having the same soil type and cropping patterns, were available (Banga, 1981); and (c) streamflow from snowmelt was carefully monitored. An important property of the watershed is that it does not have large elements of depressional storage and therefore the gross area of the basin can be taken as a close approximation of the contributing drainage area. The general topography of the watershed may be classed as rolling to gently undulating with approximately 85% of the area under the cultivation of cereal grains by dryland farming.

The two winters, 1973-74 and 1974-75 had contrasting snowcover and premelt soil moisture conditions. The winter of 1973-74 was a year of near-record snowfall, which produced an average depth of snowcover on the watershed of 556 mm and a snowcover water equivalent of approximately 143 mm. It was preceded by a warm, dry fall and the average moisture content of the surface layer of soil (0-300 mm) was very low (~15% by volume), especially in those land units cropped the preceding summer. Fallow and grass lands were classified in the "Limited" category while stubble lands were considered to have an "Unlimited" infiltration potential. In contrast, conditions during the winter of 1974-75 could be likened more closely to "normal". The average depth and water equivalent of the snowcover were 299 mm and 71 mm respectively, and the average fall soil moisture content was 27.4% by volume. All land use units within the watershed were classified in the "Limited" category.

The tests compared the total volume of runoff, calculated as the difference between the areally-weighted snowcover water equivalent and infiltration ($Q_{cal} = SWE - INF$), with the measured volume determined from the streamflow hydrograph (Q_{meas}). The ratio of $Q_{cal}:Q_{meas}$ was 1.02 in 1974 and 1.17 in 1975. The residual (SWE-INF-measured runoff), expressed as an equivalent average depth of water over the

area, was 1.0 mm in 1974 and 5.8 mm in 1975. These values compare favorably with the expected error of the estimate found when the model was used to obtain infiltration at a point and on small plots.

INTERFACING WITH EXISTING OPERATIONAL SYSTEMS

Computer programs were written to interface the infiltration model with the U.S. National Weather Service River Forecasting System, Sacramento Model (NWSRFS) and the U.S. Army Corps of Engineers Streamflow Simulation and Reservoir Regulation model (SSARR). Gray et al. (1984, 1985b, c) describe different interfacing procedures that have been considered and the reader is referred to these publications for greater detail. Only a brief description of the methodology employed in the current study is provided herein.

Sequencing Infiltration Quantities

In order to apply the model in operational practice the variation in infiltration rate with time during the melt period must be assumed. Granger et al. (1984) showed that the pattern of infiltration depends on many factors: the rates of snowmelt and snowcover runoff; the depth, temperature regime and water transmission characteristics of the snowcover; the amount and distribution of ice in the frozen soil; the soil temperature regime and others. Gray et al. (1985b) analysed the infiltration curves from melt of a Prairie snowcover and showed that two general patterns are dominant: an "advanced" pattern, in which most of the infiltration occurs early in the melt sequence, and a "delayed" pattern, in which the infiltration rate progressively increases through the melt period. The advanced pattern typifies infiltration from the rapid melt of a shallow snowcover. The delayed pattern reflects an increase in infiltration with time primarily due to an increase in the melt rate because of increases in net radiation and the amount of energy advected from snow-free areas and changes to the physical properties of the snow cover and frozen soil which occur over the period of ablation.

In view of the strong dependency of infiltration on the melt process it is logical to allow the output of meltwater from the snowcover generated by the ablation subroutine of a model to be a dominant factor in sequencing infiltration. Gray et al. (1985b), using the results from runoff simulations on the Creighton Tributary, suggest the use of an index approach and a snowmelt infiltration index to define the time of runoff. Runoff does not begin until the rate of release of meltwater from the snowcover is greater than the snowmelt infiltration index. They suggest an initial value for the "daily" snowmelt infiltration index equal to the snowmelt infiltration potential (from Eq. 1) divided by 6 days. When the daily meltwater flux exceeds the index, infiltration is calculated by multiplying the amount of meltwater produced by the ratio of the snowmelt infiltration potential to the snowcover water equivalent at that time.

CONTRIBUTING AREA

It is emphasized that the performance of any model in simulating streamflow from snowmelt is directly related to the snow-covered-area contributing runoff to the channel. Hence, it is important to have a reliable estimate of the volume of snow water, that is the product of contributing area * snowcover water equivalent, as input to the system.

Runoff from a Prairie watershed is not generated uniformly from all parts enclosed by the topographical divide. Prairie lands are relatively flat and their natural drainage systems are usually poorly developed and unconnected. In many years there may be no contribution of snowcover runoff to streamflow from a large part of a watershed because of the shallow snowcover and large amounts of depressional storage. In low snow years the source of runoff is snow collected in the poorly-defined channels and depressions that feed the main drainageway. Conversely, meltwater produced by a deep snowcover will generally satisfy depressional storage and overflow into the channels. Thus, a Prairie basin has a variable "contributing" area whose magnitude varies with such factors as the depth of snowfall and antecedent soil moisture

and surface storage conditions. In this regard hydrologists have made use of the concept of "Effective" and "Gross" drainage areas. The "Effective" area is that portion of a basin which might be expected to entirely contribute runoff to the main stream during a flood with a return period of two years; the "Gross" area is the plane area enclosed by the drainage divide which might be expected to contribute runoff to the outlet under extremely wet conditions (Godwin and Martin, 1975). The "Effective" area includes the major drainage channels and land immediately adjacent to defined drainageways. It is the snowcover in these areas that needs to be surveyed and used as input to a model in low snow years; in snowier winters this component of the average basin snowcover becomes less important because of the larger area of a basin contributing to runoff.

Gray et al. (1985c) studied the interaction between runoff potential, runoff volume and "apparent" contributing area for a Prairie basin. Runoff potential was defined as the sum of the snowcover water equivalent (SWE) plus precipitation occurring during the melt period (PPT) less the volume of infiltration (INF) calculated by Eq. 1. The "apparent" contributing area was the area of the basin that produced the observed runoff volume with the unit runoff potential (i.e., "apparent" area = observed runoff / unit runoff potential). Their results suggest that a relationship does exist between these variables; however, there was insufficient data to allow them to define the relationship. They indicate that further research is needed into the interaction of snowfall, snowcover and topographical aspects, and contributing area for Prairie watershed.

PERFORMANCE OF OPERATIONAL SYSTEMS WITH THE INFILTRATION MODEL

NWSRFS

An algorithm of the infiltration model was interfaced with the NWSRFS and the revised system was used to synthesize streamflow from snowmelt on the Wascana watershed at Sedley, Saskatchewan. The basin is located approximately 50 km southeast of Regina in the Dark Brown soil

zone. Approximately 85% of the watershed is under cultivation of cereal grains by dryland farming; the remaining area is pasture, woody vegetation, roads, farmyards and townsites. The topography is flat to gently rolling and because of the poor relief and drainage development the portion of the "gross" area that contributes to annual streamflow from snowmelt can vary widely. The "effective" and "gross" drainage areas of the watershed are 125 km² and 350 km², respectively.

Figure 3 shows the observed streamflow hydrographs from a low flow year, 1972 (Fig. 3a) and a high flow year, 1982 (Fig. 3b) plotted with three hydrographs generated with the NWSRFS: (1) Land - the system with its original "LAND" subroutine and a contributing area of 125 km², the "effective" area; (2) REVISED, 125 - the NWSRFS with the LAND subroutine replaced by the infiltration algorithm and a drainage area equal to the "effective" area and (3) REVISED, 144 (Fig. 3a) and REVISED, 296 (Fig. 3b) - the same as (2), but with "apparent" drainage areas of 144 km² and 296 km² respectively for the low and high flow years. In the simulations, all model parameters, except drainage area, were the same.

The results in Fig. 3 show:

- (1) The NWSRFS with its LAND subroutine grossly underestimates the observed volume of runoff. For example, in 1972 the observed runoff, expressed as an equivalent depth of water on the effective drainage area of 125 km², was 29 mm compared with a depth of 1.3 mm simulated by the LAND subroutine.
- (2) The infiltration model significantly improves the performance of the NWSRFS in simulating streamflow from snowmelt over that obtained with the LAND subroutine. A measure of the improvement is obtained by comparing the observed and simulated discharge rates using the non-dimensional parameter R² defined by the equation (Nash and Sutcliffe, 1970):

$$R^2 = 1 - \frac{\sum_{i=1}^n (q_{oi} - q_{si})^2}{\sum_{i=1}^n (q_{oi} - \bar{q}_o)^2} \quad (3)$$

where:

- n = number of values at evenly-spaced time intervals,

q_{oi} = observed discharge rate,
 q_{si} = simulated discharge rate, and
 q_o = mean of the observed values.

R^2 , termed efficiency, can be likened to the coefficient of determination used in statistics. The closer the positive value is to unity, the closer the agreement between observed and simulated hydrographs. With a drainage area of 125 km², the R^2 -values for hydrographs generated with the LAND routine in 1972 and 1982 were -0.32 and -0.15, respectively, compared with R^2 -values of 0.70 and 0.48 for the corresponding hydrographs generated by the REVISED NWSRFS. The poor simulation obtained with LAND can be directly linked to manner in which the routine evaluates infiltration to frozen soils. As shown by Gray et al. (1984) the performance of the system can be markedly improved by adjusting the soil moisture accounting routine to reduce the Upper Zone soil moisture capacity and by setting the Lower Zone percolation rate to a very small value, if possible equal to zero.

The agreement between the shapes and time elements of the hydrographs simulated using the infiltration algorithm and observed hydrographs vary in the two years, with the agreement being significantly better in the high flow year, 1982. Because the NWSRFS has a high degree of flexibility the "fit" could have been improved by changing different parameters in the model. However, such changes would only serve to mask the effects of the infiltration model in improving model performance. Previous work with the NWSRFS (Division of Hydrology, 1977) has shown that a major factor contributing to poor agreement between simulated and observed hydrographs when the system is applied to prairie watersheds is an incorrect simulation of the ablation process. For example, the manner in which the system accounts for changes in the internal energy of a shallow snowcover; differences in the magnitude of the melt factor and water transmission properties of the snowcover; the use of a temperature index for calculating melt and other factors. It is suspected that the larger differences between simulated and observed hydrographs in years of low snowcover reflects a problem

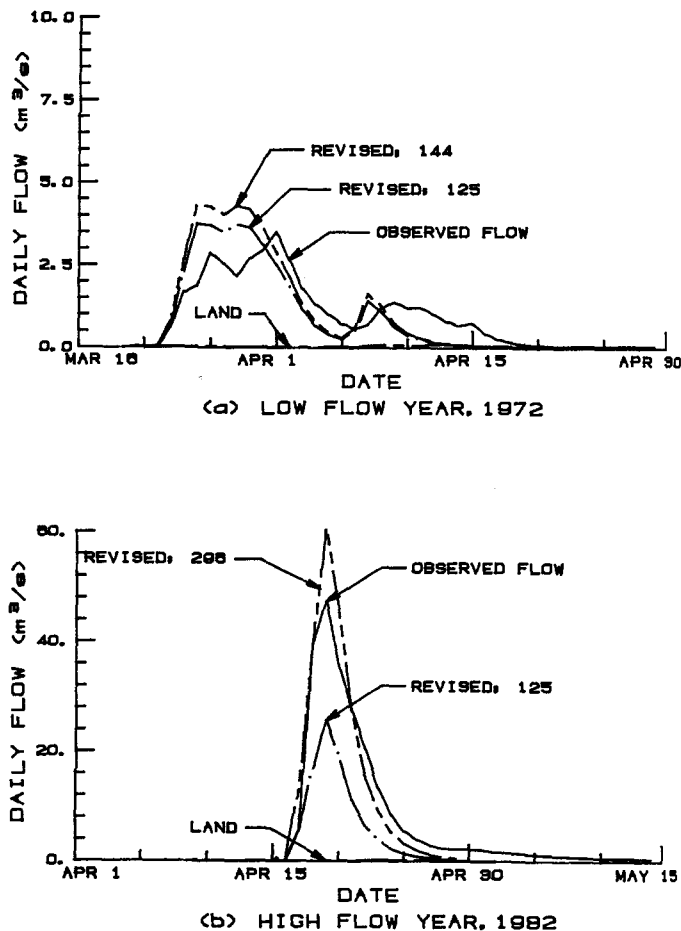


Figure 3. Observed and simulated hydrographs from snowmelt for Wascana Creek at Sedley, Saskatchewan: (a) low flow year, 1972 and (b) high flow year, 1982. LAND - the NWSRFS operated with its LAND subroutine and a contributing area of 125 km²; REVISED 125, 144 and 296 - the NWSRFS with the infiltration algorithm and contributing areas of 125 km² (effective area) and 144 or 296 km²; areas that produced the observed volume of runoff with the NWSRFS.

in simulating the meltwater release and water transmission properties of snow-filled channels.

(3) In years of low flow the "effective" area of the watershed is a better estimator of the "apparent" area contributing to the peak discharge; in years of high flow a contributing area equal to or less than the "gross" area gives the better simulation.

An algorithm of the infiltration model was also developed and interfaced with the U.S. Army Corps of Engineers Streamflow Simulation and Reservoir Regulation (SSARR) model. The procedures followed in calculating and simulating infiltration quantities by the algorithm were identical to those used with the NWSRFS and discussed above.

The revised SSARR was used to synthesize streamflow from snowmelt on the Wascana watershed. Figure 4 shows the observed streamflow hydrographs plotted with the simulated hydrographs generated by the SSARR and Revised SSARR models for a low flow year, 1972 (Fig. 4a) and a high flow year, 1982 (Fig. 4b); the same runoff events used in the tests with the NWSRFS (Fig. 3). The "apparent" drainage areas determined from the results of the tests with the NWSRFS were used, that is 144 km² in 1972 (Fig. 4a) and 296 km² in 1982 (Fig. 4b).

For the low flow year (Fig. 4a) the agreement in shapes of observed and simulated hydrographs is poor and may be attributed to a host of factors: poor choice of melt factor, an incorrect base temperature and, as with the NWSRFS, incorrect simulation of other factors affecting snowcover ablation in and runoff from in-channel accumulations. Despite the poor agreement in shapes of the curves it was found that at the end of active snowmelt the streamflow volume simulated with the REVISED SSARR was only 4% less than the observed, whereas with the SSARR it was 48% less.

In the high flow year (Fig. 4b) the agreement of the hydrographs in both shape and timing is markedly improved over the results obtained in 1972. Further, it is obvious that the simulation with REVISED SSARR is better than that obtained with SSARR. The R²-value for the REVISED SSARR was 0.79 compared with 0.63 with SSARR and the volume of runoff simulated with the revised system was only 12% less than the observed whereas SSARR underestimated the flow by 34%.

Simulation of streamflow with the two models was also undertaken for 1974, 1979 and 1980. Table 1 compares the "observed" and "simulated" volumes for the five years and it can be seen that in all years

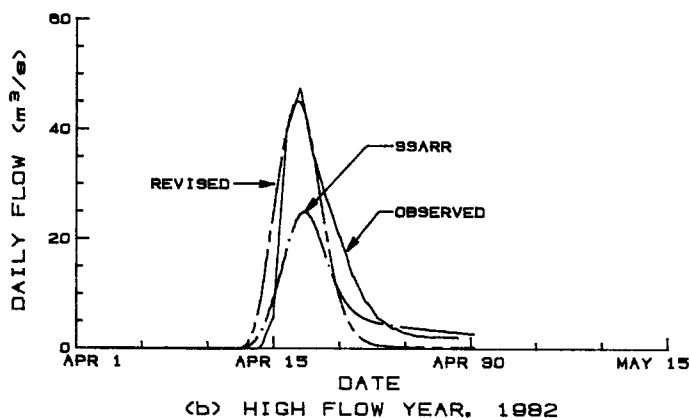
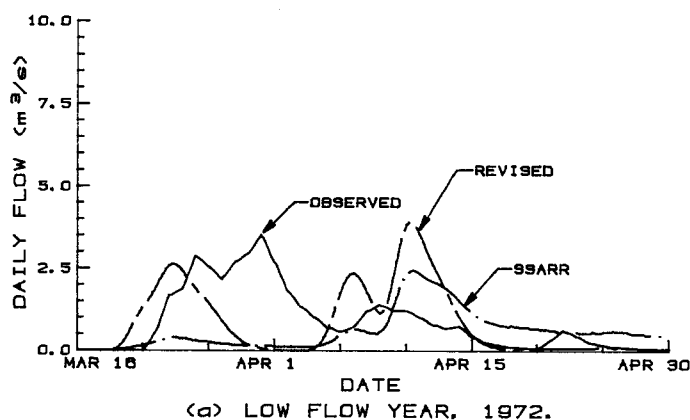


Figure 4. Observed and simulated hydrographs from snowmelt for Wascana Creek at Sedley, Saskatchewan: (a) low flow year, 1972 and (b) high flow year, 1982. REVISED SSARR - SSARR with the infiltration algorithm and SSARR - the model operated in its original mode. The contributing areas were 144 km² in 1972 and 296 km² in 1982.

except 1980 the relative error in predicting the runoff volumes was substantially smaller with REVISED SSARR than with SSARR. On average, the infiltration algorithm reduced the relative error in estimating volume by a factor of ~2, from 34 to 15%. Also the simulated volumes, except that calculated by REVISED SSARR in 1980, are less than the observed flow. This result was surprising inasmuch as the contributing areas used in the simulations were those values that gave the observed flow with the Revised NWSRFS and the same meteorological inputs, initial soil moisture contents and initial snow water

Table 1. Comparison of observed flow volume and volumes simulated with Revised SSARR and SSARR models for five years of snowmelt runoff on Wascana Creek near Sedley, Saskatchewan.

Year	Observed Flow (cmsd)	Revised SSARR		SSARR	
		Flow (cmsd)	Error %	Flow (cmsd)	Error %
1972	38.9	37.4	4	20.2	48
1974	327.5	254.2	22	231.7	29
1979	152.7	127.5	17	85.7	44
1980	47.9	58.1	21	40.4	16
1982	219.7	193.3	12	145.9	34
	Mean		15.2		34.2
	Std. Deviation		7.4		12.7

equivalents. The underprediction of runoff volume by SSARR, compared with the NWSRFS, can be attributed to differences in the manner the two models treat snow accumulation and ablation. Because SSARR uses a low-level cut-off value of snowfall depth to eliminate very small events, in many years the maximum snow water equivalent (MAXSWE) used by the model is less than the corresponding value used by the NWSRFS. Table 2 compares values of MAXSWE given by the two "revised" systems. Only in 1980 was the MAXSWE with SSARR greater than for NWSRFS and this was due to the fact that SSARR predicted a later date of snowmelt and precipitation from a late-occurring event was added to the snowpack. The result, as shown in Table 1, was to cause the runoff volume simulated by the Revised SSARR to be greater than the observed.

Table 2. Comparison of MAXSWE for the "revised" NWSRFS and SSARR.

Year	NWSRFS mm	SSARR mm	$\frac{\text{NWSRFS}}{\text{SSARR}}$
1972	45	41	1.10
1974	137	129	1.06
1979	83	77	1.08
1980	51	57	.89
1982	99	94	1.05

This paper presents a simple, physically based model of infiltration to frozen soils. The model is based on the concept that for practical purposes frozen soils may be grouped into three broad categories with respect to their infiltration potential, namely: Unlimited - cracked or highly porous soils which are capable of infiltrating most of the snow water; Limited - the infiltration potential of a soil depends primarily on the snowcover water equivalent and the ice content of the soil layer, 0-300 mm, at the time of melt and Restricted - a soil containing an impermeable layer that inhibits infiltration. Field measurements of soil water changes made during snowcover ablation are presented to support the delineation of "Restricted" and "Unlimited" classes and an empirical equation relating infiltration to snowcover water equivalent and the moisture (ice) content of the soil layer 0-300 mm is given for the Limited class.

Several validation tests of the model in estimating "point" and "areal" infiltration amounts are given. As an example, it is shown that the potential volume of runoff, calculated as the difference: snowcover water equivalent less infiltration for two years of widely-different snowcover and antecedent soil moisture conditions agreed within 17 percent of the observed streamflow from a heterogeneous 11.4 km² watershed. The results of the tests supported the proposition that the model would provide estimates of infiltration suitable for practical management use.

Procedures and methodologies of interfacing the model with operational streamflow forecasting systems are described. It is shown that the performance of the U.S. National Weather Service River Forecasting System (NWSRFS) and the U.S. Army Corps of Engineers Streamflow Simulation and Reservoir Regulation model in simulating streamflow from snowmelt on a Prairie watershed is markedly improved with use of the model. The improvement being primarily due to a better estimate of runoff volume from that obtained with the original systems. For example, on average the infiltration algorithm in SSARR reduced the relative error by the system in estimating observed flow by a factor of ~2,

from 34 to 15%.

The need for correct evaluation of the snow-covered area contributing to streamflow in order to obtain a good simulation of runoff from a Prairie watershed is emphasized.

LITERATURE CITED

- Anderson, E.A., 1973. National Weather Service river forecast system - snow accumulation and ablation model. Technical Memorandum NWS HYDRO-17, National Oceanic and Atmospheric Administration (NOAA), Silver Springs, Maryland.
- Anderson, E.A. and P.J. Neuman, 1984. Inclusion of frozen ground effects in a flood forecasting model. *In: Proceedings of the 5th Northern Basin Symposium and Workshop, Vierumaki, Finland.*
- Banga, A.B., 1981. Spatial variability of soil moisture in a Prairie environment. M.Sc. Thesis, University of Saskatchewan, Saskatoon, Saskatchewan, 86 pp.
- Bergström, S., 1979. Spring flood forecasting by conceptual models in Sweden. *In: Proceedings of Modeling Snow Cover Runoff, 1978, S.C. Colbeck and M. Ray (Editors), U.S. Army Corps of Engineers Cold Regions Research and Engineering Laboratory, Hanover, New Hampshire, pp. 397-405.*
- Division of Hydrology, 1977. An examination of the U.S. NWS River Forecast System snow accumulation and ablation model under Prairie snowmelt conditions. Unpublished Internal Report, Division of Hydrology, University of Saskatchewan, Saskatoon, Saskatchewan, 26 pp.
- Gillies, J.A., 1968. Infiltration in frozen soils. M.Sc. Thesis, University of Saskatchewan, Saskatoon, Saskatchewan, 136 pp.
- Godwin, R.B. and F.R.J. Martin, 1975. Calculation of gross and effective drainage areas for the Prairie Provinces. *In: Proceedings of the Canadian Hydrology Symposium:75. National Research Council of Canada, Ottawa, Ontario, pp.218-223.*
- Granger, R.J. and G.E. Dyck, 1980. Report of the 1979/80 investigations of infiltration and runoff from snowmelt. Internal Report, Division of Hydrology, University of Saskatchewan, Saskatoon, Saskatchewan, 67 pp.
- Granger, R.J., D.M. Gray and G.E. Dyck, 1984. Snowmelt infiltration to frozen Prairie soils. *Canadian J. Earth Sciences* 21(6):669-677.
- Gray, D.M., R.J. Granger and G.E. Dyck, 1985a. Overwinter soil moisture changes. *Transactions Amer. Society Agricultural Engineers* 28(2):442-447.
- Gray, D.M., P.G. Landine and R.J. Granger, 1984. An infiltration model for frozen Prairie soils. Paper No. 84-313 presented at the 1984 Annual Meeting of the Canadian Society of Agricultural Engineers, Winnipeg, Manitoba. 15 pp.
- Gray, D.M., P.G. Landine and R.J. Granger, 1985b. Simulating infiltration into frozen Prairie soils in streamflow models. *Canadian J. Earth Sciences* 22:464-474.
- Gray, D.M., P.G. Landine and G.A. McKay, 1985c. Forecasting streamflow runoff from snowmelt in a Prairie environment. *In: Proceedings of the 7th Canadian Hydrotechnical Conference, Canadian Society of Civil Engineers* 1A:213-231.
- Holtan, H.N., 1961. A concept for infiltration estimates in watershed engineering. U.S. Department of Agriculture, Agriculture Research Service Report 41-51, 25 pp.
- Holtan, H.N., G.J. Stiltner, W.H. Henson and N.C. Lopez, 1975. USDAHL-74, Revised model of watershed hydrology. U.S. Department of Agriculture, Agricultural Research Service Technical Bulletin 1518.
- Horton, R.E., 1940. An approach to the physical interpretation of infiltration capacity. *Soil Science Society of America Proceedings* 5:399-417.
- Kane, D.L., 1980. Snowmelt infiltration into seasonally frozen soils. *Cold Regions Science and Technology* 3:153-161.
- Kane, D.L. and J. Stein, 1983. Water movement into seasonally frozen soils. *Water Resources Research* 19(6):1544-1557.
- Kuznik, I.A. and A.I. Bezmenov, 1963. Infiltration of meltwater into frozen soil. *Soviet Soil Science* Number 6, pp. 665-671.
- Motovilov, Yu.G., 1978. Mathematical model of water infiltration into frozen soils. *Soviet Hydrology* 17(1):62-66.
- Motovilov, Yu.G., 1979. Simulation of meltwater losses through infiltration into soil. *Soviet Hydrology* 18(3):217-221.

- Nash, J.E. and J.V. Sutcliffe, 1970. River flow forecasting through conceptual models. *J. Hydrology* 10:282.
- Peck, E.L., 1976. Catchment modelling and initial parameter estimation for the National Weather Service River Forecast System. NOAA Technical Memorandum NWS HYDRO-31, Office of Hydrology, Washington, DC. pp. 1-24, plus Appendices.
- Popov, E.G., 1973. Snowmelt runoff forecasts - theoretical problems. *In: Role of Snow and Ice in Hydrology, 1972. Proceedings of the Banff Symposia, UNESCO-WMO-IAHS, 2:829-839.*
- Quick, M.C. and A. Pipes, 1973. Daily and seasonal runoff forecasting with a water budget model. *In: Role of Snow and Ice in Hydrology, 1972. Proceedings of the Banff Symposia, UNESCO-WMO-IAHS, 2:1017-1024.*
- Romanov, V.V., K.K. Pavlova, and I.L. Kalyuzhnyy, 1974. Meltwater losses through infiltration into podzolic soils and chernozems. *Soviet Hydrology Selected Papers Number 1, pp. 32-42.*
- Shipak, I.S., 1969. Relationship between the runoff coefficient and the moisture content and depth of freezing soil. *Soviet Soil Science, pp. 702-706.*
- Steppuhn, H. and G.E. Dyck, 1974. Estimating true basin snowcover. *In: Advanced Concepts and Techniques in the Study of Snow and Ice Resources. Interdisciplinary Symposium, U.S. National Academy of Science, Washington DC., pp. 314-324.*
- United States Army Corps of Engineers, 1972. Program description and users manual for SSARR model program 724-KJ-G0010. North Pacific Division, Portland, Oregon.
- United States Army Corps of Engineers, 1973. HEC-1, Flood Hydrograph Package Users Manual. Hydrological Engineering Center, Davis, California.
- United States Department of Commerce, 1972. National Weather Service River Forecast Procedures. Technical Memorandum NWS HYDRO-14, Silver Springs, Maryland, pp. 1-1 to 1-20.
- Willis, W.O., C.W. Carlson, J. Alessi and H.J. Haas, 1961. Depth of freezing and spring runoff as related to fall soil-moisture level. *Canadian J. Soil Science* 41:115-123.

USING REAL-TIME (SNOTEL) DATA IN THE NWSRFS MODEL

Keith R. Cooley*

ABSTRACT: Physical process simulation models and real-time snowpack data show promise for enhanced water supply forecasts yielding complete hydrographs rather than the traditional seasonal volume forecasts based on regression techniques and monthly snow course readings. Hydrograph forecasts are especially important for efficient reservoir operation and flood peak estimates. The National Weather Service River Forecast System (NWSRFS) model which is capable of simulating snow accumulation and melt, and streamflow was tested using snowpack and climatological data from sites in Idaho and Montana. Several approaches for using real-time SNOTEL data in the NWSRFS model were also tested. Results indicated that using SNOTEL data did not improve forecasts in most cases. However, modification of standard calibration procedures to more nearly reflect the relationship between snow pillow data and streamflow could improve results. Results also emphasize the expedience of properly locating precipitation and snow water equivalent monitoring equipment.

(KEY TERMS: simulation models; water supply forecasts; snowmelt; streamflow; snow pillow, precipitation.)

INTRODUCTION

Most of the annual streamflow in the western United States occurs during the spring and summer months, and is found to be a product of the water accumulated during the winter in the snowpack and soil profile. Knowledge of the amount of water

that will be available is essential for efficient use. Even a few months' notice allows managers to optimize reservoir operations for the multitude of competing users. Adequate water supply forecasts also let farmers decide how much acreage to plant and to which crops. Even more critical are accurate and timely forecasts during extreme years when droughts or floods occur.

Water supply forecasts have traditionally been made using multivariate regression techniques based on monthly snow course readings. These forecasts produced estimates of seasonal (i.e., April through July) runoff volume, and except in extreme years, were quite accurate. In recent years mathematical models designed to simulate physical processes have received more attention. These simulation models are of particular interest to streamflow forecasters because they produce a continuous record of streamflow volume with respect to time, which is essential to good flood prediction and reservoir operation.

Another recent development that makes simulation models attractive is the availability of continuous snowpack information provided by on-site sensors and transmitters like those used in the SCS SNOW TELEmetry (SNOTEL) system (Crook, 1985). Snowpack snow water equivalent (SWE), accumulated precipitation, and air temperature are now available for several hundred stations in the western United States at intervals of 15 minutes or greater. Simulation model forecasts could be updated or initiated at any time using

*Hydrologist, Northwest Watershed Research Center, Agricultural Research Service, U.S. Department of Agriculture, 270 South Orchard, Boise, Idaho 83705.

SNOTEL data, as opposed to the once monthly forecasts normally provided by regression methods.

The objectives of this study were to: 1) test a snow accumulation and melt model; and 2) evaluate methods of using real-time (SNOTEL) data in a simulation model for water supply forecasting.

PROCEDURE AND METHODS

Following a literature review, a snow model developed by Eric Anderson of the National Weather Service was selected for testing. The model, HYDRO-17 (Anderson, 1973), is a conceptual model of the significant physical processes affecting snow accumulation and snowmelt. It uses air temperature as an index to energy exchange across the snow-air interface and was selected because: 1) air temperature data are readily available; 2) the approach appeared to be technically sound; 3) the model has been tested in several climatic regions within the United States; and 4) an expected range of values for the calibration parameters was provided for a variety of conditions.

The HYDRO-17 snowmelt model is part of the National Weather Service River Forecast System model (NWSRFS), which consists of modular units that can be used singly or in combination for simulating various parts of the hydrologic cycle. The NWSRFS model offers both a snow accumulation and melt algorithm (HYDRO-17), and a basis for evaluating the use of real-time data in water supply forecasting. Therefore it was used for both aspects of this study.

Three evaluations of the HYDRO-17 model were made using snow water equivalent data from snow course or snow pillow sites in Idaho and Montana. In the evaluations, HYDRO-17 was calibrated by adjusting parameter values until simulated and observed SWE were essentially the same during one to five year periods. Runs were then made using the calibration parameter values for additional periods that represented above normal, normal, and below normal snow accumulation years.

The entire model was calibrated by matching simulated and observed streamflow using 1973 to 1978 water year data from Lower Willow Creek, Montana. The modules of the NWSRFS model used were: 1)

HYDRO-17 - Snow accumulation and melt; 2) SAC-SMA - Soil moisture accounting; and 3) UNIT-HG - Unit hydrograph shape.

Lower Willow Creek was divided into upper and lower zones (areas above and below 1860 m), and parameter values in HYDRO-17, SAC-SMA, and UNIT-HG were adjusted in both zones during the calibration runs as suggested by NWS model documentation (unpublished users manual).

The SNOTEL data were used in the NWSRFS model in three different ways. These were:

1) After long-term calibration parameter values were established, the snow correction factor (SCF) values were changed each year to produce simulated snow water equivalent (SWE) values equal to observed SWE values on April 1st. The model was then run for the April through July forecast period using observed temperature and precipitation data from Drummond, Montana.

2) The NWSRFS model was initiated on January 1st, February 1st, or March 1st each year using observed SWE on these starting dates and actual Drummond temperature and precipitation data for the forecast period from the starting date through July.

3) Actual SNOTEL SWE data were used (in place of HYDRO-17 simulated SWE) along with rainfall as input to the SAC-SMA soil moisture accounting subroutine.

DESCRIPTION OF SITES AND DATA SETS

Data for testing the HYDRO-17 snow model were obtained from an Idaho snow course and two Montana snow pillow sites. The snow course, Reynolds Mountain, is located at an elevation of 2073 meters on the upper end of the Reynolds Creek Experimental Watershed near Boise, Idaho. The surrounding area is predominantly sagebrush mountain meadows with a few scattered stands of willows, aspen, and Douglas fir. Mean annual precipitation is 1016 mm, most of which (60 - 70%) occurs as snowfall, and is accompanied by southwesterly winds. In addition to the SWE data provided by the snow course readings, daily maximum and minimum air temperature and precipitation records are available for most of the period since 1966.

The two snow pillows are located on the Lower Willow Creek basin near Hall, Montana (Fig. 1). The Combination site is located at an elevation of 1700 meters near a main tributary in a mixed conifer setting, and represents the lower end of a conifer forest. Average annual precipitation at the site is about 560 mm based on six years of record. Records of SWE are available for the 1973-1984 period, but precipitation data are available only for the 1979-1984 period.

The Black Pine site is located at an elevation of 2164 meters on the southerly upper end of the basin. Average annual precipitation for a six year period (1979-1984) was 716 mm. Records of SWE are available for the 1966-1984 period. The Black Pine site is located in a dense conifer setting and represents a continuous conifer forest.

The Lower Willow Creek basin was selected for evaluating the NWSRFS model simulations using SNOTEL data. This basin encompasses an area of 190 square kilometers above the reservoir. Elevation ranges from 1430 m above sea level at the reservoir to over 2400 m at the highest point. Average annual precipitation varies from 350 mm at the lower elevations to over 760 mm at the higher elevations.

Streamflow records are available for portions of each year from 1967 through 1984.

Because only SWE and 1979-1984 precipitation data were available from the Combination and Black Pine SNOTEL sites, Drummond temperature and precipitation data were used when needed as input to the model. Long-term climatological records from the Drummond weather station were the most complete and produced the best overall results of three stations within the general area of Lower Willow Creek. Drummond is about 16 km northeast of the basin at an elevation of 1200 m. Drummond records were used as input to the HYDRO-17 model for both snow pillow sites and the upper and lower zones of Lower Willow Creek.

TESTS OF HYDRO-17 SNOW MODEL

Tests of HYDRO-17 using snow course data from the Reynolds Mountain site were described by Cooley, et al. (1983). They found that simulated SWE values could be made to essentially duplicate observed values for a given year. However, when the same parameter values were used for simulations in other years, results did not match as well. Even so, HYDRO-17 produced better results than four other models tested on the same data set (Huber, 1983).

Figure 2 illustrates the results based on a five year calibration period at the Combination site (results for the Black Pine site were similar). These results suggest that when one set of parameter values is used for several years, simulated values will be high some years, low some years, and about the same as observed other years. The ambient temperature sometimes fails as a reliable index of the physical processes that cause the snow to accumulate and melt. The inclusion of additional variables such as solar radiation, wind run, and vapor pressure may be necessary to improve the model. Since these data are seldom available at the sites requiring simulation, the temperature data must suffice and this limitation of the model is recognized.



Figure 1. Lower Willow Creek Watershed Near Hall, Montana.

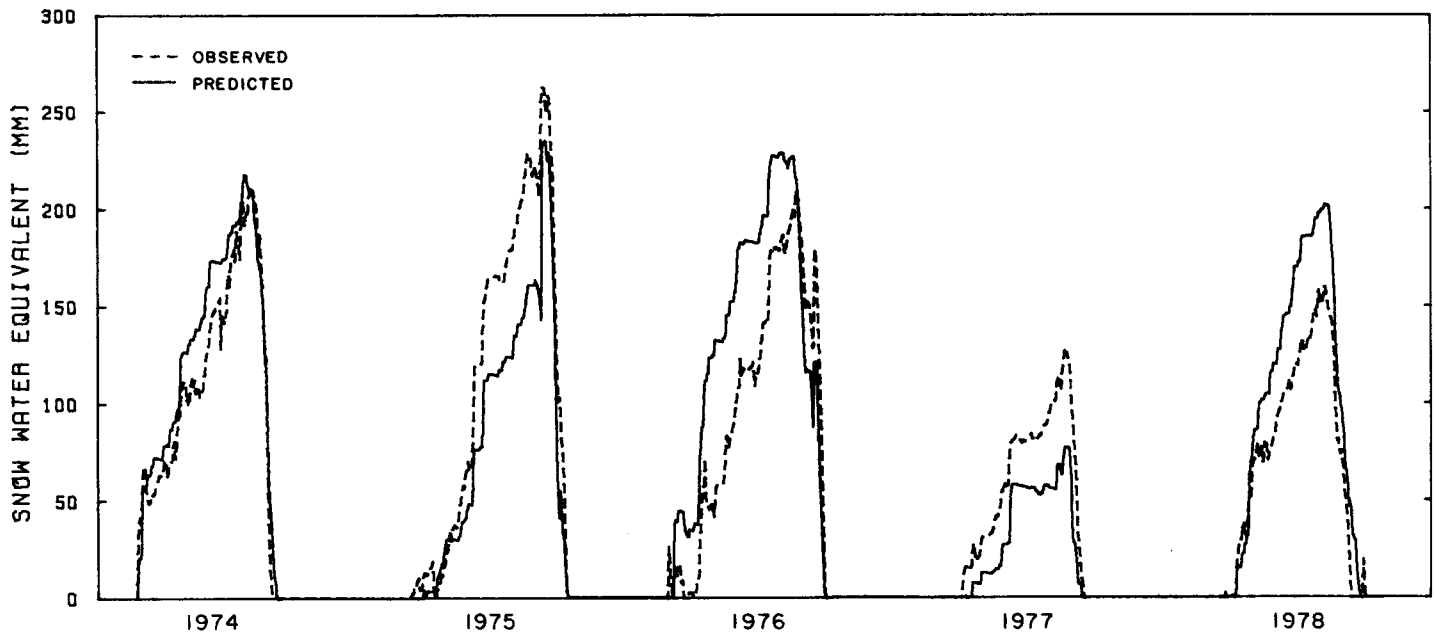


Figure 2. Simulated Snow Water Equivalent at Combination Snow Pillow Using Drummond Weather Station Precipitation and Temperature Data, Compared to Observed Snow Water Equivalent at Combination Snow Pillow (----- Observed; ——— Simulated).

USING SNOTEL DATA IN THE NWSRFS MODEL

In order to evaluate the effectiveness of using SNOTEL data to improve model simulated streamflow forecasts, it was first necessary to run the model using normally available data to produce streamflow forecasts which could be used as a basis for comparison. A twelve year record (1973-1984) of snow pillow and streamflow data at Lower Willow Creek, and corresponding temperature and precipitation data at Drummond, were available for the tests. In this case, a six year (1973-1978) calibration and a six year (1979-1984) test period were selected. Both six year periods contained high, low, and average years of streamflow.

Relationships between precipitation at Drummond and the snow pillow sites were derived using the precipitation data collected at the pillow sites after the 1979 gage installations. Monthly and annual ratios of snow pillow precipitation to Drummond precipitation were used as first estimates for snow correction factor (SCF) and precipitation adjustment factor (PXADJ) values in the calibration runs. Precipitation-elevation relationships may also be used as a basis for estimating these parameters which alter volume but not time of occurrence.

Since the monthly ratios varied considerably during the year, seasonal ratios seemed to be more realistic than average annual values. However, it isn't possible to change parameter values during the year without stopping a run, re-initializing parameters, and starting again at the stopping date. Therefore, PXADJ was selected to represent the summer ratio between the snow pillow sites and Drummond precipitation, and SCF was used to adjust for the increased ratio noted during the winter when precipitation was predominately snowfall. The SCF parameter is thus raised above its normal range to account for not only snowfall loss from unshielded gages, but also to represent the greater seasonal ratio noted for the winter period.

Other initial parameter values used in the model were based on actual data when possible, i.e., potential evapotranspiration was based on data from Bozeman, Montana. The observed and model simulated runoff traces for the 1973-1978 calibration years are presented in Figure 3. In general, simulated values of runoff matched observed values better during the calibration period than during the test period. Simulated runoff volume was greater than observed runoff volume during most of the test years. The magnitude of

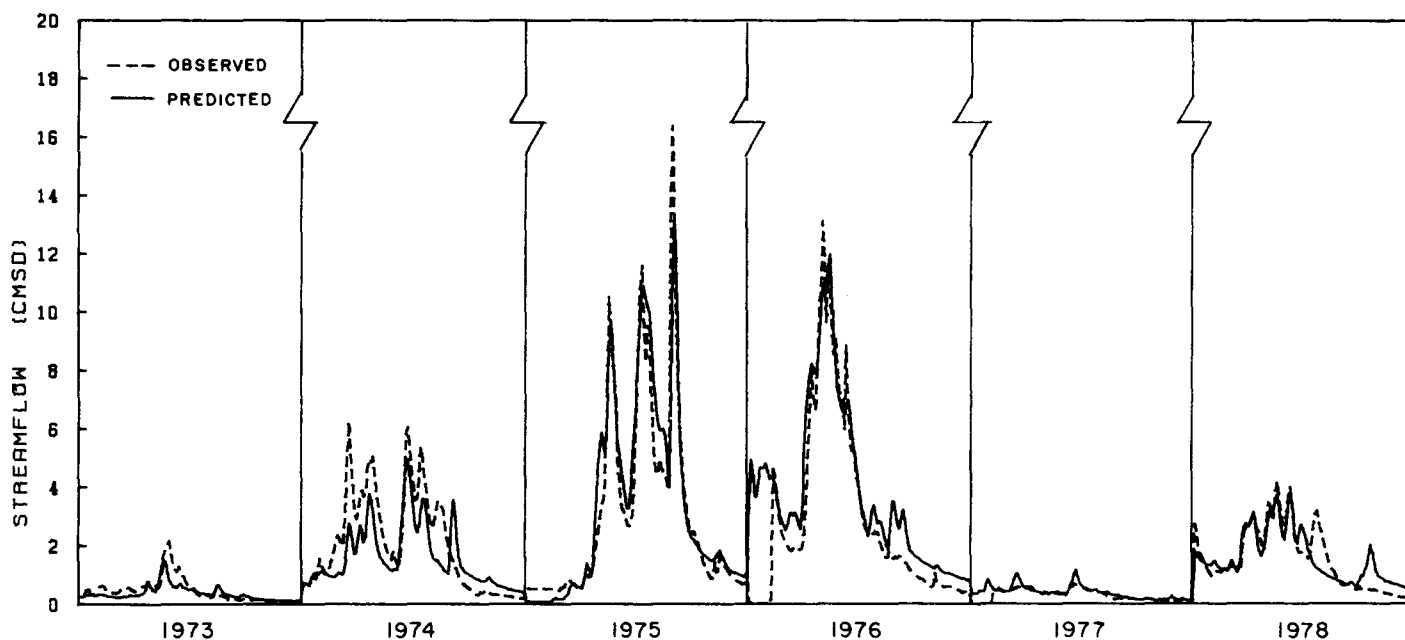


Figure 3. April Through July Observed and Simulated Streamflow at Lower Willow Creek, Montana for the 1973-1978 Calibration Period.

the overprediction during the test period tended to be greater than the differences noted for the calibration period. These differences could be due in part to a change in the relationship between precipitation on the basin and that at Drummond during the two six year periods. Unfortunately, data are not available prior to 1979 to provide verification.

Although differences between observed and simulated runoff volume were rather large some years, the timing of major events (peaks) normally produced by spring snowmelt, was in quite close agreement. One problem noted several times during the summer or fall (late June through September) was the appearance of a simulated runoff event when there was no indication of a change in observed runoff. These simulated events seem to be produced by thunderstorm rainfall recorded at Drummond and simulated by the model which, when adjusted by PXADJ, are significant enough to produce runoff from rainfall. Since there is no indication of an observed event, the storms either did not occur on the watershed or they were not of sufficient magnitude to produce overland flow and a change in streamflow. These discrepancies serve to emphasize the need for on-site precipitation data to improve model results.

Simulating Observed Snow Water Equivalent (SWE) on April 1st by Adjusting the Snow Correction Factor (SCF)

Calibration values of the snow model parameters SCF and PXADJ were based on relationships between seasonal precipitation volumes at the snow pillow sites and Drummond. If these relationships changed from year to year because of variations in storm tracks, inversions, or other meteorological conditions, this could affect yearly simulation accuracy based on long-term averages. A possible method of accounting for this variability consists of adjusting the values of SCF and/or PXADJ each year while holding all other parameter values fixed. In this case, only SCF was adjusted since comparisons were made on spring runoff which was mainly produced by snowmelt. The value of SCF was adjusted each year so that model simulated SWE on April 1st matched observed SWE at each snow pillow site.

The simulated runoff hydrographs produced using the adjusted SCF values are presented in Figure 4, along with observed runoff for the April through July period for 1975, 1976, 1980, and 1983. The simulated runoff again exceeds observed runoff in most cases, while the timing of simulated and observed peaks matches

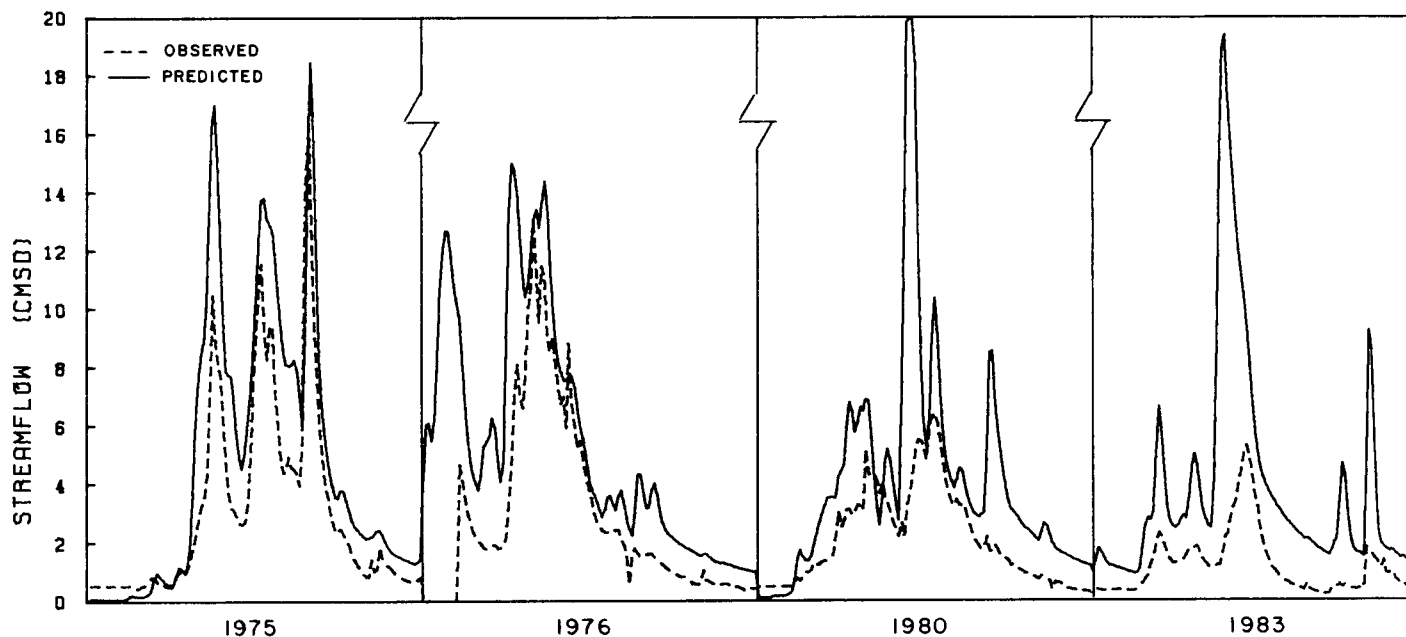


Figure 4. April Through July Observed and Simulated Streamflow at Lower Willow Creek, Montana for the 1975, 1976, 1980, and 1983 Water Years. SCF is Adjusted so that Simulated SWE Matches Observed SWE at the Snow Pillow Sites on April 1st Each Year.

rather closely. The SCF values required to make simulated SWE match observed SWE on April 1st each year, are presented in Table 1 for the two zones used in the model. Also presented in Table 1 are statistical and runoff volume comparisons. The 1973 values are somewhat questionable, since October through December water year data were not available, and estimates of initial conditions on January 1st could affect these results. Omitting 1973, the range of SCF values required in the upper zone did not vary greatly from the value of 2.10 used in the calibration. However, the SCF values needed in the lower zone were all above the 1.25 value obtained during calibration, some by almost three times.

These results suggest that April 1st SWE may not be a good index of spring runoff volume, especially from the lower zone where in most years some snowmelt has already occurred. Since snowpack conditions vary each year, matching maximum snow accumulation in each zone may provide a better index of later snowmelt runoff. However, it would be more difficult to use in forecast procedures since it would occur at different times in each zone and for each year.

Using SNOTEL SWE to Initialize the NWSRFS Model

Another approach that could improve model simulated results would be to use SNOTEL snow water equivalent data for updating the model whenever a forecast is desired. In this study, SWE as recorded at the pillow sites, on January 1st, February 1st, or March 1st was used to initialize the model. The model was then used to simulate April through July runoff, which was compared to observed runoff for the same period. The calibration values of model parameters were used, and the status of other conditions, such as soil water storage in the upper and lower soil zones, was estimated. Drummond temperature and precipitation data for the years tested were again used as input for the forecast periods.

The four years which produced the greatest difference between simulated and observed runoff during the calibration and test periods (1975, 1976, 1980, and 1983) were selected for this test. The simulated runoff that was produced when the model was initiated on January 1st of the 1975 and 1980 years and the observed runoff for corresponding years is

TABLE 1. Snow Correction Factors (SCF) Required to Match Observed SWE at the Combination and Black Pine Sites, and Simulated Runoff Compared to Observed Runoff at Lower Willow Creek, Montana.

	SCF		April-July Runoff (mm)			Daily Errors (mm)		
	Lower Zone	Upper Zone	OBS	SIM	DIFF	RMS ¹	AVG-ABS ²	r ³
1973	5.90	3.20	25.7	44.4	18.7	0.16	0.12	0.935
1974	1.75	1.93	113.5	103.7	-9.8	0.35	0.26	0.911
1975	1.71	2.35	174.0	262.7	88.7	1.06	0.72	0.926
1976	1.90	2.05	160.5	243.6	83.1	0.90	0.59	0.919
1977	2.84	2.46	16.4	37.5	21.1	0.18	0.13	0.913
1978	1.75	2.42	83.6	125.7	42.1	0.34	0.25	0.911
1979	1.56	1.71	65.1	74.0	8.9	0.18	0.13	0.943
1980	1.76	2.14	118.8	235.5	116.7	1.35	0.59	0.732
1981	2.93	2.02	86.5	156.5	70.0	0.58	0.45	0.863
1982	1.30	1.55	130.9 ⁴	173.5 ⁴	42.6 ⁴	0.45	0.31	0.945
1983	3.42	2.35	66.9	213.6	146.7	1.22	0.61	0.752
1984	3.25	2.05	115.9	174.1	58.2	0.90	0.46	0.661
Total	24.17	23.03						
Average	2.20	2.09						

¹Daily root mean square error.

²Daily average absolute error.

³Correlation coefficient for daily flows.

⁴April data missing.

presented in Figure 5. Plots of the runoff traces produced when the model was initiated on February 1st and March 1st are not presented. These traces were essentially the same as the January 1st trace, in timing, but were of greater magnitude in volume, especially peak values. Comparisons of runoff volume and statistical measures are presented in Table 2 for the various starting dates. Also included for comparison are the results obtained during the calibration and prior test periods.

In all cases tested, model simulated runoff exceeded observed runoff. It is interesting to note that snowpack conditions on the earliest starting date (January 1st) produced the best results, followed by the next earliest date. Also, this updating scheme improved results over those obtained in the calibration and

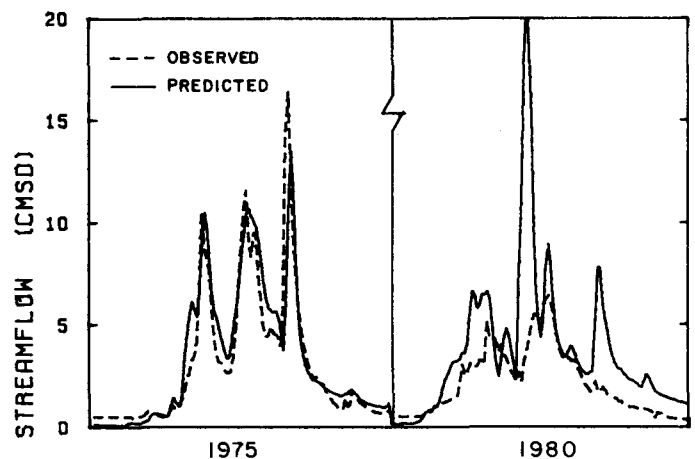


Figure 5. April Through July Observed and Simulated Streamflow at Lower Willow Creek, Montana for 1975 and 1980. Model Initialized on January 1st Using Observed SWE at the Snow Pillow Sites.

TABLE 2. Runoff volume and statistical comparisons for various model-run starting dates at Lower Willow Creek, Montana.

		April-July Runoff (mm)			Daily Errors (mm)		
		OBS	SIM	DIFF	RMS ¹	AVG-ABS ¹	r ¹
1975	JAN 1st	174.0	184.8	10.8	0.56	0.34	0.924
	FEB 1st	174.0	218.6	44.6	0.70	0.48	0.930
	MAR 1st	174.0	215.8	41.8	0.69	0.46	0.928
	CALIB.	174.0	184.4	10.4	0.54	0.33	0.929
1976	JAN 1st	160.5	170.9	10.4	0.35	0.26	0.973
	FEB 1st	160.5	171.0	10.5	0.34	0.25	0.974
	MAR 1st	160.5	180.7	20.2	0.40	0.30	0.965
	CALIB.	160.5	187.5	27.0	0.38	0.29	0.971
1980	JAN 1st	118.8	208.4	89.6	1.26	0.62	0.703
	FEB 1st	118.8	215.8	97.0	1.32	0.66	0.707
	MAR 1st	118.8	227.5	108.7	1.45	0.72	0.699
	TEST	118.8	198.6	79.8	1.04	0.44	0.732
1983	JAN 1st	66.9	77.1	10.2	0.35	0.22	0.688
	FEB 1st	66.9	77.4	10.5	0.35	0.22	0.687
	MAR 1st	66.9	93.7	26.8	0.43	0.28	0.699
	APR 1st	66.9	132.3	65.4	0.62	0.42	0.825
	TEST	66.9	77.2	10.3	0.26	0.16	0.781

¹See Table 1 for definitions.

prior test runs in only the 1976 water year. However, results were essentially the same in the January 1st starting date runs for 1975 and 1983.

Two factors that could have significant impact on the simulated results are the method of calibration used and the non-continuous data base available. If the model had been calibrated on the snow pillow data prior to calibration based on runoff, the SWE values may have been a better index of subsequent runoff. The problems associated with initiating a model run without a continuous record of input data such as runoff, soil moisture storage, etc., could also significantly affect the simulation results. In all cases where data are not available, the status of the various water storage and conveyance components must be estimated, thus impacting the results accordingly.

Using the NWSRFS Model with Daily SNOTEL SWE in Place of HYDRO-17 Simulated SWE

One of the great advantages of the SNOTEL system over traditional snow course surveys is the ability to obtain real time data rather than biweekly or monthly SWE readings. Although the NWSRFS model was not originally designed to use SNOTEL information as input, it is possible to modify the normal procedures and make use of this more timely data. The procedure used in this study was to replace the simulated snowmelt plus rain output of the HYDRO-17 subroutine with actual daily snowmelt determined from the snow pillow readings and rainfall. In other words, only the soil moisture accounting and unit hydrograph submodels were used.

The above procedure was tested on the 1975 water year. The model runs were initiated using April 1st watershed conditions as determined from SNOTEL data and calibration runs. Model parameters as determined for the calibration period were used in the first run and results are presented in Figure 6 and Table 3. Both timing and volume are noted to be quite different than observed. A second run was made in an attempt to correct these discrepancies. The precipitation adjustment factor PXADJ included in the soil moisture submodel was adjusted to compensate for the differences in runoff volume noted during the first run.

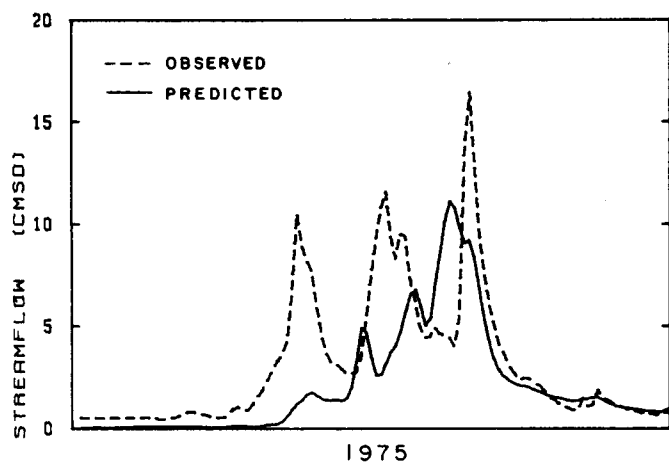


Figure 6. April Through July Observed and Simulated Streamflow at Lower Willow Creek, Montana for 1975. Model Initialized April 1st Using Calibration Parameter Values, Observed SWE, and Actual Snowmelt at the Snow Pillow Sites Plus Drummond Rainfall as Input.

Results of the second run are presented in Figure 7 and Table 3. As noted the observed and simulated runoff volumes are essentially identical, the daily errors are smaller, and the correlation coefficient (r) has increased. However, the timing of runoff peaks is still not as good as that obtained during the calibration runs using HYDRO-17 results rather than observed snow pillow melt. Part of the difference observed could be due to the calibration being based on runoff rather than snow pillow data as previously mentioned. However, the large errors

noted at the end of May and first of June, may be greater than one could adjust for by changing soil moisture reservoir amounts and transmission times. If this was the case, it would again indicate that either the snow pillow sites do not represent the zones selected, or Drummond precipitation is not a good measure of precipitation on the watershed at this time. In either case, the importance of on-site climatological data and representative SNOTEL sites is imperative for increased modeling accuracy.

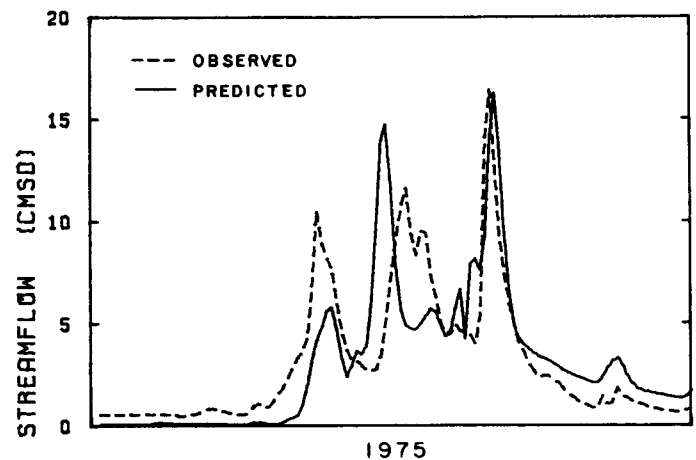


Figure 7. April Through July Observed and Simulated Streamflow at Lower Willow Creek, Montana for 1975. Model initialized April 1st Using "Best Fit" Parameter Values, Observed SWE, and Actual Snowmelt at the Snow Pillow Sites Plus Drummond Rainfall as Input.

DISCUSSION

The outcome of the studies was less than anticipated except for the calibration and test period results. However, the procedures were tested and proved to be operationally possible, and several main problems were identified that could be avoided in future studies. The first problem relates to the study site and the data set that was available. The lack of a continuous streamflow record made it difficult to develop calibration parameters related to baseflow conditions.

TABLE 3. Simulated and observed runoff comparisons for the April through July periods obtained from actual snowmelt measurements at the Black Pine and Combination snow pillow sites at Lower Willow Creek, Montana.

		PXADJ		April-July Runoff (mm)			Daily Errors (mm)		
		Lower Zone	Upper Zone	OBS	SIM	DIFF	RMS ¹	AVG-ABS ¹	r ¹
1975	(1)	1.000	1.00	174	115.6	-58.4	1.26	0.77	0.660
	(2)	1.420	0.800	174	174.2	0.2	1.10	0.73	0.755

¹See Table 1 for definitions.

Also, the discontinuous record made it necessary to assume initial watershed conditions at the beginning of each run and could have added to the magnitude of the errors.

The second problem seemed to be a product of the method used to calibrate the model. In this case, the entire model was calibrated with respect to observed runoff. This may not have resulted in any problems were it not for the attempts to use actual snow water equivalent and snowmelt data as inputs for initializing and updating the model. A better approach might have been to calibrate the HYDRO-17 submodel with respect to data available at the snow pillow sites. Then using the calibration parameter values thus obtained for HYDRO-17, the parameter values in the soil moisture accounting and unit hydrograph submodels could be adjusted (calibrated) with respect to observed streamflow. The tests described should then be more meaningful and produce better results.

Acknowledgements. I wish to express my appreciation for the extra effort given by Dave Robertson in making computer runs, and providing suggestions while working with the NWSRFS model. I also wish to thank Bernie Shafer, Phil Farnes, Don Jensen, Shari Hennefer, Sue Jackson, Beth Pirrong, Apryl Wilson, and Leon Huber for their assistance.

LITERATURE CITED

- Anderson, E. A., 1973. National Weather Service River Forecast System--Snow Accumulation and Ablation Model. NOAA Technical Memorandum NWS HYDRO-17. U.S. Dept. of Commerce, Silver Spring, Maryland. 217 pp.
- Cooley, K. R., E. P. Springer, and A. L. Huber, 1983. SPUR Hydrology Component: Snowmelt, p. 45-61. In: SPUR--Simulation of Production and Utilization of Rangelands: A rangeland model for management and research, J. R. Wight (Editor). USDA-ARS, Misc. Publ. No. 1431, Feb.
- Crook, A. G., 1985. Operational Experience in Meteor Burst Telemetry - Eight Years of SNOTEL Project Observations. In: Proceedings of International Workshop on Hydrologic Applications of Space Technology. Cocoa Beach, Florida. (In Press.)
- Huber, A. L., 1983. A Comparison of Several Snow Accumulation and Ablation Algorithms Used in Watershed Modeling, p. 76-88. In: Proceedings of Western Snow Conference, April 19-22, 1983. Vancouver, Washington.

THEORETICAL BASIS AND PERFORMANCE EVALUATION OF CURRENT
SNOWMELT-RUNOFF SIMULATION MODELS

T.W. Tesche*

ABSTRACT: Since the early 1970's, computer simulation of snowpack accumulation, metamorphism, and snowmelt has emerged as a viable tool in water resources management. Snowpack modeling has also been employed in such diverse fields as the description of snow avalanche and simulation of the fate of acidic materials transported over large distances in the atmosphere prior to accumulation in seasonal snow cover (i.e., acid deposition). In this paper we review representative examples of empirical and numerical snowpack simulation models that have been developed since the pioneering work of Leaf and Brink (1973a). Present day snowpack simulation models are examined on the basis of their treatment of physical processes, operational features, data requirements, and results of past verification studies. Critical areas of model development, data acquisition, calibration, and model evaluation are discussed.

(KEY TERMS: snowmelt, modeling, performance evaluation, runoff)

INTRODUCTION

Hydrologic simulation models have developed over the last two decades into sophisticated, widely accepted tools used regularly in water resources management studies worldwide. Whether for flood prediction, reservoir operations, water supply forecasting or for studying water quality issues, these models have provided engineers and scientists with a

powerful means with which to study hydrologic processes. Watershed models, designed to predict or forecast watershed response to precipitation (solid or liquid), have been formulated using a variety of mathematical representations of the fundamental conservation relations for mass and energy. In the design and implementation of most watershed models, principal concern has been in relating basic precipitation to runoff. Simulation of the physical processes affecting snow accumulation, snow metamorphism, and the thermodynamic processes of snowmelt have been accorded secondary emphasis. In this paper, however, the focus is directed mainly toward models of the processes governing snowpack melt and the hydrologic processes leading to water delivery from a basin.

The following section outlines the basic conceptual approaches that have been taken in developing snowmelt-runoff simulation models. Included is a survey of several representative snowmelt models exemplifying the different model types. While not exhaustive, the codes included in the review represent the range available in sophistication and diversity of application.

MODEL CONCEPTS

Development of a simulation model of snowmelt-runoff requires (1) identifying the relevant physical processes and (2) determining the most appropriate mathematical representation for all or a subset of these phenomena.

Basic Physical Processes

Important physical processes in snowmelt modeling include snow accumulation on the ground, snow metamorphism, snowmelt, and runoff. Excellent summaries of the state of knowledge in each of these disciplines is available. Male (1980), for example provides a detailed overview of the processes of snow accumulation. Comprehensive treatments of theoretical and experimental aspects of snow metamorphism are presented by Colbeck (1982, 1983), Mellor (1964), Sommerfeld and LaChapelle (1970), and Yen (1979). Anderson (1968), Bengtsson (1982), Fohn (1973), and Colbeck (1973, 1978) present snow energy budgets and authoritative discussions on various aspects of snow melt processes. Finally, the collection of papers presented at the 1978 conference on Modeling of Snow Cover Runoff (Colbeck and Ray, 1978) amply summarize the physical processes governing runoff (e.g., surface runoff, infiltration, evapotranspiration and subsurface flow).

While the thermodynamics and microphysics of snow on the ground have been studied for decades and are now fairly well understood (Perla and Martinelli, 1976), the incorporation of this knowledge into operational models for estimating snowmelt discharge remains highly empirical.

Types of Snowmelt Models

Watershed simulation models are often classified according to one of three different categories - transfer function, lumped parameter, or distributed parameter - depending upon the degree of temporal and spatial averaging of the hydraulic processes governing runoff (Shafer and Skaggs, 1983). An alternative scheme, adopted in this analysis, is based upon the degree of predictability assumed to exist in the system. Statistical models are predicated upon the assumption that the basic physical cause-effect relationships are somehow contained in the empirical data used to derive these models. These empirical models are based upon indices or correlations developed from observations. In

contrast, deterministic models are founded upon mathematical forms of the fundamental conservation relations governing mass, momentum, and energy. Through various spatial and temporal averaging procedures, the governing equations are reduced to a set that may be solved analytically, graphically, or numerically depending upon the particular model's formulation.

The advantages and limitations of these alternative conceptual frameworks are well known. Based upon observational data, statistical models are attractive because they directly link routinely measurable quantities (e.g, the maximum or mean daily air temperature) with desired output information (the daily snowmelt). Among their limitations, the statistical models are poorly suited to the characterization of extreme hydrometeorological events. Deterministic models, while conceptually more appealing since they explicitly treat physically-based cause-effect relationships, are more complicated to use and require significantly more data for model operation.

In the following section, we review a number of contemporary snowmelt-runoff models. Included are both statistical models (based upon indices and correlations) and deterministic models, formulated on the basis of either water or energy budgets (or both).

SURVEY OF SNOWMELT-RUNOFF SIMULATION MODELS

UC Davis Model (UCDM)

Merritt (1978) developed a deterministic snow accumulation and ablation model based upon the heat balance equation approach first presented by the U.S. Army Corps of Engineers, (1956). The snowpack accumulation and ablation algorithm in the UCDM was taken from the Amorocho and Espildora (1966) model (a lumped parameter model applicable to a single hydrologic unit). An energy budget was written for net longwave radiation, absorbed solar radiation, convective heat transfer, latent heat of vaporization, sensible heat change, rainwater heat content,

ground heat conduction, and cold content of the pack. The model consists of three layers - an active upper layer, and upper and lower passive layers. Input requirements of UCDM consist of initial snow depth and water equivalent, continuous air temperature, dewpoint temperature, wind speed and long- and short-wave radiation estimates. The model predicts daily basin runoff, snow depths and water equivalent in the hydrologic unit throughout the spring meltout period.

Hydrologic Engineering Center (HEC-1)

The HEC-1 is a deterministic, lumped parameter watershed model which includes a snowmelt-runoff calculation. The model is intended to simulate individual storms or events (i.e., runoff from one sustained event). Snowmelt is computed from empirical equations governing periods with or without rain. For example, the daily snowmelt rate is written as a linear function of rainfall intensity, air temperature, surface layer wind speed, and an empirical constant to reflect the "exposure" of the snowcovered area to wind. The snowmelt calculation is thus based upon the degree-day or energy budget method. HEC-1 utilizes the unit hydrograph approach for flow generation and any one of several routing equations are available. One of the limitations of the model is the inability to treat temporal and spatial variations in precipitation over the hydrologic basin.

Ontario Ministry of the Environment (OME)

Logan (1976) presented a lumped parameter deterministic snowmelt model for predicting melt in a single hydrologic unit. The snowmelt computation is based upon an energy balance method. Energy and mass transfer mechanisms are simulated at the snow-ground and snow-atmosphere interfaces and across the average pack thickness. Although the model equations represent the energy balance and melting process at a point, numerical interpolation/extrapolation procedures can be used to extend the spatial coverage of the model to a drainage basin. Principal model output

consists of ground surface free water production.

Snowmelt Runoff Model (SRM)

The Snowmelt-Runoff Model (SRM) is a deterministic, lumped parameter model formulated on an energy-balance concept. It utilizes the degree-day temperature index as the basic independent variable. In use for nearly a decade (see, for example Martinec, 1975; Martinec, et al., 1983; Rango, 1980; Rango and Martinec, 1981), this model is intended for use under conditions where snowmelt is the major contributor to runoff in mountain basins of significant relief. A given day's runoff is estimated from the sum of the recession flow and a simple empirical relationship involving a runoff coefficient, a degree-day factor, the number of degree-days, snow coverage and number of days. Although the model equation pertains, strictly speaking, to a specific point, the calculation may be generalized to cover a much broader range of geographic conditions through the use of detailed ground truth or remote sensing data. The model is capable of supplying forecasts from one day to several weeks depending upon the accuracy and range of the temperature forecasts. When the model is used in the forecast mode, it can be "nudged" or "updated" with measured discharge data at intervals throughout the simulation to improve the prediction.

Tangborn

Tangborn (1977, 1980) presented a lumped parameter snowmelt model based on the water-budget approach. The model is designed for short term predictions (1-15 days) although it may be used for the entire snowmelt season. The model, based upon an empirical treatment of snow storage and ablation, assumes that snowmelt-runoff may be determined from:

- Calculated amount of water stored as snow in the basin
- Estimated snow ablation just prior to the forecast period
- Temperature and precipitation predictions for the forecast period.

Model inputs include daily stream discharge, gaged precipitation, diurnal air temperature maxima and minima. From these synoptic inputs, the model, once calibrated using regression analysis, estimates the timing and volume of basin runoff. Possible refinements to the model include treatment of the storage and movement of liquid water in the pack, and separating the basin into distinct hydrologic subunits.

Beven and Dunne

The deterministic snowmelt-runoff model developed by Beven and Dunne (1982) is a distributed parameter model which focuses on the physics of meltwater flow through the pack. Mass transport in the slope parallel direction is treated in one dimension; in the slope normal direction, unsaturated flow to and into the soil mantle is simulated. Realistic hydrologic units are modeled by providing for a variable slope width. In principal, the model can accommodate the three dimensional structure of a snow field over simplified topography.

BURP2

The BURP2 model, developed by the U.S. Forest service (USFS, 1968) is a deterministic watershed/snowmelt model supplying continuous discharge forecasts on a daily basis for large scale forested watersheds. A distributed parameter model, BURP2 computes snowmelt through the use of a degree-day factor; the water balance is performed on a hydrologic basin comprised of several subunits of varying size. The model accounts for snowpack slope and aspect through a temperature adjustment factor. The model has several algorithms for calculating evapotranspiration and calibration is generally unnecessary. Routing of excess rainfall and infiltration processes are not treated in BURP2; the model predicts total water yield from a unit of land, but does not differentiate between surface runoff, streamflow, or ground water recharge.

MELTMOD

Leaf and Brink (1973a,b) developed a deterministic, lumped parameter snowmelt model for applications to subalpine watersheds in Colorado. MELTMOD is based on an energy balance approach, simulating winter snow accumulation, heat energy balance, snow pack conditions in terms of energy content and free water state, and resultant snowmelt (temporally and spatially resolved), for a variety of terrain aspects, slopes, elevations, and vegetative characteristics. MELTMOD treats the snowpack as a dynamic heat reservoir. Heat is added algebraically during precipitation. Only when the pack becomes isothermal and saturated does melt occur. Unsteady heat transfer theory is used in the energy budget computation. The daily minimum temperature is used as an index in segregating precipitation into snow, rain, or both. The model was designed primarily for mountain conditions where there are distinct accumulation and melt phases during the winter; the model has no provisions for a snowpack ripening and subsequently reverting back to a colder unsaturated pack.

SNOWMELT

SNOWMELT is basically a modified version of the MELTMOD code. Developed by Solomon et al, (1975, 1976), SNOWMELT simulates winter snow accumulation, an energy balance, snowpack conditions, and resultant snowmelt. Its principal improvements over the MELTMOD model are that treats alternate freezing and thawing patterns during snow accumulation and melt phases, it does not tend to keep the snow pack excessively cold during the snow accumulation phase, and it has reduced input data requirements (e.g., daily solar radiation). In addition, SNOWMELT may be applied in situations involving a discontinuous snowpack. The model is dependent upon four daily input variables: maximum and minimum temperatures, precipitation, and shortwave radiation. Only limited knowledge of local watershed and snowpack structure is needed for model initialization.

Judson, Leaf and Brink

As part of a long term research effort into avalanche prediction and hazard evaluation, Judson, Leaf, and Brink (1980) extended the capabilities of the MELTMOD snowmelt model to include more details of snowpack physics. Specifically, the MELTMOD code was extended to simulate layer depth, age, densification, temperature gradient and equitemperature metamorphism, melt-freeze metamorphism, snow pack accumulation, and wind loading and redistribution. The output of this deterministic model includes, in addition to melt rates (if dictated by the conditions), snow pack stratigraphy, and weighted average loading rates from the previous one to three days. The model treats the vertical variation in snow pack water and energy exchanges in detail and can accommodate changing topography in the downslope direction. This model has the potential for routine application as an operational snowmelt-runoff model but the sophisticated treatment of the loading and metamorphic processes associated with snow slab instability (Judson and King, 1985), would require simplification in order to yield reasonable computing costs.

Weissman

Weissman (1977) developed a model of the melting of a snow pack due to warm air advection. Assuming a ripe, saturated pack, this model calculates the heat and momentum fluxes in the thermal internal boundary layer over a horizontal snowpack. Principal model output is the total average melt over the pack and the variation in melt as a function of downwind distance from the upstream edge of the snow field. Conventional mixing length theory is used to model the turbulent momentum and energy fluxes in the atmospheric boundary layer over the snow surface.

Akan

Recently, Akan (1984) formulated a time-dependent, distributed parameter mathematical model of snowmelt runoff based upon a numerical finite difference

solution of the diffusion equation. The model concept includes two physical layers resting on an inclined slope. In the upper unsaturated zone, the processes of heat and mass exchange, phase change, percolation, conduction, and vapor diffusion are simulated. In the saturated zone, basal flow is modeled. The unsaturated zone is assumed incompressible and the melt layer is assumed not to settle. Detailed empirical treatment of microphysical processes are included in the model for the coefficients of hydraulic conductivity, thermal conductivity, and vapor diffusion in snow; variations in snow porosity and grain size due to phase changes; and constitutive relations for liquid water pressure, snow temperature, and water vapor content. The model is two dimensional (i.e., variation in the slope normal and parallel directions) and predicts melt and snowmelt runoff on 30 to 60 minute intervals.

Jordan (1983)

Jordan (1983) developed a distributed parameter, deterministic model to study the physics of snow melt and vertical mass transport in deep, mature mountain snowpacks. The model is a one-dimensional, unsaturated, transient code which solves the diffusion equation in a homogeneous, rigid, porous medium. The principal objective of this model is the study of the propagation of meltwater flux waves down through the pack as a function of time.

CALIBRATION AND EVALUATION

In the literature the terms "model validity," "model evaluation," and "model verification," are frequently interchanged, at times obscuring the true nature of the comparison between prediction and observation. Here we provide the following definitions:

1. Model Calibration - the adjustment of empirical model constants or parameters in order to optimize the agreement between prediction and

observation, with limited regard to the physical meaning or reasonableness of the value(s) ultimately chosen.

2. Model Validity - the degree of agreement between model predictions and corresponding observations, given perfect specification of model inputs. This concept refers to the scientific soundness and implementation of the model's formulation.
3. Model Evaluation - the process of examining and quantifying the performance of a snowmelt-runoff model. Use of the terms "validation" and "verification" to refer to this process should be avoided.
4. Model Verification - the successful evaluation of the model; that is the imposed standards of performance have been met.

In considering present snowmelt-runoff models, we are primarily interested in model calibration efforts and in subsequent model evaluation results. Validation of current generation models is unlikely due to the typical time and space averaging (lumping) that underlies most model's formulations. Verification of models is also unlikely at present since few if any standards of model performance have been established against which to judge quantitatively the acceptability of a model for usage.

A wide variety of snowmelt-runoff model evaluation studies are reported in the literature and most of them include some form of calibration. Solomon et al (1976) present evaluation results in three subjective categories - good, average, and poor correlation between predicted and measured water equivalents. They note the difficulty in developing statistical "goodness of fit" measures with serially dependent data yet declare the model to perform "satisfactory."

Price and Dunne (1976) compared predicted and measured daily runoff results from a subarctic study plot using a physically-based energy balance model.

The ratio of observed melt rates to predicted rates were examined as a function of time and the two rates were compared through linear regression. Based upon an r value of 0.85 and a sigma of 0.71 cm/day, they conclude that the model's performance is "quite satisfactory and within the currently accepted limits in snowmelt hydrology."

Baker and Carder (1977) compared the BURP, ECOWAT, SNOWMELT, and USDAHL-85 models. The models were first calibrated by varying threshold temperatures, temperature and precipitation "factors," degree-day coefficients, and snowfall temperatures. Time series of model predictions of daily snowmelt were compared with data from the White Mountains snow course for 1966-1969. Only very limited data comparisons are presented.

Haverly, Wolford and Brooks (1978) present a similar, but slightly more rigorous evaluation study of the HEC-1, USACE, and SNOWMELT models with data from northwestern Minnesota. Predicted and observed snowmelts were compared statistically for two seasons of data on open and forested plots. R squared values ranged between 0.489 to 0.924 prompting the researchers to conclude that the models were of comparable accuracy. In addition, the HEC-1 model was recommended for operational streamflow forecasting because it "requires little calibration time and fewer data."

More recently, Gottlieb (1980) compared calculated and observed daily snowmelt discharges from the Peyto Glacier Basin using a detailed energy budget model. The r squared (explained variance) for the basin was computed for each of eight years based upon computed and observed daily runoff. The r squared values ranged between 0.56 and 0.83. Time series plots of daily calculated and observed discharge were also presented and were declared to be quite satisfactory.

Rango (1980) modeled snowmelt in the Wind River Range of Wyoming with SRM and matched seasonal runoff volumes with the model to within 5 percent. 82-86 percent of the daily variance in snowmelt was explained by model prediction, using "goodness-of-fit" statistics.

An evaluation of the Bengtsson (1982) model of vertical snowmelt percolation through the pack was performed using data obtained in runoff experiments conducted over a 22 hour period. Hourly average runoff rates were compared with model predictions. The discrepancies in the hydrograph were attributed to either measurements errors or an incorrect energy balance.

Rango (1985) also presents SRM model evaluation results for fourteen snow-covered basins in the U.S. and seven foreign countries. His statistical comparisons include absolute differences in calculated and observed seasonal discharge volumes, and coefficient of variation statistics based on daily flows. The model evaluation results are also stratified according to whether the snow-cover inputs are derived from visual or Landsat observations, snow course records, aircraft orthophotos, or NOAA satellite observations. The average variance across all basins simulated by SRM, was 0.86 (0.73 to 0.96).

Review of the snowmelt-runoff model evaluation literature reveals that qualitative comparisons of the computed and observed hydrographs is the basis for most summaries of model performance. While statistical summaries of the hydrographs are important in assessing the overall accuracy of the model calibration and subsequent evaluation (on independent data sets), they by no means present the whole picture. Among the measures of performance that provide insight into the adequacy of a models performance are estimates of bias, error, accuracy of the peak discharge, total discharge volume, and temporal and spatial correlation in snowmelt-runoff rates. Furthermore, these statistical measures provide additional insight when calculated over daily, weekly, flow interval, and seasonal periods. Additional insight into the performance characteristics of present snowmelt-runoff models can be developed through more rigorous statistical evaluations than have been reported to date.

Current procedures for evaluating the predictive performance of air quality simulation models may be worth adopting (in suitably modified form) in the

development of more refined snowmelt model calibration and evaluation methods.

SUMMARY

In the dozen or so years since introduction of the distributed parameter, deterministic snowmelt-runoff models of Leaf and Brink (1973a,b) and Solomon et al (1975, 1976) few model developers have attempted to extend these simulation techniques to new models offering greater temporal and spatial resolution in treatment of the governing physical processes. In other fields in the physical and earth sciences (i.e., atmospheric chemistry and transport, ground water flow and contaminant dispersion, surface water quality) the last decade has been one of intensive development of progressively more sophisticated mathematical modeling and simulation techniques, fostered largely by advances in computer technology. One reason, perhaps, for the less advanced state of development in snowmelt simulation models is the lack of a lead governmental agency in the U.S. to coordinate snow science research. Because studies of seasonal snow cover embrace so many geophysical disciplines - the physical, earth, chemical, hydrological and atmospheric sciences - the problems associated with managing research in this field are apparently outside the scope of any one agency or department. Moreover, prospects for centralization of seasonal snowpack research within the government to not appear bright, especially in light of the growing trend of governmental agencies to deemphasize certain areas of snow hydrology research. The closing of the U.S. Forest Service Avalanche Research Station in Fort Collins is one recent example.

Nonetheless, research and applications in the study of seasonal snow cover will continue. The following areas continue to provide significant research opportunities:

Snow Distribution and Accumulation Models

Research opportunities exist in developing improved descriptions of the processes governing snow formation,

transport, deposition, and redistribution by wind on the ground surface. Terrain and vegetative cover inhomogeneities play an important role in the local snowfall accumulation and redistribution patterns (Thomsen, 1980). Refinement of atmospheric transport models (for complex terrain), improved models of orographic snowfall, better descriptions of the effects of local topography and vegetation on snow distribution, and improved measurement methods of snowpack properties are all areas where refinements to snowmelt-runoff models and their inputs can be achieved.

Snow Pack Energy Budgets

Few previous studies have investigated in detail the several energy transfer processes simultaneously occurring within the snowpack at a given time and how they relate to mesoscale atmospheric circulations. Due to the large costs of data acquisition, it is important that field experiments be designed and study sites selected so as to maximize the generality of point measurements to areas of larger scale. In particular, in-situ measurements of radiant, sensible, latent, and geothermal heat fluxes and snowpack heat content properties need to be performed in such a way that they (1) support detailed analysis of evaporation, sublimation, condensation, sensible heat transfer, (2) permit the correlation between microscale energy transfers and mesoscale atmospheric circulations, and (3) aid in the investigation of concurrent snow metamorphic changes.

Snow Metamorphism

The microphysics of snow metamorphism have been studied in detail in the laboratory and to a lesser extent in the field, the latter associated mainly with snowpack stability and avalanche release (Perla and Martinelli, 1976). There is a pressing need to extend the current knowledge of the metamorphic processes which occur at a point in the pack (and under idealized conditions) to the more general metamorphic changes which occur on

realistic, non-uniform packs of differing slopes, aspects, vegetative cover, etc. The processes of temperature gradient, equitemperature gradient, melt-freeze, and radiation-recrystallization metamorphism need to be formulated into mathematical models which can be operated with relatively simple climatic data inputs (either from routine measurements or supplied by numerical weather prediction or mesoscale meteorological models).

Physical Properties of Snow

The physical properties of snow are reasonable well understood, notwithstanding the extremely broad range of shapes and densities the substance may assume. However, improvements in present capabilities for in-situ and remote sensing (e.g., Rango et al 1979), of seasonal snowcover's physical properties remain one of the principal challenges in snow hydrology research. Needed are improved techniques for determining the aerial extent, depth, density, water content, and stratigraphy of the snowpack. These properties are directly related to improved knowledge of snowmelt processes. Related information on snowpack spectral reflectivity, infrared emissions, radiation scattering properties, microwave emissions, and dielectric properties may also prove valuable.

Physical Properties During Melt

The thermodynamics of snowmelt have been studied intensively in the laboratory for early two decades. Advances in this area of snow microphysics need to be incorporated into the mathematical formulation of snowmelt, meltwater percolation, and runoff processes. Improved model formulation of the meltwater thermodynamics and percolation processes will require complete snow-profile descriptions including pack depth, density, freewater content, grain shape, grain size, and temperature in each layer of the pack.

Complexity in Model Formulation

The rapidly expanding capabilities of today's supercomputers has stimulated

in some a tendency to promote significantly expanded complexity in model detail (e.g., temporal and spatial resolution, number of physiochemical processes considered). This tendency should be avoided in those situations where added model complexity is obtained at the expense of physical insight into the system under study. Complex simulation models play an important role in snow hydrology; an obvious example is in the estimation of and design for extreme snowmelt-runoff events, for which the more lumped-parameter empirically based techniques are poorly equipped. However, judicious selection is needed in obtaining the proper balance between mathematical complexity of the simulated system and the conceptual understanding of the relevant physical processes of greatest importance in a given application.

LITERATURE CITED

- Akan, A.O., 1984, "Simulation of Runoff From Snow-Covered Hillslopes," Water Resources Research, Vol. 20, No. 6 pp. 707-713.
- Amoroch, J. and B. Espildora 1966, "Mathematical Simulation of the Snow Melting Process," Water Science and Engineering Paper No. 2001, University of California, Davis.
- Anderson, E.A. 1968, "Development and Testing of Snowpack Energy Balance Equations," Water Resources Research, Vol. 4, pp. 19-37.
- Baker, M.B. and D.R. Carder, 1977, "Comparative Evaluations of Four Snow Models," proceedings 45th Annual Western Snow Conference.
- Beven, K. and T. Dunne, 1982, "Modeling the Effect of Runoff Processes on Snowmelt Hydrographs," International Symposium on Rainfall-Runoff Modeling, May 18-21, Mississippi State University, Mississippi State, MS.
- Bengtsson, L, 1982, "Percolation of Meltwater Through a Snowpack," Cold Regions Science and Technology, Vol. 6, pp. 73-81.
- Colbeck, S.C., 1973, "Theory of Metamorphism of Wet Snow," Res. Rep. 313, U.S. Army Cold Region Res. and Engr. Lab., Hanover, N.H.
- Colbeck, S.C., 1978, "Physical Aspects of Water Flow Through Snow," Advances in Hydroscience II, Academic Press, New York, NY.
- Colbeck, S.C., 1982, "An Overview of Seasonal Snow Metamorphism," Reviews of Geophysics and Space Physics, Vol. 20, No. 1, pp. 45-71.
- Colbeck, S.C. 1983, "Theory of Metamorphism of Dry Snow," Journal of Geophysical Research, Vol. 88, No. C9, pp. 5475-82.
- Colbeck, S.C. and M. Ray 1978, "Modeling of Snow Cover Runoff," proceedings of a meeting on Modeling of Snow Cover Runoff, 26-28 September 1978, CRREL, Hanover, N.A., America-Geophysical Union and American Meteorological Society.
- Fohn, P.M.B., 1973, "Short-Term Snow Melt and Ablation Derived From Heat- and Mass-Balance Measurements," Journal of Glaciology, Vol. 12, No. 65.
- Gottlieb, L., 1980, "Development and Applications of a Runoff Model for Snow-covered and Glacierized Basins," Nordic Hydrology, Vol. 11, pp. 255-272.
- Haverly, B. A., R.A. Wolford, and K.N. Brooks 1978, "A Comparison of Three Snowmelt Prediction Models," proceedings 46th annual Western Snow Conference.
- Jordan, P., 1983, "Meltwater Movement in a Deep Snowpack 2. Simulation Model," Water Resources Research, Vol. 19, No. 4, pp. 979-985.
- Judson, A., C. F. Leaf, and G.E. Brink, 1980, "A Process-Oriented Model for Simulating Avalanche Danger," Journal of Glaciology, Vol. 26, No. 94, pp. 53-63.
- Judson, A., and R. King, 1985, "An Index of Regional Snow-Pack Stability Based on Natural Slab Avalanches," Journal of Glaciology, Vol. 31, No. 108.

- Leaf, C.F. and G.E. Brink, 1973a, "Computer Simulation of Snowmelt Within a Colorado Subalpine Watershed," USDA Forest Service, RM-99, Fort Collins, CO.
- Leaf, C.F. and G.E. Brink, 1973b, "Hydrologic Simulation Model of Colorado Subalpine Forest," USDA Forest Service, RM-103, Fort Collins, CO.
- Logan, L.A. 1976, "A Computer-Aided Snowmelt Model for Augmenting Winter Streamflow Simulation in a Southern Ontario Drainage Basin," Canadian Journal of Civil Engineering, Vol. 3, pp. 531-554.
- Male, D.H., 1980, "The Seasonal Snow-cover," in Dynamics of Snow and Ice Masses, Academic Press.
- Martinec, J. 1975, "Snowmelt-Runoff Model for Stream Flow Forecasts," Nordic Hydrology, Vol. 6, No. 3, pp. 145-154.
- Martinec, J., A. Rango, and E. Major, 1983, "The Snowmelt-Runoff Model (SRM) User's Manual," NASA reference Publication No. 110, Goddard Space Flight Center, Greenbelt, MD.
- Mellor, M. 1964, "Properties of Snow," Cold Region Science and Engineering, Part III-A1, Hanover, NH.
- Merritt, R.G., 1978, "Digital Simulation of Snowmelt Runoff," University of Nevada, Desert Research Institute, PB 293252, Reno, NV.
- Perla, R.I., and M. Martinelli, 1976, "Avalanche Handbook," Rocky Mountain Forest and Range Experiment Station, Fort Collins, CO.
- Price, A.G. and T. Dunne, 1976, "Energy Balance Computations of Snowmelt in a Subarctic Area," Water Resources Research, Vol. 12, No. 4.
- Rango, A. 1980, "Remote Sensing of Snow Covered Area for Runoff Modeling," proceedings of the Oxford Symposium, IASH-AISH Publ. No. 129., pp. 291-297.
- Rango, A. and J. Martinec, 1981, "Accuracy of Snowmelt Runoff Simulation," Nordic Hydrology, Vol. 12, pp. 265-274.
- Rango, A., A.T.C. Chang, and J.L. Foster, 1979, "The Utilization of Space Microwave Radiometers for Monitoring Snowpack Properties," Nordic Hydrology, Vol. 10, pp. 25-40.
- Rango, A., 1985, "Assessment of Remote Sensing Input to Hydrologic Models," Water Resources Bulletin, Vol. 21, No. 3.
- Shafer, J.M. and R.L. Skaggs, 1983, "Identification and Characterization of Watershed Models for Evaluation of Impacts of Climate Change on Hydrology," Battelle Pacific Northwest Laboratories, PNL-SA-11924.
- Solomon, R.M. et al, 1975, "Characterization of Snowmelt Runoff Efficiencies," Watershed Management Symposium ASCE Irrigation Drainage Division Proc. 1975, pp. 306-326.
- Solomon, R.M. et al, 1976, "Computer Simulation of Snowmelt," USDA Forest Service, RM-174, Fort Collins, CO.
- Sommerfeld R.H., and E.R. LaChapelle, 1970, "The Classification of Snow Metamorphism," Journal of Glaciology, Vol. 9, No. 55, pp. 3-17.
- Tangborn, W.V. 1977, "Application of a New Hydrometeorological Streamflow Prediction Model," proceedings 45th Annual Western Snow Conference.
- Tangborn, W.V. 1980, "A Model to Forecast Short-Term Snowmelt Runoff Using Synoptic Observations of Streamflow, Temperature, and Precipitation," Water Resources Research, Vol. 16, No. 4, pp. 778-786.
- Thomsen, A.G., 1980, "Spatial Simulation of Snow Processes," Nordic Hydrology, Vol. 11, pp. 273-284.
- U.S. Forest Service, 1968, "BURP: A Water Balance Program," Watershed Systems Development Unit, Berkeley, CA.
- U.S. Army Corps of Engineers, 1956, "Snow Hydrology," North Pacific Division, Portland, OR.

Weisman, R.N. 1977, "Snowmelt: A Two-Dimensional Turbulent Diffusion Model," Water Resources Research, Vol. 13, No. 2, pp. 337-342.

Yen, Y.C. 1979, "Recent Studies in Snow Properties," Advances in Hydroscience, Vol. 5, pp. 173-214.

RECENT DEVELOPMENTS IN SNOWMELT-RUNOFF SIMULATION

Sten Bergström¹

ABSTRACT: Some tendencies in recent development of snowmelt simulation models are reviewed with special emphasis on the problem of model complexity versus data availability and model performance. The possibility to use new sources of areal snow water equivalent information is discussed, and the need for reliable cost-benefit analyses is stressed. Finally a few important research needs for improved snowmelt simulation models are identified. (KEY TERMS: Snowmelt simulation; conceptual model; basin snow water equivalent.)

INTRODUCTION

Snowmelt-runoff simulation models are major components of hydrological forecasting systems and water management schemes in many parts of the world today. Their direct economic importance is maybe easiest to quantify in connection with stream-flow forecasting for reservoir operation, where damage can be avoided, and water can be put into productive use instead of leaving the reservoirs through the spillways. For design purposes, the models have a great value, as they are used to create longer runoff records and thereby more reliable runoff statistics in areas, where long climatological records are available.

Recently, interest in the use of runoff models for the interpretation of hydrochemical records of flowing waters has grown, because these records show a wide natural variation, that strongly depends on the hydrological situation. For example, the analysis of pH or alkalinity can be very confusing, unless high and low flow situations are treated differently.

Along with the development of handy desk-top computer systems and more customer-oriented soft-ware, conceptual runoff models are becoming more generally available for all categories of users. This has made it possible for local offices to run operational models independently, a fact, which is likely to have strong impact on the future use of conceptual models.

CONCEPTUAL SNOWMELT MODELS

A physically correct way to approach the snow modelling problem would be from the total heat budget of the snowpack, as discussed by, for example, U.S. Corps of Engineers (1956) and (1960), Kuz'min (1972) and Morris (1985). The general equation would be of the form:

$$W_{sw} + W_{lw} + W_c + W_l + W_g + W_p + W_t + W_m = 0 \quad (1)$$

where:

- W_{sw} = absorbed short wave radiation,
- W_{lw} = net long wave radiation,
- W_c = convective heat flux,
- W_l = latent heat flux
(condensation and evaporation),
- W_g = heat flux from the ground,
- W_p = contribution of heat from precipitation,
- W_t = change in the energy content of the snowpack,
- W_m = heat equivalent of the snowmelt.

¹Swedish Meteorological and Hydrological Institute, S-601 76 Norrköping, Sweden

Many modellers, who have attempted to model eq. 1 both at a point and on a basin scale, have experienced that its data requirements are difficult to fulfil and that some of the physical processes are very complex. This has led to the development of a number of simplified conceptual snowmelt models, which treat the meteorological variables more as indices of the physical processes that govern snowmelt rather than input to exact energy balance computations. The best known of these index methods is the commonly used and long-lived degree-day approach according to the following expression:

$$M = C_o (T - T_o) \quad (2)$$

where:

- M = snowmelt (mm),
- C_o = degree-day melt factor (mm/°C),
- T = surface air temperature (°C),
- T_o = threshold value of the air temperature (°C).

Equation 2 is normally used on daily data or data with higher resolution. When applied to runoff models, it is often combined with various options in attempts to make it more physically correct. These options vary a lot from one model to another, but the following may serve as examples:

- Liquid water holding capacity, which delays runoff from melting snow.
- Seasonal variation of the degree-day factor, which accounts for variations in insolation, albedo and thermal properties of snow.
- Separation of rainy and clear days to account for differences in the energy exchange processes.
- Introduction of wind speed and/or vapour pressure of the air into the equation to obtain a more realistic expression for energy exchange.
- Use of daily air temperature range as an index of radiation.

- Differentiation into forested and open areas to account for differences in energy exchange.
- Computation of the thermal conditions in the snowpack and/or in the ground.
- Introduction of a statistical distribution function in order to account for redistribution of snow on the ground.
- Use of elevation zones in combination with temperature and precipitation lapse rates.

OPTIMUM COMPLEXITY OF SNOWMELT MODELS

Many modellers have tried to find the optimum complexity of snowmelt models by comparative test runs on well controlled data bases. Anderson (1976) found that an energy balance equation was superior to an index model in well defined open areas and under extreme conditions. His results are to some degree supported by Braun (1985), whose results indicate that some improvements may be obtained by energy balance models in small basins in Switzerland.

Contradictory to these results, Kuusisto (1978) partly failed to show improvements when moving from a simple index model to a more energy-balance-like approach on snowpillow data from Finland. Vehviläinen (1985) also in Finland, and Lundquist (1981) in Norway came to a similar conclusion when applying a conceptual runoff model with snowmelt routines of increasing complexity to small basins in their respective countries.

Between 1976 and 1983 the World Meteorological Organization, WMO, performed a well controlled intercomparison of models of snowmelt runoff in order to examine their performances under various conditions. Altogether 11 models, varying in complexity from simple degree-day approaches with a water holding capacity option to more complex energy balance computations, were tested on data from 6 basins with snowmelt as a significant hydrological component (Tables 1 and 2).

Table 1. Models participating in the WMO Intercomparison of Models of Snowmelt Runoff.

1. UBC Watershed Model (Canada)	(Quick and Pipes, 1972)
2. CEQUEAU Model (Canada)	(Charbonneau, Fortin and Morin, 1977)
3. ERM Model (Czechoslovakia)	(Turčan, 1981)
4. NAM-II (Denmark)	(Nielsen and Hansen, 1973)
5. TANK Model (Japan)	(Sugawara et al., 1974)
6. HBV Model (Sweden)	(Bergström, 1976)
7. SRM Model (Switzerland)	(Rango and Martinec, 1979)
8. IHDM Model (United Kingdom)	(Morris, 1980)
9. SSARR Model (USA)	(U.S. Corps of Engineers, 1972)
10. PRMS Model (USA)	(Leavsley and Striffler, 1978)
11. NWSRFS Model (USA)	(Anderson, 1973)

Table 2. Test basins in the WMO Intercomparison of Models of Snowmelt Runoff.

1. Durance (France)	2 170	km ²
2. W3-Watershed (USA)	8.4	km ²
3. Dunajec River (Poland)	680	km ²
4. Dischma Basin (Switzerland)	43.3	km ²
5. Illecilleweat River (Canada)	1 100	km ²
6. Kultsjön (Sweden)	1 110	km ²

The models were calibrated to each basin over a six years period, and four remaining years were used for verification. This produced a wealth of information, varying from various statistical criteria of agreement between the models and the observations to linear scale plots of the simulations and flow duration curves.

At a final meeting in Norrköping, Sweden, in September, 1983, the modellers had the opportunity to compare their results, and many valuable conclusions were drawn. On the question of optimal model complexity the following statement was made:

"On the basis of available information, it was not possible to rank the tested models or classes of models in order of performance. The complexity of the structure of the models could not be related to the quality of the simulation results." (WMO, 1986)

AREAL VARIABILITIES

One reason why often only moderate success is achieved when increasing snowmelt modelling complexity on a basin scale is lack of detailed knowledge of the physical processes involved. Another reason, maybe more important, is the areal variability of snow conditions and of the cli-

matological variables, which serve as input to the models. The latter problem can be illustrated by the following simple case:

In most operational applications in mountainous areas, the climate stations are situated in the lower parts of the basins, as illustrated by an example from Sweden in Figure 1.

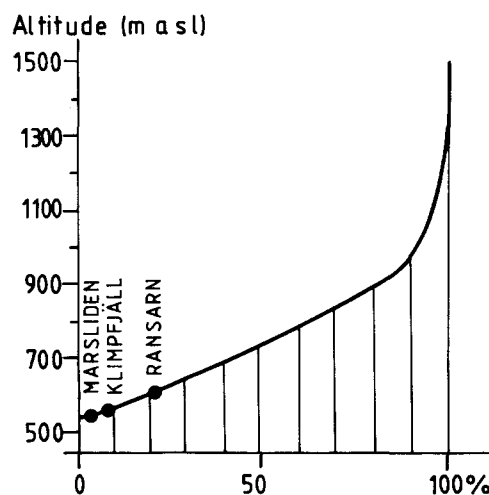


Figure 1. Example of poor altitude representativeness of climatological stations. Hypsometric curve and location of stations in the 1 109 km² Kultsjön basin in Northern Sweden.

The data therefore have to be extrapolated to higher elevations by the use of lapse rates. For air temperatures a constant lapse rate of $-0.6^{\circ}\text{C}/100\text{ m}$ elevation is often used, sometimes with a seasonal variation, as suggested, for example by Konovalov (1979). In fact, this temperature lapse rate shows strong day-to-day variation, depending on the meteorological conditions. The values normally stay around $-0.6^{\circ}\text{C}/100\text{ m}$ as an average at temperatures around freezing and higher. At lower air temperatures, however, inversions frequently will turn the temperature lapse rate positive, as shown by an example in Figure 2.

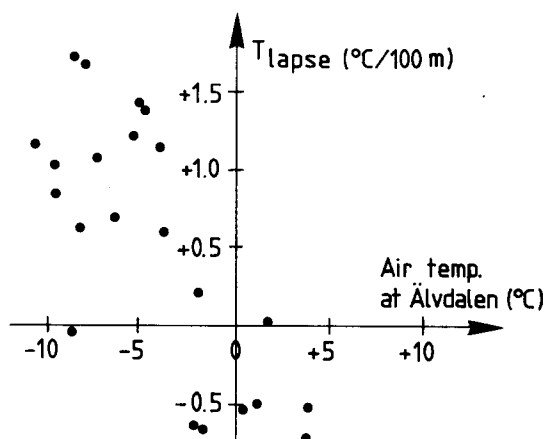


Figure 2. Example of the dependence of the temperature lapse rate on air temperature in Sweden. Data from the stations Kräckelbäcken at 670 m.a.s.l. and Älvdalen at 250 m.a.s.l.

The consequence of this is that even a very modest attempt to model the thermal properties of the snowpack or the ground will be physically obscure and is likely to fail at high elevations, unless a more realistic temperature lapse rate is adopted. Models without routines for thermal properties will suffer less from this problem and are therefore likely to be more physically correct in spite of their simplicity.

The problem of areal variability of the snowpack is particularly pronounced above the timber line, which shows up clearly, if snow water equivalent is plotted against elevation as in Figure 3.

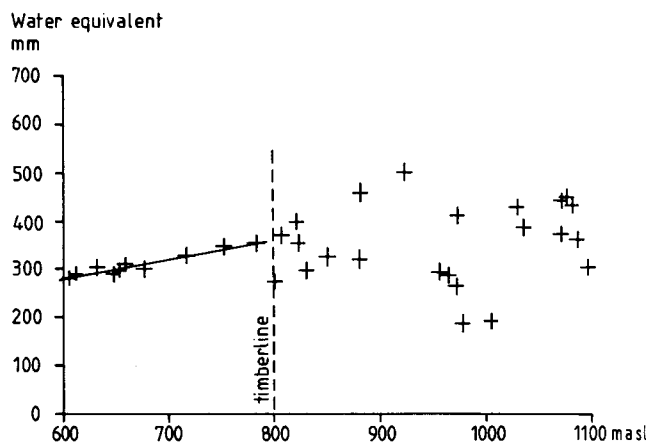


Figure 3. Plotting of snow water equivalent against elevation in the Kultsjön basin in Northern Sweden. The snow water equivalents are measured by gamma-ray technique (Bergström and Brandt, 1984).

It is the redistribution of the snow on the ground that causes the great variations above timber line. Figure 3 illustrates that a constant precipitation lapse rate can only be recommended in forested areas. This has, for example, led Killingtveit and Aam (1978) to modify the HBV Model when applying it to high elevation areas in Norway, by the introduction of a statistically distributed snow routine, as shown in Figure 4. The authors reported significant improvements by this modification, which resembles the areal depletion curve used by, for example, Anderson (1973).

It is possible that we have to accept the above statistical approach in areas with very complex snow accumulation patterns, like in wind-blown rugged terrain. Fortunately, as shown by Killingtveit and Aam (1978), the distribution pattern is very consistent from one year to another, which simplifies the modelling approach. On the other hand, the great variability in these terrains makes it difficult to justify melt equations that are too complex.

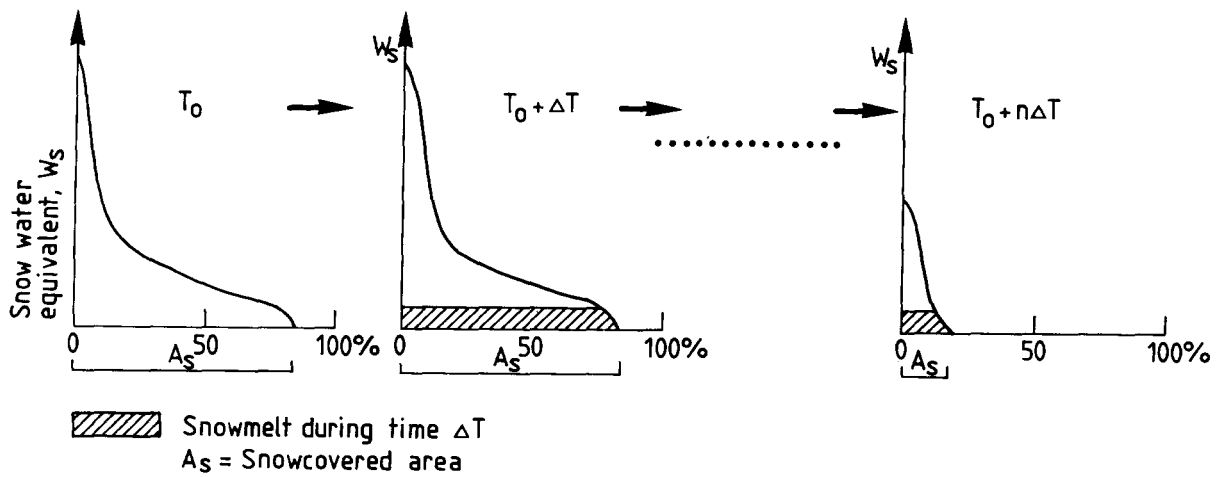


Figure 4. Principles of the statistically distributed snow routine according to Killington and Aam (1978).

LOSSES

When conceptual models are used for year-around simulation, the development of the snowpack is normally computed by an accumulation of all precipitation that falls at air temperatures below a given threshold value. Most models then use an empirically derived snowfall-correction factor to make the water balance match during the melt season. This correction factor, normally expressed as a percentage of falling snow, accounts for all kinds of losses, lack of representativeness of the precipitation gauge, poor estimates of the precipitation lapse rate and other systematic errors. The simple snowfall correction factor is thus the dominating model parameter for the forecasts of total inflow to a reservoir during a snowmelt season.

Considering the high value of correct forecasts of the total inflow to a reservoir during snowmelt and the fact that these forecasts often show errors, which are difficult to explain, it is surprising that the simple correction factor is accepted by so many modellers, while greater efforts are spent on better detailed snowmelt computations.

One reason for the lack of interest in losses may be a general feeling that there is a physical limit to possible evaporation from a snowpack due to its low surface temperature (see, for example, Bengtsson, 1980). If we regard a basin

at mid-melt as a mix of snowfields, patches and bare ground, this physical constraint is no longer valid. On a sunny day, evaporation from warm patches of bare ground can very well reach high values, in particular as these areas are fed with water from adjacent melting snow.

Better understanding of the losses that may occur from the snowpack or patches of snow and bare ground during extreme weather conditions, is an important future field for research. If this research is successful, it will pay off in very short time by improved long term forecasts.

NEW SOURCES OF BASIN SNOW DATA

The lack of detailed information about the areal variability of the snowpack and the climatological variables is probably the main reason why rather few successful modifications of the established operational snowmelt-runoff models can be found in recent literature. There seems to be a consensus among modellers that we need better input data before the models can be improved further.

As a consequence, there is growing interest in new techniques for obtaining information on the snow condition in the field. In Western United States this has resulted in a very extensive network of automated snow observation stations, SNOTEL, as described by Barton and Crook (1980). The interest in use of sat-

elite imagery has also grown, and some success in modifying traditional snowmelt forecasting methods have been reported by, for example, Rango (1985). Attempts with satellite updating of conceptual snowmelt models have also been reported from Denmark (Danish Hydraulic Institute, 1985).

Two main drawbacks of satellites for updating of conceptual models are their incapability under cloudy conditions and the fact that, for the time being, they can only give us information about the areal extent of snowcover. We will probably have to wait for more advanced microwave sensors, until we get what we really want: direct information about the snow water equivalent over the basin. But when these data are available on a routine basin, it will be a major break-through for remote sensing in snow simulation.

Attempts to measure snow by gamma-ray techniques have been made in the USA, in Canada, Norway, Finland, the USSR and Sweden (see, for example, WMO, 1979), and an impulse radar system has been successfully applied by Ulriksen (1982) in Sweden and Norway.

These techniques can be operated from airplanes at low elevation (gamma technique) or from helicopters (impulsive radar) and are therefore very expensive. On the other hand, they provide snow water equivalents more or less continuously along the flight lines and are therefore producing a wealth of data, as compared to conventional snowcourses.

In the future we can expect that weather-radar systems will be more generally available, which will provide hydrologists with direct areal precipitation information. Problems remain, like the bright-band effect of melting snowflakes and the penetration of the radar-beam through low clouds, but a wise combination of ground-information and the radar image may give us the opportunity to model areal snow accumulation in a better way than with the small point measurements of today.

The new sources of basin-wide snow-data provide us with more detailed information about the basin snowpack than is possible from point climate observations. If these data are to be used to update conceptual models, they have to be developed in a more distributed way while re-

maining simple enough to accept the rather incomplete data coverage that is generally available throughout the year. This balance between complexity and areal distribution on one hand and simplicity and limited data demand on the other will always be important and requires both field experience and a feeling for physical realities.

THE NEED FOR COST-BENEFIT ANALYSES

The introduction of new sources of areal snow data is often connected with relatively high costs both for development of new routines and for operation. It is therefore of great importance that their cost-effectiveness is investigated along with their potential for improved forecasts.

The cost-benefit analysis has to show favourable figures in comparison with existing, less expensive methods before we can expect that the new techniques will be fully accepted. This is a difficult task considering the very low costs (in Sweden in the order of \$ 500/forecast) for a forecast based on a conventional conceptual model and an existing national climatological network. As a matter of fact, the Swedish programme for gamma-ray measurements in the Kultsjön basin (Bergström and Brandt, 1985) has now been terminated because the cost for this technique did not justify the relatively small and sometimes inconsistent improvements that were obtained when using the technique to update a conventional conceptual model used in the area.

Gaining confidence in the use of new techniques finally means that they have to be verified in a forecasting mode where all possible conventional updating has been made, rather than in a simulation mode, where large volume errors in spring, for example, may remain due to poor simulation of the beginning of the accumulation phase in fall.

CONCLUSIONS

There is little doubt about the benefits of research in the field of snowmelt-runoff simulation in a society that is more and more

trying to control its water resources. Important areas are reservoir operation for water supply, power production, flood control, navigation and recreation, but simulation models are also important tools for design studies.

The development of conceptual snowmelt-runoff simulation models now seems to have reached a point, where further development is hindered by lack of knowledge about the areal variability of the climatological variables and of the snowpack itself. New techniques are under way, and this will demand models, which have a more realistic areal distribution than present lumped or semi-lumped models. These models must represent a balance between sophistication and simplicity, as they will have to be run on the conventional climatological network during periods when basin-wide snow data are not available.

One basic research need is associated with the areal variability of climatological variables within a basin. It is, for example, necessary to avoid crude constant lapse rates of air temperature and precipitation, if a more advanced energy and mass balance is to be computed at various elevations. Due to the complexity of basin-wide snow conditions, it may be fruitful to introduce a statistical approach into the computations, in particular above the timber line. One important task is then to find the optimum combination of snowmelt equations for a point and the proper statistical distribution of the snowpack.

Another basic research need is better understanding of the processes associated with losses from the snowpack and adjacent ground during the snow season.

The future use of satellite-based sensors, which are capable of informing about the basin snow water equivalent directly, might very well become a breakthrough for remote sensing in snow simulation. The research field is on the technical side, but hydrologists will have to provide adequate ground truth for the verification of this new technique and will also be responsible for the development of proper models.

The introduction of the new databases and models requires careful cost-benefit analyses based on verified forecasting results instead of just simulations.

ACKNOWLEDGEMENTS

The paper summarizes experience from both research and operational applications of conceptual snowmelt models at SMHI. Financial support from the Swedish Association of River Regulation Enterprises is greatly acknowledged.

LITERATURE CITED

- Anderson, E.A., 1973. National Weather Service River Forecast System - Snow Accumulation and Ablation Model. NOAA Technical Memorandum NWS HYDRO-17, Silver Spring, M.D.
- Anderson, E.A., 1976. A Point Energy and Mass Balance Model of a Snow Cover. NOAA Technical Report NWS 19, Silver Spring, M.D.
- Barton, M., and Crook, A.G., 1980. Operational Experiences with the SNOTEL System. ASCE Annual Convention, Hollywood-by-the-Sea, Florida.
- Bengtsson, L., 1980. Evaporation from a Snow Cover. *Nordic Hydrology* 11:221 - 234.
- Bergström, S., 1976. Development and Application of a Conceptual Runoff Model for Scandinavian Catchments. Swedish Meteorological and Hydrological Institute, RHO 7, Norrköping, Sweden.
- Bergström, S., and Brandt, M., 1984. Snömätning med flygburen gammaspektrometer i Kultsjöns avrinningsområde. Swedish Meteorological and Hydrological Institute, HO 21, Norrköping, Sweden.
- Bergström, S., and Brandt, M., 1985. Measurement of Areal Water Equivalent of Snow by Natural Gamma Radiation - Experiences from Northern Sweden. *Hydrological Sciences Journal*, No.4, December.
- Braun, L.N., 1985. Simulation of Snowmelt-Runoff in Lowland and Lower Alpine Regions of Switzerland. *Züricher Geographische Schriften*, Heft 21, Zürich.
- Charbonneau, R., Fortin, J.P., Morin, G., 1977. The CEQUEAU Model: Description and Examples of its Use in Problems Related to Water Resources Management. *Hydrological Sciences Bulletin*, IAHS, 22(1).

- Danish Hydraulic Institute, 1985. A Hydrological Modelling System for Operational Use of Satellite Snowcover Observations. Internal Report, Hørsholm, Denmark.
- Killingtveit, Å., and Aam, S., 1978. En fordelt modell for snöackumulering og -avsmelting. EFI-Institutt for Vassbygging, NTH, Trondheim, Norway.
- Konovalov, V.G., 1979. Calculation and Forecast of Glacier Melt in Middle Asia. (In Russian.) Gidrometeoroidat, Leningrad, USSR.
- Kuusisto, E., 1978. Optimal Complexity of a Point Snowmelt Model. Proceedings: Modelling of Snow Cover Runoff, Hanover, New Hampshire. U.S. Army, CRRL.
- Kuz'min, P.P., 1972. Melting of Snow Cover. U.S. Department of Commerce, National Technical Information Service. Translated from Russian by the Israel Program for Scientific Translations, Jerusalem.
- Leavesley, G.H., and Striffler, W.D., 1978. A Mountain Watershed Simulation Model. Proceedings of Meeting/Workshop on Modelling of Snow Cover Runoff, Hanover, New Hampshire, U.S. Army, CRREL.
- Lundquist, D., 1981. Snömodellstudier i Dyrdaalen. Norwegian Hydrological Committee, Internal Report No. 5, Oslo, Norway.
- Morris, E.M., 1980. Forecasting Flood Flows in Grassy and Forested Basins Using a Deterministic Distributed Mathematical Model. Proceedings of the Oxford Symposium on Hydrological Forecasting, April, 1980. IAHS-AISH Publ. No. 129.
- Morris, E.M., 1985. Snow and Ice. In: Hydrological Forecasting, edited by Anderson, M.G., and Bart, T.P. John Wiley and Sons, Chichester.
- Nielsen, S.D., and Hansen, E., 1973. Numerical Simulation of the Rainfall-Runoff Process on a Daily Basin. Nordic Hydrology, Vol. 4, No. 3.
- Quick, M.C., and Pipes, A., 1972. Daily and Seasonal Runoff Forecasting with a Water Budget Model. UNESCO/WMO, International Symposium on the Role of Snow and Ice in Hydrology, Measurement and Forecasting. Banff.
- Rango, A., 1985. Assessment of Remote Sensing Input to Hydrologic Models. Water Resources Bulletin, Vol. 21, No. 3.
- Rango, A., and Martinec, J., 1979. Application of a Snowmelt-Runoff Model Using Landsat Data. Nordic Hydrology, Vol. 10, No.4.
- Turčan, J., 1981. Empirical-Regressive Forecasting Runoff Model. Proceedings of Conference VUVH, Bratislava, 1981.
- Sugawara, M., Ozaki, E., Watanabe, I., and Katsuyama, Y., 1974. TANK-Model and its Application to Bird Creek, Wollenski Brook, Bihin River, Kitsu River, Sanaga River and Nam Mune. Research Notes of the National Center for Disaster Prevention, No. 11, Tokyo.
- Ulriksen, C.P.F., 1982. Application of Impulse Radar to Civil Engineering. Doctoral Thesis, Lund University of Technology, Department of Engineering Geology, Lund, Sweden.
- U.S. Corps of Engineers, 1956. Snow Hydrology. North Pacific Division, Portland.
- U.S. Corps of Engineers, 1960. Runoff from Snowmelt. EM 1110-2-1406, Washington, D.C.
- U.S. Corps of Engineers, 1972. Program Description and Users Manual for SSARR Model. U.S. Army Engineering Division, North Pacific, Portland.
- Vehviläinen, B., 1985. Snömodellering och prognoser - Finska erfarenheter. Vatten i Norden No. 4, 1985.
- WMO, 1979. Workshop on Remote Sensing of Snow and Soil Moisture by Nuclear Techniques. Technical papers presented at the workshop convened by WMO and organized in cooperation with IAHS and Norwegian National Committee for Hydrology, Voss, Norway.
- WMO, 1986. Intercomparison of Conceptual Models of Snowmelt Runoff. Operational Hydrology Report No. 23, Genève. (In press.)

GLACIER HYDROLOGY

THE ROLE OF GLACIERIZED BASINS IN ALASKAN HYDROLOGY

C. Benson, W. Harrison, J. Gosink, S. Bowling, L. Mayo and D. Trabant¹

ABSTRACT: This paper summarizes the results and recommendations of the International Workshop on Alaskan Hydrology: Problems Related to Glacierized Basins, held in Eagle River, Alaska, during April, 1985. Hydrology in Alaska is strongly influenced by problems associated with snow, ice and permafrost which will become increasingly important as economic development proceeds. The Scandinavian countries, Switzerland and Canada have preceded Alaska in developing hydrological resources that depend on glaciers for their sources, and Alaskans can learn from their experience. The international workshop sought to capitalize on this expertise and experience from abroad, and to help bridge the communication gap between scientific and engineering/management groups by having both groups participate. The subjects considered were: runoff from glacierized basins, sediments in glacial streams, hazards associated with glaciers, ice problems on rivers and reservoirs, and selected aspects of permafrost hydrology in glacierized basins. Two days of the workshop were devoted to presentations by the participants, followed by intensive meetings of five subgroups. This paper contains the conclusions and recommendations of the subgroups. (KEY TERMS: hydrology, glaciers, sediments, river ice, glaciological hazards, permafrost.)

INTRODUCTION

This paper summarizes the results and recommendations of an international workshop on Alaskan Hydrology: Problems Related to Glacierized Basins. The workshop was held in Eagle River, Alaska, from 8-12 April 1985. It was sponsored by: The U.S. National Science Foundation (Grant DPP84-17549), the Governor of Alaska, the Division of Geological and Geophysical Surveys (DGGs) of the Alaska Department of Natural Resources, the Alaska Power Authority, the U.S. Army Cold Regions Research and Engineering Laboratory (CRREL), the Geophysical Institute of the University of Alaska, and the Vice Chancellor for Research and Advanced Study, University of Alaska,

Fairbanks. It was attended by 49 people: 13 from Scandinavia and Europe, 5 from Canada, 9 from the U.S. and 22 from Alaska.

Hydrology in Alaska is strongly influenced by a broad range of problems associated with snow, ice and permafrost. Since relatively little economic development has occurred in Alaska, few of these problems have been faced by hydrologists, managers and planners. It is timely to address these problems now, because Alaska is on the verge of developing hydrological resources that depend on glaciers for their sources. Norway, Switzerland, Iceland, Canada and Greenland (Denmark) have preceded Alaska in these ventures and Alaskans can learn from their experiences. There is also a need for glaciological and ice management information, which is primarily in the scientific and basic engineering literature, to be made more available to planners, managers and engineers.

The workshop was motivated by such problems. Its intent was to capitalize on expertise and experience from abroad, and to help bridge the communication gap between scientific and engineering/management groups by the participation of both groups. We hope that this will help us in Alaska to utilize our vast, glacier-derived water resources more effectively and to mitigate the associated hazards.

The first two days were devoted to presentations by the participants; summaries of these presentations are included as an appendix to the report on the workshop (Benson et al., 1986). The remainder of the week was devoted to intensive meetings of five subgroups, identified in the next section, except for half a day spent on a chartered flight over heavily glacierized regions of south central Alaska. Plenary sessions were held each day to communicate progress of the subgroups to all participants. The status reports of the subgroups comprise five chapters of the final report on the workshop. Each chapter contains a set of recommendations and an extensive bibliography.

¹C. Benson, W. Harrison, J. Gosink and S. Bowling, Geophysical Institute, University of Alaska-Fairbanks, Fairbanks, Alaska 99775-0800; L. Mayo and D. Trabant, U.S. Geological Survey, Cold Regions Hydrology Project Office, Fairbanks, Alaska 99701.

It is useful to begin with some general introductory comments on the five selected facets of Alaska's snow, ice and permafrost problems which were treated in the workshop.

The Alaska-Yukon Glaciers

For brevity, the glaciers of Alaska and adjacent Canada (i.e., Yukon Territory and British Columbia) will be referred to as Alaska-Yukon glaciers. These glaciers cover an area of about 102,000 km², three quarters of which is in Alaska. For perspective, twelve states in the U.S. have smaller areas than this.

About 80% of the fresh water on Earth is in the form of glacier ice. Most of this ice, by far, is contained in the Antarctic (1.3 x 10⁷ km²) and Greenland (1.7 x 10⁶ km²) ice sheets which are remote from large human populations. The third and fourth largest ice masses (10⁵ km² each) are the Queen Elizabeth Islands, of the Canadian high arctic, and the Alaska-Yukon glaciers. Either of the latter systems of glaciers covers more than twice the glacierized area of the Himalaya and Karakorum ranges combined.

The Alaska-Yukon glaciers are significantly different from the other large ice masses for several reasons. They lie in a region of dynamic and ever-increasing human activity. The mass flux of these glaciers is among the highest in the world, and many of them are composed primarily of temperate ice (0°C throughout). In contrast to this, the Queen Elizabeth Islands are nearly as remote as the large ice sheets and their glaciers are polar, i.e., ice temperatures are well below 0°C. The Alaska-Yukon glaciers are also located in an exceptionally dynamic physical setting. They are far more active than polar glaciers because many of them form a part of a major climatic barrier on the rim of the North Pacific and receive extraordinarily heavy precipitation from the Gulf of Alaska, one of the two most vigorous storm centers in the Northern Hemisphere (the other one being in the North Atlantic). The climate of North America may be significantly affected by processes of storm and air mass modification which occur at this glacierized border of the North Pacific. Also, the oceanographic effects of copious meltwater runoff along the southern Alaska coast are being increasingly appreciated.

In spite of the exceptional features of the Alaska-Yukon system of glaciers, they still must be considered largely unexplored:

"There have been few attempts to discuss the glaciers of Alaska and adjoining parts of Canada on a regional basis. Most accounts tend to deal with single glaciers or groups of glaciers in relatively small areas; even general descriptions of the ice cover of individual mountain ranges are lacking." (Field, 1975, p. 3)

Given a random glacier in this system, the chances are that very little is known about its most basic properties: mass balance (both ice and water balances), the energy balance, recent changes in volume, mode of flow, facies and temperature distributions, sediment production, and so forth. Although we do not know a great deal about most of these glaciers, we do know that they include vastly different types. For example, in the coastal regions of Alaska the glaciers may receive 10 m or more of snow and are temperate, while in the Brooks Range they receive less than a meter of snow and the temperature of most of the ice volume is below 0°C. Therefore, within the system we have glaciers with completely different hydrologic, ice-flow, and sediment regimes.

Glaciers and Hydroelectric Energy

It has become abundantly clear in the last decade that Alaska will ultimately experience massive economic development. This means that resource management will become even more critical in the years ahead. Although most attention so far has been given to the petroleum industry, it is clear that there is a vast hydroelectric potential. Most prominent is the proposal to dam the Susitna River at a cost in excess of 5 billion dollars. On the average, Alaska-Yukon glaciers and high-altitude, snow-covered regions supply roughly a third of the total runoff, and exert a significant control on the flow and water quality of all major Alaskan rivers except the Colville. The value of knowledge about the hydrology of glacierized basins is increasingly being appreciated by engineers and planners involved with hydroelectric projects; yet in spite of the need for this basic knowledge, it does not exist today. By misjudging the contributions to long-term runoff from glaciers, one can make costly errors (Bezing, 1979).

Alaska's Seasonal Snow

Snow forms a thin veneer on the earth's surface over most of Alaska for 1/2 to 3/4 of the year. The Alaskan snow differs from the hydrologically important mountainous snow of the western United States in that its temperatures are lower, steeper temperature gradients occur in it, and it lasts longer and enters more directly into human activity as snow itself, rather than serving primarily as a cold storage water reservoir.

Although Alaska is famous for its glaciers, it is especially well suited for the study of seasonal snow cover. Indeed, Alaska's glaciers, extensive as they are, cover only 5% of the total area—all of which is subjected to seasonal snow. Alaska has three distinct types of snow because it contains maritime, extreme continental, and Arctic climatic zones in proximity. Striking differences exist in the snow cover from one climatic zone to the next. Our knowledge of the amount of snowfall at high

altitudes and on the Arctic Slope, and of the flux of wind-blown snow needs considerable refinement.

THE EFFECTS OF GLACIERS ON RUNOFF AND RUNOFF FORECASTING

Alaska's River and Reservoir Ice

The site of virtually all water resource development projects in Alaska will be along the rivers. These projects will be subjected to severe ice problems for substantial portions of the year. Ice jams on the rivers can result in flooding, severe erosion, and destructive ice forces. The construction of a reservoir can alter the natural river regime adversely both thermodynamically and in terms of water quality, and these problems are exacerbated by the presence of ice for long periods of the year. It is critical that the limitations to our knowledge of river and reservoir ice processes, the state-of-the-art of current research, and the capability for predicting the ice problems be delineated. For example, little is known about winter stage-discharge relationships of Alaskan rivers. The patterns of recurring ice jams have never been compiled for any Alaskan rivers. No well-developed models exist for the prediction of erosion and scour in braided or ice-covered streams. Research models of aulfs growth have been devised from laboratory studies, but field verification has not taken place. These are only a few of the examples of the need for continued study of river and reservoir ice in Alaska.

It is clear that a knowledge of the available theory, practice and technology for the avoidance or mitigation of river ice problems is essential for water resource planners, engineers and managers in Alaska in order to prevent costly, inappropriate and possibly dangerous development and construction.

Alaska's Permafrost

Both seasonally and perennially frozen ground (permafrost) give rise to scientific and engineering problems of great importance to Alaska. About 80% of Alaska is underlain by permafrost, of which 25% is continuous; all of Alaska is subjected to seasonal freezing. Only selected aspects, pertinent to glacierized basins in permafrost regions, were considered in the workshop. These topics dealt mainly with the effects of permafrost on subsurface drainage and runoff. Implicit in this concern is the dearth of knowledge and the lack of a well-defined theory describing moisture migration in freezing and thawing soils. While empirical models of the geotechnical aspects of permafrost (such as frost heaving) exist, considerably less is known regarding basic transport phenomena in a freezing soil.

A "glaciated" basin is one which shows evidence of having had glaciers present in it in the past while a "glacierized" basin has glaciers in it now. Glacierized basins tend to have less variability in runoff than do non-glacierized basins on a short-term, year-to-year basis. However, on longer time scales of 30 to 100 years, changes in the mass balance of glaciers can significantly modify runoff from glacierized basins as the amount of ice in storage changes.

The lag between precipitation and runoff is measured in hours, days or possibly weeks where no snow cover is present. With a seasonal snow cover, precipitation may accumulate over several months before it melts and appears as runoff. In a glacierized basin, precipitation falling as snow above the equilibrium line on a glacier may not appear as runoff for years, decades or even centuries. Runoff from a glacier may be almost independent of recent precipitation. Situations even exist where negative correlations exist between precipitation and runoff. For example, heavy winter snowfall may delay the exposure of relatively low-albedo glacier ice, and thus reduce the total amount of runoff the following season. Precipitation during the ablation season is normally associated with cloudy conditions, which again may reduce ablation. On the other hand, during hot sunny weather, when non-glacier sources of runoff tend to dry up, glacier melting accelerates. Thus, runoff from the glaciers themselves is likely to be greatest when runoff from the rest of the basin is least, and vice versa.

If glaciers never changed their sizes, their existence would have no major effect on long-term changes in runoff. In the real world, glacier volumes do change, due to both climatic factors and internal instabilities. Records show that considerable glacier variations have occurred in the past, and it is only prudent to expect similar variations in the future. As a non-tidewater glacier shrinks, the ice lost to the glacier appears as runoff over and above that due to recent precipitation. As it grows, some of the annual precipitation enters into long-term storage as glacier ice rather than appearing as runoff that year.

Although U.S. hydropower development has taken place in areas with heavy seasonal snow packs, few projects have been in glacierized basins. Also, the glacierized basins in the conterminous U.S. lie in the Pacific Northwest where the climate has a winter precipitation peak and a relatively long ablation period. By contrast, the mainland of Alaska has a summer precipitation peak and a relatively brief ablation period. This means that a different approach to runoff modelling may be required for Alaska.

Estimates of glacier depletion and its effects on runoff have been given for Switzerland (Kasser, 1973), Scandinavia (Østrem, 1973) and Canada (Young and Ommanney, 1984). The rate of wastage of glaciers varies from region to region (e.g., major

losses of glacier volume in the Eastern Alps and only minor losses in the Western Alps) and during the course of time (e.g., glaciers can re-advance after many years of wastage).

Over the past hundred years, glaciers in Alaska and around the world have suffered an overall loss of mass (Meier, 1984). This means that glaciers, as natural reservoirs, have been generally depleted, so less water will be available for the future. Meier also concluded that the loss of water from glaciers in Alaska during this century may have been greater than the world average. Water has been withdrawn from glacier storage and added to annual streamflow in varying amounts. Thus streamflow records obtained during the last few decades include this added component but do not specifically identify it. In planning projects which may have lifetimes of decades to a century or more, information is needed on the extent to which glacier variations or stabilization may affect future water availability and quality.

A summary of the recommendations follows:

ONE

MAINTAIN AND EXPAND UPON CURRENT DATA COLLECTION EFFORTS

Understanding of fundamental processes on both long and short time scales is very important, and dependent on the existence of an adequate data base. Therefore, steps should be taken to address this need by ensuring continuity of data collection. In particular, the existing data collection efforts at Gulkana and Wolverine glaciers should be continued, and new stations should be initiated in several other major climatic divisions of Alaska. Key areas to be added are southeastern Alaska, where Lemon Creek Glacier is a possible choice, the Brooks Range, where some data exist on McCall Glacier, and at least one glacierized basin near the west coast of Alaska. Companies or agencies operating power projects should be required to continue gathering hydrological, meteorological and glaciological data within project areas after a project is operational.

TWO

DEVELOP THE CAPABILITY OF FORECASTING RUNOFF

Models developed for other areas should be investigated for their applicability to Alaskan conditions. It is anticipated that in most cases problems will arise from the lack of necessary input data rather than from inadequate or inapplicable theory, and that the results of this investigation will therefore feed back into the priorities of the data collection program recommended above. One area in which local research will be necessary is the release of water from englacial (or glacially-dammed) storage.

THREE

DEVELOP NEW MEASUREMENT TECHNIQUES WHERE EXISTING TECHNIQUES ARE INADEQUATE FOR THE ATTAINMENT OF OBJECTIVE (1) ABOVE

At the present time, no good methods exist for measuring winter precipitation with good time resolution in the coastal mountains of Alaska, or winter discharges while there are substantial amounts of ice in streams. Improvements are needed in the continuous monitoring of snow and firm temperatures and the telemetry of hourly or daily meteorological, hydrological and glaciological conditions. Reliable telemetered data are likely to be of great importance to the application of forecasting techniques for glacially-mediated flood events.

FOUR

ASCERTAIN REGIONAL MASS BALANCE PATTERNS FOR THE MAJOR GLACIER SYSTEMS OF ALASKA

This goal probably cannot be achieved even with the long-term data collection stations recommended in ONE. Short-term studies in other basins, lasting several years, are probably needed to provide the basis for interpolation between the long-term stations.

FIVE

ANALYZE THE EXISTING CLIMATE/GLACIER VOLUME RECORD

Comparison of old aerial photos of Alaskan glaciers with new ones permits volume change to be estimated. Comparison with climatic records from existing low-lying climate stations could greatly improve our understanding of the variability of glacier response to climate over the state.

NATURAL HAZARDS CAUSED BY GLACIERS

As high-altitude storage reservoirs in the hydrological cycle, glaciers contain enormous potential energy. Relatively small amounts of this energy can be released in ways which produce major hazards. Once released, the potential energy is restored by climate so the hazards are usually recurring events. Even though the existence of these hazards can often be foreseen, they generally cannot be predicted accurately.

A "hazard" is an event that is potentially dangerous. A "risk" arises when people place structures in a position where a hazard creates a threat to life and property. The study of hazards is a matter of science; the study of risks involves science, economics, engineering, human aspirations, and politics.

The primary hazards associated with glaciers are from floods, landslides, avalanches and icebergs. Glaciers store water on top, within, beneath

and beside them; the most obvious cases are glacier-dammed lakes. Post and Mayo (1971) identified about 750 Alaskan glacier-dammed lakes and their flood paths. When a glacier water reservoir discharges it produces an outburst flood for which the Icelandic term Jökulhlaup has become widely used. Jökulhlaups involve large discharges for several days and they are often highly charged with snow, ice and rock. The retreat of a glacier may leave unstable slopes of debris which had been supported by glacier ice; this magnifies the potential hazards from landslides which may be triggered by large earthquakes (Miller, 1960). Some attention has been paid to hazards from snow avalanches in Alaska but very little attention has been given to potential ice avalanches from glaciers, yet these have caused loss of life and damage to property in Switzerland.

Alaska has 90% of the explosive volcanoes in the United States. Large amounts of water, snow and ice are mobilized rapidly during an eruption. But it is important to recognize that the effects of volcanism on glaciers are not limited to spectacular eruptions. Variable volcanic heat flux produces basal meltwater at high altitudes which interacts with the volcano in ways which are potentially hazardous but not well understood. Glaciers may take decades to recover from perturbations produced by eruptions, and the recovery process itself may create secondary hazards (Sturm, Benson and MacKeith, 1986). There is much for Alaskans to learn from case histories in other parts of the world, especially from the Andes, from Iceland and from Kamchatka (USSR).

In most areas of Earth, natural hazard research comes as a consequence of direct threat or damage to established economic improvements already at risk. This provides only an emergency response where the damages are very much more costly than the research. In Alaska, the reverse situation exists in most cases. Studies can be used to direct development away from known dangerous situations and thus avoid the hazards without having to endure the risks and costly damages. The economic and political justifications for the Alaska case require considerable insight, but the rewards for this are not small.

A summary of the recommendations follows:

ONE

PUBLISH ATLASES OF ALASKAN GLACIER HAZARDS

Most types of glacier hazards are known to occur in Alaska. Statewide assessments showing the distribution of surging glaciers and outburst flooding have been published, but require periodic updating to report new knowledge and changing natural situations. No statewide atlases have been published for other hazards. Special problems are associated with Alaska's many glacier-covered volcanoes, most of which are explosive. Our recommendation for attention to glacier-covered volcanoes

dovetails well with Resolution No. 7, on explosive volcanism, of the national workshop on Seismic, Volcanic and Tsunami Hazards in Alaska (Davies, 1983). Projects to produce these atlases should be organized and funded.

An advisory group should be assigned to steer individual research efforts along fruitful lines and ensure that the efforts of many individual projects over many years would produce a coherent set of published products that would be of direct benefit to the users.

TWO

CONDUCT MODEST RESEARCH IN THE NEAR FUTURE, TO ENSURE THAT THE KNOWLEDGE TO ATTACK EMERGENCY PROBLEMS WILL BE AVAILABLE WHEN NEEDED

Research sites should be selected from the hazard atlases to conduct priority research on those glaciological processes which, once understood, could provide predictive methods. During this work, a series of selected research individuals would evolve. To be available immediately, and most effectively, they should be resident in Alaska. These scientists would be knowledgeable about the hazards and equipped to work on emergency situations should they occur.

THREE

CREATE EMERGENCY TRAVEL FUNDS TO BE AVAILABLE FOR SELECTED SCIENTISTS TO STUDY HAZARDOUS PROCESSES AS THEY ARE DEVELOPING

The Alaska Council of Science and Technology, when it existed, considered carefully the problem of geologic hazards, including glacier hazards. One outstanding suggestion was that mission-ready scientists be listed for contact when a short-term hazardous situation is suspected. Any member of the team would be capable of charging transportation and subsistence cost for a short time to an account established in the State of Alaska government for the purpose of emergency scientific investigations of short-term phenomena, especially when the evidence of what is occurring would be otherwise lost. This list of investigators and a modest supporting fund should be established.

FOUR

INTEGRATE GLACIER HAZARD INFORMATION INTO LAND-USE PLANNING

An authority should be made responsible to bring general knowledge gained from geologic and hydrologic hazard and risk assessment research into the public planning process. The U.S. Army Corps of Engineers and other agencies have limited authority. The broader Authority will need a professional advisory group established (possibly the same group as recommended above) to work with them on reviewing required studies and setting priorities. The Authority would prepare overviews for making deci-

sions based on risk assessments, planning defenses from natural events, and keeping legislators and the public informed about the benefits to them of this research.

FIVE

DEVELOP CONTINUOUSLY TELEMETERING RIVER STAGE GAGES THAT OPERATE IN WINTER IN ALASKA BELOW HAZARDOUS GLACIER DAMMED LAKES AND VOLCANOES

Techniques for the operation of flood warning gages from glaciers during the long winters in Alaska do not exist. Such gages could also provide important new information about the normal winter flow regime of rivers at standard river gage sites.

GLACIERS AND SEDIMENT

The sediment transported by Alaskan rivers poses problems for hydropower or other engineering developments, but is also a valuable resource both as a construction material and as an intrinsic part of the river environment, affecting hydrology and biological activity. Sediment in glacier and non-glacier rivers is quite different, in quantity, variability, size distribution and mineralogy. This distinction is obviously important in Alaska where glaciers contribute to all the major rivers except the Colville, glacier surges are common, the bedrock is often friable and shattered, and there are important glacier-volcano interactions.

The present understanding of the sediment regimes of Alaskan rivers is unsatisfactory. The existing measurements (for example, U.S. Geological Survey, 1950-60a, 1950-60b, 1961-84; Harrold and Burrows, 1983; Neill et al., 1984; R & M, 1982; Lipscomb and Knott, 1985) are almost entirely well downstream from the glacier sources; their relation to the sources and to the transport processes in the intervening stretches of river is unknown. Reconnaissance measurements at a few glacier termini have been made (Gaddis, 1974) but the magnitude of the glacier sources remains virtually unknown. Measurements at the terminus of Variegated Glacier, Alaska (Humphrey, 1986; Humphrey et al., 1986) indicate an important connection between sediment supply and hydraulics and motion of the glacier, under both surge and non-surge conditions. The suspended sediment alone during the 1982-3 surge of the glacier was equivalent to about 1/2 m of rock erosion under the glacier.

It appears that a place as large and sparsely populated as Alaska stands to benefit from an understanding of sediment processes on a fairly basic level, because of the near impossibility of evaluating every possible development in detail. As a start one needs to know, at least approximately, the magnitude of the glacier input sources. This in turn would be facilitated by an understanding of the basic processes of sediment generation, storage, and transport within glaciers. Little is known of these processes yet, but they are closely linked to

problems of glacier motion and internal hydrology. If these are studied simultaneously with sediment production at the terminus, a deeper and probably more useful picture of the glacier sediment source will result.

Even if the glacier and other source problems were completely understood, we would not understand the sediment regimes of the rivers without an understanding of the downstream transport processes. Efforts by glaciologists to understand the source mechanisms and those by others to understand sediment dynamics in rivers therefore need to be coordinated. The observation of sediments produced by the surge of Variegated Glacier is an Alaskan example of how glaciologists can contribute, but there is need for similar measurements to be made at a glacier located on a major river, and for these to be related to sediment transport and channel changes downstream.

Generally, very intensive data collection is required to define sediment-transport characteristics adequately, especially where high variability exists. This is certainly true of glacierized basins, where there is ample evidence that the glacier sources are extremely variable (Østrem et al., 1967, for example). Whether carried out at glacier terminus or downstream, sampling frequency should always be intensive at the beginning of study, and adjusted only after some idea of the variability is obtained. Gurnell (1982) has reviewed the design of glacier sediment sampling programs and investigated the implications of spatial and temporal variations in suspended sediment and stream discharge in the design of sampling programs. The sediment studies carried out at glacier termini by the Norwegian Water Resources and Electricity Board could possibly serve as models (Roland and Haakensen, 1985). Daily, including sometimes hourly, sampling for an entire year would greatly increase our knowledge of variability of suspended sediment in Alaskan rivers. As well as long-term studies to evaluate annual variation, high frequency sampling of flow events provides better understanding of the mechanics of transport, especially as pertains to bedload. Synoptic, accurate measurements of hydraulics and channel geometry with suspended sediment and bedload sampling are essential to further our understanding of the dynamics of sediment movement in natural rivers.

Measurement of channel geometry, for which aerial photography is a useful method, and determination of the composition of bed material over long periods of time provide a great deal of information on how rivers change. Simply resurveying a few cross-sections and evaluating the size distribution of bed materials in the channel only once a year for ten years may provide the necessary information to tell whether a river reach is aggrading, continually moving laterally in one direction, or that the bed material is becoming coarser or finer over the long term. This, combined with discharge records alone helps predict future changes. Ideally, sediment data would also be collected.

An excellent candidate for a fairly intensive study of glacier sediment source would be Phelan Creek below Gulkana Glacier. Mass balance studies began in 1960 (Meier et al., 1971; Tangborn et al., 1977); stream flow records exist from 1966 to 1978, and from 1983 to present; some sediment data were collected at the Phelan Creek gage in 1973 (Gaddis, 1974); and this basin is tributary to the Delta River which flows into the Tanana River, where there is fairly long-term suspended sediment data downstream. Probably the best candidate for an intensive study below a glacier with the immediate potential to surge would be the short creek between Black Rapids Glacier and the Delta River. This study would also benefit from downstream sediment data on the Tanana River, and there is considerable unpublished glacier data from Black Rapids Glacier from ongoing U.S. Geological Survey and University of Alaska studies which include daily motion. Other promising sites would be Wolverine Creek below Wolverine Glacier, which has long-term glacier balance (Meier et al., 1971; Tangborn et al., 1977; Mayo et al., 1985) and stream flow data but no downstream sediment information, or one of the tributary basins of the Susitna, where stream flow, sediment and some glacier data are available (Knott and Lipscomb, 1983; Lipscomb and Knott, 1985; Harrison et al., 1983; Clarke et al., 1985; Clarke, 1986). It is likely that much could be learned by comparing the sediment production of different glaciers with different sizes in different settings, and with different flow regimes (surge and non-surge, for example).

A summary of the recommendations follows:

ONE

DEVELOP AN UNDERSTANDING OF BASIC PROCESSES AS A LONG-TERM GOAL

This long-term goal is particularly appropriate for Alaska because of the near impossibility of studying every situation in detail, and because of the limitations of statistical methods.

TWO

INITIATE SEDIMENT STUDIES NEAR THE TERMINI OF REPRESENTATIVE GLACIERS, AND RELATE THEM TO DOWNSTREAM SEDIMENT TRANSPORT STUDIES

One of these glaciers should be likely to surge, and be located on a major river. The long-term purpose of the measurements should be to define the magnitude and character of glacier sediment sources in Alaska.

THREE

RELATE SEDIMENT STUDIES AT GLACIER TERMINI TO STUDIES OF THE DYNAMICS, HYDROLOGY AND HYDRAULICS OF THE GLACIER ITSELF

The measurements at glacier termini would therefore be related to internal glacier processes and motion, and, as TWO implies, to downstream transport processes.

FOUR

INITIATE STUDIES RELATED TO SPECIFIC PROPOSED DEVELOPMENTS WELL IN ADVANCE OF NEED

This is necessary because of the high variability of sediment supply and transport.

FIVE

IMPROVE AUTOMATIC SAMPLING TECHNIQUES

This is particularly important for Alaska because of difficulty and expense of field operations.

ICE PROBLEMS ASSOCIATED WITH RIVERS AND RESERVOIRS

Water resource development in Alaska involves special problems because of the presence of ice for long periods of the year on rivers, lakes, ponds and reservoirs. The important physical phenomena associated with ice on rivers and reservoirs include: frazil ice, aufeis, anchor ice, sheet ice and the mechanical, thermal and chemical effects that these ice forms have on water bodies and the surrounding basin.

Frazil ice, which forms when water temperature supercools by a few hundredths of a degree below 0.0°C, are initially observed as discs in the range from 0.1 to 5 mm in diameter. These discs agglomerate into frazil flocs and pans when river turbulence is low. Frazil pans can exceed 1 or 2 m in diameter in small rivers like the Tanana River; in the Yukon River, the pans often exceed 10 m.

Frazil ice is known to deposit on the underside of an ice cover where the river bottom slope decreases substantially. Thus, frazil ice may accumulate in a "hanging dam" at the entrance to slow reaches in the river or in pools downstream from rapids or steeper reaches. These dams are a potential hazard causing winter flooding, overflows and associated aufeis formation. Aufeis (meaning ice on ice) formations develop when water flows over and freezes on surface ice or frigid ground. Subpermafrost groundwater and groundwater from thaw bulbs near streams are an additional source of water for aufeis (Kane, 1981). Aufeis formations approaching 10 m in thickness can be generated in this fashion (Sloan, Zenone and Mayo, 1976).

Anchor ice (ice anchored or fixed in position in the flow, as on the river bed) is generally

believed to be initiated by the attachment of frazil ice crystals to the river bed and to objects in the flow (Osterkamp and Gosink, 1983). In this manner, anchor ice can cover extensive sections of a river bed. The bonding between anchor ice and the river bed may be released if sufficient heat from radiation or groundwater is available; then the buoyant anchor ice will lift from the river bed, carrying with it sediment, gravel and on occasion, heavy rocks. This process causes an ice run which can cause severe damage to downstream hydraulic structures.

Break-up flooding is a major problem in Alaska which annually raises the prospect of loss of life and damage to property. Continued research into basic river ice dynamics, mitigation techniques and ice jam processes should eventually lower the risk of this flooding. For the present it is essential that the early warning system of the National Weather Service for break-up flooding be maintained, and if possible expanded.

Sheet ice forms on slowly-moving or quiescent water as a consequence of heat loss to the atmosphere. In this case the water turbulence is insufficient to draw the ice formed at the surface into suspension, so that ice growth propagates across the water surface rather than within the body of the water. Lakes and ponds may contain frazil ice, formed during windy conditions, and sheet ice, formed during calm periods, and snow ice, formed by the flooding of a snow layer. Consequently the morphological structure of the ice may be complex, resulting in complex thermal, mechanical and optical properties.

Most deep northern lakes can be classified as dimictic, characterized by strong stratification in the summer and stratification under the ice cover in winter. In spring, the melting ice becomes porous and weakened with vertical channels and assumes an appearance known as "candied ice." The stability of the water column is altered by short-wave penetration through the candied ice cover, and, at least in one instance, there is evidence to indicate that normal spring overturn was impeded by the stable thermal gradient, resulting in the potential for hypolimnetic oxygen depletion (La Ferriere, 1981). In glacierized basins, the turbidity of the water strongly affects short-wave radiative penetration as well as density structure. This also may have a significant effect on water temperature and quality.

Water resource development projects in cold climates and the subsequent effects on the ice conditions and the hydrological regime were considered in the workshop. A set of guidelines to define the relevant ice problems for engineers and managers, to assess the state-of-the-art for prediction or modeling, and to consider mitigation techniques presently used in northern climates, is presented in tabular form in the report on the workshop.

Recommendations

Several important documents have defined recommendations for research related to ice problems in rivers, lakes and ponds, and reservoirs. These include a National Academy of Science Report (National Research Council, 1983), and the results of a National Research Council Symposium in Canada (National Research Council Canada, 1979). These documents form a general framework for research needs related to ice. In addition to the recommendations of these documents, several other points particularly relevant to water resource development in Alaska were proposed at the workshop. The intent of these supplementary recommendations is to obtain the most cost-effective use of limited resources and, simultaneously, to assure that critical concerns, related to safety, environment and economic well-being, are not overlooked.

The recommendations particularly important for Alaska water resource development fall into two general categories: the first concerns the long-term state interests, and the second is related to site-specific investigations during the planning and feasibility stage of water resource projects.

A. Alaskan long-term interests.

Better use should be made of existing state and federal agencies and University of Alaska capabilities. Particular examples include the following:

ONE

MEASUREMENTS OF DISCHARGE AS WELL AS STAGE SHOULD BE RECORDED THROUGHOUT THE YEAR.

The U.S.G.S. presently records stage measurements at a number of sites throughout the year in Alaska, but determines stage-discharge relationships for the open water season only. For models of ice jam processes, break-up and winter flooding, it is essential that the additional measurements be made.

TWO

SUPPORT SHOULD BE PROVIDED FOR THE TRAINING OF GRADUATE STUDENTS IN ALL ASPECTS OF COLD REGION HYDROLOGY.

This is an extremely cost effective use of state resources both over the short and long term. These students will in time become scientists and engineers resident in Alaska with respect for Alaska's best interests, and well prepared for long-term water resource planning.

SOME OF THE DATA REQUIRED FOR THE CALIBRATION OF VARIOUS MODELS IS PRESENTLY COLLECTED BY A VARIETY OF STATE AND FEDERAL AGENCIES. THESE DATA SHOULD BE COMPILED AND ORGANIZED FOR BETTER ACCESSIBILITY.

Two examples include: the encoding of all U.S.G.S. data on floppy disc for easy and rapid access, and the determination of recurrent ice bridging locations on Alaskan rivers through aerial photographic surveys.

FOUR

THE NEED FOR LONG-TERM CONTINUOUS MONITORING OF SPECIFIC PHENOMENA SHOULD BE RECOGNIZED AS AN ESSENTIAL PART OF PLANNING AND DEVELOPMENT.

These measurements are required both for the basic formulation of models and for the determination of long term changes. Some specific examples include ice jam dynamics, erosion processes, permafrost degradation and frazil ice formation and growth mechanisms. These efforts should be directed toward the development of comprehensive river freeze-up and break-up models.

B. Site-specific research.

Planners, managers and engineers must be made aware that standards and models developed for temperate-zone water resource projects are often inadequate in cold climates, and furthermore, that the data needed for analysis of projects in Alaska are often not available. In addition, it is important to note that remedial techniques to remove specific ice problems may inadvertently create new problems.

ONE

AS A FIRST STEP, AN INVESTIGATION TO DETERMINE THE SCOPE OF THE MAJOR ICE PROCESSES AND PROBLEMS SHOULD BE UNDERTAKEN. THIS STUDY SHOULD HELP TO DEFINE THE APPROPRIATE LEVEL OF DETAILED MODELING REQUIRED AT THE SITE AND SPECIFY THE DATA NEEDED FOR THESE MODELS.

For example, high turbidity levels may indicate the need for a two-dimensional reservoir model rather than a more widely used one-dimensional model, or, the presence of heavy aufeis deposits may suggest the need for extensive topographic and ground water studies of the flood plain. It may also be necessary to devise new models to assess local critical concerns, for example, erosion in braided streams, ice formation in estuaries, frazil ice discharge and ice bridging processes.

ALTHOUGH DATA NEEDS DEPEND ON LOCAL CONDITIONS AND ON THE PARTICULAR WATER RESOURCE PROJECT, MODELING CAN BE USED TO HELP ESTABLISH THE EXTENT AND FREQUENCY OF THE REQUIRED DATA BY A PROCESS KNOWN AS "NUMERICAL EXPERIMENTATION".

With this process, a variety of field conditions and the associated ice problems can be tested for sensitivity. If a particular situation is found to produce critical conditions, then a clear mandate is set for further field investigations. For example, if a certain ice discharge produces consolidated and grounded ice jams with flooding at a given site, then more intense field work is needed to define ice bridging locations and frazil ice production rates. Alternatively, if reservoir temperatures are particularly sensitive to light-extinction coefficients, then further investigations of turbidity levels and erosion processes are clearly warranted. It is important that these eventualities be considered to make the most cost effective use of the resources available, and to eliminate costly remedial procedures.

THREE

THE BASIC DATA NEEDS FOR EXISTING RIVER AND RESERVOIR MODELS ARE:

i. Rivers

Discharge: (daily)
 Meteorology: air temperature, wind velocity, precipitation, relative humidity, cloud cover, short-wave and long-wave radiation (daily)
 Basin geometry: adequate river cross-sections, river slope
 In stream: water temperature, water quality, water levels, sediment bed and suspended loads (daily)
 Ice conditions: bridging locations, anchor and edge ice growth, ice discharge (during freeze-up); leading edge advance, ice cover thickness, aufeis growth (during winter); break-up locations and ice jam locations (during break-up)

ii. Lakes

Inflow and outflow: temperature, conductivity, suspended sediment concentration
 Meteorological: air temperature, wind velocity, precipitation, relative humidity, cloud cover, short-wave and long-wave radiation (daily)
 Basin geometry: area, volume and depth relations, river slope and bed angle

In-lake: water temperature, conductivity, suspended sediment, light extinction, water level (daily)
Ice conditions: snow and ice thickness (weekly)
Ground conditions: extent of permafrost, ground water table

PERMAFROST

The presence of permafrost introduces a wide range of scientific and engineering problems. Since 1963, these have received attention in four international permafrost conferences. The vast range of problems extends well beyond the scope of our workshop. However, some effects of permafrost on hydrology and water quality that are related to the primary theme of the workshop were considered.

Although 5% of Alaska is covered by glaciers, 80% of it is underlain by continuous or discontinuous permafrost and all of it is subjected to seasonally frozen ground. The one major drainage basin which is underlain by continuous permafrost is also the only one which is not affected by glacier runoff; this is the Colville River drainage on Alaska's Arctic Slope.

The differences in hydrographs between rivers lying in glacierized and non-glacierized basins within the zone of continuous permafrost may be more extreme than in non-permafrost regions. This is expected because permafrost impedes subsurface drainage, increases runoff and virtually eliminates subsurface contributions. Hydrographic data for rivers on Alaska's Arctic Slope are rare and no data base exists for comparison of discharge from glacierized and non-glacierized basins. So far the available hydrological measurements on the Arctic Slope have largely been responses to ad hoc, applied needs. When the immediate need is removed, the observations cease. Such procedure would be more appropriate if it supplemented a designed, long-term regional monitoring program. Unfortunately, the long-term program with basic scientific goals does not exist.

One special feature in the continuous permafrost zone is the formation of extensive *aufels* deposits. Dean (1984) mapped these features throughout Alaska on Landsat images and found the largest deposits and most frequent occurrences were on the north side of the Brooks Range. Some of these deposits exceed 400 km² in area (Dean, 1984) and thicknesses of 5 to 6 m have been measured (U.S. Geological Survey, 1985). Upstream reaches of the Sagavanirktok River, where the Ribdon, Echooka and Ivashak rivers join it, are subjected to a total areal *aufels* coverage of about 1000 km². This, plus high altitude snow packs and some glacier contribution to runoff, are probably responsible for the sustained base flow of the Sagavanirktok River at Prudhoe Bay which differs markedly from the sharply peaked hydrographs with low base flow of the Kuparuk and Putuligayak rivers (Carlson and Kane, 1975). Large *aufels* deposits act as glaciers in their

sustained contribution to river discharge; some of the deposits persist from year to year. The Colville River, which is the major drainage of the Arctic Slope, has less effect from *aufels* and high altitude snow packs (and not any from glaciers) than smaller rivers to the east of it.

There is a need to determine all basic hydrological parameters on the Arctic Slope. The amount of winter precipitation which comes as snow has apparently been underestimated by a factor of three; the wind transport of this snow and the amount lost by evaporation are also being reassessed (Benson, 1982). The contribution to runoff from long-term changes in the permafrost ice mass is virtually unknown.

South of the Arctic Slope, the majority of the glacierized basins lie within the zone of discontinuous permafrost, and in most drainages the glacierized area covers only a small proportion of the total basin. Only a few stream gaging sites have been established in basins with more than 50% glacier cover and in the majority of the larger basins, the glacierized area is less than 10% (Lamke, 1979). Glaciers may have a larger influence on the hydrology of a basin than would be indicated by proportion of glacier coverage. The glaciers may perform a moderating effect on streamflow by increasing runoff during hot, dry summers by glacier melt; during cool, wet summers glacier melt would be retarded (Krimmel and Tangborn, 1974; Fountain and Tangborn, 1985). The permafrost areas of the basin have the opposite effect. The hydrologic response of the permafrost areas can be highly variable and is dependent on the thaw season climate (Dingman, 1975). Except for very dry seasons when runoff is dramatically reduced, permafrost runoff responds very rapidly and has slow recessions when compared to non-permafrost areas (Dingman, 1971; Haugen et al., 1982). The hydrologic response to summer precipitation events may be attributable to thick organic soils associated with permafrost (Dingman, 1975; Slaughter and Kane, 1979). In basins with a large proportion of permafrost area relative to glacierized area, much of the glacier influence may be offset by the permafrost hydrology. To date, the study of permafrost hydrology has been limited to small research basins or study plots due primarily to the difficulty in mapping permafrost in large basins (Dingman, 1971). A full understanding of the hydrology of Alaska's drainage basins cannot be achieved without considering the influence of the permafrost areas.

A summary of recommendations follows:

ONE

COMPARE HYDROGRAPHS OF RIVERS IN GLACIERIZED AND NON-GLACIERIZED BASINS IN THE CONTINUOUS PERMAFROST OF THE ARCTIC SLOPE

The differences in hydrographs between rivers lying in glacierized and non-glacierized basins within the zone of continuous permafrost is expected to be greater than in non-permafrost regions. The Jago and Meade rivers are excellent candidates for comparison of glacierized and non-glacierized basins, respectively. These rivers are situated in proximity to existing logistical facilities.

TWO

COMPARE RUNOFF PROCESSES FROM PERMAFROST AND NON-PERMAFROST AREAS IN GLACIERIZED BASINS

The hydrology of permafrost regions differs from that of non-permafrost regions and both contrast sharply with the hydrology of glaciers. Often the extent of permafrost is not known in a given drainage basin; techniques for mapping the extent of the various sub-units of a glacierized basin must be refined as a first step in dealing with this recommendation.

THREE

DETERMINE THE BASIC HYDROLOGIC PARAMETERS ON ALASKA'S ARCTIC SLOPE

The questions of winter precipitation need special attention because of uncertainties in its quantity, the extent of wind transport and the evaporative losses.

FOUR

DETERMINE THE LONG-TERM HYDROLOGIC CYCLE OF THE COLVILLE RIVER AS THE MAJOR DRAINAGE SYSTEM OF THE ARCTIC SLOPE

In addition to the Colville, a river such as the Meade River which drains the tundra, but does not include mountain runoff should be selected for long-term monitoring. Hydrologic information from these rivers, lying completely within the zone of continuous permafrost, is needed as a contrast to that from glacier-fed Alaskan rivers.

REFERENCES

- Benson, C., 1982. Reassessment of winter precipitation on Alaska's Arctic Slope and measurements of the flux of windblown snow. Geophysical Institute Report UAG-R-288, University of Alaska, Fairbanks, 26 pp.
- Benson, C., W. Harrison, J. Gosink, S. Bowling, L. Mayo and D. Trabant, 1986. Workshop on Alaskan hydrology: problems related to glacierized basins. Geophysical Institute, University of Alaska, report in preparation.
- Bezinge, A., 1979. Grand Dixence et son hydrologie. La collecte de données hydrologiques de base en Suisse, Association Suisse pour l'aménagement des eaux, Service hydrologique national, 19 pp.
- Carlson, R. F. and D. L. Kane, 1975. Hydrology of Alaska's Arctic, in: Climate of the Arctic: Proceedings of the AAAS-AMS Conference, Fairbanks, Alaska, August 1973, Geophysical Institute, University of Alaska, Fairbanks, p. 367-373.
- Clarke, T. S., 1986. Glacier runoff, balance and dynamics in the upper Susitna River Basin, Alaska. M.S. Thesis, University of Alaska, Fairbanks, May 1986, 98 pp.
- Clarke, T. S., D. Johnson and W. D. Harrison, 1985. Glacier runoff in the Upper Susitna and Susitna River basins, Alaska, in: Resolving Alaska's Water Resources Conflicts, Institute of Water Resources Report IWR-108, University of Alaska, Fairbanks, AK 99775-1760, p. 99-111.
- Davies, J. N., 1983. Seismic, volcanic and tsunami mitigation in Alaska - an unmet need. Report of Investigations 83-11, Alaska Dept. of Natural Resources, Division of Geological and Geophysical Surveys, 13 pp.
- Dean, K., 1984. Stream-icing zones in Alaska, Report of Investigations 84-16. Alaska Department of Natural Resources, Division of Geological and Geophysical Surveys, 20 pp.
- Dingman, S. L., 1971. Hydrology of the Glenn Creek watershed Tanana River Basin, central Alaska. USA CRREL Research Report 297.
- Dingman, S. L., 1975. Hydrological effects of frozen ground: literature review and synthesis, CRREL Special Report 218.
- Field, W. O., 1975. Mountain glaciers of the northern hemisphere (2 volumes plus atlas), edited by W. O. Field American Geographical Society, published by CRREL, Hanover, NH.
- Fountain, A. G. and W. V. Tangborn, 1985. The effect of glaciers on streamflow variations. Water Resources Research Vol. 21., No. 4, p. 579-586.
- Gaddis, B. L., 1974. Suspended-sediment transport relationships for four Alaskan glacier streams. M.S. Thesis, University of Alaska, Fairbanks, 102 pp.
- Gurnell, A. M., 1982. The dynamics of suspended sediment concentration in an Alpine pro-glacial stream network. International Association of Hydrological Sciences, Publication No. 138, p. 319-330.
- Harrold, P. E. and R. L. Burrows, 1983. Sediment transport in the Tanana River near Fairbanks, Alaska, 1982. U.S. Geological Survey Water Resources Investigations Report 83-4213, 53 pp.

- Harrison, W. D., B. T. Drage, S. Bredthauer, D. Johnson, C. Schock and A. B. Follett, 1983. Reconnaissance of the glaciers of the Susitna River Basin in connection with proposed hydroelectric development. *Annals of Glaciology*, Vol. 4, p. 99-104.
- Haugen, R. K., C. W. Slaughter, H. E. Howe and S. L. Dingman, 1982. Hydrology and climatology of the Caribou-Poker Creeks Research watershed, Alaska. USA CRREL Report 82-26.
- Humphrey, N. F., 1986. Suspended sediment discharge from Variegated Glacier during its pre-surge and surge phases of motion, in: Benson et al., Workshop on Alaskan Hydrology: Problems Related to Glacierized Basins. Geophysical Institute, University of Alaska, report in preparation.
- Humphrey, N., C. Raymond and W. Harrison, 1986. Discharges of turbid water during mini-surges of Variegated Glacier, Alaska, submitted to *Journal of Glaciology*.
- Kane, D. L., 1981. Physical mechanics of aulis growth, *Canadian Journal of Civil Engineering*, Vol. 8, No. 2, p. 186-195.
- Kasser, P., 1973. Influences of changes in the glaciated area on summer runoff in the Porte due Sceaux drainage basin of the Rhone, in: Symposium on the hydrology of glaciers, IASH Publ. No. 95, p. 221-225.
- Knott, J. M. and S. W. Lipscomb, 1983. Sediment discharge data for selected sites in the Susitna River basin, Alaska, 1981-1982, U.S. Geological Survey Open-File Report 83-870, 45 pp.
- Krimmel, R. M. and W. V. Tangborn, 1974. South Cascade Glacier: the moderating effect of glaciers on runoff, in: Proceedings of the Western Snow Conference, 42nd Annual Meeting, Colorado State University, Fort Collins, 1974, p. 9-13.
- Lamke, R. D., 1979. Flood characteristics of Alaskan Streams, USGS Water Resources Investigations 78-129.
- LaPerriere, J. D., 1981. Vernal Overturn and Stratification of a Deep Lake in the High Subarctic under Ice, Proceedings of Int. Assoc. for Theoretical and Applied Limnology, Congress in Japan, 1980, p. 288-292.
- Lipscomb, S. W. and J. M. Knott, 1985. Sediment transport in the Susitna River Basin, 1982-1983, in: Resolving Alaska's Water Resources Conflicts, Institute of Water Resources Report IWR-108, University of Alaska, Fairbanks, AK 99775-1760, p. 191-204.
- Mayo, L. R., R. S. March and D. C. Trabant, 1985. Growth of Wolverine Glacier, Alaska, determined from surface altitude measurements, 1974 and 1985, in: Resolving Alaska's Water Resources Conflicts, Institute of Water Resources Report IWR-108, Nov. 1985, University of Alaska, Fairbanks, AK 99775-1760, p. 113-121.
- Meier, M. F., 1984. Contribution of small glaciers to global sea level. *Science* 266, 1418-1421.
- Meier, M. F., W. V. Tangborn, L. R. Mayo and A. Post, 1971. Combined ice and water balances of Gulkana and Wolverine glaciers, Alaska, and South Cascade Glacier, Washington, 1965 and 1966 hydrologic years. Ice and Water Balances at Selected Glaciers in the United States, U.S. Geological Survey Professional Paper 715-A, 23 pp. with maps.
- Miller, D. J., 1960. Giant waves in Lituya Bay, Alaska: U.S. Geological Survey Prof. Paper 354-C, p. 51-86.
- National Research Council, 1983. Snow and Ice Research, an Assessment. Committee on Glaciology Polar Research Board, Commission on Physical Sciences, Mathematics and Resources, National Research Council, National Academy Press, Washington, D.C., p. 1-123.
- National Research Council Canada, 1979. Proceedings of Canadian Hydrology Symposium: 79 - Cold Climate Hydrology, Ottawa, Canada, K1A 0R6.
- Neill, C. R., T. S. Buska, E. R. Chacho, C. M. Collins and L. W. Gatto, 1984. Overview of Tanana River monitoring and research studies near Fairbanks, AK. U.S. Army Cold Regions Research and Engineering Laboratory Special Report 84-37.
- Osterkamp, T. E. and J. P. Gosink, 1983. Frazil Ice Formation and Ice Cover Development in Interior Alaska Streams. *Cold Regions Science and Technology* (1983), p. 43-56.
- Østrem, G., 1973. Runoff forecasts for highly glacierized basins, in: International Hydrological Decade -- The role of snow and ice in hydrology. Proceedings of the Banff Symposia, Sept. 1972. Paris, UNESCO; Geneva, WMO; Budapest, IAHS, Vol. 2, pp. 1111-1132. (Publication No. 107 de l'Association Internationale d'Hydrologie Scientifique.)
- Østrem, G., C. W. Bridge and W. F. Rennie, 1967. Glaciology, discharge and sediment transport in the Decade Glacier area, Baffin Island, N.W.T., *Geografiska Annaler*, Vol. 49, Ser. A, p. 268-282.
- Post, A. and L. R. Mayo, 1971. Glacier dammed lakes and outburst floods in Alaska: U.S. Geological Survey Hydrologic Atlas HA-455, 10 pp., 3 pl.
- Roland, E. and N. Haakensen, 1985. Glaciologiske Undersøkelser i Norge 1982. Norges Vassdrags- og Elektrisitetsvesen Rapport nr. 1-85, with English summary.
- R & M, 1982. Alaska Power Authority Susitna hydroelectric project; task 3 - hydrology; subtask 3.07 - closeout report - reservoir sedimentation. Report for Acres American Inc., Buffalo, N.Y.
- Slaughter, C. W. and D. L. Kane, 1979. Hydrologic role of shallow organic soils in cold climates. *Canadian Hydrology Symposium: 79 - Cold Climate Hydrology*, p. 380-389.
- Sloan, C. E., C. Zenone and L. R. Mayo, 1976. Icings along the Trans-Alaska Pipeline Route, U.S. Geological Survey Professional Paper 979.

- Sturm, M., C. Benson and P. MacKeith, 1986. Effects of the 1966-68 Eruptions of Mt. Redoubt on the flow of the Drift Glacier. Submitted to: Journal of Glaciology.
- Tangborn, W. V., L. R. Mayo, D. R. Scully and R. M. Krimmel, 1977. Combined ice and water balances of Maclure Glacier, California, South Cascade Glacier, Washington, and Wolverine and Gulkana glaciers, Alaska, 1967 hydrologic year. Ice and Water Balances at Selected Glaciers in the United States. U.S. Geological Survey Professional Paper 715-B, 20 pp. with maps.
- U.S. Geological Survey, 1950-1960a. Compilation of records of quantity and quality of surface waters of Alaska. U.S. Geol. Survey Water Supply Papers 1372 and 1740.
- U.S. Geological Survey, 1950-1960b. Quantity and quality of surface waters of Alaska. U.S. Geol. Survey Water Supply Papers 1466, 1486, 1500, 1570, 1640 and 1720.
- U.S. Geological Survey, 1961-1984. Water resources data, Alaska, water years 1961-1984, published annually.
- U.S. Geological Survey, 1985. U.S. Geological Survey Open File Report 85-332. Alaska Index: Stream flow and water quality records to Sept. 30, 1983.
- Young, G. J. and C. S. L. Ommanney, 1984. Canadian glacier hydrology and mass balance studies; a history of accomplishments and recommendations for future work. Geografiska Annaler Vol. 66A, No. 3, p. 169-182.

GLACIER-CLIMATE RESEARCH FOR PLANNING HYDROPOWER IN GREENLAND

Roger J. Braithwaite and Ole B. Olesen

ABSTRACT: A program of glacier-climate research is being carried out in Greenland for the planning of possible hydropower stations. The program is based upon the parallel collection and correlation of glaciological and climatological data. The present results confirm the importance of air temperature for calculating ablation and have already been used for the simulation of runoff from glacierized areas.

(**KEY TERMS:** Greenland, hydropower, glaciers, climate, runoff.)

INTRODUCTION

Since the mid-1970s, Danish state agencies have been investigating the feasibility of hydropower stations in Greenland. Hydrological conditions in Greenland are, however, still poorly understood, e.g. because of sparcity and shortness of records as well as the effects of the arctic climate upon the runoff cycle (Gottlieb & Braithwaite, 1985). Many of the possible hydropower sites are also influenced by glaciers. The program therefore includes glaciological investigations which are carried out by the Geological Survey of Greenland (GGU) as described by Weidick (1984). An important objective of the glaciological work is to understand the effects of glaciers upon runoff. For this purpose improved knowledge of glacier-climate relations is needed.

TABLE 1. Locations of the three glacier-climate stations operated in West Greenland by the Geological Survey of Greenland.

STATION	NORTH	WEST	PERIOD
Johan Dahl Land	61°27'	45°22'	1977-83
Qamanârssûp sermia	64°29'	49°32'	1979-
Tasersiaq	66° 7'	50° 7'	1981-

The basis of the glacier-climate program is the measurement of glacier accumulation and ablation at several field stations in parallel with climatological observations. The first station was established by O.B. Olesen in late-1977 in Johan Dahl Land, South Greenland, and was manned for six summers until closed in late 1983 (Clement, 1984). The other two stations at Qamanârssûp sermia and Taser-siaq were opened by O.B. Olesen in late 1979 and late 1981 respectively and are still continuing (Braithwaite, 1985a; Olesen, 1985). The locations of the three glacier-climate stations are given in Table 1 and fig. 1. Glaciological observations are also made at several places by mobile teams, i.e. without detailed climatological measurements, but will not be discussed here.

GLACIOLOGY PROGRAM

The glaciological measurements are made in a network of stakes drilled into

The Geological Survey of Greenland, DK-1350 Copenhagen K, Denmark.

the ice which are visited at least twice yearly to measure transient balances, i.e. roughly at the beginning and end of the summer which essentially extends over the three months June to August. At Johan Dahl Land and at Qamanârssûp sermia, the main glaciological measurements are made upon large outlet glaciers from the Greenland ice sheet while the measurements at Taser-siaq are made on local ice caps but in all three cases the study areas cover hundreds of square kilometers. The data therefore refer to balances measured in sparse stake networks.

TABLE 2: Net ablation deviations for Qamanârssûp sermia for various combinations of stakes. Units are meters of water equivalent.

YEAR	A1	A2	A3	A4
1979/80	0.3			-0.3
1980/81	0.4	0.5	0.5	0.4
1981/82	0.4	0.3	0.4	0.3
1982/83	-0.4	-0.5	-0.5	-0.6
1983/84	-0.4	-0.4	-0.4	-0.1
1984/85	1.1	0.9		1.5

A1 = Based on 6 stakes for 6 years

A2 = Based on 11 stakes for 5 years

A3 = Based on 13 stakes for 4 years

A4 = Based on 3 stakes for 6 years

The stations in Johan Dahl Land and at Qamanârssûp sermia are located beside the lower ablation zone and, because of the difficulties of travelling and the distances involved, the stake networks only extend to the lower parts of the accumulation zone. The accumulation zone is also poorly delineated at both places because of the inaccuracies of mapping the surface topography on the ice sheet. For these two reasons, the data cannot be expressed in the area-averaged form generally used in glaciology (Anonymous, 1969). Braithwaite (1985b & 1986a) used a simplified version of the method by Lliboutry (1974) to analyse such data. The results are shown in Table 2 for various combinations of stakes. Although there are some substantial differences between deviations for the same year, it is clear that 1984/85 had exceptionally high ablation while 1982/83 had low ablation.

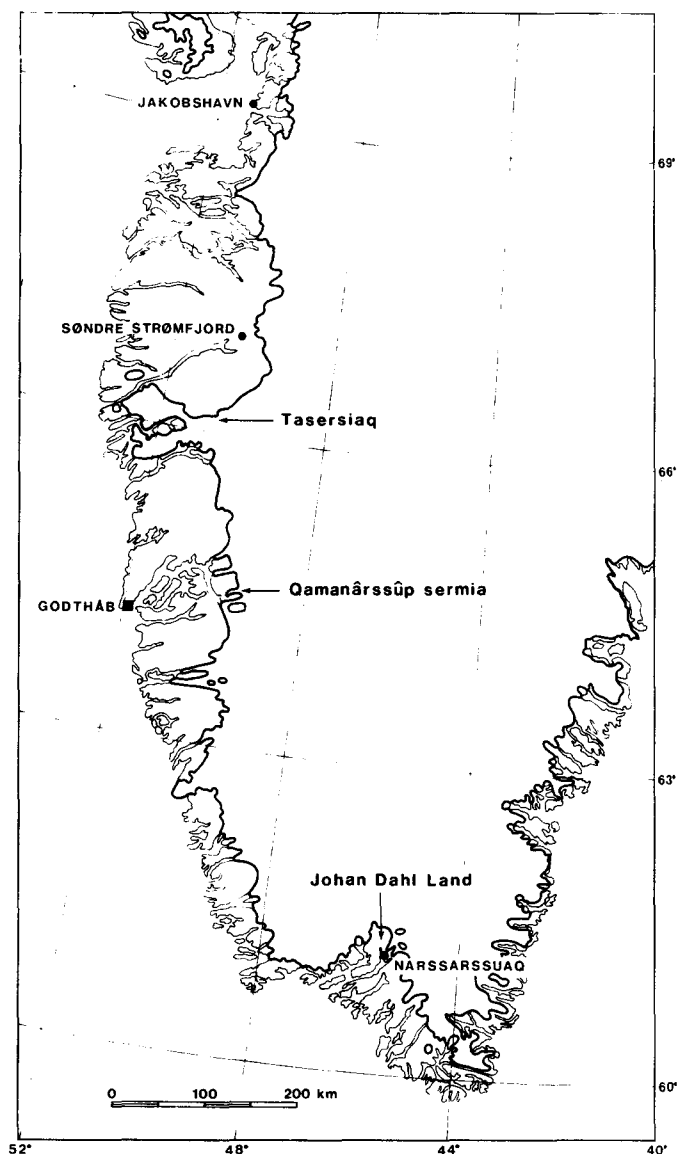


Figure 1. Locations of the three glacier-climate stations in West Greenland

The measurements are supplemented by daily readings of ice ablation at stakes located close to the field stations in Johan Dahl Land and at Qamanârssûp sermia. The readings on these stakes are used for detailed correlations with the climatological readings at the field stations. Similar measurements are also attempted at the Taser-siaq station. However, this station is located in an area with more durable snowcover so that the measurements refer mainly to snow ablation and are less detailed than the ice ablation measurements in Johan Dahl Land and at Qamanârssûp sermia.

CLIMATOLOGY PROGRAM

The climatological program is designed to be simple but comprehensive enough for glacier-climate research. Recordings of air temperature and humidity, precipitation, wind, sunshine and global radiation are made with clockwork recorders at the base camps, supplemented by hand readings twice a day, i.e. in the morning and the evening. Such a program gives daily averages or totals for the various elements and leaves the field team free for other work during the day. The combined glaciological and climatological programs can therefore be carried out by only 2-3 persons while a full program of synoptic observations would be more demanding.

Several remote thermohygrograph and raingauge stations are operated around the base camps, e.g. on glaciers at the same elevation as the base camps to measure the glacier "cooling effect". These stations are visited at intervals of 7-10 days to recover data.

The core period for the climatological observations is the ablation season which falls roughly in the three months June to August. However, in most years the hand-collected climatological observations extend from mid-May to mid-September.

A Danish-designed automatic climate station has also been tested at Qamanârssûp sermia in parallel to the hand observations (Braithwaite, 1983). Six summers of comparisons of data from automatic and manned stations have shown excellent agreement for elements like air temperature and wind speed (note: there is little or no rime formation in this area). There are still problems with the measurement of precipitation however, especially in the form of snow. Despite this, automatic climate stations will be relied upon more in the future as their relatively low running costs, compared to manned stations, offset their high capital costs. The good performance of the automatic station at Qamanârssûp sermia has allowed the measurement of temperature through most of the winter periods so that ablation can be compared with temperature on an annual basis as, for example, in Table 3.

TABLE 3. Annual ice ablation A (mm water equivalent) compared with annual melting degree-day total T (deg d) at Qamanârssûp sermia. The glaciological year is from 1 September to 31 August.

YEAR	A	T	A/T
1979/80	4090	635	6.4
1980/81	4690	617	7.6
1981/82	4660	599	7.8
1982/83	3740	426	8.8
1983/84	4260	594	7.2
1984/85	5880	728	8.1
Mean	4550	600	7.6
c.v.	+16%	+16%	+10%

SOME RESULTS

Although the field program is still continuing some results can be briefly summarized.

There is a useful, although by no means perfect, relation between ice ablation and air temperatures expressed as melting degree-day totals. The degree-day factor relating ice ablation to temperature is a fluctuating parameter rather than a constant (Braithwaite, 1986b). However, it shows no systematic variation between Johan Dahl Land and Qamanârssûp sermia, e.g. no simple variation with latitude; nor does it show sinusoidal seasonal variation as suggested, for example, by Gottlieb (1980) or Lundquist (1982). The variations of annual ablation and degree-days at Qamanârssûp sermia are shown in Table 3 where A/T is the degree-day factor in mm/deg d. This annual degree-day factor has a year-to-year fluctuation of about +10 % the reasons for which are still not fully understood although Braithwaite & Olesen (1986) suggest that they may be a result of covariations between the various sources of ablation energy.

There is only a weak correlation between ice ablation and global radiation in West Greenland although global radiation is the main source of ablation energy. Braithwaite & Olesen (1986) suggest that the long-wave radiation balance

acts in opposition to the short-wave radiation to suppress correlations between ablation and radiation. This means that there will only be a slight benefit to including radiation in future ablation models.

The relation between snow ablation and climate is more complex than for ice ablation so that less progress has been made. For example, it is much more difficult to measure mass changes in the lower accumulation area than on ice because meltwater can percolate to great depths before refreezing. It is likely that data from Tasersiaq will be more useful for snow ablation studies than those from the two older stations where most of the data refer to ice ablation. The ubiquity of refreezing means that there is little or no runoff from the accumulation area of the ice sheet, i.e. there is a "runoff line" located close to the equilibrium line. It also means that the effects of re-frozen meltwater must be included in ablation models.

There is a glacier "cooling effect" whereby the air over a glacier surface is cooler than the air over land at the same altitude. There is also an "inland" effect whereby air is heated between the coast and the edge of the Greenland ice sheet during the summer and is cooled during the winter. Both of these effects must be taken into account when calculating ablation on the Greenland ice sheet using temperatures extrapolated from the coast.

APPLICATIONS

Although there are still problems to solve, some results have been incorporated in runoff models using temperature and precipitation data from weather stations on the coast of Greenland. For example, Braithwaite & Thomsen (1984a & 1984b) and Thomsen & Jørgensen (1984) have calculated ablation for planning hydropower stations near Christianshåb and Jakobshavn, central West Greenland, where runoff from the ice sheet is the chief water source.

The present emphasis in Greenland hydrology is upon the planning of hydropower stations. Runoff models, including

glacier effects, are being used to artificially extend the short measurement series to provide a more reliable basis for dimensioning the planned hydropower stations. A decision may be made soon to build hydropower stations in Greenland, e.g. at Jakobshavn, to come on-line in the early 1990s. The priority for Greenland hydrology will then shift to problems of forecasting runoff. The continuation of the present glacier-climate research will contribute to the development of suitable forecasting methods.

ACKNOWLEDGMENTS

This paper is published by permission of The Director, The Geological Survey of Greenland. The field station in Johan Dahl Land 1977-1983 was partly funded by the European Economic Community (EEC) and by the Energy Ministry, Denmark while the other stations were wholly supported by the Geological Survey of Greenland. The work in Johan Dahl Land in the period 1979-83 was lead by Cand. Scient. Poul Clement.

REFERENCES

- Anonymous 1969. Mass-balance terms. *J. Glaciol.* 52(8), 3-7.
- Braithwaite, R.J. 1983. Comparisons between automatic and manual climate stations at Qamanârssûp sermia. *Grønlands geol. Unders. Gletscher-hydrol. Meddr* 83/5, 17 pp.
- Braithwaite, R.J. 1985a. Glacier-climate investigations in 1984 at Qamanârssûp sermia, West Greenland. Report of Activities 1984. *Rapp. Grønlands geol. Unders.* 125, 108-112.
- Braithwaite, R.J. 1985b. Relations between annual runoff and climate, Johan Dahl Land, South Greenland. *Grønlands geol. Unders. Gletscher-hydrol. Meddr* 85/2, 25 pp.
- Braithwaite, R.J. 1986a. Assessment of mass-balance variations within a sparse stake network, Qamanârssûp sermia, West

- Greenland. J. Glaciology. (In press).
- Braithwaite, R.J. 1986b. Exceptionally high ablation in 1985 at Qamanârssûp sermia, West Greenland. Report of Activities 1985. Rapp. Grønlands geol. Unders. 130 (In press).
- Braithwaite, R.J. & Thomsen, H.H. 1984a. Runoff conditions at Kuussuup Tasia, Christianshåb, estimated by modelling. Grønlands geol. Unders. Gletscher-hydrol. Meddr 84/2, 24 pp.
- Braithwaite, R.J. & Thomsen, H.H. 1984b. Runoff conditions at Paakitsup Akuliarusersua, Jakobshavn, estimated by modelling. Grønlands geol. Unders. Gletscher-hydrol. Meddr 84/3, 22 pp.
- Braithwaite, R.J. & Olesen, O.B. 1986. Ice ablation in West Greenland in relation to air temperature and global radiation. Zeitschrift für Gletscherkunde und Glazialgeologie 20(2) (In press).
- Clement, P. 1984. Glaciological activities in the Johan Dahl Land area, South Greenland, as a basis for mapping hydropower potential. Report of Activities 1983. Rapp. Grønlands geol. Unders. 120, 113-121.
- Gottlieb, L. 1980. Development and applications of a runoff model for snowcovered and glacierized basins. Nordic Hydrology 11(1980), 255-272.
- Gottlieb, L. & Braithwaite, R.J. 1985. Greenland case study: water supply. In Techniques for Prediction of Runoff from Glacierized Areas. Int. Assoc. Hydrol. Sci. Publ. 149, 73-80.
- Lliboutry, L. 1974. Multivariate statistical analysis of glacier annual balances. J. Glaciology 69(13), 371-392.
- Lundquist, D. 1982. Modelling runoff from a glacierized basin. In Hydrological Aspects of Alpine and High Mountain Areas. Int. Assoc. Hydrol. Sci. Publ. 138, 131-136.
- Olesen, O.B. 1985. Glaciological investigations in 1984 at Tasersiaq and Qapiarfiup sermia, West Greenland. Report of Activities 1984. Rapp. Grønlands geol. Unders. 125, 104-107.
- Thomsen, T. & Jørgensen, G.H. 1984. Hydrological data-model in Greenland. Nordic Hydrology 15(1984), 39-56.
- Weidick, A. 1984. Studies of glacier behaviour and glacier mass balance in Greenland - a review. Geografiska Annaler 66A(3), 183-195.

A FORECAST PROCEDURE FOR JOKULHLAUPS ON SNOW RIVER IN
SOUTHCENTRAL ALASKADavid L. Chapman¹

ABSTRACT: Snow River jokulhlaups are outburst floods caused by the rapid release of water from a glacier-dammed lake. These events occur at two- to four-year intervals, but it has not been possible to predict accurately when a jokulhlaup will begin. The forecast procedure presented here will not predict when a jokulhlaup will start; however, once a jokulhlaup has begun and is recognized as such, the procedure will forecast the hydrograph of the remainder of the event. Usually, some five days advance notice of the severity of expected flooding can be provided to downstream residents. The forecast procedure is based upon the observation that the cross-sectional area of the glacier-dammed lake outlet is proportional to the amount of water that has passed through the outlet since the beginning of the event. A log-log plot of a function of the cross-sectional area versus accumulated outflow results in a linear relationship that can be determined early in the event and used to forecast the discharge through the rest of the jokulhlaup. A tabulation of the hydrographs of all fourteen of the Snow River jokulhlaups that have occurred since 1947 is also presented. (KEY TERMS: jokulhlaup forecast; glacier-dammed lake; outburst.)

INTRODUCTION

Snow River is located at the head of the Kenai River on the eastern side of the Kenai Peninsula in southcentral Alaska. Figure 1 shows the locations of pertinent features in the Kenai River basin. Snow River jokulhlaups are outburst floods caused by the rapid release of water from a lake which was formed by the main valley glacier damming a tributary valley. During summer, runoff from rainfall, snowmelt, and some glacier melt accumulate in the lake. In winter, snowfall adds depth to the lake, as does continued drainage of glacier meltwater from earlier seasons. In the course of two to four years, the lake fills to a depth of 80 to 160 meters and creates a hydrostatic head sufficient to initiate the self-dumping process. On at least one occasion, this was when the height of the lake surface was about 0.9 of the height of the ice dam, which suggests that lifting of the dam may take place. Once begun, the flowing water enlarges its escape route and the discharge accelerates until the head is insufficient to support acceleration. At that point, the lake is nearly empty and the discharge drops abruptly. The volume of water stored in the lake at the beginning of jokulhlaup events has

¹Hydrologist, National Weather Service, Alaskan River Forecast Center, 701 C Street, Box 23, Anchorage, Alaska 99513.

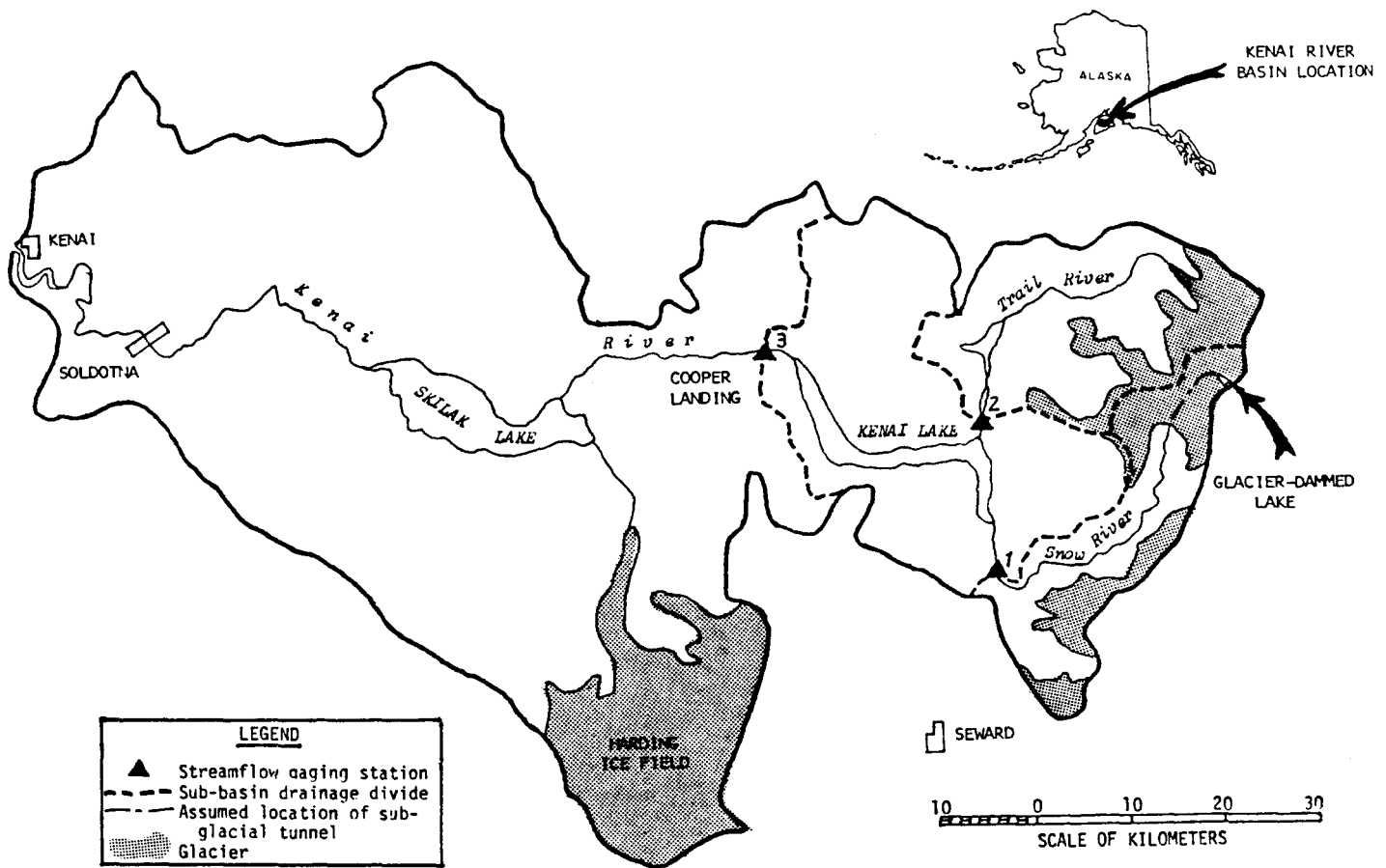


Figure 1. Location Map of the Kenai River Basin

ranged from 96 million to 240 million cubic meters. The elapsed time from the time the outflow becomes recognizable as a jokulhlaup until it reaches its peak rate is five to ten days; however, many other glacier-dammed lakes dump much more rapidly. With five or more days advance notice, a valuable forecast of river levels at downstream locations can be made, which provides time for property owners to move items to high ground if needed, or saves them the effort and expense if the river levels will not be so high. This requires an accurate forecast of the jokulhlaup hydrograph, not just its peak discharge.

GLACIER-DAMMED LAKE CAPACITY

One of the tools needed for a

jokulhlaup forecast is a storage-elevation relationship. Unlike common lakes and reservoirs for which fairly accurate storage versus pool elevation relationships can be determined from surveys, such relationships can change in glacier-dammed lakes. The lake may change size due to changes in the damming glacier. Floating ice is equivalent to a change in storage since large amounts of ice are usually left in the lake at the end of a dump. As the lake approaches its dumping level, the ice dam domes up and arcuate cracks appear in the glacier surface near the lake. A considerable volume of water may be stored in or under the glacier. Therefore, even though the lake might have been surveyed at some time when it was empty, no firm storage versus pool elevation relationship can be developed.

Instead, a gross estimate was made. The lake geometry was simplified to a truncated triangular pyramid designed to have approximately the correct surface area, head, and volume when full. The storage versus head relationship was reduced to the simple equations:

$$S = 5.06(h + 228)^3 - 6.00 \times 10^7 \quad (1)$$

$$h = [(S + 6.00 \times 10^7) / 5.06]^{1/3} - 228 \quad (2)$$

where:

3

S is storage in m³; and
h is head in m.

Accuracy to three significant figures is not implied. Very little accuracy is claimed but the equations are necessary tools in the procedures that follow. Fortunately, storage and head are not very sensitive parameters in those procedures.

THE SUBGLACIAL OUTLET

The Snow River glacier-dammed lake drains from the bottom of the lake and the water issues from under the glacier terminus about eight kilometers down the valley. Little else is known about the lake outlet. It is convenient to think of it as a tunnel, part of which may remain open between jokulhlaup events. In any case, some mechanism plugs the outlet and causes the lake to fill. Some other mechanism triggers the jokulhlaup, be it lifting, fracturing, or any of several things, that allows the water to begin flowing out. Once begun, the tunnel, or more specifically the hydraulic control, is enlarged by melting with most of the heat being derived from the potential energy of the very high head. The water temperature in the lake is probably very near freezing because the lake is always in contact with the glacier and there is at least partial ice cover at all times. Some erosion must also

occur by physical scouring due to high velocity flow. Post and Mayo (1971) state that the cross-sectional area of the tunnel is proportional to the volume of water that has already passed through it, providing no collapse or closure takes place.

A tunnel eight kilometers long could hardly be called an orifice. Nevertheless, considering the small outlet relative to the very high head, the orifice flow formula applies reasonably well and is certainly convenient. The formula states:

$$Q = CA(2gh)^{1/2} \quad (3)$$

where:

Q is discharge in m³/s;
C is coefficient of discharge;
A is cross-sectional area of

the orifice in m²;

g is 9.8 m/s²; and
h is head in m, the depth of water that produces discharge.

The initial head can be determined by flying over the lake and estimating the lake level based on visible markers. The coefficient, C, and the area, A, are both unknown, but it is not necessary to determine them separately. It is only necessary to determine their product, CA, and the procedure for doing that follows.

COMPUTATION OF SNOW RIVER JOKULHLAUP HYDROGRAPHS

The glacier-dammed lake drains under the glacier for a distance of eight kilometers to the glacier terminus. From that point the water flows down Snow River a distance of 48 kilometers to Kenai Lake. During some of the jokulhlaup events, the U.S. Geological Survey operated a stream gage at the railroad bridge near the mouth

of Snow River. The flood wave at that location is necessarily very similar to the hydrograph at the glacier terminus because Snow River flow is supercritical through most of its length, slowing down only for a few kilometers through Paradise Valley and arriving at the gage about three hours after leaving the glacier. For those events when the gage was operating, the jokulhlaup hydrographs were clearly superimposed upon the other Snow River flow. Separation of the flows into jokulhlaup flow and non-jokulhlaup flow was simple.

Two other gages were used to derive the other jokulhlaup hydrographs. Kenai River at Cooper Landing is located on the Sterling Highway bridge at the outlet of Kenai Lake. Trail River near Lawing is near the mouth of Trail River which empties into Kenai Lake. Both gages began operation in 1947 and although the U.S. Geological Survey discontinued operation of the Trail River gage, the National Weather Service has maintained records during the open water season. For those events when no Snow River record is available, a reverse routing procedure was applied to Kenai Lake outflows, i.e., the flows recorded at the Kenai River at Cooper Landing gage, to obtain a Kenai Lake inflow hydrograph. The inflow was separated into Snow River flow and non-Snow River flow by applying drainage area ratio to the Trail River gage records to determine the ungedged area flows. In most cases there was no significant rainfall during the events and the non-jokulhlaup flow was steady. Having the Snow River flow determined, that part attributed to lake drainage was separated.

Table 1 lists the volumes and peaks of all the jokulhlaups since 1947 along with the peak flows at the Snow River gage and at the Cooper Landing gage. Table 2 lists the daily-flow hydrographs of those jokulhlaups along with accumulated outflow, the water volume remaining

in the glacier-dammed lake, the head as computed by equation (2), and CA computed as explained below. Except for the events of 1982 and 1985, the jokulhlaup hydrographs were published in Chapman (1981) along with the resulting reconstitutions of Cooper Landing hydrographs as proof of the effectuality of the methods used.

COMPUTATION OF OUTLET TUNNEL EXPANSION

There is no practical way to measure or otherwise determine the outlet tunnel dimensions during a jokulhlaup. It is a simple procedure, however, to compute the product CA, which is a function of the cross-sectional area, by transposing equation (3) as:

$$CA = Q / (2gh)^{1/2} \quad (4)$$

Table 2 shows a straightforward accounting of the volume of water remaining in the lake at the end of each day. Applying equation (2) provides the head, h. This is the head that produces the instantaneous end-of-day discharge, Q. Entering these values into equation (4) yields the value of CA. All of the values mentioned above plus the 24-hour outflow volume and the accumulated outflow at the end of each day are shown in Table 2.

A log-log plot of CA versus accumulated outflow results in a straight line up to the point at which orifice control is lost. Figure 2 (following Table 2) illustrates that relationship for two events when the Snow River gage was operating, which eliminates most of the possibility of author bias. The different slopes of the lines show that different events have different rates of increase in outflow from the glacier. The apparent straight line relationship verifies that the cross-sectional area of the tunnel is proportional to the volume of water that has passed through the tunnel since the

TABLE 1. Snow River Jokulhlaups Volume and Peak Outflow
With Peak Flow at Snow River Gage and at Cooper Landing.

Year	Glacier Dammed Lake		Snow R nr Seward		Kenai R at Cooper Landing		
	Jokulhlaup Incl. Dates	Estimated Volume (10^6 m^3)	Est. Peak Outflow (m^3/sec)	Peak Flow (m^3/sec)	Date	Peak Flow (m^3/sec)	Date
1949	18 Oct - 29 Oct	143.6	422	464 (1)	27 Oct	328 (2)	28 Oct
1951	05 Nov - 20 Nov	96.2	311	326 (1)	17 Nov	177 (5)	18 Nov
1953	04 Dec - 19 Dec	98.8	198	207 (1)	15 Dec	125 (5)	17 Dec
1956	18 Oct - 01 Nov	129.8	354	365 (1)	29 Oct	207 (5)	30 Oct
1958	06 Oct - 20 Oct	128.9	394	402 (1)	17 Oct	236 (5)	17 Oct
1961	28 Sep - 08 Oct	175.2	544	566 (3)	07 Oct (3)	396 (2)	08 Oct
1964	15 Sep - 27 Sep	154.9	450	507 (2)	23 Sep	402 (2)	24 Sep
1967	26 Aug - 02 Sep	150.5	760	810 (4)	31 Aug	609 (2)	01 Sep
1970	08 Sep - 24 Sep	188.7	481	504 (2)	22 Sep	343 (5)	23 Sep
1974	09 Sep - 22 Sep	240.5	708	748 (2)	20 Sep	654 (2)	21 Sep
1977	29 Aug - 08 Sep	151.1	394	473 (2)	05 Sep	422 (5)	06 Sep
1979	18 Oct - 24 Oct	127.0	419	445 (1)	24 Oct	362 (6)	24 Oct
1982	17 Sep - 01 Oct	177.6	388	456 (1)	29 Sep	439 (2)	29 Sep
1985	21 Nov - 05 Dec	159.2	334	340 (7)	02 Dec	233 (6)	03 Dec

NOTES:

- (1) Inferred by downstream gages.
- (2) Published by U.S. Geological Survey.
- (3) Peak flow and date shown are inferred by downstream gages. The 1964 Surface Water Records of Alaska show peak flow of $708 \text{ m}^3/\text{sec}$ on 30 Sep 1961. That date cannot be supported by Cooper Landing flow records.
- (4) Peak flow and date shown are inferred by downstream gages. The 1970 Water Resources Data for Alaska show $1,557 \text{ m}^3/\text{sec}$ on 31 Aug 1967.
- (5) Daily flows, not necessarily peak flows.
- (6) From unpublished National Weather Service records.
- (7) Measured by U.S. Geological Survey.

TABLE 2. Snow River Jokulhlaups - Glacier-dammed Lake Daily and Accumulated Outflow, Computed Head, and CA.

Date	Lake at End of Day	Outflow 24-hr	Accum Outflow	Volume Remaining	Head	CA	Date	Lake at End of Day	Outflow 24-hr	Accum Outflow	Volume Remaining	Head	CA
	m ³ /sec	Volume 10 ⁶ m ³	10 ⁶ m ³	10 ⁶ m ³	m	m ²		m ³ /sec	Volume 10 ⁶ m ³	10 ⁶ m ³	10 ⁶ m ³	m	m ²
1949							1961						
18 Oct	0.0	0.00	0.00	143.57	114.7	0.00	28 Sep	0.0	0.00	0.00	175.15	131.5	0.00
19 Oct	9.9	0.66	0.66	142.91	114.3	0.21	29 Sep	14.2	0.56	0.56	174.59	131.2	0.28
20 Oct	19.3	1.13	1.79	141.78	113.6	0.41	30 Sep	90.6	5.33	5.89	169.26	128.5	1.81
21 Oct	38.2	2.67	4.46	139.11	112.1	0.81	01 Oct	155.6	11.40	17.29	157.86	122.5	3.18
22 Oct	82.3	4.53	8.99	134.58	109.5	1.78	02 Oct	185.9	15.49	32.78	142.37	114.0	3.93
23 Oct	144.4	9.69	18.68	124.89	103.8	3.20	03 Oct	214.0	16.64	49.42	125.73	104.3	4.73
24 Oct	214.0	15.85	34.53	109.04	94.1	4.98	04 Oct	266.0	20.31	69.73	105.42	91.8	6.27
25 Oct	288.0	21.14	55.67	87.90	80.0	7.27	05 Oct	349.0	25.59	95.32	79.83	74.3	9.15
26 Oct	364.0	28.63	84.30	59.27	58.7	10.73	06 Oct	499.0	34.69	130.01	45.14	46.9	16.46
27 Oct	422.0	34.25	118.55	25.02	28.1	17.98	07 Oct	261.0	41.59	171.60	3.55	4.4	28.11
28 Oct	85.0	22.70	141.25	2.32	2.9	-	08 Oct	0.0	3.55	175.15	0.00	0.0	-
29 Oct	0.0	2.32	143.57	0.00	0.0	-	1964						
1951							15 Sep	0.0	0.00	0.00	154.94	120.9	0.00
05 Nov	0.0	0.00	0.00	96.22	85.7	0.00	16 Sep	0.7	0.01	0.01	154.93	120.9	0.01
06 Nov	1.4	0.05	0.05	96.17	85.7	0.03	17 Sep	8.5	0.12	0.13	154.81	120.8	0.17
07 Nov	3.4	0.24	0.29	95.93	85.5	0.08	18 Sep	80.0	4.65	4.78	150.16	118.3	1.66
08 Nov	7.1	0.49	0.78	95.44	85.2	0.17	19 Sep	150.1	9.17	13.95	140.99	113.2	3.19
09 Nov	9.9	0.73	1.51	94.71	84.7	0.24	20 Sep	258.0	16.76	30.71	124.23	103.4	5.73
10 Nov	19.8	0.98	2.49	93.73	84.0	0.49	21 Sep	350.0	27.87	58.58	96.36	85.8	8.53
11 Nov	40.9	2.43	4.92	91.30	82.4	1.02	22 Sep	397.0	32.66	91.24	63.70	62.2	11.37
12 Nov	78.2	4.62	9.54	86.68	79.2	1.98	23 Sep	396.0	35.92	127.16	27.78	30.9	16.09
13 Nov	100.8	8.89	18.43	77.79	72.9	2.67	24 Sep	85.0	23.29	150.45	4.49	5.6	-
14 Nov	117.6	8.51	26.94	69.28	66.5	3.26	25 Sep	25.9	3.74	154.19	0.75	1.0	-
15 Nov	169.8	11.80	38.74	57.48	57.3	5.07	26 Sep	4.3	0.73	154.92	0.02	0.1	-
16 Nov	253.0	17.54	56.28	39.94	42.3	8.79	27 Sep	0.0	0.02	154.94	0.00	0.0	-
17 Nov	283.0	26.18	82.46	13.76	16.3	15.83	1967						
18 Nov	56.6	12.48	94.94	1.28	1.6	-	26 Aug	0.0	0.00	0.00	150.48	118.5	0.00
19 Nov	7.5	1.22	96.16	0.06	0.1	-	27 Aug	8.5	0.24	0.24	150.24	118.4	0.18
20 Nov	0.0	0.06	96.22	0.00	0.0	-	28 Aug	175.6	8.32	8.56	141.92	113.7	3.72
1953							29 Aug	391.0	24.71	33.27	117.21	99.2	8.87
04 Dec	0.0	0.00	0.00	98.81	87.4	0.00	30 Aug	617.0	40.61	73.88	76.60	72.0	16.42
05 Dec	2.1	0.06	0.06	98.75	87.4	0.05	31 Aug	719.0	62.88	136.76	13.72	16.2	40.35
06 Dec	8.5	0.37	0.43	98.38	87.1	0.21	01 Sep	22.7	13.70	150.46	0.02	0.1	-
07 Dec	20.5	1.10	1.53	97.28	86.4	0.50	02 Sep	0.0	0.02	150.48	0.00	0.0	-
08 Dec	40.4	2.45	3.98	94.83	84.8	0.99	1970						
09 Dec	63.7	4.53	8.51	90.30	81.7	1.59	08 Sep	0.0	0.00	0.00	188.72	138.3	0.00
10 Dec	89.0	6.48	14.99	83.82	77.2	2.29	09 Sep	0.8	0.02	0.02	188.70	138.3	0.02
11 Dec	115.9	8.89	23.88	74.93	70.8	3.11	10 Sep	3.4	0.15	0.17	188.55	138.1	0.06
12 Dec	140.9	11.13	35.01	63.80	62.3	4.03	11 Sep	7.4	0.44	0.61	188.11	138.0	0.14
13 Dec	165.7	13.21	48.22	50.59	51.6	5.21	12 Sep	13.7	0.83	1.44	187.28	137.6	0.26
14 Dec	184.1	15.41	63.63	35.18	37.9	6.75	13 Sep	26.2	1.54	2.98	185.74	136.8	0.51
15 Dec	160.0	15.65	79.28	19.53	22.5	7.62	14 Sep	45.9	2.98	5.96	182.76	135.4	0.89
16 Dec	103.4	11.99	91.27	7.54	9.2	7.70	15 Sep	76.4	4.94	10.90	177.82	132.9	1.40
17 Dec	42.5	5.87	97.14	1.67	2.1	-	16 Sep	106.2	7.39	18.29	170.43	129.1	2.11
18 Dec	9.9	1.47	98.61	0.20	0.3	-	17 Sep	157.2	10.96	29.25	159.47	123.4	3.20
19 Dec	0.0	0.20	98.81	0.00	0.0	-	18 Sep	229.0	16.20	45.45	143.27	114.5	4.83
1956							19 Sep	314.0	23.29	68.74	119.98	100.9	7.06
18 Oct	0.0	0.00	0.00	129.78	106.7	0.00	20 Sep	386.0	30.97	99.71	89.01	80.8	9.70
19 Oct	2.3	0.02	0.02	129.76	106.7	0.05	21 Sep	430.0	35.72	135.43	53.29	53.8	13.24
20 Oct	8.5	0.44	0.46	129.32	106.5	0.19	22 Sep	299.0	38.51	173.94	14.78	17.4	16.19
21 Oct	24.1	1.35	1.81	127.97	105.7	0.53	23 Sep	84.4	13.09	187.03	1.69	2.2	-
22 Oct	46.6	2.81	4.62	125.16	104.0	0.89	24 Sep	0.0	1.69	188.72	0.00	0.0	-
23 Oct	75.3	5.24	9.86	119.92	100.8	1.69	1974						
24 Oct	114.5	7.78	17.64	112.14	96.0	2.64	09 Sep	0.0	0.00	0.00	240.52	162.2	0.00
25 Oct	161.5	12.01	29.65	100.13	88.3	3.88	10 Sep	7.5	0.24	0.24	240.28	162.1	0.13
26 Oct	205.0	15.90	45.55	84.23	77.5	5.26	11 Sep	19.5	1.05	1.29	239.23	161.6	0.35
27 Oct	250.0	19.55	65.10	64.68	63.0	7.11	12 Sep	49.6	2.32	3.61	236.91	160.6	0.88
28 Oct	299.0	23.71	88.81	40.97	43.2	10.28	13 Sep	86.9	6.24	9.85	230.67	157.8	1.56
29 Oct	300.0	27.99	116.80	12.98	15.4	17.27	14 Sep	121.6	8.78	18.63	221.89	153.9	2.21
30 Oct	56.6	10.50	127.30	2.48	3.1	-	15 Sep	167.1	12.23	30.86	209.66	148.3	3.10
31 Oct	14.3	2.10	129.40	0.38	0.5	-	16 Sep	231.0	16.64	47.50	193.02	140.4	4.40
01 Nov	0.0	0.38	129.78	0.00	0.0	-	17 Sep	324.0	23.24	70.74	169.78	128.8	6.45
1958							18 Sep	459.0	32.78	103.52	137.00	110.9	9.85
06 Oct	0.0	0.00	0.00	128.91	106.2	0.00	19 Sep	592.0	46.49	150.01	90.51	81.8	14.78
07 Oct	0.3	0.01	0.01	128.90	106.2	0.01	20 Sep	510.0	55.78	205.79	34.73	37.5	18.84
08 Oct	11.0	0.69	0.70	128.21	105.8	0.24	21 Sep	104.8	32.30	238.09	2.43	3.1	-
09 Oct	29.7	1.83	2.53	126.38	104.7	0.66	22 Sep	0.0	2.43	240.52	0.00	0.0	-
10 Oct	48.4	3.30	5.83	123.08	102.7	1.08	1977						
11 Oct	71.6	5.06	10.89	118.02	99.7	1.62	29 Aug	0.0	0.00	0.00	151.10	118.8	0.00
12 Oct	109.6	7.32	18.21	110.70	95.1	2.54	30 Aug	38.2	1.96	1.96	149.14	117.8	0.79
13 Oct	163.8	11.62	29.83	99.08	87.6	3.95	31 Aug	78.4	4.65	6.61	144.49	115.2	1.65
14 Oct	220.0	16.69	46.52	82.39	76.2	5.69	01 Sep	132.2	8.91	15.52	135.58	110.1	2.85
15 Oct	280.0	21.38	67.90	61.01	60.1	8.16	02 Sep	205.0	13.95	29.47	121.63	101.9	4.59
16 Oct	340.0	27.06	94.96	33.95	36.8	12.66	03 Sep	287.0	21.53	51.00	100.10	88.3	6.90
17 Oct	164.2	27.11	122.07	6.84	8.4	12.80	04 Sep	348.0	28.14	79.14	71.96	68.5	9.50
18 Oct	39.1	6.43	128.50	0.41	0.6	-	05 Sep	394.0	32.05	111.19	39.91	42.3	13.68
19 Oct	2.4	0.32	128.82	0.09	0.1	-	06 Sep	214.0	26.18	137.37	13.73	16.3	-
20 Oct	0.0	0.09	128.91	0.00	0.0	-	07 Sep	79.6	10.79	148.16	2.94	3.7	-
							08 Sep	0.0	2.94	151.10	0.00	0.0	-

Table 2 (continued)

Date	Lake at End of Day	Outflow 24-hr Volume	Accum Outflow	Volume Remaining	Head	CA
	m	$10^6 m^3$	$10^6 m^3$	$10^6 m^3$	m	m^2
1979						
18 Oct	0.0	0.00	0.00	127.04	105.1	0.00
19 Oct	56.6	3.18	3.18	123.86	103.2	1.26
20 Oct	212.0	16.15	19.33	107.71	93.2	4.96
21 Oct	280.0	20.55	39.88	87.16	79.5	7.09
22 Oct	351.0	27.89	67.77	59.27	58.7	10.35
23 Oct	408.0	32.78	100.55	26.49	29.6	16.94
24 Oct	0.0	26.49	127.04	0.00	0.0	-
1982						
17 Sep	0.0	0.00	0.00	177.56	132.8	0.00
18 Sep	23.2	1.00	1.00	176.56	132.2	0.46
19 Sep	30.9	2.35	3.35	174.21	131.0	0.61
20 Sep	40.5	3.08	6.43	171.13	129.5	0.80
21 Sep	44.5	3.67	10.10	167.46	127.6	0.89
22 Sep	65.1	4.75	14.85	162.71	125.1	1.31
23 Sep	93.4	6.85	21.70	155.86	121.4	1.91
24 Sep	133.1	9.79	31.49	146.07	116.0	2.79
25 Sep	184.1	13.70	45.19	132.37	108.2	4.00
26 Sep	255.0	18.96	64.15	113.41	96.8	5.85
27 Sep	326.0	25.08	89.23	88.33	80.3	8.22
28 Sep	382.0	30.58	119.81	57.75	57.5	11.38
29 Sep	340.0	32.40	152.21	25.35	28.5	14.39
30 Sep	169.9	22.72	174.93	2.63	3.3	21.13
01 Oct	0.0	2.63	177.56	0.00	0.0	-
1985						
21 Nov	0.0	0.00	0.00	159.24	123.2	0.00
22 Nov	3.1	0.13	0.13	159.11	123.2	0.06
23 Nov	15.0	0.78	0.91	158.33	122.7	0.31
24 Nov	28.6	1.88	2.79	156.45	121.7	0.59
25 Nov	45.6	3.21	6.00	153.24	120.0	0.94
26 Nov	55.5	4.37	10.37	148.87	117.6	1.16
27 Nov	98.3	6.64	17.01	142.23	113.9	2.08
28 Nov	141.0	10.34	27.35	131.89	108.0	3.06
29 Nov	183.8	14.03	41.38	117.86	99.6	4.16
30 Nov	226.0	17.71	59.09	100.15	88.3	5.43
01 Dec	269.0	21.40	80.49	78.75	73.6	7.08
02 Dec	334.0	26.03	106.52	52.72	53.4	10.32
03 Dec	311.0	27.84	134.36	24.88	28.0	13.28
04 Dec	143.0	19.61	153.97	5.27	6.5	-
05 Dec	0.0	5.27	159.24	0.00	0.0	-

beginning of the jokulhlaup event. It also provides a basis upon which a forecast procedure can be developed.

JOKULHLAUP FORECAST PROCEDURE

In 1969 and in subsequent years, several lake-level markers were installed which are visible from the air. National Weather Service hydrologists periodically fly over the lake to determine whether it is near the level at which it may dump. If it has reached a high level, a jokulhlaup may be imminent, but it is not possible to predict just when it will occur. The frequency of aerial observation is then increased, while noting the lake level, photographing whatever might be of value in later studies, looking closely at the lake edges for evidence of falling stage, and observing the glacier terminus for signs of lake drainage. At the River Forecast Center, the operational, i.e., current, Snow River hydrograph is watched for a change that might indicate the start of the jokulhlaup. When such a change appears, an aerial reconnaissance will be made, weather permitting, to verify that the jokulhlaup has started. The river observer will be asked to make two or more stage readings per day through the event.

On the second or third day, while the lake outflow is still small, the CA versus accumulated outflow relationship will already have been established and the total remaining jokulhlaup hydrograph can be forecast. The forecast procedure is simple, but tedious if done manually. A computer program has been developed which requires as input the observed Snow River flows up to date, the forecast non-jokulhlaup flows (same as routine daily runoff forecast), and the beginning lake elevation or storage. The program computes the equation of the CA versus accumulated outflow relationship based on observed values to date. The program fore-

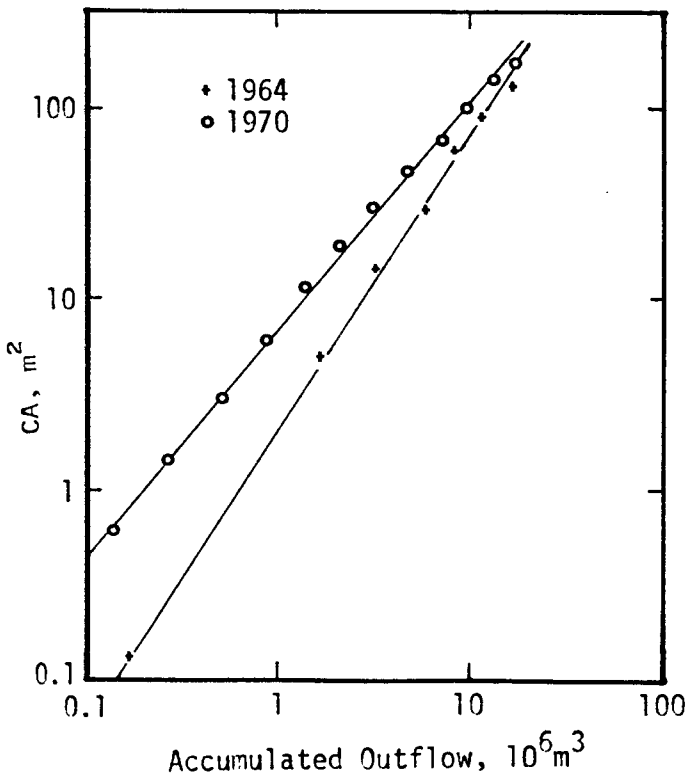


Figure 2. Glacier-dammed Lake Accumulated Outflow versus CA.

casts by selecting a discharge expected 24 hours after the last observation or determination. The average of that selected discharge and the previous discharge determines the volume of outflow for the day, which in turn determines the remaining lake volume. Applying equation (2) yields the head which corresponds to the selected discharge. A value of CA is obtained from equation (4). Another value of CA is obtained from the CA versus accumulated outflow relationship. If the two values of CA are alike (within 1%), the selected discharge is deemed correct. If they are not alike, another discharge is systematically selected and the procedure repeated until agreement is reached. The program then proceeds to the next day and the next. Eventually, agreement cannot be reached because orifice control will have been lost due to low head. The program then projects the hydrograph in a straight line to zero flow, the line being sloped to contain the remaining lake volume, which is small. The forecast is updated daily as better definition of the CA versus accumulated outflow relationship evolves.

JOKULHLAUP FORECAST EXAMPLE

The 1985 jokulhlaup was chosen to illustrate the results of applying the forecast procedure, primarily because it was free of unrelated precipitation events and most other perturbations in the hydrographs. As it was very late in the season, the Kenai River gage at Cooper Landing was the only gage in the upper Kenai River system that was still operating; all other stations had shut down for the winter. On 25 November, a small rise on the Kenai River was unexplained by weather, although the weather did prevent flying a reconnaissance of Snow River.

Kenai Lake inflows were determined that would produce the observed flows at Cooper Landing.

All streams in the vicinity were known to be low and steady, so the Kenai Lake inflows were assumed to be composed of steady flows from Trail River, Snow River below the glacier, and other intervening areas. All of the increase in flow was attributed to dumping of the glacier-dammed lake. All flow values so determined were entered into the jokulhlaup forecast program along with an estimate of the lake storage. From earlier flights over the lake, it was estimated that the head on 25 November was probably 130 or 131 meters. However, it was also observed that the glacier had extended into the lake area, and the storage would be less than would be computed by equation (1). The storage was estimated to be 160 million cubic meters; and the resulting head computed by equation (2) and shown in Table 2 is not accurate. Post-event analysis of the hydrograph at Cooper Landing showed that storage estimate to be nearly correct.

Figures 3 and 4 show the hydrographs of the first forecast, which was made on 25 November, compared with the actual hydrographs at the glacier terminus and at Cooper Landing. Figure 4 shows the minor rise of 23-25 November that alerted the River Forecast Center of the beginning of a hydrologic event suspected of being a jokulhlaup. That rise was sufficient to establish the CA versus accumulated outflow relationship upon which the forecast was based. While the first forecast was not especially good, the peak flow from the glacier-dammed lake was predicted within 10 percent, and the crest stage at Cooper Landing was very close.

Over the next two days, 26 and 27 November, high wind produced a considerable setup, or wind tide, and transported some of the Kenai Lake ice cover past the telemetered Cooper Landing stream gage, which produced an anomaly in its hydrograph. On 28 November, calm conditions returned, and a new forecast

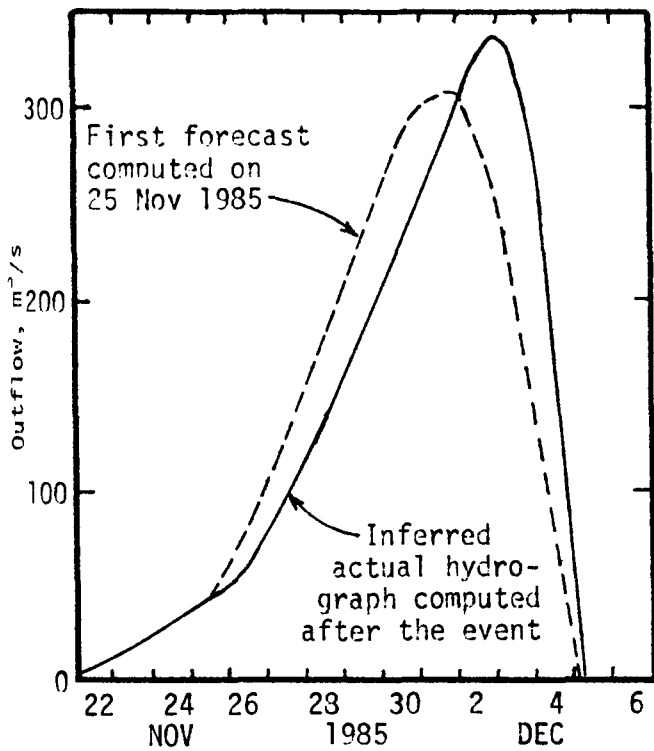


Figure 3. First Forecast and Inferred Actual Hydrographs of Glacier-dammed Lake Outflow of 1985.

was made based upon a better defined CA versus accumulated outflow relationship. That forecast is not shown as it was nearly perfect, mostly coinciding with the actual hydrographs.

As shown in Figure 4, the river stage, or gage height, is the height of the water surface above an arbitrary datum; it is not necessarily a measure of the depth of the water. The gage telemetry reports in units of feet and the records are kept in feet. The rise shown in Figure 4 is very close to 5.0 feet, or 1.5 meters.

CONCLUSION

It has been demonstrated that, during a jokulhlaup on Snow River, the cross-sectional area of the outlet of the glacier-dammed lake is proportional to the amount of water that has passed through the outlet. That proportion differs from event to event but it reveals itself early in each event, and that enables forecasting the remainder of the jokulhlaup several days in advance of the peak flow.

REFERENCES

- Chapman, D. L., 1981. Jokulhlaups on Snow River in Southcentral Alaska. NOAA Technical Memorandum, NWS AR-31, National Weather Service, Anchorage, Alaska.
- Post, A. and L. R. Mayo, 1971. Glacier Dammed Lakes and Outburst Floods in Alaska. Hydrologic Investigation Atlas, HA-455, U.S. Geological Survey, Washington, D.C.

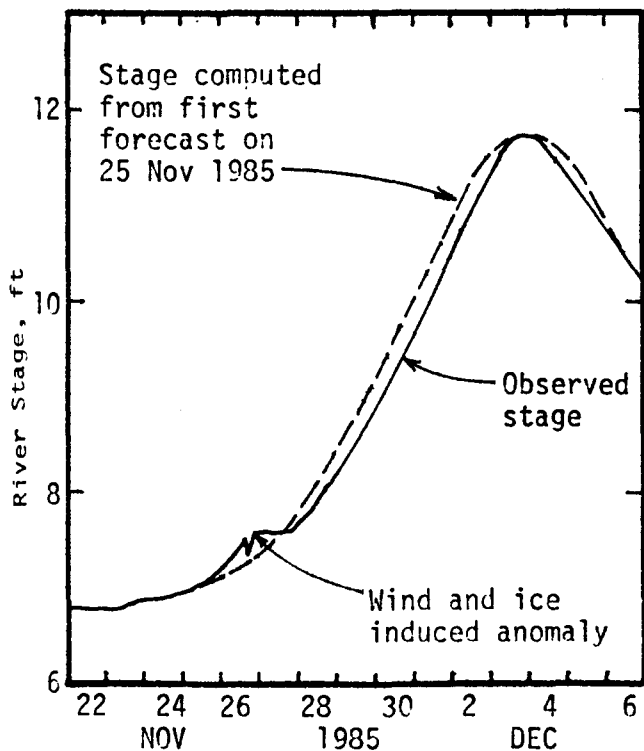


Figure 4. First Forecast and Observed Stage Hydrographs of Kenai River at Cooper Landing.

SUSPENDED SEDIMENT BUDGET OF A GLACIER-FED LAKE - EKLUTNA LAKE, ALASKA

Jeffrey H. Coffin and William S. Ashton*

ABSTRACT: Suspended sediment data from Eklutna Lake, a glacier-fed lake in southcentral Alaska, were analyzed to determine the annual sediment budget of the lake. The data may be more valuable than previously published methods for estimating suspended sediment yield from small to moderate glacier-covered basins in the region or in similar areas.

Streamflow and sediment measurements were made on two major inflow streams and the lake outflow. Instantaneous values of discharge and total suspended sediment concentration (TSS) were used to develop regression relationships for each of the inflow streams.

Observed suspended sediment concentrations ranged from 0.15 to 570 mg/l in the inflow streams and from 0.50 to 36 mg/l in the outflow. The suspended sediment entering Eklutna Lake for the one-year period from October 1983 through September 1984 was 42,000 metric tons (46,000 tons). The amount leaving the lake during the same period was 940 metric tons (1030 tons), indicating a trap efficiency of 98%. Good agreement was found with Brune's trap efficiency relationship, but poor agreement was observed with Guymon's sediment yield relationship. (KEY TERMS: suspended sediment; sediment budget; trap efficiency; glacial lake; Eklutna Lake; Alaska.)

INTRODUCTION

Suspended sediment and water discharge measurements were made on two major inflow streams and the outflow stream of Eklutna Lake during a one-year period.

Information on behavior of suspended sediment within a glacier-fed lake was collected to assess environmental impacts of suspended sediment within a proposed hydroelectric reservoir on the glacier-fed Susitna River in southcentral Alaska. A reservoir simulation model was tested on Eklutna Lake and then applied to the proposed Susitna reservoir (Wei and Hamblin, 1986). Values of reservoir trap efficiency and regional sediment yield were computed for Eklutna Lake and compared with published values (Brune, 1953; Guymon, 1974).

STUDY AREA

Eklutna Lake is a glacier-fed lake near Anchorage, Alaska (Figure 1). Twenty percent of the lake's 287 square km (111 sq mi) watershed is covered by glaciers. The glacier-covered area is drained by two primary tributaries which merge approximately 1 km upstream from the lake's southeast end. One tributary originates from Eklutna Glacier and was designated Glacier Fork in this study; the other was called East Fork. Twenty percent of East Fork's 104 sq km (40 sq mi) basin is glacier-covered, and fifty-four percent of Glacier Fork's 70 sq km (27 sq mi) basin is glacier-covered. Although these two creeks drain about 50% of the lake's watershed, they provide about 90% of the lake inflow (based on flow data for the current study period). Elevations within the Eklutna Lake drainage basin range from 260 to 2440 m (850 to 8000 ft) above the mean sea level.

Eklutna Lake's depth reaches a maxi-

* Respectively, Senior Civil Engineer/Hydrologist and Hydrologist, R&M Consultants, Inc., 5024 Cordova Street, Anchorage, Alaska 99503



FIGURE 1. LOCATION MAP

mum of 60 m (200 ft) in several areas around the center, at a full-pool elevation of 264 m (R&M Consultants, 1982). The lake is approximately 11 km (7 mi) long and 1 km (0.7 mi) wide (Figure 2). The lake is a reservoir for a 33-megawatt hydroelectric powerplant. The powerplant is supplied by a power tunnel which has its intake at the northwest end of the lake. The only other lake outlet is an uncontrolled spillway which has discharged only very infrequently since its construction in the 1950's.

The lake water surface elevation typically ranges from a high of 264 m (868 ft) above sea level during September or October to a low of 252 m (828 ft) during June. Peak outflow for power production occurs during the winter and spring months

(January-June). The average hydraulic residence time of the lake (lake volume divided by mean annual inflow) is 1.8 years (R&M Consultants, 1982), and the residence time was 2.0 years for the 1984 study period.

FIELD DATA COLLECTION METHODS

A stilling well, float, and strip-chart water-level recorder were installed in East Fork and Glacier Fork and operated through the open-water season of 1984. Periodic discharge measurements were made to determine stage-discharge relationships. A one-liter, depth-integrated water sample was collected twice per week at each gaging station

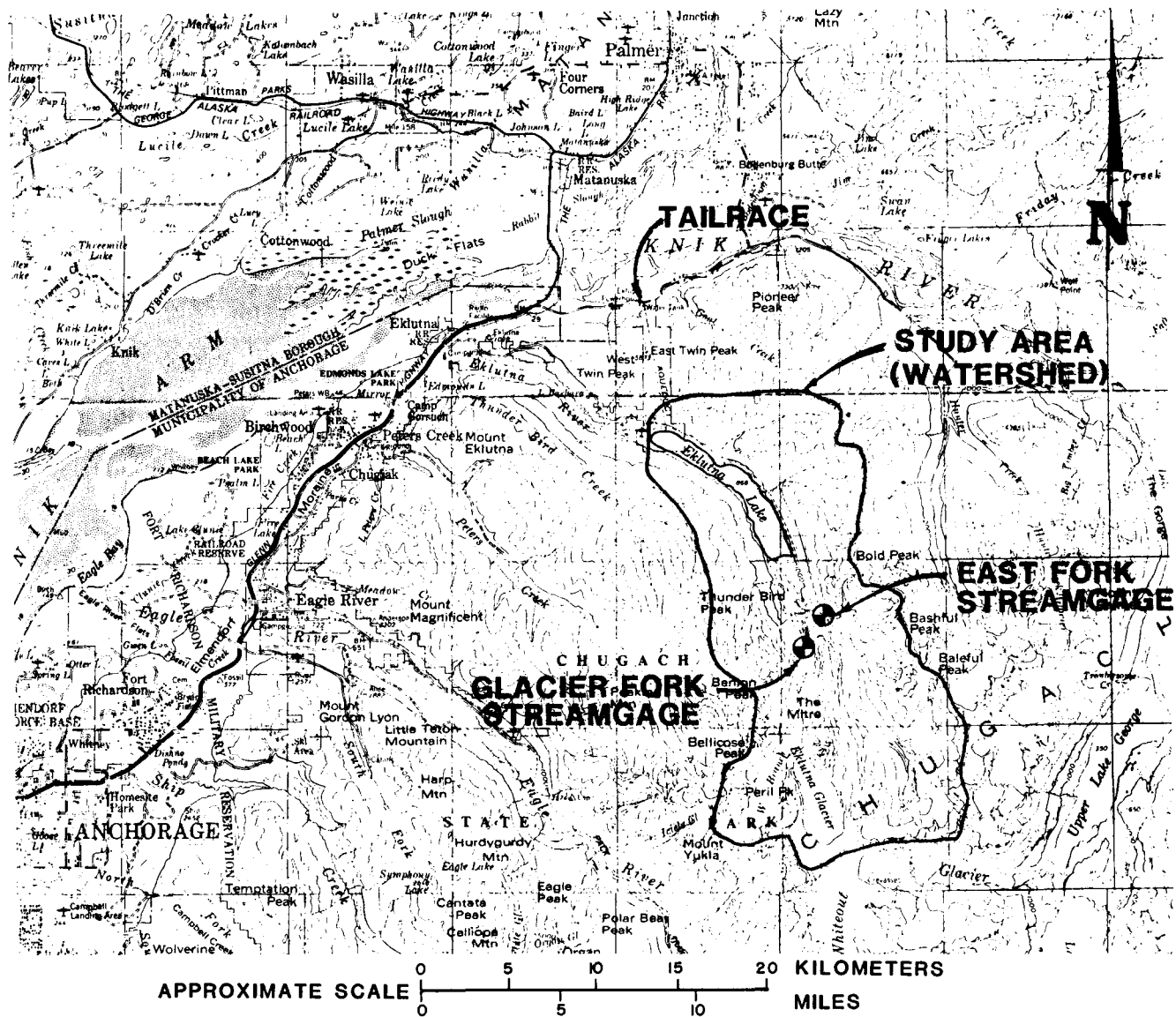


FIGURE 2. VICINITY MAP SHOWING EKLUTNA LAKE WATERSHED AND POWERPLANT TAILRACE

from early June through freeze-up (about mid-November) and analyzed for total suspended solids (TSS) concentration. A hand-held DH-48 sampler was used for sampling, and TSS determinations were made with 0.45-micron filters using standard procedures for detection of nonfilterable residue (APHA et. al., 1981).

Measurements of daily lake outflows

were provided by the Eklutna Hydroelectric Project, Alaska Power Administration. Depth-integrated samples were taken twice per week from the lake outflow in the powerplant tailrace on the same dates the inflow streams were sampled, and TSS concentrations were determined in the laboratory in the same manner as for the inflow samples.

ANALYTICAL METHODS

The TSS concentrations determined for each of the inflow streams were matched with the instantaneous streamflows at the times of sampling. These data pairs were then related to derive a regression equation of TSS as a function of discharge. The regression equations were used to predict mean daily TSS concentrations from mean daily discharges for each stream for the open-water period. The daily values for discharge and TSS were then used to compute each site's daily sediment inflow to the lake. Changes in flow and TSS were assumed to be negligible between the gaging sites and the lake.

During the ice-covered season, different relationships were used because the TSS and streamflow were both very low. Winter flows were estimated from extrapolated recessions of the fall hydrographs and from occasional winter discharge measurements, made approximately once per month. TSS concentrations were estimated by interpolating between concentrations sampled at the times of discharge measurements.

Monthly-averaged TSS concentrations for the outflow were computed from the sampled concentrations, which had been obtained twice per week during the open-water season and once per month during the winter season. The total release of sediment from the lake was computed from the monthly outflow volume and the average TSS concentration (Table 1).

RESULTS

Good relationships were observed between TSS and discharge on both inflow streams, with correlation coefficients of 0.88 and 0.91 for East Fork and Glacier Fork, respectively (Figure 3). Measured suspended sediment concentrations ranged from 0.15 to 570 mg/l in the inflow streams and from 0.50 to 36 mg/l in outflow (R&M Consultants, 1985).

The sampled inflow data for East Fork and Glacier Fork are plotted in Figure 4. The graphs show mean daily discharge and instantaneous values of TSS concentration for each site, indicating the period June

through August to be most prominent for contributing flow and sediment to the lake. Figure 5 shows TSS concentration of the outflow for the same period. Little variation is seen around the base level of 2-4 mg/l, except for a few "spikes" in the plot in July and August. The outflow's TSS concentration varied fairly smoothly through the year, as the lake diluted the high concentrations observed in the inflow streams.

Table 1 summarizes all the inflow and outflow suspended sediment data for the study period on a monthly basis. Examination of the monthly totals of sediment transport (thousands of kg) reveals that over 90% of the inflow sediment occurs during July and August and over 99% occurs during June through September. The outflow of sediment, however, is relatively uniformly distributed throughout the year.

DISCUSSION

Eklutna Lake's trap efficiency of 98% is in good agreement with generalized curves of trap efficiency developed by Brune (1953). Brune's curves, which relate trap efficiency to hydraulic residence time, give a median trap efficiency of 97.5%, with envelope curves at 95 and 100% for Eklutna Lake's 2-year residence time.

Suspended sediment data from the Eklutna Lake basin show differences from the regional suspended sediment yield relationship developed by Guymon (1974) by an order of magnitude. Eklutna Lake's 42,000 metric tons (46,000 tons) of sediment input from 174 sq km (67 sq mi) above the two gaging stations equates to 248 metric tons (tonnes) per sq km (707 tons per sq mi). When each tributary is considered individually, Guymon's relationship indicates theoretical yields of about 182,000 tonnes (200,000 tons) per year from East Fork and about 364,000 tonnes (400,000 tons) per year from Glacier Fork (using distances to the glaciers of 10 miles and 3 miles for East Fork and Glacier Fork, respectively).

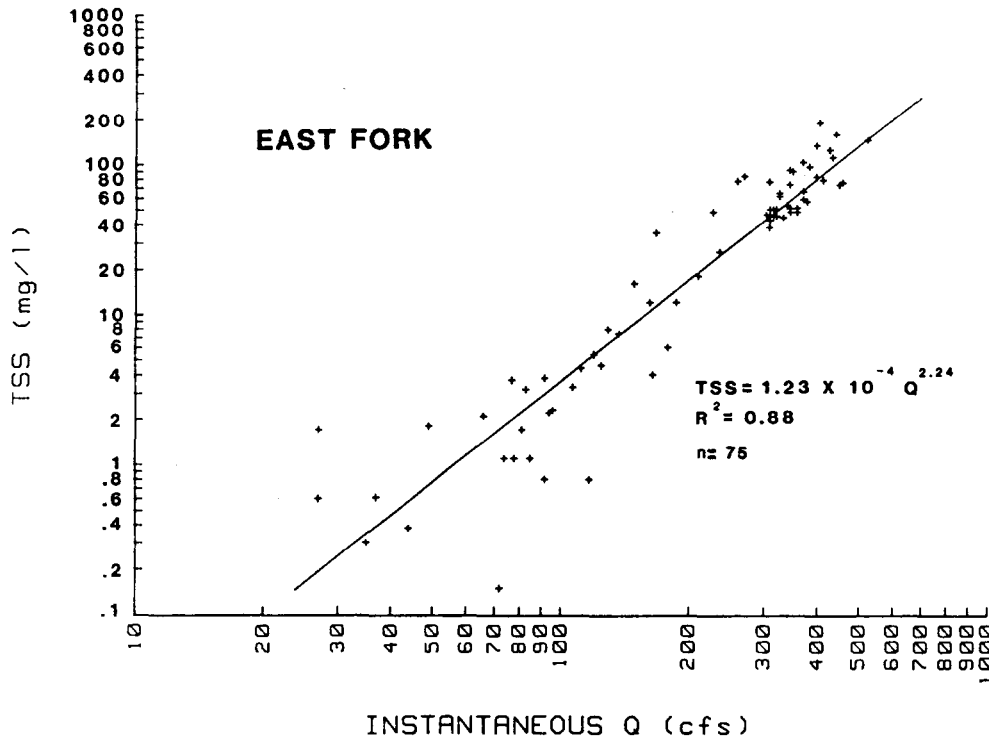
The values of Guymon's (1974) λ computed (50 and 5.5 miles, 31 and 3.4 km) are at and below the low limit of Guymon's data, indicating the relationship may not

Table 1. Eklutna Lake Sediment Inflow and Outflow for Water Year 1984

MONTH	INFLOW			OUTFLOW			BALANCE	
	Avg. Water Flow Rate (m ³ /sec)	Avg. TSS Concn. (mg/l)	Sediment Inflow (SEDIN) (1000 kg)	Avg. Water Flow Rate (m ³ /sec)	Avg. TSS Concn. (mg/l)	Sediment Outflow (SEDOUT) (1000 kg)	Net Sediment Input (SEDIN-SEDOUT) (1000 kg)	Cumulative Sediment Input (SEDIN-SEDOUT) (1000 kg)
OCT 83	4.6	21.0	259	3.3	3.8*	34	225	225
NOV 83	1.3	4.0	13	4.0	4.6*	48	-35	190
DEC 83	1.4	4.0	15	6.3	3.0*	51	-36	154
JAN 84	0.9	3.0	7	10.9	2.5*	73	-66	88
FEB 84	0.8	3.0	6	12.3	2.5*	74	-68	20
MAR 84	0.6	3.0	5	13.1	2.0*	70	-65	-45
APR 84	0.7	3.0	5	13.0	2.5*	84	-79	-124
MAY 84	3.0	4.4	35	9.4	2.5	63	-28	-152
JUN 84	10.6	78.9	2,168	10.1	2.0	52	2,116	1,964
JUL 84	25.0	215.4	14,423	5.8	11.0	171	14,252	16,216
AUG 84	30.2	295.7	23,918	4.2	10.0	112	23,806	40,022
SEP 84	7.4	61.7	1,183	4.3	5.6	62	1,121	41,143
TOTALS			42,037			894		41,143

*TSS concentration estimated with data from Water Year 1985.

$$[\text{Trap Efficiency} = \frac{(\text{SEDIN}-\text{SEDOUT})}{(\text{SEDIN})} = \frac{42,037-894}{42,037} = 98\%]$$



(NOTE: 1.0 CU FT/SEC IS 0.0283 CU M/SEC)

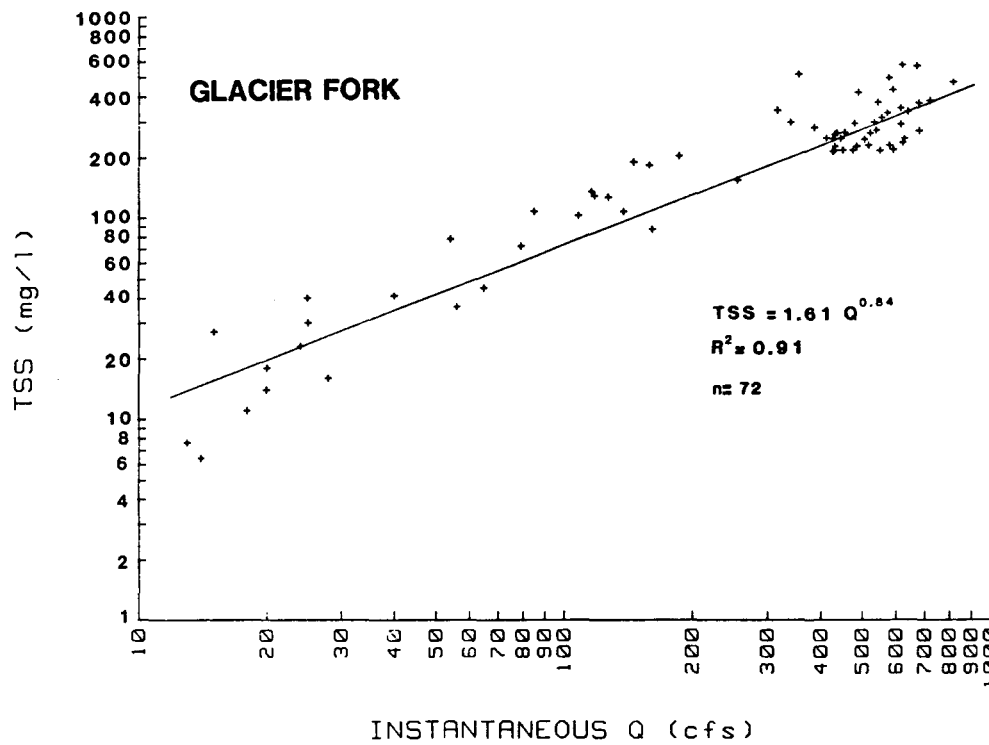


Figure 3. Regression Relationships Between Total Suspended Sediment Concentration and Instantaneous Flow for East Fork and Glacier Fork, Using 1984 Data.

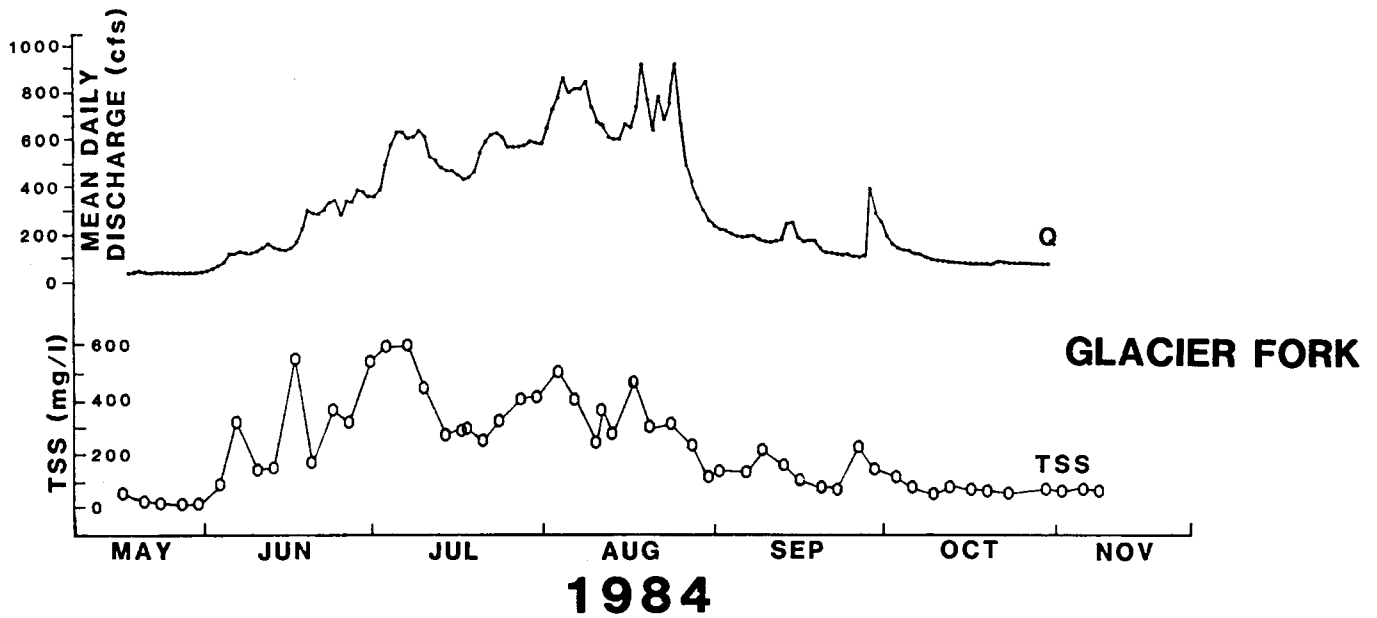
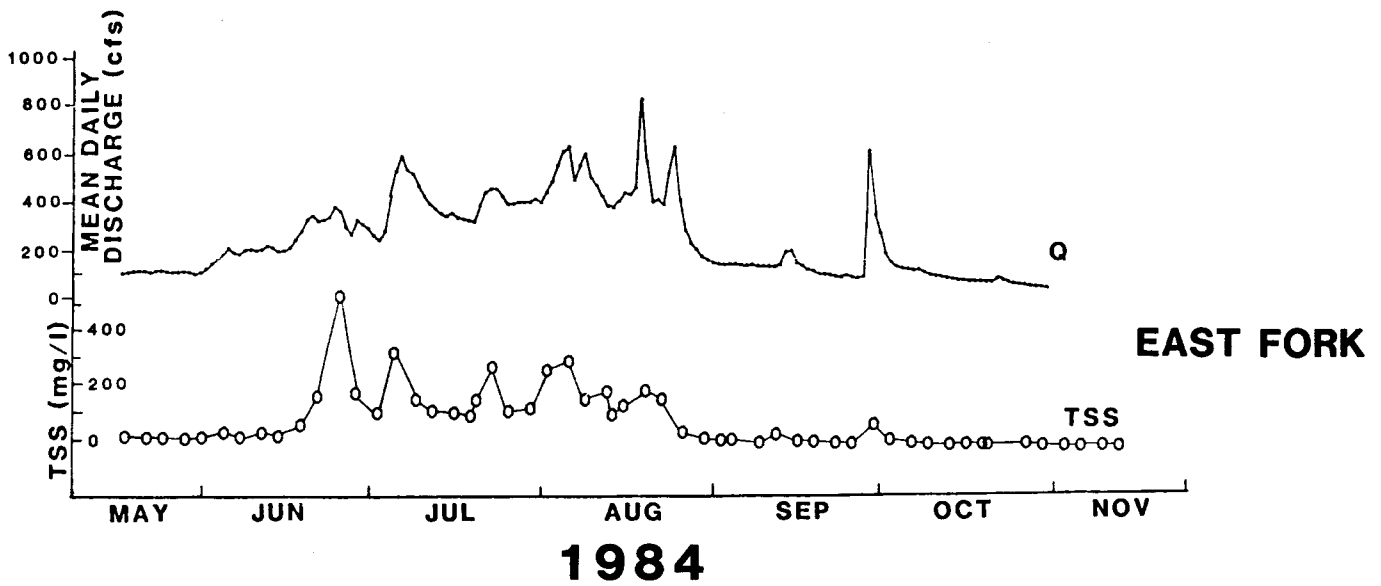


Figure 4. Mean Daily Discharge and Instantaneous Sampled Concentrations of Total Suspended Sediment for East Fork and Glacier Fork for 1984 Open-Water Season.

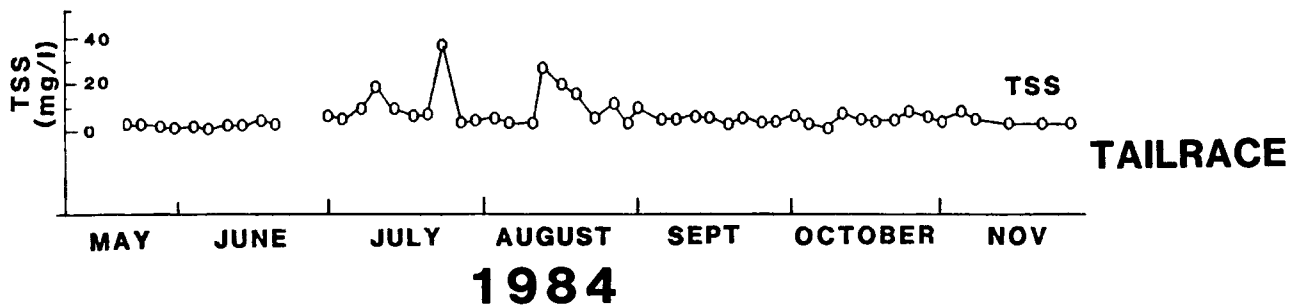


Figure 5. Instantaneous Sampled Concentration of Total Suspended Sediment for Eklutna Lake Outflow (Tailrace) for 1984 Open-Water Season.

LITERATURE CITED

be valid for drainage basins this small, with this high a percentage of glacier cover, or gaged this close to the glaciers (all factors which contribute to a low λ and a high theoretical sediment yield and which were outside the values of Guymon's data).

Another possibility is that 1984 was far below average in terms of sediment yield at Eklutna, but this would not likely explain the order of magnitude difference. Guymon's report was the only prior study found which had published values for regional sediment yield in Alaska.

The data presented here may be more valuable than previously published methods for estimating yield of suspended sediment from glacier-covered basins of small to moderate size (e.g. less than 250 sq km or 100 sq mi) in southcentral Alaska or in an area with similar geological and climatological conditions. The presentation of the data on quantities of suspended sediment entering and leaving the lake may also be useful for making estimates of sedimentation in other glacier-fed reservoirs. Comparison with previous studies indicates that trap efficiency of a glacier-fed lake may be more easily extended to other study areas than is annual sediment yield of a glacier-covered drainage basin.

ACKNOWLEDGMENTS

The field work and primary data reduction for this project were performed for the Alaska Power Authority under contract to Harza-Ebasco Susitna Joint Venture for the Susitna Hydroelectric Project. The Alaska Division of Parks and Chugach State Park rangers were very gracious for permitting installation and operation of the field instrumentation within the park. The Eklutna Hydroelectric Project, Alaska Power Administration, was very helpful in providing data on lake outflow through the powerplant. Analyses of suspended sediment concentration were performed by Chemical and Geological Laboratories of Alaska, Inc., in Anchorage. We thank Jim Munter and an anonymous reviewer for their review comments.

- American Public Health Association (APHA), American Water Works Association and Water Pollution Control Federation. 1981. Standard methods for the examination of water and wastewater. Fifteenth edition, 1980. APHA, Washington, D.C.
- Brune, C.M. 1953. Trap efficiency of reservoirs. Trans. Am. Geophys. Union, June, p. 884.
- Guymon, G.L. 1974. Regional sediment yield analysis of Alaska streams. Journal of the Hydraulics Division, American Society of Civil Engineers, Vol. 100, No. HY1, Proc. Paper 10255. January 1974. pp. 41-51.
- R&M Consultants, Inc. 1982. Glacial lake studies, interim report. Prepared for Alaska Power Authority under contract to Acres American, Inc. December.
- R&M Consultants, Inc. 1985. Glacial lake physical limnology studies, Eklutna Lake, Alaska (Draft). Prepared for Alaska Power Authority under contract to Harza-Ebasco Susitna Joint Venture. June.
- Wei, C.Y. and P.F. Hamblin. 1986. Reservoir water quality simulation in cold regions. In: Proceedings of the Cold Regions Hydrology Symposium, American Water Resources Association. July.

ANNUAL RUNOFF RATE FROM GLACIERS IN ALASKA;
A MODEL USING THE ALTITUDE OF GLACIER MASS BALANCE EQUILIBRIUM

Lawrence R. Mayo*

ABSTRACT: Glaciers in Alaska occur in high precipitation areas where the runoff is difficult to measure, yet hydrologically important. The spatial variability of glacier runoff is understood poorly. The equilibrium line altitude (ELA) of glaciers is related inversely to the average precipitation rate. Therefore, information about the average runoff from individual glaciers is contained in ELA data. This newly evaluated information about runoff is available from topographic maps. An ELA runoff model proposed determines average annual runoff from basins in Alaska. As a test the runoff rate was calculated for the Knik River basin, Alaska, using the model is 2.0 m/yr which compares with the average rate of 2.03 m/yr measured from 1959 to 1985.

Applied to an ungaged site in Alaska, the Bering Glacier drainage basin, the ELA model indicates that 34 km³ of water is produced annually from this basin which contains Alaska's largest glacier. Furthermore, Bering Glacier is the source of 76 percent of the discharge from the drainage basin and the average discharge of the Bering Glacier drainage into the Gulf of Alaska is about 1080 m³/s.

(KEY TERMS: glaciers; runoff; Alaska; snow and ice melt; estimation technique.)

INTRODUCTION

Glaciers in Alaska occur in areas of high precipitation, most of which arrives as wind-blown snow. Measuring that precipitation is difficult. Much of the precipitation remains in storage for time

periods ranging from a few hours to centuries, but eventually runs off.

Runoff from glaciers is almost as difficult to measure as is precipitation because glacier-fed rivers are shifting-bed, braided streams that are rarely stable gaging sites. Even though areas with glaciers are widespread and therefore important, relatively little is known about their runoff.

Estimates of runoff from basins with glaciers at ungaged locations are often needed. For example, most of the glacier runoff from areas such as the St. Elias Mountains, cannot be gaged because part of the water flows via innumerable short, braided rivers to the coast, and part of the water flows sub-glacially directly into the ocean. Knowledge of that runoff is important, however, to other scientific problems such as understanding the dynamics of the coastal North Pacific gyre circulation (Royer, 1982), and developing reliable weather forecasting models.

Multivariate regression analyses used to generate equations for estimating annual river discharge in Alaska have been proposed (Parks and Madison, 1985, p. 20). Their analyses obtained the highest success ($r^2=0.98$) for gaged basins using drainage area and precipitation as independent variables. Basin area, however, is not a truly independent variable because discharge is equal to runoff rate times drainage area. Furthermore, the precipitation map they used (U.S. National Weather Service, 1972) is not independent from discharge data because it was drawn by the present author to conform with the runoff data.

*U.S. Geological Survey, 101 12th Ave., Box 11, Fairbanks, Alaska 99701.

Input for a runoff model must be independent from existing runoff data and must be influenced strongly by precipitation. The model results would be most useful if they could be obtained from existing, readily available information for extensive remote areas where the cost of field investigations is high. Runoff

data from three research glacier basins, Wolverine, Gulkana, and McCall (Figure 1) are analysed in this paper to provide a simple model whereby glacier runoff can be estimated reliably in Alaska.

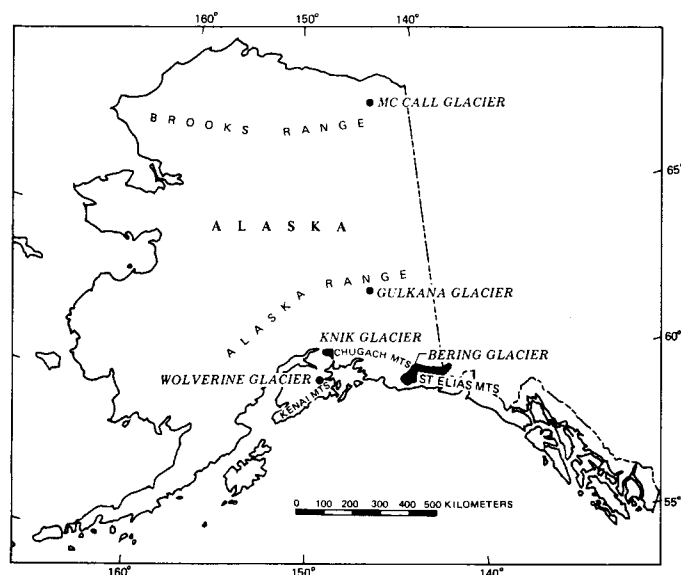


Figure 1. Locations of Glaciers used in this study.

GLACIER MASS BALANCE EQUILIBRIUM ALTITUDE

Information about spatial variations of precipitation and runoff rates is potentially contained in analyses of variations of glacier equilibrium line altitude. The equilibrium line altitude, or ELA, is the altitude at which snow accumulation is equal to snow melt. Meier and Post (1962) recognized that ELA is a function of precipitation. Increased snowfall tends to lower the ELA. Glaciers in a high precipitation climate receive considerably more snow than do glaciers in a drier, more continental climate. For a limited range of latitude, the average ELA in high precipitation areas is at relatively low altitude, and higher where drier.

Péwe and Reger (1972) and Østrem et al. (1981) used the relation of glacier ELA in Alaska to analyse precipitation patterns. However, ELA information has not been applied previously to studies of runoff.

DETERMINATION OF ELA FROM TOPOGRAPHIC MAPS

Time-averaged equilibrium line altitudes (ELA) of glaciers can be determined from topographic maps with varying degrees of precision depending on quality of the maps and the presence of mappable geomorphic indicators of glacier mass balance equilibrium. Using U.S. Geological Survey topographic maps of Alaska, the highest quality information is available at the largest scale, 1:63,360. These maps are readily available, accurate, and cover almost all glacierized areas of Alaska.

The ELA is the altitude of the boundary between a glacier's accumulation zone and its ablation zone. These two zones can be identified on high-quality topographic maps. Snow accumulation together with glacier flow in the accumulation zone cause dust and rock debris on the glacier from surrounding mountains to submerge into the glacier. The surface is therefore almost always relatively clean, smooth snow. Friction at the glacier edge retards this submergence, leaving a thin up-turned glacier edge against the adjoining mountain slope.

Ice from the accumulation zone flows into the ablation zone replacing (only approximately) the melt losses from the glacier. In this zone, the previously-deposited snow mass and rock debris emerges to the glacier surface. In late summer when the ablation zone is bare of snow and the old ice, mantled with accumulated rock debris, is exposed. This accumulation of rock is called supraglacial till and forms medial moraines. On the air photos the topographic maps are compiled from, this rock debris usually appears black, in contrast to the white color of the ice, and is mapped with a stipple pattern. Friction at the glacier ablation zone edge retards emergence flow, leaving a narrow valley between the glacier and the adjoining mountain slope.

The rock debris and edge valleys of the ablation zone, and the upturned glacier edges in the accumulation zone are not small features; they show prominently on high-quality topographic maps. The central part of Gannett Glacier (Figure 2) near Knik Glacier illustrates these features.

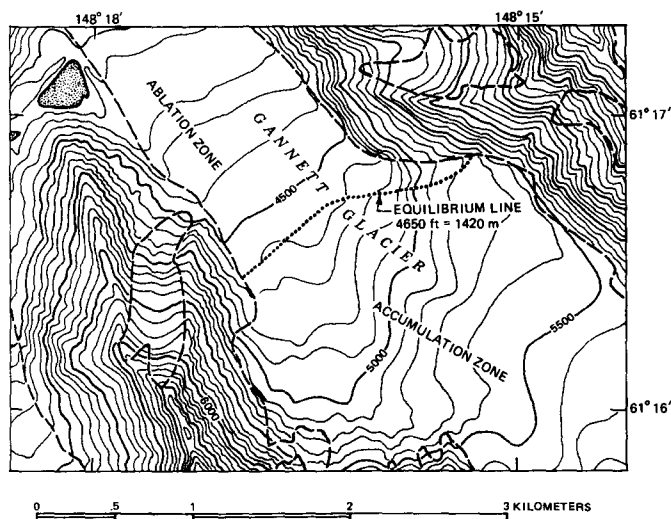


Figure 2. Central area of Gannett Glacier showing topographic features used to determine the glacier equilibrium line. Contour interval, 100 feet (30.48 meters).

The glacier zones determined from topographic maps represent the average glacier mass balance conditions over a period of many years, probably decades, because significant glacier flow responses to changing climatic conditions requires time. It is, therefore, useful for analysing only average runoff conditions.

RELATION OF ELA TO ANNUAL RUNOFF

Research by the U.S. Geological Survey at Wolverine Glacier, Kenai Peninsula, and Gulkana Glacier, Alaska Range; and by the University of Alaska at McCall Glacier, Brooks Range provide measurements of the glacier component of runoff in Alaska. Runoff from the glaciers originates from snow and ice ablation, rainfall, and condensation. Annual ablation, the dominant source of runoff, was determined from glacier mass balance measurements. Runoff from alpine (non-glacier) areas of the basins is small because part of the

precipitation which falls on these areas as snow is redistributed onto the glacier by wind and avalanche action. Continuous streamflow data are available for the three glacier research basins.

In this paper, runoff rate is expressed as a vertical velocity, m/yr (meters per year) for the average over the surface considered. This is similar to the practice of reporting precipitation and glacier mass balance rates as a vertical velocity. Runoff flux rate, or discharge, is runoff rate times area, expressed here as km^3/yr (cubic kilometers of water per year) for the area specified. All runoff rates are considered to be averages in both space and time.

Runoff measurements are available for several glaciers in Alaska. The U.S. Geological Survey has monitored Gulkana and Wolverine Glaciers from 1966 to the present. Continuous streamflow information is available during the period 1967 to 1978, so this analysis is limited to that period for those glaciers.

The average measured runoff rate from all sources at Wolverine Glacier basin in southern Alaska, from 1967 to 1978, was 3.14 m/yr (meters per year) (U.S. Geological Survey, 1979). During this same period, the measured average ablation rate from snow, old firn, and ice on the glacier was 2.72 m/yr, or about 62 percent of the runoff. Rain and condensation on the glacier produce 25 percent of the basin runoff, and the alpine area contributes only 13 percent to the basin runoff. The average ELA, from yearly measurements during the period, was 1150 meters.

At Gulkana Glacier, in the Alaska Range of interior Alaska, the measured average runoff rate from 1967 to 1978 was 1.97 m/yr (U.S. Geological Survey, 1969) indicating that the climate at Gulkana is drier than at Wolverine, but still quite maritime compared with most of interior Alaska which typically has only 0.25 m/yr average runoff. The average ELA at Gulkana during the same period was 1180 meters. The total glacier area in the basin is 22.2 km^2 , of which Gulkana Glacier is 19.3 km^2 . Measured average ablation of Gulkana Glacier was 1.88 m/yr for the same period. This ablation with

rainfall added resulted in the glacier runoff rate of 2.38 m/yr, 85 percent of the measured runoff. Rain on the glaciers was the source of 18 percent of the runoff. The alpine area produced only 15 percent of the runoff.

Glacier ablation and runoff rates at McCall Glacier in the Brooks Range were measured in 1969 and 1970 by Wendler et al. (1973). Although the data cover only about half the ablation season for each of only two years, the information is quite useful because it indicates the magnitude of glacier runoff in a climatic setting that is different from that at either Gulkana or Wolverine Glaciers. The glacier ablation volume rate reported here (Table 1) is calculated from data presented by Wendler et al. (1973, p. 421-422). They also measured the runoff rate, which they reported was 9.1 liters per second per square kilometer, which is equivalent to 0.28 m/yr. An error in determining glacier area may have been made (Trabant, oral communication, 1986), so the glacier and basin areas reported here were determined by this author. The total area of glaciers in the basin is 10.1 km², of which McCall Glacier is 7.2 km². McCall Glacier produces only 0.62 m/yr runoff and the non-glacier area produces only 0.11 m/yr. In this relatively dry climate, the ELA of 2050 m is much higher than at either Gulkana or Wolverine Glaciers.

Table 1. Equilibrium line altitude and runoff measurements for three glaciers in Alaska. The alpine area is the non-glacier area. Measurements at Gulkana and Wolverine Glaciers by the author; at McCall Glacier by Wendler et al. (1973).

	Wolverine 1967-1978		Gulkana 1967-1978		McCall 1969-1970	
Equilibrium Line Altitude	1150 m		1780 m		2050 m	
Glacier	m/yr	km ³ /yr	%	m/yr	km ³ /yr	%
Measured Ablation	2.72	.0482	62	1.88	.0417	67
Estimated Rainfall	1.10	.0195	25	0.50	.0111	18
Calculated Runoff	3.82	.0676	87	2.38	.0528	85
Basin	m/yr	km ³ /yr	%	m/yr	km ³ /yr	%
Est. Alpine Runoff	1.40	.0097	13	1.00	.0094	15
Measured Runoff	3.14	.0773	100	1.97	.0622	100
	km ²	%		km ²	%	
Glacier Area	17.7	72		22.2	70	
Alpine Area	6.9	28		9.4	23	
Basin Area	24.6	100		31.6	100	
	km ²	%		km ²	%	
Glacier Area	10.1	33		10.1	33	
Alpine Area	6.9	28		6.9	28	
Basin Area	17.0	100		17.0	100	

The glacier and alpine components of the measured runoff were estimated (Table 1) from measurements of R, the basin runoff rate based on the equation:

$$R = (NS_n + G S_g) / (S_n + S_g) \quad (1)$$

where:

- N is non-glacier alpine runoff rate;
- S_n is the non-glacier alpine area;
- G is glacier runoff rate; and
- S_g is the glacier area.

If glacier mass balance data are available, the glacier runoff, G, can be estimated as follows:

$$G = A - K + C + P_r \quad (2)$$

where:

- A is measured annual ablation;
- K is freezing of water in the glacier;
- C is condensation on the glacier; and
- P_r is estimated annual rainfall.

Freezing of water in a glacier removes liquid from that available for runoff, and condensation adds to runoff. Both quantities are relatively small. In this analysis, condensation and internal freezing are not considered further, because they tend to cancel each other for runoff, although they can be important to glacier mass and heat balances.

The estimated quantities, N and P_r, are not uniquely determined, but the total of the two estimated quantities is known, so the estimates are constrained by the data. The estimated values of N and P_r were adjusted (Table 1) so that the calculated runoff is equal to the measured runoff. An assumption made in the process is that rain runoff from glacier and alpine areas are approximately equal because rain is not redistributed by wind to the extent that snow is. Furthermore, alpine runoff must be larger than glacier rain runoff because there is, in addition, snow melt runoff from alpine areas. The resulting uncertainty in the calculated glacier runoff is small because the snow and ice ablation from glaciers dominates the runoff from these basins.

The interpreted runoff and ELA data (Table 1) from the research glaciers indicates a well-defined inverse relationship of runoff rate to ELA exists in Alaska, as shown in Figure 3.

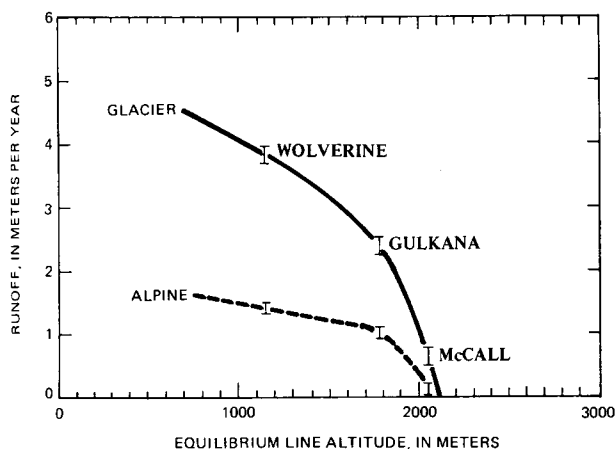


Figure 3. Relationship of average glacier equilibrium line altitude to the average runoff rate. Dashed line is the runoff from the alpine part of the basin adjacent to the glacier.

PROPOSED ELA RUNOFF ESTIMATION MODEL

It is proposed here that the relationship of runoff rate to ELA shown by Figure 3 is a general relationship over much of Alaska and it is, therefore, useful for calculating glacier runoff. The ELA Runoff Model proposed is the application of the measured relationship between ELA and runoff to other basins in Alaska.

The ELA Runoff Model is developed as follows:

The basin average runoff rate, R , is calculated by first determining the glacier and alpine runoff rate from the graph (Figure 1) for each hydrologically different area in the basin; determining the area of each unit from the map; multiplying runoff rate by area to obtain runoff volume rate; and then dividing by the total basin area. If a basin has forested lowlands, the runoff of that part of the basin must be estimated from other studies.

Thus, for a basin with glaciers, equation (1) stated previously here applies, that:

$$R = (NS_n + G S_g) / (S_n + S_g) \quad (1)$$

For a single glacier or a set of glaciers with a representative ELA, the annual glacier and alpine runoff rates, G and A , are determined from Figure 3.

ELA variations within a drainage basin are so large in some cases that no single ELA is representative. In this situation, the basin can be sub-divided into zones where representative ELA values can be obtained. The basin average runoff rate is calculated by first determining the runoff volume rate for each subdivision; then the total runoff volume rate is accumulated before dividing by basin area. If a basin has forested lowland areas, the runoff from those areas must be estimated from other studies.

The ELA runoff model provides time- and area-average runoff rates, which is new hydrologic information for vast ungaged areas of Alaska. It should be recognized, however, that the is quite limited. In this model, for example, annual variations of glacier runoff have not been demonstrated to be related to annual variations in ELA. Furthermore, runoff calculated using the ELA model cannot be used directly to construct contour maps of runoff rate because glacier runoff varies inversely with altitude on individual glaciers. Snow and ice melt is the primary source of glacier runoff and the melt rate generally decreases with altitude. Additional techniques must be developed before glacier runoff contours over large areas of Alaska can be drawn using ELA as part of the argument. The estimated accuracy of the model is not known, but cannot be more accurate than about 0.2 m/y

ELA RUNOFF MODEL TEST AT A GAGED BASIN

As a test of the ELA runoff model, runoff was calculated for the Knik River basin near Palmer, Alaska. Water flowing from the Knik River Basin has been gaged continuously since 1959 (U.S. Geological Survey, 1959-1985). In the Knik basin, glacier equilibrium altitudes range widely from 670 m in the southern part of the basin to 2100 m in the northern part of the basin (Figure 4). This large variation of ELA indicates that a strong

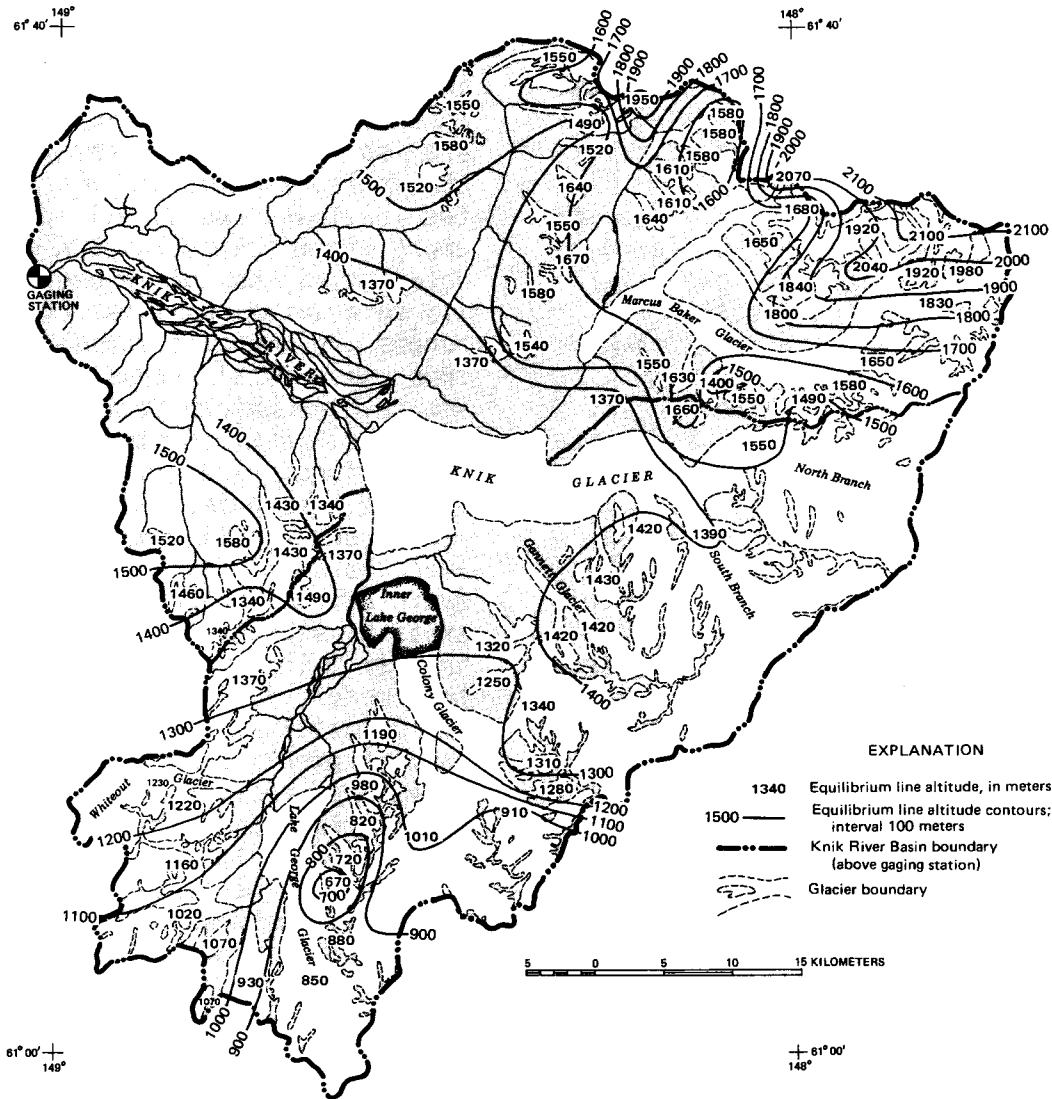


Figure 4. Distribution of the equilibrium line altitude in the Knik River Basin. Altitudes in meters.

precipitation shadow occurs in the Marcus Baker Glacier area and that precipitation and runoff are probably quite high in the southern part of the basin.

The Knik basin can be divided into three parts (Figure 4), the North sub-basin with the highest ELAs, the Knik Glacier sub-basin dominated by Knik Glacier, and the south sub-basin which has low ELAs. Each sub-basin contains a major glacier, other small glaciers, rock with alpine tundra vegetation, and forested lowland.

To apply the ELA model, the areas of glacier, alpine, and forested terrain in each sub-basin were measured from the map and shown in Table 2. The average ELA's

of glaciers in each sub-basin were determined from the ELA graph (Figure 4); then used to determine runoff rates (Figure 5). ELA contours represent an imaginary surface above which glaciers form only where the land or glacier surface is higher. Runoff from the forested lowlands was estimated to be approximately half that from alpine areas because the annual precipitation measured nearby at Palmer is only 0.35 m/yr. The accuracy of this estimate is relatively unimportant, however, because the runoff from the forested lowlands is only 6 percent of the basin total.

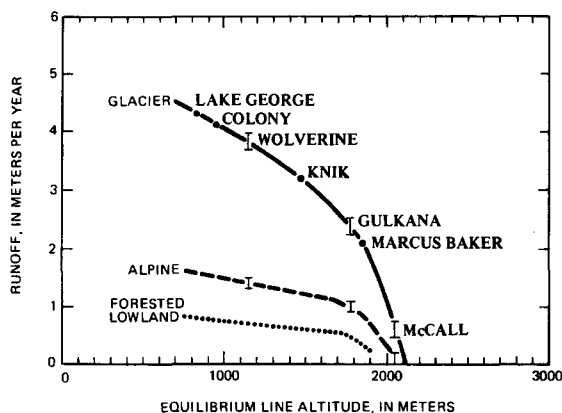


Figure 5. ELA model interpretation of runoff rate for Knik River Basin using glacier equilibrium line altitude information (see Figure 4).

During the calculation process (Table 2) high accuracy is shown only to avoid committing rounding errors during the calculation. Reportable results should be rounded. The ELA model calculation (Table 2) indicates that the basin average runoff rate is 2.0 m/yr. The measured 24-year average runoff rate for the Knik River from 1960 to present is 2.03 m/yr. This remarkable agreement, at least for this one case, indicates that the technique potentially can produce valid results.

Other interesting results, such as the percentage of runoff from each identified source, also come from the ELA model at Knik River basin. Glaciers occupy 47 percent of the basin area yet contribute 77 percent of the runoff. Glaciers occupy high local precipitation areas and also serve as effective precipitation traps in the windy climate. Furthermore, the south sub-basin, which is closer to the coast, contributes more water than the larger north sub-basin. Knik Glacier (14 percent of the basin) is the source of 23 percent of the river flow.

ESTIMATION OF GLACIER RUNOFF FROM AN UNGAGED BASIN

The ELA runoff model can be applied to other hydrologically important areas in Alaska, such as the St. Elias Mountains, where runoff measurements are sparse yet considerable runoff occurs. The basin chosen for an application example is the

Table 2.-- Average annual runoff from Knik River Basin, Alaska, calculated by the ELA runoff model. ELA and area data from Figure 4 (map); estimated runoff (one decimal) from Figure 5 (graph); calculated runoff (two decimals). All calculations carried out to full accuracy. Apparent errors in totals are not real, but are due to rounding.

	Data from map		ELA m	Model predicted RUNOFF RATE		
	AREA km ²	%		m/yr	km ² /yr	%
NORTH SUB-BASIN						
Marcus Baker Glacier	270	9	1830	2.1	0.57	9
Other Glaciers	160	5	1500	3.2	0.51	8
Alpine	760	25		0.9	0.68	11
Forested lowland	500	17		0.45	0.23	4
Subtotal	1690	56		1.18	1.99	33
KNIK GLACIER SUB-BASIN						
Knik Glacier	430	14	1470	3.2	1.38	23
Other Glaciers	20	1	1450	3.3	0.07	1
Alpine	60	2		1.2	0.07	1
Subtotal	510	17		2.97	1.51	25
SOUTH SUB-BASIN						
Colony Glacier	160	5	950	4.1	0.66	11
Lake George Glacier	200	7	830	4.3	0.86	14
Other Glaciers	180	6	1170	3.7	0.67	11
Alpine	140	5		1.6	0.22	4
Forested lowland	140	5		0.8	0.11	2
Subtotal	820	27		3.07	2.52	41
KNIK RIVER BASIN SUMMARY						
Glaciers	1420	47		3.31	4.70	78
Alpine	960	32		1.02	0.98	16
Forested lowland	640	21		0.53	0.34	6
TOTAL	3020	100		1.99	6.02	100
				Measured runoff	2.03 m/yr	

Bering Glacier basin. Runoff from the basin would be particularly difficult if not impossible to gage because the glacier runoff forms 12 rivers that flow into the Gulf of Alaska along 100 km of shoreline before they can gather into a single large river.

Bering Glacier, 6540 km² area, is a complex system of ice streams (see Figure 6) that includes the Bagley Icefield and the Stellar Glacier as a tributary. Even without considering the Stellar tributary, 830 km², the Bering is still the largest glacier in North America. The ELA rises dramatically with increasing distance from the ocean (Figure 6), indicating that precipitation decreases significantly over a relatively short distance.

A small, low altitude basin, Dick Creek, at the west edge of the basin, gaged from 1970-1981, had an average of 5.9 m/yr

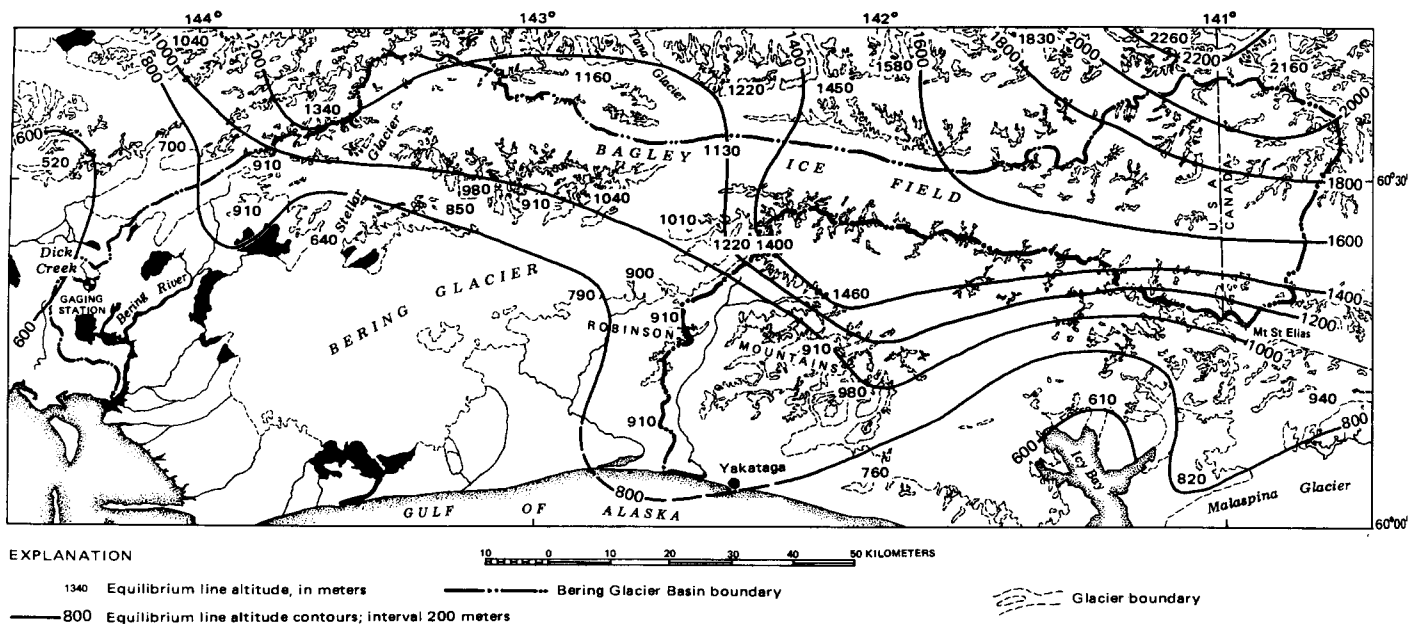


Figure 6. Equilibrium line altitude in the Bering Glacier basin. Contour interval, 200 m.

runoff (U.S. Geological Survey, 1982). Precipitation at nearby Yakutat (2.1 m/yr) and Yakataga (3.1 m/yr) average 2.6 m/yr. The sparse precipitation and runoff measurements indicate that the average runoff rate from the forested lowlands in this region is probably very high, between 3 and 4 m/yr.

To apply the ELA Runoff Model to the Bering Glacier basin, the area was subdivided into 3 glacier and 2 non-glacier areas. The Bering Glacier and Stellar Glacier tributary were separated because the ELA of the Bering is 1100 m, whereas it is only 640 for the Stellar. Other small glaciers (210 km²), alpine, and forested lowland areas were also considered separately. ELA model calculations (Table 3) indicate that the Bering Glacier basin produces a considerable amount of water, 34 km³/yr (1080 m³/s, or 38,000 ft³/s), 79 percent of which comes from the glaciers.

The average runoff rate indicated by the ELA model for the Bering basin is 3.8 m/yr. Royer (1982, p. 2018) estimated the average runoff rate to be 2.4 m/yr for the same region based on sparse precipitation and oceanographic data, but concluded that this was probably an underestimate of the actual amount.

Table 3. Average annual runoff calculated for the Bering Glacier drainage area. The equivalent average river discharge rates are also given in units of cubic meters per second, m³/s, and cubic feet per second, ft³/s, for comparison.

	AREA	ELA	RUNOFF RATE					
	km ²	%	m	m/yr	km ³ /yr	%	m ³ /s	ft ³ /s
GLACIER SYSTEM								
Bering tributary	5710	63	1100	3.9	22.3	65	707	25000
Stellar tributary	830	9	640	4.5	3.7	11	117	4100
Bering/Stellar	6540	72		4.0	26.0	76	824	29100
Other glaciers	210	2	910	4.1	0.9	3	29	1000
TOTAL	6750	74		4.0	26.9	79	852	30100
NON-GLACIER AREAS								
Alpine	550	6	900	1.6	0.9	3	29	1000
Forested lowland	1770	20		3.5	6.2	18	196	6900
TOTAL	2320	26		3.1	7.1	21	225	7900
BASIN TOTAL	9070	100		3.8	34.0	100	1078	38000

DISCUSSION

The relationship of runoff to ELA, Figure 3, suggests that the highest expected ELA in Alaska is about 2100 m. No glaciers in Alaska have ELA's higher than 2200 m. In a study of the refreezing of water in glaciers, Trabandt and Mayo (1985) showed that almost all glacier meltwater above 2100 m altitude refreezes in cold, permeable glacier firn where it remains as glacier accumulation, which

explains the altitude limit. Rock areas above about 2100 m altitude shed most precipitation by avalanching rather than by liquid runoff. Thus, little liquid runoff occurs from glaciers or alpine areas above that altitude. Most precipitation above 2100 m flows by avalanching and glacier ice motion.

Precipitation in mountainous areas tends to increase with altitude. This generalization does not, however, apply well to Bering Glacier. The ELA runoff model of the Bering area indicates that precipitation and runoff from this large glacier are less than the runoff measured at Dick Creek, the small, lower altitude sub-basin. Thus, the zone of maximum precipitation adjacent the Pacific Ocean in this part of Alaska may be as low as only 500 m altitude.

The ELA runoff model for Alaska can be expected to give good estimates of runoff from unglaciated basins that contain glaciers. The model as calibrated in this paper is restricted to the latitude band from 60° to 70° North in northwestern North America, and can be expected to overestimate runoff north of this band and underestimate runoff to the south. Where glacier ablation and runoff data are available for other areas, the ELA runoff model could be recalibrated.

Among the five basins studied in Alaska, snow and ice melt produced substantially more runoff than did rainfall, and glaciers produced from 74 to 87 percent of the total runoff.

The ELA model provides a means of estimating the runoff from all glaciers in Alaska, which can be compared to the total runoff of the nation. Glaciers occupy 73,000 km², or about 5 percent of Alaska. The average ELA of these is not known precisely, but is between that of Gulkana and Wolverine Glaciers. Thus, the average runoff rate from Alaskan glaciers is approximately 3 m/yr, or 220 km³/yr. Average runoff from the conterminous states has been estimated to be 1,230 billion gallons per day (U.S. Geological Survey, 1984), or 1550 km³/yr. R.D. Lamke (oral comm., 1986) estimated the average runoff from Alaska to be 620 km³/yr.

Bering Glacier produces 4.2 percent of Alaska's runoff and 1.2 percent of the

national runoff including Alaska. Glaciers in Alaska produce approximately 35 percent of Alaska's runoff; an amount equal to 14 percent of that from the conterminous states; and 10 percent of the total runoff from the nation.

ACKNOWLEDGMENTS

The author thanks T.C. Royer, Chester Zenone, and R.M. Krimmel for offering many helpful suggestions in this study. Krimmel, using Landsat images, verified the Knik basin ELA map (Figure 4).

LITERATURE CITED

- Meier, M.F., and A.S. Post, 1962. Recent variations in mass net budgets of glaciers in western North America. *Int. Assoc. Scientific Hydrology Pub.* 58/A:251-260.
- Østrem, G., N. Haakensen, and T. Eriksson, 1981. The Glaciation Level in Southern Alaska. *Geograf. Ann.* 63/A:251-260.
- Parks, B.P., and R.J. Madison, 1985. Estimation of Selected Flow and Water-Quality Characteristics of Alaskan Streams. U.S. Geological Survey Water-Resources Investigations Report 84-4247.
- Péwé, T.L., and R.D. Reger, 1972. Modern and Wisconsinan Snowlines in Alaska. 24th International Geological Congress, Montreal, Proceedings 12:187-197.
- Royer, T.C., 1982. Coastal Fresh Water Discharge in The Northeast Pacific. *Jour. Geophysical Research* 87:2017-2021.
- Trabant, D.C., and L.R. Mayo, 1985. Estimation and Effects of Internal Accumulation on Five Glaciers in Alaska. *Annals of Glaciology* 6:113-117.
- U.S. Geological Survey, 1959-1985. Water Resources Data, Alaska. U.S. Geological Survey Hydrologic Data Series, Published Annually.
- U.S. Geological Survey, 1984. National Water Summary 1983--Hydrologic events and issues: U.S. Geological Survey Water Supply Paper 2250, 243 p.
- U.S. National Weather Service, 1972. Mean Annual Precipitation-Inches; Alaska. Map 73-2446. 1 sheet.
- Wendler, G., D. Trabant, and C. Benson, 1973. Hydrology of a Partly Glacier-Covered Arctic Watershed. *Int. Assoc.*

REMOTE SENSING

SEASONAL AND INTERANNUAL OBSERVATIONS AND MODELING OF THE SNOWPACK ON
THE ARCTIC COASTAL PLAIN OF ALASKA USING SATELLITE DATADorothy K. Hall, Alfred T. C. Chang, James L. Foster¹

ABSTRACT: Snow is a dynamic component of the global hydrologic cycle. Measurement of approximate snow extent and depth on a global scale is possible using passive microwave data from the Nimbus-7 Scanning Multichannel Microwave Radiometer (SMMR). Improvement of snow depth measurement is dependent partly upon our ability to recognize the influence of snow structure on microwave signatures. Multiple linear correlations of microwave brightness temperature (T_B) from the SMMR, snow depth and air temperature have been performed for the Arctic Coastal Plain of Alaska. The portion of the T_B variability that cannot be explained by snow depth and air temperature is most likely due to physical differences in the snowpacks among the 4 years studied. Results from a snow energy balance model show that the temperature profiles of the snowpacks on the Arctic Coastal Plain can be quite different between years. The depth hoar layer which is comprised of large crystals is influenced by the snowpack temperature gradient. The presence and variability of a depth hoar layer may be detected by passive microwave satellite sensors and can be modeled using a radiative transfer model and a snow energy balance model. (KEY TERMS: depth hoar, passive microwave, SMMR, snow depth.)

BACKGROUND

The world-wide snow cover is one of the most dynamic and poorly understood features on the Earth's surface. It is quite variable in terms of depth, density, duration and stratigraphic characteristics. Through the use of remote sensing techniques we are gaining an improved understanding of snow extent and depth on local, regional and especially global scales and the role of snow in the Global Hydrologic Cycle.

Physically-based models have been developed which allow us to estimate snow depth, and to simulate changing snow structure and snowmelt processes. In this paper, some of the major sources of error in the determination of snow depth on the Arctic Coastal Plain of Alaska using microwave radiometry are assessed. Modeling is shown to be an effective tool in accomplishing this.

The Arctic Coastal Plain of Alaska is a good region in which to study annual and interannual snow characteristics because it is a large area that is flat and treeless. The snow cover on the Arctic Coastal Plain of Alaska is quite shallow and generally begins to form by early October and lasts through May. Depth hoar which is common in the snowpack on the Arctic Coastal Plain is comprised of large

¹Laboratory for Terrestrial Physics, Code 624, NASA/Goddard Space Flight Center, Greenbelt, MD 20771

(1 to 15 mm in size) crystals that form as a result of a temperature gradient in the snowpack (Benson et al., 1975). The physical temperature at the base of the snowpack is warmer than at the surface of the snowpack. Vapor diffusion (a result of the temperature gradient) occurs from the lower to upper portions of the snowpack where sublimation from crystals in the lower layers gives way to redeposition in the upper layers.

The thickness of the depth hoar layer and the size of the depth hoar crystals are dependent upon the meteorological conditions during snowpack build-up and the degree of snow surface cooling throughout the winter. Date and amount of first snowfall, and ground surface temperature at the time of the first snowfall will help to determine the amount of heat that will be retained by the ground and will thus influence the temperature profile within the snowpack. A steeper temperature gradient will lead to a better developed depth hoar layer in a given year. Satellite passive microwave observations of the snow on the Arctic Coastal Plain provide the opportunity to study inter-annual changes in snow cover and depth on a regional scale, and the use of a radiative transfer model and a snowmelt energy balance model allow inferences to be made about snowpack structure.

PREVIOUS WORK

Passive microwave data from the Nimbus-7 Scanning Multichannel Microwave Radiometer (SMMR) are useful for estimation of global snow extent (Chang, 1986) and snow depth (Kunzi et al., 1981). Studies have shown that there is an inverse relationship between snow depth and passive microwave brightness temperature (T_B) as measured by satellite sensors under dry snow conditions (Foster

et al., 1984). Snow crystals scatter the upwelling emission and thus deeper snow which contains more snow crystals will permit more scattering and will result in a lower T_B .

Recent studies have shown that the microwave response of certain types of snow structure can be modeled successfully using a radiative transfer model (Hall et al., in press) leading to an improved ability to estimate snow depth in selected regions using microwave radiometry. Radiative transfer modeling has shown that snow depth, temperature and grain size are important parameters which govern the T_B , where the T_B is a function of emissivity and temperature of the snow. In addition, it has been shown that large snow grain sizes reduce the microwave emission from a snowpack and increase scattering which results in a lower T_B (Chang et al., 1982; Hall et al., in press). The large snow crystals in the depth hoar layer contribute to a low microwave T_B . Thus, two snowpacks of equal depth may have different T_B s due to different grain size distributions.

Use of a two-layer radiative transfer model (Chang et al., 1976) permits the effect of grain size of the upper and lower layers in a snowpack to be analyzed. Larger grain sizes can be assigned to the lower layer to simulate a depth hoar layer. The thickness of the depth hoar layer can be increased through time when modeling a time series of data. Hall (in press) found that the coefficients of correlation between observed and modeled T_B correlated well when the thickness of the depth hoar layer was allowed to increase by 0.5 cm per week during a 3 month study period in each of 4 years studied.

Energy balance modeling of snow has been accomplished by several authors (Choudhury et al., 1980; Anderson, 1976; Dozier, 1984). The energy balance model used in this paper is a one-dimensional,

time-dependent numerical integration model based on the surface energy balance, heat transport within the snowpack and snow density variation equations. It incorporates the effects of snow melt, liquid water retention, liquid water percolation and refreezing. However it does not incorporate different snow structure effects except as can be inferred by temperature profiles which are produced by the model. Numerical integrations are carried out for specified periods of time by dividing the snowpack into finite layers. Input parameters which influence the thermal structure of snowpacks are: air pressure, air temperature, humidity, wind speed and solar heating. Air temperature, wind speed and solar heating are the major controlling factors (Choudhury et al., 1980). The temperature and density profiles are simulated. As mentioned previously, temperature profiles are important because they influence depth hoar development.

METHODOLOGY

In this paper, the snow cover on the Arctic Coastal Plain is studied during each of 4 winters: 1979-80, 1980-81, 1981-82 and 1982-83 using horizontally-polarized passive microwave SMMR data at the 0.81 cm wavelength (37 GHz frequency) obtained from 5 day T_B averages from late September through early June in each year. These data are plotted and shown in Figure 1. The SMMR data represent the average of 15 T_B grid cells each of which represents an area that is $1/2^\circ$ latitude x $1/2^\circ$ longitude in area. The T_B data were located approximately between $70 - 70.5^\circ$ N and $152 - 159^\circ$ W.

The T_B s are used in single and multiple linear correlations with air temperature (which is used to infer snow temperature) and snow depth. Air temperatures and snow depth measurements are obtained from the Barrow, Alaska meteorological station (NOAA, 1979a - 1983a; NOAA, 1979b-1982b).

The energy balance model which was described previously, employs meteorological data from Barrow, Alaska. The model is employed in order to determine if the negative temperature gradient in the snowpack could be maintained given initial snowpack conditions that were assumed for early in the snow season for the first 5 days of November in each year of the study. A negative temperature gradient allows the depth hoar layer in a snowpack to be maintained.

RESULTS

Note in Figure 1 that just prior to snow accumulation (mid-September), the T_B s in each year are $210 \pm 5^\circ$ K. Similarly, just after snowmelt in early June, the T_B s are $220 \pm 5^\circ$ K. As soon as the snow begins to accumulate each fall, significant changes in T_B appear due to the presence of snow. For example, in mid-February there is a 35K difference in T_B between the 1981-82 snowpack (166K) and the 1979-80 snowpack (201K).

Analysis of a time series of Nimbus-7 SMMR T_B data of snow on the Arctic Coastal Plain shows that seasonal variability in T_B is correlated with snow depth and air temperature (Tables 1 and 2). In some years, these correlations can be very good. For example, the correlation between snow depth and microwave T_B was $R = -0.84$ in 1981-82 (Table 1). In other years, the correlation is poorer, e.g. $R = -0.52$ in 1980-81.

Linear and multiple linear regressions were performed using the T_B data and meteorological data obtained from Barrow, Alaska. Part of the interannual variability in T_B can be explained on the basis of snow depth and temperature differences between years. Table 2 shows the results of the multiple linear correlation using air temperature, snow depth and T_B . Note the addition of air temperature

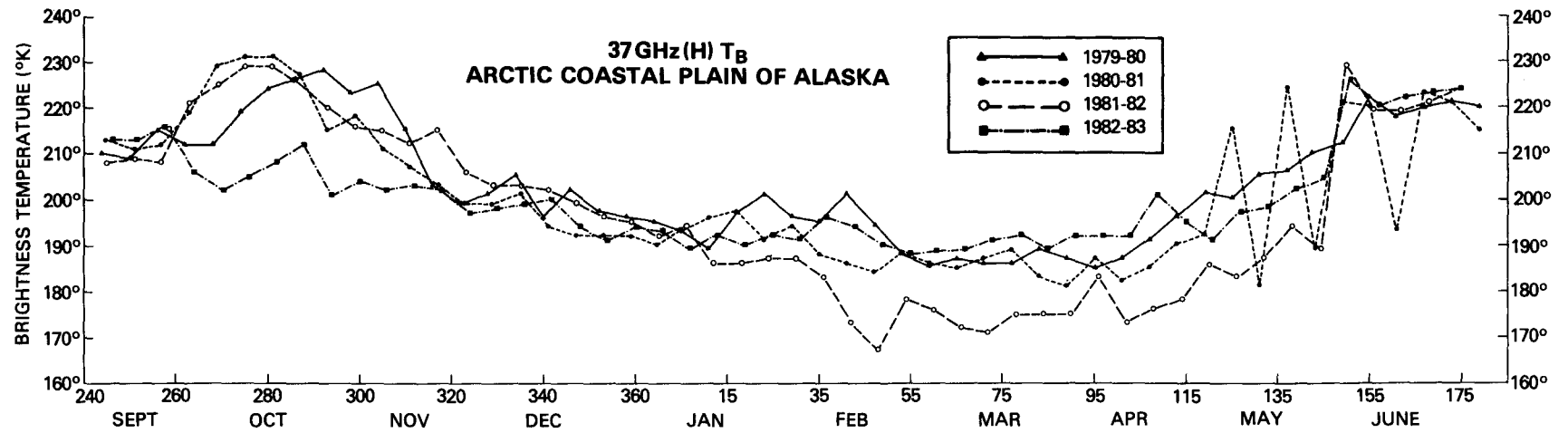


Figure 1. Plots of horizontally-polarized 0.81 cm (37 GHz) SMMR brightness temperature versus time, 1979-1983.

(Table 2) improves the correlations in 3 out of the 4 years studied.

Especially in some years, there is a substantial portion of the T_B variability that cannot be explained by snow depth and/or air temperature (Table 2). Major factors which contribute to this variability are: atmospheric effects, variability in snow depth within a SMMR resolution element, and snow structure variability. Atmospheric effects are considered to be quite minor during the winter in northern Alaska because the liquid water in the atmosphere which would affect the microwave emission is negligible. Ice crystals in clouds do not have a measurable effect on the microwave T_B at the 0.81 cm wavelength (Wilheit, 1972). Other factors also may affect the microwave emissivity of snow but are not considered here.

TABLE 1. Correlation of T_B and Snow Depth

Winter	R	R ²	Standard Error
1979-80	-0.76	0.58	8.041
1980-81	-0.52	0.27	12.313
1981-82	-0.84	0.71	9.471
1982-83	-0.64	0.40	4.708

TABLE 2. Multiple Linear Correlation of T_B , Snow Depth and Air Temperature

Winter	R	R ²	Standard Error
1979-80	0.77	0.59	7.990
1980-81	0.69	0.47	5.872
1981-82	0.84	0.71	4.600
1982-83	0.70	0.49	2.524

The variability in snow depth in a resolution element of the SMMR data (in this case, $1/2^\circ$ latitude x $1/2^\circ$ longitude) is a source of error. The SMMR will record an "average" T_B for each resolution element. Benson

(1982) reports that some snow drifts along river banks can be > 10 m deep. Snow on the flat tundra is generally less than 40 cm deep. This large areal variability in snow depth will contribute to the unexplained errors in the linear correlations between T_B and snow depth because of the need to assign one snow depth value to a large ($1/2^\circ \times 1/2^\circ$) area. Thus the average snow depth is underestimated by using the reported point source values. This is especially true if the meteorological station lies in a precipitation shadow.

Finally, there is an error which is due to snow structure variability. The snow structure will change if the thickness of the depth hoar layer and the grain size distribution within the snowpack change. The variability in the thickness of the depth hoar layer and the size of the depth hoar crystals contributes to T_B changes since greater depth hoar development causes more microwave scattering and thus lower T_B s (Hall et al., in press).

In order to study the inter-annual differences in snow structure, energy balance modeling was performed in addition to the modeling of the microwave emission using a radiative transfer model. Temperature profiles simulated from the energy balance model are shown in Figures 2, 3, 4 and 5. The initial (given) temperature profile and the temperature profile for the end of each 6-day period (total = 4 years) is shown. Note that the steep, negative temperature gradient is maintained throughout the 6 day period in each year according to results from the energy balance model. A steep, negative temperature gradient, if maintained, permits increased development of depth hoar layer thickness and size of the depth hoar crystals as the winter progresses. Initial snowpack conditions were estimated and based on a snowpack with a steep negative temperature profile which is typical

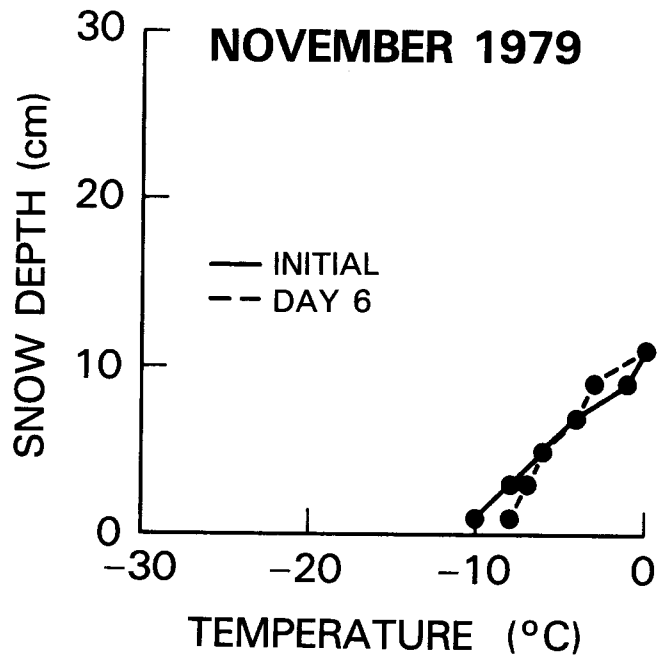


Figure 2. Temperature profiles of the snowpack on the Arctic Coastal Plain of Alaska. The initial snowpack profile (based on measured snow depth) was assumed for November 1, 1979 and input into the energy balance model. The profile on day 6, November 6, 1979, was simulated by the model.

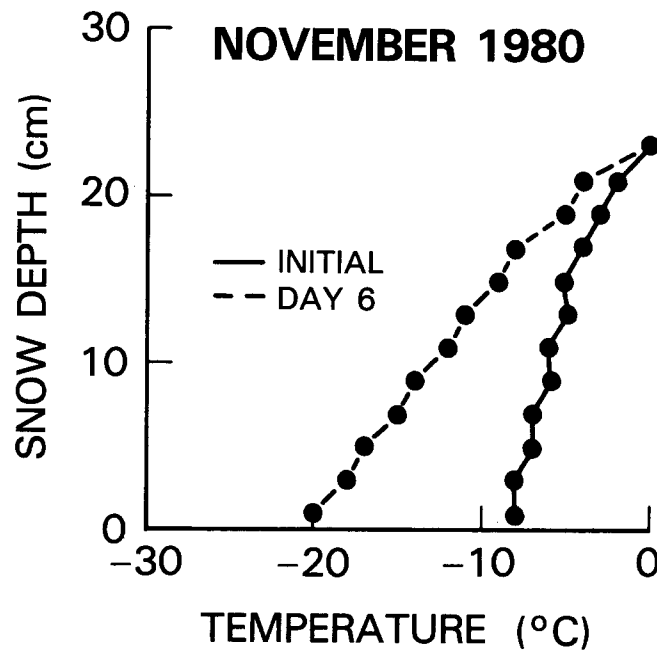


Figure 3. Temperature profiles of the snowpack on the Arctic Coastal Plain of Alaska. The initial snowpack profile (based on measured snow depth) was assumed for November 1, 1980 and input into the energy balance model. The profile on Day 6, November 6, 1980, was simulated by the model.

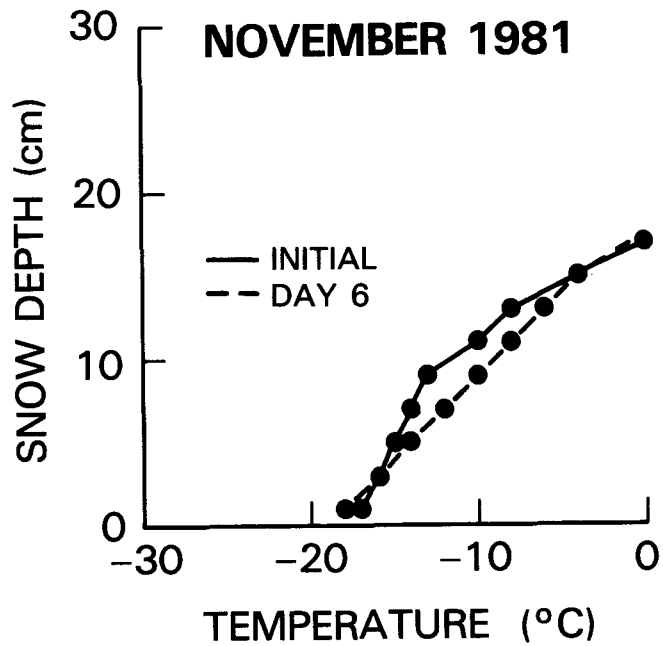


Figure 4. Temperature profiles of the snowpack on the Arctic Coastal Plain of Alaska. The initial snowpack profile (based on measured snow depth) was assumed for November 1, 1981 and input into the energy balance model. The profile on Day 6, November 6, 1981, was simulated by the model.

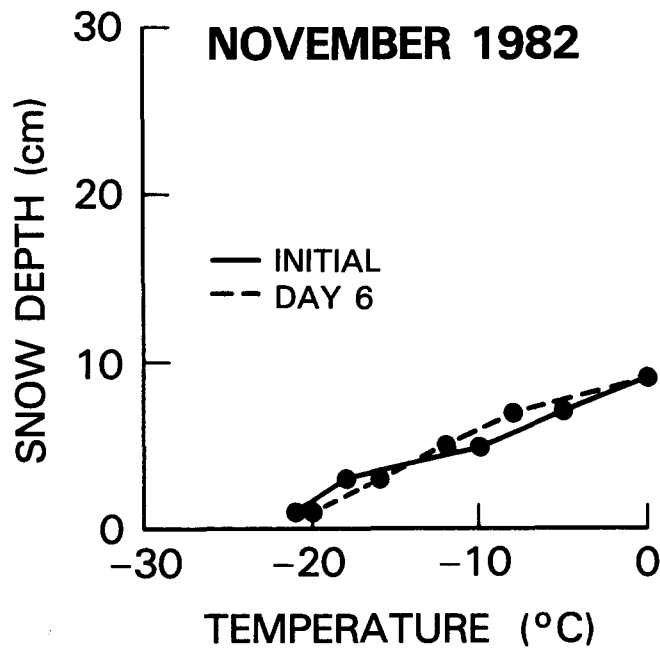


Figure 5. Temperature profiles of the snowpack on the Arctic Coastal Plain of Alaska. The initial snowpack profile (based on measured snow depth) was assumed for November 1, 1982 and input into the energy balance model. The profile on day 6, November 6, 1982, was simulated by the model.

for the Arctic Coastal Plain as discussed in Benson et al. (1975).

Comparison of the simulated temperature profiles among the 4 years reveals considerable differences in the steepness of the gradient. This can be attributed to varying snow depths and variable meteorological conditions among years. Thus, one can see that this would lead to significant differences in snowpack structure (in terms of depth hoar development) from year to year. This snow structure variability, which can be observed in the field or modeled using energy balance modeling, helps to explain the annual variability in T_B which is evident in the SMMR data. Large variations in T_B between years are apparent (Figure 1) particularly beginning in mid-January and continuing until snowmelt in the spring.

DISCUSSION AND CONCLUSION

Analysis of the errors that are present in the simple and multiple linear correlations between microwave T_B and snow depth and air temperature has revealed that the major sources of error are primarily due to variability in snow depth and the physical conditions within the snowpack on the Arctic Coastal Plain of Alaska. Atmospheric effects are probably not significant during this study period. Unrepresentative snow depth measurement and snow depth variability due to drifting are problems that should be solvable with better in-situ snow measurement techniques. Areal variability in snow depth would be less of a problem with higher resolution sensors which should be considered for future satellites.

The snow structure variability that affects the microwave signal on the Arctic Coastal Plain is largely a result of changes in the thickness of the depth hoar layer

and is believed to represent a large part of the unexplained error from coefficient of determination studies. As described, this depth hoar variability results from meteorological conditions which differ from year to year.

Use of a snowmelt energy balance model has allowed us to simulate snowpack temperature profiles given a set of initial conditions. Results of the model show considerable variability in snowpack temperature profiles between years resulting from interannual variations in snow depth and meteorological conditions, thus resulting in interannual variability in depth hoar development.

Snowpack structure and depth vary from region to region due to differing meteorological and topographic conditions. In snowpacks of equal depth, the microwave emissivity can vary due to snowpack structure. In the case of depth hoar, a common component of snowpack structure, the effect on the microwave emission can be understood through modeling. Snowpack structure effects such as ice lenses and layers are not as easily understood in terms of their microwave response. Additional analysis and modeling may help to explain these and other snow structure effects in the future.

Though errors remain in the measurement of snow depth from microwave satellite sensors, analysis of these errors through radiative transfer modeling and snow energy balance modeling is providing valuable information on regional snow depth and structure characteristics. Extensive depth hoar development is known to be present in seasonal snowpacks throughout the world. As we gain a better understanding of the interactions between microwaves and snow structure, the ability to determine regional snow depth using passive microwave satellite data will improve dramatically.

REFERENCES

- Anderson, E. A., 1976. A Point Energy and Mass Balance Model of a Snow Cover. NOAA Technical Report NWS 19, 150 pp.
- Benson, C., B. Holmgren, R. Timmer, G. Weller and S. Parrish, 1975. Observations on the Seasonal Snow Cover and Radiation Climate at Prudhoe Bay, Alaska during 1972. In Ecological Investigations of the Tundra Biome in the Prudhoe Bay Region, Alaska (J. Brown, ed.), Biological Papers of the University of Alaska Special Report Number 2, October, 1975, pp. 13-50.
- Benson, C. S., 1982. Reassessment of Winter Precipitation on Alaska's Arctic Slope and Measurements of the Flux of Wind Blown Snow. Geophysical Institute University of Alaska UAG R-288, 26 pp.
- Chang, A. T. C., P. Gloersen, T. Schmugge, T. T. Wilheit and H. J. Zwally, 1976. Microwave Emission from Snow and Glacier Ice. Journal of Glaciology, V. 16, pp. 23-39.
- Chang, A. T. C., J. L. Foster, D. K. Hall, A. Rango and B. K. Hartline, 1982. Snow Water Equivalent Estimation by Microwave Radiometry. Cold Regions Science and Technology, V. 5, pp. 259-267.
- Chang, A. T. C., 1986. Nimbus-7 SMMR Snow Cover Data. Proceedings of the Snow Watch 1985 Workshop on CO₂ Snow Interaction, 28-30 October 1985, College Park, MD.
- Choudhury, B. J., C. S. Cheng and A. T. C. Chang, 1980. Numerical Simulation of the Thermal Structure of Snowpacks using an Energy Balance Model: Model Description and Parameter Test. NASA Technical Memorandum 82044, 30 pp.
- Dozier, J., 1984. Snow Reflectance from Landsat-4 Thematic Mapper. IEEE Transactions on Geoscience and Remote Sensing, V. GE-22, pp. 323-328.
- Foster, J. L., D. K. Hall, A. T. C. Chang and A. Rango, 1984. An Overview of Passive Microwave Snow Research and Results. Reviews of Geophysics and Space Physics, V. 22, pp. 195-208.
- Hall, D. K., A. T. C. Chang and J. L. Foster (in press). Detection of Depth Hoar Layer in the Snowpack on the Arctic Coastal Plain of Alaska Using Satellite Data. Journal of Glaciology.
- Hall, D. K. (in press). Influence of Changing Depth Hoar Structure on Microwave Emission from Snow in Northern Alaska 1980-1983. Submitted for publication.
- Kunzi, K. F., S. Patil and H. Rott, 1982. Snow-cover Parameters Retrieval from Nimbus-7 Scanning Multichannel Microwave Radiometer (SMMR) Data. IEEE Transactions on Geoscience and Remote Sensing, GE-20 (4), pp. 452-467.
- NOAA, 1979a-1983a. Climatological Data - Alaska, NOAA, Asheville, N.C.
- NOAA, 1979b-1982b. Local Climatological Data, Barrow, Alaska, NOAA, Asheville, N.C.
- Wilheit, T. T., 1972. The Electrically Scanned Microwave Radiometer (ESMR) Experiment. The Nimbus-5 User's Guide, pp. 59-105.

OPERATIONAL DEMONSTRATION OF MONITORING SNOWPACK CONDITIONS UTILIZING
DIGITAL GEOSTATIONARY SATELLITE DATA ON AN INTERACTIVE COMPUTER SYSTEM

Milan W. Allen and Frederick R. Mosher¹

ABSTRACT: The National Severe Storms Forecast Center (NSSFC) collects and maintains real-time data bases of atmospheric and surface observations in addition to full resolution GOES data with the Centralized Storm Information System (CSIS). These data sets and analyses derived from these data sets are then combined with topographic, hydrologic and/or geopolitical boundaries to assist hydrologic users as well as the primary severe storm forecasting users. During the 1985 snowmelt season, the Satellite Field Services Station (SFSS) began utilizing CSIS capabilities to derive operational digital snowcover maps from 1 km. visible GOES data. The snowcover mapping technique is based on the fact that snowcover increases the brightness of a land area. Snow free/cloud free data sets are adjusted to account for daily and seasonal solar illumination angle differences between the reference time and the snowmapping time. In 1986, snowmapping services will be expanded from 350,000 sq. km to 1.2 million sq. km to meet increasing user requirements. An optional 1986 service will be snowcover mapping by elevation zones while development work is conducted to

determine the feasibility of deriving solar insolation, skin temperature over snowcovered areas and free atmospheric conditions (temperature, relative humidity, wind speed and direction) at specified elevations. (KEY TERMS: interactive processing; digital data; satellite hydrology, snowcover mapping.)

INTRODUCTION

Traditionally, water resources forecasters have relied upon point measurements of snow water equivalent, temperature, and precipitation collected from manual snow courses, cooperative observers, climatological stations, and remotely sensed platforms for snowpack monitoring. These point measurements are extrapolated to derive mean areal values for individual hydrologic units (river basins). Regression analyses, lapse rates and empirically derived curves are also applied to these data sets to account for the effects of large topographic and physical features such as mountains and lakes.

Spatial data sets became available with the launch of the

¹Respectively, Satellite Hydrologist SFSS and Director, Techniques Development Unit, National Severe Storms Forecast Center, Room 1728, Federal Building, 601 E. 12th Street, Kansas City, Missouri 64106.

first meteorological satellites. Snow cover maps derived from satellite imagery provided forecasters with information on snowpack location and extent. During the last five years there have been two important development phases in the transition from manual photointerpretation techniques to digital techniques. The original digitally derived maps were alphanumeric computer printouts utilizing relatively coarse 4 km GOES visible data sets. Processing required a batch processing system to access the National Environmental Satellite Data and Information Services (NESDIS) data bases on the IBM 360/195 computers in Washington, D.C. Currently, snowmapping operations utilize real-time full resolution 1 km GOES data on the Interactive Centralized Storm Information System (CSIS) at the National Severe Storms Forecast Center (NSSFC) in Kansas City. CSIS processing capabilities have enabled the NSSFC satellite hydrologist to begin developing more diversified products and services to monitor snowpack conditions in addition to expanding areal coverage with the more detailed snowcover maps.

Visual Snowcover Mapping Techniques

Prior to 1978, NESDIS employed photointerpretation techniques to produce operational snowcover maps. The technique utilized a Zoom Transfer Scope (ZTS) to register a rectified and enlarged visible image from NOAA polar orbiting satellites to a basin outline by aligning landmarks (lakes, rivers, etc.). The snowline was traced onto the basin map and percent snowcover was calculated using a planimeter or electronic density slicer. These visually derived analyses were labor intensive and accuracy was directly related to the analyst's familiarity with each basin's topography, canopy, and skills

interpreting the effects of varying illumination angles on features (forests, etc.) within each basin.

Snowcover Mapping with Digital Data

From 1978 to 1981, NESDIS began conducting snowmapping tests utilizing digital GOES data on interactive and batch processing systems to increase the timeliness, effectiveness, accuracy and expand the areal coverage to meet user requests.

Results of tests conducted on interactive systems using GOES imagery and basin boundary overlays displayed on video terminals were somewhat mixed. This visual technique enhanced the analyst's ability to eliminate clouds and measure snowcovered area by pixel counting. However, complex snowlines and discontinuous snowcover required superior eye-hand coordination by the analyst. Limitations with existing hardware and software resulted in emphasis being placed on the digital snowmapping technique being concurrently developed on the NOAA main computers.

This batch processing all digital procedure was tested operationally during the spring of 1981. This procedure developed snowfree/cloudfree data sets (masks) for each basin. The darkest (lowest count value) pixel within each basin was chosen as the "threshold value" used to reference every pixel in each basin. During the snowmapping season a new threshold value was selected to brighten or darken the mask to account for varying solar illumination angles.

On cloudfree days the program was submitted through a Remote Job Entry (RJE) terminal to the NOAA main computers in Suitland, MD. Repetitive submissions are required to exactly align the mask and the visible data and then produce a series of snowcover maps. The initial threshold

value was added to each pixel in the mask and compared to each pixel retrieved from the GOES data set. If the mask plus threshold value is less than the GOES value, the pixel is assumed to be snowcovered. The number of snowcovered pixels was divided by the total number of pixels in the basin to derive percent snowcover.

Between December, 1981 and July, 1984, the SFSS generated and distributed 691 snowcover analyses covering 16 basins in the western United States. Because the procedure required visible data from a GOES satellite at 135°W, the program was significantly affected by the failure of three GOES satellites beginning in November, 1982. The failure of GOES-5 and the decision to move GOES-6 to a more central location threatened to leave the SFSS without the ability to generate digital snowcover analyses. After months of reviewing the digital snowcover mapping software it was decided the man-hours required to modify existing software and write new software for the reduced resolution data would not be worth the effort.

CURRENT SNOWMAPPING OPERATION

Centralized Storm Information System (CSIS)

CSIS is a developmental system which exists in an operational environment and supports the operational mission at the National Severe Storms Forecast Center (NSSFC). CSIS is a spin-off of the University of Wisconsin's Space Science and Engineering Center's (SSEC) Man computer Interactive Data Access System (McIDAS). While the ultimate goal of CSIS is to improve NSSFC's ability to forecast severe weather, it also represents another phase in the NWS effort to develop a system to ingest, analyze, integrate and display real

time data from all available sources.

The CSIS system consists of a GOES receiving antenna system, four Harris slash-6 computers, five interactive video terminals, conventional surface and upper air data, dial-up radar inputs, 1600 bpi magnetic tape drives used for data archiving and four 300 mb hard disks, an interface to other NSSFC computers and a phone link with the SSEC McIDAS for Visible Infrared Spin Scan Radiometer (VISSR) Atmospheric Sounder (VAS) data access.

System flexibility gives the analyst a diverse menu of options and capabilities including: real-time stretched data from the GOES VISSR; color enhancement of satellite imagery; the ability to superimpose data and analyses on satellite imagery; locating of points on the imagery using earth, satellite, and screen coordinates; a macro language facility for defining a sequence of commands; color graphics; the capability to overlay a variety of maps over satellite data, to change the gray scale of imagery and remap data to different map projections; a statistical analysis of data; data archival on magnetic tape; and black and white hardcopy of graphics and/or imagery.

CSIS Snowcover Mapping

The CSIS snowcover mapping technique is based on the fact that snowcover increases the brightness of a land area. The following are the procedures used in the CSIS snowcover mapping technique:

- o Identify areas to be mapped and select data sectors.
- o Develop an automated system to collect full resolution data.
- o Set up seven day rotating

- files to archive the data.
- o Input United States Geological Survey (USGS) catalog units for basin delineation over areas to be mapped.
- o Prepare snowfree/cloudfree reference data bases (masks).
- o Remap GOES data into mask projection.
- o Exactly align the mask and GOES data.
- o Adjust the brightness of the mask to reflect the difference in solar illumination angle of the GOES data.
- o Composite two images to eliminate clouds.
- o Compare each pixel in the mask and image to produce a snow/no snow image.
- o Sub-divide each sector into mapping scenes.
- o Eliminate cloud contamination manually with the cursor.
- o Overlay basin boundaries and digitally compute percent snowcover.
- o Overlay percent snowcover tables for each basin.
- o Hardcopy the snow/no snow image with basin boundaries and tables.
- o Archive GOES data used for mapping on magnetic tape.
- o Disseminate maps via first class mail and rapifax.

Real time full resolution GOES data are received directly from satellite and stored on the CSIS Data Base Manager (DBM). A clock controlled scheduler then "sectorizes" these data and sends them to another CPU where they are stored for real time or future display on an interactive terminal. Snowcover mapping data are stored in two seven-day rotating files,

one for each time period. During the winter and early spring, data are archived at 1700Z and 1800Z (GMT). From early Spring through July, data are archived earlier at 1600Z and 1700Z to reduce the possibility of small cloud contamination. Software was written to allow the analyst to manipulate file parameters and display the files with one line keylins.

The USGS basin boundary tape has 27,000 sectors representing regions, sub-regions, accounting units, and catalog units for the contiguous 48 states. The highly detailed boundaries are defined by latitude/longitude pairs of points that are line segments between individual basins. Software developed by the NWS Office of Hydrology (OH) was modified to read the data into CSIS. Additional software was written to convert the data to CSIS geographical format, and display various configurations of regions, sub-regions, accounting units, and catalog units in addition to the snowmapping basins.

Full resolution GOES-5

visible data for September 24 and 25, 1983 were aligned and composited to create snowfree/cloudfree images. These images were then remapped into a projection of the satellite at its winter longitude (108°W). Navigation coordinate data were then exactly aligned with the imagery using landmark coordinates derived from 1:1000000 Lambert Conformal Operational Navigation Charts.

The satellite visible images need to be corrected for brightness changes due to the daily and seasonal change of the sun angle. It has been assumed that the land and snow reflect sunlight in an isotropic manner. This is a good first order approximation to these surfaces as long as extreme sun angles are avoided. The visible brightness counts on the GOES

satellite have been digitized with a square root digitization technique. The solar zenith angles θ were calculated for the center of the basin of interest for the reference image and the current image and the entire satellite image was then multiplied by the correction factor

$$\sqrt{\frac{\cos \theta_1}{\cos \theta_2}}$$

To reduce the amount of time required to manually align the GOES imagery a reference mask software was developed to align the imagery with the mask resulting in the alignment of the digital data bases. The entire operation requires one command and two single letter keyins. GOES data and the reference mask are loaded on "opposite frames" of a terminal. This allows the analyst to flicker between the two images using a one letter keyin as the toggle switch to check their alignment and look for landmarks visible on both images. A cursor is placed directly over the landmark in the GOES imagery by moving a pen over a data tablet connected to the terminal. The one letter keyin is entered and the reference mask is displayed. The operation is repeated on the reference mask. The GOES data are repositioned and all pixels are now given the navigation, satellite, and earth coordinates of the reference mask. The repositioned image is loaded and alignment is checked by flickering between the realigned image and the mask.

Compositing two images to eliminate clouds is a combination of the two previous steps. Brightness levels of one image are scaled to match the illumination angle of the other. Pixels on each image contaminated by cloud shadows are set to zero using a cursor data function. The two images are

aligned and every pixel in each image is compared. The darkest pixel value is then selected to produce the composited image.

Snowcover sectors are produced by comparing every pixel in the sector with every pixel in the scaled mask. If the sector pixel is brighter than the mask pixel, the sector pixel is classified as being snowcovered and its count value is used to build the snowcover sector. If the sector pixel is less than or equal to the mask value, the pixel in the snowcover sector is given a count value equal to zero.

Each snowcover map in a sector is then displayed and checked again for cloud contamination. If contamination exists, it is removed interactively using a cursor data function which sets the contaminated values to zero or the threshold stripping program can be rerun with the background increased by a small delta to determine the snow/no snow threshold. Each catalog unit boundary is overlaid over the snowmap and a statistical discrimination function is used to derive percent snowcover by dividing the number of non-zero pixels by the total number of pixels inside each boundary. Percentages are then entered into a macro, written to overlay a table of percent snowcover values on each map. An interactive enhancement function is used to convert all non-zero pixels to white and change catalog boundaries to gray. Hard copies are made using a Honeywell VGR 4000 Video Graphics Recorder. Snowcover maps are disseminated via first class mail and rapifax. GOES image sectors used to derive snowcover maps are archived on magnetic tape.

During 1985, the 16 basins mapped using reduced resolution NESDIS data were subdivided into 68 USGS hydrologic catalog units and

service was expanded to include 17 additional catalog units in Idaho. The catalog units range in size from 800 to 12,000 sq. km. and cover 350,000 sq. km. From late February through June 1985, the SFSS derived and disseminated 773 snowcover analyses for 85 catalog units in the western U.S.

CSIS Snowcover Mapping in Perspective

Many factors affect the accuracy of satellite areal snowcover measurements, including data resolution, methodology, exactness of basin boundaries, precision of registration of boundaries to imagery, measuring techniques, and the skill of the analyst applying the tools and procedures. There are four critical time components that affect the operational utilization of these data: frequency of observation, the time between data collection and availability for analysis, time required to do the analysis, and the time required to deliver the product to the users. The principal costs of the product are data acquisition, data processing and product delivery.

In terms of accuracy, the GOES interactive digital snowcover mapping technique has many distinct advantages over manual photointerpretation procedures except in the area of data resolution. LANDSAT's 30 m resolution is clearly superior to the NOAA polar orbiting data (1000 m at Nadir) and GOES (1000 m at the Equator). The digital technique has the ability to overcome the complexity of reflected light on various types of terrain from constantly changing solar illumination angles. Navigation and geographic data bases in CSIS enable the analyst to register imagery and basin boundaries more accurately (± 1 km) than a ZTS, and pixel counting is far more reliable than a planimeter or density slicer. The digital tech-

nique is not affected by complex, broken, or spotty snow fields. The digital technique also has considerably shorter processing times per basin than planimeter techniques. All other factors can be considered equal.

"Finding the clear spots" between cloud cover is one of the greatest advantages of using GOES data, because visible imagery is collected every 1/2 hour during daylight hours and is available for analysis within five minutes time. The wide range of possible collection times allows more frequent and reliable data collection. Analyses for 29 basins can be completed within 40 minutes of the data collection time. Maps can be disseminated within one hour of data collection time using a rapifax and within 24 hours using overnight express mail service.

While the CSIS technique has many advantages over other procedures, its' accuracy in heavily forested areas must be verified and documented through a cooperative program with UH and the users.

SERVICE REQUIREMENTS

Background

During the 1970's, the National Aeronautics and Space Administration (NASA) sponsored the Applications Systems Verification and Transfer (ASVT) snowmapping program. This five year user cooperative effort used four test sites in Arizona, California, Colorado and the northwestern United States to perform operational evaluations of the effects of technological capabilities (in existence at that time) on water resources forecasting.

Study results show that sixtyeight percent (68%) of the surface water in the 11 western states is derived from snowmelt

runoff. The total value of snowmelt runoff water is subdivided into the following categories:

Irrigation & hydroelectric energy	- 87%
Municipal & Industrial	- 9%
Flood Damage	- 4%
Other Uses	- <1%

Test results show that a minimum 6% improvement in forecast accuracy was achieved using satellite derived snowcover maps. This six percent improvement in forecasting snowmelt runoff would result in a total annual benefit of \$36.5 million (1981) dollars for irrigated agriculture and hydroelectric energy for the 11 western states. Estimated annual cost for the 2,195,250 km² area impacted by snowmelt forecasting was \$0.23/km². These costs were derived from the Colorado ASTV and are based upon acquiring eight sets of Landsat imagery (\$400), 16 man-days to interpret the imagery (\$800), eight man-days to implement the data (\$600) and the cost of a zoom transfer scope (ZTS) (\$10,000) with 25% utilization and amortized over 10 years. CSIS snowmapping costs during 1985 were \$0.14/km² of area mapped.

User Survey

The user community for snowcover maps is diverse in mission and, therefore, product utilization varies. Field and research offices of the National Weather Service (NWS), Corps of Engineers (COE), Bureau of Reclamation (BOR), Soil Conservation Service (SCS), Agricultural Research Service (ARS), and the Forest Service can utilize these data for real-time, medium range and seasonal streamflow forecasting, reservoir regulation and a variety of other water resources and agricultural services at regional and local levels. Additionally, many

agencies will utilize these data to develop, expand and calibrate hydrologic models.

During the summer of 1985, the SFSS surveyed existing and potential satellite hydrology users to prioritize expansion and development work on CSIS. Products and services listed for operational testing and development were percent snowcover per basin, percent snowcover per elevation zone per basin, solar insolation and precipitation, skin temperature over snowcovered area, atmospheric data (temperature, wind speed and direction), and historic data sets of all these products.

Additional information was also solicited for user requirements for product format, resolution, frequency of observations, seasonal coverage, and timely dissemination.

Survey Results - Non-Weather Service Users

Surveys were distributed to existing snowcover users and new agencies that had requested coverage during the 1986 snowmelt season. Therefore, the results cannot be interpreted as being representative of the entire hydrologic community. In fact, the results stated here will only cover non-NWS users.

In general, percent snowcover was requested by operational users plus historic data sets, while nonoperational users engaged in model development and calibration requested all or parts of the products surveyed. New areal snowcover mapping service was requested for 561,000 sq. km in the Western United States, 516,000 sq. km in the Great Lakes Basin and 176,000 sq. km in the Appalachian mountain range from Pennsylvania to Alabama. Elevation zone snowmapping services were generally

confined to basins above 6,000 ft.

Solar insolation was the most requested product in terms of total areal coverage and regional diversity. Data was requested for 2,823,000 sq. km, including large areas such as the Great Lakes Basin, Great Plains, and Appalachians, in addition to requests on the sub-regional and basin levels from West Virginia to California.

Skin temperature data was requested for 979,000 sq. km in the Great Lakes, Missouri headwaters, Appalachians, Rio Grande headwater, Salmon River, Death Valley, and Salt River Project. Half of the interest in the data is to see if it will help identify those portions of the snowpack where melt has begun.

The other half is for year-round monitoring of skin temperatures for vegetative and soil moisture stress on a real-time basis.

Upper air data was requested for 753,000 sq. km in the Great Lakes, Missouri headwaters, Sierras and Death Valley areas. These data will be used to develop, calibrate and drive operational models year-round. These data are needed on a real-time basis.

One of the most significant results of the survey has been requests by at least one office from the ARS, BOR, COE, USFS and USGS for all or most of the products surveyed. These data sets will be utilized to develop, calibrate and test a variety of hydrologic models. Output from these models will enable us to assess the value of these data sets and the validity of the scientific principles and techniques used to derive these data. These studies will play an integral role in prioritizing and implementing the data operationally.

CURRENT SERVICE OBJECTIVES

Areal Snowcover Mapping

During the 1986 snowmelt season, snowcover mapping services will be expanded to include an additional 561,000 sq. km in the Western United States and 128,000 sq. km for Lake Superior drainage. These new areas are almost double the 350,000 sq. km mapped during 1985. This expansion of service area is made possible by new software that will enable the hydrologist to display, combine and analyze imagery and geographical data bases more efficiently. Selected basins will be analyzed under snowfree and snowcovered conditions to assess the combined effects of various solar illumination angles, slope orientations, and terrain on visible brightness levels.

Snowcover Mapping by Elevation Zones

The Rio Grande River above Del Norte, Colorado, Salmon River above Whitebird, Idaho and possibly the Boise River above Lucky Peak Dam will be mapped by elevation zones. Digital elevation data sets will be remapped into the satellite projection of the snowfree/cloud-free mask. Each pixel in the mask which has a corresponding pixel in the elevation data set will then be level discriminated with the elevation pixel to produce a gray scaled elevation image. The derived snowcover image, elevation range and the hydrologic boundary data set will be combined to produce images of snowcover area and the percent of snowcover by elevation zone per hydrologic unit. These maps will only require one additional step and one minute of time to the existing procedure.

Solar Insolation

The metamorphosis of a

snowpack can be modeled by monitoring the energy balance of incoming solar radiation, escaping longwave radiation, sensible heat advection, and precipitation. Techniques developed by Gauthier *et al.* (1980), and Gauthier (1982) have shown the feasibility of measuring solar insolation from geostationary satellite data and detecting mesoscale variability in energy balance. One of the primary influences on the radiation balance is cloud cover, and one of the techniques used to determine snow-cover was developed to identify cloud cover. Elevation data sets will also be utilized to account for terrain orientation (snow lasts longer on the north slope of a mountain than on the south slope) and to adjust the data sets to more accurately estimate these parameters. We plan to investigate the possibility of monitoring the conditions on CSIS.

CONCLUSIONS

Interactive digital snowcover mapping with 1 km visible GOES data is an accurate, timely, and cost effective means of acquiring basin snowcover area to assess, allocate and forecast water resources from snowmelt runoff because:

- o It can overcome the complexities of reflected light on various types of terrain from constantly changing solar illumination angles.
- o Imagery and basin boundaries can be accurately registered (\pm km).
- o Pixel counting is a fast, accurate and reliable measuring technique.
- o Data collection is more frequent and reliable.
- o Cloud contamination can be minimized more effectively.
- o Up to 30 snowcover analyses can be completed within 40 minutes of the data collec-

tion time.

- o Digital data can be archived easily and inexpensively.
- o Analyses only cost \$140 per 1000 sq. km. per year during 1985.

Today's long and short range snowmelt runoff forecasting systems are dependent upon a variety of point hydrometeorological observations which are then statistically weighted and/or extrapolated to derive areally distributed data sets. Escalating costs for data collection have made snowpack monitoring with an interactive geostationary satellite system the most cost-effective means of acquiring temporally and spatially complete data sets to enhance the value of all other data.

REFERENCES

- Allen, M.W. and F.R. Mosher, 1985. Interactive Snowcover Mapping with Geostationary Satellite Data Over the Western United States. In: Summaries, Nineteenth International Symposium On Remote Sensing of Environment. p.
- Gautier, C., G. Diak, and S. Masse, 1980. A Simple Physical Model to Estimate Incident Solar Radiation at the Surface From GOES Satellite Data. J. Appl. Meteor., 17: 1005-1012.
- _____, 1982. Mesoscale Insolation Variability Derived From Satellite Data. Meteor., 21: 51-58.
- Tarpley, J.D., Schneider, S.R., and Danaher, E.J., 1979. An All Digital Approach to Snow Mapping Using Geostationary Satellite Data. In Proceedings of the Final Workshop on the Operational Applications of Satellite Snowcover Observations (Sparks,

Nevada), NASA Conference
Publication 2116, National
Aeronautics and Space
Administration, Washington,
D.C.

Castruccio, P., Loats, H., Lloyd,
D., and Newman, P., 1981.
Applications Systems
Verification and Transfer
Project Volume VII: Cost/
Benefit Analysis for the
ASVT on Operational Applica-
tions of Satellite Snowcover
Observations, NASA Technical
Paper 1828.

APPLYING A SNOWMELT-RUNOFF MODEL WHICH
UTILIZES LANDSAT DATA IN UTAH'S WASATCH MOUNTAINSWoodruff Miller¹

ABSTRACT: The Martinec-Rango Snowmelt-Runoff Model (SRM) was applied to the 130 km² American Fork, Utah basin in order to simulate the daily streamflow. The year 1983 was chosen to be investigated because of the record-breaking snowpack and peak discharges which uniquely tested the model. Landsat images were used to determine the snow-cover areas within the basin zones. While all model parameters were generally within the suggested numerical range and temporal sequence, some variations were necessary in order to generate the best correspondence between simulated and measured discharges. Because the recession coefficient is a function of historical streamflow data, an extensive analysis was required in order to approximate the all-time maximum flowrate. The simulation accuracy was very good as evidenced by the high hydrograph visual correspondence, the large daily discharge R² value of 0.85, and the small runoff volume D_v value of 3.7%. These statistics are in line with SRM average values from other basins.

(KEY TERMS: snowmelt-runoff model; snow cover; Landsat; simulation; recession coefficient.)

INTRODUCTION

Over the past two decades many stream-flow models have been developed in various countries which utilize snowmelt as the major runoff source. These usually

compute day-to-day flows taking advantage also of the daily cycles of temperature and solar radiation. The models are generally operational in a simulation and/or forecast mode. Simulations are used to produce discharge in ungaged basins or to compute snowmelt runoff for hypothetical climatic conditions. The forecast mode uses real time data to predict the runoff into the future. Applicability of these models has developed and improved as they have been tested on river basins with differing physical characteristics and climatological conditions.

The snowmelt-runoff model (SRM) developed by J. Martinec and A. Rango is one of these models. SRM is designed to simulate and forecast daily streamflow in mountain basins where snowmelt is a major runoff component. A unique feature of SRM is that Landsat imagery can be utilized to identify snow extent (Rango and Martinec, 1979). Description and information on application of the model are given in a published user manual (Martinec et al., 1983).

The model has been applied successfully to basins ranging in size from 3 to 4000 km² but may not be as applicable to non-mountain basins. SRM has been used for climate conditions from humid to semi-arid but tends to be less accurate when there are significant amounts of rainfall during the snowmelt period (Martinec et al., 1983). In a recent comparison among eleven snowmelt-runoff models conducted by the World Meteorological Organization

¹Associate Professor, Department of Civil Engineering, Brigham Young University, 368 K Clyde Building, Provo, Utah 84602.

(WMO), SRM performed very well. The results were consistent with earlier tests, the statistical evaluation parameters were good, and the potential for forecasting and year-round simulation were found to be promising (Rango, 1985).

BACKGROUND

The Snowmelt-Runoff Model was applied to the American Fork, Utah basin for the 1983 runoff period in order to evaluate the model under somewhat extreme conditions. The American Fork River basin is located near the center of the Wasatch Mountain range which runs north-south almost the entire length of Utah (Figure 1). This semi-arid basin has an area of 130 km² and ranges in elevation from 3580 m at the summit of Mount Timpanogos to 1820 m at the gaging station called "American Fork above Upper Power-Plant". American Fork River flows southwest into Utah Lake which drains to the north into Great Salt Lake through the Jordan River.

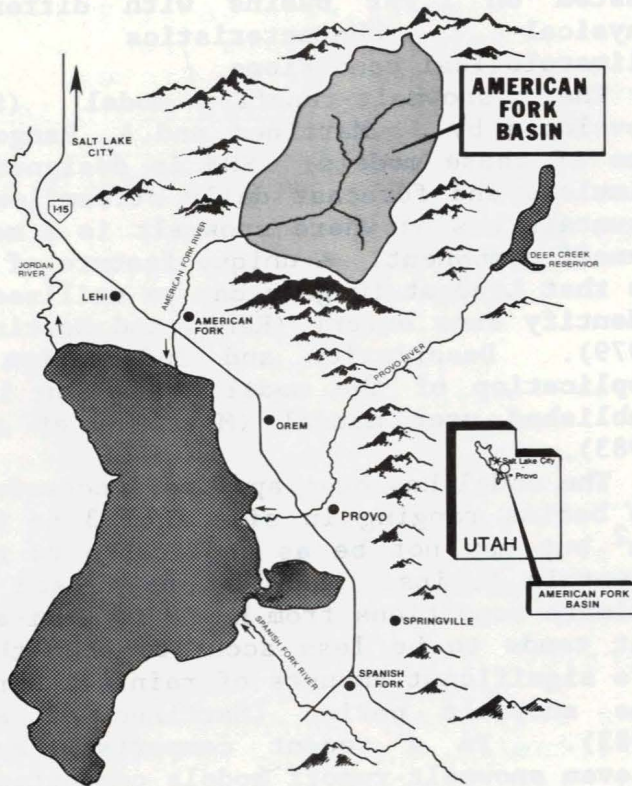


Figure 1. Location of American Fork Basin in Central Utah's Wasatch Mountains.

Snow depths in the American Fork basin have been observed to be well over 300 cm near the summits. High-elevation snow course maximum depths average approximately 180 cm and low-elevation snow course maximum depths average approximately 80 cm. The snowpack generally lasts well into June or July and on occasion remains throughout the summer at the higher elevations. Snowmelt is the major runoff component as evidenced by the fact that the American Fork River becomes almost dry in the late summer and fall.

Snow depths in the basin during the winter of 1982-83 were among the greatest on record and both the American Fork River volume of runoff and peak flowrate were the all-time maxima. The flooding was aggravated by the rapid temperature rise and above normal rainfall in late May along the Wasatch Mountains. Discharges from American Fork River and other tributaries caused Utah Lake to rise 2 m above its normal elevation and flood thousands of acres of prime agricultural land.

Parameter values used in the SRM which are based upon historical data were uncertain because of the record-breaking snowpack and runoff. This resulted in a unique use of the model and will contribute to the growing set of applications. The results of this test should be helpful in applying the SRM on basins with deep snowpacks which remain well into the summer months.

MODEL PARAMETERS

SRM is a deterministic runoff model with all parameters to be predetermined. Four elevation zones of approximately 440 m were established and the areas of each zone were determined. The other measured variables are: number of degree-days (T), ratio of snow-covered area to the total area (S), and precipitation contributing to runoff (P). For the American Fork study, T and P data were obtained from the weather station within the basin at Timpanogos Cave National Monument. Landsat scenes for May 30 and July 17, 1983 were used to develop S data (Figure 2). The percent of snow-covered area in

each zone on these dates was plotted and curves were drawn to estimate the daily percent of snow-covered area for the simulation period (Figure 3). More Landsat data would have been useful in establishing these curves but no other cloud-free scenes were available.

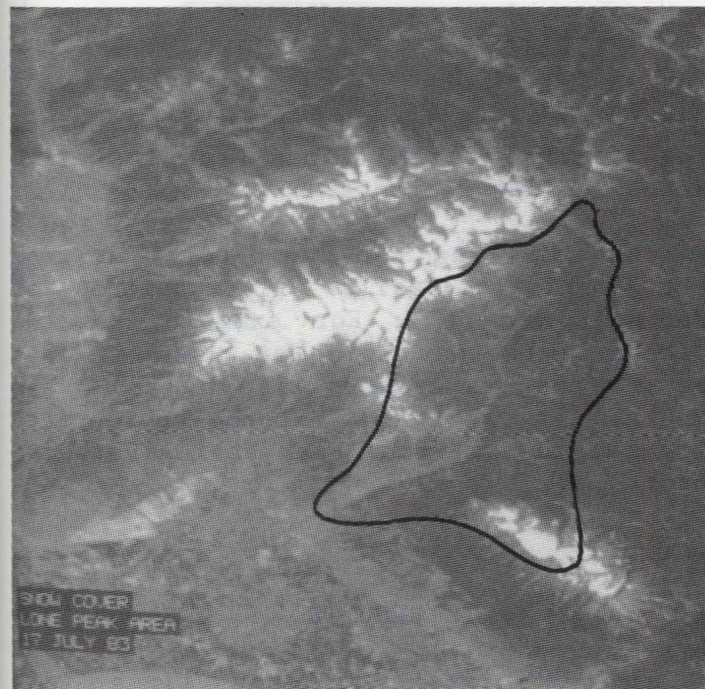
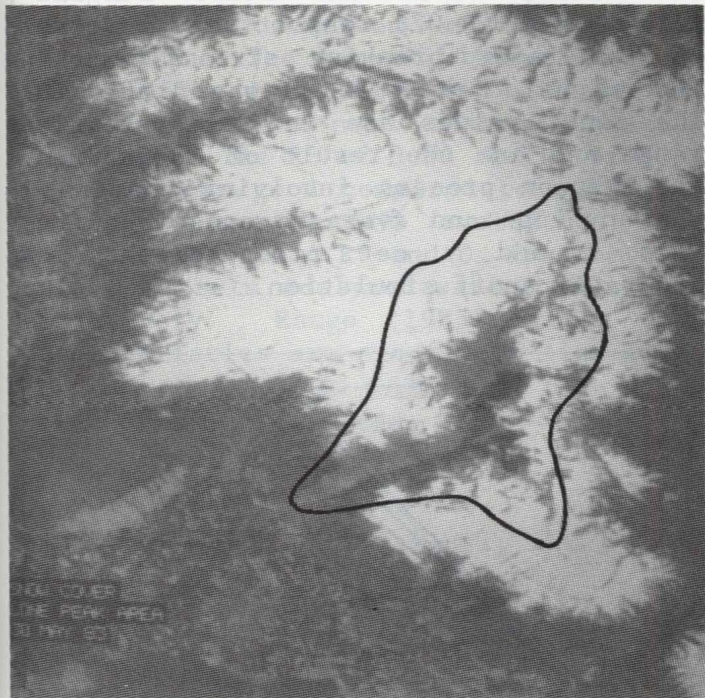


Figure 2. May 30 and July 17, 1983 Landsat Scenes with the Snow-Cover on American Fork Basin.

The model parameters to be calculated are: snow and rain runoff coefficients (C_s & C_r), degree-day factor (α) indicating the snowmelt depth from one degree-day, temperature lapse rate (γ), critical rain/snow threshold temperature (T_c), recession coefficient (k) indicating the decline of discharge, and the lag time (L).

Typically C_s values are suggested to be near 1.0 at the start of the snowmelt season, decrease to 0.5 or 0.4 in midsummer and may increase somewhat at the end of the runoff period. The C_r values are usually slightly lower than C_s values and decrease similarly but without a late season increase. (Martinec & Rango, 1986)

In the American Fork case, during April and May, the soil profile was relatively dry and there was significant recharge along with snowpack retention which called for lower than usual C_s values. There are also two small reservoirs in the basin which were holding a portion of the early runoff. During June, the C_s values were slightly higher than suggested because of the saturated conditions. Low values appropriate for late runoff were used for July and August. C_r values paralleled the C_s pattern at slightly lower magnitudes.

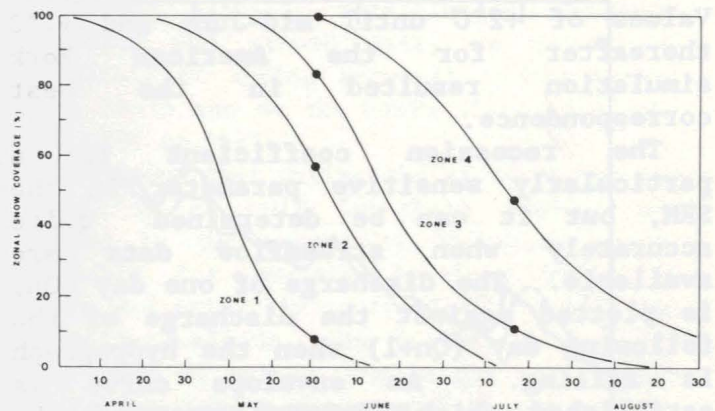


Figure 3. Landsat-Derived Snow-Cover Depletion Curves for American Fork Basin.

In SRM computations, α is determined by the empirical relation; $\alpha = 1.1 \rho_s / \rho_w$, where ρ_s and ρ_w are snow and water densities. Factors usually range from 0.35 to 0.6 $\text{cm}/^\circ\text{C-day}$ with the lower values earlier in the season (new snow) and at higher elevations (Martinec & Rango, 1986).

Values for the American Fork study varied from 0.3 to 0.6 through the snowmelt season, but were constant for all

elevations. The density ratios as calculated from snow course data in the lower two zones were also used for the higher two zones. Varying the α 's with elevation decreased the runoff simulation accuracy.

Without temperature stations at different elevations, the lapse rate must be evaluated with regard to climatic conditions. SRM simulations in the Rocky Mountains (of which the Wasatch are a part) have successfully used 0.75 to 0.95 °C per 100 m which increase throughout the season (Martinec & Rango, 1986). In the American Fork study, γ was held constant at 0.95 except for a ten day period in late May. During this time, there was an unseasonal warm period which apparently altered the temperature profile requiring a much lower lapse rate value.

Critical threshold temperature determines for each day of the snowmelt period whether measured precipitation was rain or snow. SRM retains rain in the snowpack in the beginning of the snowmelt season so that only the rain falling on snow-free areas contributes to runoff. Later, SRM allows the rain to penetrate the snow cover and become part of the runoff. T_c is suggested to decrease from +3°C to +0.5°C from April to August. Values of +2°C until mid-June and +1°C thereafter for the American Fork simulation resulted in the best correspondence.

The recession coefficient is a particularly sensitive parameter in the SRM, but it can be determined quite accurately when streamflow data are available. The discharge of one day (Q_n) is plotted against the discharge of the following day (Q_{n+1}) when the hydrograph is falling. An envelope curve is established which includes most of the points but not the extreme values. Then an average line between the lower envelope and the 1:1 line is drawn. By determining two k values from the usual equation, $k = Q_{n+1}/Q_n$, at two different discharges on the plot and substituting into the equations;

$$\begin{aligned} \log k_1 &= \log x + y \log Q_1 \text{ and} \\ \log k_2 &= \log x + y \log Q_2, \end{aligned}$$

values of x and y can be calculated. (Martinec et al. 1983). SRM uses x and y along with the current discharge to

determine a variable recession coefficient from the equation,

$$k_{n+1} = xQ_n^y$$

Figure 4 shows the recession flow plot for American Fork from 10 years of recession data. The envelope and average lines are shown and the values of x and y are 0.916 & -0.026 respectively. Because of the record-breaking streamflows, the determination of x and y was difficult. The final values are in the appropriate range and are the result of an extensive calibration process involving changes in the envelope and average recession lines. This x and y set produced the most accurate runoff simulation.

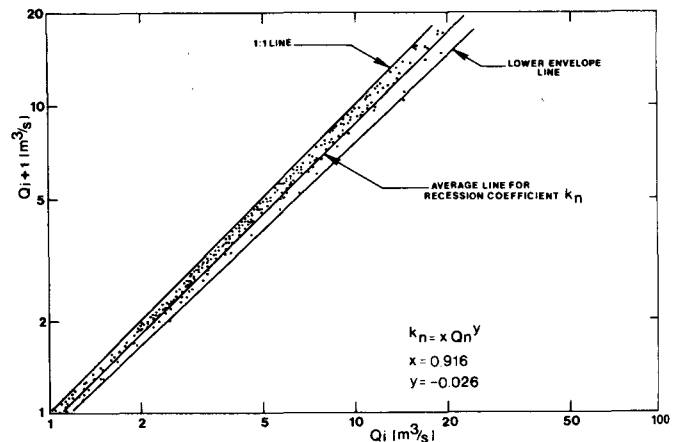


Figure 4. Recession Flow Plot for American Fork Basin with the Lines Used to Derive Recession Coefficients.

The time lag can be determined from characteristic daily fluctuations of snowmelt runoff. For example, if the discharge begins rising at noon, it lags behind the temperature rise by about six hours. It was found that the appropriate lag for the American Fork basin is twelve hours.

RESULTS

The SRM was run many times with different parameter values as part of the calibration process. Each iteration evaluation was based on three criteria. First, the graphical plot of simulated versus observed daily discharge was

examined for overall correspondence and to identify major simulation errors. Second, the coefficient of determination (R^2) value was examined for relative accuracy of daily discharge values. Finally, the percentage difference between the total measured and simulated runoff (D_v) was examined.

Figure 5 shows the final plot of the simulated and observed snowmelt season hydrographs. The temporal correspondence of streamflow peaks is good, although the magnitudes are not always exactly comparable. The R^2 of 0.90 and D_v of 1.7% are also very good compared to other SRM results. In the WMO evaluation, the average calibration R^2 and D_v for the four basin data sets analyzed were 0.85 and 5% respectively. Rango (1985) states that these statistics are exactly in line with SRM average values from all the other basins previously tested.

CONCLUSIONS

Based upon the American Fork study, the conclusion is made that the SRM can fairly accurately simulate streamflows and runoff volumes from a basin of deep and long-lasting snowpacks. A total runoff volume which had never been accumulated before was closely computed and a peak discharge which had never been gaged before was nearly reached by the model. This was accomplished with all model parameter values within the physically realistic ranges and without the benefit of more complete Landsat snow-cover area information.

Continuation of this investigation is ongoing. Some alternatives which are being pursued include choosing a year with more Landsat images, choosing a larger basin, choosing a year with minimum snowpack, and running the model for several years and on a year-round basis if data are available. Within Utah's Wasatch Mountains are ideal river basin locations for these future studies.

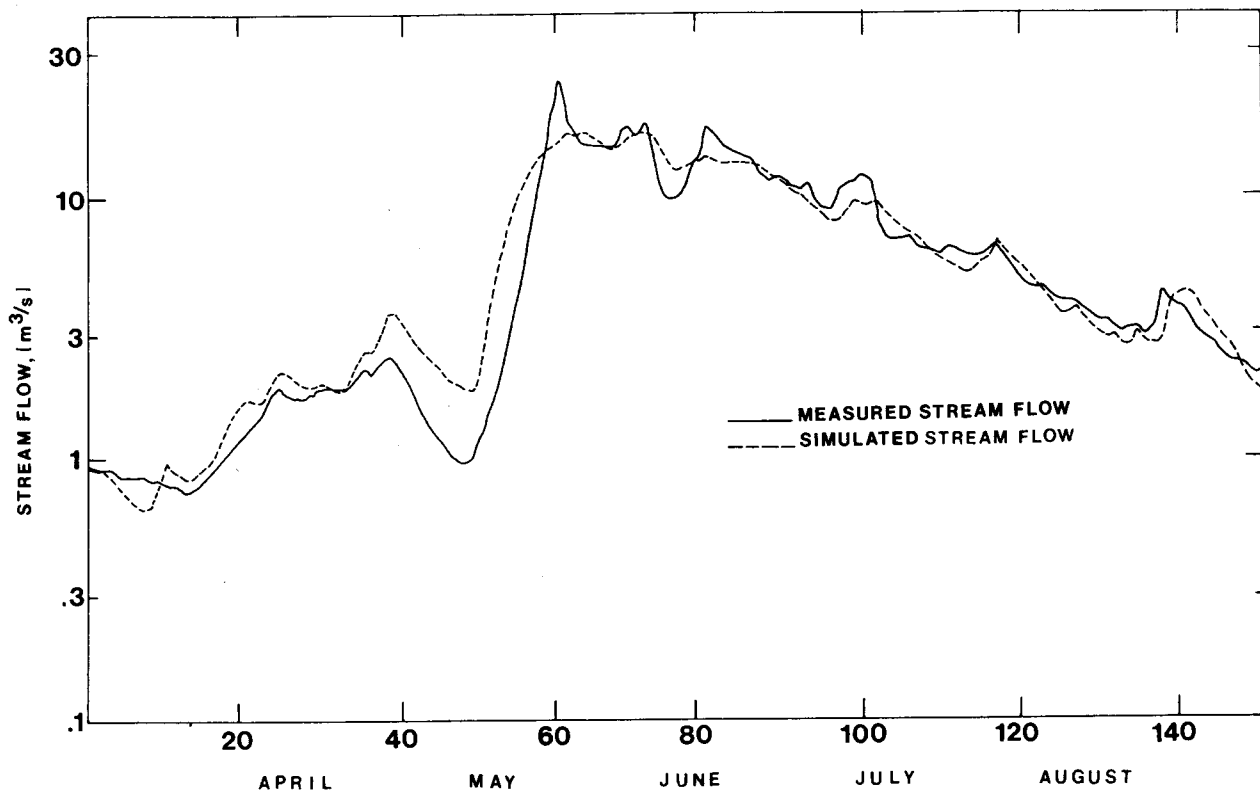


Figure 5. Daily Simulated and Observed Hydrographs during the Snowmelt-Runoff Season for American Fork Basin.

REFERENCES

- Martinec, J., A. Rango, and E. Major, 1983. The Snowmelt-Runoff Model (SRM) User's Manual. NASA Reference Publication 1100. 118 pp.
- Martinec, J. and A. Rango, 1986. Parameter Values for Snowmelt Runoff Modeling. Journal of Hydrology.
- Rango, A. and J. Martinec, 1979. Application of a Snowmelt-Runoff Model Using Landsat Data. Nordic Hydrology 10:4:225-238.
- Rango, A, 1985. Results of the Snowmelt-Runoff Model in an International Test. Proceedings of the Western Snow Conference, Boulder, Colorado.

INITIATION OF SPRING SNOWMELT OVER ARCTIC LANDS

David A. Robinson¹

ABSTRACT: The springtime initiation of snowmelt in the Tanana River Basin and over the North Slope of Alaska was found to correlate with daily regionally averaged values of parameterized absorbed shortwave radiation at the ground (Q) of from 6-8 MJm^{-2} and 2.5-4.5 MJm^{-2} , respectively. These values are a function of solar insolation, surface albedo and atmospheric screening factors. Results are based on analyses of satellite imagery and ground station data from 1978-1985. During these springs, the date melt started ranged from 3/27 to 4/23 (ave. 4/10) in the Basin and from 4/13 to 5/28 (ave. 5/10) on the Slope. An early or late melt in the Basin was not paralleled on the Slope. Regional albedo at the start of melt was approximately 0.35 in the Basin and 0.75 on the Slope. As the two regions differ by only several degrees of latitude, this difference in albedo appears to be the primary explanation for the considerably later date at which melt commenced on the Slope. In both regions, an early start of melt appeared to be caused by abnormally warm air advected into a region. On the Slope, regardless of the starting date, the most rapid interval of decreasing albedo occurred once a secondary threshold of 6-8 $\text{MJm}^{-2}\text{day}^{-1}$ was reached. Correlations between Q and local and regional temperatures appeared strongest on the Slope.

(KEY TERMS: snowmelt, absorbed shortwave radiation, albedo, temperature, runoff)

INTRODUCTION

The impact of spring snowmelt on hydrologic regimes in the arctic and subarctic depends on the water content of the snowpack and on the timing and duration of the melt period. An early, rapid, melt might result in spring flooding, followed by drought in summer.

While considerable effort has gone into improving estimates of the potential runoff from a snowpack (eg. Rango *et al.*, 1975; Ostrem *et al.*, 1979; Shafer *et al.*, 1979), less attention has been paid to the prediction of the start and duration of snowmelt, with some notable exceptions (eg. Carlson *et al.*, 1974; Rasmussen and Ffolliott, 1979). Here, using shortwave satellite and ground data, we report on variations of spring snowmelt in the Tanana River Basin and on the North Slope of Alaska from 1978 to 1985.

We found that during the study period the initiation of melt in these regions was related to the amount of shortwave energy available for surface heating, which in spring was primarily controlled by insolation and surface albedo. The latter, in turn, is a function of relief, the height and density of the vegetation canopy and of the extent, depth and physical characteristics of the snowpack (Kung *et al.*, 1964; Robinson and Kukla, 1984). The latter properties depend on the age of the upper layers of the pack. The timing and duration of snowmelt was monitored by observing regional changes in surface brightness using satellite data.

¹Lamont-Doherty Geological Observatory of Columbia University, Palisades, New York 10964.

DATA

Imagery from NOAA TIROS and Defense Meteorological Satellite Program (DMSP) near-polar orbiting satellites was examined. The Advanced Very High Resolution Radiometer onboard the NOAA satellites provided imagery with a resolution of 1 km in both visible (0.55-0.68 μ m) and infrared (10.5-11.5 μ m) channels. Daily data covering Alaska were available throughout the study period. Direct readout DMSP imagery was used for scattered intervals during the period. Spectral ranges are 0.4-1.1 μ m and 10.5-12.5 μ m. Resolution is 0.6 km.

Daily data of surface air temperature and snow depth were taken from Climatological Data for Alaska (NOAA, 1978-85).

METHOD

Daily sets of surface albedo, temperature, snow depth, cloudiness and absorbed shortwave radiation at the surface were assembled for the Tanana Basin and North Slope regions (Figure 1) from March 15 to May 15 and April 15 to June 15 of each study

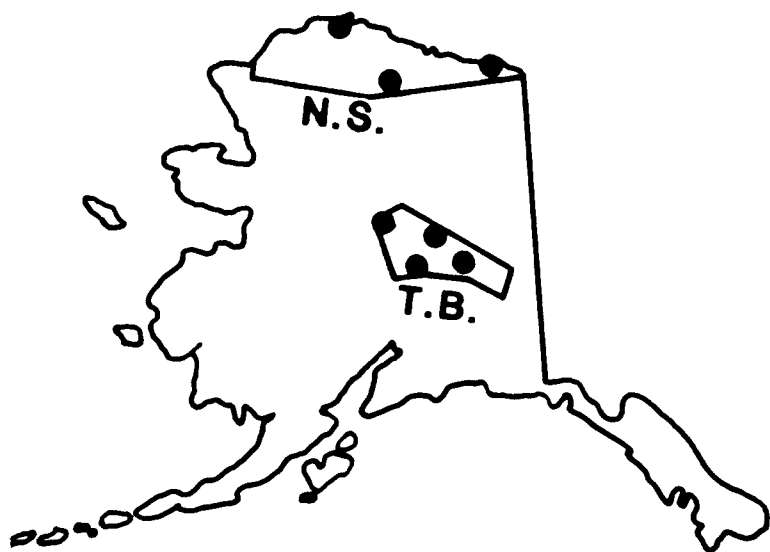


Figure 1. State of Alaska, showing the locations of the North Slope (NS) and Tanana Basin (TB) study regions. The locations of climate stations used in the study are marked with dots.

year, respectively, as follows:

1. Surface albedo: Clear-sky shortwave AVHRR scenes close to the satellite subtrack and showing different stages of progressing snowmelt were selected from the eight year data base to create a "master melt progression set" for each region. The average surface brightness of each scene of the sequential set was measured on an image processor. Specular reflectance is minimal over the surfaces measured at spring solar zenith angles in Alaska and at the satellite viewing angle (Taylor and Stowe, 1984). Surface albedo was computed from brightness data by linear interpolation between homogeneous bright and dark snow-covered or snow-free targets in each scene, whose surface albedos were estimated from data gathered in Alaska and elsewhere (eg. Larsson and Orvig, 1962; McFadden and Ragotzkie, 1967; Weller *et al.*, 1972; Maykut and Church, 1973; Robinson and Kukla, 1984). This method effectively eliminates differences in brightness between images resulting from variations in image production. Shine and Henderson-Sellers (1983), using a radiative transfer scheme, showed that this approach works well with satellite imagery, regardless of channel width. Albedos so calculated on an independent image may be up to 0.10 too low or 0.05 too high (Robinson and Kukla, 1985). However, monitoring the time progression of brightness histogram statistics throughout the melt period, such as standard deviation, skewness and kurtosis, narrowed the error range.

The albedo of a study region on a specific day during the eight year period was obtained by visual comparison of a clear-sky image for that day with the measured "master melt progression set". Where clouds prevented analysis, albedo was estimated by linear interpolation from the closest clear-sky dates.

2. Temperature and snow depth: Daily regional averages of high and low temperature and snow depth were calculated by averaging reports from stations evenly distributed within the study regions (Figure 1). The Tanana Basin stations included Big Delta, Fairbanks, McKinley Park and Tanana. Barrow, Barter Island and Umiat comprised the North Slope network.

3. Absorbed radiation: Daily parameterized shortwave radiation available for surface heating or evaporation was computed

from a simple model, whose inputs were regional surface albedo (a), insolation at the top of the atmosphere (I) and a parameterized regional atmospheric screening factor (S) (equation 1).

$$Q = (1-a) I S \quad (1)$$

Since an analysis of cloud cover from the polar orbiter imagery showed no seasonal trends in either region, the average observed cloud coverage during the eight melt seasons was used to derive a mean atmospheric screening factor of 0.47 in the Basin and 0.44 on the Slope. The preceding values were obtained from once-a-day visual estimates of areal cloud cover in each study region, following a method previously employed over arctic sea ice (Robinson *et al.*, 1985). This involved a visual inspection and charting of clouds in shortwave and infrared imagery, determining a fraction of cloud-covered area in the study region and estimating relative cloud thickness from the degree to which the clouds obscured the underlying surface contrast. Clouds were classified as thin, moderately thick or thick. Features under thin clouds were clearly recognizable but with reduced contrast. Features were marginally recognizable through moderately thick clouds and fully obscured under thick clouds. Cloud-class screening factors used in calculating regional screening factors were 0.6 (thin clouds), 0.4 (moderate) and 0.2 (thick) and clear skies 0.7. These highly approximate values were based on measurements in other regions at solar zenith angles of between 40° and 70° (Robinson, unpublished), the range of spring midday angles in the study regions. As only one morning or midday image per day was available for analysis, the cloudiness statistics do not take into account any potential diurnal cycle of cloud cover.

RESULTS

North Slope

In the early spring each year, regional surface brightness was homogeneous, with surface albedo close to 0.80. Subsequently, rivers began to appear as dark ribbons through the snow-covered region, as snowmelt runoff from the foothills of the Brooks Range reached the area (cf. Holmgren *et al.* (1975)

for a detailed description of breakup on the North Slope). As a result, regional albedo decreased to about 0.75. Once the paths of streams originating in the tundra began to appear, albedo fell below 0.75. At this time we considered regional melt to be underway. When albedo reached approximately 0.25, only a few patches of snow and numerous frozen ponds were recognized on the imagery as being brighter than the surrounding snow-free tundra. At this point the major period of melt was considered over.

The timing and duration of the North Slope melt varied by up to 45 and 38 days, respectively, during the 1978-1985 period (Table 1). When melt began in late April to mid-May (Figure 2) it tended to last longer than when it commenced later in May (Figure 3).

TABLE 1. Dates on which the major period of snowmelt started (albedo fell below 0.75) and ended (albedo reached 0.25) on the North Slope. The duration (Dura.) of melt and the daily parameterized absorbed shortwave radiation at the ground (Q) ($MJm^{-2}day^{-1}$) in the region on the date melt commenced and at the start of the most rapid 10 day period of albedo decrease are also given.

Year	Start Date	Q	End	Dura. (days)	Rapid start: Date	Q
1978	5/24	4.4	6/13	20	6/5	7.2
1979	4/19	2.8	6/4	46	5/28	10.9
1980	5/21	4.2	6/15	25	6/6	7.3
1981	5/6	3.6	6/13	38	5/28	8.1
1982	5/29	4.5	6/18	20	5/31	6.1
1983	4/13	2.5	6/7	55	5/29	7.8
1984	5/28	4.5	6/14	17	6/6	6.9
1985	5/16	4.2	6/3	18	5/24	6.7

Early melt was associated with abnormally warm temperatures. On the average, highs were near $0^\circ C$ during the period of initial slow albedo decreases of from about 0.75 to 0.55. Following this, an interval of stable albedo and colder temperatures was common. In the last week of May, the albedo again dropped at an increased rate. The major melt

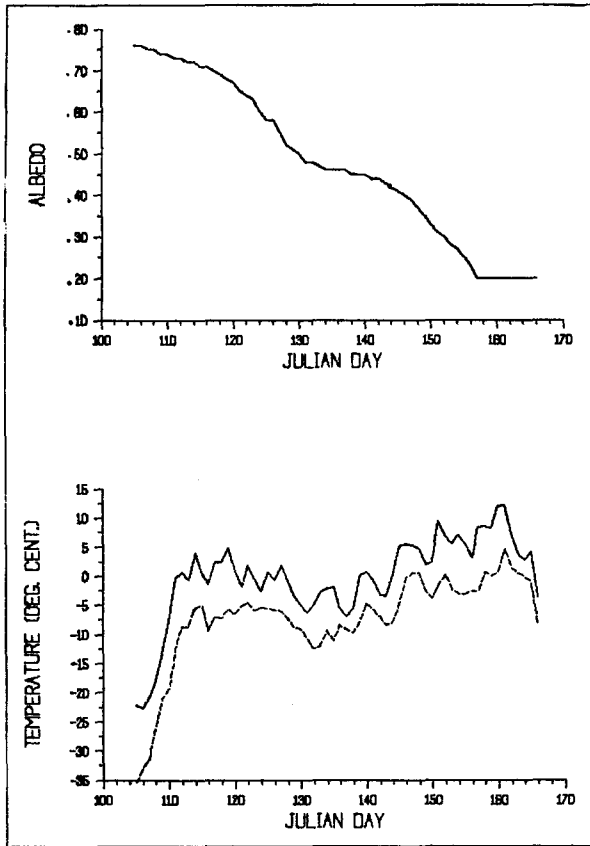


Figure 2. Daily regional surface albedo (top) and regionally averaged high and low temperatures (bottom) from April 15 (Julian day 105) to June 15 (Julian day 166), 1979 on the North Slope.

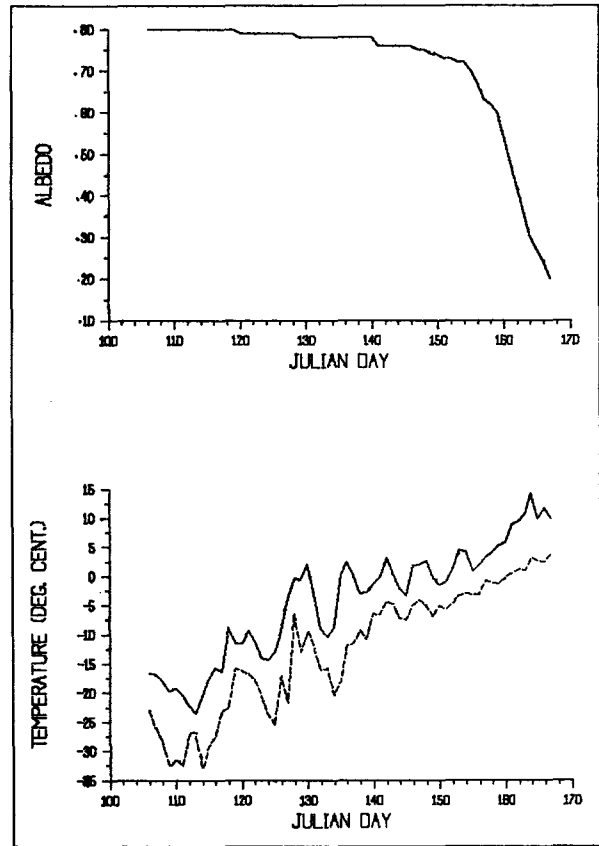


Figure 3. Same as Figure 2, but for 1984 (Julian days 106 to 167).

ended between June 3 and 13. High temperatures were close to $+5^{\circ}\text{C}$ during the last active phase of melt and frequently rose above 5°C following the melt. Low temperatures generally remained below 0°C until melt was complete. In years with a later start of melt, temperatures prior to, during and following the melt were similar to those for the early start years. However, in late years melt was most active in early June and ended between June 13 and 18.

There was no relationship between snow depth measured at the start of melt at the three Slope stations and the satellite-derived timing and duration of the regional melt. It is uncertain, however, to what degree these stations represent regional conditions.

Daily parameterized absorbed shortwave radiation at the ground at the commencement

of regional melt ranged from $2.5\text{--}4.2 \text{ MJm}^{-2}$ ($1\text{J}=0.239\text{cal}$) in early melt years and $4.2\text{--}4.5 \text{ MJm}^{-2}$ in late melt years (Table 1). At the beginning of the most rapid 10 day decline in surface albedo, albedo values ranged from 0.53 to 0.65 and daily Q values were between 6.1 and 8.1 MJm^{-2} . The only exception was the 10.9 MJm^{-2} value in 1979, when albedo was 0.37.

There was a large range between the daily values of Q over the North Slope in the earliest and latest melt cases (Figure 4). On average, over twice as much radiation was absorbed on a given date in late May or early June in 1979 than in 1984. Correspondingly, in May 1979, Slope temperatures were 4°C higher than in 1984. Within the region, high temperatures in May 1979 differed by 10°C between Umiat, where the high averaged $+5^{\circ}\text{C}$, and Barrow, where the high averaged -5°C . Albedo during this month was considerably lower in the vicinity of Umiat than at Barrow. In 1984 the Slope remained snow

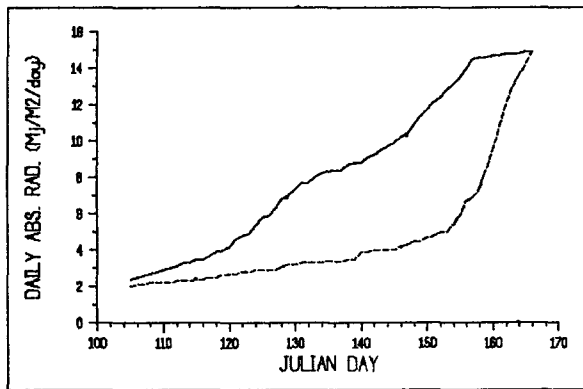


Figure 4. Daily parameterized absorbed shortwave radiation at the ground in the North Slope test region from April 15 to June 15 in 1979 (top curve) and during the same period in 1984 (bottom curve). Results based on a model which incorporates realistic surface albedo, top of atmosphere insolation and parameterized mean eight year surface radiation income. Bottom axis shows Julian days in 1979. Add one day to get Julian days in 1984.

covered throughout May and the mean Umiat high (-1°C) was only 4°C higher than Barrow's (-5°C).

Tanana Basin

In late March and early April of the eight studied years, surface albedo in the Tanana Basin ranged between 0.32 and 0.38. The higher value appeared to come close to the Basin's potential maximum, while the lower value was the result of meager snow cover in upstream valley regions. Once the surface brightness began to continuously decrease, the melt was considered to be underway. The rate at which albedo decreased remained relatively constant until the regional surface albedo was close to 0.20. This was considered the active period of melt. When albedo reached 0.20, snow cover was only visible on the higher ground and occasionally in downstream portions of the Basin and the major melt period was considered over.

The timing and duration of Basin melt varied by up to 27 and 19 days, respectively, between 1978-1985 (Table 2). Melt commenced between April 6 and 14 in six of the eight

TABLE 2. Dates on which the major period of snowmelt started (albedo fell and stayed below the spring maximum) and ended (albedo reached 0.20) in the Tanana Basin. The duration (Dura.) of melt and the daily parameterized absorbed shortwave radiation at the ground (Q) ($\text{MJm}^{-2}\text{day}^{-1}$) in the region on the date melt commenced are also given.

Year	Start Date	Q	End	Dura. (days)
1978	4/9	7.2	4/28	19
1979	4/14	7.9	5/2	18
1980	3/27	5.9	4/29	33
1981	4/14	8.1	4/28	14
1982	4/6	6.6	5/13	37
1983	4/9	7.2	4/30	21
1984	4/10	7.5	5/8	28
1985	4/23	8.5	5/20	27

years, with 1980 (March 27) (Figure 5) and 1985 (April 23) (Figure 6) being the only exceptions. There was some indication that the melt took longer when it began earlier, but snow depth, which on a regional scale was poorly known, may also have affected the duration. In 1981, when the depth of the snowpack at the four Basin stations averaged the lowest (17cm), the melt duration was the shortest (14 days). Conversely, in 1985, when the pack was deepest (64cm), the duration was relatively long (24 days), despite having the latest starting date.

High temperatures during the early stages of melt were generally within several degrees of freezing. Only in 1980, when there was a persistent period of abnormal highs of about $+5^{\circ}\text{C}$ in late March and early April, were temperatures noticeably higher at the beginning of melt. In all years, highs were usually between $+5^{\circ}\text{C}$ and 10°C during the middle and later stages of melt and regularly above 10° following melt. Low temperatures generally remained below 0°C until melt was complete.

Daily parameterized values of Q were between 6.6 and 8.1 MJm^{-2} at the commencement of melt in six of the eight years (Table 2). Only in 1980 (5.9 MJm^{-2}) and in 1985 (8.5 MJm^{-2}) did they fall outside of this range. These two years exhibited the largest

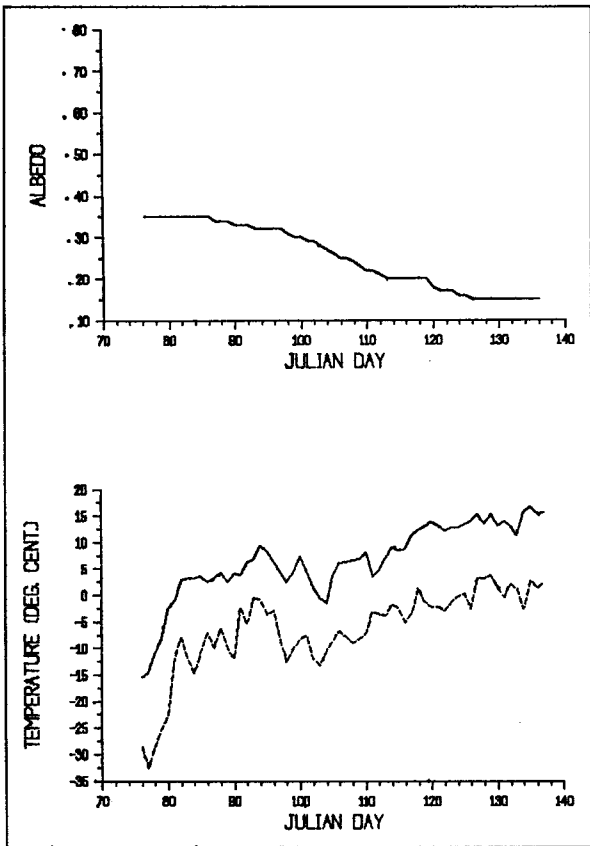


Figure 5. Daily regional surface albedo (top) and regionally averaged high and low temperatures (bottom) from March 15 (Julian day 75) to May 15 (Julian day 136), 1980 in the Tanana Basin.

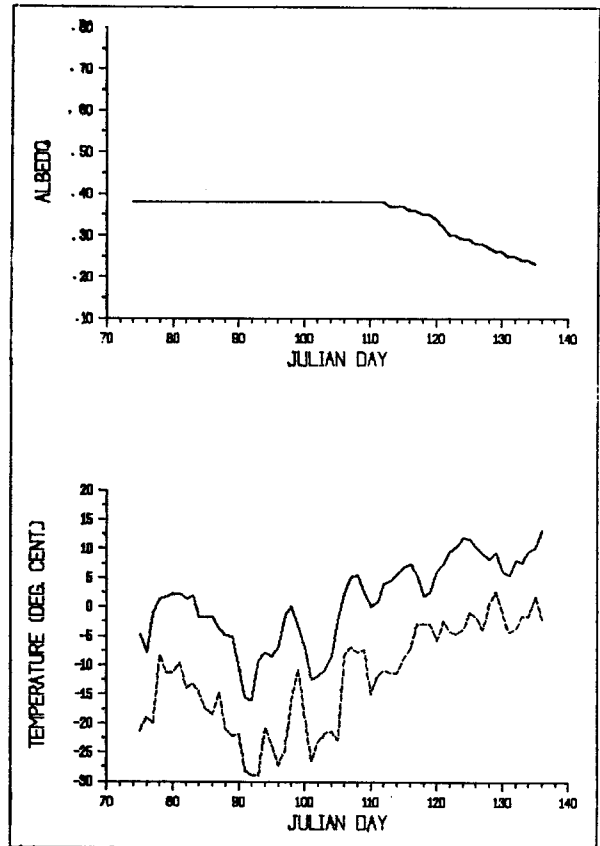


Figure 6. Same as Figure 5, but for 1985 (Julian days 74 to 135).

differences in daily Q amongst the years studied (Figure 7). In the latter half of April, daily values differed by close to 2.5 MJm^{-2} , with 1985 values lagging about 2 weeks behind those in 1980 (Figure 7). In April 1980, the mean temperature in the region was $+1^\circ\text{C}$, while in April 1985 it was -8°C .

DISCUSSION

The approximately six degree difference in latitude of the Tanana Basin (64°N) and North Slope (70°N) study regions results in the Slope receiving 16% less daily insolation at the top of the atmosphere than over the Basin on April 1 and 6% less on May 1. Thus, there would be a difference of only several days in melt initiation between the two

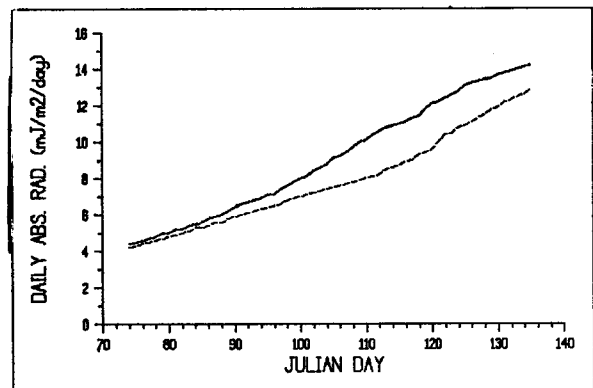


Figure 7. Daily parameterized absorbed shortwave radiation at the ground in the Tanana Basin study area from March 15 to May 15 in 1980 (top curve) and in 1985 (bottom curve). See Figure 4 for model description. Bottom axis shows Julian days in 1985. Add one day to get Julian days in 1980.

regions in April if regional snow-covered albedos were the same. By late May, the Slope receives more insolation at the top of the atmosphere than the Basin. Therefore, the difference in the regional albedos of the two regions when snow covered appears to be the primary reason why the most active period of melt in the open country of the Slope began an average of 51 days later than the start of the active period of melt in the forested Basin. In each region, there was a threshold₂ range of daily Q of approximately 6-8 MJm⁻² reached before the most active period of decreasing albedo began. This threshold range was reached in mid-April in the Basin but in the last week of May or first week of June on the Slope.

An early or late start of melt in the Basin did not necessarily correlate with the relative timing of initial melt on the Slope. The starting date of initial melt in the two regions differed by as few as 4 days and as many as 55 days. This range was generally a reflection of the widely ranging starting dates on the North Slope. There was also no relationship between the two regions regarding the time at which melt ended. This differed from 14-57 days.

An early commencement of melt on the North Slope in April or early May did not trigger the rapid demise of snow cover over the entire Slope, apparently because of the low values of absorbed radiation which exist at that time of spring. Insolation is considerably below its late spring values and the albedo, despite a partial decrease from its maximum, remains relatively high.

Correlations between absorbed radiation and the most active period of melt and between absorbed radiation and local and regional temperatures appear strongest on the North Slope. This is likely due to the greater simplicity of the boundary layer dynamics on the Slope compared to the Basin. In the latter, the water content of the snowpack is more variable in an absolute sense in a given year as well as between years. The forests in the Basin add to the complexity of the radiation budget, as does its more variable topography and frequent inversions. The radiation budget of the Slope is more singularly and directly affected by the snowpack.

Several of the study results stand out as being of importance to the hydrologic community. 1) There is not a parallel

relationship between an early or late melt in the Basin and on the Slope. 2) The major period of snowmelt runoff can not be expected to occur in either region until the initial shortwave radiation threshold is reached. 3) When₂ the₁ secondary threshold of 6-8 MJm⁻² day⁻¹ is reached on the Slope, the subsequent runoff should be reduced in years when the melt starts early. 4) The duration of melt in the Basin appears to be more sensitive to the initial water content of the snowpack than on the Slope.

ACKNOWLEDGMENTS

Appreciation is expressed to Mark Serreze and George Kukla for their contributions to this study. This work was supported by Air Force grant AFOSR 86-0053 and National Science Foundation grant ATM 85-05558. This is LDGO contribution 3972.

LITERATURE CITED

- Carlson, R.F., W. Norton and J. McDougall, 1974. Modeling Snowmelt Runoff in an Arctic Coastal Plain. University of Alaska Institute of Water Resources Report IWR-43, 72pp.
- Holmgren, B., C. Benson and G. Weller, 1975. A Study of the Breakup on the Arctic Slope of Alaska by Ground, Air and satellite Observations. In: Climate of the Arctic, G. Weller and S.A. Bowling (Editors). Twenty-Fourth Alaska Science Conference, 15-17 Aug. 1973, 358-366.
- Kung, E.C., R.A. Bryson and D.H. Lenschow, 1964. Study of a Continental Surface Albedo on the Basis of Flight Measurements and Structure of the Earth's Surface Cover Over North America. Mon. Wea. Rev. 22:543-564.
- Larsson, P. and S. Orvig, 1962. Albedo of Arctic Surfaces. Arctic Meteorology Research Group, McGill University, Publication in Meteorology No. 54, 33pp.
- Maykut, G.A. and P.E. Church, 1973. Radiation Climate of Barrow, Alaska, 1962-66. J. Appl. Met. 12:620-628.
- McFadden, J.D. and R.A. Ragotzkie, 1967. Climatological Significance of Albedo in Central Canada. J. Geophys. Res. 72:1135-1143.
- NOAA, 1978-1985. Climatological Data,

- Alaska, v.64-71.
- Ostrem, G., T. Andersen and H. Odegaard, 1979. Operational Use of Satellite Data for Snow Inventory and Runoff Forecast. In: Satellite Hydrology, M. Deutsch, D.R. Wiesnet and A. Rango (Editors). American Water Resources Association, 230-234.
- Rango, A., V.V. Salomonson and J.L. Foster, 1975. Employment of Satellite Snowcover Observations for Improving Seasonal Runoff Estimates. In: Operational Applications of Satellite Snowcover Observations, A. Rango (Editor). NASA, 157-174.
- Rasmussen, W.O. and P.F. Ffolliott, 1979. Prediction of Water Yield Using Satellite Imagery and a Snowmelt Simulation Model. In: Satellite Hydrology, M. Deutsch, D.R. Wiesnet and A. Rango (Editors). American Water Resources Association, 193-196.
- Robinson, D.A. and G. Kukla, 1984. Albedo of a Dissipating Snow Cover. J. Cl. and Appl. Met. 23:1626-1634.
- Robinson, D.A. and G. Kukla, 1985. Maximum Surface Albedo of Seasonally Snow-Covered Lands in the Northern Hemisphere. J. Cl. and Appl. Met. 24:402-411.
- Robinson, D.A., G.J. Kukla and M.C. Serreze, 1985. Arctic Cloud Cover During the Summers of 1977-1979. Lamont-Doherty Geological Observatory of Columbia University Technical Report LDCO-85-5, 175pp.
- Shafer, G.A., C.F. Leaf and J.K. Marron, 1979. Landsat Derived Snow Cover as an Input Variable for Snow Melt Runoff Forecasting in South Central Colorado. In: Satellite Hydrology, M. Deutsch, D.R. Wiesnet and A. Rango (Editors). American Water Resources Association, 218-224.
- Shine, K.P. and A. Henderson-Sellers, 1983. Cryosphere-Cloud Interactions Near the Snow/Ice Limit: Sensitivity Testing of Model Parameterizations. Final Report NSF Grant ATM 80-18898, University of Liverpool, 158pp.
- Taylor, V.R. and L.L. Stowe, 1984. Reflectance Characteristics of Uniform Earth and Cloud Surfaces Derived From Nimbus-7 ERB. J. Geophys. Res. 89:4987-4996.
- Weller, G., S. Cubley, S. Parker, D. Trabant and C. Benson, 1972. The Tundra Microclimate During Snow-melt at Barrow, Alaska. Arctic 25:291-300.

RIVER ICE HYDRAULICS

FORECASTING THE EFFECTS ON RIVER ICE
DUE TO THE PROPOSED SUSITNA HYDROELECTRIC PROJECT

Ned W. Paschke and H.W. Coleman*

ABSTRACT: River ice processes affect the physical and hydraulic properties of many of the world's rivers. Although winter flows are characteristically low, the additional friction and ice displacement within an ice-covered river can greatly increase the water surface elevation. The Susitna River, located in south-central Alaska, is generally subject to river ice processes for 6 or 7 months of each year. Environmental studies in connection with the proposed Susitna Hydroelectric Project (Alaska Power Authority, 1985) included documentation of natural (pre-project) river ice conditions and forecasting the effects of the project on river ice. In this regard, a numerical river ice model was calibrated and applied to an 85-mile reach of the Susitna River downstream of the proposed project. This paper presents a summary of the river ice modeling process, observed trends in natural ice conditions and the expected effects of the proposed project.

(KEY TERMS: cold regions; river ice; winter hydro operation, river ice modeling.)

INTRODUCTION

Proposed Susitna Hydroelectric Project

The proposed Susitna Hydroelectric Project includes the construction of two large dams on the Susitna River (Figure 1). Watana Dam, an earthfill structure with an ultimate planned height of 885 feet, would be located 184 river miles upstream from the river mouth at Cook Inlet (i.e., "RM 184"). Devil Canyon Dam, a 645-foot high concrete arch structure, would be located at RM 152, i.e., 32 miles downstream of Watana Dam.

The project is planned for construction in 3 stages as follows:

- Stage I - Watana Dam would be constructed to an initial height of 700 feet.
- Stage II - Devil Canyon Dam (full height) would be constructed.
- Stage III - Watana Dam would be raised to its ultimate height of 885 feet.

* Respectively, Hydraulic Engineer, Harza Engineering Company, 150 South Wacker Drive, Chicago, Illinois 60606 (Presently, Assistant Director of Engineering and Planning, Madison Metropolitan Sewerage District, 1610 Moorland Road, Madison, Wisconsin 53713); and Head, Hydraulic Analysis and Design Section, Harza Engineering Company, 150 South Wacker Drive, Chicago, Illinois 60606.

Stage I is planned to begin operation in the year 1999. Stages II and III would be added in accordance with energy demand.

project in operation, changes from the natural flows and stream temperatures will affect the river ice conditions and the frequency and severity of the slough overtopping events. The river ice model therefore focuses on the timing and magnitude of ice-induced river stage variations at the slough and side channel locations.

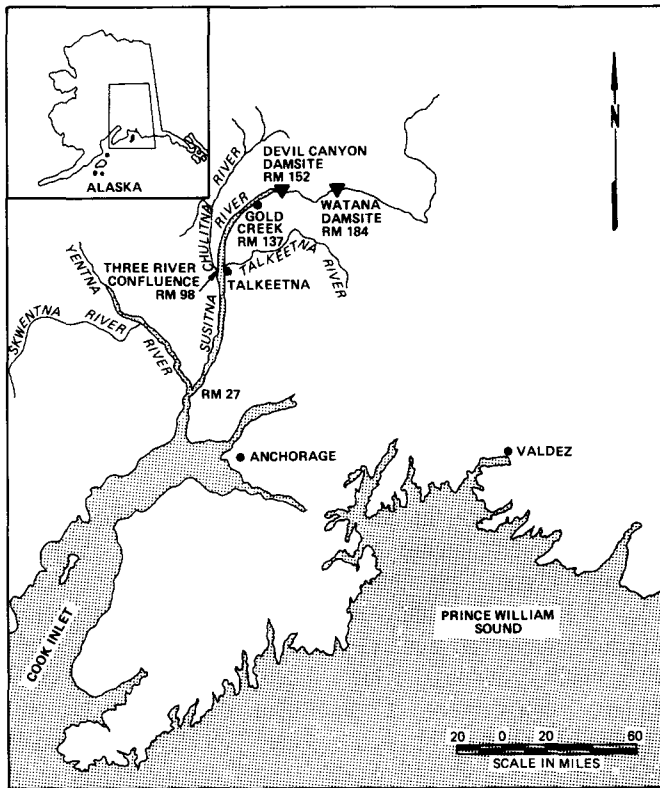


Figure 1. Susitna River Location Map

METHODOLOGY

Study Reach

River ice modeling was limited to the "middle reach" of the Susitna River, i.e., the 85-mile reach from the Watana dams site to the "three-river confluence" formed by the Susitna, Chulitna and Talkeetna Rivers (Figure 1). Downstream of this confluence, the substantial incoming tributaries are expected to lessen the relative effects of the future project. Typical natural river flow rates in the vicinity of the damsites range from 30,000 cfs in June to less than 2,000 cfs in March. With the project operating reservoir releases would generally be 8,000 to 13,000 cfs year-round.

Environmental Background

Environmental concerns regarding ice processes on the Susitna River include potential effects on the salmon population. A number of slough and side channel areas along the river provide habitat for spawning and juvenile overwintering. These areas are generally isolated from the mainstem by a natural berm at the upstream entrance to the slough or side channel. During the winter, these areas are often warmer than the mainstem due to upwelling of relatively warm (e.g. 3°C) groundwater. Ice-induced stage increases periodically overtop some of the berms under natural conditions, flooding the slough with 0°C mainstem water and possibly harming the developing salmon. With the proposed

Susitna River Ice Observations

Ice observations on the Susitna River have been documented for the past five winters (R&M Consultants 1981, 1982, 1983, 1984, 1985). Natural ice processes on the Susitna typically begin in early October with the generation of frazil ice, i.e., small ice crystals probably formed in supercooled surface water exposed to subfreezing air temperatures (Ashton, 1978). Frazil ice is first observed in the middle and upper reaches of the Susitna which are subject to the coldest air temperatures. Reaches of low solar radiation and high water turbulence appear to be highest in frazil ice production.

As the frazil is carried downstream, it coalesces into pans or rafts of "slush" ice which are often 2 to 5 feet in diameter and which may cover as much

as 80% of the river surface. Border ice is observed to form as some of the slush ice pans come to rest and freeze together in low velocity zones along the river banks.

Typically late in October, an accumulation of slush ice becomes jammed and freezes together near the river mouth, forming a stationary ice bridge across the river. Formation of the ice bridge appears to be triggered by a high concentration of slush ice pans, low air temperatures and a high tide event in Cook Inlet which substantially reduces river velocities for several miles upstream. Following formation of the ice bridge, slush ice pans accumulate against its upstream edge and thereby advance the ice cover in an upstream direction. Some slush is observed to be swept beneath the ice front and is apparently deposited downstream on the underside of the cover, thereby thickening the ice cover. Periodic mechanical compression or "shoving" of the advancing ice cover (Pariset et. al., 1966) is observed, whereby as much as 2000 feet of the slush ice cover consolidates and thickens.

The advancing ice cover often reaches the three-river confluence (RM 98) in November and the vicinity of Gold Creek (RM 137) in late December or January, but varies with weather and flow conditions. Observed ice front progression rates in the middle reach typically range from 0 to 2 miles per day. Ice front progression generally becomes undefined upstream of Gold Creek, where intermittent bridging of border ice precedes the arrival of the ice front.

River stage increases of 2 to 6 feet in the middle reach are common during progression of the ice front, and overtopping of some slough and side channel areas has been observed. Slush ice cover thicknesses are observed to vary substantially along the river and particularly across the channel width. Often little or no ice is observed in a central, high velocity core area whereas accumulations as great as 12 feet thick reaching the channel bottom have been observed closer to the river banks. Following progression, the upper surface of the slush ice cover begins to freeze into solid ice. The solid ice portion of the ice cover is observed to reach typical thicknesses of

2 to 4 feet by February or March.

Spring breakup of the ice cover typically occurs in early May and is largely due to the natural flow increases which lift and fracture the cover. Sporadic ice jams caused by blocks of the fractured ice cover are observed to cause greater stage increases and more frequent slough overtoppings than those of the initial ice cover progression.

River Ice Model

The numerical river ice model was based on the work of Calkins (1984) on the Ottawaquechee River and was modified and calibrated by Harza-Ebasco (1984) for application to the Susitna River. The model provides a daily summary of hydraulic and ice conditions throughout the study reach during the period from November 1 to April 30. A detailed description of the model and its governing equations has been presented by Calkins (1984). The general features of the model are briefly summarized as follows:

1. Hydraulic profiles are computed daily based on the Bernoulli and Manning equations (standard step method). Computations include the effects of the ice cover and border ice where appropriate.
2. Frazil ice production within reaches of 0°C open water is computed by a heat transfer coefficient approach (Ashton, 1978). Cumulative frazil flow rates are tabulated as the ice travels downstream.
3. Border ice growth is computed as a function of air temperature and water velocity and is calibrated to Susitna observations.
4. Hydraulic conditions at the ice front determine if the slush ice pans are swept beneath the ice cover or accumulated at its upstream edge, thereby advancing the ice front (Figure 2). Deposition of slush ice beneath the cover is computed based on the ice supply and water velocity under the ice cover. Thicknesses of the advancing ice cover are computed in accordance with

Pariset, et. al. (1966). Ice front progression rates are based on river geometry and the supply of ice reaching the front.

5. Solid ice growth within the slush ice cover is computed (Figure 2).
6. Melting of the ice cover and retreat of the ice front are computed when warm water (i.e. above 0°C) reaches the ice front. Water temperature decay beneath the ice cover is also computed. Mechanical breakup of the ice cover is not simulated by the model.

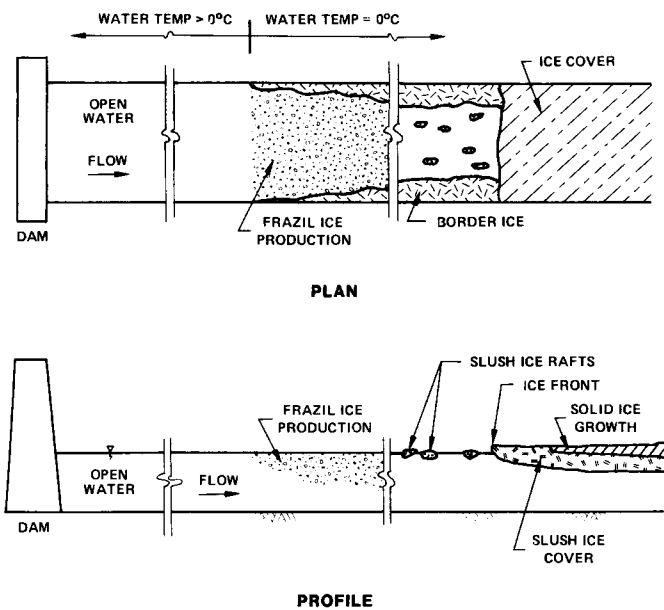


Figure 2. River Ice Schematic

Surveyed river cross-sections at 102 locations between Watana damsite (RM 184) and the "three-river confluence" (RM 98) were used in the model. Manning's "n" values ranging from .022 to .065 were selected to calibrate the open-channel portion of the model to stage-discharge measurements. Daily air temperatures and wind speeds recorded at 3 locations along the study reach were used for the various ice processes in the model. For simulations of natural (pre-project) conditions, daily flow rates and frazil ice discharges were input at the upstream boundary based on observations at Gold

Creek (RM 137). For with-project conditions, flow rates and water temperatures upstream of the ice front were provided by corresponding reservoir and stream temperature simulations. Starting dates for the simulated with-project ice front progression at the three-river confluence were based on tabulation of the total ice volumes supplied to the lower Susitna River and the time required to advance the lower Susitna ice front from Cook Inlet to the three-river confluence.

The river ice model is primarily intended to simulate the timing and magnitude of river stage variations associated with ice. Simulated natural ice conditions show reasonably good agreement with field observations (Figure 3). Limitations of the model relate primarily to its one-dimensional nature. Velocities and ice cover thicknesses computed by the model are mean or characteristic values intended to represent an entire cross-section. Actual velocities and ice thicknesses are likely to be quite non-uniform within the cross-section.

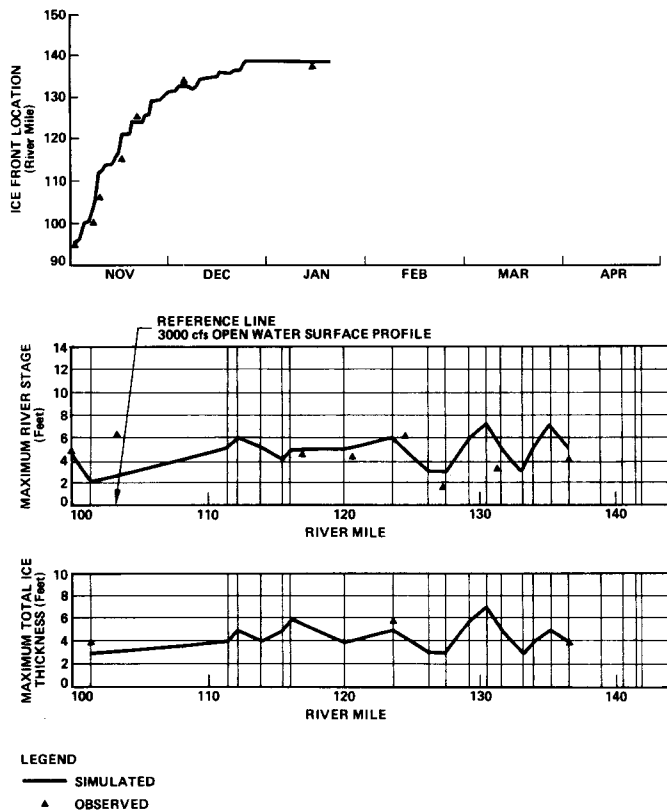


Figure 3. Sample River Ice Calibration Winter 1982-1983

RESULTS

Sample results of river ice simulations for natural conditions and the three stages of the project are shown in Figures 4 and 5. These simulations are based on weather conditions of 1981-82 (an average winter in terms of mean air temperatures) and show typical trends.

With Stage I in operation, ice front progression at the "three-river confluence" during an average winter is expected to be delayed until mid-December, about 3 weeks later than that of natural conditions (Figure 4). With the operation of the project Stages II and III, respectively, the ice cover progression is expected to be further delayed until late December or early January (Figure 5).

Spring meltout in the middle reach of the Susitna River with Stage I operating is expected to be completed by late April (Figure 4), about 2 weeks earlier than the natural breakup. With operation of

Stages II and III, the meltout would be further advanced (Figure 5), occurring in late to early March, respectively. The delayed ice front progression and the earlier-than-natural ice meltout with the project operating is due primarily to warmer-than-natural water temperatures released from the project reservoirs during the winter months.

The maximum upstream extent of the ice cover during an average winter is expected to be in the vicinity of RM 139 with Stage I operating. This ice cover extent would be reduced to near RM 133 with Stage II operating and further reduced to the vicinity of RM 114 with Stage III operating (Figure 5). Little or no ice is expected upstream of these locations with the project operating, whereas under natural conditions these reaches become covered by border ice growth.

The total thickness of the river ice cover with Stage I operating is expected to be generally similar to that of natural conditions (Figure 4). Ice cover

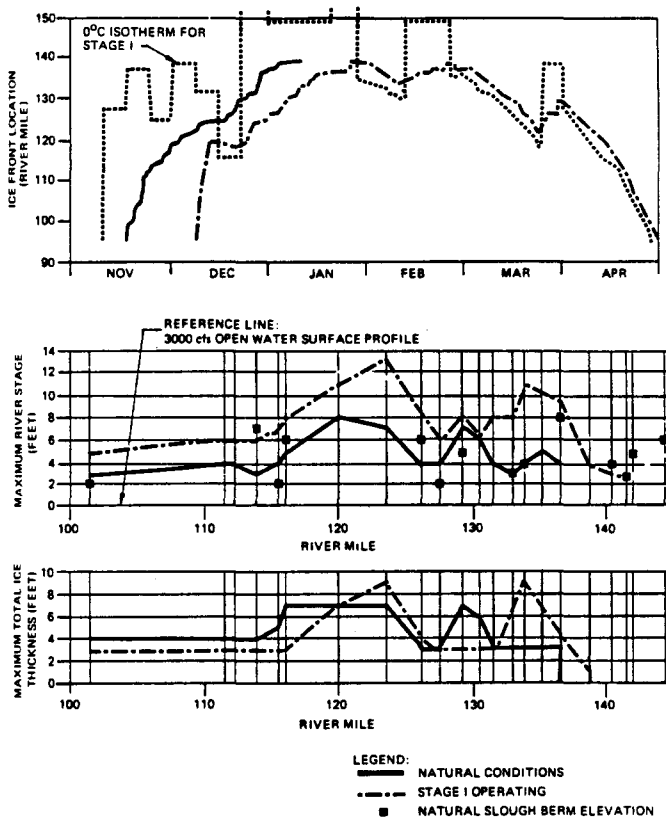


Figure 4. Simulated River Ice Conditions Stage I vs. Natural 1981-1982 Weather Conditions

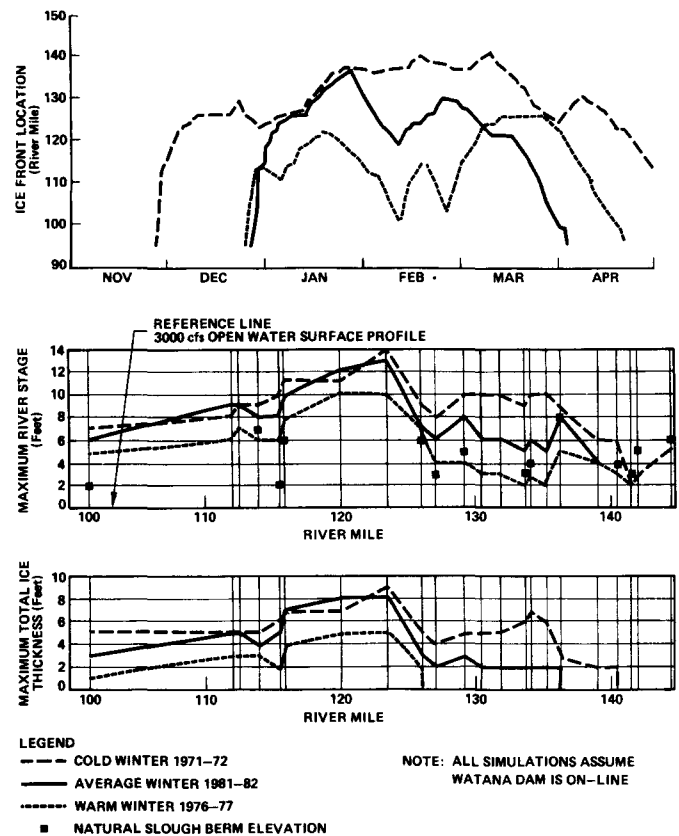


Figure 5. Simulated River Ice Conditions Stages I, II and III 1981-1982 Weather Conditions

thicknesses are expected to be progressively reduced with the addition of Stages II and III (Figure 5). The reduced extent and thicknesses of the ice cover with the project operation again primarily reflect the warmer-than-natural reservoir release temperatures.

Maximum river stages within the ice-covered reaches during operation of Stages I, II and III are expected to be generally several feet higher than those of natural conditions. This is due primarily to the greater-than-natural flow rates with the project in operation. The frequency and magnitude of the slough overtopping events upstream of the ice front with the project operating are therefore expected to be less than or equal to those of natural conditions.

The simulation results discussed above are based on the average winter weather conditions of 1981-82. Simulations were also made for a cold winter (1971-72) and a warm winter (1976-77). Although these simulations (Figure 6) were based on a different construction and operational schedule than Figures 4 and 5, they serve to indicate the sensitivity of the simulated river ice processes to weather conditions. With the project in operation during a cold winter, for example, the ice front would be expected to begin several weeks earlier and would extend several miles further upstream than for an average winter. Maximum ice cover thicknesses and river stages during a cold winter would also be about 2 feet greater than those during an average winter. During a warm winter, conversely, ice cover thicknesses and river stages are likely to be about 2 feet less than for the average winter.

SUMMARY

A numerical river ice model was applied to the Susitna River to forecast the effects of the proposed Susitna Hydroelectric Project. The model simulations predicted delayed ice cover formation, reduced ice cover extent and earlier and milder spring meltout relative to natural conditions. Greater than natural river stages were predicted for

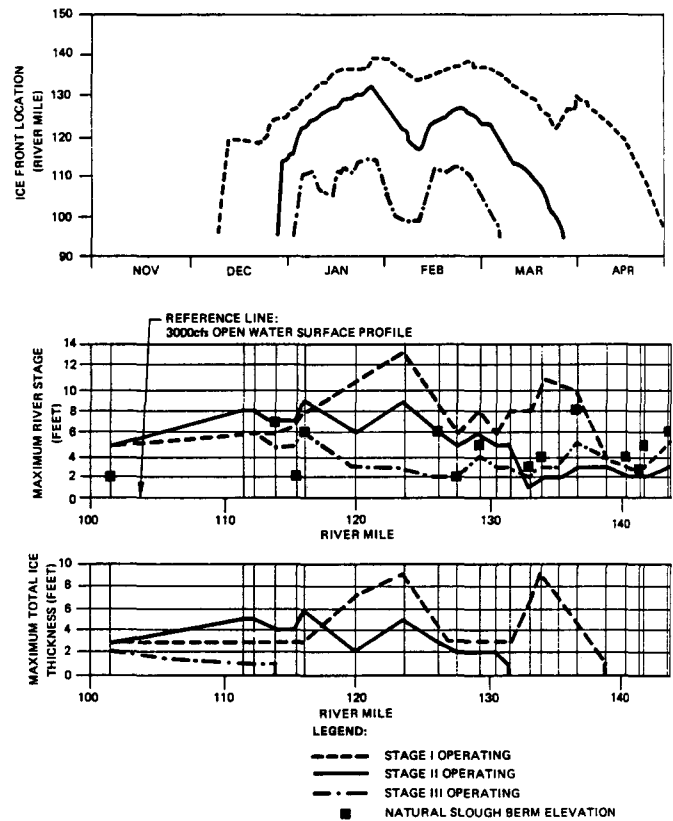


Figure 6. Simulated River Ice Results For Various Weather Conditions

some reaches, and mitigation measures will be proposed therein. Weather conditions and project stage were shown to substantially affect the expected river ice conditions.

REFERENCES

- Alaska Power Authority, 1985, Amendment to the Application for Major License, The Susitna Hydroelectric Project (Draft), prepared by Harza-Ebasco Susitna Joint Venture.
- Ashton, George D., 1978, "River Ice", Annual Reviews in Fluid Mechanics, Vol. 10, pp 369-392.
- Calkins, D.J., 1984, "Numerical Simulation of Freezeup on the Ottawaquechee River", Workshop on Hydraulics of River Ice, June 20-21, 1984, Fredericton, New Brunswick, pp 247-277.
- Gerard, R., 1984, Notes from short course "Ice Engineering for Rivers and

Lakes", University of Wisconsin.
Harza-Ebasco Susitna Joint Venture, 1984,
"Instream Ice Simulation Study" for
Alaska Power Authority.
Harza-Ebasco Susitna Joint Venture, 1985,
"Instream Ice Simulations; Supplemen-
tary Studies for Middle Susitna
River", for Alaska Power Authority.
Pariset, E., Rene Hausser and Andre
Gagnon, 1966, "Formation of Ice Covers
and Ice Jams in Rivers", ASCE Journal
of Hydraulics Division, Vol. 92, HY6.
R&M Consultants, Inc., 1981, "Ice Obser-
vations, 1980-81", for Acres American
for Alaska Power Authority.
R&M Consultants, Inc., 1982, "Winter
1981-82, Ice Observations Report", for
Acres American for Alaska Power
Authority.
R&M Consultants, Inc., 1983, "Susitna
River Ice Study, 1982-83", for Harza-
Ebasco for Alaska Power Authority.
R&M Consultants, Inc., 1985, "Susitna
River Ice Study, 1983-84", for Harza-
Ebasco for Alaska Power Authority.
R&M Consultants, Inc., 1985, "Susitna
River Ice Study, 1984 Freeze-Up",
Draft Report for Harza-Ebasco for
Alaska Power Authority.

A STRUCTURE TO CONTROL ICE FORMATION AND ICE JAM
 FLOODING ON CAZENOVIA CREEK, NEW YORK

Steven R. Predmore¹

ABSTRACT: Cazenovia Creek, in Western New York State, frequently ice jam floods the communities of West Seneca and Buffalo. This report describes the ice characteristics of Cazenovia Creek and an ice control structure (ICS) proposed by the U.S. Army Corps of Engineers to (1) modify the creek's ice formation, (2) restrict and control Cazenovia Creek ice runs, and (3) eliminate ice jam flooding in downstream residential and business areas.

The ICS, to be located just upstream of the urban development in West Seneca, consists of a 6 ft (1.8 m) high, 250 ft (76 m) long weir (dam). Extending 6 ft (1.8 m) above the weir are nine concrete piers, spaced 25 ft (7.6 m) apart, which will prevent ice runs from moving downstream. The weir and its concrete piers comprise the principal spillway for the ICS. Adjacent to this spillway are a 225 ft (69 m) long elevated weir and a 225 ft (69 m) long elevated floodway for passing high flows.

(KEY TERMS: ice control structure; ice retention structure; ice jam flooding.)

INTRODUCTION

The western New York communities of West Seneca and Buffalo, located along the lower reaches of Cazenovia Creek, are annually affected by the creek's late winter and early spring ice jam floods. The creek's peak discharges, which are

often less than channel capacity under free-flow conditions, cause significant residential and business flooding as a result of ice jams which raise stream stages above bank level. In response to the ice jam flooding, the U.S. Army Corps of Engineers has designed and physically modelled an ice control structure (ICS) which will reduce ice formation in West Seneca and Buffalo and eliminate ice jam flooding in these communities. This report describes the ice formation and ice-run characteristics of Cazenovia Creek and the design and operation of the ICS which will eliminate ice jam flood damage.

CAZENOVIA CREEK

Watershed Description

The Cazenovia Creek watershed is about 30 mi (48 km) long and has a maximum width of 10 mi (16 km) as shown in Figure 1. The creek is composed of two main branches and a main stem which drain 130 mi² (357 km²) into the Buffalo River and downstream Lake Erie. The east and west branches, in the headwaters of the watershed, are steeply sloped and rural, while the lower reaches along the main stem in West Seneca and downstream Buffalo are flat and urban developed.

The stream varies in width from 100-200 ft (30-60 m). Its average discharge over 44 years of record is 230 ft³/s (6.4 m³/s) and its maximum recorded

¹Hydrologist, U.S. Army Corps of Engineers, Buffalo District, 1776 Niagara Street, Buffalo, NY 14207.

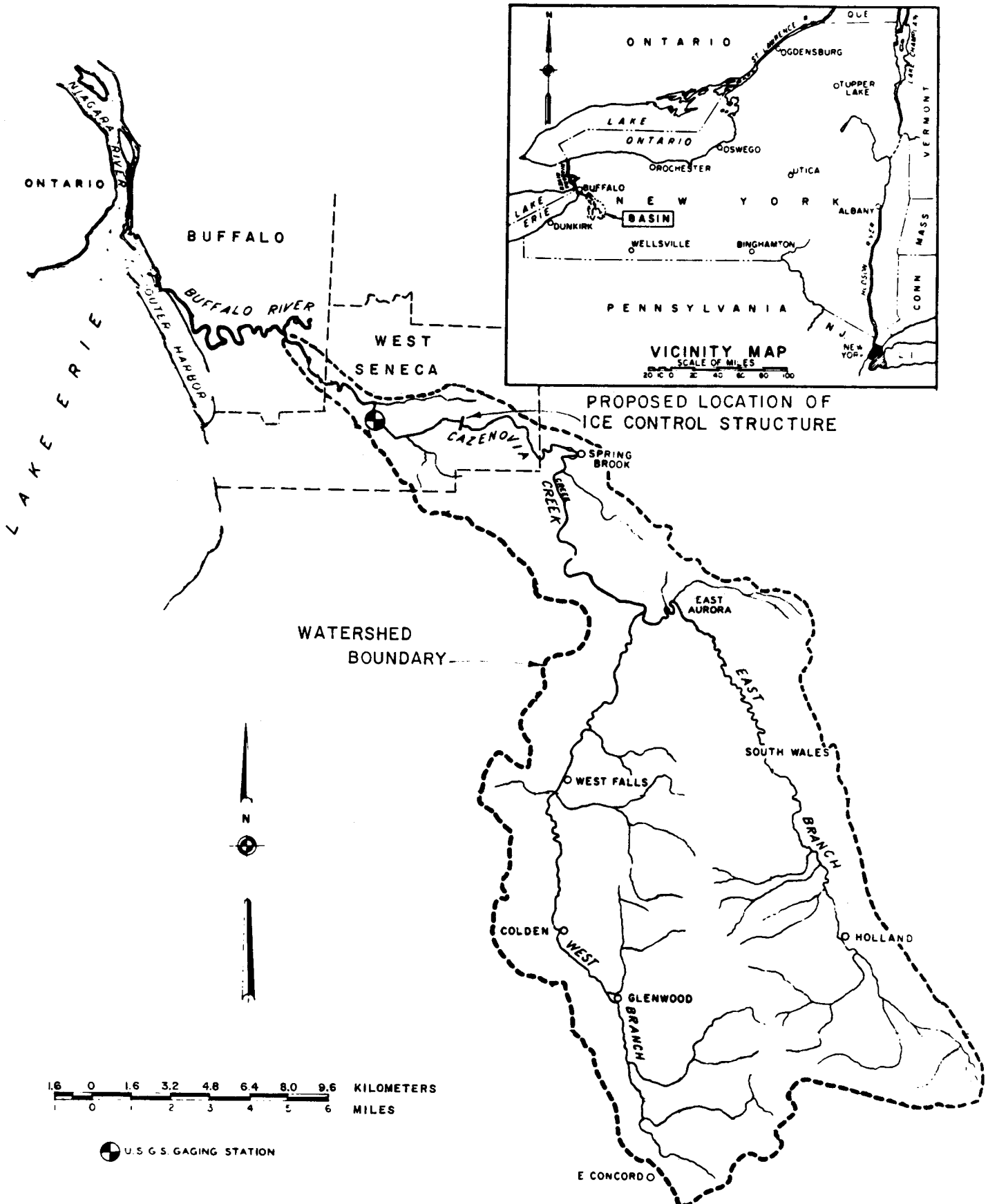


FIGURE 1. CAZENOVIA CREEK WATERSHED.

discharge is 13,500 ft³/s (382 m³/s).

A reach of very still water extends from the mouth of the creek to a point about 1 mi (1.6 km) upstream. This still-water reach is created by a deepened channel and the back-water effect of Lake Erie. Stream velocities in this reach are very low. Upstream from the still-water area, Cazenovia Creek is only 2 ft (0.6 m) deep at low discharge and exhibits stream velocities of 1-4 ft/s (0.3-1.2 m/s). The different velocity characteristics of the still-water area near the mouth and the upstream fast water area result in different ice formation characteristics in the two areas.

Ice Formation

The ice cover on Cazenovia Creek first forms as sheet ice in the 1 mi (1.6 km) long still-water reach near the mouth. Frazil ice generated in the faster waters upstream, is transported to the upstream end of the sheet ice where it is carried beneath the ice to form a hanging dam. Eventually, the frazil ice bridges the creek at the upstream end of the sheet ice and with its downstream movement halted, forms a complete ice cover which extends upstream for 7-30 mi (11-48 km), depending on the severity of the winter. Cold temperatures then solidify the surface of the frazil ice, resulting in 1.5-9 in (4-23 cm) of solid ice underlain by up to 2 ft (0.6 m) of frazil.

Ice Break-up

Because the headwaters of Cazenovia Creek are composed of two branches, the Cazenovia Creek ice break-up is often characterized by two separate ice runs. The East Branch of Cazenovia Creek experiences break-up first. The East Branch ice run subsequently enters the main stem, frequently jamming and flooding as it moves downstream. The jams cause no damage in the undeveloped upper reaches but cause significant residential and business damage when, at 6 mi (10 km) above the mouth, they reach West Seneca and then Buffalo. Following the first run, a second ice run occurs as ice vacates the West Branch and moves relatively unrestricted to the mouth.

The average annual damage due to Cazenovia Creek flooding is \$427,000, of which over \$300,000 is caused by ice jam flooding (USACE, 1985). The remainder is due to free-flow flooding. The ice control structure (ICS) proposed by the U.S. Army Corps of Engineers will alleviate the ice jam flooding in the urban-residential areas adjacent to the creek.

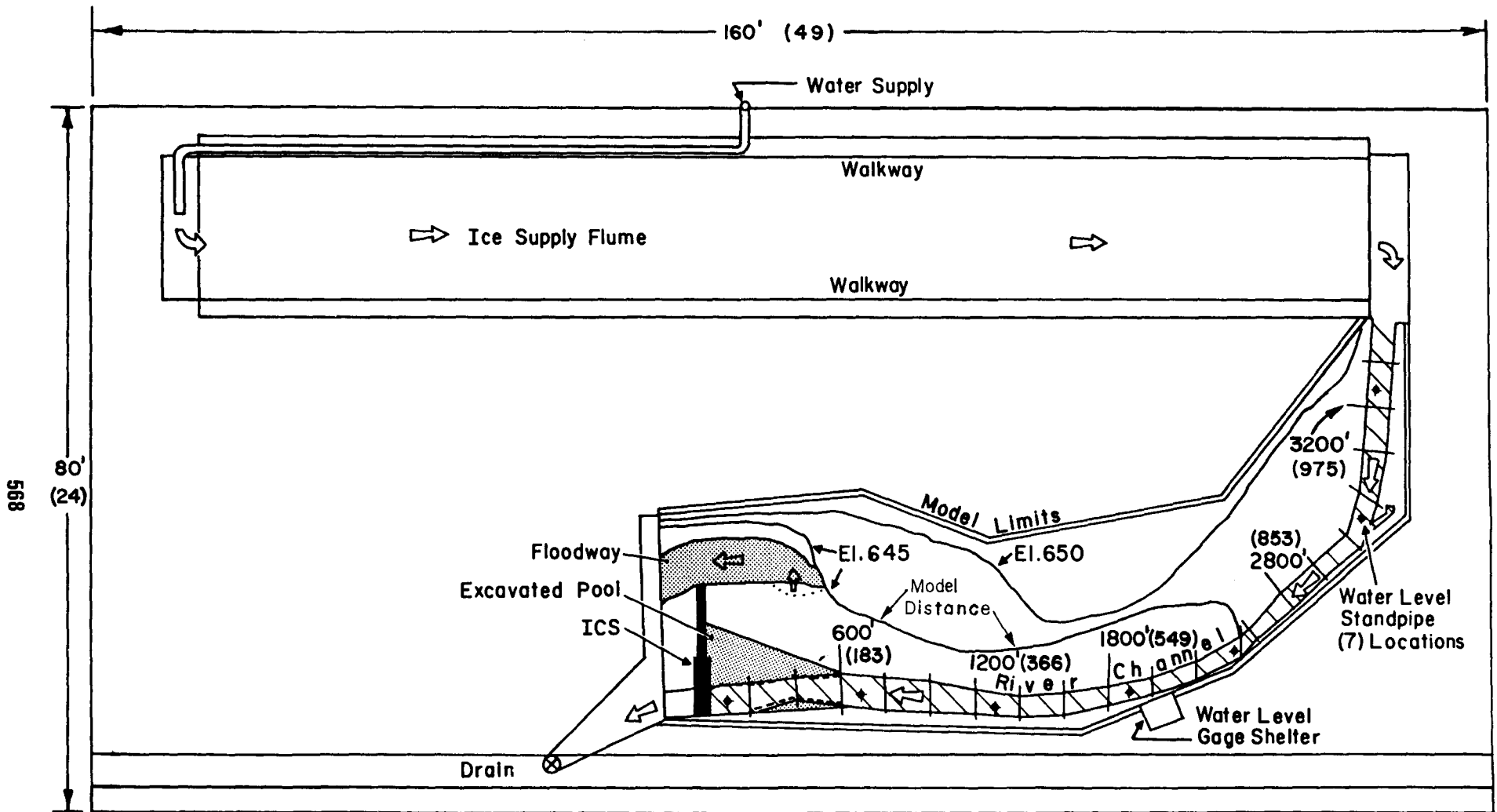
ICE CONTROL STRUCTURE

Design

The ice control structure was designed and modeled in 1984 by David S. Deck of the U.S Army Corps of Engineers, Cold Regions Research and Engineering Laboratory (CRREL), in Hanover, NH, with design assistance from the U.S. Army Corps of Engineers, Buffalo District, Buffalo, NY. The model, which simulated about 4,400 ft (1,341 m) of the creek at the proposed ICS location upstream of West Seneca development, was constructed using the conventional method of sandfill, templates, and mortar skim, and sealed with epoxy paint (Figure 2) (Deck, 1985). Constructed in CRREL's refrigerated laboratory, the model was designed using Froude criterion scaling, and used real ice doped with urea to properly scale the flexural strength of the ice. The pump used to supply water to the model provided a model discharge of up to 6,000 ft³/s (170 m³/s) which was fully adequate for designing the structure.

A variety of ICS designs were tested, with the final ICS design shown in Figure 3. The ICS is a three stage weir. The lowest weir (dam) is 6 ft (1.8 m) high, 250 ft (76 m) long and has a crest elevation of 641 ft (195.4 m) National Geodetic Vertical Datum (NGVD). Associated with this low weir are nine concrete piers, spaced 25 ft (7.6 m) apart, which are 12 ft (3.7 m) high, 3 ft (0.9 m) thick, and extend 6 ft (1.8 m) above the top of the low weir. The piers will restrict ice movement downstream. Together, the low weir and piers comprise the principal spillway of the structure.

The second stage is a 225 ft (69 m)



NOTE:
 NOT TO SCALE
 NUMBERS WITHIN () ARE METERS

FIGURE 2. PLAN VIEW OF CAZENOVIA CREEK PHYSICAL MODEL (DECK, 1985).

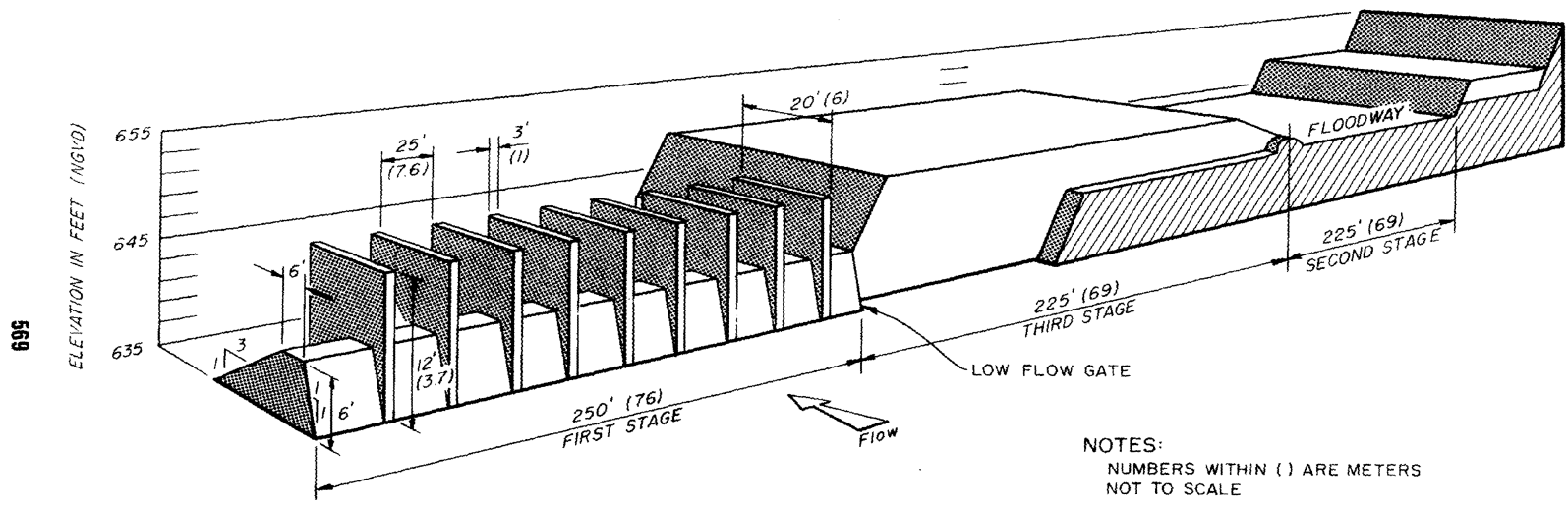


FIGURE 3. CAZENOVIA CREEK ICE CONTROL STRUCTURE (DECK, 1985 MODIFIED).

wide side-channel floodway at elevation 643 ft (196.0 m) NGVD, and will be utilized when the streamflow exceeds 3,300 ft³/s (93 m³/s). The third and highest stage of the ICS is a 225 ft (69 m) long weir which bridges the principle spillway (low weir and piers) and the side-channel floodway. The elevation of the third stage weir is 649 ft (196.6 m) NGVD.

Additional features include (USACE, 1985):

(1) A pool area, just upstream of the ICS, excavated to elevation 635 ft (193.5 m) NGVD. It is 400 ft (122 m) wide at the dam and tapers linearly to the natural stream width at a point 600 ft (183 m) upstream of the dam.

(2) A gated low-flow opening, located at one end of the low weir. The gate will be closed early in the winter to create the 6 ft (1.8 m) deep pool behind the dam. The gate will be opened to drain the pool each Spring when the threat of ice jamming has passed. The sill elevation of the opening will be 1 ft (0.3 m) lower than the pool bottom elevation. A low-flow channel will be excavated to direct summertime flows through the excavated pool to the opening.

(3) Training levees which confine excess discharges to the floodway channel.

(4) A 20 ft (6 m) long concrete splash apron immediately downstream of the low weir. The apron inhibits erosion caused by water falling from the top of the weir.

(5) An after bay excavated to 635 ft (193.5 m) NGVD extending 600 ft (183 m) downstream of the dam.

(6) An access road used for construction and subsequent maintenance of ICS.

Operation

The ICS will (1) reduce downstream ice formation, (2) initiate ice jamming in the undeveloped reach upstream of the structure, and (3) restrict ice runs from progressing to downstream developed areas.

During the winter, the 6 ft (1.8 m) deep, 30 ac (12 ha) pool will trap frazil ice which is generated in upstream reaches. By preventing the frazil ice from moving downstream, the ICS will effectively reduce the ice cover in the lower reaches of Cazenovia Creek. In addition, the stable ice cover on the pool will restrict the downstream movement of the ice run and cause the jam to occur upstream of the structure and deposit ice in the undeveloped flood plain.

Ice movement past the ICS will be restricted by the piers on top of the low weir. Further, when inflow to the structure exceeds 3,300 ft³/s (93 m³/s), and water and ice begin flowing to the floodway adjacent to the main spillway, natural vegetation (trees and brush), located just upstream of the floodway, will restrict ice movement through the floodway.

Buffalo District hydraulic studies show that the ICS piers will be overtopped when discharge reaches 10,500 ft³/s (298 m³/s). However, no ice jam flooding downstream from the ICS is expected to occur at discharges greater than 10,500 ft³/s (298 m³/s) for two reasons: modeling of the structure revealed that most of the retained ice will melt before pier overtopping occurs, and any ice passing downstream of the structure will experience relatively unrestricted flow to the mouth of the creek due to the reduced ice formation downstream of the structure and the evacuation of the ice cover from the channel prior to 10,500 ft³/s (298 m³/s).

Cost

The cost of constructing the ICS is \$1.8 million. The benefit-to-cost ratio for the project is 1.6 to 1.0. Construction may begin in 1988 and be completed in 1989.

CONCLUSION

Based on physical model tests, the proposed ICS for Cazenovia Creek will be effective in eliminating ice jam flooding in the urban developed areas of West Seneca and Buffalo, NY. The ICS design may also prove useful for ICS's in other similar cold region streams.

REFERENCES

Deck, D.S., 1985. Cazenovia Creek Physical Ice Model Study, U.S. Army Corps of Engineers, Cold Regions Research and Engineering Laboratory, Hanover, NH.

U.S. Army Corps of Engineers (USACE), Buffalo District. 1985. Draft Detailed Project Report and Environmental Impact Statement for Cazenovia Creek, West Seneca, NY, Section 205.

FREEZEUP PROCESSES ALONG THE SUSITNA RIVER, ALASKA

Stephen R. Bredthauer and G. Carl Schoch *

ABSTRACT: Operation of the proposed Susitna Hydroelectric Project in south-central Alaska would significantly alter the flow, thermal, and ice regimes of the river downstream of the projects, potentially causing significant environmental impacts. Consequently, the ice regime of the Susitna River has been monitored since 1980 to document natural ice processes and their environmental effects, and to obtain calibration data for ice modelling of certain segments of the river. This paper describes the different freeze-up characteristics along the river's length which result from the significant variations in climate, morphology, and gradient along the river.

(KEY TERMS: river ice; Alaska; Susitna River.)

INTRODUCTION

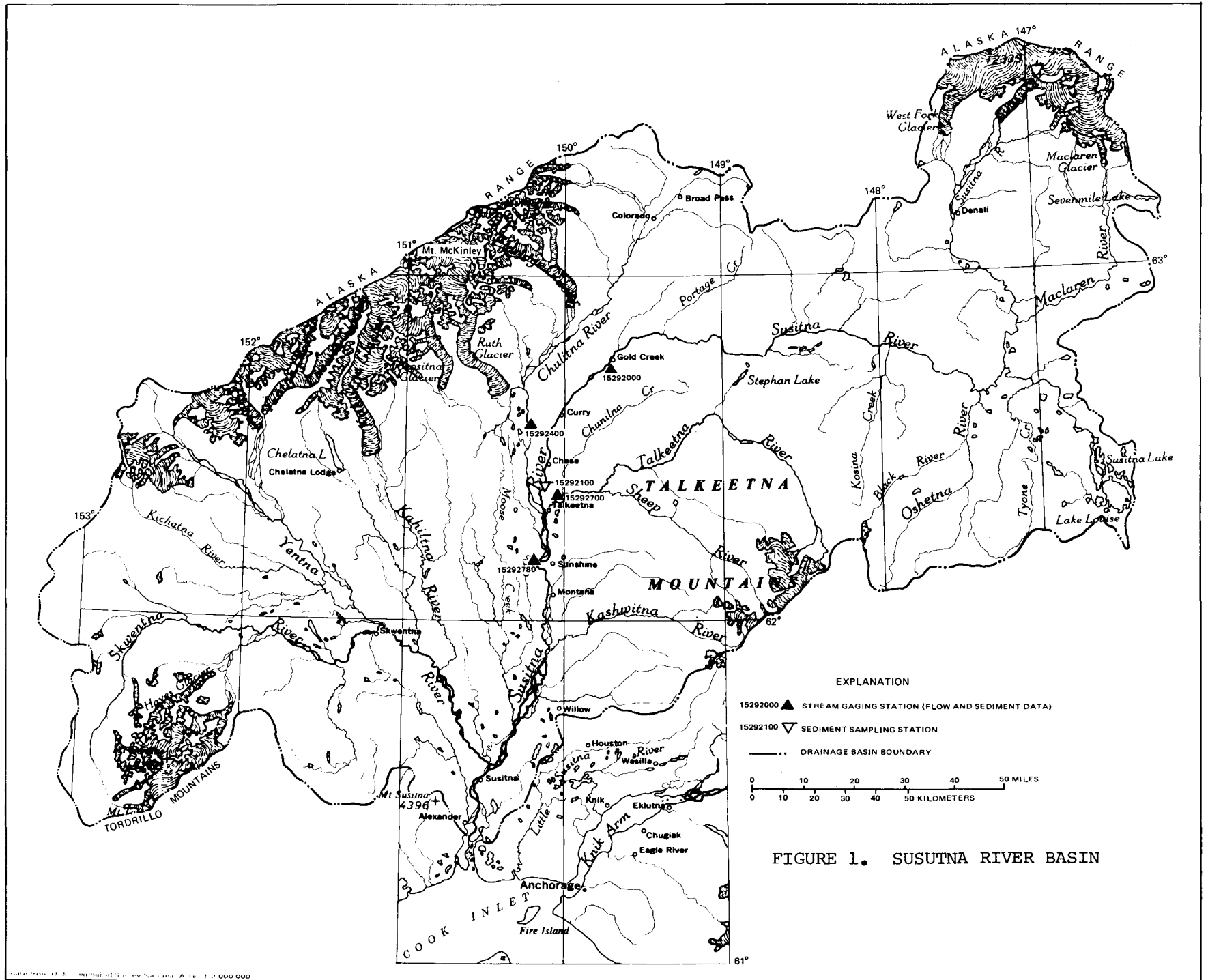
The Susitna River basin is located in southcentral Alaska, originating from glaciers on the southern flank of the Alaska Range (Figure 1). The drainage basin covers 19,600 sq. mi. (50,760 sq. km.), and is the sixth largest in Alaska.

The upper basin upstream of the damsites is in the Continental climate zone, with climate characteristics of cold, dry winters and warm, moderately wet summers. The lower basin is in the Transition climate zone (between the Continental and Maritime zones), where temperature is less variable and precipitation is greater than in the Continental zone.

The Susitna River travels a distance of about 318 mi (512 km) from its glacial

headwaters to Cook Inlet. Just downstream from the headwater glaciers, the river is highly braided. About 18 mi (29 km) downstream from the glaciers, the river develops a split channel configuration which continues for 53 mi (85 km). This initial reach, known as the upper Susitna River, has colder air temperatures than the downstream reaches due to its higher elevation and latitude. However, it also receives a substantial amount of solar radiation during freezeup because of its north-south orientation. The river then flows through a series of steep-walled canyons for about 96 mi (154 km) to the mouth of Devil Canyon. This reach, known as the impoundment zone, contains the Watana and Devil Canyon damsites at river mile (RM) 184.4 and RM 151.6, respectively. The river then emerges from the canyon into the middle Susitna River, which flows through a broad glacial U-shaped valley to the confluence with the Chulitna River (RM 98), about 50 mi (80 km) downstream. The Talkeetna River enters about one mile downstream (RM 97). Steep canyon walls along the impoundment zone and the middle Susitna River tend to shade the turbulent water surface for much of the winter. Average winter flow (November through April) in this reach is 1,600 cfs (45 cms). The river again becomes highly braided at the confluence with the Chulitna River. Average winter flow downstream of the Chulitna and Talkeetna rivers is 4,500 cfs (127 cms). The braided pattern continues for the 98 mi (157 km) downstream to the mouth of the river, with a few intermittent reaches of well-defined single or multiple channels. The Yentna River, the largest tributary to

* Respectively, Senior Civil Engineer and Hydrologist, R&M Consultants, 5024 Cordova Street, Anchorage, Alaska 99503.



the Susitna River, enters at RM 28.

ICE COVER FORMATION PROCESSES

Progression of an ice cover on the Susitna River begins in late October near the mouth at Cook Inlet. Frazil ice pans from the Yentna River, the middle and lower Susitna Rivers, and the Talkeetna and Chulitna Rivers jam to form a bridge near the mouth. This occurs during a high tide period when the air temperatures are significantly below freezing throughout the basin and frazil ice discharge is high. After the ice bridge forms, the incoming frazil ice accumulates at the upstream or leading edge of the ice cover, or at natural lodgement points such as shallows or islands, and causes the ice cover to progress upstream.

The ice cover advances upstream by different mechanisms, depending on the air temperature, volume of incoming ice, and river hydrodynamics. The mechanisms of upstream progression have been described by Calkins (1983). Additional descriptions of these mechanisms may be found in Pariset *et al* (1966) and Ashton (1978). The mechanisms are described below, along with observations of processes on the Susitna River.

(1) Progression by juxtaposition of arriving floes with no subsequent thickening, leading to a rapid ice cover development. This occurs at water velocities less than some critical value required to submerge incoming ice floes below the ice cover. On the Susitna River, this has been observed to be approximately 2 ft/sec (0.6 m/sec). Ice cover thickness equals slush floe thickness. On the Susitna River, this is the predominant process of progression upstream to about RM 25. Slush ice floes drifting through this reach have been on the water surface and exposed to cold air temperature long enough to form a solid surface layer, significantly strengthening the floes so that they resist crushing or breaking apart.

(2) Hydraulic thickening, in which slush floes arriving at the leading edge thicken to a greater value than the original ice floe thickness. The ice thickness is sufficient to transmit hydraulic forces to the banks. The ratio

of ice cover thickness to flow depth is usually less than 0.33. A related process also described by Calkins (1983) and often observed on the Susitna River is mechanical thickening or shoving of an ice cover already in place. This apparently occurs due to an instability within the ice cover relative to water velocity and increased upstream water levels which increase the pressure on the ice cover. A portion of the ice cover that has progressed by juxtaposition or hydraulic thickening may suddenly fail and move downstream, thickening as the surface area decreases. The ice cover thickness created by hydraulic processes is not sufficient to withstand the forces acting on it during its progression. The ice cover thus breaks and moves downstream, being mechanically thickened until it can withstand the forces imposed on it. The momentum of the moving ice mass may cause the ice thicknesses to be greater than the hydraulic stability requirement. The ratio of ice cover thickness to flow depth usually exceeds 0.33. Shoving usually causes a downstream progression, sometimes moving the leading edge downstream as far as 1 mile (1.61 km). This process usually occurs where water velocities exceed 4 ft/sec. (1.2 m/sec.). Hydraulic thickening and shoving are the primary processes of ice cover advance from RM 25 upstream to near RM 130. Compressions may occur repeatedly, creating higher upstream water levels and lower velocities, until progression can resume.

(3) Arriving slush floes are compressed and added to the cover, but some also submerge and break apart, eventually being deposited underneath the ice cover further downstream if lower velocities occur.

(4) Arriving slush floes do not accumulate at the ice front, but are subducted beneath the cover. They may be deposited some distance downstream.

The process of undercover deposition is difficult to document, but most likely occurs on the Susitna River. Juxtaposition and hydraulic thickening seem to be the dominant progression processes on the Susitna River, with undercover deposition and shoving the primary thickening processes.

Two other processes are also common, but do not significantly affect ice cover

progression in the reach between the river mouth and Gold Creek (RM 137). These are anchor ice and border ice formation.

Anchor ice formation is common in shallows throughout and downstream of a turbulent reach. Anchor ice is particularly prevalent upstream from RM 120, where the river may not develop an ice cover until late December. Anchor ice dams up to 2 feet thick have been documented between RM 130 and RM 149.

Border ice forms along the banks of the river as a result of (a) freezing of water in shallow areas, (b) accumulation of frazil pans in eddies and on obstructions such as bars or tree limbs, or (c) shearing of moving frazil pans on the river banks or on the border ice shelves. Border ice does not generally close the river downstream of RM 137, but may result in raising of water levels and obstructions to the downstream passage of frazil ice pans. This may lead to intermittent bridging of the river, resulting in the ice cover progressing upstream of the bridge prior to the downstream ice cover completely forming.

Border and anchor ice processes are more dominant in the reach upstream of Gold Creek (RM 137), due to the high velocities and to the fact that the ice cover normally does not progress upstream to this reach.

SEQUENCE OF ICE COVER PROGRESSION LOWER SUSITNA RIVER

Frazil ice usually first appears by October in the upper Susitna River. This ice drifts downriver, often accumulating into loosely bonded slush ice floes, until it either melts or exits from the lower Susitna River into Cook Inlet. The initiation of ice cover progression usually occurs in late October. An ice bridge forms near the mouth of the Susitna River during a period of high tide and high slush ice discharge. Initial ice bridges have been observed at RM 1.9, RM 5, and RM 9.

During the freeze-up period, the Yentna River (RM 26) often contributes from 50 to 60 percent of the total estimated ice volume below the Yentna-Susitna confluence (R&M Consultants, 1985a,b). Upstream of the Yentna River, about 80

percent of the ice is contributed by the middle Susitna River, with the Chulitna and Talkeetna Rivers contributing only about 20 percent (R&M Consultants, 1985a,b).

The ice cover progression the lower Susitna River occurs primarily by juxtaposition to about RM 25 and by hydraulic thickening upstream to about RM 130. Intermittent bridging may occur at natural lodgements points, such as shallows and islands. When this happens, the ice cover may progress upstream before the river downstream is fully ice covered. Depending on weather conditions, the ice cover will reach Talkeetna between early November and early December.

As the ice cover progresses upstream, the water level increases (stages) due to the increased resistance of flow and the displacement of the ice. Water levels generally increase about 2 to 4 feet (0.6 to 1.2 m) in the lower Susitna River due to ice, although increases of up to 8 feet (2.4 m) have been observed at the mouth of Montana Creek (R&M Consultants, 1985ab). The increased water levels due to ice are illustrated for a number of sites on the lower Susitna River in Figure 2.

The increased water levels often result in the overtopping of previously dewatered or isolated side channel entrances. The increased water flow caused by overtopping may wash out the snow cover and fracture existing ice. Slush ice from the mainstem will generally not flow into the side channel unless the overtopping depth at the overtopped upstream berm exceeds about one foot (0.3 m). If slush ice flows into the side channel, an ice cover forms rapidly in a manner similar to that described for the mainstem. Otherwise, the ice cover forms by border ice growth, which may take several weeks.

Many of the side channels dewater prior to freezeup. Others have separate water sources from tributaries or groundwater seeps. However, the groundwater seepage is greatly reduced from summer levels due to the lower flow and water level in the mainstem. During ice cover progression, the increase in mainstem water levels raises the groundwater levels in the river alluvium. Consequently, even if the entrance to a side channel is not overtopped, the increased groundwater levels may result in seepage flow in the

RELATIVE STAGE LEVELS AT SELECTED SITES DURING 1983

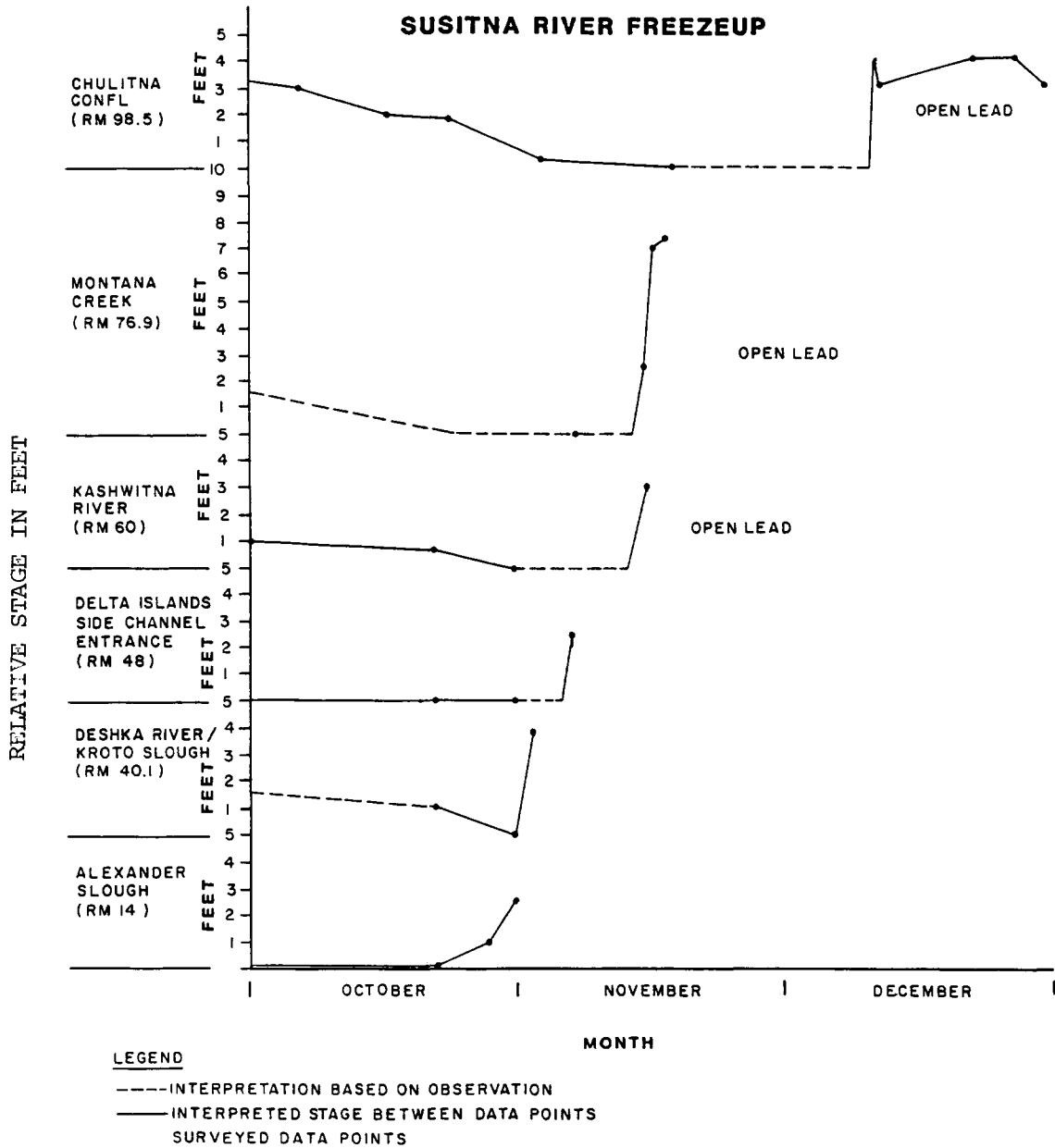


FIGURE 2. RELATIVE STAGE LEVELS AT SELECTED SITES DURING 1983 SUSITNA RIVER FREEZEUP

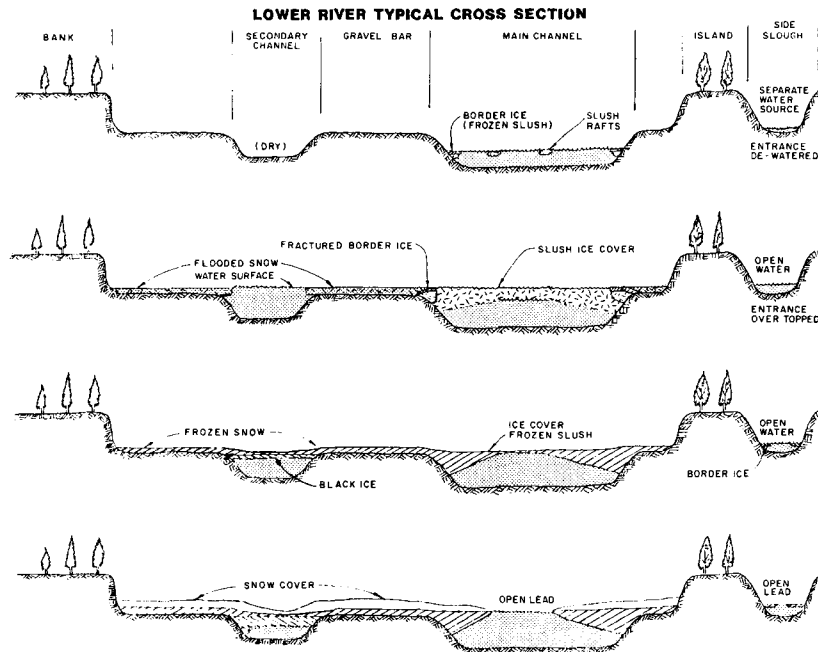


FIGURE 3. TYPICAL ICE COVER DEVELOPMENT, LOWER SUSITNA RIVER.

channel.

Major tributaries of the Susitna River (such as the Yentna, Deshka, Talkeetna, and Chulitna rivers) form an ice cover by surface accumulations of frazil slush ice after their mouths are blocked by the ice cover on the Susitna River. Smaller tributaries generally develop an ice cover by border ice and anchor ice accumulations. These minor tributaries are generally too shallow and turbulent to form a stable ice cover.

Following freezeup on the mainstem, the ice cover sags due to a gradual decrease in discharge, ice cover erosion, and bank storage. Open leads may persist in the mainstem and side channels due either to high velocity or to the thermal effects of warm groundwater.

Typical ice cover development on the lower Susitna River is illustrated in Figure 3. The days numbered on the left indicate the approximate passage of time since the leading edge of the progressing ice cover advanced upstream past each cross-section. These cross-sections are only schematics and do not represent the actual river. The lower river is much

wider than shown here, with widths exceeding 6,000 feet (1,829 m), so that the depth-to-width ratio is not representative. The schematic illustrates many of the processes of ice cover development documented on the Susitna River.

Day 1 shows slush ice rafts drifting downstream in the mainstem. The discharge has dropped low enough to dewater secondary channels and side sloughs. The drifting slush ice rafts have accumulated in low-velocity flow margins or eddies and subsequently frozen to form border ice. Little additional border ice growth occurs until water velocities decrease further. Open water exists in side sloughs, since this water is generally warm, flowing from seeps or springs. The ice front progresses to the area on Day 2, resulting in a rapid increase in water level, flooding of the surrounding gravel bars, and overtopping of the side slough. The secondary channel is inundated and now conveys water that bypasses the ice-choked mainstem. Snow on the floodplain is saturated, eventually freezing into snow ice. The ice accumulation and compressions in the mainstem have fractured the existing

border ice, which was either shoved laterally or incorporated into the cover. By Day 10, the slush ice cover has probably frozen solid, black ice has grown under the new ice, and the side channel is beginning to freeze over by border ice growth. Within about one month after the ice cover has formed over the mainstem, few additional changes will occur for the remainder of the winter. Open channel leads will typically erode through the ice cover. Depressions over the secondary channels are typical. The side channels are essentially ice-covered, but may retain an open lead.

SEQUENCE OF ICE COVER PROGRESSION MIDDLE SUSITNA RIVER

When an ice bridge forms at the Chulitna confluence (RM 98.6), ice cover progression continues upstream to the vicinity of RM 137. Depending on flow rate, ice concentrations, climatic conditions, and channel morphology, this bridge may form either when ice cover progression on the lower Susitna River reaches the confluence, or else independently of the lower river progression at a point just upstream of the Susitna-Chulitna confluence. Flow in the middle Susitna River during this period is typically about 2,000 - 3,000 cfs (610 - 914 m). In very cold years, one or more secondary bridges may form upstream of this bridge, resulting in secondary progressions of the ice cover.

Ice cover shoving, sagging, open lead development and secondary ice cover progression predominate through the reach from the Chulitna confluence to about RM 137. The ice cover progresses by juxtaposition and hydraulic thickening until encountering a critical velocity, which causes leading edge instability and failure of the ice cover. The subsequent consolidation results in ice cover stabilization due to a shortening of the ice cover, substantial thickening as the ice is compressed, a stage increase, and lateral expansion (telescoping). As the stage increases, the entire ice cover lifts, and pressures are then relieved by lateral expansion of the ice across the river channel. This process of lateral telescoping can continue until the ice

cover has expanded bank to bank or else has encountered some other obstruction (such as gravel islands) on which the ice becomes stranded.

Ice cover sag, collapse, and open lead development usually occur within days after a slush ice cover stabilizes. A steady decrease in streamflow gradually lowers the ice surface along the entire river. Prior to breakup, much of the ice rests on the channel bottom.

The typical ice cover development on the middle Susitna River is shown on Figure 4. The sequence is essentially the same as on the lower Susitna River, with the primary difference being the higher degree of staging and compression of the ice cover. The slush ice cover is shoved laterally, often to the top of the bank and vegetation line. Some ice may be eroded in high velocity areas, and redeposited where velocities are lower. As the ice is redistributed into a more hydraulically efficient cross-section, the water level recedes, causing the cover to sag, often conforming to the configuration of the channel bottom. Open channel leads are typical through this reach, but often freeze over by early March. The progression rate decreases as the ice front moves upriver, due to the increasing river gradient and the decreasing amounts of ice flowing downstream as the upper river freezes over.

The reach from RM 137 to Devil Canyon (RM 150) gradually freezes over, with complete coverage occurring much later than further downstream. The reach has a steep gradient, high velocities, and a single channel in winter. The most significant freezeup characteristics include extensive anchor ice, wide border ice layers, ice dams and snow ice.

Anchor ice dams have been observed at several locations which are constricted by border ice. The dams and constrictions create a backwater area by restricting the streamflow, subsequently causing extensive overflow onto border ice. The overflow bypasses the ice dam and re-enters the channel further downstream. Within the backwater area, slush ice accumulates in a thin layer from bank to bank and eventually freezes.

The processes of ice cover progression described for the reach downstream of RM 137 generally do not occur in

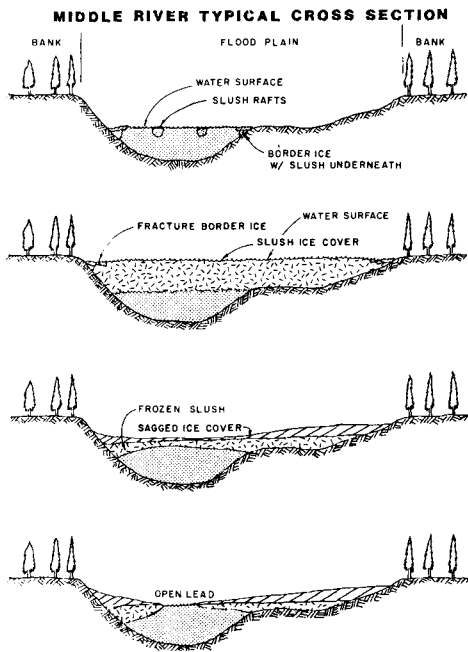


FIGURE 4. TYPICAL ICE COVER DEVELOPMENT MIDDLE SUSITNA RIVER.

this reach. There are only minimal water level increases due to anchor ice growth on the channel bottom. Sloughs and side channels are generally not breached. Open leads exist in the main channel, primarily in high-velocity areas between ice bridges.

Ice processes in Devil Canyon (RM 150 to RM 151.5) create the thickest ice along the Susitna River, with observed thicknesses of up to 23 feet (7 m) (R&M Consultants, 1981). Large volumes of slush ice enter the canyon, generated by upstream rapids or by heavy snowfall. Additional frazil ice forms in the extreme turbulence within the canyon. The slush ice repeatedly jams in a plunge pool near RM 150 and an ice cover progresses upstream, eventually staging more than 25 feet (7.6 m) above the open water level. However, slush ice has little strength, and the center of the ice cover rapidly collapses after the downstream jam disappears and the water drains from beneath the ice. Some slush ice freezes to the canyon walls, increasing in thickness with each staging repetition. The ice cover forms and erodes several times during the winter

(R&M Consultants, 1984).

Upstream of Devil Canyon, the Susitna River generally has a steep single channel with banks rising gradually from the water surface to the vegetation trim line. Low discharges through the winter result in generally shallow water. Numerous boulders exist along the channel margin, providing anchors for slush ice that drifts along the banks. Shore ice develops rapidly into the channel until water velocities exceed about 1-2 ft/sec (0.3 - 0.6 m/sec). As streamflow decreases, there is a gradual filling of the narrow open channel into a continuous ice cover.

Anchor ice thicknesses exceed 2 feet (0.6 m) in some areas, raising the water level accordingly. The rising water either fractures the border ice or overflows on top. When overflow occurs, snow on the shore ice is flooded and eventually freezes, significantly thickening the border ice.

CONCLUDING REMARKS

The paper discusses the various types of ice formation processes documented along the length of the Susitna River, a major Alaskan river being considered for hydroelectric development. Operation of the proposed Susitna Hydroelectric Project would significantly alter the flow, thermal, and ice regimes of the river downstream of the project. The studies have been conducted to document the natural physical processes on the Susitna River, both to determine their environmental effects and to provide calibration for ice modelling of with-project conditions. Since ice processes play a major role in the natural regime of northern rivers, knowledge of the effects of water resource development on the ice regime is necessary before any assessment of the environmental impacts of the project can be made.

ACKNOWLEDGMENTS

Ice studies of the Susitna River were funded by the Alaska Power Authority for licensing and design of the Susitna Hydroelectric Project. Field work was performed by R&M Consultants, Inc. under

contract to Acres American, Inc. (1980-82) and to the Harza-Ebasco Susitna Joint Venture (1983-1986).

REFERENCES

- Ashton, G. 1978. River ice. Annual Review of Fluid Mechanics. 10: 369-92.
- Calkins, D.J. 1983. Hydraulics, mechanics and heat transfer for winter freezeup river conditions. Class notes for: Ice Engineering for Rivers and Lakes, University of Wisconsin, Madison, Wisconsin.
- Pariset, E., Hauser, R. and A. Gagnon. 1966. Formation of ice covers and ice jams in rivers. Journal of the Hydraulics Division ASCE. 92: 1-24.
- R&M Consultants, Inc. 1981. Ice observations 1980-1981. Alaska Power Authority. Susitna Hydroelectric Project. Anchorage, Alaska.
- R&M Consultants, Inc. 1982. Ice observations 1981-1982. Alaska Power Authority. Susitna Hydroelectric Project. Anchorage, Alaska.
- R&M Consultants, Inc. 1984. Susitna River ice study, 1982-1983. Alaska Power Authority. Susitna Hydroelectric Project. Anchorage, Alaska.
- R&M Consultants, Inc. 1985a. Susitna River ice study 1983-1984. Alaska Power Authority. Susitna Hydroelectric Project. Anchorage, Alaska.
- R&M Consultants, Inc. 1985b. Susitna River ice study, 1984-1985. Alaska Power Authority, Susitna Hydroelectric Project. Anchorage, Alaska.

GROWTH AND DECAY OF RIVER ICE COVERS

Hung Tao Shen and A.M. Wasantha Lal¹

ABSTRACT: In this paper a mathematical model for calculating the thermal growth and decay of river ice covers is developed. The model takes into consideration the insulation effect of snow and frazil ice, the formation of snow ice, and is able to provide a continuous description of the ice cover thickness throughout the winter. Applications of the simulation model to ice covers at two different locations are also presented. (KEY TERMS: ice cover thickness; snow ice; capillary rise; black ice; heat exchange.)

INTRODUCTION

Since the classical work of Stefan (1889), studies of the thermal effect on river ice cover have generally been limited to approximate analytical solutions and empirical degree-day methods (Michel, 1971; Pivovarov, 1973). In recent years, simple finite-difference models have been developed for calculating river ice cover thickness (Ashton, 1982). These models, which correctly treated the boundary condition at the air-snow or air-ice interface and the insulation effects of snow and frazil ice, are relatively easy to use. However, these models are still restricted in that: a) all of these models consider only the growth of the ice cover, and are

not able to describe the variation of the cover thickness during the melting period; b) the formation of snow ice due to the freezing of snow slush are not considered. Studies by Lepparanta (1983) and Bengtsson (1984) considered the effect of snow ice formation. However, further refinements to these studies are needed. The existence of the capillary fringe in the snow slush, which can affect the snow ice thickness, were neglected in both of these studies. In Lepparanta's model snow slush was directly transformed into snow ice whether frozen or not. The snow surface temperature was assumed to be the same as the air temperature. Bengtsson correctly included the effect of the surface thermal resistance in calculating the black ice growth. The growth of single layer snow ice was calculated by considering the heat transfer process in the cover neglecting the surface thermal resistance. Snow slush between layers of white ice was directly transformed to snow ice.

In this paper, a generalized model for the thermal growth and decay of a river ice cover is developed and compared with field observations. The model takes into consideration the insulation effects due to the snow cover and the frazil ice as well as the possible formation of snow ice. The model also provides a continuous description

¹Respectively, Professor and Research Assistant, Department of Civil and Environmental Engineering, Clarkson University, Potsdam, N.Y. 13676.

of the ice cover thickness variation and its composition throughout the entire winter.

ANALYTICAL TREATMENT

The thermal growth and decay of an ice cover is governed by the heat exchange at the air-snow or the ice-air interface, the heat transfer through the snow and ice layers and the composition of the cover (Shen, 1985). For the ice cover shown in Fig. 1a the submergence depth h_w can be calculated by:

$$h_w = [(1-e_s)\rho_i h_s + \rho_i h_i + (1-e_f)\rho_i h_f + e_f \rho_w h_f] / \rho_w \quad (1)$$

in which, h_w = submergence depth defined as the difference between the water level and the elevation of the bottom surface of the frazil accumulation; h_s , h_i , h_f = thickness of snow, ice, and frazil layers, respectively; ρ_i , ρ_w = density of ice and water, respectively; e_s , e_f = porosity of snow and frazil respectively. In this equation, the density of the solid fraction of snow, and frazil are assumed to be the same as the density of ice. If the submergence depth is greater than the combined thickness of the ice cover and the frazil ice, then part of the snow will be submerged to become snow slush. This critical condition, $h_w > (h_i + h_f)$, is equivalent to

$$h_s > \frac{\Delta\rho(h_i + (1-e_f)h_f)}{(1-e_s)\rho_i} \quad (2)$$

in which $\Delta\rho = \rho_w - \rho_i$. For $e_s = 0.67$, and $h_f = 0$, Eq. 2 gives $h_s > 0.27 h_i$, which indicates that a relatively small snow cover thickness is required in order for an ice cover to be submerged.

Once submerged, a snow slush layer will form. The thickness of the slush layer can be calculated

from the hydrostatic balance by including the effect of the capillary fringe above the phreatic surface. The slush layer will freeze from the upper surface of the capillary fringe downward to form white ice. The thickness of the slush layer is

$$h_{sw} = \{CR\rho_w + (1-e_s)\rho_i h_{sd} - \Delta\rho[h_{ib} - (1-e_f)h_f]\} / (\rho_w - \rho_{sw}) \quad (3)$$

in which ρ_{sw} = density of slush = $(1-e_s)\rho_i + S e_s \rho_w$; CR = capillary rise; S = water saturation of the slush; h_{sd} = thickness of the dry snow. Due to the small difference between ρ_w and ρ_{sw} , the slush thickness h_{sw} will be much larger than CR. With additional snow fall, the white ice may be flooded with another slush layer forming on top of it. If the submergence of the white ice occurs before the slush layer underneath it completely turns into ice, a new layer of snow ice will be formed from the top of the new slush layer above the flooded white ice layer. This process may continue during the growth period leading to the formation of multiple layers of white ice sandwiched between slush layers. If the submergence of the white ice occurs after the slush underneath the white ice completely turned into ice, this layered white ice-slush structure will not form. Fig. 1b shows the structure of a river ice cover consists of layers of dry snow, snow slush, white ice, black ice, and frazil ice.

Surface Heat Flux

To calculate the rate of change of the cover thickness, the heat exchange with the atmosphere at the top surface of the cover must first be determined. Using the linearized form of Dingman and Assur (1967), the surface heat exchange rate can

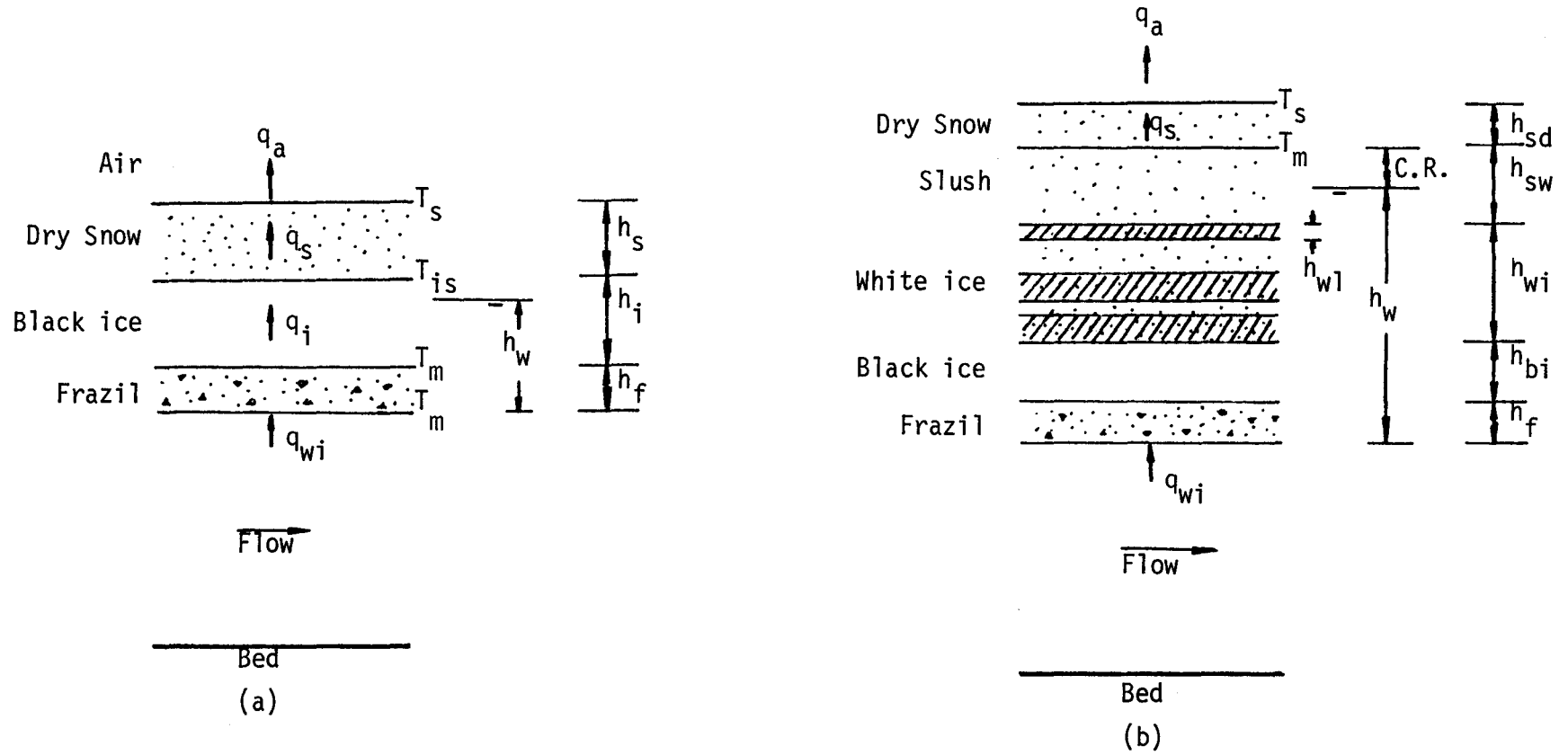


Figure 1. Thermal growth and decay of river ice cover: a) black ice growth without snow slush; b) white ice growth with snow slush and layered white ice-slush structure.

be expressed as:

$$q_a = -\phi_R + \alpha + \beta(T_s - T_a) \quad (4)$$

in which q_a = heat flux to the atmosphere from the cover surface; ϕ_R = solar radiation; T_s = surface temperature; T_a = air temperature; and α, β = coefficients which can be derived from the complete surface heat exchange processes including radiation, evaporation and sensible heat transfer. To further simplify the analysis, the solar radiation effect is sometimes lumped into the coefficients α' and β' , thus

$$q_a = \alpha' + \beta'(T_s - T_a) \quad (5)$$

Since ϕ_R varies with latitude, Eq. 5 can only apply to sites located in the same latitude for a given set of α' and β' values.

Ice Thickness Variations

The thickening and melting of the cover can be analyzed by assuming a quasi-steady linear temperature distributions in each layer of the cover. The quasi-steady assumption has shown to be acceptable for river ice covers (Greene, 1979; Ashton, 1982). In the following discussion, the formulation for the ice cover thickness variation will be presented separately for cases with or without snow slush. The surface heat flux q_a is expressed in the form of Eq. 4. The resulting formulas can be applied when q_a is approximated by Eq. 5, by setting ϕ_R to be zero and α and β to be α' and β' .

Ice Thickness Variation without Slush Layer - In this case, the surface temperature, T_s , can be determined by the conservation of heat flux across interfaces between various layers in the cover.

$$T_s = \left[\left(\frac{h_i}{h_s} + \frac{h_s}{k_s} \right) (T_a + \frac{\phi_R - \alpha}{\beta} + \frac{T_m}{\beta}) / \left(\frac{h_i}{k_i} + \frac{h_s}{k_s} + \frac{1}{\beta} \right) \right] \quad (6)$$

in which, T_m = the melting point, 0°C ; and k_i, k_s = thermal conductivities of snow and black ice, $0.3 \text{ wm}^{-1} \text{ }^\circ\text{C}^{-1}$ and $2.24 \text{ wm}^{-1} \text{ }^\circ\text{C}^{-1}$, respectively. When the ice layer consists of both the white ice and the black ice, then h_i and k_i becomes $h_i = h_{wi} + h_{bi}$ and $k_i = h_i / (h_{wi}/k_{wi} + h_{bi}/k_{bi})$, in which subscripts wi and bi represent white ice and black ice, respectively.

In the absence of frazil accumulation on the underside of the ice cover, the rate of growth of black ice, when $T_s < T_m$ is given by

$$\rho_i L_i \frac{dh_i}{dt} = \left[(T_m - T_s) / \left(\frac{h_s}{k_s} + \frac{h_i}{k_i} \right) \right] - q_{wi} \quad (7)$$

in which L_i = the latent heat of fusion of water, $3.4 \times 10^5 \text{ J kg}^{-1}$, and, q_{wi} = heat flux from the water to the ice. For the present analysis, this heat flux is taken as (Ashton, 1983)

$$q_{wi} = h_{wi} (T_w - T_m) \quad (8)$$

in which, T_w = the water temperature; and h_{wi} = a heat transfer coefficient which can be evaluated by the formula (Ashton, 1982)

$$h_{wi} = C_{wi} U_w^{0.8} D_w^{-0.2} \quad (9)$$

in which $C_{wi} = 1662 \text{ WS}^{0.8} \text{ m}^{-2.6} \text{ }^\circ\text{C}^{-1}$; D_w = flow depth, m; and U_w = the average flow velocity, m/s. The coefficient C_{wi} may increase by up to 50% when relief features form on the underside of the cover. Eqs. 6 and 7 are also valid when there is no snow cover by setting

$h_s=0$. When the surface heat flux q_a becomes negative, the surface temperature, T_s , calculated from Eq. 2 will be greater than T_m . Under this condition, T_s should be set equal to T_m , and melting of the snow cover and the ice cover can be calculated by Eqs. 10 and 11.

$$(1-e_s)\rho_i L_i \frac{dh_s}{dt} = -\phi_R + \alpha + \beta(T_s - T_a) \quad (10)$$

$$\rho_i L_i \frac{dh_i}{dt} = -h_{wi}(T_w - T_m) \quad (11)$$

When the snow cover is melted completely, melting will occur on the top and the bottom surfaces of the ice cover, the melting rate when there is no frazil accumulation becomes

$$\rho_i L_i \frac{dh_i}{dt} = -\phi_R + \alpha + \beta(T_s - T_a) - h_{wi}(T_w - T_m) \quad (12)$$

In the above analysis the water resulting from the melting of the snow or ice cover is assumed to be drained through the cover. Wake and Rumer (1979) have examined the magnitude of the error introduced by the assumption of well-drained ice surface compared to an undrained ice surface. Their analysis indicates that the effect of accumulated water over melting ice on the melting rate may be insignificant.

In the presence of a frazil ice layer on the underside of the ice cover, the growth of ice cover thickness will be accelerated (Calkins, 1979). This is because the frazil ice layer insulates the ice cover from the warm water below, as well as the fact that only the porewater in the frazil layer needs to be solidified for the downward growth of the ice cover. During the growth period, when $T_s < T_m$, the rate of growth of

the ice cover is

$$\frac{dh_i}{dt} = (T_m - T_s) / [e_f \rho_i L_i (\frac{h_s}{k_s} + \frac{h_i}{k_i})] \quad (13)$$

The rate of reduction of the frazil layer at its bottom is

$$\frac{dh'_f}{dt} = -h_{wi}(T_w - T_m) / [\rho_i L_i (1 - e_f)] \quad (14)$$

Hence, the total rate of reduction of the frazil layer is

$$\frac{dh_f}{dt} = \frac{dh'_f}{dt} - \frac{dh_i}{dt} \quad (15)$$

During the melting period, when $T_s > T_m$, the rate of reduction of the snow cover and the frazil layers can be calculated using Eqs. 10, 11 and 14, respectively. The melting at the bottom of the ice cover can occur only in the absence of the frazil layer and can be determined by Eq. 11. The rate of melting at the upper surface of the ice cover in the absence of a snow cover is

$$\frac{dh_i}{dt} = [-\phi_R + \alpha + \beta(T_s - T_a)] / \rho_i L_i \quad (16)$$

Ice Thickness Variation with Slush Layer - The major consequence of the presence of the slush layer formed by the submergence of the snow cover is the formation of white ice. In this case, the portion of the cover below the top surface of the slush layer is isothermal, and maintains a temperature at the freezing point. For the case shown in Fig. 1b, white ice will grow downward from the top surface of the slush layer. The cover surface temperature, T_s , is calculated with Eq. 17 by considering the balance of the upward heat flow in the dry, snow cover and at the snow-air interface

$$T_s = \left[\frac{h_{sd}}{k_s} \left(T_a + \frac{\phi_R^{-\alpha}}{\beta} \right) + \frac{T_m}{\beta} \right] / \left(\frac{h_{sd}}{k_s} + \frac{1}{\beta} \right) \quad (17)$$

If $T_s < T_m$, then the growth of white ice can be calculated by the equation

$$\rho_i L_i e_s S \frac{dh_{wi}}{dt} = k_s (T_m - T_s) / h_{sd} \quad (18)$$

In addition to the case shown in Fig. 1b, other cases with slush layer are possible. When the phreatic surface is close to the snow surface all of the snow will turn into slush due to the capillary rise. In this case white ice will grow downward from the top surface of the snow cover, at a rate

$$\frac{dh_{wi}}{dt} = (T_m - T_a + \frac{\alpha - \phi_R}{\beta}) / \left[\rho_i L_i e_s S \left(\frac{1}{\beta} + \frac{h_{wi}}{k_{wi}} \right) \right] \quad (19)$$

When the water level is located below the top surface of the uppermost white ice layer, the growth rate of the white ice from the bottom of this layer is

$$\frac{dh_{wl}}{dt} = (T_m - T_a + \frac{\alpha - \phi_R}{\beta}) / \left[\rho_i L_i e_s S \left(\frac{1}{\beta} + \frac{h_s}{k_s} + \frac{h_{wl}}{k_{wi}} \right) \right] \quad (20)$$

in which, h_{wl} = the thickness of the uppermost white ice layer. It should be noted that the black ice growth can occur only after the entire snow slush layer turned into white ice. The growth rate of black ice can then be calculated by Eq. 13. The melting of snow cover,

frazil layer, and the ice cover at both the upper and the lower surfaces can be calculated as discussed in the case with no slush layer.

MODEL APPLICATIONS

The thermal growth and decay of river ice covers can be computed through stepwise numerical integrations. The model is applied to the ice covers in the upper St. Lawrence River near Massena, N.Y. (Shen and Chiang, 1984, Shen and Yapa, 1985), and the ice cover on the Finnish coast of Bothnian Bay at Virpinieme (Lepparanta, 1983).

Fig. 2 shows the comparison between the observed and simulated ice thickness variations for four stations along the St. Lawrence River for the winter of 1977-78. In the simulation the surface heat exchange at the snow-air interface is calculated from Eq. 5 with $\alpha' = 14.92 \text{ wm}^{-2}$ and $\beta' = 12.62 \text{ wm}^{-2} \text{ } ^\circ\text{C}^{-1}$. Fig. 3 shows the comparison between the observed and simulated cover thickness at Virpinieme for the winter of 1976-66. The surface heat exchange is calculated based on Eq. 4. The α and β values on the snow-air interface can be calculated from

$$\alpha = 196.77 + 6.62 V_a - 1.72 RH - 0.28 CC^2 \quad (21)$$

$$\beta = 0.185 T_a + 4.61 V_a + 0.11 RH \quad (22)$$

On the ice-air interface

$$\alpha = 154.90 + 2.88 V_a - 1.11 RH - 0.32 CC^2 \quad (23)$$

$$\beta = 0.098 T_a + 2.47 V_a + 0.08 RH \quad (24)$$

in which T_a = air temperature, $^\circ\text{C}$;

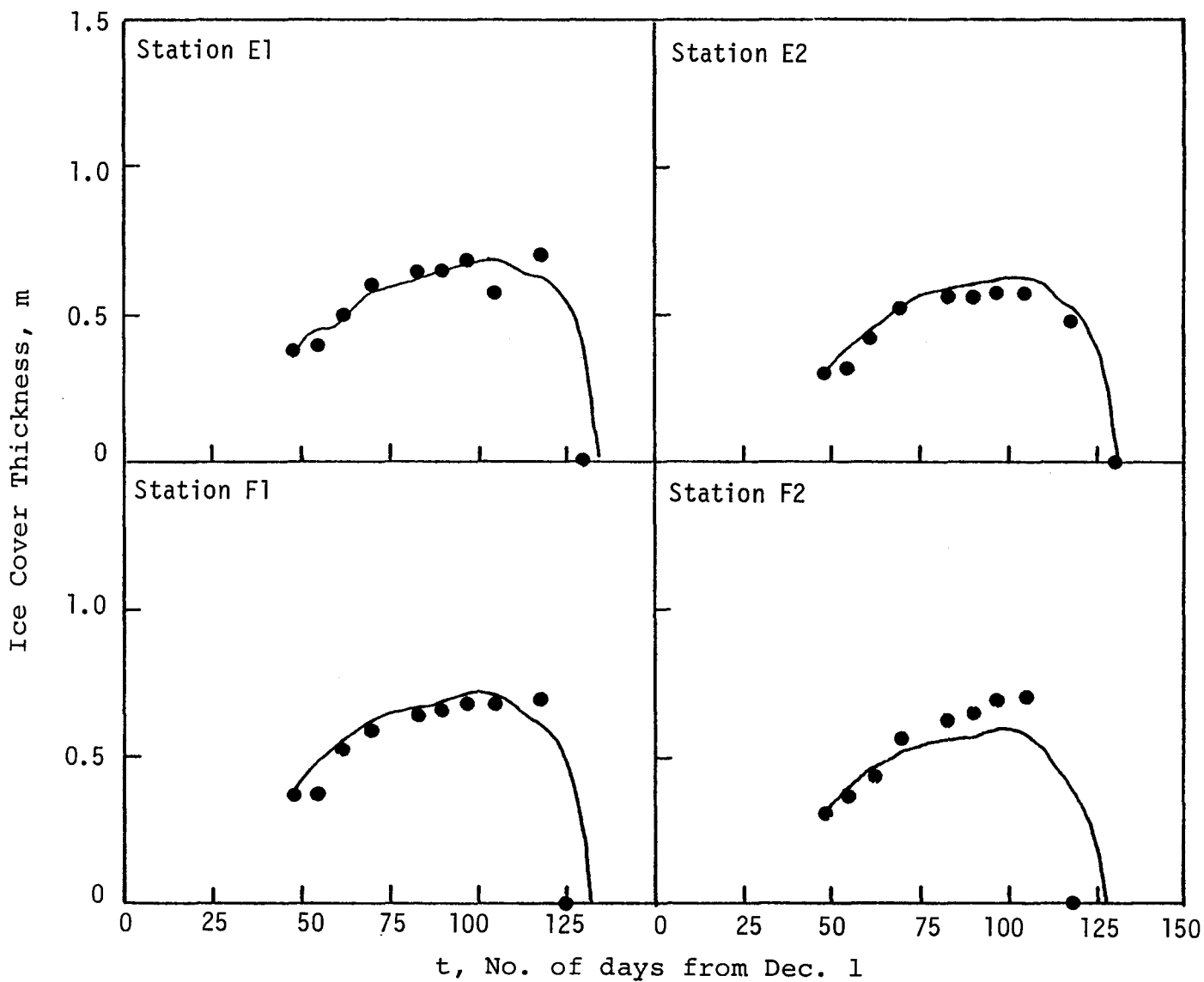


Figure 2. Comparison between observed (●) and simulated (—) ice cover thickness, St. Lawrence River, Winter of 1977-78.

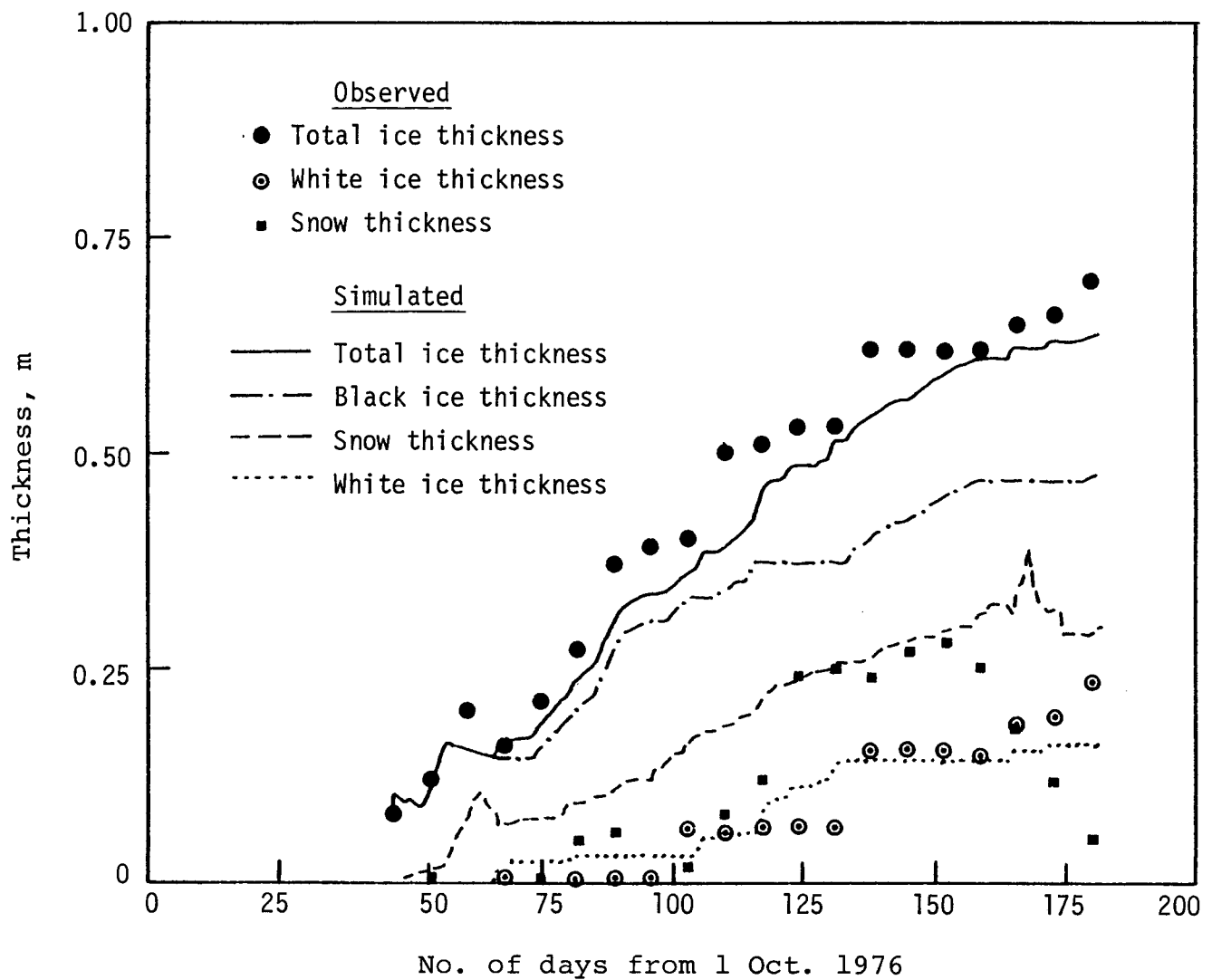


Figure 3. Comparison between observed and simulated cover thickness, Virpinieme, Finland, Winter of 1976-77.

V = wind velocity, m/sec; RH = relative humidity, %; and CC = cloud cover in tenths. Other constants used in the computations are: $k_{wi} = 2.1 \text{ wm}^{-1} \text{ }^\circ\text{C}^{-1}$, $\rho_w = 1.0 \text{ gcm}^{-3}$, $\rho_i = 0.916 \text{ gcm}^{-3}$, $e_s = 0.8$, $S = 0.94$, $CR = 1.75 \text{ cm}$, and $\rho_{wi} = \rho_i [e_s S + (1 - e_s)] = 0.872 \text{ gcm}^{-3}$. These results show that the model can provide good simulations for the growth and decay of an ice cover. Refinements by including variable snow properties due to the packing effect, (Lepparanta 1983) and the effect of the refreezing of undrained meltwater may be considered for further studies.

ACKNOWLEDGEMENT

This study is partially supported by the U.S. Army Cold Regions Research and Engineering Laboratory under Contract No. DACA 89-84-K-0008. The writers would like to thank S.C. Colbeck, C.A. Knight, and M. Lepparanta for valuable discussions. M. Lepparanta provided data at the Virpinieme site.

REFERENCES

- Ashton, G.D., 1982. Theory of Thermal Control and Prevention of Ice in Rivers and Lakes. *Advances in Hydrosience*. Vol. 13:131-185.
- Bengtsson, L., 1984. Forecasting Snow and Black Ice Growth from Temperature and Precipitation. *IAHR Ice Symposium, Hamburg*. 173-185.
- Calkins, D.J., 1979. Accelerated Ice Growth in Rivers. *CRREL Report 79-14, Cold Regions Research and Engineering Laboratory, Hanover, NH*, 4 pp.
- Greene, G.M., 1981. Simulation of Ice Cover Growth and Decay in One-Dimensional on the Upper St. Lawrence River. *NOAA TM ERL GLERL:36, Great Lakes Environmental Research Lab., Ann Arbor, MI*, 82 pp.
- Lepparanta, M., 1983. A Growth Model for Black Ice, Snow Ice and Snow Thickness in Subarctic Basins. *Nordic Hydrology*, 14: 59-70.
- Michel, B., 1971. Winter Regime of Rivers and Lakes. *Cold Regions Science and Engineering Monograph, III-Bla, U.S. Army Cold Regions Laboratory, Hanover, NH*, 131 pp.
- Pivovarov, A.A., 1973. Thermal Conditions in Freezing Lakes and Rivers. *John Wiley and Sons, New York, NY*, 136 pp.
- Shen, H.T. and Chiang, L.A., 1984. Simulation of Growth and Decay of River Ice Cover. *Journal of Hydraulic Engineering, ASCE*, 110: 958-971.
- Shen, H.T., and Yapa, P.D., 1985. A Unified Degree Day Method for River Ice Cover Thickness Simulation. *Canadian Journal of Civil Engineering*, Vol. 12:54-62.
- Shen, H.T., 1985. Hydraulics of River Ice. Report No. 85-1, Department of Civil and Environ. Engineering, Clarkson University, Potsdam, NY, 80 pp.
- Stefan, J., 1889. *Über die Theorien des Eisbildung insbesondere über die Eisbildung in Polarmure*. *Wien Sitzunber. Akad. Wiss., Ser. A, Pt. 2*: 965-983.
- Wake, A., and Rumer, R.R., Jr., 1979. Effect of Surface Melt Water Accumulation on the Dissipation of Lake Ice. *Water Resources Research*, 15(2): 430-434.

ICE JAMS IN REGULATED RIVERS IN NORWAY, EXPERIENCES AND PREDICTIONS

Randi Pytte Asvall¹

ABSTRACT: Developing water-courses for power production may cause severe ice problems in the areas involved. The general theory of ice formation in rivers is described.

Possible influences of power development on ice formation are discussed. Of special importance is the amount and temperature of the discharged water flow, and sudden increases in discharge flows during the ice period.

Experiences from selected regulated rivers in Norway are then described.

In the upper Glomma river and in Otta river there has been an increase of winter discharge in order to transport reservoir water from the upper reservoir to intake dams further down the river. This caused initially various problems with ice runs, ice jamming and flooding. By modifications of the scheme of water discharge the main problems have been overcome in most cases.

In the river Nea there has been an increase in discharge downstream from a power station in the upper part of the water-course. The problems here, which to a certain degree were expected, could only be dealt with by further developing the river downstream.

In the river Alta, which is presently being developed, and Stjørdal, which is being planned, recommended schemes of water discharge to avoid ice problems downstream from the power stations are described. These schemes will be reviewed following a 5 year trial period.

(KEY TERMS: ice conditions, frazil, ice run, ice jam, flooding.)

ICE FORMATION IN RIVERS

In slow flowing rivers with a vertical temperature gradient the formation of an ice cover is similar to that in lakes. When the flow is turbulent, however, the temperature differences within the water body are very small. In cold weather the whole water body will be cooled down to the freezing point. The water surface will be supercooled and this supercooled water film will traverse through the 0°C water body. When it comes in contact with any nuclei, frazil will be formed. When the supercooled film meets the bottom, frazil will form there and fasten to the bottom as bottom ice (Figure 1).

If there are large rocks or other obstacles on the river bed these may then be natural foundations for ice dams, often referred to as anchor ice dams. Such ice dams may develop at more or less regular intervals and divide a rapid stretch into a staircase-like system. The dams will form small reservoirs which will soon be covered by surface ice. The ice cover then stops the supercooling. Following this, a slow thaw, due to the

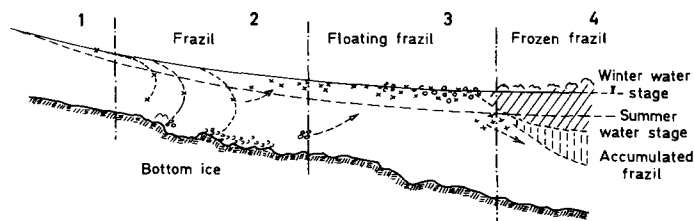


Figure 1. Formation and accumulation of frazil.

¹Norwegian Water Resources and Energy Administration.

energy change, gradually opens a narrow passage through the ice dams. After this stage the ice condition is said to be stabilized. However, before the process has reached the stage where most of such a stretch has become ice covered, large amounts of ice have been produced. The ice masses are carried further along and frequently cause problems downstream.

Ice formation in rivers with moderate current takes place mainly by the ice growing out from the shore edges or upwards from already established ice fronts. The critical values of the water velocity for this type of ice formation are about 0,4 m/s and 0,6 m/s for shore ice and front ice, respectively. At greater velocities drifting ice or frazil, often produced in turbulent flowing water upstream, does not adhere to or remain with former ice fronts. Instead it dips down under the ice and is transported further downstream. When reaching areas where the water current is reduced, the ice will accumulate under the ice cover and reduce the available cross section for water transportation. These accumulations are frequently called hanging ice dams. The whole river might gradually be clogged by ice and thus cause flooding upstream.

With changes in meteorological conditions, particularly increased temperatures or with increased water discharges, an ice dam may break down, causing step bursts, and initiating an ice run in the river. The floating ice may then accumulate further down, often where the river narrows or in a river bend, or where the slope gets smaller. This may cause an ice jam and subsequent flooding upstream. Such occurrences are known to take place in several natural rivers in Norway, and more frequently in some rivers than others.

CHANGES IN ICE FORMATION DUE TO POWER DEVELOPMENT

A power development will cause increased winter flow in rivers downstream from the power station. Normally the water temperature of the discharged water is also increased. Between the reservoir and the power station the river winter

flow may often be reduced.

Generally there is a danger of more severe ice conditions when the winter discharge is increased and the water temperature is close to 0°C. The temperature of the discharged water depends on the design of the power development. The size and relative location of the reservoirs are of special importance. Discharged water temperature in the range of 3-1°C in the beginning of the winter, gradually decreasing to 0,5°C or colder is common to many Norwegian power developments. Substantial variations in discharge temperature between plants and also from year to year are frequent.

The evaluation of future discharge water temperature following a water power development is therefore of large importance in judging the consequences on the ice formation. This is often done by modelling the temperature in the future reservoirs, based on observations of actual temperatures in existing lakes. Temperature above 0°C in the river downstream of the discharge will result in ice free stretches downstream. The extent of these stretches is often very limited, and as soon as the water masses are cooled down to 0°C ice production commences.

It may be very important to evaluate the area of such an open water stretch following a power development. In recent years several theoretical models describing the cooling of water masses under various meteorological conditions have been developed. For practical purposes, however, we have found the following simple formula presented by O. Devik in 1931 to be adequate:

$$F \cdot S = Q \cdot t$$

where F = cooling surface, S = specific heat loss, Q = water discharge and t = discharge water temperature.

Based on calculations and measurements in several Norwegian rivers Devik also established values for specific heat loss from a water surface at 0°C for various meteorological conditions. For meteorological conditions referred to as medium cold, e. g. air temperature -10°C, no clouds and no wind, or air temperature -20°C, cloudy and no wind, an average

specific heat loss in the order of 200 W/m² is used. For meteorological conditions referred to as strong cold, e.g. air temperature -20°C, clear sky and no wind, or air temperature -30°C, cloudy and no wind, an average specific heat loss in the order of 400 W/m² is used.

The area of open water (F) needed to cool a stream from 1°C down to the freezing point by medium cold, strong cold and given flow (Q) will then be as follows:

Q m ³ /s	Medium cold F(10 ³ m ²)	Strong cold F(10 ³ m ²)
1	20	10
10	200	100
50	1000	500

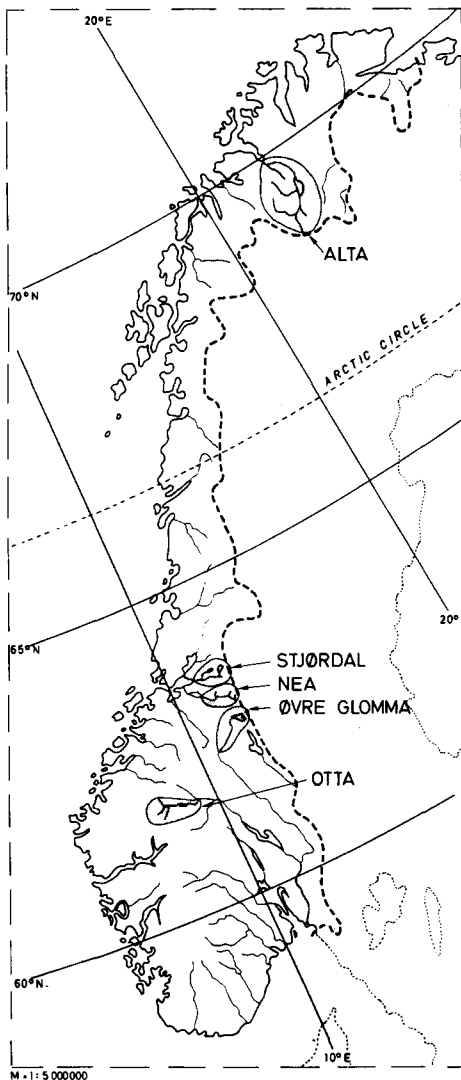


Figure 2. Location of the rivers dealt with.

As mentioned an increased winter flow of water with a temperature close to freezing will generally increase frazil formation in a turbulent flowing river. The increased flow will also cause longer stretches of the river to get turbulent flow conditions and thus expose larger areas for frazil formation. The building up of ice dams sufficiently large to stabilize the river will also take a longer time. The risk for ice dams to break down before the river is stabilized will consequently increase.

With a relatively small winter discharge the breakdown of an ice dam may often be a local event. With an increased winter flow, however, a series of ice dams may simultaneously break down. Due to the larger flow and larger ice masses stored in the river bed the damages may then be more severe.

Upstream from the discharge of the power plant, the winter flow may often be reduced. This reduction depends on the design of the power plant, but is fairly common to larger and newer developments. The river stretches thus getting a reduced flow frequently have experienced turbulent flow and subsequently large ice production before the regulation. In such areas the ice production will diminish after the regulation.

NORWEGIAN EXPERIENCES ON RIVER ICE PROBLEMS

In the following some examples of Norwegian experiences regarding ice problems in regulated rivers are described. Expected ice conditions for projects currently being built or planned are also commented on (Figure 2).

Glomma

Glomma was the first river in Norway where changed ice conditions due to power development was experienced to be a problem (Figure 3). Glomma is the longest river in Norway. The valley runs north-south in the eastern part of the country. The upper part, which is dealt with here has a typical continental climate and often very cold winters.

Aursunden, a lake in the very upper part of the water-course, was regulated

for power production on January 1. 1924. Average water discharge from Aursunden before regulation was normally about 12 m³/s on November 1. and gradually decreasing to about 5 m³/s by the first of January. The natural water flow from Aursunden just before the reservoir was taken into use, was 4 m³/s. Upon starting on January 1. the release of water was gradually increased to 20 m³/s by January 25. An ice run was initiated, this caused the upper 8 km to be ice free and flooding of the ice further downwards. Due to this, winter transport on the ice, previously common, was prevented down to Os.

The next winter the discharge was kept steady at 13 m³/s from November 15. until April 15. No ice problems were reported this winter, which was extremely mild.

The following winter the release from Aursunden was started November 15. at 13 m³/s, which was kept unchanged until December 17. From then on the release was increased gradually to 21 m³/s by January 2., and from then on kept constant until April 10. The ice situation was, however, not stabilized from Hummel-

voll to Eidsfoss, where the river is very turbulent. Several ice runs took place in connection with the increase of discharge.

The next two winters the release from Aursunden was started in October/November at 18-19 m³/s. This flow was kept until the end of January, and from then on gradually reduced. Several severe ice runs were experienced in December these two winters, both in this upper part of the river (Tolga area) and in another turbulent river stretch further down the valley.

After these years with severe damages due to ice problems it was claimed by the inhabitants in the adjacent area that the increased winter flow had increased the possibilities for ice runs in the river. A state commission was then established to study the problem.

Each breakdown of an ice dam and following ice run was analysed and compared with the meteorological situation. In all cases there had been meteorological changes that theoretically could have promoted breakdown of ice dams. Comparisons were also made with the situation in the neighbouring water-course

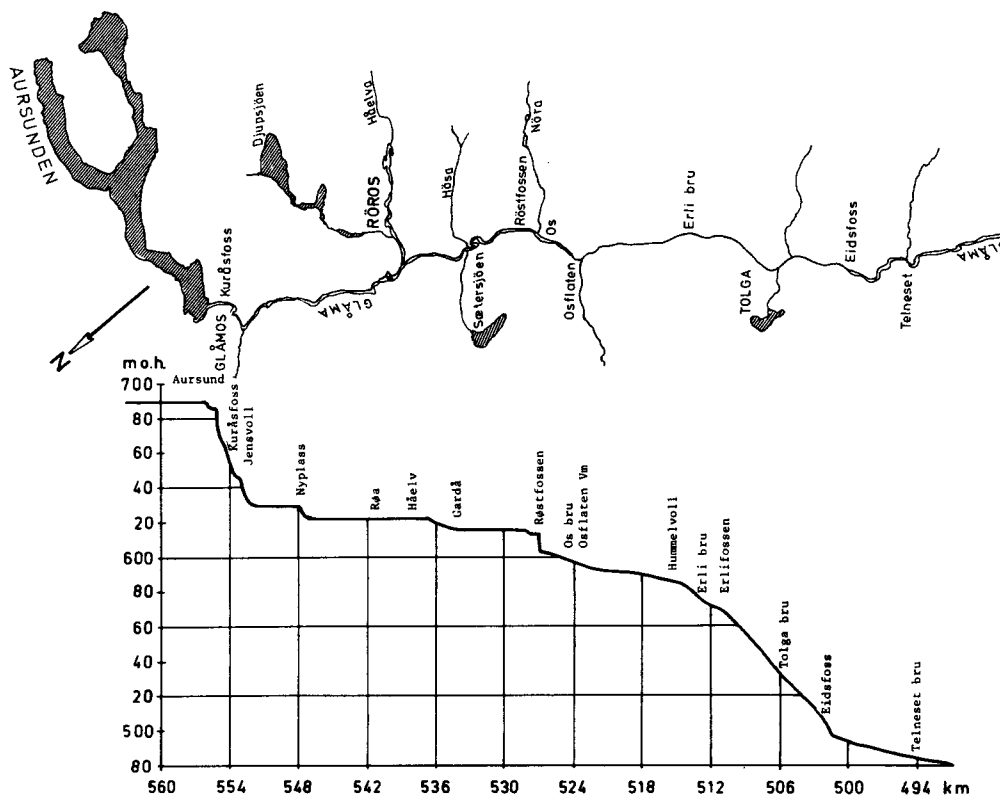


Figure 3. The upper part of Glomma river. Below the elevation and distance from the ocean.

Trysil, which was not regulated. A great similarity could be seen regarding breakdown of ice dams within the two water-courses these two years.

The formation of an ice dam was not found to be much influenced by the size of the water flow. During formation ice dams are being built just strong enough to keep the water masses accumulated by each dam, and the strength thus adjusted to the water flow. An increase in flow after the dams are established, however, will often break them down. The commission therefore arrived at the conclusion that the breakdown of ice dams and following initiation of ice runs was not due to the larger winter flow, but to changes in the meteorological conditions. The consequences of the ice runs, however, were realized to be much more severe with the increased winter flow. Therefore the commission proposed to build lenses or thresholds across the river on critical points. These should promote an early formation of a stable ice cover, reduce the slope of the river, and thus prevent possible ice runs further down the river.

Another problem in connection with the regulation was increased flooding and icing, especially in two areas, Os and Koppang (Koppang is outside the map area). The slope at both places is very gentle. The commission found that the increased winter flow had created more open river stretches, thereby increasing the formation of bottom ice and frazil, and causing jamming of the river. This increased the water stage and flooding of the river beds. Flooding of cellars was also frequent in these areas.

To avoid these problems the commission proposed to reduce the discharge from the lake Aursunden to previous unregulated winter conditions. This has later been changed to a release of $10 \text{ m}^3/\text{s}$ during the period from the start of ice formation until the river is stabilized. This normally takes place mid December. From then on it is allowed to gradually increase the release. This has been the general scheme for regulation of lake Aursunden since then, and major ice problems have generally been avoided.

Nea

The river Nea originates in Sweden and runs north-west-wards through Selbusjøen and further towards Trondheim draining into Trondheimsfjorden. The upper part of the watershed has generally a continental climate, but westerly winds may cause mild coastal weather, even with rains high up in the valley (Figure 4).

Even before regulation the river Nea experienced fairly large ice production. Problems associated with this were accepted by the population. The large and sudden changes in the meteorologic situation which the valley often experiences during winter further promote ice problems.

During the period 1941-1950 various lakes in the upper part of the water-course were regulated for power production purposes in existing power plants downstream from Selbusjøen, in the very low parts of the water-course. The corresponding increase in winter flow was fairly small and did not give noticeable changes in the ice conditions in the valley.

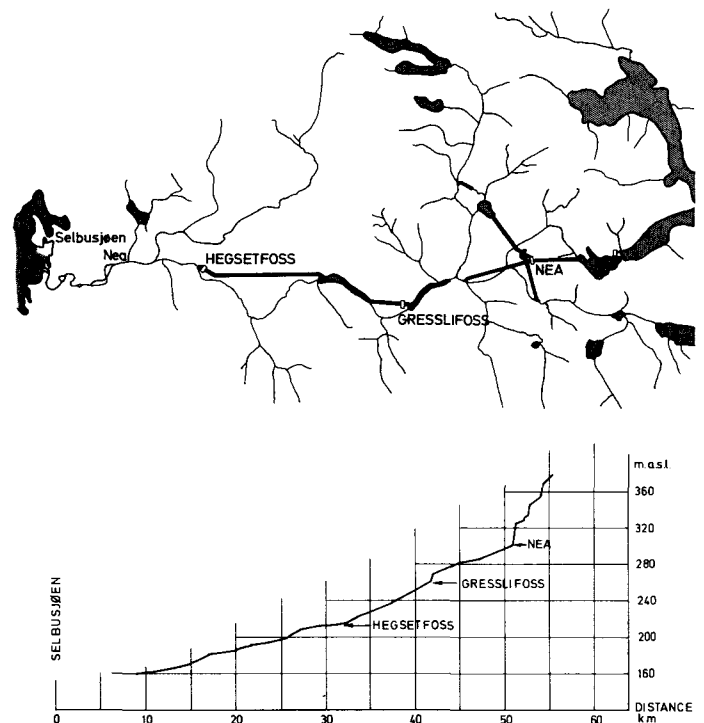


Figure 4. The Nea river with the locations of existing power stations and levelling of the main river.

about 10 to about 40 m³/s by management of the existing reservoirs. The water temperature at Eidefoss is very close to 0°C. Every winter there is frazil production, large bottom ice formation and building up of ice dams with following increased water stage along the river. The river is not stabilized every year. Under special meteorological conditions ice runs may occur, occasionally causing serious threats to the village Otta. This demonstrates that the present winter discharge is very close to the maximum acceptable level for this river. Only minor variations in discharge or meteorological conditions may consequently affect the ice conditions. The power plant management is well aware of this, but even though special care always is taken damages due to ice jams do occur.

Several alternatives for further exploitation of the upper part of the water-course have been investigated. Possible influences on the ice situation have been a part of these investigations. The present alternatives will eliminate the ice problems in the Skjåk area, but introduce new problems in the Otta area unless the river from Eidefoss and downwards is also utilized. Being aware of

this, all plans for further power production of the upper part of the water-course include simultaneous utilization also of the lower Otta river.

Alta

In the river Alta the Alta power plant is now under construction. During the planning stage of this power development ice problems were also of major consideration.

Although the area has a fairly gentle climate considering the latitude, the winter temperature is generally low, and being north of the arctic circle there is no daylight for part of the winter. Occasionally there are intrusions of milder weather in the lower part of the valley, particularly during the ice-forming period.

The water-course drains part of the Finnmark plateau. It runs northwards through the lake Vir'dnejav'ri (250 m.a.s.l.) descending a steep narrow canyon to Sav'co (80 m.a.s.l.) in the Alta valley. Alta power station utilizes the fall between Vir'dnejav'ri and Sav'co. The lake Vir'dnejav'ri is the only reservoir, and there is about 46 km

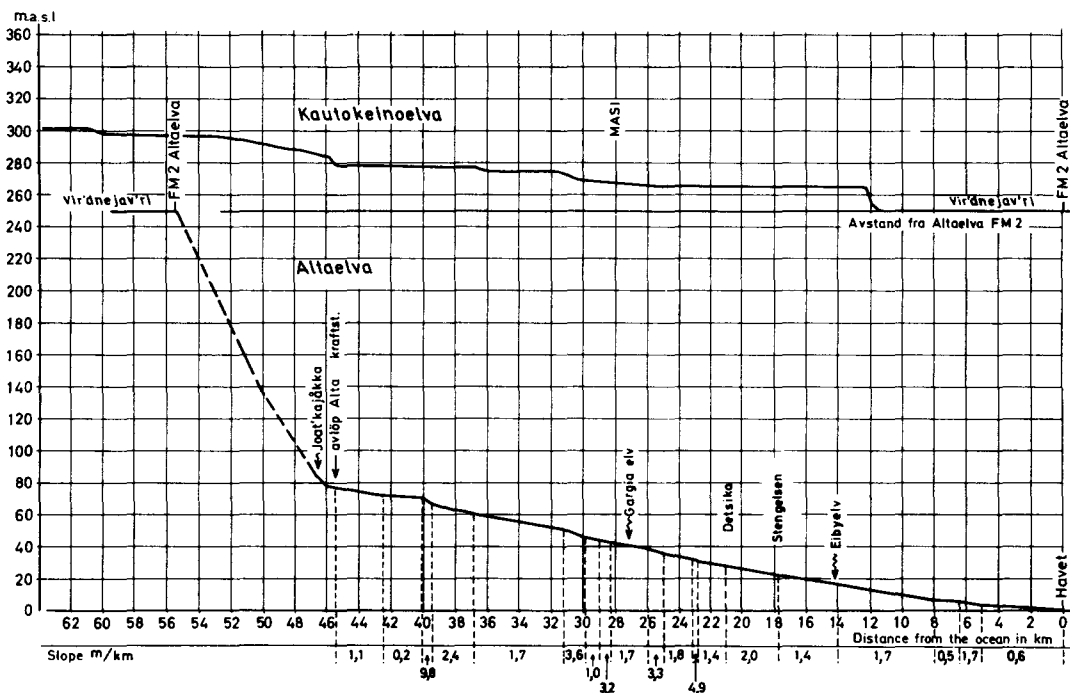


Figure 6. Levelling of the Alta river. Average slope of separate sections are shown below.

from the power station discharge to the river's outlet in Altafjord, located at approximately 70°N. The average slope is 1,7 m/km, varying between stretches with white water and more gently flowing river (Figure 6).

The question raised concerning the ice conditions was how much water could be utilized during the winter period.

Every winter there is large ice production in the river, and the rise in water stage due to ice is considerable (Figure 7). Ice jams of some kind form every winter. Normally the river will develop a stabilized ice condition, and generally be ice covered during November or December. Occasionally, however, the river has experienced severe ice runs with subsequent flooding and icing, which have delayed the stabilizing of the river.

Experiences from other water-courses in Norway have, as already mentioned, indicated that power plant generation with an increased winter flow may affect the ice conditions, often causing serious damage. The Alta river was considered to be very sensitive in this respect, mainly due to the extremely cold weather that often occurs in the winter.

The known ice runs in the river were analysed with regard to the discharge and

the meteorological situation. Only 6-8 larger winter ice runs were reported in the lower part of the river. It was known, however, that breakdown of ice dams that did not give larger ice runs were often not reported. There are certain areas where ice jams formed in this manner often occur.

Water temperature measurements were made in the Vir'dnejav'ri reservoir, and the discharge temperature was judged to be 1-2°C in the beginning of the winter season. This will give positive water temperatures a distance of some 6-10 km downstream from the discharge, depending somewhat on the meteorological conditions and the release of water. There is however in this area a fairly long river stretch with an average slope of 2,4 m/km. A stronger current here following increased flow will further retard a stabilization of the ice conditions.

In the more gentle flowing areas of the river considerable amounts of ice often accumulates at present. By increasing the winter flow, and thus creating larger ice free areas, it was feared that the ice production might be so large that it would cause severe problems, especially in the lower and most populated part of the valley. By analysing the ice situation experienced so far no connection was found between the discharge and the registered ice runs in the river, as in the Glomma case.

Even a smaller increase in discharge during the ice-forming period may, however, easily break down ice dams that are being established. It is therefore considered of major importance to avoid sudden increases in the discharge, even if these are small, at any time after ice production has started. It was also concluded that it was preferable to maintain fairly high discharge within the natural range of variation during the ice-forming period. The main discharge pattern should be similar to that during natural conditions. The reservoir should be used so that no artificial increases in discharge occur. Natural increases during this period should be eliminated or reduced as much as possible.

On these grounds it was recommended to permit a discharge during the ice-forming period in the order of the 75 percentile

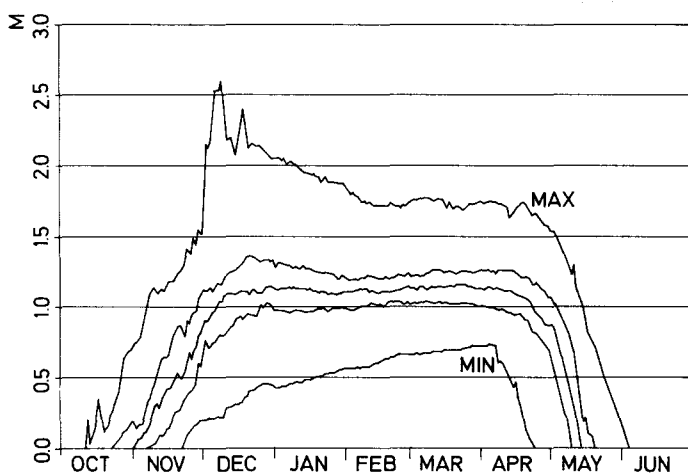


Figure 7. Characteristic values (min., 25 pc, med., 75 pc and max.) of rise in water stage due to ice in the river (1914-1968).

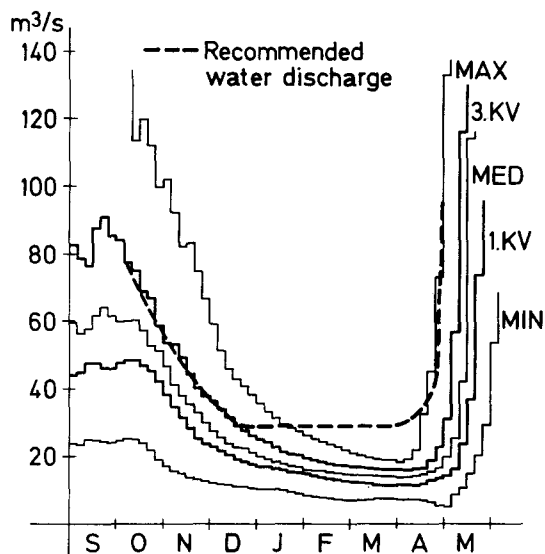


Figure 8. Recommended regulated discharge compared to natural discharge.

of natural discharge until the river is stabilized. This is expected to happen by the middle of December at a discharge of about 30 m³/s (Figure 8). This discharge may then be kept throughout the winter. If the discharge for some reason is reduced during the winter it can not be increased again without special considerations of the ice conditions.

This larger winter discharge is expected to give an earlier ice break-up in the spring and thus give the possibility for an earlier increase in discharge than the normal spring flood. In this way possible unused water in the reservoir may be used at this time. The Alta river is also a very important salmon river, and this winter scheme of discharge was acceptable also for these interests.

Usage of the reservoir according to these recommendations were concessioned for a trial period of 5 years. Upon this the control scheme will be reviewed. During the trial period the ice situation of course will be studied closely.

The power plant is planned to be commissioned in 1988. The jurisdictional survey evaluating damages and inconveniences for the population has already started. Due to the general hydrological situation and the reservoir capacity it is agreed to maintain a winter discharge somewhat lower than the official per-

mission stated above. This scheme will impose fairly large annual variations in discharge. This may be of particular interest for the coming studies.

Stjørdal

The river Stjørdalselva drains the mountainous areas close to the Swedish border, and runs westwards towards Trondheimsfjorden (Figure 9). Similar to the neighbouring Nea river described earlier, this area has generally a cold winter climate. Mild weather with rain up to fairly high altitude may occur during the winter period. This is of course very promoting for ice runs, and severe damages due to ice problems do occur.

The upper part of the water-course was regulated in 1890-1915. The existing regulation consists of several smaller power plants along the Kopperå river. The river stretches and intake reservoirs within the various plants are generally not ice covered. The water temperature is gradually decreased so that the discharge water from the lowest plant, Nustadfoss, normally has a temperature of 0,5°C or colder during winter. The discharge is fairly even and amounts to 10-12 m³/s during the winter period. This is approximately a doubling of the natural discharge. The upper river stretch, from Nustadfoss and somewhat downstream from Funna, has a very gentle slope. Then

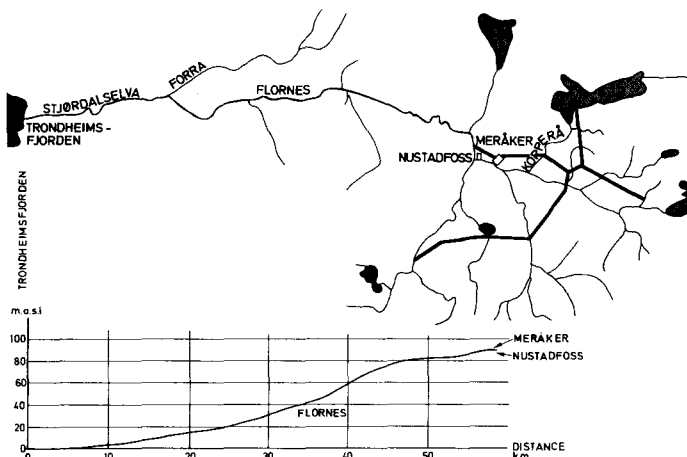


Figure 9. Stjørdalselva with planned power development. Below elevation and distance from the ocean.

there is a relatively steep river stretch down to the area of Flornes.

The somewhat newer development of the river Funna has a winter discharge of $3 \text{ m}^3/\text{s}$ with a temperature normally in the order of 2°C the first part of the winter. This gives an open area downstream of the inlet to the main river.

Before any regulation was introduced in the water-course the main river was ice covered and used for winter transport all the way up to Nustadfoss. The larger ice problems that did occur in the river was mainly due to ice runs originating in the tributaries in the lower part of the water-course. When the ice flowed into the main river it caused jamming and subsequent flooding upstream in the main river.

The introduction of Nustadfoss power plant, and thus increased winter flow downstream, reduced the ice cover on the river. The relatively steep river stretch down to Flornes became an area of fairly large frazil and bottom ice production. Series of ice dams are now being formed, and the river stretch is normally stabilized very late in the winter. Only in winters with very cold weather and a small natural discharge this river stretch will now be completely ice covered. In recent years several ice runs have started in this river stretch which have caused jamming with subsequent flooding and other damages, especially in the area around Flornes.

Further development of the power potential in the upper part of the watershed is now being planned. Larger reservoir capacity is being introduced. The planned new power plant is designed to take the reservoir water mainly through tunnels, thereby reducing the heat loss of the water. The discharge from the lowest power station, Meråker, will be approximately at the same location as the present discharge of Nustadfoss power station.

The question to be answered in this development, as was the case in Alta, is the consequences on the ice situation of a larger winter discharge downstream from the power station. How large a winter discharge that can be accepted without causing severe ice problems is of particular interest. As this is a salmon

river proper care has also to be taken of the fishing interests of the river.

This new power development is expected to give a discharge water temperature in the order of 2°C for the first part of the winter and then gradually decrease. Depending somewhat on the climatological conditions and the discharge this will prevent the ice cover on a river stretch downstream the station. It is however expected that the water temperature will be reduced to the freezing point by reaching the area of steeper slope. Here there will be frazil production and formation of ice dams. One main question is whether it is possible to run the power plant without breaking down ice dams and initiating an ice run in this area. Because of this it is extremely important to avoid any further increases in the discharge during the ice period. Meråker power station will be controlling the discharge from a far larger part of the watershed than Nustadfoss power station is today. By a careful management of the Meråker power station it is expected possible to avoid or at least reduce even natural increases in discharge during the ice-forming period. By this the possibilities for initiating ice runs on the river stretch above Flornes should be reduced.

On these grounds it will be recommended for a scheme of regulation similar to that for Alta. The discharge is gradually to be decreased according to the pattern of natural discharge during the ice-forming period. When the river is stabilized it is expected that a constant winter discharge can be kept through the winter. A winter discharge in the order of $25\text{--}30 \text{ m}^3/\text{s}$ will probably be proposed for a trial period of 5 years also in this case. The ice situation will then be observed closely. A final scheme of regulation based on actual experiences may then be established.

HYDROLOGIC ASPECTS OF ICE JAMS

Darryl Calkins*

ABSTRACT: The hydrologic aspects of ice jams have received very little attention. During the last 30 years, the major emphasis has been placed on understanding the hydraulics and mechanics of ice jams and determining their "flood" levels. However, a parameter that should be known with reasonable accuracy is the flow discharge at the ice jam location. This paper examines hydrologic information that is important for analyzing ice jam flooding problems, such as flow measurements under the ice cover and winter stage rating curves, frequency analysis of winter flow records, watershed cooling and natural river thermal regimes, ice discharge and snowmelt runoff prediction. The significance of each of these areas is addressed and suggested research opportunities are examined.

(KEY TERMS: ice jams, river ice, snowmelt, thermal analysis, winter hydrology.)

INTRODUCTION

The first question one might ask is: What is really meant by the term "hydrologic aspects" of ice jams? The International Association for Hydraulic Research, after years of heated debate, published with still much dispute the definition of an ice jam as "a stationary accumulation of fragmented ice or frazil which obstructs a waterway." The hydrologic aspects within this definition can probably be as broad and include the "quantity and quality of water and ice that reaches an ice jam site."

The hydrologic aspects of ice jams

have not been heavily researched. In the past two decades there have been considerable advances in understanding the mechanics and hydraulics of floating ice jams, mainly clarifying and applying existing theories to solving engineering problems (Pariset et al., 1966, Uzuner and Kennedy, 1976, Calkins, 1983, Beltaos, 1983). Numerical modeling of the ice processes and hydraulics has been expanded to offer greatly improved predictions of the water levels associated with ice covers and ice jams (Pashke and Schoch, 1985, Shen and Yappa, 1984, Calkins, 1984, Petryk, 1981). However, the significance of the hydrologic input to the ice jam has been neglected. For example, the prediction of the hydrograph and the associated water temperature at a certain location from rain on frozen ground or rain on snow or snowmelt is an important feature that needs attention. Anderson and Neuman (1984) recognized the importance of frozen ground on the runoff processes and proposed a frost index correction to the National Weather Service flood prediction model. This is a start in the process but, as they indicate, a more physically based model is necessary before significant gains can be made. Hydrologic models that can predict both the flow rate and the temperature during the winter season have not been developed because of a lack of understanding of some of the basic hydrologic processes.

POTENTIAL RESEARCH OPPORTUNITIES

Several areas have been identified that are deficient in knowledge or lack

*U.S. Army Cold Regions Research and Engineering Laboratory, Hanover, New Hampshire 03755-1290.

sufficient accuracy in the data when dealing with ice jams. These areas are flow discharge measurements, flood frequency analysis of flows and stages, watershed cooling and freeze-up flow prediction, natural river thermal regimes in winter, ice discharge, and snowmelt runoff predictions. The latter has received much attention from a mass prediction viewpoint, but very little has been done on the quantity of heat available during these events. For example, melting of the ice in a river occurs every year and is often the only relief from ice jam flooding, yet little is known on the temperature distribution and its timing during the runoff period.

Flow measurements and winter records

There are ongoing programs within the U.S. and Canadian Water Survey Agencies that are addressing the issue of poor records for the winter season. At a recent conference in Michigan, researchers and engineers presented their work on how flow measurements were conducted under the ice and how the stage records were adjusted to account for the ice cover.

A major difficulty in conducting flow discharge measurements under the ice cover has been the uncertainty of whether the current meter was functioning properly due to ice accumulation on the cups. Vane current meters are now being used with only minimal problems. In some of the frazil-laden rivers, finding the flow zone was a major problem; simply putting down 20 holes evenly spaced across the river does not adequately find the flow area.

An area that still needs research is in the conversion of river stage data to flow discharge. Most countries adjust their records in a similar manner taking into account other basin flow records, air temperature, precipitation, and usually one discharge reading during the winter. The actual details of correcting to the proper stage will not be given. The flow records during freeze-up are probably more accurate than those during break-up because of the non-dynamic conditions of the ice and water and the noticeable trend of declining discharge as the winter season begins.

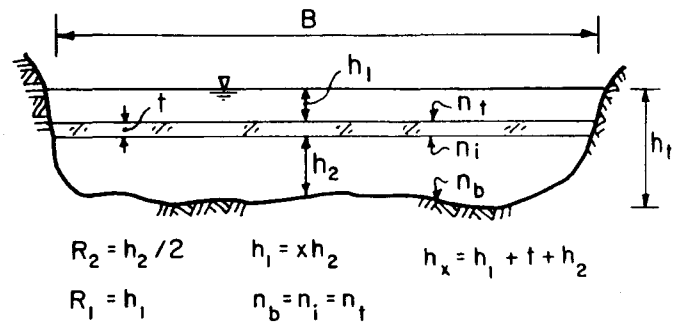


Figure 1. An example of flow occurring beneath and over the ice sheet.

Flow records during break-up can be improved by accounting for the mechanics of the ice cover and ice jam conditions. For smaller rivers the ice cover prior to break-up may flood with water over the top. Figure 1 is an example of flow occurring beneath and over the ice sheet. The flow hydraulics can easily be written for both areas, as uniform flow can still be assumed in both zones and there is no pressure flow in the lower zone.

The Manning equation is applied to the two flow areas. For ease in presentation, the bed and ice cover roughnesses (both top and bottom) are assumed the same, $n_i = n_b = n_t$. The river with a uniform slope S is sufficiently wide to assume that the wetted perimeter is nearly equal to the river width B . The flow depth over the top of the ice is represented as some fraction (x) of the flow depth below the ice cover, $h_1 = x h_2$. For the flow over and under a horizontal ice cover, the discharge is

$$Q = \frac{B S^{1/2} h_2^{5/3}}{n_b} (x^{5/3} + 0.63).$$

A potential error could arise when calculating the discharge if the flow over the top of the ice is ignored, and this is computed on the basis of the ratio Q_c / Q_u where Q_c is the total flow (under and over the ice) and Q_u is the flow under the ice at the same stage.

The flow under the ice cover is

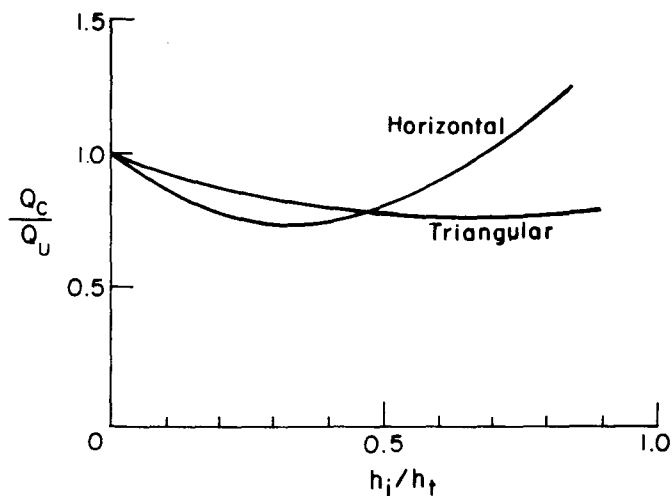


Figure 2. Error in actual discharge by not accounting for flow over the top of the ice.

$$Q_u = 0.63 \frac{BS^{1/2}}{n_b} h_t^{5/3}$$

where the ice cover thickness t is assumed to be negligible in the definition of the total stage, $h_t = h_1 + h_2 + t$.

By plotting Q_c/Q_u versus h_1/h_t in Figure 2, the error in actual discharge is seen. For example, if the flow depth over the ice cover is only one half the total depth, the calculated discharge, if one assumes the cover was fully floating, is about 20% low. When the ratio $h_1/h_t > 0.70$, then the flow discharge will be greater than that assumed for the floating cover.

The ice sheet will not remain horizontal but will deform due to the buoyancy. It has been assumed for this example that a triangular shape will represent this deformation and that the ice sheet bends at the midpoint of the channel and rises with the water level (Fig. 3). The combined flow discharge is now

$$Q_c = \frac{BS}{n_b}^{1/2} \left(\frac{h_2}{2}\right)^{5/3} \left[2 \left(\left(1 + \frac{x}{2}\right) \left(1 + \frac{x}{2}\right)^{2/3} \right) + x^{5/3} \right]$$

If the same ratio of flows Q_c/Q_u is developed for the triangular-shaped ice cover, the relationship improves slightly (Fig. 2). The triangular-shaped formulation would improve the estimate for the discharge up to $h_1/h_t = 0.5$, but thereafter the use of a triangular representation will always underestimate the flow. A time-dependency creep model could be developed to predict this shape, which would be more like that shown in Figure 4. Realistically, the error in calculating the discharge is probably between these two curves up to $h_1/h_t = 0.5$ for a finite portion of time, and this is why a time-dependency model would be more useful. Beyond $h_1/h_t > 0.5$ the discharge computation should depend upon the ice sheet shape in the channel.

Field observations by the writer in New England have indicated that when the width is in excess of 100 m, no significant water flow over the ice exists. There is a critical river width that is related to the stiffness (characteristic length) of the ice sheet, which would be a function of the ice thickness and stage rise.

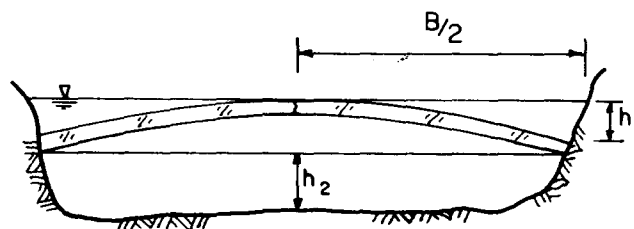


Figure 3. Triangular representation of ice cover.

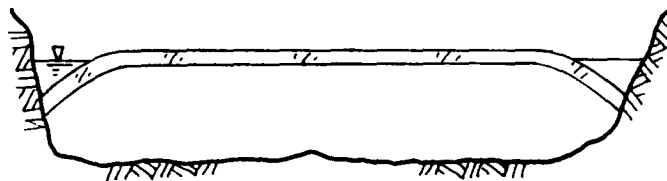


Figure 4. A more realistic representation of the ice shape in a river.

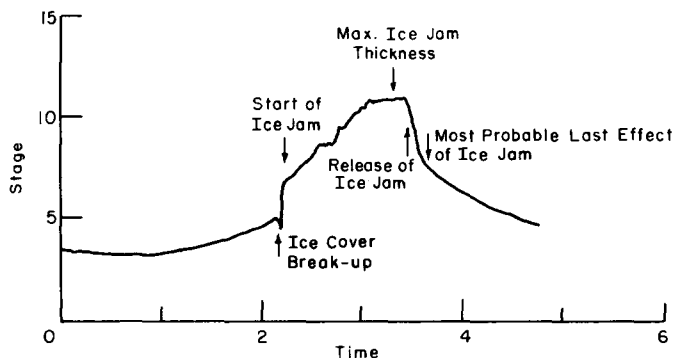


Figure 5. A typical break-up hydrograph.

During ice jam conditions, the flow estimates should be checked versus the flow computations one would get using the knowledge from the equilibrium theory for ice jam thicknesses (Beltaos, 1983, Calkins, 1983). At this time one would still have to rely on the judgement of the individual reviewing the stage records to determine when the ice cover went from a single-layered sheet to a multi-layered ice jam, which is not hard to determine from the stage records. Further research in the analysis of break-up hydrographs would help selecting the times when break-up and ice jam conditions were present. Beltaos (1984) has taken the records from one hydrometric station to evaluate the river ice break-up using the stage records for the winter period and a simple thermal energy factor. This type of analysis needs to be extended to many more sites for further evaluation. In Figure 5 is a typical break-up hydrograph where the sharp decline represents the initial break-up (water and ice moving out of storage), the next steep vertical rise indicates that the ice jam has stalled or is moving very slowly (positive wave moving upstream), and the rapid decline again indicates that the jam has moved downstream (water and ice coming out of storage). River water surface gradients during this period will be very steep and a single looped rating curve is probably not applicable.

Frequency Analysis

The frequency analysis of maximum annual winter stage and winter discharge records is becoming recognized as important for studies such as ice jam flooding,

hydro-electric winter flows or ice control, water supply regulation, etc. The population of peak flows occurring in the ice-covered and non-ice-covered seasons can be separated into "winter" and "summer" events and treated as independent sources because the processes for peak open channel floods are hydrologically based without the influence of ice on the river or runoff from snowmelt or frozen ground conditions. The winter season is defined as beginning with the day ice first forms on the river to the day of ice out. Distinctions of flow periods within the winter season are also recognized, e.g. the freeze-up versus the break-up period. Techniques for analyzing the stage and discharge frequencies have been presented in several recent papers (Gerard and Karpuk, 1978, Gerard and Calkins, 1984).

Research is needed to determine the type of distribution the winter flows follow. Can the distributions be regionally characterized? Another area that needs attention is the proper use of limited data bases and the kind of confidence limits or risks that are associated with these data sets.

Freeze-up flow prediction and watershed cooling

The prediction of flow during the freeze-up period is critical when trying to assess an ice jam flooding problem that occurs as a result of the excessive ice production. This type of flooding problem usually occurs when there has been sufficient cold weather to have frozen ground and little or no snow on the ground. A warm front then moves through the watershed bringing rain on frozen ground. The warm front is then immediately followed by a cold front that cools the river water to its freezing point, and ice generation begins with the river at relatively high flows for that time of year.

The prediction of runoff at the beginning of the winter has received little attention. Predicting the water temperature of the runoff requires knowledge of the effect of frozen ground on basin runoff and the heat loss experienced. There are algorithms for use with various hydro-

logic models that incorporate the effect of the frozen ground (Anderson and Neuman, 1984) on the response of watershed runoff, but the heat flow associated with the runoff has not been evaluated.

This writer has not been able to locate many references that address the cooling of watersheds and the impact it has on the runoff. Groundwater and other shallow source zones are under the influence of the cold front that penetrates into the soil column, but how these sources influence the river water temperature during freeze-up has not been quantified. There have been some observations on river water temperature and corresponding groundwater temperatures in nearby wells, and the definite lag in the ground water temperatures versus the river water is clearly evident.

River thermal regimes

The cooling and heating of river flows has been studied for many years in relation to excess thermal energy supplied from such users as nuclear power plants, sewage treatment outflows and heavy industry. The natural cooling regimes in rivers have not been studied in detail because of the complexity of this process. Shen and Yapa (1984) have used a convection-diffusion model for the cooling of the river flow in the St. Lawrence River. At this time the model does not account for lateral inflow and its temperature.

The cooling of the river water to its freezing temperature is important for predicting the onset of ice production and the subsequent ice cover formation. In assessing ice jam flooding, the solution that is often reached, because no other option is available, is to let the jam melt and the water levels subside. The question is, how long does the jam take to melt? If the water temperature and flow discharge are known or can be predicted, then the available heat to melt the ice jam can be computed, as well as the time. Water temperature immediately following break-up is extremely important. Parkinson (1982) reports that the water temperature at the leading edge of the break-up ice jam on the Mackenzie River was in excess of +8°C. Which is the major heat

source: short wave solar radiation, sensible heat, groundwater contribution, tributary flow or all of the above? Pangburn (personal communication) has recently measured the water temperature during the 1986 snowmelt season at the Sleepers River Watershed in Danville, Vermont.

There is a tremendous shortage of data on the temperature regimes of natural rivers immediately prior to freeze-up or just after break-up. With the use of precision thermistors, accuracies of 0.05°C are easily attainable and are necessary for research in this area. Portable water temperature instrumentation with data logging capability is now available.

Ice Discharge

One of the unknown quantities of river flow during freeze-up is the ice discharge, but it is an extremely important factor when trying to predict the water levels and the ice cover progression rates. Very little field data have been collected and limited analytical development on the heat loss at the water/air interface has been performed. A few studies have been undertaken to understand how surface and frazil ice is incorporated into the shore ice and anchor ice. Attempts have been made to measure the ice discharge on the Susitna River (personal observations, Carl Schoch, R&M Consultants), but conclusive results have not been achieved as yet when compared with analytical computations and field measurements of ice cover progression rates.

Another important aspect of the river ice discharge is the role it plays in determining the locations of the initial ice bridges that start the progression of the ice cover. Predicting the first ice bridge and its location is important and significant to any modeling effort when one is attempting to change the hydraulic regime in some manner, i.e. increased flows or channel modification. An equally important consideration is how much ice can be expected to reach a jam site during break-up.

The first step in improving our knowledge is to develop field equipment and techniques for measuring the freeze-up

ice discharge. Sampling and measuring the collected ice will be the problem. Is a full depth sampling apparatus necessary or does only the upper few centimeters of the flow depth need to be considered? How many samples in a cross section are needed? Is using a calorimeter the only method that ensures that trapped water around the ice crystals is not included in the calculation? How will the ice that is trapped in the shore ice or anchor ice be accounted for in the heat budget approach to calculating the total ice produced? As one can see, there are many questions to answer.

Snowmelt runoff prediction

This paper will not go into much detail on this subject, but the reader is referred to recent conferences and symposia that have focused specifically on the subject material, for example Unesco-WMO-IAHS 1972, CRREL 1978, the Northern Research Basins Symposiums, the Eastern and Western Snow Conferences, etc. and other journal articles. The one area that needs consideration is the prediction of water temperature along with the flow discharge, and this has been addressed in another section.

SUMMARY AND CONCLUSIONS

The importance and significance of hydrologic information for the analysis of ice jams has been emphasized. Areas of research to strengthen the quality of the hydrologic input have been suggested. These major areas are:

1. Discharge calculations during the ice cover break-up and ice jam periods based on the mechanics of the ice cover and equilibrium thickness of ice jams.

2. Statistical distributions for winter peak flows and enhanced analytical techniques for sparsely populated samples.

3. Runoff prediction for freeze-up periods where the impact of frozen ground is important.

4. Field data on the water temperature of natural streams and analytical methods for predicting the cooling of water and melting of the river ice in these streams.

5. Field measurements on the quantity of ice being generated and transported in rivers, both at freeze-up and break-up.

REFERENCES

- Anderson, E.A. and Neuman P.J., 1984. Inclusion of frozen effects in a flood forecasting model. Proceedings of the Fifth Northern Research Basins Symposium. The role of snow and ice in Northern Basin Hydrology, Viermak, Finland, March 19-23, 1984.
- Beltaos, S., 1983. River ice jam - Theory, case studies and applications. Journal of Hydraulic Engineering, ASCE, Vol. 109, No. 10, pp. 1338-1359.
- Beltaos, S., 1984. Study of river ice break-up using hydrometric station records. Proceedings of the Workshop on the Hydraulics of River Ice, June 20-21, Fredericton, N.B., pp. 41-64.
- Calkins, D.J., 1983. Ice jams in shallow rivers with floodplain flow. Canadian Journal of Civil Engineering, Vol. 10, No. 3, pp. 538-548.
- Calkins, D.J., 1984. Numerical simulation of freeze-up on the Ottawaquechee River. Proceedings of the Workshop on the Hydraulics of River Ice, June 20-21, Fredericton, N.B., pp. 247-278.
- Gerard, R. and E.W. Karpuk, 1978. Probability analysis of historical flood data. ASCE Journal of Hydraulic Division, Vol. 105, No. HY9, Sept., pp. 1153-1165.
- Gerard, R. and D.J. Calkins, 1984. Ice Related Flood Frequency Analysis: Application of Analytical Techniques. Proceedings of Cold Regions Engineering Specialty Conference, CSCE, Montreal, pp. 85-101.

- Pariset, E., R. Hauser and A. Gagnon, 1966. Formation of ice covers and ice jam in rivers. ASCE, Journal of the Hydraulics Division, Vol. 92, No. HY6, pp. 1-24.
- Parkinson, F.E., 1982. Water temperature observations during break-up on the Liard-Mackenzie River System. Proceedings of the Workshop on Hydraulics of Ice Covered Rivers. June 1-2, Edmonton, Alberta, pp. 252-265.
- Paskhe, N.W. and C. Schoch, 1985. Simulation of river ice processes on Alaska's Susitna River. Paper presented at Waterpower 85, Sept. 25-27, 1985, Las Vegas, Nevada. Proceedings to be published by ASCE.
- Petryk, S., 1981. Numerical modeling and predictability of ice regime in rivers.
- Proc. IAHR Int'l Symp. on Ice, Quebec, vol. 1, pp. 426-436.
- Shen, H.T. and D.D. Yapa, 1984. Computer simulation of ice cover formation in the upper St. Lawrence River. Proceedings, Workshop on Hydraulics of River Ice, NRCC subcommittee on Hydraulics of Ice Covered Rivers, June 20-21, Fredericton, N.B., pp. 227-245.
- Smith, K., 1974. Water temperature variations within a major river system. Nordic Hydrology, vol. 6, pp. 155-169.
- Uzuner, M.S. and J.F. Kennedy, 1976. Theoretical model of river ice jams. ASCE, Journal of the Hydraulics Division, Vol. 102, No. 9, pp. 1365-1383.

AUTHOR INDEX

Alger, George R.	275	Harleman, Donald R. F.	39
Allen, Milan W.	531	Harrison, William D.	329, 471
Ashton, William S.	415, 501	Ishikawa, N.	305
Asvall, Randi Pytte	593	Janowicz, J. Richard	313
Benson, C. S.	101, 471	Johnson, Douglas	329
Berg, Neil	201	Jones, K. C.	13
Bergman, James A.	367	Kane, Douglas L.	283, 321
Bergström, Sten	461	Kattelman, Richard C.	359, 377
Bjerklie, David	345	Kettle, Dr. Roger J.	113
Boone, Richard L.	263	Koenings, J. P.	179
Bowling, S.	471	Kobayashi, D.	297
Bradley, N. Elizabeth	407	Kojima, K.	297, 305
Braithwaite, Roger J.	485	Kraeger-Rovey, Catherine	93
Bredthauer, Stephen R.	415, 573	Kyle, Gary B.	179
Burkett, R. D.	179	Kuusisto, Esko	397
Calkins, Darryl	603	Lal, A. M. Wasantha	583
Campana, Michael E.	263	LaPerriere, Jacqueline D.	31, 143
Carlson, Robert	345	Landine, P. G.	427
Chang, Alfred T. C.	521	Latkovich, Vito J.	131
Chapman, David L.	491	Lindsay, Robert E.	221
Clark, Michael A.	113	Louie, David S.	63
Clarke, Theodore S.	329	Marron, J. K.	13
Cobb, Ernest D.	135	Marsh, P.	23
Coffin, Jeffrey H.	501	Martin, Donald C.	143
Coleman, H. Wayne	63, 557	Mayo, Lawrence R.	471, 509
Cooley, Keith R.	439	McGurk, Bruce J.	359
Cooper, David J.	93	Miller, Woodruff	541
Dean, K. G.	339	Mosher, Frederick R.	531
D'Souza, Giles	113	Motoyama, H.	297, 305
Edmundson, Jim A.	179	Munter, James A.	245
Edmundson, John M.	179	Olesen, Ole B.	485
Farnes, P. E.	13	Panfilova, V. K.	293
Feinstein, Joel I.	3	Pansic, Nicholas	221
Foster, James L.	521	Parks, Bruce	135
Futrell II, James C.	131	Paschke, Ned W.	557
Gemperline, Eugene J.	3, 63, 73	Petrik, William A.	253
Gieck, Robert E., Jr.	283	Pott, David B.	221
Gosink, J. P.	31, 471	Predmore, Steven R.	565
Granger, R. J.	427	Prowse, Terry D.	121
Gray, D. M.	427	Rhodes, Jonathan J.	157
Greenlee, D. L.	157	Robinson, David A.	547
Gross, Harry	121	Rothwell, R. L.	231
Hall, Dorothy K.	521	Rovey, Edward W.	93
Hamblin, P. F.	167	Rowe, Timothy G.	213

Rundquist, Larry A.	407
Sand, Knut	321
Santeford, Henry S.	275
Schmidt, R. A.	355
Schoch, G. Carl	573
Shafer, B. A.	13
Shen, Hung Tao	583
Sherstone, David A.	121
Skau, C. M.	157
Slaughter, C. W.	101
Sturges, David L.	53, 387
Swanson, L. E.	231
Tabler, Ronald D.	53
Tesche, T. W.	449
Theurer, F. D.	13
Trabant, D.	471
Wege, Russell E.	87
Whitfield, Paul H.	149
Whitley, W. G.	149
Wei, C. Y.	167
Woo, Sheri	201
Woods, Paul F.	195, 213
Wu, Yaohuang	3
Zuzel, John F.	237